

N O T I C E

THIS DOCUMENT HAS BEEN REPRODUCED FROM
MICROFICHE. ALTHOUGH IT IS RECOGNIZED THAT
CERTAIN PORTIONS ARE ILLEGIBLE, IT IS BEING RELEASED
IN THE INTEREST OF MAKING AVAILABLE AS MUCH
INFORMATION AS POSSIBLE

SEP

NASA TECHNICAL MEMORANDUM 79162

(NASA-TM-79162) BIBLIOGRAPHY OF LEWIS
RESEARCH CENTER TECHNICAL PUBLICATIONS
ANNOUNCED IN 1978 (NASA) 367 p
HC A16/MF A01

N81-17943

CSSL 05B

Unclas

G3/82 15676



BIBLIOGRAPHY OF LEWIS RESEARCH CENTER TECHNICAL
PUBLICATIONS ANNOUNCED IN 1978

Lewis Research Center
Cleveland, Ohio 44135
May 1979



NASA

PREFACE

In 1978, the Lewis publications output was 213 research reports and 243 journal articles and conference presentations. The number of conference presentations (199) that were given at seminars and society symposiums was the highest in the Center's history. The production of 267 contractor reports increased 16 percent over that of 1977. In addition, 50 patent applications were filed and 35 patents issued.

In 1977, the Lewis Director initiated the Annual Award for Best Lewis Publication. The purpose of the award is to encourage and reward outstanding research and technology contributions by Lewis staff members. The criteria for selection are quality and innovativeness, potential impact on the research and technology field, and the excellence of the presentation. The publication date must be between July 1 of the preceding year and June 30 of the award year. The winning publication is selected by the Lewis Research Advisory Board. The award is a framed certificate and \$1000.

In 1977, the first year of the award, the Best Lewis Publication was "Isothermal Elastohydrodynamic Lubrication Point Contacts, Parts III and IV" by Bernard J. Hamrock and Duncan Dowson (TN's D-8317 and D-8318). They are described in Abstracts N77-11400 (p. 111) and N76-35509 (p. 89) of the "Bibliography of Lewis Research Center Publications Announced in 1977" and the "Bibliography of Lewis Research Center Publications Announced in 1976," respectively.

In 1978, the Annual Award for Best Lewis Publication was presented for the following two papers: "Unsteady Flow in a Supersonic Cascade with Strong In-Passage Shocks" by Marvin E. Goldstein, Willis Braun, and J. J. Adamczyk, which is described in Abstract A78-17270 (p. 6) and "Models for Some Aspects of Atmospheric Vortices" by Robert G. Deissler, which is described in Abstract A78-14581 (p. 150).

All the publications in this collection were announced in the 1978 issues of STAR (Scientific and Technical Aerospace Reports) and/or IAA (International Aerospace Abstracts).

The arrangement of the material is by NASA subject category, as noted in the Contents. The Lewis-authored items are listed first, followed by the contractor items. Within each of these groups is listed report literature, in N-number sequence, followed by the journal and conference presentations, in A-number sequence.

The various indexes will help locate specific publications by subject, author, contractor organization, contract number, and report number.

CONTENTS

	Page
AERONAUTICS (GENERAL)	1
AERODYNAMICS	3
AIR TRANSPORTATION AND SAFETY	9
AIRCRAFT DESIGN, TESTING AND PERFORMANCE	10
AIRCRAFT INSTRUMENTATION	11
AIRCRAFT PROPULSION AND POWER	12
AIRCRAFT STABILITY AND CONTROL	34
RESEARCH AND SUPPORT FACILITIES (AIR)	35
ASTRONAUTICS (GENERAL)	36
ASTRODYNAMICS	39
GROUND SUPPORT SYSTEMS AND FACILITIES (SPACE)	40
LAUNCH VEHICLES AND SPACE VEHICLES	41
SPACECRAFT COMMUNICATIONS, COMMAND AND TRACKING	43
SPACECRAFT DESIGN, TESTING AND PERFORMANCE	44
SPACECRAFT INSTRUMENTATION	46
SPACECRAFT PROPULSION AND POWER	47
CHEMISTRY AND MATERIALS (GENERAL)	56
COMPOSITE MATERIALS	57
INORGANIC AND PHYSICAL CHEMISTRY	64
METALLIC MATERIALS	68
NONMETALLIC MATERIALS	80
PROPELLANTS AND FUELS	88
ENGINEERING (GENERAL)	91
COMMUNICATIONS	93
ELECTRONICS AND ELECTRICAL ENGINEERING	96
FLUID MECHANICS AND HEAT TRANSFER	101
INSTRUMENTATION AND PHOTOGRAPHY	109
LASERS AND MASERS	111
MECHANICAL ENGINEERING	113
QUALITY ASSURANCE AND RELIABILITY	124
STRUCTURAL MECHANICS	125
EARTH RESOURCES	129
ENERGY PRODUCTION AND CONVERSION	130
ENVIRONMENT POLLUTION	147
GEOPHYSICS	148
METEOROLOGY AND CLIMATOLOGY	150
OCEANOGRAPHY	151
LIFE SCIENCES (GENERAL)	152
AEROSPACE MEDICINE	153
MAN/SYSTEM TECHNOLOGY AND LIFE SUPPORT	154
COMPUTER OPERATIONS AND HARDWARE	155
COMPUTER PROGRAMMING AND SOFTWARE	156
CYBERNETICS	158

	Page
NUMERICAL ANALYSIS	159
STATISTICS AND PROBABILITY	160
SYSTEMS ANALYSIS	161
PHYSICS (GENERAL)	162
ACOUSTICS	163
ATOMIC AND MOLECULAR PHYSICS	169
NUCLEAR AND HIGH-ENERGY PHYSICS	170
PLASMA PHYSICS	171
SOLID-STATE PHYSICS	175
ADMINISTRATION AND MANAGEMENT	176
DOCUMENTATION AND INFORMATION SCIENCE	177
URBAN TECHNOLOGY AND TRANSPORTATION	178
SPACE SCIENCES (GENERAL)	183
SOLAR PHYSICS	184
GENERAL	185
SUBJECT INDEX (KEYWORDS)	A-1
PERSONAL AUTHOR INDEX (INCLUDES LEWIS AND CONTRACTOR AUTHORS)	B-1
CORPORATE SOURCE INDEX (CONTRACTOR ORGANIZATIONS)	C-1
CONTRACT NUMBER INDEX	D-1
REPORT/ACCESSION NUMBER INDEX (INCLUDES PATENTS)	E-1

01 AERONAUTICS (GENERAL)

N78-25049* National Aeronautics and Space Administration, Lewis Research Center, Cleveland, Ohio

INTERACTION OF A TURBULENT-JET NOISE SOURCE WITH TRANSVERSE MODES IN A RECTANGULAR DUCT
George P. Succi (MIT, Cambridge, Mass.), Kenneth J. Baumeister, and K. Uno Ingard (MIT, Cambridge, Mass.) Jun. 1978 42 p refs
(NASA-TP-1248; E-9482) Avail: NTIS HC A03/MF A01 CSCL 20A

A turbulent jet was used to excite transverse acoustic modes in a rectangular duct. The pressure spectrum showed asymmetric singularities (pressure spikes) at the resonant frequencies of the duct modes. This validates previously published theoretical results. These pressure spikes occurred over a range of jet velocities, orientations, and inlet turbulence levels. At the frequency of the spike, the measured transverse pressure shape matched the resonant mode shape. Author

N78-27048* National Aeronautics and Space Administration, Lewis Research Center, Cleveland, Ohio

ACEE PROPULSION OVERVIEW c07
Donald L. Nored In NASA, Langley Res. Center, CTOL Transport Technol., 1978 Jun. 1978 p 9-23 refs (For primary document see N78-27046 18-01)
Avail: NTIS HC A22/MF A01 CSCL 21E

Technology for fuel-efficient subsonic CTOL transport aircraft is discussed. The engine component improvement project, the energy efficient engine project, and the advanced turboprop project are included. The overall goals and objectives of each project are reviewed and the approach and schedule for accomplishing these project goals and objectives are given. J.M.S.

N78-27055* National Aeronautics and Space Administration, Lewis Research Center, Cleveland, Ohio

STATUS OF ADVANCED TURBOPROP TECHNOLOGY c07
J. F. Dugan, B. A. Miller, and D. A. Sagerser In NASA, Langley Res. Center, CTOL Transport Technol., 1978 Jun. 1978 p 139-166 refs (For primary document see N78-27046 18-01)
Avail: NTIS HC A22/MF A01 CSCL 21E

Research is reviewed in the following areas: turboprop powered transport aircraft, wind tunnel aerodynamic and acoustics tests of model propellers, turboprop maintenance, and wind tunnel tests on airframe-turboprop interactions. Continued development of the technology for advanced turboprop transport was emphasized. J.M.S.

N78-27056* National Aeronautics and Space Administration, Lewis Research Center, Cleveland, Ohio

PROPULSION SYSTEMS NOISE TECHNOLOGY c07
C. E. Feiler In NASA, Langley Res. Center, CTOL Transport Technol., 1978 Jun. 1978 p 167-185 refs (For primary document see N78-27046 18-01)
Avail: NTIS HC A22/MF A01 CSCL 21E

Turboprop engine noise research relevant to conventional aircraft is discussed. In the area of fan noise, static to flight noise differences were discussed and data were presented for two different ways of simulating flight behavior. Experimental results from a swept rotor fan design are presented which show that this concept has potential for reducing the multiple-pure-tone or buzz-saw noise related to the shock waves on a fan operating at supersonic tip speeds. Acoustic suppressor research objectives centered around the effect of the wave system generated by the fan stage that is the input to the treatment. A simplifying and unifying parameter, mode cutoff ratio was described. Results are presented which show that suppressor performance can be improved if the input wave is more precisely described. In jet noise, calculated results showing the potential noise reduction from the use of internal mixer nozzles rather than separate flow nozzles are presented. J.M.S.

N78-27067* National Aeronautics and Space Administration, Lewis Research Center, Cleveland, Ohio

ADVANCED MATERIALS RESEARCH FOR LONG-HAUL AIRCRAFT TURBINE ENGINES c07
R. A. Signomili and C. P. Blankenship In NASA, Langley Res. Center, CTOL Transport Technol., 1978 Jun. 1978 p 187-204 refs (For primary document see N78-27046 18-01)
Avail: NTIS HC A22/MF A01 CSCL 21E

The status of research efforts to apply low to intermediate temperature composite materials and advanced high temperature materials to engine components is reviewed. Emerging materials technologies and their potential benefits to aircraft gas turbines were emphasized. The problems were identified, and the general state of the technology for near term use was assessed. J.M.S.

N78-27068* National Aeronautics and Space Administration, Lewis Research Center, Cleveland, Ohio

GAS TURBINE ENGINE EMISSION REDUCTION TECHNOLOGY PROGRAM c07
Donald A. Petrash and Larry A. Diehl In NASA, Langley Res. Center, CTOL Transport Technol., 1978 Jun. 1978 p 205-216 (For primary document see N78-27046 18-01)
Avail: NTIS HC A22/MF A01 CSCL 21E

Progress in the development of combustor technology to meet the standards for the allowable pollutant emission levels of aircraft gas turbine engines is reported. The high-bypass-ratio turbofan engines which power the large commercial aircraft were emphasized along with efforts to reduce emission for near term applications. Recommendations for continuing research to reduce emissions to meet far term needs are given. J.M.S.

N78-15987* Nielsen Engineering and Research, Inc., Mountain View, Calif.

PERTURBATION SOLUTIONS FOR TRANSONIC FLOW ON THE BLADE-TO-BLADE SURFACE OF COMPRESSOR BLADE ROWS Final Report

Stephen S. Stahara, Denny S. Chaussee, and John R. Spreiter
Jan. 1978 71 p refs
(Contract NAS3-19738)
(NASA-CR-2941; NEAR-TR-136) Avail: NTIS HC A04/MF A01 CSCL 21E

A preliminary investigation was conducted to establish the theoretical basis of perturbation techniques with the objective of minimizing computational requirements associated with parametric studies of transonic flows in turbomachines. The theoretical analysis involved the development of perturbation methods for determining first order changes in the flow solution due to variations of one or more geometrical or flow parameters. The formulation is primarily directed toward transonic flows on the blade to blade surface of a single blade row compressor. Two different perturbation approaches were identified and studied. Applications and results of these methods for various perturbations are presented for selected two dimensional transonic cascade flows to illustrate the advantages and disadvantages of each technique. Additionally, it was found that, for flows with shock waves, proper account of shock displacement was crucial. Author

N78-15988* Pratt and Whitney Aircraft, East Hartford, Conn.
AERO-ACOUSTIC TESTS OF DUCT-BURNING TURBOFAN EXHAUST NOZZLES. COMPREHENSIVE DATA REPORT. VOLUME 1: MODEL SCALE ACOUSTIC DATA Final Report

Hilary Kozlowski and Allan B. Packman Feb. 1977 440 p
 3 Vol
 (Contract NAS3-17866)
 (NASA-CR-134910, PWA-5336) Avail: NTIS
 HC A19/MF A01 CSCL 02A

A compilation of all the detailed acoustic and aerodynamic data covering static aero-acoustic tests of duct-burning turbofan exhaust nozzles is presented. The basic model scale acoustic data and acoustic data scaled to full size is tabulated. In addition, perceived noise levels are shown at various sideline distances. A graphical presentation of the data is also given. Author

N78-15989* Pratt and Whitney Aircraft, East Hartford, Conn.
AERO-ACOUSTIC TESTS OF DUCT-BURNING TURBOFAN EXHAUST NOZZLES. COMPREHENSIVE DATA REPORT. VOLUME 2: ACOUSTIC AND AERODYNAMIC DATA Final Report

Hilary Kozlowski and Allan B. Packman Feb. 1977 570 p
 3 Vol
 (Contract NAS3-17866)
 (NASA-CR-134910, PWA-5336) Avail: NTIS
 HC A24/MF A01 CSCL 02A

For abstract, see N78-15988.

N78-15990* Pratt and Whitney Aircraft, East Hartford, Conn.
AERO-ACOUSTIC TESTS OF DUCT-BURNING TURBOFAN EXHAUST NOZZLES. COMPREHENSIVE DATA REPORT. VOLUME 3: ACOUSTIC AND AERODYNAMIC DATA CURVES Final Report

Hilary Kozlowski and Allan B. Packman Feb. 1977 427 p
 3 Vol
 (Contract NAS3-17866)
 (NASA-CR-134910, PWA-5336) Avail: NTIS
 HC A19/MF A01 CSCL 02A

For abstract, see N78-15988.

N78-21044* General Electric Co., Cincinnati, Ohio
WIND TUNNEL PERFORMANCE TESTS OF COANNULAR PLUG NOZZLES Final Report

Paul S. Staid, Washington, NASA Apr. 1978 116 p refs
 (Contract NAS3-19777)
 (NASA-CR-2990, Rept. 77AEG596) Avail: NTIS
 HC A06/MF A01 CSCL 02A

Wind tunnel performance test results and data analyses are presented for dual-flow plug nozzles applicable to supersonic cruise aircraft during takeoff and low-speed flight operation. Outer exhaust stream pressure ratios from 1.5 to 3.5 were tested, inner exhaust stream conditions were varied from very low, or bleed flow rates, up to a pressure ratio of 3.5. Mach numbers tested ranged from zero to 0.45. Measured thrust coefficients for the eight model configurations, operating at an external Mach number of 0.36 and an outer flow pressure ratio of 2.5, varied from 0.95 to 0.974 for high inner flow rates. At low inner flow, the performance ranged from 0.88 to 0.97 for the same operating conditions. The primary design variables influencing the performance levels were the annular height of the inner and outer nozzle throats (denoted by radius ratio - the ratio of inner to outer flowpath diameter at the nozzle throat), the plug geometry, and the inner stream flow rate. Author

N78-28043* General Electric Co., Cincinnati, Ohio Aircraft Engine Group

ACOUSTIC TESTS OF DUCT-BURNING TURBOFAN JET NOISE SIMULATION Final Report

P. R. Knott, E. J. Stringas, J. F. Brausch, P. S. Staid, P. H. Heck, and D. Latham Jul. 1978 345 p refs
 (Contract NAS3-18008)
 (NASA-CR-2986, DOC-R77AEG524) Avail: NTIS
 HC A15/MF A01 CSCL 20A

The results of a static acoustic and aerodynamic performance, model-scale test program on coannular unsuppressed and multielement fan suppressed nozzle configurations are summarized. The results of the static acoustic tests show a very beneficial interaction effect. When the measured noise levels were compared with the predicted noise levels of two independent but equivalent conical nozzle flow streams, noise reductions for the unsuppressed coannular nozzles were of the order of 10 PNdB; high levels of suppression (8 PNdB) were still maintained even when only a small amount of core stream flow was used. The multielement fan suppressed coannular nozzle tests showed 15 PNdB noise reductions and up to 18 PNdB noise reductions when a treated ejector was added. The static aerodynamic performance tests showed that the unsuppressed coannular plug nozzles obtained gross thrust coefficients of 0.972, with 1.2 to 1.7 percent lower levels for the multielement fan-suppressed coannular flow nozzles. For the first time anywhere, laser velocimeter velocity profile measurements were made on these types of nozzle configurations and with supersonic heated flow conditions. Measurements showed that a very rapid decay in the mean velocity occurs for the nozzle tested. J.M.S.

02 AERODYNAMICS

Includes aerodynamics of bodies, combinations, wings, rotors, and control surfaces; and internal flow in ducts and turbomachinery.

For related information see also 34 *Fluid Mechanics and Heat Transfer*.

N78-10026* National Aeronautics and Space Administration, Lewis Research Center, Cleveland, Ohio.

ATMOSPHERIC EFFECTS ON INLETS FOR SUPERSONIC CRUISE AIRCRAFT

Gary L. Cole 1977 14 p refs Presented at 13th Prop. Conf., Orlando, Fla., 11-13 Jul. 1977; sponsored by AIAA and Soc. of Automotive Engr. (NASA-TM-X-73847; E-9154) Avail: NTIS HC A02/MF A01 CSCL 01A

Mixed-compression inlet dynamic behavior in the vicinity of unstart, was simulated and analyzed to investigate time response of an inlet's normal shock to independent disturbances in ambient temperature and pressure and relative velocity (longitudinal gust), with and without inlet controls active. The results indicate that atmospheric disturbances may be more important than internal disturbances in setting inlet controls requirements because they are usually not anticipated and because normal shock response to rapid atmospheric disturbances is not attenuated by the inlet, as it is for engine induced disturbances. However, before inlet control requirements can be fully assessed, more statistics on extreme atmospheric disturbances are needed. Author

N78-11002* National Aeronautics and Space Administration, Lewis Research Center, Cleveland, Ohio.

EXPERIMENTAL PERFORMANCE OF A 13.65-CENTIMETER-TIP-DIAMETER TANDEM-BLADED SWEEP-BACK CENTRIFUGAL COMPRESSOR DESIGNED FOR A PRESSURE RATIO OF 8

Hugh A. Klassen, Jerry R. Wood (Army Air Mobility Res. and Develop. Lab., Cleveland), and Lawrence F. Schumann (Army Air Mobility Res. and Develop. Lab., Cleveland) Nov 1977 27 p refs (NASA-TP-1091) Avail: NTIS HC A03/MF A01 CSCL 01A

A 13.65 cm tip diameter backswep centrifugal impeller having a tandem inducer and a design mass flow rate of 0.907 kg/sec was experimentally investigated to establish stage and impeller characteristics. Tests were conducted with both a cascade diffuser and a vaneless diffuser. A pressure ratio of 5.9 was obtained near surge for the smallest clearance tested. Flow range at design speed was 63 percent for the smallest clearance test. Impeller exit to shroud axial clearance at design speed was varied to determine the effect on stage and impeller performance. Author

N78-11008* National Aeronautics and Space Administration, Lewis Research Center, Cleveland, Ohio.

EFFECT OF COOLANT FLOW EJECTION ON AERODYNAMIC PERFORMANCE OF LOW-ASPECT-RATIO VANES. 2: PERFORMANCE WITH COOLANT FLOW EJECTION AT TEMPERATURE RATIOS UP TO 2

Jeffrey E. Haas (Army Air Mobility Res. and Develop. Lab., Cleveland) and Milton G. Kofskey Oct 1977 34 p refs (NASA-TP-1057; E-9213) Avail: NTIS HC A03/MF A01 CSCL 21E

The aerodynamic performance of a 0.5 aspect ratio turbine vane configuration with coolant flow ejection was experimentally determined in a full annular cascade. The vanes were tested at a nominal mean section ideal critical velocity ratio of 0.850 over a range of primary to coolant total temperature ratio from 1.0 to 2.08 and a range of coolant to primary total pressure ratio from 1.0 to 1.4 which corresponded to coolant flows from 3.0 to 10.7 percent of the primary flow. The variations in primary and thermodynamic efficiency and exit flow conditions with circumferential and radial position were obtained. Author

N78-14898* National Aeronautics and Space Administration, Lewis Research Center, Cleveland, Ohio.

COLD-AIR PERFORMANCE OF A TIP TURBINE DESIGNED TO DRIVE A LIFT FAN

Jeffrey E. Haas, Milton G. Kofskey, and Glen M. Hotz Jan 1978 23 p refs (NASA-TP-1126; E-9293) Avail: NTIS HC A02/MF A01 CSCL 20E

Performance was obtained over a range of speeds and pressure ratios for a 0.4 linear scale version of the LF460 lift fan turbine with the rotor radial tip clearance reduced to about 2.5 percent of the rotor blade height. These tests covered a range of speeds from 60 to 140 percent of design equivalent speed and a range of scroll inlet total to diffuser exit static pressure ratios from 2.6 to 4.2. Results are presented in terms of equivalent mass flow, equivalent torque, equivalent specific work, and efficiency. Author

N78-16001* National Aeronautics and Space Administration, Lewis Research Center, Cleveland, Ohio.

COLD-AIR PERFORMANCE OF A TIP TURBINE DESIGNED TO DRIVE A LIFT FAN. 3: EFFECT OF SIMULATED FAN LEAKAGE ON TURBINE PERFORMANCE

Jeffrey E. Haas (Army R and T Labs.), Milton G. Kofskey, Glen M. Hotz, and Samuel M. Futra, Jr. Jan 1978 28 p refs (NASA-TP-1109; E-9331) Avail: NTIS HC A03/MF A01 CSCL 01A

Performance data were obtained experimentally for a 0.4 linear scale version of the LF460 lift fan turbine for a range of scroll inlet total to diffuser exit static pressure ratios at design equivalent speed with simulated fan leakage air. Tests were conducted for full and partial admission operation with three separate combinations of rotor inlet and rotor exit leakage air. Data were compared to the results obtained from previous investigations in which no leakage air was present. Results are presented in terms of mass flow, torque, and efficiency. Author

N78-17001* National Aeronautics and Space Administration, Lewis Research Center, Cleveland, Ohio.

SYNTHESIS OF BLADE FLUTTER VIBRATORY PATTERNS USING STATIONARY TRANSDUCERS

A. Kurkov and J. Dicus Mar 1977 26 p refs Proposed for presentation at Gas Turbine Conf., London, Engl., 9-13 Apr. 1978; sponsored by Am. Soc. of Mechan. Engineers (NASA-TM-73821; E-9410) Avail: NTIS HC A03/MF A01 CSCL 01A

Flutter frequency was determined and rotor vibratory amplitude and phase distributions during flutter were reconstructed from stationary aerodynamic type measurements. A previously reported optical method for measuring blade-tip displacement during flutter was extended by means of digital analysis. Displacement amplitudes and phase angles were determined based on this method. For selected blades, spectral results were also obtained from strain gage measurements. The results from these three types of measurement were compared and critically evaluated. Author

N78-17898* National Aeronautics and Space Administration, Lewis Research Center, Cleveland, Ohio.

EFFECT OF DESIGN CHANGES ON AERODYNAMIC AND ACOUSTIC PERFORMANCE OF TRANSLATING-CENTERBODY SONIC INLETS

Brent A. Miller Feb 1978 49 p refs (NASA-TP-1132; E-9283) Avail: NTIS HC A03/MF A01 CSCL 01A

An experimental investigation was conducted to determine the effect of design changes on the aerodynamic and acoustic performance of translating centerbody sonic inlets. Scale model inlets were tested in the Lewis Research Center's V/STOL wind tunnel. The effects of centerbody position, entry lip contraction ratio, diffuser length, and diffuser area ratio on inlet total pressure recovery, distortion, and noise suppression were investigated at static conditions and at forward velocity and angle of attack. With the centerbody in the takeoff position (retracted), good aerodynamic and acoustic performance was attained at static

conditions and at forward velocity. At 0 deg incidence angle with a sound pressure level reduction of 20 dB, the total pressure recovery was 0.986. Pressure recovery at 50 deg was 0.981. With the centerbody in the approach position (extended), diffuser flow separation occurred at an incidence angle of approximately 20 deg. However, good performance was attained at lower angles. With the centerbody in the takeoff position the ability of the inlet to tolerate high incidence angles was improved by increasing the lip contraction ratio. However, at static conditions with the centerbody in the approach position, an optimum lip contraction ratio appears to exist, with both thinner and thicker lips yielding reduced performance. Author

N78-19067* National Aeronautics and Space Administration, Lewis Research Center, Cleveland, Ohio.

PERFORMANCE CHARACTERISTICS OF TWO ANNULAR DUMP DIFFUSERS USING SUCTION-STABILIZED VORTEX FLOW CONTROL

A. J. Juhasz and J. M. Smith 1978 14 p refs In ENGLISH; FRENCH summary Proposed for Presentation at the Joint Symp. on Design and Operation of Fluid Machinery, Fort Collins, Colo., 12-14 Jun. 1978

(NASA-TM-73857) Avail: NTIS HC A02/MF A01 CSCL 01A

Test results are described for two abrupt area change annular diffusers with provisions for maintaining suction stabilized toroidal vortices at the area discontinuity. Both diffusers had an overall area ratio of 4.0 with the prediffuser area ratio being 1.18 for diffuser A and 1.4 for diffuser B. Performance was evaluated at near atmospheric pressure and temperature for a range of inlet Mach numbers from 0.18 to 0.41 and suction rates from 0 to 16%. Static pressure recovery improved significantly as the suction rate was increased to approximately 11%. Results obtained with diffuser A were superior to that obtained with diffuser B. Flat radial profiles of exit velocity were not obtained since the flow showed preferential hub or tip attachment at moderate suction rates. At high suction rates the diffuser exit flow became circumferentially nonuniform and unstable. Author

N78-20080* National Aeronautics and Space Administration, Lewis Research Center, Cleveland, Ohio.

EFFECT OF COOLING-HOLE GEOMETRY ON AERODYNAMIC PERFORMANCE OF A FILM-COOLED TURBINE VANE TESTED WITH COLD AIR IN A TWO-DIMENSIONAL CASCADE

John F. Kline, Roy G. Stabe, and Thomas P. Moffitt Mar. 1978 49 p refs

(NASA-TP-1136: E-9174) Avail: NTIS HC A03/MF A01 CSCL 01A

The effect of the orientation and cooling-hole size on turbine-vane aerodynamic losses was evaluated. The contribution of individual vane regions to the overall effect was also investigated. Test configurations were based upon a representative configuration having 45 spanwise rows of holes spaced about the entire vane profile. Nominal hole diameters of 0.0254 and 0.0356 cm and nominal hole orientations of 35 deg, 45 deg, and 55 deg from the local vane surface and 0 deg, 45 deg, and 90 deg from the main-stream flow direction were investigated. Flow conditions and aerodynamic losses were determined by vane-exit surveys of total pressure, static pressure, and flow angle. Author

N78-24058* National Aeronautics and Space Administration, Lewis Research Center, Cleveland, Ohio.

EFFECTS OF NOZZLE DESIGN AND POWER ON CRUISE DRAG FOR UPPER-SURFACE-BLOWING AIRCRAFT

Edward T. Meleason In NASA, Langley Res. Center Powered-Lift Aerodyn and Acoustics 1976 p 183-196 refs (For availability see N78-24046 15-02)

Avail: NTIS HC A22/MF A01 CSCL 01A

A high speed wind tunnel investigation was conducted on a series of upper surface blowing nozzles with D-shaped exits installed on a representative short haul aircraft model. Both two

and four engine configurations were investigated. Powered engine simulators were used to properly represent nacelle flows. Large differences in cruise drag penalties associated with the various nozzle designs were seen. Some geometric parameters influencing nozzle cruise drag are identified. Author

N78-24063* National Aeronautics and Space Administration, Lewis Research Center, Cleveland, Ohio.

ANALYTICAL MODELING OF UNDER-THE-WING EXTERNALLY BLOWN FLAP POWERED-LIFT NOISE

Daniel J. McKinzie, Jr. In NASA, Langley Res. Center Powered-Lift Aerodyn and Acoustics 1976 p 263-282 refs (For availability see N78-24046 15-02)

Avail: NTIS HC A22/MF A01 CSCL 01A

The sound field produced by the interaction of a subsonic jet with a large-scale model of the under the wing externally blown flap in an approach attitude was analyzed. The analysis was performed to obtain a better understanding of the dominant noise sources and the mechanisms governing the peak sound pressure level frequencies of the broadband spectra. An analytical expression is derived which incorporates two available theories and experimental data; the expression predicts the sound field along a circular arc of approximately 120 deg measured from the upstream jet axis in the fly-over plane. The analysis compares favorably with test results obtained from two large-scale models, one using cold air from a conical nozzle and the other using hot gas from a TF-34 turbofan engine having a conical exhaust nozzle with a 12 lobe internal forced mixer. The frequency at which the peak sound pressure level occurs appears to be governed by a phenomenon which produces periodic formation and shedding of large-scale turbulence structures from the nozzle lip. Author

N78-24066* National Aeronautics and Space Administration, Lewis Research Center, Cleveland, Ohio.

OVERVIEW OF THE QCSEE PROGRAM

Carl C. Ciepluch In NASA, Langley Res. Center Powered Lift Aerodyn and Acoustics 1976 p 325-333 refs (For availability see N78-24046 15-02)

Avail: NTIS HC A22/MF A01 CSCL 01A

Externally blown flap and upper surface blown flap powered lift concepts were investigated in the Quiet Clean Short-Haul Experimental Engine Program and briefly discussed along with propulsion system requirements. Noise limits, emission standards, thrust requirements, and thrust-to-weight ratios are among the factors considered. J.M.S.

N78-24067* National Aeronautics and Space Administration, Lewis Research Center, Cleveland, Ohio.

ACOUSTIC DESIGN OF THE QCSEE PROPULSION SYSTEMS

Irvin J. Loeffler, Edward B. Smith (GE Co., Fairfield, Conn.), and Harry D. Sowers (GE Co., Fairfield, Conn.) In NASA, Langley Res. Center Powered-Lift Aerodyn and Acoustics 1976 p 335-356 refs (For availability see N78-24046 15-02)

Avail: NTIS HC A22/MF A01 CSCL 01A

Acoustic design features and techniques employed in the Quiet Clean Short-Haul Experimental Engine (QCSEE) Program are described. The role of jet/flap noise in selecting the engine fan pressure ratio for powered lift propulsion systems is discussed. The QCSEE acoustic design features include a hybrid inlet (near-sonic throat velocity with acoustic treatment); low fan and core pressure ratios; low fan tip speeds; gear-driven fans; high and low frequency stacked core noise treatment; multiple-thickness treatment, bulk absorber treatment; and treatment on the stator vanes. The QCSEE designs represent and anticipated acoustic technology improvement of 12 to 16 PNdB relative to the noise levels of the low-noise engines used on current wide-body commercial jet transport aircraft. Author

N78-24069* National Aeronautics and Space Administration, Lewis Research Center, Cleveland, Ohio.

INLET TECHNOLOGY FOR POWERED-LIFT AIRCRAFT

Roger W. Luidens *In* NASA Langley Res. Center. Powered-Lift Aerodyn and Acoustics 1976 p 369-385 refs (For availability see N78-24046 15-02)

Avail: NTIS HC A22/MF A01 CSCL 01A

The concepts, analytical tools, and experimental data available for designing inlets for powered lift aircraft are discussed. It is shown that inlets can be designed to meet noise, distortion, and cruise drag requirements at the flight and engine operating conditions of a powered lift aircraft. The penalty in pressure recovery for achieving the required noise suppression was 0.3 percent. Author

N78-24070* National Aeronautics and Space Administration, Lewis Research Center, Cleveland, Ohio.

REVERSE-THRUST TECHNOLOGY FOR VARIABLE-PITCH FAN PROPULSION SYSTEMS

David A. Sagerser, John W. Schaefer, and Donald A. Dietrich *In* NASA Langley Res. Center. Powered-Lift Aerodyn and Acoustics 1976 p 387-402 refs (For availability see N78-24046 15-02)

Avail: NTIS HC A22/MF A01 CSCL 01A

Tests conducted to develop the technology necessary to meet the unique reverse-thrust performance requirements of a variable pitch fan propulsion system are discussed. The losses and distortion associated with the air entering the fan and core compressor from the rear of the engine, the direction of fan blade pitch rotation for best reverse-thrust aerodynamic performance, and engine response and operating characteristics during forward- to reverse-thrust transients are among the factors studied. The test results of several scale fan models as well as a full-size variable pitch fan engine are summarized. Results show the following: a flared exhaust nozzle makes a good reverse-thrust inlet, acceptable core inlet duct recovery and distortion levels in reverse flow were demonstrated; adequate thrust levels were achieved; forward- to reverse-thrust response time achieved was better than the goal; thrust and noise levels strongly favor reverse through feather pitch; and finally, flight-type inlets make the establishment of reverse flow more difficult. Author

N78-26098* National Aeronautics and Space Administration, Lewis Research Center, Cleveland, Ohio.

COLD-AIR PERFORMANCE OF THE COMPRESSOR-DRIVE TURBINE OF THE DEPARTMENT OF ENERGY BASELINE AUTOMOBILE GAS-TURBINE ENGINE Final Report

Richard J. Roelke and Kerry L. McLallin Jul. 1978 24 p refs (Contract EC-77-A-31-1011)

(NASA-TM-78894; E-9480; DOE/NASA/1011-78/25) Avail: NTIS HC A02/MF A01 CSCL 01A

The aerodynamic performance of the compressor-drive turbine of the DOE baseline gas-turbine engine was determined over a range of pressure ratios and speeds. In addition, static pressures were measured in the diffusing transition duct located immediately downstream of the turbine. Results are presented in terms of mass flow, torque, specific work, and efficiency for the turbine and in terms of pressure recovery and effectiveness for the transition duct. Author

N78-26099* National Aeronautics and Space Administration, Lewis Research Center, Cleveland, Ohio.

VSTOL TILT NACELLE AERODYNAMICS AND ITS RELATION TO FAN BLADE STRESSES

Robert J. Shaw, Robert C. Willis, and Joseph L. Koncsek (Boeing Mil. Airplane Develop.) Jul. 1978 15 p refs Proposed for presentation at the 14th Joint Propulsion Conf., Las Vegas, Nev., 25-27 Jul. 1978; sponsored by the AIAA and the Soc. of Automotive Engr (NASA-TM-78899; E-9635) Avail: NTIS HC A02/MF A01 CSCL 10A

A scale model of a VSTOL tilt nacelle with a 0.508 m single stage fan was tested in a low speed wind tunnel to ascertain inlet aerodynamic and fan aeromechanical performance over the low speed flight envelope. Fan blade stress maxima occurred at discrete rotational speeds corresponding to integral engine order vibrations of the first flatwise bending mode. Increased fan blade stress levels coincided with internal boundary layer separation but became severe only when the separation location had progressed to the entry lip region of the inlet. G.G.

N78-26100* National Aeronautics and Space Administration, Lewis Research Center, Cleveland, Ohio.

A VISCOUS-INVISCID INTERACTIVE COMPRESSOR CALCULATIONS

William Johnston (Case Western Reserve Univ.) and Peter M. Sockol Jul. 1978 14 p refs Presented at 11th Fluid and Plasma Dynamics Conf., Seattle, Washington, 10-12 Jul. 1978; sponsored by AIAA

(NASA-TM-78920; E-9658) Avail: NTIS HC A02/MF A01 CSCL 01A

A viscous-inviscid interactive procedure for subsonic flow is developed and applied to an axial compressor stage. Calculations are carried out on a two-dimensional blade-to-blade region of constant radius assumed to occupy a mid-span location. Hub and tip effects are neglected. The Euler equations are solved by MacCormack's method, a viscous marching procedure is used in the boundary layers and wake, and an iterative interaction scheme is constructed that matches them in a way that incorporates information related to momentum and enthalpy thicknesses as well as the displacement thickness. The calculations are quasi-three-dimensional in the sense that the boundary layer and wake solutions allow for the presence of spanwise (radial) velocities. Author

N78-27083* National Aeronautics and Space Administration, Lewis Research Center, Cleveland, Ohio.

COMPUTER PROGRAMS FOR CALCULATING TWO-DIMENSIONAL POTENTIAL FLOW IN AND ABOUT PROPULSION SYSTEM INLETS

J. Dennis Hawk, Norbert O. Stockman, and Charles A. Fauril, Jr. Jun 1978 366 p refs

(NASA-TM-78930; E-0671) Avail: NTIS HC A16/MF A01 CSCL 01A

Incompressible potential flow calculations are presented that were corrected for compressibility in two-dimensional inlets at arbitrary operating conditions. Included are a statement of the problem to be solved, a description of each of the computer programs, and sufficient documentation, including a test case, to enable a user to run the program. G.G.

N78-30057* National Aeronautics and Space Administration, Lewis Research Center, Cleveland, Ohio.

PERFORMANCE WITH AND WITHOUT INLET RADIAL DISTORTION OF A TRANSONIC FAN STAGE DESIGNED FOR REDUCED LOADING IN THE TIP REGION

James F. Schmidt and Robert S. Ruggeri Aug. 1978 84 p refs

(NASA-TP-1294; E-9246) Avail: NTIS HC A05/MF A01 CSCL 01A

A transonic compressor stage designed for a reduced loading in the tip region of the rotor blades was tested with and without inlet radial distortion. The rotor was 50 cm in diameter and designed for an operating tip speed of 420 m/sec. Although the rotor blade loading in the tip region was reduced to provide

additional operating range, analysis of the data indicates that the flow around the damper appears to be critical and limited the stable operating range of this stage. For all levels of tip and hub radial distortion, there was a large reduction in the rotor stall margin. Author

N78-32062* National Aeronautics and Space Administration, Lewis Research Center, Cleveland, Ohio.
WIND TUNNEL EVALUATION OF YF-12 INLET RESPONSE TO INTERNAL AIRFLOW DISTURBANCES WITH AND WITHOUT CONTROL

Gary L. Cole, George H. Neiner, and Miles O. Dustin. In NASA Dryden Flight Res. Center YF-12 Experiments Symp., Vol. 1 Aug. 1978, p. 157-192. refs. (For primary document see N78-32055 23-02)

Avail. NTIS HC A13/MF A01 CSCL 01A

The response of terminal-shock position and static pressures in the subsonic duct of a YF-12 aircraft flight-hardware inlet to perturbations in simulated engine corrected airflow were obtained with and without inlet control. Frequency response data, obtained with inlet controls inactive, indicated the general nature of the inherent inlet dynamics, assisted in the design of controls, and provided a baseline reference for responses with active controls. All the control laws were implemented by means of a digital computer that could be programmed to behave like the flight inlet's existing analog control. The experimental controls were designed using an analytical optimization technique. The capabilities of the controls were limited primarily by the actuation hardware. The experimental controls provided somewhat better attenuation of terminal shock excursions than did the YF-13 inlet control. Controls using both the forward and aft bypass systems also provided somewhat better attenuation than those using just the forward bypass. The main advantage of using both bypasses is in the greater control flexibility that is achieved. A.R.H.

A78-12289* Calculation of 3-dimensional choking mass flow in turbomachinery with 2-dimensional flow models. T. Katsaris (NASA, Lewis Research Center, Cleveland, Ohio). In: Transonic flow problems in turbomachinery; Proceedings of the Workshop, Monterey, Calif., February 11, 12, 1976. (A78-12286 02-02) Washington, D.C., Hemisphere Publishing Corp., 1977, p. 60-67; Discussion, p. 67-69.

An approach is considered for obtaining an approximate flow solution in the case of a cross-sectional flow surface within a guided channel, taking into account a pair of typical turbine blades with three-dimensional orthogonal surfaces across the flow passage, the calculation of the mass flow across the throat in the case of a 2-D passage with curved walls, and the determination of the choking mass flow. It is pointed out that the choking solution for a three-dimensional guided passage in a blade row can be obtained in a very similar manner by satisfying momentum equations for the blade-to-blade and the hub-to-tip direction. A considered example involves the calculation of the choking mass flow for a centrifugal compressor impeller in an automotive application. G.R.

A78-12312* Review of experimental work on transonic flow in turbomachinery. W. D. McNally (NASA, Lewis Research Center, Cleveland, Ohio). In: Transonic flow problems in turbomachinery; Proceedings of the Workshop, Monterey, Calif., February 11, 12, 1976. (A78-12286 02-02) Washington, D.C., Hemisphere Publishing Corp., 1977, p. 457-484; Discussion, p. 484, 51 refs.

The review is primarily concerned with modern experimental techniques of high response and laser supported instrumentation. The considered techniques make it possible to obtain detailed data of steady and unsteady processes occurring inside transonic blade rows and in the vicinity of the rows. Such data are needed for the verification of computer codes used for the study of the operational characteristics of turbomachinery. Attention is given to high response transducers, hot wire probes, hot film gauges, laser Doppler velocimeter systems, laser fluorescence, and laser holography. G.R.

A78-17270* Unsteady flow in a supersonic cascade with strong in-passage shocks. M. E. Goldstein, W. Braun, and J. J. Adamczyk (NASA, Lewis Research Center, Cleveland, Ohio). *Journal of Fluid Mechanics*, vol. 83, Dec. 5, 1977, p. 569-604, 21 refs.

Linearized theory is used to study the unsteady flow in a supersonic cascade with in-passage shock waves. We use the Wiener-Hopf technique to obtain a closed-form analytical solution for the supersonic region. To obtain a solution for the rotational flow in the subsonic region we must solve an infinite set of linear algebraic equations. The analysis shows that it is possible to correlate quantitatively the oscillatory shock motion with the Kutta condition at the trailing edges of the blades. This feature allows us to account for the effect of shock motion on the stability of the cascade. Unlike the theory for a completely supersonic flow, the present study predicts the occurrence of supersonic bending flutter. It therefore provides a possible explanation for the bending flutter that has recently been detected in aircraft-engine compressors at higher blade loadings. (Author)

A78-20701* Development and test of an inlet and duct to provide airflow for a wing boundary layer control system. D. W. Gunnarson (Boeing Commercial Airplane Co., Seattle, Wash.) and J. C. McArdle (NASA, Lewis Research Center, Cleveland, Ohio). *American Institute of Aeronautics and Astronautics, Aerospace Sciences Meeting, 16th, Huntsville, Ala., Jan. 16-18, 1978, Paper 78-141*, 9 p. NASA-sponsored research.

The boundary layer control (BLC) system of the quiet short-haul research airplane (QSRA) requires significant amounts of pressurized airflow for successful operation. An inlet and duct were successfully developed which removed airflow from the engine fan duct for the BLC system at or above the required total pressure of 99% of the average fan duct total pressure. The design was constrained by the tight space limitations of the QSRA nacelle. Potential flow with boundary layer analysis techniques were used as an aid to select the inlet and duct geometries. Airflow and total pressure profile data were obtained during development tests. (Author)

A78-20702* A combined potential and viscous flow solution for V/STOL engine inlets. A. H. Ybarra, W. W. Rhoades (Vought Corp., Dallas, Tex.), and N. O. Stockman (NASA, Lewis Research Center, Cleveland, Ohio). *American Institute of Aeronautics and Astronautics, Aerospace Sciences Meeting, 16th, Huntsville, Ala., Jan. 16-18, 1978, Paper 78-142*, 8 p. 5 refs.

A potential flow routine and a viscous boundary layer routine have been combined into a single routine for estimating the flow in and around subsonic inlets. In this combined routine, the viscous flow solution about the inlet body is obtained by adding the viscous displacement thickness to the inlet geometry. Combination of the two flow solutions has resulted in cost savings, both in preparation time and in computer time. This routine is a useful tool in optimizing lip shapes for V/STOL inlets. The method of combining the routine, comparison with NASA test data, and utilization of the routine for V/STOL inlet design are presented. (Author)

A78-41843* A viscous-inviscid interactive compressor calculation. W. A. Johnston (Case Western Reserve University, Cleveland, Ohio) and P. M. Sockol (NASA, Lewis Research Center, Cleveland, Ohio). *American Institute of Aeronautics and Astronautics, Fluid and Plasma Dynamics Conference, 11th, Seattle, Wash., July 10-12, 1978, Paper 78-1140*, 10 p. 24 refs. NASA-supported research.

A viscous-inviscid interactive procedure for subsonic flow is developed and applied to an axial compressor stage. Calculations are carried out on a two-dimensional blade-to-blade region of constant radius assumed to occupy a mid-span location. Hub and tip effects are neglected. The Euler Equations are solved by MacCormack's method; a viscous matching procedure is used in the boundary layers and wake, and an iterative interaction scheme is constructed that

matches them in a way that incorporates information related to momentum and enthalpy thicknesses as well as the displacement thickness. The calculations are quasi-three-dimensional in the sense that the boundary layer and wake solutions allow for the presence of spanwise (radial) velocities. (Author)

A78-43520 * # **VSTOL tilt nacelle aerodynamics and its relation to fan blade stresses.** R. J. Shaw, R. C. Williams (NASA, Lewis Research Center, Cleveland, Ohio), and J. L. Koncek (Boeing Aerospace Co., Boeing Military Airplane Development, Seattle, Wash.). *American Institute of Aeronautics and Astronautics and Society of Automotive Engineers, Joint Propulsion Conference, 14th, Las Vegas, Nev., July 25-27, 1978, AIAA Paper 78-958.* 11 p. 9 refs.

A scale model of a VSTOL tilt nacelle with a 0.508 m single stage fan was tested in the NASA Lewis 9x15 Low Speed Wind Tunnel to ascertain inlet aerodynamic and fan aeromechanical performance over the low speed flight envelope. Fan blade stress maxima occurred at discrete rotational speeds corresponding to integral engine order vibrations of the first flatwise bending mode. Increased fan blade stress levels coincided with internal boundary layer separation occurring but became severe only when the separation location had progressed to the entry lip region of the inlet. The inlet/fan system could operate within the low speed flight envelope without incurring fan blade stress limits although boundary layer separation did occur for certain operating conditions. (Author)

A78-45096 * # **Inlet-engine matching for SCAR including application of a bicone variable geometry inlet.** J. F. Wasserbauer and W. H. Gerstenmaier (NASA, Lewis Research Center, Cleveland, Ohio). *American Institute of Aeronautics and Astronautics and Society of Automotive Engineers, Joint Propulsion Conference, 14th, Las Vegas, Nev., July 25-27, 1978, AIAA Paper 78-961.* 22 p. 15 refs.

Airflow characteristics of variable cycle engines (VCE) designed for Mach 2.32 can have transonic airflow requirements as high as 1.6 times the cruise airflow. This is a formidable requirement for conventional, high performance axisymmetric, translating centerbody mixed compression inlets. An alternate inlet is defined where the second cone of a two cone centerbody collapses to the initial cone angle to provide a large off-design airflow capability, and incorporates modest centerbody translation to minimize spillage drag. Estimates of transonic spillage drag are competitive with those of conventional translating centerbody inlets. The inlet's cruise performance exhibits very low bleed requirements with good recovery and high angle of attack capability. (Author)

A78-45133 * # **End-wall boundary layer prediction for axial compressors.** P. M. Sockol (NASA, Lewis Research Center, Cleveland, Ohio). *American Institute of Aeronautics and Astronautics, Fluid and Plasma Dynamics Conference, 11th, Seattle, Wash., July 10-12, 1978, Paper 78-1139.* 19 p. 15 refs.

An integral boundary layer procedure has been developed for the computation of viscous and secondary flows along the annulus walls of an axial compressor. The procedure is an outgrowth and extension of the pitch-averaged methods of Mellor and Horlock. In the present work secondary flow theory is used to develop approximations for the velocity profiles inside a rotating blade row and for the blade force deficit terms in the momentum integral equations. The computer code based on this procedure has been iteratively coupled to a quasi-one-dimensional model for the external inviscid flow. Computed results are compared with measurements in a compressor cascade. (Author)

A78-46537 * # **Methods for calculating the transonic boundary layer separation for V/STOL inlets at high incidence angles.** D. C. Chou, H. C. Lee (Iowa, University, Iowa City, Iowa), F. W. Luidens, and N. O. Stockman (NASA, Lewis Research Center, Cleveland, Ohio). In: *Atmospheric Flight Mechanics Conference, Palo Alto, Calif., August 7-9, 1978, Technical Papers.* (A78-46526 20-08) New York, American Institute of Aeronautics and Astronautics, Inc., 1978, p. 100-106. 10 refs. Grant No. NSG-3117. (AIAA 78-1340)

A semi-empirical scheme for the prediction of transonic pressure distribution on the surface of V/STOL inlets at high incidence angles has been developed. The investigation is intended to improve the boundary layer calculation and separation prediction by including the effects of shock wave-boundary layer interaction into the Lewis Inlet Viscous Computer Program. Wind-tunnel results and theoretical pressure calculation for critical cases are used in constructing the transonic pressure distribution. The program, which describes the development of the boundary layer and predicts the possible flow separation, can handle the cases of inlets at high incidence angles where local supersonic region may occur in the flow. (Author)

N78-12034*# **Advanced Technology Labs., Inc., Westbury, N. Y.**

COMPUTATION OF UNSTEADY TRANSONIC FLOWS THROUGH ROTATING AND STATIONARY CASCADES. 2: USER'S GUIDE TO FORTRAN PROGRAM B2DATL Final Report

Edgar Aizner and Paul P. Kalben Nov. 1977 81 p refs (Contract NAS3-16807)

(NASA-CR-2901, ATL-TR-205-Vol-2) Avail: NTIS HC A03/MF A01 CSCL 01A

Documentation for the FORTRAN program B2DATL is provided. The program input, output, and operational procedures are described; a dictionary of the principal FORTRAN variables is provided; the function of all subroutines is outlined and flow charts of the principal subroutines and the main program are presented. Author

N78-12035*# **Advanced Technology Labs., Inc., Westbury, N. Y.**

COMPUTATION OF UNSTEADY TRANSONIC FLOWS THROUGH ROTATING AND STATIONARY CASCADES. 3: ACOUSTIC FAR-FIELD ANALYSIS Final Report

Simon Slutsky, Dietrich Fischer, and John I. Erdos Nov. 1977 56 p refs

(Contract NAS3-16807)

(NASA-CR-2902, ATL-TR-205-Vol-3) Avail: NTIS HC A04/MF A01 CSCL 01A

A small perturbation type analysis has been developed for the acoustic far field in an infinite duct extending upstream and downstream of an axial turbomachinery stage. The analysis is designed to interface with a numerical solution of the near field of the blade rows and, thereby, to provide the necessary closure condition to complete the statement of infinite duct boundary conditions for the subject problem. The present analysis differs from conventional inlet duct analyses in that a simple harmonic time dependence was not assumed, since a transient signal is generated by the numerical near-field solution and periodicity is attained only asymptotically. A description of the computer code developed to carry out the necessary convolutions numerically is included, as well as the results of a sample application using an impulsively initiated harmonic signal. Author

N78-17991*# **Pratt and Whitney Aircraft, East Hartford, Conn. Commercial Products Div**

MEAN VELOCITY, TURBULENCE INTENSITY AND TURBULENCE CONVECTION VELOCITY MEASUREMENTS FOR A CONVERGENT NOZZLE IN A FREE JET WIND TUNNEL COMPREHENSIVE DATA REPORT

C. J. McColgan and R. S. Larson Apr 1977 262 p

(Contract NAS3-17866)

(NASA CR 135238, PWA-5516)

Avail: NTIS

HC A12/MF A01 CSCL 01A

The effect of light on the mean flow and turbulence properties of a 0.056 m circular jet were determined in a free jet wind tunnel. The nozzle exit velocity was 122 m/sec, and the wind tunnel velocity was set at 0, 12, 37, and 61 m/sec. Measurements of flow properties including mean velocity, turbulence intensity and spectra, and eddy convection velocity were carried out using two linearized hot wire anemometers. This report contains the raw data and graphical presentations. The final technical report includes a description of the test facilities, test hardware, along with significant test results and conclusions. Author

N78-20082* Advanced Technology Labs., Inc., Westbury, N. Y.
COMPUTATION OF UNSTEADY TRANSONIC FLOWS THROUGH ROTATING AND STATIONARY CASCADES. 1: METHOD OF ANALYSIS Final Report

John I. Erdos and Edgar Alzner Dec. 1977 131 p refs
 (Contract NAS3-16807)
 (NASA-CR-2900; ATL-TR-205-Vol-1) Avail: NTIS
 HC A07/MF A01 CSCL 01A

A numerical method of solution of the inviscid, compressible, two-dimensional unsteady flow on a blade-to-blade stream surface through a stage (rotor and stator) or a single blade row of an axial flow compressor or fan is described. A cyclic procedure has been developed for representation of adjacent blade-to-blade passages which asymptotically achieves the correct phase between all passages of a stage. A shock-capturing finite difference method is employed in the interior of the passage, and a method of characteristics technique is used at the boundaries. The blade slipstreams form two of the passage boundaries and are treated as moving contact surfaces capable of supporting jumps in entropy and tangential velocity. The Kutta condition is imposed by requiring the slipstreams to originate at the trailing edges, which are assumed to be sharp. Results are presented for several transonic fan rotors and compared with available experimental data, consisting of holographic observations of shock structure and pressure contour maps. A subcritical stator solution is also compared with results from a relaxation method. Finally, a periodic solution for a stage consisting of 44 rotor blades and 46 stator blades is discussed. Author

N78-21068* Pratt and Whitney Aircraft Group, East Hartford, Conn.

MEAN VELOCITY, TURBULENCE INTENSITY AND TURBULENCE CONVECTION VELOCITY MEASUREMENTS FOR A CONVERGENT NOZZLE IN A FREE JET WIND TUNNEL Final Report

C. J. McColgan and R. S. Larson Apr. 1978 31 p refs
 (Contract NAS3-17866)
 (NASA-CR-2949; PWA-5506) Avail: NTIS HC A03/MF A01 CSCL 01A

The effect of light on the mean flow and turbulence properties of a 0.056 m circular jet were determined in a free jet wind tunnel. The nozzle exit velocity was 122 m/sec, and the wind tunnel velocity was set at 0, 12, 37, and 61 m/sec. Measurements of flow properties including mean velocity, turbulence intensity and spectra, and eddy convection velocity were carried out using two linearized hot wire anemometers. Normalization factors were determined for the mean velocity and turbulence convection velocity. Author

N78-32066* Hamilton Standard, Windsor Locks, Conn.
AERODYNAMIC DESIGN AND PERFORMANCE TESTING OF AN ADVANCED 30 DEG SWEEP, EIGHT BLADED PROPELLER AT MACH NUMBERS FROM 0.2 TO 0.85 Final Report

D. M. Black, R. W. Mentha, and H. S. Wainauski Sep. 1978 119 p refs
 (Contract NAS3-20219)
 (NASA-CR-3047) Avail: NTIS HC A06/MF A01 CSCL 01A

The increased emphasis on fuel conservation in the world has stimulated a series of studies of both conventional and unconventional propulsion systems for commercial aircraft. Preliminary results from these studies indicate that a fuel saving of from 15 to 28 percent may be realized by the use of an advanced high speed turboprop. The turboprop must be capable

of high efficiency at Mach 0.8 above 10.68 km (35,000 ft) altitude if it is to compete with turbofan powered commercial aircraft. An advanced turboprop concept was wind tunnel tested. The model included such concepts as an aerodynamically integrated propeller/nacelle, blade sweep and power (disk) loadings approximately three times higher than conventional propeller designs. The aerodynamic design for the model is discussed. Test results are presented which indicate propeller net efficiencies near 80 percent were obtained at high disk loadings at Mach 0.8. B.B.

N78-33344* United Technologies Research Center, East Hartford, Conn.

DERIVATION AND EVALUATION OF AN APPROXIMATE ANALYSIS FOR THREE-DIMENSIONAL VISCOUS SUBSONIC FLOW WITH LARGE SECONDARY VELOCITIES Final Report

O. L. Anderson, W. R. Brolley, and H. McDonald Oct. 1978 84 p refs
 (Contract NAS3-19752)
 (NASA-CR-159430; UTRC78-106) Avail: NTIS
 HC A05/MF A01 CSCL 01A

An approximate analysis is presented for calculating three-dimensional, low Mach number, laminar viscous flows in curved passages with large secondary flows and corner boundary layers. The analysis is based on the decomposition of the overall velocity field into inviscid and viscous components with the overall velocity being determined from superposition. An incompressible vorticity transport equation is used to estimate inviscid secondary flow velocities to be used as corrections to the potential flow velocity field. A parabolized streamwise momentum equation coupled to an adiabatic energy equation and global continuity equation is used to obtain an approximate viscous correction to the pressure and longitudinal velocity fields. A collateral flow assumption is invoked to estimate the viscous correction to the transverse velocity fields. The approximate analysis is solved numerically using an implicit ADI solution for the viscous pressure and velocity fields. An iterative ADI procedure is used to solve for the inviscid secondary vorticity and velocity fields. This method was applied to computing the flow within a turbine vane passage with inlet flow conditions of $M = 0.1$ and $M = 0.25$, $Re = 1000$ and adiabatic walls, and for a constant radius curved rectangular duct with $R/D = 12$ and 14 and with inlet flow conditions of $M = 0.1$, $Re = 1000$, and adiabatic walls. A.R.H.

A78-12307* Perturbation solutions for blade-to-blade surfaces of a transonic compressor. S. S. Stahara, D. S. Chaussee (Nielsen Engineering and Research, Inc., Mountain View, Calif.), and J. R. Spreiter (Stanford University, Stanford, Calif.). In: Transonic flow problems in turbomachinery; Proceedings of the Workshop, Monterey, Calif., February 11, 12, 1976. (A78-12286 02-02) Washington, D.C., Hemisphere Publishing Corp., 1977, p. 359-366; Discussion, p. 366-368. Contract No. NAS3-19738.

The paper describes a perturbation method for turbomachinery calculations, particularly where it is necessary to carry out a number of calculations for closely-related flows such as are needed in a parametric study. The method is applied for solving a model problem involving blade-to-blade surfaces of a transonic compressor. Basically, the method makes use of a previously calculated base solution to determine first-order changes in the flow field due to variations in one or more of a variety of geometrical or flow field parameters. The fundamental assumption associated with the perturbation solution is that the magnitude of the deviations from the base solution lies within the range of a linear perturbation analysis. Comparisons are made for results obtained, by varying the thickness ratio of an unstaggered nonlifting cascade composed of biconvex profiles in a flow with an oncoming freestream Mach number of 0.60. S.D.

03 AIR TRANSPORTATION AND SAFETY

Includes passenger and cargo air transport operations; and aircraft accidents.

For related information see also *16 Space Transportation* and *85 Urban Technology and Transportation*.

N78-31061* National Aeronautics and Space Administration
Lewis Research Center, Cleveland, Ohio.

SIMULTANEOUS MEASUREMENTS OF OZONE OUTSIDE AND INSIDE CABINS OF TWO B-747 AIRLINERS AND A GATES LEARJET BUSINESS JET

Porter J. Perkins and Daniel Briat 1978 11 p refs Proposed for presentation at the Conf. on Atmospheric Environ. of Aerospace Systems and Appl. Meteorology, New York, 13-16 Nov. 1978; sponsored by the Am. Meteorol. Soc. and the AIAA (NASA-TM-78983; E-9760) Avail: NTIS HC A02/MF A01 CSCL 06T

The average amount of ozone measured in the cabins of two B-747 airliners varied from 40 percent to 80 percent of the atmospheric concentrations without special ozone destruction systems. A charcoal filter in the cabin air inlet system of one B-747 reduced the ozone to about 5 percent of the atmospheric concentration. A Learjet 23 was also instrumented with monitors to measure simultaneously the atmospheric and ozone concentrations. Results indicate that a significant portion of the atmospheric ozone is not destroyed in the pressurization system and remains in the aircraft cabin of the Learjet. For the two cabin configurations tested, the ozone retentions were 63 and 41 percent of the atmospheric ozone concentrations. Ozone concentrations measured in the cabin near the conditioned-air outlets were reduced only slightly from atmospheric ozone concentrations. It is concluded that a constant difference between ozone concentrations inside and outside the cabin does not exist.

G.G.

N78-11024* General Electric Co. Pittsfield, Mass.

LIGHTNING PROTECTION OF AIRCRAFT

Franklin A. Fisher and J. Anderson Plumer Oct. 1977 530 p refs

(Contract NAS3-19080)

(NASA-RP-1008) Avail: NTIS HC A23/MF A01 CSCL 01C

The current knowledge concerning potential lightning effects on aircraft and the means that are available to designers and operators to protect against these effects are summarized. The increased use of nonmetallic materials in the structure of aircraft and the constant trend toward using electronic equipment to handle flight-critical control and navigation functions have served as impetus for this study. For individual titles, see N78-11025 through N78-11041.

05 AIRCRAFT DESIGN, TESTING AND PERFORMANCE

Includes aircraft simulation technology.
For related information see also 18 *Spacecraft Design, Testing and Performance* and 39 *Structural Mechanics*.

N78-17041* National Aeronautics and Space Administration, Lewis Research Center, Cleveland, Ohio.
PRELIMINARY STUDY OF PROPULSION SYSTEMS AND AIRPLANE WEIGHT PARAMETERS FOR A US NAVY SUBSONIC V/STOL AIRCRAFT

C. L. Zola, L. H. Fishbach, and J. L. Allen Feb. 1978 42 p refs

(NASA-TM-73652; E-9519) Avail NTIS HC A03/MF A01 CSCL 01C

Two V/STOL propulsion concepts were evaluated in a common aircraft configuration. One propulsion system consists of cross coupled turboshaft engines driving variable pitch fans. The other system is a gas coupled combination of turbojet gas generators and tip turbine fixed pitch fans. Evaluations were made of endurance at low altitude, low speed loiter with equal takeoff fuel loads. Effects of propulsion system sizing, bypass ratio, and aircraft wing planform parameters were investigated and compared. Shaft driven propulsion systems appear to result in better overall performance, although at higher installed weight, than gas systems. Author

N78-25080* Sikorsky Aircraft, Stratford, Conn.
OIL-AIR MIST LUBRICATION FOR HELICOPTER GEARING
Final Report

F. McGrogan Dec 1976 52 p refs

(Contract NAS3-18538)

(NASA-CR-135031, SER-50959) Avail NTIS HC A04/MF A01 CSCL 01C

The applicability of a once-through oil mist system to the lubrication of helicopter spur gears was investigated and compared to conventional jet spray lubrication. In the mist lubrication mode, cooling air was supplied at 366K (200 F) to the out of mesh location of the gear sets. The mist air was also supplied at 366K (200 F) to the radial position mist nozzle at a constant rate of 0.0632 mol/s (3 SCFM) per nozzle. The lubricant contained in the mist air varied between 32 - 44 cc/hour. In the recirculating jet spray mode, the flow rate was varied between 1893 - 2650 cc/hour. Visual inspection revealed the jet spray mode produced a superior surface finish on the gear teeth but a thermal energy survey showed a 15 - 20% increase in heat generated. The gear tooth condition in the mist lubrication mode system could be improved if the cooling air and lubricant/air flow ratio were increased. The test gear-box and the procedure used are described. Author

06 AIRCRAFT INSTRUMENTATION

Includes cockpit and cabin display devices; and flight instruments.

For related information see also *19 Spacecraft Instrumentation and Photography*.

N78-17062* National Aeronautics and Space Administration, Lewis Research Center, Cleveland, Ohio.
INSTRUMENTATION FOR PROPULSION SYSTEMS DEVELOPMENT

Isidore Warshawsky 1978 24 p refs Presented at the Soc. of Automotive Engr. Congr. (Meeting 1M21), Detroit, 27 Feb. - 3 Mar. 1978

(NASA-TM-73840) Avail. NTIS HC A02/MF A01 CSCL 01D

Apparatus and techniques developed or used by NASA-Lewis to make steady state or dynamic measurements of gas temperature, pressure, and velocity and of the temperature, tip clearance, and vibration of the blades of high-speed fans or turbines are described. The advantages and limitations of each instrument and technique are discussed and the possibility of modifying them for use in developing various propulsion systems is suggested.

Author

N78-24137* National Aeronautics and Space Administration, Lewis Research Center, Cleveland, Ohio.

ON THE USE OF RELATIVE VELOCITY EXPONENTS FOR JET ENGINE EXHAUST NOISE

James R Stone 1978 17 p refs Presented at 95th Meeting of Acoust Soc of Am., Providence, R I, 16-19 May 1978

(NASA-TM-78873, E-9605) Avail. NTIS HC A02/MF A01 CSCL 20A

The effect of flight on jet engine exhaust noise has often been presented in terms of a relative velocity exponent, n , as a function of radiation angle. The value of n is given by the OASPL reduction due to relative velocity divided by 10 times the logarithm of the ratio of relative jet velocity to absolute jet velocity. In such terms, classical subsonic jet noise theory would result in a value of n being approximately 7 at 90 degree angle to the jet axis with n decreasing, but remaining positive, as the inlet axis is approached and increasing as the jet axis is approached. However, flight tests have shown a wide range of results, including negative values of n in some cases. In this paper it is shown that the exponent n is positive for pure subsonic jet mixing noise and varies, in a systematic manner, as a function of flight conditions and jet velocity.

Author

N78-24138* National Aeronautics and Space Administration, Lewis Research Center, Cleveland, Ohio

DESIGN AND PRELIMINARY RESULTS OF A SEMITRANSPIRATION COOLED (LAMILLOY) LINER FOR A HIGH-PRESSURE HIGH-TEMPERATURE COMBUSTOR

Jerrold D Wear, Arthur M. Trout, John M. Smith, and Robert E Jones 1978 13 p refs To be presented at the 14th Propulsion Conf., Las Vegas, Nev., 25-27 Jul. 1978, sponsored by AIAA and SAE

(NASA-TM-78874; E-9607) Avail. NTIS HC A02/MF A01 CSCL 21E

A Lamilloy combustor liner was designed, fabricated and tested in a combustor at pressures up to 8 atmospheres. The liner was fabricated of a three layer Lamilloy structure and designed to replace a conventional step louver liner. The liner is to be used in a combustor that provides hot gases to a turbine cooling test facility at pressures up to 40 atmospheres. The Lamilloy liner was tested extensively at lower pressures and demonstrated lower metal temperatures than the conventional liner, while at the same time requiring about 40 percent less cooling air flow. Tests conducted at combustor exit temperatures in excess of 2200 K have not indicated any cooling or durability problems with the Lamilloy liner.

Author

N78-24139* National Aeronautics and Space Administration, Lewis Research Center, Cleveland, Ohio.

GENERAL AVIATION INTERNAL-COMBUSTION ENGINE RESEARCH PROGRAMS AT NASA-LEWIS RESEARCH CENTER

Edward A. Willis 1978 23 p refs Proposed for presentation at 14th Propulsion Conf., Las Vegas, Nev., 25-27 Jul. 1978; cosponsored by AIAA and SAE

(NASA-TM-78891; E-9628) Avail. NTIS HC A02/MF A01 CSCL 21A

An update is presented of non-turbine general aviation engine programs. The program encompasses conventional, lightweight diesel and rotary engines. It's three major thrusts are: (1) reduced SFC's; (2) improved fuels tolerance; and (3) reduced emissions. Current and planned future programs in such areas as lean operation, improved fuel management, advanced cooling techniques and advanced engine concepts, are described. These are expected to lay the technology base, by the mid to latter 1980's, for engines whose life cycle fuel costs are 30 to 50% lower than today's conventional engines.

Author

07 AIRCRAFT PROPULSION AND POWER

Includes prime propulsion systems and systems components, e.g., gas turbine engines and compressors; and on-board auxiliary power plants for aircraft.

For related information see also 20 *Spacecraft Propulsion and Power*, 28 *Propellants and Fuels*, and 44 *Energy Production and Conversion*.

N78-10086* National Aeronautics and Space Administration Lewis Research Center, Cleveland, Ohio.

CONCEPTS FOR THE DEVELOPMENT OF LIGHT-WEIGHT COMPOSITE STRUCTURES FOR ROTOR BURST CONTAINMENT

Arthur G. Holms *In MIT An Assessment of Technol for Turbojet Engine Rotor Failures* Mar. 1977 p 295-330 refs (For availability see N78-10088 01-07)

Avail NTIS HC A18/MF A01 CSCL 21E

Published results on rotor burst containment with single materials, and on body armor using composite materials were used to establish a set of hypotheses about what variables might control the design of a weight-efficient protective device. Based on modern concepts for the design and analysis of small optimum sealing experiments, a particular experiment for evaluating the hypotheses and materials was designed. The design and methods for the analysis of results are described. The consequence of such hypotheses is that the device should consist of as many as four concentric rings, each to consist of a material uniquely chosen for its position in the penetration sequence. Author

N78-10088* National Aeronautics and Space Administration Lewis Research Center, Cleveland, Ohio.

APPLICATION OF A FLIGHT-LINE DISK CRACK DETECTOR TO A SMALL ENGINE

John R Berranger *In MIT An Assessment of Technol for Turbojet Engine Rotor Failures* Mar 1977 383-388 (For availability see N78-10088 01-07)

Avail NTIS HC A18/MF A01 CSCL 21E

A disk crack detector was developed and applied to a small military engine for use as a flight-line turbine crack monitor. The system consists of an eddy current type sensor and its cables within the engine, external connecting cables and a remotely located electrical capacitance-conductance bridge and signal analyzer. As the turbine spins, the rotor is monitored by the sensor for radial surface cracks emanating from the interblade region of the rotor. Author

N78-10089* National Aeronautics and Space Administration Lewis Research Center, Cleveland, Ohio.

TURBINE DISKS FOR IMPROVED RELIABILITY

Albert Kaufman *In MIT An Assessment of Technol for Turbojet Engine Rotor Failures* Mar 1977 p 389-411 (For availability see N78-10088 01-07)

Avail NTIS HC A18/MF A01 CSCL 21E

Advanced disk structural concepts were employed to improve the cyclic lives and reliability of turbine disks. Analytical studies were conducted to evaluate bore entry disks as potential replacements for the existing first stage turbine disks in the CF6-50 and JT8D-17 engines. Results of low cycle fatigue, burst fracture mechanics, and fragment energy analyses are summarized for the advanced disk designs and the existing disk designs with both conventional and advanced disk materials. Other disk concepts such as composite laminated link, multibore, multidisk, and spline disks were also evaluated for the CF6-50 engine. Author

N78-10087* National Aeronautics and Space Administration Lewis Research Center, Cleveland, Ohio.

EVALUATION OF AN F100 MULTIVARIABLE CONTROL USING A REAL-TIME ENGINE SIMULATION

John R. Szuch, Charles Skira (AFSC), and James F. Soader 1977 17 p refs Presented at 13th Propulsion Conf., Orlando, Fla., 11-13 Jul. 1977; sponsored by AIAA and Soc. of Automotive Engrs

(NASA-TM-X-73648; E-9155) Avail NTIS HC A02/MF A01 CSCL 21E

A multivariable control design for the F100 turbofan engine was evaluated, as part of the F100 multivariable control synthesis (MVCS) program. The evaluation utilized a real-time, hybrid computer simulation of the engine and a digital computer implementation of the control. Significant results of the evaluation are presented and recommendations concerning future engine testing of the control are made. Author

N78-10085* National Aeronautics and Space Administration Lewis Research Center, Cleveland, Ohio.

THE PROMISE OF EUTECTICS FOR AIRCRAFT TURBINES

Hugh R Gray 1977 21 p refs Presented at Mater. Show and Conf., Chicago, 25-27 Oct 1977, sponsored by ASM (NASA-TM-73714; E-9258) Avail NTIS HC A02/MF A01 CSCL 21E

The current status of the first generation eutectics, gamma/gamma transition - delta and NiTaC-13, is described in detail. Several second generation systems, such as gamma/gamma transition - alpha and NiTaC 3-116A, gamma - beta, and COTAC 74 are also reviewed with particular emphasis on their critical physical and mechanical properties, future research directions, and potential applications. Results of recent cost-benefit analyses of eutectic turbine blades are discussed. Author

N78-11063* National Aeronautics and Space Administration Lewis Research Center, Cleveland, Ohio.

AIRCRAFT ENGINE EMISSIONS

Oct 1977 452 p Conf held in Cleveland, 18-19 May 1977 (NASA-CP-2021; E-9262) Avail NTIS HC A20/MF A01 CSCL 21E

A conference on aircraft engine emissions was held to present the results of recent and current work. Such diverse areas as components, controls, energy efficient engine designs, and noise and pollution reduction are discussed. For individual titles, see N78-11064 through N78-11080.

N78-11085* National Aeronautics and Space Administration Lewis Research Center, Cleveland, Ohio.

EMISSIONS REDUCTION TECHNOLOGY PROGRAM

Robert E Jones *In Aircraft Eng Emissions* Oct 1977 p 19-58 (For availability see N78-11063 02-07)

Avail NTIS HC A20/MF A01 CSCL 21E

Combustor concepts having the potential for significantly lower emissions levels were investigated. The combustor emissions reduction was measured in an engine test. Emission characteristics common to all engine classes are shown. Multiple-burning zone combustors, specifically the double annular and swirl-can combustors were studied. Airblast and air assist fuel injection techniques were evaluated for emissions control potential. The combustor screening and refining phases are summarized. Author

N78-11067* National Aeronautics and Space Administration, Lewis Research Center, Cleveland, Ohio
POLLUTION REDUCTION TECHNOLOGY PROGRAM FOR CLASS T4(JT8D) ENGINES

R. Roberts (Pratt and Whitney Aircraft Group, East Hartford, Conn.), A. J. Fiorentino (Pratt and Whitney Aircraft Group, East Hartford, Conn.), and L. A. Diehl *In its Aircraft Eng. Emissions* Oct 1977 p 29-89 refs (For availability see N78-11063 02-07)

Avail NTIS HC A20/MF A01 CSCL 21E

The technology required to develop commercial gas turbine engines with reduced exhaust emissions was demonstrated. Can-annular combustor systems for the JT8D engine family (EPA class T4) were investigated. The JT8D turbofan engine is an axial-flow, dual-spool, moderate-bypass-ratio design. It has a two-stage fan, a four-stage low-pressure compressor driven by a three-stage low-pressure turbine, and a seven-stage high-pressure compressor driven by a single-stage high-pressure turbine. A cross section of the JT8D-17 showing the mechanical configuration is given. Key specifications for this engine are listed.

Author

N78-11071* National Aeronautics and Space Administration, Lewis Research Center, Cleveland, Ohio
SUMMARY OF EMISSIONS REDUCTION TECHNOLOGY PROGRAMS

Richard W. Niedzwiecki *In its Aircraft Eng. Emissions* Oct 1977 p 181-202 (For availability see N78-11063 02-07)

Avail NTIS HC A20/MF A01 CSCL 21E

The NASA emissions reduction contract programs for EPA aircraft engine classes P2 (turbojet engines), T1 (jet engines with thrust under 8000 lb), T4 (JT8D) engines, and T2 (jet engines with thrust over 8000 lb) are discussed. The most important aspects of these programs, the commonality of approaches used, the test results, and assessments regarding applications of the derived technology are summarized.

Author

N78-11072* National Aeronautics and Space Administration, Lewis Research Center, Cleveland, Ohio
EMISSIONS CONTROL FOR GROUND POWER GAS TURBINES

Richard A. Rudney, Richard J. Pnem, Albert J. Juhasz, David N. Anderson, Thaddeus S. Mroz, and Edward J. Mularz *In its Aircraft Eng. Emissions* Oct 1977 p 203-242 refs (For availability see N78-11063 02-07)

Avail NTIS HC A20/MF A01 CSCL 21E

The similarities and differences of emissions reduction technology for aircraft and ground power gas turbines is described. The capability of this technology to reduce ground power emissions to meet existing and proposed emissions standards is presented and discussed. Those areas where the developing aircraft gas turbine technology may have direct application to ground power and those areas where the needed technology may be unique to the ground power mission are pointed out. Emissions reduction technology varying from simple combustor modifications to the use of advanced combustor concepts, such as catalysis is described and discussed.

Author

N78-11073* National Aeronautics and Space Administration, Lewis Research Center, Cleveland, Ohio
GENERAL AVIATION PISTON-ENGINE EXHAUST EMISSION REDUCTION

Erwin E. Kempke Jr., William H. Houtman (EPA, Washington, D. C.), William T. Westfield (FAA, Washington, D. C.), Larry C. Duke (AVCO Lycoming, Williamsport, Pa.), and Bernard J. Rezy (Teledyne Continental Motors, Los Angeles) *In its Aircraft Eng. Emissions* Oct 1977 p 243-275 refs (For availability see N78-11063 02-07)

Avail NTIS HC A20/MF A01 CSCL 21E

To support the promulgation of aircraft regulations, two airports were examined: Van Nuys and Tamiami. It was determined that the carbon monoxide (CO) emissions from piston engine aircraft have a significant influence on the CO levels in the ambient air in and around airports where workers and travelers would be exposed. Emissions standards were set up for control

of emissions from aircraft piston engines manufactured after December 31, 1978. The standards selected were based on a technologically feasible and economically reasonable control of carbon monoxide. It was concluded that substantial CO reductions could be realized if the range of typical fuel-air ratios could be narrowed. Thus, improvements in fuel management were determined as reasonable controls.

Author

N78-11074* National Aeronautics and Space Administration, Lewis Research Center, Cleveland, Ohio

ALTERNATIVE FUELS

Jack S. Grobman, Helmut F. Butze, Robert Friedman, Albert C. Antoine, and Thane W. Reynolds *In its Aircraft Eng. Emissions* Oct 1977 p 277-308 refs (For availability see N78-11063 02-07)

Avail NTIS HC A20/MF A01 CSCL 21E

Potential problems related to the use of alternative aviation turbine fuels are discussed and both ongoing and required research into these fuels is described. This discussion is limited to aviation turbine fuels composed of liquid hydrocarbons. The advantages and disadvantages of the various solutions to the problems are summarized. The first solution is to continue to develop the necessary technology at the refinery to produce specification jet fuels regardless of the crude source. The second solution is to minimize energy consumption at the refinery and keep fuel costs down by relaxing specifications.

Author

N78-11076* National Aeronautics and Space Administration, Lewis Research Center, Cleveland, Ohio

GLOBAL ATMOSPHERIC SAMPLING PROGRAM

Erwin A. Lazberg, Porter J. Perkins, David R. Englund, Daniel J. Gwintner, and James D. Holdeman *In its Aircraft Eng. Emissions* Oct 1977 p 323-355 refs (For availability see N78-11063 02-07)

Avail NTIS HC A20/MF A01 CSCL 21E

Automated instruments were installed on a commercial B-747 aircraft, during the program, to obtain baseline data and to monitor key atmospheric constituents associated with emissions of aircraft engines in order to determine if aircraft are contributing to pollution of the upper atmosphere. Data thus acquired on a global basis over the commercial air routes for 5 to 10 years will be analyzed. Ozone measurements in the 29,000 to 45,000 foot altitude were expanded over what has been available from ozonesondes. Limited aerosol composition measurements from filter samples show low levels of sulfates and nitrates in the upper troposphere. Recently installed instruments for measurement of carbon monoxide and condensation nuclei are beginning to return data.

Author

N78-11077* National Aeronautics and Space Administration, Lewis Research Center, Cleveland, Ohio

STRATOSPHERIC CRUISE EMISSION REDUCTION PROGRAM

Larry A. Diehl, Gregory M. Reck, Cecil J. Marek, and Andrew J. Szanislo *In its Aircraft Eng. Emissions* Oct 1977 p 357-391 (For availability see N78-11063 02-07)

Avail NTIS HC A20/MF A01 CSCL 21E

A recently implemented NASA effort specifically aimed at reducing cruise oxides of nitrogen from high-altitude aircraft is discussed. The desired emission levels and the combustor technology required to achieve them are discussed. A brief overview of the SCERP operating plan is given. Lean pre-mixed, pre-vaporized combustion and some of the potential difficulties that are associated with applying this technique to gas turbine combustors are examined. Base technology was developed in several key areas. These fundamental studies are viewed as a requirement for successful implementation of the lean pre-mixed combustion technique.

Author

N78-11078* National Aeronautics and Space Administration, Lewis Research Center, Cleveland, Ohio.

ADVANCED LOW-NO(x) COMBUSTORS FOR SUPERSONIC HIGH-ALTITUDE GAS TURBINES

Peter B. Roberts (International Harvester, Chicago) *In its Aircraft Eng. Emissions* Oct. 1977 p 393-415 ref (For availability see N78-11063 02-07)

Avail NTIS HC A20/MF A01 CSCL 21E

The impact of gas-turbine-engine-powered aircraft on worldwide pollution was defined within two major areas of contribution. First, the contribution of aircraft to the local air pollution of metropolitan areas and, second, the long-term effects on the chemical balance of the stratosphere of pollutants emitted from future generations of high-altitude, supersonic commercial and military aircraft. Preliminary findings indicate that stratospheric oxides of nitrogen (NO_x) emissions may have to be limited to very low levels if, for example, ozone depletion with concomitant increases in sea-level radiation, are to be avoided. Theoretical considerations suggest that (NO_x) levels as low as 10 gram per kilogram of fuel and less should be attainable from an idealized premixed type of combustor. Experimental studies were intended to explore new combustor concepts designed to minimize the formation of (NO_x) in aircraft gas turbines and to define their major operational problems and limitations. Author

N78-11090* National Aeronautics and Space Administration, Lewis Research Center, Cleveland, Ohio.

EFFECT OF ENDWALL COOLING ON SECONDARY FLOWS IN TURBINE STATOR VANES

Louis J. Goldman and Kerry L. McLellan *In AGARD Secondary Flows in Turbomachines* Sep. 1977 29 p refs (For availability see N78-11083 02-07)

Avail NTIS HC A14/MF A01 CSCL 21E

An experimental investigation was performed to determine the effect of endwall cooling on the secondary flow behavior and the aerodynamic performance of a core-turbine stator vane. The investigation was conducted in a cold-air, full-annular cascade, where three-dimensional effects could be obtained. Two endwall cooling configurations were tested. In the first configuration, the cooling holes were oriented so that the coolant was injected in line with the inviscid streamline direction. In the second configuration, the coolant was injected at an angle of 15 deg to the inviscid streamline direction and oriented toward the vane pressure surface. In both cases the stator vanes were solid and uncooled so that the effect of endwall cooling could be obtained directly. Total pressure surveys were taken downstream of the stator vanes over a range of cooling flows at the design mean-radius critical velocity ratio of 0.778. Changes in the total pressure contours downstream of the vanes were used to obtain the effect of endwall cooling on the secondary flows in the stator. Comparisons were made between the two cooled-endwall configurations and with the results obtained previously for solid endwalls. Author

N78-11106* National Aeronautics and Space Administration, Lewis Research Center, Cleveland, Ohio.

ALTITUDE TEST OF SEVERAL AFTERBURNER CONFIGURATIONS ON A TURBOFAN ENGINE WITH A HYDROGEN HEATER TO SIMULATE AN ELEVATED TURBINE DISCHARGE TEMPERATURE

Fry L. Johnsen and Richard P. Cullom. Nov. 1977 57 p refs (NASA-TP-1068, E-9207) Avail NTIS HC A04/MF A01 CSCL 21E

A performance test of several experimental afterburner configurations was conducted with a mixed flow turbofan engine in an altitude facility. The simulated flight conditions were for Mach 1.4 at two altitudes 12,190 and 14,630 meters. Turbine discharge temperatures of 889 and 1056 K were used. A production afterburner was tested for comparison. The research afterburners included partial forced mixers with V-gutter flameholders; a carbureted V-gutter flameholder; and a triple ring V-gutter flameholder with four swirl-can fuel mixers. Fuel injection variations were included. Performance data shown include augmented thrust ratio, thrust specific fuel consumption, combustion efficiency, and total pressure drop across the afterburner. Author

N78-13066* National Aeronautics and Space Administration, Lewis Research Center, Cleveland, Ohio.

EFFECT OF FUEL PROPERTIES ON PERFORMANCE OF SINGLE AIRCRAFT TURBOJET COMBUSTOR AT SIMULATED IDLE, CRUISE, AND TAKEOFF CONDITIONS

Helmut F. Butze and Arthur L. Smith. Sep. 1977 21 p refs (NASA-TM-73780, E-9336) Avail NTIS HC A02/MF A01 CSCL 21E

The performance of a single-can JT8D combustor was investigated with a number of fuels exhibiting wide variations in chemical composition and volatility. Performance parameters investigated were combustion efficiency, emissions of CO, unburned hydrocarbons and nitrogen oxides, as well as liner temperatures and smoke. The most pronounced effects of changes in fuel composition were observed at simulated cruise and takeoff conditions where smoke and liner temperatures increased significantly as the hydrogen content of the fuel decreased. At the simulated idle condition, emissions of CO and unburned hydrocarbons increased slightly and, accordingly, combustion efficiencies decreased slightly as the hydrogen content of the fuels decreased. Author

N78-13080* National Aeronautics and Space Administration, Lewis Research Center, Cleveland, Ohio.

FLIGHT-EFFECTS ON PREDICTED FAN FLY-BY NOISE

Marcus F. Heidmann and Bruce J. Clark. 1977 24 p refs. Presented at 94th Meeting of the Acoustical Soc. of Am., Miami, Fla., 13-16 Dec. 1977.

(NASA-TM-73798) Avail NTIS HC A02/MF A01 CSCL 20A

The impact on PNL (Perceived Noise Level, Tone corrected) and Fly-by EPNL (Effective Perceived Noise Level) when forward motion reduces the noise generated by the bypass fan of an aircraft engine was studied. Calculated noise spectra for a typical subsonic tip speed fan designed for blade passage frequency (BPF) tone cutoff were translated in frequency by systematically varying the BPF from 0.5 to 8 kHz. Two cases of predicted flight-effects on fan source noises were considered: reduced BPF tone level of 8 db and reduced broadband noise level of about 2 db in addition to reduced tone level. The maximum reduction in PNL of the noise as emitted from the fan occurred when the BPF was at 4 kHz where the reductions were 7.4 and 10.0 db. The maximum reduction in EPNL of the noise as received during a 500-foot altitude fly-by occurred when the BPF was at 2.5 kHz where the reductions were 5.0 and 7.8 db. Author

N78-13081* National Aeronautics and Space Administration, Lewis Research Center, Cleveland, Ohio.

AN EMPIRICAL MODEL FOR INVERTED-VELOCITY-PROFILE JET NOISE PREDICTION

James R. Stone. 1977 30 p refs. Presented at 94th Meeting of the Acoustical Soc. of Am., Miami, Fla., 13-16 Dec. 1977 (NASA-TM-73838, E-9425) Avail NTIS HC A03/MF A01 CSCL 20A

An empirical model for predicting the noise from inverted-velocity-profile coaxial or conical jets is presented and compared with small-scale static and simulated flight data. The model considered the combined contributions of as many as four uncorrelated constituent sources: the premerged jet/ambient mixing region, the merged jet/ambient mixing region, outer stream shock/turbulence interaction, and inner stream shock/turbulence interaction. The noise from the merged region occurs at relatively low frequency and is modeled as the contribution of a circular jet at merged conditions and total exhaust area, with the high frequencies attenuated. The noise from the premerged region occurs at high frequency and is modeled as the contribution of an equivalent plug nozzle at outer stream conditions, with the low frequencies attenuated. Author

N78-13082* National Aeronautics and Space Administration, Lewis Research Center, Cleveland, Ohio.

AN OVERVIEW OF AEROSPACE GAS TURBINE TECHNOLOGY OF RELEVANCE TO 1st DEVELOPMENT OF THE AUTOMOTIVE GAS TURBINE ENGINE

D. G. Evans and T. J. Miller. 1978 52 p refs. Presented at Ann Meeting of the Soc. of Automotive Engineers, Detroit, Mich.,

27 Feb. - 3 Mar. 1978

(NASA-TM-73849) Avail: NTIS HC A04/MF A01 CSCL 21E

Technology areas related to gas turbine propulsion systems with potential for application to the automotive gas turbine engine are discussed. Areas included are: system steady-state and transient performance prediction techniques, compressor and turbine design and performance prediction programs and effects of geometry, combustor technology and advanced concepts, and ceramic coatings and materials technology. Author

N78-13083* National Aeronautics and Space Administration, Lewis Research Center, Cleveland, Ohio.

MECHANICAL CHARACTERISTICS OF STABILITY-BLEED VALVES FOR A SUPERSONIC INLET

George H. Neiner, Miles O. Dustin, and Gary L. Cole Washington Dec. 1977 39 p refs

(NASA-TM-X-3483; E-8852) Avail: NTIS HC A03/MF A01 CSCL 21E

Mechanical characteristics of a set of direct-operated relief valves used in a throat-bypass stability-bleed system designed for the YF-12 aircraft inlet are described. A comparison of data taken before and after the windtunnel tests (at room temperature) showed that both the effective spring rate and the piston friction had decreased during the wind tunnel tests. In neither the effective spring rate nor the piston friction was the magnitude of change great enough to cause significant impairment of overall system effectiveness. No major valve mechanical problems were encountered in any of the tests. During high temperature bench tests, piston frictional drag increased. The friction returned to its initial room temperature value when the stability-bleed valve was disassembled and reassembled. The problem might be solved by using a different material for the piston sleeve bearing and the piston rings. Author

N78-13084* National Aeronautics and Space Administration, Lewis Research Center, Cleveland, Ohio.

INFLUENCE OF OIL SQUEEZE FILM DAMPING ON STEADY-STATE RESPONSE OF FLEXIBLE ROTOR OPERATING TO SUPERCRITICAL SPEEDS

Robert E. Cunningham Dec 1977 44 p refs
(NASA-TP-1094; E-9091) Avail: NTIS HC A03/MF A01 CSCL 21E

Experimental data were obtained for the unbalance response of a flexible rotor to speeds above the third lateral bending critical. Squeeze-film damping coefficients calculated from measured data showed good agreement with short-journal-bearing approximations over a frequency range from 5000 to 31,000 cpm. Response of a rotor to varying amounts of unbalance was investigated. A very lightly damped rotor was compared with one where oil-squeeze dampers were applied. Author

N78-18042* National Aeronautics and Space Administration, Lewis Research Center, Cleveland, Ohio.

PRELIMINARY QCSEE PROGRAM TEST RESULTS

Carl C. Ciepluch 1977 22 p refs Presented at 1977 Aerospace Meeting, Los Angeles, 14-17 Nov. 1977; sponsored by SAE (NASA-TM-73732) Avail: NTIS HC A02/MF A01 CSCL 21E

The QCSEE (Quiet, Clean, Short-Haul Experimental Engine) program has entered the engine test phase. Overall design and advanced technology incorporated into the two engines in the program were described. In addition, preliminary engine test results are presented and compared to the technical requirements the engines were designed to meet. Author

N78-18043* National Aeronautics and Space Administration, Lewis Research Center, Cleveland, Ohio.

COMPUTER PROGRAM FOR CALCULATION OF A GAS TEMPERATURE PROFILE BY INFRARED EMISSION: ABSORPTION SPECTROSCOPY

Donald R. Buchele Dec 1977 85 p refs
(NASA-TM-73848; E-9436) Avail: NTIS HC A05/MF A01 CSCL 21E

A computer program to calculate the temperature profile of

a flame or hot gas was presented in detail. Emphasis was on profiles found in jet engine or rocket engine exhaust streams containing H₂O or CO₂ radiating gases. The temperature profile was assumed axisymmetric with an assumed functional form controlled by two variable parameters. The parameters were calculated using measurements of gas radiation at two wavelengths in the infrared. The program also gave some information on the pressure profile. A method of selection of wavelengths was given that is likely to lead to an accurate determination of the parameters. The program is written in FORTRAN 4 language and runs in less than 60 seconds on a Univac 1100 computer. Author

N78-18044* National Aeronautics and Space Administration, Lewis Research Center, Cleveland, Ohio.

TEMPERATURE DISTRIBUTIONS AND THERMAL STRESSES IN A GRADED ZIRCONIA/METAL GAS PATH SEAL SYSTEM FOR AIRCRAFT GAS TURBINE ENGINES

Christopher M. Taylor (Leeds Univ.) and Robert C. Bill (Army R and T Labs., Cleveland) 1978 19 p refs Presented at the Conf. on Air-Breathing Propulsion Systems, Huntsville, Ala., 18-18 Jan. 1978; sponsored by AIAA (NASA-TM-73818) Avail: NTIS HC A02/MF A01 CSCL 21E

A ceramic/metallic aircraft gas turbine outer gas path seal designed for improved engine performance was studied. Transient temperature and stress profiles in a test seal geometry were determined by numerical analysis. During a simulated engine deceleration cycle from sea-level takeoff to idle conditions, the maximum seal temperature occurred below the seal surface, therefore the top layer of the seal was probably subjected to tensile stresses exceeding the modulus of rupture. In the stress analysis both two- and three-dimensional finite element computer programs were used. Predicted trends of the simpler and more easily usable two-dimensional element programs were borne out by the three-dimensional finite element program results. Author

N78-18045* National Aeronautics and Space Administration, Lewis Research Center, Cleveland, Ohio.

A COMPUTER PROGRAM FOR THE TRANSIENT THERMAL ANALYSIS OF AN IMPINGEMENT COOLED TURBINE BLADE

Raymond E. Gaugler 1978 10 p refs Presented at Aerospace Sci. Meeting, Huntsville, Ala., 18-18 Jan. 1978; sponsored by AIAA (NASA-TM-73819) Avail: NTIS HC A02/MF A01 CSCL 21E

A computer program to calculate transient and steady state temperatures, pressures, and coolant flows in a cooled turbine blade or vane with an impingement insert is described. Input to the program includes a description of the blade geometry, coolant supply conditions, outside thermal boundary conditions and wheel speed. Coolant-side heat transfer coefficients are calculated internally in the program, with the user specifying the mode of heat transfer at each internal flow station. Program output includes the temperature at each node, the coolant pressures and flow rates, and the inside heat transfer coefficients. A sample problem is discussed. Author

N78-18063* National Aeronautics and Space Administration, Lewis Research Center, Cleveland, Ohio.

COLD-AIR PERFORMANCE OF FREE-POWER TURBINE DESIGNED FOR 112-KILOWATT AUTOMOTIVE GAS-TURBINE ENGINE. 1: DESIGN STATOR-VANE-CHORD SETTING ANGLE OF 35 DEG

Milton G. Kofsky and William J. Nusbaum Jan 1978 23 p refs
(NASA-TP-1007 CONS/1011-12; E-8964) Avail: NTIS HC A02/MF A01 CSCL 21E

A cold air experimental investigation of a free power turbine designed for a 112-kW automotive gas turbine was made over a range of speeds from 0 to 130 percent of design equivalent speeds and over a range of pressure ratio from 1.11 to 2.45. Results are presented in terms of equivalent power, torque, mass flow, and efficiency for the design power point setting of the variable stator. Author

N78-18066* National Aeronautics and Space Administration
Lewis Research Center, Cleveland, Ohio
A REVIEW OF NASA'S PROPULSION PROGRAMS FOR AVIATION

Warner L. Stewart, Harry W. Johnson, and Richard J. Weber
1978 21 p refs Presented at the 16th Aerospace Sci. Meeting,
Huntsville, Ala., 16-18 Jan., sponsored by AIAA

(NASA-TM-73831) Avail: NTIS HC A02/MF A01 CSCL 21A

A review of five NASA engine-oriented propulsion programs of major importance to civil aviation are presented and discussed. Included are programs directed at exploring propulsion system concepts for (1) energy conservation subsonic aircraft (improved current turbofans, advanced turbofans, and advanced turboprops); (2) supersonic cruise aircraft (variable cycle engines); (3) general aviation aircraft (improved reciprocating engines and small gas turbines); (4) powered lift aircraft (advanced turbofans); and (5) advanced rotorcraft. Author

N78-17066* National Aeronautics and Space Administration,
Lewis Research Center, Cleveland, Ohio.

VARIABLE THRUST NOZZLE FOR QUIET TURBOFAN ENGINE AND METHOD OF OPERATING SAME Patent

Arthur P. Adamson, inventor (to NASA) (GE, Cincinnati, Ohio)
Issued 17 Jan. 1978 7 p Filed 29 May 1975 Sponsored by NASA

(NASA-Case-LEW-12317-1; US-Patent-4,068,469;
US-Patent-Appl-SN-581750; US-Patent-Class-60-204;
US-Patent-Class-60-226R; US-Patent-Class-60-271) Avail: US
Patent Office CSCL 21E

An improved method of operating a gas turbine engine is presented wherein engine-generated noise is maintained at a reduced level during reduced thrust operation. Fan speed was maintained at a constant level while fan nozzle area was increased. This maintained high inlet Mach numbers for reduced forward noise propagation and also permitted reduced nozzle exhaust velocity for reduced shear noise. In another embodiment, airflow was increased by means of a fan blade pitch change or speed increase while the fan nozzle area was increased, yielding both a net reduction in engine thrust and noise.

Official Gazette of the U.S. Patent Office

N78-17066* National Aeronautics and Space Administration,
Lewis Research Center, Cleveland, Ohio.

GAS TURBINE ENGINE WITH CONVERTIBLE ACCESSORIES Patent

Donald F. Sargisson (GE, Cincinnati, Ohio) and Arthur P. Adamson,
inventors (to NASA) Issued 17 Jan. 1978 6 p Filed 8 Nov.
1974 Sponsored by NASA

(NASA-Case-LEW-12390-1; US-Patent-4,068,470;
US-Patent-Appl-SN-522109; US-Patent-Class-60-226R;
US-Patent-Class-74-385; US-Patent-Class-74-417) Avail: US
Patent Office CSCL 21E

Drive means for connecting a gas turbine engine to its accessories are so constructed as to allow the accessories to be selectively positioned to any one of several predetermined circumferential positions about the perimeter of the engine. This feature permits convenient mounting of the same engine upon vehicles demanding radically different engine mounting arrangements.

Official Gazette of the U.S. Patent Office

N78-17066* National Aeronautics and Space Administration,
Lewis Research Center, Cleveland, Ohio.

CERAMICS IN GAS TURBINE: POWDER AND PROCESS CHARACTERIZATION

Sunil Dutta 1977 16 p refs Presented at the Conf. on
Composites and Advanced Materials, Cocoa Beach, Fla., 17-19 Jan.
1977; Sponsored by Am. Ceramic Soc.
(NASA-TM-73875; E-9475) Avail: NTIS HC A02/MF A01
CSCL 21E

Some of the intrinsic properties of various forms of Si₃N₄ and SiC are listed and limitations of such materials' availability are pointed out. The essential features/parameters to characterize a batch of powder are discussed including the standard techniques for such characterization. In process characterization, parameters

in sintering, reaction sintering, and hot pressing processes are discussed including the factors responsible for strength limitations in ceramic bodies. Significant improvements in material properties can be achieved by reducing or eliminating the strength limiting factors with consistent powder and process characterization along with process control. Author

N78-17066* National Aeronautics and Space Administration
Lewis Research Center, Cleveland, Ohio.

GENERAL AVIATION ENERGY-CONSERVATION RESEARCH PROGRAMS AT NASA-LEWIS RESEARCH CENTER

Edward A. Willis 1977 26 p refs Presented at the Conf. on
Energy Conserv. in Gen. Aviation, Kalamazoo, Mich., 10-11 Oct.
1977; sponsored by Western Michigan Univ.

(NASA-TM-73884) Avail: NTIS HC A03/MF A01 CSCL 21E

The major thrust of NASA's nonturbine general aviation engine programs is directed toward (1) reduced specific fuel consumption, (2) improved fuel tolerance, and (3) emission reduction. Current and planned future programs in such areas as lean operation, improved fuel management, advanced cooling techniques and advanced engine concepts, are described. These are expected to lay the technology base, by the mid to latter 1980's, for engines whose total fuel costs are as much as 30% lower than today's conventional engines. Author

N78-18066* National Aeronautics and Space Administration,
Lewis Research Center, Cleveland, Ohio.

INTEGRATED GAS TURBINE ENGINE-NACELLE Patent

Arthur P. Adamson, Donald F. Sargisson, and Charles L. Stotler,
Jr., inventors (to NASA) Issued 25 Oct. 1977 9 p Filed
3 Nov. 1975 Division of US Patent Appl. SN-522108, filed
8 Nov. 1974

(NASA-Case-LEW-12389-2; US-Patent-4,055,041;
US-Patent-Appl-SN-628221; US-Patent-Class-60-226R;
US-Patent-Class-60-39.31; US-Patent-Class-244-53A;
US-Patent-Class-244-54) Avail: US Patent Office CSCL 21E

A nacelle for use with a gas turbine engine is presented. An integral webbed structure resembling a spoked wheel for rigidly interconnecting the nacelle and engine, provides lightweight support. The inner surface of the nacelle defines the outer limits of the engine motive fluid flow annulus while the outer surface of the nacelle defines a streamlined envelope for the engine.

Official Gazette of the U.S. Patent Office

N78-18066* National Aeronautics and Space Administration,
Lewis Research Center, Cleveland, Ohio.

VARIABLE MIXER PROPULSION CYCLE Patent

Dan Joseph Rundell (GE, Cleveland), Donald Patrick McHugh
(GE, Cleveland), Tom Foster (GE, Cleveland), and Ralph Harold
Brown, inventors (to NASA) (GE, Cleveland) Issued 24 Jan.
1978 10 p Filed 2 Jun. 1975 Sponsored by NASA

(NASA-Case-LEW-12917-1; US-Patent-4,069,661;
US-Patent-Appl-SN-583055; US-Patent-Class-60-204;
US-Patent-Class-60-262) Avail: US Patent Office CSCL 21E

A design technique, method, and apparatus are delineated for controlling the bypass gas stream pressure and varying the bypass ratio of a mixed flow gas turbine engine in order to achieve improved performance. The disclosed embodiments each include a mixing device for combining the core and bypass gas streams. The variable area mixing device permits the static pressures of the core and bypass streams to be balanced prior to mixing at widely varying bypass stream pressure levels. The mixed flow gas turbine engine therefore operates efficiently over a wide range of bypass ratios and the dynamic pressure of the bypass stream is maintained at a level which will keep the engine inlet airflow matched to an optimum design level throughout a wide range of engine thrust settings.

Official Gazette of the U.S. Patent Office

N78-19167* National Aeronautics and Space Administration, Lewis Research Center, Cleveland, Ohio.

PREDICTED INLET GAS TEMPERATURES FOR TUNGSTEN FIBER REINFORCED SUPERALLOY TURBINE BLADES

Edward A. Winea, Leonard J. Westfall, and Donald W. Petrasiek 1978 23 p refs Presented at 2d Intern. Conf. on Composite Materials, Toronto, Canada, 16-20 Apr. 1978; sponsored by Am. Inst. of Mining, Metallurgical, and Petroleum Engineers (NASA-TM-73842) Avail: NTIS HC A02/MF A01 CSCL 21E

Tungsten fiber reinforced superalloy composites (TFRS) impingement cooled turbine blade inlet gas temperatures were calculated taking into account material spanwise strength, thermal conductivity, material oxidation resistance, fiber-matrix interaction, and coolant flow. Measured values of TFRS thermal conductivities are presented. Calculations indicate that blades made of 30 volume percent fiber content TFRS having a 12.0/0 N-m/kg stress-to-density ratio while operating at 40 atmospheres and a 0.06 coolant flow ratio could permit a turbine blade inlet gas temperature of over 1900K. This is more than 150K greater than similar superalloy blades. Author

N78-19168* National Aeronautics and Space Administration, Lewis Research Center, Cleveland, Ohio.

HIGH TEMPERATURE ENVIRONMENTAL EFFECTS ON METALS

S. J. Grisaffe, C. E. Lowell, and C. A. Stearns 1977 19 p refs Presented at 24th Sagamore Army Materials Res. Conf. Risk and Failure Analysis for Reliability, Bolton Landing, N. Y., 22-26 Aug. 1977

(NASA-TM-73878) Avail: NTIS HC A02/MF A01 CSCL 21E

The gas turbine engine was used as an example to predict high temperature environmental attack on metals. Environmental attack in a gas turbine engine derives from high temperature, combustion products of the air and fuel burned, and impurities. Of all the modes of attack associated with impurity effects, hot corrosion was the most complicated mechanistically. Solutions to the hot corrosion problem were sought semi-empirically in: (1) improved alloys or ceramics; (2) protective surface coating; (3) use of additives to the engine environment; and (4) air/fuel cleanup to eliminate harmful impurities. J.C.S.

N78-19161* National Aeronautics and Space Administration, Lewis Research Center, Cleveland, Ohio.

EXPERIMENTAL DETERMINATION OF TRANSIENT STRAIN IN A THERMALLY-CYCLED SIMULATED TURBINE BLADE UTILIZING A NON-CONTACT TECHNIQUE

Frederick D. Calfo and Peter T. Bizon Jan. 1978 31 p refs (NASA-TM-73888; E-9500) Avail: NTIS HC A03/MF A01 CSCL 21E

A type of noncontacting electro-optical extensometer was used to measure the displacement between parallel targets mounted on the leading edge of a simulated turbine blade throughout a complete heating and cooling cycle. The blade was cyclically heated and cooled by moving it into and out of a Mach 1 hot gas stream. The principle of operation and measurement procedure of the electro-optics extensometer are described. Author

N78-20130* National Aeronautics and Space Administration, Lewis Research Center, Cleveland, Ohio.

TWO-DIMENSIONAL COLD-AIR CASCADE STUDY OF A FILM-COOLED TURBINE STATOR BLADE. 4: COMPARISON OF EXPERIMENTAL AND ANALYTICAL AERODYNAMIC RESULTS FOR BLADE WITH 12 ROWS OF 0.078-CENTIMETER-(0.030-INCH-) DIAMETER HOLES HAVING STREAMWISE EJECTION ANGLES

Herman W. Prust, Jr. Mar. 1978 30 p refs (NASA-TP-1151; E-9187) Avail: NTIS HC A03/MF A01 CSCL 21E

Previously published experimental aerodynamic efficiency results for a film cooled turbine stator blade are compared with analytical results computed from two published analytical methods. One method was used as published; the other was modified for certain cases of coolant discharge from the blade suction surface. For coolant ejection from blade surface regions where

the surface static pressures are higher than the blade exit pressure, both methods predict the experimental results quite well. However, for ejection from regions with surface static pressures lower than the blade exit pressure, both methods predict too small a change in efficiency. The modified method gives the better prediction. Author

N78-20131* National Aeronautics and Space Administration, Lewis Research Center, Cleveland, Ohio.

PERFORMANCE OF A SHORT ANNULAR DUMP DIFFUSER USING SUCTION-STABILIZED VORTICES AT INLET MACH NUMBERS TO 0.41

John M. Smith and Albert J. Juhasz Apr. 1978 40 p refs (NASA-TP-1194; E-9332) Avail: NTIS HC A03/MF A01 CSCL 21E

A short, annular dump diffuser was designed to use suction to establish stabilized vortices on both walls for improved flow expansion in the region of an abrupt area change. The diffuser was tested at near ambient inlet pressure and temperature. The overall diffuser area ratio was 4.0. The inlet height was 2.54 cm and the exit pitot-static rakes were located at a distance from the vortex fence equal to two or six times the inlet height. Performance data were taken at near ambient temperature and pressure for nominal inlet Mach numbers of 0.18 to 0.41 with suction rates of 0 to 18 percent of the total inlet airflow. The exit velocity profile could be shifted toward either wall by adjusting the inner- or outer-wall suction rate. Symmetrical exit velocity profiles were unstable, with a tendency to shift back to hub- or tip-weighted profile. Diffuser effectiveness was increased from about 47 percent without suction to over 85 percent at a total suction rate of about 14 percent. The diffuser total pressure losses at inlet Mach numbers of 0.18 and 0.41 decreased from 1.1 and 5.6 percent without suction to 0.48 and 5.2 percent at total suction rates of 14.4 and 5.6 percent, respectively. Author

N78-20132* National Aeronautics and Space Administration, Lewis Research Center, Cleveland, Ohio.

SIMULATED FLIGHT EFFECTS ON NOISE CHARACTERISTICS OF A FAN INLET WITH HIGH THROAT MACH NUMBER

Howard L. Wesoky, Donald A. Dietrich, and John M. Abbott Apr. 1978 45 p refs (NASA-TP-1199; E-9253) Avail: NTIS HC A03/MF A01 CSCL 21E

An anechoic wind tunnel experiment was conducted to determine the effects of simulated flight on the noise characteristics of a high throat Mach number fan inlet. Comparisons were made with the performance of a conventional low throat Mach number inlet with the same 50.8 cm fan noise source. Simulated forward velocity of 41 m/sec reduced perceived noise levels for both inlets, the largest effect being more than 3 db for the high throat Mach number inlet. The high throat Mach number inlet was as much as 7.5 db quieter than the low throat Mach number inlet with tunnel airflow and about 6 db quieter without tunnel airflow. Effects of inlet flow angles up to 30 deg were seemingly irregular and difficult to characterize because of the complex flow fields and generally small noise variations. Some modifications of tones and directivity at blade passage harmonics resulting from inlet flow angle variation were noted. Author

N78-20133* National Aeronautics and Space Administration, Lewis Research Center, Cleveland, Ohio.

TWO-DIMENSIONAL COLD-AIR CASCADE STUDY OF A FILM-COOLED TURBINE STATOR BLADE. 5: COMPARISON OF EXPERIMENTAL AND ANALYTICAL AERODYNAMIC RESULTS FOR BLADE WITH 12 ROWS OF 0.038-CENTIMETER-(0.015 INCH) DIAMETER COOLANT HOLES HAVING STREAMWISE EJECTION ANGLES

Herman W. Prust, Jr. Apr. 1978 23 p refs (NASA-TP-1204; E-9342) Avail: NTIS HC A02/MF A01 CSCL 21E

Published experimental aerodynamic efficiency results were compared with results predicted from two published analytical methods. This is the second of two such comparisons. One of the analytical methods was used as published; the other was

modified for certain cases of coolant discharge from the blade suction surface. The results show that for 23 cases of single row and multirow discharge covering coolant fractions from 0 to about 9 percent, the difference between the experimental and predicted results was no greater than about 1 percent in any case and less than 1/2 percent in most cases. Author

N78-21108* National Aeronautics and Space Administration, Lewis Research Center, Cleveland, Ohio.

COMPARISON OF THE NOISE CHARACTERISTICS OF TWO LOW PRESSURE RATIO FANS WITH A HIGH THROAT MACH NUMBER INLET

Howard L. Wesoky, John M. Abbott, and Donald A. Dietrich Jan. 1978 31 p refs (NASA-TM-73880; E-9489) Avail: NTIS HC A03/MF A01 CSCL 21E

Acoustics data obtained in experiments with two low pressure ratio 50.8 cm (20 in.) diameter model fans differing in design tip speed were compared. Determination of the average throat Mach number used to compare high Mach inlet noise reduction characteristics was based on a correlation of inlet wall static pressure measurements with a flow field calculation. The largest noise reductions were generally obtained with the higher tip speed fan. At a throat Mach number of 0.79, the difference in noise reduction was about 3.5 db with static test conditions. Although the noise reduction increased for the lower tip speed fan with a simulated flight velocity of 41 m/sec (80 knots), it was still about 2 db less than that of the high tip speed fan which was only tested at the static condition. However, variations in acoustic performance could not be absolutely attributed to the different fan designs because of differences in inlet lip contours which resulted in small variations of peak wall Mach number and axial extent of supersonic and near-sonic flow. Author

N78-21109* National Aeronautics and Space Administration, Lewis Research Center, Cleveland, Ohio.

GAS PATH SEALING IN TURBINE ENGINES

Lawrence P. Ludwig 1978 44 p refs Presented at AGARD Power, Energetics, and Propulsion Panel Meeting on Seal Technol. in Gas Turbine Engines, London, 6-7 Apr. 1978 (NASA-TM-73890; E-9505) Avail: NTIS HC A03/MF A01 CSCL 21E

A survey of gas path seals is presented with particular attention given to sealing clearance effects on engine component efficiency. The effects on compressor pressure ratio and stall margin are pointed out. Various case-rotor relative displacements, which affect gas path seal clearances, are identified. Forces produced by nonuniform sealing clearances and their effect on rotor stability are discussed qualitatively, and recent work on turbine-blade-tip sealing for high temperature is described. The need for active clearance control and for engine structural analysis is discussed. The functions of the internal-flow system and its seals are reviewed. Author

N78-21110* National Aeronautics and Space Administration, Lewis Research Center, Cleveland, Ohio.

PHOTOGRAPHIC CHARACTERIZATION OF SPARK-IGNITION ENGINE FUEL INJECTORS

Peggy L. Evanich Feb. 1978 27 p refs (NASA-TM-78830; E-9535) Avail: NTIS HC A03/MF A01 CSCL 21E

Manifold port fuel injectors suitable for use in general aviation spark-ignition engines were evaluated qualitatively on the basis of fuel spray characteristics. Photographs were taken at various fuel flow rates or pressure levels. Mechanically and electronically operated pintle injectors generally produced the most atomization. The plain-orifice injectors used on most fuel-injected general aviation engines did not atomize the fuel when sprayed into quiescent air. Author

N78-21112* National Aeronautics and Space Administration, Lewis Research Center, Cleveland, Ohio.

AIRFLOW AND THRUST CALIBRATION OF AN F100 ENGINE, S/N P680059, AT SELECTED FLIGHT CONDITIONS

Thomas J. Biesiadny, Douglas Lee, and Jose R. Rodriguez Apr. 1978 27 p refs (NASA-TP-1069; E-9257) Avail: NTIS HC A03/MF A01 CSCL 21E

An airflow and thrust calibration of an F100 engine, S/N P680059, was conducted to study airframe propulsion system integration losses in turbofan-powered high-performance aircraft. The tests were conducted with and without thrust augmentation for a variety of simulated flight conditions with emphasis on the transonic regime. The resulting corrected airflow data generalized into one curve with corrected fan speed while corrected gross thrust increased as simulated flight conditions increased. Overall agreement between measured data and computed results was 1 percent for corrected airflow and -1 1/2 percent for gross thrust. The results of an uncertainty analysis are presented for both parameters at each simulated flight condition. Author

N78-21114* National Aeronautics and Space Administration, Lewis Research Center, Cleveland, Ohio.

THEORETICAL FLOW CHARACTERISTICS OF INLETS FOR TILTING-NACELLE VTOL AIRCRAFT

Michael A. Boles, Rogers W. Luidens, and Norbert O. Stockman Apr. 1978 31 p refs (NASA-TP-1205; E-9387) Avail: NTIS HC A03/MF A01 CSCL 21E

The results of a theoretical investigation of geometric variables for lift-cruise-fan, tilting nacelle inlets operating at high incidence angles are presented. These geometric variables are investigated for their effects on surface static to free stream pressure ratio, and the separation parameters of maximum to diffuser exit surface velocity ratio and maximum surface Mach number for low speed operating conditions. The geometric parameters varied were the internal lip contraction ratio, external forebody to diffuser exit diameter ratio external forebody length to diameter ratio and internal lip major to minor axis ratio. Author

N78-21122* National Aeronautics and Space Administration, Lewis Research Center, Cleveland, Ohio.

PROGRESS IN ADVANCED HIGH TEMPERATURE TURBINE MATERIALS, COATINGS, AND TECHNOLOGY

John C. Freche and G. Marvin Ault In AGARD High Temp. Probl. in Gas Turbine Eng. Feb. 1978 31 p refs (For availability see N78-21118 12-07)

Avail: NTIS HC A25/MF A01 CSCL 21E

Advanced materials, coatings, and cooling technology is assessed in terms of improved aircraft turbine engine performance. High cycle operating temperatures, lighter structural components, and adequate resistance to the various environmental factors associated with aircraft gas turbine engines are among the factors considered. Emphasis is placed on progress in development of high temperature materials for coating protection against oxidation, hot corrosion and erosion, and in turbine cooling technology. Specific topics discussed include metal matrix composites, superalloys, directionally solidified eutectics, and ceramics J.M.S

N78-22007* National Aeronautics and Space Administration, Lewis Research Center, Cleveland, Ohio.

IMPACT BEHAVIOR OF FILAMENT WOUND GRAPHITE/EPOXY FAN BLADES

Kenneth J. Bowles 1978 19 p refs Presented at the 23d Natl. SAMPE Symp. and Exhibition, Anaheim, Calif., 2-4 May 1978

(NASA-TM-78845; E-9562) Avail: NTIS HC A02/MF A01 CSCL 21E

The fabrication and impact tests of graphite/epoxy filament wound fan blades are discussed. Blades which were spin tested at tip speeds up to 305 meters per second retained their structural integrity. Two blades were each impacted with a 454 gram slice of a 908 gram simulated bird at a tip speed of 263 meters

per second and impact angles of 22 and 32 deg. The impact tests were recorded with high-speed movie film. The blade which was impacted at 22 deg sustained some root delamination but remained intact. The 32 deg impact separated the blade from the root. No local damage other than leading edge debonding was observed for either blade. Results of a failure mode analysis are also discussed. Author

N78-22088* National Aeronautics and Space Administration, Lewis Research Center, Cleveland, Ohio.
REDUCTION OF AIRCRAFT GAS TURBINE ENGINE POLLUTANT EMISSIONS Status Report
 Larry A. Diehl 1978 17 p refs Proposed for presentation at 71st Ann. Meeting of the Air Pollution Control Assoc., Houston, Tex., 26-30 Jun. 1978
 (NASA-TM-78870; E-9601) Avail: NTIS HC A02/MF A01 CSCL 21E

To accomplish simultaneous reduction of unburned hydrocarbons, carbon monoxide, and oxides of nitrogen, required major modifications to the combustor. The modification most commonly used was a staged combustion technique. While these designs are more complicated than production combustors, no insurmountable operational difficulties were encountered in either high pressure rig or engine tests which could not be resolved with additional normal development. The emission reduction results indicate that reductions in unburned hydrocarbons were sufficient to satisfy both near and far-term EPA requirements. Although substantial reductions were observed, the success in achieving the CO and NOx standards was mixed and depended heavily on the engine/engine cycle or which it was employed. Technology for near term CO reduction was satisfactory or marginally satisfactory. Considerable doubt exists if this technology will satisfy all far-term requirements. Author

N78-22093* National Aeronautics and Space Administration, Lewis Research Center, Cleveland, Ohio.
LEAN COMBUSTION LIMITS OF A CONFINED PREMIXED-PREVAPORIZED PROPANE JET
 Kenneth L. Huck and Cecil J. Marek Apr. 1978 23 p refs
 (NASA-TM-78868; E-9453) Avail: NTIS HC A02/MF A01 CSCL 21B

Lean blowout limits were reported for a premixed prevaporized propane jet issuing into a cylindrical combustor. A single hole in a flat plate was used as a flameholder. Flameholders with various hole diameters were used. Jet velocities were varied from 3 to 290 meters per second. The combustor cross sectional area was changed by using different quartz liners of 12.7 and 22.2 millimeters diameters. As a result the combustor Reynolds number varied from 1000 to 9000. Stability was achieved at laminar as well as turbulent conditions. Three zones of flame stability were observed. The blowout equivalence ratio varied with step size and the combustor and jet Reynolds numbers. The combustor inlet mixture temperature was 395 K, and the combustor pressure was 1 atmosphere. Author

N78-22101* National Aeronautics and Space Administration, Lewis Research Center, Cleveland, Ohio.
IN-PLACE RECALIBRATION TECHNIQUE APPLIED TO A CAPACITANCE-TYPE SYSTEM FOR MEASURING ROTOR BLADE TIP CLEARANCE
 John P. Barranger Apr. 1978 35 p refs
 (NASA-TP-1110; E-9395) Avail: NTIS HC A03/MF A01 CSCL 20E

The rotor blade tip clearance measurement system consists of a capacitance sensing probe with self contained tuning elements, a connecting coaxial cable, and remotely located electronics. Tests show that the accuracy of the system suffers from a strong dependence on probe tip temperature and humidity. A novel in-place recalibration technique was presented which partly overcomes this problem through a simple modification of the electronics that permits a scale factor correction. This technique, when applied to a commercial system significantly reduced errors under varying conditions of humidity and temperature. Equations were also found that characterize the important cable and probe design quantities. Author

N78-23023* National Aeronautics and Space Administration, Lewis Research Center, Cleveland, Ohio.
NORMAL SHOCK AND RESTART CONTROLS FOR A SUPERSONIC AIRBREATHING PROPULSION SYSTEM
 George H. Nainer, Gary L. Cole, and Francis J. Paulovich In NASA, Washington Fourth Inter-Center Control Systems Conf. Jan. 1978 p 299-321 refs (For availability see N78-23010 13-99)
 Avail: NTIS HC A22/MF A01 CSCL 21E

N78-23024* National Aeronautics and Space Administration, Lewis Research Center, Cleveland, Ohio.
OPTIMAL CONTROL OF A SUPERSONIC INLET TO MINIMIZE FREQUENCY OF INLET UNSTART
 Bruce Lehtinen, John R. Zeller, and Lucille C. Geysler In NASA, Washington Fourth Inter-Center Control Systems Conf. Jan. 1978 p 323-335 refs (For availability see N78-23010 13-99)
 Avail: NTIS HC A22/MF A01 CSCL 21E

N78-23068* National Aeronautics and Space Administration, Lewis Research Center, Cleveland, Ohio.
SUPERSONIC THROUGH-FLOW FAN ENGINES FOR SUPERSONIC CRUISE AIRCRAFT
 Leo C. Franciscus Apr. 1978 53 p refs
 (NASA-TM-78889; E-9626) Avail: NTIS HC A04/MF A01 CSCL 21E

Engine performance, weight and mission studies were carried out for supersonic through flow fan engine concepts. The mission used was a Mach 2.32 cruise mission. The advantages of supersonic through flow fan engines were evaluated in terms of mission range comparisons between the supersonic through flow fan engines and a more conventional turbofan engine. The specific fuel consumption of the supersonic through flow fan engines was 12 percent lower than the more conventional turbofan. The aircraft mission range was increased by 20 percent with the supersonic fan engines compared to the conventional turbofan. Author

N78-23095* National Aeronautics and Space Administration, Lewis Research Center, Cleveland, Ohio.
ALTITUDE CALIBRATION OF AN F100, S/N P680063, TURBOFAN ENGINE
 Thomas J. Biesiadny, Douglas Lee, and Jose R. Rodriguez May 1978 23 p refs
 (NASA-TP-1228; E-9355) Avail: NTIS HC A02/MF A01 CSCL 21E

An airflow and thrust calibration of an F100 engine was conducted in coordination with a flight test program to study airframe-propulsion system integration characteristics of turbofan-powered high-performance aircraft. The tests were conducted with and without augmentation for a variety of simulated flight conditions with emphasis on the transonic regime. Test results for all conditions are presented in terms of corrected airflow and corrected gross thrust as functions of corrected fan speed for nonaugmented power and an augmented thrust ratio as a function of fuel-air ratio for augmented power. Comparisons of measured and predicted data are presented along with the results of an uncertainty analysis for both corrected airflow and gross thrust. Author

N78-25089* National Aeronautics and Space Administration, Lewis Research Center, Cleveland, Ohio.
GAS TURBINE ENGINE WITH RECIRCULATING BLEED Patent
 Arthur P. Adamson, inventor (to NASA) (GE, Cincinnati, Ohio) Issued 11 Apr. 1978 5 p Filed 14 Jun. 1976 Sponsored by NASA
 (NASA-Case-LEW-12452-1; US Patent-4,083,181; US Patent-Appl-SN-695513; US Patent-Class-60-39,52; US Patent-Class-60-226R) Avail: US Patent Office CSCL 21E

Carbon monoxide and unburned hydrocarbon emissions in a gas turbine engine are reduced by bleeding hot air from the

engine cycle and introducing it back into the engine upstream of the bleed location and upstream of the combustor inlet. As this hot inlet air is recycled, the combustor inlet temperature rises rapidly at a constant engine thrust level. In most combustors, this will reduce carbon monoxide and unburned hydrocarbon emissions significantly. The preferred locations for hot air extraction are at the compressor discharge or from within the turbine, whereas the preferred reentry location is at the compressor inlet.

Official Gazette of the U.S. Patent Office

N78-26090* National Aeronautics and Space Administration, Lewis Research Center, Cleveland, Ohio.
COUNTER PUMPING DEBRIS EXCLUDER AND SEPARATOR Patent

Lawrence P. Ludwig, inventor (to NASA) Issued 18 Apr. 1978 5 p Filed 31 Mar. 1976 Supersedes N78-20487 (14 - 11, p 1394)

(NASA-Case-LEW-11855-1; US-Patent-4,084,825; US-Patent-Appl-SN-872222; US-Patent-Class-277-25; US-Patent-Class-277-134) Avail: US Patent Office CSCL 21E

A dirt separator and excluder for removing entrained debris from gas turbine shaft seals is described. A helical groove pattern is constructed on the rotating shaft with the pumping pattern such that it tends to pump seal pressurizing gas toward the gas turbine seal. A second helical groove pattern is provided on the stationary housing or counter rotating member coaxial with the shaft, and this pattern is designed to provide pumping in the direction opposite from that of the groove pattern on the shaft. Gas with entrained debris entering this grooved area will be subjected to high centrifugal forces due to the swirl motion induced by the groove pattern and the rotation of the shaft. This debris is centrifuged outwardly into the outer groove pattern on the housing or counter rotating member. Because the outer groove pattern has a pumping direction opposite from that of the seal, dirt is pumped away from the seal and can be collected in a suitable debris trap remote from the seal location.

Official Gazette of the U.S. Patent Office

N78-26143* National Aeronautics and Space Administration, Lewis Research Center, Cleveland, Ohio.
COMBUSTOR CONCEPTS FOR AIRCRAFT GAS TURBINE LOW-POWER EMISSIONS REDUCTION

E. J. Mularz, C. C. Gleason (G.E. Co., Evandale, Ohio), and W. J. Dodds (G.E. Co., Evandale, Ohio) Jul. 1978 20 p refs Presented at the 14th Propulsion Conf., Las Vegas, Nev., 25-27 Jul. 1978; co-sponsored by the AIAA and the Soc. of Automotive Engrs.

(NASA-TM-78875; AVRADCOM-TR-78-23(PL); AIAA-Paper-78-999) Avail: NTIS HC A02/MF A01 CSCL 20E

Several combustor concepts were designed and tested to demonstrate significant reductions in aircraft engine idle pollutant emissions. Each concept used a different approach for pollutant reductions: the hot wall combustor employs a thermal barrier coating and impingement cooled liners; the recuperative cooling combustor preheats the air before entering the combustion chamber; and the catalytic converter combustor is composed of a conventional primary zone followed by a catalytic bed for pollutant cleanup. The designs are discussed in detail and test results are presented for a range of aircraft engine idle conditions. The results indicate that ultralow levels of unburned hydrocarbons and carbon monoxide emissions can be achieved.

R.R.

N78-26144* National Aeronautics and Space Administration, Lewis Research Center, Cleveland, Ohio.
END-WALL BOUNDARY LAYER PREDICTION FOR AXIAL COMPRESSORS

Peter M. Sockol 19 p refs Presented at the 11th Fluid and Plasma Dynamics Conf., Seattle, 10-12 Jul. 1978; sponsored by AIAA

(NASA-TM-78928; E-9688) Avail: NTIS HC A02/MF A01 CSCL 21E

An integral boundary layer procedure was developed for the computation of viscous and secondary flows along the annulus

walls of an axial compressor. The procedure is an outgrowth and extension of the pitch-averaged methods of Mellor and Horlock. In the present work secondary flow theory is used to develop approximations for the velocity profiles inside a rotating blade row and for the blade force deficit terms in the momentum integral equations. The computer code based on this procedure was iteratively coupled to a quasi-one-dimensional model for the external inviscid flow. Computed results are compared with measurements in a compressor cascade.

Author

N78-26145* National Aeronautics and Space Administration, Lewis Research Center, Cleveland, Ohio.
LIQUID-COOLING TECHNOLOGY FOR GAS TURBINES REVIEW AND STATUS

G. James VanFossen, Jr. (Army Res. and Technol. Labs.) and Francis S. Stepha Aug. 1978 14 p refs Proposed for presentation at the 13th Intersoc. Energy Conversion Eng. Conf., San Diego, Calif., 20-25 Aug. 1978; sponsored by the SAE, ACS, AIAA, ASME, IEEE, AICHE, and ANS (NASA-TM-78906; AVRADCOM-TR-78-28(PL); E-9517-1) Avail: NTIS HC A02/MF A01 CSCL 21E

A review of research related to liquid cooling of gas turbines was conducted and an assessment of the state of the art was made. Various methods of liquid cooling turbines were reviewed. Examples and results with test and demonstrator turbines utilizing these methods along with the advantages and disadvantages of the various methods are discussed.

B.B.

N78-26146* National Aeronautics and Space Administration, Lewis Research Center, Cleveland, Ohio.
EMITTANCE AND ABSORPTANCE OF NASA CERAMIC THERMAL BARRIER COATING SYSTEM

Curt H. Liebert Jun. 1978 31 p refs Presented in part at the Intern. Conf. on Met. Coatings, San Francisco, 3-7 Apr. 1978; sponsored by the Am. Vacuum Soc. (NASA-TP-1190; E-9474) Avail: NTIS HC A03/MF A01 CSCL 20E

Spectral emittance measurements were made on a two-layer ceramic thermal barrier coating system: consisting of a metal substrate, a NiCrAl_y bond coating and a yttria-stabilized zirconia ceramic coating. Spectral emittance data were obtained for the coating system at temperatures of 300 to 1590 K, ceramic thickness of zero to 0.076 centimeter, and wavelengths of 0.4 to 14.6 micrometers. The data were transformed into total hemispherical emittance values and correlated with respect to ceramic coating thickness and temperature using multiple regression curve fitting techniques. The results show that the ceramic thermal barrier coating system is highly reflective and significantly reduces radiation heat loads on cooled gas turbine engine components. Calculation of the radiant heat transfer within the nonisothermal, translucent ceramic coating material shows that the gas-side ceramic coating surface temperature can be used in heat transfer analysis of radiation heat loads on the coating system.

Author

N78-27122* National Aeronautics and Space Administration, Lewis Research Center, Cleveland, Ohio.
SUPERCRITICAL FUEL INJECTION SYSTEM Patent Application

C. J. Marek and L. P. Cooper, inventors (to NASA) Filed 19 Jun. 1978 10 p (NASA-Case-LEW-12990-1; US-Patent-Appl-SN-916654) Avail: NTIS HC A02/MF/A01 CSCL 21E

A fuel injection system for gas turbines or the like which includes a pair of high pressure pumps which provide fuel and a carrier fluid such as air at pressures above the critical pressure of the fuel was developed. A supercritical mixing chamber mixes the fuel and carrier fluid and the mixture is sprayed into a combustion chamber for burning therein. The use of fuel and a carrier fluid at supercritical pressures promotes rapid mixing of the fuel in the combustion chamber so as to reduce the formation of pollutants and promote cleaner burning.

NASA

N78-27126* National Aeronautics and Space Administration, Lewis Research Center, Cleveland, Ohio.

INLET-ENGINE MATCHING FOR SCAR INCLUDING APPLICATION OF A BICONE VARIABLE GEOMETRY INLET

Joseph F. Wasserbauer and William H. Gerstenmaier 1978 23 p refs Presented at the 14th Propulsion Conf., Las Vegas, Nev. 25-27 Jul. 1978; cosponsored by the AIAA and the SAE Engr (NASA-TM-78955; E-9706) Avail: NTIS HC A02/MF A01 CSCL 21E

Airflow characteristics of variable cycle engines (VCE) designed for Mach 2.32 can have transonic airflow requirements as high as 1.6 times the cruise airflow. This is a formidable requirement for conventional, high performance, axisymmetric, translating centerbody mixed compression inlets. An alternate inlet is defined, where the second cone of a two cone center body collapses to the initial cone angle to provide a large off-design airflow capability, and incorporates modest centerbody translation to minimize spillage drag. Estimates of transonic spillage drag are competitive with those of conventional translating centerbody inlets. The inlet's cruise performance exhibits very low bleed requirements with good recovery and high angle of attack capability. Author

N78-27126* National Aeronautics and Space Administration, Lewis Research Center, Cleveland, Ohio.

A COMPUTER PROGRAM FOR FULL-COVERAGE FILM-COOLED BLADING ANALYSIS INCLUDING THE EFFECTS OF A THERMAL BARRIER COATING

Jun 1978 11 p refs To be presented at the Winter Ann. Meeting of ASME, San Francisco, 10-15 Dec. 1978 (NASA-TM-78951; AVRADCOM-TR-78-31(PL); E-9696) Avail: NTIS HC A02/MF A01 CSCL 21E

The program input, coolant flow and heat transfer model, and the program output are discussed. As an example, sections of the suction and pressure sides of a high temperature, high pressure turbine vane are analyzed to show the effects of a thermal barrier coating. Compared to the uncoated design, the coating halves the required coolant flow, while simultaneously reducing metal outer temperatures by over 111 K. Author

N78-27127* National Aeronautics and Space Administration, Lewis Research Center, Cleveland, Ohio.

FUEL COMPENSATIVE AIRCRAFT ENGINE TECHNOLOGY

Donald L. Nelson 1978 39 p refs Proposed for presentation at 11th Cong. of the Intern. Council of Aeronautical Sci., Lisbon, Portugal, 10-16 Sep. 1978; sponsored by AIAA (NASA-TM-78962; E-9719) Avail: NTIS HC A03/MF A01 CSCL 21E

Technology developments for more fuel-efficient subsonic transport aircraft are reported. Three major propulsion projects were considered: (1) engine component improvement - directed at current engines; (2) energy efficient engine - directed at new turbofan engines; and (3) advanced turboprops - directed at technology for advanced turboprop powered aircraft. Each project is reviewed and some of the technologies and recent accomplishments are described. G.G.

N78-27130* National Aeronautics and Space Administration, Lewis Research Center, Cleveland, Ohio.

REVERSE-FLOW COMBUSTOR FOR SMALL GAS TURBINES WITH PRESSURE-ATOMIZING FUEL INJECTORS

Carl T. Norgrin, Edward J. Mularz (AVRADCOM Res and Technol Labs), and Stephen M. Riddlebaugh Aug. 1978 30 p refs (NASA-TP-1260; AVRADCOM-TR-78-22(PL); E-9458) Avail: NTIS HC A03/MF A01 CSCL 21E

A reverse flow combustor suitable for a small gas turbine (2 to 3 kg/s mass flow) was used to evaluate the effect of pressure atomizing fuel injectors on combustor performance. In these tests an experimental combustor was designed to operate with 18 simplex pressure atomizing fuel injectors at sea level takeoff conditions. To improve performance at low power

conditions, fuel was redistributed so that only every other injector was operational. Combustor performance, emissions, and liner temperature were compared over a range of pressure and inlet air temperatures corresponding to simulated idle, cruise, and takeoff conditions typical of a 16 to 1 pressure ratio turbine engine. B.B.

N78-28088* National Aeronautics and Space Administration, Lewis Research Center, Cleveland, Ohio.

FORTAN PROGRAM FOR CALCULATING COOLANT FLOW AND METAL TEMPERATURES OF A FULL-COVERAGE FILM-COOLED VANE OR BLADE

Peter L. Meitner (AVRADCOM R and T Labs., Cleveland) Jul. 1978 92 p refs (NASA-TP-1259; E-9491; AVRADCOM-TR-78-19(PL)) Avail: NTIS HC A05/MF A01 CSCL 21E

A computer program that calculates the coolant flow and the metal temperatures of a full-coverage-film-cooled vane or blade was developed. The analysis was based on compressible, one-dimensional fluid flow and on one-dimensional heat transfer and treats the vane or blade shell as a porous wall. The calculated temperatures are average values for the shell outer-surface area associated with each film-cooling hole row. A thermal-barrier coating may be specified on the shell outer surface, and centrifugal effects can be included for blade calculations. The program is written in FORTRAN 4 and is operational on a UNIVAC 1100/42 computer. The method of analysis, the program input, the program output, and two sample problems are provided. G.G.

N78-28100* National Aeronautics and Space Administration, Lewis Research Center, Cleveland, Ohio.

EFFECT OF AIR TEMPERATURE AND RELATIVE HUMIDITY AT VARIOUS FUEL-AIR RATIOS ON EXHAUST EMISSIONS ON A PER-MODE BASIS OF AN AVCO LYCOMING O-320 DIAD LIGHT AIRCRAFT ENGINE: VOLUME 1: RESULTS AND PLOTTED DATA

Michael Skorobetsky, Donald V. Cosgrove, Phillip R. Meng, and Erwin E. Kempf, Jr. Jul. 1978 109 p refs (NASA-TM-73507-Vol.1; E-8916-2) Avail: NTIS HC E08/MF A01 CSCL 21E

A carbureted four cylinder air cooled O-320 DIAD Lycoming aircraft engine was tested to establish the effects of air temperature and humidity at various fuel-air ratios on the exhaust emissions on a per-mode basis. The test conditions include carburetor lean out at air temperatures of 50, 59, 80, and 100 F at relative humidities of 0, 30, 60, and 80 percent. Temperature humidity effects at the higher values of air temperature and relative humidity tested indicated that the HC and CO emissions increased significantly, while the NOx emissions decreased. Even at a fixed fuel air ratio, the HC emissions increase and the NOx emissions decrease at the higher values of air temperature and humidity. B.B.

N78-31103* National Aeronautics and Space Administration, Lewis Research Center, Cleveland, Ohio.

GAS PATH SEAL Patent Application

Robert C. Bill and Lawrence P. Ludwig, inventors (to NASA) Filed 4 Aug. 1978 9 p (NASA-Case-Law-12131-2; US-Patent-Appi-SN-931090) Avail: NTIS HC A02/MF A01 CSCL 21E

A gas path seal for a turbine engine or compressor is provided. The gas path seal comprises a shroud of material wearable or abradable relative to the material of the turbine or compressor blades and closely spaced from the blade tips. A compliant backing, preferably of several layers of corrugated metal or a compliant material covered with a thin layer of ductile material, is provided about the shroud, and a rigid mounting surrounds the compliant backing. The novel feature is a compliant backing between the shroud and mounting. As a result normal forces during a blade rub are limited and wear is reduced and the life of the shroud is lengthened for a design of comparable clearance of blade to shroud. NASA

N78-31100* National Aeronautics and Space Administration, Lewis Research Center, Cleveland, Ohio.

ANALYSIS OF METAL TEMPERATURE AND COOLANT FLOW WITH A THERMAL-BARRIER COATING ON A FULL-COVERAGE-FILM-COOLED TURBINE VANE

Peter L. Meitner (AVRADCOM Res. and Technol. Labs.) Aug. 1978 15 p refs
(NASA-TP-1310; AVRADCOM-TR-78-20; Avail: NTIS HC A02/MF A01 CSCL 21E

The potential benefits of combining full-coverage film cooling with a thermal-barrier coating were investigated analytically for sections on the suction and pressure sides a high-temperature, high-pressure turbine vane. Metal and ceramic coating temperatures were calculated as a function of coating thickness and coolant flow. With a thermal-barrier coating, the coolant flows required for the chosen sections were half those of an uncoated design, and the metal outer temperatures were simultaneously reduced by over 111 K (200 F). For comparison, transpiration cooling was also investigated. Full-coverage film cooling of a coated vane required more coolant flow than did transpiration cooling. Author

N78-31101* National Aeronautics and Space Administration, Lewis Research Center, Cleveland, Ohio.

REDUNDANT DISC Patent

William N. Barack (GE, Cincinnati), Paul A. Domes (GE, Cincinnati), and Stephen W. Beakman, inventors (to NASA) (GE, Cincinnati) Issued 27 Jun. 1978 7 p Filed 22 Mar. 1976 Sponsored by NASA

(NASA-Case-LEW-12496-1; US-Patent-4,097,194; US-Patent-Appl-SN-668971; US-Patent-Class-416-244A; US-Patent-Class-416-214A; US-Patent-Class-74-572; US-Patent-Class-29-463) Avail: US Patent Office CSCL 21E

A rotatable disc is described that consists of parallel plates tightly joined together for rotation about a hub. Each plate is provided with several angularly projecting spaced lands. The lands of each plate are interposed in alternating relationship between the lands of the next adjacent plate. In this manner, circumferential displacement of adjacent sectors in any one plate is prevented in the event that a crack develops. Each plate is redundantly sized so that, in event of structural failure of one plate, the remaining plates support a proportionate share of the load of the failed plate. The plates are prevented from separating laterally through the inclusion of generally radially extending splines which are inserted to interlock cooperating, circumferentially adjacent lands. Official Gazette of the U.S. Patent Office

N78-33102* National Aeronautics and Space Administration, Lewis Research Center, Cleveland, Ohio.

RESULTS AND STATUS OF THE NASA AIRCRAFT ENGINE EMISSION REDUCTION TECHNOLOGY PROGRAMS

R. E. Jones, L. A. Diehl, D. A. Petresh, and J. Grobman Oct. 1978 53 p refs
(NASA-TM-79009; E-9793) Avail: NTIS HC A04/MF A01 CSCL 21E

The results of an aircraft engine emission reduction study are reviewed in detail. The capability of combustor concepts to produce significantly lower levels of exhaust emissions than present production combustors was evaluated. The development status of each combustor concept is discussed relative to its potential for implementation in aircraft engines. Also, the ability of these combustor concepts to achieve proposed NME and NCE EPA standards is discussed. B.B.

N78-33107* National Aeronautics and Space Administration, Lewis Research Center, Cleveland, Ohio

PERFORMANCE OF A TRANSONIC FAN STAGE DESIGNED FOR A LOW MERIDIONAL VELOCITY RATIO

Royce D. Moore, George W. Lewis, Jr., and Walter M. Osborn Nov. 1978 83 p refs
(NASA-TP-1298; E-8994) Avail: NTIS HC A05/MF A01 CSCL 21E

The aerodynamic performance and design parameters of a transonic fan stage are presented. The fan stage was designed for a meridional velocity ratio of 0.8 across the tip of the stage,

a pressure ratio of 1.57, a flow of 29.5 kilograms per second, and a tip speed of 426 meters per second. Radial surveys were obtained over the stable operating range from 60 to 100 percent of design speed. The measured, peak efficiency (0.81) of the stage occurred at a pressure ratio of 1.58 and a flow of 28.7 kilograms per second. L.S.

N78-33108* National Aeronautics and Space Administration, Lewis Research Center, Cleveland, Ohio.

DESIGN AND OVERALL PERFORMANCE OF FOUR HIGHLY LOADED, HIGH SPEED INLET STAGES FOR AN ADVANCED HIGH-PRESSURE-RATIO CORE COMPRESSOR

Lonnice Reid and Royce D. Moore Oct. 1978 122 p refs
(NASA-TP-1337; E-9302) Avail: NTIS HC A06/MF A01 CSCL 21E

The detailed design and overall performances of four inlet stages for an advanced core compressor are presented. These four stages represent two levels of design total pressure ratio (1.82 and 2.05), two levels of rotor aspect ratio (1.19 and 1.63), and two levels of stator aspect ratio (1.26 and 1.78). The individual stages were tested over the stable operating flow range at 70, 90, and 100 percent of design speeds. The performances of the low aspect ratio configurations were substantially better than those of the high aspect ratio configurations. The two low aspect ratio configurations achieved peak efficiencies of 0.876 and 0.872 and corresponding stage efficiencies of 0.845 and 0.840. The high aspect ratio configurations achieved peak ratio efficiencies of 0.851 and 0.849 and corresponding stage efficiencies of 0.821 and 0.831. Author

N78-33109* National Aeronautics and Space Administration, Lewis Research Center, Cleveland, Ohio.

DESIGN AND PERFORMANCE OF A 427-METER-PER-SECOND-TIP-SPEED TWO-STAGE FAN HAVING A 2.40 PRESSURE RATIO

Walter S. Cunnan, William Stevens, and Donald C. Ursek Oct. 1978 96 p refs
(NASA-TP-1314; E-9005) Avail: NTIS HC A05/MF A01 CSCL 21E

The aerodynamic design and the overall and blade-element performances are presented of a 427-meter-per-second-tip-speed two-stage fan designed with axially spaced blade rows to reduce noise transmitted upstream of the fan. At design speed the highest recorded adiabatic efficiency was 0.796 at a pressure of 2.30. Peak efficiency was not established at design speed because of a damper failure which terminated testing prematurely. The overall efficiencies, at 60 and 80 percent of design speed, peaked at approximately 0.83. Author

N78-33110* National Aeronautics and Space Administration, Lewis Research Center, Cleveland, Ohio.

DYGABCD: A PROGRAM FOR CALCULATING LINEAR A, B, C, AND D MATRICES FROM A NONLINEAR DYNAMIC ENGINE SIMULATION

Lucille C. Geyser Sep. 1978 203 p refs
(NASA-TP-1295; E-9464) Avail: NTIS HC A10/MF A01 CSCL 21E

A digital computer program, DYGABCD, was developed that generates linearized, dynamic models of simulated turbofan and turbojet engines. DYGABCD is based on an earlier computer program, DYNGEN, that is capable of calculating simulated nonlinear steady-state and transient performance of one and two-spool turbojet engines or two- and three-spool turbofan engines. Most control design techniques require linear system descriptions. For multiple-input/multiple-output systems such as turbine engines, state space matrix descriptions of the system are often desirable. DYGABCD computes the state space matrices commonly referred to as the A, B, C, and D matrices required for a linear system description. The report discusses the analytical approach and provides a users manual, FORTRAN listings, and a sample case. L.S.

A78-20851 * # A review of NASA's propulsion programs for civil aviation. W. L. Stewart (NASA, Lewis Research Center, Cleveland, Ohio), H. W. Johnson (NASA, Aeronautical Propulsion Div., Washington, D.C.), and R. J. Weber (NASA, Lewis Research Center, Mission Analysis Branch, Cleveland, Ohio). *American Institute of Aeronautics and Astronautics, Aerospace Sciences Meeting, 16th, Huntsville, Ala., Jan. 16-18, 1978, Paper 78-43*. 14 p. 19 refs.

Five NASA engine-oriented propulsion programs of major importance to civil aviation are presented and discussed. Included are programs directed at exploring propulsion-system concepts for (1) energy-conservative subsonic aircraft (improved current turbofans, advanced turbofans, and advanced turboprops), (2) supersonic cruise aircraft (variable-cycle engines), (3) general aviation aircraft (improved reciprocating engines and small gas turbines), (4) powered-lift aircraft (advanced turbofans), and (5) advanced rotorcraft. These programs reflect the opportunities still existing for significant improvements in civil aviation through the application of advanced propulsion concepts. (Author)

A78-23840 * Preliminary QCSEE program - Test results. C. C. Ciepluch (NASA, Lewis Research Center, Cleveland, Ohio). *Society of Automotive Engineers, Aerospace Meeting, Los Angeles, Calif., Nov. 14-17, 1977, Paper 771008*. 11 p.

Preliminary results are reported for the Quiet Clean Short-haul Experimental Engine (QCSEE) program initiated by NASA in 1974 to develop propulsion system technology suitable for powered-lift short-range commercial aircraft. The QCSEE technology also has applications to the proposed U.S. Navy V/STOL aircraft. Emphasis in the QCSEE program is placed on developing engines with low noise characteristics; in addition, the power plants are required to conform to EPA 1979 pollutant emissions standards. Thrust performance, fan design, and thrust/weight ratio are discussed for both the over-the-wing and under-the-wing engine configurations under study. J.M.B.

A78-23891 * The application of the Routh approximation method to turbofan engine models. W. C. Merrill (NASA, Lewis Research Center, Cleveland, Ohio). In: Joint Automatic Control Conference, San Francisco, Calif., June 22-24, 1977 Proceedings. Volume 2. (A78-23851 08-63) New York, Institute of Electrical and Electronics Engineers, Inc., 1977, p. 1019-1028. 9 refs.

The Routh approximation technique is applied in the frequency domain to a 16th order state variable turbofan engine model. The results obtained motivate the extension of the frequency domain formulation of the Routh method to the time domain to handle the state variable formulation directly. The time domain formulation is derived and a new characterization, which specifies all possible Routh similarity transformations, is given. This characterization is computed by the solution of two eigenvalue-eigenvector problems. The application of the time domain Routh technique to the state variable engine model is described and some results are given. Additional computational problems are discussed including an optimization procedure which can improve the approximation accuracy by taking advantage of the transformation characterization. (Author)

A78-23892 * Minimum-time acceleration of aircraft turbofan engines. F. Teron (NASA, Lewis Research Center, Cleveland, Ohio). In: Joint Automatic Control Conference, San Francisco, Calif., June 22-24, 1977, Proceedings. Volume 2. (A78-23851 08-63) New York, Institute of Electrical and Electronics Engineers, Inc., 1977, p. 1029-1037. 12 refs.

Minimum-time accelerations of the F100 turbofan engine are presented. A piecewise-linear engine model, having three state variables and four control variables, is used to obtain the minimum-time solutions. The linear model which applies at a given time in the trajectory is determined by calculating a normalized 'distance' from

the current state to the equilibrium state associated with each linear model. The linear model associated with the closest equilibrium point is then used. The control histories for the minimum-time solutions are used as input to a nonlinear simulation of the F100 engine to verify the accuracy of the piecewise-linear solutions.

(Author)

A78-23907 * Design of turbofan engine controls using output feedback regulator theory. W. C. Merrill (NASA, Lewis Research Center, Cleveland, Ohio). In: Joint Automatic Control Conference, San Francisco, Calif., June 22-24, 1977, Proceedings. Volume 2. (A78-23851 08-63) New York, Institute of Electrical and Electronics Engineers, Inc., 1977, p. 1504-1509. 9 refs.

A multivariable control design procedure based on output feedback regulator (OFR) theory is applied to the F100 turbofan engine. Results for the OFR design are compared to a design based on linear quadratic regulator (LQR) theory. This LQR design was obtained as part of the F100 Multivariable Control Synthesis (MVCS) program. In the MVCS program the LQR feedback control was designed in a reduced dimension state space and then applied to the original system. However, the OFR feedback control is designed in the full order state space and thus eliminates any need for model reduction techniques. Using the performance measure and control structure of the MVCS program LQR design, an equivalent OFR feedback control is obtained. The flexibility of the OFR as a control design procedure is demonstrated and differing feedback control structures are evaluated. (Author)

A78-24877 * # Noise of deflectors used for flow attachment with STOL-OTW configurations. U. von Glahn and D. Groesbeck (NASA, Lewis Research Center, Cleveland, Ohio). *Acoustical Society of America, Meeting, 94th, Miami Beach, Fla., Dec. 13-16, 1977, Paper*. 16 p.

Future STOL aircraft may utilize engine-over-the-wing (OTW) installations in which the exhaust nozzles are located above and separated from the upper surface of the wing. An external jet-flux deflector can be used with such installations to provide flow attachment to the wing/flap surfaces for lift augmentation. In the present work, the deflector noise in the flyover plane measured with several model-scale nozzle/deflector/wing configurations is examined. The deflector-associated noise is correlated in terms of velocity and geometry parameters. The data also indicate that the effective overall sound pressure level of the deflector-associated noise peaks in the forward quadrant near 40 deg from the inlet axis. (Author)

A78-24878 * # Combustor fluctuating pressure measurements in-engine and in a component test facility - A preliminary comparison. M. Reshko and A. Karchmer (NASA, Lewis Research Center, Cleveland, Ohio). *Acoustical Society of America, Meeting, 94th, Miami Beach, Fla., Dec. 13-16, 1977, Paper*. 18 p. 5 refs.

Combustor internal fluctuating pressure and far-field noise generated in a YF-102 turbofan engine are investigated; combustor internal measurements are also made in a duct-component test facility operating over a range of conditions encompassing those characteristic of the aircraft engine. Although directly measured spectra for the engine and the duct-component test facility show discrepancies, the results of coherence function, transfer function and phase relationship comparisons suggest that the internal dynamics of the combustor as an acoustic source may be preserved in a component test facility. J.M.B.

A78-24179 * # An empirical model for inverted-velocity profile jet noise prediction. J. R. Stone (NASA, Lewis Research Center, Cleveland, Ohio). *Acoustical Society of America, Meeting, 94th, Miami Beach, Fla., Dec. 13-16, 1977, Paper*. 28 p. 12 refs.

It is known that the noise generated by inverted-velocity-profile coaxial (without center plug) and coannular (with center plug) nozzles should be modeled as the combined contributions of various

source regions and noise generation mechanisms. In this paper, an empirical noise-prediction model is described which considers the noise generated by two jet-mixing regions and two potential regions of shock/turbulence interaction. Results calculated from the empirical model are compared with model-scale experimental data for static and simulated flight conditions. These comparisons are made for cases where both streams are subsonic, where the outer stream is supersonic with the inner stream subsonic, and where both streams are supersonic. The cases considered cover a range of inner-to-outer-stream area ratios and include both coaxial and coannular nozzles. It is shown that the model gives reasonable predictions of absolute noise spectra and even better predictions of incremental changes.

S.D.

A78-24880 * # Effectiveness of an inlet flow turbulence control device to simulate flight fan noise in an anechoic chamber. R. P. Woodward, J. A. Wazyaniak, L. M. Shaw, and M. J. MacKinnon (NASA, Lewis Research Center, Cleveland, Ohio). *Acoustical Society of America, Meeting, 94th, Miami Beach, Fla., Dec. 13-16, 1977, Paper. 21 p.* 13 refs.

A hemispherical inlet flow control device was tested on a 50.8 cm. (20-inch) diameter fan stage in the NASA-Lewis Anechoic Chamber. The control device used honeycomb and wire mesh to reduce turbulence intensities entering the fan. Far field acoustic power level results showed about a 5 dB reduction in blade passing tone and about 10 dB reduction in multiple pure tone sound power at 90% design fan speed with the inlet device in place. Hot film cross probes were inserted in the inlet to obtain data for two components of the turbulence at 65 and 90% design fan speed. Without the flow control device the axial intensities were below 1.0%, while the circumferential intensities were almost twice this value. The inflow control device significantly reduced the circumferential turbulence intensities and also reduced the axial length scale. (Author)

A78-24898 * # Output feedback regulator design for jet engine control systems. W. Merrill (NASA, Lewis Research Center, Cleveland, Ohio). *National Electronics Conference, Chicago, Ill., Oct. 13, 14, 1977, Paper. 13 p.* 6 refs.

A multivariable control design procedure based on the output feedback regulator formulation is described and applied to an F100 turbofan engine model. Full order model dynamics are incorporated in the example design. The effect of actuator dynamics on closed loop performance is investigated. Also, the importance of turbine inlet temperature as an element of the dynamic feedback is studied. Step responses are given to indicate the improvement in system performance with this control. Calculation times for all experiments are given in CPU seconds for comparison purposes. (Author)

A78-29330 * # General aviation energy-conservation research programs at NASA-Lewis Research Center. E. A. Willis (NASA, Lewis Research Center, Cleveland, Ohio). *Western Michigan University, Conference on Energy Conservation in General Aviation, Kalamazoo, Mich., Oct. 10, 11, 1977, Paper. 23 p.* 14 refs.

A review is presented of non-turbine general aviation engine programs underway at the NASA-Lewis Research Center in Cleveland, Ohio. The program encompasses conventional, lightweight diesel and rotary engines. Its three major thrusts are, in order of priority: (1) reduced SFCs; (2) improved fuels tolerance; and (3) reducing emissions. Current and planned future programs in such areas as lean operation, improved fuel management, advanced cooling techniques and advanced engine concepts, are described. These are expected to lay the technology base, by the mid to latter 1980s, for engines whose total fuel costs are as much as 30% lower than today's conventional engines. (Author)

A78-33111 * # Effect of airstream velocity on mean drop diameters of water sprays produced by pressure and air atomizing nozzles. R. D. Ingebo (NASA, Lewis Research Center, Cleveland, Ohio). In: *Gas turbine combustion and fuels technology: Proceedings of the Winter Annual Meeting, Atlanta, Ga., November 27-December 2, 1977. (A78-33108 13-31)* New York, American Society of Mechanical Engineers, 1977, p. 31-35. 6 refs.

A scanning radiometer was used to determine the effect of airstream velocity on the mean drop diameter of water sprays produced by pressure atomizing and air atomizing fuel nozzles used in previous combustion studies. Increasing airstream velocity from 23 to 53.4 meters per second reduced the Sauter mean diameter by approximately 50 percent with both types of fuel nozzles. The use of a sonic cup attached to the tip of an air assist nozzle reduced the Sauter mean diameter by approximately 40 percent. Test conditions included airstream velocities of 23 to 53.4 meters per second at 293 K and atmospheric pressure. (Author)

A78-33218 * # Gas path sealing in turbine engines. L. P. Ludwig (NASA, Lewis Research Center, Cleveland, Ohio). *NATO, AGARD, Power, Energetics, and Propulsion Panel Meeting on Seal Technology in Gas Turbine Engines, London, England, Apr. 6, 7, 1973, Paper. 45 p.* 54 refs.

Survey of gas path seals is presented with particular attention given to sealing clearance effects on engine component efficiency. The effects on compressor pressure ratio and stall margin are pointed out. Various case-rotor relative displacements, which affect gas path seal clearances, are identified. Forces produced by nonuniform sealing clearances and their effect on rotor stability are discussed qualitatively, and recent work on turbine-blade-tip sealing for high temperatures is described. The need for active clearance control and for engine structural analysis is discussed. The functions of the internal-flow system and its seals are reviewed. (Author)

A78-33355 * # State-of-the-art of turbofan engine noise control. W. L. Jones and J. F. Groeneweg (NASA, Lewis Research Center, Cleveland, Ohio). In: *NOISE-CON 77; Proceedings of the National Conference on Noise Control Engineering, Hampton, Va., October 17-19, 1977. (A78-35651 14-01)* New York, Noise Control Foundation, 1977, p. 361-380. 22 refs.

A description is presented of some of the recent advances in the technology of turbofan engine noise reduction, taking into account turbomachinery noise sources, new fans for low noise, fan and core noise suppression, and a new program for improving static noise testing of fans and engines. The problem of jet noise has been substantially reduced in connection with the lower jet velocities employed in the case of the high bypass turbofan engines. The dominant noise sources are now related to the turbomachinery with the fan stage, the compressor, and the turbine. Since the fan stage is the primary source of turbomachinery noise, it has been considered in a major part of the investigations designed to reduce turbofan engine noise. G.R.

A78-37683 * # On the use of relative velocity exponents for jet engine exhaust noise. J. R. Stone (NASA, Lewis Research Center, Cleveland, Ohio). *Acoustical Society of America, Meeting, 95th, Providence, R.I., May 16-19, 1978, Paper. 16 p.* 14 refs.

The effect of flight on jet engine exhaust noise has often been presented in terms of a relative velocity exponent n , as a function of radiation angle. The value of n is given by the OASPL reduction due to relative velocity divided by 10 times the logarithm of the ratio of relative jet velocity to absolute jet velocity. It is shown in this paper that the exponent n is positive for pure subsonic jet mixing noise and varies, in a systematic manner, as a function of flight conditions and jet velocity. On the basis of calculations from simple empirical models for jet mixing noise, shock noise and internally-generated noise, it is shown that when other sources are present, the resulting range of n is increased over the range for jet mixing noise, and in some cases negative values of n are obtained. (Author)

A78-43380 * # Propulsion. D. L. Nored (NASA, Lewis Research Center, Energy Conservative Engines Office, Cleveland, Ohio). *Aeronautics and Astronautics*, vol. 16, July-Aug. 1978, p. 47-54, 119. 14 refs.

NASA aims at developing propulsion technology to reduce the fuel consumption of present engines by 8%, that of new engines of the late 1980s by at least 12%, and that of an advanced early 1990s turboprop by an additional 16%. This paper reviews three separate NASA programs which take up these aims. They are, respectively, Engine Component Improvement, Energy Efficient Engine, and Advanced Turboprops. B.J.

A78-43504 * # Design approaches to more energy efficient engines. N. T. Saunders, R. S. Colladay, and L. E. Maciocci (NASA, Lewis Research Center, Cleveland, Ohio). *American Institute of Aeronautics and Astronautics and Society of Automotive Engineers, Joint Propulsion Conference, 14th, Las Vegas, Nev., July 25-27, 1978, AIAA Paper 78-937*. 10 p. 5 refs.

In 1976 NASA initiated the Aircraft Energy Efficiency (ACEE) Program to assist in the development of technology for more fuel-efficient aircraft for commercial airline use. The Energy Efficient Engine (EEE) Project of the ACEE program is intended to lay the advanced-technology foundation for a new generation of turbofan engine. This project, planned as a seven-year cooperative government-industry effort, is aimed at developing and demonstrating advanced component and systems technologies for engines that could be introduced into airline service by the late 1980s or early 1990s. In addition to fuel savings, new engines must offer potential for being economically attractive to the airline users and environmentally acceptable. A description is presented of conceptual energy-efficient engine designs which offer potential for achieving all of the goals established for the EEE Project. G.R.

A78-43505 * # General aviation internal combustion engine research programs at NASA-Lewis Research Center. E. A. Willis (NASA, Lewis Research Center, Cleveland, Ohio). *American Institute of Aeronautics and Astronautics and Society of Automotive Engineers, Joint Propulsion Conference, 14th, Las Vegas, Nev., July 25-27, 1978, AIAA Paper 78-932*. 15 p. 17 refs.

An update is presented of non-turbine general aviation engine programs underway at the NASA-Lewis Research Center in Cleveland, Ohio. The program encompasses conventional, lightweight diesel and rotary engines. Its three major thrusts are: (a) reduced SFC's; (b) improved fuels tolerance; and (c) reducing emissions. Current and planned future programs in such areas as lean operation, improved fuel management, advanced cooling techniques and advanced engine concepts, are described. These are expected to lay the technology base, by the mid to late 1980's, for engines whose life cycle fuel costs are 30 to 50% lower than today's conventional

A78-43544 * # Design and preliminary results of a semi-transpiration cooled [Lamilloy] liner for a high-pressure high-temperature combustor. J. D. Wear, A. M. Trout, J. M. Smith, and R. E. Jones (NASA, Lewis Research Center, Cleveland, Ohio). *American Institute of Aeronautics and Astronautics and Society of Automotive Engineers, Joint Propulsion Conference, 14th, Las Vegas, Nev., July 25-27, 1978, AIAA Paper 78-997*. 8 p. 5 refs.

A Lamilloy combustor liner has been designed, fabricated and tested in a combustor at pressures up to 8 atmospheres. The liner was fabricated of a three layer Lamilloy structure and designed to replace a conventional step-louver liner. The liner will be used in a combustor that provides hot gases to a turbine cooling test facility at pressures up to 40 atmospheres. The Lamilloy liner was tested extensively at lower pressures and demonstrated lower metal temperatures than the conventional liner, while at the same time requiring about 40 percent less cooling air flow. Tests conducted at combustor exit temperatures in excess of 2200 K have not indicated any cooling or durability problems with the Lamilloy liner. (Author)

A78-43218 * # Combustor concepts for aircraft gas turbine low-power emissions reduction. E. J. Mularz (NASA, Lewis Research Center; U.S. Army, Air Mobility Research and Development Laboratory, Cleveland, Ohio), C. C. Gleason, and W. J. Dodds (NASA, Lewis Research Center, Cleveland; General Electric Co., Evendale, Ohio). *American Institute of Aeronautics and Astronautics and Society of Automotive Engineers, Joint Propulsion Conference, 14th, Las Vegas, Nev., July 25-27, 1978, AIAA Paper 78-959*. 11 p. 6 refs. Contract No. NAS3-20680.

Three combustor concepts have been designed and tested to demonstrate significant reductions in aircraft engine idle pollutant emissions. Each concept used a different approach for pollutant reductions: the Hot Wall Combustor employs a thermal barrier coating and impingement cooled liners, the Recuperative Cooling Combustor preheats the air before entering the combustion chamber, and the Catalytic Converter Combustor is composed of a conventional primary zone followed by a catalytic bed for pollutant cleanup. The designs are discussed in detail and test results are presented for a range of aircraft engine idle conditions. The results indicate that ultra-low levels of unburned hydrocarbons and carbon monoxide emissions can be achieved with this technology. (Author)

A78-45098 * # NASA/General Electric Engine Component Improvement Program. A. J. Albright, D. J. Leonard (General Electric Co., Cincinnati, Ohio), and J. A. Ziemianski (NASA, Lewis Research Center, Cleveland, Ohio). *American Institute of Aeronautics and Astronautics and Society of Automotive Engineers, Joint Propulsion Conference, 14th, Las Vegas, Nev., July 25-27, 1978, AIAA Paper 78-929*. 7 p. Contracts No. NAS3-20629; No. NAS3-20631.

The Engine Component Improvement (ECI) Program has been initiated in connection with projects designed to reduce the impact of the world-wide energy crisis in the area of aviation. The two parts of the ECI program have the overall objective to identify and quantify the sources and causes of CF6 engine performance deterioration, and to reduce the fuel consumption of CF6 engines through the development and the incorporation of various performance improvement concepts. The CF6 high-bypass turbofan engine was selected as a basis for this effort, since it is expected to be a significant fuel user in commercial revenue service for the next 15 to 20 years. The first part of the ECI program represents the initial step in an effort to achieve a goal of five percent reduction in fuel usage for CF6 engines in the 1979-82 time period. The first performance improvement concept selected is an improved efficiency fan blade. Other improvements are related to a short core exhaust system and an improved high pressure turbine. G.R.

A78-48452 * # NASA engine system technology programs - An overview. H. W. Johnson (NASA, Aeronautical Propulsion Div., Washington, D.C.) and E. W. Conrad (NASA, Lewis Research Center, Energy Conservation Engines Office, Cleveland, Ohio). *American Institute of Aeronautics and Astronautics and Society of Automotive Engineers, Joint Propulsion Conference, 14th, Las Vegas, Nev., July 25-27, 1978, AIAA Paper 78-928*. 5 p.

The various propulsion systems technology programs are examined. The Stratospheric Cruise Emission Reduction program has the objective to explore and demonstrate advanced technology fuel preparation and combustion systems which produce very low emission levels, particularly with respect to the oxides of nitrogen, during high altitude cruising flight. Other programs considered include the Quiet, Clean, General Aviation Turbofan program, the Variable Cycle Engine Technology program, the Helicopter Transmission Technology program, the Broad Specification Fuels Technology program, the Engine Component Improvement program, the Advanced Turboprop Technology program, the Supersonic Cruise Propulsion Technology program, the Materials for Advanced Turbine Engines program, and the Aeroelasticity of Turbine Engines program. G.R.

N78-10082* TRW, Inc., Cleveland, Ohio
COST ANALYSIS OF ADVANCED TURBINE BLADE MANUFACTURING PROCESSES Final Report, Oct. 1976 - April 1977

C. F. Barth, D. E. Blake, and T. S. Stelson Oct 1977 89 p refs

(NASA-20378)
 (NASA-CR-135203) TRW-1ER-7930 Avail NTIS
 HC A06/MF A01 CSCL 21E

A rigorous analysis was conducted to estimate relative manufacturing costs for high technology gas turbine blades prepared by three candidate materials process systems. The manufacturing costs for the same turbine blade configuration of directionally solidified eutectic alloy, an oxide dispersion strengthened superalloy, and a fiber reinforced superalloy, were compared on a relative basis to the costs of the same blade currently in production utilizing the directional solidification process. An analytical process cost model was developed to quantitatively perform the cost comparisons. The impact of individual process yield factors on costs was also assessed as well as effects of process parameters, raw materials, labor rates and consumable items. Author

N78-10083* Douglas Aircraft Co., Inc., Long Beach, Calif
EFFECT OF FORWARD MOTION ON ENGINE NOISE

G. L. Blankenship, J. K. C. Low, J. A. Watkins, and J. E. Merriam Oct. 1977 198 p refs

(Contract NAS3-20031)
 (NASA-CR-134954) MDC-J7708 Avail NTIS
 HC A09/MF A01 CSCL 20A

Methods used to determine a procedure for correcting static engine data for the effects of forward motion are described. Data were analyzed from airplane flyover and static engine tests with a JT8D-109 low-bypass-ratio turbofan engine installed on a DC-9-30, with a CF6-8D high-bypass-ratio turbofan engine installed on a DC-10-10, and with a JT9D-59A high-bypass-ratio turbofan engine installed on a DC-10-40. The observed differences between the static and the flyover data bases are discussed in terms of noise generation, convective amplification, atmospheric propagation, and engine installation. The results indicate that each noise source must be adjusted separately for forward-motion and installation effects and then projected to flight conditions as a function of source-path angle, directivity angle, and acoustic range relative to the microphones on the ground. Author

N78-11082* Pratt and Whitney Aircraft Group, East Hartford, Conn. Commercial Products Div
ADVANCED SUPERSONIC PROPULSION STUDY, PHASE 4 Final Report

R. A. Howlett Sep 1977 109 p

(Contract NAS3 19540)
 (NASA-CR-135273) PWA 5547-4 Avail NTIS
 HC A06/MF A01 CSCL 21E

Installation characteristics for a Variable Stream Control Engine (VSCE) were studied for three advanced supersonic airplane designs. Sensitivity of the VSCE concept to change in technology projections was evaluated in terms of impact on overall installed performance. Based on these sensitivity results, critical technology requirements were reviewed, resulting in the reaffirmation of the following requirements: low noise nozzle system, a high performance low emissions duct burner and main burner, hot section technology, variable geometry components, and propulsion integration features including an integrated electronic control system. Author

N78-11081* General Electric Co., Cincinnati, Ohio
COST BENEFIT STUDY OF ADVANCED MATERIALS TECHNOLOGY FOR AIRCRAFT TURBINE ENGINES

R. V. Hilery and R. P. Johnston Sep 1977 89 p refs

(Contract NAS3 20074)
 (NASA-CR-135235) Avail NTIS HC A05/MF A01 CSCL 21E

The cost benefits of eight advanced materials technologies

were evaluated for two aircraft missions. The overall study was based on a time frame of commercial engine use of the advanced material technologies by 1985. The material technologies evaluated were eutectic turbine blades, titanium aluminum components, ceramic vanes, shrouds and combustor liners, tungsten composite FeCrAlY blades, gamma prime oxide dispersion strengthened (ODS) alloy blades, and no coat ODS alloy combustor liners. They were evaluated in two conventional takeoff and landing missions, one transcontinental and one inter-continental. Author

N78-11082* Rocketdyne, Canoga Park, Calif
LINEAR AEROSPIKE ENGINE STUDY Final Report, Jun. 1976 - Apr. 1977

M. G. Diem and F. M. Kirby Nov 1977 236 p refs

(Contract NAS3 20114)
 (NASA-CR-135231) RI/RD77-170 Avail NTIS
 HC A11/MF A01 CSCL 21A

Parametric data on split-combustor linear engine propulsion systems are presented for use in mixed mode single-stage-to-orbit (SSTO) vehicle studies. Preliminary design data for two selected engine systems are included. The split combustor was investigated for mixed-mode operations with oxygen/hydrogen propellants used in the inner combustor in Mode 2 and in conjunction with either oxygen/RF-1, oxygen/RJ-5, O₂/CH₄, or O₂/H₂ propellants in the outer combustor for Mode 1. Both gas generator and staged combustion power cycles were analyzed for providing power to the turbopumps of the inner and outer combustors. Numerous cooling circuits and cooling fluids (propellants) were analyzed and hydrogen was selected as the preferred coolant for both combustors and the linear aerospace nozzle. The maximum operating chamber pressure was determined to be limited by the availability of hydrogen coolant pressure drop in the coolant circuit. Author

N78-12081* Pratt and Whitney Aircraft Group, West Palm Beach, Fla. Government Products Div
EVALUATION OF A LOW ASPECT RATIO SMALL AXIAL COMPRESSOR STAGE, VOLUME 1 Final Report

C. W. Sawyer III Nov 1977 148 p refs

(Contract NAS3 19424)
 (NASA-CR-135240) PWA FR-8499-Vol 1 Avail NTIS
 HC A07/MF A01 CSCL 21E

A program was conducted to evaluate the effects of scaling, tip clearance, and IGV reset on the performance of a low aspect ratio compressor stage. Stage design was obtained by scaling an existing single stage compressor by a linear factor of 0.304. The design objective was to maintain the meanline velocity field of the base machine in the smaller size. Adjustments were made to account for predicted blockage differences and to chord lengths and airfoil edge radii to obtain reasonable blade geometries. Meanline velocity diagrams of the base stage were not maintained at the scaled size. At design speed and flowrate the scaled stage achieved a pressure ratio of 1.423, adiabatic efficiency of 0.822 and surge margin of 18.5%. The corresponding performance parameters for the base stage were 1.480, 0.872 and 25.2%, respectively. The base stage demonstrated a peak efficiency at design speed of 0.872, the scaled stage achieved a level of 0.838. When the scaled stage rotor and stator tip clearances were doubled, the stage achieved a pressure ratio of 1.413, efficiency of 0.799 and surge margin of 16.0% at the design flowrate. The peak stage efficiency at design speed was 0.825 with the increased clearance. Increased prewhirl lowered the stage pressure ratio as expected. Stage efficiency was maintained with ten degrees of increased prewhirl and then decreased substantially with ten additional degrees of reset. Author

N78-12082* Pratt and Whitney Aircraft Group, West Palm Beach, Fla. Government Products Div
EVALUATION OF A LOW ASPECT RATIO SMALL AXIAL COMPRESSOR STAGE, VOLUME 2 Final Report

C. W. Sawyer III Nov 1977 222 p refs

(Contract NAS3 19424)
 (NASA-CR-135241) PWA FR-8499-Vol 2 Avail NTIS
 HC A10/MF A01 CSCL 21E

For abstract, see N78-12081

N78-12882* AResearch Mfg. Co., Phoenix, Ariz.
COST/BENEFIT ANALYSIS OF ADVANCED MATERIAL TECHNOLOGIES FOR SMALL AIRCRAFT TURBINE ENGINES

D. H. Conroy Sep 1977 68 p refs
 (Contract NAS3-20073)
 (NASA-CR-135285; AResearch-21-2381) Avail. NTIS
 HC A04/MF A01 CSCL 21E

Cost/benefit studies were conducted on ten advanced material technologies applicable to small aircraft gas turbine engines to be produced in the 1985 time frame. The cost/benefit studies were applied to a two engine, business-type jet aircraft in the 6800- to 9100-Kg (15,000- to 20,000-lb) gross weight class. The new material technologies are intended to provide improvements in the areas of high-pressure turbine rotor components, high-pressure turbine rotor components, high-pressure turbine stator airfoils, and static structural components. The cost/benefit of each technology is presented in terms of relative value, which is defined as a change in life cycle cost times probability of success divided by development cost. Technologies showing the most promising cost/benefits based on relative value are uncooled single crystal MAR-M 247 turbine blades, cooled DS MAR-M 247 turbine blades, and cooled ODS TiCrAl laminate turbine stator vanes. Author

N78-12087* General Electric Co., Cincinnati, Ohio
AUGMENTOR EMISSIONS REDUCTION TECHNOLOGY PROGRAM Final Report

W. C. Colley, M. J. Kenworthy, and D. W. Bahr Nov 1977
 185 p refs
 (Contract NAS3 19737)
 (NASA CR 135215; R77AEG593) Avail. NTIS
 HC A08/MF A01 CSCL 21E

Technology to reduce pollutant emissions from duct burner type augmentors for use on advanced supersonic cruise aircraft was investigated. Test configurations representing variations of two duct burner design concepts, were tested in a rectangular sector rig at inlet temperature and pressure conditions corresponding to takeoff, transonic climb, and supersonic cruise flight conditions. Both design concepts used pilot flameholders to stabilize combustion of lean, premixed fuel/air mixtures. The concepts differed in the flameholder type used. High combustion efficiency (97%) and low levels of emissions (1.19 g/kg fuel) were achieved. The detailed measurements suggested the direction that future development efforts should take to obtain further reductions in emission levels and associated improvements in combustion efficiency over an increased range of temperature rise conditions. Author

N78-13068* General Electric Co., Cincinnati, Ohio Aircraft Engine Group
ADVANCED SUPERSONIC PROPULSION STUDY, PHASES 3 AND 4

Roy D. Allan and Warren Joy Nov 1977 297 p refs
 (Contract NAS3 19544)
 (NASA CR 135236; R77AEG635) Avail. NTIS
 HC A13/MF A01 CSCL 21E

An evaluation of various advanced propulsion concepts for supersonic cruise aircraft resulted in the identification of the double bypass variable cycle engine as the most promising concept. This engine design utilizes special variable geometry components and an annular exhaust nozzle to provide high take off thrust and low jet noise. The engine also provides good performance at both supersonic cruise and subsonic cruise. Emission characteristics are excellent. The advanced technology double bypass variable cycle engine offers an improvement in aircraft range performance relative to earlier supersonic jet engine designs and yet at a lower level of engine noise. Research and technology programs required in certain design areas for this engine concept to realize its potential benefits include refined parametric analysis of selected variable cycle engines, screening of additional unconventional concepts and engine preliminary design studies. Required critical technology programs are summarized. Author

N78-13089* Pratt and Whitney Aircraft Group, East Hartford, Conn. Commercial Products Div.
HIGH FREQUENCY DYNAMIC ENGINE SIMULATION
 J. A. Scherman, K. E. Fischer, and P. W. McLaughlin Jul 1977 166 p refs

(Contract NAS3-20292)
 (NASA-CR-135313; PWA-5543) Avail. NTIS
 HC A08/MF A01 CSCL 21E

A digital computer simulation of a mixed flow twin spool turbofan engine was assembled to evaluate and improve the dynamic characteristics of the engine simulation to disturbance frequencies of at least 100 Hz. One dimensional forms of the dynamic mass, momentum and energy equations were used to model the engine. A TF30 engine was simulated so that dynamic characteristics could be evaluated against results obtained from testing of the TF30 engine at the NASA Lewis Research Center. Dynamic characteristics of the engine simulation were improved by modifying the compression system model. Modifications to the compression system model were established by investigating the influence of size and number of finite dynamic elements. Based on the results of this program, high frequency engine simulations using finite dynamic elements can be assembled so that the engine dynamic configuration is optimum with respect to dynamic characteristics and computer execution time. Resizing of the compression systems finite elements improved the dynamic characteristics of the engine simulation but showed that additional refinements are required to obtain close agreement simulation and actual engine dynamic characteristics. Author

N78-14047* Solar Turbines International, San Diego, Calif.
WIDE RANGE OPERATION OF ADVANCED LOW NOx COMBUSTORS FOR SUPERSONIC HIGH-ALTITUDE AIRCRAFT GAS TURBINES Technical Report, Nov. 1975 - Aug. 1977

P. B. Roberts and R. J. Fiorito Oct 1977 44 p
 (Contract NAS3 19770)
 (NASA-CR-135297; RDR 1817 22) Avail. NTIS
 HC A03/MF A01 CSCL 21E

An initial rig program tested the Jet Induced Circulation (JIC) and Vortex Air Blast (VAB) systems in small can combustor configurations for NOx emissions at a simulated high altitude, supersonic cruise condition. The VAB combustor demonstrated the capability of meeting the NOx goal of 1.0 g NO2/kg fuel at the cruise condition. In addition, the program served to demonstrate the limited low-emissions range available from the lean premixed combustor. A follow-on effort was concerned with the problem of operating these lean, premixed combustors with acceptable emissions at simulated engine idle conditions. Various techniques have been demonstrated that allow satisfactory operation on both the JIC and VAB combustors at idle with CO emissions below 20 g/kg fuel. The VAB combustor was limited by flashback, autoignition phenomena at the cruise conditions to a pressure of 8 atmospheres. The JIC combustor was operated up to the full design cruise pressure of 14 atmospheres without encountering an autoignition limitation although the NOx levels, in the 2-3 g NO2/kg fuel range, exceeded the program goal. Author

N78-15041* Pratt and Whitney Aircraft Group, East Hartford, Conn. Commercial Products Div.
EXPERIMENTAL CLEAN COMBUSTOR PROGRAM: TURBULENCE CHARACTERISTICS OF COMPRESSOR DISCHARGE FLOWS

P. S. Follansbee and R. R. Dils Oct 1977 43 p refs
 (Contract NAS3 19447)
 (NASA CR 135277; PWA 5540) Avail. NTIS
 HC A03/MF A01 CSCL 21E

The results of turbulence measurements at the entrance to the compressor duct of a large gas turbine are presented. Hot film and hot wire measurements were conducted over a compressor discharge temperature range of 450K to 608K. It was found that the turbulent intensity at the 1D and midspan locations increases gradually from 6% or 1 percent at idle to 7% or 1 percent at approach, the turbulent intensity at the OD location increases from 7.5% or 0.5 percent at idle to 15% or 0.5 percent at approach. The energy in the velocity waves is

uniformly distributed over a 0.1 to 5 kHz bandwidth, and the cut-off frequency is not a strong function of the engine operation. The axial length of the Fourier components within this bandwidth varies from 0.021 to 1.05m. The turbulence near the diffuser O.D. is of sufficient amplitude and scale to effect the flow to the front end sections of the burner. Author

N78-16052* Fiber Science, Inc., Gardena, Calif
FILAMENT-WINDING FABRICATION OF QCSEE CONFIGURATION FAN BLADES
 Sam Yao Jan 1978 22 p
 (Contract NAS3-20099)
 (NASA-CR-135332) Avail: NTIS HC A02/MF A01 CSCL 21E

The design and fabrication of twelve NASA-QCSEE type composite fan blades utilizing wet filament winding fabrication techniques is described. All composite fibers were continuous and attached to the root end. All components were formed, bonded, and co-cured in one molding process. Advanced fiber materials used in the blade fabrication were Thornei-300, Carbolon Z-2-1, and Carbolon Z-3 graphite in an epoxy resin matrix. Author

N78-16054* Pratt and Whitney Aircraft Group, East Hartford, Conn. Commercial Products Div
AN ANALYTICAL STUDY OF THERMAL BARRIER COATED FIRST STAGE BLADES IN A JT9D ENGINE
 William R. Savcik and Barry L. Stoner Jan 1978 31 p refs
 (Contract NAS3-21033)
 (NASA-CR-135360) PWA-55901 Avail: NTIS HC A03/MF A01 CSCL 21E

Steady state and transient heat transfer and structural calculations were completed to determine the coating and base alloy temperatures and strains. Results indicate potential for increased turbine life using thin durable thermal barrier coatings on turbine airfoils due to a significant reduction in blade average and maximum temperatures and alloy strain range. An interpretation of the analytical results is compared to the experimental engine test data. Author

N78-17066* Pratt and Whitney Aircraft, West Palm Beach, Fla. Government Products Div
ANALYTICAL STUDY OF THERMAL BARRIER COATED FIRST-STAGE BLADES IN AN F100 ENGINE Progress Report, 1 Sep. 1977 - 31 Jan. 1978
 D. E. Andreas Feb 1978 27 p
 (Contract NAS3-21032)
 (NASA-CR-135359; FR-9609) Avail: NTIS HC A03/MF A01 CSCL 21E

Heat transfer and stress analyses were performed on two sections of a thermal barrier coated (TBC) F100 1st-stage turbine blade. Results of the analyses indicate that the TBC on the leading edges of both sections experience the highest elastic strain ranges and these occur during transient engine operation. Further study is recommended to determine the effects of plastic deformation (creep) and creep-fatigue interaction on coating life. Author

N78-17064* Pratt and Whitney Aircraft Group, East Hartford, Conn. Commercial Products Div
METHOD OF FAN SOUND MODE STRUCTURE DETERMINATION Final Report
 G. F. Pickett, T. G. Sofrin, and R. W. Wells Aug 1977 160 p refs
 (Contract NAS3-20047)
 (NASA-CR-135293) PWA 5554-31 Avail: NTIS HC A08/MF A01 CSCL 21E

A method for the determination of fan sound mode structure in the inlet of turbofan engines using in-duct acoustic pressure measurements is presented. The method is based on the simultaneous solution of a set of equations whose unknowns are modal amplitude and phase. A computer program for the solution of the equation set was developed. An additional computer

program was developed which calculates microphone locations the use of which results in an equation set that does not give rise to numerical instabilities. In addition to the development of a method for determination of coherent modal structure, experimental and analytical approaches are developed for the determination of the amplitude frequency spectrum of randomly generated sound models for use in narrow annulus ducts. Two approaches are defined: one based on the use of cross-spectral techniques and the other based on the use of an array of microphones. Author

N78-17065* Pratt and Whitney Aircraft Group, East Hartford, Conn. Commercial Products Div
METHOD OF FAN SOUND MODE STRUCTURE DETERMINATION COMPUTER PROGRAM USER'S MANUAL: MICROPHONE LOCATION PROGRAM
 G. F. Pickett, R. A. Wells, and R. A. Love Aug 1977 72 p refs
 (Contract NAS3-20047)
 (NASA-CR-135294) PWA-5554-4 Avail: NTIS HC A04/MF A01 CSCL 21E

A computer user's manual describing the operation and the essential features of the microphone location program is presented. The Microphone Location Program determines microphone locations that ensure accurate and stable results from the equation system used to calculate modal structures. As part of the computational procedure for the Microphone Location Program, a first-order measure of the stability of the equation system was indicated by a matrix 'conditioning' number. Author

N78-17068* Pratt and Whitney Aircraft Group, East Hartford, Conn. Commercial Products Div
METHOD OF FAN SOUND MODE STRUCTURE DETERMINATION COMPUTER PROGRAM USER'S MANUAL: MODAL CALCULATION PROGRAM
 G. F. Pickett, R. A. Wells, and R. A. Love Aug 1977 74 p refs
 (Contract NAS3-20047)
 (NASA-CR-135295) PWA 5554-5 Avail: NTIS HC A04/MF A01 CSCL 21E

A computer user's manual describing the operation and the essential features of the Modal Calculation Program is presented. The Modal Calculation Program calculates the amplitude and phase of modal structures by means of acoustic pressure measurements obtained from microphones placed at selected locations within the fan inlet duct. In addition, the Modal Calculation Program also calculates the first order errors in the modal coefficients that are due to tolerances in microphone location coordinates and inaccuracies in the acoustic pressure measurements. Author

N78-18070* Pratt and Whitney Aircraft Group, West Palm Beach, Fla. Government Products Div
F-15/NONAXISYMMETRIC NOZZLE SYSTEM INTEGRATION STUDY SUPPORT PROGRAM Contractor Report, 24 Feb. 1977 - 30 Sep. 1977
 H. L. Stevens Feb 1978 171 p ref.
 (Contract NAS3-20608)
 (NASA-CR-136252; FR-9232) Avail: NTIS HC A08/MF A01 CSCL 21E

Nozzle and cooling methods were defined and analyzed to provide a viable system for demonstration. 2-D nozzle technology on the F-15 aircraft. Two candidate cooling systems applied to each nozzle were evaluated. The F-100 engine mount and case modifications requirements were analyzed and the actuator and control system requirements for two dimensional nozzles were defined. Nozzle performance changes relative to the axisymmetric baseline nozzle were evaluated and performance and weight characteristics for axisymmetric reference configurations were estimated. The infrared radiation characteristics of these nozzles installed on the F-100 engine were predicted. A full scale development plan with associated costs to carry the F100 engine/two-dimensional (2-D) nozzle through flight tests was defined. Author

N78-19183* Cincinnati Univ., Ohio. Dept. of Aerospace Engineering and Applied Mechanics.
ANALYSIS OF THE CROSS FLOW IN A RADIAL INFLOW TURBINE SCROLL

A Hamed, S. Abdallah, and W. Tabakoff Nov. 1977 61 p
 (Grant NoG-3068)
 (NASA-CR-135320) Avail: NTIS HC A04/MF A01 CSCL 21E

Equations of motion were derived, and a computational procedure is presented, for determining the nonviscous flow characteristics in the cross-sectional planes of a curved channel due to continuous mass discharge or mass addition. An analysis was applied to the radial inflow turbine scroll to study the effects of scroll geometry and the through flow velocity profile on the flow behavior. The computed flow velocity component in the scroll cross-sectional plane, together with the through flow velocity profile which can be determined in a separate analysis, provide a complete description of the three dimensional flow in the scroll. Author

N78-19184* Cincinnati Univ., Ohio. Dept. of Aerospace Engineering and Applied Mechanics.

COMPUTER PROGRAM FOR THE ANALYSIS OF THE CROSS FLOW IN A RADIAL INFLOW TURBINE SCROLL
 A Hamed, S. Abdallah, and W. Tabakoff Nov. 1977 56 p
 (Grant NoG-3068)
 (NASA-CR-135321) Avail: NTIS HC A04/MF A01 CSCL 21E

A computer program was used to solve the governing of the potential flow in the cross sectional planes of a radial inflow turbine scroll. A list of the main program, the subroutines, and typical output example are included. Author

N78-19180* Pratt and Whitney Aircraft, East Hartford, Conn. Commercial Products Div.
VCE TESTBED PROGRAM PLANNING AND DEFINITION STUDY Final Report

J. S. Westmoreland and J. Godston Jan 1978 82 p
 (Contract NAS3-20C48)
 (NASA-CR-135382; PWA-5546-7) Avail: NTIS HC A05/MF A01 CSCL 21E

The flight definition of the Variable Stream Control Engine (VSCE) was updated to reflect design improvements in the two key components: (1) the low emissions duct burner, and (2) the annular exhaust nozzle. The testbed design was defined and plans for the overall program were formulated. The effect of these improvements was evaluated for performance, emissions, noise, weight, and length. For experimental large scale testing of the duct burner and annular nozzle, a design definition of the VCE testbed configuration was made. This included selecting the core engine, determining instrumentation requirements, and selecting the test facilities, in addition to defining control system and assembly requirements. Plans for a comprehensive test program to demonstrate the duct burner and nozzle technologies were formulated. The plans include both aeroacoustic and emissions testing. Author

N78-20129* General Electric Co., Cincinnati, Ohio. Aircraft Engine Group.
LONG-TERM CF6 ENGINE PERFORMANCE DETERIORATION: EVALUATION OF ENGINE S/N 481-479 Final Report

W. H. Kramer and J. J. Smith Feb 1978 118 p
 (Contract NAS3-20631)
 (NASA-CR-135381) Avail: NTIS HC A06/MF A01 CSCL 21E

The performance testing and analytical teardown of CF6-6D engine is summarized. This engine had completed its initial installation on DC-10 aircraft. The investigative test program was conducted inbound prior to normal overhaul/refurbishment. The performance testing included an inbound test, a test following cleaning of the low pressure turbine airfoils, and a final test after leading edge rework and cleaning the stage one fan blades. The analytical teardown consisted of detailed disassembly inspection measurements and airfoil surface finish checks of the

as received deteriorated hardware. Included in this report is a detailed analysis of the test cell performance data, a complete analytical teardown report with a detailed description of all observed hardware distress, and an analytical assessment of the performance loss (deterioration) relating measured hardware conditions to losses in both SFC (specific fuel consumption) and EGT (exhaust gas temperature). Author

N78-21111* Pratt and Whitney Aircraft Group, East Hartford, Conn. Commercial Products Div.

EVALUATION OF FEDERAL AVIATION ADMINISTRATION ION ENGINE EXHAUST SAMPLING RAKE Final Report
 A. J. Fiorentino, W. Greene, and R. Roberts Jun. 1977 61 p
 ref

(Contracts NAS3-19447; DOT-FA77WAI-708)
 (NASA-CR-135213; PWA-5534; FAA-RD-77-115) Avail: NTIS HC A04/MF A01 CSCL 21E

A FAA exhaust emissions rake was tested in the Experimental Clean Combustor Program, Phase 3 to permit comparison of the values of gaseous emissions and smoke measured by the FAA rake with those measured with the NASA Pratt and Whitney Aircraft (P and WA) rake used in the Phase 3 Experimental Clean Combustor Program and with station seven probes. The results showed that the levels of CO, THC, NOx and smoke measured by the FAA and NASA/P and WA rakes agree well at high power, but that CO emissions measured by the FAA rake were approximately 10 percent higher than those measured by the NASA/P and WA rake at low power. Author

N78-21147* General Electric Co., Evendale, Ohio. Aircraft Engine Group.

EFFECTS OF FILM INJECTION ON PERFORMANCE OF A COOLED TURBINE

James D. McDonel and James E. Eiswerth. In AGAFD High Temp. Probl. in Gas Turbine Eng. Feb. 1978 11 p refs (For availability see N78-21118 12-07)
 (Contract NAS3-16732)

Avail: NTIS HC A25/MF A01

Tests were conducted in a 20 inch diameter single stage air cooled turbine designed to evaluate the effects of film cooling air on turbine aerodynamic performance. A comparison was made of the experimental results and an analytical method of evaluating film injection effects on turbine performance. The results are used to determine the effects of film cooling on overall engine performance for selected cycle conditions. The engine performance studies are used to show the cycle benefits of increased gas temperature at various coolant flow rates. Author

N78-22086* Pratt and Whitney Aircraft Group, East Hartford, Conn.

F100(3) PARALLEL COMPRESSOR COMPUTER CODE AND USER'S MANUAL Contractor Report, Mar. 1977 - Feb. 1978

R. S. Mazzawy, D. A. Fulkerson, D. E. Haddad, and T. A. Clark May 1978 52 p refs

(Contract NAS3-20610)
 (NASA-CR-135388; PWA-5549-8) Avail: NTIS HC A04/MF A01 CSCL 21E

The Pratt & Whitney Aircraft multiple segment parallel compressor model has been modified to include the influence of variable compressor vane geometry on the sensitivity to circumferential flow distortion. Further, performance characteristics of the F100 (3) compression system have been incorporated into the model on a blade row basis. In this modified form, the distortion's circumferential location is referenced relative to the variable vane controlling sensors of the F100 (3) engine so that the proper solution can be obtained regardless of distortion orientation. This feature is particularly important for the analysis of inlet temperature distortion. Competibility with fixed geometry compressor applications has been maintained in the model. Author

N78-23089* General Electric Co., Cincinnati, Ohio.
QCSEE TASK 2: ENGINE AND INSTALLATION PRELIMINARY DESIGN Final Report
 R. Neitzel, R. Lee, and A. J. Charnay Jun. 1973 350 p refs
 (Contract NAS3-16728)
 (NASA-CR-134738) Avail: NTIS HC A15/MF A01 CSCL 21E

High-bypass turbofan engines with features required for commercial short haul powered lift transports were designed. Two engines were configured for each of the externally blown flap installations, under-the-wing and over-the-wing. Estimates of installed and uninstalled performance, noise, and weight were defined for each propulsion system. Author

N78-24141* Pratt and Whitney Aircraft Group, East Hartford, Conn. Commercial Products Div.
DEVELOPMENT OF A PLASMA SPRAYED CERAMIC GAS PATH SEAL FOR HIGH PRESSURE TURBINE APPLICATION Final Report, 9 Jun. 1977 - 9 Jan. 1978
 L. T. Shembob May 1978 86 p
 (Contract NAS3-20623)
 (NASA-CR-135387; PWA-5569-12) Avail: NTIS HC A05/MF A01 CSCL 21E

Development of the plasma sprayed graded, layered ZrO₂/CoCrAlY seal system for gas turbine engine blade tip seal applications up to 1589 K (2400 °F) surface temperature was continued. The effect of changing ZrO₂/CoCrAlY ratios in the intermediate layers on thermal stresses was evaluated analytically with the goal of identifying the materials combinations which would minimize thermal stresses in the seal system. Three methods of inducing compressive residual stresses in the sprayed seal materials to offset tensile thermal stresses were analyzed. The most promising method, thermal prestraining, was selected based upon potential, feasibility and complexity considerations. The plasma spray equipment was modified to heat, control and monitor the substrate temperature during spraying. Specimens were fabricated and experimentally evaluated to (1) substantiate the capability of the thermal prestrain method to develop compressive residual stresses in the sprayed structure and (2) define the effect of spraying on a heated substrate on abrasibility, erosion and thermal shock characteristics of the seal system. Thermal stress analysis, including residual stresses and material properties variations, was performed and correlated with thermal shock test results. Seal system performance was assessed and recommendations for further development were made. Author

N78-26147* General Applied Science Labs., Inc., Westbury, N. Y.
EXPERIMENTAL STUDY OF THE EFFECTS OF FLAMEHOLDER GEOMETRY ON EMISSIONS AND PERFORMANCE OF LEAN PREMIXED COMBUSTORS Final Report
 Gerald Rolfe and K. S. Venkataramani Apr. 1978 89 p refs
 (Contract NAS3-20603)
 (NASA-CR-135424; GASL-TR-249) Avail: NTIS HC A05/MF A01 CSCL 21E

Emissions of NO_x, CO, and unburned hydrocarbons (UHC) are reported for a lean premixed propane-air system at inlet conditions of 800K and 1MPa using twelve flameholder designs. The flameholders tested represent six design concepts with two values of blockage for each concept. Data were obtained at reference velocities of 35 m/s, 25 m/s and 20 m/s at combustor stations 10 cm and 30 cm downstream of the flameholders. Flameholder pressure drop was found to be a principal determinant of emissions performance. Designs producing larger pressure drops also produced less NO_x, CO, and UHC emissions. The lean stability limit equivalence ratio was found to be approximately 0.35 for all designs. Flashback velocities (axial components in the flameholder passages) varied between 30 m/s and 40 m/s. A perforated plate flameholder was operated with a velocity as low as 23 m/s through the perforations at equivalence ratio 0.7 without producing flashback. Author

N78-27126* Boeing Commercial Airplane Co., Seattle, Wash.
JT9D ENGINE DIAGNOSTICS, TASK 2: FEASIBILITY STUDY OF MEASURING IN-SERVICE FLIGHT LOADS
 P. G. Kafka, M. A. Skibo, and J. L. White 15 Oct 1977 68 p refs
 (Contract NAS3 20632)
 (NASA-CR-135395; D5-44664) Avail: NTIS HC A04/MF A01 CSCL 21E

The feasibility of measuring JT9D propulsion system flight inertia loads on a 747 airplane is studied. Flight loads background is discussed including the current status of 747/JT9D loads knowledge. An instrumentation and test plan is formulated for an airline-owned in-service airplane and the Boeing-owned RA001 test airplane. Technical and cost comparisons are made between these two options. An overall technical feasibility evaluation is made and a cost summary presented. Conclusions and recommendations are presented in regard to using existing inertia loads data versus conducting a flight test to measure inertia loads. Author

N78-27129* Pratt and Whitney Aircraft Group, East Hartford, Conn. Commercial Products Div.
FABRICATION AND TEST OF DIGITAL OUTPUT INTERFACE DEVICES FOR GAS TURBINE ELECTRONIC CONTROLS Final Report
 D. M. Newirth and E. W. Koenig May 1978 59 p
 (Contract NAS3-19898)
 (NASA-CR-135427; PWA-5544-13) Avail: NTIS HC A04/MF A01 CSCL 21E

A program was conducted to develop an innovative digital output interface device, a digital effector with optical feedback of the fuel metering valve position, for future electronic controls for gas turbine engines. A digital effector (on-off solenoids driven directly by on-off signals from a digital electronic controller) with optical position feedback was fabricated, coupled with the fuel metering valve, and tested under simulated engine operating conditions. The testing indicated that a digital effector with optical position feedback is a suitable candidate, with proper development, for future digital electronic gas turbine controls. The testing also identified several problem areas which would have to be overcome in a final production configuration. Author

N78-28086* General Electric Co., Cincinnati, Ohio. Aircraft Engine Group.
ACOUSTIC TESTS OF DUCT-BURNING TURBOFAN JET NOISE SIMULATION: COMPREHENSIVE DATA REPORT, VOLUME 1, SECTION 2: FULL SIZE DATA Final Report
 P. H. Heck, D. Latham, J. F. Brausch, E. J. Stringas, P. S. Staid, and P. R. Knott Aug. 1978 832 p
 (Contract NAS3-18008)
 (NASA-CR-135239-Vol-1-Sept-2) Avail: NTIS HC A99/MF A01 CSCL 21E

Acoustic data are presented scaled to a full size engine by a factor of 8 on a 96.9 m (320 ft) arc and a 731.5 m (2400 ft) sideline. D.L.G.

N78-28086* General Electric Co., Cincinnati, Ohio. Aircraft Engine Group.
ACOUSTIC TESTS OF DUCT-BURNING TURBOFAN JET NOISE SIMULATION: COMPREHENSIVE DATA REPORT, VOLUME 1, SECTION 3: DATA PLOTS Final Report
 P. H. Heck, D. Latham, J. F. Brausch, E. J. Stringas, P. S. Staid, and P. R. Knott Aug 1978 520 p
 (Contract NAS3-18008)
 (NASA-CR-135239-Vol-1-Sept-3) Avail: NTIS HC A22/MF A01 CSCL 21E

Acoustic data plots are presented which were obtained in the tests on scale nozzles for use on duct-burning turbofan engines. D.L.G.

N78-28087* General Electric Co., Cincinnati, Ohio. Aircraft Engine Group.

ACOUSTIC TESTS OF DUCT-BURNING TURBOFAN JET NOISE SIMULATION: COMPREHENSIVE DATA REPORT. VOLUME 2: MODEL DESIGN AND AERODYNAMIC TEST RESULTS Final Report

P. H. Heck, D. Latham, J. F. Brauch, E. J. Stringas, P. S. Stald, and P. R. Knott Aug. 1978 229 p refs
(Contract NAS3-18008)
(NASA-CR-135239-Vol-2) Avail: NTIS HC A11/MF A01 CSCL 21E

The selection procedure is described which was used to arrive at the configurations tested, and the performance characteristics of the test nozzles are given. D.L.G.

N78-28088* General Applied Science Labs., Inc., Westbury, N. Y.

EXPERIMENTAL STUDY OF THE EFFECT OF CYCLE PRESSURE ON LEAN COMBUSTION EMISSIONS Final Report

Gerald Roffe and K. S. Venkataramani Washington NASA Jul. 1978 51 p
(Contract NAS3-20581)
(NASA-CR-3032: GASL-TR-248) Avail: NTIS HC A04/MF A01 CSCL 21E

Experiments were conducted in which a stream of premixed propane and air was burned under conditions representative of gas turbine operation. Emissions of NO_x, CO, and unburned hydrocarbons (UHC) were measured over a range of combustor inlet temperature, pressure, and residence time at equivalence ratios from 0.7 down to the lean stability limit. At an inlet temperature of 600 K, observed NO_x levels dropped markedly with decreasing pressure for pressures below 20 atm. The NO_x levels are proportional to combustor residence time and formation rates were principally a function of adiabatic flame temperature. For adiabatic flame temperatures of 2050 K and higher, CO reached chemical equilibrium within 2 msec. Unburned hydrocarbon species dropped to a negligible level within 2 msec regardless of inlet temperature, pressure, or equivalence ratio. For a combustor residence time of 2.5 msec, combustion inefficiency became less than 0.01% at an adiabatic flame temperature of 2050 K. The maximum combustion inefficiency observed was on the order of 1% and corresponded to conditions near the lean stability limit. Using a perforated plate flameholder, this limit is well represented by the condition of 1800 K adiabatic flame temperature. Author

N78-29089* General Electric Co., Cincinnati, Ohio. Aircraft Engine Group.

CORE COMPRESSOR EXIT STAGE STUDY. VOLUME 1: BLADING DESIGN Design Report, Oct. 1976 - Apr. 1977

D. C. Wisler Dec. 1977 67 p refs
(Contract NAS3-20070)
(NASA-CR-135391: Doc-R77AEG400-Vol-1) Avail: NTIS HC A04/MF A01 CSCL 21E

A baseline compressor test stage was designed as well as a candidate rotor and two candidate stators that have the potential of reducing endwall losses relative to the baseline stage. These test stages are typical of those required in the rear stages of advanced, highly-loaded core compressors. The baseline Stage A is a low-speed model of Stage 7 of the 10 stage AMAC compressor. Candidate Rotor B uses a type of meanline in the tip region that unloads the leading edge and loads the trailing edge relative to the baseline Rotor A design. Candidate Stator B embodies twist gradients in the endwall region. Candidate Stator C embodies airfoil sections near the endwalls that have reduced trailing edge loading relative to Stator A. Tests will be conducted using four identical stages of blading so that the designs described will operate in a true multistage environment. A.R.H.

N78-29103* General Electric Co., Cincinnati, Ohio. Aircraft Engine Group.

LONG-TERM CF6 ENGINE PERFORMANCE DETERIORATION: EVALUATION OF ENGINE S/N 42-380 Final Report

W. H. Kramer and J. J. Smith Aug. 1978 112 p
(Contract NAS3-20631)
(NASA-CR-159390) Avail: NTIS HC A06/MF A01 CSCL 21E

The performance testing and analytical teardown of CF6-8D engine serial number 451-380 which was recently removed from a DC-10 aircraft is summarized. The investigative test program was conducted inbound prior to normal overhaul/refurbishment. The performance testing included an inbound test, a test following cleaning of the low pressure turbine airfoils, and a final test after leading edge rework and clearing the stage one fan blades. The analytical teardown consisted of detailed disassembly inspection measurements and airfoil surface finish checks of the as-received deteriorated hardware. Aspects discussed include the analysis of the test cell performance data, a complete analytical teardown report with a detailed description of all observed hardware distress, and an analytical assessment of the performance loss (deterioration) relating measured hardware conditions to losses in both specific fuel consumption and exhaust gas temperature. A.R.H.

N78-29104* General Electric Co., Cincinnati, Ohio. DESIGN OF IMPACT-RESISTANT BORON/ALUMINUM LARGE FAN BLADE

C. T. Salemma and S. A. Yokel Jul. 1978 93 p refs
(Contract NAS3-21041)
(NASA-CR-135417) Avail: NTIS HC A05/MF A01 CSCL 21E

The technical program was comprised of two technical tasks. Task 1 encompassed the preliminary boron/aluminum fan blade design effort. Two preliminary designs were evolved. An initial design consisted of 32 blades per stage and was based on material properties extracted from manufactured blades. A final design of 36 blades per stage was based on rule-of-mixture material properties. In Task 2, the selected preliminary blade design was refined via more sophisticated analytical tools. Detailed finite element stress analysis and aero performance analysis were carried out to determine blade material frequencies and directional stresses. L.S.

N78-29105* Pratt and Whitney Aircraft Group, East Hartford, Conn. Commercial Products Div.

EFFECT OF STEADY FLIGHT LOADS ON JT9D-7 PERFORMANCE DETERIORATION

A. Jay and E. S. Todd 9 Jun. 1978 103 p refs
(Contract NAS3-20632)
(NASA-CR-135407: PWA-5512-24) Avail: NTIS HC A06/MF A01 CSCL 21E

Short term engine deterioration occurs in less than 250 flights on a new engine and in the first flights following engine repair; while long term deterioration involves primarily hot section distress and compression system losses which occur at a somewhat slower rate. The causes for short-term deterioration are associated with clearance changes which occur in the flight environment. Analytical techniques utilized to examine the effects of flight loads and engine operating conditions on performance deterioration are presented. The role of gyroscopic, gravitational, and aerodynamic loads are discussed along with the effect of variations in engine build clearances. These analytical results are compared to engine test data along with the correlation between analytically predicted and measured clearances and rub patterns. Conclusions are drawn and important issues are discussed. A.R.H.

N78-31163* Pratt and Whitney Aircraft Group, West Palm Beach, Fla. Government Products Div.
ADVANCED OPTICAL BLADE TIP CLEARANCE MEASUREMENT SYSTEM

M. J. Ford, R. E. Honeycutt, R. E. Nordlund, and W. W. Robinson
 Jul. 1978 85 p refs
 (Contract NAS3-20479)
 (NASA-CR-159402; FR-10200A) Avail: NTIS
 HC A06/MF A01 CSCL 21E

An advanced electro-optical system was developed to measure single blade tip clearances and average blade tip clearances between a rotor and its gas path seal in an operating gas turbine engine. This system is applicable to fan, compressor, and turbine blade tip clearance measurement requirements, and the system probe is particularly suitable for operation in the extreme turbine environment. A study of optical properties of blade tips was conducted to establish measurement system application limitations. A series of laboratory tests was conducted to determine the measurement system's operational performance characteristics and to demonstrate system capability under simulated operating gas turbine environmental conditions. Operational and environmental performance test data are presented. Author

N78-31166* General Electric Co., Cincinnati, Ohio. Aircraft Engine Group.

ENERGY EFFICIENT ENGINE: PRELIMINARY DESIGN AND INTEGRATION STUDIES Final Report, Jan. 1977 - Apr. 1978

R. P. Johnston, R. Hirschkrone, C. C. Koch, R. E. Neitzel, and P. W. Vinson Sep. 1978 417 p refs
 (Contract NAS3-20627)
 (NASA-CR-135444; R78AEG510) Avail: NTIS
 HC A18/MF A01 CSCL 21E

Parametric design and mission evaluations of advanced turbolan configurations were conducted for future transport aircraft application. Economics, environmental suitability and fuel efficiency were investigated and compared with goals set by NASA. Of the candidate engines which included mixed- and separate-flow, direct-drive and geared configurations, an advanced mixed-flow direct-drive configuration was selected for further design and evaluation. All goals were judged to have been met except the acoustic goal. Also conducted was a performance risk analysis and a preliminary aerodynamic design of the 10 stage 23:1 pressure ratio compressor used in the study engines. Author

N78-32086* Pratt and Whitney Aircraft Group, East Hartford, Conn. Commercial Products Div.
COMPRESSOR SEAL RUB ENERGETICS STUDY
 Final Report, 8 Apr. 1977 - 8 Apr. 1978

W. F. Lavery May 1978 139 p refs
 (Contract NAS 3-20613)
 (NASA-CR-159424; PWA-5618) Avail: NTIS
 HC A07/MF A01 CSCL 21E

The rub mechanics of compressor abraable blade tip seals at simulated engine conditions were investigated. Twelve statistically planned, instrumented rub tests were conducted with titanium blades and Feltmetal fibermetal rubstrips. The tests were conducted with single stationary blades rubbing against seal material bonded to rotating test disks. The instantaneous rub torque, speed, incursion rate and blade temperatures were continuously measured and recorded. Basic rub parameters (incursion rate, rub depth, abraable density, blade thickness and rub velocity) were varied to determine the effects on rub energy and heat split between the blade, rubstrip surface and rub debris. The test data was reduced, energies were determined and statistical analyses were completed to determine the primary and interactive effects. Wear surface morphology, profile measurements and metallographic analysis were used to determine wear, glazing, melting and material transfer. The rub energies for these tests were most significantly affected by the incursion rate while rub velocity and blade thickness were of secondary importance. The ratios of blade wear to seal wear were representative of those experienced in engine operation of these seal system materials. Author

N78-32087* General Electric Co., Cincinnati, Ohio.
AIRCRAFT GAS TURBINE LOW-POWER EMISSIONS REDUCTION TECHNOLOGY PROGRAM Final Report
 W. J. Dodds, C. C. Gleason, and D. W. Bahw Oct. 1978 161 p refs

(Contract NAS3-20680)
 (NASA-CR-135434; Doc-R78AEG408) Avail: NTIS
 HC A06/MF A01 CSCL 21E

Advanced aircraft turbine engine combustor technology was used to reduce low-power emissions of carbon monoxide and unburned hydrocarbons to levels significantly lower than those which were achieved with current technology. Three combustor design concepts, which were designated as the hot-wall liner concept, the recuperative-cooled liner concept, and the catalyst converter concept, were evaluated in a series of CF8-50 engine size 40 degree-sector combustor rig tests. Twenty-one configurations were tested at operating conditions spanning the design condition which was an inlet temperature and pressure of 422 K and 304 kPa, a reference velocity of 23 m/s and a fuel-air-ratio of 10.5 g/kg. At the design condition typical of aircraft turbine engine ground idle operation, the best configurations of all three concepts met the stringent emission goals which were 10, 1, and 4 g/kg for CO, HC, and Nox, respectively. G.G.

N78-33163* General Electric Co., Cincinnati, Ohio. Aircraft Engine Group.

BLADE ROW DYNAMIC DIGITAL COMPRESSION PROGRAM. VOLUME 2: JSC CIRCUMFERENTIAL DISTORTION REDISTRIBUTION MODEL, EFFECT OF STATOR CHARACTERISTICS, AND STAGE CHARACTERISTICS SENSITIVITY STUDY

W. A. Tesch and W. G. Steenken Jul. 1978 76 p refs
 (Contract NAS3-18526)
 (NASA-CR-134953; R78AEG484-Vol-2) Avail: NTIS
 HC A04/MF A01 CSCL 21E

The results of dynamic digital blade row compressor model studies of a J85-13 engine are reported. The initial portion of the study was concerned with the calculation of the circumferential redistribution effects in the blade-free volumes forward and aft of the compression component. Although blade-free redistribution effects were estimated, no significant improvement over the parallel-compressor type solution in the prediction of total-pressure inlet distortion stability limit was obtained for the J85-13 engine. Further analysis was directed to identifying the rotor dynamic response to spatial circumferential distortions. Inclusion of the rotor dynamic response led to a considerable gain in the ability of the model to match the test data. The impact of variable stator loss on the prediction of the stability limit was evaluated. An assessment of measurement error on the derivation of the stage characteristics and predicted stability limit of the compressor was also performed. Author

N78-33104* AiResearch Mfg. Co., Phoenix, Ariz.
POLLUTION REDUCTION TECHNOLOGY PROGRAM FOR SMALL JET AIRCRAFT ENGINES. PHASE 2 Final Report
 T. W. Bruce, F. G. Davis, T. E. Kuhn, and H. C. Mongis Sep. 1978 187 p refs
 (Contract NAS3-20044)
 (NASA-CR-159415; AiResearch-21-2817) Avail: NTIS
 HC A06/MF A01 CSCL 21A

A series of iterative combustor pressure rig tests were conducted on two combustor concepts applied to the AiResearch TFE731-2 turbofan engine combustion system for the purpose of optimizing combustor performance and operating characteristics consistent with low emissions. The two concepts were an axial air-assisted airblast fuel injection configuration with variable geometry air swirlers and a staged premix/prevaporization configuration. The iterative rig testing and modification sequence on both concepts was intended to provide operational compatibility with the engine and determine one concept for further evaluation in a TFE731-2 engine. Author

A78-17396 * Sound separation probes for flowing duct noise measurements. M. T. Moore (General Electric Co., Aircraft Engine Group, Cincinnati, Ohio). In: *International Instrumentation Symposium, 23rd, Las Vegas, Nev., May 1-5, 1977, Proceedings.* (A78-17351 05-35) Pittsburgh, Pa., Instrument Society of America, 1977, p. 451-459. Contract No. NAS3-18021.

In order to understand the propagation of broadband sound from a device such as a jet engine, it is necessary to make fluctuating pressure measurements in the ducted airstream. However, in a flowing duct, fluctuating pressure energy can be due to both turbulence and sound travelling in the duct. By using the principal that sound waves and turbulent flow pressure perturbations travel at different velocities, a probe has been developed that provides the data necessary to separate the energy due to sound from that due to turbulence. A mini-computer based FFT analysis of the probe measurements provides the overall level of the broadband sound in the duct as well as the spectral distribution of the sound energy.

(Author)

A78-23893 * Optimal controls for an advanced turbofan engine. G. L. Slater (Cincinnati, University, Cincinnati, Ohio). In: *Joint Automatic Control Conference, San Francisco, Calif., June 22-24, 1977, Proceedings, Volume 2.* (A78-23851 08-63) New York, Institute of Electrical and Electronics Engineers, Inc., 1977, p. 1038-1043. 10 refs. Contract No. NAS3-18021.

Linear optimal control theory is applied to the control synthesis of a high bypass ratio, variable pitch, turbofan engine. The basic control philosophy is to use only a low order dynamic model of the plant coupled with the concept of integral-output states so as to maintain control simplicity yet guarantee integral control of thrust, turbine temperature and other important engine outputs. Linear simulation results indicate that the control system developed provides rapid control of small thrust perturbations and quickly eliminates the effect of unmodelled thrust and temperature disturbances. Large thrust accelerations are obtained in about one half second while the control maintains negligible overshoot in temperature and stall margins.

(Author)

A78-23518 * # Failure detection and correction for turbofan engines. R. C. Corley (General Electric Co., Group Engineering Div., Cincinnati, Ohio) and H. A. Spang, III (GE Research and Development Center, Schenectady, N.Y.). *AIChE, ASME, IEEE, ISA, and SME, Joint Automatic Control Conference, San Francisco, Calif., June 22-24, 1977, Paper.* 7 p. Contract No. NAS3-18021.

In this paper, a failure detection and correction strategy for turbofan engines is discussed. This strategy allows continuing control of the engines in the event of a sensor failure. An extended Kalman filter is used to provide the best estimate of the state of the engine based on currently available sensor outputs. Should a sensor failure occur the control is based on the best estimate rather than the sensor output. The extended Kalman filter consists of essentially two parts, a nonlinear model of the engine and up-date logic which causes the model to track the actual engine. Details on the model and up-date logic are presented. To allow implementation, approximations are made to the feedback gain matrix which result in a single feedback matrix which is suitable for use over the entire flight envelope. The effect of these approximations on stability and response is discussed. Results from a detailed nonlinear simulation indicate that good control can be maintained even under multiple failures. (Author)

A78-24902 * # Effects of film injection on performance of a cooled turbine. J. D. McDonel and J. E. Eiswerth (General Electric Co., Aircraft Engine Group, Evendale, Ohio). *NATO, AGARD, Propulsion and Energetics Panel Meeting, 50th, Middle East Technical University, Ankara, Turkey, Sept. 19-23, 1977, Paper.* 10 p. Contract No. NAS3-16732.

Some of the most dramatic increases in the performance of turbojet and turbofan aircraft engines have been obtained as a result of increased thermodynamic cycle temperature made possible by the use of film cooling techniques. The realization of the potential performance gains, however, is only possible if the quantity of cooling air and the aerodynamic mixing losses resulting from the injection of coolant in the form of film on the flowpath surfaces are minimized. Such a minimization requires a more complete understanding of the relationship between cooling and aerodynamics. A review is conducted of tests which have been conducted to determine the effects of coolant injection on turbine performance. The results obtained in the tests are compared with an analytical technique developed for predicting coolant injection effects. Particular attention is given to the effects of turbine cooling on overall cycle thermodynamic efficiency, taking into account incremental changes in turbine thermodynamic efficiency for various incremental changes in coolant flow rate. G.R.

A78-45097 * # Fuel consumption improvement in current transport engines. R. W. Hines (United Technologies Corp., Pratt and Whitney Aircraft Group, East Hartford, Conn.) and J. A. Ziemanski (NASA, Lewis Research Center, Cleveland, Ohio). *American Institute of Aeronautics and Astronautics and Society of Automotive Engineers, Joint Propulsion Conference, 14th, Las Vegas, Nev., July 25-27, 1978, AIAA Paper 78-930.* 7 p. 7 refs. Contracts No. NAS3-20630; No. NAS3-20632.

A review is conducted of improvements which can be made with respect to the fuel consumption of current engines and new production versions of current engines. A description is presented of an engine diagnostics program which has the objective to identify and quantify the causes and sources of performance deterioration in the JT9D turbofan engine and to develop basic data which will be applied to minimize performance degradation of current and future engines. General areas where performance losses occur are examined, taking into account seals, blades and vanes, and cases. Potential performance improvement concepts are related to improved component aerodynamics, improved flowpath sealing, blade tip clearance control, improved turbine cooling effectiveness, improved turbine materials and coatings, duct and nozzle aerodynamic refinements, nacelle aerodynamic refinements, forced exhaust mixers, advanced nacelle materials, and advanced fuel control. G.R.

08 AIRCRAFT STABILITY AND CONTROL

Includes aircraft handling qualities; piloting; flight controls;
and autopilots

N78-27137* National Aeronautics and Space Administration,
Lewis Research Center, Cleveland, Ohio.

REAL TIME DIGITAL PROPULSION SYSTEM SIMULATION FOR MANNED FLIGHT SIMULATORS

James R. Mihalow and Clint E. Hart 1978 45 p refs Presented
at the 14th Propulsion Conf., Las Vegas, Nev., 25-27 Jul. 1978;
sponsored by AIAA and the Soc. of Automotive Engr.
(NASA-TM-78958; E-9710) Avail: NTIS HC A03/MF A01
CSCL 01C

A real time digital simulation of a STOL propulsion system
was developed which generates significant dynamics and internal
variables needed to evaluate system performance and aircraft
interactions using manned flight simulators. The simulation ran
at a real-to-execution time ratio of 8.8. The model was used in
a piloted NASA flight simulator program to evaluate the simulation
technique and the propulsion system digital control. The simulation
is described and results shown. Limited results of the flight
simulation program are also presented. Author

09 RESEARCH AND SUPPORT FACILITIES (AIR)

Includes airports, hangars and runways; aircraft repair and overhaul facilities; wind tunnels; shock tube facilities; and engine test blocks.

For related information see also 14 *Ground Support Systems and Facilities (Space)*.

simulation which could be integrated into a multiengine aircraft simulation. A summary of the accomplishments which have been made in this program. G.R.

N78-13077* National Aeronautics and Space Administration, Lewis Research Center, Cleveland, Ohio.

COMBUSTOR FLUCTUATING PRESSURE MEASUREMENTS IN-ENGINE AND IN A COMPONENT TEST FACILITY: A PRELIMINARY COMPARISON

Meyer Reshotko and Allen Karchmer 1977 19 p refs Presented at 94th Meeting of the Acoust. Soc. Am., Miami Beach, Fla., 13-16 Dec. 1977

(NASA-TM-73845: E-8432) Avail: NTIS HC A02/MF A01 CSCL 14B

In a program to investigate combustor noise, measurements were made with a YF-102 engine of combustor internal fluctuating pressure and far field noise. The relationship of far field noise to engine internal measurement was ascertained. The relationships between combustor internal measurements obtained in an engine and those obtained in a component test facility were established by using a YF-102 combustor, instrumented identically with that used in the engine tests. The combustor was operated in a component test facility over a range of conditions encompassing engine operation. A comparison of the directly measured spectra at corresponding locations in the two tests showed significant differences. The results of two point signal analyses within each combustor, were similar for both tests, indicating that the internal dynamics of the combustor as an acoustic source are preserved in a component test facility. Author

N78-18069* National Aeronautics and Space Administration, Lewis Research Center, Cleveland, Ohio.

THE ERDA/LeRC PHOTOVOLTAIC SYSTEMS TEST FACILITY

Americo F. Forestieri Sep. 1977 12 p refs Presented at 1977 Photovoltaics Solar Energy Conf., Comm. of the European Communities, Luxembourg, 27-30 Sep. 1977

(Contract E(49-26)-1022)

(NASA-TM-73787: ERDA/NASA-1022/77/19) Avail: NTIS HC A02/MF A01 CSCL 14B

A test facility was designed, and built to provide a place where photovoltaic systems may be assembled and electrically configured, to evaluate system performance and characteristics. The facility consists of a solar cell array of an initial 10-kW peak power rating, test hardware for several alternate methods of power conditioning, a variety of loads, an electrical energy storage system, and an instrumentation and data acquisition system. Author

A78-45095* Real time digital propulsion system simulation for manned flight simulators. J. R. Mihalow and C. E. Hart (NASA, Lewis Research Center, Cleveland, Ohio). *American Institute of Aeronautics and Astronautics and Society of Automotive Engineers, Joint Propulsion Conference, 14th, Las Vegas, Nev., July 25-27, 1978, AIAA Paper 78-927*, 44 p. 7 refs.

The QCSEE (Quiet, Clean Short-haul Experimental Engine) Program was initiated by NASA to develop and demonstrate propulsion system technology for an advanced commercial STOL aircraft. One of the specific technical objectives was to provide technology for digital electronic control of future commercial engines. An element of this technology development was to evaluate the digital control in a simulated flight environment. In this connection a simulation program was initiated to evaluate the QCSEE UTW (Under the Wing) digital control system over a range of conditions encountered in typical airport operations. The goal of the simulation effort was to derive a real time digital propulsion

12 ASTRONAUTICS (GENERAL)

For extraterrestrial exploration see 91 Lunar and Planetary Exploration.

N78-10129* National Aeronautics and Space Administration, Lewis Research Center, Cleveland, Ohio.

PROCEEDINGS OF THE SPACECRAFT CHARGING TECHNOLOGY CONFERENCE Interim Report
C. P. Pike, ed. and R. R. Lovell, ed. 24 Feb. 1977 885 p
refs Conf. held at Colorado, 27-29 Oct. 1976; Sponsored by NASA and AFGL
(AF Proj. 7861)

(NASA-TM-X-73537; AFGL-TR-77-0061; AFSG-364) Avail:
NTIS HC A99/MF A01 CSCL 22B

Over 50 papers from the spacecraft charging conference are included on subjects such as: (1) geosynchronous plasma environment, (2) spacecraft modeling, (3) spacecraft materials characterization, (4) spacecraft materials development, and (5) satellite design and test. For individual titles, see N78-10130 through N78-10182.

N78-10135* National Aeronautics and Space Administration, Lewis Research Center, Cleveland, Ohio.

PRELIMINARY REPORT ON THE CTS TRANSIENT EVENT COUNTER PERFORMANCE THROUGH THE 1976 SPRING ECLIPSE SEASON c18

N. John Stevens, Robert R. Lovell, and Vernon W. Klinecft *In its Proc. of the Spacecraft Charging Technol. Conf.* 24 Feb. 1977 p 81-105 refs (For availability see N78-10129 01-12)

Avail: NTIS HC A99/MF A01 CSCL 22A

The transient event counter is described, defining its operational characteristics, and presenting the preliminary results obtained through the first 90 days of operation including the Spring 1976 eclipse season. The results show that the CTS was charged to the point where discharges have occurred. The discharge induced transients have not caused any anomalous events in spacecraft operation. The data indicate that discharges can occur at any time during the day without preference to any local time quadrant. The number of discharges occurring in the 1 sec sample interval are greater than anticipated. Author

N78-10136* National Aeronautics and Space Administration, Lewis Research Center, Cleveland, Ohio.

ACTIVE CONTROL OF SPACECRAFT CHARGING ON ATS-5 AND ATS-6 c16

Carolyn K. Purvis, Robert O. Bartlett (NASA, Goddard Space Flight Center), and Sherman E. DeForest (California Univ., La Jolla) *In its Proc. of the Spacecraft Charging Technol. Conf.* 24 Feb. 1977 p 107-120 refs (For availability see N78-10129 01-12)

Avail: NTIS HC A99/MF A01 CSCL 22B

Effects on spacecraft ground potential of active emission of charged particles are being investigated through experiments using the ATS-5 and ATS-6 spacecraft. Each spacecraft is equipped with ion engine neutralizers which emit low energy charged particles. Despite great differences in design between the two spacecraft, they attain similar potentials in similar environments. Therefore, effects on spacecraft potential of neutralizer operations can be used to compare the effects of operating the two different neutralizers (hot wire filament and plasma bridge). The neutralizers on both spacecraft were operated in eclipse. Results of these operations are presented and spacecraft responses compared.

Author

N78-10186* National Aeronautics and Space Administration, Lewis Research Center, Cleveland, Ohio.

THE LEWIS RESEARCH CENTER GEOMAGNETIC SUBSTORM SIMULATION FACILITY c14

Frank D. Berkopec, N. John Stevens, and John C. Sturman *In its Proc. of the Spacecraft Charging Technol. Conf.* 24 Feb. 1977 p 423-430 refs (For availability see N78-10129 01-12)

Avail: NTIS HC A99/MF A01 CSCL 14B

A simulation facility was established to determine the response of typical spacecraft materials to the geomagnetic substorm environment and to evaluate instrumentation that will be used to monitor spacecraft system response to this environment. Space environment conditions simulated include the thermal-vacuum conditions of space, solar simulation, geomagnetic substorm electron fluxes and energies, and the low energy plasma environment. Measurements for spacecraft material tests include sample currents, sample surface potentials, and the cumulative number of discharges. Discharge transients are measured by means of current probes and oscilloscopes and are verified by a photomultiplier. Details of this facility and typical operating procedures are presented.

Author

N78-10188* National Aeronautics and Space Administration, Lewis Research Center, Cleveland, Ohio.

TESTING OF TYPICAL SPACECRAFT MATERIALS IN A SIMULATED SUBSTORM ENVIRONMENT c18

N. John Stevens, Frank D. Berkopec, John V. Staskus, Richard A. Blech, and Steven J. Narciso *In its Proc. of the Spacecraft Charging Technol. Conf.* 24 Feb. 1977 p 431-457 refs (For availability see N78-10129 01-12)

Avail: NTIS HC A99/MF A01 CSCL 11G

The test specimens were spacecraft paints, silvered Teflon, thermal blankets, and solar array segments. The samples, ranging in size from 300 to 1000 sq cm were exposed to monoenergetic electron energies from 2 to 20 keV at a current density of 1 NA/sq cm. The samples generally behaved as capacitors with strong voltage gradient at their edges. The charging characteristics of the silvered Teflon, Kapton, and solar cell covers were controlled by the secondary emission characteristic. Insulators that did not discharge were the spacecraft paints and the quartz fiber cloth thermal blanket sample. All other samples did experience discharges when the surface voltage reached -8 to -18kV. The discharges were photographed. The breakdown voltage for each sample was determined and the average energy lost in the discharge was computed.

Author

N78-10187* National Aeronautics and Space Administration, Lewis Research Center, Cleveland, Ohio.

CHARGING CHARACTERISTICS OF MATERIALS: COMPARISON OF EXPERIMENTAL RESULTS WITH SIMPLE ANALYTICAL MODELS c28

Carolyn K. Purvis, N. John Stevens, and Jon C. Oglebay *In its Proc. of the Spacecraft Charging Technol. Conf.* 24 Feb. 1977 p 458-436 refs (For availability see N78-10129 01-12)

Avail: NTIS HC A99/MF A01 CSCL 11G

A one-dimensional model for charging of samples is used in conjunction with experimental data taken to develop material charging characteristics for silvered Teflon. These characteristics are then used in a one dimensional model for charging in space to examine expected response. Relative charging rates as well as relative charging levels for silvered Teflon and metal are discussed.

Author

N78-10173* National Aeronautics and Space Administration, Lewis Research Center, Cleveland, Ohio.

PROVISIONAL SPECIFICATION FOR SATELLITE TIME IN A GEOMAGNETIC ENVIRONMENT c13

N. John Stevens, Robert R. Lovell, and Carolyn K. Purvis *In its Proc. of the Spacecraft Charging Technol. Conf.* 24 Feb. 1977 p 735-744 refs (For availability see N78-10129 01-12)

Avail: NTIS HC A99/MF A01 CSCL 22B

Satellites in geosynchronous orbit were experiencing operational anomalies. These anomalies are believed to be due to the environment charging the spacecraft surfaces to a point where discharges occur. In designing future satellites for long term operation at geosynchronous altitude, it is important that designers have a specification that will give the total time per year, the particle flux density and particle energies that their satellites can be expected to encounter in these substorm environmental conditions. The limited data currently available on the environmental conditions are used to generate the provisional specification given in this report.

Author

N78-10174* National Aeronautics and Space Administration, Lewis Research Center, Cleveland, Ohio.

DEVELOPMENT OF ENVIRONMENTAL CHARGING EFFECT MONITORS FOR OPERATIONAL SATELLITES c15

N. John Stevens, John C. Sturman, and Frank D. Berkopec *In its Proc. of the Spacecraft Charging Technol. Conf.* 24 Feb. 1977 p 745-751 refs (For availability see N78-10129 01-12) Avail: NTIS HC A99/MF A01 CSCL 22B

Design details and design goals are given of an instrumentation package to monitor the effects of the environmental charging of spacecraft surfaces on the systems of operational spacecraft.

Author

N78-10175* National Aeronautics and Space Administration, Lewis Research Center, Cleveland, Ohio.

VIKING AND STP P78-2 ELECTROSTATIC CHARGING DESIGNS AND TESTING c15

R. O. Lewis, Jr. *In its Proc. of the Spacecraft Charging Technol. Conf.* 24 Feb. 1977 p 753-772 Lakewood, Colo. (For availability see N78-10129 01-12)

Avail: NTIS HC A99/MF A01 CSCL 22B

The design provisions of the Viking and the P78-2 (SCATHA) vehicles and a mathematical analysis of the effect of arcing on typical interface circuits are given. Results of verification testing of the analysis are presented as well as vehicle testing for tolerance to arcing.

Author

N78-16076* National Aeronautics and Space Administration, Lewis Research Center, Cleveland, Ohio

INTERACTION OF LARGE, HIGH POWER SYSTEMS WITH OPERATIONAL ORBIT CHARGED PARTICLE ENVIRONMENTS

Carolyn K. Purvis, N. John Stevens, and Frank D. Berkopec 1977 19 p refs Presented at the Meeting on Long Range Planning for the Ind. Phase of Space Exploration, San Francisco, 18-20 Oct. 1977. Sponsored by the Am Astronautical Soc (NASA-TM-73867; E-9459) Avail: NTIS HC A02/MF A01 CSCL 22A

A potentially hazardous spacecraft environment interaction is discussed. The interaction of large high voltage systems with low energy (less than 50 eV) plasmas which can result in loss of power and/or arcing was examined. The impact of this class of interactions where the ambient operation is most severe at low orbits where the ambient plasmas are densest. Results of experimental work and predictions of simple analytical models were presented and their implications for design of space systems were reviewed.

Author

N78-27142* National Aeronautics and Space Administration, Lewis Research Center, Cleveland, Ohio

INVESTIGATION OF MEANS FOR PERTURBING THE FLOW FIELD IN A SUPERSONIC WIND TUNNEL

Gary L. Cole and Warren R. Hingst Jun. 1978 30 p refs (NASA-TM-78954; E-9703) Avail: NTIS HC A03/MF A01 CSCL 14B

The development status of a device for generating atmospheric-type turbulences in supersonic inlet testing is summarized. Elaborated are desired aerodynamic and activation capabilities of the device, and the techniques that were considered and their drawbacks.

G.G.

N78-27143* National Aeronautics and Space Administration, Lewis Research Center, Cleveland, Ohio

DESIGN OF AN AIR EJECTOR FOR BOUNDARY-LAYER BLEED OF AN ACOUSTICALLY TREATED TURBOFAN ENGINE INLET DURING GROUND TESTING

Edward G. Etakolch Jun. 1978 21 p refs (NASA TM 78917; E-9655) Avail: NTIS HC A02/MF A01 CSCL 14B

An air ejector was designed and built to remove the boundary-layer air from the inlet a turbofan engine during an acoustic ground test program. This report describes: (1) how

the ejector was sized; (2) how the ejector performed; and (3) the performance of a scale model ejector built and tested to verify the design. With proper acoustic insulation, the ejector was effective in reducing boundary layer thickness in the inlet of the turbofan engine while obtaining the desired acoustic test conditions.

Author

N78-10180* Systems Science and Software, La Jolla, Calif. Plasma Physics Group.

DYNAMIC MODELING OF SPACECRAFT IN A COLLISIONLESS PLASMA c15

Ira Katz, Donald E. Parks, Sergio Wang, and Andrew Wilson *In NASA, Lewis Res. Center Proc. of the Spacecraft Charging Technol. Conf.* 24 Feb. 1977 p 319-330 refs (For availability see N78-10129 01-12)

(Contracts NAS3-20119; DNA001-76-C-0121)

Avail: NTIS HC A99/MF A01 CSCL 22B

A new computational model is described which can simulate the charging of complex geometrical objects in three dimensions. Two sample calculations are presented. In the first problem, the capacitance to infinity of a complex object similar to a satellite with solar array paddles is calculated. The second problem concerns the dynamic charging of a conducting cube partially covered with a thin dielectric film. In this calculation, the photoemission results in differential charging of the object.

Author

N78-14063* General Dynamics/Convair, San Diego, Calif. **CONCEPTUAL DESIGN FOR SPACELAB TWO-PHASE FLOW EXPERIMENTS**

R. D. Bradshaw and C. D. King Dec. 1977 88 p refs

(Contract NAS3-20389)

(NASA-CR-135327; CASD-NAS-77-025)

Avail: NTIS

HC A05/MF A01 CSCL 22A

KC-135 aircraft tests confirmed the gravity sensitivity of two phase flow correlations. The prime component of the apparatus is a 1.5 cm dia by 90 cm fused quartz tube test section selected for visual observation. The water-cabin air system with water recycle was a clear choice for a flow regime pressure drop test since it was used satisfactorily on KC-135 tests. Freon-11 with either overboard dump or with liquid-recycle will be used for the heat transfer test. The two experiments use common hardware. The experimental plan covers 120 data points in six hours with mass velocities from 10 to 640 kg/sec-sq m and qualities 0.01 to 0.64. The apparatus with pump, separator, storage tank and controls is mounted in a double spacelab rack. Supporting hardware, procedures, measured variables and program costs are defined.

Author

N78-20180* Kentucky Univ., Lexington. Boiling and Phase Change Lab.

CONCEPTUAL DESIGN FOR SPACELAB POOL BOILING EXPERIMENT

John H. Lienhard and Robert E. Peck Mar. 1978 71 p refs

(Contract NAS3-20397)

(NASA-CR-135378; UKY-TR106-78-ME15)

Avail: NTIS

HC A04/MF A01 CSCL 22A

A pool boiling heat transfer experiment to be incorporated with a larger two-phase flow experiment on Spacelab was designed to confirm (or alter) the results of earth-normal gravity experiments which indicate that the hydrodynamic peak and minimum pool boiling heat fluxes vanish at very low gravity. Twelve small sealed test cells containing water, methanol or Freon 113 and cylindrical heaters of various sizes are to be built. Each cell will be subjected to one or more 45 sec tests in which the surface heat flux on the heaters is increased linearly until the surface temperature reaches a limiting value of 500 C. The entire boiling process will be photographed in slow-motion. Boiling curves will be constructed from thermocouple and electric input data, for comparison with the motion picture records. The conduct of the experiment will require no more than a few hours of operator time.

Author

N78-25106* Business and Technological Systems, Inc.
Seabrook, Md.

**SEP ENCKE-87 AND HALLEY RENDEZVOUS STUDIES AND
IMPROVED S/C MODEL IMPLEMENTATION IN HILTOP
Final Report**

J. L. Horsewood and F. I. Mann Feb. 1978 29 p refs

(Contract NAS3-20850)

(NASA-CR-135414; BTS-TR-78-55-Pt-1) Avail. NTIS
HC A03/MF A01 CSCL 22A

Studies were conducted to determine the performance requirements for projected state-of-the-art SEP spacecrafts boosted by the Shuttle/IUS to perform a rendezvous with the comet Halley and a rendezvous with the comet Encke during its 1977 apparition. The spacecraft model of the standard HILTOP computer program was assumed. Numerical and graphical results summarizing the studies are presented. Author

N78-25106* Business and Technological Systems, Inc.
Seabrook, Md.

**HELIOCENTRIC INTERPLANETARY LOW THRUST TRAJECTORY
OPTIMIZATION PROGRAM. SUPPLEMENT 1,
PART 2 Final Report**

F. I. Mann and J. L. Horsewood Feb. 1978 103 p refs

(Contract NAS3-20850)

(NASA-CR-135414-App. BTS-TR-78-54-Suppl-1-Pt-2) Avail.
NTIS HC A06/MF A01 CSCL 22A

The improvements made to the HILTOP electric propulsion trajectory computer program are described. A more realistic propulsion system model was implemented in which various thrust subsystem efficiencies and specific impulse are modeled as variable functions of power available to the propulsion system. The number of operating thrusters are staged, and the beam voltage is selected from a set of five (or less) constant voltages, based upon the application of variational calculus. The constant beam voltages may be optimized individually or collectively. The propulsion system logic is activated by a single program input key in such a manner as to preserve the HILTOP logic. An analysis describing these features, a complete description of program input quantities, and sample cases of computer output illustrating the program capabilities are presented. Author

13 ASTRODYNAMICS

Includes powered and free-flight trajectories; and orbit and launching dynamics.

A78-32756 * * 12-cm magneto-electrostatic containment argon/xenon ion source development. W. D. Ramsey (Xerox Electro-Optical Systems, Pasadena, Calif.). *American Institute of Aeronautics and Astronautics and Deutsche Gesellschaft für Luft- und Raumfahrt, International Electric Propulsion Conference, 13th, San Diego, Calif., Apr. 25-27, 1978, AIAA Paper 78-681*. 9 p. 8 refs. Contract No. NAS3-20393.

The original 12 cm hexagonal magneto-electrostatic containment (MESC) discharge chamber described by Moore in 1969 has been optimized for argon and xenon operation. Argon mass utilization efficiencies of 65 to 77 percent were achieved at keeper plus main discharge energy consumptions of 244 to 422 eV/ion respectively. Xenon performance of 86 to 96 percent mass utilization were realized at 203 to 350 eV/ion. The paper discusses the optimization process and test results. (Author)

14 GROUND SUPPORT SYSTEMS AND FACILITIES (SPACE)

Includes launch complexes, research and production facilities, ground support equipment, e.g., mobile transporters, and simulators.

For related information see also *09 Research and Support Facilities (Air)*.

A78-37431 * * A mission profile life test facility. E. James (Xerox Electro-Optical Systems, Pasadena, Calif.), R. Vetrone, and R. Bechtel (NASA, Lewis Research Center, Cleveland, Ohio), *American Institute of Aeronautics and Astronautics and Deutsche Gesellschaft für Luft- und Raumfahrt, International Electric Propulsion Conference, 13th, San Diego, Calif., Apr. 25-27, 1978, AIAA Paper 78-671*, 10 p. Contract No. NAS3-20380.

A test facility is being prepared for a 16,000 hour mission profile life test of multiple electric propulsion thrust subsystems. The facility will be capable of simultaneously operating three 27 kW, 30 cm mercury ion thrusters and their power processing. The facility will permit conduction of a program of long-term tests to document thruster characteristics as a function of time and operating points to allow prediction of thruster performance for any mission profile. The thruster will be tested in a 7m by 10m vacuum chamber. Each thruster will be installed in a separate lock chamber so that it can be extended into, or extracted from the main chamber without violating the vacuum integrity of the other thruster. The thrusters will exhaust into a 3m by 5m frozen mercury target. The target and an array of cryopanels to collect sputtered target material will be liquid nitrogen chilled. Power processor units will be tested in an adjacent 1.5m by 2m vacuum chamber and will be temperature controlled by simulated heat pipes. (Author)

A78-37441 * * Economics of ion propulsion for large space systems. T. D. Masek, J. W. Ward (Hughes Research Laboratories, Malibu, Calif.) and V. K. Raelin (NASA, Lewis Research Center, Cleveland, Ohio), *American Institute of Aeronautics and Astronautics and Deutsche Gesellschaft für Luft- und Raumfahrt, International Electric Propulsion Conference, 13th, San Diego, Calif., Apr. 25-27, 1978, AIAA Paper 78-698*, 19 p. Contract No. NAS3-20101.

This study of advanced electrostatic ion thrusters for space propulsion was initiated to determine the suitability of the baseline 30-cm thruster for future missions and to identify other thruster concepts that would better satisfy mission requirements. The general scope of the study was to review mission requirements, select thruster designs to meet these requirements, assess the associated thruster technology requirements, and recommend short and long term technology directions that would support future thruster needs. Preliminary design concepts for several advanced thrusters were developed to assess the potential practical difficulties of a new design. This study produced useful general methodologies for assessing both planetary and earth orbit missions. For planetary missions, the assessment is in terms of payload performance as a function of propulsion system technology level. For earth orbit missions, the assessment is made on the basis of cost (cost sensitivity to propulsion system technology level). (Author)

15 LAUNCH VEHICLES AND SPACE VEHICLES

Includes booster, manned orbital laboratories, reusable vehicles, and space stations.

N78-13187* National Aeronautics and Space Administration
Lewis Research Center, Cleveland, Ohio

CTS (HERMES): UNITED STATES EXPERIMENTS AND OPERATIONS SUMMARY

Patrick L. Donoughe and Harry R. Hunczak. 1977. 27 p. refs. Presented at Symp. on Hermes (Communications Technol. Satellite), its Performance and Applications, Ottawa, 29 Nov-1 Dec 1977, sponsored by Royal Soc. of Canada, Canadian Dept. of Communications and NASA (NASA-TM-73830) Avail. NTIS HC A03/MF A01 CSCL 22A

The Communications Technology Satellite, launched in January 1976 and embodying the highest power transmitter in a communications satellite, was considered as a joint program between the U.S. and Canada, close coordination of the two countries was necessitated since the management and control of experiments were done in real time. Criteria used by NASA for acceptance of the United States experiments are noted and acceptance procedures are discussed. The category for each accepted experiment is given. The modes employed for the U.S. experiments in the areas of management, coordination, lesson, and real time operation are described. Some of the highlights associated with satellite utilization are given. Author.

N78-17127* National Aeronautics and Space Administration
Lewis Research Center, Cleveland, Ohio

PURGING OF A TANK-MOUNTED MULTILAYER INSULATION SYSTEM BY GAS DIFFUSION

Irving E. Sumner. Jan 1978. 59 p. refs. (NASA TP 1127 E-9286) Avail. NTIS HC A04/MF A01 CSCL 22B

The investigation was conducted on a multilayer insulation (MLI) system mounted on a spherical liquid hydrogen propellant tank. The MLI consisted of two blankets of insulation each containing 15 double-aluminized Mylar radiation shields separated by double silk net spacers. The gaseous nitrogen initially contained within the MLI system and vacuum chamber was purged with gaseous helium introduced both underneath the MLI and into the vacuum chamber. The MLI panels were assumed to be purged primarily by means of gas diffusion. Overall test results indicated that nitrogen concentrations well below 1 percent could be achieved everywhere within the MLI system. Typical times to achieve 1 percent nitrogen concentration within the MLI panels ranged from 69 minutes at the top of the tank to 158 minutes at the bottom of the tank. Four space hold thermal performance tests indicated no significant thermal degradation of the MLI system had occurred due to the purge tests conducted. The final measured heat input attributed to the MLI was 7.23 watts as compared to 7.18 watts for the initial baseline thermal performance test. Author.

N78-21188* National Aeronautics and Space Administration
Lewis Research Center, Cleveland, Ohio

THE PLASMA INTERACTION EXPERIMENT (PIX) DESCRIPTION AND TEST PROGRAM

Louis R. Ignaczak, Fred A. Halsey, Edward J. Domino, David H. Culp, and Francis J. Shekar. 1978. 20 p. Presented at the 13th Intern. Elec. Propulsion Conf., San Diego, Calif., 25-27 Apr 1978, cosponsored by AIAA and DGLK (NASA TM 78863 E-9594) Avail. NTIS HC A02/MF A01 CSCL 22A

The plasma interaction experiment (PIX) is a battery powered preprogrammed auxiliary payload on the LANDSAT-C launch. This experiment is part of a larger program to investigate space plasma interactions with spacecraft surfaces and components. The varying plasma densities encountered during available telemetry coverage periods are deemed sufficient to determine first order interactions between the space plasma environment

and the biased experimental surfaces. The specific objectives of the PIX flight experiment are to measure the plasma coupling current and the negative voltage breakdown characteristics of a solar array segment and a gold plated steel disk. Measurements will be made over a range of surface voltages up to plus or minus kilovolt. The orbital environment will provide a range of plasma densities. The experimental surfaces will be voltage biased in a preprogrammed step sequence to optimize the data returned for each plasma region and for the available telemetry coverage. Author.

N78-21189* National Aeronautics and Space Administration
Lewis Research Center, Cleveland, Ohio

COMPARISON OF REUSABLE INSULATION SYSTEMS FOR CRYOGENICALLY-TANKED EARTH-BASED SPACE VEHICLES

Irving E. Sumner and James R. Barber. 1978. 21 p. refs. Presented at 2d Thermophys. and Heat Transfer Conf., Palo Alto, Calif., 24-26 May 1978, cosponsored by AIAA and ASME (NASA-TM-73868 E-9192) Avail. NTIS HC A02/MF A01 CSCL 22B

Three reusable insulation systems concepts were developed for use with cryogenic tanks of earth-based space vehicles. Two concepts utilized double-goldized Kapton (DGK) or double-aluminized Mylar (DAM) multilayer insulation (MLI), while the third utilized a hollow-glass-microsphere, loadbearing insulation (LBI). Thermal performance measurements were made under space-hold (vacuum) conditions for insulating warm boundary temperatures of approximately 291 K. The resulting effective thermal conductivity was approximately 0.0006 W/m-K (W = weight, Kg m = measured, K = temperature) for the MLI systems (liquid hydrogen test results) and 0.00054 W/m-K for the LBI system (liquid nitrogen test results corrected to liquid hydrogen temperature). Author.

N78-28188* National Aeronautics and Space Administration
Lewis Research Center, Cleveland, Ohio

PRELIMINARY CONCEPT, SPECIFICATIONS, AND REQUIREMENTS FOR A ZERO-GRAVITY COMBUSTION FACILITY FOR SPACELAB

Richard L. DeWitt. Jun 1978. 51 p. refs. (NASA-TM-78910 E-9646) Avail. NTIS HC A04/MF A01 CSCL 22B

The preliminary concept, specifications, and requirements of a reusable zero gravity combustion facility (O-GCF) for use by experimenters aboard the spacelab payload of the space transportation system (STS) orbiter are described. The facility will be amenable to any mission of the STS orbiter in which a spacelab habitable segment and pallet segment are integral and for which orbital mission plans specify induced accelerations of 0.0001 g or less for sufficiently long periods so as not to impact experiment performance. Author.

N78-18144* George Inst. of Tech., Atlanta. Engineering Experiment Station

MILLIMETER WAVE SATELLITE CONCEPTS, VOLUME 1

Ned B. Hilsen, L. D. Holland, R. E. Thomas, R. W. Wallace, and J. G. Gallagher. Sep 1977. 238 p. refs.

(Contract NAS3-20110) (NASA-CR-135227, GT-A1855-Vol-1) Avail. NTIS HC A11/MF A01 CSCL 22B

The identification of technologies necessary for development of millimeter spectrum communication satellites was examined from a system point of view. Development of methodology based on the technical requirements of potential services that might be assigned to millimeter wave bands for identifying the viable and appropriate technologies for future NASA millimeter research and development programs and testing of this methodology with selected user applications and services were the goals of the program. The entire communications network, both ground and space subsystems was studied. Cost, weight, and performance models for the subsystems, conceptual design for point-to-point and broadcast communications satellites, and analytic relationships between subsystem parameters and an overall link performance

are discussed along with baseline conceptual systems, sensitivity studies, model adjustment analyses, identification of critical technologies and their risks, and brief research and development program scenarios for the technologies judged to be moderate or extensive risks. Identification of technologies for millimeter satellite communication systems, and assessment of the relative risks of these technologies, was accomplished through subsystem modeling and link optimization for both point-to-point and broadcast applications. Author

878-31141*/ Dayton Univ., Ohio. Research Inst.
CONTINUATION OF THE COMPENDIUM OF APPLICATIONS TECHNOLOGY SATELLITE AND COMMUNICATIONS TECHNOLOGY SATELLITE USER EXPERIMENTS 1967-1977. VOLUME 1 Final Report
 Nicholas A. Engler, John F. Nash, and Jerry D. Strange May 1978 203 p refs
 (Contract NAS3-20302)
 (NASA-CR-135416-Vol-1; UDR-TR-78-67-Vol-1) Avail: NTIS HC A10/MF A01 CSCL 22A

User experiments conducted utilizing the Applications Technology Satellites (ATS) 1, 3, 5, and 6 and the Communications Technology Satellites are summarized. The experiments are grouped by type of service offered. For example: education, health services, and data transmission. Particular emphasis is given to summarizing and evaluating user attitudes toward the ATS program. J.M.S.

878-31142*/ Dayton Univ., Ohio. Research Inst.
CONTINUATION OF THE COMPENDIUM OF APPLICATIONS TECHNOLOGY SATELLITE AND COMMUNICATIONS TECHNOLOGY SATELLITE USER EXPERIMENTS 1967-1977. VOLUME 2 Final Report
 Nicholas A. Engler, John F. Nash, and Jerry D. Strange May 1978 455 p refs
 (Contract NAS3-20382)
 (NASA-CR-135416-Vol-2; UDR-TR-78-67-Vol-2) Avail: NTIS HC A20/MF A01 CSCL 22A

Approximately 453 reports, papers, and articles catalogued into an information retrieval system, covering communications experiments and demonstrations conducted, utilizing the Communications Technology Satellite and the Applications Technology Satellites 1, 3, 5, and 6 are listed. J.M.S.

878-31143*/ Raytheon Co., Weyland, Mass. Microwave and Power Tube Div
DESIGN, FABRICATION AND TESTING OF A CFA FOR USE IN THE SCALAR POWER SATELLITE Final Report
 William C. Brown Aug 1978 152 p refs
 (Contract NAS3-20374)
 (NASA-CR 159410, PT-5228) Avail: NTIS HC A08/MF A01 CSCL 228

A crossed field amplifier was designed to meet the performance objectives of high signal to noise ratio, an efficiency of 85%, a CW microwave power output of 5-8 kW, and a frequency of 2450 MHz. The signal to noise ratio achieved was better than 60 db/MHz in a 2000 MHz band centered on the carrier. High circuit efficiency of 97% and a sharp knee on voltage current characteristic was achieved. The basic problem of maintaining good transfer of heat to the external radiator while providing for adequate connections to input and output was solved. Maximum efficiency achieved was 70.6% and gain and power level were below objectives. An investigation of causes of poor performance indicated the poor field pattern in the cathode anode interaction area of the tube was a major cause. B.B.

17 SPACECRAFT COMMUNICATIONS, COMMAND AND TRACKING

Includes telemetry; space communications networks; astro-
navigation; and radio blackout.

For related information see also *04 Aircraft Communi-
cations and Navigation* and *32 Communications*.

N78-28188* National Aeronautics and Space Administration,
Lewis Research Center, Cleveland, Ohio.

CARRIER-INTERFERENCE RATIOS FOR FREQUENCY SHARING BETWEEN FREQUENCY-MODULATED AMPLI- TITUDE-MODULATED-VESTIGIAL-SIDEBAND TELEVISION SYSTEMS

Scott P. Barnes and Edward F. Miller Aug. 1978 29 p refs
(NASA-TP-1264; E-9478) Avail: NTIS HCA03/MFA01 CSCL
17B

For just perceptible interference, an FM television signal interfering with another FM television signal must have an average signal power that is 26 to 37 db less than the wanted signal power. For an AM-VSB television signal interfering with an FM television signal, the AM-VSB television's sync peak average power must be 18 to 31 db below the FM television signal's average power. Also, when an FM television signal interferes with an AM-VSB signal, the average signal power of the FM signal should be 56 to 59 db below the sync peak average power of the AM-VSB television signal. The range of power ratios occur as a result of different TV scenes used in the tests and different FM-signal frequency deviations used. All tests were performed using 525 line, system M, color-television signals.

G.G.

N78-23137* National Aeronautics and Space Administration,
Lewis Research Center, Cleveland, Ohio.

THERMAL CHARACTERISTICS OF THE 12-GIGAWATT, 200-WATT OUTPUT STAGE TUBE FOR THE COMMUNICA- TION TECHNOLOGY SATELLITE

Arthur N. Curren Oct. 1978 39 p refs
(NASA-TP-1344; E-9560) Avail: NTIS HCA03/MFA01 CSCL
17B

A description of the methods used to measure component temperatures and heat-rejection rates in a simulated space environment on output stage tubes (OSTs) developed for the Communications Technology Satellite is presented along with summaries of experimentally determined values. The OSTs were operated over the entire anticipated operating drive range, from the dc beam (zero drive) condition to the 6-db overdrive condition. The baseplate temperature was varied from -10 to 58 C with emphasis placed on the testing done at 45 C, the normal anticipated operating temperature. The heat-rejection rate of the OST baseplate ranged from 7.6 W at the dc beam condition to 184.5 W at the 6-db overdrive condition, the heat-rejection rate of the multistage depressed collector (MDC) cover ranged from 192.2 to 155.9 W for the same conditions. The maximum OST temperature measured on the MDC cover was 227 C during a dc beam test. The minimum temperature measured, also on the MDC cover, was -67.5 C at the end of an extended simulated eclipse test period. No effects were observed on the OST thermal characteristics due to vibration testing or temperature-reversal cycle testing.

Author

18 SPACECRAFT DESIGN, TESTING AND PERFORMANCE

Includes spacecraft thermal and environmental control; and attitude control.

For life support systems see *54 Man/System Technology and Life Support*. For related information see also *05 Aircraft Design, Testing and Performance* and *39 Structural Mechanics*.

N78-21198* National Aeronautics and Space Administration, Lewis Research Center, Cleveland, Ohio.

CHARGING OF FLEXIBLE SOLAR ARRAY SUBSTRATES IN KILOVOLT ELECTRON BEAMS

John V. Stekous and Steven J. Narciso Mar. 1978 32 p refs (NASA-TM-73865; E-9455) Avail: NTIS HC A03/MF A01 CSDL 10A

A series of survey tests were conducted to evaluate samples of flexible solar arrays. The samples used woven carbon fibers and/or coatings to increase the surface conductivity of the KAPTON substrate and thereby reduce surface charging. Four different samples were evaluated by exposing them to monoenergetic electron beams of 2 to 20 KeV at a current density of 1 nA sq cm. Simulated eclipse tests were also conducted. The results were as expected: the more continuous the conductive pattern, the lower the surface charging. Author

A78-19567* NASCAP, a three-dimensional Charging Analyzer Program for complex spacecraft. I. Katz, D. E. Parks, M. J. Mandell, J. M. Harvey, S. S. Wang (Systems Science and Software, La Jolla, Calif.), and J. C. Roche (NASA, Lewis Research Center, Cleveland, Ohio). (*Institute of Electrical and Electronics Engineers, Annual Conference on Nuclear and Space Radiation Effects, 14th, Williamsburg, Va., July 12-15, 1977.*) *IEEE Transactions on Nuclear Science*, vol. NS-24, Dec. 1977, p. 2276-2280.

A computer code, NASCAP (NASA Charging Analyzer Program), has been developed by Systems, Science and Software under contract to NASA-LeRC to simulate the charging of a complex spacecraft in geosynchronous orbit. The capabilities of the NASCAP code include a fully three-dimensional solution of Poisson's equation about an object having considerable geometrical and material complexity, particle tracking, shadowing in sunlight, calculation of secondary emission, backscatter and photoemission, and graphical output. A model calculation shows how the NASCAP code may be used to improve our understanding of the spacecraft-plasma interaction. (Author)

A78-33220* NASA Charging Analyzer Program - A computer tool that can evaluate electrostatic contamination. N. J. Stevens, J. C. Roche (NASA, Lewis Research Center, Cleveland, Ohio), and M. J. Mandell (Systems, Science and Software, La Jolla, Calif.). *U.S. Air Force and NASA, International Spacecraft Contamination Conference, Colorado Springs, Colo., Mar. 7-9, 1978, Paper 13* p. 17 refs.

The data from the ATS 5 and 6 Auroral Particles Experiments have shown that the environment at geosynchronous orbit can charge spacecraft surfaces to appreciable negative values. Such surface charges could have undesirable effects on satellite equipment and the data obtained in satellite experiments. A computer program, the NASA Charging Analyzer Program (NASCAP), has, in this connection, been developed to determine the surface charging of spacecraft when encountering geomagnetic substorm conditions. Once a model of a spacecraft has been developed in the NASCAP code, the surface charging can be computed for any environmental input flux. On the basis of the obtained information regarding the surface charging, charged particle trajectories can be computed to determine if it is possible for a particle to return to a satellite surface. It is pointed out that the computer runs conducted with the NASCAP code represent the first attempts to use a self-consistent program to study the behavior of spacecraft surfaces experiencing a geomagnetic substorm condition. G.R.

A78-35590* Evaluation of commercially-available spacecraft-type heat pipes. W. B. Kaufman and L. K. Tower (NASA, Lewis Research Center, Cleveland, Ohio). In: *International Heat Pipe Conference, 3rd, Palo Alto, Calif., May 22-24, 1978, Technical Papers. (A78-35576 14-34)* New York, American Institute of Aeronautics and Astronautics, Inc., 1978, p. 88-95. 5 refs. (AIAA 78-397)

As part of an effort to develop reliable, cost effective spacecraft thermal control heat pipes, Lewis Research Center of NASA is conducting life tests on 30 commercially-available heat pipes in 10 groups of different design and material combinations. Materials are aluminum and stainless steel, and working fluids are methanol and ammonia. The formation of noncondensable gas is observed for times exceeding 11,000 hours. The heat transport capacities of the pipes are also determined. Considerable gas is found in two groups of methanol pipes; one group shows no gas. One group of ammonia pipes has no observable gas. Another group has much gas. Manufacturers' processing schedules are examined for differences explaining the presence of gas. Heat transport capacity is found to be severely reduced in some pipes containing gas. (Author)

A78-36004* Comparison of reusable insulation systems for cryogenically-tanked earth-based space vehicles. I. E. Sumner and J. R. Barber (NASA, Lewis Research Center, Cleveland, Ohio). *American Institute of Aeronautics and Astronautics and American Society of Mechanical Engineers, Thermophysics and Heat Transfer Conference, 2nd, Palo Alto, Calif., May 24-26, 1978, AIAA Paper 78-877. 15 p. 8 refs.*

Three reusable insulation systems concepts have been developed for use with cryogenic tanks of earth-based space vehicles. Two concepts utilized double-goldized Kapton (DGK) or double-aluminized Mylar (DAM) multilayer insulation (MLI), while the third utilized a hollow-glass-microsphere, load-bearing insulation (LBI). All three insulation systems have recently undergone experimental testing and evaluation under NASA-sponsored programs. Thermal performance measurements were made under space-hold (vacuum) conditions for insulation warm boundary temperatures of approximately 291 K. The resulting effective thermal conductivity was approximately .00008 W/m-K for the MLI systems (liquid hydrogen test results) and .00054 W/m-K for the LBI system (liquid nitrogen test results corrected to liquid hydrogen temperature). The DGK MLI system experienced a maximum thermal degradation of 38 percent, the DAM MLI system 14 percent, and the LBI system 6.7 percent due to repeated thermal cycling representing typical space flight conditions. Repeated exposure of the DAM MLI system to a high humidity environment for periods as long as 8 weeks provided a maximum degradation of only 24 percent. (Author)

A78-36719* Interaction of large, high power systems with operational orbit charged particle environments. C. K. Purvis, N. J. Stevens, and F. D. Berkopec (NASA, Lewis Research Center, Cleveland, Ohio). In: *The Industrialization of Space; Proceedings of the Twenty-third Annual Meeting, San Francisco, Calif., October 18-20, 1977, Part 1. (A78-36701 15-12)* San Diego, Calif., American Astronautical Society; Univelt, Inc., 1978, p. 429-446. 18 refs. (AAS 77-243)

Concepts are presently being advanced for space systems to be used for such activities as manufacturing, earth observations, scientific exploration, power generation and human habitation, in locations ranging from low earth orbit (300-500 km) to geosynchronous orbit and beyond. Many of these systems concepts envision large structures and high power levels, and consequently higher operating voltages than have been used in space to date. The potential impact of interactions of space systems with their operational orbit charged particle environments on the systems' performance must be accounted for in the design process. A potentially hazardous spacecraft-environment interaction is discussed, namely the interaction of large high voltage systems with low energy (less than 50 eV) plasmas which can result in loss of power, and/or arcing. The impact of this class of interactions on system operation is most severe at low orbits where the ambient plasmas are densest. Results of experimental work and predictions of simple analytical models are presented and their implications for design of space systems are discussed. (Author)

A78-43500 * # **Effect of vibration on retention characteristics of screen acquisition systems.** J. R. Tegart (Martin Marietta Aerospace, Denver, Colo.) and J. C. Aydelott (NASA, Lewis Research Center, Cleveland, Ohio). *American Institute of Aeronautics and Astronautics and Society of Automotive Engineers, Joint Propulsion Conference, 14th, Las Vegas, Nev., July 25-27, 1978, AIAA Paper 78-1030* 12 p. 8 refs. Contract No. NAS3-20097.

The design of surface tension propellant acquisition systems using fine-mesh screen must take into account all factors that influence the liquid pressure differentials within the system. One of those factors is spacecraft vibration. Analytical models to predict the effects of vibration have been developed. A test program to verify the analytical models and to allow a comparative evaluation of the parameters influencing the response to vibration was performed. Screen specimens were tested under conditions simulating the operation of an acquisition system, considering the effects of such parameters as screen orientation and configuration, screen support method, screen mesh, liquid flow and liquid properties. An analytical model, based on empirical coefficients, was most successful in predicting the effects of vibration. (Author)

A78-14991 * # **ADDJUST - An automated system for steering Centaur launch vehicles in measured winds.** D. C. Swanson (General Dynamics Corp., Convair Div., San Diego, Calif.). In: *Conference on Aerospace and Aeronautical Meteorology, 7th, and Symposium on Remote Sensing from Satellites, Melbourne, Fla., November 16-19, 1976, Preprints. (A78-14952 03-47)* Boston, Mass., American Meteorological Society, 1977, p. 210-213. Contract No. NAS3-13514.

ADDJUST (Automatic Determination and Dissemination of Just-Updated Steering Terms) is an automated computer and communication system designed to provide Atlas/Centaur and Titan Centaur launch vehicles with booster-phase steering data on launch day. Wind soundings are first obtained, from which a smoothed wind velocity vs altitude relationship is established. Design for conditions at the end of the boost phase with initial pitch and yaw maneuvers, followed by zero total angle of attack through the filtered wind establishes the required vehicle attitude as a function of altitude. Polynomial coefficients for pitch and yaw attitude vs altitude are determined and are transmitted for validation and loading into the Centaur airborne computer. The system has enabled 14 consecutive launches without a flight wind delay. V.P.

A78-36005 * # **An ultralightweight, evacuated, load-bearing, high-performance insulation system.** R. T. Parmley and G. R. Cunningham, Jr. (Lockheed Research Laboratories, Palo Alto, Calif.). *American Institute of Aeronautics and Astronautics and American Society of Mechanical Engineers, Thermophysics and Heat Transfer Conference, 2nd, Palo Alto, Calif., May 24-26, 1978, AIAA Paper 78-878* 6 p. 19 refs. Contract No. NAS3 17817.

A new hollow glass microsphere insulation and a flexible stainless steel vacuum jacket were demonstrated on a flight-weight cryogenic test tank, 1.17 m in diameter. The weight of the system is three times lighter than the most advanced vacuum-jacketed design demonstrated to date, a free-standing honeycomb hard shell with a multilayer insulation system (for a Space Tug application). Design characteristics of the flexible vacuum jacket are presented along with a model describing the insulation thermal performance as a function of boundary temperatures and emittance, compressive load on the insulation and insulation gas pressure. Test data are compared with model predictions and with prior flat-plate calorimeter test results. Potential applications for this insulation system or a derivative of this system include the cryogenic Space Tug, the Single-Stage-to-Orbit Space Shuttle, LH₂ fueled subsonic and hypersonic aircraft, and LNG applications. (Author)

19 SPACECRAFT INSTRUMENTATION

For related information see also *06 Aircraft Instrumentation* and *35 Instrumentation and Photography*.

N78-17148* National Aeronautics and Space Administration, Lewis Research Center, Cleveland, Ohio.

DESIGN AND FABRICATION OF A LOW-SPECIFIC-WEIGHT PARABOLIC DISH SOLAR CONCENTRATOR

Carl W. Richter, Arthur G. Birchenough, Gerald A. Marquis, and Thaddeus S. Mroz Jan. 1978 18 p refs
(NASA-TP-1152; E-9339) Avail: NTIS HC A02/MF A01 CSCL 10A

A segmented design and fabrication and assembly techniques were developed for a 1.8 m (6 ft) diameter parabolic concentrator for space application. This design and these techniques were adaptable to a low cost, mass-produced concentrator. Minimal machining was required. Concentrator segments of formed magnesium were used. The concentrator weighed only 1.6 kg/sq m (0.32 lbf/sq ft). Author

A78-19566* Summary of the CTS Transient Event Counter data after one year of operation. N. J. Stevens, V. W. Klinec (NASA, Lewis Research Center, Cleveland, Ohio), and J. V. Gore (NASA, Lewis Research Center, Cleveland, Ohio; Department of Communications, Communications Research Centre, Ottawa, Canada). (*Institute of Electrical and Electronics Engineers, Annual Conference on Nuclear and Space Radiation Effects, 14th, Williamsburg, Va., July 12-15, 1977*) *IEEE Transactions on Nuclear Science*, vol. NS-24, Dec. 1977, p. 2270-2275. 16 refs.

The environmental charging of satellite surfaces during geomagnetic substorms is the apparent cause of a significant number of anomalous events occurring on geosynchronous satellites since the early 1970's. Electromagnetic pulses produced in connection with the differential charging of insulators can couple into the spacecraft harness and cause electronic switching anomalies. An investigation conducted to determine the response of the spacecraft surfaces to substorm particle fluxes makes use of a harness transient detector. The harness transient detector, called the Transient Event Counter (TEC) was built and integrated into the Canadian-American Communications Technology Satellite (CTS). A description of the TEC and its operational characteristics is given and the obtained data are discussed. The data show that the satellite surfaces appear to be charged to the point that discharges occur and that the discharge-induced transients couple into the wire harnesses. G.R.

20 SPACECRAFT PROPULSION AND POWER

Includes main propulsion systems and components, e.g., rocket engines; and spacecraft auxiliary power sources.

For related information see also 07 Aircraft Propulsion and Power, 28 Propellants and Fuels, and 44 Energy Production and Conversion.

N78-13124* National Aeronautics and Space Administration, Lewis Research Center, Cleveland, Ohio.

HYDROGEN FILM COOLING OF A SMALL HYDROGEN-OXYGEN THRUST CHAMBER AND ITS EFFECT ON EROSION RATES OF VARIOUS ABLATIVE MATERIALS
Ned Hannum, William E. Roberts, and Louis M. Russell Dec. 1977 27 p refs

(NASA-TP-1098; E-8909) Avail: NTIS HC A03/MF A01 CSDL 21H

An experimental investigation was conducted to determine what arrangement of film-coolant injection orifices should be used to decrease the erosion rates of small, high temperature, high pressure ablative thrust chambers without incurring a large penalty in combustion performance. All of the film cooling was supplied through holes in a ring between the outer row of injector elements and the chamber wall. The best arrangement, which had twice the number of holes as there were outer row injection elements, was also the simplest. The performance penalties, presented as a reduction in characteristic exhaust velocity efficiency, were 0.8 and 2.8 percentage points for the 10 and 20 percent cooling flows, respectively. The best film-coolant injector was then used to obtain erosion rates for 19 ablative materials. The throat erosion rate was reduced by a factor of 2.5 with a 10 percent coolant flow. Only the more expensive silica phenolic materials had low enough erosion rates to be considered for use in the nozzle throat. However, some of the cheaper materials might qualify for use in other areas of small nozzles with large throat diameters where the higher erosion rates are more acceptable.

Author

N78-18089* National Aeronautics and Space Administration, Lewis Research Center, Cleveland, Ohio.

LIQUID ROCKET LINES, BELLOWES, FLEXIBLE HOSES, AND FILTERS NASA Space Vehicle Design Criteria (Chemical Propulsion)

Apr 1977 186 p refs Prepared by Hosiastyme, Canoga Park, Calif.

(NASA-SP-8123) Avail: NTIS HC A09/MF A01 CSDL 21H

Fluid-flow components in a liquid propellant rocket engine and the rocket vehicle which it propels are interconnected by lines, bellows, and flexible hoses. Elements involved in the successful design of these components are identified and current technologies pertaining to these elements are reviewed, assessed, and summarized to provide a technology base for a checklist of rules to be followed by project managers in guiding a design or assessing its adequacy. Recommended procedures for satisfying each of the design criteria are included.

A.R.H.

N78-20251* National Aeronautics and Space Administration, Lewis Research Center, Cleveland, Ohio.

STATUS OF SERT II SPACECRAFT AND ION THRUSTERS, 1978

W. R. Kerslake and L. R. Igneczek 1978 10 p refs Presented at the 13th Intern. Elec. Propulsion Conf., San Diego, Calif., 25-27 Apr. 1978; sponsored in part by AIAA and DGLR (NASA-TM-78827; E-9531) Avail: NTIS HC A02/MF A01 CSDL 21C

The historical record of the SERT 2 spacecraft and ion thruster systems for 8 years since the February 1970 launch is reviewed. The original SERT 2 mission, one year duration, was planned with the spacecraft in a continuous sunlight orbit to provide continuous solar power. An extended mission, using intermittent power available from an earth shadowed orbit was performed during the past 5 years while waiting for the orbit to change again to continuous sunlight in early 1979. Continuous thruster

testing is planned in 1979. Both spacecraft and ion thruster systems are near-fully functional when the solar array is illuminated. Thruster system 2 is fully operational. Thruster system 1 continues to demonstrate reight capability, but the high-voltage-grid short remains.

Author

N78-21202* National Aeronautics and Space Administration, Lewis Research Center, Cleveland, Ohio.

EVOLUTION OF THE 1-mib MERCURY ION THRUSTER SUBSYSTEM

W. R. Kerslake and B. A. Banks 1978 25 p refs Presented at the 13th Intern. Elec. Propulsion Conf., San Diego, Calif., 25-27 Apr. 1978; cosponsored by AIAA and DGLR (NASA-TM-73733; E-9278) Avail: NTIS HC A02/MF A01 CSDL 21C

The developmental history, performance, and major lifetests of each component of the present 1-mib (4.5 mN) thruster system are traced over the past 10 years. The 1-mib thruster subsystem consists of an 8 cm diameter ion thruster mounted on 2 axis gimbels, a mercury propellant tank, a power electronics unit, a controller/digital interface unit, and necessary electrical harnesses plus propellant tankage and feed lines.

Author

N78-21203* National Aeronautics and Space Administration, Lewis Research Center, Cleveland, Ohio.

PULSE IGNITION CHARACTERIZATION OF MERCURY ION THRUSTER HOLLOW CATHODE USING AN IMPROVED PULSE IGNITOR

E. G. Wintucky and R. P. Gruber 1978 20 p refs Presented at the 13th Intern. Elec. Propulsion Conf., San Diego, Calif., 25-27 Apr. 1978; cosponsored by AIAA and DGLR (NASA-TM-78858; E-9592) Avail: NTIS HC A02/MF A01 CSDL 21C

An investigation of the high voltage pulse ignition characteristics of the 8 cm mercury ion thruster neutralizer cathode identified a low rate of voltage rise and long pulse duration as desirable factors for reliable cathode starting. Cathode starting breakdown voltages were measured over a range of mercury flow rates and tip heater powers for pulses with five different rates of voltage rise. Breakdown voltage requirements for the fastest rising pulse (2.5 to 3.0 kV/micro sec) were substantially higher (2 kV or more) than for the slowest rising pulse (0.3 to 0.5 kV/micro sec) for the same starting conditions. Also described is an improved, low impedance pulse ignitor circuit which reduces power losses and eliminates problems with control and packaging associated with earlier designs.

Author

N78-21204* National Aeronautics and Space Administration, Lewis Research Center, Cleveland, Ohio.

PLANNED FLIGHT TEST OF A MERCURY ION AUXILIARY PROPULSION SYSTEM. 1: OBJECTIVES, SYSTEMS DESCRIPTIONS, AND MISSION OPERATIONS

John C. Power 1978 46 p refs Presented at the 13th Intern. Elec. Propulsion Conf., San Diego, Calif., 25-27 Apr. 1978; cosponsored by AIAA and DGLR

(NASA-TM-78859; E-9589) Avail: NTIS HC A03/MF A01 CSDL 21C

A planned flight test of an 8 cm diameter, electron-bombardment mercury ion thruster system is described. The primary objective of the test is to flight qualify the 5 mN (1 mib.) thruster system for auxiliary propulsion applications. A seven year north-south stationkeeping mission was selected as the basis for the flight test operating profile. The flight test, which will employ two thruster systems, will also generate thruster system space performance data, measure thruster-spacecraft interactions, and demonstrate thruster operation in a number of operating modes. The flight test is designated as SAMSO-601 and will be flown aboard the shuttle-launched Air Force space test program P80-1 satellite in 1981. The spacecraft will be 3-axis stabilized in its final 740 km circular orbit, which will have an inclination of approximately greater than 73 degrees. The spacecraft design lifetime is three years.

Author

N78-21208* National Aeronautics and Space Administration, Lewis Research Center, Cleveland, Ohio.

EFFECT OF FACILITY BACKGROUND GASES ON INTERNAL EROSION OF THE 30-cm Hg ION THRUSTER

Vincent K. Rawlin and Maris A. Mentenicks 1978 31 p refs Presented at the 13th Intern. Elec. Propulsion Conf., San Diego, Calif., 25-27 Apr. 1978; sponsored by AIAA and DGLR (NASA-TM-78803; E-9584; AIAA-78-665) Avail: NTIS HC A03/MF A01 CSCL 21C

Sputtering erosion of the upstream side of the molybdenum screen grid by discharge chamber ions in mercury bombardment thrusters was considered. Data which revealed that the screen grid erosion was very sensitive to the partial pressure of certain background gases in the space simulation vacuum facility were presented along with results of tests conducted to evaluate this effect. It is shown from estimates of the screen grid erosion in space that adequate lifetime for proposed missions exists.

Author

N78-21208* National Aeronautics and Space Administration, Lewis Research Center, Cleveland, Ohio.

A REVIEW OF ELECTRON BOMBARDMENT THRUSTER SYSTEMS/SPACECRAFT FIELD AND PARTICLE INTERFACES

David C. Byers 1978 36 p refs Presented at the 13th Intern. Elec. Propulsion Conf., San Diego, Calif., 25-27 Apr. 1978; sponsored by AIAA and DGLR (NASA-TM-78850; E-9571) Avail: NTIS HC A03/MF A01 CSCL 21C

Information on the field and particle interfaces of electron bombardment ion thruster systems was summarized. Major areas discussed were the nonpropellant particles, neutral propellant, ion beam, low energy plasma, and fields. Spacecraft functions and subsystems reviewed were solar arrays, thermal control systems, optical sensors, communications, science, structures and materials, and potential control.

Author

N78-21207* National Aeronautics and Space Administration, Lewis Research Center, Cleveland, Ohio.

DIAGNOSTIC EVALUATIONS OF A BEAM-SHIELDED 8-cm MERCURY ION THRUSTER

S. Nakaniishi 1978 25 p refs Presented at the 13th Intern. Elec. Propulsion Conf., San Diego, Calif., 25-27 Apr. 1978; sponsored by AIAA and DGLR (NASA-TM-78855; E-9581) Avail: NTIS HC A02/MF A01 CSCL 21C

An engineering model thruster fitted with a remotely actuated graphite fiber polyimide composite beam shield was tested in a 3- by 8.5-meter vacuum facility for in situ assessment of beam shield effects on thruster performance. Accelerator drain current neutralizer floating potential and ion beam floating potential increased slightly when the shield was moved into position. A target exposed to the low density regions of the ion beam was used to map the boundaries of energetic fringe ions capable of sputtering. The particle efflux was evaluated by measurement of film deposits on cold, heated, bare, and enclosed glass slides.

Author

N78-21208* National Aeronautics and Space Administration, Lewis Research Center, Cleveland, Ohio.

THE 5200 CYCLE TEST OF AN 8-cm DIAMETER Hg ION THRUSTER

M. A. Mentenicks and E. G. Wintucky 1978 27 p refs Presented at the 13th Intern. Elec. Propulsion Conf., San Diego, Calif., 25-27 Apr. 1978; sponsored by AIAA and DGLR (NASA-TM-78860; E-9590) Avail: NTIS HC A03/MF A01 CSCL 21C

An accelerated cycle test was conducted in which an 8-cm Engineering Model Thruster (EMT) prototype successfully completed 5200 on-off cycles and a total of more than 1300 hours of thruster operation at a 4.5 mN thrust level. Cathode tip heater powers required for starting and keeper voltages

remained well within acceptable limits. The discharge chamber utilization and electrical efficiency were nearly constant over the duration of the test. It was concluded that on-off cyclic operation by itself does not appreciably degrade starting capability or performance of the 8-cm EMT.

Author

N78-21208* National Aeronautics and Space Administration, Lewis Research Center, Cleveland, Ohio.

PLANNED FLIGHT TEST OF A MERCURY ION AUXILIARY PROPULSION SYSTEM. PART 2: INTEGRATION WITH HOST SPACECRAFT

Rodney M. Knight 1978 16 p refs Presented at the 13th Intern. Elec. Propulsion Conf., San Diego, Calif., 25-27 Apr. 1978; sponsored by AIAA and DGLR (NASA-TM-78869; E-9599) Avail: NTIS HC A02/MF A01 CSCL 21C

The objectives of the flight test and a description on how those objectives are in support of an overall program goal of attaining user application were described. The approach to accomplishment was presented as it applies to integrating the propulsion system with the host spacecraft. A number of known interface design considerations which affect the propulsion system and the spacecraft were discussed. Analogies were drawn comparing the relationship of the organizations involved with this flight test with those anticipated for future operational missions. The paper also expanded upon objectives, system description, mission operations, and measurement of plume effects.

Author

N78-21211* National Aeronautics and Space Administration, Lewis Research Center, Cleveland, Ohio.

LIQUID ROCKET ENGINE SELF-COOLED COMBUSTION CHAMBERS Space Vehicle Design Criteria

Sep. 1977 130 p refs (NASA-SP-8124) Avail: NTIS HC A07/MF A01 CSCL 21H

Self-cooled combustion chambers are chambers in which the chamber wall temperature is controlled by methods other than fluid flow within the chamber wall supplied from an external source. In such chambers, adiabatic wall temperature may be controlled by use of upstream fluid components such as the injector or a film-coolant ring, or by internal flow of self-contained materials; e.g. pyrolysis gas flow in charring ablaters, and the flow of infiltrated liquid metals in porous matrices. Five types of self-cooled chambers are considered in this monograph. The name identifying the chamber is indicative of the method (mechanism) by which the chamber is cooled, as follows: ablative; radiation cooled; internally regenerative (intergen); heat sink; adiabatic wall. Except for the intergen and heat sink concepts, each chamber type is discussed separately. A separate and final section of the monograph deals with heat transfer to the chamber wall and treats Stanton number evaluation, film cooling, and film-coolant injection techniques, since these subjects are common to all chamber types. Techniques for analysis of gas film cooling and liquid film cooling are presented.

Author

N78-22148* National Aeronautics and Space Administration, Lewis Research Center, Cleveland, Ohio.

CLOSED LOOP SOLAR ARRAY-ION THRUSTER SYSTEM WITH POWER CONTROL CIRCUITRY Patent Application

Robert P. Gruber, inventor (to NASA) Filed 29 Mar. 1978 20 p (NASA-Case-LEW-12780-1; US-Patent-Appl-SN-891370) Avail: NTIS HC A02/MF A01 CSCL 21C

A solar array-ion thruster system is described which includes a power control circuit that permits use of the thruster itself in operating the solar array at its maximum power point. The power control circuit, connected between the solar array and the ion thruster and receiving voltage and current signals from the former, multiplies the voltage and current signals together to produce a power signal which is differentiated with respect to time. The differentiator output is detected by a zero crossing detector and, after suitable shaping, the detector output is

phase compared with a crack in a phase demodulator. An integrator receives no output from the phase demodulator when the operating point is at the maximum power point, but is driven toward the maximum power point for non-optimum operation. A ramp generator provides minor variations in the beam current reference signal produced by the integrator in order to obtain the first derivative of power. NASA

N78-23142* National Aeronautics and Space Administration, Lewis Research Center, Cleveland, Ohio.
A MECHANICAL THERMAL AND ELECTRICAL PACKAGING DESIGN FOR A PROTOTYPE POWER MANAGEMENT AND CONTROL SYSTEM FOR THE 30 cm MERCURY ION THRUSTER

G. Richard Sharp, Louis Gadeon, Jon C. Oglebay, Francis S. Shaker, and Clifford E. Siegert 1978 31 p refs Presented at the 13th Intern. Elec. Propulsion Conf., San Diego, Calif., 25-27 Apr. 1978; sponsored by AIAA and DGLR (NASA-TM-78862; E-9593) Avail: NTIS HC A03/MF A01 CSDL 21C

A prototype electric power management and thruster control system for a 30 cm ion thruster is described. The system meets all of the requirements necessary to operate a thruster in a fully automatic mode. Power input to the system can vary over a full two to one dynamic range (200 to 400 V) for the solar array or other power source. The power management and control system is designed to protect the thruster, the flight system and itself from arcs and is fully compatible with standard spacecraft electronics. The system is easily integrated into flight systems which can operate over a thermal environment ranging from 0.3 to 5 AU. The complete power management and control system measures 45.7 cm (18 in.) x 15.2 cm (6 in.) x 114.8 cm (45.2 in.) and weighs 36.2 kg (79.7 lb). At full power the overall efficiency of the system is estimated to be 87.4 percent. Three systems are currently being built and a full schedule of environmental and electrical testing is planned. Author

N78-23143* National Aeronautics and Space Administration, Lewis Research Center, Cleveland, Ohio.

A 30-cm MERCURY ION THRUSTER PERFORMANCE WITH A 1 kW CAPACITOR-DIODE VOLTAGE MULTIPLIER BEAM SUPPLY

F. F. Terdan and W. T. Harrigill, Jr. 27 Apr. 1978 17 p refs Presented at the 13th Intern. Elec. Propulsion Conf., San Diego, Calif., 25-27 Apr. 1978; sponsored by AIAA and DGLR (NASA-TM-78864; E-9595; AIAA-Paper-78-886) Avail: NTIS HC A02/MF A01 CSDL 21C

A 1 kW solar array and capacitor-diode voltage multiplier converter (S/A-CDVM) was successfully integrated with a 30 cm diameter mercury ion thruster system to provide ion beam power. Measurements were made to compare steady state and transient response performance of a conventional bridge converter with the S/A-CDVM converter used for the ion beam supply. The ability to recover from screen to accelerator arcs and promptly re-establish stable thruster performance was demonstrated. Solar array transient response to thruster arcing was measured. Author

N78-23144* National Aeronautics and Space Administration, Lewis Research Center, Cleveland, Ohio.

SENSITIVITY OF 30-cm MERCURY BOMBARDMENT ION THRUSTER CHARACTERISTICS TO ACCELERATOR GRID DESIGN

V. K. Rawlin 1978 29 p refs Presented at the 13th Intern. Elec. Propulsion Conf., San Diego, Calif., 25-27 Apr. 1978; sponsored by AIAA and DGLR (NASA-TM-78861; E-9591; AIAA-Paper-78-868) Avail: NTIS HC A03/MF A01 CSDL 21C

The design of ion optics for bombardment thrusters strongly influences overall performance and lifetime. The operation of a 30 cm thruster with accelerator grid open area fractions ranging from 43 to 24 percent, was evaluated and compared with experimental and theoretical results. Ion optics properties measured included the beam current extraction capability, the minimum accelerator grid voltage to prevent backstreaming, ion

beamlet diameter as a function of radial position on the grid and accelerator grid hole diameter, and the high energy, high angle ion beam edge location. Discharge chamber properties evaluated were propellant utilization efficiency, minimum discharge power per beam amp, and minimum discharge voltage. Author

N78-26173* National Aeronautics and Space Administration, Lewis Research Center, Cleveland, Ohio.

INVESTIGATION OF THE EFFECT OF CERAMIC COATINGS ON ROCKET THRUST CHAMBER LIFE

R. J. Quentmeyer, H. J. Kasper, and J. M. Kazaroff 1978 26 p refs Presented at the 14th Propulsion Conf., Las Vegas, Nev., 25-27 Jul. 1978; sponsored by AIAA and the Soc. of Automotive Engr. (NASA-TM-78892; E-9630; AIAA-Paper-78-1034) Avail: NTIS HC A03/MF A01 CSDL 21H

Cylindrical rocket thrust chamber cylinders were coated with a 0.203 mm (0.008 in.) layer of zirconium oxide using a process that employed electrodeposition of metal to a spray coated mandrel. The cylinders were cyclically tested using hydrogen oxygen propellants at a nominal chamber pressure of 4.14 MN/sq m (600 psia) to show the effect of the coating on life. Both cylinders failed prematurely due to causes unrelated to the coatings. Post destructive analysis showed no cooling passage wall deformation. Where erosion of the coating occurred, the coating thickness stabilized at 0.081 mm (0.0024 in.) within 80 cycles and remained well adhered throughout the tests.

Author

N78-27170* National Aeronautics and Space Administration, Lewis Research Center, Cleveland, Ohio.

STATUS OF THE NASA-LEWIS RESEARCH CENTER SPACECRAFT CHARGING INVESTIGATION

N. John Stevens, Frank D. Berkopac, and Carolyn K. Purvis 1978 25 p refs Presented at the Spacecraft Electromagnetic Compatibility Seminar, Noordwijk, The Netherlands, 24-26 May 1978; sponsored by the European Space Research and Technology Centre (ESTEC) (NASA-TM-78938; E-9682) Avail: NTIS HC A02/MF A01 CSDL 22B

The technology necessary to control the absolute and differential charging of spacecraft surfaces is detailed for developing ground simulation facilities, characterizing the charging and discharging characteristics of spacecraft materials, deriving analytical modelling tools and issuing design guideline documents. Facilities were developed and testing of various materials was completed. Comparisons between experimental results, space results and predictions from models were made. Harness transient monitors were flown on satellites. G.G.

N78-27174* National Aeronautics and Space Administration, Lewis Research Center, Cleveland, Ohio.

PERFORMANCE OF A THERMIONIC CONVERTER MODULE UTILIZING EMITTER AND COLLECTOR HEAT PIPES

Erich Kroeger, James Morris, Gabor Miskolcay (Thermo Electron Corp.), David P. Lieb (Thermo Electron Corp.), and Douglass B. Goodale (Thermo Electron Corp.) Jun 1978 38 p refs (Contract NAS3-20270) (NASA-TM-78941; E-9705) Avail: NTIS HC A03/MF A01 CSDL 10A

A thermionic converter module simulating a configuration for an out-of-core thermionic nuclear reactor was designed, fabricated, and tested. The module consists of three cylindrical thermionic converters. The tungsten emitter of the converter is heated by a tungsten, lithium heat pipe. The emitter heat pipes are immersed in a furnace, insulated by MULTI-FOIL thermal insulation, and heated by tungsten radiation filaments. The performance of each thermionic converter was characterized before assembly into the module. Dynamic voltage, current curves were taken using a 60 Hz sweep and computerized data acquisition over a range of emitter, collector, and cesium-reservoir temperatures. An output power of 215 W was observed at an emitter temperature of 1750 K and a collector temperature of 855 K for a two diode module. With a three diode module, an output power of 270 W was observed at an average emitter temperature of 1800 K and a collector temperature of 875 K. J.M.S.

N78-31183* National Aeronautics and Space Administration, Lewis Research Center, Cleveland, Ohio.

LIQUID ROCKET ENGINE AXIAL-FLOW TURBOPUMPS Space Vehicle Design Criteria (Chemical Propulsion)

D. D. Scheer, M. C. Huppert (Rocketdyne), F. Viteri (Aerojet Liquid Rocket Co.), J. Farquhar (Aerojet Liquid Rocket Co.), and Russell B. Keller, Jr., ed. Apr. 1978 127 p. refs

(NASA-SP-8125) Avail: NTIS HC A07/MF A01 CSCL 21H

The axial pump is considered in terms of the total turbopump assembly. Stage hydrodynamic design, pump rotor assembly, pump materials for liquid hydrogen applications, and safety factors as utilized in state of the art pumps are among the topics discussed. Axial pump applications are included.

J.M.S.

A78-32734* Planned flight test of a mercury ion auxiliary propulsion system. I - Objectives, systems descriptions, and mission operations. J. L. Power (NASA, Lewis Research Center, Cleveland, Ohio). *American Institute of Aeronautics and Astronautics and Deutsche Gesellschaft für Luft- und Raumfahrt, International Electric Propulsion Conference, 13th, San Diego, Calif., Apr. 25-27, 1978, AIAA Paper 78-647-1.* 45 p. 22 refs.

A planned flight test of an 8-cm diameter, electron-bombardment mercury ion thruster system is described. The primary objective of the test is to flight qualify the 5 mN thruster system for auxiliary propulsion applications. A seven year north-south station-keeping mission was selected as the basis for the flight test operating profile. The flight test, which will employ two thruster systems, will also generate thruster system space performance data, measure thruster-spacecraft interactions, and demonstrate thruster operation in a number of operating modes. The flight test is designated as SAMS0-601 and will be flown aboard the Shuttle-launched Air Force Space Test Program P80-1 satellite in 1981. The spacecraft will be 3-axis stabilized in its final 740 km circular orbit, which will have an inclination of at least 73 degrees. The spacecraft design lifetime is three years.

(Author)

A78-32735* Planned flight test of a mercury ion auxiliary propulsion system. II - Integration with host spacecraft. R. M. Knight (NASA, Lewis Research Center, Cleveland, Ohio). *American Institute of Aeronautics and Astronautics and Deutsche Gesellschaft für Luft- und Raumfahrt, International Electric Propulsion Conference, 13th, San Diego, Calif., Apr. 25-27, 1978, AIAA Paper 78-647-11.* 15 p. 5 refs.

This is part II of a three-part paper describing the approved flight test of a mercury ion auxiliary propulsion system. The objectives of the flight test are summarized with reference to user application. The approach to accomplishment is presented as it applies to integrating the propulsion system with the host spacecraft, USAF's STP P80-1. A number of known interface design considerations which affect the propulsion system and the spacecraft are discussed. Finally, analogies are drawn comparing the relationship of the organizations involved with this flight test with those anticipated for future operational missions. Attention is given to the viewpoint of the project office.

(Author)

A78-32736* 5200 cycle of an 8-cm diameter Hg ion thruster. M. A. Manteniaks and E. G. Wintucky (NASA, Lewis Research Center, Cleveland, Ohio). *American Institute of Aeronautics and Astronautics and Deutsche Gesellschaft für Luft- und Raumfahrt, International Electric Propulsion Conference, 13th, San Diego, Calif., Apr. 25-27, 1978, AIAA Paper 78-649.* 26 p. 12 refs.

An accelerated cycle test was conducted in which an 8-cm Engineering Model Thruster (EMT) prototype successfully completed 5200 on-off cycles and a total of more than 1300 hours of thruster operation at a 4.5 mN thrust level. Cathode tip heater powers required for starting and keeper voltages remained well within acceptable limits. The discharge chamber utilization and electrical efficiency were nearly constant over the duration of the test. It is concluded that on-off cyclic operation by itself does not appreciably degrade starting capability or performance of the 8-cm EMT.

(Author)

A78-32743* Status of SERT II spacecraft and ion thrusters - 1978. W. R. Kerlake and L. R. Ignaczak (NASA, Lewis Research Center, Cleveland, Ohio). *American Institute of Aeronautics and Astronautics and Deutsche Gesellschaft für Luft- und Raumfahrt, International Electric Propulsion Conference, 13th, San Diego, Calif., Apr. 25-27, 1978, AIAA Paper 78-662.* 7 p. 6 refs.

The historical record of the SERT II spacecraft and ion thruster systems for 8 years since the February 1970 launch is reviewed. The original SERT II mission, one year duration, was planned with the spacecraft in a continuous sunlight orbit to provide continuous solar power. An extended mission, using intermittent power available from an earth shadowed orbit has been performed during the past 5 years while waiting for the orbit to change again to continuous sunlight in early 1979. Continuous thruster testing is planned in 1979. Both spacecraft and ion thruster systems are near-fully functional when the solar array is illuminated. Thruster system 2 is fully operational. Thruster system 1 continues to demonstrate reliable capability, but the high-voltage-grid short remains.

(Author)

A78-32745* Effect of facility background gases on internal erosion of the 30-cm Hg ion thruster. V. K. Rawlin and M. A. Manteniaks (NASA, Lewis Research Center, Cleveland, Ohio). *American Institute of Aeronautics and Astronautics and Deutsche Gesellschaft für Luft- und Raumfahrt, International Electric Propulsion Conference, 13th, San Diego, Calif., Apr. 25-27, 1978, AIAA Paper 78-665.* 30 p. 26 refs.

One life limiting phenomenon of mercury bombardment thrusters is sputtering erosion of the upstream side of the molybdenum screen grid by discharge chamber ions. Data were obtained which revealed that the screen grid erosion was very sensitive to the partial pressure of certain background gases in the space simulation vacuum facility. The results of tests conducted to evaluate this effect are presented. An estimate of the screen grid erosion in space was made which showed that adequate lifetime for proposed missions exists.

(Author)

A78-32747* Sensitivity of 30-cm mercury bombardment ion thruster characteristics to accelerator grid design. V. K. Rawlin (NASA, Lewis Research Center, Cleveland, Ohio). *American Institute of Aeronautics and Astronautics and Deutsche Gesellschaft für Luft- und Raumfahrt, International Electric Propulsion Conference, 13th, San Diego, Calif., Apr. 25-27, 1978, AIAA Paper 78-668.* 28 p. 20 refs.

The design of ion optics for bombardment thrusters strongly influences overall performance and lifetime. The operation of a 30-cm thruster with accelerator grid open area fractions ranging from 43 to 24 percent, was evaluated and compared with previously published experimental and theoretical results. Ion optics properties measured included the beam current extraction capability, the minimum accelerator grid voltage to prevent backstreaming, ion beamlet diameter as a function of radial position on the grid and accelerator grid hole diameter, and the high energy, high angle ion beam edge location. Discharge chamber properties evaluated were propellant utilization efficiency, minimum discharge power per beam amp, and minimum discharge voltage.

(Author)

A78-32750* Investigation of high voltage spacecraft system interactions with plasma environments. N. J. Stevens, F. D. Berkopec, C. K. Purvis, N. Griet, and J. Staskus (NASA, Lewis Research Center, Cleveland, Ohio). *American Institute of Aeronautics and Astronautics and Deutsche Gesellschaft für Luft- und Raumfahrt, International Electric Propulsion Conference, 13th, San Diego, Calif., Apr. 25-27, 1978, AIAA Paper 78-672.* 14 p. 29 refs.

The exposure of high voltage spacecraft systems to the charged particle environment of space can produce interactions that will influence system operation. An experimental investigation of these interactions has been undertaken for insulator and conductor test surfaces biased up to plus or minus 1 kV in a simulated low earth orbit charged particle environment. It has been found that these interactions are controlled by the insulator surfaces surrounding the

biased conductors. For positive applied voltages the electron current collection can be enhanced by the insulators. For negative applied voltages the insulator surface confines the voltage to the conductor region; this can cause arcing. Understanding these interactions and the technology to control their impact on system operation is essential to the design of solar cell arrays for ion drive propulsion applications that use direct drive power processing. (Author)

A78-32752 * # The Plasma Interaction Experiment (PIX) Description and flight qualification test program. L. R. Ignaczak, F. A. Haley, E. J. Domino, D. H. Culp, and F. J. Shaker (NASA, Lewis Research Center, Cleveland, Ohio). *American Institute of Aeronautics and Astronautics and Deutsche Gesellschaft für Luft- und Raumfahrt, International Electric Propulsion Conference, 13th, San Diego, Calif., Apr. 25-27, 1978, AIAA Paper 78-674*. 19 p.

The Plasma Interaction Experiment (PIX) is a battery powered preprogrammed auxiliary payload on the Landsat-C launch. This experiment is part of a larger program to investigate space plasma interactions with spacecraft surfaces and components. The varying plasma densities encountered during available telemetry coverage periods are deemed sufficient to determine first order interactions between the space plasma environment and the biased experimental surfaces. The specific objectives of the PIX flight experiment are to measure the plasma coupling current and the negative voltage breakdown characteristics of a solar array segment and a gold plated steel disk. Measurements will be made over a range of surface voltages up to plus or minus 1 kilovolt. The orbital environment will provide a range of plasma densities. The experimental surfaces will be voltage-biased in a preprogrammed step sequence to optimize the data returned for each plasma region and for the available telemetry coverage. (Author)

A78-32754 * # A review of electron bombardment thruster systems/spacecraft field and particle interfaces. D. C. Byers (NASA, Lewis Research Center, Cleveland, Ohio). *American Institute of Aeronautics and Astronautics and Deutsche Gesellschaft für Luft- und Raumfahrt, International Electric Propulsion Conference, 13th, San Diego, Calif., Apr. 25-27, 1978, AIAA Paper 78-677*. 35 p. 76 refs.

This paper collates and summarizes information on the field and particle interfaces of electron bombardment ion thruster systems. Major areas discussed are the propellant particles, neutral propellant, ion beam, low energy plasma, and fields. Spacecraft functions and subsystems reviewed are solar arrays, thermal control systems, optical sensors, communications, science, structures and materials, and potential control. An appendix is included to facilitate identification of specific interaction areas. (Author)

A78-32759 * # A mechanical, thermal and electrical packaging design for a prototype power management and control system for the 30 cm mercury ion thruster. G. R. Sharp, L. Gadeon, J. C. Oglebay, F. S. Shaker, and C. E. Sigert (NASA, Lewis Research Center, Cleveland, Ohio). *American Institute of Aeronautics and Astronautics and Deutsche Gesellschaft für Luft- und Raumfahrt, International Electric Propulsion Conference, 13th, San Diego, Calif., Apr. 25-27, 1978, AIAA Paper 78-585*. 31 p. 12 refs.

A prototype Electric Power Management and Thruster Control System for a 30 cm ion thruster has been built and is ready to support a first mission application. The system meets all of the requirements necessary to operate a thruster in a fully automatic mode. Power input to the system can vary over a full two to one dynamic range (200 to 400 V) for the solar array or other power source. The Power Management and Control system is designed to protect the thruster, the flight system and itself from arcs and is fully compatible with standard spacecraft electronics. The system is designed to be easily integrated into flight systems which can operate over a thermal environment ranging from 0.3 to 5 AU. The complete

Power Management and Control system measures 45.7 cm x 15.2 cm x 114.8 cm and weighs 36.2 kg. At full power the overall efficiency of the system is estimated to be 87.4 percent. Three systems are currently being built and a full schedule of environmental and electrical testing is planned. (Author)

A78-32760 * # 30-cm mercury ion thruster performance with a 1 kW capacitor-diode voltage multiplier beam supply. F. S. Terdan and W. T. Herrigill, Jr. (NASA, Lewis Research Center Cleveland, Ohio). *American Institute of Aeronautics and Astronautics and Deutsche Gesellschaft für Luft- und Raumfahrt, International Electric Propulsion Conference, 13th, San Diego, Calif., Apr. 25-27, 1978, AIAA Paper 78-686*. 16 p. 19 refs.

A 1 kW Solar Array and Capacitor-Diode Voltage Multiplier Converter (S/A-CDVM) has been successfully integrated with a 30 cm-diameter mercury ion thruster system to provide ion beam power. Measurements were made to compare steady state and transient response performance of a conventional bridge converter with the S/A-CDVM converter used for the ion beam supply. The ability to recover from screen to accelerator arcs and promptly re-establish stable thruster performance was demonstrated. Solar array transient response to thruster arcing was also measured. (Author)

A78-32768 * # Diagnostic evaluations of a beam-shielded 8-cm mercury ion thruster. S. Nakanishi (NASA, Lewis Research Center, Cleveland, Ohio). *American Institute of Aeronautics and Astronautics and Deutsche Gesellschaft für Luft- und Raumfahrt, International Electric Propulsion Conference, 13th, San Diego, Calif., Apr. 25-27, 1978, AIAA Paper 78-702*. 24 p. 8 refs.

An engineering model thruster fitted with a remotely actuated graphite fiber polyimide composite beam shield was tested in a 3- by 6.5-meter vacuum facility for in-situ assessment of beam shield effects on thruster performance. Accelerator drain current, neutralizer floating potential and ion beam floating potential increased slightly when the shield was moved into position. A target exposed to the low density regions of the ion beam was used to map the boundaries of energetic fringe ions capable of sputtering. The particle efflux was evaluated by measurement of film deposits on cold, heated, bare, and enclosed glass slides. (Author)

A78-32773 * # Pulse ignition characterization of mercury ion thruster hollow cathode using an improved pulse ignitor. E. G. Wintucky and R. P. Gruber (NASA, Lewis Research Center, Cleveland, Ohio). *American Institute of Aeronautics and Astronautics and Deutsche Gesellschaft für Luft- und Raumfahrt, International Electric Propulsion Conference, 13th, San Diego, Calif., Apr. 25-27, 1978, AIAA Paper 78-709*. 19 p. 12 refs.

An investigation of the high voltage pulse ignition characteristics of the 8-cm mercury ion thruster neutralizer cathode identified a low rate of voltage rise and long pulse duration as desirable factors for reliable cathode starting. Cathode starting breakdown voltages were measured over a range of mercury flow rates and tip heater powers for pulses with five different rates of voltage rise. Breakdown voltage requirements for the fastest rising pulse (2.5 to 3.0 kV/microsec) were substantially higher (2 kV or more) than for the slowest rising pulse (0.3 to 0.5 kV/microsec) for the same starting conditions. The paper also describes an improved, low impedance pulse ignitor circuit which reduces power losses and eliminates problems with control and packaging associated with earlier designs. (Author)

A78-32776 * # Evolution of the 1-mlb mercury ion thruster subsystem. W. R. Kerlake and B. A. Banks (NASA, Lewis Research Center, Cleveland, Ohio). *American Institute of Aeronautics and Astronautics and Deutsche Gesellschaft für Luft- und Raumfahrt, International Electric Propulsion Conference, 13th, San Diego, Calif., Apr. 25-27, 1978, AIAA Paper 78-711B*. 24 p. 30 refs.

A general description and review of the auxiliary Electric

Propulsion program, which led to the present 1-mib (4.5 mN) thruster system, is presented. The developmental history, performance, and major life-tests of each component of the system are traced over the past 10 years. Major components include the 8-cm diameter ion thruster, the power processor, and the propellant reservoir and distribution system. (Author)

A78-40828 * Comment on: Mass-pipe reactors for space power applications. R. E. English (NASA, Lewis Research Center, Cleveland, Ohio). *Journal of Energy*, vol. 2, May-June 1978, p. 191, 192. Authors' Reply, p. 192.

N78-10306* Hughes Research Labs., Malibu, Calif. Ion Physics Dept.
EXTENDED PERFORMANCE SOLAR ELECTRIC PROPULSION THRUST SYSTEM STUDY. VOLUME 1: EXECUTIVE SUMMARY Final Report
R. L. Poeschel and E. I. Hawthorne Sep 1977 108 p refs (Contract NAS3-20395) (NASA-CR-135281) Avail NTIS HC A08/MF A01 CSCL 21C

Several thrust system design concepts were evaluated and compared using the specifications of the most advanced 30 cm engineering model thruster as the technology base. The extensions in thruster performance required for the Halley's comet mission were defined and alternative thrust system concepts were designed. Confirmation testing and analysis of thruster and power-processing components were performed, and the feasibility of achieving extended performance requirements was verified. A baseline design was selected from the alternatives considered, and the design analysis and documentation were refined. A program development plan was formulated that outlines the work structure considered necessary for developing, qualifying, and fabricating the flight hardware for the baseline thrust system within the time frame of a project to rendezvous with Halley's comet. An assessment was made of the costs and risks associated with a baseline thrust system as provided to the mission project under this plan. Critical procurements and interfaces were identified and defined. Results are presented. (Author)

N78-11192* Hughes Research Labs., Malibu, Calif.
EXTENDED PERFORMANCE SOLAR ELECTRIC PROPULSION THRUST SYSTEM STUDY. VOLUME 1: EXECUTIVE SUMMARY Final Report, 14 Feb. - 29 Aug. 1977
R. L. Poeschel, E. I. Hawthorne, Y. C. Wesman, M. Friman, G. C. Benson, R. J. McGrath, R. M. Martinich, T. L. Linsenhardt, and J. R. Beattie Sep 1977 110 p refs. Prepared in cooperation with Hughes Space and Communications Group, Los Angeles (Contract NAS3-20395) (NASA-CR-135281) Avail NTIS HC A08/MF A01 CSCL 21C

Several ion thrust system design concepts were evaluated and compared using the specifications of the most advanced 30 cm engineering model thruster as the technology base. Emphasis was placed on relatively high-power missions (80 to 100 kW) such as a Halley's comet rendezvous. The extensions in thruster performance required for the Halley's comet mission were defined and alternative thrust system concepts were designed in sufficient detail for comparing mass efficiency, reliability, structure, and thermal characteristics. Confirmation testing and analysis of thruster and power-processing components were performed. A baseline design was selected from the alternatives considered and the design analysis and documentation were refined. The baseline thrust system design features modular construction, conventional power processing, and a concentrator solar collector and is designed to interface with the Space Shuttle. A program development plan was formulated that outlines the work structure considered necessary for developing, qualifying, and fabricating the flight hardware for the baseline thrust system of a mission to rendezvous with Halley's comet during December 1985. (Author)

N78-12148* TRW Defense and Space Systems Group, Redondo Beach, Calif.
ION BEAM PLUME AND EFFLUX CHARACTERIZATION FLIGHT EXPERIMENT STUDY Final Report, 1 Jan.-1 Dec. 1977

J. M. Sellen, Jr., S. Zakari, A. Cole, G. Rowak, and G. K. Komatsu 1 Dec 1977 166 p refs (Contract NAS3-30287) (NASA-CR-135275) Avail NTIS HC A08/MF A01 CSCL 21C

A flight experiment and flight experiment package for a shuttle-borne flight test of an 8-cm mercury ion thruster was designed to obtain charged particle and neutral particle material transport data that cannot be obtained in conventional ground based laboratory testing facilities. By the use of both ground and space testing of ion thrusters, the flight worthiness of these ion thrusters for other spacecraft applications may be demonstrated. The flight experiment definition for the ion thruster initially defined a broadly ranging series of flight experiments and flight test sensors. From this larger test series and sensor list, an initial flight test configuration was selected with measurements in charged particle material transport, condensable neutral material transport, thruster internal erosion, ion beam neutralization and ion thrust beam/space plasma electrical equilibrium. These measurement areas may all be examined for a seven day shuttle borne mission and for available test time in the 50-100 hour period. (Author)

N78-13122* Systems Science and Software, La Jolla, Calif.
SOLAR ELECTRIC PROPULSION THRUSTER INTERACTIONS WITH SOLAR ARRAYS Contractor Report, Jul. 1978 - Jul. 1977

Donald E. Parks and Ira Katz Aug 1977 258 p refs (Contract NAS3-20119) (NASA-CR-135257) SSS-R 78-3420 Avail NTIS HC A12/MF A01 CSCL 21C

The effect of interactions of spacecraft-generated and naturally occurring plasmas with high voltage solar array components on an advanced solar electric propulsion system proposed for the Halley's Comet rendezvous mission was investigated. The spacecraft-generated plasma consists of mercury ions and neutralizing electrons resulting from the operation of ion thrusters (the charge-exchange plasma) and associated hollow cathode neutralizers. Quantitative results are given for parasitic currents and power coupled into solar arrays with voltage bias as a function of position on the array. (Author)

N78-13123* Colorado State Univ., Fort Collins, Dept. of Mechanical Engineering
CHARGE-EXCHANGE PLASMA GENERATED BY AN ION THRUSTER Annual Report 1 Nov. 1978 - 31 Dec. 1977
Harold R. Kaufman Dec 1977 41 p refs (Grant NAG 3008) (NASA-CR-135318) Avail NTIS HC A03/MF A01 CSCL 21C

The charge exchange plasma generated by an ion thruster was investigated experimentally using both 5 cm and 15 cm thrusters. Results are shown for wide ranges of radial distance from the thruster and angle from the beam direction. Considerations of test environment as well as distance from the thruster indicate that a valid simulation of a thruster on a spacecraft was obtained. A calculation procedure and a sample calculation of charge exchange plasma density and saturation electron current density are included. (Author)

N78-18167* Colorado State Univ., Fort Collins, Dept. of Mechanical Engineering
MERCURY ION THRUSTER RESEARCH, 1977 Annual Report, 1 Dec 1978 - 1 Dec 1977
Paul J. Wilbur Dec 1977 163 p refs (Grant NGR 06 002 112) (NASA-CR-135317) Avail NTIS HC A08/MF A01 CSCL 21C

The measured ion beam divergence characteristics of two and three-grid multiperforated accelerators are presented.

The effects of permeance geometry net-to-total accelerating voltage discharge voltage and propellant are examined. The applicability of a model describing doubly-charged ion densities in mercury thrusters is demonstrated for an 8-cm diameter thruster. The results of detailed Langmuir probing of the interior of an operating cathode are given and used to determine the ionization fraction as a function of position upstream of the cathode orifice. A mathematical model of discharge chamber electron diffusion and collector processes is presented along with scaling laws useful in estimating performance of large diameter and/or high specific impulse thrusters. A model describing the production of ionized molecular nitrogen in ion thrusters is included. Author

NTS 16100* TRW Defense and Space Systems Group, Redondo Beach, Calif

ION ENGINE AUXILIARY PROPULSION APPLICATIONS AND INTEGRATION STUDY

S. Zahra ed. 7 Jul 1977. 280 p. refs.

(Contract NAS3-20113)

(NASA CR 135312 TRW 29989-6013 RU 00) Avail NTIS HC A13/MF A01 CSCL 21C

The benefits derived from application of the 8 cm mercury electron bombardment ion thruster were assessed. Two specific spacecraft missions were studied. A thruster was tested to provide additional needed information on its efflux characteristics and interactive effects. A Users Manual was then prepared describing how to integrate the thruster for auxiliary propulsion on geosynchronous satellites. By incorporating ion engines on an advanced communications mission, the weight available for added payload increases by about 62 kg (138 lb) for a 100 kg (2200 lb) satellite which otherwise uses electrothermal hydrazine ion engines. Ion engines can be integrated into a high performance propulsion module that is compatible with the multimission modular spacecraft and can be used for both geosynchronous and low earth orbit applications. The low disturbance torques introduced by the ion engines permit accurate spacecraft pointing with the payload in operation during thrusting periods. The feasibility of using the thrusters' neutralizer assembly for neutralization of differentially charged spacecraft surfaces at geosynchronous altitude was demonstrated during the testing program. Author

NTS 16080* Hughes Research Labs, Malibu, Calif
EXTENDED PERFORMANCE SOLAR ELECTRIC PROPULSION THRUST SYSTEM STUDY VOLUME 4 THRUSTER TECHNOLOGY EVALUATION Final Report, 14 Feb - 29 Aug, 1977

R. L. Poesche, E. J. Hawthorne, V. J. Weisman, M. Friman, G. C. Bensch, R. J. McGloth, R. M. Martinek, T. L. Unsenberut and J. R. Beattie. Sep. 1977. 110 p. refs. Prepared in cooperation with Hughes Space and Communications Group, Los Angeles. (Contract NAS3-20395)

(NASA CR 135281) Avail NTIS HC A06/MF A01 CSCL 21C

Several thrust system design concepts were evaluated and compared using the specifications of the most advanced 30 cm engineering model thruster as the technology base. Emphasis was placed on relatively high power missions, 60 to 100 kW, such as a Halley's comet rendezvous. The extensions in thruster performance required for the Halley's comet mission were defined and alternative thrust system concepts were designed in sufficient detail for comparing mass, efficiency, reliability, structure and thermal characteristics. Confirmation testing and analysis of thruster and power processing components were performed and the feasibility of satisfying extended performance requirements was verified. A baseline design was selected from the alternatives considered and the design analysis and documentation were refined. The baseline thrust system design features modular construction, compact power processing, and a concentrator solar array concept and is designed to interface with the Space Shuttle. Author

NTS 16080* Hughes Research Labs, Malibu, Calif Ion Physics Dept Staff

EXTENDED PERFORMANCE SOLAR ELECTRIC PROPULSION THRUST SYSTEM STUDY VOLUME 6: CAPACITOR-DODE VOLTAGE MULTIPLIER: TECHNOLOGY EVALUATION Final Report

R. M. Martinek. Sep. 1977. 74 p.

(Contract NAS3-20395)

(NASA CR 135281-Vol-6) Avail NTIS HC A04/MF A01 CSCL 21C

A 1-kW capacitor-dode voltage multiplier (CDVM) was designed, fabricated and tested to demonstrate the power of feasibility of high power CDVM's and to verify the analytical techniques that had been used to predict the performance characteristics of a 6-bar CDVM. High efficiency (98.2%), a low ratio of component weight to power (0.55 kg/kW), and low output ripple voltage (less than 1%, peak to peak) were obtained during the operation of a 1-kW CDVM versus input line, load current, and load fault conditions. Author

NTS 16100* Hughes Research Labs, Malibu, Calif
EXTENDED PERFORMANCE SOLAR ELECTRIC PROPULSION THRUST SYSTEM STUDY VOLUME 3: TRADEOFF STUDIES OF ALTERNATE THRUST SYSTEM CONFIGURATIONS Final Report, 14 Feb - 29 Aug, 1977

E. J. Hawthorne. Dec. 1977. 157 p. refs.

(Contract NAS3-20395)

(NASA CR 135281-Vol-3) Avail NTIS HC A06/MF A01 CSCL 21C

Several thrust system design concepts were evaluated and compared using the specifications of the most advanced 30 cm engineering model thruster as the technology base. Emphasis was placed on relatively high power missions. The extensions in thruster performance required for the Halley's comet mission were defined and alternative thrust system concepts were designed in sufficient detail for comparing mass, efficiency, reliability, structure and thermal characteristics. Confirmation testing and analysis of thruster and power processing components were performed. A baseline design was selected from the alternatives considered and the design analysis and documentation were refined. A program development plan was formulated that outlines the work structure considered necessary for developing, qualifying, and fabricating the flight hardware for the baseline thrust system within the time frame of a project to rendezvous with Halley's comet. An assessment was made of the costs and risks associated with a baseline thrust system as provided to the mission project under the plan. Critical procurements and interfaces were identified and defined. Author

NTS 16100* Colorado State Univ., Fort Collins, Dept of Mechanical Engineering

INERT GAS THRUSTERS Annual Report, 1 Aug. 1976 - 30 Jul. 1977

Harold R. Kaufman. Jul. 1977. 78 p. refs.

(Grant NSG 3011)

(NASA CR 135226) Avail NTIS HC A05/MF A01 CSCL 21C

Inert gases, particularly argon and xenon, are of interest as possible alternatives to the usual electric thruster propellants of mercury and cesium. Hollow cathode data were obtained for a wide range of operating conditions. Some test conditions gave plasma coupling voltages at or below the sputtering threshold, hence should permit long operating lifetimes. All observations of hollow cathode operation were consistent with a single theory of operation in which a significant amount of the total electron emission is from localized areas within the orifice. This mode of emission is also supported by scanning electron microscope photographs that indicate local temperatures at or near the melting temperature of the tungsten tip. Experimental hollow cathode performance was correlated for two orifice diameters, three inert gas propellants, and a range of flow rates for each propellant. The basic theory for the production of doubly ionized argon and xenon was completed. Experimental measurements of the doubly ionized fraction agree with theory within about plus or minus 20 percent. High voltage isolators were studied for the propellant feed line. The breakdown voltage per segment ranged from 300 to over 500 V with argon. Author

N78-18285* TRW Defense and Space Systems Group, Redondo Beach, Calif

ELECTRIC PROTOTYPE POWER PROCESSOR FOR A 30CM ION THRUSTER Final Report, 1 Apr. 1976 - 1 Mar. 1977
J J Bess, L Y Inouye, and A D Schoenfeld Mar 1977
104 p

(Contract NAS3-19730)
(NASA CR-136287 TRW-28014-6001-TU-00) Avail NTIS
HC A08/MF A01 CSCL 21C

An electrical prototype power processor unit was designed, fabricated and tested with a 30 cm mercury ion engine for primary space propulsion. The power processor unit used the thyristor series resonant inverter as the basic power stage for the high power beam and discharge supplies. A transistorized series resonant inverter processed the remaining power for the low power outputs. The power processor included a digital interface unit to process all input commands and external telemetry signals so that electric propulsion systems could be operated with a central computer system. The electrical prototype unit included design improvement in the power components such as thyristors, transistors, filters and resonant capacitors, and power transformers and inductors in order to reduce component weight, to minimize losses, and to control the component temperature rise. A design analysis for the electrical prototype is also presented on the component weight, losses, part count and reliability estimate. The electrical prototype was tested in a thermal vacuum environment. Integration tests were performed with a 30 cm ion engine and demonstrated operational compatibility. Electromagnetic interference data was also recorded on the design to provide information for spacecraft integration. Author

N78-20280* TRW Defense and Space Systems Group, Redondo Beach, Calif Power Conversion Electronics Dept
EXTENDED PERFORMANCE ELECTRIC PROPULSION POWER PROCESSOR DESIGN STUDY, VOLUME 1: EXECUTIVE SUMMARY Final Report, 1 May - 25 Oct. 1977

J J Bess, L Y Inouye, and A D Schoenfeld Nov. 1977
83 p

(Contract NAS3 20403)
(NASA CR 135357 TRW-31526-000-Vol-1) Avail NTIS
HC A05, MF A01 CSCL 21C

Several power processor design concepts were evaluated and compared. Emphasis was placed on a 30cm ion thruster power processor with a beam supply rating of 2 kW to 10kW. Extensions in power processor performance were defined and were designed in sufficient detail to determine efficiency, component weight, part count, reliability and thermal control. Preliminary electrical design, mechanical design, and thermal analysis were performed on a 6kW power transformer for the beam supply. Bi-Mod mechanical, structural, and thermal control configurations were evaluated for the power processor, and preliminary estimates of mechanical weight were determined. A program development plan was formulated that outlines the work breakdown structure for the development, qualification and fabrication of the power processor flight hardware. Author

N78-22148* Texas A&I Univ., Kingsville
INVESTIGATION OF THE BURNING CONFIGURATION OF A COAXIAL INJECTOR IN A COMBUSTION CHAMBER
J OHara Feb 1978 26 p refs
(Grant NSG-3112)
(NASA CR-135383) Avail NTIS HC A03/MF A01 CSCL 21H

An analytical investigation was made into the stability of the burning configuration of a single coaxial injector surrounded by similar injectors. The stability criteria was based on an average pressure difference along the boundaries of the adjacent stream tubes as calculated using Spaulding's numerical method. The results indicate qualitatively that there is a tendency for the injectors to have different burning configurations. It is believed that the configuration achieved is random, however once the burning configuration is established, it is believed to persist.

N78-24278* Rocketdyne, Canoga Park, Calif
PREBURNER OF STAGED COMBUSTION ROCKET ENGINE

Final Report Jul. 1976 - Dec. 1977
M C Yost Feb 1978 280 p refs

(Contract NAS3-19713)
(NASA CR-136356 RI/RD78-114) Avail NTIS
HC A13/MF A01 CSCL 21H

A regeneratively cooled LOX/hydrogen staged combustion assembly system with a 400:1 expansion area ratio nozzle utilizing an 89 000 Newton (20 000 pound) thrust regeneratively cooled thrust chamber and 175:1 tubular nozzle was analyzed, assembled, and tested. The components for this assembly include two spark/torch oxygen hydrogen igniters, two servo-controlled LOX valves, a preburner injector, a preburner combustor, a main propellant injector, a regeneratively cooled combustion chamber, a regeneratively cooled tubular nozzle with an expansion area ratio of 175:1, an uncooled heavy-wall steel nozzle with an expansion area ratio of 400:1, and interconnecting ducting. The analytical effort was performed to optimize the thermal and structural characteristics of each of the new components and the ducting, and to verify the capabilities of the previously fabricated components. The testing effort provided a demonstration of the preburner/combustor chamber operation, chamber combustion efficiency and stability, and chamber and nozzle heat transfer. Author

N78-24280* Hughes Research Labs., Malibu, Calif Ion Physics Dept

THE 30-CM ION THRUSTER POWER PROCESSOR

Final Report
B G Herron and D J Hopper Apr 1978 77 p refs

(Contract NAS3 172231)
(NASA CR 135401) Avail NTIS HC A05/MF A01 CSCL 21C

A power processor unit for powering and controlling the 30 cm Mercury Electron-Bombardment Ion Thruster was designed, fabricated and tested. The unit uses a unique and highly efficient transistor bridge inverter power stage in its implementation. The system operated from a 200 to 400 V dc input power bus, provides 12 independently controllable and closely regulated dc power outputs, and has an overall power conditioning capacity of 3.5 kW. Protective circuitry was incorporated as an integral part of the design to assure failure-free operation during transient and steady state load faults. The implemented unit demonstrated an electrical efficiency between 31.5 and 91.9 at its nominal rated load over the 200 to 400 V dc input bus range. Author

N78-25127* Rocketdyne, Canoga Park, Calif Advanced and Propulsion Engineering Units

ADVANCED SPACE ENGINE POWERHEAD BREADBOARD ASSEMBLY SYSTEM STUDY Final Report, Dec. 1976 - Jun. 1977

R G Campbell Mar 1978 170 p refs

(Contract NAS3 20386)
(NASA CR 135232 RI/RD77-192) Avail NTIS
HC A08/MF A01 CSCL 21H

The objective of this study was to establish a preliminary design of a Powerhead Breadboard Assembly (PBA) for an 88 964 Newton (20 000 pound) thrust oxygen, hydrogen staged combustion cycle engine for use in orbital transfer vehicle propulsion. Existing turbopump, preburner, and thrust chamber components were integrated with interconnecting ducting, a heat exchanger, and a control system to complete the PBA design. Cycle studies were conducted to define starting transients and steady state balances for the completed design. Specifications were developed for all valve applications and the conditions required for the control system integration with the facility for system test were defined. Author

A78-32751 * **Spacecraft-generated plasma interaction with high voltage solar array.** D. E. Parks and I. Ketz (Systems, Science and Software, La Jolla, Calif.). *American Institute of Aeronautics and Astronautics and Deutsche Gesellschaft für Luft- und Raumfahrt, International Electric Propulsion Conference, 13th, San Diego, Calif., Apr. 25-27, 1978, AIAA Paper 78-673*. 9 p. 11 refs. Contract No. NAS3-20119.

Calculations are made of the effect of interactions of spacecraft-generated plasmas and high voltage solar array components on an advanced Solar Electric Propulsion system. The plasma consists of mercury ions and electrons resulting from the operation of ion thrusters and associated hollow cathode neutralizers. Because large areas of the solar array are at high potential and not completely insulated from the surrounding plasma, the array can, under some conditions, collect excessive electron currents. Results are given for the parasitic currents collected by the solar arrays and means for reducing these currents are considered. (Author)

A78-32753 * **Ion beam plume and efflux measurements of an 8-cm mercury ion thruster.** G. K. Komatsu, J. M. Sellen, Jr. and S. Zahran (TRW Defense and Space Systems Group, Redondo Beach, Calif.). *American Institute of Aeronautics and Astronautics and Deutsche Gesellschaft für Luft- und Raumfahrt, International Electric Propulsion Conference, 13th, San Diego, Calif., Apr. 25-27, 1978, AIAA Paper 78-676*. 9 p. Contract No. NAS3-20113.

Measurements of the ion beam plume and efflux constituents of an 8-cm mercury ion thruster have been carried out in the TRW 5 x 10 foot testing chamber. Charged components (ion beam plume) were measured with an array of movable position Faraday cups and retarding potential analyzers yielding both current density and particle energy determination. Neutral components (ion beam efflux) were determined with a movable position ionization gauge. Measurements of the ion beam plume were performed for a thruster both with and without a sputter shield. Analysis of data in terms of normalized effluxes has been carried out and has been applied to an example calculation of efflux compatibility with a communications spacecraft. (Author)

A78-37430 * **Extended performance solar electric propulsion thrust system design.** J. E. Cake (NASA, Lewis Research Center, Cleveland, Ohio), E. I. Hawthorne (Hughes Aircraft Co., Space and Communications Group, Los Angeles, Calif.), and R. L. Poeschel (Hughes Research Laboratories, Malibu, Calif.). *American Institute of Aeronautics and Astronautics and Deutsche Gesellschaft für Luft- und Raumfahrt, International Electric Propulsion Conference, 13th, San Diego, Calif., Apr. 25-27, 1978, AIAA Paper 78-643*. 14 p. 19 refs. Contract No. NAS3-20395.

A thrust system design has been established for an extended performance technology, 6.4 kW, 4800 sec specific impulse ion thruster. The configuration is comprised of ten thrusters configured with a power management and control subsystem in a modular thrust system design. The system design approach is an adaptation of that previously established for the baseline technology 2.7 kW, 3000 sec specific impulse ion thruster. The power management and control subsystem design includes a combination of individual electronics for each thruster and a set of electronics with redundancy that are common to all thrusters. The thermal dissipation from all electronics is removed with a common heat pipe/radiator assembly. (Author)

A78-37434 * **Engineering Model 8-cm Thruster System.** B. G. Herron (Hughes Aircraft Co., Technology Div., El Segundo, Calif.), J. Hyman, Jr., D. J. Hopper, W. S. Williamson, C. R. Dulgeroff, and C. R. Collett (Hughes Research Laboratories, Malibu, Calif.). *American Institute of Aeronautics and Astronautics and Deutsche Gesellschaft für Luft- und Raumfahrt, International Electric Propulsion Conference, 13th, San Diego, Calif., Apr. 25-27, 1978, AIAA Paper 78-646*. 11 p. 8 refs. Contracts No. NAS3-18917; No. NAS3-21023.

Development of an Engineering Model 8-cm Mercury Ion Thruster System for Satellite Control has been successfully completed. This system operates at a specific impulse in excess of 2600 sec, produces a thrust of 5 mN with a total input power of 165 W; it has a dry mass of 16.6 kg and a mercury-propellant-reservoir capacity of 8.75 kg. This paper summarizes the development work, the system characteristics and performance, and the testing undertaken to verify the design. (Author)

A78-37436 * **Extended-performance thruster technology evaluation.** J. R. Beattie, R. L. Poeschel (Hughes Research Laboratories, Malibu, Calif.), and R. T. Bechtel (NASA, Lewis Research Center, Solar Electric Propulsion Office, Cleveland, Ohio). *American Institute of Aeronautics and Astronautics and Deutsche Gesellschaft für Luft- und Raumfahrt, International Electric Propulsion Conference, 13th, San Diego, Calif., Apr. 25-27, 1978, AIAA Paper 78-666*. 14 p. 15 refs. Contract No. NAS3-20395.

Two 30-cm ion thruster technology areas are investigated in support of the extended-performance thruster operation required for the Halley's comet rendezvous mission. These areas include an evaluation of the thruster performance and lifetime characteristics at increased specific impulse and power levels, and the design and evaluation of a high-voltage propellant electrical isolator. Experimental results are presented indicating that all elements of the thruster design function well at the higher specific impulse and power levels. It is shown that the only thruster modifications required for extended-performance operation are a respacing of the ion optics assembly and a redesign of the propellant isolators. Experimental results obtained from three isolator designs are presented, and it is concluded that the design and development of a high-voltage isolator is possible using existing technology. (Author)

A78-37439 * **Electrical Prototype Power Processor for the 30-cm Mercury electric propulsion engine.** J. J. Biess (TRW Defense and Space Systems Group, Redondo Beach, Calif.) and R. J. Frye (NASA, Lewis Research Center, Cleveland, Ohio). *American Institute of Aeronautics and Astronautics and Deutsche Gesellschaft für Luft- und Raumfahrt, International Electric Propulsion Conference, 13th, San Diego, Calif., Apr. 25-27, 1978, AIAA Paper 78-684*. 9 p. 9 refs. Contracts No. NAS3-19730; No. NAS3-20403.

An Electrical Prototype Power Processor has been designed to the latest electrical and performance requirements for a flight-type 30-cm ion engine and includes all the necessary power, command, telemetry and control interfaces for a typical electric propulsion subsystem. The power processor was configured into seven separate mechanical modules that would allow subassembly fabrication, test and integration into a complete power processor unit assembly. The conceptual mechanical packaging of the electrical prototype power processor unit demonstrated the relative location of power, high voltage and control electronic components to minimize electrical interactions and to provide adequate thermal control in a vacuum environment. Thermal control was accomplished with a heat pipe simulator attached to the base of the modules. (Author)

23 CHEMISTRY AND MATERIALS (GENERAL)

Includes biochemistry and organic chemistry.

N78-22167* National Aeronautics and Space Administration, Lewis Research Center, Cleveland, Ohio
IN SITU SELF CROSS-LINKING OF POLYVINYL ALCOHOL BATTERY SEPARATORS Patent Application
 Warren H. Philipp, L. C. Hou, and D. W. Shebley, inventors (to NASA) Filed 19 Apr. 1978 13 p
 (NASA-Case-LEW-12972-1, US-Patent-AppI-SN-897829) Avail: NTIS HC A02/MF A01 CSCL 07C

The method disclosed is used to produce a polyvinyl alcohol sheet material wherein the polyvinyl alcohol is substantially free of 1,2 diol units, and has an acetal self cross-linked structure wherein the acetal content is determined by the 1,2 diol content in the sheet material prior to cross-linking. The sheet material product exhibits high conductivity and oxidation resistance, as well as minimal distortion of the prefabricated polyvinyl alcohol sheet material.

NASA

N78-26172* National Aeronautics and Space Administration, Lewis Research Center, Cleveland, Ohio
ION PROPULSION FOR SPACECRAFT
 W R Kerstake et al 1977 27 p refs
 (NASA-TM-79502) Avail: NTIS HC A03/MF A01 CSCL 21C

The theory of the ion-thruster propulsion system is discussed along with the Space Electric Rocket Test 1 and 2. The use of electric propulsion for stationkeeping and attitude control function of geosynchronous satellites is described, and a comparison of thruster systems is presented.

F.O.S.

N78-26177* National Aeronautics and Space Administration, Lewis Research Center, Cleveland, Ohio
THE FRICTION AND WEAR PROPERTIES OF SPUTTERED HARD REFRACTORY COMPOUNDS
 William A. Branard Aug 1978 17 p refs. Proposed for presentation at the 2d Intern Conf on Solid Lubrication, Denver, 14-18 Aug 1978, sponsored by the Am Soc of Lub Engr (NASA-TM-78895, E-9368) Avail: NTIS HC A02/MF A01 CSCL 11D

Several refractory silicide, boride, and carbide coatings were examined. The coatings were applied to type 440C steel surfaces by radio-frequency sputtering. The friction and wear properties of the coatings were found to be related to stoichiometry and impurity content of the bulk coating as well as the degree of interfacial adherence between coating and substrate. Bulk coating stoichiometry could to a large extent be controlled by the application of a negative bias voltage during deposition. Adherence was promoted by the formation of an oxidized layer at the interface. Deliberate preoxidizing of the 440C produced enhanced adherence for many compounds which are related to the formation of a mixed oxide transition region.

Author

N78-26178* National Aeronautics and Space Administration, Lewis Research Center, Cleveland, Ohio
FRICTION AND WEAR OF CARBON-GRAPHITE MATERIALS FOR HIGH-ENERGY BRAKES

Robert C. Bill Aug 1978 21 p refs. Proposed for presentation at the 2d Intern Conf on Solid Lubrication, Denver, 14-18 Aug 1978, sponsored by the Am Soc of Lubrication Engr (NASA-TM-78903, AVRADCOM-TR-78-27(PL), E-8259-1) Avail: NTIS HC A02/MF A01 CSCL 11D

Caliper type brake simulation experiments were conducted on seven different carbon graphite materials formulations against a steel disk material and against a carbon graphite disk material. The effects of binder level, boron carbide (B4C) additions, SiC additions, graphite fiber additions, and graphite cloth reinforcement on friction and wear behavior were investigated. Reductions in binder level, additions of B4C, and additions of SiC each resulted in increased wear. The wear rate was not affected by the addition of graphite fibers. Transition to severe wear and high friction was observed in the case of graphite-cloth-reinforced carbon sliding against a disk of similar composition. The transition was related to the disruption of a continuous graphite shear film that must form on the sliding surfaces if low wear is to occur.

B.B.

A78-24910 * Progress in advanced high temperature turbine materials, coatings, and technology. J. C. Freche and G. M. Ault (NASA, Lewis Research Center, Cleveland, Ohio). *NATO, AGARD, Propulsion and Energetics Panel Meeting, 50th, Middle East Technical University, Ankara, Turkey, Sept. 19-23, 1977, Paper, 43 p.* 89 refs.

Several NASA-sponsored benefit-cost studies have shown that very substantial benefits can be obtained by increasing material capability for aircraft gas turbines. Prealloyed powder processing holds promise for providing superalloys with increased strength for turbine disk applications. The development of advanced powder metallurgy disk alloys must be based on a design of optimum processing and heat treating procedures. Materials considered for high temperature application include oxide dispersion strengthened (ODS) alloys, directionally solidified superalloys, ceramics, directionally solidified eutectics, materials combining the high strength of a gamma prime strengthened alloy with the elevated temperature strength of an ODS, and composites. Attention is also given to the use of high pressure turbine seals, approaches for promoting environmental protection, and turbine cooling technology.

G.R.

N78-16094* Gelles (S H) Associates, Columbus, Ohio
MATERIALS SCIENCE EXPERIMENTS IN SPACE
 Final Report
 S H Gelles, B C Giesser, M E Glicksman, J L Margrave, H Markovitz, A S Nowick, J D Verhoeven, and A F Witt Jan 1978 84 p refs
 (Contract NAS3-20049)

(NASA CR 2842) Avail: NTIS HC A05/MF A01 CSCL 22A
 The criteria for the selection of the experimental areas and individual experiments were that the experiment or area must make a meaningful contribution to the field of material science and that the space environment was either an absolute requirement for the successful execution of the experiment or that the experiment can be more economically or more conveniently performed in space. A number of experimental areas and individual experiments were recommended for further consideration as space experiments. Areas not considered to be fruitful and others needing additional analysis in order to determine their suitability for conduct in space are also listed. Recommendations were made concerning the manner in which these materials science experiments are carried out and the related studies that should be pursued.

Author

24 COMPOSITE MATERIALS

Includes laminates.

N78-10217* National Aeronautics and Space Administration Lewis Research Center, Cleveland, Ohio

CONSOLIDATION OF SILICON NITRIDE WITHOUT ADDITIVES

Paul F Sikora and Hun C. Yeh 1977 13 p refs Presented at Fall Meeting of the Am. Ceramic Soc., San Francisco, 31 Oct - 3 Nov 1978

(NASA-TM-73693, E-9229) Avail NTIS HC A02/MF A01 CSCL 11D

The feasibility of producing a sound, dense Si₃N₄ body without additives was explored, using conventional gas hot isostatic pressing techniques and an uncommon hydraulic hot isostatic pressing technique. These two techniques produce much higher pressure 275-413 MN/m² (40,000 - 60,000 psi) than hot pressing techniques. Evaluation was based on density measurement, microscopic examination, both optical and electron and X-ray diffraction analysis. The results are summarized as follows: (1) Si₃N₄ can be densified to high density, greater than 95% of theoretical, without additions. (2) The higher density Si₃N₄ specimens appear to be associated with a greater amount of alpha to beta transformation. (3) Under high pressure, the alpha to beta transformation can occur at a temperature as low as 1150 C. (4) Grain deformation and subsequent recrystallization and grain refinement result from hot isostatic pressing of Si₃N₄.

Author

N78-13136* National Aeronautics and Space Administration Lewis Research Center, Cleveland, Ohio

EFFECT OF DISCONTINUITIES AS A MEANS TO ALLEVIATE THERMAL EXPANSION MISMATCH DAMAGE IN LAMINAR COMPOSITES

Charles A Hoffman Nov 1977 17 p refs

(NASA-TM-73739, E-9259) Avail NTIS HC A02/MF A01 CSCL 11D

An investigation of Nichrome/tungsten laminar composites showed that intentionally introduced discontinuities, such as perforations through or grooves on the surface of the matrix laminae, improved thermal expansion mismatch damage resistance. It was found that specimens having smooth matrix laminae surfaces were virtually destroyed by delamination in 21 or fewer fast cool cycles in which they were water quenched from 981 C. Specimens having interior matrix laminae with discontinuities and relatively thin, non-discontinuous surface matrix laminae resisted 50 similar cycles without evident delamination damage.

Author

N78-13137* National Aeronautics and Space Administration Lewis Research Center, Cleveland, Ohio

FRACTURE SURFACE CHARACTERISTICS OF OFF-AXIS COMPOSITES

J. H. Sinclair and C. C. Chamis 1977 23 p refs Presented at 14th Ann. Meeting of the Soc. of Engr. Sci., Inc., Bethlehem, Pa., 14-16 Nov 1977

(NASA-TM-73700, E-9085-2) Avail NTIS HC A02/MF A01 CSCL 11D

The fracture surface characteristics of off-axis high modulus graphite fiber epoxy composite specimens were studied using a scanning electron microscope (SEM). The specimens were subjected to tensile loading at various angles (0 deg - 90 deg) to the fiber direction. SEM photomicrographs of the fractured surfaces revealed three different load angle regions with distinct fracture characteristics. Based on these revelations, criteria were established which can be used to characterize fracture surfaces with respect to a predominant single stress fracture mode.

Author

N78-13138* National Aeronautics and Space Administration Lewis Research Center, Cleveland, Ohio

MECHANICAL BEHAVIOR AND FRACTURE CHARACTERISTICS OF OFF-AXIS FIBER COMPOSITES. 1: EXPERIMENTAL INVESTIGATION

John H. Sinclair and Christos C. Chamis Dec 1977 36 p refs

(NASA-TP-1081, E-9085) Avail NTIS HC A03/MF A01 CSCL 11D

The mechanical behavior, fracture surfaces, and fracture modes of unidirectional high-modulus graphite-fiber/epoxy composites subjected to off-axis tensile loads were investigated experimentally. The investigation included the generation of stress-strain-to-fracture data and scanning electron microscope studies of the fractured surfaces. The results led to the identification of fracture modes and distinct fracture surface characteristics for off-axis tensile loading. The results also led to the formulation of criteria for identifying and characterizing these fracture modes and their associated fracture surfaces. The results presented and discussed herein were used in the theoretical investigation and comparisons described in Part 2. These results should also provide a good foundation for identifying, characterizing, and quantifying fracture modes in both off-axis and angle-ply laminates.

Author

N78-10086* National Aeronautics and Space Administration Lewis Research Center, Cleveland, Ohio

MECHANICAL BEHAVIOR AND FRACTURE CHARACTERISTICS OF OFF-AXIS FIBER COMPOSITES. 2: THEORY AND COMPARISONS

Christos C. Chamis and John H. Sinclair Jan 1978 29 p refs

(NASA-TP-1082, E-9269) Avail NTIS HC A03/MF A01 CSCL 11D

The mechanical behavior and stresses inducing fracture modes of unidirectional high-modulus graphite-fiber epoxy composites subjected to off-axis tensile loads were investigated theoretically. The investigation included the use of composite mechanics, combined-stress failure criteria, and finite-element stress analysis. The results are compared with experimental data and led to the formulation of criteria and convenient plotting procedures for identifying, characterizing, and quantifying these fracture modes.

Author

N78-17152* National Aeronautics and Space Administration Lewis Research Center, Cleveland, Ohio

ADHESIVE COHESIVE STRENGTH OF A ZrO₂-1.2 w/o Y₂O₃ NiCrAlY THERMAL BARRIER COATING

Stanley R Levine 1978 26 p refs Proposed for presentation at the 80th Ann. Meeting of the Am. Ceramic Soc., Detroit, MI, 11 May 1978

(NASA-TM-73792, E-9359) Avail NTIS HC A03/MF A01 CSCL 11D

The room temperature adhesive cohesive strength of a 0.05 cm thick ZrO₂-1.2 w/o Y₂O₃ 0.013 cm thick NiCrAlY thermal barrier coating system (TBC) was investigated. The weakest link was the oxide/NiCrAlY interface region with a strength of 6.2 MN/sq m. The fracture was about half cohesive oxide failure, half oxide/NiCrAlY adhesive failure and 1 percent cohesive NiCrAlY failure. The TBC failed in a similar manner in 950 C tensile and compression tests. The oxide stripped from the TBC had a cohesive strength of 24.6 MN/sq m. The NiCrAlY had a cohesive strength of 25.1 MN/sq m. The NiCrAlY and oxide failed primarily at interparticle boundaries.

Author

N78-17153* National Aeronautics and Space Administration Lewis Research Center, Cleveland, Ohio

THE EFFECTS OF ECCENTRICITIES ON THE FRACTURE OF OFF-AXIS FIBER COMPOSITES

C. C. Chamis and J. H. Sinclair 1978 17 p refs Presented at the 33rd Ann. Conf. of the Soc. of the Plastics Ind., Reinforced Plastics Composites Inst., Washington, D. C., 7-10 Feb 1978

(NASA-TM-73826, E-9269-1) Avail NTIS HC A02/MF A01 CSCL 11D

Finite element analyses were performed to investigate theoretic

ically the effects of in-plane and out-of-plane eccentricities, bending or twisting, and thickness nonuniformity on the axial stress and strain variations across the width of off-axis specimens. The results are compared with measured data and are also used to assess the effects of these eccentricities on the fracture stress of off-axis fiber composites. Guidelines for detecting and minimizing the presence of eccentricities are described. Author

N78-17184* National Aeronautics and Space Administration
Lewis Research Center, Cleveland, Ohio
MECHANICAL AND PHYSICAL PROPERTIES OF MODERN BORON FIBERS

James A DiCarlo 1978 20 p refs Proposed for presentation at the 2d Intern Conf on Composite Mater, Toronto, 16-20 Apr 1978, sponsored by the Met Soc of AIME (NASA-TM-73882, E-9494) Avail NTIS HC A02/MF A01 CSCI 11D

The results of accurate measurements of the modern boron fiber's Young's modulus, flexural modulus, shear modulus, and Poisson's ratio are reported. Physical property data concerning fiber density, thermal expansion, and resistance obtained during the course of the mechanical studies are also given. Author

N78-17185* National Aeronautics and Space Administration
Lewis Research Center, Cleveland, Ohio
THERMAL ENVIRONMENT EFFECTS ON STRENGTH AND IMPACT PROPERTIES OF BORON-ALUMINUM COMPOSITES

H H Grimes, R A Lad, and J E Marsel (Cleveland State Univ, Ohio) 1977 20 p refs Proposed for presentation at the 2d Intern Conf on Composite Materials, Toronto, Canada, 16-20 Apr 1978, sponsored by the Am Inst of Mining, Met and Petrol Engrs (NASA-TM-73885, E-9498) Avail NTIS HC A02/MF A01 CSCI 11D

Thermal effects on fracture strength and impact energy were studied in 50 volume percent unidirectional composites of 143 and 203 micron boron fibers in 6061 and 1100 aluminum matrices. For 6061 matrix composites, strength was maintained to approximately 400 C in the cyclic tests and higher than 400 C in the static tests. For the 1100 matrix composites, strength degradation appeared near 260 C after cycling and higher than 260 C in static heating. This composite strength degradation is explained by a fiber degradation mechanism resulting from a boron-aluminum interface reaction. The impact energy absorption degraded significantly only above 400 C for both matrix alloys. Thus, while impact loss for the 6061 composite correlates with the fiber strength loss, other energy absorption processes appear to extend the impact resistance of the 1100 matrix composites to temperatures beyond where its strength is degraded. Interrupted impact tests on as-received and thermally cycled composites define the range of load over which the fibers break in the impact event. Author

N78-18204* National Aeronautics and Space Administration
Lewis Research Center, Cleveland, Ohio
AXIAL RESIDUAL STRESSES IN BORON FIBERS

Donald H Behrendt 1978 19 p refs Presented at 2d Intern Conf on Composite Materials, Toronto, Canada, 16-20 Apr 1978

(NASA-TM-73894) Avail NTIS HC A02/MF A01 CSCI 11D

The axial residual stress distribution as a function of radius was determined from the fiber surface to the core including the average residual stress in the core. Such measurements on boron on tungsten (B/W) fibers show that the residual stresses for 102, 142, 203, and 386 micron diameter fibers were similar, being compressive at the surface and changing monotonically to a region of tensile within the boron. At approximately 25 percent of the original radius, the stress reaches a maximum tensile stress of about 860 mn/sq m and then decreases to a compressive stress near the tungsten boride core. Data were presented for 203 micron diameter B/W fibers that show annealing above 900 C reduces the residual stresses. A comparison

between 102 micron diameter B/W and boron on carbon (b/C) shows that the residual stresses were similar in the outer regions of the fibers, but that large differences near and in the core were observed. The effects of these residual stresses on the fracture of boron fibers were discussed. Author

N78-18205* National Aeronautics and Space Administration
Lewis Research Center, Cleveland, Ohio
RESIDUAL STRESSES IN ANGLEPLYED LAMINATES AND THEIR EFFECTS ON LAMINATE BEHAVIOR

C C Chermis 1978 24 p refs Presented at the 2d Intern Conf on Composite Mater, Toronto, 16-23 Apr 1978 (NASA-TM-78835) Avail NTIS HC A02/MF A01 CSCI 11D

Evidence of the presence of lamination residual stresses in angleplyed laminates were transply cracks and warpage of unsymmetric laminates which occur prior to application of any mechanical load. Lamination residual strains were measured using the embedded strain gage technique. These strains result from the temperature differences between cure and room temperature and vary linearly within this temperature range. Lamination residual stresses were usually present in angleplyed fiber composites laminates; they were also present in unidirectional hybrids and superhybrids. For specific applications, the magnitudes of lamination residual stresses were determined and evaluated relative to the anticipated applied stresses. Particular attention was given to cyclic thermal loadings in applications where the thermal cycling takes place over a wide temperature range. Author

N78-20254* National Aeronautics and Space Administration
Lewis Research Center, Cleveland, Ohio

MEASUREMENT OF THE TIME-TEMPERATURE DEPENDENT DYNAMIC MECHANICAL PROPERTIES OF BORON/ALUMINUM COMPOSITES

J A DiCarlo and J E Marsel (Cleveland State Univ) 1978 43 p refs Presented at the 5th Conf on Composite Mater Testing and Design, New Orleans, 20-23 Mar 1978; sponsored by Am Soc for Testing and Mater (NASA-TM-78837, E-9548) Avail NTIS HC A03/MF A01 CSCI 11D

A flexural vibration test and associated equipment were developed to accurately measure the low strain dynamic modulus and damping of composite materials from -200 C to over 500 C. The basic test method involves the forced vibration of composite bars at their resonant free-free flexural modes in a high vacuum cryostat furnace. The accuracy of these expressions and the flexural test was verified by dynamic moduli and damping capacity measurements on 50 fiber volume percent boron/aluminum (B/Al) composites vibrating near 2000 Hz. The phase results were summarized to permit predictions of the B/Al dynamic behavior as a function of frequency, temperature, and fiber volume fraction. Author

N78-20255* National Aeronautics and Space Administration
Lewis Research Center, Cleveland, Ohio

CORRELATION OF FIBER COMPOSITE TENSILE STRENGTH WITH THE ULTRASONIC STRESS WAVE FACTOR

Alex Vary and Raymond F Lark 1978 23 p refs Presented at the 1978 Spring Conf, New Orleans, 3-7 Apr 1978; sponsored by Am Soc for Nondestructive Testing

(NASA-TM-78846, E-9564) Avail NTIS HC A03/MF A01 CSCI 11D

An ultrasonic acoustic technique was used to indicate the strength variations of tensile specimens of a graphite epoxy composite. A stress wave factor was determined and its value was found to depend on variations of the fiber-resin bonding as well as fiber orientation. The fiber orientations studied were 0 deg (longitudinal), 10 deg (off axis), 90 deg (transverse) [0 deg or -45 deg/0 deg] symmetrical and [+ or -45 deg] symmetrical. The stress wave factor can indicate variations of the tensile and shear strengths of composite materials. The stress wave factor was also found to be sensitive to strength variations associated with microporosity and differences in fiber-resin ratio. Author

N78-21220* National Aeronautics and Space Administration, Lewis Research Center, Cleveland, Ohio.

IN SITU PLY STRENGTH: AN INITIAL ASSESSMENT

C. C. Chamis and T. L. Sullivan 1978 19 p refs Presented at the 5th Conf. on Composite Mater.: Testing and design, New Orleans, 20-22 Mar. 1978; sponsored by Am. Soc. for Testing and Mater.

(NASA-TM-73771; E-9238) Avail: NTIS HC A02/MF A01 CSCL 11D

The in situ ply strengths in several composites were calculated using laminate fracture data for appropriate low modulus, and high modulus fiber composites were used in conjunction with the least squares method. The laminate fracture data were obtained from tests on Modmor-1 graphite/epoxy, AS-graphite/epoxy, boron/epoxy and E-glass/epoxy. The results show that the calculated in situ ply strengths can be considerably different from those measured in unidirectional composites, especially the transverse strengths and those in angleplied laminates with transply cracks. Author

N78-21211* National Aeronautics and Space Administration, Lewis Research Center, Cleveland, Ohio.

TITANIUM/BERYLLIUM LAMINATES: FABRICATION, MECHANICAL PROPERTIES, AND POTENTIAL AERO-SPACE APPLICATIONS

C. C. Chamis and R. F. Lark May 1978 25 p refs Presented at the 23d Natl. SAMPE Symp. and Exhibition, Anaheim, Calif., 2-4 May 1978

(NASA-TM-73891; E-9508) Avail: NTIS HC A02/MF A01 CSCL 11D

The investigation indicated that structural laminates can be made which have a modulus of elasticity comparable to steel, fracture strength comparable to the yield strength of titanium, density comparable to aluminum, impact resistance comparable to titanium, and little or no notch sensitivity. These laminates can have stiffness and weight advantages over other materials including advanced fiber composites, in some aerospace applications where buckling resistance, vibration frequencies, and weight considerations control the design. Author

N78-22163* National Aeronautics and Space Administration, Lewis Research Center, Cleveland, Ohio.

METHOD FOR ALLEVIATING THERMAL STRESS DAMAGE IN LAMINATES Patent Application

C. A. Hoffman, J. W. Weston, and N. W. Orth, inventors (to NASA) Filed 6 Apr. 1978 16 p

(NASA-Case-LEW-12493-1; US-Patent-Appl-SN-893857) Avail: NTIS HC A02/MF A01 CSCL 11D

According to the method of the invention discontinuities are positively introduced into the interface between layers so as to reduce the thermal stress produced by unequal expansion of the materials which make up the composite. Although a plurality of discrete elements could be used to form one of the layers and thus carry out this purpose, the discontinuities are preferably produced by simply drilling holes in the metallic matrix layer or by forming grooves in a grid pattern in this layer. The apparent novel feature of the invention is the use of geometrical considerations to introduce discontinuities in the matrix of a composite material. This provides for the control of stresses that would otherwise unbound the constituents, cause peeling of the outer layers, and cause the loss of strength properties of the composite when it is subjected to one or more thermal cycles. NASA

N78-24291* National Aeronautics and Space Administration, Lewis Research Center, Cleveland, Ohio.

THERMAL BARRIER COATINGS

S. J. Grasse, S. R. Levine, and J. S. Clark 1978 21 p refs Presented at the 23d Ann. Intern. Gas Turbine Conf., London, 9-13 Apr. 1978; sponsored by ASME

(NASA-TM-78R48) Avail: NTIS HC A02/MF A01 CSCL 11D

Thermal barrier coatings offer gas turbines one way to reach fuel flexibility and improved efficiency. Test/analytical results are encouraging for this young technology. Author

N78-32181* National Aeronautics and Space Administration, Lewis Research Center, Cleveland, Ohio.

EFFECTS OF MOISTURE PROFILES AND LAMINATE CONFIGURATION ON THE HYGRO STRESSES IN ADVANCED COMPOSITES

C. C. Chamis, J. H. Sinclair, and R. F. Lark 1978 18 p ref Presented at the 10th Natl. Tech. Conf., Kiamesha Lake, New York, 17-19 Oct. 1978. Sponsored by the Soc. for the Advan. of Mater. and Process Eng.

(NASA-TM-78978; E-9755) Avail: NTIS HC A02/MF A01 CSCL 11D

An integrated hygrothermo-mechanical theory was used to predict the effects of three moisture profiles on the ply hygro stresses in angleplied laminates. The moisture profiles were linear, parabolic and hyperbolic. Moisture content varied from 1 percent in the exposed ply to zero in the protected ply. The angleplied laminates were of two generic configurations. The results obtained are summarized graphically to illustrate the effects of both moisture profile and laminate configuration. The results indicate that ply transverse tensile hygro stresses may reach sufficiently high magnitudes to cause transply cracking. A.R.H.

N78-33148* National Aeronautics and Space Administration, Lewis Research Center, Cleveland, Ohio.

ANALYSIS/DESIGN OF STRIP REINFORCED RANDOM COMPOSITES (STRIP HYBRIDS)

C. C. Chamis and J. H. Sinclair 1978 23 p refs To be presented at the Annual Meeting of ASME, San Francisco, Calif., 10-15 Dec. 1978

(NASA-TM-78985; E-9733) Avail: NTIS HC A02/MF A01 CSCL 11D

Advanced analysis methods and composite mechanics were applied to a strip-reinforced random composite square panel with fixed ends to illustrate the use of these methods for the a priori assessment of the composite panel when subjected to complex loading conditions. The panel was assumed to be of E-glass random composite. The strips were assumed to be of three advanced unidirectional composites to cover a range of low, intermediate, and high modulus stiffness. The panels were assumed to be subjected to complex loadings to assess their adequacy as load-carrying members in auto body, aircraft engine nacelle and windmill blade applications. The results show that strip hybrid panels can be several times more structurally efficient than the random composite base materials. Some of the results are presented in graphical form and procedures are described for use of these graphs as guides for preliminary design of strip hybrids. A.R.H.

N78-33160* National Aeronautics and Space Administration, Lewis Research Center, Cleveland, Ohio.

ACOUSTIC EMISSION TESTING OF COMPOSITE VESSELS UNDER SUSTAINED LOADING

R. F. Lark and P. E. Moorhead 1978 25 p refs Presented at the Symp. on Nondestructive Evaluation and Flaw Criticality for Composite Mater., Philadelphia 10-11 Oct. 1978. Sponsored by the Am. Soc. for Testing Mater.

(NASA-TM-78981; E-9759) Avail: NTIS HC A02/MF A01 CSCL 11D

Acoustic emissions (AE) generated from Kevlar 49/epoxy composite pressure vessels subjected to sustained load-to-failure tests were studied. Data from two different transducer locations on the vessels were compared. It was found that AE from vessel wall-mounted transducers showed a wide variance from those for identical vessels subjected to the same pressure loading. Emissions from boss-mounted transducers did, however, yield values that were relatively consistent. It appears that the signals from the boss-mounted transducers represent an integrated average of the emissions generated by fibers fracturing during the vessel tests. The AE from boss-mounted transducers were also independent of time for vessel failure. This suggests that a similar number of fiber fractures must occur prior to initiation of vessel failure. These studies indicate a potential for developing an AE test procedure for predicting the residual service life or integrity of composite vessels. A.R.H.

A78-33161* National Aeronautics and Space Administration, Lewis Research Center, Cleveland, Ohio.

ION BEAM SPUTTERING OF FLUOROPOLYMERS

J. S. Sovey 1978 15 p refs To be presented at the 25th Natl. Vacuum Symp., San Francisco, 28 Nov. 1978 - 1 Dec. 1978 Sponsored by the Am. Vacuum Soc.

(NASA-TM-79000: E-9784) Avail: NTIS HC A02/MF A01 CSCL 11D

Ion beam sputter processing rates as well as pertinent characteristics of etched targets and films are described. An argon ion beam source was used to sputter etch and deposit the fluoropolymers PTFE, FEP, and CTFE. Ion beam energy, current density, and target temperature were varied to examine effects on etch and deposition rates. The ion etched fluoropolymers yield cone or spire-like surface structures which vary depending upon the type of polymer, ion beam power density, etch time, and target temperature. Sputter target and film characteristics documented by spectral transmittance measurements. X-ray diffraction, ESCA, and SEM photomicrographs are included.

A.R.H.

A78-24892* A Weibull characterization for tensile fracture of multicomponent brittle fibers. R. G. Barrows (NASA, Lewis Research Center; U.S. Army, Air Mobility Research and Development Laboratory, Cleveland, Ohio). *Metallurgical Society of AIME, Fall Metals Conference, Chicago, Ill., Oct. 24-27, 1977, Paper. 30 p. 25 refs.*

Necessary to the development and understanding of brittle fiber reinforced composites is a means to statistically describe fiber strength and strain-to-failure behavior. A statistical characterization for multicomponent brittle fibers is presented. The method, which is an extension of usual Weibull distribution procedures, statistically considers the components making up a fiber (e.g. substrate, sheath, and surface) as separate entities and taken together as in a fiber. Tensile data for silicon carbide fiber and for an experimental carbon-boron alloy fiber are evaluated in terms of the proposed multicomponent Weibull characterization. (Author)

A78-24905* An integrated theory for predicting the hydrothermomechanical response of advanced composite structural components. C. C. Chamis, R. F. Lark, and J. H. Sinclair (NASA, Lewis Research Center, Cleveland, Ohio). *American Society for Testing and Materials, Technical Specialists Conference on Environmental Effects on Advanced Composite Materials, Dayton, Ohio, Sept. 29, 30, 1977, Paper. 43 p. 18 refs.*

A theory is developed for predicting the hydrothermomechanical response of advanced composite structural components. The combined hydrothermal effects on the mechanical properties of unidirectional composites loaded along the material axis and off-axis, and of angleplied laminates are also evaluated. The materials investigated consist of neat PR-288 epoxy matrix resin and an AS-type graphite fiber/PR-288 resin unidirectional composite. S.C.S.

A78-25191* Effect of processing parameters on autoclaved PMR polyimide composites. R. D. Vannucci (NASA, Lewis Research Center, Cleveland, Ohio). In: *Materials and processes - In service performance; Proceedings of the Ninth National Technical Conference, Atlanta, Ga., October 4-6, 1977. (A78-25176 09-23)* Azusa, Calif., Society for the Advancement of Material and Process Engineering, 1977, p. 177-199.

A study was conducted to determine the effect of processing parameters on the processability and properties of autoclaved fiber reinforced PMR polyimide composites. Composites were fabricated from commercially available graphite fabric and glass fabric PMR polyimide prepreg materials. Process parameters investigated included degree of resin advancement, heating rate, and cure pressure. Composites were inspected for porosity by ultrasonic 'C' scan and photomicrographic examination. Processing characteristics for each set of process parameters and the effect of process parameters on composite mechanical properties at room temperature and 600 F are described. (Author)

A78-33201* Residual stresses in angleplied laminates and their effects on laminate behavior. C. C. Chamis (NASA, Lewis Research Center, Cleveland, Ohio). *Metallurgical Society of AIME, International Conference on Composite Materials, 2nd, Toronto, Canada, Apr. 16-20, 1978, Paper. 23 p. 17 refs.*

NASA Lewis Research Center research in the field of composite laminate residual stresses is reviewed and summarized. The origin of lamination residual stresses, evidence of their presence, experimental methods for measuring them, and theoretical methods for predicting them are described. Typical results are presented which show the magnitudes of residual stresses in various laminates including hybrids and superhybrids, and in other complex composite components. Results are also presented which show the effects of lamination residual stresses on laminate warpage and on laminate mechanical properties including fracture stresses. Finally, the major findings and conclusions derived therefrom are summarized. (Author)

A78-33203* Predicted inlet gas temperatures for tungsten fiber reinforced superalloy turbine blades. E. A. Winsa, L. J. Westfall, and D. W. Petrasek (NASA, Lewis Research Center, Cleveland, Ohio). *Metallurgical Society of AIME, International Conference on Composite Materials, 2nd, Toronto, Canada, Apr. 16-20, 1978, Paper. 22 p. 23 refs.*

Tungsten fiber-reinforced superalloy composite (TFRS) impingement-cooled turbine blade inlet gas temperatures were calculated taking into account material spanwise strength, thermal conductivity, material oxidation resistance, fiber-matrix interaction, and coolant flow. Measured values of TFRS thermal conductivities are presented. Calculations indicate that blades made of 30 volume percent fiber content TFRS having a 12,000 N-m/kg stress-to-density ratio while operating at 40 atm and a 0.06 coolant flow ratio could permit a turbine blade inlet gas temperature of over 1900 K. This is more than 150 K greater than similar superalloy blades. (Author)

A78-33204* Thermal environment effects on strength and impact properties of boron-aluminum composites. H. H. Grimes, R. A. Lad (NASA, Lewis Research Center, Cleveland, Ohio), and J. E. Maisel (Cleveland State University, Cleveland, Ohio). *Metallurgical Society of AIME, International Conference on Composite Materials, 2nd, Toronto, Canada, Apr. 16-20, 1978, Paper. 19 p.*

A systematic study was conducted regarding the degradation of fracture strength and impact energy in commercial B-Al composites in both static and cyclic thermal environments. The composites used in the study contained approximately 50 vol % boron fibers, unidirectionally aligned in either a 6061 Al or 1100 Al matrix. The tensile strengths of the composites after 3000 thermal cycles as a function of upper cycle temperature are presented in graphs. The temperature at which the strengths of 6061 Al matrix, B-Al composites were significantly degraded after 3000 cycles was noticeably higher than that for the 1100 Al matrix composites. Static heating at 420 C resulted in no significant strength degradation for the 6061 Al matrix composites. In the case of 1100 matrix composites, some degradation was observed at 420 C but markedly less than in the composites cycled to 420 C. G.R.

A78-33207* Correlation of fiber composite tensile strength with the ultrasonic stress wave factor. A. Vary and R. F. Lark (NASA, Lewis Research Center, Cleveland, Ohio). *American Society for Nondestructive Testing, Spring Conference, New Orleans, La., Apr. 3-7, 1978, Paper. 22 p. 9 refs.*

An ultrasonic-acoustic technique was used to indicate the strength variations of tensile specimens of a graphite-epoxy composite. A 'stress wave factor' was determined and its value was found to depend on variations of the fiber-resin bonding as well as fiber orientation. The fiber orientations studied were 0 deg (longitudinal), 10 deg (off axis), 90 deg (transverse), (0 deg⁺ or - 45 deg 0) symmetrical, and (+ or - 45 deg) symmetrical. The stress wave factor can indicate variations of the tensile and shear strengths of composite materials. The stress wave factor was also found to be sensitive to strength variations associated with microporosity and differences in fiber-resin ratio. (Author)

A78-33209 * Shear strength of metal - SiO₂ contacts. S. V. Pepper (NASA, Lewis Research Center, Cleveland, Ohio). *American Physical Society, U.S. Navy, and ARPA, International Topical Conference on the Physics of SiO₂ and Its Interfaces, Yorktown Heights, N.Y., Mar. 22-24, 1978, Paper. 5 p. 11 refs.*

The strength of the bond between metals and SiO₂ is studied by measuring the static coefficient of friction of metals contacting alpha-quartz in ultrahigh vacuum. It was found that copper with either chemisorbed oxygen, nitrogen or sulphur exhibited higher contact strength on stoichiometric SiO₂ than did clean copper. Since the surface density of states induced by these species on copper is similar, it appears that the strength of the interfacial bond can be related to the density of states on the metal surface. (Author)

A78-33210 * Kinetics of imidization and crosslinking in PMR-polyimide resin. R. W. Lauver (NASA, Lewis Research Center, Cleveland, Ohio). *American Chemical Society, Central Regional Meeting, 9th, Charleston, W. Va., Oct. 12-14, 1977, Paper. 23 p. 14 refs.*

A78-33213 * Principles of ESCA and applications to metal corrosion, coating and lubrication. D. R. Wheeler (NASA, Lewis Research Center, Cleveland, Ohio). *American Society for Metals Symposium on Modern Metallographic Techniques and Their Applications, Cleveland, Ohio, Apr. 10, 11, 1978, Paper. 14 p. 10 refs.*

The principles of ESCA (electron spectroscopy for chemical analysis) are described by comparison with other spectroscopic techniques. The advantages and disadvantages of ESCA as compared to other surface sensitive analytical techniques are evaluated. The use of ESCA is illustrated by actual applications to oxidation of steel and René 41, the chemistry of lubricant additives on steel, and the composition of sputter deposited hard coatings. Finally, a bibliography of material that is useful for further study of ESCA is presented and commented upon. (Author)

A78-33222 * Measurement of the time-temperature dependent dynamic mechanical properties of boron/aluminum composites. J. A. DiCarlo (NASA, Lewis Research Center, Material Science Branch, Cleveland, Ohio) and J. E. Maisel (Cleveland State University, Cleveland, Ohio). *American Society for Testing and Materials, Conference on Composite Materials: Testing and Design, 5th, New Orleans, La., Mar. 20-23, 1978, Paper. 42 p. 20 refs.*

A relatively simple flexural vibration test is developed for accurate measurement of the low-strain dynamic modulus and damping capacity of B-Al composite bar specimens from -200 C to over 500 C. The specimens are prepared from 8-ply unidirectional panels containing 50 volume percent fibers composed of 203-micron commercial boron-on-tungsten fibers. The basic test technique consists of the forced flexural vibration of the composite bar specimens at their two lowest free-free symmetrical resonant modes in a high-vacuum cryostat furnace. Specimen damping is determined from oscilloscope photographs of the free decay obtained after simultaneously removing the resonant drive signal and grounding the vibration-drive electrode. The availability of time-temperature dynamic data coupled with the predictive accuracy of composite theory suggests a future potential for using such data in examining environmental effects on composite macrostructure and microstructure. S. D.

A78-33223 * In situ ply strengths - An initial assessment. C. C. Chamis and T. L. Sullivan (NASA, Lewis Research Center, Cleveland, Ohio). *American Society for Testing and Materials, Conference on Composite Materials: Testing and Design, 5th, New Orleans, La., Mar. 20-23, 1978, Paper. 18 p. 14 refs.*

The in situ ply strengths in several composites were calculated using a computational procedure developed for this purpose. Laminate fracture data for appropriate low modulus and high modulus fiber composites were used in the laminate analysis in

conjunction with the method of least squares. The laminate fracture data were obtained from tests on Modmor-I graphite/epoxy, AS-graphite/epoxy, boron/epoxy and E-glass/epoxy. The results obtained show that the calculated in situ ply strengths can be considerably different from those measured in unidirectional composites, especially the transverse strengths and those in angled ply laminates with transverse cracks. (Author)

A78-33436 * Recent advances in lightweight, filament-wound composite pressure vessel technology. R. F. Lark (NASA, Lewis Research Center, Cleveland, Ohio). In: *Composites in pressure vessels and piping; Proceedings of the Energy Technology Conference, Houston, Tex., September 18-23, 1977. (A78-33435 13-24) New York, American Society of Mechanical Engineers, 1977, p. 17-49. 8 refs.*

A review of recent advances is presented for lightweight, high-performance composite pressure vessel technology that covers the areas of design concepts, fabrication procedures, applications, and performance of vessels subjected to single-cycle burst and cyclic fatigue loading. Filament-wound fiber/epoxy composite vessels were made from S-glass, graphite, and Kevlar 49 fibers and were equipped with both structural and nonstructural liners. Pressure vessel structural efficiencies were attained which represented weight savings, using different liners, of 40 to 60 percent over all-titanium pressure vessels. Significant findings in each area are summarized including data from current NASA-Lewis Research Center contractual and in-house programs. (Author)

A78-37686 * The use of an ion-beam source to alter the surface morphology of biological implant materials. A. J. Weigand (NASA, Lewis Research Center, Cleveland, Ohio). *Society for Biomaterials, Conference, San Antonio, Tex., Apr. 29-May 2, 1978, Paper. 27 p. 21 refs.*

An electron-bombardment ion-thruster was used as a neutralized-ion-beam sputtering source to texture the surfaces of biological implant materials. The materials investigated included 316 stainless steel; titanium-6% aluminum, 4% vanadium; cobalt-20% chromium, 15% tungsten; cobalt-35% nickel, 20% chromium, 10% molybdenum; polytetrafluoroethylene; polyoxymethylene; silicone and polyurethane copolymer; 32% carbon-impregnated polyolefin; segmented polyurethane; silicone rubber; and alumina. Scanning electron microscopy was used to determine surface morphology changes of all materials after ion-texturing. Electron spectroscopy for chemical analysis was used to determine the effects of ion-texturing on the surface chemical composition of some polymers. Liquid contact angle data were obtained for ion-textured and untextured polymer samples. Results of tensile and fatigue tests of ion-textured metal alloys are presented. Preliminary data of tissue response to ion-textured surfaces of some metals, polytetrafluoroethylene, alumina, and segmented polyurethane have been obtained. (Author)

A78-40310 * Effect of preload on the fatigue and static strength of composite laminates with defects. T. R. Porter (Boeing Aerospace Co., Seattle, Wash.) and G. T. Smith (NASA, Lewis Research Center, Cleveland, Ohio). In: *Recent advances in engineering science; Proceedings of the Fourteenth Annual Meeting, Bethlehem, Pa., November 14-16, 1977. (A78-40301 17-31) Bethlehem, Pa., Lehigh University, 1977, p. 267-270.*

The effect of a preload cycle on the structural performance of three graphite-epoxy composite laminates was studied. The laminates studied were a laminate typical of general purpose structures (L1), a laminate representative of a filament wound tank (L2), and a laminate representative of turboengine fan blades. The effects of three sizes of simulated initial defects were studied. The tests developed static strength data, fatigue to failure data, and residual static data after application of a predetermined number of fatigue cycles. For L1 specimens, there was a slight trend for the static

strength to be greater for preloaded specimens. After application of cyclic loading, however, the influence of preloading was insignificant. In L2 and L3 specimens there was no consistent difference in the static or fatigue results between preloaded and nonpreloaded specimens. P.T.H.

A78-50325* Impetus of composite mechanics on test methods for fiber composites. C. C. Chamis (NASA, Lewis Research Center, Cleveland, Ohio). *U.S.-USSR Seminar on Fracture of Composite Materials, Riga, Latvian SSR, Sept. 4-7, 1978, Paper. 30 p. 14 refs.*

Significant contributions of the three major areas of composite mechanics to the development of test methods are illustrated with selected examples. The areas of composite mechanics include composite micromechanics, composite macromechanics, and laminate theory. The examples can be considered to be representative of the contribution of composite mechanics to the development of composite test methods. The specific examples describe contributions such as criteria for selecting resin matrices for improved composite strength, the 10 deg off-axis tensile test, procedures for configuring hybrids, and the concept of 'reduced bending rigidities'. The pertinent composite mechanics equations associated with each contribution are given and supplemented by tabular and/or graphical data which illustrate the significance of the contribution. G.R.

N78-11197* Massachusetts Inst. of Tech., Cambridge
ANALYSIS OF DELAMINATION IN UNIDIRECTIONAL AND CROSSPLYED FIBER COMPOSITES CONTAINING SURFACE CRACKS Interim Report

S. S. Wang and J. F. Mandell May 1977 35 p refs

(Grant NsG-3044)

(NASA-CR-135248) Avail: NTIS HC A03/MF A01 CSCL 11D

A two-dimensional hybrid stress finite element analysis is described which was used to study the local stress field around delamination cracks in composite materials. The analysis employs a crack tip singularity element which is embedded in a matrix interlayer between plies of the laminate. Results are given for a unidirectional graphite/epoxy laminate containing a delamination emanating from a surface crack through the outside ply. The results illustrate several aspects of delamination cracks: (1) the localization of the singular stress domain within the interlayer, (2) the local concentration of stress in the ply adjacent to the crack; (3) the nature of the transverse normal and interlaminar shear stress distributions; and (4) the relative magnitudes of $K_{sub 1}$ and $K_{sub 2}$ associated with the delamination. A simple example of the use of the analysis in predicting delamination crack growth is demonstrated for a glass/epoxy laminate. The comparisons with experimental data show good agreement. Author

N78-13134* Westinghouse Electric Corp., Pittsburgh, Pa
Research and Development Center

CHARACTERIZATION, SHAPING, AND JOINING OF SiC/SUPERALLOY SHEET FOR EXHAUST SYSTEM COMPONENTS Final Report

J. A. Cornie 20 Jul 1977 82 p refs

(Contract NAS3-19735)

(NASA-CR-135301) Rept-9D4-NASIC-R1) Avail: NTIS HC A05/MF A01 CSCL 11D

Hafnium carbide was shown to be virtually inert when in contact with silicon carbide and Waspaloy for at least 200 hr at 1093 C (2000 F). Extensive interaction was noted with other superalloys such as HA-188. A continuous CVD HfC deposition process was developed for deposition of up to 8 microns on 14 mm (0.056 in.) SiC tungsten core filament at rates as high as 8 m/min. The rate can be increased by increasing the length of the reactor and the output of the power supply used in resistive heating of the filament substrate. The strength of HfC coated filament varies with thickness in a Griffith-like manner. This strength reduction was greater for HfC coatings than for tungsten coatings, presumably because of the greater ductility of tungsten. Author

N78-14089* General Electric Co., Cincinnati, Ohio.
IMPACT RESISTANT BORON/ALUMINUM COMPOSITES FOR LARGE FAN BLADES

T. L. Oller, C. T. Salemme, J. H. Bowden, G. S. Doble, and P. Melnyk Dec 1977 127 p ref

(Contract NAS3-19728)

(NASA-CR-135274) R77AEG667)

Avail: NTIS

HC A07/MF A01 CSCL 11D

Blade-like specimens were subjected to static ballistic impact testing to determine their relative FOD impact resistance levels. It was determined that a plus or minus 15 deg layup exhibited good impact resistance. The design of a large solid boron/aluminum fan blade was conducted based on the FOD test results. The CF6 fan blade was used as a baseline for these design studies. The solid boron/aluminum fan blade design was used to fabricate two blades. This effort enabled the assessment of the scale up of existing blade manufacturing details for the fabrication of a large B/Al fan blade. Existing CF6 fan blade tooling was modified for use in fabricating these blades. Author

N78-18103* Cornell Univ., Ithaca, N. Y. Dept of Theoretical and Applied Mechanics

IMPACT ON MULTILAYERED COMPOSITE PLATES

Final Report, Sep. 1976 - Dec. 1976

B. S. Kim and F. C. Moon Apr. 1977 121 p refs

(Grant NsG-3080)

(NASA-CR-135247) Avail: NTIS HC A06/MF A01 CSCL 11D

Stress wave propagation in a multilayer composite plate due to impact was examined by means of the anisotropic elasticity theory. The plate was modeled as a number of identical anisotropic layers and the approximate plate theory of Mindlin was then applied to each layer to obtain a set of difference-differential equations of motion. Dispersion relations for harmonic waves and correction factors were found. The governing equations were reduced to difference equations via integral transforms. With given impact boundary conditions these equations were solved for an arbitrary number of layers in the plate and the transient propagation of waves was calculated by means of a Fast Fourier Transform algorithm. The multilayered plate problem was extended to examine the effect of damping layers present between two elastic layers. A reduction of the interlaminar normal stress was significant when the thickness of damping layer was increased but the effect was mostly due to the softness of the damping layer. Finally, the problem of a composite plate with a crack on the interlaminar boundary was formulated. Author

N78-18131* Fiber Science, Inc., Gardena, Calif.
COMPOSITE HUB/METAL BLADE COMPRESSOR ROTOR

Contractor Report, Dec. 1974 - Oct. 1975

Sam Yao Jan. 1978 25 p

(Contract NAS3-18926)

(NASA-CR-135343) Avail: NTIS HC A02/MF A01 CSCL 11D

A low cost compressor rotor was designed and fabricated for a small jet engine. The rotor hub and blade keepers were compression molded with graphite epoxy. Each pair of metallic blades was held in the hub by a keeper. All keepers were locked in the hub with circumferential windings. Feasibility of fabrication was demonstrated in this program. Author

N78-20257* General Dynamics/Convair, San Diego, Calif.
THERMAL PERFORMANCE OF A CUSTOMIZED MULTI-LAYER INSULATION (MLI). DESIGN AND FABRICATION OF TEST FACILITY HARDWARE Final Report

K. E. Leonhard 15 Aug 1975 67 p refs

(Contract NAS3-17756)

(NASA-CR-135051) CASD-NAS-75-006)

Avail: NTIS

HC A04/MF A01 CSCL 11D

The design, fabrication, and assembly of hardware for testing the performance of a customized multilayer insulation are discussed. System components described include the thermal payload simulator, the modified cryoshroud, and a tank back pressure control device designed to maintain a constant liquid

boiling point during the thermal evaluation of the multilayer insulation. The thermal payload simulator will provide a constant temperature surface in the range of 20.5 to 417K (37 to 750R) for the insulated tank to view. The cryostat was modified to establish a low temperature black body cavity while limiting liquid hydrogen usage to a minimum feasible rate. Author

N78-22164* Norton Co., Worcester, Mass.
IMPROVED REACTION SINTERED SILICON NITRIDE
 Final Report
 H. R. Baumgartner Mar. 1978 83 p refs
 (Contract NAS3-19723)
 (NASA CR-135291) Avail: NTIS HC A06/MF A01 CSCL 110

Processing treatments were applied to as-nitrided reaction sintered silicon nitride (RSSN) with the purpose of improving strength after processing to above 350 MN/m² and improving strength after oxidation exposure. The experimental procedures are divided into three broad classifications: sintering of surface-applied powders; impregnation of solution followed by further thermal processing; and infiltration of molten silicon and subsequent carburization or nitridation of the silicon. The impregnation of RSSN with solutions of aluminum nitrate and zirconyl chloride, followed by heating at 1400-1500 C in a nitrogen atmosphere containing silicon monoxide, improved RSSN strength and oxidation resistance. The room temperature bend strength of RSSN was increased nearly fifty percent above the untreated strength with mean absolute strengths up to 420 MN/m². Strengths of treated samples that were measured after a 12 hour oxidation exposure in air were up to 90 percent of the original as-nitrided strength, as compared to retained strengths in the range of 35 to 60 percent for untreated RSSN after the same oxidation exposure. Author

N78-26132* TRW Equipment Labs., Cleveland, Ohio
FIBER REINFORCED PMR POLYIMIDE COMPOSITES
 Final Report, 28 Jun. 1978 - 31 Oct. 1977
 P. J. Cayano and W. E. Winters 15 May 1978 103 p refs
 (Contract NAS3-20366)
 (NASA CR-135377; TRW-ER-7884F) Avail: NTIS HC A06/MF A01 CSCL 110

Commercially obtained PMR-15 polyimide prepregs with S-glass and graphite fiber reinforcements were evaluated along with in-house prepared glass and graphite cloth PMR 2 materials. A novel autoclave approach was conceived and used to demonstrate that both the PMR systems respond to 14 MPa (200 psi) autoclave pressures to produce void free composites equivalent to die molded laminates. Isothermal gravimetric analysis and subsequent mechanical property tests indicated that the PMR 2 system was significantly superior in thermo oxidative stability, and that S-glass reinforcements may contribute to the accelerated degradation of composites at 316 C (600 F) when compared to graphite fiber reinforced composites. Fully reversed bending fatigue experiments were conducted with a type of fixture unused for organic matrix composites. These studies indicated that the graphite fiber composites were clearly superior in fatigue resistance to the glass fiber reinforced material and that PMR matrix composite systems yield performance of the same order as composite materials employing other families of matrices. Author

A78-18903* Evaluation of low cost/high temperature fiber and blanket insulation. E. L. Straus (Martin Marietta Aerospace, Denver, Colo.). In: Diversity - Technology explosion; Proceedings of the Twenty-second National Symposium and Exhibition, San Diego, Calif., April 26-28, 1977. (A78-18870 04-23) Azusa, Calif., Society for the Advancement of Material and Process Engineering, 1977, p. 466-485. 8 refs. Contract No. NAS3-18900.

Twelve fiber materials comprising water-felted fiber cakes and blanket insulation were subjected to furnace exposures at 1000, 1200, 1400, and 1600 C for up to 500 hours to establish the time-temperature limits below which these insulation materials can withstand repeated thermal cycles without detrimental shrinkage, thermal conductivity increase, or physical changes. Test samples were inspected periodically during the exposure cycles and weight loss and dimensional shrinkage were measured. Density, fiber crystallography, and thermal conductivity were measured after exposure and properties were compared with those of unexposed controls. (Author)

A78-26683* Evaluation of flawed composite structure under static and cyclic loading. T. R. Porter (Boeing Aerospace Co., Seattle, Wash.). In: Fatigue of filamentary composite materials; Proceedings of the Symposium, Denver, Colo., November 15, 16, 1976. (A78-26673 10-24) Philadelphia, Pa., American Society for Testing and Materials, 1977, p. 152-170. Contract No. NAS3-19709.

This paper presents the results of a program investigating the effects of initial defects on the fatigue and fracture response of composite laminates. The structural laminates investigated were a typical angle-ply laminate, a polar/hoop-wound pressure vessel laminate, and a typical engine fan blade laminate. Defects investigated were full- and half-penetration circular holes, full- and half-penetration slits, and countersink holes. Results are presented showing the effects of the defect size and type on the static fracture strength, fatigue performance, and residual static strength. The results of inspection procedures are shown, describing the effect of cyclic and static loadings on damage propagation in composite laminates. The data in this study were used to define proof test levels as a qualification procedure in composite structure subjected to cyclic loading. (Author)

25 INORGANIC AND PHYSICAL CHEMISTRY

Includes chemical analysis, e.g., chromatography; combustion theory; electrochemistry; and photochemistry.

For related information see also 77 *Thermodynamics and Statistical Physics*.

N78-10224* National Aeronautics and Space Administration, Lewis Research Center, Cleveland, Ohio.

FUEL COMBUSTION Patent

Cecil J. Marek, inventor (to NASA) Issued 4 Oct. 1977 5 p Filed 31 Mar. 1976 Supersedes N76-20215 (14 - 11, p 1358)

(NASA-Case-LEW-12137-1; US-Patent-4,052,144; US-Patent-Appl-SN-672210; US-Patent-Class-431-352; US-Patent-Class-431-158; US-Patent-Class-60-39,51R; US-Patent-165-106) Avail: US Patent Office CSCL 218

A fuel combustor comprises a chamber with air and fuel inlets and a combustion gas outlet. The fuel is supplied to a vaporization zone and fuel and air are mixed in a pair of mixing chambers, each exemplified by a swirl can. The resultant mixture is directed into a combustion zone within the combustor. Heat pipes are arranged with one end portion substantially in the combustion zone and the other end in the vaporization zone of its appropriate mixing chamber. Some of the heat of combustion is thus carried back upstream into the swirl cans, to vaporize the fuel as it enters the vaporization zone in the swirl can, thereby improving vaporization and fuel mixing.

Official Gazette of the U.S. Patent Office

N78-12167* National Aeronautics and Space Administration, Lewis Research Center, Cleveland, Ohio.

EFFECT OF TRICHLOROFUOROMETHANE AND MOLECULAR CHLORINE ON OZONE FORMATION BY SIMULATED SOLAR RADIATION

David A. Britter and Edgar L. Wong Nov. 1977 22 p refs (NASA-TP-1093; E-9078) Avail: NTIS HC A02/MF A01 CSCL 04A

Mixtures of air with either Cl₂ or CFC₃ were photolyzed in a reaction chamber by simulated solar radiation. Ozone formation was temporarily inhibited by Cl₂ and permanently inhibited by CFC₃. A chemical mechanism including gas phase and wall reactions is proposed to explain these results. The CFC₃ is assumed to be adsorbed on the chamber walls and to poison the sites for O₃ destruction. Author

N78-13157* National Aeronautics and Space Administration, Lewis Research Center, Cleveland, Ohio.

FORMATION OF Na₂SO₄ AND K₂SO₄ IN FLAMES DOPED WITH SULFUR AND ALKALI CHLORIDES AND CARBONATES

George C. Fryburg, Robert A. Miller, Carl A. Stearns, and Fred J. Kohl 1977 19 p refs Presented at Symp. on High Temp. Metal Halide Chem., Atlanta, 9-14 Oct. 1977; sponsored by Electrochem. Soc.

(NASA-TM-73794) Avail: NTIS HC A02/MF A01 CSCL 218

High pressure, free-jet expansion, mass spectrometric sampling was used to identify directly and to measure reaction products formed in doped methane-oxygen flames. Flames were doped with SO₂ or CH₃SH and sodium or potassium chlorides or carbonates. Gaseous Na₂SO₄ or K₂SO₄ molecules were formed in residence times on the order of msec for each combination of dopants used. Composition profiles of combustion products were measured and compared with equilibrium thermodynamic calculations of product composition. Author

N78-13158* National Aeronautics and Space Administration, Lewis Research Center, Cleveland, Ohio.

VOLATILE PRODUCTS FROM THE INTERACTION OF KCl(g) WITH Cr₂O₃ AND La₂O₃ IN OXIDIZING ENVIRONMENTS

Fred J. Kohl, Robert A. Miller, Carl A. Stearns, George C. Fryburg, and John G. Dillard 1977 15 p refs Presented at Symp. on High Temp. Metal Halide Chem., Atlanta, 9-14 Oct. 1977; sponsored by Electrochem. Soc.

(NASA-TM-73795) Avail: NTIS HC A02/MF A01 CSCL 07D

Cooled target collection techniques and high pressure mass spectrometric sampling were used to measure the relative rates of oxidative vaporization and to identify the volatile products emanating from samples of chromia and Mg-doped lanthanum chromite. The materials were exposed to partial pressures of KCl with and without H₂O in one atmosphere of slowly flowing oxygen at elevated temperatures. Chromia and fresh samples of lanthanum chromite exhibited enhanced rates of oxidative vaporization upon exposure to these reactants. Mass spectrometric identification showed that the enhancements resulted from the heterogeneous formation of complex molecules of the type KCl sub 1,2,3 CrO₃ and KOH sub 1,2 CrO₃. Lanthanum chromite that had undergone prolonged oxidative vaporization exhibited no enhanced oxidation upon exposure to the reactants. Author

N78-13159* National Aeronautics and Space Administration, Lewis Research Center, Cleveland, Ohio.

INTERACTION OF NaCl(g) AND HCl(g) WITH CONDENSED Na₂SO₄

Carl A. Stearns, Fred J. Kohl, George C. Fryburg, and Robert A. Miller 1977 21 p refs Presented at Symp. on High Temp. Metal Halide Chem., Atlanta, Ga., 9-14 Oct. 1977; sponsored by Electrochemical Soc.

(NASA-TM-73796) Avail: NTIS HC A02/MF A01 CSCL 07D

The interaction of Na₂SO₄(l) with NaCl(g), HCl(g), and H₂O(g) was studied in atmospheric pressure flowing air and oxygen at Na₂SO₄(l) temperatures of 900 and 1600 C. Thermogravimetric and high pressure mass spectrometric sampling techniques were used. Experimental results establish that previously reported enhanced rates of weight loss of Na₂SO₄(l) in the presence of NaCl(g) are due to the reaction: Na₂SO₄(c) + 2HCl(g) = 2NaCl(g) + SO₂(g) + H₂O(g) + 1/2O₂(g) being driven to the right in flowing gas systems. The HCl(g) is the product of hydrolysis of NaCl caused by small but significant amounts of H₂O(g) present in the system. Thermochemical calculations are used to show that even with sub-ppm levels of H₂O(g) present, significant quantities of HCl(g) are produced. Author

N78-16211* National Aeronautics and Space Administration, Lewis Research Center, Cleveland, Ohio.

THE FLUORINATION OF COBALT AND ZINC

Patricia Marie O'Donnell Jul. 1976 111 p refs

(NASA-TM-X-73478; E-C233) Avail: NTIS HC A06/MF A01 CSCL 07D

The reaction of cobalt and zinc with gaseous fluorine was studied. Both temperature and pressure were variables, ranging from 298 to 773 K and 50 to 625 torr. Both reactions were described by the parabolic rate law. The reaction was both temperature and pressure dependent. In the zinc reaction the vaporization rate of zinc above 573 K complicated the kinetics. The cobalt reaction was complex due to the formation of two fluorides. Parabolic rate constants were calculated and from the temperature dependence of the reaction a heat of reaction of 2.8 kcal/mole superscript -1 for zinc and 4.8 kcal/mole superscript -1 for cobalt in the low temperature range was estimated. A theoretical analysis indicated the most probable mechanism for both reactions is cation diffusion through cation vacancies. Comparisons with reported oxidation kinetics were given. Author

N78-17172* National Aeronautics and Space Administration
Lewis Research Center, Cleveland, Ohio.
**RELEASE OF DISSOLVED NITROGEN FROM WATER
DURING DEPRESSURIZATION**

R. J. Simoneau 1978 20 p refs To be Presented at the
14th Ann. Meeting of the Southeastern Seminar on Thermal
Sci., Raleigh, N. C. 6-7 Apr 1978
(NASA-TM-73822, E-1411-1) Avail: NTIS HC A02/MF A01
CSCL 07D

Experiments were run to study depressurization of water
containing various concentrations of dissolved nitrogen gas. The
primary case being room temperature water saturated with
nitrogen at 4 MPa. In a static depressurization experiment, water
with very high nitrogen content was depressurized at rates from
0.09 to 0.50 MPa per second and photographed with high
speed movies. The pictures showed that the bubble population
at a given pressure increased strongly with decreasing depres-
surization rate. Flow experiments were performed in an axisym-
metric converging-diverging nozzle and in a two-dimensional
converging nozzle with glass sidewalls. Depressurization gradi-
ents were roughly 500 to 1200 MPa per second. Both nozzles
exhibited choked flow behavior even at nitrogen concentration
levels as low as 4 percent of saturated. The flow rates were
independent of concentration level and could be computed as
incompressible water flow based on the difference between
stagnation and throat pressures; however, the throat pressures
were significantly different between the two nozzles. Author

N78-18237* National Aeronautics and Space Administration,
Lewis Research Center, Cleveland, Ohio.

**DEFINITION AND EFFECT OF CHEMICAL PROPERTIES OF
SURFACES IN FRICTION, WEAR, AND LUBRICATION**

Donald H. Buckley 1978 40 p refs Proposed for Presentation
at the Intern. Conf. on Tribology, Cambridge, Mass., 19-23 June
1978; sponsored by ONR, AROD, ARPA, and MIT
(NASA-TM-73806) Avail: NTIS HC A03/MF A01 CSCL 07D

Chemical properties relative to their role in adhesion, friction,
wear and lubrication discussed in this paper will include: (1)
adsorption, both physical and chemical; (2) orientation of the
solid as well as the lubricant; (3) surface energy; (4) surface
segregation; (5) surface versus bulk metallurgical effects; (6)
electronic nature of the surface; and (7) bonding mechanisms.
Author

N78-20281* National Aeronautics and Space Administration,
Lewis Research Center, Cleveland, Ohio.

**EFFECT OF NITRIC OXIDE ON PHOTOCHEMICAL OZONE
FORMATION IN MIXTURES OF AIR WITH MOLECULAR
CHLORINE AND WITH TRICHLOROFLUOROMETHANE**

David A. Bittker and Edgar L. Wong Apr. 1978 25 p refs
(NASA-TP-1192, E-9297) Avail: NTIS HC A02/MF A01 CSCL
07D

Ozone formation in a reaction chamber at room temperature
and atmospheric pressure was studied for the photolysis of
mixtures of NO with either Cl₂ or CFC13 in air. Both Cl₂ + NO
and CFC13 + NO in air strongly inhibited O₃ formation during
the entire 3 to 4 hour reaction. A chemical mechanism that
explains the results was presented. An important part of this
mechanism was the formation and destruction of chlorine nitrate.
Computations were performed with this same mechanism for
CFC13-NO-air mixtures at stratospheric temperatures, pressures,
and concentrations. Results showed large reductions in steady-
state O₃ concentrations in these mixtures as compared with
pure air. Author

N78-25148* National Aeronautics and Space Administration,
Lewis Research Center, Cleveland, Ohio.

**APPARATUS FOR EXT. ACTION AND SEPARATION OF A
PREFERENTIALLY PHOTO-DISSOCIATED MOLECULAR
ISOTOPE INTO POSITIVE AND NEGATIVE IONS BY MEANS
OF AN ELECTRIC FIELD Patent**

Horst E. Wilhelm inventor (to NASA) (Colo. State Univ., Ft
Collins) Issued 18 Apr 1978 5 p Sponsored by NASA
(NASA-Case-LEW-12465-1, US-Patent-4,085,332.

US-Patent-Appl-SN-692413, US Patent-Class-250-528;
US-Patent-Class-55-2, US-Patent-Class-55-100;
US-Patent-Class-55-101; US-Patent-Class-250-531;
US-Patent-Class-250-423P) Avail: US Patent Office CSCL
07D

Molecules of one and the same isotope were preferentially
photodissociated by a laser and an ultraviolet source, or by
multiphoton absorption of laser radiation. The resultant ions were
confined with a magnetic field, moved in opposite directions by
an electric field, extracted from the photodissociation region by
means of screening and accelerating grids, and collected in
ducts. Official Gazette of the U.S. Patent Office

N78-25149* National Aeronautics and Space Administration,
Lewis Research Center, Cleveland, Ohio.

**FORMULATED PLASTIC SEPARATORS FOR SOLUBLE
ELECTRODE CELLS Patent Application**

Dean W. Sheibley, inventor (to NASA) Filed 3 Nov. 1977
22 p

(NASA-Case-LEW-12358-2; US-Patent-Appl-SN-848428) Avail:
NTIS HC A02/MF A01 CSCL 07D

Membranes comprising a hydrochloric acid-insoluble sheet
of a mixture of a rubber and a powered ion transport material
were designed for use in oxidation-reduction (REDOX) electrical
accumulator cells. The sheet of thermoplastic rubber and an ion
transport material, which may be in the form of a film on a
flexible substrate such as asbestos or paper was made by
dissolving the rubber in a solvent and mixing with the ion transport
material which is 20-50 volume percent as compared with
80-50 volume percent rubber. Preferred ion transport materials
include a salt or a chloride anion; a phosphonium, tertiary
ammonium or quaternary ammonium, cation; a metal oxide, and
a silicate or boric acid. NASA

N78-26185* National Aeronautics and Space Administration,
Lewis Research Center, Cleveland, Ohio.

**APPLICATION OF ESCA TO THE DETERMINATION OF
STOICHIOMETRY IN SPUTTERED COATINGS AND
INTERFACE REGIONS**

Donald R. Wheeler Aug. 1978 15 p refs Proposed for
presentation at the 2d Intern. Conf. on Solid Lubrication, Denver,
14-18 Aug. 1978; sponsored by the Am. Soc. of Lubrication
Engr.

(NASA-TM-78896, E-9367) Avail: NTIS HC A02/MF A01
CSCL 07D

X-ray photoelectron spectroscopy was used to characterize
radiofrequency sputter deposited films of several refractory
compounds. Both the bulk film properties such as purity and
stoichiometry and the character of the interfacial region between
the film and substrate were examined. The materials were CrB₂,
MoS₂, Mo₂C, and Mo₂B₅ deposited on 440C steel. It was
found that oxygen from the sputtering target was the primary
impurity in all cases. Biasing improves the film purity. The effect
of biasing on film stoichiometry is different for each compound.
Comparison of the interfacial composition with friction data
suggests that adhesion of these films is improved if a region of
mixed film and iron oxides can be formed. Author

N78-27226* National Aeronautics and Space Administration,
Lewis Research Center, Cleveland, Ohio.

TARGETS FOR PRODUCING HIGH PURITY I-123 Patent

James W. Blue, inventor (to NASA) Issued 9 May 1978 7 p
Filed 4 Sep 1973 Supersedes N74-1047b (12-1, p 0060)
Continuation-in-part of abandoned US Patent Appl. SN-266927,
filed 28 Jun 1972, which is a continuation in-part of US appl.
SN-863280, filed 2 Oct 1969, US Patent-3,694,313

(NASA-Case-LEW-10518-3, US-Patent-4,088,532,
US-Patent-Appl-SN-394207, US-Patent-Class-176-11,
US-Patent-Class-176-16, US-Patent-Class-250-400,
US-Patent-Class-250-429, US-Patent-Class-250-492B;
US-Patent-3,694,313, US-Patent-Appl-SN-266927,
US-Patent-Appl-SN-863280) Avail: US Patent Office CSCL
07D

Tellurium powder in improved targets is bombarded with a
cyclotron beam to produce Xe-123. Flowing gas streams carry

the Xe 123 through one cold trap which removes Xe-123 that subsequently decays to I-123. During this bombardment energy is deposited in the target material causing its temperature to rise. Some of the tellurium vaporizes and subsequently condenses on surfaces that are cooler than the vaporization temperature. Provision is made for the repeated bombardment of this condensed tellurium.

Official Gazette of the U.S. Patent Office

A78-24887 * Volatile products from the interaction of $KCl(g)$ with Cr_2O_3 and La_2O_3 in oxidizing environments. F. J. Kohl, R. A. Miller, C. A. Stearns, G. C. Fryburg (NASA, Lewis Research Center, Cleveland, Ohio), and J. G. Dillard. *Electrochemical Society, Symposium on High Temperature Metal Halide Chemistry, Atlanta, Ga., Oct. 9-14, 1977, Paper 14 p. 9 refs.*

Based on cooled target collection methods and high pressure mass spectrometer sampling, oxidative vaporization rates and emanating volatile products were evaluated for interactions of $KCl(g)$ with Cr_2O_3 and La_2O_3 in oxidizing environments. It was found that: (1) increased rates of oxidative vaporization upon exposure to the reactants are exhibited by chromia and fresh lanthanum chromite samples, and (2) these increased rates result from the heterogeneous formation of complex molecules such as KCl sub $1,2,3CrO_3$ and KOH sub $1,2CrO_3$. No increased rates were observed for lanthanum chromite subjected to prolonged oxidative vaporization. S.G.S.

A78-24888 * Interaction of $NaCl(g)$ and $HCl(g)$ with condensed Na_2SO_4 . C. A. Stearns, F. J. Kohl, G. C. Fryburg, and R. A. Miller (NASA, Lewis Research Center, Cleveland, Ohio). *Electrochemical Society, Symposium on High Temperature Metal Halide Chemistry, Atlanta, Ga., Oct. 9-14, 1977, Paper 20 p. 17 refs.*

$Na_2SO_4(l)-NaCl(g)$ interactions were studied at a total pressure of one atmosphere of air or oxygen for various temperatures of $Na_2SO_4(l)$ and for various partial pressures of $NaCl(g)$ and $H_2O(g)$. Mass spectrometric sampling techniques were used to identify and monitor gas phase species. Continuous recording thermogravimetric measurements were conducted to determine condensed phase weight change rates. Experimental measurements were supplemented with thermodynamic calculations. Numerous experiments were performed at sample temperatures of 900 and 1000 C with 300 ppm $NaCl(g)$. In these experiments, the reproducibility of the Na_2SO_4 vaporization weight loss rate and initial weight gain upon addition of $NaCl(g)$ were found to be satisfactory. It was found that the addition of $NaCl(g)$ to air flowing over $Na_2SO_4(l)$ at 900 and 1000 C enhances the rate of weight loss of the $Na_2SO_4(l)$. This enhancement increases when $H_2O(g)$ is also added to the air flow. G.R.

A78-24889 * Formation of Na_2SO_4 and K_2SO_4 in flames doped with sulfur and alkali chlorides and carbonates. G. C. Fryburg, R. A. Miller, C. A. Stearns, and F. J. Kohl (NASA, Lewis Research Center, Cleveland, Ohio). *Electrochemical Society, Symposium on High Temperature Metal Halide Chemistry, Atlanta, Ga., Oct. 9-14, 1977, Paper 18 p. 27 refs.*

High pressure, free-jet expansion, mass spectrometric sampling was used to identify directly and to measure reaction products formed in doped methane-oxygen flames. Flames were doped with SO_2 or CH_3SH and sodium or potassium chlorides or carbonates. Gaseous Na_2SO_4 or K_2SO_4 molecules were formed in residence times on the order of 1 msec for each combination of dopants used. Composition profiles of combustion products were measured and compared with equilibrium thermodynamic calculations of product composition. (Author)

A78-31438 * X-ray photoelectron spectroscopic study of surface chemistry of dibenzyl disulfide on steel under mild and severe wear conditions. D. R. Wheeler (NASA, Lewis Research Center, Cleveland, Ohio). *Wear, vol. 47, Apr. 1978, p. 243-264, 16 refs.*

X-ray photoelectron spectroscopy was used to characterize the chemical composition of 304 stainless steel surfaces run in oil containing dibenzyl disulfide under both mild and severe wear conditions. In severe wear a sulfide was formed at the expense of the normal oxide. This was due to either chemical attack on the oxide or reaction with clean metal exposed by the wear process. In the mild wear scars there was no evidence of either sulfide or mercaptide. The oxide, however, was approximately twice as thick as the normal oxide on an unworn surface. The change in surface chemistry was primarily a function of wear rate rather than load. (Author)

A78-33221 * Effluent characterization from a conical pressurized fluid bed. R. J. Priem, R. J. Rothblut, and R. W. Paton (NASA, Lewis Research Center, Cleveland, Ohio). *International Conference on Fluidized-Bed Combustion, 5th, Washington, D.C., Dec. 12-14, 1977, Paper 14 p. 10 refs.*

An important factor regarding the use of a pressurized coal burning fluidized bed (PFB) providing gases for driving a gas turbine is the turbine blade lifetime. However, very little data are currently available to predict erosion and corrosion rates produced by the effluent from a PFB. To assess the potential of alloys developed for aeronautical applications to resist this environment it was decided to build a coal burning fluidized bed that could be employed to measure erosion and corrosion rates. Tests were conducted with a conical fluidized bed to obtain some degree of filtration through the top of the bed. A description is presented of the data obtained in the first 138 hours of testing to characterize the effluent from the bed under different test conditions. The considered tests had been made to determine the best operating conditions prior to using the bed in a determination of the erosion and corrosion rates of typical turbine blade materials. G.R.

A78-33224 * Release of dissolved nitrogen from water during depressurization. R. J. Simons (NASA, Lewis Research Center, Cleveland, Ohio). *Southeastern Seminar on Thermal Sciences, Annual Meeting, 14th, Raleigh, N.C., Apr. 6-7, 1978, Paper 19 p. 7 refs.*

Experiments were run to study depressurization of water containing various concentrations of dissolved nitrogen gas, the primary case being room temperature water saturated with nitrogen at 4 MPa. In a static depressurization experiment, water with very high nitrogen content was depressurized at rates from 0.09 to 0.50 MPa per second and photographed with high-speed movies. The pictures showed that the bubble population at a given pressure increased strongly with decreasing depressurization rate. Bubbles rarely appeared before the pressure reached half the initial pool pressure. Flow experiments were performed in an axisymmetric converging-diverging nozzle and in a two-dimensional converging nozzle with glass sidewalls. Depressurization gaugents were roughly 500 to 1200 MPa per second. Both nozzles exhibited choked flow behavior even at nitrogen concentration levels as low as 4 percent of saturated. The flow rates were independent of concentration level and could be computed as incompressible water flow based on the difference between stagnation and throat pressures; however, the throat pressures were significantly different between the two nozzles. (Author)

26 METALLIC MATERIALS

Includes physical, chemical, and mechanical properties of metals, e.g., cohesion, and metallurgy.

N78-11220* National Aeronautics and Space Administration
Lewis Research Center, Cleveland, Ohio

SECONDARY-ELECTRON-EMISSION PROPERTIES OF CONDUCTING SURFACES WITH APPLICATION TO MULTISTAGE DEPRESSED COLLECTORS FOR MICROWAVE AMPLIFIERS

Ralph Forman Nov 1977 33 p refs
(NASA-TP-1097, E-9233) Avail NTIS HC A03/MF A01 CSCL 11F

To improve the efficiency of high power microwave tubes, low secondary electron yield electrode surface for use in depressed collectors are needed. The secondary emission characteristics of a number of materials were investigated. The materials studied were beryllium, carbon (soot and pyrolytic graphite), copper, titanium carbide, and tantalum. Both total secondary yield delta and relative reflected primary yield were measured. These measurements were made in conjunction with Auger spectroscopy so that the secondary emission characteristics could be determined as a function of surface contamination or purity. The results show that low atomic weight elements, such as beryllium and carbon, have the lowest reflected primary yield and that roughening the surface of an electrode can markedly decrease secondary yield both for delta and reflected primaries. All factors considered a roughened pyrolytic graphite surface showed the greatest potential for use as an electrode surface in depressed collectors.

Author

N78-13181* National Aeronautics and Space Administration
Lewis Research Center, Cleveland, Ohio

MECHANICAL PROPERTIES OF ION-BEAM-TEXTURED SURGICAL IMPLANT ALLOYS

A J Weigand 1977 24 p refs. Presented at 24th Natl Symp, Boston, 8-11 Nov 1977, sponsored by Am Vacuum Soc
(NASA-TM-73742, E-9056-1) Avail NTIS HC A02/MF A01 CSCL 11F

An electron bombardment Hg ion thruster was used as an ion source to texture surfaces of materials used to make orthopedic and/or dental prostheses or implants. The materials textured include 316 stainless steel, titanium-6% aluminum, 4% vanadium, and cobalt-20% chromium, 15% tungsten. To determine the effect of ion texturing on the ultimate strength and yield strength, stainless steel and Co-Cr-W alloy samples were tensile tested to failure. Three types of samples of both materials were tested. One type was ion textured (the process also heats each sample to 300 C), another type was simply heated to 300 C in an oven, and the third type was untreated. Stress-strain diagrams, 0.2% offset yield strength data, total elongation data, and area reduction data are presented. Fatigue specimens of ion textured and untextured 316 stainless steel and Ti-6% Al-4% V were tested. Included as an ion textured sample is a Ti-6% Al-4% V sample which was ion machined by means of Ni screen mask so as to produce an array of 140 mu m x 140 mu m x 60 mu m deep pits. Scanning electron microscopy was used to characterize the ion textured surfaces.

Author

N78-13182* National Aeronautics and Space Administration
Lewis Research Center, Cleveland, Ohio

ROOM TEMPERATURE CRACK GROWTH RATES AND -20 DEG F FRACTURE TOUGHNESS OF WELDED 1 1/4 INCH A-285 STEEL PLATE

John L Shannon, Jr and Walter Rzasnicki Nov 1977 22 p refs
(NASA-TM-73847, E-9435) Avail NTIS HC A02/MF A01 CSCL 11F

Data are presented which were developed in support of a structural assessment of NASA-LEWIS' 10-foot by 10-foot supersonic wind tunnel, critical portions of which are fabricated from rolled and welded 1 1/4 inch thick A-285 steel plate.

Test material was flame cut from the tunnel wall and included longitudinal and circumferential weld joints. Parent metal, welds, and weld heat affected zone were tested. Tensile strength and fracture toughness were determined at -20 F, the estimated lowest tunnel operating temperature. Crack growth rates were measured at room temperature, where growth rates in service are expected to be highest.

Author

N78-13183* National Aeronautics and Space Administration
Lewis Research Center, Cleveland, Ohio

CYCLIC STRESS-STRAIN CURVE DETERMINATION FOR DBAC STEEL BY THREE METHODS

Alfred J. Nachtigal [1977] 6 p refs
(NASA-TM-73815, E-9402) Avail NTIS HC A02/MF A01 CSCL 11F

The room temperature cyclic stress-strain was determined for DBAC low alloy steel by three different methods. The method that involves the use of a single specimen monotonic tension test after cyclic straining provided the best agreement with the accepted basic method which requires a number of companion specimen tests. The single specimen test is also the simplest to conduct.

Author

N78-15229* National Aeronautics and Space Administration
Lewis Research Center, Cleveland, Ohio

FRICTION AND WEAR OF SEVERAL COMPRESSOR GAS-PATH SEAL MOVEMENTS

Robert C Bill and Donald W Wisander Jan 1978 42 p refs
(NASA-TP-1128, E-9276) Avail NTIS HC A03/MF A01 CSCL 11A

Rub interaction experiments were conducted on a series of sintered and plasma sprayed compressor gas path seal materials in contact with Ti-6Al-4V blade tip and knife edge rotors. The most rub tolerant materials investigated were sintered Nichrome and plasma sprayed nickel 25 percent graphite. The effectiveness of providing a compliant substrate for dense seal material coatings was also demonstrated. In general it was observed that rotor wear and high frictional energy generation rates accompanied smearing or surface densification of the materials investigated. The onset of smearing was sensitive to rub interaction parameters and seal geometry. Two complementary models were proposed to account for the smearing trends. One is based on thermal effects, the other on particulate escape effects. They were shown to be consistent with the experimental evidence at hand and together they predict that smearing, with the onset of high energy rub conditions, is favored when incursion rates (radial motion) are low, incursion depths are high, the seal geometry is of a knife edge character, and the seal particle size is small.

Author

N78-15230* National Aeronautics and Space Administration
Lewis Research Center, Cleveland, Ohio

FEASIBILITY STUDY OF TUNGSTEN AS A DIFFUSION BARRIER BETWEEN NICKEL-CHROMIUM-ALUMINUM AND GAMMA-GAMMA PRIME-DELTA EUTECTIC ALLOYS

Stanley G Young and Glenn R Zellars Jan 1978 35 p refs
(NASA-TP-1131, E-9271) Avail NTIS HC A03/MF A01 CSCL 11F

Coating systems proposed for potential use on eutectic alloy components in high-temperature gas turbine engines were studied with emphasis on deterioration of such systems by diffusion. A 1-mil thick W sheet was placed between eutectic alloys and a NiCrAl layer. Layered test specimens were aged at 1100 C for as long as 500 hours. Without the W barrier, the delta phase of the eutectic deteriorated by diffusion of Nb into the NiCrAl. Insertion of the W barrier stopped the diffusion of Nb from delta. Chromium diffusion from the NiCrAl into the gamma/gamma prime phase of the eutectic was greatly reduced by the barrier. However, the barrier thickness decreased with time, and W diffused into both the NiCrAl and the eutectic. When the delta platelets were aligned parallel to the NiCrAl layer rather than perpendicular, diffusion into the eutectic was reduced.

Author

N78-15235* National Aeronautics and Space Administration
Lewis Research Center, Cleveland, Ohio

THE INFLUENCE OF COMPOSITION, ANNEALING TREATMENT, AND TEXTURE ON THE FRACTURE TOUGHNESS OF Ti-6Al-2.5Sn PLATE AT CRYOGENIC TEMPERATURES
R. H. VanStone (GE, Schenectady, N. Y.), J. L. Shannon, Jr., W. S. Pierce, and J. R. Low, Jr. (Carnegie-Mellon Univ.) May 1977
46 p refs Presented at Symp on Toughness and Fracture Behavior of Titanium, Toronto, Ontario, 2-3 May 1977, sponsored by Am Soc Testing and Mater
(NASA TM 73872) Avail NTIS HC A03/MF A01 CSCL 11F

The plane strain fracture toughness $K_{sub Ic}$ and conventional tensile properties of two commercially produced one-inch thick Ti-6Al-2.5Sn plates were determined at cryogenic temperatures. One plate was extra-low interstitial (ELI) grade, the other normal interstitial. Portions of each plate were mill annealed at 1088 K (1500 F) followed by either air cooling or furnace cooling. The tensile properties, flow curves, and $K_{sub Ic}$ of these plates were determined at 295 K (room temperature), 77 K (liquid nitrogen temperature), and 20 K (liquid hydrogen temperature)

Author

N78-17187* National Aeronautics and Space Administration
Lewis Research Center, Cleveland, Ohio

MATERIALS TECHNOLOGY ASSESSMENT FOR STIRLING ENGINES

Joseph R. Stephens, Walter R. Witzke, Gordon K. Watson, James R. Johnston, and William J. Croft (Army Materials and Mechanics Res Center, Watertown, Mass.) Oct 1977 16 p refs Presented at Dept of Energy Highway Vehicle Sys Contractors' Coordination Meeting, Dearborn, Mich, 4-6 Oct 1977
(Contract EC-77-A-31-1011)

(NASA TM 73789, E-9356, CONS/1011-22) Avail NTIS HC A02 MF A01 CSCL 11F

A materials technology assessment of high temperature components in the improved (metal) and advanced (ceramic) Stirling engines was undertaken to evaluate the current state-of-the-art of metals and ceramics, identify materials research and development required to support the development of automotive Stirling engines, and to recommend materials technology programs to assure material readiness concurrent with engine system development programs. The most critical component for each engine is identified and some of the material problem areas are discussed

Author

N78-17189* National Aeronautics and Space Administration
Lewis Research Center, Cleveland, Ohio

ELEVATED-TEMPERATURE TENSILE AND CREEP PROPERTIES OF SEVERAL FERRITIC STAINLESS STEELS

J. Daniel Whittenberger Dec 1977 22 p refs
(NASA-TM 73853, E-9440) Avail NTIS HC A02/MF A01 CSCL 11F

The elevated temperature mechanical properties of several ferritic stainless steels were determined. The alloys evaluated included Armco 18SR, GE 1541, and NASA 18TA. Tensile and creep strength properties at 1073 and 1273 K and residual room temperature tensile properties after creep testing were measured. In addition, 1273 K tensile and creep tests and residual property testing were conducted with Armco 18SR and GE 1541 which were exposed for 200 hours to a severe oxidizing environment in automotive thermal reactors. Aside from the residual tensile properties for Armco 18SR, prior exposures did not affect the mechanical properties of either alloy. The 1273 K creep strength parallel to the sheet rolling direction was similar for all three alloys. At 1073 K, NASA 18TA had better creep strength than either Armco 18SR or GE 1541. NASA 18TA possesses better residual properties after creep testing than either Armco 18SR or GE 1541

Author

N78-17190* National Aeronautics and Space Administration
Lewis Research Center, Cleveland, Ohio

ELEVATED-TEMPERATURE FLOW STRENGTH, CREEP RESISTANCE AND DIFFUSION WELDING CHARACTERISTICS OF Ti-6Al-2Nb-1Ta-0.8Mo

J. Daniel Whittenberger and Thomas J. Moore Dec 1977

31 p refs

(NASA-TM-73854, E-9441) Avail NTIS HC A03/MF A01 CSCL 11F

A study of the flow strength, creep resistance and diffusion welding characteristics of the titanium alloy Ti-6Al-2Nb-1Ta-0.8Mo was conducted. Two mill-processed forms of this alloy were examined. The forged material was essentially processed above the beta transus while the rolled form was subjected to considerable work below the beta transus. Between 1150 and 1250 K, the forged material was stronger and more creep resistant than the rolled alloy. Both forms exhibit superplastic characteristics in this temperature range. Strain measurements during diffusion welding experiments at 1200 K reveal that weld interfaces have no measurable effect on the overall creep deformation. Significant deformation appears to be necessary to produce a quality diffusion weld between superplastic materials. A 'soft' interlayer inserted between forging surfaces would seemingly allow manufacture of quality diffusion welds with little overall deformation.

Author

N78-18182* National Aeronautics and Space Administration
Lewis Research Center, Cleveland, Ohio

TANTALUM MODIFIED FERRITIC IRON BASE ALLOYS Patent

Robert E. Oldreave and Charles P. Blankenship, inventors (to NASA) Issued 25 Oct 1977 3 p Filed 21 Jan 1976
Supersedes N78-17233 (14-08, p 0958)
(NASA-Case-LEW-12095-1; US-Patent-4,065,416, US-Patent-App'l-SN-651009; US-Patent-Class-75-124, US-Patent-Class-75-126D; US-Patent-Class-75-126F, US-Patent-Class-75-126G; US-Patent-Class-75-128T) Avail: US Patent Office CSCL 11F

Strong ferritic alloys of the Fe-Cr-Al type containing 0.4% to 2% tantalum were developed. These alloys have improved fabricability without sacrificing high temperature strength and oxidation resistance in the 800 C (1475 F) to 1040 C (1900 F) range.

Official Gazette of the U.S. Patent Office

N78-18183* National Aeronautics and Space Administration
Lewis Research Center, Cleveland, Ohio

DIRECTIONALLY SOLIDIFIED EUTECTIC GAMMA-GAMMA NICKEL-BASE SUPERALLOYS Patent

Melvin R. Jackson, inventor (to NASA) Issued 25 Oct 1977 7 p Filed 7 May 1976
(NASA-Case-LEW-12905-1, US-Patent-4,065,447,

US-Patent-App'l-SN 684171, US-Patent-Class-148-32; US-Patent-Class-75-170, US-Patent-Class-148-32.5) Avail: US Patent Office CSCL 11F

A directionally solidified multivariant eutectic gamma-gamma prime nickel-base superalloy casting having improved high temperature properties was developed. The alloy is comprised of a two phase eutectic structure consisting essentially of, on a weight percent basis, 6.0 - 9.0 aluminum, 5.0 - 17.0 tantalum, 0-10 cobalt, 0-6 vanadium, 0-6 rhenium, 2.0-6.0 tungsten, and the balance being nickel, subject to the proviso that the sum of the atomic percentages of aluminum plus tantalum is within the range of from 19-22, and the ratio of atomic percentages of tantalum to aluminum plus tantalum is within the range of from 0.12 - 0.23. Embedded within the gamma nickel-base matrix are aligned eutectic gamma prime phase (primarily nickel-aluminum-tantalum) reinforcing fibers.

Official Gazette of the U.S. Patent Office

N78-18261* National Aeronautics and Space Administration
Lewis Research Center, Cleveland, Ohio

CORRELATIONS BETWEEN ULTRASONIC AND FRACTURE TOUGHNESS FACTORS IN METALLIC MATERIALS

Alex Vary 1978 18 p refs Proposed for Presentation at the 11th Symp on Fracture Mech., Blacksburg, Va., 12-14 Jun 1978

(NASA-TM-73805) Avail NTIS HC A02/MF A01 CSCL 11F

A heuristic mathematical basis was proposed for the experimental correlations found between ultrasonic propagation factors and fracture toughness factors in metallic materials. A crack extension model was developed wherein spontaneous stress

A78-40371* Fracture surface characteristics of off-axis composites. J. H. Sillier and C. C. Charns (NASA Lewis Research Center, Cleveland, Ohio) *Society of Engineering Science, Annual Meeting, 14th, Lehigh University, Bethlehem, Pa., Nov. 14-16, 1977, Paper 22 p.*

The fracture surface characteristics of off-axis high modulus graphite fiber epoxy composite specimens were studied using a scanning electron microscope (SEM). The specimens were subjected to tensile loading at various angles (0-90 deg) to the fiber direction. SEM photomicrographs of the fractured surfaces revealed three different load angle regions with distinct fracture characteristics. Based on these revelations, criteria were established which can be used to characterize fracture surfaces with respect to a predominant 'single stress' fracture mode. (Author)

N78-14118* West Virginia Univ. Morgantown Coll. of Engineering

FLUIDIZED BED COMBUSTOR MODELING

M. Monro, P. Ranganathan, R. Krishnan, and C. Y. Wen. Jan. 1977. 214 p. refs.

(Contract NAS3-19725)

(NASA CR 135164) Avail. NTIS HC A10/MF A01 CSCL 21B

A general mathematical model for the prediction of performance of a fluidized bed coal combustor (FBC) is developed. The basic elements of the model consist of: (1) hydrodynamics of gas and solids in the combustor, (2) description of gas and solids contacting pattern, (3) kinetics of combustion and (4) absorption of SO₂ by limestone in the bed. The model is capable of calculating the combustion efficiency, axial bed temperature profile, carbon hold-up in the bed, oxygen and SO₂ concentrations in the bubble and emulsion phases, sulfur retention efficiency and particulate carry over by elutriation. The effects of bed geometry, excess air, location of heat transfer coils in the bed, calcium to sulfur ratio in the feeds, etc. are examined. The calculated results are compared with experimental data. Agreement between the calculated results and the observed data are satisfactory in most cases. Recommendations to enhance the accuracy of prediction of the model are suggested. (Author)

N78-25150* Notre Dame Univ. Ind. Dept. of Aerospace and Mechanical Engineering

BURNING OF LIQUID POOLS IN REDUCED GRAVITY
Final Report, Mar. 1976 - Feb. 1977

A. Murty Kanury. Jun. 1977. 141 p. refs.

(Contract NAS3-20087)

(NASA CR 135234 TR 77-33) Avail. NTIS HC A07/MF A01 CSCL 21B

The existing literature on the combustion of liquid fuel pools is reviewed to identify the physical and chemical aspects which require an improved understanding. Among the pre-, trans- and post-ignition processes, a delineation was made of those which seem to uniquely benefit from studies in the essential environment offered by spacelab. The role played by the gravitational constant in analytical and experimental justifications was developed. The analytical justifications were based on hypotheses, models and dimensional analyses, whereas the experimental justifications were based on an examination of the range of gravity and gravity-dependent variables possible in the earth-based laboratories. Some preliminary expositions into the questions of feasibility of the proposed spacelab experiment are also reported. (Author)

A78-41901* Analytical study of laser-supported combustion waves in hydrogen. N. H. Kemp and R. G. Root (Physical Sciences Inc., Woburn, Mass.) *American Institute of Aeronautics and Astronautics, Fluid and Plasma Dynamics Conference, 11th, Seattle, Wash., July 10-12, 1978, Paper 78-1219, 14 p., 15 refs.* Contract No. NAS3-20381

Laser supported combustion (LSC) waves are an important ingredient in the fluid mechanics of CW laser propulsion using a hydrogen propellant and 10.6 micron lasers. Therefore, a computer model has been constructed to solve the one-dimensional energy equation with constant pressure and area. Physical processes considered include convection, conduction, absorption of laser energy, radiation energy loss, and accurate properties of equilibrium hydrogen. Calculations for 1, 3, 10 and 30 atm were made for intensities of 10 to the 4th to 10 to the 6th W/sq cm, which gave temperature profiles, wave speed, etc. To pursue the propulsion application, a second computer model was developed to describe the acceleration of the gas emerging from the LSC wave into a variable-pressure, converging streamtube, still including all the above mentioned physical processes. The results show very high temperatures in LSC waves which absorb all the laser energy, and high radiative losses. (Author)

(elastic) waves produced during microcracking are instrumental in promoting the onset of unstable crack extension. Material microstructural factors involved in the process are measurable by ultrasonic probing. Experimental results indicate that ultrasonic attenuation and velocity measurements will produce significant correlations with fracture toughness properties and also yield strength. Author

N78-18282* National Aeronautics and Space Administration
Lewis Research Center, Cleveland, Ohio

PRINCIPLES OF ESCA AND APPLICATION TO METAL CORROSION, COATING AND LUBRICATION

Donald R. Wheeler 1978 15 p refs Presented at the Symp on Mod Mt alloy Tech and Ther Appl, Cleveland, 10-11 Apr 1978

(NASA TM-78839) Avail NTIS HC A02/MF A01 CSCL 11F

The principles of ESCA (electron spectroscopy for chemical analysis) were described by comparison with other spectroscopic techniques. The advantages and disadvantages of ESCA as compared to other surface sensitive analytical techniques were evaluated. The use of ESCA was illustrated by actual applications to oxidation of steel and Rene 41, the chemistry of lubricant additives on steel and the composition of sputter deposited hard coatings. A bibliography of material that was useful for further study of ESCA was presented and commented upon. Author

N78-21286* National Aeronautics and Space Administration
Lewis Research Center, Cleveland, Ohio

STRENGTH ENHANCEMENT PROCESS FOR PREALLOYED POWDER SUPERALLOYS

William J. Waters and John C. Freche 1977 31 p refs Presented at the TMS AIME Fall Meeting, Chicago, 24-27 Oct 1977

(NASA TM-78834, E-8544) Avail NTIS HC A03/MF A01 CSCL 11F

A technique involving superplastic processing and high pressure autoclaving was applied to a nickel base prealloyed powder alloy. Tensile strengths as high as 2865 MN sq m at 480 C were obtained with as superplastically deformed material. Appropriate treatments yielding materials with high temperature tensile and stress rupture strengths were also devised. Author

N78-21287* National Aeronautics and Space Administration
Lewis Research Center, Cleveland, Ohio

STRAINRANGE PARTITIONING BEHAVIOR OF THE NICKEL BASE SUPERALLOYS, RENE 80 AND IN 100

G. R. Halford and A. J. Nachtigal 1978 17 p refs Presented at the 46th Meeting of the Struct and Mater Panel of AGARD Specialists Meeting on Characterization of Low Cycle High Temp Fatigue by Strainrange Partitioning Method, Aalborg, Denmark, 9-14 Apr 1978

(NASA TM-78828) Avail NTIS HC A02/MF A01 CSCL 11F

A study was made to assess the ability of the method of Strainrange Partitioning (SRP) to both correlate and predict high temperature, low cycle fatigue lives of nickel base superalloys for gas turbine applications. The partitioned strainrange versus life relationships for uncoated Rene 80 and cast IN 100 were also determined from the ductility normalized Strainrange Partitioning equations. These were used to predict the cyclic lives of the baseline tests. The life predictability of the method was verified for cast IN 100 by applying the baseline results to the cyclic life prediction of a series of complex strain cycling tests with multiple hold periods at constant strain. It was concluded that the method of SRP can correlate and predict the cyclic lives of laboratory specimens of the nickel base superalloys evaluated in this program. Author

N78-21288* National Aeronautics and Space Administration
Lewis Research Center, Cleveland, Ohio

INFLUENCE OF FRETTING ON FLEXURAL FATIGUE OF 304 STAINLESS STEEL AND MILD STEEL

Robert C. Bill, Arny R. and T. Labal and Douglas A. Rohn 1978 19 p refs

(NASA-TP-1193, C-9414) Avail NTIS HC A02/MF A01 CSCL 11F

Fretting fatigue experiments conducted on 304 stainless steel using a flexural fatigue test arrangement with bolted on fretting pads demonstrated that fatigue life is reduced by at least a factor of 10 in the 286 to 334 MPa (38,500 to 48,500 psi) nominal flexural fatigue stress range. In addition, experiments in which the fretting pads were removed after selected numbers of cycles, followed by continued flexural fatigue without fretting show that continued fretting beyond 50,000 cycles does not significantly further reduce fatigue life of 304 stainless steel at 317 MPa (46,000 psi). Microscopic examination of the fretted contact areas revealed fracture initiation sites as well as numerous cracks that did not propagate to failure. Flexural fretting fatigue experiments performed on mild steel showed an insensitivity of fatigue life to the incidence of fretting under flexural stress conditions of from 162 to 217 MPa (23,500 to 31,500 psi). Author

N78-22288* National Aeronautics and Space Administration
Lewis Research Center, Cleveland, Ohio

HIGH TOUGHNESS-HIGH STRENGTH IRON ALLOY Patent Application

J. R. Stephens and W. R. Wittke, inventors (to NASA) Filed 13 Dec 1977 12 p

(NASA Case-LEW 12542-2, US Patent Appl-SN-860406) Avail NTIS HC A02/MF A01 CSCL 11F

A steel alloy is provided which exhibits excellent strength and toughness characteristics at cryogenic temperatures. The alloy consists essentially of about 10 to 18 percent by weight nickel, about 0.1 to 1.0 percent by weight aluminum, and 0 to about 3 percent by weight of at least one of the following additional elements: copper, lanthanum, niobium, tantalum, titanium, vanadium, yttrium, zirconium, and the rare earth metals, the balance being essentially iron. The steel alloy is produced by a process which includes using cold rolling at room temperature and subsequent heat treatment at temperatures ranging from 500 to 650 C and possesses a fracture toughness ranging from 200 to 230 ksi square root of (in.) and yield strength up to 230 ksi. NASA

N78-23193* National Aeronautics and Space Administration
Lewis Research Center, Cleveland, Ohio

THE ROLE OF THERMAL SHOCK IN CYCLIC OXIDATION

Carl E. Lowell and Daniel L. Deedmore 1978 14 p refs Presented at 153d Meeting of the Electrochem Soc, Seattle, 21-26 May 1978

(NASA TM-78876, E-9610) Avail NTIS HC A02/MF A01 CSCL 11F

The effect of thermal shock on the spalling of oxides from the surfaces of several commercial alloys was determined. The average cooling rate was varied from approximately 240 C per second to less than 1.0 C per second during cyclic oxidator tests in air. The tests consisted of one hundred cycles of one hour at the maximum temperature (1100 or 1200 C). The alloys were H05 B75, TD Ni-CrAl, IN 601, IN 702, and B 1900, plus HF. All of these alloys exhibited partial spalling within the oxide rather than total oxide loss down to bare metal. Thermal shock resulted in deformation of the metal which in turn resulted in most cases in changing the oxide failure mode from compressive to tensile. Tensile failures were characterized by cracking of the oxide and little loss, while compressive failures were characterized by explosive loss of platelets of oxide. This behavior was confirmed by examination of mechanically stressed oxide scales. The thermally shocked oxides spalled less than the slow cooled oxides, with the exception of TD Ni-CrAl. This material failed in a brittle manner rather than by plastic deformation. Author

N78-24326* National Aeronautics and Space Administration
Lewis Research Center, Cleveland, Ohio

NEW ALLOYS TO CONSERVE CRITICAL ELEMENTS

Joseph R. Stephens 1978 15 p refs Presented at the Intern Eng Conf and Tool Exposition, Philadelphia, 8-11 May 1978, sponsored by the Soc of Manufacturing Engrs

(NASA TM 78840 E 9551) Avail NTIS HC A02/MF A01 CSCI 11F

Based on availability of domestic reserves chromium is one of the most critical elements within the US metal industry. New alloys having reduced chromium contents which offer potential as substitutes for higher chromium alloys are currently in use are being investigated. This paper focuses primarily on modified Type 304 stainless steels having one third less chromium but maintaining comparable oxidation and corrosion properties to that of type 304 stainless steel the largest single use of chromium. Substitutes for chromium in these modified Type 304 stainless steel alloys include silicon and aluminum plus molybdenum. Author

N78-24336* National Aeronautics and Space Administration Lewis Research Center, Cleveland, Ohio
CYCLIC OXIDATION OF COATED OXIDE DISPERSION STRENGTHENED (ODS) ALLOYS IN HIGH VELOCITY GAS STREAMS AT 1100 DEG C

Michael A Gedwill May 1979 20 p refs
(NASA TM 78877 E 9611) Avail NTIS HC A02/MF A01 CSCI 11F

Several overlay coatings on ODS NiCrAl were tested in Mach 1 and Mach 0.3 burner rigs to examine oxidation and thermal fatigue performance. The coatings were applied by various methods. Based on weight change, macroscopic and metallographic observations in Mach 1 tests Nascoat 70 on TD NiCrAl exhibited the best oxidation resistance. In Mach 0.3 tests PWA 267 and A10-1 about equally were the best coatings on YD NiCrAl (Nascoat 70 was not tested in Mach 0.3 rigs). Author

N78 26198* National Aeronautics and Space Administration Lewis Research Center, Cleveland, Ohio
ROLE OF ALLOYING ELEMENTS IN ADHESIVE TRANSFER AND FRICTION OF COPPER BASE ALLOYS

Donald H Buckley Jun 1978 19 p refs
(NASA TP 1256 E 9471) Avail NTIS HC A02/MF A01 CSCI 11F

Sliding friction experiments were conducted in a vacuum with binary copper alloy riders sliding against a conventional bearing steel surface with normal residual oxides present. The binary alloys contained 1 atomic percent of various alloying elements. Auger spectroscopy analysis was used to monitor the adhesive transfer of the copper alloys to the bearing steel surface. A relation was found to exist between adhesive transfer and the reaction potential and free energy of formation of the alloying element in the copper. The more chemically active the element and the more stable its oxide, the greater was the adhesive transfer and wear of the copper alloy. Transfer occurred in all the alloys except copper-gold after relatively few (25) passes across the steel surface. Author

N78 26199* National Aeronautics and Space Administration Lewis Research Center, Cleveland, Ohio
MORPHOLOGY OF GOLD AND COPPER ION-PLATED COATINGS

Talivaldis Spalvins Jun 1978 17 p refs
(NASA-TP 1262 E 9528) Avail NTIS HC A02/MF A01 CSCI 11F

Copper and gold films (0.2 to 2 microns thick) were ion plated onto polished 304 stainless steel glass mica surfaces. These coatings were examined by SEM for defects in their morphological growth. Three types of defects were distinguished: nodular growth, abnormal or runaway growth, and spits. The cause for each type of defect was investigated. Nodular growth is due to inherent substrate microdefects, abnormal or runaway growth is due to external surface inclusions, and spits are due to nonuniform evaporation (ejection of droplets). All these defects induce stresses and produce porosity in the coatings and thus weaken their mechanical properties. During surface rubbing, large nodules are pulled out, leaving vacancies in the coatings. Author

N78 26226* National Aeronautics and Space Administration Lewis Research Center, Cleveland, Ohio

EROSION /CORROSION OF TURBINE AIRFOIL MATERIALS IN THE HIGH-VELOCITY EFFLUENT OF A PRESSURIZED FLUIDIZED COAL COMBUSTOR

Glenn R Zellars, Anne P Lowe, and Carl E Lowell Jul 1978 33 p refs
(NASA TP 1274 E 9507) Avail NTIS HC A03/MF A01 CSCI 11F

Four candidate turbine airfoil superalloys were exposed to the effluent of a pressurized fluidized bed with a solids loading of 2 to 4 g/scm for up to 100 hours at two gas velocities, 150 and 270 m/sec, and two temperatures, 730 deg and 795 C. Under these conditions both erosion and corrosion occurred. The damaged specimens were examined by cross section measurements, scanning electron and light microscopy, and X ray analysis to evaluate the effects of temperature, velocity, particle loading, and alloy material. Results indicate that for a given solids loading the extent of erosion is primarily dependent on gas velocity. Corrosion occurred only at the higher temperature. There was little difference in the erosion/corrosion damage to the four alloys tested under these severe conditions. G G

N78-29214* National Aeronautics and Space Administration Lewis Research Center, Cleveland, Ohio

ADHESION OF A BIMETALLIC INTERFACE Ph D. Thesis - Case Western Reserve Univ.

John Ferrante Jun 1978 332 p refs
(NASA TM 78890) Avail NTIS HC A15/MF A01 CSCI 11A

The Hohenberg-Kohn and Kohn-Sham formalisms are used to examine binding (binding energy as a function of separation) for combinations of the simple metals Al(111), Zn(0001), Mg(0001), and Na(110) in contact. Similar metal contacts between Al, Zn, Mg, and Na are examined self-consistently in an ab initio calculation using the Kohn-Sham formalism. Crystallinity is included using the Ashcroft pseudopotential via first order perturbation theory for the electron-ion interaction, and the ion-ion interaction is included exactly via a lattice sum. Binding energy was determined both in the local density approximation and including gradient corrections to the exchange and correlation energy. Binding was found in all cases. In dissimilar metal contacts interfacial bonding was greater than that in the weaker material predicting the possibility of metallic transfer. The nonzero position of the energy minimum in like metal contacts is explained in terms of consistency between the Ashcroft pseudopotential and the bulk charge density. Good agreement with experimental surface energies is obtained in the self-consistent calculation when nonlocal terms are included. Author

N78 29215* National Aeronautics and Space Administration Lewis Research Center, Cleveland, Ohio

RUB TOLERANCE EVALUATION OF TWO SINTERED NiCrAl GAS PATH SEAL MATERIALS

Robert C Bill Jul 1978 12 p
(NASA TM 78967 AVRADCOM TR 78 39(PL) E 9726) Avail NTIS HC A02/MF A01 CSCI 11F

Two strength level variations of sintered NiCrAl (about 40 percent dense), candidate high pressure turbine seal materials were subject to rub tolerance testing against AM 355 steel blade tips. The high strength material (17 N/sq mm tensile strength) showed frictional and radial loads that were 20 to 50 percent higher than those measured for the low strength material (15.5 N/sq mm tensile strength). Measured wear to the AM 355 blade tips was not significantly different for the two sintered NiCrAl seal materials. Wear of the sintered NiCrAl was characterized by material removal to a depth greater than the depth to which blade tips were driven into the seal, indicating self-erosion effects. Author

N78-29216* National Aeronautics and Space Administration Lewis Research Center, Cleveland, Ohio

REACTIONS OF YTTRIA-STABILIZED ZIRCONIA WITH OXIDES AND SULFATES OF VARIOUS ELEMENTS Final Report

Isidor Zaplatynsky Jul 1978 16 p refs

(Contract EF 77 A 01 2593)
 (NASA TM 78942, DOE/NASA/2593 78/1, E 9689) Avail
 NTIS HC A02/MF A01 CSCL 11B

The reactions between partially stabilized zirconia, containing 8 weight percent yttria, and oxides and sulfates of various elements were studied at 1200, 1300, and 1400 C for times to 800, 400 and 200 hours, respectively. These oxides and sulfates represent impurities and additives potentially present in gas turbine fuels or impurities in the turbine combustion air as well as the elements of the substrate alloys in contact with zirconia. Based on the results, these compounds can be classified in four groups: (1) compounds which did not react with zirconia (Na₂SO₄, K₂SO₄, Cr₂O₃, Al₂O₃ and NiO), (2) compounds that reacted completely with both zirconia phases (CaO, BaO, and BaSO₄), (3) compounds that reacted preferentially with monoclinic zirconia (Na₂O, K₂O, CoO, Fe₂O₃, MgO, SiO₂, and ZnO), and (4) compounds that reacted preferentially with cubic zirconia (V₂O₅, P₂O₅) Author

N78-30205* National Aeronautics and Space Administration
 Lewis Research Center, Cleveland, Ohio

SIMULATION MODEL OF A SINGLE-STAGE LITHIUM BROMIDE WATER ABSORPTION COOLING UNIT

David Miao Aug 1978 44 p refs
 (NASA TP 1296, E 9547) Avail NTIS HC A03/MF A01 CSCL 20K

A computer model of a LiBr-H₂O single stage absorption machine was developed. The model, utilizing a given set of design data such as water flow rates and inlet or outlet temperatures of these flow rates but without knowing the interior characteristics of the machine (heat transfer rates and surface areas) can be used to predict or simulate off design performance. Results from 130 off-design cases for a given commercial machine agree with the published data within 2 percent. Author

N78-30206* National Aeronautics and Space Administration
 Lewis Research Center, Cleveland, Ohio

EFFECT OF OXYGEN, METHYL MERCAPTAN, AND METHYL CHLORIDE ON FRICTION BEHAVIOR OF COPPER-IRON CONTACTS

Donald H Buckley Aug 1978 19 p refs
 (NASA TP 1309, E 9606) Avail NTIS HC A02/MF A01 CSCL 11F

Sliding friction experiments were conducted with an iron rider on a copper disk and a copper rider on an iron disk. The sputter cleaned iron and copper disk surfaces were saturated with oxygen, methyl mercaptan, and methyl chloride at atmospheric pressure. Auger emission spectroscopy was used to monitor the surfaces. Lower friction was obtained in all experiments with the copper rider sliding on the iron disk than when the couple was reversed. For both iron and copper disks, methyl mercaptan gave the best surface coverage and was most effective in reducing friction. For both iron and copper disks, methyl chloride was the least effective in reducing friction. With sliding, copper transferred to iron and iron to copper. Author

N78-31208* National Aeronautics and Space Administration
 Lewis Research Center, Cleveland, Ohio

INHIBITION OF HOT SALT CORROSION BY METALLIC ADDITIVES

Daniel L Deadmore and Carl E Lowell Jul 1978 20 p refs
 (Contract EF-77-A-01-2593)
 (NASA TM 78966, E 9725, DOE/NASA/2953 78/2) Avail
 NTIS HC A02/MF A01 CSCL 07D

The effectiveness of several potential fuel additives in reducing the effects of sodium sulfate induced hot corrosion was evaluated in a cyclic Mach 0.3 burner rig. The potential inhibitors examined were salts of Al, Si, Cr, Fe, Zn, Mg, Ca, and Ba. The alloys tested were IN 100, U 700, IN 738, IN 792, Mar M 509, and 304 stainless steel. Each alloy was exposed for 100 cycles of 1 hour each at 900 C in combustion gases doped with the corrodant and inhibitor salts and the extent of attack was determined by measuring maximum metal thickness loss. The most effective and consistent inhibitor additive was Ba (NO₃)₂ which reduced the hot corrosion attack to nearly that of simple oxidation. Author

N78-31209* National Aeronautics and Space Administration
 Lewis Research Center, Cleveland, Ohio

REVIEW OF THE AGARD S AND M PANEL EVALUATION PROGRAM OF THE NASA-LEWIS SRP APPROACH TO HIGH-TEMPERATURE LCF LIFE PREDICTION

Marvin H Hirschberg 1978 11 p refs Proposed for presentation at the 52d Meeting of the Propulsion and Energetics Panel, Cleveland, 23-27 Oct 1978, sponsored by AGARD
 (NASA TM 78877, E 9772) Avail NTIS HC A02/MF A01 CSCL 11F

Twenty laboratories in six countries participated in testing their own materials of interest under their own laboratory conditions. In this way the results obtained provided validation of the Strainrange Partitioning (SRP) method for a wide range of materials and insured maximum usefulness to each of the participating laboratories. The various investigators shared their findings, thus providing the basis for an in-depth evaluation of the SRP method. While the results were variable from laboratory to laboratory, most investigators agreed that the SRP method was a significant step toward life prediction in the presence of high temperature and cyclic stresses. L S

N78-31210* National Aeronautics and Space Administration
 Lewis Research Center, Cleveland, Ohio

THE EFFECT OF FUEL-TO-AIR RATIO ON BURNER-RIG HOT CORROSION

Daniel L Deadmore, Carl E Lowell, and Fred J Kohl Jul 1978 20 p refs
 (NASA TM 78960, E 9649) Avail NTIS HC A02/MF A01 CSCL 07A

Samples of a cobalt base alloy Mar M 509, were subjected to hot corrosion in a Mach 0.3 burner rig. The corrodant was NaCl added as an aqueous solution to the combustion products of a sulfur containing Jet A fuel. The metal temperature was fixed at 900 C. The extent of hot corrosion increased by a factor of three as the fuel-to-air mass ratio was increased from 0.033 to 0.050. Because the depositing salt was always Na₂SO₄, the increased attack appeared to be related to the gas composition. Author

N78-31211* National Aeronautics and Space Administration
 Lewis Research Center, Cleveland, Ohio

LONGITUDINAL SHEAR BEHAVIOR OF SEVERAL OXIDE DISPERSION STRENGTHENED ALLOYS

T K Glasgow Aug 1978 20 p refs Proposed for presentation at the Fall Meeting of the Am Inst of Mining, Metallurgical and Petrol Engr, Chicago, 24-27 Oct 1978
 (NASA TM 78973, E 9746) Avail NTIS HC A02/MF A01 CSCL 11F

Two commercial oxide dispersion strengthened (ODS) alloys, MA 753 and MA 754, and three experimental ODS alloys, MA 757E, MA 755E, and MA 6000E were tested in shear at 760 C. Comparisons were made with other turbine blade and vane alloys. All of the ODS alloys exhibited less shear strength than directionally solidified Mar M 200. Hf or then conventionally cast B 1900. The strongest ODS alloy tested, MA 755E, was comparable in both shear and tensile strength to the lamellar directionally solidified eutectic alloy gamma/gamma prime - delta. Substantial improvements in shear resistance were found for all alloys tested when the geometry of the specimen was changed from one generating a transverse tensile stress in the shear area to one generating a transverse compressive stress. Finally, 760 C shear strength as a fraction of tensile strength was found to increase linearly with the log of the transverse tensile ductility. Author

N78-31212* National Aeronautics and Space Administration
 Lewis Research Center, Cleveland, Ohio

EFFECTS OF COMPOSITIONAL CHANGES ON THE PERFORMANCE OF A THERMAL BARRIER COATING SYSTEM

Stephan Stecura Aug 1978 33 p refs Proposed for presentation at the 3d Ann Conf on Composite and Advanced Mater, Merritt Island, Fla, 21-24 Jan 1979
 (NASA TM 78976, E 9751) Avail NTIS HC A03/MF A01 CSCL 11F

Currently proposed thermal barrier systems for aircraft gas turbine engines consist of NiCrAlY bond coating covered with an insulating oxide layer of yttria stabilized zirconia. The effect of yttrium concentration (from 0.15 to 1.08 w/o) in the bond coating and the yttria concentration (4 to 24.4 w/o) in the oxide layer were evaluated. Furnace, natural gas oxygen torch, and Mach 1.0 burner rig cyclic tests on solid specimens and air cooled blades were used to identify trends in coating behavior. Results indicate that the combinations of yttrium levels between 0.15 to 0.35 w/o in the bond coating and the yttria concentration between 6 to 8 w/o in the zirconium oxide layer were the most adherent and resistant to high temperature cyclic exposure.

Author

N78-31213* National Aeronautics and Space Administration Lewis Research Center, Cleveland, Ohio
EFFECTS OF THERMOMECHANICAL PROCESSING ON STRENGTH AND TOUGHNESS OF IRON-12-PERCENT-NICKEL REACTIVE METAL ALLOYS AT -196 C
 Joseph R. Stephens and Walter R. Witzke, Aug. 1978, 36 p, refs.
 (NASA TP 1308, E 9583) Avail. NTIS HC A03/MF A01 CSCL 11f

Thermomechanical processing (TMP) was evaluated as a method of strengthening normally tough iron-12-nickel reactive metal alloys at cryogenic temperatures. Five iron-12-nickel alloys with reactive metal additions of aluminum, niobium, titanium, vanadium, and aluminum plus niobium were investigated. Primary evaluation was based on the yield strength and fracture toughness of the thermomechanically processed alloys at 196 C. B B

N78-33196* National Aeronautics and Space Administration Lewis Research Center, Cleveland, Ohio
LONG TERM HOT HARDNESS CHARACTERISTICS OF FIVE THROUGH HARDENED BEARING STEELS
 Neil E. Anderson, Oct. 1978, 20 p, refs. Prepared in cooperation with US Army Aviation Research and Development Command, St. Louis, Mo.
 (NASA TP 1341, E 9533) Avail. NTIS HC A02/MF A01 CSCL 11f

Five vacuum melted bearing steels tempered to various room temperature hardnesses, AISI 52100 and the tool steels AISI M1, AISI M50 Halmo, and WB 49 were studied. Hardness measurements were taken on AISI 52100 at room temperature and at elevated temperatures after soaking it at temperatures to 478 K (400 F) for as long as 1000 hours. Hardness measurements were also taken on the tool steels after soaking them at temperatures to 700 K (800 F) for as long as 1000 hours. None of the tool steel tempered during soaking and AISI 52100 did not temper when soaked at 366 K (200 F) for 1000 hours. However, AISI 52100 that was initially hardened to room temperature hardness of 62.5 or 64.5 lost hardness during the first 500 hours of the 1000 hour soak tests at temperatures greater than 394 K (250 F) but it maintained its hardness during the final 500 hours of soaking. Similarly, AISI 52100 initially hardened to room temperature hardness of 60.5 lost hardness during the first 500 hours of the 1000 hour soaking at temperatures greater than 422 K (300 F) but it maintained its hardness during the final 500 hours of soaking. A R H

A78-15335* An experimental P/M wrought superalloy for advanced temperature service, R. V. Miner (NASA, Lewis Research Center, Cleveland, Ohio) and W. B. Kent (Cyclops Corp., Bridgeville, Pa.), *International Journal of Powder Metallurgy and Powder Technology*, vol. 13, Oct. 1977, p. 293-294, 296 (6 ff.), 7 refs.

A study was undertaken in order to adapt HB-11 (an experimental wrought superalloy with high temperature strength) to manufacture via powder metallurgy techniques, and to improve its microstructural stability. Three compositional modifications were produced and evaluated. Among the conclusions reached it was found that: (1) HB-11 having a low C and low Hf alloy content is suitable for advanced temperature turbine disks, and is applicable to fabrication by powder metallurgy techniques; (2) HB-11, when compared to modifications with higher C and/or higher Hf, is

somewhat weaker in tension at intermediate temperatures but superior in tensile ductility, rupture strength and ductility, and stability during long-time heating; (3) increases in the cross-rolling temperature increase the grain size of alloys after solution treatment, and (4) both the lower C modifications develop larger grain sizes than the higher C modification. S.C.S.

A78-15826* Cryogenic properties of a new tough-strong iron alloy, J. R. Stephens and W. R. Witzke (NASA, Lewis Research Center, Cleveland, Ohio), *National Bureau of Standards, International Cryogenic Materials Conference, University of Colorado, Boulder, Colo., Aug. 2-5, 1977, Paper*, 12 p, 5 refs.

A program was undertaken to develop an iron base alloy having a fracture toughness of 220 MPa $\sqrt{\text{cm}}$ root meters with a corresponding yield stress of 1.4 GPa (200 ksi) at -196 C. An Fe-12Ni alloy was selected as the base alloy. Factors considered include reactive metal additions, effects of interstitial impurities, strengthening mechanisms, and weldability. The goals of this program were met in an Fe-12Ni-0.5Al alloy strengthened by thermomechanical processing or by precipitate strengthening with 2 percent Cu. The alloy is weldable with the weld metal and heat affected zone in the post-weld annealed condition having toughness equivalent to the base alloy. (Author)

A78-18631* Volatilization of oxides during oxidation of some superalloys at 1200 C, I. Zaplatynsky (NASA, Lewis Research Center, Cleveland, Ohio), *Oxidation of Metals*, vol. 11, Dec. 1977, p. 289-301, 15 refs.

Volatilization of oxides during cyclic oxidation of commercial Nichrome, Inconel 750, Rene 41, Stellite 6B, and GE 1541 was studied at 1200 C in static air. Quantitative analysis of oxide vapor deposits revealed that oxides of tungsten, molybdenum, niobium, manganese, and chromium volatilized preferentially from the oxide scales. Aluminum and silicon were not detected in vapor deposits. For all the alloys except GE 1541 chromium was found to be the most metallic element in the oxide scales. (Author)

A78-18792* Effects of heat treating PM Rene' 95 slightly below the gamma-prime solvus, R. L. Dreshfield (NASA, Lewis Research Center, Cleveland, Ohio), *American Institute of Mining, Metallurgical and Petroleum Engineers, Annual Meeting 106th, Atlanta, Ga., Mar. 6-10, 1977, Paper*, 18 p, 5 refs.

An investigation was performed on As HIP Rene' 95 to obtain additional information on the variation of the amount of gamma-prime with solutioning temperatures near the gamma-prime solvus temperature and the resulting effects on tensile and stress-rupture strengths of As HIP Rene' 95. The amount of gamma-prime phase was found to increase at a rate of about 0.5% per degree Celsius as the temperature decreased from the solvus temperature to about 50 C below the gamma-prime solvus temperature. The change in the amount of gamma-prime phase with decreasing solutioning temperature was observed to be primarily associated with decreasing solubilities of Al+Ti+Ni and increasing solubility of Cr in the gamma phase. For As HIP Rene' 95 solutioned at either 1107 or 1135 C and subsequently water quenched and double aged for 4 hours at 815 C followed by 24 hours at 650 C, the higher solution temperature resulted in significantly greater yield strengths at room temperature and 650 C as well as a greater room temperature ultimate strength. Also, longer stress-rupture lives at 650 C were associated with the higher solution temperature. (Author)

A78-18793* Burner rig alkali salt corrosion of several high temperature alloys, D. Deadmore and C. Lowell (NASA, Lewis Research Center, Cleveland, Ohio), *Electrochemical Society Meeting 151st Philadelphia, Pa., May 8-13, 1977, Paper*, 19 p, 17 refs.

The hot corrosion of five alloys was studied in cyclic tests in a Mach 0.3 burner rig to whose combustion chamber various aqueous salt solutions were injected. Three nickel base alloys (IN 792, IN 738, and IN 160), a cobalt base alloy (MM 509), and an iron base

alloy (304 stainless steel) were studied at temperatures of 700, 800, 900, and 1000 C with various salt concentrations and compositions. The relative resistance of the alloys to hot corrosion attack was found to vary with temperature and with both the concentration and composition of the injected salt solution. Results indicate that the corrosion of these alloys is a function of both the presence of salt condensed as a liquid on the surface and of the composition of the gas phases present. (Author)

A78-21431 * Effect of prior creep at 1365 K on the room temperature tensile properties of several oxide dispersion strengthened alloys. J. D. Whittenberger (NASA, Lewis Research Center, Cleveland, Ohio) *Metallurgical Transactions A - Physical Metallurgy and Materials Science*, vol. 8A, Dec. 1977, p. 1863-1870. 21 refs.

An experimental study was conducted to determine whether oxide dispersion strengthened (ODS) Ni-base alloys in wrought bar form are subject to creep degradation effects similar to those found in thin-gage sheet. The bar products evaluated included ODS Ni, ODS-NiCr, and advanced ODS NiCrAl types, the alloys included microstructures ranging from an essentially perfect single crystal to a structure consisting of very small elongated grains. Tensile test specimens were exposed to creep at various stress levels at 1365 K and then tensile tested at room temperature. Low residual tensile properties, change in fracture mode, appearance of dispersoid free bands, grain boundary cavitation, and/or internal oxidation are interpreted as creep degradation effects. The amount of degradation depends on creep strain, and degradation appears to be due to diffusional creep which produces dispersoid free bands around grain boundaries acting as vacancy sources. S.D.

A78-21439 * Effects of silicon on the oxidation, hot corrosion, and mechanical behavior of two cast nickel base superalloys. R. V. Miner, Jr. (NASA, Lewis Research Center, Cleveland, Ohio) *Metallurgical Transactions A - Physical Metallurgy and Materials Science*, vol. 8A, Dec. 1977, p. 1949-1954. 6 refs.

Cast specimens of nickel base superalloys 713C and Mar M200 with nominal additions of 0, 0.5, and 1 wt% Si were evaluated for oxidation and corrosion resistance, tensile and stress rupture properties, microstructure, and phase relations. Results are compared with those of an earlier study of the effects of Si in B-1900. Si had similar effects on all three superalloys. It improves oxidation resistance but the improvement in 713C and Mar M200 was considerably less than in B-1900. Hot corrosion resistance is also improved somewhat. Si is, however, detrimental to mechanical properties, in particular rupture strength and tensile ductility. Si has two obvious microstructural effects. It increases the amount of gamma prime precipitated in eutectic nodules and promotes a Mo(Ni₃Si)₂ Laves phase in the alloys containing Mo. These microstructural effects do not appear responsible for the degradation of mechanical properties, however. (Author)

A78-21858 * Tensile and creep properties of the experimental oxide dispersion strengthened iron-base sheet alloy MA 956E at 1365 K. J. D. Whittenberger (NASA, Lewis Research Center, Cleveland, Ohio) *Metallurgical Transactions A - Physical Metallurgy and Materials Science*, vol. 9A, Jan. 1978, p. 101-110. 13 refs.

A study of the 1365 K tensile properties, creep characteristics and residual room temperature properties after creep testing of the experimental oxide dispersion strengthened iron base alloy MA 956E (Fe-20Cr-4.5Al-0.5Ti-0.5Y₂O₃) was conducted. The 1365 K tensile properties, particularly ductility, are strongly dependent on strain rate. It appears that MA 956E does not easily undergo slow plastic deformation. Rather than deform under creep loading conditions, the alloy apparently fails by a crack nucleation and growth mechanism. Fortunately, there appears to be a threshold stress below which crack nucleation and/or growth does not occur. (Author)

A78-23461 * Friction and wear of sintered fibermetal abrasion seal materials. R. C. Bill (NASA, Lewis Research Center; U.S. Army, Mobility Research and Development Laboratory, Cleveland, Ohio) and L. T. Shimbob (United Technologies Corp., Pratt and Whitney Aircraft Group, East Hartford, Conn.). *ASME, ASTM, ASM, SME, ASLE, and SAE, International Conference on Wear of Materials, St. Louis, Mo., Apr. 25-28, 1977, Paper 26*. p. 10 refs.

Three abrasion seal material systems based on a sintered NiCrAlY fiber metal structure were evaluated under a range of wear conditions representative of those likely to be encountered in various knife edge seal (labyrinth or shrouded turbine) applications. Conditions leading to undesirable wear of the rotating knife were identified, and a model proposed based on thermal effects arising under different rub conditions. It was found, and predicted by the model, that low incursion (plunge) rates tended to promote smearing of the low density sintered material with consequent wear to the knife edge. Tradeoff benefits between baseline 19 percent dense material, a similar material of increased density, and a self-lubricating coating applied to the 19 percent dense material were identified on the basis of relative rub tolerance and erosion resistance. (Author)

A78-24369 * Volume fraction determination in cast superalloys and directionally solidified eutectic alloys by a new manual point count practice. C. W. Andrews (NASA, Lewis Research Center, Electron Optics and Microscopy Unit, Cleveland, Ohio) *Journal of Testing and Evaluation*, vol. 6, Jan. 1978, p. 20-28. 6 refs.

A78-24370 * Load displacement measurement and work determination in three-point bend tests of notched or precracked specimens. R. J. Buzzard and D. M. Fisher (NASA, Lewis Research Center, Cleveland, Ohio) *Journal of Testing and Evaluation*, vol. 6, Jan. 1978, p. 35-39.

Suggestions for testing of notched or cracked three-point bend specimens are presented that (1) correct displacement measurement errors resulting from misalignment between the load applicator and specimen, (2) account for coincidental strains not associated with the work of crack extension, (3) simplify record analysis and processing, and (4) extend displacement gage range without sacrifice of sensitivity or accuracy. These testing details are particularly applicable to procedures in which the crack extension force $J(I)$ is determined from the work done on the specimen. (Author)

A78-24372 * Comparison of equivalent energy and energy per unit area W (bar/A) data with valid fracture toughness data for iron, aluminum, and titanium alloys. W. R. Witzke and J. R. Stephens (NASA, Lewis Research Center, Cleveland, Ohio) *Journal of Testing and Evaluation*, vol. 6, Jan. 1978, p. 75-79. 15 refs.

A78-24882 * The promise of eutectics for aircraft turbines. H. R. Gray (NASA, Lewis Research Center, Cleveland, Ohio). *American Society for Metals, Materials Show and Conference, Chicago, Ill., Oct. 25-27, 1977, Paper 20*. p. 13 refs.

Gas turbine blades and vanes for the 1980s call for new materials with higher operational temperature capabilities. The potential increase of from 40 to 110 C in operational temperature capabilities predicted for directionally solidified eutectics is a larger increment over currently available alloys than previously obtained in any new turbine blade alloy. The paper discusses the properties of gamma/gamma prime delta and NiTaC-13 directionally solidified first-generation eutectics for use as gas turbine blade materials. A few of the more promising second-generation eutectics for blade applications (gamma/gamma prime alpha, NiTaC-3-116A) and for vane applications (gamma beta, COTAC 74) are also discussed. Attention is given to mechanical properties, such as transverse ductility and shear strength, that can be inherently critical in a directionally solidified eutectic. Further R&D requirements for properties, coatings, and lower cost processing technology are identified. S.D.

A78-28423 * # Rolling element fatigue life of AMS 5749 corrosion resistant, high temperature bearing steel. R. J. Parker (NASA, Lewis Research Center, Cleveland, Ohio) and R. S. Hodder (Larrobe Steel Co., Larrobe, Pa.). *American Society of Lubrication Engineers and American Society of Mechanical Engineers, Joint Lubrication Conference, Kansas City, Mo., Oct. 3-5, 1977, ASME Paper 77-Lub-30*, 7 p. 9 refs. Members, \$1.50; nonmembers, \$3.00.

A78-29329 * # High temperature environmental effects on metals. S. J. Grisaffo, C. E. Lowell, and C. A. Stearns (NASA, Lewis Research Center, Cleveland, Ohio). *U.S. Army, Sagamore Army Materials Research Conference on Risk and Failure Analysis for Reliability, 24th, Bolton Landing, N.Y., Aug. 22-26, 1977, Paper*, 18 p. 25 refs.

The current status of knowledge and ability to predict high-temperature environmental attack of metals is reviewed with particular reference to the gas turbine engine. Environmental attack is caused by high temperatures, combustion products, and impurities. A schematic representation of life-limiting factors of turbine components shows that environmental attack can lead to very early failures. Attention is given to high temperature oxidation with prevailing modes of oxidation attack, and to hot corrosion and other impurity effects. Erosion attack results from the direct mechanical removal of component material by impact of hard substances like ash, sand, or dirt. Solutions to hot-corrosion problems can be found semiempirically by using improved alloys or ceramics, protective surface coatings, additives to the engine environment, and air/fuel cleanup to eliminate detrimental impurities. S.D.

A78-30112 * Oxide morphology and spalling model for NiAl. J. L. Smialek (NASA, Lewis Research Center, Cleveland, Ohio). *Metallurgical Transactions A - Physical Metallurgy and Materials Science*, vol. 9A, Mar. 1978, p. 309-320. 17 refs.

A scanning electron microscope equipped with an energy dispersive spectrographic unit was used to study in detail the Al₂O₃ oxide morphology and oxide-metal interface of a nickel-rich NiAl alloy (Ni 42 at% Al) with a view toward providing information relevant to spalling theories in the MCrAlY system. In addition, the kinetics of spalling was studied for critical evaluation of one of the step-process spall models and for collection of pertinent experimental data. Cyclic oxidation tests were run in 1-atm air at about 1100 C, and isothermal specimens were examined from 2 min to 200 hr of exposure. It is shown that oxide spalling occurs primarily at the oxide-metal interface in an intergranular mode, that crystallographic Kirkendall voids arise as a result of oxidation, and that the fractional area of spalled oxide varies widely in cyclic tests but increases with the square of oxide thickness for isothermal tests. A spall model is developed in the form of a summation series. S.D.

A78-32319 * Investigation of the fracture mechanism of Ti-5Al-2.5Sn at cryogenic temperatures. R. H. Van Stone (GE Research and Development Center, Schenectady, N.Y.), J. R. Low, Jr., and J. L. Shannon, Jr. (NASA, Lewis Research Center, Strength of Materials Section, Cleveland, Ohio). *Metallurgical Transactions A - Physical Metallurgy and Materials Science*, vol. 9A, Apr. 1978, p. 539-552. 56 refs. Grant No. NGR-39-087-047.

Fractography and metallographic sectioning were used to investigate the influence of microstructure on the fracture mechanism and fracture toughness (K_{1C}) of normal interstitial and extra low interstitial (ELI) Ti-5Al-2.5Sn at 20 K (-423 F) and 77 K (-320 F). Plates of each grade were mill annealed at 815 C followed by either air or furnace cooling. These variations in composition and cooling rate resulted in differences in the volume fraction and internal structure of the dispersed beta phase and in the ordering of the alpha matrix. The ELI alloys were tougher than the normal interstitial plates. K_{1C} of the furnace-cooled ELI plate was 25% lower than that of the air-cooled ELI material. Variations in cooling rate had no influence of K_{1C} of the normal interstitial alloys. Fractography showed that a large portion of the fracture surfaces

were covered with elongated dimples. Metallographic sections of specimens deformed at 77 K showed that these features form at the intersections of slip bands or deformation twins with grain or twin boundaries. Ordering and higher interstitial levels increase the local strain in slip bands resulting in void nucleation at lower macroscopic strains and lower K_{1C} values. (Author)

A78-33214 * Strain range partitioning behavior of the nickel base superalloys, Rene 30 and 100. G. R. Halford and A. J. Nachtigall (NASA, Lewis Research Center, Cleveland, Ohio). *NAIOP AGARD, Specialists Meeting on Characterization of Low Cycle High Temperature Fatigue by Strain Range Partitioning Method, Aalborg, Denmark, Apr. 9-14, 1978, Paper*, 16 p. 18 refs.

A study has been made to assess the ability of the method of Strain Range Partitioning (SRP) to both correlate and predict high-temperature low cycle fatigue lives of nickel base superalloys for gas turbine applications. SRP is shown to correlate the cyclic lives of the baseline tests to within factors of nearly two. The partitioned strain range versus life relationships for uncoated Rene 30 and cast IN 100 have also been determined from the ductility normalized strain range partitioning equations. These were used to predict the cyclic lives of the baseline tests. Predicted and observed cyclic lives agreed to within factors of nearly three. The life predictability of the method is also verified for cast IN 100 by applying the baseline results to the cyclic life prediction of a series of complex strain cycling tests with multiple hold periods at constant strain. It is concluded that the method of SRP can correlate and predict the cyclic lives of laboratory specimens of the nickel base superalloys evaluated in this program. (Author)

A78-33216 * Strength enhancement process for prealloyed powder superalloys. W. J. Waters and J. C. Friehe (NASA, Lewis Research Center, Cleveland, Ohio). *Metallurgical Society of AIME, Fall Meeting, Chicago III, Oct. 24-27, 1977, Paper*, 30 p. 11 refs.

A technique involving superplastic processing and high pressure autoclaving was applied to a nickel base prealloyed powder alloy. Tensile strengths as high as 2865 MN/cm² (415 ksi) at 480 C (900 F) were obtained with a superplastically deformed material. Appropriate treatments yielding materials with high temperature tensile and stress rupture strengths (980 C (1800 F)) were also tested. (Author)

A78-35394 * Surface-crack shape change in bending fatigue using an inexpensive resonant fatiguing apparatus. W. S. Pierce and J. L. Shannon, Jr. (NASA, Lewis Research Center, Strength of Materials Section, Cleveland, Ohio). *Journal of Testing and Evaluation*, vol. 6, May 1978, p. 183-188. 5 refs.

An inexpensive device for producing surface cracks of controlled size and shape is described along with results of its use which show how the shape of the surface crack changes as it grows in bending fatigue from a variety of crack starter shapes. The growth pattern for any crack is uniquely defined by the crack starter configuration and appears to be independent of alloy. Shape changes are substantial and all growth curves tend toward a common growth curve. Circular cracks tend to become elliptical with an associated increase in stress intensity factor. This increase accelerates the crack growth rate and proximity to the critical flaw size. Through cracks produced by the extension of a surface crack in a bending stress field will have length ten times the section thickness. The results demonstrate the necessity of taking into account changing crack shape in the calculation of structural life when bending is a significant component of the stress field. (Author)

A78-36045 * Mechanical properties on ion beam-textured surgical implant alloys. A. J. Weigand (NASA, Lewis Research Center, Cleveland, Ohio). *(American Vacuum Society, National Symposium, 24th, and Conference on Microbalance Techniques, 15th, Boston, Mass., Nov. 8-11, 1977.) Journal of Vacuum Science and Technology*, vol. 15, Mar.-Apr. 1978, p. 718-724. 14 refs.

ORIGINAL PAGE IS
OF POOR QUALITY

A78-37076 * # The effect of microstructure on hydrogen embrittlement of the nickel base superalloy, Udimet 700. H. R. Gray (NASA, Lewis Research Center, Cleveland, Ohio). In Structures, Structural Dynamics and Materials Conference, 19th, Bethesda, Md., April 3-5, 1978, Technical Papers, New York, American Institute of Aeronautics and Astronautics, Inc., 1978, 31 p. 12 refs.

Material from a single heat of cast and wrought Udimet 700 was processed and/or heat treated to produce five material conditions with identical chemical compositions but with distinct microstructural variations, and then evaluated for susceptibility to hydrogen embrittlement. Two prealloyed powder conditions exhibited significantly improved resistance to hydrogen embrittlement, as compared to wrought material. No degradation in notch or smooth tensile strengths occurred, and average ductilities of 25 percent reduction of area were determined for 2 hydrogen evaluation procedures. For the most severe hydrogenation procedure, ductility levels were reduced to 15 percent. These improvements were attributed to cleaner grain boundaries and decreased grain size.

(Author)

A78-37676 * # The role of thermal shock in cyclic oxidation. C. E. Lowell and D. L. Deadmore (NASA, Lewis Research Center, Cleveland, Ohio). *Electrochemical Society, Meeting, 153rd, Seattle, Wash., May 21-26, 1978, Paper*, 13 p. 11 refs.

The effect of thermal shock on the spalling of oxides from the surfaces of several commercial alloys was determined. The average cooling rate was varied from approximately 240 C/sec to less than 1.0 C/sec during cyclic oxidation tests in air. The tests consisted of one hundred cycles of one hour at the maximum temperature (1100 or 1200 C). The alloys were HOS-875, TD-Ni, TD NiCrAl, IN-601, IN-702, and B 1900 plus Hf. Thermal shock resulted in deformation of the metal which in turn resulted, in most cases, in changing the oxide failure mode from compressive to tensile. Tensile failures were characterized by cracking of the oxide and little loss, while compressive failures were characterized by explosive loss of platelets of oxide. The thermally shocked oxides spalled less than the slow cooled samples with the exception of TD NiCrAl. This material failed in a brittle manner rather than by plastic deformation. The HOS-875 and the TD-Ni did not spall during either type of cooling. Thus, the effect of thermal shock on spalling is determined, in large part, by the mechanical properties of the metal.

(Author)

A78-37680 * # New alloys to conserve critical elements. J. R. Stephens (NASA, Lewis Research Center, Cleveland, Ohio). *Society of Manufacturing Engineers, International Engineering Conference and Tool Exposition, Philadelphia, Pa., May 8-11, 1978, Paper*, 14 p. 12 refs.

Previous studies and surveys on availability of domestic reserves have shown that chromium is a most critical element within the U.S. metal industry. More precisely, the bulk of chromium is consumed in the production of stainless steels, specifically Type 304 stainless steel (304SS) which contains 18% Cr. The present paper deals with means of reducing chromium in commercial stainless steels by substituting more abundant or less expensive elements with the intent of maintaining the properties of 304SS. The discussion focuses on some of the oxidation and corrosion properties of new substitute stainless steels with only 12% Cr, which represents a potential saving of 33% of the chromium consumed in the production of 304SS. The alloying elements substituted for Cr in 304SS are selected according to their potential for protective oxide formation during high temperature oxidation; these are Al, Si, Ti, Y, and misch metal which is 99.7% rare-earth metals containing 50 to 55% cerium. Other alloying elements to impart corrosion resistance are Mn, Mo, and V. S.D.

A78-41400 * Cleaning process for contaminated superalloy powders. A. E. Anglin (NASA, Lewis Research Center, Cleveland, Ohio). *Powder Technology*, vol. 20, 1978, p. 137, 138

A cleaning process for removing interstitial contaminants from superalloy powders after wet grinding is described. Typical analyses of oxygen, carbon, nitrogen, and hydrogen in ball milled WAZ 20

superalloy samples after hydrogen plus vacuum cleaning are presented. The hydrogen cleaning step involves heating retorts containing superalloy powder twice under flowing hydrogen with a 24 hour hold at each temperature. The vacuum step involves heating cold-pressed billets two hours at an elevated temperature at a pressure of 10 microPa. It is suggested that the hydrogen plus vacuum cleaning procedure can be applied to superalloys contaminated by other substances in other industrial processes. M. L.

A78-41465 * Development of strong and tough cryogenic Fe-12Ni alloys containing reactive metal additions. W. R. Witke and J. R. Stephens (NASA, Lewis Research Center, Cleveland, Ohio). *Cryogenics*, vol. 17, Dec 1977, p. 681-688, 17 refs.

The fracture toughness and tensile behaviour of arc melted and hot rolled Fe-12Ni alloys containing up to 4 atomic percent reactive metal additions of Al, Nb, Ti, or V were determined at 77 K. Cryogenic toughness was improved up to 7.5 times that of binary Fe-12Ni, depending on the reactive metal, its concentration, and annealing temperature. (Author)

A78-45426 * Interpolation and extrapolation of creep rupture data by the minimum commitment method. II - Oblique translation. S. S. Manson (Case Western Reserve University, Cleveland, Ohio) and C. R. Ensign (NASA, Lewis Research Center, Cleveland, Ohio). *American Society of Mechanical Engineers and Canadian Society of Mechanical Engineers, Pressure Vessels and Piping Conference, Montreal, Canada, June 26-29, 1978, Paper*, 28 p. 5 refs. Research supported by the Electric Power Research Institute and NASA.

An outline is presented of a new procedure, termed the oblique translation method, which emerged in the development of the focal point convergence method. Approaches for implementing the oblique translation method are discussed. It is shown that the new method is essentially a minimum commitment method when manually graphically implemented, in the sense that the form of the functions involved are not forced into particular analytical forms. The individual constants and functions are independently determined. The minimum commitment concept is extended to the analysis of creep rupture data wherein each isothermal is to be generated by an oblique translation of the 'master curve' when plotted. Attention is given to a manual graphical analysis, the preassessment of data, and an analysis by computer code. G. R.

A78-45427 * Interpolation and extrapolation of creep rupture data by the minimum commitment method. I - Focal point convergence. S. S. Manson (Case Western Reserve University, Cleveland, Ohio) and C. R. Ensign (NASA, Lewis Research Center, Cleveland, Ohio). *American Society of Mechanical Engineers and Canadian Society of Mechanical Engineers, Pressure Vessels and Piping Conference, Montreal, Canada, June 26-29, 1978, Paper*, 100 p. 16 refs. Research supported by the Electric Power Research Institute and NASA.

The minimum commitment method has been applied to the analysis of creep rupture data. The method is based on a parameter representing the focal point of convergence of all isothermals when extended to the long or short times necessary for such convergence to occur. The technique may be applied by manual graphic analysis or computer code. It is illustrated for the nickel base alloy Astroloy. S. C. S.

A78-45428 * Interpolation and extrapolation of creep rupture data by the minimum commitment method. III - Analysis of multiheats. S. S. Manson (Case Western Reserve University, Cleveland, Ohio) and C. R. Ensign (NASA, Lewis Research Center, Cleveland, Ohio). *American Society of Mechanical Engineers and Canadian Society of Mechanical Engineers, Pressure Vessels and Piping Conference, Montreal, Canada, June 26-29, 1978, Paper*, 32 p. 5 refs. Research supported by the Electric Power Research Institute.

and NASA.

An outline is presented of approaches for treating multiheats on the basis of the focal point convergence method. The method has been employed in the case of two highly characterized multiheats, including a 304 stainless steel studied in Japan and a low alloy carbon steel studied in England. The method makes use of the same functional form for all materials. Only the constants are varied for each multiheat. Completely computerized procedures are employed for the determination of the constants. Once the basic analysis has been performed, the representation of various members in the same system is achieved by adding linear expressions of log stress, changing only two constants in the equations to represent a selected heat.

G.R.

A78-45434 * Correlations between ultrasonic and fracture toughness factors in metallic materials. A. Vary (NASA, Lewis Research Center, Cleveland, Ohio). *Symposium on Fracture Mechanics, 11th, Blacksburg, Va., June 12-14, 1978, Paper*. 17 p. 18 refs.

A heuristic mathematical basis is proposed for the experimental correlations found between ultrasonic propagation factors and fracture toughness factors in metallic materials. A crack extension model is proposed wherein spontaneous stress (elastic) waves produced during microcracking are instrumental in promoting the onset of unstable crack extension. Material microstructural factors involved in this process are measurable by ultrasonic probing. Experimental results indicate that ultrasonic attenuation and velocity measurements will produce significant correlations with fracture toughness properties and also yield strength. (Author)

A78-50086 * The cyclic oxidation resistance of cobalt chromium-aluminum alloys at 1100 and 1200 C and a comparison with the nickel-chromium-aluminum alloy system. C. A. Barrett and C. E. Lowell (NASA, Lewis Research Center, Cleveland, Ohio). *Oxidation of Metals*, vol. 12, Aug. 1978, p. 293-311. 13 refs.

A78-51714 * Substitution for chromium in 301 stainless steel. J. R. Stephens and C. A. Barrett (NASA, Lewis Research Center, Cleveland, Ohio). In: *Environmental degradation of engineering materials, Proceedings of the Conference, Blacksburg, Va., October 10-12, 1977.* (A78-51701 23-23) Blacksburg, Va., Virginia Polytechnic Institute and State University, 1978, p. 257-266. 5 refs.

An investigation was conducted to determine the effects of substituting less strategic elements for Cr on oxidation and corrosion resistance of AISI 304 stainless steel. Cyclic oxidation resistance was evaluated at 870 C. Corrosion resistance was determined by exposure of specimens to a boiling copper-rich solution of copper sulfate and sulfuric acid. Alloy substitutes for Cr include Al, Mn, Mo, Si, Ti, V, Y, and misch metal. A level of about 12% Cr was the minimum amount of Cr required for adequate oxidation and corrosion resistance in the modified composition 304 stainless steels. This represents a Cr saving of 33 percent. Two alloys containing 12% Cr plus 2% Al plus 2% Mo and 12% Cr plus 2.65% Si were identified which exhibited oxidation and corrosion resistance comparable to AISI 304 stainless steel. (Author)

A78-51716 * 10,000-hour cyclic oxidation behavior at 815 C (1500 F) of 33 high-temperature alloys. C. A. Barrett (NASA, Lewis Research Center, Cleveland, Ohio). In: *Environmental degradation of engineering materials, Proceedings of the Conference, Blacksburg, Va., October 10-12, 1977.* (A78-51701 23-23) Blacksburg, Va., Virginia Polytechnic Institute and State University, 1978, p. 319-327.

Thirty-three commercial high-temperature Fe-, Ni-, and Co-base alloys were oxidized in air at 815 C (1500 F) for ten 1000-hour cycles. Specific weight change versus time curves were derived and the 10,000-hour surface oxides were analyzed by X-ray diffraction. The alloys were ranked by a combination of appearance and metal loss estimates derived from gravimetric data. (Author)

A78-51739 * Ductility normalized-strain-range partitioning life relations for creep-fatigue life predictions. G. R. Halford, J. F. Sautman, and M. H. Hirschberg (NASA, Lewis Research Center, Cleveland, Ohio). In: *Environmental degradation of engineering materials; Proceedings of the Conference, Blacksburg, Va., October 10-12, 1977.* (A78-51701 23-23) Blacksburg, Va., Virginia Polytechnic Institute and State University, 1978, p. 599-612. 24 refs.

Techniques utilizing strainrange partitioning may be used to estimate the effects of the environment on the high-temperature, low-cycle, creep-fatigue resistance of alloys. Three levels of ductility-normalized strainrange-partitioning life relations are discussed: (1) strainrange partitioning relations from ductility data, (2) strainrange partitioning relations scaled by ductility ratios, and (3) strainrange partitioning life relations with measured PP lines. The procedures have demonstrated good agreement with available creep-fatigue data.

S.C.S.

A78-53063 * Reaction diffusion in the NiCrAl and CoCrAl systems. S. R. Levine (NASA, Lewis Research Center, Coatings Section, Cleveland, Ohio). *Metallurgical Transactions A: Physical Metallurgy and Materials Science*, vol. 9A, Sept. 1978, p. 1237-1250. 18 refs.

The paper assesses the effect of overlay coating and substrate composition on the kinetics of coating depletion by interdiffusion. This is accomplished by examining the constitution, kinetics and activation energies for a series of diffusion couples primarily of the NiCrAl/Ni-10Cr or CoCrAl/Ni-10Cr type annealed at temperatures in the range 1000-1205 C for times up to 500 hr. A general procedure is developed for analyzing diffusion in multicomponent multiphase systems. It is shown that by introducing the concept of beta-solution strength, which can be determined from appropriate phase diagrams, the Wagner solution for consumption of a second phase in a semiinfinite couple is successfully applied to the analysis of MCrAl couples. Thus, correlation of beta-recession rate constants with couple composition, total and diffusional activation energies, and interdiffusion coefficients are determined. S.D.

A78-11232* General Electric Co., Cincinnati, Ohio. Material and Process Technology Labs
MANUFACTURE AND ENGINE TEST OF ADVANCED OXIDE DISPERSION STRENGTHENED ALLOY TURBINE VANES
Final Report
P G Bailey Oct 1977 158 p refs
(Contract NAS3-18915)
(NASA-CR-135289, R77AEG569) Avail: NTIS HC A08/MF A01 CSCL 11F

Oxide-Dispersion-strengthened (ODS) Ni-Cr-Al alloy systems were exploited for turbine engine vanes which would be used for the space shuttle thermal protection system. Available commercial and developmental advanced ODS alloys were evaluated, and three were selected based on established vane property goals and manufacturing criteria. The selected alloys were evaluated in an engine test. Candidate alloys were screened by strength, thermal fatigue resistance, oxidation and sulfidation resistance. The Ni-16Cr (3 to 5)Al-ThO₂ system was identified as having attractive high temperature oxidation resistance. Subsequent work also indicated exceptional sulfidation resistance for these alloys. G.D.H.

A78-14143* Ford Motor Co., Dearborn, Mich. Engineering and Research Staff
FABRICATION OF THIN LAYER BETA ALUMINA
Gerald J Tennenhouse [1977] 41 p refs
(Contract NAS3-19782)
(NASA-CR-135308) Avail: NTIS HC A03/MF A01 CSCL 11F

Beta alumina tubes having walls 700 microns, 300 microns, and 140 microns were processed by extrusion and sintering utilizing Ford proprietary binder and fabrication systems. Tubes prepared by this method have properties similar to tubes prepared by isostatic pressing and sintering, i.e. density greater than 98% of theoretical and a helium leak rate less than 3×10^{-10} to the

8th power cc/sq cm/sec. Ford ultrasonic bonding techniques were used for bonding beta alumina end caps to open ended beta alumina tubes prior to sintering. After sintering, the bond was hermetic, and the integrity of the bonded area was comparable to the body of the tube. Author

N78-16233* IIT Research Inst., Chicago, Ill. Metals Research Div.

THERMAL FATIGUE AND OXIDATION DATA OF SUPERALLOYS INCLUDING DIRECTIONALLY SOLIDIFIED EUTECTICS

V. L. Hill and V. E. Humphreys Jun. 1977 66 p refs (Contract NAS3-17787)

(NASA-CR-135272; IITRI-B6124-48) Avail: NTIS HC A04/MF A01 CSCL 11F

Thermal fatigue and oxidation data were obtained on 61 specimens, representing 15 discrete alloy compositions or fabricating techniques and three coating systems. Conventionally fabricated alloys included V57, MM 200, Rene 77, Rene 125, MM 248, MM 509, IN-738, IN-792 + Hf, and MM 200 + Hf. The directionally solidified alloys were MM 200, MM 200 single crystal, MM 200 bicrystal, cellular gamma/gamma' - delta and lamellar gamma/gamma' - delta. The coatings systems included NiCrAlY on IN-738, IN-792 + Hf, MM 200 DS, MM 200 DS single crystal, and cellular gamma/gamma' - delta and NiCrAlY/Pt on lamellar gamma/gamma' - delta. Crack initiation survival rates were recorded for all alloys, with and without coatings. All uncoated alloys, except MM 509, exhibited significant oxidation weight loss in 75,000 to 15,000 cycles. MM 509 specimens had weight losses only slightly higher than coated specimens through 7,500 cycles. All coated specimens had low weight loss. Author

N78-16234* Massachusetts Inst of Tech., Cambridge Aeroelastic and Structures Research Lab

EXPERIMENTAL TRANSIENT AND PERMANENT DEFORMATION STUDIES OF STEEL SPHERE-IMPACTED OR EXPLOSIVELY-IMPULSED ALUMINUM PANELS

Emmett A. Witmer, Fred Merlis, Jose J. A. Rodal, and Thomas R. Stagliano May 1977 144 p refs

(Grant NGR 22 009 339) (NASA CR-135315; ASRL-TR 154-12) Avail: NTIS HC A07/MF A01 CSCL 11F

The sheet explosive loading technique (SELT) was employed to obtain elastic-plastic large deflection 3-d transient and/or permanent strain data on simple well defined structural specimens and materials. Initially flat 6061-T651 aluminum panels with all four sides ideally clamped via integral construction. The SELT loading technique was chosen since it is both convenient and provides forcing function information of small uncertainty. These data will be useful for evaluating pertinent 3-d structural response prediction methods. Author

N78-16149* IIT Research Inst. Chicago Ill.

THERMAL FATIGUE AND OXIDATION DATA FOR ALLOY/BRAZE COMBINATIONS Technical Report, May 1975 - May 1977

V. L. Hill and V. E. Humphreys Jun. 1977 55 p refs (Contract NAS3 18942)

(NASA CR 135299; IITRI-B6134-25) Avail: NTIS HC A04/MF A01 CSCL 11F

Thermal fatigue and oxidation data were obtained for 62 brazed specimens of 3 iron, 3 nickel, and 1 cobalt-base alloy. Fluidized bed thermal cycling was conducted over the range 740-25°C employing 10 cm long single edge wedge specimens. Immersion time was always 4 minutes in each bed. Types of test specimens employed in the program include those with brazed overlays on the specimen radius, those butt brazed at midspan and those with a brazed foil overlay on the specimen radius. Of the 18 braze overlay specimens, 5 generated fatigue cracks by 7,000 cycles. Thermal cracking of butt brazed specimens occurred exclusively through the butt braze. Of the 23 butt brazed

specimens, 7 survived 11,000 thermal cycles without cracking. Only 2 of the 21 foil overlaid specimens exhibiting cracking in 7,000 cycles. Blistering of the foil did occur for 2 alloys by 500 cycles. Oxidation of the alloy/braze combination was limited at the test maximum test temperature of 740°C. Author

N78-16150* Carnegie-Mellon Univ., Pittsburgh, Pa. Dept. of Metallurgy and Materials Science

THE EFFECT OF MICROSTRUCTURE AND STRENGTH ON THE FRACTURE TOUGHNESS OF AN 18 Ni, 300 GRADE MARAGING STEEL Final Report

J. A. Psioda and J. R. Low, Jr. Nov. 1977 94 p refs (Grant NGR-39-087-003)

(NASA-CR-135288; CMU-NASA-8) Avail: NTIS HC A05/MF A01 CSCL 11F

Fractography and metallographic sectioning were used to investigate the influence of microstructure and strength on the fracture toughness (K_{Ic}) and fracture mechanism of an 18 Ni, 300 grade maraging steel. Increased yield strength from 1442 to 2070 MN/m squared through precipitation hardening results in a K_{Ic} loss from 143 to 55 MN/m superscript 3/2. Ti (C,N) Ti2S, and TiC inclusions in sizes from 1 to 8, 1 to 15, and 0.1 to 2 microns respectively serve as sites for void nucleation and lead to fracture by the dimpled rupture process in all strength levels considered. TiC nucleated dimples occupy more than half the fracture in all conditions. Void nucleation rate and resultant number of dimples per unit area of fracture increase with increasing yield strength. Average dimple size decreases with increasing strength and/or overaging which follows from the decreasing amount of stable void growth measured by sectioning tensile specimens. Void growth is assisted by crack branching along a path of TiC inclusions. Coalescence occurs in the highest strength materials by a combination of TiC void nucleation and premature separation at strengthening precipitates. Author

N78-19288* Kentucky Univ., Lexington, Dept. of Metallurgical Engineering and Materials Science.

THE EFFECT OF MINOR ADDITIONS OF TITANIUM ON THE FRACTURE TOUGHNESS OF Fe-12Ni ALLOYS AT 77K Final Report, 1 Nov. 1976 - 31 Oct. 1977

H. Conrad, C. Yin, and G. Sargent 16 Jan. 1978 92 p refs (Grant NaG-3125)

(NASA-CR-135351) Avail: NTIS HC A05/MF A01 CSCL 11F

Titanium additions ranging from 0.18 to 0.99 atomic percent and heat treatments of 2 hours at 550, 685 and 820°C respectively followed by a water quench were considered. Cubic and rectangular shaped inclusions were noted in the SEM fractographs of the alloys with the Ti additions. A fine precipitate was observed by TEM for the Fe-12Ni-0.18Ti alloys heat treated at 550°C; this precipitate was not observed for the 685 and 820°C heat treatments of the same alloy. Auger mappings of the fracture surfaces indicated a weak to moderate association of the interstitials C, N and O with Ti, the degree of which depended on the particular interstitial and the heat treatment temperature. Author

N78-20310* California Univ., Berkeley, Lawrence Berkeley Lab

THE DESIGN OF AN Fe-12Mn-0.2Ti ALLOY STEEL FOR LOW TEMPERATURE USE Final Report

S. K. Hwang and J. W. Morris, Jr. 6 Dec 1977 107 p (Grant NGR-05-003-562)

(NASA-CR-135310) Avail: NTIS HC A06/MF A01 CSCL 11F

An investigation was made to improve the low temperature mechanical properties of Fe-8 approximately 12% Mn-0.2Ti alloy steels. A two-phase (alpha + gamma) tempering in combination with cold working or hot working was identified as an effective treatment. A potential application as a Ni-free cryogenic steel was shown for this alloy. It was also shown that an Fe-8Mn steel could be grain refined by a purely thermal treatment because of its dislocated martensitic structure and absence of epsilon phase. A significant reduction of the ductile brittle transition temperature was obtained in this alloy. The nature and origin of

brittle fracture in Fe-Mn alloys were also investigated. Two embrittling regions were found in a cooling curve of an Fe-12Mn-C 2Ti steel which was shown to be responsible for intergranular fracture. Auger electron spectroscopy identified no segregation during solution-annealing treatment. Avoiding the embrittling zones by controlled cooling led to a high cryogenic toughness in a solution-annealed condition. Author

N78-21285* Colt Industries, Inc., Pittsburgh, Pa. Crucible Materials Research Center.

FABRICATION OF STAINLESS STEEL CLAD TUBING
Final Report

C. W. Kovach 7 Apr. 1978 102 p
(Contract NAS3-20098)

(NASA-CP-135347) Avail: NTIS HC A08/MF A01 CSCL 11F

The feasibility of producing stainless steel clad carbon steel tubing by a gas pressure bonding process was evaluated. Such a tube product could provide substantial chromium savings over monolithic stainless tubing in the event of a serious chromium shortage. The process consists of the initial assembly of three component tubets from conventionally produced tubing, the formation of a strong metallurgical bond between the three components by gas pressure bonding, and conventional cold draw and anneal processing to final size. The quality of the tubes produced was excellent from the standpoint of bond strength, mechanical, and forming properties. The only significant quality problem encountered was carburization of the stainless clad by the carbon steel core which can be overcome by further refinement through at least three different approaches. The estimated cost of clad tubing produced by this process is greater than that for monolithic stainless tubing, but not so high as to make the process impractical as a chromium conservation method. Author

N78-21286* United Technologies Research Center, East Hartford, Conn.

STUDY OF THE EFFECTS OF GASEOUS ENVIRONMENTS ON SULFIDATION ATTACK OF SUPERALLOYS
Final Report

John G. Smeggil and Norman S. Bornstein Nov. 1977 166 p refs

(Contract NAS3-20039)

(NASA-CN-135348; R77-912613-5) Avail: NTIS HC A08/MF A01 CSCL 11F

Studies were conducted to examine the effect of the gaseous corrodents NaCl, HCl, and NaOH on the high temperature oxidation and Na₂SO₄-induced corrosion behavior of the alumina former NiAl, the chromia former Ni-25 wt % Cr, elemental Cr, and the superalloy B-1900. Experiments were conducted at 900 and 1050 C in air in the presence and absence of the gaseous corrodents. Effects involving both reaction rates and microstructural changes in oxide morphology were observed due to the presence of these corrodents at levels anticipated to be present in operating industrial and marine gas turbines. The effect of gaseous NaCl, HCl, and possibly NaOH on NiAl in simple oxidation was to remove aluminum from below the protective alumina layer and to simultaneously weaken the adherence of the protective alumina oxide scale to the substrate. The aluminum removed from below the oxide scale was redeposited on its surface as alpha-Al₂O₃ whiskers. With respect to the chromia formers, gaseous NaCl and HCl promoted breakaway oxidation kinetics and changes in the microstructures of the oxide scales. Author

N78-25188* Pratt and Whitney Aircraft Group, East Hartford, Conn. Commercial Products Div

MANUFACTURE OF ASTROLOY TURBINE DISK SHAPES BY HOT ISOSTATIC PRESSING, VOLUME 1 Final Report

R. D. Eng and D. J. Evans Mar. 1978 89 p refs
(Contract NAS3-20072)

(NASA-CR-135408; PWA-5574-12-Vol-1) Avail: NTIS HC A05/MF A01 CSCL 11F

The Materials in Advanced Turbine Engines project was conducted to demonstrate container technology and establish manufacturing procedures for fabricating direct Hot Isostatic Pressing (HIP) of low carbon Astroloy to ultrasonic disk shapes. The HIP processing procedures including powder manufacture and handling, container design and fabrication, and HIP consolidation techniques were established by manufacturing five HIP disks. Based upon dimensional analysis of the first three disks, container technology was refined by modifying container tooling which resulted in closer conformity of the HIP surfaces to the sonic shape. The microstructure, chemistry and mechanical properties of two HIP low carbon Astroloy disks were characterized. One disk was subjected to a ground base experimental engine test, and the results of HIP low carbon Astroloy were analyzed and compared to conventionally forged Waspaloy. The mechanical properties of direct HIP low carbon Astroloy exceeded all property goals and the objectives of reduction in material input weight and reduction in cost were achieved. Author

A78-24901* # The effect of NaCl(g) on the Na₂SO₄-induced

hot corrosion of NiAl. J. G. Smeggil, N. S. Bornstein, and M. A. DeCrescente (United Technologies Research Center, East Hartford, Conn.). *Engineering Foundation, Conference on Ash Deposits and Corrosion: Due to Impurities in Combustion Gases, Henniker, N.H., June 26-July 1, 1977, Paper.* 14 p, 33 refs. Contract No. NAS3-20039.

Studies have been performed to examine the effect of NaCl vapor on the Na₂SO₄-induced hot corrosion of the alumina former NiAl. In the incubation period associated with such hot corrosion, NaCl(g) has been shown to be effective in removing aluminum from below the protective alumina scale and redepositing it as Al₂O₃ whiskers on the surface of the Na₂SO₄-coated sample. Similar effects seen in simple oxidation are associated with isothermal rupturing of the protective alumina scale. (Author)

27 NONMETALLIC MATERIALS

Includes physical, chemical, and mechanical properties of plastics, elastomers, lubricants, polymers, textiles, adhesives, and ceramic materials.

N78-10294* National Aeronautics and Space Administration, Lewis Research Center, Cleveland, Ohio.

IMPROVED PERFORMANCE OF SILICON NITRIDE-BASED HIGH TEMPERATURE CERAMICS

Richard L. Ashbrook 1977 26 p refs Presented at Mater. Show and Conf., Chicago, 25-27 Oct. 1977; sponsored by ASM

(NASA-TM-73719; E-9268) Avail: NTIS HC A03/MF A01 CSCL 11B

Recent progress in the production of Si₃N₄ based ceramics is reviewed. (1) high temperature strength and toughness of hot pressed Si₃N₄ were improved by using high purity powder and a stabilized ZrO₂ additive. (2) impact resistance of hot pressed Si₃N₄ was increased by the use of a crushable energy absorbing layer. (3) the oxidation resistance and strength of reaction sintered Si₃N₄ were increased by impregnation of reaction sintered silicon nitride with solutions that oxidize Al₂O₃ or ZrO₂. (4) beta prime SiAlON compositions and sintering aids were developed for improved oxidation resistance or improved high temperature strength.

Author

N78-10295* National Aeronautics and Space Administration, Lewis Research Center, Cleveland, Ohio.

FRICITION AND WEAR OF SINGLE-CRYSTAL AND POLYCRYSTALLINE MANGANESE-ZINC FERRITE IN CONTACT WITH VARIOUS METALS

Kazuhiisa Miyoshi (Kanazawa Univ.) and Donald H. Buckley 1977 28 p refs

(NASA-TP-1059) Avail: NTIS HC A03/MF A01 CSCL 209

Sliding friction experiments were conducted with single-crystal (SCF) and hot-pressed polycrystalline (HPF) manganese-zinc ferrite in contact with various metals. Results indicate that the coefficients of friction for SCF and HPF are related to the relative chemical activity of those metals in high vacuum. The more active the metal, the higher the coefficient of friction. The coefficients of friction for both SCF and HPF were the same and much higher in vacuum than in argon at atmospheric pressure. All the metals tested transferred to the surface of both SCF and HPF in sliding. Both SCF and HPF exhibited cracking and fracture with sliding. Cracking in SCF is dependent on crystallographic characteristics. In HPF, cracking depends on the orientation of the individual crystallites.

Author

N78-12222* National Aeronautics and Space Administration, Lewis Research Center, Cleveland, Ohio.

EFFECTIVENESS OF VARIOUS ORGANOMETALLICS AS ANTIWEAR ADDITIVES IN MINERAL OIL

Donald H. Buckley Nov. 1977 20 p refs

(NASA-TP-1096) Avail: NTIS HC A02/MF A01 CSCL 11H

Sliding friction experiments were conducted with 1045 steel contacting 302 stainless steel and lubricated with various organometallics in mineral oil. Auger emission spectroscopy was used to determine the element present in the wear contact zone. The results indicate that there are organometallics which are as effective an antiwear additives as the commonly used zinc dialkyl dithiophosphate. These include dimethyl cadmium, triphenyl lead thiomethoxide, and triphenyl tin chloride. The additives were examined in concentrations to 1 weight percent. With dimethyl cadmium at concentrations of 0.5 weight percent, and above, cadmium was detected in the contact zone. Coincident with the detection of cadmium, a marked decrease in the friction coefficient was observed. All additives examined reduced friction, but only the aforementioned reduced wear to a level comparable to that observed with zinc dialkyl dithiophosphate.

Author

N78-15277* National Aeronautics and Space Administration, Lewis Research Center, Cleveland, Ohio.

EFFECT OF THERMAL EXPOSURE ON LUBRICATING PROPERTIES OF POLYIMIDE FILMS AND POLYIMIDE-BONDED GRAPHITE FLUORIDE FILMS

Robert L. Fusaro Jan. 1978 26 p refs

(NASA-TP-1125; D-9179) Avail: NTIS HC A03/MF A01 CSCL 11G

The effect of thermal exposure on the weight loss, adherence, friction, and wear properties of polyimide films and polyimide bonded graphite fluoride films was investigated. Films bonded to 304 stainless steel or 440C-HT steel were thermally exposed at temperatures of 315, 345, 370, or 400 C for 100 hours or more and then evaluated, using a pin-on-disk machine, at temperatures of 25, 315, or 345 C in atmospheres of dry or moist air. Polyimide films were brittle after thermal exposure. Polyimide bonded graphite fluoride films had adherence and gave low friction and wear results, thus, they appear to be good candidates for solid lubrication applications where long thermal soaks are prevalent.

Author

N78-15276* National Aeronautics and Space Administration, Lewis Research Center, Cleveland, Ohio.

TRIMERIZATION OF AROMATIC NITRILES Patent

Li-Chen Hsu, inventor (to NASA); Issued 6 Dec. 1977 18 p Filed 10 Oct. 1974 Supersedes N74-34579 (12 - 24, p. 2914)

(NASA-Case-LEW-12053-1; US-Patent-4,061,856.

US-Patent-Appi-SN-513613; US-Patent-Class-544-193.

US-Patent-Class-260-2R; US-Patent-Class-526-193.

US-Patent-Class-526-225) Avail: US Patent Office CSCL 07C

Triazine compounds and cross-linked polymer compositions were made by heating aromatic nitriles to a temperature in the range of about 100 C to about 700 C, in the presence of a catalyst or mixture of catalysts. Aromatic nitrile-modified (terminated and/or appended) imide, benzimidazole, imidazopyrrolone, quinoxaline, and other condensation type prepolymers or their prepolymers were made which were trimerized with or without a filler by the aforementioned catalytic trimerization process.

Official Gazette of the U.S. Patent Office

N78-15278* National Aeronautics and Space Administration, Lewis Research Center, Cleveland, Ohio.

FRICITION AND WEAR OF POLYETHYLENE OXIDE POLYMER HAVING A RANGE OF MOLECULAR WEIGHTS

Donald H. Buckley Jan. 1978 17 p refs

(NASA-TP-1129; E-9261) Avail: NTIS HC A02/MF A01 CSCL 11G

Sliding friction and wear experiments were conducted at light loads (25 to 250 g) with various molecular weights of the polyethylene oxide polymer sliding on itself and iron. Results of the experimental investigation indicate that (1) the coefficient of friction for the polymer decreases with increasing molecular weight, (2) the friction coefficient is higher for the polymer sliding on itself than it is for the polymer sliding on iron, (3) at sufficiently high loads localized surface melting occurs and the friction coefficient is the same for the polymer sliding on itself and iron, (4) fracture cracks develop in the sliding wear track at higher, but not lower sliding velocities, reflecting a strain rate sensitivity to crack initiation, and (5) the friction coefficient for the polymer sliding on iron increases with the formation of a polymer film on the iron surface.

Author

N78-15280* National Aeronautics and Space Administration, Lewis Research Center, Cleveland, Ohio.

PRELIMINARY STUDY OF CYCLIC THERMAL SHOCK RESISTANCE OF PLASMA SPRAYED ZIRCONIUM OXIDE TURBINE OUTER AIR SEAL SHROUDS

Robert G. Ehl, Arno R. and J. Lab. and Donald W. Vanderschueren Dec. 1977 14 p refs

(NASA-TM-73852; E-9404) Avail: NTIS HC A02/MF A01 CSCL 11A

Several experimental methods representing potential high pressure turbine seal material systems were subjected to cyclic

thermal shock exposures similar to those that might be encountered under severe engine start-up and shut-down sequences. All of the experimental concepts consisted of plasma-sprayed yttria stabilized ZrO₂ on the high temperature side of the blade tip seal shroud. Between the ZrO₂ and a cooled dense metal backing, various intermediate layer concepts intended to mitigate thermal stresses were incorporated. Performance was judged on the basis of the number of thermal shock cycles required to cause loss of seal material through spallation. The most effective approach was to include a low modulus sintered metal pad between the ZrO₂ and the metallic backing. It was also found that reducing the density of the ZrO₂ layer significantly improved the performance of specimens with plasma-sprayed metal/ceramic composite intermediate layers. Author

N78-17220* National Aeronautics and Space Administration, Lewis Research Center, Cleveland, Ohio
EFFECTS OF HYDROTHERMAL EXPOSURE ON A LOW-TEMPERATURE CURED EPOXY
 Richard W. Lauer 1978 12 p refs Presented at the 33rd Ann Conf. of Reinforced Plastics/Composites Inst. of the Soc of the Plastics Ind., Inc., Wash., D. C., 7-10 Feb. 1978 (NASA-TM-73841; E-9428) Avail: NTIS HC A02/MF A01 CSCL 11C

Thermal mechanical analysis was employed to monitor the penetration temperature of a low-temperature epoxy resin. Both neat resin and E-glass composite samples were examined. The effects of cure temperature variation and moisture content on the apparent glass transition temperature were determined. Author

N78-17221* National Aeronautics and Space Administration, Lewis Research Center, Cleveland, Ohio
PMR POLYIMIDE PREPREG WITH IMPROVED TACK CHARACTERISTICS
 Tito T. Serafini and Peter Delvigs 1978 13 p refs Proposed for presentation at 2d Intern Conf on Composite Materials, Toronto, Can., 16-21 Apr. 1978, sponsored by Am Inst of Mining, Metallurgical and Petroleum Engineers (NASA TM 73898) Avail: NTIS HC A02/MF A01 CSCL 11C

Current PMR Polyimide prepreg technology utilizes methanol or ethanol solvents for preparation of the PMR prepreg solutions. The volatility of these solvents limits the tack and drape retention characteristics of unprotected prepreg exposed to ambient conditions. Studies conducted to achieve PMR 15 Polyimide prepreg with improved tack and drape characteristics were described. Improved tack and drape retention were obtained by incorporation of an additional monomer. The effects of various levels of the added monomer on the thermo-oxidative stability and mechanical properties of graphite fiber reinforced PMR 15 composites exposed and tested at 316 C (600 F) were discussed. Author

N78-20333* National Aeronautics and Space Administration, Lewis Research Center, Cleveland, Ohio
COATINGS FOR WEAR AND LUBRICATION
 Tevaldas Spahn 1978 33 p refs Presented at the 3d Intern Conf on Metallurgical Coatings, San Francisco, 3-7 Apr. 1978, sponsored by Am Vacuum Soc, Inc. (NASA TM 78341) Avail: NTIS HC A03/MF A01 CSCL 11G

Recent advances in the tribological uses of rf sputtered and ion plated films of solid film lubricants (laminar solids, soft metals, organic polymers) and wear resistant refractory compounds (carbides, nitrides, oxides) are reviewed. The sputtering and ion plating potentials and the corresponding coatings formed were evaluated relative to the friction coefficient, wear endurance life and mechanical properties. The tribological and mechanical properties for each kind of film are discussed in terms of film adherence, coherence, density, grain size, morphology, internal stresses, thickness and substrate conditions such as temperature, topography, chemistry and cleaning. The ion plated materials in addition (1) improved tribological properties may have better mechanical properties such as tensile strength and fatigue life. Author

N78-20336* National Aeronautics and Space Administration, Lewis Research Center, Cleveland, Ohio
X-RAY PHOTOELECTRON SPECTROSCOPY STUDY OF RADIOFREQUENCY-SPUTTERED REFRACTORY COMPOUND STEEL INTERFACES
 Donald R. Wheeler and William A. Brainard Feb. 1978 20 p refs (NASA-TP-1181; E-9374) Avail: NTIS HC A02/MF A01 CSCL 11G

Radiofrequency sputtering was used to deposit Mo₂C, Mo₂B₅, and MoSi₂ coatings on 440C steel substrates. Both sputter etched and preoxidized substrates were used, and the films were deposited with and without a substrate bias of -300 V. The composition of the coatings was measured as a function of depth by X-ray photoelectron spectroscopy combined with argon ion etching. In the interfacial region there was evidence that bias produced a graded interface in Mo₂B₅ but not in Mo₂C. Oxides of iron and of all film constituents except carbon were present in all cases but the iron oxide concentration was higher and the layer thicker on the preoxidized substrates. The film and iron oxides were mixed in the MoSi₂ and Mo₂C films but layered in the Mo₂B₅ film. The presence of mixed oxides correlates with enhanced film adhesion. Author

N78-20337* National Aeronautics and Space Administration, Lewis Research Center, Cleveland, Ohio
LUBRICATION AND FAILURE MECHANISMS OF GRAPHITE FLUORIDE FILMS
 Robert L. Fusaro Apr. 1978 32 p refs (NASA-TP-1197; E-9346) Avail: NTIS HC A03/MF A01 CSCL 11H

An optical microscope, equipped with a vertical illuminator and two polaroid filters (one rotatable), was used to visually study 440C HT steel surfaces lubricated with rubbed graphite fluoride films. Friction and wear results were compared to visual observations as a function of sliding distance for films applied to three surface finishes - polished, sanded, and sand-blasted. In general, the lubricating process was one of initial deformation or wear of metallic asperities into flat plateaus and then the formation of thin, layer-like dynamic films which sheared between the flats and eventually flowed through the contact area. Failure was due to depletion of the graphite fluoride with the subsequent formation of excessive powdery metallic debris that formed a heavy, powdery film on both the roller and disk surfaces. Author

N78-20338* National Aeronautics and Space Administration, Lewis Research Center, Cleveland, Ohio
FRICION AND WEAR OF RADIOFREQUENCY-SPUTTERED BORIDES, SILICIDES, AND CARBIDES
 William A. Brainard and Donald R. Wheeler Apr. 1978 19 p refs (NASA-TP-1156; E-9384) Avail: NTIS HC A02/MF A01 CSCL 11G

The friction and wear properties of several refractory compound coatings were examined. These compounds were applied to 440 C bearing steel surfaces by radiofrequency (RF) sputtering. The refractory compounds were the titanium and molybdenum borides, the titanium and molybdenum silicides and the titanium, molybdenum, and boron carbides. Friction testing was done with a pin on disk wear apparatus at loads from 0.1 to 5.0 newtons. Generally the best wear properties were obtained when the coatings were bias sputtered onto 440 C disks that had been pre-oxidized. Adherence was improved because of the better bonding of the coatings to the iron oxide formed during preoxidation. As a disk, the carbides provided wear protection to the highest loads. Titanium boride coatings provided low friction and good wear properties to moderate loads. Author

N78-21294* National Aeronautics and Space Administration
Lewis Research Center, Cleveland, Ohio
FRICTION AND METAL TRANSFER FOR SINGLE-CRYSTAL SILICON CARBIDE IN CONTACT WITH VARIOUS METALS IN VACUUM

Kazuhisa Miyoshi (Kanazawa Univ. Japan) and Donald H. Buckley
Apr. 1978 27 p refs
(NASA-TP-1191; E-9307) Avail. NTIS HC A03/MF A01 CSCL 11G

Sliding friction experiments were conducted with single-crystal silicon carbide in contact with transition metals (tungsten, iron, rhodium, nickel, titanium, and cobalt), copper, and aluminum. Results indicate the coefficient of friction for a silicon carbide-metal system is related to the d bond character and relative chemical activity of the metal. The more active the metal, the higher the coefficient of friction. All the metals examined transferred to the surface of silicon carbide in sliding. The chemical activity of metal to silicon and carbon and shear modulus of the metal may play important roles in metal transfer and the form of the wear debris. The less active and greater resistance to shear the metal has, with the exception of rhodium and tungsten, the less transfer to silicon carbide. Author

N78-21295* National Aeronautics and Space Administration
Lewis Research Center, Cleveland, Ohio

WEAR OF SINGLE-CRYSTAL SILICON CARBIDE IN CONTACT WITH VARIOUS METALS IN VACUUM

Kazuhisa Miyoshi and Donald H. Buckley Apr. 1978 24 p refs
(NASA-TP-1198; E-9360) Avail. NTIS HC A02/MF A01 CSCL 11G

Sliding friction experiments were conducted in vacuum with single crystal silicon carbide (0001) surface in contact with transition metals (tungsten, iron, rhodium, nickel, titanium, and cobalt), copper, and aluminum. The hexagon shaped cracking and fracturing of silicon carbide that occurred is believed to be due to cleavages of both the prismatic and basal planes. The silicon carbide wear debris, which was produced by brittle fracture, shears or rolls on both the metal and silicon carbide and produces grooves and indentations on these surfaces. The wear scars of aluminum and titanium, which have much stronger chemical affinity for silicon and carbon, are generally rougher than those of the other metals. Fracturing and cracking along the grain boundary of rhodium and tungsten were observed. These may be primarily due to the greater shear modulus of the metals. Author

N78-22232* National Aeronautics and Space Administration
Lewis Research Center, Cleveland, Ohio
THE EFFECT OF MICROSTRUCTURE ON HYDROGEN EMBRITTLEMENT OF THE NICKEL-BASE SUPERALLOY, UDIMET 700

Hugh R. Gray 1978 32 p refs Presented at the 19th Struct. Structural Dyn and Mater Conf. Bethesda Md 3-5 Apr 1978 sponsored by the AIAA and the Am Soc of Mech Engrs
(NASA TM 73772; E-9574) Avail. NTIS HC A03/MF A01 CSCL 11F

Material from a single heat of cast and wrought Udimet 700 was processed and/or heat treated to produce five material conditions with identical chemical compositions but with distinct microstructural variations and then evaluated for susceptibility to hydrogen embrittlement. Two prealloyed powder conditions exhibited significantly improved resistance to hydrogen embrittlement as compared to wrought material. No degradation in notch or smooth tensile strengths occurred and average ductilities of 25 percent reduction of area were determined for 2 hydrogen evaluation procedures. For the most severe hydrogenation procedure ductility levels were reduced to 15 percent. These improvements were attributed to cleaner grain boundaries and decreases grain size. Author

N78-22243* National Aeronautics and Space Administration
Lewis Research Center, Cleveland, Ohio
EXPERIMENTAL EVALUATION OF FUEL PREPARATION SYSTEMS FOR AN AUTOMOTIVE GAS TURBINE CATALYTIC COMBUSTOR

Robert R. Tacina 1977 22 p refs Presented at the 2d Workshop on Catalytic Combust., Raleigh, N. C.; sponsored by EPA Prepared for DOE
(NASA-TM-78856; DOE/NASA-1011-78/23; E-9585) Avail. NTIS HC A02/MF A01 CSCL 21D

Spatial fuel distributions, degree of vaporization, pressure drop and air velocity profiles were measured. Three airblast injectors and an air-assist nozzle were tested. Air swirlers were used to improve the spatial fuel-air distribution. The work was done in a tubular duct. Test conditions were a pressure of 0.3 MPa, inlet air temperatures up to 800 K, air velocity of 20 m/s and fuel-air ratios up to 0.020. The fuel vaporizer used multiple cones to provide high velocity air for atomization and also straightened the inlet airflow. With this configuration, uniform spatial fuel-air distributions were obtained with mixing lengths greater than 17.8 cm. In this length, vaporization of the fuel was 98.5 percent complete at an inlet air temperature of 700 K. The total pressure loss was 1.0 percent with a reference velocity of 20 m/s and 0.25 percent at 10 m/s. The air velocity was uniform across the duct and no autoignition reactions were observed. Author

N78-23231* National Aeronautics and Space Administration
Lewis Research Center, Cleveland, Ohio
KINETICS OF IMIDIZATION AND CROSSLINKING IN PMR-POLYIMIDE RESIN

Richard W. Lauer 1977 24 p refs Presented at the 9th Central Reg Meeting of the Am Chem Soc. Charleston, W. Va. 12-14 Oct 1977. Submitted for publication
(NASA TM 78844; E-9561) Avail. NTIS HC A02/MF A01 CSCL 11D

Infrared spectroscopy and differential scanning calorimetry were employed to study the imidization and crosslinking kinetics of norbornenyli capped addition type polyimide resins (designated PMR for polymerization of monomer reactants). The spatial and thermal analyses were performed on resin specimens which had been isothermally aged at temperatures appropriate for imidization (120 to 204 C) and crosslinking (275 to 325 C). Imidization occurs rapidly (approximately 0.01 min) at short times, while at times longer than approximately 0.5 hour, the rate decreases significantly (approximately 0.001 min). The crosslinking reaction exhibits first order kinetics during the initial portion of the reaction and its rate appears to be limited by the reversion of the norbornenyli Diels Alder adduct. The total heat evolved per mole of endcap during crosslinking shows an inverse dependence on the molecular weight of the imide prepolymer. This reflects the effect of endcap dilution and decreased mobility of the larger oligomers. Author

N78-25215* National Aeronautics and Space Administration
Lewis Research Center, Cleveland, Ohio
PRESSURELESS SINTERED SIALONS WITH LOW AMOUNTS OF SINTERING AID

Alan Aras Jun 1978 16 p refs
(NASA TP 1246; E-9502) Avail. NTIS HC A02/MF A01 CSCL 11G

Two beta phase Sialons of composition Si₂6Al₂O₁₃Y₂O₃ (Si₂6Al₂O₁₃Y₂O₃)₆ and Si₂6Al₂O₁₃Y₂O₃ (Si₂6Al₂O₁₃Y₂O₃)₆ were pressureless sintered from mixtures of Y₂O₃ and separately mixed Beta-Sialon-Al₂O₃ and SiO₂. These Sialons had densities of over 98% of the theoretical, four point bend strengths of 460 and 155 MPa at room temperature and 1400 C, respectively, and 1400 C oxidation rates lower than those reported for hot pressed Si₃N₄ and for a stronger Sialon with 2.5 weight percentage Y₂O₃. Author

N78-26236* National Aeronautics and Space Administration, Lewis Research Center, Cleveland, Ohio
CATALYTIC DECOMPOSITION OF METHANOL FOR ONBOARD HYDROGEN GENERATION
 Theodore Brabbs Jun 1978 47 p refs
 (NASA-TP-1247; E-9472) Avail NTIS HC A03/MF A01 CSCL 210

The steam reformation of an equimolar mixture of methanol and water on a copper chromite catalyst was studied at three furnace temperatures and at feed space velocities from 800 to 2600 per hour. The hydrogen space velocity could be related to the reactor temperature by the equation $Sv = A \exp(-\omega/T)$, where A and omega are constants determined for each value of alpha and T is temperature. At a methanol conversion of 0.87 and a reactor temperature of 589 K, the extrapolated value of the hydrogen space velocity was 9400 per hour. This velocity was used to estimate the size of an onboard hydrogen reactor for automotive applications. Such a reactor would need only about 0.8 liter of catalyst to produce 7630 STP liters (1.5 lb) of hydrogen per hour. This quantity of catalyst would fit into nine tubes 17.8 centimeters long and 2.54 centimeters in inside diameter, which is smaller than most mufflers. The reactor products would contain 12 to 13 percent more chemical energy than the incoming methanol and water. Author

N78-26214* National Aeronautics and Space Administration, Lewis Research Center, Cleveland, Ohio
SPUTTERING TECHNOLOGY IN SOLID FILM LUBRICATION

Talivaldis Spalvins 1978 18 p refs To be presented at the 2d Intern. Conf. on Solid Lubrication, Denver, 14-18 Aug 1978, sponsored by the Am. Soc. of Lub. Engr.
 (NASA-TM-78914) Avail NTIS HC A02/MF A01 CSCL 11H

Potential and present sputtering technology is discussed as it applies to the deposition of solid film lubricants, particularly MoS₂, WS₂, and PTFE. Since the sputtered films are very thin, the selection of the sputtering parameters and substrate condition is very critical as reflected by the lubricating properties. It was shown with sputtered MoS₂ films that the lubricating characteristics are directly affected by the selected sputtering parameters (power density, pressure, sputter etching, dc biasing, etc.) and the substrate temperature, chemistry, topography, and the environmental conditions during the friction tests. Electron microscopy and other surface sensitive analytical techniques illustrate the resulting changes in sputtered MoS₂ film morphology and chemistry which directly influence the film adherence and frictional properties. G.G.

N78-26215* National Aeronautics and Space Administration, Lewis Research Center, Cleveland, Ohio
A COMPARISON OF THE LUBRICATING MECHANISMS OF GRAPHITE FLUORIDE AND MOLYBDENUM DISULFIDE FILMS

Robert L. Fusaro Aug 1978 42 p refs Proposed for presentation at the 2d Intern. Conf. on Solid Lubrication, Denver, 14-18 Aug 1978, sponsored by the Am. Soc. of Lubrication Engr.
 (NASA-TM-78897; E-9533) Avail NTIS HC A03/MF A01 CSCL 11H

A microscopic study of 440C steel sliding surfaces lubricated by graphite fluoride or molybdenum disulfide solid lubricant rubbed films was conducted. The sliding surfaces, along with the friction wear and wear life were observed as a function of the number of sliding revolutions in three different atmospheres: moist air, dry air, or dry argon. In general, the lubricating mechanisms of the two solid lubricants were found to be relatively similar; that is, a dynamic thin layer-like film was formed between the two metallic surfaces. The mechanisms of failure were found to be somewhat different; however, failure of MoS₂ films was very dependent on atmospheric degradation while that of graphite fluoride films was more dependent on flow of the lubricant film out of the contact zone. Author

N78-27274* National Aeronautics and Space Administration, Lewis Research Center, Cleveland, Ohio
EFFECTS OF PRESSURE AND TEMPERATURE ON HOT PRESSING A SIALON

Hun C. Yeh 1977 18 p refs Presented at the Fall Meeting of the Basic Sci. Div. of the Am. Ceram. Soc., Hyannis, Mass., 25-28 Sep. 1977
 (NASA-TM-78945; E-9692) Avail NTIS HC A02/MF A01 CSCL 11D

Mixed powders (60 m/o Al₂O₃-40 m/o Si₃N₄) were hot pressed at temperatures and pressures from 1360 to 1750 C and 3.5 to 27.5 MPa (0.5 to 4.0 ksi). Fully dense sialon bodies are obtainable at temperatures and pressures as low as 1550 C and 0.5 ksi. The fully dense bodies contain beta prime and x-phase. There is some evidence that plastic deformation has contributed to densification. Author

N78-27257* National Aeronautics and Space Administration, Lewis Research Center, Cleveland, Ohio

THE USE OF ION BEAM CLEANING TO OBTAIN HIGH QUALITY COLD WELDS WITH MINIMAL DEFORMATION

Bernard Sater and Thomas J. Moore 1978 13 p refs Presented at 10th Natl. Technical Conf., N.Y., 17-19 Oct. 1978, sponsored by Soc. for the Advancement of Material and Process Engineering
 (NASA-TM-78933; E-9676) Avail NTIS HC A02/MF A01 CSCL 11F

A variation of cold welding is described which utilizes an ion beam to clean mating surfaces prior to joining in a vacuum environment. High quality solid state welds were produced with minimal deformation. L.S.

N78-28247* National Aeronautics and Space Administration, Lewis Research Center, Cleveland, Ohio

EFFECT OF OXYGEN AND NITROGEN INTERACTIONS ON FRICTION OF SINGLE-CRYSTAL SILICON CARBIDE

Kazuhiisa Miyoshi and Donald H. Euckley (Kanazawa Univ., Japan) Jul. 1978 22 p refs
 (NASA-TP-1265; E-9424) Avail NTIS HC A02/MF A01 CSCL 11G

Friction studies were conducted with single-crystal silicon carbide contacting silicon carbide and titanium after having been exposed to oxygen and nitrogen in various forms. After they had been sputter cleaned, the surfaces were (1) exposed to gaseous oxygen and nitrogen (adsorption), (2) ion bombarded with oxygen and nitrogen, or (3) reacted with oxygen (SiC only). Auger emission spectroscopy was used to determine the presence of oxygen and nitrogen. The results indicate that the surfaces of silicon carbide with reacted and ion-bombarded oxygen ions give higher coefficients of friction than do argon sputter-cleaned surfaces. The effects of oxygen on friction may be related to the relative chemical, thermodynamic properties of silicon, carbon, and titanium for oxygen. The adsorbed films of oxygen, nitrogen, and mixed gases of oxygen and nitrogen on sputter-cleaned, oxygen-ion bombarded, and oxygen-reacted surfaces generally reduce friction. Adsorption to silicon carbide is relatively weak. Author

N78-28246* National Aeronautics and Space Administration, Lewis Research Center, Cleveland, Ohio

PRESSURELESS SINTERED BETA PRIME Si₃N₄ SOLID SOLUTION: FABRICATION, MICROSTRUCTURE, AND STRENGTH

Sunil Dutta 1977 19 p refs Presented at the Fall Meeting of the Basic Sci. Div. of the Am. Ceram. Soc., Hyannis, Mass., 25-28 Sep. 1977

(NASA-TM-78950) Avail NTIS HC A02/MF A01 CSCL 11B

Si₃N₄, AlN, and Al₂O₃ were used as basic constituents in a study of the pressureless sintering of beta prime Si₃N₄ solid solution as a function of temperature. Y₂O₃-SiO₂ additions were used to promote liquid phase sintering. The sintered specimens were characterized with respect to density, microstructure, strength, oxidation, and thermal shock resistance. Density greater than 98 percent of theoretical was achieved by pressureless sintering at 1750 C. The microstructure consisted

essentially of fine-grained beta prime-Si₃N₄ solid solution as the major phase. Modulus of rupture strengths up to 483 MPa were achieved at moderate temperature (1000 C), but decreased to 228 MPa at 1380 C. This substantial strength loss was attributed to a glassy grain boundary phase formed during cooling from the sintering temperature. The best oxidation resistance was exhibited by a composition containing 3 mol % Y₂O₃-SiO₂ additives. Water quench thermal shock resistance was equivalent to that of reaction sintered silicon nitride but lower than hot-pressed silicon nitride. A.R.H.

N78-28248* National Aeronautics and Space Administration, Lewis Research Center, Cleveland, Ohio
SUBSTITUTION OF CERAMICS FOR HIGH TEMPERATURE ALLOYS

H. B. Probst 1978 19 p refs. Presented at the 14th State-of-the-Art Symp on Scarce and Critical Mater., Washington, D. C., 5-7 June 1978, sponsored in part by the Am. Chem. Soc., the Federation of Mater. Soc. and the Am. Soc. for Metals (NASA-TM-78931, E-9674) Avail. NTIS HC A02/MF A01 CSCL 11C

The high temperature capability of ceramics such as silicon nitride and silicon carbide can result in turbine engines of improved efficiency. Other advantages when compared to the nickel and cobalt alloys in current use are raw material availability, lower weight, erosion/corrosion resistance, and potentially lower cost. The use of ceramics in three different sizes of gas turbine is considered, these are the large utility turbines, advanced aircraft turbines, and small automotive turbines. Special considerations, unique to each of these applications arise when one considers substituting ceramics for high temperature alloys. The effects of material substitutions are reviewed in terms of engine performance, operating economy, and secondary effects. A.R.H.

N78-30238* National Aeronautics and Space Administration, Lewis Research Center, Cleveland, Ohio

FRICTION AND WEAR OF METALS WITH A SINGLE-CRYSTAL ABRASIVE GRIT OF SILICON CARBIDE: EFFECT OF SHEAR STRENGTH OF METAL

Kazuhisa Miyachi (Kanazawa Univ., Japan) and Donald H. Buckley Aug 1976 27 p refs (NASA-TP-1293, E-9499) Avail. NTIS HC A03/MF A01 CSCL 11G

Sliding friction experiments were conducted with spherical, single-crystal silicon carbide riders in contact with various metals and with metal riders in contact with silicon carbide flats. Results indicate that (1) the friction force in the plowing of metal and (2) the groove height (corresponding to the volume of the groove) are related to the shear strength of the metal. That is, they decrease linearly as the shear strength of the bulk metal increases. Grooves are formed in metals primarily from plastic deformation, with occasional metal removal. The relation between the groove width D and the load W can be expressed by $W = kD^n$, superscript n which satisfies Meyer's law. Author

N78-31238* National Aeronautics and Space Administration, Lewis Research Center, Cleveland, Ohio

EFFECT OF ATTRITION MILLING ON THE REACTION SINTERING OF SILICON NITRIDE

T. P. Herbell, T. K. Glasgow, and H. C. Yeh (Cleveland State Univ.) 1978 21 p refs. Presented at the 80th Ann Meeting of the Am. Ceram. Soc. Detroit, 7-12 May 1978 (Contract EC 77 A 31-1040)

(NASA TM 78985, E 9723, DOE/NASA/1040-78/2) Avail. NTIS HC A02/MF A01 CSCL 11G

Silicon powder was ground in a steel attrition mill under nitrogen. Air exposed powder was compacted, pre-fired in helium, and reaction sintered in nitrogen & v o hydrogen. For longer grinding times oxygen content, surface area and compactability of the powder increased, and both alpha/beta ratio and degree of nitridation during sintering increased. Iron content remained constant. Author

A78-11847* Directionally solidified ceramic eutectics. R. L. Ashbrook (NASA, Lewis Research Center, Cleveland, Ohio). *American Ceramic Society, Journal*, vol. 60, Sept.-Oct. 1977, p. 428-435. 29 refs.

The aligned structures which result from the directional solidification (DS) of ceramic eutectics are of interest because of their potential for use in electronic devices and as structural materials. Techniques for growing DS ceramic eutectics are briefly discussed. The principles and controlling parameters of DS eutectic growth are described. The criteria for plane-front growth and the effect of growth rate on interlamellar or interfiber spacing are discussed. Examples of the effect of growth parameters on the alignment of the microstructure are given. Examples of the mechanical properties of directionally solidified oxide-oxide ceramics are also cited. (Author)

A78-17456* Microstructure of hot-pressed Al₂O₃-Si₃N₄ mixtures as a function of holding temperature. H. C. Yeh (NASA, Lewis Research Center, Cleveland State University, Cleveland, Ohio). In: *Ceramic microstructures '76: With emphasis on energy related applications*, Proceedings of the Sixth International Materials Symposium, Berkeley, Calif., August 24-27, 1976. (A78-17451 05-27) Boulder, Colo., Westview Press, Inc., 1977, p. 444-455. 9 refs.

Powder mixtures of 40 mol Si₃N₄-60 mol Al₂O₃ were hot-pressed at 4000 psi at various holding temperatures from 1100 C to 1700 C. Scanning and transmission electron microscopy results were correlated to X-ray phase analysis and density measurements. The progressively developed microstructure was used to interpret the densification behavior of SiAlON. (Author)

A78-18787* Two-layer thermal barrier coating for high temperature components. S. Secura (NASA, Lewis Research Center, Surface Protection Branch, Cleveland, Ohio). *American Ceramic Society, Joint Fall Meeting of the Basic Science, San Francisco, Calif., Nov. 1, 1976, Paper 31-BEN-76P*. *American Ceramic Society Bulletin*, vol. 56, Dec. 1977, p. 1082-1085, 1089. 12 refs.

A simple two-layer plasma sprayed thermal barrier coating system was developed which has the potential for protecting high temperature air-cooled gas turbine components. Of the initially examined coatings, the most promising system is an Ni-16Cr-6Al-0.6Y (in wt%) bond coating (about 0.005 to 0.010 cm thick) and a ZrO₂-12Y₂O₃ (in wt%) thermal barrier coating (about 0.025 to 0.064 cm thick). This thermal barrier substantially lowered the metal temperature of the air-cooled airfoil. The coating withstood 3200 cycles (80 s at 1280 C surface temperature) and 275 cycles (1 hr at 1490 C surface temperature) without cracking or spalling. No separation of the thermal barrier from the bond coating or the bond coating from the substrate was observed. (Author)

A78-23445* Microstructural and wear properties of sputtered carbides and silicides. T. Spalvins (NASA, Lewis Research Center, Cleveland, Ohio). In: *Wear of materials - 1977*; Proceedings of the International Conference, St. Louis, Mo., April 25-28, 1977. (A78-23426 08-37) New York, American Society of Mechanical Engineers, 1977, p. 358-363. 6 refs.

Sputtered Cr₃C₂, Cr₃S₂, and MoSi₂ wear-resistant films (0.05 to 3.5 microns thick) were deposited on metal and glass surfaces. Electron transmission, electron diffraction, and scanning electron microscopy were used to determine the microstructural appearance. Strong adherence was obtained with these sputtered films. Internal stresses and defect crystallographic growth structures of various configurations within the film have progressively more undesirable effects for film thicknesses greater than 1.5 microns. Sliding contact and rolling element bearing tests were also performed with these sputtered films. (Author)

A78-24895 * Consolidation of silicon nitride without additives. P. F. Sikora (NASA, Lewis Research Center, Cleveland, Ohio) and H. C. Yeh (NASA, Lewis Research Center, Cleveland State University, Cleveland, Ohio). *American Ceramic Society, Fall Meeting, San Francisco, Calif., Oct. 31-Nov. 3, 1975, Paper*. 12 p. 6 refs.

The use of ceramics for gas turbine engine construction might make it possible to increase engine efficiency by raising operational temperatures to values beyond those which can be tolerated by metallic alloys. The most promising ceramics being investigated in this connection are Si₃N₄ and SiC. A description is presented of a study which had the objective to produce dense Si₃N₄. The two most common methods of consolidating Si₃N₄ currently being used include hot pressing and reaction sintering. The feasibility was explored of producing a sound, dense Si₃N₄ body without additives by means of conventional gas hot isostatic pressing techniques and an uncommon hydraulic hot isostatic pressing technique. It was found that Si₃N₄ can be densified without additions to a density which exceeds 95% of the theoretical value. G.R.

A78-24908 * Optical and electrical properties of ion beam textured Kapton and Teflon. M. J. Mirtich and J. S. Sovey (NASA, Lewis Research Center, Cleveland, Ohio). *American Vacuum Society, National Vacuum Symposium, 24th, Boston, Mass., Nov. 8-11, 1977, Paper*. 15 p. 10 refs.

Results are given for ion beam texturing of polyimide (Kapton) and fluorinated ethylene propylene (Teflon) by means of a 30-cm diam electron bombardment argon ion source. Ion beam-textured Kapton and Teflon surfaces are evaluated for various beam energies, current densities, and exposure times. The optical properties and sheet resistance are measured after each exposure. Provided in the paper are optical spectral data, resistivity measurements, calculated absorbance and emittance measurements, and surface structure SEM micrographs or various exposures to argon ions. It is found that Kapton becomes conducting and Teflon nonconducting when ion beam-textured. Textured Kapton exhibits large changes in the transmittance and solar absorbance, but only slight changes in reflectance. Surface texturing of Teflon may allow better adherence of subsequent sputtered metallic films for a high absorbance value. The results are valuable in spacecraft charging applications. S.D.

A78-28438 * Friction, deformation and fracture of single-crystal silicon carbide. K. Miyoshi (Kanazawa University, Kanazawa, Japan) and D. H. Buckley (NASA, Lewis Research Center, Cleveland, Ohio). *American Society of Lubrication Engineers and American Society of Mechanical Engineers, Joint Lubrication Conference, Kansas City, Mo., Oct. 3-5, 1977, ASLE Preprint 77-LC-5C-3*. 10 p. 14 refs.

An investigation was conducted to determine the nature of the deformation and fracture of silicon carbide and its effects on friction properties. Friction experiments were conducted with hemispherical and conical diamond riders sliding on the basal plane of silicon carbide. The results indicate that, when deformation is primarily elastic, the friction does not depend on crystallographic orientation and there is no detectable fracture or cracking. When, however, plastic deformation occurs, silicon carbide exhibits anisotropic friction and deformation behavior. Surface fracture crack patterns surrounding wear tracks are observed to be of three types. The crack geometries of two types are generally independent of orientation, the third crack, however, depends on the orientation. All surface cracks extend into subsurface. (Author)

A78-29328 * Ceramics in gas turbines - Powder and process characterization. S. Dutta (NASA, Lewis Research Center, Cleveland, Ohio). *American Ceramic Society, Conference on Composites and Advanced Materials, Cocoa Beach, Fla., Jan. 17-19, 1977, Paper*. 15 p. 5 refs.

The role of powder and process characterization in producing high quality silicon nitride and silicon carbide components, for gas turbine applications, is described. Some of the intrinsic properties of various forms of Si₃N₄ and SiC are listed and limitations of such

materials' availability have been pointed out. The essential features/parameters to characterize a batch of powder have been discussed including the standard techniques for such characterization. In process characterization, parameters in sintering, reaction sintering, and hot pressing processes are discussed including the factors responsible for strength limitations in ceramic bodies. It is inevitable that significant improvements in material properties can be achieved by rectifying or eliminating the strength limiting factors with consistent powder and process characterization along with process control. (Author)

A78-30301 * Composition of RF-sputtered refractory compounds determined by X-ray photoelectron spectroscopy. D. R. Wheeler and W. A. Brainard (NASA, Lewis Research Center, Cleveland, Ohio). *Journal of Vacuum Science and Technology*, vol. 15, Jan.-Feb. 1978, p. 24-30. 17 refs.

RF-sputtered coatings of CrB₂, MoSi₂, Mo₂C, TiC, and MoS₂ were examined by X-ray photoelectron spectroscopy (XPS). Data on stoichiometry, impurity content, and chemical bonding were obtained. The influences of sputtering target history, deposition time, RF power level, and substrate bias were studied. Significant deviations from stoichiometry and high oxide levels were related to target outgassing. The effect of substrate bias depended on the particular coating material studied. (Author)

A78-33206 * Mechanical and physical properties of modern boron fibers. J. A. DiCarlo (NASA, Lewis Research Center, Cleveland, Ohio). *Metallurgical Society of AIME, International Conference on Composite Materials, 2nd, Toronto, Canada, Apr. 16-20, 1978, Paper*. 19 p. 22 refs.

Measurements of the Young's modulus, flexural modulus, shear modulus and Poisson's ratio for boron fibers prepared by modern deposition techniques are reported. Physical properties of the boron fibers, including density, thermal expansion and resistance, are also surveyed. In addition, prediction of the total deformation strain in an anelastic boron fiber subjected to tensile or flexural stress is discussed. J.M.B.

A78-37684 * Ion beam sputter etching and deposition of fluoropolymers. B. A. Banks, J. S. Sovey, T. B. Miller, and K. S. Grandall (NASA, Lewis Research Center, Cleveland, Ohio). *Electrochemical Society, International Conference on Electron and Ion Beam Science and Technology, 8th, Seattle, Wash., May 21-26, 1978, Paper*. 16 p. 21 refs.

Fluoropolymer etching and deposition techniques including thermal evaporation, RF sputtering, plasma polymerization, and ion beam sputtering are reviewed. Etching and deposition mechanisms and material characteristics are discussed. Ion beam sputter etch rates for polytetrafluoroethylene (PTFE) were determined as a function of ion energy, current density and ion beam power density. Peel strengths were measured for epoxy bonds to various ion beam sputtered fluoropolymers. Coefficients of static and dynamic friction were measured for fluoropolymers deposited from ion bombardment PTFE. (Author)

A78-38706 * High temperature compressive cracking in hot-pressed silicon nitride. W. A. Sanders (NASA, Lewis Research Center, Cleveland, Ohio). *American Ceramic Society, Journal*, vol. 61, May-June 1978, p. 278, 279. 5 refs.

Results are presented for high-temperature (1370, 1430, 1540, 1590 C) slow strain-rate compression tests on cylindrical specimens of hot-pressed Si₃N₄ of the HS 130 brand under various compressive loads. The results are presented in terms of number of longitudinal cracks, percent increase in diameter, percent decrease in length, and percent loss in weight. Scanning electron micrographs are presented of cylindrical surfaces of compression specimens tested at 1430 C for

640 MN/m² and at 1590 C for 220 MN/m². As compared to results obtained by other investigators, it appears more likely that the cracks resulting from compressive loading are due to subsurface crack growth caused by circumferential tensile stresses acting across grain boundaries that contain a viscous silicate glass phase. S.D.

A78-44095 * Friction and wear behavior of single-crystal silicon carbide in sliding contact with various metals. K. Miyoshi and D. H. Buckley, (NASA, Lewis Research Center, Cleveland, Ohio). *American Society of Lubrication Engineers Annual Meeting, 33rd, Dearborn Mich. Apr. 17-20, 1978, Paper, 27 p. 11 refs.*

Sliding friction experiments were conducted with single crystal silicon carbide in contact with various metals. Results indicate the coefficient of friction is related to the relative chemical activity of the metals. The more active the metal, the higher the coefficient of friction. All the metals examined transferred to silicon carbide. The chemical activity of the metal and its shear modulus may play important roles in metal transfer, the form of the wear debris and the surface roughness of the metal wear scar. The more active the metal and the less resistance to shear, the greater the transfer to silicon carbide and the rougher the wear scar on the surface of the metal. Hexagonal shaped cracking and fracturing formed by cleavage of both prismatic and basal planes is observed on the silicon carbide surface. (Author)

A78-47595 * Pressureless sintered beta-prime-Si₃N₄ solid solution - Fabrication, microstructure, and strength. S. Dutta (NASA, Lewis Research Center, Cleveland, Ohio). *American Ceramic Society Fall Meeting, Hyannis, Mass., Sept. 25-28, 1977, Paper, 19 p. 26 refs.*

Pressureless sintering of beta-prime-Si₃N₄ solid solution was studied as a function of temperature using Si₃N₄-AlN, and Al₂O₃ as basic constituents, Y₂O₃-SiO₂ additions were used to promote liquid-phase sintering. The sintered specimens were characterized with respect to density, microstructure, strength, oxidation, and thermal shock resistance. Density greater than 98 percent of theoretical was achieved by pressureless sintering at 1750 C. The microstructure consisted essentially of fine grained beta-prime Si₃N₄ solid solution as the major phase. Modulus of rupture strengths up to 483 M Pa were achieved at moderate temperature (1000 C), but decreased to 228 M Pa at 1380 C. This substantial strength loss was attributed to a "glassy" grain boundary phase formed during cooling from the sintering temperature. The best oxidation resistance was exhibited by a composition containing 3 mol % Y₂O₃-SiO₂ additives. Water quench thermal shock resistance was equivalent to that of reaction sintered silicon nitride but lower than hot-pressed silicon nitride. (Author)

A78-47596 * Substitution of ceramics for high temperature alloys. H. B. Probst (NASA, Lewis Research Center, Cleveland, Ohio). *American Chemical Society, Federal and Materials Societies and American Society for Metals, State-of-the-Art Symposium on Silicon and Ceramic Materials, 14th, Washington, D.C., June 5-7, 1978, Paper, 17 p. 20 refs.*

Ceramics such as silicon nitride and silicon carbide are currently receiving a great deal of attention as potential materials for advanced gas turbine engines. The primary advantage offered by ceramics is their high temperature capability which can result in turbine engines of improved efficiency. Other advantages when compared to the nickel and cobalt alloys in current use are raw material availability, lower weight, erosion-corrosion resistance, and potentially lower cost. The use of ceramics in three different sizes of gas turbine engines is considered, these are the large utility turbines, advanced aircraft turbines, and small automotive turbines. The effects of material substitution are reviewed in terms of engine performance, operating economy, and secondary effects. (Author)

A78-50524 * Effect of attrition milling on the reaction sintering of silicon nitride. T. P. Herbell, T. K. Glasgow (NASA, Lewis Research Center, Cleveland, Ohio), and H. C. Yeh (Cleveland State University, Cleveland, Ohio). *American Ceramic Society Annual Meeting 80th, Detroit, Mich., May 7-12, 1978, Paper, 18 p. 8 refs. Contract No. EC 77-A-31-1040.*

Silicon powder was ground in a steel attrition mill under nitrogen. Air-exposed powder was compacted, pre-fired in helium, and reaction-sintered in nitrogen-4 v/o hydrogen. For longer grinding times, oxygen content, surface area and compactability of the powder increased, and both alpha/beta ratio and degree of nitridation during sintering increased. Iron content remained constant. (Author)

N78-10291* Owens-Illinois, Inc., Toledo, Ohio
IMPROVED CERAMIC HEAT EXCHANGE MATERIAL
Interim Report
H. L. McCollister Sep 1977 40 p
(Contracts NAS3-19733; EC-77-A-31-1011)
(NASA-CR-135262; CONS/733-1) Avail NTIS
HC A03/MF A01 CSCL 11B

Improved corrosion resistant ceramic materials that are suitable for use as regenerative heat exchangers for vehicular gas turbines is reported. Two glass-ceramic materials, C-144 and C-145, have superior durability towards sulfuric acid and sodium sulfate compared to lithium aluminosilicate (LAS) Corning heat exchange material 9455. Material C-144 is a leached LAS material whose major crystalline phase is silica keatite plus mullite, and C-145 is a LAS keatite solid solution (SS) material. In comparison to material 9455, material C-144 is two orders of magnitude better in dimensional stability to sulfuric acid at 300 C, and one order of magnitude better in stability to sodium sulfate at 1000 C. Material C-145 is initially two times better in stability to sulfuric acid, and about one order of magnitude better in stability to sodium sulfate. Both C-144 and C-145 have less than 300 ppm delta L/L thermal expansion from ambient to 1000 C, and good dimensional stability of less than approximately 100 ppm delta L/L after exposure to 1000 C for 100 hours. The glass-ceramic fabrication process produced a hexagonal honeycomb matrix having an 85% open frontal area, 50 micrometer wall thickness, and less than 5% porosity. Author

N78-13200* General Electric Co., Philadelphia, Pa.
IMPROVED CERAMIC HEAT EXCHANGER MATERIAL
Interim Report
H. W. Rauch Nov. 1977 35 p ref
(Contracts NAS3-19698; EC-77-A-31-1011)
(NASA-CR-135292; CONS/9698-1) Avail: NTIS
HC A03/MF A01 CSCL 11C

Various ceramic materials in the form of small, monolithic bars were screened as candidate materials in heat exchanger structures for automotive gas turbine engines. Small bar-shaped specimens of the honeycomb were used to measure thermal, chemical, and mechanical properties and for macro- and microstructure examinations. Cylindrical honeycomb specimens about 15.2 cm diameter and 10.2 in. thick are currently being tested in a gas turbine engine. Data obtained from testing the bar-shaped honeycomb specimens of GE-3200 and from testing bar-shaped honeycomb specimens of Corning 9455 were compared. Results indicate that GE-3200 has significantly better resistance to sulfuric acid and to sodium chloride than Corning 9455; thermal expansion of GE-3200 is higher than that of Corning 9455; mechanical properties of GE-3200 are higher in the tangential direction, but lower in the radial direction than Corning 9455, and during thermal cycling between RT-1000 C and RT-1100 C, GE-3200 tends to elongate while Corning 9455 tends to slightly contract. Overall assessment of GE-3200 properties, ease of material preparation, ready adaptability to honeycomb fabrication, and refractoriness qualify this new material as a candidate for heat exchanger application in automotive gas turbine engines. Author

N78-17216* United Technologies Research Center, East Hartford, Conn.
DEVELOPMENT OF Si3N4 AND SiC OF IMPROVED TOUGHNESS Final Report
 John J. Brennan and Charles O. Hulse 25 Oct 1977 148 p refs
 (Contract NAS3-19731)
 (NASA-CR-135306 R77-912252-23) Avail NTIS
 HC A07/MF A01 CSCL 11B

The application of energy absorbing surface layers to Si3N4 and SiC was investigated. Among the layers studied were microcracked materials such as iron titanate and a silica-zircon mixture and porous materials such as reaction sintered Si3N4. Energy absorption due to microcrack extension upon impact was found not to be an important mechanism. Instead, the fivefold improvement in Charpy and ballistic impact at elevated temperature (1250 C and 1370 C) found for Fe2TiO5 was due to plastic deformation while similar improvement found for silica-zircon mixtures at RT was due to crushing of the porous material. Due to thermal expansion mismatch, these two materials could not withstand thermal cycling when used as energy absorbing surface layers on Si3N4. Reaction sintered Si3N4 layers on dense Si3N4 were found to give up to a sevenfold increase in ballistic impact resistance due to crushing of the layer upon impact. High porosity (45%), large particle size R5 Si3N4 layers fabricated from -100, -200 mesh Si powder gave better impact improvement than less porous (30%), small particle size layers fabricated from -325 mesh Si powder. Author

N78-21289* United Technologies Research Center, East Hartford, Conn.
DEVELOPMENT OF SiAlON MATERIALS Contractor Report.
 Jun. 1975 - Sep. 1977
 G. K. Layden Dec. 1977 142 p refs
 (Contract NAS3-19712)
 (NASA-CR-135290 R77-912184-21) Avail NTIS
 HC A07/MF A01 CSCL 11B

Cold pressing and sintering techniques were used to produce ceramic bodies in which the major phase was beta prime Si3-Al-O-N4 solid solution. A variety of foreign oxides were used to promote liquid phase sintering, and this resulted in the incorporation of additional solid phases in the ceramic bodies which controlled elevated temperature properties. None of the bodies studied to date exhibited both adequate high temperature mechanical properties and oxidation resistance. Criteria are suggested to guide the formulation of bodies with improved high temperature properties. Author

N78-31235* Ultrasonics, Inc., Irvine, Calif.
SYNTHESIS OF PERFLUOROALKYLENE AROMATIC DIAMINES Final Report, 14 Apr. 1977 - 12 May, 1975
 K. L. Paciorek, T. I. Ito, J. H. Nakahara, and R. H. Kratzer Aug. 1978 52 p refs
 (Contract NAS3-20400)
 (NASA-CR-159403 SN-8320-F) Avail NTIS
 HC A04/MF A01 CSCL 07C

Analogues of methylene diamines were synthesized, in which the methylene group between the two aromatic nuclei was replaced by various perfluoroalkylene linkages. The hydrolytic, thermal, and thermal oxidative stabilities of PMR polyimides derived from these diamines were determined. Three types of PMR polyimide discs were fabricated from the dimethyl ester of 3,3',4,4' benzophenonetetracarboxylic acid, the methyl ester of 5-norbornene-2,3-dicarboxylic acid, and one of the following three diamines: methyl dianiline, 1,3-bis(4-aminophenyl)hexafluoropropane, and 2,2-bis(4-aminophenyl)hexafluoropropane. The polyimide based on 2,2-bis(4-aminophenyl)hexafluoropropane exhibited the best hydrolytic, thermal, and thermal oxidative stability as determined by moisture uptake and thermogravimetric analysis. Author

N78-31238* International Harvester Co., San Diego, Calif.
 Solar Div
ADVANCED CERAMIC MATERIAL FOR HIGH TEMPERATURE TURBINE TIP SEALS Interim Technical Progress Report, Feb. 1976 - Nov. 1977
 N. G. Solomon and J. W. Vogan Jan. 1978 60 p
 (Contract NAS3-20061)
 (NASA-CR-136317 RDR-1831-23) Avail NTIS
 HC A04/MF A01 CSCL 11B

Ceramic material systems are being considered for potential use as turbine blade tip gas path seals at temperatures up to 1370 1/4 C. Silicon carbide and silicon nitride structures were selected for study since an initial analysis of the problem gave these materials the greatest potential for development into a successful materials system. Segments of silicon nitride and silicon carbide materials over a range of densities, processed by various methods, a honeycomb structure of silicon nitride and ceramic blade tip inserts fabricated from both materials by hot pressing were tested singly and in combination. The evaluations included wear under simulated engine blade tip rub conditions, thermal stability, impact resistance, machinability, hot gas erosion and feasibility of fabrication into engine components. The silicon nitride honeycomb and low-density silicon carbide using a selected grain size distribution gave the most promising results as rub-tolerant shroud liners. Ceramic blade tip inserts made from hot-pressed silicon nitride gave excellent test results. Their behavior closely simulated metal tips. Wear was similar to that of metals but reduced by a factor of six. Author

A78-24881* Improved performance of silicon nitride-based high temperature ceramics. R. L. Ashbrook (NASA, Lewis Research Center, Cleveland, Ohio). *American Society for Metals, Materials Show and Conference, Chicago, Ill., Oct. 25-27, 1977, Paper*, 25 p. 11 refs. Contracts No. NAS3-17768; No. NAS3-19731; No. NAS3-19723; No. NAS3-19712.

Results are presented regarding experiments intended for improving the strength and toughness of hot-pressed Si3N4 (HPSN), improving the strength and oxidation resistance of reaction-sintered Si3N4 (RSSN), and improving the strength and oxidation resistance of sinterable Si-Al-O-N compositions. It is shown that the use of ZrO2 instead of MgO as a sintering aid improved the room-temperature and high-temperature flexural strength of HPSN, in addition to enhancing the rupture strength and Charpy impact resistance. The use of crushable energy absorbing layers increased the impact resistance of HPSN. Impregnation of RSSN with solutions that oxidize to Al2O3 or ZrO2 resulted in increased bending strength at room temperature. Beta-prime Si-Al-O-N sintered to full density by means of the sintering aids CeO2, Y2O3, and ZrO2 yielded the greatest strength with Y2O3 and the greatest oxidation resistance with ZrO2. S.D.

A78-40997* Traction and lubricant film temperature as related to the glass transition temperature and solidification. J. L. Layer and M. E. Peterkin (Suntech, Inc., Marcus Hook, Pa.). *(American Society of Lubrication Engineers, Annual Meeting, 32nd, Montreal, Canada, May 9-12, 1977.) ASLE Transactions*, vol. 21, July 1978, p. 250-256. 16 refs. Contracts No. F44620-74-C-0038; No. NAS3-19758.

Does a traction fluid have to be a glass or solid under operating conditions. Infrared spectra on dynamic EHD contacts of several types of fluid were used to determine the surface and oil film temperatures. Polarized spectral runs were made to study molecular alignment. Static glass transition pressures at appropriate temperatures were between 0.1 and 2.0 GPa, with the traction fluid showing the highest. In the EHD contact region, the traction fluid showed both the highest film temperatures as well as the greatest degree of molecular alignment. A plot of the difference between the film and surface temperatures vs. shear rate resulted in a master plot valid for all the fluids. From this work, the authors propose a model of 'fluid' traction where friction between parallel rough molecules produces the traction. (Author)

28 PROPELLANTS AND FUELS

Includes rocket propellants, igniters, and oxidizers; storage and handling; and aircraft fuels.

For related information see also *07 Aircraft Propulsion and Power*, *20 Spacecraft Propulsion and Power*, and *44 Energy Production and Conversion*.

N78-13233* National Aeronautics and Space Administration, Lewis Research Center, Cleveland, Ohio.
HYDROCARBON GROUP TYPE DETERMINATION IN JET FUELS BY HIGH PERFORMANCE LIQUID CHROMATOGRAPHY

Albert C. Antoine 1977 13 p refs Presented at 4th Ann Meeting of the Federation of Analytical Chem and Spectroscopy Soc. (FACSS 4), Detroit, Mich., 7-11 Nov. 1977 (NASA-TM-73829, E-9418) Avail: NTIS HC A02/MF A01 CSCL 21D

Thirty-two jet and diesel fuel samples of varying chemical composition and physical properties were prepared from oil shale and coal syncrudes. Hydrocarbon types in these samples were determined by a fluorescent indicator adsorption analysis, and the results from three laboratories are presented and compared. Two methods of rapid high performance liquid chromatography were used to analyze some of the samples, and these results are also presented and compared. Two samples of petroleum-based Jet A fuel are similarly analyzed. Author

N78-14177* National Aeronautics and Space Administration, Lewis Research Center, Cleveland, Ohio.

PERFORMANCE AND EMISSIONS OF A CATALYTIC REACTOR WITH PROPANE, DIESEL AND JET A FUELS
 David N. Anderson Sep 1977 26 p refs Presented at the Fall Meeting, Western States Section of the Combust. Inst., Stanford, Calif., 17-18 Oct. 1977 (Contract EC-77-A-31-1011) (NASA-TM-73786; CONS/1011-20; E-9349) Avail: NTIS HC A03/MF A01 CSCL 21D

Tests were made to determine the performance and emissions of a catalytic reactor operated with propane, No. 2 diesel, and Jet A fuels. A 12-cm diameter and 18-cm long catalytic reactor using a proprietary noble metal catalyst was operated at an inlet temperature of 800 K, a pressure of 300,000 Pa and reference velocities of 10 to 15 m/s. No significant differences between the performance of the three fuels were observed when 98.5 percent purity propane was used. The combustion efficiency for 99.8-percent purity propane tested later was significantly lower, however. The diesel fuel contained 135 ppm of bound nitrogen and consequently produced the highest NO_x emissions of the three fuels. As much as 85 percent of the bound nitrogen was converted to NO_x. Steady-state emissions goals based on half the most stringent proposed automotive standards were met when the reactor was operated at an adiabatic combustion temperature higher than 1350 K with all fuels except the 99.8-percent purity propane. With that fuel, a minimum temperature of 1480 K was required. Author

N78-17229* National Aeronautics and Space Administration, Lewis Research Center, Cleveland, Ohio.

ALTERNATIVE AIRCRAFT FUELS
 J. P. Longwell (MIT, Cambridge) and J. Grobman Jun 1977 22 p refs Proposed for presentation at 23d Ann Intern. Gas Turbine Conf., London, Engl., 9-13 Apr. 1978; sponsored by Am Soc of Machan Engineers (NASA-TM-73836) Avail: NTIS HC A02/MF A01 CSCL 21D

The efficient utilization of fossil fuels by future jet aircraft may necessitate the broadening of current aviation turbine fuel specifications. The most significant changes in specifications would be an increased aromatics content and a higher final boiling point in order to minimize refinery energy consumption and costs. These changes would increase the freezing point and might lower

the thermal stability of the fuel, and could cause increased pollutant emissions, increased combustor liner temperatures, and poorer ignition characteristics. The effects that broadened specification fuels may have on present-day jet aircraft and engine components and the technology required to use fuels with broadened specifications are discussed. Author

N78-19325* National Aeronautics and Space Administration, Lewis Research Center, Cleveland, Ohio.

JET AIRCRAFT HYDROCARBON FUELS TECHNOLOGY
 John P. Longwell, ed. 1978 64 p Workshop held at Cleveland, Ohio, 7-9 Jun. 1977 (NASA-CP-20(33; E-9457) Avail: NTIS HC A04/MF A01 CSCL 21D

A broad specification, reference fuel was proposed for research and development. This fuel has a lower, closely specified hydrogen content and higher final boiling point and freezing point than ASTM Jet A. The workshop recommended various priority items for fuel research and development. Key items include prediction of tradeoffs among fuel refining, distribution, and aircraft operating costs; combustor liner temperature and emissions studies; and practical simulator investigations of the effect of high freezing point and low thermal stability fuels on aircraft fuel systems. Author

N78-20361* National Aeronautics and Space Administration, Lewis Research Center, Cleveland, Ohio.

COMPUTER PROGRAM FOR OBTAINING THERMODYNAMIC AND TRANSPORT PROPERTIES OF AIR AND PRODUCTS OF COMBUSTION OF ASTM-A-1 FUEL AND AIR

Steven A. Hippensteele and Raymond S. Colclay Mar. 1978 56 p (NASA-TP-1160; E-9371) Avail: NTIS HC A04/MF A01 CSCL 21B

A computer program for determining desired thermodynamic and transport property values by means of a three-dimensional (pressure, fuel-air ratio, and either enthalpy or temperature) interpolation routine was developed. The program calculates temperature (or enthalpy), molecular weight, viscosity, specific heat at constant pressure, thermal conductivity, isentropic exponent (equal to the specific heat ratio at conditions where gases do not react), Prandtl number, and entropy for air and a combustion gas mixture of ASTM-A-1 fuel and air over fuel-air ratios from zero to stoichiometric, pressures from 1 to 40 atm, and temperatures from 250 to 2800 K. Author

N78-24358* National Aeronautics and Space Administration, Lewis Research Center, Cleveland, Ohio.

ION BEAM SPUTTER ETCHING AND DEPOSITION OF FLUOROPOLYMERS

Bruce A. Banks, James S. Sovey, Thomas B. Miller, and Karen S. Crandall 1978 17 p refs Presented at the 8th Intern. Conf on Electron and Ion Beam Sci and Tech., Seattle, 21-26 May 1978, sponsored by the Electrochemical Soc., Inc (NASA-TM-78888) Avail: NTIS HC A02/MF A01 CSCL 07D

Fluoropolymer etching and deposition techniques including thermal evaporation, RF sputtering, plasma polymerization, and ion beam sputtering are reviewed. Etching and deposition mechanism and material characteristics are discussed. Ion beam sputter etch rates for polytetrafluoroethylene (PTFE) were determined as a function of ion energy, current density and ion beam power density. Peel strengths were measured for epoxy bonds to various ion beam sputtered fluoropolymers. Coefficients of static and dynamic friction were measured for fluoropolymers deposited from ion bombarded PTFE. Author

N78-24366* National Aeronautics and Space Administration
Lewis Research Center, Cleveland, Ohio.
ATOMIC HYDROGEN STORAGE METHOD AND APPARATUS Patent

John A. Wooliam, inventor (to NASA) Issued 7 Mar 1978
4 p Filed 13 Apr 1976 Supersedes N78-22399 (14 - 13,
p 1644)

(NASA Case-LEW-12081-1; US-Patent-4,077,788;
US-Patent Appl-SN-676432; US-Patent-Class-62-48;
US-Patent-Class-34-15; US-Patent-Class-62-100;
US-Patent-Class-250-492R; US-Patent-Class-423-648R) Avail:
US Patent Office CSCL 21D

Atomic hydrogen, for use as a fuel or as an explosive, is stored in the presence of a strong magnetic field in exfoliated layered compounds such as molybdenum disulfide or an elemental layer material such as graphite. The compound is maintained at liquid helium temperatures and the atomic hydrogen is collected on the surfaces of the layered compound which are exposed during delamination (exfoliation). The strong magnetic field and the low temperature combine to prevent the atoms of hydrogen from recombining to form molecules.

Official Gazette of the U.S. Patent Office

N78-24369* National Aeronautics and Space Administration
Lewis Research Center, Cleveland, Ohio
IMPACT OF FUTURE FUEL PROPERTIES ON AIRCRAFT ENGINES AND FUEL SYSTEMS

R. A. Rudey and J. S. Grobman 1978 33 p refs To be presented at Lecture Ser 96, Paris, Munich, and London, 12-20 Oct 1978, sponsored by AGARD (NASA-TM 78866, E-9597) Avail: NTIS HC A03/MF A01 CSCL 21D

This paper describes and discusses the propulsion-system problems that will most likely be encountered if the specifications of hydrocarbon-based jet fuels must undergo significant changes in the future and, correspondingly, the advances in technology that will be required to minimize the adverse impact of these problems. Several investigations conducted are summarized. Illustrations are used to describe the relative effects of selected fuel properties on the behavior of propulsion-system components and fuel systems. The selected fuel properties are those that are most likely to be relaxed in future fuel specifications. Illustrations are also used to describe technological advances that may be needed in the future. Finally, the technological areas needing the most attention are described, and programs that are under way to address these needs are briefly discussed.

Author

N78-24370* National Aeronautics and Space Administration
Lewis Research Center, Cleveland, Ohio
CHARACTERISTICS AND COMBUSTION OF FUTURE HYDROCARBON FUELS

R. A. Rudey and J. S. Grobman 1978 26 p Proposed for presentation at Lecture Series 96, Paris, Munich, London, 12-20 Oct 1978, sponsored by AGARD (NASA-TM 78865, E-9596) Avail: NTIS HC A03/MF A01 CSCL 21D

As the world supply of petroleum crude oil is being depleted, the supply of high-quality crude oil is also dwindling. This dwindling supply is beginning to manifest itself in the form of crude oils containing higher percentages of aromatic compounds, sulphur, nitrogen, and trace constituents. The result of this trend is described and the change in important crude oil characteristics, as related to aircraft fuels, is discussed. As available petroleum is further depleted, the use of synthetic crude oils (those derived from coal and oil shale) may be required. The principal properties of these syncrudes and the fuels that can be derived from them are described. In addition to the changes in the supply of crude oil, increasing competition for middle-distillate fuels may require that specifications be broadened in future fuels. The impact that the resultant potential changes in fuel properties may have on combustion and thermal stability characteristics is illustrated and discussed in terms of ignition, soot formation, carbon deposition, flame radiation, and emissions.

Author

N78-27088* National Aeronautics and Space Administration
Lewis Research Center, Cleveland, Ohio
IMPACT OF BROAD-SPECIFICATION FUELS ON FUTURE JET AIRCRAFT

Jack Grobman In NASA Langley Res Center CTOL Transport Technol 1978 Jun 1978 p 217-233 refs (For primary document see N78-27046 18-01)

Avail: NTIS HC A22/MF A01 CSCL 21D

The effects that broad specification fuels have on airframe and engine components were discussed along with the improvements in component technology required to use broad specification fuels without sacrificing performance, reliability, maintainability, or safety.

J M S

A78-17482* = Simulation of the heat transfer characteristics of LOX. R. C. Hendricks (NASA, Lewis Research Center, Cleveland, Ohio). *American Institute of Chemical Engineers and American Society of Mechanical Engineers, Heat Transfer Conference, Salt Lake City, Utah, Aug. 15-17, 1977, ASME Paper 77-HT-9*. 8 p. 10 refs. Members, \$1.50, nonmembers, \$3.00.

In connection with proposals for a second generation shuttle vehicle it has been suggested that the engine regenerative coolant be the oxidizer rather than a fuel. The feasibility of such an approach depends on the suitability of oxygen for the cooling functions. The information currently available concerning the heat transfer characteristics of liquid oxygen (LOX) in the near critical region at elevated pressures is not sufficient for an evaluation. It is, therefore, proposed to make use of data from similar fluids for a simulation of the heat transfer characteristics of LOX. Graphs are presented which demonstrate that experimental heat transfer results for fluid nitrogen can be used qualitatively to simulate heat transfer to liquid oxygen. Quantitative agreement appears satisfactory provided the proper level of adjusting constant can be determined.

G. R.

A78-24906* = Hydrocarbon group type determination in jet fuels by high performance liquid chromatography. A. C. Antoine (NASA, Lewis Research Center, Cleveland, Ohio). *Federation of Analytical Chemistry and Spectroscopy Societies, Annual Meeting, 4th, Detroit, Mich., Nov. 7-11, 1977, Paper*. 12 p.

Results are given for the analysis of some jet and diesel fuel samples which were prepared from oil shale and coal syncrudes. Thirty-two samples of varying chemical composition and physical properties were obtained. Hydrocarbon types in these samples were determined by fluorescent indicator adsorption (FIA) analysis, and the results from three laboratories are presented and compared. Recently, rapid high performance liquid chromatography (HPLC) methods have been proposed for hydrocarbon group type analysis, with some suggestion for their use as a replacement of the FIA technique. Two of these methods were used to analyze some of the samples, and these results are also presented and compared. Two samples of petroleum-based Jet A fuel are similarly analyzed.

(Author)

N78-16194* United Technologies Research Center East
Hartford Conn

**DEVELOPMENT OF AN EXPERIMENT FOR DETERMINING
THE AUTOIGNITION CHARACTERISTICS OF AIRCRAFT-
TYPE FUELS**

Louis J. Spadecchini Sep 1977 30 p refs

(Contract NAS3-20066)

(NASA-CR-135329 R78-912881-2)

Avail NTIS

HC A03/MF A01 CSCL 21D

An experimental test apparatus was developed to determine the autoignition characteristics of aircraft-type fuels in premixing prevaporizing passages at elevated temperatures and pressures. The experiment was designed to permit independent variation and evaluation of the experimental variables of pressure, temperature, flow rate, and fuel-air ratio. A comprehensive review of the autoignition literature is presented. Performance verification tests consisting of measurements of the ignition delay times for several lean fuel-air mixture ratios were conducted using Jet-A fuel at inlet air temperatures in the range 600 K to 900 K and pressures in the range 9 atm to 30 atm.

Author

N78-19326* Gordian Associates, Inc., New York
**COMPUTER MODEL FOR REFINERY OPERATIONS WITH
EMPHASIS ON JET FUEL PRODUCTION. VOLUME 2:
DATA AND TECHNICAL BASES** Final Report

Daniel N. Dunbar and Barry G. Tunnah 21 Feb. 1978 55 p
refs

(Contract NAS3-20620)

(NASA-CR-135334 Rept-1099-1)

Avail: NTIS

HC A04/MF A01 CSCL 21D

The FORTRAN computing program predicts the flow streams and material, energy, and economic balances of a typical petroleum refinery, with particular emphasis on production of aviation turbine fuel of varying end point and hydrogen content specifications. The program has provision for shale oil and coal oil in addition to petroleum crudes. A case study feature permits dependent cases to be run for parametric or optimization studies by input of only the variables which are changed from the base case. The report has sufficient detail for the information of most readers.

Author

N78-20360* Gordian Associates, Inc., New York
**COMPUTER MODEL FOR REFINERY OPERATIONS WITH
EMPHASIS ON JET FUEL PRODUCTION. VOLUME 1:
PROGRAM DESCRIPTION** Final Report

Daniel N. Dunbar and Barry G. Tunnah 14 Feb. 1978 127 p
refs

(Contract NAS3-20620)

(NASA-CR-135333 Rept-1099-1-Vol-1)

Avail: NTIS

HC A07/MF A01 CSCL 21D

A FORTRAN computer program is described for predicting the flow streams and material, energy, and economic balances of a typical petroleum refinery, with particular emphasis on production of aviation turbine fuel of varying end point and hydrogen content specifications. The program has provision for shale oil and coal oil in addition to petroleum crudes. A case study feature permits dependent cases to be run for parametric or optimization studies by input of only the variables which are changed from the base case.

Author

N78-26236* Gordian Associates, Inc., New York
**COMPUTER MODEL FOR REFINERY OPERATIONS WITH
EMPHASIS ON JET FUEL PRODUCTION. VOLUME 3:
DETAILED SYSTEMS AND PROGRAMMING DOCUMENTA-
TION** Final Report

Daniel N. Dunbar and Barry G. Tunnah 27 Jun 1978 53 p

(Contract NAS3-20620)

(NASA-CR-135335 Rept-1099-1-Vol-3)

Avail NTIS

HC A04/MF A01 CSCL 21D

The FORTRAN computing program predicts flow streams and material, energy, and economic balances of a typical petroleum refinery, with particular emphasis on production of aviation turbine fuels of varying end point and hydrogen content specifications. The program has a provision for shale oil and coal oil in addition to petroleum crudes. A case study feature permits dependent cases to be run for parametric or optimization studies by input of only the variables which are changed from the base case.

Author

A78-43415* Jet fuels from synthetic crudes. A. C. Antoine (NASA, Lewis Research Center, Cleveland, Ohio) and J. P. Gallagher (Atlantic Richfield Co., Harvey, Ill.). In: Coal processing technology, Volume 3. (A78-43403-19-44) New York: American Institute of Chemical Engineers, 1977, p. 107-114. Contract No. NAS3-19747.

An investigation was conducted to determine the technical problems in the conversion of a significant portion of a barrel of either a shale oil or a coal synthetic crude oil into a suitable aviation turbine fuel. Three syncrudes were used, one from shale and two from coal, chosen as representative of typical crudes from future commercial production. The material was used to produce jet fuels of varying specifications by distillation, hydrotreating, and hydrocracking. Attention is given to process requirements, hydrotreating process conditions, the methods used to analyze the final products, the conditions for shale oil processing, and the coal liquid processing conditions. The results of the investigation show that jet fuels of defined specifications can be made from oil shale and coal syncrudes using readily available commercial processes.

G.R.

31 ENGINEERING (GENERAL)

Includes vacuum technology, control engineering; display engineering; and cryogenics.

N78-17227* National Aeronautics and Space Administration
Lewis Research Center, Cleveland, Ohio
CLOSED LOOP SPRAY COOLING APPARATUS Patent
Donald L. Alger, William B. Schwab, and Edward R. Furman,
inventors (to NASA) Issued 17 Jan 1978 4 p Filed 31 Mar.
1976 Supersedes n78-20486 (14-1); p 1394
(NASA Case-LEW-11981-1; US-Patent-4,068,495.
US Patent Appl-SN 672220; US Patent-Class-112-376.
US Patent Class 62-514R, US-Patent-Class-313-22) Avail: US
Patent Office CSCL 13G

A closed loop apparatus for spraying coolant against the back of a radiation target is described. The coolant was circulated through a closed loop with a bubble of inert gas being maintained around the spray. Mesh material was disposed between the bubble and the surface of the liquid coolant which was below the bubble at a predetermined level. In a second embodiment, no inert gas was used, the bubble consisting of a vapor produced when the coolant was sprayed against the target.

Official Gazette of the U.S. Patent Office

N78-22267* National Aeronautics and Space Administration,
Lewis Research Center, Cleveland, Ohio.
APPLIED ROUTH APPROXIMATION
Walter C. Merrill Apr 1978 40 p refs
(NASA-TP-1231; E-9114) Avail: NTIS HC A03/MF A01 CSCL
12B

The Routh approximation technique for reducing the complexity of system models was applied in the frequency domain to a 18th order, state variable model of the F100 engine and to a 43d order, transfer function model of a launch vehicle boost pump pressure regulator. The results motivate extending the frequency domain formulation of the Routh method to the time domain in order to handle the state variable formulation directly. The time domain formulation was derived and a characterization that specifies all possible Routh similarity transformations was given. The characterization was computed by solving two eigenvalue-eigenvector problems. The application of the time domain Routh technique to the state variable engine model is described, and some results are given. Additional computational problems are discussed, including an optimization procedure that can improve the approximation accuracy by taking advantage of the transformation characterization.

Author

N78-30303* National Aeronautics and Space Administration,
Lewis Research Center, Cleveland, Ohio.
GAS TURBINE PROJECT STATUS c37
W. E. Goette In DOE Highway Vehicle Systems Mar 1978
p 125-129 (For primary document see N78-30293 21-31)
Avail: NTIS HC A20/MF A01 CSCL 21A

The state-of-the-art of automobile gas turbine technology, particularly with respect to fuel economy and emissions, was defined. An advanced gas turbine system is proposed which incorporates significant advances in technology and has a fifty to sixty percent gain in fuel economy over the spark ignition engine, while meeting the same goals of the improved gas turbine engine.

J.A.M.

N78-30333* National Aeronautics and Space Administration
Lewis Research Center, Cleveland, Ohio

**CATALYTIC COMBUSTION FOR THE AUTOMOTIVE GAS
TURBINE ENGINE** c37

D. N. Anderson /in NATO Proc. of the 4th Intern. Symp. on
Automotive Propulsion Systems, Vol. 1 Feb. 1978 p 47-54
(For primary document see N78-30332 21-31)

Avail NTIS HC A23/MF A01 CSCL 21A

Fuel-air premixing-preevaporizing systems and commercial catalysts were studied as part of a demonstration of a low emissions combustor for an automotive gas turbine engine. A fuel preparation system which would supply a fuel-air mixture which was uniform to within + or - 10 percent of the mean fuel-air ratio, with 90 percent fuel vaporization and with no autoignition is described. The catalytic reactor was required to produce emissions which were low enough to meet the most stringent proposed U.S. automotive standards. The overall pressure drop for both systems was to be less than 3 percent, with 1 percent allowed in the fuel-air preparation system and the remainder in the catalytic reactor. B.B.

N78-18251* Lockheed Missiles and Space Co., Palo Alto,
Calif. Research Lab.

**EVACUATED LOAD-BEARING HIGH PERFORMANCE
INSULATION STUDY Final Report, May 1974 - Aug. 1977**

R. T. Parmley and G. R. Cunningham Dec. 1977 264 p refs
(Contract NAS3-17817)

(NASA-CR-135342; LMSC-D564116) Avail: NTIS
HC A12/MF A01 CSCL 22B

A light weight, vacuum jacketed, load bearing cryogenic insulation system was developed and tested on a 1.17-m (46-in.) spherical test tank. The vacuum jacket consists of 0.08 mm (0.03 in.) thick 3.11 stainless steel formed into a wedge design that allows elastic jacket movements as the tank shrinks (cools) or expands (warms up or is pressurized). Hollow glass spheres, approximately 80 micrometers in diameter with a bulk density of 0.069 g/cc (4.3 lb cubic foot), provide the insulating qualities and one atmosphere load bearing capability required. The design, fabrication, and test effort developed the manufacturing methods and engineering data needed to scale the system to other tank sizes, shapes, and applications. The program demonstrated that thin wall jackets can be formed and welded to maintain the required vacuum level of 0.13 Pa yet flex elastically for multiple reuses. No significant shifting or breakage of the microspheres occurred after 13 simulated Space Tug flight cycles on the test tank and a hundred 1 atmosphere load cycles in a flat plate calorimeter. The test data were then scaled to the Space Tug L02 and LH2 tanks, and weight, thermal performance, payload performance, and costs were compared with a helium purged multilayer insulation system. Author

N78-29276* Horizons Research, Inc., Cleveland, Ohio
**HIGH RESOLUTION MASKS FOR ION MILLING PORES
THROUGH SUBSTRATES OF BIOLOGICAL INTEREST**

Sandra S. Donovan Jun. 1978 41 p refs

(Contract NAS3-21054)

(NASA-CR-135435, HRI-391) Avail: NTIS HC A03/MF A01
CSCL 13H

The feasibility was investigated of electrochemically oxidizing vapor deposited aluminum coatings to produce porous aluminum oxide coatings with submicron pore diameters and with straight channels normal to the substrate surface. Porous aluminum oxide coatings were produced from vapor deposited aluminum coatings on thin stainless steel (304), copper, Teflon (FEP) and Kapton substrates and also on pure aluminum substrates. Scanning electron microscope examination indicated that porous oxide coatings can be produced with straight channels, appropriate pore diameters and none or minimal intervening residual aluminum. The oxide coatings on the copper and Kapton substrates had the straightest channels and in general were superior to those fabricated on the other substrate materials. For oxide coatings fabricated at 600 V and 300 V, pore diameters were 0.4-0.6 and 0.3 micron with center-to-center spacing of 0.7-0.8 and 0.4 micron, respectively. Estimated direct labor and materials costs to prepare an oxide mask is anticipated to be about \$4-\$6 per square foot. F.O.S.

32 COMMUNICATIONS

Includes land and global communications; communications theory; and optical communications.

For related information see also *04 Aircraft Communications and Navigation* and *17 Spacecraft Communications, Command and Tracking*.

N78-10346* National Aeronautics and Space Administration, Lewis Research Center, Cleveland, Ohio.

DISASTER WARNING SYSTEM STUDY SUMMARY

B. F. LeRoy, J. E. Maloy, R. C. Braley, C. E. Provencher, H. A. Schumaker, and M. E. Valgora Oct. 1977 21 p
(NASA-TM-73797; E-9366) Avail: NTIS HC A02/MF A01 CSCL 17B

A conceptual satellite system to replace or complement NOAA's data collection, internal communications, and public information dissemination systems for the mid-1980's was defined. Program cost and cost sensitivity to variations in communications functions are analyzed. Author

N78-13282* National Aeronautics and Space Administration, Lewis Research Center, Cleveland, Ohio.

PERFORMANCE OF THE 12GHz, 200 WATT TRANSMITTER EXPERIMENT PACKAGE FOR THE HERMES SATELLITE

Robert S. Alexovich 1977 34 p refs Presented at Symp. on Hermes (Communications Technol. Satellite) its Performance and Applications, Ottawa, 29 Nov. - 1 Dec. 1977; sponsored by Royal Soc. of Canada, Canadian Dept. of Communications and NASA
(NASA-TM-73804; E-9385) Avail: NTIS HC A04/MF A01 CSCL 17B

Performance characteristics from on-orbit tests of the Transmitter Experiment Package (TEP) for the Hermes Satellite are presented. The TEP consists of a Power Processing System (PPS), an Output Stage Tube (OST) and a Variable Conductance Heat Pipe System (VCHPS), all of which are described. The OST is a coupled-cavity Traveling Wave Tube (TWT) with a Multistage Depressed Collector (MDC) and a stepped velocity-tapered slow wave structure for efficiency enhancement. It has an RF output power of 233 watts and overall efficiency of 50.75 percent at a center band frequency of 12.080 GHz. The PPS provides the required operating voltages, regulation, control and protection for the OST. The VCHPS consists of a fin radiator and three dual-artery stainless steel heat pipes using methanol and a mixture of inert gases. Test results presented include efficiencies, RF output power and body current. A discussion of thermal anomalies which occurred is presented. Author

N78-13263* National Aeronautics and Space Administration, Lewis Research Center, Cleveland, Ohio.

A DIGITALLY IMPLEMENTED COMMUNICATIONS EXPERIMENT UTILIZING THE HERMES (CTS) SATELLITE

H. D. Jackson and J. Fiala 1977 20 p refs Presented at Symp. on Hermes (Comm Technol. Satellite) its Performance and Appl., Ottawa, Ontario, 29 Nov. - 1 Dec. 1977; Sponsored by The Royal Soc. of Canada, Canadian Dept. of Commun., and NASA

(NASA-TM-73827) Avail: NTIS HC A02/MF A01 CSCL 17B
The Hermes (CTS) experiment program made possible a significant effort directed toward new developments which will reduce the costs associated with the distribution of satellite services. Advanced satellite transponder technology and small inexpensive earth terminals were demonstrated as part of the Hermes program. Another system element that holds promise for reduced transmission cost is associated with the communication link implementation. An experiment is described which uses CTS to demonstrate digital link implementation and its advantages over conventional analog systems. A Digitally Implemented Communications experiment which demonstrates the flexibility and efficiency of digital transmission of television video and audio,

telephone voice and high-bit-rate data is also described. Presentation of the experiment concept which concentrates on the evaluation of full-duplex digital television in the teleconferencing environment is followed by a description of unique equipment that was developed. Author

N78-18326* National Aeronautics and Space Administration, Lewis Research Center, Cleveland, Ohio.

UTILIZATION OF NASA LEWIS MOBILE TERMINALS FOR THE HERMES SATELLITE

E. A. Edelman, J. L. Fiala, and L. Rizzolla 1977 30 p refs Presented at Symp. of Hermes, Commun. Technol. Satellite: Its Performance and Appl., Ottawa, 29 Nov. - 1 Dec. 1977; sponsored by NASA, Roy. Soc. Can. and Can. Dept. of Commun.
(NASA-TM-73859; E-9448) Avail: NTIS HC A03/MF A01 CSCL 17B

The high power of the Hermes satellite enables two-way television and voice communication with small ground terminals. The Portable Earth Terminal (PET) and the Transportable Earth Terminal (TET) were developed and built by NASA-Lewis to provide communications capability to short-term users. The NASA-Lewis mobile terminals are described in terms of vehicles and onboard equipment, as well as operation aspects, including use in the field. The section on demonstrations divides the uses into categories of medicine, education, technology and government. Applications of special interest within each category are briefly described. Author

N78-26373* National Aeronautics and Space Administration, Lewis Research Center, Cleveland, Ohio.

MEDIUM POWER VOLTAGE MULTIPLIERS WITH A LARGE NUMBER OF STAGES

W. T. Harrigill and I. T. Myers Jun. 1978 9 p refs Presented at Power Electron. Specialists Conf., Syracuse, N. Y., 13-15 Jun. 1978; sponsored by IEEE
(NASA-TM-78900; E-9636) Avail: NTIS HC A02/MF A01 CSCL 10C

Voltage multiplier techniques are extended at medium power levels to larger multiplication ratios. A series of dc-dc converters were built, with from 20 to 45 stages and with power levels up to 100 watts. Maximum output voltages were about 10,000 volts. Author

N78-31323* National Aeronautics and Space Administration, Lewis Research Center, Cleveland, Ohio.

THE 20/30 GHz SATELLITE SYSTEMS TECHNOLOGY NEEDS ASSESSMENT

Grady Stevens and David Wright 1978 13 p refs Proposed for presentation at the Intern. Telemetry Conf., Los Angeles, 14-16 Nov. 1978; sponsored by Instrumen; Soc. of Am.
(NASA-TM-78975; E-9750) Avail: NTIS HC A02/MF A01 CSCL 17B

Rain attenuation in the 20/30 GHz bands, and the resultant impact on system user costs were estimated for a variety of satellite communication system concepts. Results of previous and current NASA Lewis contractual and in-house studies on system design are reported as well as market studies conducted to evaluate the concepts and test their relevancy against forecasted market needs. The 20/30 GHz bands appear attractive economically and, with certain technology, appear to offer a virtually unlimited spectrum resource. This attractiveness is especially relevant to high density trunking where there is sufficient traffic to justify dual-station site diversity. A.R.H.

N78-33283* National Aeronautics and Space Administration, Lewis Research Center, Cleveland, Ohio.

AN AIRBORNE METEOROLOGICAL DATA COLLECTION SYSTEM USING SATELLITE RELAY (ASDAR)

James W. Bagwell and Bruce G. Linoow 1978 17 p ref Proposed for presentation at the Intern. Telemetry Conf., Los Angeles, 14-16 Nov. 1978; sponsored by the Instr. Soc. of America
(NASA-TM-78992; E-9768) Avail: NTIS HC A02/MF A01 CSCL 17B

The National Aeronautics and Space Administration (NASA) has developed an airborne data acquisition and communication system for the National Oceanic and Atmospheric Administration (NOAA). This system known as ASDAR, the Aircraft to Satellite Data Relay, consists of a microprocessor based controller, time clock, transmitter and antenna. Together they acquire meteorological and position information from existing aircraft systems on B-747 aircraft, convert and format these, and transmit them to the ground via the GOES meteorological satellite series. The development and application of the ASDAR system is described with emphasis on unique features. Performance to date is exceptional, providing horizon-to-horizon coverage of aircraft flights. The data collected is of high quality and is considered a valuable addition to the data base from which NOAA generates its weather forecasts. Author

A78-24384 * # A digitally implemented communications experiment utilizing the Hermes /CTS/ satellite. H. D. Jackson and J. Fiala (NASA, Lewis Research Center, Cleveland, Ohio). *Royal Society of Canada, Symposium on Hermes (Communications Technology Satellite): Its Performance and Applications, Ottawa, Canada, Nov. 29-Dec. 1, 1977, Paper. 19 p. 7 refs.*

Attention is given to an investigation being conducted by NASA-Lewis and Comsat Laboratories which uses the Hermes (CTS) satellite to explain digital link implementation and the advantages it provides over conventional analog systems. The experiment concentrates on developing several video, audio, and data digital communications techniques. S.C.S.

A78-24885 * # Utilization of NASA Lewis mobile terminals for the Hermes satellite. E. A. Edelman, J. L. Fiala, and L. Rizzolla (NASA, Lewis Research Center, Cleveland, Ohio). *Royal Society of Canada, Symposium on Hermes (Communications Technology Satellite): Its Performance and Applications, Ottawa, Canada, Nov. 29-Dec. 1, 1977, Paper. 29 p.*

The paper describes the portable earth terminal (PET) and the transportable earth terminal (TET) which enable two-way television and voice communication. Both terminals were developed by NASA and utilize the high power of the Hermes satellite. PET is a bus-type vehicle which has receiving equipment for full duplex color television and which can transmit programs originating in either the on-board PET studio or in nearby buildings. PET has a collapsible 2.4-m diameter parabolic antenna interfacing with a 500-watt 14-GHz wideband TV transmitter and a 12-GHz wideband TV receiver system. TET uses two parabolic reflector antennas, 3 m and 1.2 m in diameter, mounted on a flat trailer towed by a truck. TET can receive and relay color TV signals, and its narrowband transmitter can serve as a return audio link permitting a question-and-answer format. Also described are uplink and downlink performance characteristics, operation procedures, and field demonstrations which enabled personnel at several hospitals to participate in a distant medical conference. M.L.

A78-24886 * # CTS /Hermes/ - United States experiments and operations summary. P. L. Donoughe and H. R. Hunczak (NASA, Lewis Research Center, Cleveland, Ohio). *Royal Society of Canada, Symposium on Hermes (Communications Technology Satellite): Its Performance and Applications, Ottawa, Canada, Nov. 29-Dec. 1, 1977, Paper. 26 p. 29 refs.*

The U.S. experiments conducted with the Communications Technology Satellite, a joint Canadian-U.S. venture launched in 1976, are discussed. The 14/12 GHz frequencies employed by the 200-W transmitter on board the satellite provide two-way television and voice communications. Applications of the satellite in the categories of health care, community services and education are considered; experiments have also made use of the special properties of the super-high frequency band (e.g. link characterization and digital communications). Time-sharing of the 14/12 GHz communication between the U.S. and Canada has functioned well. J.M.B.

A78-15616 * A forecast of broadcast satellite communications. J. P. Martino and R. C. Lenz, Jr. (Dayton, University Research Institute, Dayton, Ohio). In: *NAECON '77: Proceedings of the National Aerospace and Electronics Conference, Dayton, Ohio, May 17-19, 1977. (A78-15651 04-33)* New York, Institute of Electrical and Electronics Engineers, Inc., 1977, p. 536-540, Contract No. NAS3-20365.

This paper presents forecasts of likely changes in broadcast satellite technology, the technology of ground terminals, and the technology of terrestrial communications competitive with satellites. The impacts of these changes in technology are then assessed, using a cross-impact model of U.S. domestic telecommunications, to determine the consequences of various possible changes in communications satellite technology. These consequences are discussed in terms of various possible services, for households, businesses, and specialized customers, which might become economically viable as a result of improvements in satellite technology. (Author)

A78-31970 * # Low cost Ku-band earth terminals for voice/data/facsimile. R. L. Kelley (Fairchild Space and Electronics Co., Germantown, Md.). *Intelcom 77 Symposium, Atlanta, Ga., Oct. 9-15, 1977, Paper. 7 p. Contract No. NAS3-23064.*

A Ku-band satellite earth terminal capable of providing two way voice/facsimile teleconferencing, 128 Kbps data, telephone, and high-speed imagery services is proposed. Optimized terminal cost and configuration are presented as a function of FDMA and TDMA approaches to multiple access. The entire terminal from the antenna to microphones, speakers and facsimile equipment is considered. Component cost versus performance has been projected as a function of size of the procurement and predicted hardware innovations and production techniques through 1985. The lowest cost combinations of components has been determined in a computer optimization algorithm. The system requirements including terminal EIRP and G/T, satellite size, power per spacecraft transponder, satellite antenna characteristics, and link propagation outage were selected using a computerized system cost/performance optimization algorithm. System cost and terminal cost and performance requirements are presented as a function of the size of a nationwide U.S. network. Service costs are compared with typical conference travel costs to show the viability of the proposed terminal. (Author)

A78-31971 * # Communication satellite services for special purpose users. D. L. Wright (NASA, Lewis Research Center, System Analysis Section, Cleveland, Ohio) and J. D. Kiesling (Fairchild Space and Electronics Co., Germantown, Md.). *Intelcom 77 Symposium, Atlanta, Ga., Oct. 9-15, 1977, Paper. 9 p. Contract No. NAS3-23064.*

The present study identifies potential satellite services, examines the technology necessary for efficient implementation of these services, and determines minimum service cost versus user network size. The generic satellite services evaluated comprise TV and radio distribution (for retransmission), video teleconferencing (interactive), audio/facsimile teleconferencing (interactive), multiplexed data/voice (point-to-point), and satellite-supported land mobile. Satellite costs are based on extrapolations from ongoing commercial satellite programs. Production methods, new technology, and effect of production quantities on present and future production costs are examined to provide information on earth station equipment cost versus the variable 'buy'. Six different launch vehicles from a Delta 2914 to a dedicated Shuttle and three frequency bands and both broadcast (no eclipse capability) and fixed service satellites are considered to assess the effect of satellite size on cost and performance. It is assumed that the user pays only for his prorata share of the space segment costs. S.D.

C-2

A78-43173 * # Low cost satellite land mobile service for nationwide applications. J. A. Weiss (Fairchild Space and Electronics Co., Germantown, Md.). *Institute of Electrical and Electronics Engineers, Vehicular Technology Conference, Denver, Colo., Mar. 22-24, 1978, Paper*. 10 p. 5 refs. Contract No. NAS3-23064.

A satellite land mobile system using mobile radios in the UHF band, and Ku-band Communications Routing Terminals (earth stations) for a nationwide connection from any mobile location to any fixed or mobile location, and from any fixed location to any mobile location is proposed. The proposed nationwide satellite land mobile service provides: telephone network quality (1 out of 100 blockage) service, complete privacy for all the users, operation similar to the telephone network, alternatives for data services up to 32 Kbps data rates, and a cost effective and practical mobile radio compatible with system sizes ranging from 10,000 to 1,000,000 users. Seven satellite alternatives (ranging from 30 ft diameter dual beam antenna to 210 ft diameter 77 beam antenna) along with mobile radios having a sensitivity figure of merit (G/T) of -15 dB/deg K are considered. Optimized mobile radio user costs are presented as a function of the number of users with the satellite and mobile radio alternatives as system parameters. (Author)

33 ELECTRONICS AND ELECTRICAL ENGINEERING

Includes test equipment and maintainability; components, e.g., tunnel diodes and transistors; microminiaturization; and integrated circuitry.

For related information see also 60 Computer Operations and Hardware and 76 Solid-State Physics.

N78-11401* National Aeronautics and Space Administration, Lewis Research Center, Cleveland, Ohio.

INSTRUMENT TO AVERAGE 100 DATA SETS

George B. Turns, Arthur G. Birchenough, and William J. Rice Oct 1977 19 p

(NASA-TP-1055; E-9159) Avail: NTIS HC A02/MF A01 CSCL 09C

An instrumentation system is currently under development which will measure many of the important parameters associated with the operation of an internal combustion engine. Some of these parameters include mass-fraction burn rate, ignition energy, and the indicated mean effective pressure. One of the characteristics of an internal combustion engine is the cycle-to-cycle variation of these parameters. A curve-averaging instrument has been produced which will generate the average curve, over 100 cycles, of any engine parameter. The average curve is described by 2048 discrete points which are displayed on an oscilloscope screen to facilitate recording and is available in real time. Input can be any parameter which is expressed as a + or - 10-volt signal. Operation of the curve-averaging instrument is defined between 100 and 6000 rpm. Provisions have also been made for averaging as many as four parameters simultaneously, with a subsequent decrease in resolution. This provides the means to correlate and perhaps interrelate the phenomena occurring in an internal combustion engine. This instrument has been used successfully on a 1975 Chevrolet V8 engine, and on a Continental 6-cylinder aircraft engine. While this instrument was designed for use on an internal combustion engine, with some modification it can be used to average any cyclically varying waveform. Author

N78-13330* National Aeronautics and Space Administration, Lewis Research Center, Cleveland, Ohio.

POTENTIAL DAMAGE TO DC SUPERCONDUCTING MAGNETS DUE TO THE HIGH FREQUENCY ELECTROMAGNETIC WAVES

G J Gabriel (Notre Dame Univ) 1977 10 p refs Presented at 7th Symp on Engineering Problems of Fusion Res., Knoxville, Tenn., 25-28 Oct 1977, sponsored by IEEE.

(NASA-TM-73808) Avail: NTIS HC A02/MF A01 CSCL 09C

Experimental data are presented in support of the hypothesis that a dc superconducting magnet coil does not behave strictly as an inductor, but as a complicated electrodynamic device capable of supporting electromagnetic waves. Travel times of nanosecond pulses and evidence of sinusoidal standing waves were observed on a prototype four-layer solenoidal coil at room temperature. Ringing observed during switching transients appears as a sequence of multiple reflected square pulses whose durations are related to the layer lengths. With sinusoidal excitation of the coil, the voltage amplitude between a pair of points on the coil exhibits maxima at those frequencies such that the distance between these points is an odd multiple of half wavelength in free space. Evidence indicates that any disturbance, such as that resulting from switching or sudden fault, initiates multiple reflections between layers, thus raising the possibility for sufficiently high voltages to cause breakdown. Author

N78-13331* National Aeronautics and Space Administration, Lewis Research Center, Cleveland, Ohio.

A SUSTAINED-ARC IGNITION SYSTEM FOR INTERNAL COMBUSTION ENGINES

Arthur G. Birchenough Nov 1977 15 p refs

(NASA-TM-73833; E-9420) Avail: NTIS HC A02/MF A01 CSCL 09C

A sustained-arc ignition system was developed for internal combustion engines. It produces a very-long-duration ignition pulse with an energy in the order of 100 millijoules. The ignition pulse waveform can be controlled to predetermined actual ignition requirements. The design of the sustained-arc ignition system is presented in the report. Author

N78-17283* National Aeronautics and Space Administration, Lewis Research Center, Cleveland, Ohio.

PARTICLE PARAMETER ANALYZING SYSTEM Patent

David O. Hansen (TRW Inc., Redondo Beach, Calif.) and Neal L. Roy, inventors (to NASA) (TRW Inc., Redondo Beach, Calif.) Issued 21 Jan. 1988 8 p Filed 28 Jan. 1986 Sponsored by NASA

(NASA-Case-XLE-06094; US-Patent-3,423,627;

US-Patent-AppI-SN-623632; US-Patent-Class-315-22) Avail: US Patent Office CSCL 09C

An X-Y plotter circuit apparatus is described which displays an input pulse representing particle parameter information, that would ordinarily appear on the screen of an oscilloscope as a rectangular pulse, as a single dot positioned on the screen where the upper right hand corner of the input pulse would have appeared. If another event occurs, and it is desired to display this event, the apparatus is provided to replace the dot with a short horizontal line.

Official Gazette of the U.S. Patent Office

N78-17286* National Aeronautics and Space Administration, Lewis Research Center, Cleveland, Ohio.

NOISE AS A TOOL FOR EVALUATING THE ACTIVATION OF CATHODES

Henry Koemehl 1978 6 p Presented at the Space Traveling Wave Tube Cathode Conf., Washington, D. C., 30 Jan. - 1 Feb. 1978; sponsored by DoD and IEEE

(NASA-TM-73895; E-9520) Avail: NTIS HC A02/MF A01 CSCL 09C

Measurements, at low frequencies, of the shot noise current from space charge limited cathodes always produced results substantially in excess of theoretical predictions. Measuring the ratio $(I_{sub\ eq})/S$ yielded a relation $(I_{sub\ eq})/S = 1288 V_{sub\ k} - 1288 k(T_{sub\ k})/e$, independent of the operating point of the diode (triode) as long as all parts of the cathode had a full space charge controlled emission. This method was so sensitive as to permit detection of cathode temperature changes by 1 K, thus it allowed a powerful screening method between well and poorly activated cathodes, superior to dip tests and other current-voltage methods. Author

N78-19387* National Aeronautics and Space Administration, Lewis Research Center, Cleveland, Ohio.

UP-DATE OF TRAVELING WAVE TUBE IMPROVEMENTS

Erik Buck 1978 15 p ref Presented at Electronic Warfare Symp., Warner Robins AFB, Ga., 20-24 Mar. 1978

(NASA-TM-78852; E-9572) Avail: NTIS HC A02/MF A01 CSCL 09C

A brief survey is presented of areas of progress on traveling wave tube designs. Data demonstrates the effect of multistage depressed collectors, the design of which is made possible by powerful NASA computer programs. Other topics include beam refocusing, RF circuit losses, and cathode testing. Author

N78-21372* National Aeronautics and Space Administration, Lewis Research Center, Cleveland, Ohio.

NASA CHARGING ANALYZER PROGRAM: A COMPUTER TOOL THAT CAN EVALUATE ELECTROSTATIC CONTAMINATION

N John Stevens, James C. Roche, and Myron J. Mandell (Systems Sci and Software, La Jolla, Calif) 1978 14 p refs Presented at Intern. Spacecraft Contamination Conf., Colorado Springs, Colo., 7-9 Mar. 1978, sponsored in part by NASA and AF

(NASA-TM-73889; E-9526) Avail: NTIS HC A02/MF A01 CSCL 09C

A computer code, the NASA Charging Analyzer Program (NASCAP), was developed to study the surface charging of bodies subjected to geomagnetic substorm conditions. This program will treat the material properties of a surface in a self-consistent manner and calculate the electric fields in space due to the surface charge. Trajectories of charged particles in this electric field can be computed to determine if these particles enhance surface contamination. A preliminary model of the Spacecraft Charging At The High Altitudes (SCATHA) satellite was developed in the NASCAP code and subjected to a geomagnetic substorm environment to investigate the possibility of electrostatic contamination. The results indicate that differential voltages will exist between the spacecraft ground surfaces and the insulator surfaces. The electric fields from this differential charging can enhance the contamination of spacecraft surfaces. Author

N78-21973* National Aeronautics and Space Administration, Lewis Research Center, Cleveland, Ohio.
INVESTIGATION OF HIGH VOLTAGE SPACECRAFT SYSTEM INTERACTIONS WITH PLASMA ENVIRONMENTS

N. John Stevens, Frank D. Berkopec, Carolyn K. Purvis, Norman Grier, and John V. Staskus. Ap: 1978 22 p refs Presented at the 13th Intern. Elec. Propulsion Conf., San Diego Calif., 25-27 Apr 1978; sponsored by AIAA and DGLR (NASA-TM-78831; E-9536) Avail: NTIS HC A02/MF A01 CSDL 09C

An experimental investigation was undertaken for insulator and conductor test surfaces biased up to + or - 1kV in a simulated low earth orbit charged particle environment. It was found that these interactions are controlled by the insulator surfaces surrounding the biased conductors. For positive applied voltages the electron current collection can be enhanced by the insulators. For negative applied voltages the insulator surface confines the voltage to the conductor region. Understanding these interactions and the technology to control their impact on system operation is essential to the design of solar cell arrays for ion drive propulsion applications that use direct drive power processing. Author

N78-25323* National Aeronautics and Space Administration, Lewis Research Center, Cleveland, Ohio.
LIQUID METAL SLIP RING Patent Application
Frank D. Berkopec, Robert R. Lovell, and David H. Culp, inventors (to NASA) Filed 17 Apr 1978 11 p (NASA Case LEW-12277-2; US Patent Appl-SN-896955) Avail: NTIS HC A02/MF A01 CSDL 09C

The liquid metal electrical device includes a rotor with a channel for retaining the liquid by tension. The device also includes a stator in the form of a brush partially immersed in the metal. The brush is bidirectionally symmetrical so that whichever direction the rotor turns, the probe presents the same physical resistance and affords the same electrical conductivity as a connection between the probe and the rotor. NASA

N78-27367* National Aeronautics and Space Administration, Lewis Research Center, Cleveland, Ohio.
DIRECT HEATING SURFACE COMBUSTOR Patent
Donald G. Beremand, Lloyd I. Shire, and Thaddeus S. Mroz, inventors (to NASA) Issued 9 May 1978 6 p. Filed 26 Jul 1976 Supersedes N76 28646 (14 19 p 2478) (NASA Case LEW 11877 1; US Patent 4 087 962; US Patent Appl SN 708660; US Patent Class 60 39 65; US Patent Class 431 7; US Patent Class 431 10; US Patent Class 431 328; US Patent Class 60 39 69H; Avail: US Patent Office CSDL 200

The combustor utilizes a non-adiabatic flame to provide low emission combustion for gas turbines. A fuel air mixture is directed through a porous wall the other side of which serves as a combustion surface. A radiant heat sink disposed adjacent to and spaced from the combustion surface controls the combustor flame temperature in order to prevent the formation of oxides of nitrogen. A secondary air flow cools the heat sink. Additionally,

up to 100% of secondary air flow is mixed with the combustion products at the direct heating surface combustor to dilute such products thereby reducing exit temperature. However, if less than 100% secondary air is mixed to the combustor, the remainder may be added to the combustion products further downstream. Official Gazette of the U.S. Patent Office

N78-32341* National Aeronautics and Space Administration, Lewis Research Center, Cleveland, Ohio.
REGULATED HIGH EFFICIENCY, LIGHTWEIGHT CAPACITOR-DIODE MULTIPLIER dc TO dc CONVERTER Patent
William T. Harrigill, Jr. and Ira T. Myers, inventors (to NASA) Issued 30 May 1978 5 p. Filed 27 May 1977 Supersedes N77-24386 (15 15, p 2011) (NASA Case-Law-12781-1; US Patent-4,082,712; US Patent-Appl-SN-801432; US Patent-Class-363-60; US Patent-Class-363-16; US Patent-Class-363-101) Avail: US Patent Office CSDL 09C

A voltage multiplier having a capacitor-diode voltage multiplying network is disclosed which is fed with voltage pulses from a dc source through a first switching means. Pulses of a second polarity are also supplied through a second switching means to the input of the capacitor-diode voltage multiplier from a second dc source whose voltage is adjustable to change the voltage of the pulses of second polarity. The switching means are alternately rendered conducting by signals from a control circuit. The second dc source may be controlled by a voltage comparator which compares the output voltage of the capacitor-diode voltage multiplier to the reference source. Official Gazette of the U.S. Patent Office

A78-15823 * Design and prototype fabrication of a 30 tesla cryogenic magnet. G. M. Prok, M. C. Swanson, and G. V. Brown (NASA, Lewis Research Center, Cleveland, Ohio). *National Bureau of Standards, Cryogenic Engineering Conference, University of Colorado, Boulder, Colo., Aug. 2-5, 1977, Paper*. 15 p.

A liquid-neon-cooled magnet has been designed to produce 30 teslas in steady operation. Its feasibility was established by a previously reported parametric study. To ensure the correctness of the heat transfer relationships used, supercritical neon heat transfer tests were made. Other tests made before the final design included tests on the effect of the magnetic field on pump motors; tensile-shear tests on the cryogenic adhesives; and simulated flow studies for the coolant. The magnet will be made of two pairs of coils, cooled by forced convection of supercritical neon. Heat from the supercritical neon will be rejected through heat exchangers which are made of roll-bonded copper panels and are submerged in a pool of saturated liquid neon. A partial mock-up coil was wound to identify the tooling required to wind the magnet. This was followed by winding a prototype pair of coils. The prototype winding established procedures for fabricating the final magnet and revealed slight changes needed in the final design. (Author)

A78 16922 * Electric vehicle power train instrumentation - Some constraints and considerations. J. E. Triner and I. G. Hansen (NASA, Lewis Research Center, Cleveland, Ohio). *Electric Vehicle Council International Electric Vehicle Exposition and Conference, 1st, Chicago, Ill., Apr. 26-29, 1977, Paper 7744*. 21 p 8 refs

The application of pulse modulation control (choppers) to dc motors creates unique instrumentation problems. In particular, the high harmonic components contained in the current waveforms require frequency response accommodations not normally considered in dc instrumentation. In addition to current sensing, accurate power measurement not only requires adequate frequency response but also must address phase errors caused by the finite bandwidths and component characteristics involved. This paper discusses the implications of these problems and reports on the degree to which they have been solved at Lewis Research Center. (Author)

A78-18282 * Use of a simple external nonreciprocal attenuator in coupled-cavity TWT's. D. J. Connolly (NASA, Lewis Research Center, Cleveland, Ohio). *IEEE Transactions on Electron Devices*, vol. ED-24, Dec. 1977, p. 1351-1353. 7 refs.

A technique has been developed for introducing a nonreciprocal sever in a traveling-wave tube design. It employs an output coupler followed by a ferrite isolator, a variable phase shifter, and an input coupler. The input and output couplers are similar to those already needed at the ends of the tube. The isolator and phase shifter are similar to commercially available waveguide components. A computer simulation has suggested the technique may yield a significant improvement in efficiency. S.C.S.

A78-18287 * A possible pole problem in the formula for klystron gap fields. H. G. Kosmahl (NASA, Lewis Research Center, Cleveland, Ohio). *IEEE Transactions on Electron Devices*, vol. ED-24, Dec. 1977, p. 1368, 1369.

In isolated cases a pole may be encountered in a previously published solution for the fields in a klystron gap. Formulas, permitting the critical combinations of parameters to be defined, are presented. It is noted that the region of inaccuracy surrounding the pole is sufficiently small and that a 0.1% change in the field changing parameter is enough to avoid it. S.C.S.

A78-23635 * Secondary electron emission properties of conducting surfaces for use in multistage depressed collectors. R. Forman (NASA, Lewis Research Center, Cleveland, Ohio). *IEEE Transactions on Electron Devices*, vol. ED-25, Jan. 1978, p. 69. 70.

An Auger spectrometer in ultrahigh vacuum was used to measure the secondary emission properties of a number of candidate collector materials including beryllium, carbon, (soot and pyrolytic graphite), copper, titanium carbide and tantalum. The advantage of the technique used is that the surface chemical constituents could be determined just before the secondary emission characteristics of the surface were measured. Pyrolytic graphite roughened by sputter etching showed the most favorable results for depressed collector use. B.J.

A78-24883 * # Performance of the 12 GHz, 200 watt Transmitter Experiment Package for the Hermes Satellite. R. E. Alexovich (NASA, Lewis Research Center, Cleveland, Ohio). *Royal Society of Canada, Symposium on Hermes (Communications Technology Satellite): Its Performance and Applications, Ottawa, Canada, Nov. 29-Dec. 1, 1977, Paper. 33 p. 6 refs.*

Performance characteristics from on-orbit tests of the Transmitter Experiment Package (TEP) for the Hermes Satellite are presented. The tests were conducted from February 8, 1976 through August 8, 1977. The TEP consists of a Power Processing System (PPS), an Output Stage Tube (OST) and a Variable Conductance Heat Pipe System (VCHPS), all of which are described. The OST is a coupled cavity traveling wave tube with a multistage depressed collector and a stepped velocity-tapered slow wave structure for efficiency enhancement. It has an RF output power of 233 W and overall efficiency of 50.75% at a center band frequency of 12.080 GHz. The PPS provides the required operating voltages, regulation, control and protection for the OST. The VCHPS consists of a fin radiator and three dual-artery stainless steel heat pipes using methanol and a mixture of inert gases. Test results presented include efficiencies, RF output power and body current. A discussion of thermal anomalies which occurred is presented. (Author)

A78-33208 * # Up-date of traveling wave tube improvements. E. Buck (NASA, Lewis Research Center, Cleveland, Ohio; USAF, Washington, D.C.). *Electronic Warfare Symposium, Warner Robins AFB, Ga., Mar. 20-24, 1978, Paper. 14 p.*

NASA research in the area of traveling wave tube technology is reviewed, with emphasis on the basic physics of guns and collectors and a computer model for the interaction between the electron beam

and the RF circuit. The design of a multistage depressed collector, capable of multiplying tube efficiency by a factor of two or more, is presented; one such design has been adopted for commercial traveling wave tube production. A three-dimensional model of electron trajectories toward the collector also receives attention, as does the problem of RF circuit losses. J.M.B.

A78-38902 * Potential damage to dc superconducting magnets due to high frequency electromagnetic waves. G. J. Gabriel (Notre Dame, University, Notre Dame, Ind.) and J. A. Burkhart (NASA, Lewis Research Center, Cleveland, Ohio). In: *Symposium on Engineering Problems of Fusion Research, 7th, Knoxville, Tenn., October 26-28, 1977, Proceedings, Volume 1. (A78-39783 17-75) Piscataway, N.J., Institute of Electrical and Electronics Engineers, Inc., 1977, p. 741-745. 7 refs. NASA-supported research.*

Studies of a d.c. superconducting magnet coil indicate that the large coil behaves as a straight waveguide structure. Voltages between layers within the coil sometimes exceeded those recorded at terminals where protective resistors are located. Protection of magnet coils against these excessive voltages could be accomplished by impedance matching throughout the coil system. The wave phenomenon associated with superconducting magnetic coils may create an instability capable of converting the energy of a quiescent d.c. superconducting coil into dissipative a.c. energy, even in cases when dielectric breakdown does not take place. J.M.B.

A78-45435 * * Medium power voltage multipliers with a large number of stages. W. T. Harrigill and I. T. Myers (NASA, Lewis Research Center, Cleveland, Ohio). *Institute of Electrical and Electronics Engineers, Power Electronics Specialists Conference, Syracuse, N.Y., June 13-15, 1978, Paper. 7 p. 13 refs.*

Voltage multiplier techniques were extended at medium power levels to larger multiplication ratios. A series of DC-DC converters were built, with from 20 to 45 stages and with power levels up to 100 watts. Maximum output voltages were about 10,000 volts.

(Author)

N78-11295* # Hughes Aircraft Co. Torrance, Calif. Electron Dynamics Div
STUDY OF 42 AND 86 GHz COUPLED CAVITY TRAVELING-WAVE TUBES FOR SPACE USE
J. B. Kennedy, I. Tammaru, and P. S. Wolcott Jun 1977
171 p refs
(Contract NAS3-19701)
(NASA-CR-134670, W-06553) Avail NTIS HC A08/MF A01 CSCL 09A

Designs were formulated for four CW, millimeter wavelength traveling-wave tubes having high efficiency and long life. Three of these tubes in the 42 to 44 GHz frequency region develop power outputs of 100 to 300 watts with overall efficiencies of typically 45 percent. Another tube, which covers the frequency range of 84 to 86 GHz provides a power output of 200 watts at 25 percent efficiency. The cathode current density in each design was 1A/sq cm. Each tube includes metal-ceramic construction, periodic permanent magnet focusing, a two step velocity taper, an electron beam refocusing section, and a radiation cooled three-stage depressed collector. The electrical and mechanical design for each tube type is discussed in detail. The results of thermal and mechanical analyses are presented.

Author

N78-13325* # Mays Development Corp. San Diego, Calif.
THE EFFECT OF ENVIRONMENTAL PLASMA INTERACTIONS ON THE PERFORMANCE OF THE SOLAR SAIL SYSTEM Contractor Report, Jul. 1976 - Jul. 1977
Marvin Douglas, Robert Laquey, and Sherman DeForest Aug 1977 104 p refs
(Contract NAS3-20119)
(NASA-CR-135258) Avail: NTIS HC A06/MF A01 CSCL 09C

Interaction between the solar sail and the natural plasma environment were examined for deleterious impacts upon the operation of the sail and its associated payload. Electrostatic charging of the sail in the solar wind and in near earth environment were examined. Deployment problems were studied. An analysis of electromechanical oscillations coupling the sail to the natural plasma was performed. As a result of these studies, it was concluded that none of these effects will have a significant negative impact upon the sail operation. The natural environment will be significantly perturbed and this will preclude measurements of electric and magnetic fields from an attached payload. Author

N78-13328* Systems Science and Software, La Jolla, Calif. **A THREE DIMENSIONAL DYNAMIC STUDY OF ELECTROSTATIC CHARGING IN MATERIALS** Contractor Report, Jul. 1978 - Jul. 1977

I. Katz, D. E. Parks, M. J. Mandell, J. M. Harvey, D. H. Brownell, Jr., S. S. Wang, and M. Rotenberg Aug. 1977 334 p refs (Contract NAS3-20119) (NASA-CR-135258; SSS-R-77-3367) Avail: NTIS HC A15/MF A01 CSCL 09C

A description is given of the physical models employed in the NASCAP (NASA Charging Analyzer Program) code, and several test cases are presented. NASCAP dynamically simulates the charging of an object made of conducting segments which may be entirely or partially covered with thin dielectric films. The object may be subject to either ground test or space user-specified environments. The simulation alternately treats (1) the tendency of materials to accumulate and emit charge when subject to plasma environment, and (2) the consequent response of the charged particle environment to an object's electrostatic field. Parameterized formulations of the emission properties of materials subject to bombardment by electrons, protons, and sunlight are presented. Values of the parameters are suggested for clean aluminum, Al₂O₃, clean magnesium, MgO, SiO₂ kapton, and teflon. A discussion of conductivity in thin dielectrics subject to radiation and high fields is given, together with a sample calculation. Author

N78-13329* Systems Science and Software, La Jolla, Calif. **NASCAP USER'S MANUAL** Contractor Report, Jul. 1978 - Jul. 1977

M. J. Mandell, J. M. Harvey, and I. Katz Aug. 1977 354 p refs (Contract NAS3 20119) (NASA CR-135259; SSS-R-77-3368) Avail: NTIS HC A16/MF A01 CSCL 09C

The NASCAP (NASA Charging Analyzer Program) code simulates the charging process for a complex object in either tenuous plasma or ground test environment. Detailed specifications needed to run the code are presented. The object definition section, OBJDEF, allows the test object to be easily defined in the cubic mesh. The test object is composed of conducting sections which may be wholly or partially covered with thin dielectric coatings. The potential section, POTENT, obtains the electrostatic potential in the space surrounding the object. It uses the conjugate gradient method to solve the finite element formulation of Poisson's equation. The CHARGE section of NASCAP treats charge redistribution among the surface cells of the object as well as charging through radiation bombardment. NASCAP has facilities for extensive graphical output, including several types of object display plots, potential contour plots, space charge density contour plots, current density plots, and particle trajectory plots. Author

N78-15397* Case Western Reserve Univ., Cleveland, Ohio. Engineering Design Center. **ADAPTATION OF ION BEAM TECHNOLOGY TO MICRO-FABRICATION OF SOLID STATE DEVICES AND TRANSDUCERS**

James A. Topich Nov. 1977 43 p refs (Grant NSG 3131) (NASA CR 135314) Avail: NTIS HC A03/MF A01 CSCL 09C

It was found that ion beam texturing of silicon surfaces can

be used to increase the effective surface area of MOS capacitors. There is, however, a problem with low dielectric breakdown. Preliminary work was begun on the fabrication of ion implanted resistors on textured surfaces and the potential improvement of wire bond strength by bonding to a textured surface. In the area of ion beam sputtering, the techniques for sputtering PVC were developed. A PVC target containing valinomycin was used to sputter an ion selective membrane on a field effect transistor to form a potassium ion sensor. Author

N78-16400* Hughes Aircraft Co., Culver City, Calif. **HIGH FREQUENCY CAPACITOR-DIODE VOLTAGE MULTIPLIER dc-dc CONVERTER DEVELOPMENT** Progress Report, 14 Jun. - 14 Jul. 1977

Jack J. Kisch and Robert M. Marinelli Sep. 1977 72 p refs (Contract NAS3-20111) (NASA-CR-135309; P77-437) Avail: NTIS HC A04/MF A01 CSCL 09C

A power conditioner was developed which used a capacitor diode voltage multiplier to provide a high voltage without the use of a step-up transformer. The power conditioner delivered 1200 Vdc at 100 watts and was operated from a 120 Vdc line. The efficiency was in excess of 90 percent. The component weight was 197 grams. A modified boost-add circuit was used for the regulation. A short circuit protection circuit was used which turns off the drive circuit upon a fault condition, and recovers within 5 ms after removal of the short. High energy density polysulfone capacitors and high speed diodes were used in the multiplier circuit. Author

N78-19382* Westinghouse Electric Corp., Pittsburgh, Pa. Research and Development Center. **NIOBIUM-GERMANIUM SUPERCONDUCTING TAPES FOR HIGH-FIELD MAGNET APPLICATIONS** Final Report, 19 Apr. 1978 - 19 Nov. 1977

A. I. Braginski, G. W. Roland, R. R. Daniel, and J. A. Woolam Nov. 1977 116 p refs (Contract NAS3-20233) (NASA-CR-135384; Rept-77-9F1-HYSUC-R9) Avail: NTIS HC A06/MF A01 CSCL 09C

A process of fabricating superconducting Nb₃Ge tapes by chemical vapor deposition (CVD) has been developed and tapes up to 10 meters long fabricated. The typical properties achieved were: critical temperature T_{sub c} = 20 K, upper critical field H_{sub c2} = 29 tesla at 4.2 K, and J_{sub c} = 3 to 4 x 10 to the 8th power A m(-2) at 4.2 K, 18 tesla. The relative depression of T_{sub c} and H_{sub c2} compared with the best thin film samples sputtered on sapphire was due to the presence of Nb₅Ge₃ second-phase particles used as flux pinning centers and to strains induced by thermal mismatch with Hastelloy B tape substrates. A peculiar field dependence of flux pinning force that was observed in both CVD and sputtered Nb₃Ge indicated a premature pin-breaking mechanism or a phase inhomogeneity. Directions of further optimization work were defined. Author

N78-24488* Hughes Aircraft Co., Culver City, Calif. **TECHNOLOGICAL DEVELOPMENT OF CYLINDRICAL AND FLAT SHAPED HIGH ENERGY DENSITY CAPACITORS** Final Technical Report, 22 Apr. 1978 - 15 Sep. 1977

Joseph A. Zelik and Robert D. Parker Dec. 1977 100 p (Contract NAS3 20090) (NASA CR 135286; P77-594) Avail: NTIS HC A05/MF A01 CSCL 09A

Cylindrical wound metallized film capacitors rated 2 micron F 500 VDC that had an energy density greater than 0.3 J/g, and flat flexible metallized film capacitors rated at 2 micron F 500 VDC that had an energy density greater than 0.1 J/g were developed. Polysulfone polycarbonate and polyvinylidene fluoride (PVF₂) were investigated as dielectrics for the cylindrical units. PVF₂ in 60 micron m thickness was employed in the final components of both types. Capacitance and dissipation factor measurements were made over the range 25 C to 100 C and 10 Hz to 10 kHz. No pre-life-test burning was performed, and

six of ten cylindrical units survived a 2500 hour AC plus DC life test. Three of the four failures were infant mortality. All but two of the flat components survived 400 hours. Finished energy densities were 0.104 J/g at 900 V and 0.200 J/g at 700 V. The energy density being limited by the availability of thin PVF2 films
Author

N78-29380* TRW Defense and Space Systems Group, Redondo Beach, Calif. Power Conversion Electronics Dept.
MODELING AND ANALYSIS OF POWER PROCESSING SYSTEMS (MAPPS), INITIAL PHASE 2 Final Report
Yuan Yu, Fred C. Lee, Herb Wengenheim, and Dan Warren
22 Dec. 1977 427 p refs
(Contract NAS3-19690)
(NASA-CR-135173; TRW-27744.000) Avail: NTIS HC A19/MF A01 CSCL 09C

The overall objective of the program is to provide the engineering tools to reduce the analysis, design, and development effort, and thus the cost, in achieving the required performances for switching regulators and dc-dc converter systems. The program was both tutorial and application oriented. Various analytical methods were described in detail and supplemented with examples, and those with standardization appeals were reduced into computer-based subprograms. Major program efforts included those concerning small and large signal control-dependent performance analysis and simulation, control circuit design, power circuit design and optimization, system configuration study, and system performance simulation. Techniques including discrete time domain, conventional frequency domain, Lagrange multiplier, nonlinear programming, and control design synthesis were employed in these efforts. To enhance interactive conversation between the modeling and analysis subprograms and the user, a working prototype of the Data Management Program was also developed to facilitate expansion as future subprogram capabilities increase.
Author

N78-29351* California Inst. of Tech., Pasadena. Dept of Electrical Engineering
MODELLING, ANALYSIS AND DESIGN OF SWITCHING CONVERTERS
Slobodan Cuk and R. D. Middlebrook [1978] 320 p refs
Prepared for TRW Defense and Space Systems Group, Redondo Beach, Calif.
(Contracts NAS3-19690, NAS3-20102)
(NASA-CR-135174; TRW-A72042-RHBE; TRW-D04803-CFCM) Avail: NTIS HC A14/MF A01 CSCL 09C

A state-space averaging method for modeling switching dc-to-dc converters for both continuous and discontinuous conduction mode is developed. In each case the starting point is the unified state-space representation, and the end result is a complete linear circuit model, for each conduction mode, which correctly represents all essential features, namely, the input, output, and transfer properties (static dc as well as dynamic ac small-signal). While the method is generally applicable to any switching converter, it is extensively illustrated for the three common power stages (buck, boost, and buck-boost). The results for these converters are then easily tabulated owing to the fixed equivalent circuit topology of their canonical circuit model. The insights that emerge from the general state-space modeling approach lead to the design of new converter topologies through the study of generic properties of the cascade connection of basic buck and boost converters.
F.O.S.

A78-18574* Solid State Remote Power Controllers for high voltage DC distribution systems. W. W. Billings (Westinghouse Electric Corp., Lima, Ohio) and G. R. Sundberg (NASA, Lewis Research Center, Cleveland, Ohio). In: NAECON '77; Proceedings of the National Aerospace and Electronics Conference, Dayton, Ohio, May 17-19, 1977. (A78-18551 04-33) New York, Institute of Electrical and Electronics Engineers, Inc., 1977, p. 186-192. 5 refs. Contract No. NAS3-20183.

Presently, hybrid Remote Power Controllers (RPC's) are in production and prototype units are available for systems utilizing 28VDC, 120VDC, 115VAC/400 Hz and 230VAC/400 Hz. This paper describes RPC development in a new area of application: HVDC distribution systems utilizing 270/300VDC. Two RPC current ratings, 1 amp and 2 amps, were selected for development as they are adequate to control 90% of projected system loads. The various aspects and trade-offs encountered in circuit development are discussed with special focus placed on the circuits that see the stresses of the high dc potentials. The comprehensive evaluation tests are summarized which confirmed the RPC compliance with the specification and with system/load compatibility requirements. In addition, present technology status and new applications are summarized.
(Author)

A78-18796* Discrete time domain modelling and analysis of dc-dc converters with continuous and discontinuous inductor current. R. P. Iwens, F. C. Lee (TRW Defense and Space Systems Group, Redondo Beach, Calif.), and J. E. Triner (NASA, Lewis Research Center, Cleveland, Ohio). *International Federation of Automatic Control, Symposium on Control in Power Electronics and Electrical Drives, 2nd, Dusseldorf, West Germany, Oct. 3-5, 1977, Preprint*. 15 p. 9 refs. Contract No. NAS3-18918.

Using discrete time state variable representation, a generalized computer-aided modeling and analysis of dc-dc converters is presented. The methodology provides exact modeling and is applicable to all types of power stages and duty-cycle control, including continuous and discontinuous inductor current operation. Converter stability, transient behavior and audio susceptibility can be analytically evaluated and predicted. The generalized theory of the proposed approach to converter modeling and analysis is presented first, followed by a demonstrative example applying the theory to a constant frequency buck converter operating in continuous and discontinuous inductor current mode. Excellent agreement with laboratory test data has been observed.
(Author)

34 FLUID MECHANICS AND HEAT TRANSFER

Includes boundary layers; hydrodynamics; fluidics; mass transfer; and ablation cooling.

For related information see also 02 *Aerodynamics and 77 Thermodynamics and Statistical Physics.*

N78-10416* National Aeronautics and Space Administration, Lewis Research Center, Cleveland, Ohio.

THE DESIGN OF HYDRAULIC PRESSURE REGULATORS THAT ARE STABLE WITHOUT THE USE OF SENSING LINE RESTRICTORS OR FRICTIONAL DAMPERS

Harold Gold 1977 22 p refs Presented at Natl. Conf. on Fluid Power, Chicago, 25-27 Oct. 1977; sponsored by IIT (NASA-TM-X-73687; E-9220) Avail NTIS HC A02/MF A01 CSCL 200

Parameters controlled in design determine the stability of hydraulic pressure regulators in service. The non-linear sensing line restrictor can provide stability, but degrades the transient response. Linear damping is not always physically realizable and is sensitive to clearance and viscosity. Design relationships are analytically derived through which regulators can be made to be stable without the use of either of these damping means. The analytical distinctions between the parameters derived and those in prior literature are discussed. An analytically derived circuit component that stabilizes an otherwise unstable regulator and its experimental verification is described. Author

N78-10418* National Aeronautics and Space Administration, Lewis Research Center, Cleveland, Ohio.

RELEASE OF DISSOLVED NITROGEN FROM WATER DURING DEPRESSURIZATION TRANSIENTS: PRELIMINARY REPORT

Robert J. Simoneau 1977 25 p refs Presented at 5th Water Reactor Safety Res Inform Meeting, Gaithersburg, Md., 7-11 Nov. 1977; sponsored by Nucl Regulatory Comm. (NASA-TM-73822; E-9411) Avail NTIS HC A02/MF A01 CSCL 200

An experiment was run to study depressurization of water containing various concentrations of dissolved nitrogen gas, the primary case being room temperature water saturated with nitrogen at 4 MPa. The experiment had two major components: both visual and static depressurization experiment and a flow through a pressure gradient experiment. In the static depressurization experiment, water which had been bubbled with nitrogen for from 1 to 28 days, was depressurized at from 0.09 to 0.50 MPa/second. The transient was photographed with high speed movies. The pictures showed that the bubble population increased strongly with decreasing depressurization rate and weakly with increased bubble time. The water was always very nearly saturated with nitrogen. Bubbles rarely appeared before the pressured reached $P_{sub\ zero/2}$ and in some instances levels of $P_{sub\ zero/5}$ would show no bubbles. Flow experiments were performed in two nozzles, an axisymmetric converging-diverging nozzle and a two-dimensional converging nozzle with glass sidewalls. Depressurization rates were roughly 0.5×1000 to 1.2×1000 MPa/second. Both nozzles exhibited choked flow behavior even at nitrogen concentration levels as low as 4 percent of saturation. Author

N78-12961* National Aeronautics and Space Administration, Lewis Research Center, Cleveland, Ohio.

ON THE LOCALNESS OF THE SPECTRAL ENERGY TRANSFER IN TURBULENCE

R. G. Densler 1977 20 p refs Presented at 13th Annu Meeting of the Fluid Mec Div of the Amer Phys Soc., Bethlehem, Penn., 21-23 Nov. 1977 (NASA-TM-73824; E-9376) Avail NTIS HC A02/MF A01 CSCL 200

By utilizing available experimental data for net energy transfer spectra for homogeneous turbulence, contributions $P(k, k' \text{ prime } 1)$ to the energy transfer at a wavenumber k from various other

wavenumbers $k' \text{ prime } 1$ are calculated. This is done by fitting a truncated power-exponential series in k and $k' \text{ prime } 1$ to the experimental data for the net energy transfer $T(k)$, and using known properties of $P(k, k' \text{ prime } 1)$. Although the contributions $P(k, k' \text{ prime } 1)$ obtained by using this procedure are not unique, the results obtained by using various assumptions do not differ significantly. It seems clear from the results that for a region where the energy entering a wavenumber band dominates that leaving, much of the energy entering the band comes from wavenumbers which are about an order of magnitude smaller. That is, the energy transfer is rather nonlocal. This result is not significantly dependent on Reynolds number. For lower wavenumbers, where more energy leaves than enters a wavenumber band, the energy transfer into the band is more local, but much of the energy then leaves at distant wavenumbers. Author

N78-13388* National Aeronautics and Space Administration, Lewis Research Center, Cleveland, Ohio.

EFFECT OF AIRSTREAM VELOCITY ON MEAN DROP DIAMETERS OF WATER SPRAYS PRODUCED BY PRESSURE AND AIR ATOMIZING NOZZLES

Robert D. Ingebo 1977 9 p refs Presented at Winter Ann. Meeting, Atlanta, Ga., 27 Nov. - 2 Dec. 1977 (NASA-TM-73740; E-9304) Avail NTIS HC A02/MF A01 CSCL 200

A scanning radiometer was used to determine the effect of airstream velocity on the mean drop diameter of water sprays produced by pressure atomizing and air atomizing fuel nozzles used in previous combustion studies. Increasing airstream velocity from 23 to 53.4 meters per second reduced the Sauter mean diameter by approximately 50 percent with both types of fuel nozzles. The use of a sonic cup attached to the tip of an air assist nozzle reduced the Sauter mean diameter by approximately 40 percent. Test conditions included airstream velocities of 23 to 53.4 meters per second at 293 K and atmospheric pressure. Author

N78-13379* National Aeronautics and Space Administration, Lewis Research Center, Cleveland, Ohio.

EFFECTS OF FILM INJECTION ANGLE ON TURBINE VANE COOLING

James W. Gauntner Dec. 1977 24 p refs (NASA-TP-1095; E-9254) Avail NTIS HC A02/MF A01 CSCL 200

Film ejection from discrete holes in the suction surface of a turbine vane was studied for hole axes (1) slanted 30 deg to the surface in the streamwise direction and (2) slanted 30 deg to the surface and 40 deg from the streamwise direction toward the hub. The holes were near the throat area in a five-row staggered array with 8-diameter spacing. Mass flux ratios were as high as 1.2. The data were obtained in an annular sector cascade at conditions where both the ratio of the boundary layer momentum thickness-to-hole diameter and the momentum thickness Reynolds number were typical of an advanced turbofan engine at both takeoff and cruise. Wall temperatures were measured downstream of each of the rows of holes. Results of this study are expressed as a comparison of cooling effectiveness between the in-line angle injection and the compound-angle injection as a function of mass flux ratio. These heat transfer results are also compared with the results of a referenced flow visualization study. Also included is a closed-form analytical solution for temperature within the film cooled wall. Author

N78-14313* National Aeronautics and Space Administration, Lewis Research Center, Cleveland, Ohio.

EXPERIMENTAL EVALUATION OF PREMIXING-PREVAPOORIZING FUEL INJECTION CONCEPTS FOR A GAS TURBINE CATALYTIC COMBUSTOR

Robert Tacina Aug 1977 19 p refs Presented at ASME Winter Ann Meeting, Atlanta, 27 Nov. - 2 Dec. 1977 (Contract EC-77-A-31-1011) (NASA-TM-73755; E-9301; CONS/1011-18) Avail NTIS HC A02/MF A01 CSCL 20A

Experiments were performed to evolve and evaluate a premixing-prevaporizing fuel system to be used with a catalytic

combustor for possible application in an automotive gas turbine. Spatial fuel distribution and degree of vaporization were measured using Jet A fuel. Three types of air blast injectors, an air assist nozzle and a simplex pressure atomizer were tested. Air swirlers with vane angles up to 30 deg were used to improve the spatial fuel distribution. The work was done in a 12-cm (4.75-in.) diameter tubular rig. Test conditions were: a pressure of 0.3 and 0.6 MPa (3 and 6 atm), inlet air temperatures up to 800 K (590 F), velocity of 20 m/sec (66 ft/sec) and fuel-air ratios of 0.01 and 0.025. Uniform spatial fuel distributions that were within plus or minus 10 percent of the mean were obtained. Complete vaporization of the fuel was achieved with air blast configurations at inlet air temperatures of 550 K (530 F) and higher. The total pressure loss was less than 0.5 percent for configurations without air swirlers and less than 1 percent for configurations with a 30 deg vane angle air swirler. Author

N78-17336* National Aeronautics and Space Administration, Lewis Research Center, Cleveland, Ohio
MAGNETIC HEAT PUMPING Patent
 Gerald V Brown, inventor (to NASA) Issued 17 Jan. 1978
 9 p Filed 30 Nov. 1976 Supersedes N77-15343 (15 - 06, p 0750)
 (NASA-Case-LEW-12508-1; US-Patent-4,069,028;
 US-Patent-Appl-SN-746580; US-Patent-Class-62-3) Avail: US Patent Office CSCL 200

A ferromagnetic or ferrimagnetic element is used to control the temperature and applied magnetic field of the element to cause the state of the element as represented on a temperature-magnetic entropy diagram to repeatedly traverse a loop. The loop may have a first portion of concurrent substantially isothermal or constant temperature and increasing applied magnetic field, a second portion of lowering temperature and constant applied magnetic field, a third portion of isothermal and decreasing applied magnetic field, and a fourth portion of increasing temperature and constant applied magnetic field. Other loops may be four sided, with two isotherms and two adiabats. Preferably, a regenerator is used to enhance desired cooling or heating effects, with varied magnetic fields, or varying temperatures including three-sided figures traversed by the representative point
 Official Gazette of the U.S. Patent Office

N78-17338* National Aeronautics and Space Administration, Lewis Research Center, Cleveland, Ohio
METHOD FOR CALCULATING CONVECTIVE HEAT-TRANSFER COEFFICIENTS OVER TURBINE VANE SURFACES
 Daniel J Gauntner and Janis Sucec Jan. 1978 18 p refs
 (NASA-TP-1134, E-9324) Avail: NTIS HC A02/MF A01 CSCL 200

A method for calculating laminar, transitional, and turbulent convective heat-transfer coefficients for turbine vane surfaces is described. An approximate integral solution method produced results in good agreement with a finite-difference solution. Comparisons between the two are presented. The integral solution results agreed well with the finite-difference solution results in the laminar and turbulent regions. Differences in calculating the start of transition produced a later starting point for the approximate integral solution's transitional flow regime. Author

N78-17340* National Aeronautics and Space Administration, Lewis Research Center, Cleveland, Ohio
HIGH TEMPERATURE SURFACE PROTECTION
 Stanley R Levine 1978 17 p refs Presented at Spring Review Conf. of the Inst. of Metallurgists, Cardiff, Wales, 7-10 Apr. 1978
 (NASA-TM-73877, E-9477) Avail: NTIS HC A02/MF A01 CSCL 200

Alloys of the MCrAlX type are the basis for high temperature surface protection systems in gas turbines. M can be one or more of Ni, Co, or Fe and X denotes a reactive metal added to enhance oxide scale adherence. The selection and formation as

well as the oxidation, hot corrosion and thermal fatigue performance of MCrAlX coatings are discussed. Coatings covered range from simple aluminides formed by pack cementation to the more advanced physical vapor deposition overlay coatings and developmental plasma spray deposited thermal barrier coatings. Author

N78-17341* National Aeronautics and Space Administration, Lewis Research Center, Cleveland, Ohio
ACCELERATED LIFE TESTS OF SPECIMEN HEAT PIPE FROM COMMUNICATION TECHNOLOGY SATELLITE (CTS) PROJECT
 Leonard K. Tower and Warner B. Kaufman Dec. 1977 27 p refs
 (NASA-TM-73846, E-9433) Avail: NTIS HC A03/MF A01 CSCL 200

A gas-loaded variable conductance heat pipe of stainless steel with methanol working fluid identical to one now on the CTS satellite was life tested in the laboratory at accelerated conditions for 14,200 hours, equivalent to about 70,000 hours at flight conditions. The noncondensable gas inventory increased about 20 percent over the original charge. The observed gas increase is estimated to increase operating temperature by about 2.2 C, insufficient to harm the electronic gear cooled by the heat pipes in the satellite. Tests of maximum heat input against evaporator elevation agree well with the manufacturer's predictions. Author

N78-18355* National Aeronautics and Space Administration, Lewis Research Center, Cleveland, Ohio
THERMAL BARRIER COATING SYSTEM Patent
 Stephan Stecura and Curt H Leibert, inventors (to NASA) Issued 25 Oct. 1977 3 p Filed 14 May 1976 Supersedes N76-23359 (14 - 14, p 1773)
 (NASA-Case-LEW-12554-1; US-Patent-4,055,705;
 US-Patent-Appl-SN-686449; US-Patent-Class-428-633;
 US-Patent-Class-428-652; US-Patent-Class-428-667;
 US-Patent-Class-427-405; US-Patent-Class-427-419A,
 US-Patent-Class-427-34; US-Patent-Class-427-423) Avail: US Patent Office CSCL 200

A coating system which contains a bond coating and a thermal barrier coating is applied to metal surfaces such as turbine blades and provides both low thermal conductivity and improved adherence when exposed to high temperature gases or liquids. The bond coating contains NiCrAlY and the thermal barrier coating contains a reflective oxide. The reflective oxides ZrO₂-Y₂O₃ and ZrO₂-MgO have demonstrated significant utility in high temperature turbine applications.
 Official Gazette of the U.S. Patent Office

N78-20488* National Aeronautics and Space Administration, Lewis Research Center, Cleveland, Ohio
THE ROLE OF DROP VELOCITY IN STATISTICAL SPRAY DESCRIPTION
 J. F. Groeneweg, M. M. El-Wakil (Wisc. Univ., Madison), P. S. Myers (Wisc. Univ., Madison), and O. A. Uyehara (Wisc. Univ., Madison) 1978 14 p refs Presented at 1st Intern. Conf. on Liquid Atomization and Spray Systems, Tokyo, 29-31 Aug. 1978
 (NASA-TM-73887, E-9502) Avail: NTIS HC A02/MF A01 CSCL 200

The justification for describing a spray by treating drop velocity as a random variable on an equal statistical basis with drop size was studied experimentally. A double exposure technique using fluorescent drop photography was used to make size and velocity measurements at selected locations in a steady ethanol spray formed by a swirl atomizer. The size velocity data were categorized to construct bivariate spray density functions to describe the spray immediately after formation and during downstream propagation. Bimodal density functions were formed by environmental interaction during downstream propagation. Large differences were also found between spatial mass density and mass flux size distribution at the same location. Author

N78-20488* National Aeronautics and Space Administration, Lewis Research Center, Cleveland, Ohio.

EVALUATION OF COMMERCIALY-AVAILABLE SPACE-CRAFT-TYPE HEAT PIPES

W. B. Kaufman and L. K. Tower 1978 16 p refs Proposed for Presentation at the 3d Intern. Heat Pipes Conf., Palo Alto, Calif., 22-24 May 1978; Sponsored by AIAA (NASA-TM-78828) Avail: NTIS HC A02/MF A01 CSCL 20D

As part of an effort to develop reliable, cost effective spacecraft thermal control heat pipes, life tests on 30 commercially available heat pipes in 10 groups of different design and material combinations were conducted. Results for seven groups were reported herein. Materials are aluminum and stainless steel, and working fluids are methanol and ammonia. The formation of noncondensable gas was observed for times exceeding 11,000 hours. The heat transport capacities of the pipes were also determined. Author

N78-21403* National Aeronautics and Space Administration, Lewis Research Center, Cleveland, Ohio.

CONSTRAINED BLOWSING OF LIQUID MERCURY IN A FLEXIBLE SPHERICAL TANK

Joseph Lestngi (Akron Univ., Ohio) and Ralph Zavesky Apr 1978 12 p refs Presented at the 13th Intern. Elec. Propulsion Conf., San Diego, Calif., 25-27 Apr. 1978; sponsored by AIAA and DGLR (NASA-TM-78833; E-9540) Avail: NTIS HC A02/MF A01 CSCL 20D

The mercury propellant tank system developed for use with solar electric propulsion was studied to analytically determine the resonant frequencies of the tank system and compare them with the anticipated control natural frequency of the spacecraft. The system consisted of a stainless steel spherical shell and a hemispherical elastomeric diaphragm. The major analytical tool used was the NASTRAN program. Six mathematical models were developed. Resonant frequencies for six harmonics were obtained for each of the six models considered. The results show that the lowest resonant frequency for the tank system is about an order of magnitude greater than the anticipated control frequency of the spacecraft. Author

N78-21404* National Aeronautics and Space Administration, Lewis Research Center, Cleveland, Ohio.

BOUNDARY LAYER ANALYSIS OF A CENTAUR STANDARD SHROUD

W. R. Hingat and C. E. Towne Mar 1978 19 p refs (NASA-TM-78843; E-9557) Avail: NTIS HC A02/MF A01 CSCL 20D

An analytical boundary layer investigation was carried out in conjunction with an experimental wind tunnel test to determine the discharge characteristics of the Centaur shroud ascent vent system on the Titan/Centaur launch vehicle. This involved estimating the effect of the local boundary layers on the vent discharge for vehicle Mach numbers ranging from 0.8 to 1.56. The growth of the boundary layer along the vehicle was influenced by the interaction with flanges protruding into the flow and by the longitudinal corrugations in the vehicle surface. The effects of the flange and corrugations were treated by approximate techniques. In addition, boundary layer calculations were made for a 3 percent model of the launch vehicle compared with experimental results. Author

N78-22329* National Aeronautics and Space Administration, Lewis Research Center, Cleveland, Ohio.

NUMERICAL SPATIAL MARCHING TECHNIQUES FOR ESTIMATING DUCT ATTENUATION AND SOURCE PRESSURE PROFILES

K. J. Reumeister 1978 38 p refs Presented at the 95th Meeting of the Acoust. Soc. of Am., Providence, 16-19 May 1978 (NASA-TM-78857; E-9586) Avail: NTIS HC A03/MF A01 CSCL 20D

A numerical method was developed that could predict the pressure distribution of a ducted source from far field pressure

inputs. Using an initial value formulation, the two-dimensional homogeneous Helmholtz wave equation (no steady flow) was solved using explicit marching techniques. The Von Neumann method was used to develop relationships which describe how sound frequency and grid spacing effect numerical stability. At the present time, stability considerations limit the approach to high frequency sound. Sample calculations for both hard and soft wall ducts compare favorably to known boundary value solutions. In addition, assuming that reflections in the duct are small, this initial value approach was successfully used to determine the attenuation of a straight soft wall duct. Compared to conventional finite difference or finite element boundary value approaches, the numerical marching technique is orders of magnitude shorter in computation time and required computer storage and can be easily employed in problems involving high frequency sound. Author

N78-23384* National Aeronautics and Space Administration, Lewis Research Center, Cleveland, Ohio.

HIGH TEMPERATURE HEAT PIPE RESEARCH AT NASA LEWIS RESEARCH CENTER

L. K. Tower and W. B. Kaufman 1978 15 p refs Presented at the 3d Intern. Heat Pipes Conf., Palo Alto, Calif., 22-24 May 1978; sponsored by AIAA (NASA-TM-78832; E-9537) Avail: NTIS HC A02/MF A01 CSCL 20D

High temperature refractory metal heat pipes with alkali metal working fluids, for use in thermionic space power systems, were studied. The main effort involved a concept for an out-of-core thermionic nuclear reactor power system. For this a lithium filled heat pipe of 335 cm length with 18 kW capacity was built in several modifications, one of them ultimately tested. Fabrication studies included the manufacture of a heat pipe tube of wire reinforced tantalum by chemical vapor deposition (CVD) and the extension to a reinforced pipe with integral arteries made by the CVD process. A lithium-filled CVD tungsten heat pipe of about 3 kW capacity ran several thousand hours above 1800 K. Materials compatibility studies of several liquid metals in tantalum alloy pipes were performed. Author

N78-23385* National Aeronautics and Space Administration, Lewis Research Center, Cleveland, Ohio.

STIFFNESS OF STRAIGHT AND TAPERED ANNULAR GAS PATH SEALS

David P. Fleming 1978 23 p refs Proposed for presentation at Lubrication Conf., Minneapolis, 24-26 Oct 1978; cosponsored by ASME and Am. Soc. Mech. Engr (NASA-TM-78872; E-9576) Avail: NTIS HC A02/MF A01 CSCL 20D

Radial stiffness of annular (ring-type) gas path seals are calculated for both constant-clearance designs and tapered designs for which the inlet clearance is larger than the outlet clearance. Under some conditions a constant-clearance seal can have a negative stiffness, this undesirable property is completely eliminated by use of tapered seals. Leakage rates are only moderately higher in tapered seals. Author

N78-24484* National Aeronautics and Space Administration, Lewis Research Center, Cleveland, Ohio.

DEGREE OF VAPORIZATION USING AN AIRBLAST TYPE INJECTOR FOR A PREMIXED-PREVAPOORIZED COMBUSTOR

Robert R. Tacina Apr 1978 12 p refs To be presented at the 1st Intern. Conf. on Liquid Atomization and Spray Systems, Tokyo, 28-31 Aug. 1978, sponsored by the Fuel Soc. of Japan (Contract EC-77-A-31-1011) (NASA-TM-78836; E-9546) Avail: NTIS HC A02/MF A01 CSCL 20D

Vaporization data that could be useful in designing premixed-prevaporized fuel preparation systems for gas turbine combustors are presented. The effect of the experimental parameters on vaporization was found to be $E = T_{sub} \ln(\tau_{0.18} (V_{sub} \text{ ref} + 38) / P_{sub} \text{ in} + 35) / 203000$ where E is the degree of vaporization in percent, T_{sub} is the inlet air temperature in K

over the range 450 to 700 K, the residence time in ms over the range 4.3 to 23.8 ms, V sub ref the reference velocity in m/s over the range 6 to 22 m/s, and P sub in the inlet pressure in MPa over the range 0.18 to 0.88 MPa. Jet A and Diesel no. 2 fuels were tested for the effect of inlet air temperature and were found to have nearly identical results. Author

N78-28381* National Aeronautics and Space Administration, Lewis Research Center, Cleveland, Ohio
FLOW COMPENSATING PRESSURE REGULATOR Patent Edward F. Beehr, inventor (to NASA) issued 19 Apr. 1978 6 p Filed 21 Mar. 1977 Supersedes N77-20408 (15 - 11, p 1453)

(NASA-Case-LEW-12718-1; US-Patent-4,084,812; US-Patent-Appl-SN-779428; US-Patent-Class-137-484.2; US-Patent-Class-137-501; US-Patent-Class-137-505.18) Avail: US Patent Office CSCL 200

An apparatus for regulating pressure of treatment fluid during ophthalmic procedures is described. Flow sensing and pressure regulating diaphragms are used to modulate a flow control valve. The pressure regulating diaphragm is connected to the flow control valve to urge the valve to an open position due to pressure being applied to the diaphragm by bias means such as a spring. The flow sensing diaphragm is mechanically connected to the flow control valve and urges it to an opened position because of the differential pressure on the diaphragm generated by a flow of incoming treatment fluid through an orifice in the diaphragm. A bypass connection with a variable restriction is connected in parallel relationship to the orifice to provide for adjusting the sensitivity of the flow sensing diaphragm. A multiple lever linkage system is utilized between the center of the second diaphragm and the flow control valve to multiply the force applied to the valve by the other diaphragm and reverse the direction of the force. Official Gazette of the U.S. Patent Office

N78-28390* National Aeronautics and Space Administration, Lewis Research Center, Cleveland, Ohio
LITHIUM AND POTASSIUM HEAT PIPES FOR THERMIONIC CONVERTERS

Gabor Miskolczi (Thermo Electron Corp., Waltham, Mass.) and Ench Kroeger 1978 7 p refs Proposed for presentation at the 13th Intersociety Energy Conversion Engr. Conf., San Diego, Calif., 20-25 Aug. 1978, sponsored by SAE, ACS, AIAA, ASME, IEEE, AIChE, and ANS (Contract NAS3-20270) (NASA-TM-78946; E-9695) Avail: NTIS HC A02/MF A01 CSCL 200

A prototypic heat pipe system for an out-of-core thermionic reactor was built and tested. The emitter of the concentric thermionic converter consists of the condenser of a tungsten heat pipe utilizing a lithium working fluid. The evaporator section of the emitter heat pipe is radiation heated to simulate the thermal input from the nuclear reactor. The emitter heat pipe thermal transport is matched to the thermionic converter input requirement. The collector heat pipe of niobium, 1% zirconium alloy uses potassium as the working fluid. The thermionic collector is coupled to the heat pipe by a tapered conical joint designed to minimize the temperature drop. The collector heat flux matches the design requirements of the thermionic converter. Author

N78 27367* National Aeronautics and Space Administration, Lewis Research Center, Cleveland, Ohio
SOME FLOW PHENOMENA IN A CONSTANT AREA DUCT WITH A BORDA TYPE INLET INCLUDING THE CRITICAL REGION

H. C. Hendricks and R. J. Simonau 1978 14 p refs Proposed for presentation at the Winter Ann. Meeting, San Francisco 10-15 Dec. 1978. Sponsored by ASME (NASA-TM-78943; E-9690) Avail: NTIS HC A02/MF A01 CSCL 200

Mass limiting flow characteristics for a 55 L/D tube with a borda type inlet were assessed over large ranges of temperature and pressure using fluid nitrogen. Under certain conditions separation and pressure drop at the inlet was sufficiently strong to permit partial vaporization and the remaining fluid flowed

through the tube as if it were a free jet. An empirical relation was determined which defines conditions under which this type of flow can occur. A flow coefficient is presented which enables estimations of flow rates over the experimental range. A flow rate stagnation pressure map for selected stagnation isotherms and pressure profiles document these flow phenomena. J.A.M.

N78-27386* National Aeronautics and Space Administration, Lewis Research Center, Cleveland, Ohio
MEASUREMENT OF CONTROL SYSTEM RESPONSE USING AN ANALOG OPERATIONAL CIRCUIT

Vincent R. Livi 1978 4 p refs Presented at the Elec./Electron. Conf. and Exposition, Cleveland, 9-11 May 1978; Sponsored by IEEE (NASA-TM-78937; E-9580) Avail: NTIS HC A02/MF A01 CSCL 48

Three basic steps are established for an analog method that measures control system response parameters. An example shows how these steps were used on a speed control portion of an auxiliary power unit. The equations and calculations necessary to describe this subsystem are given. The mechanization schematic and simulation diagram for obtaining the measured response parameters of the control system using an analog circuit are explained. Methods for investigating the various effects of the control parameters are described. It is concluded that the optimum system should be underdamped enough to be slightly oscillatory during transients. Author

N78-28372* National Aeronautics and Space Administration, Lewis Research Center, Cleveland, Ohio
VELOCITY, TEMPERATURE, AND ELECTRICAL CONDUCTIVITY PROFILES IN HYDROGEN-OXYGEN MHD DUCT FLOWS

Mahesh S. Greywall and Carlton C. P. Pian 1978 11 p refs To be presented at the Winter Ann. Meeting of the ASME, San Francisco, 10-15 Dec. 1978. Prepared in cooperation with Wichita State Univ. (Grant NoG-3186; Contract EF-77-A-01-2647) (NASA-TM-78958; E-9717) Avail: NTIS HC A02/MF A01 CSCL 200

Two-dimensional duct flow computations for radial distributions of velocity, temperature, and electrical conductivity are reported. Calculations were carried out for the flow conditions representative of a hydrogen-oxygen combustion driven MHD duct. Results are presented for profiles of developing flow in a smooth duct, and for profiles of fully developed pipe flow with a specified streamwise shear stress distribution. The predicted temperature and electrical conductivity profiles for the developing flows compare well with available experimental data. G.G.

N78-28374* National Aeronautics and Space Administration, Lewis Research Center, Cleveland, Ohio

TACT1, A COMPUTER PROGRAM FOR THE TRANSIENT THERMAL ANALYSIS OF A COOLED TURBINE BLADE OR VANE EQUIPPED WITH A COOLANT INSERT. 1. USERS MANUAL

Raymond E. Gaugler Aug. 1978 78 p refs (NASA-TP-1271; E-9554) Avail: NTIS HC A05/MF A01 CSCL 21E

A computer program to calculate transient and steady state temperatures, pressures, and coolant flows in a cooled axial flow turbine blade or vane with an impingement insert is described. Coolant side heat transfer coefficients are calculated internally in the program, with the user specifying either impingement or convection heat transfer at each internal flow station. Spent impingement air flows in a chordwise direction and is discharged through the trailing edge and through film cooling holes. The ability of the program to handle film cooling is limited by the internal flow model. Sample problems, with tables of input and output are included in the report. Input to the program includes a description of the blade geometry, coolant supply conditions,

outside thermal boundary conditions, and wheel speed. The blade wall can have two layers of different materials, such as a ceramic thermal barrier coating over a metallic substrate. Program output includes the temperature at each node, the coolant pressures and flow rates, and the inside heat-transfer coefficients. Author

N78-28407* National Aeronautics and Space Administration, Lewis Research Center, Cleveland, Ohio
LIQUID PROPELLANT REORIENTATION IN A LOW-GRAVITY ENVIRONMENT

Irving E Sumner Jul 1978 52 p
 (NASA-TM-78959; E-9716) Avail NTIS HC A04/MF A01
 CSCL 20D

An existing empirical analysis relating to the reorientation of liquids in cylindrical tanks due to propulsive settling in a low gravity environment was extended to include the effects of geyser formation in the Weber number range from 4 to 10. Estimates of the minimum velocity increment required to be imposed on the propellant tank to achieve liquid reorientation were made. The resulting Bond numbers, based on tank radius, were found to be in the range from 3 to 5, depending upon the initial liquid fill level, with higher Bond number required for high initial fill levels. The resulting Weber numbers, based on tank radius and the velocity of the liquid leading edge, were calculated to be in the range from 6.5 to 8.5 for cylindrical tanks having a fineness ratio of 2.0, with Weber numbers of somewhat greater values for longer cylindrical tanks. It, therefore, appeared to be advantageous to allow small geysers to form and then desupate into the surface of the collected liquid in order to achieve the minimum velocity increment. The Bond numbers which defined the separation between regions in which geyser formation did and did not occur due to propulsive settling in a spherical tank configuration ranged from 2 to 9 depending upon the liquid fill level. 3 B

N78-23399* National Aeronautics and Space Administration, Lewis Research Center, Cleveland, Ohio
ENGINEERING IN THE 21ST CENTURY

John F. McCarthy, Jr. 1978 15 p refs. Presented at the 25th Annv Conf of the Am. Astronautical Soc., Houston, Tex., 30 Oct 1978 - 2 Nov 1978
 (NASA-TM-79010; E-9714) Avail NTIS HC A02/MF A01
 CSCL 12B

Reasonable evolutionary trends in federal outlays for aerospace research and development predict a continuing decline in real resources (1970 dollars) until the mid eighties, and a growth thereafter to the 1970 level by 2000, still well below the 1966 peak. Employment levels will parallel this trend with no shortage of available personnel foreseen. These trends characterize a maturing industry. Shifts in outlook toward the economic use of resources, rather than minimum risk at any cost, and toward missions aligned with societal needs and broad national goals will accompany these trends. These shifts in outlook will arise in part in academia, and will, in turn, influence engineering education. By 2000 space technology will have achieved major advances in the management of information, in space transportation, in space structures, and in energy. The economics of space systems must be the primary consideration if the space program foreseen for the 21st century is to become an actuality. Author

A78 15725 * Revised international representations for the viscosity of water and steam and new representations for the surface tension of water. R. C. Hendricks (NASA, Lewis Research Center, Cleveland, Ohio), R. B. McClintock (General Electric Co., Schenectady, N. Y.), and G. J. Silvestri (Westinghouse Electric Corp., Philadelphia, Pa.) *ASME Transactions Series A: Journal of Engineering for Power*, vol. 99, Oct. 1977, p. 664-678, 11 refs.

A78-15820 * # Boiling incipience and convective boiling of neon and nitrogen. S. S. Papell and R. C. Hendricks (NASA, Lewis Research Center, Cleveland, Ohio). *National Bureau of Standards, Cryogenic Engineering Conference, University of Colorado, Boulder, Colo., Aug. 2-5, 1977, Paper*. 17 p. 6 refs.

Forced convection and subcooled boiling heat transfer data for liquid nitrogen and liquid neon were obtained in support of a design study for a 30 tesla cryo-magnet cooled by forced convection of liquid neon. This design precludes nucleate boiling in the flow channels as they are too small to handle vapor flow. Consequently, it was necessary to determine boiling incipience under the operating conditions of the magnet system. The cryogen data obtained over a range of system pressures, fluid flow rates, and applied heat fluxes were used to develop correlations for predicting boiling incipience and convective boiling heat transfer coefficients in uniformly heated flow channels. The accuracy of the correlating equations was then evaluated. A technique was also developed to calculate the position of boiling incipience in a uniformly heated flow channel. Comparisons made with the experimental data showed a prediction accuracy of plus or minus 15 percent. (Author)

A78-15821 * # Effect of ice contamination on liquid-nitrogen drops in film boiling. G. J. Schoenow (NASA, Lewis Research Center, Cleveland, Ohio; Florida, University, Gainesville, Fla.), C. E. Chmielewski (NASA, Lewis Research Center, Cleveland, Ohio; Indiana Public Service Co., Plainfield, Ind.), and K. J. Baumeister (NASA, Lewis Research Center, Cleveland, Ohio). *National Bureau of Standards, Cryogenic Engineering Conference, University of Colorado, Boulder, Colo., Aug. 2-5, 1977, Paper*. 11 p. 8 refs.

Previously reported vaporization time data of liquid nitrogen drops in film boiling on a flat plate are about 30 percent shorter than predicted from standard laminar film boiling theory. This theory, however, had been found to successfully correlate the data for conventional fluids such as water, ethanol, benzene, or carbon tetrachloride. This paper presents experimental evidence that some of the discrepancy for cryogenic fluids results from ice contamination due to condensation. The data indicate a fairly linear decrease in droplet evaporation time with the diameter of the ice crystal residue. After correcting the raw data for ice contamination along with convection, a comparison of theory with experiment shows good agreement. (Author)

A78-15822 * # Estimating surface temperature in forced convection nucleate boiling - A simplified method. R. C. Hendricks and S. S. Papell (NASA, Lewis Research Center, Cleveland, Ohio). *National Bureau of Standards, Cryogenic Engineering Conference, University of Colorado, Boulder, Colo., Aug. 2-5, 1977, Paper*. 7 p. 9 refs.

A simplified expression to estimate surface temperatures in forced convection boiling was developed using a liquid nitrogen data base. Using the principal of corresponding states and the Kutateladze relation for maximum pool boiling heat flux, the expression was normalized for use with other fluids. The expression was applied also to neon and water. For the neon data base, the agreement was acceptable with the exclusion of one set suspected to be in the transition boiling regime. For the water data base at reduced pressure greater than 0.05 the agreement is generally good. At lower reduced pressures, the water data scatter and the calculated temperature becomes a function of flow rate. (Author)

A78-15824 * # Two phase choked flow in tubes with very large L/D. A. C. Hendricks and R. J. Simoneau (NASA, Lewis Research Center, Cleveland, Ohio). *National Bureau of Standards, Cryogenic Engineering Conference, University of Colorado, Boulder, Colo., Aug. 2-5, 1977, Paper*. 21 p. 19 refs.

Two phase and gaseous choked flow data for fluid nitrogen were obtained for a test section which was a long constant area duct of 16 200 L/D with a diverging diffuser attached to the exit. Flow rate data were taken along five isotherms (reduced temperature of 0.81, 0.96, 1.06, 1.12, and 2.34) for reduced pressures to 3. The flow rate

data were mapped in the usual manner using stagnation conditions at the inlet mixing chamber upstream of the entrance length. The results are predictable by a two-phase homogeneous equilibrium choking flow model which includes wall friction. A simplified theory which in essence decouples the long tube region from the high acceleration choking region also appears to predict the data reasonably well, but about 16 percent low. (Author)

A78-17481 * Velocity and temperature profiles in near-critical nitrogen flowing past a horizontal flat plate. R. J. Simoneau (NASA, Lewis Research Center, Cleveland, Ohio). *American Institute of Chemical Engineers and American Society of Mechanical Engineers, Heat Transfer Conference, Salt Lake City, Utah, Aug. 15-17, 1977, ASME Paper 77-HT-7*. 8 p. 11 refs. Members, \$1.50; nonmembers, \$3.00.

Boundary layer velocity and temperature profiles were measured for nitrogen near its thermodynamic critical point flowing past a horizontal flat plate. The heated surface was oriented both facing upward and downward. The results were compared to earlier work in which measurements were made for vertically upward flow. The boundary layer temperatures ranged from below to above the thermodynamic critical temperature. For wall temperatures below the thermodynamic critical temperature there was little variation between the velocity and temperature profiles in the three orientations. In all three orientations the point of crossing into the critical temperature region is marked by a significant flattening of the velocity and temperature profiles and also a decrease in heat transfer coefficient. As the heat flux and, consequently, wall temperature are further increased significant changes occur in the velocity and temperature profiles. Examination of near-critical heat transfer in these three flow orientations offers insights into the relative role of buoyancy forces in this regime. (Author)

A78-17508 * Thermally driven oscillations and wave motion of a liquid drop. K. J. Baumeister, R. C. Hendricks (NASA, Lewis Research Center, Cleveland, Ohio), and G. J. Schoessow (Florida University, Gainesville, Fla.). *American Institute of Chemical Engineers and American Society of Mechanical Engineers, Heat Transfer Conference, Salt Lake City, Utah, Aug. 15-17, 1977, Paper*. 11 p. 16 refs. Members, \$1.50; nonmembers, \$3.00.

In the state of Leidenfrost boiling, liquid drops are observed to vibrate in a variety of modal patterns. Theories are presented which predict the frequency of oscillation and show that the observed modal patterns of drops correspond to the minimum energy oscillatory excitation state. High speed photographic techniques were used to record these motions and substantiate the theories. An incipient temperature was also found for water drops in film boiling below which free oscillations do not exist. In addition to these oscillations, photographic sequences are presented which show that wave motion can exist along the circumference of the drop. Following the study of free oscillations, the system was mounted on a shaker table and the drop subjected to a range of forced frequencies and accelerations. (Author)

A78-20682 * A computer program for the transient thermal analysis of an impingement cooled turbine blade. R. E. Gaugler (NASA, Lewis Research Center, Cleveland, Ohio). *American Institute of Aeronautics and Astronautics, Aerospace Sciences Meeting, 16th, Huntsville, Ala., Jan. 16-18, 1978, Paper 78-92*. 9 p. 8 refs.

A computer program to calculate transient and steady state temperatures, pressures, and coolant flows in a cooled turbine blade or vane with an impingement insert is described. Input to the program includes a description of the blade geometry, coolant supply conditions, outside thermal boundary conditions and wheel speed. Coolant side heat transfer coefficients are calculated internally in the program, with the user specifying the mode of heat transfer at each internal flow station. Program output includes the temperature at each node, the coolant pressures and flow rates, and the inside heat transfer coefficients. A sample problem is discussed. (Author)

A78-23246 * Characteristics of the unsteady motion on transversely sheared mean flows. M. E. Goldstein (NASA, Lewis Research Center, Cleveland, Ohio). *Journal of Fluid Mechanics*, vol. 84, Jan. 30, 1978, p. 306-329. 15 refs.

An explicit representation for the unsteady motion on a transversely sheared mean flow is obtained which corresponds to the gustline motion on a uniform mean flow. The important features of this motion are discussed. It is shown that its velocity, pressure and vorticity are all induced by a certain disturbance field that is a linear combination of the vorticity and particle-displacement fields and is everywhere frozen in the mean flow. The general ideas are illustrated by considering the scattering of a gust by a half-plane embedded in a shear flow. (Author)

A78-24000 * On the localness of the spectral energy transfer in turbulence. R. G. Deissler (NASA, Lewis Research Center, Cleveland, Ohio). *American Physical Society, Anniversary Meeting of the Fluid Mechanics Division, 30th, Bethlehem, Pa., Nov. 21-23, 1977, Paper*. 19 p. 12 refs.

Data for the energy transfer function are used to estimate the degree of localness of energy transfer in homogeneous turbulence. It is found that in regions where the energy which enters a wavenumber band is greater than the energy leaving, much of the energy entering the band is produced by wavenumbers an order of magnitude smaller. Thus for both low and high Reynolds numbers, spectral energy transfer is nonlocal. The tendency of the energy to jump between separated wavenumber regions agrees with the theory that turbulence forms concentrated regions of large velocity gradients. It is also felt that the universal equilibrium theory may be applicable if the Reynolds number of the turbulence is very high. S.C.S.

A78-32749 * Constrained sloshing of liquid mercury in a flexible spherical tank. J. Lestingi (Akron, University, Akron, Ohio) and R. Zavesky (NASA, Lewis Research Center, Mechanical Engineering Section, Cleveland, Ohio). *American Institute of Aeronautics and Astronautics and Deutsche Gesellschaft für Luft- und Raumfahrt, International Electric Propulsion Conference, 13th, San Diego, Calif., Apr. 25-27, 1978, AIAA Paper 78-670*. 8 p. 7 refs.

The mercury propellant tank system developed for use with solar electric propulsion was studied to analytically determine the resonant frequencies of the tank system and compare them with the anticipated control natural frequency of the spacecraft. The system consisted of a stainless steel spherical shell and a hemispherical elastomeric diaphragm which separates the mercury propellant and the gaseous nitrogen pressurant. The major analytical tool used was the NASTRAN program. Six mathematical models, which represent various amounts of mercury in the tank system were developed. Resonant frequencies for six harmonics were obtained for each of the six models considered. The results show that the lowest resonant frequency for the tank system is about an order of magnitude greater than the anticipated control frequency of the spacecraft. (Author)

A78-35618 * High temperature heat pipe research at NASA Lewis Research Center. I. K. Tower and W. B. Kaufman (NASA, Lewis Research Center, Cleveland, Ohio). In: *International Heat Pipe Conference, 3rd, Palo Alto, Calif., May 22-24, 1978, Technical Papers (A78-35676-14-34)*. New York, American Institute of Aeronautics and Astronautics, Inc., 1978, p. 303-311 (AIAA 78-438).

In the course of studies of thermionic power plants for space applications, high temperature refractory metal heat pipes have been designed and built for alkali metal working fluids. Fabrication of tungsten wire reinforced tantalum pipes by chemical vapor deposition is discussed, the development of reinforced pipes with integral arteries produced by chemical vapor deposition is also mentioned. The feasibility of using lithium, sodium, potassium, cesium or mercury as the working fluid in the heat pipes is also reviewed. Operation of a lithium filled heat pipe of about 3 kW capacity for several thousand hours is reported. J.M.B.

A78-40983 * Turbulence processes and simple closure schemes. R. G. Deissler (NASA, Lewis Research Center, Cleveland, Ohio). In: Handbook of turbulence. Volume 1 Fundamentals and applications. (A78-40976 17-34) New York, Plenum Press, 1977, p. 165-186. 23 refs.

The problem of closure in turbulence in the case of two-point correlations resides in the existence of two unknowns E and W, the energy spectrum function and the transfer function, respectively, in the spectrum equation. In the case of weak turbulence, W is negligible. In case of higher correlations, closure can be effective by neglecting the inertia term in the highest order term used. Specifying a certain number of spectra at an initial time is also a way of getting around the closure problem. A simple case of turbulent shear flow is then considered, where two-point correlation equations are used and the velocity is broken into mean and fluctuating components. This yields a differential equation for the energy spectrum, the three terms of which are the energy spectrum, production term and dissipation term. They are plotted for a particular time. Similar analyses and comparisons with experiment are made for pipe and boundary layer flows. P.T.H.

A78-41154 * # Liquid jet impingement normal to a disk in zero gravity. T. L. Labus (NASA, Lewis Research Center, Cleveland, Ohio) and K. J. DeWitt (Toledo, University, Toledo, Ohio). (American Society of Mechanical Engineers, Paper 78-WA/FE-1, 1978.) ASME, Transactions, Journal of Fluids Engineering, vol. 100, June 1978, p. 204-209. 27 refs.

An experimental and analytical investigation was conducted to determine the free surface shapes of circular jets impinging normal to sharp-edged disks in zero gravity. Experiments conducted in a zero gravity drop tower yielded three distinct flow patterns which were classified in terms of the relative effects of surface tension and inertial forces. An order of magnitude analysis was conducted indicating regions where viscous forces were not significant when computing free surface shapes. The free surface analysis was simplified by transforming the governing potential flow equations and boundary conditions into the inverse plane. The resulting nonlinear equations were solved numerically and comparisons were made with the experimental data for the inertia dominated regime. (Author)

A78-45431 * # Performance characteristics of two annular dump diffusers using suction-stabilized vortex flow control. A. J. Juhasz and J. M. Smith (NASA, Lewis Research Center, Cleveland, Ohio). International Association for Hydraulic Research, ASME, and ASCE, Joint Symposium on Design and Operation of Fluid Machinery, Fort Collins, Colo., June 12-14, 1978, Paper, 13 p. 7 refs.

The two diffusers employed in the investigation had the same overall area ratio but different prediffuser area ratios and suction slot geometries. Velocity profile and diffuser pressure recovery performance data were obtained at ambient pressure and temperature, with inlet Mach numbers ranging from 0.18 to 0.41 and suction rate varying from zero to 18% of total inlet mass flow rate. On the basis of the reported investigation it is concluded that suction stabilized vortex flow diffusers show promise for application in combustors because of relatively high static pressure recovery and low total pressure loss obtained in a short length. Performance obtained using a narrow angle (7 degree) prediffuser was superior to that obtained with a prediffuser having a 14 degree included angle. G.R.

A78-50322 * # Degree of vaporization using an airblast type fuel injector for a premixed prevaporized combustor. R. R. Tacina (NASA, Lewis Research Center, Cleveland, Ohio). Fuel Society of Japan. International Conference on Liquid Atomization and Spray Systems, 1st, Tokyo, Japan, Aug. 28-31, 1978, Paper, 11 p. 9 refs. Contract No. EC-77-A-31-1011.

Vaporization data are presented which could be useful in designing premixed-prevaporized fuel preparation systems for gas turbine combustors. Lean, premixed prevaporized combustion systems are being developed because they operate with low flame

temperatures and, therefore, produce low levels of nitrogen oxides. Parametric tests of the effect of inlet air temperature, length (residence time), reference velocity, pressure and fuel-air ratio on the degree of vaporization are reported. Jet A and Diesel no. 2 fuel were tested. A formula is provided which shows the effect of inlet air temperature, residence time, reference velocity, and pressure on the degree of vaporization for a constant fuel-air ratio of 0.020. The results of the effect of inlet air temperature on the degree of vaporization using Jet A and Diesel no. 2 are nearly identical. G.R.

A78-50323 * # The role of drop velocity in statistical spray description. J. F. Groeneweg (NASA, Lewis Research Center, Cleveland, Ohio), M. M. El-Wakil, P. S. Myers, and O. A. Uyehara (Wisconsin, University, Madison, Wis.). Fuel Society of Japan, International Conference on Liquid Atomization and Spray Systems, 1st, Tokyo, Japan, Aug. 28-31, 1978, Paper, 16 p. 15 refs.

The justification for describing a spray by treating drop velocity as a random variable on an equal statistical basis with drop size was studied experimentally. A double-exposure technique using fluorescent drop photography was used to make size and velocity measurements at selected locations in a steady ethanol spray formed by a swirl atomizer. The size-velocity data were categorized to construct bivariate spray density functions to describe the spray immediately after formation and during downstream propagation. It was found that a statistical treatment of drop velocity was supported by the data. Spray density function shapes and modal characteristics depended strongly on position and the amount of droplet-gas interaction that had occurred. Bimodal density functions were formed by environmental interaction during downstream propagation. Large differences were also found between spatial mass density and mass flux size distributions at the same location. (Author)

N78-12384 #/ Martin Marietta Corp., Denver, Colo. EFFECT OF VIBRATION ON RETENTION CHARACTERISTICS OF SCREEN ACQUISITION SYSTEMS Final Report. May 1976 - Jun. 1977

J. R. Tegart and A. C. Park Oct. 1977 167 p refs (Contract NAS3-20097)

(NASA-CR-135264; MCR-77-253) Avail: NTIS HC A08/MF A01 CSCL 20D

An analytical and experimental investigation of the effect of vibration on the retention characteristics of screen acquisition systems was performed. The functioning of surface tension devices using fine-mesh screens requires that the pressure differential acting on the screen be less than its pressure retention capability. When exceeded, screen breakdown will occur and gas-free expulsion of propellant will no longer be possible. An analytical approach to predicting the effect of vibration was developed. This approach considers the transmission of the vibration to the screens of the device and the coupling of the liquid and the screen in establishing the screen response. A method of evaluating the transient response of the gas/liquid interface within the screen was also developed. (Author)

N78-16329 # Sigma Research, Inc., Richland, Wash. TWO-PHASE WORKING FLUIDS FOR THE TEMPERATURE RANGE 60 TO 350 C Final Report

Eric v. Saaski and Peter C Owzarski Jun. 1977 103 p refs (Contract NAS3-20222)

(NASA-CR-135255) Avail: NTIS HC A06/MF A01 CSCL 20D

The decomposition and corrosion of two-phase heat transfer liquids and metal envelopes have been investigated on the basis of molecular bond strengths and chemical thermodynamics. Potentially stable heat transfer fluids for the temperature range 100 C to 350 C have been identified and reflux heat pipes tests initiated with 10 fluids and carbon steel and aluminum envelopes to experimentally establish corrosion behavior and noncondensable gas generation rates. (Author)

N78-17342* Aerojet Liquid Rocket Co., Sacramento, Calif.
SUPERCritical OXYGEN HEAT TRANSFER Final Report
 R. G. Spencer and D. C. Rouser Nov. 1977 95 p refs
 (Contract NAS3-20384)
 (NASA-CR-135339) Avail: NTIS HC A05/MF A01 CSDL
 200

Heat transfer to supercritical oxygen was experimentally measured in electrical heated tubes. Experimental data were obtained for pressures ranging from 17 to 34.6 MPa (2460 to 5000 psia), and heat fluxes from 2 to 90 million w/sq cm (1.2 to 55 Btu/(sq in. sec)). Bulk temperatures ranged from 98 to 217 K (173 to 391 R). Experimental data obtained by other investigators were added to this to increase the range of pressure down to 2 MPa (290 psia) and increase the range of bulk temperature up to 566 K (1019 R). From this compilation of experimental data a correlating equation was developed which predicts over 95% of the experimental data within + or - 30%.
 Author

N78-29410* TRW Defense and Space Systems Group, Redondo Beach, Calif.
CTS TEP THERMAL ANOMALIES: HEAT PIPE SYSTEM PERFORMANCE Final Report
 S. D. Marcus 30 Nov. 1977 61 p refs
 (Contract NAS3-21012)
 (NASA-CR-159413) Avail: NTIS HC A04/MF A01 CSDL
 200

A part of the investigation is summarized of the thermal anomalies of the transmitter experiment package (TEP) on the Communications Technology Satellite (CTS) which were observed on four occasions in 1977. Specifically, the possible failure modes of the variable conductance heat pipe system (VCHPS) used for principal thermal control of the high-power traveling wave tube in the TEP are considered. Further, the investigation examines how those malfunctions may have given rise to the TEP thermal anomalies. Using CTS flight data information, ground test results, analysis conclusions, and other relevant information, the investigation concentrated on artery depriving as the most likely VCHPS failure mode. Included in the study as possible depriving mechanisms were freezing of the working fluid, Marangoni flow, and gas evolution within the arteries. The report concludes that while depriving of the heat pipe arteries is consistent with the bulk of the observed data, the factors which cause the arteries to deprive have yet to be identified.
 LS

N78-31380* General Dynamics/Convair, San Diego, Calif.
FILLING OF ORBITAL FLUID MANAGEMENT SYSTEMS
 F. Merrin, M. H. Blatt, and N. C. Thies Jul. 1978 117 p refs
 (Contract NAS3-21021)
 (NASA-CR-159404; CASD-NAS-78-010) Avail: NTIS
 HC A06/MF A01 CSDL 200

A study was performed with three objectives (1) analyze fluid management system fill under orbital conditions, (2) determine what experimentation is needed, and (3) develop an experimental program. The fluid management system was a 1.06m (41.7 in) diameter pressure vessel with screen channel device. Analyses were conducted using liquid hydrogen and N2O4. The influence of helium and autogenous pressurization systems was considered. Analyses showed that fluid management system fill will be more difficult with a cryogen than with an earth storable. The key to a successful fill with cryogen is in devising techniques for filling without vent liquid, and removing trapped vapor from the screen device at tank fill completion. This will be accomplished with prechill, fill, and vapor condensation processes. Refill will require a vent and purge process, to dilute the residual helium, prior to introducing liquid. Neither prechill, chill, nor purge processes will be required for earth storables.
 Author

N78-33366* Colorado State Univ., Fort Collins. Fluid Mechanics and Wind Engineering Program.
A VISUAL INVESTIGATION OF TURBULENCE IN STAGNATION FLOW ABOUT A CIRCULAR CYLINDER Final Report
 Wafiq Z. Sedeh and Herbert J. Brauer Oct. 1978 62 p refs
 Film supplement Number C-288 to this report is available on loan from Chief Management Services Division (S-5), National Aeronautics and Space Administration, Lewis Research Center, 2100 Brookpark Road, Cleveland, Ohio 44135
 (Grant NoG-3127)
 (NASA-CR-3019; CSU-FMWEP-NASLRC-1;
 CER-77-78WZS-HG1322) Avail: NTIS HC A04/MF A01 CSDL
 200

A visual investigation of turbulence in stagnation flow around a circular cylinder was carried out in order to gain a physical insight into the model advocated by the continuity-amplification theory. Motion pictures were taken from three different viewpoints, and a frame by frame examination of selected movie strips was conducted. Qualitative and quantitative analyses of the flow events focused on tracing the temporal and spatial evolution of a cross-vortex tube outlined by the entrained smoke filaments. The visualization supplied evidence verifying: (1) the selective stretching of cross-vortex tubes which is responsible for the amplification of cross vorticity and, hence, of streamwise turbulence; (2) the streamwise tilting of stretched cross-vortex tubes; (3) the existence of a coherent array of vortices near the stagnation zone; (4) the interaction of the amplified vorticity with the body laminar boundary layer; and, (5) the growth of a turbulent boundary layer.
 Author

A78-42877* Flow of liquid jets through closely woven screens. F. T. Dodge and R. E. Ricker (Southwest Research Institute, San Antonio, Tex.). *Journal of Spacecraft and Rockets*, vol. 15, July-Aug. 1978, p. 213-218, 9 refs. Contract No. NAS3-20086.

Previously developed analytical models relate pressure drop across a fine-mesh screen to throughflow velocity for duct systems. These models are shown to be unreliable for an unconfined flow, such as a free jet, impinging on a screen. A new model is developed for these kinds of systems, incorporating the important influence of liquid deflection by the screen. A new parameter, the boundary-layer blockage coefficient, is introduced. This coefficient, which depends on the screen weave geometry and the jet impingement angle, accounts for the increase in fluid path length through the screen resulting from the flow deflection. Comparisons are made with previous experimental studies to determine empirical values of the blockage coefficient. It is concluded that the new model reliably predicts the bulk flow and penetration characteristics of an impinging liquid jet interacting with a screen.
 (Author)

A78-48716* Convection due to surface-tension gradients. S. Ostrach (Case Western Reserve University, Cleveland, Ohio). *COSPAR Plenary Meeting, 21st, Innsbruck, Austria, May 29 June 10, 1978, Paper*, 9 p. 19 refs. Contract No. NAS3-21046.

The use of dimensionless parameters to study fluid motions that could occur in a reduced-gravity environment is discussed. The significance of the Marangoni instability is considered and the use of dimensionless parameters to investigate problems such as thermo and diffusocapillary flows is described. Characteristics of fluid flow in space are described, and the relation and interaction of motions due to capillarity and buoyancy is examined.
 M.L.

35 INSTRUMENTATION AND PHOTOGRAPHY

Includes remote sensors; measuring instruments and gages; detectors; cameras and photographic supplies; and holography.

For aerial photography see 43 *Earth Resources*. For related information see also 06 *Aircraft Instrumentation and 13 Spacecraft Instrumentation*.

N78-13467* National Aeronautics and Space Administration, Lewis Research Center, Cleveland, Ohio.

RELIABILITY ANALYSIS OF FORTY-FIVE STRAIN-GAGE SYSTEMS MOUNTED ON THE FIRST FAN STAGE OF A YF-100 ENGINE

Raymond Holanda and Lloyd M. Frause Sep. 1977 20 p refs
(NASA-TM-73724; E-9274) Avail: NTIS HC A02/MF A01 CSCL 14B

The reliability of 45 state-of-the-art strain gage systems under full scale engine testing was investigated. The flame spray process was used to install 23 systems on the first fan rotor of a YF-100 engine, the others were epoxy cemented. A total of 56 percent of the systems failed in 11 hours of engine operation. Flame spray system failures were primarily due to high gage resistance, probably caused by high stress levels. Epoxy system failures were principally erosion failures, but only on the concave side of the blade. Lead-wire failures between the blade-to-disk jump and the control room could not be analyzed. Author

N78-16463* National Aeronautics and Space Administration, Lewis Research Center, Cleveland, Ohio.

RECOVERY AND RADIATION CORRECTIONS AND TIME CONSTANTS OF SEVERAL SIZES OF SHIELDED AND UNSHIELDED THERMOCOUPLE PROBES FOR MEASURING GAS TEMPERATURE

George E. Glawe, Raymond Holanda, and Lloyd N. Krause Jan 1978 30 p refs
(NASA-TP-1099; E-9289) Avail: NTIS HC A03/MF A01 CSCL 14B

Performance characteristics were experimentally determined for several sizes of a shielded and unshielded thermocouple probe design. The probes are of swaged construction and were made of type K wire with a stainless steel sheath and shield and MgO insulation. The wire sizes ranged from 0.03- to 1.02-mm diameter for the unshielded design and from 0.16- to 0.81-mm diameter for the shielded design. The probes were tested through a Mach number range of 0.2 to 0.9, through a temperature range of room ambient to 1420 K, and through a total-pressure range of 0.03 to 0.22 MPa (0.3 to 22 atm). Tables and graphs are presented to aid in selecting a particular type and size. Recovery corrections, radiation corrections, and time constants were determined. Author

N78-23028* National Aeronautics and Space Administration, Lewis Research Center, Cleveland, Ohio.

APPLICATION OF FLUIDICS TO NEW CONTROL COMPONENTS

Miles O. Dustin, Vernon D. Gebben, and Robert E. Wellhagen In NASA, Washington Fourth Inter-Center Control Systems Conf. Jan. 1978 p 365-386 refs (For availability see N78-23010 13-99)

Avail: NTIS HC A22/MF A01 CSCL 20D

A78-11382* A low cost, portable instrument for measuring emittance. G. McDonald (NASA, Lewis Research Center, Cleveland, Ohio). *International Solar Energy Society, Annual Meeting, Orlando, Fla., June 6-10, 1977, Paper*. 10 p.

A low cost, portable instrument has been developed with which emittance can be measured by comparison to a standard. A reflector collects infra-red radiation from a heated sample onto a low mass, black detector and the temperature rise of the black detector is measured with a thermocouple and meter. Graphical examples are presented for determination of emittance from measurements made on a sample at any known temperature. (Author)

A78-17397* Miniature drag force anemometer. L. N. Krause and G. C. Fraick (NASA, Lewis Research Center, Cleveland, Ohio). In: *International Instrumentation Symposium*, 23rd, Las Vegas, Nev., May 1-5, 1977, Proceedings. (A78-17351 05-35) Pittsburgh, Pa., Instrument Society of America, 1977, p. 461-467. 7 refs.

A miniature drag force anemometer is described which is capable of measuring dynamic velocity head and flow direction. The anemometer consists of a silicon cantilevered beam 2.5 mm long, 1.5 mm wide, and 0.25 mm thick with an integrated diffused strain gage bridge, located at the base of the beam, as the force measuring element. The dynamics of the beam are like that of a second order system with a natural frequency of about 42 kHz and a damping coefficient of 0.007. The anemometer can be used in both forward and reversed flow. Measured flow characteristics up to Mach 0.6 are presented along with application examples including turbulence measurements. (Author)

A78-23625* Development of a drift-correction procedure for a photoelectric spectrometer. G. B. Chapman, II and W. A. Gordon (NASA, Lewis Research Center, Cleveland, Ohio). *Applied Spectroscopy*, vol. 32, Jan.-Feb. 1978, p. 46-53. 6 refs.

A technique has been developed to automatically correct for drifts in the radiometric sensitivity of the detector channels in a direct-reading emission spectrometer. The method utilizes a 1000 W tungsten-halogen reference lamp to illuminate the detectors through the same optical path as that traversed during the analysis of the sample. Detector channel responses to the light are compared to those for the same light intensity at the time of analytical calibration. This corrects for the drift. It is noted that with the exception of positioning the lamp, the procedure is fully automatic. S.C.S.

A78-33365* Instrumentation for propulsion systems development. I. Warshawsky (NASA, Lewis Research Center, Cleveland, Ohio). *Society of Automotive Engineers, Congress and Exposition, Detroit, Mich., Feb. 27-Mar. 3, 1978, Paper 780076*. 11 p. 20 refs.

Various types of instrumentation for the development of propulsion systems are discussed. For the steady-state measurement of local temperature, pressure and flow velocity in gases the devices include: a multielement probe, calibrated thermocouple probes, thermocouple probes designed for low gas velocities, pressure measuring devices for high-speed rotors, and instruments for data pickup from rotating members. For the dynamic measurements of the same factors attention is given to 2-mm diameter pressure transducers, flush-diaphragm transducers, resistance thermometers or thermocouples, and miniature transducers for velocity measurements. Instruments for compressor and turbine blade instrumentation are described with reference to a pyrometer for mapping turbine blade surface temperature, a capacitance method for making rotor clearance measurements, and optical detection procedures for blade vibration amplitude. S.C.S.

A78-38826* Ultraviolet spectrophotometer for measuring columnar atmospheric ozone from aircraft. F. A. Hanser, B. Sellers (Panametrics, Inc., Waltham, Mass.), and D. C. Briehl (NASA, Lewis Research Center, Cleveland, Ohio). *Applied Optics*, vol. 17, May 15, 1978, p. 1649-1656. 40 refs.

An ultraviolet spectrophotometer (UVS) to measure downward solar fluxes from an aircraft or other high altitude platform is described. The UVS uses an ultraviolet diffuser to obtain large angular response with no aiming requirement, a twelve-position filter wheel with narrow (2-nm) and broad (20-nm) bandpass filters, and an ultraviolet photodiode. The columnar atmospheric ozone above the UVS (aircraft) is calculated from the ratios of the measured ultraviolet fluxes. Comparison with some Dobson station measurements gives agreement to 2%. Some UVS measured ozone profiles over the Pacific Ocean for November 1976 are shown to illustrate the instrument's performance. (Author)

N78-11368*/ Teledyne Systems Co. Northridge, Calif
STRAPDOWN GYRO TEST PROGRAM Final Report, 1 Jun. 1978 - 1 Sep. 1977

R B Irvine and R VanAlstine Oct. 1977 59 p refs
(Contract NAS3-31909)
(NASA-CR-150458) Avail. NTIS HC A04/MF A01 CSCL 14B

The power spectral noise characteristic performance of the Teledyne two-degree-of-freedom dry tuned gimbal gyroscope was determined. Tests were conducted using a current configuration SDG-5 gyro in conjunction with test equipment with minor modification. Long term bias stability tests were conducted as well as some first difference performance tests. The gyro, test equipment, and the tests performed are described. Results are presented. (Author)

A78-41464* Compact electron-beam source for formation of neutral beams of very low vapor pressure materials. J. A. Rutherford and D. A. Vroom (IRT Corp., San Diego, Calif.). *Review of Scientific Instruments*, vol. 49, July 1978, p. 1008-1010. Contract No. NAS3-17759.

In order to form metal vapors for neutral beam studies, an electron-beam heater and a power supply have been designed. The source, which measures about 30 x 50 x 70 mm, consists of a filament, accelerating plate (defined by pole pieces), and a supported target. The electrons from the filament are focused by the field penetration through a 2 mm slit in the high-voltage cage. They are then accelerated to about 5 kV to a ground plate. The electrons then follow a path in the magnetic field and strike the sample to be heated on its front surface. The assembly is attached to a water-cooled base plate. The electron beam source has produced beams of Ta and C particles with densities of about 10 to the 8th power/cu cm. S.C.S.

36 LASERS AND MASERS

Includes parametric amplifiers.

N78-13421* National Aeronautics and Space Administration, Lewis Research Center, Cleveland, Ohio.

SMALL-SIGNAL GAIN DIAGNOSTIC MEASUREMENTS IN A FLOWING CO₂ PIN DISCHARGE LASER

R. A. Blech, E. J. Manista, and J. W. Dunning, Jr. Nov. 1977
17 p refs
(NASA-TM-73843; E-9430) Avail: NTIS HC A02/MF A01 CSCL 20E

Small-signal gain diagnostic measurements were conducted on closed loop, high power, carbon dioxide laser to assess the coupling between gas flow velocity and resonator saturation. Parameters investigated included optical cavity and discharge power. Results of gain measurements within and downstream of the excitation volume are presented for a laser gas composition He:N₂:CO₂ of 10:7:1 at 90 torr. The gain at constant discharge power was observed to be dependent upon discharge power level and time. An important result of this study is that the effects of gain swept downstream of the discharge region must be considered in the resonator design if efficient extraction of stored optical energy is desired. Author

N78-14386* National Aeronautics and Space Administration, Lewis Research Center, Cleveland, Ohio.

DISTRIBUTION OF E/N AND N SUB e IN A CROSS-FLOW ELECTRIC DISCHARGE LASER

John W. Dunning, Jr., Richard B. Lancashire, and Eugene J. Manista 1976 17 p refs Presented at 29th Ann. Gaseous Electron. Conf., Cleveland, 19-22 Oct. 1976; sponsored by GE and Am. Phys. Soc.
(NASA-TM-73807; E-9390) Avail: NTIS HC A02/MF A01 CSCL 20E

The spatial distribution of the ratio of electric field to neutral gas density on a flowing gas, multiple pin-to-plane discharge was measured in a high-power, closed loop laser. The laser was operated at a pressure of 140 torr (1:7:20, CO₂, N₂, He) with typically a 100 meter/second velocity in the 5 x 8 x 135 centimeter discharge volume. E/N ratios ranged from 2.7 x 10 to the minus 16th power to 1.4 x 10 to the minus 16th power volts/cm along the discharge while the electron density ranged from 2.8 x 10 to the 10th power to 1.2 x 10 to the 10th power cm³. Author

N78-21441* National Aeronautics and Space Administration, Lewis Research Center, Cleveland, Ohio.

A REVIEW OF THE THERMOELECTRONIC LASER ENERGY CONVERTER (TELEC) PROGRAM AT LEWIS RESEARCH CENTER

D. L. Alger, E. J. Manista, and R. W. Thompson 1978 19 p refs Presented at 3d Conf. on Radiation Energy Conversion, Moffett Field, Calif., 26-27 Jan. 1978; sponsored by NASA
(NASA-TM-73888; E-9503) Avail: NTIS HC A02/MF A01 CSCL 20E

The investigation of the Thermoelectronic Laser Energy Converter (TELEC) concept began with a feasibility study of a 1 megawatt sized TELEC system. The TELEC was to use either cesium vapor or hydrogen as the plasma medium. The cesium vapor TELEC appears to be the more practical device studied with an overall calculated conversion efficiency of greater than 48%. Following this study, a small TELEC cell was fabricated which demonstrated the conversion of a small amount of laser power to electrical power. The cell developed a short circuit current of 0.7 amperes and an open circuit voltage, as extrapolated from volt-ampere curves, of about 1.5 volts. Author

A78-24886* Distribution of E/N and N/e in a cross-flow electric discharge laser. J. W. Dunning, Jr., R. B. Lancashire, and E. J. Manista (NASA, Lewis Research Center, Cleveland, Ohio). *General Electric Co. and American Physical Society, Annual Gaseous Electronics Conference, 29th, Cleveland, Ohio, Oct. 19-22, 1976*, Paper. 16 p. 5 refs.

Measurements have been conducted of the effect of the convection of ions and electrons on the discharge characteristics in a large scale laser. The results are presented for one particular distribution of ballast resistance. Values of electric field, current density, input power density, ratio of electric field to neutral gas density (E/N), and electron number density were calculated on the basis of measurements of the discharge properties. In a number of graphs, the E/N ratio, current density, power density, and electron density are plotted as a function of row number (downstream position) with total discharge current and gas velocity as parameters. From the dependence of the current distribution on the total current, it appears that the electron production in the first two rows significantly affects the current flowing in the succeeding rows. G.R.

N78-13420* Rockwell International Corp., Anaheim, Calif. ANALYSIS AND DESIGN OF A HIGH POWER LASER ADAPTIVE PHASED ARRAY TRANSMITTER Final Report G. E. Meyers, J. F. Suohoo, J. Winocur, N. A. Messie, W. H. Southwell, R. A. Brandewie, and C. L. Hayes Dec. 1977 190 p refs

(Contract NAS3-18937)
(NASA-CR-134952; C75-537/501) Avail: NTIS HC A13/MF A01 CSCL 20E

The feasibility of delivering substantial quantities of optical power to a satellite in low earth orbit from a ground based high energy laser (HEL) coupled to an adaptive antenna was investigated. Diffraction effects, atmospheric transmission efficiency, adaptive compensation for atmospheric turbulence effects, including the servo bandwidth requirements for this correction, and the adaptive compensation for thermal blooming were examined. To evaluate possible HEL sources, atmospheric investigations were performed for the CO₂, (C-12)(O-18)2 isotope, CO and DF wavelengths using output antenna locations of both sea level and mountain top. Results indicate that both excellent atmospheric and adaptive efficiency can be obtained for mountain top operation with a micron isotope laser operating at 9.1 um, or a CO laser operating single line (P10) at about 5.0 (C-12)(O-18)2um, which was a close second in the evaluation. Four adaptive power transmitter system concepts were generated and evaluated, based on overall system efficiency, reliability, size and weight, advanced technology requirements and potential cost. A multiple source phased array was selected for detailed conceptual design. The system uses a unique adaption technique of phase locking independent laser oscillators which allows it to be both relatively inexpensive and most reliable with a predicted overall power transfer efficiency of 53%. Author

N78-19611* Avco-Everett Research Lab., Everett, Mass.
LASER ABSORPTION PHENOMENA IN FLOWING GAS DEVICES Final Technical Report
 P. K. Chapman and J. H. Otis Jun. 1978 126 p refs
 (Contract NAS3-18859)
 (NASA-CR-135129) Avail: NTIS HC A06/MF A01 CSCL 20E

A theoretical and experimental investigation is presented of inverse Bremsstrahlung absorption of CW CO₂ laser radiation in flowing gases seeded with alkali metals. In order to motivate this development, some simple models are described of several space missions which could use laser powered rocket vehicles. Design considerations are given for a test cell to be used with a welding laser, using a diamond window for admission of laser radiation at power levels in excess of 10 kW. A detailed analysis of absorption conditions in the test cell is included. The experimental apparatus and test setup are described and the results of experiments presented. Injection of alkali seedant and steady state absorption of the laser radiation were successfully demonstrated, but problems with the durability of the diamond windows at higher powers prevented operation of the test cell as an effective laser powered thruster. Author

N78-19480* Hughes Research Labs., Malibu, Calif.
EXCIMER LASERS Final Report, 30 May 1978 - 10 Jun. 1978
 A. J. Palmer, L. D. Hess, R. R. Stephens, and D. M. Pepper
 Nov. 1977 129 p refs
 (Contract NAS3-18707)
 (NASA-CR-155949) Avail: NTIS HC A07/MF A01 CSCL 20E

The results of a two-year investigation into the possibility of developing continuous wave excimer lasers are reported. The program included the evaluation and selection of candidate molecular systems and discharge pumping techniques. The K Ar/K₂ excimer dimer molecules and the xenon fluoride excimer molecule were selected for study; each used a transverse and capillary discharges pumping technique. Experimental and theoretical studies of each of the two discharge techniques applied to each of the two molecular systems are reported. Discharge stability and fluorine consumption were found to be the principle impediments to extending the XeF excimer laser into the continuous wave regime. Potassium vapor handling problems were the principal difficulty in achieving laser action on the K Ar/K₂ system. Of the four molecular systems and pumping techniques explored, the capillary discharge pumped K Ar/K₂ system appears to be the most likely candidate for demonstrating continuous wave excimer laser action primarily because of its predicted lower pumping threshold and a demonstrated discharge stability advantage. Author

N78-20489* Physical Sciences, Inc., Woburn, Mass.
ANALYTICAL STUDY OF LASER SUPPORTED COMBUSTION WAVES IN HYDROGEN Final Report, 10 Dec. 1978 - 4 Dec. 1977
 N. H. Kemp and R. G. Root Aug. 1977 119 p refs
 (Contract NAS3-20381)
 (NASA-CR-135349; PSI-TR-97) Avail: NTIS HC A06/MF A01 CSCL 20E

A one-dimensional energy equation, with constant pressure and area, was used to model the LSC wave. This equation balances convection, conduction, laser energy absorption, radiation energy loss and radiation energy transport. Solutions of this energy equation were obtained to give profiles of temperature and other properties, as well as the relation between laser intensity and mass flux through the wave. The flow through the LSC wave was then conducted through a variable pressure, variable area streamtube to accelerate it to high speed, with the propulsion application in mind. A numerical method for coupling the LSC wave model to the streamtube flow was developed and a sample calculation was performed. The result shows that 42% of the

laser power has been radiated away by the time the gas reaches the throat. It was concluded that in the radially confined flows of interest for propulsion applications, transverse velocities would be less important than in the unconfined flows where air experiments have been conducted. Author

N78-25407* Hughes Aircraft Co., Culver City, Calif.
CLOSED CYCLE ELECTRIC DISCHARGE LASER DESIGN INVESTIGATION Final Report

Philip K. Barty and Richard C. Smith Mar. 1978 95 p refs
 (Contract NAS3-20100)
 (NASA-CR-135408; P78-128) Avail: NTIS HC A05/MF A01 CSCL 20E

Closed cycle CO₂ and CO electric discharge lasers were studied. An analytical investigation assessed scale-up parameters and design features for CO₂, closed cycle, continuous wave, unstable resonator, electric discharge lasing systems operating in space and airborne environments. A space based CO system was also examined. The program objectives were the conceptual designs of six CO₂ systems and one CO system. Three airborne CO₂ designs, with one, five, and ten megawatt outputs, were produced. These designs were based upon five minute run times. Three space based CO₂ designs, with the same output levels, were also produced, but based upon one year run times. In addition, a conceptual design for a one megawatt space based CO laser system was also produced. These designs include the flow loop, compressor, and heat exchanger, as well as the laser cavity itself. The designs resulted in a laser loop weight for the space based five megawatt system that is within the space shuttle capacity. For the one megawatt systems, the estimated weight of the entire system including laser loop, solar power generator, and heat radiator is less than the shuttle capacity. Author

N78-26870* National Aeronautics and Space Administration
 Lewis Research Center, Cleveland, Ohio.
CONSIDERATIONS TO ACHIEVE DIRECTIONALITY FOR GAMMA RAY LASERS
 e36
 S. Jha (Cincinnati Univ.) and J. Blue (Princeton Univ. Partially Ionized Plasmas, Including the 3rd Symp. on Uranium Plasmas Sep. 1976 p 275-279 refs (For availability see N78-26837 17-70)
 (Grant N6G-3091)
 Avail: NTIS HC A13/MF A01 CSCL 20E

A method of alignment of nuclei for a gamma ray laser and a means of achieving preferential emission of radiation along the crystal axis are studied. Atomic alignment was achieved by materials researchers who made composite structures composed of needle-like single crystals all with the same orientation and all pointing in the same direction contained in a matrix of cobalt or nickel. The proposed method of preferential emission of radiation along the aligned needles is to have a symmetric field gradient at the nucleus and a sequence of excited levels of spin and parity 2(+) and 0(+). The proposed scheme reduces the density of excited states required for lasing and reduces the linewidth due to inhomogeneous broadening. Mossbauer absorption experiments intended to test these ideas are outlined. Author

37 MECHANICAL ENGINEERING

Includes auxiliary systems (non-power); machine elements and processes; and mechanical equipment.

N78-10467^o National Aeronautics and Space Administration Lewis Research Center, Cleveland, Ohio OIL COOLING SYSTEM FOR A GAS TURBINE ENGINE Patent

George A. Coffinberry (GE, Cincinnati) and Howard B. Kast, inventors (to NASA) (GE, Cincinnati) Issued 18 Aug. 1977 10 p Filed 17 Jul. 1975 Sponsored by NASA (NASA-Case-LEW-12321-1; US-Patent-4,041,697; US-Patent-Appl-SN-598641; US-Patent-Class-60-39-28R; US-Patent-Class-60-39-66; US-Patent-Class-415-180; US-Patent-Class-123-41-33; US-Patent-Class-123-122E; US-Patent-Class-137-104) Avail: US Patent Office CSCL 21E

A gas turbine engine fuel delivery and control system is provided with means to recirculate all fuel in excess of fuel control requirements back to aircraft fuel tank, thereby increasing the fuel pump heat sink and decreasing the pump temperature rise without the addition of valving other than that normally employed. A fuel/oil heat exchanger and associated circuitry is provided to maintain the hot engine oil in heat exchange relationship with the cool engine fuel. Where anti-icing of the fuel filter is required, means are provided to maintain the fuel temperature entering the filter at or above a minimum level to prevent freezing thereof. Fluid circuitry is provided to route hot engine oil through a plurality of heat exchangers disposed within the system to provide for selective cooling of the oil.

Official Gazette of the U.S. Patent Office

N78-10468^o National Aeronautics and Space Administration Lewis Research Center, Cleveland, Ohio IMPACT ABSORBING BLADE MOUNTS FOR VARIABLE PITCH BLADES Patent

Richard Ravenhall (GE, Cincinnati), Charles T. Salemme (GE, Cincinnati), and Arthur P. Adamson, inventors (to NASA) (GE, Cincinnati) Issued 13 Sep. 1977 6 p Filed 29 May 1975 Sponsored by NASA (NASA-Case-LEW-12313-1; US-Patent-4,047,840; US-Patent-Appl-SN-581751; US-Patent-Class-416-135; US-Patent-Class-416-141; US-Patent-Class-416-220R; US-Patent-Class-416-248) Avail: US Patent Office CSCL 131

A variable pitch blade and blade mount are provided that are suitable for propellers, fans and the like and which have improved impact resistance. Composite fan blades and blade mounting arrangements permit the blades to pivot relative to a turbine hub about an axis generally parallel to the centerline of the engine upon impact of a large foreign object, such as a bird. Centrifugal force recovery becomes the principal energy absorbing mechanism and a blade having improved impact strength is obtained.

Official Gazette of the U.S. Patent Office

N78-10474^o National Aeronautics and Space Administration Lewis Research Center, Cleveland, Ohio STABILITY OF NUMERICAL INTEGRATION TECHNIQUES FOR TRANSIENT ROTOR DYNAMICS

Albert F. Kasck 1977 22 p refs (NASA-TP-1092; E-9252) Avail: NTIS HC A02/MF A01 CSCL 21E

A finite element model of a rotor bearing system was analyzed to determine the stability limits of the forward backward, and centered Euler Runge-Kutta, Milne, and Adams numerical integration techniques. The analysis concludes that the highest frequency mode determines the maximum time step for a stable solution. Thus, the number of mass elements should be minimized. Increasing the damping can sometimes cause numerical instability. For a uniform shaft, with 10 mass elements, operating at approximately the first critical speed, the maximum time step for the Runge-Kutta, Milne, and Adams methods is that which corresponds to approximately 1 degree of shaft movement. This is independent of rotor dimensions.

Author

N78-18438^o National Aeronautics and Space Administration Lewis Research Center, Cleveland, Ohio

METHOD OF FORMING METAL HYDRIDE FILMS Patent Robert Steinberg, Donald L. Alger, and Dale W. Cooper, inventors (to NASA) Issued 25 Oct. 1977 5 p Filed 20 Feb. Supersedes N78-18262 (14 - 09, p 1100)

(NASA-Case-LEW-12083-1; US-Patent-4,055,686; US-Patent-Appl-SN-859882; US-Patent-Class-427-124; US-Patent-Class-427-126; US-Patent-Class-427-256; US-Patent-Class-427-248E; US-Patent-Class-427-260; US-Patent-Class-250-489; US-Patent-Class-313-618) Avail: US Patent Office CSCL 13H

The substrate to be coated (which may be of metal, glass or the like) is cleaned, both chemically and by off-sputtering in a vacuum chamber. In an ultra-high vacuum system, vapor deposition by a sublimator or vaporizer coats a cooled shroud disposed around the substrate with a thin film of hydride forming metal which getters any contaminant gas molecules. A shutter is then opened to allow hydride forming metal to be deposited as a film or coating on the substrate. After the hydride forming metal coating is formed, deuterium or other hydrogen isotopes are bled into the vacuum system and diffused into the metal film or coating to form a hydride of metal film. Higher substrate temperatures and pressures may be used if various parameters are appropriately adjusted.

Official Gazette of the U.S. Patent Office

N78-13438^o National Aeronautics and Space Administration Lewis Research Center, Cleveland, Ohio

DESIGN CONSIDERATIONS IN MECHANICAL FACE SEALS FOR IMPROVED PERFORMANCE. 1: BASIC CONFIGURATIONS

Lawrence P. Ludwig and Harold F. Greiner (Sealol, Inc., Providence, R. I.) 1977 20 p refs Presented at Winter Annual Meeting, Atlanta, Ga., 27 Nov. - 2 Dec. 1977 (NASA-TM-73735; E-9298-1) Avail: NTIS HC A02/MF A01 CSCL 11A

Basic assembly configurations of the mechanical face seal are described and some advantages associated with each are listed. The various forms of seal components are illustrated, and functions pointed out. The technique of seal pressure balancing and its application are described; and the concept of the PV factor, its different forms and limitations are discussed. Brief attention is given to seal lubrication, since it is covered in detail in a companion paper. Finally, the operating conditions for various applications of low pressure seals (aircraft transmissions) are listed, and the seal failure mode of a particular application is discussed.

Author

N78-17384^o National Aeronautics and Space Administration Lewis Research Center, Cleveland, Ohio

VARIABLE CYCLE GAS TURBINE ENGINES Patent

James Edward Johnson (GE, Cincinnati) and Tom Foster, inventors (to NASA) (GE, Cincinnati) Issued 27 Dec. 1977 10 p Filed 2 Jun. 1975 Sponsored by NASA

(NASA-Case-LEW-12916-1; US-Patent-4,064,892; US-Patent-Appl-SN-583056; US-Patent-Class-60-261; US-Patent-Class-60-262; US-Patent-Class-60-271) Avail: US Patent Office CSCL 21E

A technique, method, and apparatus were designed for varying the bypass ratio and modulating the flow of a gas turbine engine in order to achieve improved mixed mission performance. Embodiments include gas flow control system for management of core and bypass stream pressure comprising diverter valve means downstream of the core engine to selectively mix or separate the core and bypass exhaust streams. The flow control system may also include variable geometry means for maintaining the engine inlet airflow at a matched design level at all flight velocities. Earth preferred embodiment thus may be converted from a high specific thrust mixed flow cycle at supersonic velocities to a lower specific thrust separated flow turbofan system at subsonic velocities with a high degree of flow variability in each mode of operation.

Official Gazette of the U.S. Patent Office

N78-17388* National Aeronautics and Space Administration. Lewis Research Center, Cleveland, Ohio.

BEARINGS, SEALS, AND LUBRICATION TECHNOLOGY
William J. Anderson 1978 24 p refs Presented at the 1978 Automotive Eng. Congr. and Exposition, Detroit, 27 Feb. - 3 Mar. 1978; sponsored by SAE

(NASA-TM-73851) Avail: NTIS HC A02/MF A01 CSCL 131

Results of selected NASA research programs on rolling-element and fluid-film bearings, gears, and elastohydrodynamic lubrication are reported. Advances in rolling-element bearing material technology, which have resulted in a significant improvement in fatigue life, and which make possible new applications for rolling bearings, are discussed. Research on whirl-resistant, fluid-film bearings, suitable for very high-speed applications, is discussed. An improved method for predicting gear pitting life is reported. An improved formula for calculating the thickness of elastohydrodynamic films (the existence of which help to define the operating regime of concentrated contact mechanisms such as bearings, gears, and cams) is described.

Author

N78-18429* National Aeronautics and Space Administration. Lewis Research Center, Cleveland, Ohio.

STATISTICAL MODEL FOR ASPERITY-CONTACT TIME FRACTION IN ELASTOHYDRODYNAMIC LUBRICATION

Steven M. Sidik and John J. Coy (US Army R and T Lab., Cleveland) Feb. 1978 41 p refs

(NASA-TP-1130; E-9265) Avail: NTIS HC A03/MF A01 CSCL 131

Relations for the asperity contact time fraction during elastohydrodynamic (EHD) lubrication of a typical ball bearing are presented. The analysis is based on a two-dimensional random surface model, and actual profile traces of the bearing surfaces were used as statistical sample records. The results of the analysis show that transition from 90 percent contact to 1 percent contact occurs within a dimensionless film thickness range of approximately 4 to 5. This thickness ratio is several times larger than reported in the literature where one-dimensional random surface models were used.

Author

N78-18512* National Aeronautics and Space Administration. Lewis Research Center, Cleveland, Ohio.

FRICTION AND WEAR BEHAVIOR OF SINGLE-CRYSTAL SILICON CARBIDE IN SLIDING CONTACT WITH VARIOUS METALS

Kazuhisa Miyoshi and Donald H. Buckley 1978 28 p refs Presented at Ann. Meeting of Am. Soc. of Lubrication Engineers, Dearborn, Mich., 17-20 Apr. 1978

(NASA-TM-73782; E-9337) Avail: NTIS HC A03/MF A01 CSCL 11D

Sliding friction experiments were conducted with single-crystal silicon carbide in contact with various metals. Results indicate the coefficient of friction is related to the relative chemical activity of the metals. The more active the metal, the higher the coefficient of friction. All the metals examined transferred to silicon carbide. The chemical activity of the metal and its shear modulus may play important roles in metal transfer, the form of the wear debris and the surface roughness of the metal wear scar. The more active the metal, and the less resistance to shear, the greater the transfer to silicon carbide and the rougher the wear scar on the surface of the metal. Hexagon shaped cracking and fracturing formed by cleavage of both prismatic and basal planes is observed on the silicon carbide surface.

Author

N78-18513* National Aeronautics and Space Administration. Lewis Research Center, Cleveland, Ohio.

SELF-ACTING SHAFT SEALS

Lawrence P. Ludwig 1978 36 p refs Presented at AGARD Power, Energy, and Propulsion Panel Meeting on Seal Technology in Gas Turbine Engines, London, 6-7 Apr. 1978

(NASA-TM-73856) Avail: NTIS HC A03/MF A01 CSCL 11A

Self-acting seals are described in detail. The mathematical models for obtaining a seal force balance and the equilibrium

operating film thickness are outlined. Particular attention is given to primary ring response (seal vibration) to rotating seal face runout. This response analysis reveals three different vibration modes with secondary seal friction being an important parameter. Leakage flow inlet pressure drop and effects of axisymmetric sealing face deformations are discussed. Experimental data on self-acting face seals operating under simulated gas turbine conditions are given. Also a spiral groove seal design operated to 244 m/sec (800 ft/sec) is described.

Author

N78-20511* National Aeronautics and Space Administration. Lewis Research Center, Cleveland, Ohio.

TRIBOLOGICAL PROPERTIES OF SURFACES

Donald H. Buckley 1978 25 p refs Presented at the Intern. Conf. on Mat. Coatings, San Francisco, 3-7 Apr. 1978; sponsored by Am. Vacuum Soc.

(NASA-TM-73896) Avail: NTIS HC A02/MF A01 CSCL 20K

The real area of contact between two solid surfaces is only a small portion of the apparent area. Deformation of these areas can result in solid state contact through surface films. For clean solid to solid contact strong adhesive bonding occurs across the interface. Under these conditions many properties of the solid such as the metallurgical and chemical nature of metals can influence adhesion, friction, and wear behavior. The presence of gases, liquids, and solid films on the surface of solids alter markedly tribological characteristics. These surface films can also considerably change the mechanical effects of solid state contact on bulk material behavior.

Author

N78-20512* National Aeronautics and Space Administration. Lewis Research Center, Cleveland, Ohio.

FRICTION AND WEAR OF SELECTED METALS AND ALLOYS IN SLIDING CONTACT WITH AISI 440 C STAINLESS STEEL IN LIQUID METHANE AND IN LIQUID NATURAL GAS

Donald W. Wisander Feb. 1978 18 p refs

(NASA-TP-1150; E-9195) Avail: NTIS HC A02/MF A01 CSCL 20K

Aluminum, titanium, beryllium, nickel, iron, copper, and several copper alloys were run in sliding contact with AISI 440C in liquid methane and natural gas. All of the metals run except copper and the copper alloys of tin and tin-lead showed severely galled wear scars. Friction coefficients varied from 0.2 to 1.0, the lowest being for copper, copper-17 wt % tin, and copper-8 wt % tin-22 wt % lead. The wear rate for copper was two orders of magnitude lower than that of the other metals run. An additional order of magnitude of wear reduction was achieved by the addition of tin and/or lead to copper.

Author

N78-20513* National Aeronautics and Space Administration. Lewis Research Center, Cleveland, Ohio.

PREDICTED AND EXPERIMENTAL PERFORMANCE OF JET-LUBRICATED 120-MILLIMETER-BORE BALL BEARINGS OPERATING TO 2.5 MILLION DN

Harold H. Coe and Erwin V. Zaretsky Apr. 1978 28 p refs (NASA-TP-1196; E-9288) Avail: NTIS HC A03/MF A01 CSCL 131

Bearing inner- and outer-face temperatures and friction power losses were calculated using two computer programs. The values obtained were compared with previously reported experimental data for 120 mm bore bearings which operated at thrust loads to 22 240 N (5000 lb), shaft speeds to 20 800 rpm, and with two lubricant flow rates. One program severely underestimated the power loss, while the other, called SHABERTH, provided a good prediction of both face temperatures and power losses.

Author

N78-21476* National Aeronautics and Space Administration, Lewis Research Center, Cleveland, Ohio.

CHARACTERIZATION OF WEAR DEBRIS GENERATED IN ACCELERATED ROLLING-ELEMENT FATIGUE TESTS

William R. Jones, Jr. and Richard J. Parker Apr. 1978 28 p refs

(NASA-TP-1203; E-9260) Avail: NTIS HC A03/MF A01 CSCL 131

A ferrographic analysis was used to determine the types and quantities of wear debris generated during accelerated rolling contact fatigue tests. The five-ball rolling contact fatigue tester was used. Ball specimens were made of a corrosion resistant, high-temperature bearing steel. The lubricant was a superrefined naphthenic mineral oil. Conditions included a maximum Hertz stress of 5.52×10^8 to the 9th power Pa and a shaft speed of 10,000 rpm. Four types of wear debris were observed: (1) normal rubbing wear particles, (2) fatigue microspall particles, (3) spheres, and (4) friction polymer deposits. The characterization of wear debris as a function of time was of limited use in predicting fatigue failures in these accelerated tests. Author

N78-21473* National Aeronautics and Space Administration, Lewis Research Center, Cleveland, Ohio.

ROLLING-ELEMENT FATIGUE LIFE OF AISI M-50 AND 18-4-1 BALLS

Richard J. Parker and Erwin V. Zaretsky Apr. 1978 19 p refs

(NASA-TP-1202; E-9350) Avail: NTIS HC A02/MF A01 CSCL 131

Rolling element fatigue studies were conducted with AISI M-50, EFR 18-4-1, and VAR 18-4-1. Groups of 12.7 mm (1/2-in) diameter balls of each material were tested in the five ball fatigue tester. Test conditions included a load of 1540 N (347 lb) giving a maximum Hertz stress of 5520 MPa (800 000 psi), a shaft speed of 10,700 rpm, and a contact angle of 30 deg. Tests were run at a race temperature of 339 K (150 F) with a type 2 ester lubricant. The rolling element fatigue life of AISI M-50 was not significantly different from that of EFR 18-4-1 or VAR 18-4-1 based on a statistical comparison of the test results. Author

N78-22377* National Aeronautics and Space Administration, Lewis Research Center, Cleveland, Ohio.

FEROGRAPHIC ANALYSIS OF WEAR PARTICLES FROM SLIDING ELASTOHYDRODYNAMIC EXPERIMENTS

William R. Jones, Jr., H. S. Nagara (Mechanical Technology, Inc., Latham, N. Y.), and Ward O. Winer (Georgia Inst. of Tech., Atlanta) Apr. 1978 31 p refs

(NASA-TP-1230; E-9300) Avail: NTIS HC A03/MF A01 CSCL 20K

The Ferrograph was used to analyze wear debris generated in a sliding elasto-hydrodynamic contact. The amount of wear debris correlates well with the ratio of film thickness to composite surface roughness (A ratio). The general wear level parameter and the wear severity index yielded similar correlations with average A ratios. Essentially all the generated wear particles were of the normal rubbing wear type. The Ferrograph was more sensitive in detecting the wear debris than was the commonly used emission spectrograph. Author

N78-24546* National Aeronautics and Space Administration, Lewis Research Center, Cleveland, Ohio.

AUTOMOTIVE GAS TURBINE FUEL CONTROL Patent

Harold Gold, inventor (to NASA) Issued 14 Mar. 1978 14 p Filed 8 Nov. 1976 Supersedes N77-13426 (15 04, p 0477)

(NASA-Case-LEW-12785-1 US-Patent-4,078,378 US-Patent-App'l-SN-739909 US-Patent-Class-60-39 28R) Avail US Patent Office CSCL 21A

A fuel control system is reported for automotive-type gas turbines and particularly advanced gas turbines utilizing variable geometry components to improve mileage and reduce pollution emission. The fuel control system compensates for fuel density variations, inlet temperature variations, turbine vane actuation, acceleration and turbine braking. These parameters are utilized to control various orifices, spool valves and pistons.

Official Gazette of the U.S. Patent Office

N78-25423* National Aeronautics and Space Administration, Lewis Research Center, Cleveland, Ohio.

SOME EFFECTS OF COMPOSITION ON FRICTION AND WEAR OF GRAPHITE-FIBER-REINFORCED POLYIMIDE LINERS IN PLAIN SPHERICAL BEARINGS

Harold E. Sliney and Thomas P. Jacobson May 1978 23 p refs

(NASA-TP-1229; E-9296) Avail: NTIS HC A02/MF A01 CSCL 131

Oscillating, plain spherical bearings with graphite-fiber-reinforced polyimide (GFRPI) liners were tested for friction and wear from 25 to 315 C. A condensation polymer was compared with an addition polymer, and a high-modulus fiber was compared with a lower cost, low-modulus fiber. All polymer fiber combinations gave friction coefficients from 0.05 to 0.18 and low wear. Adding CdO and CdI₂ reduced the wear of degassed bearings in dry air. These additives were not needed when the bearing liners contained adsorbed moisture. Although, at 25 C, MoS₂ reduced the friction and wear of the base composite at unit loads above 70,000,000 N/m squared (10,000 psi), it had no beneficial effect at lighter loads. Author

N78-26442* National Aeronautics and Space Administration, Lewis Research Center, Cleveland, Ohio.

DESIGN APPROACHES TO MORE ENERGY EFFICIENT ENGINES

Neal T. Saunders, Raymond S. Colleday, and Lawrence E. Macioco Jul. 1978 13 p refs Presented at the 14th Propulsion Conf., Las Vegas, Nev., 25-27 Jul. 1978; cosponsored by AIAA and SAE

(NASA-TM-78893) Avail: NTIS HC A02/MF A01 CSCL 10B

The status of NASA's Energy Efficient Engine Project, a comparative government-industry effort aimed at advancing the technology base for the next generation of large turbofan engines for civil aircraft transports is summarized. Results of recently completed studies are reviewed. These studies involved selection of engine cycles and configurations that offer potential for at least 12% lower fuel consumption than current engines and also are economically attractive and environmentally acceptable. Emphasis is on the advancements required in component technologies and systems design concepts to permit future development of these more energy efficient engines. G.Y.

N78-26443* National Aeronautics and Space Administration, Lewis Research Center, Cleveland, Ohio.

ADDITIONAL ASPECTS OF ELASTOHYDRODYNAMIC LUBRICATION

Bernard J. Hamrock Jun. 1978 15 p refs Presented at the Intern. Conf. Fundamentals of Tribology, Cambridge, Mass., 19-22 Jun. 1978, sponsored by ARO, DARPA, MIT, and ONR

(NASA-TM-78898; E-9634) Avail: NTIS HC A02/MF A01 CSCL 11H

An up-to-date review of the varying aspects of elasto-hydrodynamic lubrication is presented. Some recent work on elasto-hydrodynamic lubrication of materials of low elastic modulus as well as on hydrodynamic lubrication is included. Both these topics are applicable for contacts with any ellipticity parameter (ranging from a circular contact to a line contact). G.G.

N78-26444* National Aeronautics and Space Administration, Lewis Research Center, Cleveland, Ohio.

PROPOSED DESIGN PROCEDURE FOR TRANSMISSION SHAFTING UNDER FATIGUE LOADING

Stuart F. Loewenthal 1978 10 p refs To be presented at the 5th Ann Meeting of the Natl. Conf. on Power Transmission, Philadelphia, 7-9 Nov. 1978, sponsored by the III. Inst. of Technol.

(NASA-TM-78927; E-9667) Avail: NTIS HC A02/MF A01 CSCL 131

A new standard for the design of transmission shafting is reported. Computed was the diameter of rotating solid steel shafts under combined cyclic bending and steady torsion is presented. The formula is based on an elliptical variation of endurance strength with torque exhibited by combined stress fatigue data. Fatigue factors are cited to correct specimen bending endurance strength data for use in the shaft formula. A design example illustrates how the method is to be applied. G.G.

N78-26445* National Aeronautics and Space Administration, Lewis Research Center, Cleveland, Ohio.
SOME LOAD LIMITS AND SELF-LUBRICATING PROPERTIES OF PLAIN SPHERICAL BEARINGS WITH MOLDED GRAPHITE FIBER REINFORCED POLYIMIDE LINERS TO 320 C

Harold E. Stiney 1978 13 p refs To be presented at the Joint Lubrication Conf., Minneapolis, 24-26 Oct. 1978; cosponsored by the Am. Soc. of Lubrication Engr. and the Am. Soc. of Mech. Engr.
 (NASA-TM-78936; E-9678) Avail: NTIS HC A02/MF A01 CSCL 131

Plain spherical bearings with molded liners of self-lubricating graphite fiber-polyimide composite were developed and their dynamic load capacities were determined. Liners were prepared by transfer molding a prepolymer resin-fiber mix into the space between the ball and outer race, the completing polymerization under heat and pressure. Bearing dynamic load capacities were in excess of 140 MPa (20,000 psi) from room temperature to 260 C and about 70 MPa (10,000 psi) at 320 C. Friction coefficients were about 0.20 at room temperatures and light loads and tended to decrease with increasing temperatures and loads to about 0.15. Thermal expansion of the liner at uniform bearing temperatures of 200 C or higher produced a bearing preload which could be alleviated by providing an initial internal diametral clearance of 0.05 to 0.10 mm. Author

N78-26446* National Aeronautics and Space Administration, Lewis Research Center, Cleveland, Ohio.
FILTRATION EFFECTS ON BALL BEARING LIFE AND CONDITION IN A CONTAMINATED LUBRICANT

Stuart H. Loewenthal and Donald W. Moyer (Tribon Mfg. Co., Cleveland) Oct. 1978 26 p refs Proposed for presentation at the Joint Lubrication Conf., Minneapolis, 24-26 Oct. 1978; sponsored by the Am. Soc. of Mech. Engr. and the Am. Soc. of Lubrication Engr.
 (NASA-TM-78907; E-9418) Avail: NTIS HC A03/MF A01 CSCL 131

Ball bearings were fatigue tested with a noncontaminated lubricant and with a contaminated lubricant under four levels of filtration. The test filters had absolute particle removal ratings of 3, 30, 49, and 105 microns. Aircraft turbine engine contaminants were injected into the filter's supply line at a constant rate of 125 milligrams per bearing hour. Bearing life and running track condition generally improved with finer filtration. The experimental lives of 3 and 30 micron filter bearings were statistically equivalent, approaching those obtained with the noncontaminated lubricant bearings. Compared to these bearings, the lives of the 49 micron bearings were statistically lower. The 105 micron bearings experienced gross wear. The degree of surface distress, weight loss, and probable failure mode were dependent on filtration level, with finer filtration being clearly beneficial. Author

N78-26447* National Aeronautics and Space Administration, Lewis Research Center, Cleveland, Ohio.
GRAPHITE-FIBER-REINFORCED POLYIMIDE LINERS OF VARIOUS COMPOSITIONS IN PLAIN SPHERICAL BEARINGS

Harold E. Stiney and Thomas P. Jacobson Aug. 1978 19 p refs Proposed for presentation at the 2d Intern Conf. on Solid Lubrication, Denver, 14-16 Aug. 1978; sponsored by the Am. Soc. of Lubrication Engr.
 (NASA-TM-78908; E-9298) Avail: NTIS HC A02/MF A01 CSCL 131

A plain spherical bearing design with a ball diameter of 28.6 mm, a race length of 12.7 mm, and a 1.7-mm-thick, molded composite liner was evaluated. The liner material is a self-lubricating composite of graphite-fiber-reinforced polyimide resin (GFRPI). The liner is prepared by transfer molding a mixture of one part chopped graphite fiber and one part partially polymerized resin into the space between the bearing ball and the outer race and then completing the polymerization under heat and pressure. Several liner compositions were evaluated: two types of polyimide, condensation and addition, two types of graphite fiber, low and high modulus, and four powder additives - cadmium

oxide, cadmium iodide, graphite fluoride, and molybdenum disulfide. The bearings were oscillated + or - 15 deg at 1 Hz for 20 kilocycles under a radial unit load of 28 MN sq m (4200 psi) in dry air at 25, 200, or 315 C. Both types of fiber and polyimide gave low friction and wear. A simple equation was developed to fit the wear-time data and adequately predicted wear to 100 kilocycles. Author

N78-27435* National Aeronautics and Space Administration, Lewis Research Center, Cleveland, Ohio.
ELASTOHYDRODYNAMIC FILM THICKNESS MEASUREMENTS OF ARTIFICIALLY PRODUCED SURFACE DENTS AND GROOVES

L. D. Wedeven and C. Cusano (Illinois Univ., Urbana) 1978 39 p refs Proposed for presentation at the Joint Lubrication Conf., Minneapolis, Minn., 24-26 Oct. 1978; Sponsored by ASME and Am. Soc. of Lubrication Engineers
 (NASA-TM-78949; E-9893) Avail: NTIS HC A03/MF A01 CSCL 131

Elastohydrodynamic (EHD) film thickness measurements using optical interferometry were made of artificially produced dents and grooves under rolling and sliding conditions. These measurements are compared to stylus traces of the dent and groove profiles to determine the local deformation associated with micro-EHD pressure generation. The surface geometry associated with the dents and grooves became intimately involved in the lubrication process itself, creating local pressure variations that substantially deformed the local surface geometry, particularly under sliding conditions. The rolling results implied surface initiated fatigue, and the sliding results showed clearly the EHD surface interactions that must occur prior to scuffing failure. J.A.M.

N78-28457* National Aeronautics and Space Administration, Lewis Research Center, Cleveland, Ohio.
EFFECT OF FILTRATION ON ROLLING-ELEMENT-BEARING LIFE IN CONTAMINATED LUBRICANT ENVIRONMENT
 Stuart H. Loewenthal, Donald W. Moyer (Tribon Bearing Co., Cleveland), and John J. Sherlock (Tribon Bearing Co., Cleveland) Jul. 1978 34 p refs
 (NASA-TP-1272; E-9418) Avail: NTIS HC A03/MF A01 CSCL 131

Fatigue tests were conducted on groups of 65 millimeter-bore ball bearings under four levels of filtration with and without a contaminated MIL-L-23699 lubricant. The baseline series used noncontaminated oil with 49 micron absolute filtration. In the remaining tests contaminants of the composition found in aircraft engine filters were injected into the filter's supply line at a constant rate of 125 milligrams per bearing-hour. The test filters had absolute particle removal ratings of 3, 30, 49, and 105 microns (0.45, 10, 30, and 70 microns nominal), respectively. Bearings were tested at 15,000 rpm under 4580 newtons radial load. Bearing life and running track condition generally improved with finer filtration. The 3 and 30 micron filter bearings in a contaminated lubricant had statistically equivalent lives, approaching those from the baseline tests. The experimental lives of 49 micron bearings were approximately half the baseline bearing's lives. Bearings tested with the 105 micron filter experienced wear failures. The degree of surface distress, weight loss, and probable failure mode were found to be dependent on filtration level, with finer filtration being clearly beneficial. Author

N78-28488* National Aeronautics and Space Administration, Lewis Research Center, Cleveland, Ohio.
ELASTOHYDRODYNAMIC LUBRICATION OF ELLIPTICAL CONTACTS FOR MATERIALS OF LOW ELASTIC MODULUS. 2: STARVED CONJUNCTION

Bernard J. Hamrock and Duncan Dowson (Leeds Univ., England) Jul. 1978 26 p refs Proposed for presentation at the Joint Lubrication Conf., Minneapolis, 24-26 Oct. 1978; sponsored by the Am. Soc. of Lubrication Engr. and the Am. Soc. of Mech. Engr.
 (NASA-TP-1273; E-9558) Avail: NTIS HC A03/MF A01 CSCL 11H

Lubricant starvation effects on minimum film thickness for low-elastic modulus materials are studied by moving the inlet boundary closer to the contact center. Contour plots of the pressure and film thickness in and around the contact were obtained for fully flooded and starved lubrication conditions. These contour plots show that the inlet pressure contours become less circular and that the film thickness decreases substantially as the severity of starvation increases. G.G.

N78-28489* National Aeronautics and Space Administration, Lewis Research Center, Cleveland, Ohio.
METHOD OF COLD WELDING USING ION BEAM TECHNOLOGY Patent Application

Bernard L. Sater, inventor (to NASA) Filed 28 Jul. 1978 10 p
 (NASA-Case-LEW-12982-1; US-Patent-Appl-SN-929084) Avail: NTIS HC A02/MF A01 CSCL 13H

A method is described for cold welding metals in a vacuum using ion beams to prepare the surfaces of metals to be joined. The figure is a schematic diagram of an ion beam apparatus for carrying out the method. An expellant gas is stored in a high pressure tank and delivered to a ion source assembly. The ion source produces a unidirectional beam of gas molecules with uniform energies which, in a vacuum environment, is directed onto each surface to be cleared and effectively sputters away the contamination oxide layer to expose clean underlying metal. When the surfaces to be joined are sufficiently clean, they are pressed together with pressure adequate to assure that their asperities are brought into intimate contact throughout the area to be joined. This process provides a solid state cold weld with metal-to-metal bonding without causing gross deformation due to plastic flow and thinning of the material at the joint. NASA

N78-30305* National Aeronautics and Space Administration, Lewis Research Center, Cleveland, Ohio.
LEWIS RESEARCH CENTER SUPPORT OF CHRYSLER UPGRADED ENGINE PROGRAM

E. L. Warren *In* DOE Highway Vehicle Systems Mar. 1978 p 143-149 (For primary document see N78-30293 21-31)
 Avail: NTIS HC A20/MF A01 CSCL 21A

N78-30314* National Aeronautics and Space Administration, Lewis Research Center, Cleveland, Ohio.
STIRLING ENGINE PROJECT STATUS

R. G. Ragdale *In* DOE Highway Vehicle Systems Mar. 1978 p 241-243 (For primary document see N78-30293 21-31)
 Avail: NTIS HC A20/MF A01 CSCL 21A

N78-30316* National Aeronautics and Space Administration, Lewis Research Center, Cleveland, Ohio

INITIAL TEST RESULTS WITH SINGLE CYLINDER RHOMBIC DRIVE STIRLING ENGINE
 James E. Carrell *In* DOE Highway Vehicle Systems Mar. 1978 p 254-258 (For primary document see N78-30293 21-31)
 Avail: NTIS HC A20/MF A01 CSCL 13I

N78-30318* National Aeronautics and Space Administration, Lewis Research Center, Cleveland, Ohio.
MATERIALS TECHNOLOGY ASSESSMENT FOR STIRLING ENGINES

Joseph R. Stephens *In* DOE Highway Vehicle Systems Mar. 1978 p 267-274 (For primary document see N78-30293 21-31)
 Avail: NTIS HC A20/MF A01 CSCL 21A

N78-30384* National Aeronautics and Space Administration, Lewis Research Center, Cleveland, Ohio.
LIQUID ROCKET ENGINE TURBOPUMP ROTATING-SHAFT SEALS NASA Space Vehicle Design Criteria, Chemical Propulsion

R. E. Burcham and Russell B. Keller, Jr., ed. Feb. 1978 160 p refs Prepared in cooperation with Rocketdyne, Canoga Park, Calif.

(NASA-SP-8121) Avail: NTIS HC A08/MF A01 CSCL 11A
 A monograph is organized and presents, for effective use in design, the significant experience and knowledge accumulated in development and operational programs to date. It reviews and assesses current practices, and from them establishes firm guidance for achieving greater consistency in design, increased reliability in the end product, and greater efficiency in the design effort. The monograph is divided into two major sections: state of the art and design criteria. G.Y.

N78-30385* National Aeronautics and Space Administration, Lewis Research Center, Cleveland, Ohio.

EFFECT OF GEOMETRY ON HYDRODYNAMIC FILM THICKNESS

David E. Brewster (AVRADCOM Res. and Technol. Labs.), Bernard J. Hamrock, and Christopher M. Taylor (Leeds Univ., England) Aug. 1978 35 p refs Proposed for presentation at ASLE-ASME Joint Lubrication Conf., Minneapolis, 24-26 Oct. 1978
 (NASA-TP-1287; E-9347; AVRADCOM-TR-78-18) Avail: NTIS HC A03/MF A01 CSCL 20K

The influence of geometry on the isothermal hydrodynamic film separating two rigid solids was investigated. Pressure-viscosity effects were not considered. The minimum film thickness is derived for fully flooded conjunctions by using the Reynolds conditions. It was found that the minimum film thickness had the same speed, viscosity, and load dependence as Kapitza's classical solution. However, the incorporation of Reynolds boundary conditions resulted in an additional geometry effect. Solutions using the parabolic film approximation are compared with those using the exact expression for the film in the analysis. Contour plots are shown that indicate in detail the pressure developed between the solids. Author

N78-33445* National Aeronautics and Space Administration, Lewis Research Center, Cleveland, Ohio.

THE PRACTICAL IMPACT OF ELASTOHYDRODYNAMIC LUBRICATION

William J. Anderson 1978 14 p refs Presented at the 8th Leeds-Lyon Symp on Tribology, Leeds, Engl., 19-22 Sep. 1978
 (NASA-TM-78987; E-9766) Avail: NTIS HC A02/MF A01 CSCL 13I

The use of elastohydrodynamics in the analysis of rolling element bearings is discussed. Relationships for minimum film thickness and tractive force were incorporated into computer codes and used for bearing performance prediction. The lambda parameter (ratio of film thickness to composite surface roughness) was shown to be important in predicting bearing life and failure mode. Results indicate that at values of lambda below 3 failure modes other than the classic subsurface initiated fatigue can occur. S.S.

N78-33467* National Aeronautics and Space Administration, Lewis Research Center, Cleveland, Ohio

MINIMUM FILM THICKNESS IN ELLIPTICAL CONTACTS FOR DIFFERENT REGIMES OF FLUID-FILM LUBRICATION

Bernard J. Hamrock and Duncan Dowson (Leeds Univ., Engl.)

Oct. 1978 26 p refs
(NASA-TP-1342; E-9687) Avail: NTIS HC A02/MF A01 C8C1
11H

The film parameter equations are provided for four fluid-film lubrication regimes found in elliptical contacts. These regimes are isoviscous-rigid; viscous-rigid; elastohydrodynamic of low-elastic-modulus materials, or isoviscous-elastic; and elastohydrodynamic, or viscous-elastic. The influence or lack of influence of elastic and viscous effects is the factor that distinguishes these regimes. The film parameter equations for the respective regimes come from earlier theoretical studies by the authors on elastohydrodynamic and hydrodynamic lubrication of elliptical conjunctions. These equations are restated and the results are presented as a map of the lubrication regimes, with film thickness contours on a log-log grid of the viscosity and elasticity parameters for five values of the ellipticity parameter. The results present a complete theoretical film-parameter solution for elliptical contacts in the four lubrication regimes. L.S.

A78-12737 * # Simplified solution for elliptical-contact deformation between two elastic solids. D. E. Brewe (U.S. Army, Air Mobility Research and Development Laboratory, Cleveland, Ohio) and B. J. Hamrock (NASA, Lewis Research Center, Cleveland, Ohio). *ASME, Transactions, Series F - Journal of Lubrication Technology*, vol. 99, Oct. 1977, p. 485-487. 10 refs.

A linear regression by the method of least squares is made on the geometric variables that occur in the equation for elliptical-contact deformation. The ellipticity and the complete elliptic integrals of the first and second kind are expressed as a function of the x,y-plane principal radii. The ellipticity was varied from 1 (circular contact) to 10 (a configuration approaching line contact). The procedure for solving these variables without the use of charts or a high-speed computer would be quite tedious. These simplified equations enable one to calculate easily the elliptical-contact deformation to within 3 percent accuracy without resorting to charts or numerical methods. (Author)

A78-20591 * # High stiffness seals for rotor critical speed control. D. P. Fleming (NASA, Lewis Research Center, Cleveland, Ohio). *American Society of Mechanical Engineers, Design Engineering Technical Conference, Chicago, Ill., Sept. 26-30, 1977, Paper 77-DET-10* 9 p. 8 refs. Members, \$1.50; nonmembers, \$3.00.

An annular seal is analyzed in which the inlet clearance is larger than the outlet clearance; the flow path may be either stepped or tapered. This design produces radial stiffnesses 1.7 to 14 times that of a constant clearance seal having the same minimum clearance. When sealing high pressure fluids, such as a seal can improve rotor stability and can be used to shift troublesome critical speeds to a more suitable location. (Author)

A78-20808 * # Study of lubricant jet flow phenomena in spur gears - Out of mesh condition. D. P. Townsend (NASA, Lewis Research Center, Cleveland, Ohio) and L. S. Akin (NASA, Lewis Research Center, Cleveland, Ohio; Western Gear Corp., Lynnwood, Calif.). *American Society of Mechanical Engineers, Design Engineering Technical Conference, Chicago, Ill., Sept. 26-30, 1977, Paper 77-DET 104* 8 p. 5 refs. Members, \$1.50; nonmembers, \$3.00.

An analysis was conducted for oil jet lubrication on the disengaging side of a gear mesh. Results of the analysis were computerized and used to determine the oil jet impingement depth for several gear ratios and oil jet to pitch line velocity ratios. An experimental program was conducted on the NASA gear test rig using high speed photography to experimentally determine the oil jet impingement depth on the disengaging side of mesh. Impingement depth reaches a maximum at gear ratio near 1.5 where chopping by the leading gear tooth limits the impingement depth. The pinion impingement depth is zero above a gear ratio of 1.172 for a jet velocity to pitch line velocity ratio of 1.0 and is similar for other velocity ratios. The impingement depth for gear and pinion are equal

and approximately one-half the maximum at a gear ratio of 1.0. Impingement depth on either the gear or pinion may be improved by relocation of the jet from the pitch line or by changing the jet angle. Results of the analysis were verified by experimental results using a high-speed camera and a well lighted oil jet. (Author)

A78-20809 * # Experimental and analytical load-life relation for AISI 9310 steel spur gears. D. P. Townsend, J. J. Coy, and E. V. Zaretsky (NASA, Lewis Research Center, Cleveland, Ohio). *American Society of Mechanical Engineers, Design Engineering Technical Conference, Chicago, Ill., Sept. 26-30, 1977, Paper 77-DET-121*. 7 p. 18 refs. Members, \$1.50; nonmembers, \$3.00.

Life tests were conducted at three different loads with three groups of 8.9 cm, pitch diameter spur gears made of vacuum arc remelted AISI 9310 steel. Life was found to vary inversely with load to the 4.3 and 5.1 power at the L-10 and L-50 life levels, respectively. The Weibull slope varied linearly with maximum Hertz contact stress, having an average value of 2.5. The test data when compared to AGMA standards showed a steeper slope for the load-life diagram. (Author)

A78-20883 * # Temperature distributions and thermal stresses in a graded zirconia/metal gas path seal system for aircraft gas turbine engines. C. M. Taylor (NASA, Lewis Research Center, Cleveland, Ohio; Leeds University, Leeds, England) and R. C. Bill (NASA, Lewis Research Center; U.S. Army, Propulsion Laboratory, Cleveland, Ohio). *American Institute of Aeronautics and Astronautics, Aerospace Sciences Meeting, 16th, Huntsville, Ala., Jan. 16-18, 1978, Paper 78-93*. 11 p. 5 refs.

A78-23362 * # The elastic distortion of the flanged inner ring of a high-speed cylindrical roller bearing. C. M. Taylor (NASA, Lewis Research Center, Cleveland, Ohio; Leeds University, Leeds, England). *American Society of Lubrication Engineers and American Society of Mechanical Engineers, Joint Lubrication Conference, Kansas City, Mo., Oct. 3-5, 1977, ASME Paper 77-Lub-8*. *ASME, Transactions, Journal of Lubrication Technology*, vol. 100, Jan. 1978, p. 18-24. 5 refs.

The elastic distortion of the inner ring of an experimental 3,000,000 DN roller bearing is investigated analytically. The geometry of this bearing is unusually complex and for this reason a bearing with an axially symmetric inner ring and shaft is also analyzed. Only the inner ring and shaft are considered using a two-dimensional finite element computer program which enables interference between these components to be accommodated. The results for the experimental bearing suggest that elastic distortions are modest in relation to the design clearances. However, the variation of the radial deflection of the raceway may be significant for some circumstances and the interference fit adopted between the ring and shaft appears to be questionably low. (Author)

A78-23364 * # Lubrication of high-speed, large bore tapered roller bearings. R. J. Parker (NASA, Lewis Research Center, Cleveland, Ohio) and H. R. Signer (Industrial Tectonics, Inc., Compton, Calif.). *American Society of Lubrication Engineers and American Society of Mechanical Engineers, Joint Lubrication Conference, Kansas City, Mo., Oct. 3-5, 1977, ASME Paper 77-Lub 13*. *ASME, Transactions, Journal of Lubrication Technology*, vol. 100, Jan. 1978, p. 31-38. 9 refs.

The performance of 120 65 mm bore tapered-roller bearings was investigated at shaft speeds up to 15,000 rpm. Temperature distribution and bearing heat generation were determined as a function of shaft speed, radial and thrust loads, lubricant flow rate, and lubricant inlet temperature. Lubricant was supplied either by jets or by a combination of holes through the cone directly to the cone-rib contact and jets at the roller small end side. Cone-rib lubrication significantly improved high-speed tapered-roller bearing

performance, yielding lower cone-face temperatures and lower power loss and allowing lower lubricant flow rates for a given speed condition. Bearing temperatures increased with increased shaft speed and decreased with increased lubricant flow rate. Bearing power loss increased with increased shaft speed and increased lubricant flow rate. (Author)

A78-23428 * The use of analytical surface tools in the fundamental study of wear. D. H. Buckley (NASA, Lewis Research Center, Lubrication Fundamentals Section, Cleveland, Ohio). In: *Wear of materials - 1977*; Proceedings of the International Conference, St. Louis, Mo., April 25-28, 1977. (A78-23426 08-37) New York, American Society of Mechanical Engineers, 1977, p. 12-29. 77 refs.

This paper reviews the various techniques and surface tools available for the study of the atomic nature of the wear of materials. These include chemical etching, X-ray diffraction, electron diffraction, scanning electron microscopy, low-energy electron diffraction, Auger emission spectroscopy analysis, electron spectroscopy for chemical analysis, field ion microscopy, and the atom probe. Properties of the surface and wear surface regions which effect wear such as surface energy, crystal structure, crystallographic orientation, mode of dislocation behavior, and cohesive bonding are discussed. A number of mechanisms involved in the generation of wear particles are identified with the aid of the aforementioned tools. (Author)

A78-24487 * The design of hydraulic pressure regulators that are stable without the use of sensing line restrictors or frictional dampers. H. Gold (NASA, Lewis Research Center, Cleveland, Ohio). *Illinois Institute of Technology, National Conference on Fluid Power, Chicago, Ill., Oct 25-27, 1977, Paper 21 p. 6 refs.*

A direct-acting hydraulic pressure regulator design which incorporates stability margin, response and droop margin is developed. The pressure regulator system does not involve a nonlinear sensing line restrictor (which may degrade transient response) or linear damping (which is sensitive to clearance and viscosity). The direct-acting hydraulic pressure regulator makes use of the technique of lead network stabilization (i.e., the tuned stabilizer concept). An analytically derived circuit pressure regulator is tested to study the stability limit under a parallel capacitive plus resistive load and the stabilizing effect of the tuned stabilizer. J.M.B.

A78-26414 * Elastohydrodynamic lubrication of elliptical contacts for materials of low elastic modulus. I - Fully flooded conjunction. B. J. Hamrock (NASA, Lewis Research Center, Cleveland, Ohio) and D. Dowson (NASA, Lewis Research Center, Cleveland, Ohio; Leeds University, Leeds, England). *American Society of Lubrication Engineers and American Society of Mechanical Engineers, Joint Lubrication Conference, Kansas City, Mo., Oct. 3-5, 1977, ASME Paper 77-Lub-10* 10 p. 12 refs. Members, \$1.50; nonmembers, \$3.00.

A complete numerical solution is presented to the problem of isothermal elastohydrodynamic lubrication of elliptical contacts for low-elastic-modulus materials operating under fully flooded conditions. No assumption is made for the pressure or film thickness within the contact, and compressibility and viscous effects are taken into account. Because of the dimensionless representation of the coordinates, the actual Hertzian contact ellipse becomes a circle regardless of the value of the ellipticity parameter. A minimum film thickness relation and a central film thickness relation are derived from examining 17 different cases. Contour plots for detailed illustration of the pressure distribution and film thickness in the conjunction are provided. S.D.

A78-26425 * Ferrographic analysis of wear debris generated in accelerated rolling element fatigue tests. W. R. Jones, Jr. and R. J. Parker (NASA, Lewis Research Center, Cleveland, Ohio). *American Society of Lubrication Engineers and American Society of Mechanical Engineers, Joint Lubrication Conference, Kansas City, Mo., Oct. 3-5, 1977, Paper 21 p. 21 refs.*

Ferrographic analysis was used to determine the types and quantities of wear particles generated during accelerated rolling contact fatigue tests. The NASA five-ball rolling contact fatigue tester was used. Ball specimens were made of AMS 6749, a corrosion-resistant high-temperature bearing steel. The lubricant was a super-refined naphthenic mineral oil. Conditions included a maximum Hertz stress of 5.52 billion Pa and a shaft speed of 10,000 rpm. Four types of wear particles were observed: normal rubbing wear particles, fatigue spall particles, spheres, and friction polymer. (Author)

A78-26926 * Steady-state unbalance response of a three-disk flexible rotor on flexible, damped supports. R. E. Cunningham (NASA, Lewis Research Center, Cleveland, Ohio). *American Society of Mechanical Engineers, Design Engineering Technical Conference, Chicago, Ill., Sept. 26-29, 1977, Paper 41 p. 15 refs.*

Experimental data are presented for the unbalance response of a flexible, ball bearing supported rotor to speeds above the third lateral bending critical. Values of squeeze film damping coefficients obtained from measured data are compared to theoretical values obtained from short bearing approximation over a frequency range from 5000 to 31,000 cycles/min. Experimental response for an undamped rotor is compared to that of one having oil squeeze film dampers at the bearings. Unbalances applied varied from 0.62 to 15.1 gm-cm. (Author)

A78-31829 * Shape of two-dimensional solidification interface during directional solidification by continuous casting. R. Siegel (NASA, Lewis Research Center, Cleveland, Ohio). *ASME, Transactions, Journal of Heat Transfer, vol. 100, Feb. 1978, p. 3-10. 11 refs.*

An analysis was made of the two-dimensional solidification of an ingot being cooled and withdrawn vertically downward from a mold consisting of parallel walls of finite length. Heat transfer analysis shows how the flatness of the interface is related to the ingot thickness, the withdrawal rate, the heat addition from the superheated liquid metal, and the temperature difference available for cooling. This provides an understanding of the conditions that will yield a maximum rate of casting while achieving the desired flatness of the interface. The results are interpreted with respect to the conditions for obtaining an aligned eutectic structure by directional solidification. In this process an additional constraint must be included that relates the ingot withdrawal rate and the heat transfer rate from the liquid metal to the solidification interface. (Author)

A78-33183 * Design considerations in mechanical face seals for improved performance. I - Basic configurations. L. P. Ludwig (NASA, Lewis Research Center, Cleveland, Ohio) and H. F. Greiner (Saiel, Inc., Providence, R.I.). *American Society of Mechanical Engineers, Winter Annual Meeting, Atlanta, Ga., Nov. 27-Dec. 2, 1977, Paper 77-WA/Lub-3* 10 p. 8 refs. Members, \$1.50; nonmembers, \$3.00.

Basic assembly configurations of the mechanical face seal are described and some advantages associated with each are listed. The various forms of seal components (the primary seal, secondary seal, etc.) are illustrated, and functions pointed out. The technique of seal pressure balancing and its application is described and the concept of the PV factor, its different forms and limitations are discussed. Brief attention is given to seal lubrication since it is covered in detail in a companion paper. Finally, the operating conditions for various applications of low pressure seals (aircraft transmissions) are listed, and the seal failure mode of a particular application is discussed. (Author)

A78-33186 * Design considerations in mechanical face seals for improved performance. H. Lubrication. L. P. Ludwig (NASA, Lewis Research Center, Cleveland, Ohio) and H. F. Greiner (Sealol, Inc., Providence, R.I.). *American Society of Mechanical Engineers, Winter Annual Meeting, Atlanta, Ga., Nov. 27-Dec. 2, 1977, Paper 77-WA/Lub-4*. 12 p. 21 refs. Members, \$1.80; nonmembers, \$3.00.

The importance of sealing technology in the U.S. industrial chemical-orientated society in regard to maintenance and environmental contamination is pointed out. It is stated that seal performance (leakage, life) is directly related to seal lubrication, which is a mechanism not well understood. Current thinking in regard to seal lubrication is reviewed, the effect of energy dissipation in the thin lubricating film separating the sealing faces is pointed out, and the results of vaporization due to heating are illustrated. Also, hydrodynamic lubrication is reviewed, and an inherent tendency for the seal to operate with angular misalignment is pointed out. Recent work on hydrostatic effects is summarized and the conditions for seal instability are discussed. Four different modes of seal lubrication are postulated with the mode type being a strong function of speed and pressure. (Author)

A78-33211 * Tribological properties of surfaces. D. H. Buckley (NASA, Lewis Research Center, Cleveland, Ohio). *American Vacuum Society, International Conference on Metallurgical Coatings, San Francisco, Calif., Apr. 3-7, 1978, Paper*. 24 p. 21 refs.

The real area of contact between two solid surfaces is only a small portion of the apparent area. Deformation of these areas can result in solid state contact through surface films. For clean solid to solid contact strong adhesive bonding occurs across the interface. Under these conditions many properties of the solid such as the metallurgical and chemical nature of metals can influence adhesion, friction, and wear behavior. The presence of gases, liquids, and solid films on the surface of solids alter markedly tribological characteristics. These surface films can also considerably change the mechanical effects of solid state contact on bulk material behavior. (Author)

A78-33219 * Self-acting shaft seals. L. P. Ludwig (NASA, Lewis Research Center, Cleveland, Ohio). *NATO, AGARD, Power, Energetics, and Propulsion Panel Meeting on Seal Technology in Gas Turbine Engines, London, England, Apr. 6, 7, 1978, Paper*. 36 p. 17 refs.

Self-acting seals are described in detail. The mathematical models for obtaining a seal force balance and the equilibrium operating film thickness are outlined. Particular attention is given to primary ring response (seal vibration) to rotating seal face runout. This response analysis reveals three different vibration modes with secondary seal friction being an important parameter. Leakage flow inlet pressure drop and effects of axisymmetric and nonaxisymmetric sealing face deformations are discussed. Experimental data on self-acting face seals operating under simulated gas turbine conditions are given, these data show the feasibility of operating the seal at conditions of 345 N/mq cm and 152 m/sec sliding speed. Also a spiral groove seal design operated to 244 m/sec is described. (Author)

A78-33364 * An overview of aerospace gas turbine technology of relevance to the development of the automotive gas turbine engine. D. G. Evans and T. J. Miller (NASA, Lewis Research Center, Cleveland, Ohio). *Society of Automotive Engineers, Congress and Exposition, Detroit, Mich., Feb. 27-Mar. 3, 1978, Paper 780075*. 23 p. 65 refs.

The NASA Lewis Research Center (LeRC) has conducted, and has sponsored with industry and universities, extensive research into many of the technology areas related to gas turbine propulsion systems. This aerospace-related technology has been developed at both the component and systems level, and may have significant potential for application to the automotive gas turbine engine. This paper summarizes this technology and lists the associated references.

The technology areas are system steady-state and transient performance prediction techniques, compressor and turbine design and performance prediction programs and effects of geometry, combustor technology and advanced concepts, and ceramic coatings and materials technology. (Author)

A78-33368 * Bearing, gearing, and lubrication technology. W. J. Anderson (NASA, Lewis Research Center, Cleveland, Ohio). *Society of Automotive Engineers, Congress and Exposition, Detroit, Mich., Feb. 27-Mar. 3, 1978, Paper 780077*. 11 p. 28 refs.

Results of selected NASA research programs on rolling-element and fluid-film bearings, gears, and elastohydrodynamic lubrication are reported. Advances in rolling-element bearing material technology, which have resulted in a significant improvement in fatigue life, and which make possible new applications for rolling bearings, are discussed. Research on whirl-resistant, fluid-film bearings, suitable for very high-speed applications, is discussed. An improved method for predicting gear pitting life is reported. An improved formula for calculating the thickness of elastohydrodynamic films (the existence of which help to define the operating regime of concentrated contact mechanisms such as bearings, gears, and cams) is described. (Author)

A78-37677 * Experimental evaluation of fuel preparation systems for an automotive gas turbine catalytic combustor. R. R. Tacina (NASA, Lewis Research Center, Cleveland, Ohio). *U.S. Environmental Protection Agency, Workshop on Catalytic Combustion, 2nd, Raleigh, N.C., June 21, 22, 1977, Paper*. 21 p. 6 refs.

Premixing-prevaporizing fuel systems were evaluated for use with a catalytic reactor for possible automotive gas turbine application. Spatial fuel-air distributions, degree of vaporization, pressure drop and air velocity profiles were measured. Three airblast injectors and an air-assist nozzle were tested. Air swirlers were used to improve the spatial fuel-air distribution. The work was done in a 12 cm tubular duct. Test conditions were: a pressure of 0.3 and 0.5 MPa, inlet air temperatures up to 800 K, air velocities of 10 and 20 m/s and fuel air ratios up to 0.020. The fuel was Jet A. The best results were obtained with an air-blast configuration that used multiple cones to provide high velocity air for atomization and also straightened the inlet airflow. With this configuration, uniform spatial fuel-air distributions were obtained with mixing lengths greater than 17.8 cm. In this length, vaporization of the fuel was 98.5 percent complete at an inlet air temperature of 700 K. The total pressure loss was 1.0 percent with a reference velocity of 20 m/s and 0.25 percent at 10 m/s. The air velocity was uniform across the duct and no autoignition reactions were observed. (Author)

A78-45430 * Additional aspects of elastohydrodynamic lubrication. B. J. Hamrck (NASA, Lewis Research Center, Cleveland, Ohio). *U.S. Army, DARPA, MIT, and U.S. Navy, International Conference on Fundamentals of Tribology, Cambridge, Mass., June 19-22, 1978, Paper*. 14 p. 14 refs.

Elastohydrodynamic lubrication (EHL) for materials of low elastic modulus is considered. Engineering applications in which EHL is important for low-elastic-modulus materials include seals, human joints, tires, and elastomeric material machine elements. Theoretical solutions of the problem of fully flooded line contacts in the case of low elastic materials are discussed. The equation regarding dimensionless minimum film thickness for fully flooded elliptical contacts for low elastic modulus is compared with the corresponding equation for materials of high elastic modulus. The powers of the dimensionless speed parameter U are quite similar in both equations, but the power of the dimensionless load parameter W is much more significant for low elastic modulus materials. Attention is given to aspects of dimensionless grouping, the isoviscous rigid regime, the viscous rigid regime, the isoviscous elastic regime, and the viscous elastic regime. G. R.

A78-45436 * # Definition and effect of chemical properties of surfaces in friction, wear, and lubrication. D. H. Buckley (NASA, Lewis Research Center, Cleveland, Ohio). U.S. Navy, U.S. Army, DARPA, and MIT, *International Conference on Fundamentals of Tribology, Cambridge, Mass., June 19-22, 1978, Paper. 39 p.* 75 refs.

Much of the data relative to the properties of surfaces that have been used in the past in analyzing, interpreting and predicting adhesion, friction and wear behavior for solid surfaces is now suspect. With the advent of analytical surface tools, careful and complete characterization of surfaces indicate that very frequently the outermost layers of solid surfaces are markedly different in chemistry than had been previously thought. These layers, as will be shown, are extremely important in adhesion, friction and wear behavior. Some of the properties to be discussed in the paper relative to their role in adhesion, friction, wear and lubrication will include: (1) adsorption, both physical and chemical; (2) orientation of the solid as well as the lubricant; (3) surface energy; (4) surface segregation; (5) surface versus bulk metallurgical effects; (6) electronic nature of the surface; and (7) bonding mechanisms. (Author)

N78-10472 * # Chrysler Corp., Detroit, Mich., **SPLITTER-BLADED CENTRIFUGAL COMPRESSOR IMPELLER DESIGNED FOR AUTOMOTIVE GAS TURBINE APPLICATION** Final Report, 1 Sep. 1976 - 30 Jun. 1977 R. C. Pampreen Jun. 1977 44 p refs (Contract NAS3-20059) (NASA-CR-135237) Avail: NTIS HC A03/MF A01 CSCL 21A

Mechanical design and fabrication of two splitter-bladed centrifugal compressor impellers were completed for rig testing at NASA Lewis Research Center. These impellers were designed for automotive gas turbine application. The mechanical design was based on NASA specifications for blade-shape and flowpath configurations. The contractor made engineering drawings and performed calculations for mass and center-of-gravity, for stress and vibration analyses, and for shaft critical speed analysis. One impeller was machined to print; the other had a blade height and exit radius of 2.54 mm larger than print dimensions. Author

N78-17387 * # Avco Lycoming Engine Group, Stratford, Conn., **DEVELOPMENT OF SPIRAL-GROOVE SELF-ACTING FACE SEALS** Final Report, 9 Feb. 1976 - 31 Mar. 1977 M. O'Brien Jun. 1977 141 p refs Sponsored in part by Army Air Mobility R and D Lab (Contract NAS3-19772) (NASA-CR-135303; LYC-77-41) Avail: NTIS HC A07/MF A01 CSCL 11A

An experimental evaluation and a 100-hour endurance test were performed on a spiral groove geometry, self-acting face seal. The seal was tested and operated successfully at maximum conditions of 243.8 m/s surface speed, 199.9 N/sq cm air pressure, and 645.4K (702 F) air temperature. The maximum speed condition of 243.8 m/s was obtained at a shaft speed of 72,500 rpm. Seal wear, gas leakage, and sealing element temperature were monitored during the test. Condition of the seal at the completion of the test was documented and found acceptable for further use. The spiral groove wear rate measured during the endurance test indicates a minimum potential seal life of over 2700 hours. Seal air leakage measured during the test program is within the range considered acceptable for consideration for use in a small gas turbine engine. Author

N78-17380 * # Stein Seal Co., Philadelphia, Pa., **FEASIBILITY STUDY OF NEGATIVE LIFT CIRCUMFERENTIAL TYPE SEAL FOR HELICOPTER TRANSMISSIONS** E. N. Goldring Oct. 1977 38 p (Contract NAS3-20598) (NASA-CR-135302) Avail: NTIS HC A03/MF A01 CSCL 11A

A new seal concept, the negative lift circumferential type seal, was evaluated under simulated helicopter transmission conditions. The bore of the circumferential seal contains step type geometry which produces a negative lift that urges the

sealing segments towards the shaft surface. The seal size was a 2.5 inch bore and the test speeds were 7000 and 14,250 rpm. During the 300 hour test at typical transmission seal pressure (to 2 psig) the leakage was within acceptable limits and generally less than 0.1 cc/hour during the last 150 hours of testing. The wear to the carbon segments during the 300 hours was negligible. Author

N78-20514 * # Mechanical Technology, Inc., Latham, N. Y., **BALANCING TECHNIQUES FOR HIGH-SPEED FLEXIBLE ROTORS** Final Report A. J. Smalley Apr. 1978 129 p refs (Contract NAS3-18520) (NASA-CR-2975; MTI-77TR2) Avail: NTIS HC A07/MF A01 CSCL 13I

Ideal and non-ideal conditions for multiplane balancing are addressed. Methodology and procedures for identifying optimum balancing configurations and for assessing, quantitatively, the penalties associated with non-optimum configurations were developed and demonstrated. The problems introduced when vibration sensors are supported on flexible mounts were assessed experimentally, and the effects of flexural asymmetry in the rotor on balancing were investigated. A general purpose method for predicting the threshold of instability of an asymmetric rotor was developed, and its predictions are compared with measurements under different degrees of asymmetry. Author

N78-21471 * # Michigan Univ., Ann Arbor, Dept. of Aerospace Engineering, **LIGHTWEIGHT, LOW COMPRESSION AIRCRAFT DIESEL ENGINE** T. L. Gaynor, M. S. Bottrell, C. D. Eagle, and C. F. Bachle Jul. 1977 103 p refs (Contract NAS3-20051) (NASA-CR-135300) Avail: NTIS HC A06/MF A01 CSCL 21G

The feasibility of converting a spark ignition aircraft engine to the diesel cycle was investigated. Procedures necessary for converting a single cylinder GTS10-520 are described as well as a single cylinder diesel engine test program. The modification of the engine for the hot port cooling concept is discussed. A digital computer graphics simulation of a twin engine aircraft incorporating the diesel engine and Hot Port concept is presented showing some potential gains in aircraft performance. Sample results of the computer program used in the simulation are included. Author

N78-21472 * # Mechanical Technology, Inc., Latham, N. Y., **HYDRODYNAMIC AIR LUBRICATED COMPLIANT SURFACE BEARING FOR AN AUTOMOTIVE GAS TURBINE ENGINE. 1: JOURNAL BEARING PERFORMANCE** Final Report D. Ruscitto, J. McCormick, and S. Gray Apr. 1978 145 p refs Prepared for DOE (Contracts NAS3-19427; EC-77-A-31-1040) (NASA-CR-135368; CONS/9427-1) Avail: NTIS HC A07/MF A01 CSCL 20E

A 38.1 mm (1.5 inch) diameter Hydresil Compliant Surface Air Lubricated Journal Bearing was designed and tested to obtain bearing performance characteristics at both room temperature and 315 C (600 F). Testing was performed at various speeds up to 80,000 rpm with varying loads. Rotating sensors provided an opportunity to examine the film characteristics of the compliant surface bearing. In addition to providing minimum film thickness values and profiles, many other insights into bearing operation were gained such as the influence of bearing fabrication accuracy and the influence of smooth foil deflection between the bumps. Author

N78-27427* Detroit Diesel Allison, Indianapolis, Ind.
**AERODYNAMIC PERFORMANCE OF CONVENTIONAL AND
 ADVANCED DESIGN LABYRINTH SEALS WITH SOLID-
 SMOOTH ABRADABLE, AND HONEYCOMB LANDS**
 Final Report, 21 Jul. 1976 - 21 Nov. 1977

H. L. Stocker, D. M. Cox, and G. F. Holle Nov. 1977 272 p
 refs

(Contract NAS3-20066)
 (NASA-CR-135307; EDR-9339) Avail NTIS
 HC A12/MF A01 CSCL 11A

Labyrinth air seal static and dynamic performance was evaluated using solid, abradable, and honeycomb lands with standard and advanced seal designs. The effects on leakage of land surface roughness, abradable land porosity, rub grooves in abradable lands, and honeycomb land cell size and depth were studied using a standard labyrinth seal. The effects of rotation on the optimum seal knife pitch were also investigated. Selected geometric and aerodynamic parameters for an advanced seal design were evaluated to derive an optimized performance configuration. The rotational energy requirements were also measured to determine the inherent friction and pumping energy absorbed by the various seal knife and land configurations tested in order to properly assess the net seal system performance level. Results indicate that: (1) seal leakage can be significantly affected with honeycomb or abradable lands, (2) rotational energy absorption does not vary significantly with the use of a solid-smooth, an abradable, or a honeycomb land, and (3) optimization of an advanced lab seal design produced a configuration that had leakage 25% below a conventional stepped seal.

ARH

N78-27428* SKF Industries, Inc., King of Prussia, Pa. Research
 Lab

**EMERGENCY AND MICROFOG LUBRICATION AND
 COOLING OF BEARINGS FOR ARMY HELICOPTERS**
 Final Report, Dec. 1972 - Jun. 1977

J. W. Rosenleb Jan. 1978 125 p refs

(Contract NAS3-17343)

(NASA-CR-135195; SKF AL77T021) Avail NTIS
 HC A06/MF A01 CSCL 13I

An analysis and system study was performed to provide design information regarding lubricant and coolant flow rates and flow paths for effective utilization of the lubricant and coolant in a once-through oil-mist (microfog) and coolant air system. A system was designed, manufactured, coupled with an existing rig and evaluation tests were performed using 48 mm bore split-inner angular-contact ball bearings under 1779N (400 lb) thrust load. An emergency lubrication aspirator system was also manufactured and tested under lost lubricant conditions. The testing demonstrated the feasibility of using a mist oil and cooling air system to lubricate and cool a high speed helicopter engine mainshaft bearing. The testing also demonstrated the feasibility of using an emergency aspirator lubrication system as a viable survivability concept for helicopter mainshaft engine bearing for periods as long as 30 minutes.

Author

N78-28486* General Motors Corp., Indianapolis, Ind. Detroit
 Diesel Allison Div.

**STUDY AND PROGRAM PLAN FOR IMPROVED HEAVY
 DUTY GAS TURBINE ENGINE CERAMIC COMPONENT
 DEVELOPMENT** Final Report

H. E. Helms May 1977 156 p refs

(Contract EX-76-A-31-101; NAS3-20064)

(NASA-CR-135230; CONS/0064-1; DDA-EDR-9068) Avail:
 NTIS HC A06/MF A01 CSCL 21A

A fuel economy of 213 mg/W (0.35 lb/hp-hr) brake specific fuel consumption by 1981 through use of ceramic materials, with conformance to current and projected Federal noise and emission standards was demonstrated and a commercially viable engine is described. Study results show that increased turbine inlet and regenerator inlet temperatures, through the use of ceramic materials, contribute the greatest amount to achieving fuel economy goals. Further, improved component efficiencies for the compressor, gasifier turbine, power turbine, and regenerator disks show significant additional gains in fuel economy. Fuel saved in a 500,000 mile engine life, risk levels involved in development, and engine related life cycle costs for fleets (100 units) of trucks and buses were used as criteria to select work goals for the planned program.

ERA

N78-28448* Mechanical Technology, Inc., Latham, N. Y.

**HYDRODYNAMIC AIR LUBRICATED COMPLIANT SUR-
 FACE BEARING FOR AN AUTOMOTIVE GAS TURBINE
 ENGINE. 2: MATERIALS AND COATINGS** Final Report

Bharat Bhushan, David Ruscitto, and Stanley Gray Jul. 1978
 139 p refs

(Contracts NAS3-19427; EC-77 A-31 1040)

(NASA-CR-135402; CONS/9427-2) Avail NTIS
 HC A07/MF A01 CSCL 11A

Material coatings for an air-lubricated, compliant journal bearing for an automotive gas turbine engine were exposed to service test temperatures of 540 C or 650 C for 300 hours, and to 10 temperature cycles from room temperatures to the service test temperatures. Selected coatings were then put on journal and partial-arc foils and tested in start-stop cycle tests at 14 kPa (2 psi) loading for 2000 cycles. Half of the test cycles were performed at a test chamber service temperature of 540 C (1000 F) or 650 C (1200 F), the other half were performed at room temperature. Based on test results, the following combinations and their service temperature limitations are recommended: HL 800 TM (CdO and graphite) on foil versus chrome carbide on journal up to 370 C (700 F); NASA PS 120 (Tribaloy 400, silver and CaF₂ on journal versus uncoated foil up to 540 C (1000 F) and Kaman DES on journal and foil up to 640 C (1200 F). Kaman DES coating system was further tested successfully at 35 kPa (5 psi) loading for 2000 start-stop cycles.

ARH

N78-31427* General Electric Co., Cincinnati, Ohio

**ROLLING ELEMENT FATIGUE TESTING OF GEAR MATERI-
 ALS**

A. H. Nahm 1 Apr. 1978 110 p refs

(Contract NAS3-14302)

(NASA-CR-135411; Doc-R78AEG289) Avail NTIS
 HC A06/MF A01 CSCL 13I

Rolling element fatigue lives of eleven alloys were evaluated. The eleven alloys studied were three nitriding alloys (Super Nitralloy, Nitralloy 135 and Nitralloy N), four case carburizing alloys (AISI 9310, CBS 600, CBS 1000M and Vasco X-2), and four throughhardening alloys (Vasco Matrix II, AISI W-1, AISI S-2 and AISI O-2). Several different heat treatments and/or melting processes were studied on the three carburizing alloy steels. Metallurgical analyses were made before and after the RC rig tests. Test data were statistically analyzed using the Weibull distribution function. B-10 lives were compared versus VIM-VAR AISI M-50 and carburized VAR AISI 9310, as reference alloys.

LS

A78-23433* Tennessee Univ. Space Inst., Tullahoma.
**TRANSIENT DYNAMICS OF A FLEXIBLE ROTOR WITH
 SQUEEZE FILM DAMPERS** Final Report
 D. F. Buono, L. D. Schlitzer, R. G. Hall, III, and D. H. Hibner
 Sep 1978 85 p refs
 (NACA-CR-3060) (NASA-CR-3060) PWA-5548-9) Avail: NTIS
 HC A05/MF A01 CSCL 131

A series of simulated blade loss tests are reported on a test rotor designed to operate above its second bending critical speed. A series of analyses were performed which predicted the transient behavior of the test rig for each of the blade loss tests. The scope of the program included the investigation of transient rotor dynamics of a flexible rotor system, similar to modern flexible jet engine rotors, both with and without squeeze film dampers. The results substantiate the effectiveness of squeeze film dampers and document the ability of available analytical methods to predict their effectiveness and behavior. (Author)

A78-27606* Dynamic tooth loads and stressing for high contact ratio spur gears. R. W. Cornell and W. W. Westervelt (United Technologies Corp., Hamilton Standard Div., Windsor Locks, Conn.). *American Society of Mechanical Engineers, Design Engineering Technical Conference, Chicago, Ill., Sept. 26-30, 1977, Paper 77-DET-101*. 8 p. 10 refs. Members, \$1.50, nonmembers, \$3.00. Contract No. NAS3-17859.

A time history, closed form solution is presented for a dynamic model of spur gear systems for all practical contact ratios. The analysis determines the dynamic response of the gear system and the associated tooth loads and stressing. The dynamic model assumes the two gears act as a rigid inertia and the teeth act as a variable spring of a dynamic system excited by the meshing action of the teeth. Included in the analysis are the effects of the nonlinearity of the tooth pair stiffness during mesh, the tooth errors, and the tooth profile modifications. Besides reviewing the features, solution, and program of this analysis, preliminary results from applying the analysis are presented, which show that tooth profile modification, system inertia and damping, and system critical speeds can affect the dynamic gear tooth loads and stressing significantly. (Author)

A78-23447* Influence of adsorbed fluids on the rolling contact deformation of MgO single crystals. K. F. Dufrane (Battelle Columbus Laboratories, Columbus, Ohio). In: *Wear of materials - 1977, Proceedings of the International Conference, St. Louis, Mo., April 25-28, 1977*. (A78-23426 08-37) New York, American Society of Mechanical Engineers, 1977, p. 446-451. 5 refs. Contract No. NAS3-6263.

Basic phenomena associated with rolling contact deformation were studied using MgO as a model bearing material. A hardened steel ball was rolled on MgO single crystals in slow-speed reciprocating motion and in high-speed circular motion. The resulting deformation was studied by dislocation etch-pit techniques. The presence of adsorbed fluids, such as silicone oil, white mineral oil, and toluene, with slow-speed sliding caused a dramatic change in slip mode and premature surface spalling compared with similar experiments in air or under water. In contrast, dimethyl formamide inhibited these slip processes. The results are consistent with the dependence of dislocation mobility on adsorbed species. High speed hydrodynamic rolling with mineral oil lubrication produced a different slip phenomena entirely from the slow speed rolling. The slip bands resembled those produced in tensile tests, and all slip apparently initiated at subsurface sites. (Author)

A78-31600* Development and fabrication of a diffusion welded Columbian alloy heat exchanger. W. F. Zimmerman, E. C. Duderstadt, D. Weir (General Electric Co., Evendale, Ohio), and R. H. Titran (NASA, Lewis Research Center, Cleveland, Ohio). *American Institute of Mining, Metallurgical, and Petroleum Engineers, Annual Meeting, 107th, Denver, Colo., Feb. 26-Mar. 2, 1978, Paper A78-61*. 18 p. Contract No. NAS3-18541.

A Mini Brayton space power generation system required the development of a Columbian alloy heat exchanger to transfer heat from a radioisotope heat source to a He/Xe working fluid. A light-weight design featured the simultaneous diffusion welding of 148 longitudinal fins in an annular heat exchanger about 9-1/2 in. in diameter, 13-1/2 in. in length and 1/4 in. in radial thickness. To complete the heat exchanger, additional gas ducting elements and attachment supports were added by GTA welding in a vacuum-purged inert atmosphere welding chamber. The development required the modification of an existing large size hot isostatic press to achieve HIP capabilities of 2800 F and 10,000 psi for at least 3 hr. Excellent diffusion welds were achieved in a high-quality component which met all system requirements. (Author)

38 QUALITY ASSURANCE AND RELIABILITY

Includes product sampling procedures and techniques; and quality control.

N78-17287* National Aeronautics and Space Administration, Lewis Research Center, Cleveland, Ohio.
USE OF AN ULTRASONIC-ACOUSTIC TECHNIQUE FOR NONDESTRUCTIVE EVALUATION OF FIBER COMPOSITE STRENGTH

Alex Vary and Kenneth J. Bowles 1978 12 p refs Presented at the 33rd Ann. Conf. of the Soc. of the Plastics Ind., Washington, D.C., 7-10 Feb. 1978 (NASA-TM-73813; E-9400) Avail: NTIS HC A02/MF A01 CSCL 14D

Details of the method used to measure the stress wave factor are described. Frequency spectra of the stress waves are analyzed in order to clarify the nature of the wave phenomena involved. The stress wave factor was measured with simple contact probes requiring only one-side access to a part. This is beneficial in nondestructive evaluations because the waves can run parallel to fiber directions and thus measure material properties in directions assumed by actual loads. The technique can be applied where conventional through transmission techniques are impractical or where more quantitative data are required. The stress wave factor was measured for a series of graphite/polyimide composite panels, and results obtained are compared with those from transmission immersion ultrasonic scans. Author

N78-24885* National Aeronautics and Space Administration, Lewis Research Center, Cleveland, Ohio.
QUANTITATIVE ULTRASONIC EVALUATION OF MECHANICAL PROPERTIES OF ENGINEERING MATERIALS

Alex Vary 1978 37 p refs Presented at 1st Intern. Symp. on Ultrasonic Meter Characterization, Gaithersburg, Md., 7-9 Jun 1978; cosponsored by NBS and Am. Soc. Nondestructive Testing. (NASA-TM-78905; E-9640) Avail: NTIS HC A03/MF A01 CSCL 14D

Progress in the application of ultrasonic techniques to nondestructive measurement of mechanical strength of engineering materials is reviewed. A dormant concept in nondestructive evaluation (NDE) is invoked. The availability of ultrasonic methods that can be applied to actual parts to assess their potential susceptibility to failure under design conditions is discussed. It was shown that ultrasonic methods yield measurements of elastic moduli, microstructure, hardness, fracture toughness, tensile strength, yield strength, and shear strength for a wide range of materials (including many types of metals, ceramics, and fiber composites). It was also indicated that although most of these methods were shown feasible in laboratory studies, more work is needed before they can be used on actual parts in processing, assembly, inspection, and maintenance lines. Author

A78-45433 * Quantitative ultrasonic evaluation of mechanical properties of engineering materials. A. Vary (NASA, Lewis Research Center, Cleveland, Ohio). *National Bureau of Standards and American Society for Nondestructive Testing, International Symposium on Ultrasonic Materials Characterization, 1st, Gaithersburg, Md., June 7-9, 1978, Paper, 37 p.* 55 refs.

Current progress in the application of ultrasonic techniques to nondestructive measurement of mechanical strength properties of engineering materials is reviewed. Even where conventional NDE techniques have shown that a part is free of overt defects, advanced NDE techniques should be available to confirm the material properties assumed in the part's design. There are many instances where metallic, composite, or ceramic parts may be free of critical defects while still being susceptible to failure under design loads due

to inadequate or degraded mechanical strength. This must be considered in any failure prevention scheme that relies on fracture analysis. This review will discuss the availability of ultrasonic methods that can be applied to actual parts to assess their potential susceptibility to failure under design conditions. (Author)

N78-18801* Westinghouse Electric Corp., Pittsburgh, Pa.
FABRICATION AND CHARACTERISTICS OF EXPERIMENTAL RADIOGRAPHIC AMPLIFIER SCREENS Final Report
 Zoltan Szepes; Jan. 1978 25 p refs
 (Contract NAS3-20742)
 (NASA-CR-2937; Rept. 77-9F9-RAPEX-R1) Avail: NTIS HC A02/MF A01 CSCL 14D

The fabrication process and transfer characteristics for solid state radiographic image transducers (radiographic amplifier screens) are described. These screens are for use in realtime nondestructive evaluation procedures that require large format radiographic images with contrast and resolution capabilities unavailable with conventional fluoroscopic screens. The screens are suitable for in-motion, on-line radiographic inspection by means of closed circuit television. Experimental effort was made to improve image quality and response to low energy (5 kV and up) X-rays. Author

N78-33463* General Electric Co., Cincinnati, Ohio. Material and Process Technology Labs.
ROLLING ELEMENT FATIGUE TESTING OF GEAR MATERIALS Final Report, Apr. 1977 - Jun. 1978
 A. H. Nahm 26 Jul 1978 124 p refs
 (Contract NAS3-14302)
 (NASA-CR-135450; R78AEG476) Avail: NTIS HC A08/MF A01 CSCL 14D

Rolling element fatigue lives of nine alloys were evaluated in Rolling Contact (RC) rigs. Test conditions included a Hertzian stress at 4,826 MPa (700 ksi), a rolling speed of 6.23 m/sec (245 in/sec.). Tests were run with a Type I oil (MIL-L-7808G) at room temperature. 8-10 lives (10% failure rate) of alloys were compared versus reference alloys, VIM-VAR AISI M-50 and VAR AISI 9310. Six case carburizing alloys (AISI 9310, CBS600, CBS1000M, EX00014, Vasco X-2 and EX00053) and three through-hardening alloys (AISI M-50, VascoMax 350 and Vasco Matrix 2) evaluated, showed RCF performance inferior or equivalent to that of AISI 9310 and AISI M-50. It was also found that the effects of vacuum melting processes, different tempering temperatures, freezing cycle during heat treating, shot peening, gold plating and chrome plating employed in the present investigation did not significantly affect RCF life. G.Y.

39 STRUCTURAL MECHANICS

Includes structural element design and weight analysis; fatigue; and thermal stress.

For applications see *05 Aircraft Design, Testing and Performance* and *18 Spacecraft Design, Testing and Performance*.

N78-12469* National Aeronautics and Space Administration, Lewis Research Center, Cleveland, Ohio.
NASTRAN USE FOR CYCLIC RESPONSE AND FATIGUE ANALYSIS OF WIND TURBINE TOWERS
 C. C. Chamis, P. Menos, J. H. Sinclair, and J. R. Winemiller *In its Sixth NASTRAN Users' Colloq* 1977 p 213-233 refs (For availability see N78-12443 03-39)

(Contract E(49-26)-1004)

Avail: NTIS HC A20/MF A01 CSCL 20K

A procedure is described which uses NASTRAN coupled with fatigue criteria via a postprocessor to determine the cyclic response and to assess the fatigue resistance (fatigue life) of wind turbine generator towers. The cyclic loads to which the tower may be subjected are entered either in a quasi-static approach through static load subcases (Rigid Format 1) or through the direct dynamic response (Rigid Format 9) features of NASTRAN. The fatigue criteria are applied to NASTRAN output data from either rigid format through an externally written user program embedded in a postprocessor. Author

N78-13477* National Aeronautics and Space Administration, Lewis Research Center, Cleveland, Ohio.
AN INTEGRATED THEORY FOR PREDICTING THE HYDROTHERMOMECHANICAL RESPONSE OF ADVANCED COMPOSITE STRUCTURAL COMPONENTS
 C. C. Chamis, R. F. Lark, and J. H. Sinclair 1977 43 p refs Presented at Tech. Specialists Conf. on Environ. Effects on Advanced Composite Mater., Dayton, Ohio, 29-30 Sep. 1977; sponsored by Am. Soc. for Testing and Mater.
 (NASA-TM-73812; E-9372) Avail: NTIS HC A03/MF A01 CSCL 20K

An integrated theory is developed for predicting the hydrothermomechanical (HDTM) response of fiber composite components. The integrated theory is based on a combined theoretical and experimental investigation. In addition to predicting the HDTM response of components, the theory is structured to assess the combined hydrothermal effects on the mechanical properties of unidirectional composites loaded along the material axis and off-axis, and those of angleply laminates. The theory developed predicts values which are in good agreement with measured data at the micromechanics, macromechanics, laminate analysis and structural analysis levels. Author

N78-19638* National Aeronautics and Space Administration, Lewis Research Center, Cleveland, Ohio.
MODE I ANALYSIS OF A FACE CRACKED PLATE SUBJECTED TO ROTATIONALLY CONSTRAINED END DISPLACEMENTS

Bernard Gross 1978 14 p refs Proposed for Presentation at the 11th Natl Symp. on Fracture Mech., Blacksburg Va., 12-14 Jun 1978

(NASA-TM-73777) Avail: NTIS HC A02/MF A01 CSCL 20K

Mode I stress intensity coefficients and crack mouth displacement coefficients were obtained by planar boundary collocation analysis of face cracked plates subjected to rotationally constrained end displacements. Results are presented for plates with height-to-width ratio varying from 1.0 to 5.0 and crack depth-to-plate width ratios in the range 0.1 to 0.8. Author

N78-19638* National Aeronautics and Space Administration, Lewis Research Center, Cleveland, Ohio.

SHEAR STRENGTH OF METAL-SiO₂ CONTACTS

Stephen V. Pepper 24 Mar. 1978 6 p refs Presented at the Intern. Topical Conf. on the Physics of SiO₂ and its Interfaces, Yorktown Heights, N. J., 22-24 Mar. 1978

(NASA-TM-78838) Avail: NTIS HC A02/MF A01 CSCL 20K

The strength of the bond between metals and SiO₂ was studied by measuring the static coefficient of friction of metals contacting alpha-quartz in ultrahigh vacuum. It was found that copper with either chemisorbed oxygen, nitrogen, or sulphur exhibited higher contact strength on stoichiometric SiO₂ than did clean copper. Since the surface density of states induced by these species on copper is similar, it appears that the strength of the interfacial bond can be related to the density of states on the metal surface. Author

N78-23471* National Aeronautics and Space Administration, Lewis Research Center, Cleveland, Ohio.

INTERPOLATION AND EXTRAPOLATION OF CREEP RUPTURE DATA BY THE MINIMUM COMMITMENT METHOD. PART 1: FOCAL-POINT CONVERGENCE

S. S. Manson (Case Western Reserve Univ.) and C. R. Ensign 1978 101 p refs Proposed for presentation at Symp. on Characterization of Mater. Intended for Serv. at Elevated Temp. at the Pressure Vessels and Piping Conf., Montreal, 26-29 Jun. 1978; cosponsored by ASME and Can. Soc. Mech. Engr. Sponsored in part by Elec. Power Res. Inst. 3 Vol.

(NASA-TM-78881; E-9614) Avail: NTIS HC A06/MF A01 CSCL 20K

A specialized variation of the minimum commitment method is obtained by expressing the relation $\log t + AP \log t + P - G$ where t is the rupture time, P a function of temperature, and G a function of stress. The term A was considered a structural stability parameter because it was found that the more unstable the material the higher was the negative value of A required to fit the data. The functional forms of P and G were still left to be determined from the station values determined by analysis. The extensions that were made through the development of the above equation are discussed. The discussion provides descriptions of how to implement the method both manually or by computer code. The method is illustrated in detail for Astroloy - a nickel base alloy for which the particular lot available showed embrittling instability involving a phase precipitation. It is also applied to a number of other steels, nickel base alloys, and aluminum alloys. Author

N78-23472* National Aeronautics and Space Administration, Lewis Research Center, Cleveland, Ohio.

INTERPOLATION AND EXTRAPOLATION OF CREEP RUPTURE DATA BY THE MINIMUM COMMITMENT METHOD. PART 2: OBLIQUE TRANSLATION

S. S. Manson (Case Western Reserve Univ.) and C. R. Ensign 1978 29 p refs Proposed for presentation at Symp. on Characterization of Mater. Intended for Serv. at Elevated Temp. at the Pressure Vessels and Piping Conf., Montreal, 26-29 Jun. 1978; cosponsored by ASME and Can. Soc. Mech. Engr. Sponsored in part by Elec. Power Res. Inst. 3 Vol.

(NASA-TM-78882; E-9615) Avail: NTIS HC A03/MF A01 CSCL 20K

A new concept is introduced whereby the creep-rupture isothermals are generated by an oblique translation of the master curve plotted on the conventional coordinates. For most materials a constant translation angle of around 5 deg relative to the horizontal axis is satisfactory. However, for highly unstable materials, such as a heat of Astroloy subject to sigma phase precipitation, an angle as high as 15 deg may be required. For best results the translation angle should depend on temperature, the lower temperatures requiring a lower angle. The method is, in fact, a generalization of other approaches but it allows for the other types of temperature effects than only those displayed by elastic modulus E . Implementation of the method can be accomplished either by manual-graphical means, or completely by computer, the major advantage being the ease of manual analysis. The method is illustrated for the unstable heat of Astroloy. Good results were obtained. Author

N78-23473* National Aeronautics and Space Administration, Lewis Research Center, Cleveland, Ohio.

INTERPOLATION AND EXTRAPOLATION OF CREEP RUPTURE DATA BY THE MINIMUM COMMITMENT METHOD. PART 3: ANALYSIS OF MULTHEATS

S. S. Manson (Case Western Reserve Univ.) and C. R. Eason
1978 33 p refs. Proposed for presentation at Symp. on Characterization of Mater. Intended for Serv. at Elevated Temp. at the Pressure Vessels and Piping Conf., Montreal, 26-29 Jun. 1978. cosponsored by ASME and Can. Soc. Mech. Engr. Sponsored in part by Elec. Power Res. Inst. 3 Vol. (NASA-TM-78883, E-9616) Avail: NTIS HC A03/MF A01 CSDL 20K

The Minimum Commitment Method was applied to two sets of data for which multiple heat information was available. For one alloy, a 304 stainless steel studied in Japan, data on nine well characterized heats were used, while for a proprietary low alloy carbon steel studied in the United Kingdom data were available on seven heats - in many cases to very long rupture times. For this preliminary study no instability factors were used. It was discovered that heat-to-heat variations would be accounted for by introducing heat identifiers in the form $A + B \log \sigma$ where σ is the stress and the constants A and B depend only on the heat. With these identifiers all the data could be collapsed onto a single master curve, even though there was considerable scatter among heats. Using these identifiers together with the average behavior of all heats made possible the determination of an accurate constitutive equation for each individual heat. Two basic approaches are discussed for applying the results of the analysis. Author

N78-27453* National Aeronautics and Space Administration, Lewis Research Center, Cleveland, Ohio.

FRACTOGRAPHIC EVALUATION OF CREEP EFFECTS ON STRAIN-CONTROLLED FATIGUE-CRACKING OF AISI 304LC AND 316 STAINLESS STEEL

Robert E. Oldrieve, Jun. 1978 22 p refs.
(NASA-TM-78913, E-9648) Avail: NTIS HC A02/MF A01 CSDL 20K

Analysis of high temperature low cycle fatigue of AISI 304LC and 316 stainless steels by the method of strainrange partitioning results in four separate strainrange versus life relationships depending upon the way in which creep-strain and plastic strain are combined within a cycle. Fractography is used in this investigation of the creep-fatigue interaction associated with these cycles. The PP and PC-cycle fractures were transgranular. The PC-cycle resulted in fewer cycles of initiation and shorter total cyclic life for the same applied inelastic strainrange. The CC-cycle had mixed transgranular and intergranular fracture, fewer cycles of initiation and shorter cycle life than PP or PC. The CP-cycle had fully intergranular cracking, and failed in fewer cycles than were required for cracks to initiate for PP, PC, and CC. Author

N78-32484* National Aeronautics and Space Administration, Lewis Research Center, Cleveland, Ohio.

IMPETUS OF COMPOSITE MECHANICS ON TEST METHODS FOR FIBER COMPOSITES

C. C. Chamis 1978 31 p refs. Presented at the US-USSR Seminar on Fracture of Composite Mater., Riga, USSR, 4-7 Sep. 1978.
(NASA-TM-78979, E-9734) Avail: NTIS HC A03/MF A01 CSDL 11D

The impetus of composite mechanics on composite test methods and/or on interpreting test results is described by using examples from composite micromechanics, composite micromechanics and laminate theory. The specific examples included contributions such as criteria for selecting resin matrices for improved composite strength, the 10 deg off axis tensile test, criteria for configuring hybrids and superhybrids for improved impact resistance and the reduced bending rigidities concept for buckling and vibration analyses. G.G.

A78-10531* Stress analysis and stress-intensity factors for finite geometry solids containing rectangular surface cracks. J. P. Gyekenyesi and A. Mendelson (NASA, Lewis Research Center, Cleveland, Ohio). (*American Society of Mechanical Engineers, Winter Annual Meeting, Atlanta, Ga., Nov. 27-Dec. 2, 1977, Paper 77-WA/APM-5.*) ASME, Transactions, Series E - Journal of Applied Mechanics, vol. 44, Sept. 1977, p. 442-448. 18 refs.

The line method of analysis is applied to the Navier-Cauchy equations of elastic equilibrium to calculate the displacement field in a finite geometry bar containing a variable depth rectangular surface crack under extensionally applied uniform loading. The application of this method to these equations leads to coupled sets of simultaneous ordinary differential equations whose solutions are obtained along sets of lines in a discretized region. Using the obtained displacement field, normal stresses, and the stress-intensity factor variation along the crack periphery are calculated for different crack depth to bar thickness ratios. Crack opening displacements and stress-intensity factors are also obtained for a through-thickness, center-cracked bar with variable thickness. The reported results show a considerable potential for using this method in calculating stress-intensity factors for commonly encountered surface crack geometries in finite solids. (Author)

A78-13817* Mode I stress intensity factors for round compact specimens. B. Gross (NASA, Lewis Research Center, Cleveland, Ohio). *Journal of Testing and Evaluation*, vol. 5, Nov. 1977, p. 457-460. 8 refs.

Mode I stress intensity factors were computed for round compact specimens by the boundary collocation method. Results are presented for ratios A_t/R_0 in the range 0.3 to 0.8, where A_t is the distance from the specimen center to the crack tip for a specimen of diameter $2R_0$. (Author)

A78-23355* Effect of wall thickness and material on flexural fatigue of hollow rolling elements. E. N. Bamberger (General Electric Co., Evendale, Ohio) and R. J. Parker (NASA, Lewis Research Center, Cleveland, Ohio). (*American Society of Lubrication Engineers and American Society of Mechanical Engineers, Joint Lubrication Conference, Kansas City, Mo., Oct. 3-5, 1977, ASME Paper 77-Lub-14.*) ASME, Transactions, Journal of Lubrication Technology, vol. 100, Jan. 1978, p. 39-46. 21 refs.

Hollow cylindrical bars were tested in a rolling-contact fatigue tester to determine the effects of material and outside diameter to inside diameter (OD/ID) ratios on fatigue failure mode and subsequent failure propagation. The range of applied loads with OD/ID ratios of 2.0, 1.6, 1.4, and 1.2 resulted in maximum tangential tensile stresses ranging from 165 to 655 MPa at the bore surface. Flexural failures of the hollow test bars occurred when this bore stress was 490 MPa or greater with AISI 52100 hollow bars and 338 MPa or greater with AISI M 50 hollow bars. Good correlation was obtained in relating the failures of these hollow bars with flexural failures of drilled balls from full-scale bearing test published previously. (Author)

A78-24903* The use of parabolic variations and the direct determination of stress intensity factors using the BIE method. A. Mendelson (NASA, Lewis Research Center, Cleveland, Ohio). *University of Southern California, Symposium on Applications of Computer Methods in Engineering, Los Angeles, Calif., Aug. 23-26, 1977, Paper, 15 p.*

Two advances in the numerical techniques of utilizing the BIE method are presented. The boundary unknowns are represented by parabolas over each interval which are integrated in closed form. These integrals are listed for easy use. For problems involving crack tip singularities, these singularities are included in the boundary integrals so that the stress intensity factor becomes just one more unknown in the set of boundary unknowns thus avoiding the uncertainties of plotting and extrapolating techniques. The method is applied to the problems of a notched beam in tension and bending with excellent results. (Author)

A78-28200 * Simplified contact analysis. D. E. Bruwe and B. J. Hamrock (NASA, Lewis Research Center, Cleveland, Ohio). *Machine Design*, vol. 50, Mar. 9, 1978, p. 119.

A simple and straightforward method for calculating the elastic deformation at the center of contact between two solids with different radii of curvature is proposed instead of the conventional contact deformation analysis for ball bearings, gears, and cams, which usually involves tedious iterative procedures or the use of design charts. Ellipticity of the contact is approximated from a least-squares power fit. Simplified expressions are derived which allow rapid calculation of deformation from the material properties and geometry of the contacting elements. S.D.

A78-29798 * # Nonlinear flap-lag-axial equations of a rotating beam with arbitrary precone angle. R. G. Kvaternik (NASA, Langley Research Center, Aerelasticity Branch, Hampton, Va.), W. F. White, Jr. (NASA, Langley Research Center; U.S. Army, Research and Technology Laboratories, Hampton, Va.), and K. R. V. Kaza (NASA, Lewis Research Center, Cleveland; Toledo, University, Toledo, Ohio). In: Structures, Structural Dynamics and Materials Conference, 19th, Bethesda, Md., April 3-5, 1978, Technical Papers. (A78-29776 11-39) New York, American Institute of Aeronautics and Astronautics, Inc., 1978, p. 214-227, 30 refs. (AIAA 78-491)

In an attempt both to unify and extend the analytical basis of several aspects of the dynamic behavior of flexible rotating beams, the second-degree nonlinear equations of motion for the coupled flapwise bending, lagwise bending, and axial extension of an untwisted, torsionally rigid, nonuniform, rotating beam having an arbitrary angle of precone with the plane perpendicular to the axis of rotation are derived using Hamilton's principle. The derivation of the equations is based on the geometric nonlinear theory of elasticity and the resulting equations are consistent with the assumption that the strains are negligible compared to unity. No restrictions are imposed on the relative displacements or angular rotations of the cross sections of the beam other than those implied by the assumption of small strains. Illustrative numerical results, obtained by using an integrating matrix as the basis for the method of solution, are presented both for the purpose of validating the present method of solution and indicating the range of applicability of the equations of motion and the method of solution. (Author)

A78-35396 * Displacement coefficients along the inner boundaries of radially cracked ring segments subject to forces and couples. B. Gross (NASA, Lewis Research Center, Cleveland, Ohio). *Journal of Testing and Evaluation*, vol. 6, May 1978, p. 196-201, 8 refs.

Displacement results of plane boundary collocation analysis are given for various locations on the inner boundaries of radially cracked ring segments (C shaped specimens) subject to two complementary types of loading. Results are presented for ratios of outer to inner radius in the range of 1.1 to 2.5 and ratios a/W in the range 0.1 to 0.8, where a is the crack length for a specimen of wall thickness W . By combination of these results the resultant displacement coefficient or the corresponding influence coefficient can be obtained for any practical load line location of a pin-loaded specimen. (Author)

N78-18460* # Mechanical Technology, Inc., Latham, N. Y. Research and Development Div
STIFFNESS AND DAMPING OF ELASTOMERIC O-RING BEARING MOUNTS Contractor Report, Sep. 1975 - Jan. 1977

A. J. Smalley Nov. 1977 75 p refs
(Contract NAS3-19751)
(NASA-CR-135328, MTI-78TR17) Avail NTIS
HC A04/MF A01 CSCL 131

A test rig to measure the dynamic stiffness and damping of elastomer O rings was described. Test results for stiffness and loss coefficient in the frequency range from 50 Hz to 1000 Hz are presented. Results are given for three different materials, for five temperatures, for three amplitudes, for five values of squeeze

for three values of stretch for three values of cross-section diameter and for three values of groove width. All test data points were plotted. In addition, trend summary plots were presented which compare the effect of material, temperature, amplitude, squeeze, stretch, cross-section diameter, and groove width. O ring deflections under a static load for different material were presented; and effective static stiffness values were compared with dynamic values. Author

N78-21483* # Boeing Aerospace Co., Seattle, Wash.
ANALYSIS AND TEST OF DEEP FLAWS IN THIN SHEETS OF ALUMINUM AND TITANIUM. VOLUME 1: PROGRAM SUMMARY AND DATA ANALYSIS Contractor Report, Jul. 1976 - Dec. 1977

R. W. Finger Apr. 1978 189 p refs 2 Vol.
(Contract NAS3-19897)
(NASA-CR-135369, D180-24613-1) Avail: NTIS
HC A09/MF A01 CSCL 20K

Six thicknesses of 2219-T87 aluminum base metal surface flaw and center crack specimens ranging from 9.53 to 0.635 mm (0.375 to 0.025 inch) were tested at temperatures ranging from 295K to 20K. Additionally, 6A1-4V STA titanium base metal specimens were tested in three thicknesses 3.18, 2.03, and 1.02 mm (0.125, 0.080 and 0.040 inch) at room temperature. All tests were conducted on uniaxial specimens. Results were analyzed and compared with previously developed data to establish a criterion for proof testing thin walled pressure vessels. The data analysis and exact flaw size dimensions are presented. Author

N78-21484* # Boeing Aerospace Co., Seattle, Wash.
ANALYSIS AND TEST OF DEEP FLAWS IN THIN SHEETS OF ALUMINUM AND TITANIUM. VOLUME 2: CRACK OPENING DISPLACEMENT AND STRESS-STRAIN DATA Contractor Report, Jul. 1976 - Dec. 1977

R. W. Finger Apr. 1978 213 p 2 Vol.
(Contract NAS3-19897)
(NASA-CR-135370, D180-24613-2) Avail: NTIS
HC A10/MF A01 CSCL 20K

Static fracture tests were performed on surface flawed specimens of aluminum and titanium alloys. A simulated proof overload cycle was applied prior to all of the cyclic tests. Variables included in each test series were flaw shapes and thickness. Additionally, test temperature was a variable for the aluminum test series. The crack opening displacement and stress-strain data obtained are presented. Author

N78-22402* # Mechanical Technology, Inc., Latham, N. Y.
DEVELOPMENT OF PROCEDURES FOR CALCULATING STIFFNESS AND DAMPING PROPERTIES OF ELASTOMERS IN ENGINEERING APPLICATIONS. PART 4: TESTING OF ELASTOMERS UNDER A ROTATING LOAD Contractor Report, Oct. 1975 - Mar. 1977

M. S. Darlow and A. J. Smalley Nov. 1977 87 p refs
(Contract NAS3-18548)
(NASA-CR-135355, MTI-78TR18-Pt-4) Avail: NTIS
HC A05/MF A01 CSCL 20K

A test rig designed to measure stiffness and damping of elastomer cartridges under a rotating load excitation is described. The test rig employs rotating unbalance in a rotor which runs to 60,000 RPM as the excitation mechanism. A variable resonant mass is supported on elastomer elements and the dynamic characteristics are determined from measurements of input and output acceleration. Five different cartridges are considered: three of these are buttons cartridges having buttons located in pairs, with 120 between each pair. Two of the cartridges consist of 360 elastomer rings with rectangular cross-sections. Dynamic stiffness and damping are measured for each cartridge and compared with predictions at different frequencies and different strains. Author

A78-32478* General Electric Co., Cincinnati, Ohio. Aircraft Engine Group.

EVALUATION OF CYCLIC BEHAVIOR OF AIRCRAFT TURBINE DISK ALLOYS Final Report, Jun. 1978 - 1978

V. Shehni and H. G. Pop Jun. 1978 202 p refs

(Contract NAS3-20368)

(NASA-CR-189433) Avail: NTIS HC A10/MF A01 CSCL 20K

An evaluation of the cyclic behavior of three aircraft engine turbine disk materials was conducted to compare their relative crack initiation and crack propagation resistance. The disk alloys investigated were Inconel 718, hot isostatically pressed and forged powder metallurgy Rene '95, and as-hot-isostatically pressed Rene '95. The objective was to compare the hot isostatically pressed powder metallurgy alloy forms with conventionally processed superalloys as represented by Inconel 718. Cyclic behavior was evaluated at 650 C both under continuously cycling and a fifteen minute tensile hold time cycle to simulate engine conditions. Analysis of the test data were made to evaluate the strain range partitioning and energy exhaustion concepts for predicting hold time effects on low cycle fatigue. Author

A78-12071* Lamination residual strains and stresses in hybrid laminates. I. M. Daniel and T. Liber (IIT Research Institute, Chicago, Ill.). In: Composite materials: Testing and design; Proceedings of the Fourth Conference, Valley Forge, Pa., May 3, 4, 1976. (A78-12051 02-24) Philadelphia, Pa., American Society for Testing and Materials, 1977, p. 330-343, 7 refs. Contract No. NAS3-16786.

An investigation is conducted of the effects of hybridization on the magnitude of lamination residual stresses. Eight-ply graphite/Kevlar 49/epoxy and graphite/S-glass/epoxy laminates were studied. The same matrix resin was selected for all basic materials to ensure compatibility and uniform curing of the various plies. The specimens, with inserted strain gages and thermocouples, were subjected to curing and postcuring cycles in an autoclave. Subsequently, the specimens were subjected to a thermal cycle from room temperature to 444 K and down to room temperature. It was found that hybridizing reduces apparently residual strains and stresses in the graphite plies. However, these strains were not affected much by the type and degree of hybridization. G.R.

43 EARTH RESOURCES

Includes remote sensing of earth resources by aircraft and spacecraft; photogrammetry; and aerial photography.
For instrumentation see 35 *Instrumentation and Photography*.

N78-14482* National Aeronautics and Space Administration, Lewis Research Center, Cleveland, Ohio.
IN-SITU LASER RETORTING OF OIL SHALE Patent
Harvey S. Bloomfield, inventor (to NASA) Issued 6 Dec. 1977
5 p Filed 28 Jan. 1977 Supersedes N77-18428 (15 - 09, p 1176)

(NASA-Case-LEW-12217-1; US-Patent-4,061,190;
US-Patent-App-SN-763753; US-Patent-Class-166-259;
US-Patent-Class-166-248) Avail: US Patent Office CSCI 081
Oil shale formations are retorted in situ and gaseous hydrocarbon products are recovered by drilling two or more wells into an oil shale formation underneath the surface of the ground. A high energy laser beam is directed into the well and fractures the region of the shale formation. A compressed gas is forced into the well that supports combustion in the flame front ignited by the laser beam, thereby, retorting the oil shale. Gaseous hydrocarbon products which permeate through the fractured region are recovered from one of the wells that were not exposed to the laser system. Official Gazette of the U.S. Patent Office

N78-33510* National Aeronautics and Space Administration, Lewis Research Center, Cleveland, Ohio.
AERIAL THERMOGRAPHY FOR ENERGY CONSERVATION
John R. Jack Sep. 1978 22 p refs Original contains color illustrations
(NASA-TM-78959; E-9711) Avail: NTIS HC A02/MF A01 CSCI 14E

Thermal infrared scanning from an aircraft is a convenient and commercially available means for determining relative rates of energy loss from building roofs. The need to conserve energy as fuel costs makes the mass survey capability of aerial thermography an attractive adjunct to community energy awareness programs. Background information on principles of aerial thermography is presented. Thermal infrared scanning systems, flight and environmental requirements for data acquisition, preparation of thermographs for display, major users and suppliers of thermography, and suggested specifications for obtaining aerial scanning services were reviewed. B.B.

44 ENERGY PRODUCTION AND CONVERSION

Includes specific energy conversion systems, e.g., fuel cells and batteries; global sources of energy; fossil fuels; geophysical conversion; hydroelectric power; and wind power.

For related information see also *07 Aircraft Propulsion and Power*, *20 Spacecraft Propulsion and Power*, *28 Propellants and Fuels*, and *85 Urban Technology and Transportation*.

N78-13527* National Aeronautics and Space Administration, Lewis Research Center, Cleveland, Ohio.

SOLAR CELL HIGH EFFICIENCY AND RADIATION DAMAGE

1977 221 p refs Conf. held at Cleveland, 18-19 May 1977 (NASA-CP-2020) Avail: NTIS HC A10/MF A01 CSCL 10A

Silicon solar cell analysis and fundamental measurements, silicon cell technology, gallium arsenide research and technology, and radiation effects on silicon and gallium arsenide cells, are reported. For individual titles, see N78-13528 through N78-13551.

N78-13528* National Aeronautics and Space Administration, Lewis Research Center, Cleveland, Ohio.

SUMMARY OF THE NASA SPACE PHOTOVOLTAIC RESEARCH AND TECHNOLOGY PROGRAM

Henry W. Brandhorst, Jr. In *Solar Cell High Efficiency and Radiation Damage* 1977 p 3-6 (For availability see N78-13527 04-44)

Avail: NTIS HC A10/MF A01 CSCL 10A

Low cost solar cells and arrays with high end-of-life efficiency are evaluated through two approaches: one, to obtain increased device efficiency at no increase in cost and two, to reduce the manufacturing costs of space solar cells and arrays. Technology efforts encompass high efficiency epitaxial cells, high efficiency wraparound contact solar cells, economical diffusion sources, automated cell fabrication and development of easily applied, durable cover glasses. The examination of ion-implanted profile tailored junctions and additional development of screen printed contact technology to cell development are also considered.

Author

N78-13534* National Aeronautics and Space Administration, Lewis Research Center, Cleveland, Ohio.

IMPURITY CONCENTRATIONS AND SURFACE CHARGE DENSITIES ON THE HEAVILY DOPED FACE OF A SILICON SOLAR CELL

I. Weinberg and Lon Hsu (Wayne State Univ.) In *NASA Lewis Res Center Solar Cell High Efficiency and Radiation Damage* 1977 p 89-79 refs (For availability see N78-13527 04-44) Avail: NTIS HC A10/MF A01 CSCL 10A

Increased solar cell efficiencies are attained by reduction of surface recombination and variation of impurity concentration profiles at the $n(+)$ surface of silicon solar cells. Diagnostic techniques are employed to evaluate the effects of specific materials preparation methodologies on surface and near surface concentrations. It is demonstrated that the MOS C-V method, when combined with a bulk measurement technique, yields more complete concentration data than are obtainable by either method alone. Specifically, new solar cell MOS C-V measurements are combined with bulk concentrations obtained by a successive layer removal technique utilizing measurements of sheet resistivity and Hall coefficient.

Author

N78-13606* National Aeronautics and Space Administration, Lewis Research Center, Cleveland, Ohio.

SOME BASIC CONSIDERATIONS OF MEASUREMENTS INVOLVING COLLIMATED DIRECT SUNLIGHT

An-Tr. Chai 1976 18 p refs Presented at Terrest PV Meas. Workshop, Baton Rouge, La., 10 Nov. 1976 (Contract EX-76-A-29-1022)

(NASA-TM-74947; TR-2-8; ERDA/NASA-1022/76/8; Conf-761129-8) Avail: NTIS HC A02/MF A01 CSCL 10A

The geometry of collimators for devices or instruments dealing with terrestrial direct sunlight is discussed. Effects of the opening angle and slope angle of a collimator on the measurements are investigated with regard to variations of turbidity and air mass. Based on this investigation, geometric dimensions for collimators and certain realistic terrestrial reference conditions are recommended for the purpose of solar cell calibration in terrestrial applications. ERA

N78-14625* National Aeronautics and Space Administration, Lewis Research Center, Cleveland, Ohio.

MULTI-CELL BATTERY PROTECTION SYSTEM Patent

Ralph D. Thomas and William J. Nagle, inventors (to NASA) Issued 6 Dec. 1977 5 p Filed 19 May 1976 Supersedes N76-23713 (14-14, p 1820)

(NASA-Case-LEW-12039-1, US-Patent-4,061,955;

US-Patent-AppI-SN-687822, US-Patent-Class-320-8;

US-Patent-Class-320-15, US-Patent-Class-320-18;

US-Patent-Class-320-40) Avail: US Patent Office CSCL 10A

A multi-cell battery protection system is described wherein each cell has its own individual protective circuit. The protective circuits consist of a solid state comparator unit and a high current switching device such as a relay. The comparator units each continuously monitor the associated cell and when the cell voltage either exceeds a predetermined high level or falls below a predetermined low level, the relay is actuated whereby a bypass circuit is completed across the cell thereby effectively removing the cell from the series of cells.

Official Gazette of the U.S. Patent Office

N78-14628* National Aeronautics and Space Administration, Lewis Research Center, Cleveland, Ohio.

REAL-TIME AND ACCELERATED OUTDOOR ENDURANCE TESTING OF SOLAR CELLS

Americo F. Forestieri and Evelyn Anagnostou Aug 1977 28 p refs Presented at 1977 Photovoltaics Solar Energy Conf., Luxembourg, 27-30 Sep 1977, sponsored by Comm. of the European Communities. Sponsored in part by ERDA (Contract E(49-26) 1022)

(NASA-TM-73743, E 9310, ERDA/NASA/1022/77/17) Avail: NTIS HC A03/MF A01 CSCL 10A

Real-time and accelerated outdoor endurance testing was performed on a variety of samples of interest to the National Photovoltaic Conversion Program. The real-time tests were performed at seven different sites and the accelerated tests were performed at one of those sites in the southwestern United States. The purpose of the tests were to help evaluate the lifetime of photovoltaic systems. Three types of samples were tested: transmission samples of possible cover materials, sub-modules constructed using these materials attached to solar cells, and solar cell modules produced by the manufacturers for the ERDA program. Results indicate that suitable cover materials are glass, FEP A and PFA. Dirt accumulation and cleanability are important factors in the selection of solar cell module covers and encapsulants.

Author

N78-14629* National Aeronautics and Space Administration, Lewis Research Center, Cleveland, Ohio.

US TERRESTRIAL SOLAR CELL CALIBRATION AND MEASUREMENT PROCEDURES

Henry W. Brandhorst, Jr. Sep 1977 16 p refs Presented at 1977 Photovoltaics Solar Energy Conf., Luxembourg, 27-30 Sep 1977, sponsored by Comm. of the European Communities. Sponsored in part by ERDA (Contract E(49-26) 1022)

(NASA-TM-73788, E 9353, ERDA/NASA/1022/77/20) Avail: NTIS HC A02/MF A01 CSCL 10A

A workshop was held in the fall of 1976, to evaluate and revise interim terrestrial solar cell calibration and measurement procedures. The revisions made to the interim testing procedures are described. The calibration of reference cells and the design of their holders are covered. Considerations include view angle and optical and thermal matching. Atmospheric factors which

affect the calibration and performance of solar cells are discussed. The most critical atmospheric parameter appears to be water vapor. Techniques for matching reference cells to cells or arrays under test are described. Data showing errors in performance under artificial sunlight simulators due to mismatch of reference and test cells are presented. Finally, measurement procedures and data transformations needed to obtain the performance of solar cells and arrays in outdoor natural sunlight are described.

Author

N78-14630* National Aeronautics and Space Administration, Lewis Research Center, Cleveland, Ohio.
SOLAR ENERGY METER

R. M. Masters Sep. 1977 12 p ref. Sponsored in part by ERDA

(Contract E(49-26)-1022)

(NASA-TM-7379), E-9358; ERDA/NASA/1022/77/21) Avail: NTIS HC A02/MF A01 CSCL 10A

An instrument was developed to continually integrate the energy available in incident light on a specifically oriented surface. The unit was designed for outdoor use in remote locations and is capable of operation over a temperature range of -20 to +60 C with good accuracy. The unit is weather resistant, requires low power, has a high input impedance, is inexpensive, and has a visual readout and an analog output for recording.

Author

N78-14631* National Aeronautics and Space Administration, Lewis Research Center, Cleveland, Ohio.

ANION EXCHANGE MEMBRANES FOR ELECTROCHEMICAL OXIDATION-REDUCTION ENERGY STORAGE SYSTEM

Patricia M. O'Donnell, Dean W. Sheibley, and Randall F. Gahn Aug. 1977 22 p refs

(Contract E(49-26)-1002)

(NASA-TM-7375), ERDA/NASA-1002/77/2; E-9222) Avail: NTIS HC A02/MF A01 CSCL 10C

Oxidation-reduction couples in concentrated solutions separated by appropriate ion selective membranes were considered as an attractive approach to bulk electrical energy storage. A key problem is the development of the membrane. Several promising types of anionic membranes are discussed which were developed and evaluated for redox energy storage systems. The copolymers of ethyleneglycoldimethacrylate with either 2-vinylpyridine or vinylbenzyl chloride gave stable resistance values compared to the copolymer of vinylbenzylchloride and divinylbenzene which served as the baseline membrane. A polyvinylchloride film aminated with tetraethylenepentamine had a low resistance but a high ion transfer rate. A slurry coated vinylpyridine had the lowest ion transfer rate. All these membranes functioned well in laboratory cells at ambient temperatures with the acidic chloride oxidant/reductant system, Fe³⁺, Fe²⁺/Ti³⁺, Ti⁴⁺.

Author

N78-15582* National Aeronautics and Space Administration, Lewis Research Center, Cleveland, Ohio.

BLACK CHROME ON COMMERCIALY ELECTROPLATED TIN AS A SOLAR SELECTING COATING

G. E. McDonald Sep. 1977 10 p refs Presented at Concentrating Collector Conf., Atlanta, 26-28 Sep. 1977

(Contract EX-76-29-1060)

(NASA-TM-73799; ERDA/NASA-1060/77/1; E-9375) Avail: NTIS HC A02/MF A01 CSCL 10A

The reflectance properties of black chrome electroplated on commercially electroplated tin were measured for various black chrome plating times for both the solar and infrared spectrum. The values of absorptance and emittance were calculated from the measured reflectance values. The results indicate that the optimum combination of the highest absorptance in the solar region and the lowest emittance in the infrared of the black chrome plated on commercially electroplated tin is obtained for a black chrome plating time of between one and two minutes.

Author

N78-15583* National Aeronautics and Space Administration, Lewis Research Center, Cleveland, Ohio.

ERDA/NASA 100 KILOWATT MOD-O WIND TURBINE OPERATIONS AND PERFORMANCE

R. L. Thomas and T. R. Richards Sep. 1977 18 p refs Presented at Conf. on Wind Energy Conversion Systems, Wash., D. C., 19-21 Sep. 1977

(Contract E(49-26)-1028)

(NASA-TM-73825; ERDA/NASA-1028/77/9) Avail: NTIS HC A02/MF A01 CSCL 10B

The ERDA/NASA 100 kW Mod-O wind turbine is operating at the NASA Plum Brook Station near Sandusky, Ohio. The operation of the wind turbine has been fully demonstrated and includes start-up, synchronization to the utility network, blade pitch control for control of power and speed, and shut-down. Also, fully automatic operation has been demonstrated by use of a remote control panel, 50 miles from the site, similar to what a utility dispatcher might use. The operation systems and experience with the wind turbine loads, electrical power and aerodynamic performance obtained from testing are described.

Author

N78-16434* National Aeronautics and Space Administration, Lewis Research Center, Cleveland, Ohio.

APPROXIMATE METHOD FOR CALCULATING FREE VIBRATIONS OF A LARGE-WIND-TURBINE TOWER STRUCTURE

Sankar C. Das and Bradford S. Linscott Dec. 1977 46 p refs

(Contract E(49-26)-1028)

(NASA-TM-73754; ERDA/NASA-1028/77/12) Avail: NTIS HC A03/MF A01 CSCL 10A

A set of ordinary differential equations were derived for a simplified structural dynamic lumped-mass model of a typical large-wind-turbine tower structure. Dunkerley's equation was used to arrive at a solution for the fundamental natural frequencies of the tower in bending and torsion. The ERDA-NASA 100-kW wind turbine tower structure was modeled, and the fundamental frequencies were determined by the simplified method described. The approximate fundamental natural frequencies for the tower agree within 18 percent with test data and predictions analyzed.

Author

N78-16435* National Aeronautics and Space Administration, Lewis Research Center, Cleveland, Ohio.

PHOTOVOLTAIC REFRIGERATION APPLICATION: ASSESSMENT OF THE NEAR-TERM MARKET

Louis Rosenblum, William J. Briano, William A. Poley, and Larry R. Scudder Dec. 1977 19 p

(Contract E(49-26)-1022)

(NASA-TM-73876; E-9476; DOE/NASA-1022/77/23) Avail: NTIS HC A02/MF A01 CSCL 10A

This foreign and domestic market assessment was performed as part of the Tests and Applications Project being conducted by NASA-LaRC as part of the Department of Energy's (DOE) National Photovoltaic Program. One of the objectives of that program was to stimulate the demand for photovoltaic power systems so that appropriate markets would be developed in concert with the increasing photovoltaic production capacity. The refrigeration application represented a possible market for photovoltaics; hence, a brief survey of potential applications was conducted. Both refrigerators and refrigeration systems were considered in the assessment although the primary emphasis is on refrigerators of 9 cu ft or less. Three user sectors were examined: (1) government, (2) commercial/institutional, and (3) general public.

Author

N78-17486* National Aeronautics and Space Administration, Lewis Research Center, Cleveland, Ohio.

WIND TURBINE GENERATOR ROTOR BLADE CONCEPTS WITH LOW COST POTENTIAL

T. L. Sullivan, T. P. Cahill, D. G. Griffie, Jr. (United Technologies Corp., Windsor Locks, Conn.) and H. W. Gewehr (Kaman Aerospace Corp.) Dec. 1977 38 p refs To be Presented at the 23rd Natl. SAMPE Symp., Anaheim, Calif., 2-4 May 1978

(Contract E(49-26) 1028)
 (NASA-TM-73836, DOE/NASA-1028-77/13, E-9422) Avail:
 NTIS HC A03/MF A01 CSCL 10A

Four processes for producing blades are examined. Two use filament winding techniques and two involve filling a mold or form to produce all or part of a blade. The processes are described and a comparison is made of cost, material properties, design and free vibration characteristics. Conclusions are made regarding the feasibility of each process to produce low cost, structurally adequate blades. Author

N78-17467* National Aeronautics and Space Administration, Lewis Research Center, Cleveland, Ohio.
SYNCHRONIZATION OF THE DOE/NASA 100-KILOWATT WIND TURBINE GENERATOR WITH A LARGE UTILITY NETWORK

Leonard J. Gilbert Dec 1977 19 p refs
 (Contract E(49-26) 1028)

(NASA-TM-73861, E-9450; DOE/NASA/1028/77/10) Avail:
 NTIS HC A02/MF A01 CSCL 10A

The DOE/NASA 100 kilowatt wind turbine generator system was synchronized with a large utility network. The system equipments and procedures associated with the synchronization process were described. Time history traces of typical synchronizations were presented indicating that power and current transients resulting from the synchronizing procedure are limited to acceptable magnitudes. Author

N78-17468* National Aeronautics and Space Administration, Lewis Research Center, Cleveland, Ohio.
STATUS OF THE DOE (STOR)-SPONSORED NATIONAL PROGRAM ON HYDROGEN PRODUCTION FROM WATER VIA THERMOCHEMICAL CYCLES

C. E. Baker 1977 16 p refs Presented at the Miami Intern. Conf. on Alternative Energy Sources, Miami Beach, Fla., 5-7 Dec. 1977; sponsored by Dept. of Energy and Miami Univ.
 (NASA-TM-78825; E-9529) Avail: NTIS HC A02/MF A01 CSCL 07D

The program structure is presented. The activities of the thermochemical cycles program are grouped according to the following categories: (1) specific cycle development, (2) support research and technology, (3) cycle evaluation. Specific objectives and status of on-going activities are discussed. Chemical reaction series for the production of hydrogen are presented. Efficiency and economic evaluations are also discussed. G.Y.

N78-17469* National Aeronautics and Space Administration, Lewis Research Center, Cleveland, Ohio.
TECHNICAL AND ECONOMIC FEASIBILITY STUDY OF SOLAR/FOSSIL HYBRID POWER SYSTEMS

Harvey S. Bloomfield and James E. Calogeres Dec. 1977 70 p refs
 (NASA-TM-73820, E-9409; Avail: NTIS HC A04/MF A01 CSCL 10B)

Results show that new hybrid systems utilizing fossil fuel augmentation of solar energy can provide significant capital and energy cost benefits when compared with solar thermal systems requiring thermal storage. These benefits accrue from a reduction of solar collection area that results from both the use of highly efficient gas and combined cycle energy conversion subsystems and elimination of the requirement for long-term energy storage subsystems. Technical feasibility and fuel savings benefits of solar hybrid retrofit to existing fossil-fired gas and vapor cycle powerplants were confirmed, however economic viability of steam cycle retrofit was found to be dependent on the thermodynamic and operational characteristics of the existing powerplant. Author

N78-18609* National Aeronautics and Space Administration, Lewis Research Center, Cleveland, Ohio.

SELECTIVE COATING FOR SOLAR PANELS Patent
 Glen E. McDonald, inventor (to NASA) Issued 26 Oct 1977
 6 p Filed 22 Dec. 1975 Supersedes N78-15603 (14 - 08, p 0741)

(NASA-Case-LEW-12159-1; US-Patent-4,055,707;
 US-Patent-Appl-SN-843041; US-Patent-Class-428-652;
 US-Patent-Class-128-270; US-Patent-Class-427-180;
 US-Patent-Class-428-667; US-Patent-Class-428-679) Avail:
 US Patent Office CSCL 10A

The energy absorbing properties of solar heating panels are improved by depositing a black chrome coating of controlled thickness on a specially prepared surface of a metal substrate. The surface is prepared by depositing a dull nickel on the substrate, and the black chrome is plated on this low emittance surface to a thickness between 0.5 micron and 2.5 microns.

Official Gazette of the U.S. Patent Office

N78-18616* National Aeronautics and Space Administration, Lewis Research Center, Cleveland, Ohio.

WIND TURBINE STRUCTURAL DYNAMICS

Dean R. Miller, ed. 1978 280 p refs Workshop held at Cleveland, 15-17 Nov. 1977; sponsored by DOE
 (NASA-CP-2034; DOE-Conf-771148; E-9518) Avail: NTIS HC A13/MF A01 CSCL 10A

A workshop on wind turbine structural dynamics was held to review and document current United States work on the dynamic behavior of large wind turbines, primarily of the horizontal-axis type, and to identify and discuss other wind turbine configurations that may have lower cost and weight. Information was exchanged on the following topics: (1) Methods for calculating dynamic loads; (2) Aeroelasticity stability; (3) Wind loads, both steady and transient; (4) Critical design conditions; (5) Drive train dynamics; and (6) Behavior of operating wind turbines. For individual titles, see N78-19617 through N78-19641.

N78-19617* National Aeronautics and Space Administration, Lewis Research Center, Cleveland, Ohio.

COMPARISON OF COMPUTER CODES FOR CALCULATING DYNAMIC LOADS IN WIND TURBINES

David A. Spers In *its* Wind Turbine Structural Dyn. 1978 p 1-13 refs (For availability see N78-19616 1C 4)
 Avail: NTIS HC A13/MF A01 CSCL 10A

The development of computer codes for calculating dynamic loads in horizontal axis wind turbines was examined, and a brief overview of each code was given. The performance of individual codes was compared against two sets of test data measured on a 100 KW Mod-0 wind turbine. All codes are aeroelastic and include loads which are gravitational, inertial and aerodynamic in origin. Author

N78-19618* National Aeronautics and Space Administration, Lewis Research Center, Cleveland, Ohio.

SIMPLIFIED MODELING FOR WIND TURBINE MODAL ANALYSIS USING NASTRAN

Timothy L. Sullivan In *its* Wind Turbine Structural Dyn. 1978 p 31-38 refs (For availability see N78-19616 10-44)
 Avail: NTIS HC A13/MF A01 CSCL 10A

A detailed finite element model of the MOD-0 wind turbine tower was reduced to six beam elements (stick model). The method used to calculate the properties of the beam elements in the stick model was explained and the accuracy of the stick model in predicting natural frequencies and mode shapes was examined. Computer times were compared and several applications where the stick model was used are described. From results obtained from the MOD-0 tower it is concluded that a tower of this type can be modeled as a simple cantilever beam for modal analysis. However, this model should be limited to tower torsional modes and tower bending modes where the mode shape resembles a cantilever beam first bending mode shape. Author

N78-18828* National Aeronautics and Space Administration, Lewis Research Center, Cleveland, Ohio.

INFLUENCE OF WIND TURBINE FOUNDATION

Suey T. Yee *In its* Wind Turbine Structural Dyn. 1978 p 103-108 (For availability see N78-18818 10-44)

Avail: NTIS HC A13/MF A01 CSCL 10A

The 200 kW Mod-0A wind turbine was modeled using a 3 lumped mass-spring system for the superstructure and a rotational spring for the foundation and supporting soil. Natural frequencies were calculated using soil elastic moduli varying from 3000 to 22,400 p.s.i. The reduction in natural frequencies from the rigid foundation case ranged up to 20 percent. Author

N78-18827* National Aeronautics and Space Administration, Lewis Research Center, Cleveland, Ohio.

SUMMARY OF STATIC LOAD TEST OF THE MOD-0 BLADE

Dean R Miller *In its* Wind Turbine Structural Dyn. 1978 p 109-116 refs (For availability see N78-18818 10-44)

Avail: NTIS HC A13/MF A01 CSCL 10A

A static load test was performed on the spare Mod-0 wind turbine blade to define load transfer at the root and end of the blade, and to validate stress analysis of this particular type of blade construction (frame and stringer). Analysis of the load transfer from the airfoil skin to the shank tube predicted a step change in spanwise stress in the airfoil skin at station 81.5 inches (STA 81.5). For flapwise bending a 40% reduction in spanwise stress was predicted, and for edgewise bending a 6% reduction. Experimental results verified the 40% reduction for flapwise bending, but indicated about a 30% reduction for edgewise bending. Author

N78-18825* National Aeronautics and Space Administration, Lewis Research Center, Cleveland, Ohio.

DOE/NASA MOD-0 100KW WIND TURBINE TEST RESULTS

John C Glasgow *In its* Wind Turbine Structural Dyn. 1978 p 117-150 refs (For availability see N78-18818 10-44)

Avail: NTIS HC A13/MF A01 CSCL 10A

The Wind Turbine demonstrates the capability of automatic unattended operation, including startup, achieving synchronism, and shutdown as dictated by wind conditions. During the course of these operations, a wealth of engineering data was generated. Some of the data which is associated with rotor and machine dynamics problems encountered, and the machine modifications incorporated as a solution are presented. These include high blade loads due to tower shadow, excessive nacelle yawing motion, and power oscillations. The results of efforts to correlate measured wind velocity with power output and wind turbine loads are also discussed. Author

N78-18829* National Aeronautics and Space Administration, Lewis Research Center, Cleveland, Ohio.

POWER OSCILLATION OF THE MOD-0 WIND TURBINE

Robert C Sedel *In its* Wind Turbine Structural Dyn. 1978 p 151-156 (For availability see N78-18818 10-44)

Avail: NTIS CSCL 10A

The Mod-0 power has noise components with varying frequency patterns. Magnitudes reach more than forty percent power at the frequency of twice per rotor revolution. Analysis of a simple torsional model of the power train predicts less than half the observed magnitude and does not explain the shifting frequencies of the noise patterns. Author

N78-18832* National Aeronautics and Space Administration, Lewis Research Center, Cleveland, Ohio.

METHODS OF ATTENUATING WIND TURBINE GENERATOR OUTPUT VARIATIONS

Harold Gold *In its* Wind Turbine Structural Dyn. 1978 p 179-186 refs (For availability see N78-18818 10-44)

Avail: NTIS HC A13/MF A01 CSCL 10A

Wind speed variation, tower blockage and structural and

inertial factors produce unsteady torque in wind turbines. Methods for modifying the turbine torque so that steady torque is delivered to the coupled ac generator are discussed. The method that may evolve will be influenced by the power use that develops and the trade-offs of cost, weight and complexity. Author

N78-18835* National Aeronautics and Space Administration, Lewis Research Center, Cleveland, Ohio.

EFFECTS OF ROTOR LOCATION, CONING, AND TILT ON CRITICAL LOADS IN LARGE WIND TURBINES

D. A. Spars and D. C. Janzke *In its* Wind Turbine Structural Dyn. 1978 p 227-236 refs (For availability see N78-18818 10-44)

Avail: NTIS HC A13/MF A01 CSCL 10A

Several large (1500 kW) horizontal rotor configurations were analyzed to determine the effects on dynamic loads of upwind downwind rotor locations, coned and radial blade positions, and tilted and horizontal rotor axis positions. Loads were calculated for a range of wind velocities at three locations in the structure: (1) the blade shank; (2) the hub shaft; and (3) the yaw drive. Blade axis coning and rotor axis tilt were found to have minor effects on loads. However, locating the rotor upwind of the tower significantly reduced loads at all locations analyzed. Author

N78-18838* National Aeronautics and Space Administration, Lewis Research Center, Cleveland, Ohio.

FIXED PITCH WIND TURBINES

David B. Fenn and Larry A. Viterna *In its* Wind Turbine Structural Dyn. 1978 p 243-254 (For availability see N78-18818 10-44)

Avail: NTIS HC A13/MF A01 CSCL 10A

Wind turbines designed for fixed pitch operation offer potential reductions in the cost of the machine by eliminating many costly components. It was shown that a rotor can be designed which produces the same energy annually as Mod-0 but which regulates its power automatically by progressively twisting the blades as wind speed increases. Effects of blade twist, taper, root cutout, and airfoil shape on performance are discussed as well as various starting techniques. Author

N78-18842* National Aeronautics and Space Administration, Lewis Research Center, Cleveland, Ohio.

EXPERIMENTAL DATA AND THEORETICAL ANALYSIS OF AN OPERATING 100 kW WIND TURBINE

Bradford S. Linacott, John C. Glasgow, William D. Anderson (Lockheed California Co., Burbank), and Robert E. Donham (Lockheed California Co., Burbank) Jan. 1978 21 p refs Presented at 12th Intersec. Energy Conversion Engr. Conf., Washington, D. C., 28 Aug. - 2 Sep. 1977; sponsored by Am. Nucl. Soc.

(Contract E(49-26)-1028)

(NASA-TM 73883, DOE/NASA/1028-78/15, E-9486) Avail: NTIS HC A02/MF A01 CSCL 10A

Experimental test data are correlated with analyses of turbine loads and complete system behavior of the ERDA-NASA 100 kW Mod-0 wind turbine generator over a broad range of steady state conditions, as well as during transient conditions. The deficit in the ambient wind field due to the upwind tower turbine support structure is found to be very significant in exciting higher harmonic loads associated with the flapping response of the blade in bending. Author

N 8-18843* National Aeronautics and Space Administration, Lewis Research Center, Cleveland, Ohio.

PHOTOVOLTAIC VILLAGE POWER APPLICATION: ASSESSMENT OF THE NEAR-TERM MARKET

Louis Rosenblum, William J. Briano, William A. Foley, and Larry R. Scudder Jan. 1978 29 p refs

(Contract E(49-26) 1022)

(NASA-TM 73883, DOE/NASA/1022-78/25, E-9510) Avail: NTIS HC A03/MF A01 CSCL 10B

The village power application represents a potential market for photovoltaics. The price of energy for photovoltaic systems

was compared to that of utility line extensions and diesel generators. The potential domestic demand was defined in both the government and commercial sectors. The foreign demand and sources of funding for village power systems in the developing countries were also discussed briefly. It was concluded that a near term domestic market of at least 12 MW min and a foreign market of about 10 GW exists. Author

N78-18844* National Aeronautics and Space Administration, Lewis Research Center, Cleveland, Ohio.
PHOTOVOLTAIC WATER PUMPING APPLICATIONS: ASSESSMENT OF THE NEAR-TERM MARKET
 Louis Rosenblum, William J. Bifano, Larry R. Scudder, William A. Potay, and James P. Cusik. Mar. 1978. 24 p refs.
 (Contract E(49-26)-1022)
 (NASA-TM-78847; E-9566; DOE/NASA/1022-78/28) Avail: NTIS HC A02/MF A01 CSCL 108

Water pumping applications represent a potential market for photovoltaics. The price of energy for photovoltaic systems was compared to that of utility line extensions and diesel generators. The potential domestic demand was defined in the government, commercial/institutional and public sectors. The foreign demand and sources of funding for water pumping systems in the developing countries were also discussed briefly. It was concluded that a near term domestic market of at least 240 megawatts and a foreign market of about 6 gigawatts exist. Author

N78-18848* National Aeronautics and Space Administration, Lewis Research Center, Cleveland, Ohio.
DETERMINATION OF THE ZINCATE DIFFUSION COEFFICIENT AND ITS APPLICATION TO ALKALINE BATTERY PROBLEMS
 Charles E. May. 1978. 20 p refs. Proposed for presentation at the Electrochemical Soc. Meeting, Pittsburgh, 15-20 Oct 1978.
 (NASA-TM 73879; E-9486) Avail: NTIS HC A02/MF A01 CSCL 10C

The diffusion coefficient for the zincate ion at 24 C was found to be 9.9×10^{-7} to the minus 7th power squared cm per sec. or .30 percent in 45 percent potassium hydroxide and 1.4×10^{-7} to the minus 7 squared cm per sec. or .25 percent in 40 percent sodium hydroxide. Comparison of these values with literature values at different potassium hydroxide concentrations show that the Stokes Einstein equation is obeyed. The diffusion coefficient is characteristic of the zincate ion (not the cation) and independent of its concentration. Calculations with the measured value of the diffusion coefficient show that the zinc concentration in an alkaline zincate half cell becomes uniform throughout in tens of hours by diffusion alone. Diffusion equations are derived which are applicable to finite size chambers. Details and discussion of the experimental method are also given. Author

N78-18868* National Aeronautics and Space Administration, Lewis Research Center, Cleveland, Ohio.
REDOX FLOW CELL DEVELOPMENT AND DEMONSTRATION PROJECT, CALENDAR YEAR 1978
 Dec 1977. 48 p refs.
 (Contract E(49-28)-1002)
 (NASA-TM 73873; F-9354; CONS/1002-3) Avail: NTIS HC A03/MF A01 CSCL 10A

The major focus of the effort was the key technology issues that directly influence the fundamental feasibility of the overall redox concept. These issues were the development of a suitable semipermeable separator membrane for the system, the screening and study of candidate redox couples to achieve optimum cell performance, and the carrying out of systems analysis and modeling to develop system performance goals and cost estimates. Author

N78-18887* National Aeronautics and Space Administration, Lewis Research Center, Cleveland, Ohio.
PHOTOVOLTAIC POWER SYSTEM TESTS ON AN 8-KILO-WATT SINGLE-PHASE LINE-COMMUTATED INVERTER
 John B. Stover. Feb. 1978. 16 p refs.
 (Contract E(49-26)-1022)
 (NASA-TM-78824; E-9527; DOE/NASA/1022-78/26) Avail: NTIS HC A02/MF A01 CSCL 10B

Efficiency and power factor were measured as functions of solar array voltage and current. The effects of input shunt capacitance and series inductance were determined. Tests were conducted from 15 to 75 percent of the 8 kW rated inverter input power. Measured efficiencies ranged from 78 percent to 88 percent at about 50 percent of rated inverter input power. Power factor ranged from 36 percent to 72 percent. Author

N78-18888* National Aeronautics and Space Administration, Lewis Research Center, Cleveland, Ohio.
RESULTS OF MODULE ELECTRICAL MEASUREMENT OF THE DOE 46-KILOWATT PROCUREMENT
 Henry B. Curtis. Feb. 1978. 20 p refs.
 (Contract E(49-26)-1022)
 (NASA-TM-78829; E-9534; DOE/NASA/1022-78/27) Avail: NTIS HC A02/MF A01 CSCL 10B

Current-voltage measurements have been made on terrestrial solar cell modules of the DOE/JPL Low Cost Silicon Solar Array procurement. Data on short circuit current, open circuit voltage, and maximum power for the four types of modules are presented in normalized form, showing distribution of the measured values. Standard deviations from the mean values are also given. Tests of the statistical significance of the data are discussed. Author

N78-21886* National Aeronautics and Space Administration, Lewis Research Center, Cleveland, Ohio.
EFFLUENT CHARACTERIZATION FROM A CONICAL PRESSURIZED FLUID BED
 R. J. Prem, R. J. Rollbuhler, and R. W. Patch. Dec. 1977. 15 p refs. Presented at the 5th Intern Conf on Fluidized-Bed Combust., Washington, D. C., 12-14 Dec 1977.
 (NASA-TM 73887; E-9524) Avail: NTIS HC A02/MF A01 CSCL 10A

To obtain useable corrosion and erosion results it was necessary to have data with several levels of particulate matter in the hot gases. One level of particulate loading was as low as possible so that ideally no erosion and only corrosion occurred. A conical fluidized bed was used to obtain some degree of filtration through the top of the bed which would not be highly fluidized. This would minimize the filtration required for the hot gases or conversely the amount of particulate matter in the hot gases after a given level of filtration by cyclones and/or filters. The data obtained during testing characterized the effluent from the bed at different test conditions. A range of bed heights, coal flows, air flows, limestone flow, and pressure are represented. These tests were made to determine the best operating conditions prior to using the bed to determine erosion and corrosion rates of typical turbine blade materials. Author

N78-22671* National Aeronautics and Space Administration, Lewis Research Center, Cleveland, Ohio.
SOME PROPERTIES OF LOW-VAPOR-PRESSURE BRAZE ALLOYS FOR THERMIONIC CONVERTERS
 Virginia Bar. 1978. 14 p refs. Presented at the Intern Plasma Sci Conf, Monterey, Calif., sponsored by IEEE.
 (NASA-TM 78867; E-9598) Avail: NTIS HC A02/MF A01 CSCL 10A

Property measurements were made for arc melted, rod shaped specimens. Density and dc electrical resistivity at 296 K were measured for various binary eutectic alloys. Thermal conductivity was inferred from the electrical conductivity using the Wiedemann-Franz Lorenz relation. Linear thermal expansion from 293 K to two thirds melting point under a helium atmosphere was measured for Zr-21.7 wt percent Ru, Zr-13 wt percent W, Zr-22.3 wt percent Nb, Nb-66.9 wt percent Ru, and Zr-25.7 wt percent Ta. Author

N78-23656* National Aeronautics and Space Administration, Lewis Research Center, Cleveland, Ohio.

COMPARISON OF COMPUTER CODES FOR CALCULATING DYNAMIC LOADS IN WIND TURBINES

David A. Spers 1977 39 p refs Presented at the 3rd Bien. Conf. and Workshop on Wind Energy Conversion Systems, Washington, D. C., 19-21 Sep. 1977

(Contract E(49-26)-1028)

(NASA-TM-73773; DOE/NASA/1028-78/16; E-9577) Avail: NTIS HC A03/MF A01 CSCL 10B

Seven computer codes for analyzing performance and loads in large, horizontal axis wind turbines were used to calculate blade bending moment loads for two operational conditions of the 100 kW Mod-0 wind turbine. Results were compared with test data on the basis of cyclic loads, peak loads, and harmonic contents. Four of the seven codes include rotor-tower interaction and three were limited to rotor analysis. With a few exceptions, all calculated loads were within 25 percent of nominal test data. Author

N78-23657* National Aeronautics and Space Administration, Lewis Research Center, Cleveland, Ohio.

PERFORMANCE POTENTIAL OF COMBINED CYCLES INTEGRATED WITH LOW-Btu GASIFIERS FOR FUTURE ELECTRIC UTILITY APPLICATIONS

Joseph J. Nainiger and Raymond K. Burns [1977] 42 p refs Presented at the 69th Ann. Meeting of the Am. Inst. of Chem. Engr., Chicago, 28 Nov - 2 Dec. 1976

(NASA-TM-73775; E-9567) Avail: NTIS HC A03/MF A01 CSCL 10A

A comparison and an assessment of 10 advanced utility power systems on a consistent basis and to a common level of detail were analyzed. Substantial emphasis was given to a combined cycle systems integrated with low-Btu gasifiers. Performance and cost results from that study were presented for these combined cycle systems, together with a comparative evaluation. The effect of the gasifier type and performance and the interface between the gasifier and the power system were discussed. Author

N78-23658* National Aeronautics and Space Administration, Lewis Research Center, Cleveland, Ohio.

WAKE CHARACTERISTICS OF A TOWER FOR THE DOE-NASA MOD-1 WIND TURBINE

Joseph M. Savino, Lee H. Wagner, and Mary Nash Apr. 1978 76 p refs

(Contract E(49-26)-1028)

(NASA-TM-78853; E-9575; DOE/NASA/1028-78/17) Avail: NTIS HC A05/MF A01 CSCL 10A

A 1/40th scale model of a tower concept designed for a MOD-1 wind power turbine was tested in a low speed wind tunnel. Wake wind speed profiles were measured, and from these were determined local values of wake minimum velocity ratio, average velocity ratio, and width over a range of tower elevations and wind approach angles. Comparison with results from two other all tubular models (MOD-0 and eight leg designs) tested earlier in the same tunnel indicated that wake width and flow blockage at the rotor plane of rotation were slightly larger for the MOD-1 tower than for the other two models. The differences in wake characteristics were attributed to differences in tower geometry and member dimensions. Author

N78-24615* National Aeronautics and Space Administration, Lewis Research Center, Cleveland, Ohio.

WAKE CHARACTERISTICS OF AN EIGHT-LEG TOWER FOR A MOD-0 TYPE WIND TURBINE

Joseph M. Savino, Lee H. Wagner, and Donald Sinclair Dec. 1977 70 p refs

(Contract E(49-26)-1028)

(NASA-TM-73868; E-9463; DOE/NASA/1028-77/14) Avail: NTIS HC A04/MF A01 CSCL 10B

Low speed wind tunnel tests were conducted to determine the flow characteristics of the wake downwind of a 1/25th scale all tubular eight leg tower concept suitable for application to the DOE-NASA MOD-0 wind power turbine. Measurements

were made of wind speed profiles, and from these were determined the wake local minimum velocity, average velocity, and width for several wind approach angles. These data are presented herein along with tower shadow photographs and comparisons with data from an earlier lattice type, four leg tower model constructed of tubular members. Values of average wake velocity defect ratio and average ratio of wake width to blade radius for the eight leg model were estimated to be around 0.17 and 0.30, respectively, at the plane of the rotor blade. These characteristics suggest that the tower wake of the eight leg concept is slightly less than that of the four leg design. Author

N78-24616* National Aeronautics and Space Administration, Lewis Research Center, Cleveland, Ohio.

RAPID, EFFICIENT CHARGING OF LEAD-ACID AND NICKEL-ZINC TRACTION CELLS

John J. Smithrick 1978 9 p refs To be presented at the 13th Intersoc. Energy Conversion Eng. Conf., San Diego, Calif., 20-25 Aug. 1978

(Contract EC-77-A-31-1011)

(NASA-TM-78901; E-9837; DOE/NASA/1011-78/26) Avail: NTIS HC A02/MF A01 CSCL 10C

Lead-acid and nickel-zinc traction cells were rapidly and efficiently charged using a high rate tapered direct current (HRTDC) charge method which could possibly be used for on-the-road service recharge of electric vehicles. The HRTDC method takes advantage of initial high cell charge acceptance and uses cell gassing rate and temperature as an indicator of charging efficiency. On the average, in these preliminary tests, 300 amp-hour nickel-zinc traction cells were given a HRTDC (initial current 500 amps, final current 100 amps) to 78 percent of rated amp-hour capacity within 53 minutes at an amp-hour efficiency of 92 percent and an energy efficiency of 52 percent. Three hundred amp-hour lead-acid traction cells were charged to 69 percent of rated amp-hour capacity within 45 minutes at an amp-hour efficiency of 91 percent with an energy efficiency of 64 percent. In order to find ways to further decrease the recharge times, the effect of periodically (0 to 400 Hz) pulse discharging cells during a constant current charging process (94% duty cycle) was investigated. Preliminary data indicate no significant effect of this type of pulse discharging during charge on charge acceptance of lead-acid or nickel-zinc cells. Author

N78-24617* National Aeronautics and Space Administration, Lewis Research Center, Cleveland, Ohio.

DIMINIODE THERMIONIC ENERGY CONVERSION WITH LANTHANUM-HEXABORIDE ELECTRODES

Erich W. Kroeger, Virginia L. Bair, and James F. Morris 1978 18 p refs Presented at the International Conference on Plasma Science, Monterey, Calif., 15-18 May 1978; sponsored by IEEE (NASA-TM-78887; E-9622) Avail: NTIS HC A02/MF A01 CSCL 10A

Thermionic conversion data obtained from a variable gap cesium diminiode with a hot pressed, sintered lanthanum hexaboride emitter and an arc melted lanthanum hexaboride collector are presented. Performance curves cover a range of temperatures, emitter 1500 to 1700 K, collector 750 to 1000 K, and cesium reservoir 370 to 510 K. Calculated values of emitter and collector work functions and barrier index are also given. Author

N78-24659* National Aeronautics and Space Administration, Lewis Research Center, Cleveland, Ohio.

ENERGY CONVERSION ALTERNATIVES STUDY (ECAS) Summary Report

Sep 1977 101 p refs Sponsored in part by NSF

(Contract E(49-18)-1751)

(NASA-TM-73871; E-8596) Avail: NTIS HC A06/MF A01 CSCL 10A

ECAS compared various advanced energy conversion systems that can use coal or coal-derived fuels for base-load electric power generation. It was conducted in two phases. Phase 1 consisted of parametric studies. From these results, 11 concepts were selected for further study in Phase 2. For each of the Phase 2 systems and a common set of ground rules, performance, cost,

environmental intrusion, and natural resource requirements were estimated. In addition, the contractors defined the state of the associated technology, identified the advances required, prepared preliminary research and development plans, and assessed other factors that would affect the implementation of each type of powerplant. The systems studied in Phase 2 include steam systems with atmospheric- and pressurized-fluidized-bed boilers; combined cycle gas turbine/steam systems with integrated gasifiers or fired by a semiclean, coal derived fuel; a potassium/steam system with a pressurized-fluidized-bed boiler; a closed-cycle gas turbine/organic system with a high-temperature, atmospheric-fluidized-bed furnace; a direct-coal-fired, open-cycle magnetohydrodynamic/steam system, and a molten-carbonate fuel cell/steam system with an integrated gasifier. The sensitivity of the results to changes in the ground rules and the impact of uncertainties in capital cost estimates were also examined.

Author

N78-25527* National Aeronautics and Space Administration, Lewis Research Center, Cleveland, Ohio.

SOLAR CELL COLLECTOR Patent

John C. Evans, Jr., inventor (to NASA) Issued 4 Apr. 1978 5 p. Filed 22 Feb. 1977 Supersedes N77-17564 (15 - 08, p 1052)

(NASA Case-LEW-12552-1; US Patent-4,082,569; US Patent-Appl-SN-770869; US Patent-Class-136-89CC; US Patent-Class-357-30; US Patent-Class-357-65; US Patent-Class-357-67; US Patent-Class-29-572; US Patent-Class-427-75; US Patent-Class-427-261) Avail: US Patent Office CSCL 10A

A method is provided for the fabrication of a photovoltaic device which possesses an efficient collector system for the conduction of the current generated by incident photons to the external circuitry of the device

Official Gazette of the U.S. Patent Office

N78-25528* National Aeronautics and Space Administration, Lewis Research Center, Cleveland, Ohio

METHOD OF MAKING ENCAPSULATED SOLAR CELL MODULES Patent

Evelyn Anagnostou and Americo F. Forester, inventors (to NASA) Issued 11 Apr. 1978 4 p. Filed 30 Nov. 1976 Supersedes N77-15490 (15 - 08, p 0769)

(NASA Case-LEW-12185-1; US Patent-4,083,097; US Patent-Appl-SN-746269; US Patent-Class-29-572; US Patent-Class-29-628; US Patent-Class-136-89P; US Patent-Class-136-89H) Avail: US Patent Office CSCL 10A

Electrical connections to solar cells in a module are made at the same time the cells are encapsulated for protection. The encapsulating material is embossed to facilitate the positioning of the cells during assembly

Official Gazette of the U.S. Patent Office

N78-25529* National Aeronautics and Space Administration, Lewis Research Center, Cleveland, Ohio

METHOD FOR PRODUCING SOLAR ENERGY PANELS BY AUTOMATION Patent

John C. Evans Jr., inventor (to NASA) Issued 18 Apr. 1978 11 p. Filed 25 Apr. 1977 Supersedes N77-22615 (15 - 13, p 1744)

(NASA Case-LEW 12541-1; US Patent 4,084,985; US Patent-Appl-SN 790637; US Patent-Class-136-89P; US Patent-Class-29-572; US Patent-Class-136-89H; US Patent-Class-136-89CC; US Patent-Class-156-633) Avail: US Patent Office CSCL 10A

A solar cell panel was fabricated by photoetching a pattern of collector grid systems with appropriate interconnections and bus bar tabs into a glass or plastic sheet. These regions were then filled with a first, thin conductive metal film followed by a layer of a mixed metal oxide, such as InAsO or InSnO. The multiplicity of solar cells were bonded between the protective sheet at the sites of the collector grid systems and a back electrode substrate by conductive metal filled epoxy to complete the fabrication of an integrated solar panel

Official Gazette of the U.S. Patent Office

N78-25530* National Aeronautics and Space Administration, Lewis Research Center, Cleveland, Ohio

INORGANIC-ORGANIC SEPARATORS FOR ALKALINE BATTERIES Patent

Dean W. Sheibley, inventor (to NASA) Issued 18 Apr. 1978 4 p. Filed 7 Sep. 1976 Supersedes N76-31674 (14 - 22, p 2890)

(NASA Case-LEW-12649-1; US Patent-4,085,241; US Patent-Appl-SN-720521; US Patent-Class-427-385B; US Patent-Class-427-385C; US Patent-Class-429-254) Avail: US Patent Office CSCL 10C

A flexible separator is reported for use between the electrodes of Ni-Cd and Ni-Zn batteries using alkaline electrolytes. The separator was made by coating a porous substrate with a battery separator composition. The coating material included a rubber-based resin copolymer, a plasticizer and inorganic and organic fillers which comprised 55% by volume or less of the coating as finally dried. One or more of the filler materials, whether organic or inorganic, is preferably active with the alkaline electrolyte to produce pores in the separator coating. The plasticizer was an organic material which is hydrolyzed by the alkaline electrolyte to improve conductivity of the separator coating.

Official Gazette of the U.S. Patent Office

N78-25551* National Aeronautics and Space Administration, Lewis Research Center, Cleveland, Ohio

PHOTON DEGRADATION EFFECTS IN TERRESTRIAL SOLAR CELLS

V. G. Weizer, H. W. Brandhorst, Jr., J. D. Broder, R. E. Hart and S. H. Lamneck 1978 14 p. refs. Presented at the 13th Photovoltaic Specialists Conf., Washington, D. C., 5-8 Jun. 1978; sponsored by IEEE

(Contract E(49-26)-1022) (NASA-TM-78924; DOE/NASA/1022-78/35; E-9664) Avail: NTIS HC A02/MF A01 CSCL 10A

Reduction in cell output was observed in Ni(+)/P cells upon exposure to illumination or upon the application of a sufficiently high forward bias. Conversely, an enhancement in output was observed when P(+)/N cells were illuminated. Investigations performed on Ni(+)/P cells indicated that a recombination center located at E sub c - 0.37 eV in the forbidden band was responsible for the loss in output. The center was electrically inactive in its ground state but was activated either by raising the minority carrier quasi-Fermi level sufficiently close to the latent center energy level in the band gap, or by direct excitation of electrons from the valence band to the latent center level. The center was identified as a complex of a lattice defect and a silver atom or cluster of atoms.

Author

N78-25553* National Aeronautics and Space Administration, Lewis Research Center, Cleveland, Ohio

SOLAR CELL SYSTEM HAVING ALTERNATING CURRENT OUTPUT Patent Application

J. C. Evans, Jr., inventor (to NASA) Filed 9 Jun. 1978 11 p. (NASA Case-LEW-12806-1; US Patent-Appl-SN-915050) Avail: NTIS HC A02/MF A01 CSCL 10A

A P-N junction solar cell modified by fabricating an integrated circuit inverter on the back of the cell to produce a device capable of generating an alternating current output was developed. In another embodiment integrated circuit power conditioning electronics is incorporated in a module containing a solar cell power supply

NASA

N78-25554* National Aeronautics and Space Administration, Lewis Research Center, Cleveland, Ohio

ELECTROCHEMICAL CELL FOR REBALANCING REDOX FLOW SYSTEM Patent Application

Lawrence H. Thaller, inventor (to NASA) Filed 9 Jun. 1978 12 p.

(NASA Case-LEW 13150-1; US Patent-Appl-SN 914260) Avail: NTIS HC A02/MF A01 CSCL 10A

Electricity producing cells which utilize reduction and oxidation of anode and cathode fluids are called REDOX cells. The fluids were aqueous solutions of HCl each including a different metal

chloride salt and were separated by a membrane which was permeable to certain ions. A provision of a rebalancing cell is provided, which utilized gas from undesirable side reactions and/or from an independent source to rebalance the anode and cathode fluids in a REDOX system. NASA

N78-26565* National Aeronautics and Space Administration, Lewis Research Center, Cleveland, Ohio.
CESIUM THERMIONIC CONVERTERS HAVING IMPROVED ELECTRODES Patent Application
 James F. Morris, inventor (to NASA) Filed 1 May 1978 9 p (NASA Case-LEW-12038-3; US-Patent-Appl-SN-901892) Avail: NTIS HC A02/MF A01 CSCL 10A

A high electric-power output thermionic converter is reported that uses a combination of lanthanum hexaboride emitter and collector electrodes in a cesium medium. The interaction between the lanthanum hexaboride electrodes and cesium vapor, which is adsorbed on the lanthanum hexaboride electrodes, results in lower emitter and collector work functions to produce a thermionic converter with high current density and voltage output. The lanthanum hexaboride emitter and collector electrodes employed in the cesium thermionic converter can be either in the monocrystalline or polycrystalline state. NASA

N78-26566* National Aeronautics and Space Administration, Lewis Research Center, Cleveland, Ohio.
IMPROVED BACK WALL CELL Patent Application
 Henry W. Brandhorst, Jr., inventor (to NASA) Filed 24 Apr. 1978 13 p (NASA Case-LEW-12236-2; US-Patent-Appl-SN-899123) Avail: NTIS HC A02/MF A01 CSCL 10A

Back-wall solar wells are described that consist of a first material of one conductivity type with one face more heavily doped to form a field region to receive radiant energy. A layer of opposite conductivity, or a metallic layer forming a Schottky barrier, was applied to the opposite face. A gridded contact previous to the radiant energy was applied to the region of the heavily doped material for electrical contact. Separate control of either the p-n junction or the Schottky diode junction provided for efficient collection of light. NASA

N78-26568* National Aeronautics and Space Administration, Lewis Research Center, Cleveland, Ohio.
METHOD FOR FABRICATING SOLAR CELLS HAVING INTEGRAL COLLECTOR GRIDS Patent Application
 John C. Evans, Jr., inventor (to NASA) Filed 23 Dec 1977 17 p (NASA Case-LEW-12819-2; US-Patent-Appl-SN-863770) Avail: NTIS HC A02/MF A01 CSCL 10A

A photovoltaic device was designed which possesses an integral mixed metal oxide coating in which is embedded a metallic network which functions as an efficient collector for electrons set in motion by the photovoltaic process. The metal grid system is formed from the metal elements of the transparent, conductive mixed metal oxide coating which is in contact with the oxide coating which constitutes the barrier of the devices with the semiconductor substrate. NASA

N78-26542* National Aeronautics and Space Administration, Lewis Research Center, Cleveland, Ohio.
TRANSIENT RESPONSE TO THREE-PHASE FAULTS ON A WIND TURBINE GENERATOR Ph.D. Thesis - Toledo Univ.
 Leonard J. Gilbert Jun 1978 146 p refs (NASA TM 78902; E-9638) Avail: NTIS HC A07/MF A01 CSCL 10A

In order to obtain a measure of its responses to short circuits a large horizontal axis wind turbine generator was modeled and its performance was simulated on a digital computer. Simulation of short circuit faults on the synchronous alternator of a wind turbine generator, without resort to the classical assumptions generally made for that analysis, indicates that

maximum clearing times for the system tied to an infinite bus are longer than the typical clearing times for equivalent capacity conventional machines. Also, maximum clearing times are independent of tower shadow and wind shear. Variation of circuit conditions produce the modifications in the transient response predicted by analysis. P.R.A.

N78-26543* National Aeronautics and Space Administration, Lewis Research Center, Cleveland, Ohio.
STATUS OF WRAPAROUND CONTACT SOLAR CELLS AND ARRAYS

Cosmo R. Barona and L. E. Young 1978 10 p refs Proposed for presentation at the 13th Intersociety Energy Conversion Engr. Conf., San Diego, Calif., 20-25 Aug 1978; sponsored by SAE, ACS, AIAA, ASME, IEEE, AICHE, and ANS (NASA-TM-78911; E-9646) Avail: NTIS HC A02/MF A01 CSCL 10A

Solar cells with wraparound contacts provide the following advantages in array assembly: (1) eliminate the need for discretely formed, damage susceptible series tabs; (2) eliminate the n gap problem by allowing the use of uniform covers over the entire cell surface; (3) allow a higher packing factor by reducing the additional series spacing formerly required for forming, and routing the series tab; and (4) allow the cell bonding to the interconnect system to be a single-side function wherein series contacts can be made at the same time parallel contacts are made. Author

N78-26544* National Aeronautics and Space Administration, Lewis Research Center, Cleveland, Ohio.
PRELIMINARY EVALUATION OF GLASS RESIN MATERIALS FOR SOLAR CELL COVER USE

Stanley J. Marsik, Clifford K. Swartz, and Cosmo R. Barona Jun 1978 7 p refs Presented at 13th Photovoltaic Specialists Conf., Washington, D. C., 5-8 Jun 1978; sponsored by IEEE (NASA-TM-78925; E-9665) Avail: NTIS HC A02/MF A01 CSCL 10A

The glass resins were deposited by several techniques on 200 micron thick cells and on 50 microns thick wafers. The covered cells were exposed to ultraviolet light in vacuum to an intensity of 10 UV energy equivalent solar constants at air mass zero for 728 hr. The exposure was followed by a single long thermal cycle from ambient temperature to -150 C. Visual inspection of the samples indicated that all samples had darkened to varying degrees. The loss in short-circuit current was found to range from 8 to 24%, depending on the resin formulation. In another test over 40 glass resin-coated silicon wafers withstood 15 thermal cycles from 100 to 196 C in one or more of the thicknesses tested. Several of the resin-coated wafers were tested at 65 C and 90% relative humidity for 170 hr. No change in physical appearance was detected. Author

N78-26545* National Aeronautics and Space Administration, Lewis Research Center, Cleveland, Ohio.
ULTRAVIOLET IRRADIATION AT ELEVATED TEMPERATURES AND THERMAL CYCLING IN VACUUM OF FEP-A COVERED SILICON SOLAR CELLS
 J. D. Broder and S. J. Marsik 1978 8 p refs Presented at the 13th Photovoltaic Specialists Conf., Washington, D. C., 5-8 Jun 1978; sponsored by IEEE (NASA-TM-78926; E-9666) Avail: NTIS HC A02/MF A01 CSCL 10A

Experiments were designed and performed on silicon solar cells covered with heat-bonded FEP-A in an effort to explain the rapid degeneration of open-circuit voltage and maximum power observed on cells of this type included in an experiment on the ATS-6 spacecraft. Solar cells were exposed to ultraviolet light in vacuum at temperatures ranging from 30 to 105 C. The samples were then subjected to thermal cycling from 130 to -130 C. Inspection following irradiation indicated that all the covers remained physically intact. However, during the temperature cycling heat-bonded covers showed cracking. The test showed that heat-bonded FEP-A covers embrittle during UV exposure and the embrittlement is dependent upon sample temperature during irradiation. The results of the experiment suggest a probable mechanism for the degradation of the FEP-A cells on ATS-6. Author

N78-26546* National Aeronautics and Space Administration, Lewis Research Center, Cleveland, Ohio.

AN IMPROVED TECHNIQUE FOR THE CALIBRATION OF SOLAR CELLS USING A HIGH ALTITUDE AIRCRAFT

Earle O. Boyer Apr. 1978 13 p refs
(NASA-TM-78871; E-9603) Avail: NTIS HC A02/MF A01 CSCL 10A

A description of a technique for the airborne calibration of solar cells is given. Aircraft modifications and data supporting the inherent advantages of the techniques are discussed. Author

N78-26547* National Aeronautics and Space Administration, Lewis Research Center, Cleveland, Ohio.

VARIATION OF SOLAR CELL SENSITIVITY AND SOLAR RADIATION ON TILTED SURFACES

Thomas M. Klucher 1978 10 p refs Presented at the 13th Photovoltaic Specialists Conf., Washington, D. C., 5-8 Jun. 1978; sponsored by IEEE

(Contract E(49-26)-1022)
(NASA-TM-78921; DOE/NASA/1022-78/32; E-9661) Avail: NTIS HC A02/MF A01 CSCL 10A

The validity is studied that one of various insolation models used to compute solar radiation incident on tilted surfaces from global data measured on horizontal surfaces. The variation of solar cell sensitivity to solar radiation is determined over a wide range of atmospheric condition. A new model was formulated that reduced the deviations between measured and predicted insolation to less than 3 percent. Evaluation of solar cell sensitivity data indicates small change (2-3 percent) in sensitivity from winter to summer for tilted cells. The feasibility of using such global data as a means for calibrating terrestrial solar cells is discussed. G.G.

N78-26548* National Aeronautics and Space Administration, Lewis Research Center, Cleveland, Ohio.

ENDURANCE TESTING OF FIRST GENERATION (BLOCK 1) COMMERCIAL SOLAR CELL MODULES

E. Anagnostou and Americo F. Forestieri 1978 9 p ref Presented at the 13th Photovoltaic Specialists Conf., Washington, D. C., 5-8 Jun. 1978; sponsored by IEEE

(Contract E(49-26)-1022)
(NASA-TM-78922; DOE/NASA/1022-78/33; E-9662) Avail: NTIS HC A02/MF A01 CSCL 10A

To determine lifetimes of the first generation (Block 1) commercial solar cell modules used in solar cell arrays, a program was initiated to expose these modules to a range of environments. The conditions endured by these modules encompassed hot and dry, hot and humid, tropical rain forests, sea-air, urban industrial and urban clean. Exposures were for periods up to 1 year. The effect of outdoor exposure on the performance of the modules was determined using current-voltage curves. Short-circuit current (I_{sc}) and maximum power ($P_{sub max}$) were the parameters monitored. In all cases, there was a loss of performance of the modules with outdoor exposure. Author

N78-26549* National Aeronautics and Space Administration, Lewis Research Center, Cleveland, Ohio.

DOE LeRC PHOTOVOLTAIC SYSTEMS TEST FACILITY

Ronald C. Cull and Americo F. Forestieri 1978 10 p refs Presented at the 13th Photovoltaic Specialists Conf., 5-8 Jun. 1978; sponsored by IEEE

(Contract E(49-26)-1022)
(NASA-TM-78923; DOE/NASA/1022-78/34; E-9663) Avail: NTIS HC A02/MF A01 CSCL 10A

The facility was designed and built and is being operated as a national facility to serve the needs of the entire DOE National Photovoltaic Program. The object of the facility is to provide a place where photovoltaic systems may be assembled and electrically configured, without specific physical configuration, for operation and testing to evaluate their performance and characteristics. The facility as a breadboard system allows investigation of operational characteristics and checkout of components, subsystems and systems before they are mounted in field experiments or demonstrations. The facility as currently configured consist of 10 kW of solar arrays built from modules,

two inverter test stations, a battery storage system, interface with local load and the utility grid, and instrumentation and control necessary to make a flexible operating facility. Expansion to 30 kW is planned for 1978. Test results and operating experience are summarized to show the variety of work that can be done with this facility. G.Y.

N78-26550* National Aeronautics and Space Administration, Lewis Research Center, Cleveland, Ohio.

IMPACT OF BALANCE OF SYSTEM (BOS) COSTS ON PHOTOVOLTAIC POWER SYSTEMS

Gerald F. Hein, James P. Cusack, and William A. Poley 1978 8 p Presented at the 13th Photovoltaic Specialists Conf., Washington, D. C., 5-8 Jun. 1978; sponsored by IEEE

(Contract E(49-26)-1022)
(NASA-TM-78939; DOE/NASA/1022-78/40; E-9685) Avail: NTIS HC A02/MF A01 CSCL 10A

The Department of Energy has developed a program to effect a large reduction in the price of photovoltaic modules, with significant progress already achieved toward the 1986 goal of 50 cents/watt (1975 dollars). Remaining elements of a P/V power system (structure, battery storage, regulation, control, and wiring) are also significant cost items. The costs of these remaining elements are commonly referred to as Balance-of-System (BOS) costs. The BOS costs are less well defined and documented than module costs. The Lewis Research Center (LeRC) in 1976/77 and with two village power experiments that will be installed in 1978. The costs were divided into five categories and analyzed. A regression analysis was performed to determine correlations of BOS Costs per peak watt with power size for these photovoltaic systems. The statistical relationship may be used for flat-plate, DC systems ranging from 100 to 4,000 peak watts. A survey of suppliers was conducted for comparison with the predicted BOS cost relationship. Author

N78-26551* National Aeronautics and Space Administration, Lewis Research Center, Cleveland, Ohio.

BASELINE TESTS OF THE KORDESH HYBRID PASSENGER VEHICLE

Richard F. Soltis, John M. Borek, Hubert J. Denington, and Miles O. Dustin Jun. 1978 69 p

(Contract EC-77-A-31-10111)
(NASA-TM 73769; CONS 1011-14; E-9604) Avail: NTIS HC A04/MF A01 CSCL 10A

Performance test results are presented for a four-passenger Austin A40 sedan that was converted to a heat engine alternator- and battery-powered hybrid. It is propelled by a conventional, gasoline fueled, heat engine-driven alternator and a traction pack powering a series wound, 10 hp direct current electric drive motor. The 16 hp gasoline engine drives the 7 kilowatt alternator, which provides electrical power to the drive motor or to the 96 volt traction battery through a rectifier. The propulsion battery consists of eight 12 volt batteries connected in series. The electric motor is coupled to a four-speed standard transmission, which drives the rear wheels. Power to the motor is controlled by a three step foot throttle, which actuates relays that control armature current and field excitation. Conventional hydraulic brakes are used. G.G.

N78-26552* National Aeronautics and Space Administration, Lewis Research Center, Cleveland, Ohio.

DESIGN AND OPERATING EXPERIENCE ON THE US DEPARTMENT OF ENERGY EXPERIMENTAL 100-KW WIND TURBINE

John C. Glasgow and Arthur G. Birchenough 1978 17 p refs Proposed for presentation at the 13th Intersoc. Energy Conversion Eng. Conf., San Diego, Calif., 20-25 Aug. 1978

(Contract E(49-26)-10281)
(NASA-TM 78915; E-9652; DOE/NASA/1028-78/18) Avail: NTIS HC A02/MF A01 CSCL 10A

The experimental wind turbine was designed and fabricated to assess technology requirements and engineering problems of large wind turbines. The machine has demonstrated successful operation in all of its design modes and served as a prototype

developmental test bed for the Mod-0A operational wind turbines which are currently used on utility networks. The mechanical and control system are described as they evolved in operational tests and some of the experience with various systems in the downwind rotor configurations are elaborated. G.G.

N78-26553* National Aeronautics and Space Administration, Lewis Research Center, Cleveland, Ohio.
DOE/NASA MOD-0A WIND TURBINE PERFORMANCE
 T. R. Richards and H. E. Neustadter 1978 8 p refs Proposed for presentation at the 13th Intersoc. Energy Conversion Eng. Conf., San Diego, Calif., 20-25 Aug. 1978
 (Contract E(49-26)-1004)
 (NASA-TM-78916; E-9654; DOE/NASA/1004-78/13) Avail: NTIS HC A02/MF A01 CSCL 10A

Design and operation of a large wind turbine at Clayton, Mexico is reported. This is the first of three identical 200 kW wind turbines to be operated on electric utility networks. A comparison between its predicted and measured power versus wind speed performance is presented. G.G.

N78-26554* National Aeronautics and Space Administration, Lewis Research Center, Cleveland, Ohio.
DESCRIPTION AND STATUS OF NASA-LERC/DOE PHOTOVOLTAIC APPLICATIONS SYSTEMS
 Anthony F. Ratajczak 1978 10 p refs Presented at the 13th Photovoltaic Specialists Conf., Washington, D. C., 5-8 Jun. 1978; sponsored by IEEE
 (Contract E(49-26)-1022)
 (NASA-TM-78936; E-9679; DOE/NASA/1022-78/38) Avail: NTIS HC A02/MF A01 CSCL 10A

Designed, fabricated and installed were 16 geographically dispersed photovoltaic systems. These systems are powering a refrigerator, highway warning sign, forest lookout towers, remote weather stations, a water chiller at a visitor center, and insect survey traps. Each of these systems is described in terms of load requirements, solar array and battery size, and instrumentation and controls. Operational experience is described and present status is given for each system. The P/V power systems have proven to be highly reliable with almost no problems with modules and very few problems overall. Author

N78-26555* National Aeronautics and Space Administration, Lewis Research Center, Cleveland, Ohio.
DESIGN AND FABRICATION OF A PHOTOVOLTAIC POWER SYSTEM FOR THE PAPAGO INDIAN VILLAGE OF SCHUCHULI (GUNSIGHT), ARIZONA
 William J. Bifano, Anthony F. Ratajczak, and William J. Ice 1978 10 p Presented at the 13th Photovoltaic Specialists Conf., Washington, D. C., 5-8 Jun. 1978; sponsored by the IEEE
 (Contract E(49-26)-1022)
 (NASA-TM-78948; E-9672; DOE/NASA/1022-78/39) Avail: NTIS HC A02/MF A01 CSCL 10A

A stand alone photovoltaic power system for installation in the Papago Indian village of Schuchuli is being designed and fabricated to provide electricity for village water pumping and basic domestic needs. The system will consist of a 3.5 kW (peak) photovoltaic array; controls, instrumentations, and storage batteries located in an electrical equipment building and a 120 volt dc village distribution network. The system will power a 2 HP dc electric motor. Author

N78-27520* National Aeronautics and Space Administration, Lewis Research Center, Cleveland, Ohio
SELF-RECONFIGURING SOLAR CELL SYSTEM Patent Application
 Robert P. Gruber, inventor (to NASA) Filed 19 Jun 1978 18 p
 (NASA-Case-LEW-12586-1, US Patent-Appf-SN-916655) Avail: NTIS HC A02/MF A01 CSCL 10A

An improved solar cell system is reported that utilizes control circuits to switch some of its cells so that they can be either in

series or in shunt within the array to match the load for maximum power transfer. Automatic control is provided by a sensor solar cell mounted into the configurable array; its open circuit voltage multiplied by a constant is equal to cell voltage at maximum power point. NASA

N78-27539* National Aeronautics and Space Administration, Lewis Research Center, Cleveland, Ohio
COST OF PHOTOVOLTAIC ENERGY SYSTEMS AS DETERMINED BY BALANCE-OF-SYSTEM COSTS
 Louis Rosenblum Jun 1978 14 p refs
 (NASA-TM-78957; E-9708) Avail: NTIS HC A02/MF A01 CSCL 10B

The effect of the balance-of-system (BOS) i.e. the total system less the modules, on photo-voltaic energy system costs is discussed for multikilowatt, flat-plate systems. Present BOS costs are in the range of 10 to 16 dollars per peak watt (1978 dollars). BOS costs represent approximately 50% of total system cost. The possibility of future BOS cost reduction is examined. It is concluded that, given the nature of BOS costs and the lack of comprehensive national effort focussed on cost reduction, it is unlikely that BOS costs will decline greatly in the next several years. This prognosis is contrasted with the expectations of the Department of Energy National Photovoltaic Program goals and pending legislation in the Congress which require a BOS cost reduction of an order of magnitude or more by the mid-1980s. Author

N78-28607* National Aeronautics and Space Administration, Lewis Research Center, Cleveland, Ohio
AN IMPROVED METHOD FOR ANALYSIS OF HYDROXIDE AND CARBONATE IN ALKALINE ELECTROLYTES CONTAINING ZINC
 Margaret A. Reid 1978 14 p refs To be presented at the 154th meeting of the Electrochem. Soc., Inc., Pittsburgh, 15-20 Oct 1978
 (NASA-TM-78961) Avail: NTIS HC A02/MF A01 CSCL 10C

A simplified method for titration of carbonate and hydroxide in alkaline battery electrolyte is presented involving a saturated KSCN solution as a complexing agent for zinc. Both hydroxide and carbonate can be determined in one titration, and the complexing reagent is readily prepared. Since the pH at the end point is shifted from 8.3 to 7.9-8.0, m cresol purple or phenol red are used as indicators rather than phenolphthalein. Bromocresol green is recommended for determination of the second end point of a pH of 4.3 to 4.4. Author

N78-28614* National Aeronautics and Space Administration, Lewis Research Center, Cleveland, Ohio
COMPARISON OF THREE EXPERIMENTAL METHODS USED IN DETERMINING THE THERMAL PERFORMANCE OF FLAT-PLATE SOLAR COLLECTORS Ph.D. Thesis - Kansas Univ.
 Gregory B. Hotchkiss Oct 1978 289 p refs
 (NASA-TM-78929; E-9669) Avail: NTIS HC A13/MF A01 CSCL 10A

Three experimental methods for evaluating the thermal performance of flat plate solar collectors are presented. The methods are classified according to the nature of the ambient conditions encountered during experimental testing. The classifications are: (1) steady state, (2) quasi-steady state, a, (3) unsteady state. Experimental tests on two solar collectors were conducted in an indoor solar simulator and also out-of-doors. From the experimental collector data, collector efficiency factors, which describe the steady state behavior of a collector, were determined for each experimental method. A parameter identification method based upon a discrete gradient optimization technique was used to determine the collector parameters from unsteady state data. Such a method would allow on line data reduction and would enable speedy determination of the collector efficiency factors from transient data. The design, construction, and operation of the test rig which was used to obtain the experimental data are also described. Author

N78-28634* National Aeronautics and Space Administration. Lewis Research Center, Cleveland, Ohio.

SOLUBILITY, STABILITY, AND ELECTROCHEMICAL STUDIES OF SULFUR-SULFIDE SOLUTIONS IN ORGANIC SOLVENTS

William L. Fielder and Joseph Singer Aug. 1978 43 p refs (NASA-TP-1246; E-9552) Avail: NTIS HC A03/MF A01 CSCL 10A

A preliminary study of the sulfur electrode in organic solvents suggests that the system warrants further investigation for use in a low temperature (100 deg to 120 C) Na-S secondary battery. A qualitative screening was undertaken at 120 C to determine the solubilities and stabilities of Na₂S and Na₂S₂ in representatives of many classes of organic solvents. From the screening and quantitative studies, two classes of solvents were selected for work: amides and cyclic polyalcohols. Voltammetric and Na-S cell charge discharge studies of sulfide solutions in organic solvents (e.g., N, N-dimethylformamide) at 120 C suggested that the reversibilities of the reactions on Pt or high density graphite were moderately poor. However, the sulfur electrode was indeed reducible (and oxidizable) through the range of elemental sulfur to Na₂S. Reactions and mechanisms are proposed for the oxidation reduction processes occurring at the sulfur electrode. Author

N78-28686* National Aeronautics and Space Administration. Lewis Research Center, Cleveland, Ohio.

PERFORMANCE AND STABILITY ANALYSIS OF A PHOTOVOLTAIC POWER SYSTEM Final Report

Walter C. Merrill, Ronald J. Blaha, and Roy L. Pickrell Aug. 1978 43 p refs (Contract E(49-28)-1022)

(NASA-TM-78880; E-9609; DOE/NASA/1022-78/30) Avail: NTIS HC A03/MF A01 CSCL 10A

The performance and stability characteristics of a 10 kVA photovoltaic power system are studied using linear Bode analysis and a nonlinear analog simulation. Power conversion efficiencies, system stability, and system transient performance results are given for system operation at various levels of solar insolation. Additionally, system operation and the modeling of system components for the purpose of computer simulation are described. F.O.S.

N78-29576* National Aeronautics and Space Administration. Lewis Research Center, Cleveland, Ohio.

LARGE WIND TURBINE GENERATORS

Ronald L. Thomas and Richard M. Donovan Mar. 1978 37 p refs Presented at 5th Energy Technol. Conf. and Exposition, Washington, D. C., 27 Feb. - 1 Mar. 1978 (Contract E(49-28)-1059)

(NASA-TM-73767; DOE/NASA/1059-78/1; E-9553) Avail: NTIS HC A03/MF A01 CSCL 10B

The development associated with large wind turbine systems is briefly described. The scope of this activity includes the development of several large wind turbines ranging in size from 100 kW to several megawatt levels. A description of the wind turbine systems, their programmatic status and a summary of their potential costs is included. L.S.

N78-29676* National Aeronautics and Space Administration. Lewis Research Center, Cleveland, Ohio.

THERMAL ENERGY STORAGE FOR INDUSTRIAL WASTE HEAT RECOVERY

H. W. Hoffman (ORNL), R. J. Kedl (ORNL), and R. A. Duscha Aug. 1978 10 p Presented at 13th Intersociety Energy Conversion Engineering Conf., San Diego, Calif., 20-25 Aug. 1978

(Contracts EC-77-A-31-1034; W-7405-eng-26) (NASA-TM-78953; DOE/NASA/1034-78/2; E-9702) Avail: NTIS HC A02/MF A01 CSCL 10C

The potential is examined for waste heat recovery and reuse through thermal energy storage in five specific industrial categories: (1) primary aluminum, (2) cement, (3) food processing, (4) paper and pulp, and (5) iron and steel. Preliminary results from Phase 1 feasibility studies suggest energy savings through fossil fuel displacement approaching 0.1 quad/yr in the 1985

period. Early implementation of recovery technologies with minimal development appears likely in the food processing and paper and pulp industries; development of the other three categories, though equally desirable, will probably require a greater investment in time and dollars. L.S.

N78-29577* National Aeronautics and Space Administration. Lewis Research Center, Cleveland, Ohio.

STORAGE SYSTEMS FOR SOLAR THERMAL POWER

James E. Cologeras and Larry H. Gordon Aug. 1978 9 p refs Presented at the 13th Intersoc. Energy Conversion Eng. Conf., San Diego, Calif., 20-25 Aug. 1978 (Contract EC-77-A-31-1034)

(NASA-TM-78952; DOE/NASA/1034-78/1; E-9698) Avail: NTIS HC A02/MF A01 CSCL 10C

The development status is reviewed of some thermal energy storage technologies specifically oriented towards providing diurnal heat storage for solar central power systems and solar total energy systems. These technologies include sensible heat storage in caverns and latent heat storage using both active and passive heat exchange processes. In addition, selected thermal storage concepts which appear promising to a variety of advanced solar thermal system applications are discussed. L.S.

N78-29578* National Aeronautics and Space Administration. Lewis Research Center, Cleveland, Ohio.

UTILIZATION OF SOLAR ENERGY IN DEVELOPING COUNTRIES: IDENTIFYING SOME POTENTIAL MARKETS

Gerald F. Hein and Toufiq A. Siddiqi (Environment and Policy Inst., Honolulu, Hawaii) Feb. 1978 13 p refs Presented at the Ann. Meeting of the Am. Assoc. for the Advan. of Sci., Washington, D. C., 12-17 Feb. 1978 (Contract E(49-28)-1022)

(NASA-TM-78964; DOE/NASA/1022-78/41) Avail: NTIS HC A02/MF A01 CSCL 10B

The potential use of solar electricity generated from photovoltaic cells is examined for nineteen developing nations. Energy and economic profiles are summarized for each country. A comparison is made between the use of cogeneration and photovoltaics in a rural area of Haiti. Author

N78-29683* National Aeronautics and Space Administration. Lewis Research Center, Cleveland, Ohio.

THE 200-KILOWATT WIND TURBINE PROJECT

Jan. 1978 17 p refs Prepared for DOE (NASA-TM-79757) Avail: NTIS HC A02/MF A01 CSCL 10B

The three 200 kilowatt wind turbines described, compose the first of three separate systems. Proposed wind turbines of the two other systems, although similar in design, are larger in both physical size and rated power generation. The overall objective of the project is to obtain early operation and performance data while gaining initial experience in the operation of large, horizontal-axis wind turbines in typical utility environments. Several of the key issues addressed include the following: (1) impact of the variable power output (due to varying wind speeds) on the utility grid (2) compatibility with utility requirements (voltage and frequency control of generated power) (3) demonstration of unattended, fail-safe operation (4) reliability of the wind turbine system (5) required maintenance and (6) initial public reaction and acceptance. L.S.

N78-31533* National Aeronautics and Space Administration. Lewis Research Center, Cleveland, Ohio.

INITIAL TEST RESULTS WITH A SINGLE-CYLINDER RHOMBIC-DRIVE STIRLING ENGINE Final Report

J. E. Cairrell, L. G. Thieme, and R. J. Walter Jul. 1978 42 p refs (Contract EC-77-A-31-1040)

(NASA-TM-78919; E-9656; DOE/NASA/1040-78/1) Avail: NTIS HC A03/MF A01 CSCL 10B

A 6 kW (8 hp), single-cylinder, rhombic-drive Stirling engine was restored to operating condition, and preliminary characteriza-

tion tests run with hydrogen and helium as the working gases. Initial tests show the engine brake specific fuel consumption (BSFC) with hydrogen working gas to be within the range of BSFC observed by the Army at Fort Belvoir, Virginia, in 1966. The minimum system specific fuel consumption (SFC) observed during the initial tests with hydrogen was 689 g/kW hr (1.1 lb/hp hr), compared with 620 g/kW hr (1.02 lb/hp hr) for the Army tests. However, the engine output power for a given mean compression-space pressure was lower than for the Army tests. The observed output power at a working-space pressure of 5 MPa (725 psig) was 3.27 kW (4.39 hp) for the initial tests and 3.80 kW (5.09 hp) for the Army tests. As expected, the engine power with helium was substantially lower than with hydrogen. J.M.S.

N78-31534* National Aeronautics and Space Administration, Lewis Research Center, Cleveland, Ohio

EFFECT OF INLET TEMPERATURE ON THE PERFORMANCE OF A CATALYTIC REACTOR

David N. Anderson: 1978 21 p refs Presented at the 3d Workshop on Catalytic Combust., Asheville, N. C., 3-4 Oct. 1978; sponsored by EPA

(Contract EC-77-A-31-1040)

(NASA-TM-78977; DOE/NASA/1040-78/3; E-9752) Avail: NTIS HC A02/MF A01 CSDL 10A

A 12 cm diameter by 15 cm long catalytic reactor was tested with No. 2 diesel fuel in a combustion test rig at inlet temperatures of 700, 800, 900, and 1000 K. Other test conditions included pressures of 3 and 6 x 10 to the 5th power Pa. reference velocities of 10, 15, and 20 m/s, and adiabatic combustion temperatures in the range 1100 to 1400 K. The combustion efficiency was calculated from measurements of carbon monoxide and unburned hydrocarbon emissions. Nitrogen oxide emissions and reactor pressure drop were also measured. At a reference velocity of 10 m/s, the CO and unburned hydrocarbons emissions, and, therefore, the combustion efficiency, were independent of inlet temperature. At an inlet temperature of 1000 K, they were independent of reference velocity. Nitrogen oxides emissions resulted from conversion of the small amount (135 ppm) of fuel-bound nitrogen in the fuel. Up to 90 percent conversion was observed with no apparent effect of any of the test variables. For typical gas turbine operating conditions, all three pollutants were below levels which would permit the most stringent proposed automotive emissions standards to be met. Author

A78-10903* A methodology for experimentally-based determination of gap shrinkage and effective lifetimes in the emitter and base of p-n-junction solar cells. F. A. Lindholm, A. Neugroschel (Florida, University, Gainesville, Fla.), C. T. Sah (Illinois, University, Urbana, Ill.), M. P. Godlewski, and H. W. Brandhorst, Jr. (NASA, Lewis Research Center, Cleveland, Ohio). In: Photovoltaic Specialists Conference, 12th, Baton Rouge, La., November 15-18, 1976, Conference Record. (A78-10902 01-44) New York, Institute of Electrical and Electronics Engineers, Inc., 1976, p. 1-8. 21 refs. Grant No. NSG-3018; Contract No. E(40-1)-5134.

A78-10904* Analysis of epitaxial drift field N on P silicon solar cells. C. R. Baraona and H. W. Brandhorst, Jr. (NASA, Lewis Research Center, Cleveland, Ohio). In: Photovoltaic Specialists Conference, 12th, Baton Rouge, La., November 15-18, 1976, Conference Record. (A78-10902 01-44) New York, Institute of Electrical and Electronics Engineers, Inc., 1976, p. 9-14. 14 refs.

A78-11014* Status of the ERDA/NASA Photovoltaic Tests and Applications Project. J. N. Deyo, H. W. Brandhorst, Jr., and A. F. Forestieri (NASA, Lewis Research Center, Cleveland, Ohio). In: Photovoltaic Specialists Conference, 12th, Baton Rouge, La., November 15-18, 1976, Conference Record. (A78-10902 01-44) New York, Institute of Electrical and Electronics Engineers, Inc., 1976, p. 698-704.

A78-11019* The Redox Flow System for solar photovoltaic energy storage. P. O'Donnell, R. F. Gahn, and W. Pfeiffer (NASA, Lewis Research Center, Cleveland, Ohio). In: Photovoltaic Specialists Conference, 12th, Baton Rouge, La., November 15-18, 1976, Conference Record. (A78-10902 01-44) New York, Institute of Electrical and Electronics Engineers, Inc., 1976, p. 733-736.

The interfacing of a Solar Photovoltaic System and a Redox Flow System for storage was workable. The Redox Flow System, which utilizes the oxidation-reduction capability of two redox couples, in this case iron and titanium, for its storage capacity, gave a relatively constant output regardless of solar activity so that a load could be run continually day and night utilizing the sun's energy. One portion of the system was connected to a bank of solar cells to electrochemically charge the solutions, while a separate part of the system was used to electrochemically discharge the stored energy.

(Author)

A78-11301* Evaluation of initial collector field performance at the Langley Solar Building Test Facility. R. J. Boyle, R. H. Knoll (NASA, Lewis Research Center, Cleveland, Ohio), and R. N. Jensen (NASA, Langley Research Center, Hampton, Va.). *International Solar Energy Society, Annual Meeting, Orlando, Fla., June 6-10, 1977, Paper, 20 p.* 6 refs.

The thermal performance of the solar collector field for the NASA Langley Solar Building Test Facility is given for October 1976 through January 1977. An 1180 square meter solar collector field with seven collector designs helped to provide hot water for the building heating system and absorption air conditioner. The collectors were arranged in 12 rows with nominally 51 collectors per row. Heat transfer rates for each row are calculated and recorded along with sensor, insolation, and weather data every 5 minutes using a mini-computer. The agreement between the experimental and predicted collector efficiencies was generally within five percentage points. (Author)

A78-16923* New batteries and their impact on electric vehicles. H. J. Schwartz (NASA, Lewis Research Center, Cleveland, Ohio). *Electric Vehicle Council, International Electric Vehicle Exposition and Conference, 1st, Chicago, Ill., Apr. 26-29, 1977, Paper, 15 p.* 18 refs.

The paper is concerned with the development of electric vehicles and electric vehicle batteries. The present and predicted performance levels of some battery systems such as lead-acid, nickel-iron, nickel-zinc, and zinc-chlorine are considered, as are the characteristics that an electric vehicle must possess in order to appeal to customers. The implications of battery improvements for manufacturers of electric vehicles are discussed. Lack of knowledge of passenger range requirements for electric vehicles is noted. M.L.

A78-20476* Effects of rotor location, zoning, and tilt on critical loads in large wind turbines. D. A. Spera and D. C. Janetzke (NASA, Lewis Research Center, Wind Turbine Analysis Section, Cleveland, Ohio). *Wind Technology Journal, vol. 1, Summer 1977, p. 5-10.* 7 refs.

Three large (1500 kW) horizontal rotor configurations were analyzed to determine the effects on dynamic loads of upwind and downwind rotor locations, coned and radial blade positions, and tilted and horizontal rotor axis positions. Loads were calculated for a range of wind velocities at three locations in the structure: the blade shank, the hub shaft, and the yaw drive. Blade axis coning and rotor axis tilt were found to have little effect on loads. However, locating the rotor upwind of the tower significantly reduced loads at all locations analyzed. (Author)

A78-24400 * Energy resources of the developing countries and some priority markets for the use of solar energy. T. A. Siddiqi (East-West Center, Honolulu, Hawaii) and G. F. Hein (NASA, Lewis Research Center, Cleveland, Ohio). *Journal of Energy and Development*, vol. 3, Autumn 1977, p. 164-189.

Energy consumption for the developed and non-developed world is expressed as a function of GNP. An almost straight-line graph results when energy consumption statistics are treated in this manner. The richest countries consume the most energy, and the poorest countries the least. It therefore follows that greater energy production in the developing countries (leading to greater energy consumption) will contribute to their economic growth. Energy resources in the developing countries are compared, including: solid fossil fuels, crude oil, natural gas, oil shale, and uranium. Mention is also made of the potential of renewable energy resources, such as solar, wind, and hydroelectric power, in the underdeveloped world; and it is these resources which offer the greatest possibilities for economic improvement if the money is forthcoming, i.e., from the world bank, to fund the necessary technology. D.M.W.

A78-26110 * # ECAS Phase I fuel cell results. M. Warshaw (NASA, Lewis Research Center, Fuel Cell Projects Office, Cleveland, Ohio). *Journal of Energy*, vol. 2, Jan.-Feb. 1978, p. 48-52. 10 refs.

This paper summarizes and discusses the fuel cell system results of Phase I of the Energy Conversion Alternatives Study (ECAS). Ten advanced electric powerplant systems for central-station baseload generation using coal were studied by NASA in ECAS. Three types of low-temperature fuel cells (solid polymer electrolyte, SPE, aqueous alkaline, and phosphoric acid) and two types of high-temperature fuel cells (molten carbonate, MC, and zirconia solid electrolyte, SE) were studied. The results indicate that (1) overall efficiency increases with fuel cell temperature, and (2) scale-up in powerplant size when it is accompanied by reduction in cost of electricity (COE) only when it is accompanied by utilization of waste fuel cell heat through a steam bottoming cycle and/or integration with a gasifier. For low-temperature fuel cell systems, the use of hydrogen results in the highest efficiency and lowest COE. In spite of higher efficiencies, because of higher fuel cell replacement costs integrated SE systems have higher projected COEs than do integrated MC systems. Present data indicate that life can be projected to over 30,000 hr for MC fuel cells, but data are not yet sufficient for similarly projecting SE fuel cell life expectancy. (Author)

A78-29331 * # Status of the DOE /STOR/-sponsored national program on hydrogen production from water via thermochemical cycles. C. E. Baker (NASA, Lewis Research Center, Cleveland, Ohio). *U.S. Department of Energy and University of Miami, Miami International Conference on Alternative Energy Sources, Miami Beach, Fla., Dec. 5-7, 1977, Paper*. 15 p. 5 refs.

A pure thermochemical cycle is a system of linked regenerative chemical reactions which accepts only water and heat and produces hydrogen. Thermochemical cycles are potentially a more efficient and cheaper means of producing hydrogen from water than is the generation of electricity followed by electrolysis. The Energy Storage Systems Division of the Department of Energy is currently funding a national program on thermochemical hydrogen production. The National Aeronautics and Space Administration is responsible for the technical management of this program. The goal is to develop a cycle which can potentially operate with an efficiency greater than 40% using a heat source providing a maximum available temperature of 1150 K. A closed bench-scale demonstration of such a cycle would follow. This cycle would be labeled a 'reference cycle' and would serve as a baseline against which future cycles would be compared. (Author)

A78-30196 * Synchronization of wind turbine generators against an infinite bus under gusting wind conditions. H. H. Hwang (Hawaii University, Honolulu, Hawaii) and L. J. Gilbert (NASA, Lewis Research Center, Cleveland, Ohio). *Institute of Electrical and Electronics Engineers, Summer Meeting, Mexico City, Mexico, July*

17-22, 1977, Paper F 77 676-2. IEEE Transactions on Power Apparatus and Systems, vol. PAS-97, Mar.-Apr. 1978, p. 536-544. 6 refs. Research supported by the Hawaii Natural Energy Institute and NASA.

Studies of synchronizing a wind turbine generator against an infinite bus are performed on a digital computer. In the digital simulation, wind gusts of different magnitudes and durations are hypothesized. Prior to the synchronization, differences of the frequency and phase position between voltages of the alternator and the bus are also included in the simulation. Solutions for rotor speed, generator power angle, electromagnetic torque, wind turbine torque, and wind turbine blade pitch angle, and armature current are simulated and presented graphically. The ERDA-NASA 100-kW wind turbine is used as a case study. The results so obtained will thus have immediate applications. (Author)

A78-33217 * # A review of the Thermo-electronic Laser Energy Converter (TELEC) Program at Lewis Research Center. D. L. Alger, E. J. Manista, and R. W. Thompson (NASA, Lewis Research Center, Cleveland, Ohio). *NASA Conference on Radiation Energy Conversion, 3rd, Moffett Field, Calif., Jan. 26, 27, 1978, Paper*. 18 p. 12 refs.

The investigation of the Thermo-electronic Laser Energy Converter (TELEC) concept at the Lewis Research Center (LeRC) began with a feasibility study of a 1 megawatt sized TELEC system. The TELEC was to use either cesium vapor or hydrogen as the plasma medium. The cesium vapor TELEC appears to be the more practical device studied with an overall calculated conversion efficiency of greater than 48%. Following this study, a small TELEC cell was fabricated which demonstrated the conversion of a small amount of laser power to electrical power. The cell developed a short circuit current of 0.7 amperes and an open circuit voltage, as extrapolated from volt-ampere curves, of about 1.5 volts. Work is now in progress to construct and test a cesium vapor TELEC capable of absorbing 20% of an incident 10 kW, 10.6 micrometer beam, and converting 35% of this power to electrical power. (Author)

A78-37678 * # Comparison of computer codes for calculating dynamic loads in wind turbines. D. A. Spera (NASA, Lewis Research Center, Cleveland, Ohio). *Biennial Conference and Workshop on Wind Energy Conversion Systems, 3rd, Washington, D.C., Sept. 19-21, 1977, Paper*. 38 p. 14 refs.

Seven computer codes for analyzing performance and loads in large, horizontal-axis wind turbines were used to calculate blade bending moment loads for two operational conditions of the 100 kW Mod-O wind turbine. Results are compared with test data on the basis of cyclic loads, peak loads, and harmonic contents. Four of the seven codes include rotor-tower interaction and three are limited to rotor analysis. With a few exceptions, all calculated loads were within 25% of nominal test data. (Author)

A78-45437 * # Utilization of solar energy in developing countries - Identifying some potential markets. G. F. Hein (NASA, Lewis Research Center, Cleveland, Ohio) and T. A. Siddiqi (Environment and Policy Institute, Honolulu, Hawaii). *American Association for the Advancement of Science, Annual Meeting, Washington, D.C., Feb. 12-17, 1978, Paper*. 11 p. 11 refs. Contract No. E(49-28)-1022.

A78-52837 * Real-time and accelerated outdoor endurance testing of solar cells. A. F. Forestieri and E. Anagnostou (NASA, Lewis Research Center, Cleveland, Ohio). In *Photovoltaic Solar Energy Conference, Luxembourg, September 27-30, 1977, Proceedings* (A78-52776 24-44) Dordrecht, D. Reidel Publishing Co., 1978, p. 656-676. 6 refs. ERDA supported research.

Materials for solar-cell module construction have been studied on the basis of limited real-time outdoor exposure evaluations. The materials tested included transmission samples, sub-modules, and

actual solar cells. The results suggest that glass, fluorinated ethylene propylene, and perfluoroalkoxy are good materials for the covering or encapsulation of solar-cell modules. In all cases, dirt accumulation and cleanliness are important factors. S.C.S.

A78-52844 * U.S. terrestrial solar cell calibration and measurement procedures. H. W. Brandhorst, Jr. (NASA, Lewis Research Center, Cleveland, Ohio). In: Photovoltaic Solar Energy Conference, Luxembourg, September 27-30, 1977, Proceedings. (A78-52776 24-44) Dordrecht, D. Reidel Publishing Co., 1978, p. 745-753. 10 refs. ERDA-supported research.

An outline is presented of changes in measurement procedures concerning solar cells. Outdoor measurements of cell performance based on pyranometer or pyrheliometer determination of intensity are discouraged. The absolute scale of irradiance is to be adopted as soon as possible. The standard atmosphere conditions are 1000 W/sq m irradiance, temperature 28 C, air mass 1.5, and precipitable water vapor content of 2 cm. The allowable light sources for solar simulation are short arc xenon lamps, pulsed xenon lamps, and dichroic filtered tungsten lamps. Key considerations in the design of a reference cell are considered and approaches for the matching of a reference cell to a test cell or modules are discussed. G.R.

A78-52851 * The ERDA/LeRC Photovoltaic Systems Test Facility. A. F. Forestieri (NASA, Lewis Research Center, Cleveland, Ohio). In: Photovoltaic Solar Energy Conference, Luxembourg, September 27-30, 1977, Proceedings. (A78-52776 24-44) Dordrecht, D. Reidel Publishing Co., 1978, p. 817-824. 5 refs. ERDA-supported research.

The ERDA/LeRC Photovoltaic Systems Test Facility (STF) provides a vital support function to the overall ERDA National Solar Photovoltaic Program. It allows preliminary investigation and check-out of components, subsystems, and complete photovoltaic systems before installation in actual service. The STF can also be used to determine optimum system configurations and operating modes. A facility description is presented, taking into account the solar cell array, the energy storage equipment, the power conditioning equipment, electric utility distribution network and loads, and instrumentation and data acquisition systems. Safety procedures which have been set up for maintenance and inspection of the solar array are discussed. Attention is also given to a number of investigations regarding the effect of environmental factors on solar cell array operation. G.R.

N78-12629# General Electric Co., Philadelphia, Pa. Valley Forge Space Center.
DESIGN STUDY OF WIND TURBINES 50 kW TO 3000 kW FOR ELECTRIC UTILITY APPLICATIONS. VOLUME 1: SUMMARY REPORT Final Report
Sep. 1976 65 p
(Contracts NAS3-19403; E(49-26)-1010)
(NASA-CR-134934; ERDA/NASA-9403-76/1-Vol-1;
Doc-SDS4287-Vol-1) Avail: NTIS HC A04/MF A01 CSCL 10B

Wind turbine configurations that would lead to generation of electrical power in a cost effective manner were considered. All possible overall system configurations, operating modes, and subsystem concepts were evaluated for both technical feasibility and compatibility with utility networks, as well as for economic attractiveness. A design optimization computer code was developed to determine the cost sensitivity of the various design features, and thus establish the configuration and design conditions that would minimize the generated energy costs. The preliminary designs of both a 500 kW unit and a 1500 kW unit operating in a 12 mph and 18 mph median wind speed respectively, were developed. The rationale employed and the key findings are summarized. Author

N78-13888# Thermo Electron Engineering Corp., Waltham, Mass.

ADVANCED THERMIONIC TECHNOLOGY PROGRAM Progress Report
Apr. 1977 21 p

(Contracts NAS3-20302; EY-76-C-02-3066)
(NASA-CR-155299; COO-3066-23; TE-4217/4220-123-77;
PR-22) Avail: NTIS HC A02/MF A01 CSCL 01B

Topics include surface studies (surface theory, basic surface experiments, and activation chamber experiments); plasma studies (converter theory and enhanced mode conversion experiments); and component development (low temperature conversion experiments, high efficiency conversion experiments, and hot shell development). ERA

N78-14632# Grumman Aerospace Corp., Bethpage, N.Y.
THERMAL ENERGY STORAGE HEAT EXCHANGER: MOLTEN SALT HEAT EXCHANGER DESIGN FOR UTILITY POWER PLANTS Final Report, Jul. 1976 - Jul. 1977
Angelo Ferrara, George Yenetchi, Robert Haslett, and Robert Kosson Oct. 1977 207 p refs
(Contract NAS3-20117)
(NASA-CR-135244) Avail: NTIS HC A10/MF A01 CSCL 10C

The use of thermal energy storage (TES) in the latent heat of molten salts as a means of conserving fossil fuels and lowering the cost of electric power was evaluated. Public utility systems provided electric power on demand. This demand is generally maximum during late weekday afternoons, with considerably lower overnight and weekend loads. Typically, the average demand is only 60% to 80% of peak load. As peak load increases, the present practice is to purchase power from other grid facilities or to bring older less efficient fossil-fuel plants on line which increase the cost of electric power. The widespread use of oil-fired boilers, gas turbine and diesel equipment to meet peaking loads depletes our oil-based energy resources. Heat exchangers utilizing molten salts can be used to level the energy consumption curve. The study begins with a demand analysis and the consideration of several existing modern fossil-fuel and nuclear power plants for use as models. Salts are evaluated for thermodynamic, economic, corrosive, and safety characteristics. Heat exchanger concepts are explored and heat exchanger designs are conceived. Finally, the economics of TES conversions in existing plants and new construction is analyzed. The study concluded that TES is feasible in electric power generation. Substantial data are presented for TES design, and reference material for further investigation of techniques is included. Author

N78-14633# Grumman Aerospace Corp., Bethpage, N.Y.
THERMAL ENERGY STORAGE HEAT EXCHANGER: MOLTEN SALT HEAT EXCHANGER DESIGN FOR UTILITY POWER PLANTS Topical Report, Jul. 1976 - Jul. 1977
Angelo Ferrara, George Yenetchi, Robert Haslett, and Robert Kosson Oct. 1977 36 p refs
(Contract NAS3-20117)
(NASA-CR-135245) Avail: NTIS HC A03/MF A01 CSCL 10C

Sizing procedures are presented for latent heat thermal energy storage systems that can be used for electric utility off-peak energy storage, solar power plants and other preliminary design applications. Author

N78-17482# General Electric Co., Philadelphia, Pa.
DESIGN STUDY OF WIND TURBINES 50 kW TO 3000 kW FOR ELECTRIC UTILITY APPLICATIONS. VOLUME 2: ANALYSIS AND DESIGN Final Report
Dec. 1976 328 p refs
(Contract NAS3-19403)
(NASA-CR-134935; ERDA/NASA-9403-76/2-Vol-2;
GE-SD-76SDS4288-Vol-2) Avail: NTIS HC A15/MF A01 CSCL 10A

All possible overall system configurations, operating modes, and subsystem concepts for a wind turbine configuration for cost effective generation of electrical power were evaluated for both technical feasibility and compatibility with utility networks.

as well as for economic attractiveness. A design optimization computer code was developed to determine the cost sensitivity of the various design features, and thus establish the configuration and design conditions that would minimize the generated energy costs. The preliminary designs of both a 500 kW unit and a 1500 kW unit operating in a 12 mph and 18 mph median wind speed respectively, were developed. The various design features and components evaluated are described, and the rationale employed to select the final design configuration is given. All pertinent technical performance data and component cost data are included. The costs of all major subassemblies are estimated and the resultant energy costs for both the 500 kW and 1500 kW units are calculated. Author

N78-17483* General Electric Co., Philadelphia, Pa.
DESIGN STUDY OF WIND TURBINES 50 kW TO 3000 kW FOR ELECTRIC UTILITY APPLICATIONS. VOLUME 3: SUPPLEMENTARY DESIGN AND ANALYSIS TASKS
Final Report

Dec 1976 62 p refs
(Contract NAS3-19403)
(NASA-CR-135121; ERDA/NASA-9403-76/3-Vol-3) Avail: NTIS HC A04/MF A01 CSCL 10A

Additional design and analysis data are provided to supplement the results of the two parallel design study efforts. The key results of the three supplemental tasks investigated are: (1) The velocity duration profile has a significant effect in determining the optimum wind turbine design parameters and the energy generation cost. (2) Modest increases in capacity factor can be achieved with small increases in energy generation costs and capital costs. (3) Reinforced concrete towers that are esthetically attractive can be designed and built at a cost comparable to those for steel truss towers. The approach used, method of analysis, assumptions made, design requirements, and the results for each task are discussed in detail. Author

N78-18515* Ionics, Inc., Watertown, Mass. Research Div.
ANION PERMEABLE MEMBRANE Summary Report
Samuel Alexander and Russell B. Hodgdon Jul. 1977 77 p
(Contract NAS3-20108)
(NASA-CR-135316) Avail: NTIS HC A05/MF A01 CSCL 10A

The objective of NAS 3-20108 was the development and evaluation of improved anion selective membranes useful as efficient separators in a redox power storage cell system being constructed. The program was divided into three parts. (a) optimization of the selected candidate membrane systems, (b) investigation of alternative membrane/polymer systems, and (c) characterization of candidate membranes. The major synthesis effort was aimed at improving and optimizing as far as possible each candidate system with respect to three critical membrane properties essential for good redox cell performance. Substantial improvements were made in 5 candidate membrane systems. The critical synthesis variables of cross-link density, monomer ratio, and solvent composition were examined over a wide range. In addition, eight alternative polymer systems were investigated, two of which attained candidate status. Three other alternatives showed potential but required further research and development. Each candidate system was optimized for selectivity. Author

N78-20803* Hawaii Univ., Honolulu
EMPLOYING STATIC EXCITATION CONTROL AND TIE LINE REACTANCE TO STABILIZE WIND TURBINE GENERATORS
Final Report
H. H. Hwang, H. V. Mozeico, and Tenhui Guo Apr. 1978 77 p refs
(Grant NoG-3132; Contract E(49-26)-1004)
(NASA-CR-135344; DOE/NASA/3132-78/1) Avail: NTIS HC A05/MF A01 CSCL 10A

An analytical representation of a wind turbine generator is presented which employs blade pitch angle feedback control. A mathematical model was formulated. With the functioning MOD-0 wind turbine serving as a practical case study, results of computer simulations of the model as applied to the problem of dynamic stability at rated load are also presented. The effect of the tower

shadow was included in the input to the system. Different configurations of the drive train, and optimal values of the tie line reactance were used in the simulations. Computer results revealed that a static excitation control system coupled with optimal values of the tie line reactance would effectively reduce oscillations of the power output, without the use of a slip clutch. Author

N78-20821* Rocketdyne, Canoga Park, Calif.
HYDROGEN TURBINE POWER CONVERSION SYSTEM ASSESSMENT Final Report, Aug. 1973 - Apr. 1976
D. E. Wright, A. D. Lucci, J. Campbell, and J. C. Lee 19 Apr. 1976 155 p refs
(Contract NAS3-20388)
(NASA-CR-135298; RI/RD77-252) Avail: NTIS HC A05/MF A01 CSCL 10A

A three part technical study was conducted whereby parametric technical and economic feasibility data were developed on several power conversion systems suitable for the generation of central station electric power through the combustion of hydrogen and the use of the resulting heat energy in turbogenerator equipment. The study assessed potential applications of hydrogen-fueled power conversion systems and identified the three most promising candidates. (1) Ericsson Cycle, (2) gas turbine, and (3) direct steam injection system for fossil fuel as well as nuclear powerplants. A technical and economic evaluation was performed on the three systems from which the direct injection system (fossil fuel only) was selected for a preliminary conceptual design of an integrated hydrogen-fired power conversion system. Author

N78-23550* Kaman Aerospace Corp., Bloomfield, Conn.
DESIGN STUDY OF WIND TURBINES, 50 kW TO 3000 kW FOR ELECTRIC UTILITY APPLICATIONS: EXECUTIVE SUMMARY Final Report
Jul. 1977 95 p

(Contracts NAS3-19404; E(49-26)-1010)
(NASA-CR-134936; R-1382; DOE/NASA/9404-7611) Avail: NTIS HC A05/MF A01 CSCL 10A

Preliminary designs of low power (50 to 500 kW) and high power (500 to 3000 kW) wind generator systems (WGS) for electric utility applications were developed. These designs provide the bases for detail design, fabrication, and experimental demonstration testing of these units at selected utility sites. Several feasible WGS configurations were evaluated, and the concept offering the lowest energy cost potential and minimum technical risk for utility applications was selected. The selected concept was optimized utilizing a parametric computer program prepared for this purpose. The utility requirements evaluation task examined the economic, operational, and institutional factors affecting the WGS in a utility environment, and provided additional guidance for the preliminary design effort. Results of the conceptual design task indicated that a rotor operating at constant speed, driving an AC generator through a gear transmission is the most cost effective WGS configuration. Author

N78-23560* Kaman Aerospace Corp., Bloomfield, Conn.
DESIGN STUDY OF WIND TURBINES 50 kW TO 3000 kW FOR ELECTRIC UTILITY APPLICATIONS: ANALYSIS AND DESIGN Final Report
Feb 1976 567 p refs

(Contracts NAS3-10094; E(49-26)-1010)
(NASA-CR-134937; R-1382; DOE/NASA/9404-76/2) Avail: NTIS HC A24/MF A01 CSCL 10A

In the conceptual design task, several feasible wind generator systems (WGS) configurations were evaluated, and the concept offering the lowest energy cost potential and minimum technical risk for utility applications was selected. In the optimization task, the selected concept was optimized utilizing a parametric computer program prepared for this purpose. In the preliminary design task, the optimized selected concept was designed and analyzed in detail. The utility requirements evaluation task examined the economic, operational, and institutional factors affecting the WGS in a utility environment, and provided additional guidance for the preliminary design effort. Results of the conceptual design

task indicated that a rotor operating at constant speed, driving an AC generator through a gear transmission is the most cost effective WGS configuration. The optimization task results led to the selection of a 500 kW rating for the low power WGS and a 1500 kW rating for the high power WGS. Author

N78-24874* Thermo Electron Corp., Waltham, Mass.
ERDA/NASA ADVANCED THERMIONIC TECHNOLOGY PROGRAM Progress Report
 May 1977 24 p refs
 (Contracts NAS3-20302; EY-76-C-02-3656)
 (NASA-CR-157117; PR-23; TE-4217/4220-140-77;
 COO-3056-25) Avail: NTIS HC A02/MF A01 CSCL 10A

Research progress is outlined in the areas of surface studies (basic experiments and direct beam chamber), plasma studies (converter theory and advanced mode conversion experiments), component development (low-temperature and high-temperature converter experiments), and component hardware (hot shell development). ERA

N78-26579* Thermo Electron Engineering Corp., Waltham, Mass.
ERDA-NASA ADVANCED THERMIONIC TECHNOLOGY PROGRAM Program Report
 Aug 1977 16 p refs
 (Contracts NAS3-20959; EY-76-C-02-3056)
 (NASA-CR-157222; PR-28; TE-4220/4233-29-78;
 COO-3056-28) Avail: NTIS HC A02/MF A01 CSCL 10B

Research is summarized on surface studies (work functions of different LaB6 surfaces), plasma studies, converter development (tungsten emitter, nickel collector and tungsten emitter La B6 collector), and hot shell development for using thermionic converters in the topping cycle of fossil-fuel plants. Author (ERA)

N78-27540* International Corp., Lawistown, Pa.
EVALUATION OF GLASS RESIN COATINGS FOR SOLAR CELL APPLICATIONS Final Report
 M B Field Apr 1978 38 p
 (Contract NAS3-20958)
 (NASA CR 159392) Avail: NTIS HC A03/MF A01 CSCL 10A

Using a variety of non-vacuum deposition techniques coatings were implemented on silicon solar cells and arrays of cells interconnected on Kapton substrates. The coatings provide both antireflection optical matching and environmental protection. Reflectance minima near 2% was achieved at a single wavelength in the visible. Reflectance averaging below 5% across the useful collection range was demonstrated. The coatings and methods of deposition were (1) Ta2O5 spun, dipped or sprayed; (2) Ta2O5 SiO2 spun, dipped or sprayed; (3) GR908 (SiO2) spun, dipped, or sprayed. Total coating thickness were in the range of 18 microns to 25 microns. The coatings and processes are compatible with single cells or cells mounted on Kapton substrates. GY

N78-27552* Thermo Electron Engineering Corp., Waltham, Mass.
ERDA-NASA ADVANCED THERMIONIC TECHNOLOGY PROGRAM Progress Report
 Sep 1977 11 p
 (Contracts NAS3-20959; EY-76-C-02-3056)
 (NASA CR 157248; TE-4220/4233-44-78; COO-3056-29; PR-27) Avail: NTIS HC A02/MF A01

Research progress is briefly outlined in the areas of activation experiments, enhanced mode conversion experiments, converter development (tungsten emitter, lanthanum hexaborate collector) and hot shell development. Author (ERA)

N78-2888* AiResearch Mfg. Co., Torrance, Calif.
PRELIMINARY DESIGN STUDY OF AN ALTERNATE HEAT SOURCE ASSEMBLY FOR A BRAYTON ISOTOPE POWER SYSTEM Final Report, Oct. 1977 - Apr. 1978
 Hal J. Strumpf May 1978 112 p refs Prepared for JPL
 (Contract NAS3-20818)
 (NASA-CR-135428; AiResearch-78-15171) Avail: NTIS HC A06/MF A01 CSCL 10A

Results are presented for a study of the preliminary design of an alternate heat source assembly (HSA) intended for use in the Brayton isotope power system (BIPS). The BIPS converts thermal energy emitted by a radioactive heat source into electrical energy by means of a closed Brayton cycle. A heat source heat exchanger configuration was selected and optimized. The design consists of a 10 turn helically wound Hastelloy X tube. Thermal analyses were performed for various operating conditions to ensure that post impact containment shell (PICS) temperatures remain within specified limits. These limits are essentially satisfied for all modes of operation except for the emergency cooling system for which the PICS temperatures are too high. Neon was found to be the best choice for a fill gas for auxiliary cooling system operation. Low cycle fatigue life, natural frequency, and dynamic loading requirements can be met with minor modifications to the existing HSA. B B

N78-28874* Ionics, Inc., Watertown, Mass. Research Div.
ANION PERMESELECTIVE MEMBRANE
 S S Alexander and R B. Hodgdon Jan. 1978 77 p
 (Contracts NAS3-20108; E(49-28)-1002)
 (NASA-CR-135316; CONS/O108-1) Avail: NTIS HC A05/MF A01 CSCL 10A

Experimental anion permselective membranes were improved and characterized for use as separators in a chemical redox power storage cell being developed at the NASA Lewis Research Center. The goal of minimal Fe(+3) ion transfer was achieved for each candidate membrane system. Minimal membrane resistivity was demonstrated by reduction of film thickness using synthetic backing materials but usefulness of thin membranes was limited by the scarcity of compatible fabrics. The most durable and useful backing fabrics were modacrylics. One membrane, a copolymer of 4-vinylpyridine and vinyl benzylchloride was outstanding in overall electrochemical and physical properties. Long term (1000 hrs) membrane chemical and thermal durability in redox environment was shown by three candidate polymers and two membranes. The remainder had good durability at ambient temperature. Manufacturing capability was demonstrated for large scale production of membrane sheets 5.5 sq ft in area for two candidate systems. Author

N78-28884* Rohr Industries, Inc., Chula Vista, Calif.
PRELIMINARY POWER TRAIN DESIGN FOR A STATE-OF-THE-ART ELECTRIC VEHICLE Final Report
 James A. Ross and Gerald A. Wooldridge Apr. 1978 222 p refs
 (Contracts NAS3-20592; EC-77-A-31-1044)
 (NASA-CR-135340; RHR-78-035; DOE/NASA/0592-78/1)
 Avail: NTIS HC A10/MF A01 CSCL 10A

The state-of-the-art (SOTA) of electric vehicles built since 1965 was reviewed to establish a base for the preliminary design of a power train for a SOTA electric vehicle. The performance of existing electric vehicles were evaluated to establish preliminary specifications for a power train design using state-of-the-art technology and commercially available components. Power train components were evaluated and selected using a computer simulation of the SAE J227a Schedule D driving cycle. Predicted range was determined for a number of motor and controller combinations in conjunction with the mechanical elements of power trains and a battery pack of sixteen lead-acid batteries - 471.7 kg at 0.093 MJ/Kg (1040 lbs at 11.7 Whr/lb). On the basis of maximum range and overall system efficiency using the Schedule D cycle, an induction motor and 3 phase inverter/controller was selected as the optimum combination when used with a two-speed transaxle and steel belted radial tires. The predicted Schedule D range is: 90.4 km (56.2 mi). Four near term improvements to the SOTA were identified, evaluated, and predicted to increase range approximately 7%. F.O.S.

N78-39827* Honeywell, Inc., Minneapolis, Minn.
DEVELOPMENT OF FLAT-PLATE SOLAR COLLECTORS FOR THE HEATING AND COOLING OF BUILDINGS: EXECUTIVE SUMMARY
 [1978] 21 p
 (Contract NAS3-17862)
 (NASA-CR-134804) Avail: NTIS HC A02/MF A01 CSDL 10A

An efficient, low cost, flat-plate solar collector was developed. Computer aided mathematical models of the heat process in the collector were used in defining absorber panel configuration; determining insulation thickness; and in selecting the number, spacing, and material of the covers. Prototypes were built and performance tested. Data from simulated operation of the collector are compared with predicted loads from a number of locations to determine the degree of solar utilization. S.B.S.

A78-10947* Application of thick-film technology to solar cell fabrication. M. B. Field (Owens-Illinois, Inc., Toledo, Ohio) and L. R. Scudder (NASA, Lewis Research Center, Cleveland, Ohio). In: Photovoltaic Specialists Conference, 12th, Baton Rouge, La., November 15-18, 1976, Conference Record. (A78-10902 01-44) New York, Institute of Electrical and Electronics Engineers, Inc., 1976, p. 303-308. Contract No. NAS3-19441.

Several uses of thick-film technology in solar cell fabrication are discussed. Wrap-around contacts are obtained by first printing and firing a dielectric over the edge and subsequently applying a low-firing temperature conductor. Interconnection of cells into arrays can be achieved by printing and co-firing thick-film pastes, soldering, or with heat-curing conductive epoxies on low-cost substrates. Despite ongoing research, printed (thick) film vitreous protective coatings do not yet offer sufficient optical uniformity and transparency for use on silicon. Ohmic contacts on n- and p-type silicon are considered. M.L.

A78-29636* Experiments with enhanced mode thermionic converters. P. E. Oettinger and F. N. Hussman (Thermo Electron Research and Development Center, Waltham, Mass.). *IEEE Transactions on Plasma Science*, vol. PS-6, Mar. 1978, p. 83-88, 8 refs. Contract No. NAS3-20302.

Reduction of the ionization and scattering losses associated with ignited mode cesium diodes is essential for high thermal-to-electrical conversion efficiency. Use of an auxiliary electrode in conjunction with a noble gas in the interelectrode space should permit more efficient ion generation for space charge neutralization. The characteristics of a thermionic triode utilizing a ring electrode and a dispenser cathode emitter have been studied as a function of xenon pressure, cesium reservoir temperature, spacing, electrode temperature and pulse parameters (i.e., potential, duration and repetition rate) applied to the auxiliary electrode. Pulsed operation significantly enhanced output power with uniform discharges appearing to be sustained at emitter-collector spacings as low as 0.5 mm. (Author)

A78-31974* Pulse battery charger employing 1000 ampere transistor switches. R. L. Steigerwald (General Electric Co., Schenectady, N.Y.). *Institute of Electrical and Electronics Engineers, Annual Conference, 12th, Los Angeles, Calif., Oct. 2-6, 1977, Paper*. 6 p. Contract No. NAS3 19750

A pulse charger which uses water-cooled 1000 amp transistor switches has been developed to determine empirically the best methods of rapidly charging large cells in the one- to two-volt range. The pulse charger is capable of delivering a positive current from 0 to 1000 amps and extracting a negative current from 0 to 1000 amps. The charger can supply a 1000-amp DC charge or can switch 1000 amps at a rate of 1000 Hz. Special attention is given to problems associated with rapid switching of high currents through use of transistors. J.M.B.

A78-33147* Open-Cycle Gas Turbine/Steam Turbine Combined Cycles with synthetic fuels from coal. R. P. Shah and J. C. Corman (General Electric Co., Schenectady, N.Y.). *American Society of Mechanical Engineers, Winter Annual Meeting, Atlanta, Ga., Nov. 27-Dec. 2, 1977, Paper 77-WA/Ener-9*. 12 p. Members, \$1.50; nonmembers, \$3.00. ERDA-NSF-sponsored research; Contract No. NAS3-19406.

The Open-Cycle Gas Turbine/Steam Turbine Combined Cycle can be an effective energy conversion system for converting coal to electricity. The intermediate step in this energy conversion process is to convert the coal into a fuel acceptable to a gas turbine. This can be accomplished by producing a synthetic gas or liquid, and by removing, in the fuel conversion step, the elements in the fuel that would be harmful to the environment if combusted. In this paper, two open-cycle gas turbine combined systems are evaluated: one employing an integrated low-Btu gasifier, and one utilizing a semi-clean liquid fuel. A consistent technical/economic information base is developed for these two systems, and is compared with a reference steam plant burning coal directly in a conventional furnace. (Author)

A78-34078* Performance and economics of advanced energy conversion systems for coal and coal-derived fuels. J. C. Corman and G. R. Fox (General Electric Co., Schenectady, N.Y.). *ASME, Transactions, Journal of Engineering for Power*, vol. 100, Apr. 1978, p. 252-259. Contract No. NAS3 19406.

The desire to establish an efficient Energy Conversion System to utilize the fossil fuel of the future coal has produced many candidate systems. A comparative technical-economic evaluation was performed on the seven most attractive advanced energy conversion systems. The evaluation maintains a cycle to cycle consistency in both performance and economic projections. The technical information base can be employed to make program decisions regarding the most attractive concept. A reference steam power plant was analyzed to the same detail and, under the same ground rules, was used as a comparison base. The power plants were all designed to utilize coal or coal derived fuels and were targeted to meet an environmental standard. The systems evaluated were two advanced steam systems, a potassium topping cycle, a closed cycle helium system, two open cycle gas turbine combined cycles, and an open cycle MHD system. (Author)

A78-53489* Dendritic web silicon for solar cell application. R. G. Sedensticker (Westinghouse Research Laboratories, Pittsburgh, Pa.). In: *Materials and energy: Selected topics*. (A78 53487 24 44) Amsterdam, North-Holland Publishing Co., 1977, p. 17-22, 18 refs. USAF supported research; Contracts No. NAS3-18034; No. NAS3-19439.

The dendritic web process for growing long thin ribbon crystals of silicon and other semiconductors is described. Growth is initiated from a thin wirelike dendrite seed which is brought into contact with the melt surface. Initially, the seed grows laterally to form a button at the melt surface; when the seed is withdrawn, needlelike dendrites propagate from each end of the button into the melt, and the web portion of the crystal is formed by the solidification of the liquid film supported by the button and the bounding dendrites. Apparatus used for dendritic web growth, material characteristics, and the two distinctly different mechanisms involved in the growth of a single crystal are examined. The performance of solar cells fabricated from dendritic web material is indistinguishable from the performance of cells fabricated from Czochralski grown material. M.L.

45 ENVIRONMENT POLLUTION

Includes air, noise, thermal and water pollution; environment monitoring; and contamination control.

A78-15826 * // Global measurements of gaseous and aerosol trace species in the upper troposphere and lower stratosphere from daily flights of 747 airliners. P. J. Perkins (NASA, Lewis Research Center, Cleveland, Ohio). *AGU, AIAA, and AMS, Joint Symposium on Nonurban Troposphere, Miami Beach, Fla., Nov. 10-12, 1978, Paper. 17 p. 8 refs.*

A description is given of the NASA Global Atmospheric Sampling Program (GASP), taking into account the onboard system which collects atmospheric data automatically, the extensive atmospheric measurement capability, and the data handling and distribution procedure. GASP was implemented to assess the environmental impact of aircraft exhaust emissions in the upper troposphere and lower stratosphere. Global air quality data are to be obtained for a period of five to ten years. Measurements of pollutants not related to aircraft exhaust emissions, such as chlorofluoromethanes, are now included. GASP systems are operating on a United Airlines 747, two Pan Am 747s, and a Qantas Airways of Australia 747. Real-time, in-situ measurements are conducted of ozone, water vapor, carbon monoxide, and oxides of nitrogen. Chlorofluoromethanes are measured by laboratory analysis. Typical GASP data show significant changes in ozone, carbon monoxide, and water vapor related to crossings of the tropopause. G.R.

46 GEOPHYSICS

Includes aeronomy; upper and lower atmosphere studies; ionospheric and magnetospheric physics; and geomagnetism. For space radiation see 93 Space Radiation.

N78-13889* National Aeronautics and Space Administration, Lewis Research Center, Cleveland, Ohio
AN ANALYSIS OF THE FIRST TWO YEARS OF GASP DATA

J. D. Holdeman, G. D. Nastrom (Control Data Corp., Minneapolis, Minn.), and P. D. Falconer (Albany Univ., N. Y.) 1977 10 p refs Presented at 4th Joint Conf. on Sensing of Environmental Pollutants New Orleans, La., 6-11 Nov. 1977; sponsored by Am. Chem. Soc. (NASA-TM-73817, E-9408) Avail: NTIS HC A02/MF A01 CSCL 04A

Distributions of mean ozone levels from the first two years of data from the NASA Global Atmospheric Sampling Program (GASP) show spatial and temporal variations in agreement with previous measurements. The standard deviations of these distributions reflect the large natural variability of ozone levels in the altitude range of the GASP measurements. Monthly mean levels of ozone below the tropopause show an annual cycle with a spring maximum which is believed to result from transport from the stratosphere. Correlations of ozone with independent meteorological parameters, and meteorological parameters obtained by the GASP systems show that this transport occurs primarily through cyclogenesis at mid-latitudes. Author

N78-13870* National Aeronautics and Space Administration, Lewis Research Center, Cleveland, Ohio
GLOBAL SENSING OF GASEOUS AND AEROSOL TRACE SPECIES USING AUTOMATED INSTRUMENTATION ON 747 AIRLINERS

Porter J. Perkins and Leonidas C. Papathetos 1977 11 p refs Presented at 4th Joint Conf. on Sensing of Environmental Pollutants, New Orleans, La., 6-11 Nov. 1977 (NASA-TM-73810, E-9398) Avail: NTIS HC A02/MF A01 CSCL 04A

The Global Atmospheric Sampling Program (GASP) by NASA is collecting and analyzing data on gaseous and aerosol trace species in the upper troposphere and lower stratosphere. Measurements are obtained from automated systems installed on four 747 airliners flying global air routes. Advances were made in airborne sampling instrumentation, improved instruments and analysis techniques are providing an expanding data base for trace species including ozone, carbon monoxide, water vapor, condensation nuclei, and mass concentrations of sulfates and nitrates. Simultaneous measurements of several trace species obtained frequently can be used to uniquely identify the source of the air mass as being typically tropospheric or stratospheric. A quantitative understanding of the tropospheric-stratospheric exchange processes leads to better knowledge of the atmospheric impact of pollution through the development of improved simulation models of the atmosphere. Author

A78-24883* Description and review of global measurements of atmospheric species from GASP. D. J. Gauntner, J. D. Holdeman, D. Briehl, and F. M. Humenik (NASA, Lewis Research Center, Cleveland, Ohio). *ASTM, AMS, APCA, EPA, International Ozone Institute, NBS, and NOAA, Conference on Air Quality Meteorology and Atmospheric Ozone, Boulder, Colo., July 31-Aug. 6, 1977, Paper 24* p. 9 refs.

A large volume of atmospheric constituent data is being collected in the global airlines by specially equipped B 747 aircraft. This NASA program also obtains data from the similarly equipped NASA CV 990 aircraft during dedicated flights such as a recent near pole-to-pole latitude survey mission. Aerosol composition data are also collected with a NASA F 106 aircraft. Present measurements include ozone, carbon monoxide, water vapor, aerosol and condensation nuclei, number densities, sulphates, nitrates, and the chlorofluoromethanes. Meteorological and flight parameters are also re-

corded for use in data analysis. The present aircraft operations obtain data between 8 and 13.5 km from 65 deg N between Europe and the North Pacific, and from 23 deg S over South America and 42 deg S over New Zealand. Typical constituent data from the aircraft operations during the first one and a half years are presented. Instrumentation is discussed. (Author)

A78-24884* Atmospheric ozone measurements made from B-747 airliners - Spring 1978. P. D. Falconer, A. D. Taylor (NOAA, Air Resources Laboratories, Silver Spring, Md.), and J. D. Holdeman (NASA, Lewis Research Center, Cleveland, Ohio). *IAMAP, WMO, and IAGA, Joint Symposium on Atmospheric Ozone, Dresden, East Germany, Aug. 9-17, 1976, Paper 29* p.

Atmospheric ozone in the upper troposphere and lower stratosphere north of the equator has been registered aboard two commercial B-747 airliners during the Spring of 1978. This monitoring is part of a much broader and continuing project developed by NASA and known as the Global Atmospheric Sampling Program (GASP). Additional flight and meteorological conditions have also been automatically recorded on board concurrent with the ozone measurements. Independently-derived tropopause pressure information was available from NMC data archives and was used to identify stratospheric and tropospheric flight. The composite ozone, flight and meteorological data are reported for selected dates in March, April, and May. Attention is drawn particularly to the vertical profiles of atmospheric ozone mixing ratio as a function of both distance from the tropopause and curvature of the streamlines. The GASP observations suggest that ozone levels typical of the lower stratosphere are often embedded in the upper troposphere, principally during occasions when cyclonic wind curvature was noted. (Author)

N78-23848* Control Data Corp., Minneapolis, Minn. Research Div.

VARIABILITY OF OZONE NEAR THE TROPOPAUSE FROM GASP DATA Research Report

G. D. Nastrom 14 Apr 1978 50 p refs (Contract NAS3-20618)

(NASA-CR-138408-RR-1) Avail: NTIS HC A03/MF A01 CSCL 04A

The first 22 months of ozone data from the Global Atmospheric Sampling Program are summarized. Variations in space and time were examined at nearly all scales permitted by the data. Case studies in the tropics suggest that local ozone maxima may be found in or near clouds. Preliminary seasonal mean maps of ozone during spring are presented for the Northern Hemisphere in the troposphere over the United States during summer. There is a distinct midcontinental ozone maximum. There is a diurnal variation in ozone in the upper troposphere and the daily range is about 5 ppbv. Correlations between ozone and other variables are given for the synoptic-scale and on a hemispheric scale. The possible bearing of these results on ozone transport computations is discussed. Author

A78-38835* Measurement of tropospheric 300 nm solar ultraviolet flux for determination of O(1D)/photoproduction rate. B. Sellers and F. A. Hanser (Parametrics, Inc., Waltham, Mass.). *Journal of the Atmospheric Sciences*, vol. 35, May 1978, p. 912-918, 23 refs. Research supported by the Georgia Institute of Technology; NSF Grant No. ENV-76-23802; Contracts No. N00014-73-C-0318; No. NAS3-20472.

The tropospheric importance of the OH radical, and the reaction scheme that leads to its formation, are now being widely investigated. Ozone photolysis at wavelengths no greater than 318 nm produces O(1D), a small fraction of which then reacts with water vapor to yield OH. Although experimental data are available for the O(1D) quantum yield, as well as the O3 absorption cross section, all previous tropospheric photochemical models have had to use theoretical calculations to determine the UV flux. Discussed in this paper are aircraft spectral measurements of the solar UV flux at two altitudes - 2 and 6 km. These results have been compared with three

theoretical approaches. The measured experimental fluxes have been combined here with recent quantum yield data to calculate the O(1D) photoproduction rate for various albedo values. This rate is larger than that used in models by about a factor of 2 for reasonable values of assumed albedo. (Author)

A78-41788 * Experiments on whistler wave filamentation and VLF hiss in a laboratory plasma. R. L. Stenzel (TRW Defense and Space Systems Group, Redondo Beach, California, University, Los Angeles, Calif.). (*European Physical Society, IUPAP, URSI, and Société Française de Physique, International Congress on Waves and Instabilities in Plasmas, 3rd, Palaiseau, Essonne, France, June 27-July 1, 1977*) *Journal de Physique*, vol. 38, Dec. 1977, Supplement, p. C6-89 to C6-102. 33 refs. Research supported by TRW Independent Research and Development Funds; Contracts No. NAS3-1175; No. NASW-2953.

With the development of a large magnetized plasma source it has become possible to investigate space plasma physics problems in the laboratory. First, the nonlinear effects associated with the excitation of a large amplitude whistler wave have been explored. It is found that the radiation pressure of the wave and thermal effects give rise to a field-aligned density depression in which the wave becomes completely trapped. Hyperfine filaments with diameters small compared with the parallel wavelength are observed. Second, the stability of oblique whistler waves in the presence of an electron beam has been studied. A broadband whistler instability is observed and identified as a Cherenkov interaction between beam electrons and whistlers propagating near the resonance cone. These observations confirm the present model for the generation of VLF hiss in the aurora. (Author)

47 METEOROLOGY AND CLIMATOLOGY

Includes weather forecasting and modification.

N78-17558* National Aeronautics and Space Administration, Lewis Research Center, Cleveland, Ohio.

AUTOMATED METEOROLOGICAL DATA FROM COMMERCIAL AIRCRAFT VIA SATELLITE: PRESENT EXPERIENCE AND FUTURE IMPLICATIONS

Robert Steinberg 1978 7 p refs Presented at Intern. Conf. on Maritime and Aeron. Satellite Commun. and Navigation, London, 7-10 Mar. 1978; sponsored by Institution of Elec. Eng. (NASA-TM-73750; E-9323) Avail. NTIS HC A02/MF A01 CSDL 04B

A low-cost communications system to provide meteorological data from commercial aircraft, in near real-time, on a fully automated basis has been developed. The complete system including the low profile antenna and all installation hardware weighs 34 kg. The prototype system was installed on a B-747 aircraft and provided meteorological data (wind angle and velocity, temperature, altitude and position as a function of time) on a fully automated basis. The results were exceptional. This concept is expected to have important implications for operational meteorology and airline route forecasting. Author

N78-19710* National Aeronautics and Space Administration, Lewis Research Center, Cleveland, Ohio.

PHOTOVOLTAIC REMOTE INSTRUMENT APPLICATIONS: ASSESSMENT OF THE NEAR-TERM MARKET

Louis Rosenblum, Larry R. Scudder, William A. Poley, and William J. Bifano Dec. 1977 19 p refs (Contract E(49-26)-1022)

(NASA-TM-73881; DOE/NASA/1022-77/24; E-9492) Avail. NTIS HC A02/MF A01 CSDL 14B

A preliminary assessment of the near term market for photovoltaic remote instrument applications is presented. Among the potential users, two market sectors are considered: government and private. However, the majority of the remote systems studied are operated by or for the federal, state, or local governments. Environmental monitoring and surveillance remote instrument systems are discussed. Based on information obtained in this preliminary market survey, a domestic, civilian market of at least 1.3 MW sub pk is forecast for remote instrument systems. This estimate is exclusive of several potentially large scale markets for remote instruments which are identified but for which no hard data is available. Author

A78-14581* Models for some aspects of atmospheric vortices. R. G. Deissler (NASA, Lewis Research Center, Cleveland, Ohio). *Journal of the Atmospheric Sciences*, vol. 34, Oct. 1977, p. 1502-1517, 31 refs.

A frictionless adiabatic model is used to study the growth of random vortices in an atmosphere with buoyant instability and vertical wind shear, taking account of the effects of axial drag, heat transfer, and precipitation-induced downdrafts. It is found that downdrafts of tornadic magnitude may occur in negatively buoyant columns. The radial-inflow velocity required to maintain a given maximum tangential velocity in a tornado is determined by using a turbulent vortex model. A tornado model which involves a rotating parent cloud as well as buoyancy and precipitation effects is also discussed. B.J.

A78-42962* Cloud effects on middle ultraviolet global radiation. J. Borkowski (Warszawa, Uniwersytet, Warsaw, Poland), A.-T. Chai (NASA, Lewis Research Center, Cleveland, Ohio), T. Mo (NASA, Goddard Institute for Space Studies, New York, N.Y.), and A. E. O. Green (Florida, University, Gainesville, Fla.). *Acta Geophysica Polonica*, vol. 25, no. 4, 1977, p. 287-301, 16 refs. Research supported by the U.S. Department of Transportation.

An Eppley radiometer and a Robertson-Berger sunburn meter are employed along with an all-sky camera setup to study cloud effects on middle ultraviolet global radiation at the ground level. Semiempirical equations to allow for cloud effects presented in previous work are compared with the experimental data. The study suggests a means of defining eigenvectors of cloud patterns and correlating them with the radiation at the ground level. (Author)

48 OCEANOGRAPHY

Includes biological, dynamic and physical oceanography; and marine resources.

A78-47223 * Numerical computation of three-dimensional circulation in Lake Erie - A comparison of a free-surface model and a rigid-lid model. Y. P. Sheng, W. Lick (Case Western Reserve University, Cleveland, Ohio), R. T. Gedney, and F. B. Molls (NASA, Lewis Research Center, Cleveland, Ohio). *Journal of Physical Oceanography*, vol. 8, July 1978, p. 713-727. 23 refs. Research supported by the U.S. Environmental Protection Agency.

ABSTRACT OF THE PAPER PRESENTED AT THE 1978 OCEANOGRAPHY MEETING, WASHINGTON, D.C., OCTOBER 1-5, 1978. THE MEETING WAS SPONSORED BY THE NATIONAL OCEANOGRAPHIC ADMINISTRATION AND THE NATIONAL ACADEMY OF SCIENCES. THE MEETING WAS HELD AT THE NATIONAL ACADEMY OF SCIENCES, WASHINGTON, D.C.

51

51 LIFE SCIENCES (GENERAL)

Includes genetics.

N78-22618* National Aeronautics and Space Administration, Lewis Research Center, Cleveland, Ohio.

THE USE OF AN ION-BEAM SOURCE TO ALTER THE SURFACE MORPHOLOGY OF BIOLOGICAL IMPLANT MATERIALS

A. J. Weigand 1978 28 p refs Presented at Soc. for Biomater. Conf., San Antonio, 29 Apr. - 2 May 1978 (NASA-TM-78851; E-9573) Avail: NTIS HC A03/MF A01 CSCL 06C

An electron bombardment, ion thruster was used as a neutralized-ion beam sputtering source to texture the surfaces of biological implant materials. Scanning electron microscopy was used to determine surface morphology changes of all materials after ion-texturing. Electron spectroscopy for chemical analysis was used to determine the effects of ion texturing on the surface chemical composition of some polymers. Liquid contact angle data were obtained for ion textured and untextured polymer samples. Results of tensile and fatigue tests of ion-textured metal alloys are presented. Preliminary data of tissue response to ion textured surfaces of some metals, polytetrafluoroethylene, alumina, and segmented polyurethane were obtained. Author

N78-31680* National Aeronautics and Space Administration, Lewis Research Center, Cleveland, Ohio.

DIGITAL ENHANCEMENT OF COMPUTERIZED AXIAL TOMOGRAMS

Ernest Roberts, Jr. 1978 6 p refs Presented at the 5th Ann. Computers in Cardiology Conf., Stanford, Calif., 12-14 Sep. 1978; cosponsored by IEEE, NIH, and Stanford Univ. School of Med.

(NASA-TM-78974; E-9748) Avail: NTIS HC A02/MF A01 CSCL 06E

A systematic evaluation was conducted of certain digital image enhancement techniques performed in image space. Three types of images were used, computer generated phantoms, tomograms of a synthetic phantom, and axial tomograms of human anatomy containing images of lesions, artificially introduced into the tomograms. Several types of smoothing, sharpening, and histogram modification were explored. It was concluded that the most useful enhancement techniques are a selective smoothing of singular picture elements, combined with contrast manipulation. The most useful tool in applying these techniques is the gray-scale histogram. L.S.

N78-10672* Case Western Reserve Univ., Cleveland, Ohio. Dept. of Biomedical Engineering.

EFFECT OF SURFACE TEXTURE BY ION BEAM SPUTTERING ON IMPLANT BIOCOMPATIBILITY AND SOFT TISSUE ATTACHMENT Annual Report

Donald F. Gibbons Dec. 1977 15 p refs (Grant NaG-3128)

(NASA-CR-135311; AR-1) Avail: NTIS HC A02/MF A01 CSCL 06C

The objectives in this report were to use the ion beam sputtering technique to produce surface textures on polymers, metals, and ceramics. The morphology of the texture was altered by varying both the width and depth of the square pits which were formed by ion beam erosion. The width of the ribs separating the pits were defined by the mask used to produce the texture. The area of the surface containing pits varies as the width was changed. The biological parameters used to evaluate the biological response to the texture were: (1) fibrous capsule and inflammatory response in subcutaneous soft tissue; (2) strength of the mechanical attachment of the textured surface by the soft tissue; and (3) morphology of the epidermal layer interfacing the textured surface of percutaneous connectors. Because the sputter yield on teflon ribs was approximately an order of magnitude larger than any other material the majority of the measurements presented in the report were obtained with teflon. Author

52 AEROSPACE MEDICINE

Includes physiological factors; biological effects of radiation; and weightlessness.

N78-14773* National Aeronautics and Space Administration, Lewis Research Center, Cleveland, Ohio

TISSUE MACERATING INSTRUMENT Patent

Edward F. Baehr and James E. Burnett, inventors (to NASA)

Issued 6 Dec. 1977 4 p Filed 15 Apr. 1976 Supersedes

N76-23837 (14 - 14, p 1836)

(NASA-Case-LEW 12668-1; US-Patent-4,061,146;

US-Patent-Appl-SN-677353; US-Patent-Class-128-305) Avail:

US Patent Office CSCL 06B

A surgical tissue macerating and removal tool is described which has a rotating rod with a cutting member at one end and which is disposed in a tube which is then contained in an extension of the tool handle. A frusto-conical member extends into the extension at the cutter member end of the rotating rod with its small end engaging the tube. The portion of the frusto-conical member outside of the extension forms a tissue engaging member and may be cut off at an angle to the axis of the rod to form a tissue engaging edge. Apertures are provided in the extension adjacent the frusto-conical member so that treatment fluid supplied in the annular space between the tube and the extension may flow to the operative site. An aperture is provided in the frustoconical member between the extension and the tube so that fluid may also flow into the tube where it mixes with macerated tissue being directed through an aperture in the tube to a passageway which may have suction applied to help remove macerated material.

Official Gazette of the U.S. Patent Office

N78-20766*J National Aeronautics and Space Administration, Lewis Research Center, Cleveland, Ohio.

TOXIC SUBSTANCES ALERT PROGRAM

Thomas L. Junod Jan. 1978 287 p refs Revised

(NASA-TM-73866; E-9456) Avail: NTIS HC A13/MF A01

CSCL 06T

A toxicity profile is provided, of 187 toxic substances procured by NASA Lewis Research Center during a 3 1/2 year period, including 27 known or suspected carcinogens. The goal of the program is to assure that the center's health and safety personnel are aware of the procurement and use of toxic substances and to alert and inform the users of these materials as to the toxic characteristics and the control measures needed to ensure their safe use. The program also provides a continuing record of the toxic substances procured, who procured them, what other toxic substances the user has obtained in the past, and where similar materials have been used elsewhere at the center.

Author

54 MAN/SYSTEM TECHNOLOGY AND LIFE SUPPORT

Includes human engineering; biotechnology; and space suits and protective clothing.

N78-24907* National Aeronautics and Space Administration, Lewis Research Center, Cleveland, Ohio.

ESCORT: A DATA ACQUISITION AND DISPLAY SYSTEM TO SUPPORT RESEARCH TESTING

Robert L. Miller 1978 10 p Presented at Electro 1978, Boston, 23-25 May 1978; sponsored by IEEE (NASA-TM-78909; E-9644) Avail: NTIS HC A02/MF A01 CSCL 09B

Primarily designed to acquire data at steady state test conditions, the system can also monitor slow transients such as those generated in moving to a new test condition. The system configuration makes use of a microcomputer at the test site which acts as a communications multiplexer between the measurement and display devices and a centrally located minicomputer. A variety of measurement and display devices are supported using a modular approach. This allows each system to be configured with the proper combination of devices to meet the specific test requirements, while still leaving the option to add special interfaces when needed. Centralization of the minicomputer improves utilization through sharing. The creation of a pool of minis to provide data acquisition and display services to a variable number of running tests also offers other important advantages.

Author

60 COMPUTER OPERATIONS AND HARDWARE

Includes computer graphics and data processing.
For components see 33 *Electronics and Electrical Engineering*.

N78-23761* National Aeronautics and Space Administration, Lewis Research Center, Cleveland, Ohio.

A DATA ACQUISITION AND HANDLING SYSTEM FOR THE MEASUREMENT OF RADIAL PLASMA TRANSPORT RATES

W. M. Krawczonek, C. E. Boyd (Tex. Univ., Austin), J. Y. Hong (Tex. Univ., Austin), and E. J. Powers (Tex. Univ., Austin) 1977 107 p refs Presented at Symp on Eng. Aspects of Fusion Res., Knoxville, Tenn., 25-28 Oct 1977

(NASA-TM-78849) Avail: NTIS HC A06/MF A01 CSCL 09B

A system which allows the transfer of experimental data from one or more transient recorders to a digital computer. The entry of calibration data and the entry of archival data is described. The overall approach is discussed and illustrated in detail.

Author

A78-37685* # Escort - A data acquisition and display system to support research testing. R. L. Miller (NASA, Lewis Research Center, Cleveland, Ohio). *Institute of Electrical and Electronics Engineers, ELECTRO '78 Conference, Boston, Mass., May 23-25, 1978, Paper*. 10 p.

A combination of a central minicomputer and test-site microcomputers has been adopted to provide on-line data acquisition and display service for a large number of different research programs. By integrating the data acquisition and recording functions in the minicomputer/microcomputer system, rapidly updated displays of selected data in terms of engineering units may be obtained. The system described here is primarily designed for steady-state test conditions, but may also provide data on slow transients associated with changing experimental conditions. Application of the system to full-scale jet engine tests, ion thruster assessments and anechoic chamber analyses are mentioned.

J.M.B.

61 COMPUTER PROGRAMMING AND SOFTWARE

Includes computer programs, routines, and algorithms.

N78-10746* National Aeronautics and Space Administration, Lewis Research Center, Cleveland, Ohio.
USER'S GUIDE FOR SFTRAN/300
 Theodore E. Fessler and William F. Ford Oct. 1977 51 p ref
 (NASA-TP-1008; E-9264) Avail: NTIS HC A04/MF A01 CSCL 09B

Extension and improvements made to SFTRAN, a structured-programming language are discussed. This improved language is implemented as a precompiler that translates from SFTRAN to FORTRAN. The SFTRAN language and its use are described. Time-Sharing System (TSS) command procedures were implemented that eliminate the complications of dealing with extra files and processing steps which the use of a precompiler would otherwise require. These command procedures are described and their use is illustrated by examples. Author

N78-15729* National Aeronautics and Space Administration, Lewis Research Center, Cleveland, Ohio.
AN AUTOMATED PROCEDURE FOR CALCULATING SYSTEM MATRICES FOR PERTURBATION DATA GENERATED BY AN EAI PACER AND 100 HYBRID COMPUTER SYSTEM
 Edward J. Milner and Susan M. Krosel Dec. 1977 44 p
 (NASA-TM-73869; E-9485) Avail: NTIS HC A03/MF A01 CSCL 09B

Techniques are presented for determining the elements of the A, B, C, and D state variable matrices for systems simulated on an EAI Pacer 100 hybrid computer. An automated procedure systematically generates disturbance data necessary to linearize the simulation model and stores these data on a floppy disk. A separate digital program verifies this data, calculates the elements of the system matrices, and prints these matrices appropriately labeled. The partial derivatives forming the elements of the state variable matrices are approximated by finite difference calculations. Author

N78-17724* National Aeronautics and Space Administration, Lewis Research Center, Cleveland, Ohio.
COMPUTER PROGRAM FOR CALCULATION OF COMPLEX CHEMICAL EQUILIBRIUM COMPOSITIONS, ROCKET PERFORMANCE, INCIDENT AND REFLECTED SHOCKS, AND CHAPMAN-JOUQUET DETONATIONS
 Sanford Gordon and Bonnie J. McBride Mar. 1976 145 p refs Revised
 (NASA-SP-273) Avail: NTIS HC A07/MF A01 CSCL 09B

A detailed description of the equations and computer program for computations involving chemical equilibria in complex systems is given. A free-energy minimization technique is used. The program permits calculations such as (1) chemical equilibrium for assigned thermodynamic states (T,P), (H,P), (S,P), (T,V), (U,V), or (S,V), (2) theoretical rocket performance for both equilibrium and frozen compositions during expansion, (3) incident and reflected shock properties, and (4) Chapman-Jouquet detonation properties. The program considers condensed species as well as gaseous species. Author

N78-20806* National Aeronautics and Space Administration, Lewis Research Center, Cleveland, Ohio.
USER'S GUIDE TO SFTRAN/1100
 William F. Ford and Theodore E. Fessler Apr. 1978 44 p refs
 (NASA-TP-1200; E-9445) Avail: NTIS HC A03/MF A01 CSCL 09B

Extensions and improvements were made to SFTRAN, a structured programming language. This language was implemented as a precompiler that translates from SFTRAN to FORTRAN. It

was available to batch and conversational users of the UNIVAC 1100 computer system. The SFTRAN language and its use are described. In addition, conversational time-sharing system command subroutines were implemented that eliminated the complications of dealing with extra files and processing steps that the use of a precompiler would otherwise require. These command subroutines are reported, and their use is illustrated by examples. Author

N78-21791* National Aeronautics and Space Administration, Lewis Research Center, Cleveland, Ohio.
FLOWNET: A COMPUTER PROGRAM FOR CALCULATING SECONDARY FLOW CONDITIONS IN A NETWORK OF TURBOMACHINERY
 James R. Ross Mar. 1978 68 p refs
 (NASA-TM-73774; E-9579) Avail: NTIS HC A04/MF A01 CSCL 09B

The program requires the network parameters, the flow component parameters, the reservoir conditions, and the gas properties as input. It will then calculate all unknown pressures and the mass flow rate in each flow component in the network. The program can treat networks containing up to fifty flow components and twenty-five unknown network pressures. The types of flow components that can be treated are face seals, narrow slots, and pipes. The program is written in both structured FORTRAN (SFTRAN) and FORTRAN 4. The program must be run in an interactive (conversational) mode. Author

N78-20802* Boeing Computer Services, Inc., Seattle, Wash. Energy Technology Applications Div.
A SIMULATION MODEL FOR WIND ENERGY STORAGE SYSTEMS. VOLUME 1: TECHNICAL REPORT Final Report
 A. W. Warren, R. W. Edsinger, and Y. K. Chan Aug. 1977 101 p refs
 (Contracts NAS3-20385; E(49-28)-1028)
 (NASA-CR-135283; BCS-40180-1-Vol-1; CONS-038-5-1) Avail: NTIS HC A08/MF A01 CSCL 09B

A comprehensive computer program for the modeling of wind energy and storage systems utilizing any combination of five types of storage (pumped hydro, battery, thermal, flywheel and pneumatic) was developed. The level of detail of Simulation Model for Wind Energy Storage (SIMWEST) is consistent with a role of evaluating the economic feasibility as well as the general performance of wind energy systems. The software package consists of two basic programs and a library of system, environmental, and load components. The first program is a precompiler which generates computer models (in FORTRAN) of complex wind source storage application systems, from user specifications using the respective library components. The second program provides the techno-economic system analysis with the respective I/O, the integration of systems dynamics, and the iteration for conveyance of variables. SIMWEST program, as described, runs on the UNIVAC 1100 series computers. Author

N78-20803* Boeing Computer Services, Inc., Seattle, Wash.
Energy Technology Applications Div.
**A SIMULATION MODEL FOR WIND ENERGY STORAGE
SYSTEMS. VOLUME 2: OPERATION MANUAL** Final
Report

A. W. Warren, R. W. Edsinger, and J. D. Burroughs Aug. 1977
421 p refs 3 Vol.

(Contracts NAS3-20385; E(49-28)-1028)

(NASA-CR-135284; BCS-40180-2-Vol-2; CONS-0385-2) Avail:
NTIS HC A18/MF A01 CSCL 09B

A comprehensive computer program (SIMWEST) developed for the modeling of wind energy/storage systems utilizing any combination of five types of storage (pumped hydro, battery, thermal, flywheel, and pneumatic) is described. Features of the program include: a precompiler which generates computer models (in FORTRAN) of complex wind source/storage/application systems, from user specifications using the respective library components; a program which provides the techno-economic system analysis with the respective I/O the integration of system dynamics, and the iteration for conveyance of variables; and capability to evaluate economic feasibility as well as general performance of wind energy systems. The SIMWEST operation manual is presented and the usage of the SIMWEST program and the design of the library components are described. A number of example simulations intended to familiarize the user with the program's operation is given along with a listing of each SIMWEST library subroutine. Author

N78-20804* Boeing Computer Services, Inc., Seattle, Wash.
Energy Technology Applications Div.
**A SIMULATION MODEL FOR WIND ENERGY STORAGE
SYSTEMS. VOLUME 3: PROGRAM DESCRIPTIONS**
Final Report

A. W. Warren, R. W. Edsinger, and J. D. Burroughs Aug. 1977
234 p 3 Vol.

(Contracts NAS3-20385; E(49-28)-1028)

(NASA-CR-135285; BCS-40180-3-Vol-3; CONS-0385-3) Avail:
NTIS HC A11/MF A01 CSCL 09B

Program descriptions, flow charts, and program listings for the SIMWEST model generation program, the simulation program, the file maintenance program, and the printer platter program are given. Author

63 CYBERNETICS

Includes feedback and control theory.
For related information see also *64 Man/System Technology and Life Support*.

A78-23909 * Solution of transient optimization problems by using an algorithm based on nonlinear programming. F. Teren (NASA, Lewis Research Center, Cleveland, Ohio). In: Joint Automatic Control Conference, San Francisco, Calif., June 22-24, 1977, Proceedings, Volume 2. (A78-23851 08-63) New York, Institute of Electrical and Electronics Engineers, Inc., 1977, p. 1549-1560. 11 refs.

A new algorithm is presented for solution of dynamic optimization problems which are nonlinear in the state variables and linear in the control variables. It is shown that the optimal control is bang-bang. A nominal bang-bang solution is found which satisfies the system equations and constraints, and influence functions are generated which check the optimality of the solution. Nonlinear optimization (gradient search) techniques are used to find the optimal solution. The algorithm is used to find a minimum time acceleration for a turbofan engine. (Author)

64 NUMERICAL ANALYSIS

Includes iteration, difference equations, and numerical approximation.

A78-16304 * Diagonal dominance using function minimization algorithms. G. G. Laininger (Toledo, University, Toledo, Ohio). In: Multivariable technological systems; International Symposium, 4th, Fredericton, New Brunswick, Canada, July 4-8, 1977, Preprints. (A78-16301 04-63) Oxford and New York, Pergamon Press, 1977, p. 106-112. 15 refs. Contract No. NAS3-17826; Grant No. NSG-3063.

A new approach to the design of multivariable control systems using the inverse Nyquist array method is proposed. The technique utilizes a conjugate direction function minimization algorithm to achieve dominance over a specified frequency range by minimizing the ratio of the moduli of the off-diagonal terms to the moduli of the diagonal term of the inverse open loop transfer function matrix. The technique is easily implemented in either a batch or interactive computer mode and will yield diagonalization when previously suggested methods fail. The proposed method has been successfully applied to design a control system for a sixteenth order state model of the F-100 turbofan engine with three inputs. (Author)

65 STATISTICS AND PROBABILITY

Includes data sampling and smoothing; Monte Carlo method; and stochastic processes.

NTS-16736* National Aeronautics and Space Administration, Lewis Research Center, Cleveland, Ohio
CHAIN POOLING MODELING SELECTION AS DEVELOPED FOR THE STATISTICAL ANALYSIS OF A ROTOR BURST PROTECTION EXPERIMENT

Arthur G. Holms Dec 1977 60 p refs Presented at 137th Ann Meeting, of the Am Statist Assoc., Chicago, 15-18 Aug 1977

(NASA-TM-73874, E-9479) Avail NTIS HC A04/MF A01 CSCL 12A

As many as three iterated statistical model deletion procedures were considered for an experiment. Population model coefficients were chosen to simulate a saturated 2 to the 4th power experiment, having an unfavorable distribution of parameter values. Using random number studies, three model selection strategies were developed, namely, (1) a strategy to be used in anticipation of large coefficients of variation, approximately 65 percent, (2) a strategy to be used in anticipation of small coefficients of variation, 4 percent or less, and (3) a security regret strategy to be used in the absence of such prior knowledge. Author

A78-29327 * # 'Chain pooling' model selection as developed for the statistical analysis of a rotor burst protection experiment. A. G. Holms (NASA, Lewis Research Center, Cleveland, Ohio). *American Statistical Association, Annual Meeting, 137th, Chicago, Ill., Aug. 15-18, 1977, Paper*. 60 p. 18 refs.

A statistical decision procedure called chain pooling had been developed for model selection in fitting the results of a two-level fixed-effects full or fractional factorial experiment not having replication. The basic strategy included the use of one nominal level of significance for a preliminary test and a second nominal level of significance for the final test. The subject has been reexamined from the point of view of using as many as three successive statistical model deletion procedures in fitting the results of a single experiment. The investigation consisted of random number studies intended to simulate the results of a proposed aircraft turbine-engine rotor-burst-protection experiment. As a conservative approach, population model coefficients were chosen to represent a saturated 2 to the 4th power experiment with a distribution of parameter values unfavorable to the decision procedures. Three model selection strategies were developed. (Author)

66 SYSTEMS ANALYSIS

Includes mathematical modeling; network analysis; and operations research.

N78-30886* National Aeronautics and Space Administration, Lewis Research Center, Cleveland, Ohio.
PROCEDURES FOR GENERATION AND REDUCTION OF LINEAR MODELS OF A TURBOFAN ENGINE
Kurt Seldner and David S. Cwynar Aug 1978 46 p refs (NASA-TP-1261, E-9460) Avail NTIS HC A03/MFA01 CSCL 12B

A real time hybrid simulation of the Pratt & Whitney F100-PW-F100 turbofan engine was used for linear-model generation. The linear models were used to analyze the effect of disturbances about an operating point on the dynamic performance of the engine. A procedure that disturbs, samples, and records the state and control variables was developed. For large systems, such as the F100 engine, the state vector is large and may contain high-frequency information not required for control. Thus, reducing the full-state to a reduced-order model may be a practicable approach to simplifying the control design. A reduction technique was developed to generate reduced-order models. Selected linear and nonlinear output responses to exhaust-nozzle area and main-burner fuel flow disturbances are presented for comparison. Author

70 PHYSICS (GENERAL)

For geophysics see 46 Geophysics. For astrophysics see 80 Astrophysics. For solar physics see 82 Solar Physics.

N78-12848* National Aeronautics and Space Administration Lewis Research Center, Cleveland, Ohio
OPTICAL AND ELECTRICAL PROPERTIES OF ION BEAM TEXTURED KAPTON AND TEFLON
 Michael J Mirtich and James S Sovey 1977 16 p refs
 Presented at 24th Natl Vacuum Symp., Boston, 8-11 Nov. 1977; sponsored by Am Vacuum Soc
 (NASA-TM 73778, E-9329) Avail. NTIS HC A02/MF A01 CSCL 11G

An electron bombardment argon ion source was used to ion etch polyimide (Kapton) and fluorinated ethylene, FEP (Teflon). Samples of polyimide and FEP were exposed to (0.5-1.0) keV Ar ions at ion current densities of (1.0-1/8) mA/sq cm for various exposure times. Changes in the optical and electrical properties of the samples were used to characterize the exposure. Spectral reflectance and transmittance measurements were made between 0.33 and 2.16 micron m using an integrating sphere after each exposure. From these measurements, values of solar absorptance were obtained. Total emittance measurements were also recorded for some samples. Surface resistivity was used to determine changes in the electrical conductivity of the etched samples. A scanning electron microscope recorded surface structure after exposure. Spectral optical data, resistivity measurements, calculated absorptance and emittance measurements are presented along with photomicrographs of the surface structure for the various exposures to Ar ions. Author

N78-32888* Suntech, Inc., Marcus Hook, Pa
STUDY OF DYNAMIC EMISSION SPECTRA FROM LUBRICANT FILMS IN AN ELASTOHYDRODYNAMIC CONTACT USING FOURIER TRANSFORM SPECTROSCOPY
 Final Report, 1 Jan. 1978 31 Dec. 1977
 J. L. Lauer (Rensselaer Polytechnic Inst., Troy, N. Y.) 28 Aug. 1978 128 p refs
 (Contract NAS3 19758)
 (NASA-CR-158418) Avail. NTIS HC A07/MF A01 CSCL 20K

Infrared emission spectra were obtained through a diamond window from lubricating fluids in an operating sliding elastohydrodynamic contact and analyzed by comparison with static absorption spectra under similar pressures. Different loads, shear rates and temperatures were used. Most of the spectra exhibited polarization characteristics, indicating directional alignment of the lubricant in the EHD contact. Among the fluids studied were a traction fluid, an advanced ester, and their mixtures, a synthetic paraffin, a naphthenic reference fluid (N 1), both neat and containing 1 percent of p tricresyl phosphate as an anti-wear additive and a Cether. Traction properties were found to be nearly proportional to mixture composition for traction fluid and ester mixtures. The anti-wear additive reduced traction and fluid temperature under low loads but increased them under higher loads, giving rise to formation of a friction polymer. GRA

71 ACOUSTICS

Includes sound generation, transmission, and attenuation.
For noise pollution see 45 *Environment Pollution*.

N78-13853* National Aeronautics and Space Administration, Lewis Research Center, Cleveland, Ohio.
NOISE OF DEFLECTORS USED FOR FLOW ATTACHMENT WITH STOL-OTW CONFIGURATIONS
U. vonGlahn and D. Grossbeck 1977 17 p refs Presented at 94th Meeting of Acoust. Soc. Am., Miami Beach, Fla., 13-16 Dec. 1977
(NASA-TM-73809; E-9382) Avail: NTIS HC A02/MF A01 CSDL 20A

Future STOL aircraft may utilize engine-over-the-wing installations in which the exhaust nozzles are located above and separated from the upper surface of the wing. An external jet flow deflector can be used with such installations to provide flow attachment to the wing/flap surfaces for lift augmentation. Deflector noise in the flyover plane measured with several modal-scale nozzle/deflector/wing configurations is examined. The deflector-associated noise is correlated in terms of velocity and geometry parameters. The data also indicate that the effective overall sound pressure level of the deflector-associated noise peaks in the forward quadrant near 40 deg from the inlet axis.

Author

N78-13854* National Aeronautics and Space Administration, Lewis Research Center, Cleveland, Ohio.
A PARAMETRIC INVESTIGATION OF AN EXISTING SUPERSONIC RELATIVE TIP SPEED PROPELLER NOISE MODEL

James H. Dittmar Nov. 1977 25 p refs
(NASA-TM-73816; E-9405) Avail: NTIS HC A02/MF A01 CSDL 20A

A high tip speed turboprop is being considered as a future energy conservative airplane. The high tip speed of the propeller combined with the cruise speed of the airplane may result in supersonic relative flow on the propeller tips. These supersonic blade sections could generate noise that is a cabin environment problem. An existing supersonic propeller noise model was parametrically investigated to identify and evaluate the noise reduction variables. Both independent and interdependent parameter variations (constant propeller thrust) were performed. The noise reductions indicated by the independent investigation varied from sizable in the case of reducing Mach number to minimal for adjusting the thickness and loading distributions. The noise reduction possibilities of decreasing relative Mach number were further investigated during the interdependent variations. The interdependent investigation indicated that significant noise reductions could be achieved by increasing the propeller diameter and/or increasing the number of propeller blades while maintaining a constant propeller thrust. Author

N78-13855* National Aeronautics and Space Administration, Lewis Research Center, Cleveland, Ohio.
FAR-FIELD MULTIMODAL ACOUSTIC RADIATION DIRECTIVITY
Arthur V. Seale and Edward J. Rice 1977 22 p refs Presented at 94th Meeting of the Acoustical Soc. of Am., Miami Beach, Fla., 12-16 Dec. 1977
(NASA-TM-73839; E-9426) Avail: NTIS HC A02/MF A01 CSDL 20A

Approximate equations for the far field acoustic radiation patterns in the forward quadrant from a flanged circular duct were compared with exact equations for both single and multimodal excitations. The single mode comparison showed good agreement between the exact and approximate equations for the principal lobes of higher radial order modes. For lower and especially for zero radial order modes, there was some error in the angular location and decibel level of principal lobe peak pressure obtained from the approximate equation. Some agreement of sidelobes was also observed although the approximate equation was not intended to simulate the sidelobes. The

multimodal approximate summation equations consisting only of a simple function of directivity angle and an acoustic power biasing function were checked against the exact equations for several distributions of modal power and showed excellent agreement with exact equations for all cases. Although many modes contribute to the final level and shape of the directivity curve, the major contributions appear to come from the higher radial order modes. Author

N78-13856* National Aeronautics and Space Administration, Lewis Research Center, Cleveland, Ohio.
EFFECTIVENESS OF AN INLET FLOW TURBULENCE CONTROL DEVICE TO SIMULATE FLIGHT NOISE FAN IN AN ANECHOIC CHAMBER
R. P. Woodward, J. A. Wazyniak, L. M. Shaw, and M. J. MacKinnon 1977 16 p refs Presented at the 94th Meeting of the Acoust. Soc. of Am., Miami, Fla., 13-16 Dec. 1977
(NASA-TM-73855; E-9444) Avail: NTIS HC A02/MF A01 CSDL 20A

A hemispherical inlet flow control device was tested on a 50.8 cm (20-inch) diameter fan stage in the NASA-Lewis anechoic chamber. The control device used honeycomb and wire mesh to reduce turbulence intensities entering the fan. Far field acoustic power level results show about a 5 db reduction in blade passing tone and about 10 dB reduction in multiple pure tone sound power at 90% design fan speed with the inlet device in place. Hot film cross probes were inserted in the inlet to obtain data for two components of the turbulence at 65 and 90% design fan speed. Without the flow control device, the axial intensities were below 1.0%, while the circumferential intensities were almost twice this value. The inflow control device significantly reduced the circumferential turbulence intensities and also reduced the axial length scale. Author

N78-15852* National Aeronautics and Space Administration, Lewis Research Center, Cleveland, Ohio.
EBF NOISE SUPPRESSION AND AERODYNAMIC PENALTIES
D. J. McKinzie, Jr. 1978 18 p refs Presented at the 16th Aerospace Sci. Meeting, Huntsville, Ala., 16-18 Jan. 1978; Sponsored by AIAA
(NASA-TM-73823; E-9412) Avail: NTIS CSDL 20A

Acoustic tests were conducted at model scale to determine the noise produced in the flyover and sideline planes at reduced separation distances between the nozzle exhaust plane and the flaps of an under-the-wing externally blown flap configuration in its approach attitude. Tests were also made to determine the noise suppression effectiveness of two types of passive devices which were located on the jet impingement surfaces of the configuration. In addition, static aerodynamic performance data were obtained to evaluate the penalties produced by these suppression devices. Author

N78-15853* National Aeronautics and Space Administration, Lewis Research Center, Cleveland, Ohio.
OPTIMUM WALL IMPEDANCE FOR SPINNING MODES: A CORRELATION WITH MODE CUT-OFF RATIO
Edward J. Rice 1978 17 p refs Presented at the 16th Aerospace Sci. Meeting, Huntsville, Ala., 16-18 Jan. 1978; Sponsored by AIAA
(NASA-TM-73862; E-9451) Avail: NTIS HC A02/MF A01 CSDL 20A

A correlating equation relating the optimum acoustic impedance for the wall lining of a circular duct to the acoustic mode cut-off ratio, is presented. The optimum impedance was correlated with cut-off ratio because the cut-off ratio appears to be the fundamental parameter governing the propagation of sound in the duct. Modes with similar cut-off ratios respond in a similar way to the acoustic liner. The correlation is a semi-empirical expression developed from an empirical modification of an equation originally derived from sound propagation theory in a thin boundary layer. This correlating equation represents a part of a simplified liner design method, based upon modal cut-off ratio, for multimodal noise propagation. Author

N78-16786* National Aeronautics and Space Administration, Lewis Research Center, Cleveland, Ohio

PROPAGATION OF SOUND WAVES THROUGH A LINEAR SHEAR LAYER: A CLOSED FORM SOLUTION

James N. Scott 1978 16 p refs Presented at 16th Aerospace Sci. Meeting Huntsville, Ala., 16-18 Jan. 1978; sponsored by AIAA (NASA-TM-73828; E-9203) Avail: NTIS HC A02/MF A01 CSCL 20A

Closed form solutions are presented for sound propagation from a line source in or near a shear layer. The analysis was exact for all frequencies and was developed assuming a linear velocity profile in the shear layer. This assumption allowed the solution to be expressed in terms of parabolic cylinder functions. The solution is presented for a line monopole source first embedded in the uniform flow and then in the shear layer. Solutions are also discussed for certain types of dipole and quadrupole sources. Asymptotic expansions of the exact solutions for small and large values of Strouhal number gave expressions which correspond to solutions previously obtained for these limiting cases. Author

N78-22880* National Aeronautics and Space Administration, Lewis Research Center, Cleveland, Ohio

REDUCTION OF FAN NOISE IN AN ANECHOIC CHAMBER BY REDUCING CHAMBER WALL INDUCED INLET FLOW DISTURBANCES

J. H. Dittmar, M. J. Mackinnon, and R. P. Woodward 1978 20 p refs Presented at Acoust. Soc. Am. Meeting, Providence, R. I., 16-19 May 1978 (NASA-TM-78854; E-9580) Avail: NTIS HC A02/MF A01 CSCL 20A

The difference between the flight and ground static noise of turbofan engines presents a significant problem in engine noise testing. The additional noise for static testing has been attributed to inlet flow disturbances or turbulence interacting with the fan rotor. In an attempt to determine a possible source of inflow disturbances entering fans tested in the Lewis Research Center anechoic chamber, the inflow field was studied using potential flow analysis. These potential flow calculations indicated that there was substantial flow over the wall directly behind the fan inlet that could produce significant inflow disturbances. Fan noise tests were run with various extensions added to the fan inlet to move the inlet away from this backwall and thereby reduce the inlet flow disturbances. Significant noise reductions were observed with increased inlet length. Over 5 db reduction of the blade passage tone sound power level was observed between the shortest and longest inlets at 90% fan speed and the first overtone was reduced 9 db. High frequency broadband noise was also reduced. Author

N78-24897* National Aeronautics and Space Administration, Lewis Research Center, Cleveland, Ohio

ACOUSTIC EVALUATION OF A NOVEL SWEEP-ROTOR FAN

James G. Lucas, Richard P. Woodward, and Michael J. Mackinnon 1978 24 p refs Proposed for Presentation at 11th Fluid and Plasma Dyn. Conf., Seattle, 10-12 Jul. 1978; sponsored by AIAA (NASA-TM-78878; E-9612; AIAA-Paper-78-1121) Avail: NTIS HC A02/MF A01 CSCL 20A

Inlet noise and aerodynamic performance are presented for a high tip speed fan designed with rotor blade leading edge sweep that gives a subsonic component of inlet Mach number normal to the edge at all radii. The intent of the design was to minimize the generation of rotor leading edge shock waves thereby minimizing multiple pure tone noise. Sound power level and spectral comparisons are made with several high-speed fans of conventional design. Results show multiple pure tone noise at levels below those of some of the other fans and this noise was initiated at a higher tip speed. Aerodynamic performance of the fan did not meet design goals for this first build which applied conventional design procedures to the swept fan geometry. Author

N78-24886* National Aeronautics and Space Administration, Lewis Research Center, Cleveland, Ohio

THREE-DIMENSIONAL EFFECTS ON PURE TONE FAN NOISE DUE TO INFLOW DISTORTION

Hiroshi Kobayashi 1978 26 p refs Proposed for presentation at the Eleventh Fluid and Plasma Dyn. Conf., Seattle, 10-12 Jul. 1978; sponsored by AIAA (NASA-TM-78885; E-9618) Avail: NTIS HC A03/MF A01 CSCL 20A

Two dimensional, quasi three dimensional and three dimensional theories for the prediction of pure tone fan noise due to the interaction of inflow distortion with a subsonic annular blade row were studied with the aid of an unsteady three dimensional lifting surface theory. The effects of compact and noncompact source distributions on pure tone fan noise in an annular cascade were investigated. Numerical results show that the strip theory and quasi three-dimensional theory are reasonably adequate for fan noise prediction. The quasi three-dimensional method is more accurate for acoustic power and model structure prediction with an acoustic power estimation error of about plus or minus 2 db. Author

N78-28878* National Aeronautics and Space Administration, Lewis Research Center, Cleveland, Ohio

VARIATION OF FAN TONE STEADINESS FOR SEVERAL INFLOW CONDITIONS

J. R. Balombin Jul. 1978 19 p refs Presented at the 11th Fluid and Dyn. Conf., Seattle, 10-12 Jul. 1978; sponsored by AIAA (NASA-TM-78886; E-9621; AIAA-Paper-78-1119) Avail: NTIS HC A02/MF A01 CSCL 20A

An amplitude probability density function analysis technique for quantifying the degree of fan noise tone steadiness has been applied to data from a fan tested under a variety of inflow conditions. The test conditions included typical static operation, inflow control by a honeycomb/screen device and forward velocity in a wind tunnel simulating flight. The ratio of mean square sinusoidal-to-random signal content in the fundamental and second harmonic tones was found to vary by more than an order-of-magnitude. Some implications of these results concerning the nature of fan noise generation mechanisms are discussed. Author

N78-28896* National Aeronautics and Space Administration, Lewis Research Center, Cleveland, Ohio

PRELIMINARY STUDY OF THE EFFECT OF THE TURBULENT FLOW FIELD AROUND COMPLEX SURFACES ON THEIR ACOUSTIC CHARACTERISTICS

W. A. Olsen and D. Boldman 1978 32 p refs Presented at the 11th Fluid and Plasma Dyn. Conf., Seattle, 10-12 Jul. 1978; sponsored by AIAA (NASA-TM-78944; E-9691; AIAA-78-1123) Avail: NTIS HC A03/MF A01 CSCL 20A

Fundamental theories for noise generated by flow over surfaces exist for only a few simple configurations. The role of turbulence in noise generation by complex surfaces should be essentially the same as for simple configurations. Examination of simple surface theories indicates that the spatial distributions of the mean velocity and turbulence properties are sufficient to define the noise emission. Measurements of these flow properties were made for a number of simple and complex surfaces. The configurations were selected because of their acoustic characteristics are quite different. The spatial distribution of the turbulent flow properties around the complex surfaces and approximate theory are used to locate and describe the noise sources, and to qualitatively explain the varied acoustic characteristics. LS.

N78-31871* National Aeronautics and Space Administration, Lewis Research Center, Cleveland, Ohio.
CORRELATION OF COMBUSTOR ACOUSTIC POWER LEVELS INFERRED FROM INTERNAL FLUCTUATING PRESSURE MEASUREMENTS

U. H. VonGlahn 1978 26 p refs Proposed for presentation at the 96th Meeting of the Acoust. Soc. of Am., Honolulu, Hawaii, 26 Nov. - 1 Dec. 1978
 (NASA-TM-78986; E-9764) Avail: NTIS HC A03/MF A01 CSCL 20A

Combustion chamber acoustic power levels inferred from internal fluctuating pressure measurements are correlated with operating conditions and chamber geometries over a wide range. The variables include considerations of chamber design (can, annular, and reverse-flow annular) and size, number of fuel nozzles, burner staging and fuel split, airflow and heat release rates, and chamber inlet pressure and temperature levels. The correlated data include those obtained with combustion component development rigs as well as engines. (Author)

A78-20735 * Optimum wall impedance for spinning modes. A correlation with mode cut-off ratio. E. J. Rice (NASA, Lewis Research Center, V-STOL and Noise Div., Cleveland, Ohio). *American Institute of Aeronautics and Astronautics, Aerospace Sciences Meeting 16th, Huntsville, Ala., Jan. 16-18, 1978, Paper 78-193*. 10 p. 18 refs.

A correlating equation relating the optimum acoustic impedance for the wall lining of a circular duct to the acoustic mode cut-off ratio is presented and compared to exact calculations. The optimum impedance was correlated with cut-off ratio because the cut-off ratio appears to be the fundamental parameter governing the propagation of sound in the duct. Modes with similar cut-off ratios respond in a similar way to the acoustic liner. The correlating equation is useful for the design of suppressors for aircraft engine inlets having a steady mean flow with a boundary layer and spinning mode noise source excitation. The correlation is a semi-empirical expression developed from an empirical modification of an equation originally derived from sound propagation theory in a thin boundary layer. Exact calculations of the optimum wall impedance were made over a wide range of frequency parameters, boundary layer thicknesses and flow Mach numbers to develop and verify the correlation. This correlating equation represents a part of a simplified liner design method, based upon modal cut-off ratio, for multimodal noise propagation. (Author)

A78-20738 * Propagation of sound waves through a linear shear layer. A closed form solution. J. N. Scott (NASA, Lewis Research Center, Cleveland, Ohio). *American Institute of Aeronautics and Astronautics, Aerospace Sciences Meeting 16th, Huntsville, Ala., Jan. 16-18, 1978, Paper 78-196*. 15 p. 19 refs.

Closed form solutions are presented for sound propagation from a line source in or near a shear layer. The analysis is exact for all frequencies and is developed assuming a linear velocity profile in the shear layer. This assumption allows the solution to be expressed in terms of parabolic cylinder functions. The solution is presented for a line monopole source first embedded in the uniform flow and then in the shear layer. Solutions are also discussed for certain types of dipole and quadrupole sources. Asymptotic expansions of the exact solutions for small and large values of Strouhal number give expressions which correspond to solutions previously obtained for these limiting cases. (Author)

A78-20783 * EBF noise suppression and aerodynamic penalties. L. J. McKinnzie, Jr. (NASA, Lewis Research Center, Cleveland, Ohio). *American Institute of Aeronautics and Astronautics, Aerospace Sciences Meeting, 16th, Huntsville, Ala., Jan. 16-18, 1978, Paper 78-240*. 13 p. 15 refs.

Acoustic tests were conducted at model scale to determine the noise produced in the flyover and sideline planes at reduced separation distances between the nozzle exhaust plane and the flaps of an under-the-wing (UTW) externally blown flap (EBF) configuration in its approach attitude. Tests were also made to determine the noise suppression effectiveness of two types of passive devices which were located on the jet impingement surfaces of the configuration. In addition, static aerodynamic performance data were obtained to evaluate the penalties produced by these suppression devices. Broadband low frequency noise reductions were achieved by reducing the separation distance between the nozzle and flaps. However, mid and high frequency noise was produced which exceeded that of the reference configuration. Two passive noise suppression devices located on the flaps produced moderate to large noise reductions at reduced separation distances. Consideration of the static aerodynamic performance data obtained for the configurations tested suggests that specific broadband noise suppression characteristics may be obtained through a trade-off with aerodynamic performance penalties by the careful selection of suppression devices. (Author)

A78-24876 * Far-field multimodal acoustic radiation directivity. A. V. Saule and E. J. Rice (NASA, Lewis Research Center, Cleveland, Ohio). *Acoustical Society of America, Meeting, 94th, Miami Beach, Fla., Dec. 13-16, 1977, Paper 21* p. 8 refs.

A comparison is made between approximate equations for far-field acoustic radiation patterns and exact equations for single and multimodal excitations in order to determine the validity range for the approximate approach. It is found that for single-mode cases: (1) the gross behavior of the primary lobes is adequately described by the approximate equations, (2) some error is found for lower and zero radial order modes, and (3) some agreement is yielded between exact and approximate sidelobes, although the approximate equation was not intended to simulate sidelobes. Multimodal approximate equations are compared to exact equations for various distributions of modal power; for all cases excellent agreement is found. For multimodal patterns it is noted that many modes influence the final level and shape of the directivity curve, although the major contributions are from the higher radial order modes. S.C.S.

A78-31224 * Sound production in a moving stream. A. P. Dowling, J. E. Ffowcs Williams (Cambridge University, Cambridge, England), and M. E. Goldstein (NASA, Lewis Research Center, Cleveland, Ohio). *Royal Society (London), Philosophical Transactions, Series A*, vol. 288, no. 1353, Mar. 23, 1978, p. 321-349. 26 refs.

Jet noise is modeled by particle-attached quadrupoles convected with the velocity of the actual fluid but positioned near a hypothetical instability-free vortex sheet. The strength of each quadrupole is Lighthill's stress tensor per unit mass. The work of Mami (1976) has shown that this type of model agrees well with experiment, and the present work establishes some of the equivalent sources needed for an exact analogy. The instability waves of the shear layer, as they grow into turbulence, are heard as sound that builds up as a precursor of the main turbulence-driven field. The circular compact jet is examined in some detail, and it is found that when the jet is very light it can provide a waveguide in which the

effects of source activity persist for some time but eventually leak out as sound. This interaction greatly distorts the free field characteristics of the turbulent sources, so that Reynolds-stress-induced waves have an intensity that scales with the fourth power of jet velocity. (Author)

A78-37681 * # Reduction of fan noise in an anechoic chamber by reducing chamber wall induced inlet flow disturbances. J. H. Dittmar, M. J. Mackinnon, and R. P. Woodward (NASA, Lewis Research Center, Cleveland, Ohio). *Acoustical Society of America, Meeting, 95th, Providence, R.I., May 16-19, 1978, Paper*. 19 p. 11 refs.

The difference between the flight and ground static noise of turbofan engines has been identified as a significant problem in engine noise testing. The additional noise for static testing has been attributed to inlet flow disturbances or turbulence interacting with the fan rotor. In an attempt to determine a possible source of inflow disturbances entering fans tested in the Lewis Research Center anechoic chamber the inflow field was studied using potential flow analysis. These potential flow calculations indicated that there was substantial flow over the wall directly behind the fan inlet that could produce significant inflow disturbances. Fan noise tests were run with various extensions added to the fan inlet to move the inlet away from this backwall and thereby reduce the inlet flow disturbances. Significant noise reductions were observed with increased inlet length. Over 5 dB reduction of the blade passage tone sound power level was observed between the shortest and longest inlets at 90% fan speed and the first overtone was reduced 9 dB. High frequency broadband noise was also reduced. (Author)

A78-37682 * # Numerical spatial marching techniques for estimating duct attenuation and source pressure profiles. K. J. Baumeister (NASA, Lewis Research Center, Cleveland, Ohio). *Acoustical Society of America, Meeting, 95th, Providence, R.I., May 16-19, 1978, Paper*. 37 p. 27 refs.

A numerical method is developed that could predict the pressure distribution of a ducted source from far-field pressure inputs. Using an initial value formulation, the two-dimensional homogeneous Helmholtz wave equation (no steady flow) is solved using explicit marching techniques. The Von Neumann method is used to develop relationships which describe how sound frequency and grid spacing effect numerical stability. At the present time, stability considerations limit the approach to high frequency sound. Sample calculations for both hard and soft wall ducts compare favorably to known boundary value solutions. In addition, assuming that reflections in the duct are small, this initial value approach is successfully used to determine the attenuation of a straight soft wall duct. Compared to conventional finite difference or finite element boundary value approaches, the numerical marching technique is orders of magnitude shorter in computation time and required computer storage and can be easily employed in problems involving high frequency sound. (Author)

A78-41829 * # Variation of fan tone steadiness for several inflow conditions. J. R. Balombin (NASA, Lewis Research Center, Cleveland, Ohio). *American Institute of Aeronautics and Astronautics, Fluid and Plasma Dynamics Conference, 11th, Seattle, Wash., July 10-12, 1978, Paper 78-1119*. 12 p. 11 refs.

An amplitude probability density function analysis technique for quantifying the degree of fan noise tone steadiness has been applied to data from a fan tested under a variety of inflow conditions. The test conditions included typical static operation, inflow control by a honeycomb screen device and forward velocity in a wind tunnel simulating flight. The ratio of mean square sinusoidal to random signal content in the fundamental and second harmonic tones was found to vary by more than an order of magnitude. Some implications of these results concerning the nature of fan noise generation mechanisms are discussed. (Author)

A78-41830 * # Three-dimensional effects on pure tone fan noise due to inflow distortion. H. Kobayashi (NASA, Lewis Research Center, Cleveland, Ohio; National Aerospace Laboratory, Tokyo, Japan). *American Institute of Aeronautics and Astronautics, Fluid and Plasma Dynamics Conference, 11th, Seattle, Wash., July 10-12, 1978, Paper 78-1120*. 16 p. 18 refs.

A theoretical analysis of pure tone fan noise generated by inflow distortion rotor interaction is carried out with the aid of the three-dimensional unsteady lifting surface theory developed by Namba (1977, 1974). Particular attention is given to a study of the accuracy of available two-dimensional theory for the prediction of pure tone fan noise due to the interaction of inflow distortion with a subsonic annular blade row. The theoretical model considered consists of a single three-dimensional annular cascade rotating at constant angular velocity in an annular rigid-wall duct of infinite axial extent. Attention is given to the fluctuating pressure induced by a rotor blade row, the fluctuating velocity induced by it, an inflow distortion with only an axial velocity component, the determination of acoustic dipole distribution, the pure tone acoustic power, and two-dimensional theory and quasi-three-dimensional theory. G.R.

A78-41831 * # Acoustic evaluation of a novel swept-rotor fan. J. G. Lucas, R. P. Woodward, and M. J. MacKinnon (NASA, Lewis Research Center, Cleveland, Ohio). *American Institute of Aeronautics and Astronautics, Fluid and Plasma Dynamics Conference, 11th, Seattle, Wash., July 10-12, 1978, Paper 78-1121*. 13 p. 12 refs.

Inlet noise and aerodynamic performance are presented for a high tip speed fan designed with rotor blade leading edge sweep that gives a subsonic component of inlet Mach number normal to the edge at all radii. The intent of the design was to minimize the generation of rotor leading edge shock waves thereby minimizing multiple pure tone noise. Sound power level and spectral comparisons are made with several high-speed fans of conventional design. Results showed multiple pure tone noise at levels below those of some of the other fans and this noise was initiated at a higher tip speed. Aerodynamic performance of the fan did not meet design goals for this first build which applied conventional design procedures to the swept fan geometry. (Author)

A78-45129 * # Preliminary study of the effect of the turbulent flow field around complex surfaces on their acoustic characteristics. W. A. Olsen and D. Boldman (NASA, Lewis Research Center, Cleveland, Ohio). *American Institute of Aeronautics and Astronautics, Fluid and Plasma Dynamics Conference, 11th, Seattle, Wash., July 10-12, 1978, Paper 78-1123*. 32 p. 19 refs.

Fairly extensive measurements have been conducted of the turbulent flow around various surfaces as a basis for a study of the acoustic characteristics involved. In the experiments the flow from a nozzle was directed upon various two-dimensional surface configurations such as the three-flap model. A turbulent flow field description is given and an estimate of the acoustic characteristics is provided. The developed equations are based upon fundamental theories for simple configurations having simple flows. Qualitative estimates are obtained regarding the radiation pattern and the velocity power law. The effect of geometry and turbulent flow distribution on the acoustic emission from simple configurations are discussed. G.R.

N78-20920*# United Technologies Research Center, East Hartford, Conn.

A METHOD FOR CALCULATING EXTERNALLY BLOWN FLAP NOISE Final Report

Martin R. Fink Mar 1978 130 p refs

(Contract NAS3-17863)

(NASA-CR-2954; R77-911739-17)

Avail: NTIS

HC A07/MF A01 CSCL 20A

Several basic noise components were described. These components are: (1) compact lift dipoles associated with the wing and flaps, (2) trailing edge noise associated with the last trailing edge, and (3) quadrupole noise associated with the undeflected exhaust jet and the free jet located downstream of

the trailing edge. These noise components were combined to allow prediction of directivity and spectra for under the wing (UTW) slotted flaps with conventional or mixer nozzles, UTW slotless flaps, upper surface blowing (USB) slotless flaps, and engine in front of the wing slotted flaps. A digital computer program listing was given for this calculation method. Directivities and spectra calculated by this method were compared with free field data for UTW and USB configurations. The UTRC method best predicted the details of the measured noise emission, but the ANOP method best estimated the noise levels directly below these configurations. Author

N78-20821* United Technologies Research Center, East Hartford, Conn.
A METHOD FOR CALCULATING STRUT AND SPLITTER PLATE NOISE IN EXIT DUCTS: THEORY AND VERIFICATION Final Report
 Martin R. Fink Mar. 1978 81 p refs
 (Contract NAS3-17863)
 (NASA-CR-2955; R77-911739-18) Avail: NTIS
 HC A05/MF A01 CSCL 20A

Portions of a four-year analytical and experimental investigation relative to noise radiation from engine internal components in turbulent flow are summarized. Spectra measured for such airfoils over a range of chord, thickness ratio, flow velocity, and turbulence level were compared with predictions made by an available rigorous thin-airfoil analytical method. This analysis included the effects of flow compressibility and source noncompactness. Generally good agreement was obtained. This noise calculation method for isolated airfoils in turbulent flow was combined with a method for calculating transmission of sound through a subsonic exit duct and with an empirical far-field directivity shape. These three elements were checked separately and were individually shown to give close agreement with data. This combination provides a method for predicting engine internally generated aft-radiated noise from radial struts and stators, and annular splitter rings. Calculated sound power spectra, directivity, and acoustic pressure spectra were compared with the best available data. These data were for noise caused by a fan exit duct annular splitter ring, larger-chord stator blades, and turbine exit struts. Author

N78-25827* Avco Lycoming Div., Stratford, Conn.
YF 102 IN-DUCT COMBUSTOR NOISE MEASUREMENT, VOLUME 1 Final Report, 24 Jul. 1976 - 31 Aug. 1977
 Craig A. Wilson Nov. 1977 72 p refs 3 Vol.
 (Contract NAS3-20052)
 (NASA-CR-135404-Vol-1; LYC-77-56-Vol-1) Avail: NTIS
 HC A04/MF A01 CSCL 20A

The combustion chamber from a YF 102 gas turbine engine was instrumented with semi-infinite acoustic wave guide probes and installed in a test rig to complement the combustor noise test. These combustor rig tests are described and the recorded data are listed. Internal dynamic pressure level measurements were made at the same locations and at the same operating conditions of the NASA YF 102 test. In addition, the combustor was operated at various off-designed points where one parameter at a time was varied. Background noise recordings were made to determine the magnitude of facility or test rig noise present. Author

N78-25828* Avco Lycoming Div., Stratford, Conn.
YF 102 IN-DUCT COMBUSTOR NOISE MEASUREMENT, VOLUME 2 Final Report, 24 Jul. 1976 - 31 Aug. 1977
 Craig A. Wilson Nov. 1977 193 p 3 Vol.
 (Contract NAS3-20052)
 (NASA-CR-135404-Vol-2; LYC-77-56-Vol-2) Avail: NTIS
 HC A09/MF A01 CSCL 20A
 For abstract, see N78-25827.

N78-25829* Avco Lycoming Div., Stratford, Conn.
YF 102 IN-DUCT COMBUSTOR NOISE MEASUREMENT, VOLUME 3 Final Report
 Craig A. Wilson Nov. 1977 194 p 3 Vol.
 (Contract NAS3-20052)
 (NASA-CR-135404-Vol-3; LYC-77-56-Vol-3) Avail: NTIS
 HC A09/MF A01 CSCL 20A
 For abstract, see N78-25827.

N78-29867* Pratt and Whitney Aircraft Group, East Hartford, Conn. Commercial Products Div.
FLIGHT EFFECTS ON THE AERODYNAMIC AND ACOUSTIC CHARACTERISTICS OF INVERTED PROFILE COANNULAR NOZZLES, VOLUME 1 Final Report
 Hilary Kozlowski and Allan B. Packman Jun. 1978 174 p 3 Vol.
 (Contract NAS3-17866)
 (NASA-CR-135189-Vol-1; PWA-5509-Vol-1) Avail: NTIS
 HC A08/MF A01 CSCL 20A

Jet noise spectra obtained at static conditions from an acoustic wind tunnel and an outdoor facility are compared. Data curves are presented for (1) the effect of relative velocity on OASPL directivity (all configurations); (2) the effect of relative velocity on noise spectra (all configurations); (3) the effect of velocity on PNL directivity (coannular nozzle configurations); (4) nozzle exhaust plume velocity profiles; and (5) the effect of relative velocity on aerodynamic performance. A.R.H.

N78-29868* Pratt and Whitney Aircraft Group, East Hartford, Conn. Commercial Products Div.
FLIGHT EFFECTS ON THE AERODYNAMIC AND ACOUSTIC CHARACTERISTICS OF INVERTED PROFILE COANNULAR NOZZLES, VOLUME 2 Final Report
 Hilary Kozlowski and Allan B. Packman Jun. 1978 478 p 3 Vol.
 (Contract NAS3-17866)
 (NASA-CR-135189-Vol-2; PWA-5509-Vol-2) Avail: NTIS
 HC A21/MF A01 CSCL 20A

Data from the acoustic tests of the convergent reference nozzle and the 0.75 area ratio coannular nozzle are presented in tables. Data processing routines used to scale the acoustic data and to correct the data for atmospheric attenuation are included. A.R.H.

N78-29869* Pratt and Whitney Aircraft Group, East Hartford, Conn. Commercial Products Div.
FLIGHT EFFECTS ON THE AERODYNAMIC AND ACOUSTIC CHARACTERISTICS OF INVERTED PROFILE COANNULAR NOZZLES, VOLUME 3 Final Report
 Hilary Kozlowski and Allan B. Packman Jun. 1978 433 p 3 Vol.
 (Contract NAS3-17866)
 (NASA-CR-135189-Vol-3; PWA-5509-Vol-3) Avail: NTIS
 HC A19/MF A01 CSCL 20A

Acoustic data from tests of the 0.75 area ratio coannular nozzle with ejector and the 1.2 area ratio coannular are presented in tables. Aerodynamic data acquired for the four test configurations are included. A.R.H.

A78-41852 * # Calculation of far-field jet noise spectra from near-field measurements using true source location. K. K. Ahuja, B. J. Tester, and H. K. Tanna (Lockheed Georgia Co., Marietta, Ga.). *American Institute of Aeronautics and Astronautics, Fluid and Plasma Dynamics Conference, 11th, Seattle, Wash., July 10-12, 1978, Paper 78-1153.* 8 p. 10 refs. Contract No. NAS3-20050.

Jet mixing noise data at different measurement distances are compared with values calculated from the Lockheed prediction method. Although the method does not include any acoustic near-field effects, the measured and predicted results agree well where the measured data deviates from the inverse square law. It is therefore suggested that departures from the inverse square law are primarily the result of (1) the non-negligible distance between the nozzle exit plane and the true axial source location and (2) the jet mixing noise directionality, as modeled in the prediction method. Allowing for these effects, jet noise data at 8 and 96 diameters over a wide range of frequencies, angles and jet conditions are shown to collapse with reasonable accuracy. (Author)

72 ATOMIC AND MOLECULAR PHYSICS

Includes atomic structure and molecular spectra.

N78-19897* National Aeronautics and Space Administration, Lewis Research Center, Cleveland, Ohio.

ATOMIC HYDROGEN STORAGE METHOD AND APPARATUS Patent Application

John A. Woolam, inventor to (NASA) Filed 29 Sep. 1977 10 p

(NASA-Case-LEW-12081-2; US-Patent-App-SN-837794) Avail: NTIS HC A02/MF A01 CSCL 20H

Atomic hydrogen, for use as a fuel or as an explosive, is stored in the presence of a strong magnetic field in exfoliated layered compounds such as molybdenum disulfide or an elemental layer material such as graphite. The compound is maintained at liquid helium temperatures and the atomic hydrogen is collected on the surfaces of the layered compound which are exposed during delamination (exfoliation). The strong magnetic field and the low temperature combine to prevent the atoms of hydrogen from recombining to form molecules. NASA

A78-16069 * Metastable states of small rare gas crystallites. R. D. Eters (NASA, Lewis Research Center, Cleveland, Ohio; Amsterdam, Universiteit, Amsterdam, Netherlands; Colorado State University, Fort Collins, Colo.), R. Danilowicz (Utica College, Utica, N.Y.), and J. Kaelberer (TRW, Inc., Redondo Beach, Calif.). *Journal of Chemical Physics*, vol. 67, Nov. 1, 1977, p. 4145-4148, 15 refs. Grant No. NGR-06-002-159.

Metastable states of rare gas crystallites containing N atoms are investigated for N = 5, 6, 7, and 8. In particular, the stability, structures, structural transformation, and binding energy versus temperature are determined using a Monte Carlo method. The square pyramid isomer for N = 5 is found to be unstable at any finite temperature. The other metastable isomers are all found to make spontaneous transitions to the ground state if the temperature is greater than about one half that of melting. Comparisons with previous work are also made. (Author)

N78-18883* Colorado State Univ., Fort Collins. Dept. of Physics.

INDUSTRIAL ION SOURCE TECHNOLOGY Annual Report

Harold R. Kaufman Nov. 1977 181 p refs

(Grant NSG-3088)

(NASA-CR-135353) Avail: NTIS HC A08/MF A01 CSCL 20H

Plasma probe surveys were conducted in a 30-cm source to verify that the uniformity in the ion beam is the result of a corresponding uniformity in the discharge-chamber plasma. A 15 cm permanent magnet multipole ion source was designed, fabricated, and demonstrated. Procedures were investigated for texturing a variety of seed and surface materials for controlling secondary electron emission, increasing electron absorption of light, and improved attachment of biological tissue for medical implants using argon and tetrafluoromethane as the working gases. The cross section for argon-argon elastic collisions in the ion-beam energy range was calculated from interaction potentials and permits calculation of beam interaction effects that can determine system pumping requirements. The data also indicate that different optimizations of ion-beam machines will be advantageous for long and short runs, with 1 mA-hr/cm being the rough dividing line for run length. The capacity to simultaneously optimize components in an ion-beam machine for a single application, a capacity that is not evident in competitive approaches such as diode sputtering is emphasized. Author

N78-32898* Pratt and Whitney Aircraft Group, East Hartford, Conn.

FLIGHT EFFECTS ON THE AERODYNAMIC AND ACOUSTIC CHARACTERISTICS OF INVERTED PROFILE COANNULAR NOZZLES Final Report

Hilary Kozlowski and Allan B. Packman Aug. 1978 197 p refs

(Contract NAS3-17868)

(NASA-CR-3018; PWA-5501) Avail: NTIS HC A08/MF A01 CSCL 20A

The effect of forward flight on the jet noise of coannular exhaust nozzles, suitable for Variable Stream Control Engines (VSCE), was investigated in a series of wind tunnel tests. The primary stream properties were maintained constant at 300 mps and 394 K. A total of 230 acoustic data points was obtained. Force measurement tests using an unheated air supply covered the same range of tunnel speeds and nozzle pressure ratios on each of the nozzle configurations. A total of 80 points was taken. The coannular nozzle OASPL and PNL noise reductions observed statically relative to synthesized values were basically retained under simulated flight conditions. The effect of fan to primary stream area ratio on flight effects was minor. At take-off speed, the peak jet noise for a VSCE was estimated to be over 6 PNdB lower than the static noise level. High static thrust coefficients were obtained for the basic coannular nozzles, with a decay of 0.75 percent at take-off speeds. LS.

73 NUCLEAR AND HIGH-ENERGY PHYSICS

Includes elementary and nuclear particles; and reactor theory.

For space radiation see 93 *Space Radiation*.

N78-17886* National Aeronautics and Space Administration, Lewis Research Center, Cleveland, Ohio.

OPTIMIZE OUT-OF-CORE THERMIONIC ENERGY CONVERSION FOR NUCLEAR ELECTRIC PROPULSION

James F. Morris Sep. 1977 15 p refs Proposed for presentation at Intern. Conf. on Plasma Sci., Monterey, Calif., 15-17 May 1978; sponsored by IEEE

(NASA-TM-73892) Avail: NTIS HC A02/MF A01 CSCL 18E

Current designs for out of core thermionic energy conversion (TEC) to power nuclear electric propulsion (NEP) were evaluated. Approaches to improve out of core TEC are emphasized and probabilities for success are indicated. TEC gains are available with higher emitter temperatures and greater power densities. Good potentialities for accommodating external high temperature, high power density TEC with heat pipe cooled reactors exist.

Author

1978-17886*

1978-17886*

1978-17886*

1978-17886*

1978-17886*

1978-17886*

75 PLASMA PHYSICS

Includes magnetohydrodynamics and plasma fusion.
For ionospheric plasmas see 46 *Geophysics*. For space plasmas see 90 *Astrophysics*.

N78-10883* National Aeronautics and Space Administration, Lewis Research Center, Cleveland, Ohio.

INWARD TRANSPORT OF A TOROIDALLY CONFINED PLASMA SUBJECT TO STRONG RADIAL ELECTRIC FIELDS

J. Reece Roth, Walter M. Krawczonak, Edward J. Powers (Texas Univ., Austin), Joe Hong (Texas Univ., Austin), and Young Kim (Texas Univ., Austin) 1977 14 p refs Presented at Ann. Meeting of the Plasma Phys. Div. of the Am. Phys. Soc., Atlanta, 7-11 Nov. 1977

(NASA-TM-73800) Avail: NTIS HC A02/MF A01 CSCL 20I

Digitally implemented spectral analysis techniques were used to investigate the frequency-dependent fluctuation-induced particle transport across a toroidal magnetic field. When the electric field pointed radially inward, the transport was inward and a significant enhancement of the plasma density and confinement time resulted. Author

N78-10884* National Aeronautics and Space Administration, Lewis Research Center, Cleveland, Ohio.

A MODEL FOR PARTICLE CONFINEMENT IN A TOROIDAL PLASMA SUBJECT TO STRONG RADIAL ELECTRIC FIELDS

J. Reece Roth 1977 25 p refs Presented at Ann. Meeting of the Plasma Phys. Div. of the Am. Phys. Soc., Atlanta, 7-11 Nov. 1977

(NASA-TM-73814; E-9401) Avail: NTIS HC A02/MF A01 CSCL 20I

A toroidal plasma is confined and heated by the simultaneous application of strong d.c. magnetic fields and electric fields. Strong radial electric fields (about 1 kilovolt per centimeter) are imposed by biasing the plasma with up to 12 negative electrode rings which surround its minor circumference. The plasma containment is consistent with a balance of two processes, a radial infusion of ions in those sectors not containing electrode rings, resulting from the radially inward electric fields; and ion losses to the electrode rings, each of which acts as a sink and draws ions out the plasma in the manner of a Langmuir probe in the ion saturation regime. The highest density on axis which has been observed so far in this steady-state plasma is 6.2×10 to the 12th power particles per cubic centimeter, for which the particle containment time is 2.5 milliseconds. The deuterium ion kinetic temperature for these conditions was in the range of 360 to 520 eV. Author

N78-13890* National Aeronautics and Space Administration, Lewis Research Center, Cleveland, Ohio.

HIGH-TEMPERATURE, HIGH-POWER-DENSITY THERMIONIC ENERGY CONVERSION FOR SPACE

James F. Morris 23 Nov. 1977 17 p refs
(NASA-TM-73844; E-9431) Avail: NTIS HC A02/MF A01 CSCL 20I

Theoretic converter outputs and efficiencies indicate the need to consider thermionic energy conversion (TEC) with greater power densities and higher temperatures within reasonable limits for space missions. Converter-output power density, voltage, and efficiency as functions of current density were determined for 1400-to-2000 K emitters with 725-to-1000 K collectors. The results encourage utilization of TEC with hotter-than-1650 K emitters and greater-than-6W/sq cm outputs to attain better efficiencies, greater voltages, and higher waste-heat-rejection temperatures for multihundred kilowatt space-power applications. For example, 1800 K, 30 A/sq cm TEC operation for NEP compared with the 1650 K, 5 A/sq cm case should allow much lower radiation weights, substantially fewer and/or smaller emitter

heat pipes, significantly reduced reactor and shield-related weights, many fewer converters and associated current-collecting bus bars, less power conditioning, and lower transmission losses. Integration of these effects should yield considerably reduced NEP specific weights. Author

N78-18905* National Aeronautics and Space Administration, Lewis Research Center, Cleveland, Ohio.

PROBE STUDIES IN A MODIFIED PENNING DISCHARGE

Chitra Sen 1976 15 p refs Presented at 18th Ann Meeting on Plasma Phys., San Francisco, 14-18 Nov. 1976; Sponsored by Am. Phys. Soc.

(NASA-TM-X-73631; E-9128) Avail: NTIS HC A02/MF A01 CSCL 20I

The axial and radial floating potential distribution in a modified Penning discharge were studied at different values of the background pressure, discharge voltage, and magnetic field. An array of small disc probes arranged radially with their planes perpendicular to the magnetic field and movable along the axial direction was inserted in the plasma through one open end of the magnetic mirror system. Results show that depending on the operating conditions, the discharge can undergo different mode transitions in which the plasma can sustain different floating potentials in the radial as well as in the axial directions. Preliminary results of measurement, using RF probes in the modified Penning discharge plasma are also discussed. Author

N78-18906* National Aeronautics and Space Administration, Lewis Research Center, Cleveland, Ohio.

LOWER HYBRID EMISSION DIAGNOSTICS ON THE NASA LEWIS BUMPY TORUS

R. Mallavarpu 1977 14 p refs Presented at 19th Ann. Meeting of the Plasma Phys. Div. of the Am. Physical Soc., Atlanta, Ga., 7-11 Jul 1977

(NASA-TM-73858; E-9447) Avail: NTIS HC A02/MF A01 CSCL 20I

The feasibility of using RF emission near the lower hybrid frequency of the NASA Lewis Bumpy Torus plasma for diagnostic purposes is examined. The emission is detected using a spectrum analyzer and a 50 ohm miniature coaxial antenna that is sensitive to the polarization of the incoming signal. The frequency shift of the lower hybrid emission peak is monitored as a function of the background pressure, electrode voltage, electrode ring configuration and the strength of the toroidal dc magnetic field. Simultaneous measurements of the average plasma density are made with a polarization duplexing microwave interferometer. Data derived from the experiment are discussed with reference to the following: (1) the strength of the dc magnetic field in the emitting region; (2) comparison of the lower hybrid plasma density with the average plasma density, and (3) validity of the cold plasma lower hybrid resonance formula in the high density operating regime of the bumpy torus plasma. Author

N78-20869* National Aeronautics and Space Administration, Lewis Research Center, Cleveland, Ohio.

TEMPERATURE DISTRIBUTIONS OF A CESIUM-SEEDED HYDROGEN-OXYGEN SUPERSONIC FREE JET

Shih-Ying Wang and J. Martin Smith Feb. 1978 24 p refs
(NASA-TP-1182; E-9267) Avail: NTIS HC A02/MF A01 CSCL 20I

The hydrogen-oxygen plasma was generated at combustion chamber pressures ranging from 0.5 to 2.0 megapascals and for various seed ratios (1 to 10 percent). The plasma was observed as the atmospheric exhaust from a Mach 2 rocket test facility. Transverse profiles of the absolute integrated intensity were measured with the optically thin CaI lines (0.5664 and 0.5636 microns) at a range of axial positions downstream of the 5-cm-diameter combustor nozzle exit. Radial profiles of the emission coefficient were obtained from the measured transverse profiles of intensity by Abel inversion. Temperatures were then determined from the emission coefficients for conditions of local thermodynamic equilibrium using particle densities generated by a two-dimensional free jet computer program. Temperature results show the inherent effects of compression and expansion pressure waves characteristic of a free jet exiting from a supersonic nozzle. Author

N78-28823* National Aeronautics and Space Administration, Lewis Research Center, Cleveland, Ohio.
PARAMETRIC DEPENDENCE OF ION TEMPERATURE AND RELATIVE DENSITY IN THE NASA LEWIS SUMMA FACILITY

A. Snyder, M. R. Lauer, and R. W. Patch 1978 36 p refs Presented at 18th Ann. Meeting on Plasma Phys., San Francisco, 14-18 Nov. 1978; sponsored by Am. Phys. Soc. (NASA-TM-73770; E-9583) Avail: NTIS HC A03/MF A01 CSDL 201

Further hot-ion plasma experiments were conducted in the SUMMA superconducting magnetic mirror facility. A steady-state ExB plasma was formed by applying a strong radially inward dc electric field between cylindrical anodes and hollow cathodes located near the magnetic mirror maxims. Extending the use of water cooling to the hollow cathodes, in addition to the anodes, resulted in higher maximum power input to the plasma. Steady-state hydrogen plasmas with ion kinetic temperatures as high as 830 eV were produced. Functional relations were obtained empirically among the plasma current, voltage, magnetic flux density, ion temperature, and relative ion density. The functional relations were deduced by use of a multiple correlation analysis. Data were obtained for midplane magnetic fields from 0.5 to 3.37 tesla and input power up to 45 kW. Also, initial absolute electron density measurements are reported from a 90 deg Thomson scattering laser system. Author

N78-28828* National Aeronautics and Space Administration, Lewis Research Center, Cleveland, Ohio.
A FLUCTUATION-INDUCED PLASMA TRANSPORT DIAGNOSTIC BASED UPON FAST-FOURIER TRANSFORM SPECTRAL ANALYSIS

E. J. Powers (Texas Univ., Austin), Y. C. Kim (Texas Univ., Austin), J. Y. Hong (Texas Univ., Austin), J. R. Roth, and W. M. Krawczonek 1978 18 p refs Presented at the Intern. Conf. on Plasma Sci., Monterey, Calif., 15-18 May 1978; sponsored by IEEE (NASA-TM-78932; E-9675) Avail: NTIS HC A02/MF A01 CSDL 201

A diagnostic, based on fast Fourier-transform spectral analysis techniques, that provides experimental insight into the relationship between the experimentally observable spectral characteristics of the fluctuations and the fluctuation-induced plasma transport is described. The model upon which the diagnostic technique is based and its experimental implementation is discussed. Some characteristic results obtained during the course of an experimental study of fluctuation-induced transport in the electric field dominated NASA Lewis bumpy torus plasma are presented. A.R.H.

N78-28827* National Aeronautics and Space Administration, Lewis Research Center, Cleveland, Ohio.
FLUCTUATION SPECTRA IN THE NASA LEWIS BUMPY-TORUS PLASMA

Chandra M. Singh, Walter M. Krawczonek, J. Reece Roth, Jae Y. Hong, and Edward J. Powers Jun. 1978 31 p refs (NASA-TP-1257; E-8696) Avail: NTIS HC A03/MF A01 CSDL 201

The electrostatic potential fluctuation spectrum in the NASA Lewis bumpy-torus plasma was studied with capacitive probes in the low pressure (high impedance) mode and in the high pressure (low impedance) mode. Under different operating conditions, the plasma exhibited electrostatic potential fluctuations (1) at a set of discrete frequencies, (2) at a continuum of frequencies, and (3) as incoherent high-frequency turbulence. The frequencies and azimuthal wave numbers were determined from digitally implemented autopower and cross-power spectra. The azimuthal dispersion characteristics of the unstable waves were examined by varying the electrode voltage, the polarity of the voltage and the neutral background density at a constant magnetic field strength. Author

N78-27914* National Aeronautics and Space Administration, Lewis Research Center, Cleveland, Ohio.
MICROWAVE RADIATION MEASUREMENTS NEAR THE ELECTRON PLASMA FREQUENCY OF THE NASA LEWIS BUMPY TORUS PLASMA

R. Malivarpu and J. R. Roth 1978 21 p refs Presented at the meeting of the Plasma Phys. Div. of the Am. Phys. Soc., Colorado Springs, Colo., 30 Oct-3 Nov 1978 (NASA-TM 78940; E-9686) Avail: NTIS HC A02/MF A01 CSDL 201

Microwave emission near the electron plasma frequency was observed, and its relation to the average electron density and the dc toroidal magnetic field was examined. The emission was detected using a spectrum analyzer and a 50 omega miniature coaxial probe. The radiation appeared as a broad amplitude peak that shifted in frequency as the plasma parameters were varied. The observed radiation scanned an average plasma density ranging from 10 million/cu cm to 8 hundred million/cu cm. A linear relation was observed between the density calculated from the emission frequency and the average plasma density measured with a microwave interferometer. With the aid of a relative density profile measurement of the plasma, it was determined that the emissions occurred from the outer periphery of the plasma. A.R.H.

N78-30844* National Aeronautics and Space Administration, Lewis Research Center, Cleveland, Ohio.
LOW-FREQUENCY FLUCTUATION SPECTRA AND ASSOCIATED PARTICLE TRANSPORT IN THE NASA LEWIS BUMPY-TORUS PLASMA

Chandra M. Singh, Walter M. Krawczonek, J. Reece Roth, Jae Y. Hong (Texas Univ., Austin), Young C. Kim (Texas Univ., Austin), and Edward J. Powers (Texas Univ., Austin) Aug. 1978 53 p refs (NASA-TP-1258; E-9665) Avail: NTIS HC A04/MF A01 CSDL 201

The strong radial electric field associated with the Penning discharge and the strong toroidal magnetic field give rise to a diversity of E/B phenomena, such as rotating waves and spokes, which in turn manifest themselves as space-time fluctuations of the plasma density and potential. Work is done to further understand the nature and origin of the fluctuations and their connection with fluctuation-induced transport. The approach is to monitor the density and potential fluctuations, to digitize the data, and to generate, with the aid of a computer, various spectral properties by means of the fast Fourier transform. Of particular interest is the computer-generated transport spectrum that indicates in a quantitative way which fluctuation spectral components contribute to transport and which do not. All experimental measurements of the spectral characteristics of the plasma are given in absolute units rather than as relative values. Preliminary measurements of the transport spectrum of the ion population are given, and it is shown that the fluctuation induced transport is in order-of-magnitude agreement with that inferred from the steady state current flowing to the electrodes that generate the plasma. L.S.

A78-24890* Inward transport of a toroidally confined plasma subject to strong radial electric fields. J. R. Roth, W. M. Krawczonek (NASA, Lewis Research Center, Cleveland, Ohio), E. J. Powers, J. Hong, and Y. Kim (Texas University, Austin, Tex.). *American Physical Society, Annual Meeting, Atlanta, Ga., Nov. 7-11, 1977, Paper.* 13 p, 11 refs.

The paper aims at showing that the density and confinement time of a toroidal plasma can be enhanced by radial electric fields far stronger than the ambipolar values, and that, if such electric fields point into the plasma, radially inward transport can result. The investigation deals with low-frequency fluctuation induced transport using digitally implemented spectral analysis techniques and with the role of strong applied radial electric fields and weak vertical magnetic fields on plasma density and particle confinement times in a Bumpy Torus geometry. Results indicate that application of sufficiently strong radially inward electric fields results in radially inward fluctuation-induced transport into the toroidal electrostatic potential well; this inward transport gives rise to higher average electron densities and longer particle confinement times in the toroidal plasma. S.D.

A78-24891 * # A model for particle confinement in a toroidal plasma subject to strong radial electric fields. J. R. Roth (NASA, Lewis Research Center, Cleveland, Ohio). *American Physical Society, Annual Meeting, Atlanta, Ga., Nov. 7-11, 1977, Paper. 24 p. 21 refs.*

The approach adopted in the NASA Lewis Bumpy Torus experiment is to confine and heat a toroidal plasma by the simultaneous application of strong dc magnetic fields and electric fields. Strong radial electric fields (about 1 kV/cm) are imposed by biasing the plasma with up to 12 negative electrode rings which surround its minor circumference. The plasma containment is consistent with a balance of two processes: a radial infusion of ions in those sectors not containing electrode rings, resulting from the radially inward electric fields; and ion losses to the electrode rings, each of which acts as a sink and draws ions out the plasma in the manner of a Langmuir probe in the ion saturation regime. The highest density on axis which has been observed so far in this steady-state plasma is 6.2 trillion particles per cu cm, for which the particle containment time is 2.5 msec. The deuterium ion kinetic temperature for these conditions was in the range of 360 to 520 eV. (Author)

A78-24904 * # Probe studies in a modified Penning discharge. C. Sen (NASA, Lewis Research Center, Cleveland, Ohio). *American Physical Society, Annual Meeting on Plasma Physics, 18th, San Francisco, Calif., Nov. 14-18, 1976, Paper. 14 p. 16 refs.*

The axial and radial floating potential distribution in a modified Penning discharge have been studied at different values of the background pressure, discharge voltage, and magnetic field. An array of small disc probes arranged radially with their planes perpendicular to the magnetic field and movable along the axial direction was inserted in the plasma through one open end of the magnetic mirror system. Results show that depending on the operating conditions, the discharge can undergo different mode transitions in which the plasma can sustain different floating potentials in the radial as well as in the axial directions. Preliminary results of measurement, using RF probes in the modified Penning discharge plasma are also discussed. (Author)

A78-28332 * # Lower hybrid emission diagnostics on the NASA Lewis Bumpy Torus. R. Mallavarpu (NASA, Lewis Research Center, Cleveland, Ohio). *American Physical Society, Annual Meeting, 19th, Atlanta, Ga., July 7-11, 1977, Paper. 13 p.*

The feasibility of using RF emission near the lower-hybrid frequency of the NASA Lewis Bumpy Torus plasma for diagnostic purposes is examined. The emission is detected using a spectrum analyzer and a 50-ohm miniature coaxial antenna that is sensitive to the polarization of the incoming signal. The frequency shift of the lower-hybrid emission peak is monitored as a function of the background pressure, electrode voltage, electrode ring configuration, and the strength of the toroidal dc magnetic field. Simultaneous measurements of the average plasma density are made with a polarization diplexing microwave interferometer. The experimental results extend previous work to include negative electrode voltages and plasma densities up to 1 trillion per cu cm. The information derived from the experiment is discussed with reference to: (1) the strength of the dc magnetic field in the emitting region, (2) a comparison of the lower-hybrid plasma density with the average plasma density, and (3) the validity of the cold-plasma lower-hybrid resonance formula in the high-density operating regime of the bumpy-torus plasma. (Author)

A78-34631 * Preliminary results on the conversion of laser energy into electricity. R. W. Thompson, E. J. Manista, and D. L. Alger (NASA, Lewis Research Center, Cleveland, Ohio). *Applied Physics Letters*, vol. 32, May 15, 1978, p. 610, 611. 11 refs.

A preliminary experiment was performed to investigate conversion of 10.6 micron laser energy to electrical energy via a laser-sustained argon plasma. Short-circuit currents of 0.7 A were measured between a thoriated-tungsten emitter and collector

electrodes immersed in the laser-sustained argon plasma. Open-circuit voltages of about 1.5 V were inferred from the current-voltage load characteristics. The dominant mechanism of laser energy conversion is uncertain at this time. Much higher output powers appear possible. (Author)

A78-36966 * Effects of applied dc radial electric fields on particle transport in a bumpy torus plasma. J. R. Roth (NASA, Lewis Research Center, Cleveland, Ohio). *IEEE Transactions on Plasma Science*, vol. PS-6, June 1978, p. 158-165. 22 refs.

The influence of applied dc radial electric fields on particle transport in a bumpy torus plasma is studied. The plasma, magnetic field, and ion heating mechanism are operated in steady state. Ion kinetic temperature is more than a factor of ten higher than electron temperature. The electric fields raise the ions to energies on the order of kilovolts and then point radially inward or outward. Plasma number density profiles are flat or triangular across the plasma diameter. It is suggested that the radial transport processes are nondiffusional and dominated by strong radial electric fields. These characteristics are caused by the absence of a second derivative in the density profile and the flat electron temperature profiles. If the electric field acting on the minor radius of the toroidal plasma points inward, plasma number density and confinement time are increased. S.C.S.

A78-37679 * # Parametric dependence of ion temperature and relative density in the NASA Lewis SUMMA facility. A. Snyder, M. R. Lauver, and R. W. Patch (NASA, Lewis Research Center, Cleveland, Ohio). *American Physical Society, Annual Meeting on Plasma Physics, 18th, San Francisco, Calif., Nov. 14-18, 1976, Paper. 35 p. 18 refs.*

Further hot-ion plasma experiments were conducted in the SUMMA superconducting magnetic mirror facility. A steady-state plasma with mutually perpendicular magnetic and electric fields was formed by applying a strong radially inward dc electric field between cylindrical anodes and hollow cathodes located near the magnetic mirror maxima. Extending the use of water cooling to the hollow cathodes, in addition to the anodes, resulted in higher maximum power input to the plasma. Steady-state hydrogen plasmas with ion kinetic temperatures as high as 830 eV were produced. Functional relations were obtained empirically among the plasma current, voltage, magnetic flux density, ion temperature, and relative ion density. The functional relations were deduced by use of a multiple correlation analysis. Data were obtained for midplane magnetic fields from 0.5 to 3.37 tesla and input power up to 45 kW. Also, initial absolute electron density measurements are reported from a 90 deg Thomson scattering laser system. (Author)

A78-39835 * A hollow cathode hydrogen ion source. J. S. Sovey and M. J. Mirtich (NASA, Lewis Research Center, Cleveland, Ohio). In: *Symposium on Engineering Problems of Fusion Research*, 7th, Knoxville, Tenn., October 25-28, 1977, Proceedings Volume 1. (A78-39783 17-75) Piscataway, N.J., Institute of Electrical and Electronics Engineers, Inc., 1977, p. 315-321. 18 refs.

High current density ion sources have been used to heat plasmas in controlled thermonuclear reaction experiments. High beam currents imply relatively high emission currents from cathodes which have generally taken the form of tungsten filaments. This paper describes a hydrogen ion source which was primarily developed to assess the emission current capability and design requirements for hollow cathodes for application in neutral injection devices. The hydrogen source produced ions by electron bombardment via a single hollow cathode. Source design followed mercury ion thruster technology, using a weak magnetic field to enhance ionization efficiency. A 1.3 cm diam hollow cathode using a low work function material dispenser performed satisfactorily over a discharge current range of 10-80 A. Cylindrical probe measurements taken without ion extraction indicate maximum ion number densities on the order of 10 trillion/cu cm. Discharge durations ranged from 30 sec to

continuous operation. Tests with beam extraction at 2.5 keV and 30 A discharge current yield average ion beam current densities of 0.1 A/sq cm over a 5-cm extraction diameter. Results of this study can be used to supply the baseline information needed to scale hollow cathodes for operation at discharge currents of hundreds of amperes using distributed cathodes. (Author)

A78-46189 * Model for interpreting Doppler broadened optical line emission measurements on axially symmetric plasma. G. W. Englert, R. W. Patch, and J. J. Reinmann (NASA, Lewis Research Center, Cleveland, Ohio). *Plasma Physics*, vol. 20, May 1978, p. 451-473. 19 refs.

A plasma model, previously developed to interpret neutral-particle analyzer measurements on E x B heating devices, is adapted to analyze Doppler broadened charge-exchange neutral lines measured by an optical monochromator. Comparison of theoretical with experimental results indicates that azimuthal drift as well as cyclotron motion are quite influential in determining line shapes and widths, and thus important in temperature determination, even when the monochromator line of sight is intersecting the plasma axis of symmetry. At this central sighting position, however, results are quite insensitive to radial ion density distribution when time lag between the charge-exchange excitation events and emission is neglected. Line shapes and widths obtained by sighting across chords of plasma at various distances from the plasma axis of symmetry indicate a strong dependence on time lag. (Author)

A78-52146 * Alternative approaches to plasma confinement. J. R. Roth (NASA, Lewis Research Center, Cleveland, Ohio). *IEEE Transactions on Plasma Science*, vol. PS-6, Sept. 1978, p. 270-295. 78 refs.

The paper discusses 20 plasma confinement schemes each representing an alternative to the tokamak fusion reactor. Attention is given to: (1) tokamak like devices (TORMAC, Topolotron, and the Extrap concept), (2) stellarator like devices (Torsatron and twisted coil stellarators), (3) mirror machines (Astron and reversed field devices, the 2XII B experiment, laser heated solenoids, the LITE experiment, the Kaktus-Surmac concept), (4) bumpy tori (hot electron bumpy torus, toroidal minimum B configurations), (5) electrostatically assisted confinement (electrostatically stuffed cusps and mirrors, electrostatically assisted toroidal confinement), (6) the Migma concept, and (7) wall confined plasmas. The plasma parameters of the devices are presented and the advantages and disadvantages of each are listed. S.C.S.

A78-33143 * * Design and calculated performance and cost of the ECAS Phase II open cycle MHD power generation system. L. P. Harris (General Electric Co., Schenectady, N.Y.). *American Society of Mechanical Engineers, Winter Annual Meeting, Atlanta, Ga., Nov. 27-Dec 2, 1977, Paper 77-WA/Ener 5*. 12 p. Members, \$1.50; nonmembers, \$3.00. ERDA-NSF-sponsored research; Contract No. NAS3-19406.

A 2000 MWe MHD/steam plant for central station applications has been designed and costed as part of the Energy Conversion Alternatives Study (ECAS). This plant is fueled by Illinois No. 6 coal, rejects heat through mechanical draft wet cooling towers, and includes coal processing equipment, seed reprocessing, electrical inversion of the MHD generator output and emission controls to current EPA standards. It yields an estimated overall efficiency of 0.483 (7066 Btu/kWe-hr), a capital cost of \$718 per kWe (1975 dollars), and a cost of electricity at 65% capacity factor of 32 mills per kWe-hr. If the assumed life and reliability could be achieved with these performance parameters, the MHD system should prove attractive. (Author)

76 SOLID-STATE PHYSICS

Includes superconductivity.
For related information see also 33 Electronics and Electrical Engineering and 36 Lasers and Masers.

A78-13010* National Aeronautics and Space Administration, Lewis Research Center, Cleveland, Ohio
CRYSTAL FIELD AND MAGNETIC PROPERTIES
D. J. Flood 1977 12 p refs Presented at 23d Ann Conf on Magnetism and Magnetic Materials, Minneapolis, Minn., 8-11 Nov 1977; sponsored by Am. Inst of Physics and IEEE (NASA-TM-73837; E-9330) Avail: NTIS HC A02/MF A01 CSCL 208

Magnetization and magnetic susceptibility measurements have been made in the temperature range 1.3 to 4.2 K on powdered samples of ErH₃. The susceptibility exhibits Curie-Weiss behavior from 4.2 to 2 K, and intercepts the negative temperature axis at theta = 1.05 + or - 0.05 K, indicating that the material is antiferromagnetic. The low field effective moment is 6.77 + or - 0.27 Bohr magnetons per ion. The magnetization exhibits a temperature independent contribution, the slope of which is (5 + or - 1.2) x 10 to the 6th Weber m/kg Tesla. The saturation moment is 3.84 + or - 0.15 Bohr magnetons per ion. The results can be qualitatively explained by the effects of crystal fields on the magnetic ions. No definitive assignment of a crystal field ground state can be given, nor can a clear choice between cubically or hexagonally symmetric crystal fields be made. For hexagonal symmetry, the first excited state is estimated to be 86 to 100 K above the ground state. For cubic symmetry, the splitting is on the order of 160 to 180 K. Author

A78-14423* Upper limit for magnetoresistance in silicon bronze and phosphor bronze wire. R. Feldman, L. Talley, M. Rojeski, T. Vold (Oberlin College, Oberlin, Ohio), and J. A. Woollam (NASA, Lewis Research Center, Cleveland, Ohio). *Cryogenics*, vol. 17, Jan. 1977, p. 31, 32, 10 refs.

The electrical resistivity of silicon bronze and phosphor bronze was measured in magnetic fields from 0 to 14 T and at temperatures between 2 and 300 K. At any fixed temperature, the change in resistivity to 14 T was less than a few parts in 100,000. Thus, these bronzes are excellent for use in high magnetic fields where constant resistance is required. Welding leads to the sample was found to be superior to soldering. The soldered contacts were subject to spurious resistivity changes that resulted from superconducting transitions in the solder. (Author)

A78-24917* Crystal field and magnetic properties of ErH₃. D. J. Flood (NASA, Lewis Research Center, Cleveland, Ohio). *American Institute of Physics and Institute of Electrical and Electronics Engineers, Annual Conference on Magnetism and Magnetic Materials, 23rd, Minneapolis, Minn., Nov. 8-11, 1977, Paper, 11 p, 6 refs.*

Magnetization and magnetic susceptibility measurements have been made in the temperature range 1.3 to 4.2 K on powdered samples of ErH₃. The susceptibility exhibits Curie-Weiss behavior from 4.2 to 2 K, and intercepts the negative temperature axis at 1.05 + or - 0.05 K, indicating that the material is antiferromagnetic. The low field effective moment is 6.77 + or - 0.27 Bohr magnetons per ion. The magnetization exhibits a temperature independent contribution, the slope of which is (5 + or - 1.2) times 10 to the minus 6 Weber m/kg Tesla. The saturation moment is 3.84 + or - 0.15 Bohr magnetons per ion. The results can be qualitatively explained by the effects of crystal fields on the magnetic ions. No definitive assignment of a crystal field ground state can be given, nor can a clear choice between cubically or hexagonally symmetric crystal fields be made. For hexagonal symmetry, the first excited state is estimated to be 86 to 100 K above the ground state. For cubic symmetry, the splitting is of the order of 160 to 180 K. (Author)

A78-27727* Physics and chemistry of MoS₂ intercalation compounds. J. A. Woollam (NASA, Lewis Research Center, Cleveland, Ohio) and R. B. Somoano (California Institute of Technology, Jet Propulsion Laboratory, Pasadena, Calif.). *Materials Science and Engineering*, vol. 31, Dec. 1977, p. 289-296, 27 refs.

An investigation is made of the physics and chemistry of MoS₂ intercalation compounds. These compounds may be separated into two groups according to their stoichiometry, structure and superconducting properties. The first group consists of Na, Ca, and Sr intercalates, and the second group consists of K, Rb, and Cs intercalates. Particular attention is given to the structure of the electronic energy band and to the normal state and superconducting properties of these compounds. S.C.S.

A78-45368* Critical currents in sputtered PbMo6S8. S. A. Alterovitz, J. A. Woollam (NASA, Lewis Research Center, Cleveland, Ohio), L. Kammerdiner, and H. L. Luo (California, University, La Jolla, Calif.). *Applied Physics Letters*, vol. 33, Aug. 1, 1978, p. 284-286, 12 refs. NSF-supported research.

Critical currents in sputtered Chevrel-phase lead molybdenum sulfide have been measured at several temperatures as a function of applied magnetic field up to 19 T. A critical current density of approximately 50 million A/sq m was obtained at 15 T and 1.8 K, and the effective upper critical field was estimated to be 30 T. The pinning force at low fields was found to be dependent on the amount of free lead. (Author)

A78-45500* Critical currents and scaling laws in sputtered copper molybdenum sulfide. S. A. Alterovitz, J. A. Woollam (NASA, Lewis Research Center, Cleveland, Ohio), L. Kammerdiner, and H. L. Luo (California, University, La Jolla, Calif.). *Journal of Low Temperature Physics*, vol. 30, no. 5-6, 1978, p. 797-812, 25 refs. Grant No. NSG-3103.

A78-53626* Upper critical field of copper molybdenum sulfide. S. A. Alterovitz and J. A. Woollam (NASA, Lewis Research Center, Cleveland, Ohio). *Solid-State Communications*, vol. 25, no. 2, 1978, p. 141-144, 18 refs.

The upper critical field of sintered and sputtered copper molybdenum sulfide Cu(x)Mo6S8 was measured and found to exceed the Werthamer, Helfand, and Hohenberg (1966) value for a type II superconductor characterized by dirty limit, weak isotropic electron-phonon coupling, and no paramagnetic limiting. It is suggested that the enhancement results from anisotropy or clean limit or both. Other ternary molybdenum sulfides appear to show similar anomalies. M.L.

A78-41922* Superconducting Nb3Ge for high field magnets. A. I. Braginski, M. R. Daniel, C. W. Roland (Westinghouse Research and Development Center, Pittsburgh, Pa.), and J. A. Woollam (NASA, Lewis Research Center, Cleveland, Ohio). *Institute of Electrical and Electronics Engineers, International Magnetism Conference, Florence, Italy, May 9-12, 1978, Paper, 3 p, 15 refs. Contract No. F44620-74-C-0042, No. NAS3-20233*

Superconducting Nb3Ge tape conductors 5 to 10 m long were fabricated by chemical vapor deposition. Such tapes could be used in high field magnet applications. Average tape properties set the upper performance limit of a magnet at 17 teslas (4.2 K). Highest critical current densities obtained in thin and layered films set the upper performance limit at 20 teslas (4.2 K). (Author)

81 ADMINISTRATION AND MANAGEMENT

Includes management planning and research.

NTB-13838* National Aeronautics and Space Administration,
Lewis Research Center, Cleveland, Ohio

THE MINE PROJECT: MINORITY INVOLVEMENT IN NASA ENGINEERING

Harrison Allen, Jr. 1977 8 p Presented at 48th Ann. Meeting
of the Natl. Technical Assoc., Inc., Hampton, Va., 2-5 Aug
1977

(NASA-TM-73811; E-9397) Avail: NTIS HC A02/MF A01
CSCL 05A

The Mine Project developed by Lewis Research Center (LRC) along with Tennessee State University and Tuskegee Institute, is described. The project calls for LRC to assemble on-going NASA university affairs programs aimed at benefiting the school, its faculty, and its student body. The schools receive grants to pursue research and technology projects that are relevant to NASA's missions. Upon request from the universities, LRC furnishes instructors and lecturers. The schools have use of surplus government equipment and access to NASA research facilities for certain projects. Both the faculty and students of the universities are eligible for summer employment at LRC through special programs. The MINE Project is designed to establish a continuing active relationship of 3 to 5 years between NASA and the universities, and will afford LRC with an opportunity to increase its recruitment of minority and women employees.

Author

82 DOCUMENTATION AND INFORMATION SCIENCE

Includes information storage and retrieval technology; micrography; and library science.

For computer documentation see 61 *Computer Programming and Software*.

N78-17921* + National Aeronautics and Space Administration, Lewis Research Center, Cleveland, Ohio.

BIBLIOGRAPHY OF LEWIS RESEARCH CENTER TECHNICAL CONTRIBUTIONS ANNOUNCED IN 1976

Dec. 1977 192 p

(NASA-TM-73860; E-9449) Avail: NTIS HC A09 CSCL 05B

Abstracts of Lewis authored publications and publications resulting from Lewis managed contracts which were announced in the 1976 issues of STAR (Scientific and Technical Aerospace Reports) and IAA (International Aerospace Abstracts) are presented. Research reports, journal articles, conference presentations, patents and patent applications, and theses are included. The arrangement is by NASA subject category. Citations indicate report literature (identified by their N-numbers) and the journal and conference presentations (identified by their A-numbers). A grouping of indexes helps locate specific publications by author (including contractor authors), contractor organization, contract number, and report number. Author

N78-28986* / National Aeronautics and Space Administration, Lewis Research Center, Cleveland, Ohio.

BIBLIOGRAPHY OF LEWIS RESEARCH CENTER TECHNICAL PUBLICATIONS ANNOUNCED IN 1977

Washington May 1978 348 p

(NASA-TM-78918; E-9449-2) Avail: NTIS HC A15/MF A01 CSCL 05B

This compilation of abstracts describes and indexes over 780 technical reports resulting from the scientific and engineering work performed and managed by the Lewis Research Center in 1977. All the publications were announced in the 1977 issues of STAR (Scientific and Technical Aerospace Reports) and/or IAA (International Aerospace Abstracts). Documents cited include technical reports, journal articles, conference presentations, patents and patent applications, and theses. A.R.H.

85 URBAN TECHNOLOGY AND TRANSPORTATION

Includes applications of space technology to urban problems; technology transfer; technology assessment; and surface and mass transportation.

For related information see *03 Air Transportation and Safety*, *16 Space Transportation*, and *44 Energy Production and Conversion*.

N78-18828* National Aeronautics and Space Administration, Lewis Research Center, Cleveland, Ohio.

BASELINE TESTS OF THE C. H. WATERMAN RENAULT 5 ELECTRIC PASSENGER VEHICLE

Noel B. Sargent, Edward F. McBrien, and Ralph Slavik Oct. 1977 58 p refs

(Contract EC-77-A-31-1011)

(NASA-TM-73759; E-9434; CONS/1011-4) Avail: NTIS HC A04/MF A01 CSCL 13F

The Waterman vehicle, a four passenger Renault 5 GTL, performance test results are presented and characterized the state-of-the-art of electric vehicles. It was powered by sixteen 6-volt traction batteries through a two-step contactor controller actuated by a foot throttle to change the voltage applied to the 6.7 kilowatt motor. The motor output shaft was connected to a front-wheel-drive transaxle that contains a four-speed manual transmission and clutch. The braking system was a conventional hydraulic braking system. Author

N78-17933* National Aeronautics and Space Administration, Lewis Research Center, Cleveland, Ohio.

BASELINE TESTS OF THE AM GENERAL DJ-5E ELECTRUCK ELECTRIC DELIVERY VAN

Miles O. Dustin, Henry B. Tryon, and Noel B. Sargent Oct. 1977 45 p refs

(Contract EC-77-A-31-1011)

(NASA-TM-73758; E-9383; CONS/1011-3) Avail: NTIS HC A03/MF A01 CSCL 13F

An electric quarter ton truck designed for use as a postal delivery vehicle was tested to characterize the state of the art of electric vehicles. Vehicle performance test results are presented. It is powered by a single-module, 54 volt industrial battery through a silicon controlled rectifier continuously adjustable controller with regenerative braking applied to a direct current compound wound motor. Author

N78-17934* National Aeronautics and Space Administration, Lewis Research Center, Cleveland, Ohio.

BASELINE TESTS OF THE ZAGATO ELCAR ELECTRIC PASSENGER VEHICLE

Noel B. Sargent, Edward A. Maslowski, Ralph J. Slavick, and Richard F. Soltis Oct. 1977 36 p refs

(Contract EC-77-A-31-1011)

(NASA-TM-73764; CONS/1011-9; E-9442) Avail: NTIS HC A03/MF A01 CSCL 13F

The Elcar vehicle performance test results are presented. The Elcar Model 2000 is a two passenger vehicle with a reinforced fiberglass body. It is powered by eight 12-volt batteries. The batteries are connected to the motor through an arrangement of contactors operated from a foot pedal in conjunction with a hand-operated switch. These contactors change the voltage applied to the 2-kilowatt motor. Acceleration tests, operating characteristics, and instrumentation are described. Author

N78-17935* National Aeronautics and Space Administration, Lewis Research Center, Cleveland, Ohio.

PHOTOVOLTAIC HIGHWAY APPLICATIONS: ASSESSMENT OF THE NEAR-TERM MARKET

Louis Rosenblum, Larry R. Scudder, William J. Bifano, and William A. Poley Dec. 1977 12 p ref

(Contract E(49-26)-1022)

(NASA-TM-73863; DOE/NASA/1022-77/22; E-9452) Avail: NTIS HC A02/MF A01 CSCL 05B

A preliminary assessment of the near-term market for photovoltaic highway applications is presented. Among the potential users, two market sectors are considered: government and commercial. Within these sectors, two possible application areas, signs and motorist aids, are discussed. Based on judgemental information, obtained by a brief survey of representatives of the two user sectors, the government sector appears more amenable to the introduction of photovoltaic power sources for highway applications in the near-term. However, considerable interest and potential opportunities were also found to exist in the commercial sector. Further studies to quantify the market for highway applications appear warranted. Author

N78-17936* National Aeronautics and Space Administration, Lewis Research Center, Cleveland, Ohio.

BASELINE TESTS OF THE POWER-TRAIN ELECTRIC DELIVERY VAN

Stacy Lumannick, Miles O. Dustin, and John M. Bozek Nov. 1977 60 p

(Contract EC-77-A-31-1011)

(NASA-TM-73765; E-9470; CONS/1011-10) Avail: NTIS HC A04/MF A01 CSCL 13F

Vehicle maximum speed, range at constant speed, range over stop-and-go driving schedules, maximum acceleration, gradeability, gradeability limit, road energy consumption, road power, indicated energy consumption, braking capability, battery charger efficiency, and battery characteristics were determined for a modified utility van powered by sixteen 6-volt batteries connected in series. A chopper controller actuated by a foot accelerator pedal changes the voltage applied to the 22-kilowatt (30-hp) series-wound drive motor. In addition to the conventional hydraulic braking system, the vehicle has hydraulic regenerative braking. Cycle tests and acceleration tests were conducted with and without hydraulic regeneration. Author

N78-17937* National Aeronautics and Space Administration, Lewis Research Center, Cleveland, Ohio.

TEST AND EVALUATION OF 23 ELECTRIC VEHICLES FOR STATE-OF-THE-ART ASSESSMENT

Miles O. Dustin and Robert J. Denington 3 Mar. 1978 24 p refs Presented at the 1978 SAE Congr., Detroit, Mich., 27 Feb. - 3 Mar. 1978

(Contract EC-77-A-31-1011)

(NASA-TM-73850; E-9438; CONS/1011-21) Avail: NTIS HC A02/MF A01 CSCL 13F

Eleven of the electric vehicles were passenger cars and 12 were commercial vans. Tests were conducted in accordance with an ERDS test procedure which is based on the SAE J227a Test Procedure. Tests included range, acceleration, coast-down, and braking. The results of the tests are presented, and comments on reliability are made. Author

N78-17938* National Aeronautics and Space Administration, Lewis Research Center, Cleveland, Ohio.

BASELINE TESTS OF THE EVA CHANGE-OF-PACE COUPE ELECTRIC PASSENGER VEHICLE

John M. Bozek, Edward A. Maslowski, and Miles O. Dustin Nov. 1977 53 p refs

(Contract EC-77-A-31-1011)

(NASA-TM-73763; E-9469; CONS/1011-8) Avail: NTIS HC A04/MF A01 CSCL 13F

The EVA Change-of-Pace Coupe is an electric passenger vehicle, to characterize the state-of-the-art of electric vehicles. The EVA Change-of-Pace Coupe is a four passenger sedan that has been converted to an electric vehicle. It is powered by twenty 6 volt traction batteries through a silicon controlled rectifier chopper controller actuated by a foot throttle to change the voltage applied to the series wound, direct current motor. Braking is accomplished with a vacuum assist hydraulic braking system. Regenerative braking is also provided. Author

N78-17929* National Aeronautics and Space Administration.
Lewis Research Center, Cleveland, Ohio.
**BASLINE TESTS OF THE EVA CONTACTOR ELECTRIC
PASSENGER VEHICLE**

John M. Bozek, Henry B. Tryon, and Ralph J. Slavick Nov.
1977 57 p refs

(Contract EC-77-A-31-1011)

(NASA-TM-73762; E-9481; CONS/1011-7) Avail: NTIS
HC A04/MF A01 CSCL 13F

The EVA Contactor four door sedan, an electric passenger vehicle, was tested to characterize the state-of-the-art of electric vehicles. It is a four passenger sedan that was converted to an electric vehicle. It is powered by 16 series connected 6 volt electric vehicle batteries through a four step contactor controller actuated by a foot accelerator pedal. The controller changes the voltage applied to a separately excited DC motor. The braking system is a vacuum assisted hydraulic braking system. Regenerative braking is provided. Author

N78-17960* National Aeronautics and Space Administration.
Lewis Research Center, Cleveland, Ohio.
**BASLINE TESTS OF THE BATTRONIC MINIVAN ELECTRIC
DELIVERY VAN**

Miles O. Dustin, Richard F. Soltis, John M. Bozek, and Edward
A. Maszkowski Dec. 1977 52 p refs

(Contract EC-77-A-31-1011)

(NASA-TM-73781; E-9483; CONS/1011-8) Avail: NTIS
HC A04/MF A01 CSCL 13F

An electric passenger vehicle was tested to develop data characterizing the state of the art of electric and hybrid vehicles. The test measured vehicle maximum speed, range at constant speed, range over stop-and-go driving schedules, maximum acceleration, gradeability and limit, road energy consumption, road power, indicated energy consumption, braking capability and battery charge efficiency. The data obtained are to serve as a baseline to compare improvements in electric and hybrid vehicle technologies and to assist in establishing performance standards. G.Y.

N78-17941* National Aeronautics and Space Administration.
Lewis Research Center, Cleveland, Ohio.
**MAKING AEROSPACE TECHNOLOGY WORK FOR THE
AUTOMOTIVE INDUSTRY. INTRODUCTION**

Walter T. Olson 1978 11 p Presented at the 1978 Congr.
and Exposition of the Soc. of Automotive Engr., Detroit,
27 Feb. - 3 Mar. 1978

(NASA-TM-73870) Avail: NTIS HC A02/MF A01 CSCL 05A

NASA derived technology already in use in the automotive industry include: (1) developments in electronics design, computer systems, and quality control methods for line testing of cars and trucks; (2) a combustion analysis computer program for automotive engine research and development; (3) an infrared scanner and television display for analyzing tire design and performance, and for studying the effects of heat on the service life of V-belts, shock mounts, brakes, and rubber bearings; (4) exhaust gas analyzers for trouble shooting and emissions certification; (5) a device for reducing noise from trucks; and (6) a low cost test vehicle for measuring highway skid resistance. Services offered by NASA to facilitate access to its technology are described. Author

N78-17942* National Aeronautics and Space Administration.
Lewis Research Center, Cleveland, Ohio.
**BASLINE TESTS OF THE C. H. WATERMAN DAF ELECTRIC
PASSENGER VEHICLE**

Noel B. Sargent, Edward A. Maszkowski, Richard F. Soltis, and
Richard M. Schuh Oct. 1977 113 p

(Contract EC-77-A-31-1011)

(NASA-TM-73757; CONS/1011-2; E-9388) Avail: NTIS
HC A06/MF A01 CSCL 13F

An electric vehicle was tested as part of an Energy Research Development Administration (ERDA) project to characterize the state-of-the-art of electric vehicles. The Waterman vehicle performance test results are presented in this report. The vehicle

is a converted four-passenger DAF 46 sedan. It is powered by sixteen 6-volt traction batteries through a three-step contactor controller actuated by a foot throttle to change the voltage applied to the 6.7 kW motor. The braking system is a conventional hydraulic braking system. Author

N78-18008* National Aeronautics and Space Administration.
Lewis Research Center, Cleveland, Ohio.
**STATE-OF-THE-ART ASSESSMENT OF ELECTRIC VEHICLES
AND HYBRID VEHICLES**

Sep. 1977 595 p refs

(Contract EC-77-A-31-1011)

(NASA-TM-73756; CONS/1011-1; E-9308) Avail: NTIS
HC A25/MF A01 CSCL 13F

The Electric and Hybrid Vehicle Research, Development, and Demonstration Act of 1976 (PL 94-413) requires that data be developed to characterize the state of the art of vehicles powered by an electric motor and those propelled by a combination of an electric motor and an internal combustion engine or other power sources. Data obtained from controlled tests of a representative number of sample vehicles, from information supplied by manufacturers or contained in the literature, and from surveys of fleet operators of individual owners of electric vehicles is discussed. The results of track and dynamometer tests conducted by NASA on 22 electric, 2 hybrid, and 5 conventional vehicles, as well as on 5 spark-ignition-engine-powered vehicles, the conventional counterparts of 5 of the vehicles, are presented. Author

N78-20021* National Aeronautics and Space Administration.
Lewis Research Center, Cleveland, Ohio.
**BASLINE TESTS OF THE VOLKSWAGEN TRANSPORTER
ELECTRIC DELIVERY VAN**

Richard F. Soltis, Edward McBrien, John M. Bozek, and Francis
Gourash Jan. 1978 56 p refs

(Contract EC-77-A-31-1011)

(NASA-TM-73766; CONS/1011-11; E-9506) Avail: NTIS
HC A04/MF A01 CSCL 13F

The Volkswagen Transporter, an electric delivery van, was tested as part of an Energy Research and Development Administration (ERDA) project to characterize the state of the art of electric vehicles. The Volkswagen Transporter is a standard Volkswagen van that has been converted to an electric vehicle. It is powered by a 144-volt traction battery. A direct current (dc) chopper controller, actuated by a conventional accelerator pedal, regulates the voltage or power applied to the 16-kilowatt (21-hp) motor. The braking system uses conventional hydraulic braking in combination with an electric regenerative braking system. The Volkswagen vehicle performance test results are presented. Author

N78-20022* National Aeronautics and Space Administration.
Lewis Research Center, Cleveland, Ohio.
**PERFORMANCE OF CONVENTIONALLY POWERED
VEHICLES TESTED TO AN ELECTRIC VEHICLE TEST
PROCEDURE**

Ralph J. Slavik, Miles O. Dustin, and Stacy Lumannick Dec.
1977 62 p refs

(Contract EC-77-A-31-1011)

(NASA-TM-73768; E-9482; CONS/1011-13) Avail: NTIS
HC A04/MF A01 CSCL 13F

A conventional Volkswagen transporter, a Renault 5, a Pacer, and a U. S. Postal Service general DJ-5 delivery van were treated to an electric vehicle test procedure in order to allow direct comparison of conventional and electric vehicles. Performance test results for the four vehicles are presented. Author

N78-20023* National Aeronautics and Space Administration, Lewis Research Center, Cleveland, Ohio.
RESPONSE OF LEAD-ACID BATTERIES TO CHOPPER-CONTROLLED DISCHARGE: PRELIMINARY RESULTS
 Robert L. Cataldo Feb. 1978 9 p refs
 (Contract EC-77-31-1044)
 (NASA-TM-73834; CONS/1044-1; E-9421) Avail: NTIS HC A02/MF A01 CSCL 10C

The preliminary results of simulated electric vehicle, chopper, speed controller discharge of a battery show energy output losses up to 25 percent compared to constant current discharges at the same average discharge current of 100 amperes. These energy losses are manifested as temperature rises during discharge, amounting to a two-fold increase for a 400-ampere pulse compared to the constant current case. Because of the potentially large energy inefficiency, the results suggest that electric vehicle battery/speed controller interaction must be carefully considered in vehicle design. Author

N78-21010* National Aeronautics and Space Administration, Lewis Research Center, Cleveland, Ohio.
BASLINE TESTS OF THE EPC HUMMINGBIRD ELECTRIC PASSENGER VEHICLE
 Ralph J. Slavik, Edward A. Maslowski, Noel B. Sargent, and Arthur Birchenough Dec. 1977 46 p Prepared for DOE
 (Contract EC-77-A-31-1011)
 (NASA-TM-73760; E-9485; CONS-1011-5) Avail: NTIS HC A03/MF A01 CSCL 13F

The rear-mounted internal combustion engine in a four-passenger Volkswagen Thing was replaced with an electric motor made by modifying an aircraft generator and powered by 12 heavy-duty, lead-acid battery modules. Vehicle performance tests were conducted to measure vehicle maximum speed, range at constant speed, range over stop-and-go driving schedules, maximum acceleration, gradeability limit, road energy consumption, road power, indicated energy consumption, braking capability, battery charger efficiency, and battery characteristics. Test results are presented in tables and charts. Author

N78-26010* National Aeronautics and Space Administration, Lewis Research Center, Cleveland, Ohio.
RESPONSE OF LEAD-ACID BATTERIES TO CHOPPER-CONTROLLED DISCHARGE
 Robert L. Cataldo [1978] 11 p refs Proposed for presentation at the 13th Intersoc. Energy Conversion Eng. Conf., San Diego, Calif., 20-25 Aug 1978 Revised
 (Contract EC 77-A-31-1044)
 (NASA-TM-73834-Rev. E-9421; CONS/1044-1) Avail: NTIS HC A02/MF A01 CSCL 13F

The preliminary results of simulated electric vehicle, chopper, speed controller discharge of a battery show energy output losses at up to 25 percent compared to constant current discharges at the same average discharge current of 100 A. These energy losses are manifested as temperature rises during discharge, amounting to a two-fold increase for a 400-A pulse compared to the constant current case. Because of the potentially large energy inefficiency the results suggest that electric vehicle battery/speed controller interaction must be carefully considered in vehicle design. Author

N78-28895* National Aeronautics and Space Administration, Lewis Research Center, Cleveland, Ohio.
AN INVERTER/CONTROLLER SUBSYSTEM OPTIMIZED FOR PHOTOVOLTAIC APPLICATIONS
 Roy Pickrell, George O'Sullivan (Abacus Controls, Inc., Somerville, N. J.), and Walter C. Merrill 1978 11 p refs Presented at 13th Photovoltaic Specialists Conf., Washington, D.C., 5-8 Jun. 1978; sponsored by IEEE
 (Contract E(49-28)-1022)
 (NASA-TM-78903; DOE/NASA/1022-78/31; E-9639) Avail: NTIS HC A02/MF A01 CSCL 13F

Conversion of solar array dc power to ac power stimulated

the specification, design, and simulation testing of an inverter/controller subsystem tailored to the photovoltaic power source characteristics. Optimization of the inverter/controller design is discussed as part of an overall photovoltaic power system designed for maximum energy extraction from the solar array. The special

N78-28896* National Aeronautics and Space Administration, Lewis Research Center, Cleveland, Ohio.
A CYCLE TIMER FOR TESTING ELECTRIC VEHICLES
 Richard F. Soltis 1978 11 p Proposed for presentation at the 5th Intern. Elec. Vehicle Symp., Philadelphia, 2-5 Oct 1978; sponsored by the Elec. Vehicle Council
 (Contract EC-77-A-31-1011)
 (NASA-TM-78934; E-9677; DOE/NASA/1011-78/27) Avail: NTIS HC A02/MF A01 CSCL 13F

A cycle timer was developed to assist the driver of an electric vehicle in more accurately following and repeating SAE driving schedules. These schedules require operating an electric vehicle in a selected stop-and-go driving cycle and repeating this cycle pattern until the vehicle ceases to meet the requirements of the cycle. The heart of the system is a programmable read-only memory (PROM) that has the required test profiles permanently recorded on plug-in cards, one card for each different driving schedule. The PROM generates a direct current analog signal that drives a speedometer displayed on one scale of a dual movement meter. The second scale of the dual movement meter displays the actual speed of the vehicle as recorded by the fifth wheel. The vehicle operator controls vehicle speed to match the desired profile speed. The PROM controls the recycle start time as well as the buzzer activation. The cycle programmer is powered by the test vehicle's 12-volt accessory battery, through a 5-volt regulator and a 12-volt dc-to-dc converter. Author

N78-27003* National Aeronautics and Space Administration, Lewis Research Center, Cleveland, Ohio.
STATE-OF-THE-ART ASSESSMENT OF ELECTRIC AND HYBRID VEHICLES
 Jan. 1978 598 p refs
 (Contract EX-76-A-31-1011)
 (NASA-TM-79509; HCP/M1011-01) Avail: NTIS HC A25/MF A01 CSCL 13F

Data are presented that were obtained from the electric and hybrid vehicles tested, information collected from users of electric vehicles, and data and information on electric and hybrid vehicles obtained on a worldwide basis from manufacturers and available literature. The data given include: (1) information and data base (electric and hybrid vehicle systems descriptions, sources of vehicle data and information, and sources of component data); (2) electric vehicles (theoretical background, electric vehicle track tests, user experience, literature data, and summary of electric vehicle status); (3) electric vehicle components (tires, differentials, transmissions, traction motors, controllers, batteries, battery chargers, and component summary); and (4) hybrid vehicles (types of hybrid vehicles, operating modes, hybrid vehicles components, and hybrid vehicles performance characteristics). ERA

N78-28894* National Aeronautics and Space Administration, Lewis Research Center, Cleveland, Ohio.
A STIRLING ENGINE COMPUTER MODEL FOR PERFORMANCE CALCULATIONS Final Report
 Roy Tew, Kent Jefferies, and David Miao Jul. 1978 102 p refs
 (Contract EC-77-A-31-1011)
 (NASA-TM-78884; DOE/NASA/1011-78/24; E-9613) Avail: NTIS HC A06/MF A01 CSCL 10B

To support the development of the Stirling engine as a possible alternative to the automobile spark-ignition engine, the thermodynamic characteristics of the Stirling engine were analyzed and modeled on a computer. The modeling techniques used are presented. The performance of an existing rhombic-drive Stirling engine was simulated by use of this computer program, and some typical results are presented. Engine tests are planned in order to evaluate this model. Author

A78-33358* Making aerospace technology work for the automotive industry - Introduction. W. T. Olson (NASA, Lewis Research Center, Cleveland, Ohio). *Society of Automotive Engineers, Congress and Exposition, Detroit, Mich., Feb. 27-Mar. 3, 1978, Paper. 10 p.*

In many cases it has been found that advances made in one technical field can contribute to other fields. An investigation in this connection conducted concerning subjects from contemporary NASA programs and projects which might have relevance and potential usefulness to the automotive industry. Examples regarding aerospace developments which have been utilized by the automotive industry are related to electronic design, computer systems, quality control experience, a NASA combustion scanner and television display, exhaust gas analyzers, and a device for suppressing noise propagated through ducts. Projects undertaken by NASA's center for propulsion and power research are examined with respect to their value for the automotive industry. As a result of some of these projects, a gas turbine engine and a Stirling engine might each become a possible alternative to the conventional spark ignition engine. G.R.

A78-33382* Test and evaluation of 23 electric vehicles for state-of-the-art assessment. M. O. Dustin and R. J. Denington (NASA, Lewis Research Center, Cleveland, Ohio). *Society of Automotive Engineers, Congress and Exposition, Detroit, Mich., Feb. 27-Mar. 3, 1978, Paper 780290. 12 p. 18 refs.*

Data developed by ERDA used to evaluate the performance parameters of modern electric vehicles is presented with reference to range, acceleration, coast-down, and braking. Eight of the tested vehicles had some type of regenerative braking system, which provided range increases from 1 to 31 percent. In comparison with conventional vehicles, performance was found to be lower, and reliability poorer. Energy consumption was the same, but electric power is less damaging to the environment than hydrocarbon fuels, and does not use up an increasingly scarce resource. D.M.W.

N78-22970* Ford Motor Co., Dearborn, Mich.
AUTOMOTIVE STIRLING ENGINE DEVELOPMENT PROGRAM Quarterly Technical Progress Report. Oct. 1977 - Dec. 1977

Ernest W. Kitzner Jan. 1978 98 p Sponsored in part by NASA
(Contract EC-77-C-02-4396)
(NASA-CR-135331; CONS/4396-1; QTPR-1) Avail: NTIS HC A05/MF A01 CSCL 13f

The Ford/DOE automotive Stirling engine development program is directed towards establishing the technological and developmental base that would enable a decision on whether an engineering program should be directed at Stirling engine production. The fuel economy assessment aims to achieve, with a high degree of confidence, the ERDA proposal estimate of 20.6 MPG (gasoline) for a 4500 lb 1WC Stirling engine passenger car. The current M-H fuel economy projection for the 170 HP Stirling engine is 15.7 MPG. The confidence level for this projection is 32%. A confidence level of 29% is projected for a 22.1 MPG estimate. If all of the planned analyses and test work is accomplished at the end of the one year effort, and the projected improvements are substantiated, the confidence levels would rise to 59% for the 20.6 MPG projection and 54% for the 22.1 MPG projection. Progress achieved thus far during the fuel economy assessment is discussed. Author

N78 23999* Joint Center for Graduate Study, Richland, Wash.
STIRLING ENGINE DESIGN MANUAL Final Report
William R. Martini Apr. 1978 359 p refs
(Grant Nsg-3152; Contract EC-77-A-31-1011)
(NASA-CR-135382; DOE/NASA/3152-78/1) Avail: NTIS HC A16/MF A01 CSCL 21G

This manual is intended to serve both as an introduction to Stirling engine analysis methods and as a key to the open literature on Stirling engines. Over 800 references are listed and these are cross referenced by date of publication, author and subject. Engine analysis is treated starting from elementary principles

and working through cycles analysis. Analysis methodologies are classified as first, second or third order depending upon degree of complexity and probable application: first order for preliminary engine studies, second order for performance prediction and engine optimization, and third order for detailed hardware evaluation and engine research. A few comparisons between theory and experiment are made. A second order design procedure is documented step by step with calculation sheets and a worked out example to follow. Current high power engines are briefly described and a directory of companies and individuals who are active in Stirling engine development is included. Much remains to be done. Some of the more complicated and potentially very useful design procedures are now only referred to. Future support will enable a more thorough job of comparing all available design procedures against experimental data which should soon be available. Author

N78-26968* Ford Motor Co., Dearborn, Mich.
CERAMIC REGENERATOR SYSTEMS DEVELOPMENT PROGRAM Progress Report. 1 Oct. 1976 - 30 Sep. 1977
J. A. Cook, C. A. Fucinari, J. N. Lingscheit, and C. J. Rahnke
Dec 1977 129 p refs Prepared for DOE
(Contract DEN-3-8)
(NASA-CR-135330; CONS/0008-1) Avail: NTIS HC A07/MF A01 CSCL 13F

Ceramic regenerator cores are considered that can be used in passenger car gas turbine engines, Stirling engines, and industrial/truck gas turbine engines. Improved materials and design concepts aimed at reducing or eliminating chemical attack were placed on durability test in Ford 707 industrial gas turbine engines. The results of 19,600 hours of turbine engine durability testing are described. Two materials, aluminum silicate and magnesium aluminum silicate continue to show promise toward achieving the durability objectives of this program. A regenerator core made from aluminum silicate showed minimal evidence of chemical attack damage after 6935 hours of engine test at 800 C and another showed little distress after 3510 hours at 982 C. Results obtained in ceramic material screening tests, aerothermodynamic performance tests, stress analysis, cost studies, and material specifications are also included. Author

N78-26997* Ford Motor Co., Dearborn, Mich.
CERAMIC REGENERATOR SYSTEMS DEVELOPMENT PROGRAM Progress Report. 1 Jan. - 31 Mar. 1978
J. A. Cook, C. A. Fucinari, J. N. Lingscheit, C. J. Rahnke, and V. D. Rao May 1978 108 p refs
(Contracts DEN3-8; EC-77-A-31-1040)
(NASA-CR-135430; CONS-0008-3) Avail: NTIS HC A06/MF A01 CSCL 11C

Ceramic regenerator cores are considered that can be used in passenger car gas turbine engines, Stirling engines, and industrial/truck gas turbine engines. Improved materials and design concepts aimed at reducing or eliminating chemical attack were placed on durability tests in industrial gas turbine engines. A regenerator core made from aluminum silicate shows minimal evidence of chemical attack damage after 7804 hours of engine test at 800 C and another showed little distress after 4983 hours at 982 C. The results obtained in ceramic material screening tests, aerothermodynamic performance tests, stress analysis, cost studies, and material specifications are also included. G.G.

NTS-28882*/ Booz-Allen and Hamilton, Inc., Cleveland, Ohio.
Design and Development Div.
**PRELIMINARY POWER TRAIN DESIGN FOR A STATE-OF-
THE-ART ELECTRIC VEHICLE Final Report**
Philip Mighdall and William F. Hahn Apr. 1978 144 p refs
(Contracts NAS3-20595; EC-77-A-31-1044)
(NASA-CR-135341; DOE/NASA/0595-78/1) Avail: NTIS
HC A07/MF A01 CSCL 13F

Power train designs which can be implemented within the current state-of-the-art were identified by means of a review of existing electric vehicles and suitable off-the-shelf components. The effect of various motor/transmission combinations on vehicle range over the SAE J227a schedule D cycle was evaluated. The selected, state-of-the-art power train employs a dc series wound motor, SCR controller, variable speed transmission, regenerative braking, drum brakes and radial ply tires. Vehicle range over the SAE cycle can be extended by approximately 20% by the further development of separately excited, shunt wound DC motors and electrical controllers. Approaches which could improve overall power train efficiency, such as AC motor systems, are identified. However, future emphasis should remain on batteries, tires and lightweight structures if substantial range improvements are to be achieved. Author

88 SPACE SCIENCES (GENERAL)

N78-32014* National Aeronautics and Space Administration,
Lewis Research Center, Cleveland, Ohio.
**SPACECRAFT CHARGING CONTROL BY THERMAL FIELD
EMISSION WITH LANTHANUM-HEXABORIDE EMITTERS**
James F. Morris Aug. 1978 26 p refs
(NASA-TM-78990; E-9773) Avail: NTIS HC A03/MF A01
CSCL 22B

Thermal field emitters of lanthanum (or perhaps cerium) hexaboride (LaB6) with temperature variability up to about 1500 K are suggested for spacecraft charging control. Such emitters operate at much lower voltages with considerably more control and add plasma-diagnostic versatility. These gains should outweigh the additional complexity of providing heat for the LaB6 thermal field emitter. L.S.

92 SOLAR PHYSICS

Includes solar activity, solar flares, solar radiation and sunspots.

N78-26028* National Aeronautics and Space Administration,
Lewis Research Center, Cleveland, Ohio.

**EVALUATION OF MODELS TO PREDICT INSOLATION ON
TILTED SURFACES**

Thomas M. Klucher Mar. 1978 30 p refs

(Contract E(49-26)-1022)

(NASA-TM-78842; E-9556) Avail: NTIS HC A03/MF A01
CSCL 10A

An empirical study was performed to evaluate the validity of various insolation models which employ either an isotropic or an anisotropic distribution approximation for sky light when predicting insolation on tilted surfaces. Data sets of measured hourly insolation values were obtained over a six-month period using pyranometers which received diffuse and total solar radiation on a horizontal plane and total radiation on surfaces tilted toward the equator at 37 deg and 60 deg angles above the horizon. Data on the horizontal surfaces were used in the insolation models to predict insolation on the tilted surface; comparisons of measured versus calculated insolation on the tilted surface were examined to test the validity of the sky light approximations. It was found that the Liu-Jordan isotropic distribution model provides a good fit to empirical data under overcast skies but underestimates the amount of solar radiation incident on tilted surface under clear and partly cloudy conditions. The anisotropic-clear-sky distribution model by Temps and Coulson provides a good prediction for clear skies but overestimates the solar radiation when used for cloudy days. An anisotropic-all-sky model was formulated in this effort which provided excellent agreement between measured and predicted insolation throughout the six-month period.

Author

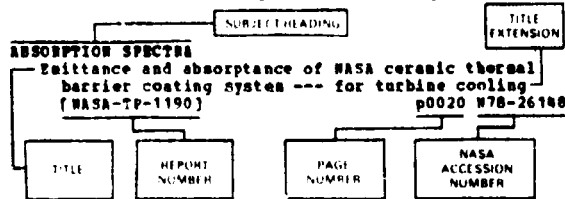
99 GENERAL

N78-23032* National Aeronautics and Space Administration,
Lewis Research Center, Cleveland, Ohio.
**DESIGN AND PERFORMANCE OF HEART ASSIST OR
ARTIFICIAL HEART CONTROL SYSTEMS** e62
John A. Webb, Jr. and Vernon D. Gebben *In* NASA, Washington
Fourth Inter-Center Control Systems Conf. Jan. 1978 p 495-506
refs (For availability see N78-23010 13-99)
Avail: NTIS HC A22/MF A01 CSCL 12B

The factors leading to the design of a controlled driving system for either a heart assist pump or artificial heart are discussed. The system provides square pressure waveform to drive a pneumatic-type blood pump. For assist usage the system uses an R-wave detector circuit that can detect the R-wave of the electrocardiogram in the presence of electrical disturbances. This circuit provides a signal useful for synchronizing an assist pump with the natural heart. It synchronizes a square wave circuit, the output of which is converted into square waveforms of pneumatic pressure suitable for driving both assist device and artificial heart. The pressure levels of the driving waveforms are controlled by means of feedback channels to maintain physiological regulation of the artificial heart's output flow. A more compact system that could achieve similar regulatory characteristics is also discussed. Author

SUBJECT INDEX

Typical Subject Index Listing



The title is used to provide a description of the subject matter. When the title is inadequately descriptive of the document content, a title extension is added separated from the title by three hyphens. The *STAR* or *JAA* accession number is included in each entry to assist the user in locating the abstract in the abstract section. If applicable, a report number is also included as an aid in identifying the document. The page and accession numbers are located beneath and to the right of the title. Under any one subject heading, the accession numbers are arranged in sequence with the *JAA* accession numbers appearing first.

A

ABSORPTION SPECTRA
Emittance and absorbance of NASA ceramic thermal barrier coating system --- for turbine cooling [NASA-TP-1190] p0020 N78-26148

ABLATIVE MATERIALS
Hydrogen film cooling of a small hydrogen-oxygen thrust chamber and its effect on erosion rates of various ablative materials [NASA-TP-1098] p0047 N78-13124

ABRASION RESISTANCE
Hub tolerance evaluation of two sintered NiCrAl gas path seal materials --- wear tests of gas turbine engine seals [NASA-TN-78967] p0071 N78-29215

ABSORBERS (MATERIALS)
WT SOLAR ENERGY ABSORBERS

ABSORPTION BANDS
U ABSORPTION SPECTRA

ABSORPTION SPECTRA
Emittance and absorbance of NASA ceramic thermal barrier coating system --- for turbine cooling [NASA-TP-1190] p0020 N78-26148

ABSTRACTS
Bibliography of Lewis Research Center technical contributions announced in 1976 [NASA-TN-73860] p0177 N78-17921

AC GENERATORS
Methods of attenuating wind turbine ac generator output variations p0133 N78-19632

Solar cell system having alternating current output [NASA-CASE-LEW-12806-1] p0136 N78-25553

ACCELERATED LIFE TESTS
Petrographic analysis of wear debris generated in accelerated rolling element fatigue tests p0119 A78-28425

5200 cycle of an 8-cm diameter Hg ion thruster [AIAA PAPER 78-649] p0050 A78-32736

Real-time and accelerated outdoor endurance testing of solar cells p0142 A78-52837

Real-time and accelerated outdoor endurance testing of solar cells [NASA-TN-73743] p0130 N78-14628

Accelerated life tests of specimen heat pipe from Communication Technology Satellite (CTS) project [NASA-TN-73846] p0102 N78-17341

ACCELERATION (PHYSICS)
WT HIGH ACCELERATION
WT PLASMA ACCELERATION

ACCELERATORS
Sensitivity of 30-cs mercury bombardment ion thruster characteristics to accelerator grid design [NASA-TN-78861] p0049 N78-23144

ACCRETION
U DEPOSITION

ACCELERATORS
WT SOLAR COLLECTORS
WT SOLAR REFLECTORS

ACOUSTIC ATTENUATION
Numerical spatial marching techniques for estimating duct attenuation and source pressure profiles p0166 A78-37682

Numerical spatial marching techniques for estimating duct attenuation and source pressure profiles [NASA-TN-78857] p0103 N78-22329

ACOUSTIC COMBUSTION
U COMBUSTION STABILITY

ACOUSTIC DUCTS
Optimum wall impedance for spinning modes - A correlation with mode cut-off ratio [AIAA PAPER 78-193] p0165 A78-20735

Numerical spatial marching techniques for estimating duct attenuation and source pressure profiles p0166 A78-37682

Optimum wall impedance for spinning modes: A correlation with mode cut-off ratio [NASA-TN-73862] p0163 N78-15853

Interaction of a turbulent-jet noise source with transverse modes in a rectangular duct [NASA-TP-1248] p0001 N78-25049

Design of an air ejector for boundary-layer bleed of an acoustically treated turbofan engine inlet during ground testing [NASA-TN-78917] p0037 N78-27143

ACOUSTIC EMISSION
Acoustic emission testing of composite vessels under sustained loading [NASA-TN-78981] p0059 N78-33150

ACOUSTIC EXCITATION
Far-field multimodal acoustic radiation directivity --- from ducted bodies [NASA-TN-73839] p0163 N78-15

ACOUSTIC IMPEDANCE
Optimum wall impedance for spinning modes - A correlation with mode cut-off ratio [AIAA PAPER 78-193] p0165 A78-20735

Optimum wall impedance for spinning modes: A correlation with mode cut-off ratio [NASA-TN-73862] p0163 N78-15853

ACOUSTIC INSTABILITY
Variation of fan tone steadiness for several inflow conditions [NASA-TN-78886] p0164 N78-26878

ACOUSTIC MEASUREMENTS
WT NOISE MEASUREMENT
Variation of fan tone steadiness for several inflow conditions [AIAA PAPER 78-1119] p0166 A78-41829

Method of fan sound mode structure determination [NASA-CR-135293] p0028 N78-17064

Use of an ultrasonic-acoustic technique for nondestructive evaluation of fiber composite strength [NASA-TN-73813] p0124 N78-17397

Acoustic evaluation of a novel swept-rotor fan --- noise reduction in turbofan engines [NASA-TN-78878] p0164 N78-24897

Three-dimensional effects on pure tone fan noise due to inflow distortion --- rotor blade noise prediction [NASA-TN-78885] p0164 N78-26898

Acoustic tests of duct-burning turbofan jet noise simulation: Comprehensive data report. Volume 1, section 2: Full size data [NASA-CR-135239-VOL-1-SECT-2] p0030 N78-28095

ACOUSTIC PROPAGATION

SUBJECT INDEX

Acoustic tests of duct-burning turbofan jet noise simulation: Comprehensive data report. Volume 1, section 3: Data plots [NASA-CR-135239-VOL-1-SECT-3] p0030 878-28096

Acoustic tests of duct-burning turbofan jet noise simulation: Comprehensive data report. Volume 2: Model design and aerodynamic test results [NASA-CR-135239-VOL-2] p0031 878-28097

Flight effects on the aerodynamic and acoustic characteristics of inverted profile conical nozzles, volume 1 --- supersonic cruise aircraft research wind tunnel tests [NASA-CR-135189-VOL-1] p0167 878-29867

Flight effects on the aerodynamic and acoustic characteristics of inverted profile conical nozzles, volume 2 --- supersonic cruise aircraft research wind tunnel tests [NASA-CR-135189-VOL-2] p0167 878-29868

Flight effects on the aerodynamic and acoustic characteristics of inverted profile conical nozzles, volume 3 --- supersonic cruise aircraft research wind tunnel tests [NASA-CR-135189-VOL-3] p0167 878-29869

Correlation of combustor acoustic power levels inferred from internal fluctuating pressure measurements [NASA-TN-78986] p0165 878-31871

ACOUSTIC PROPAGATION
Propagation of sound waves through a linear shear layer: A closed form solution [NASA-TN-73828] p0164 878-16766

ACOUSTIC PROPERTIES
ST ACOUSTIC IMPEDANCE
ST ACOUSTIC INSTABILITY
Effect of design changes on aerodynamic and acoustic performance of translating-centerbody sonic inlets [NASA-TN-1132] p0003 878-17996

Preliminary study of the effect of the turbulent flow field around complex surfaces on their acoustic characteristics [NASA-TN-78948] p0164 878-28886

Flight effects on the aerodynamic and acoustic characteristics of inverted profile conical nozzles [NASA-CR-3018] p0169 878-32836

ACOUSTIC RADIATION
U SOUND WAVES
ACOUSTIC SOUNDING
Far-field multiaxial acoustic radiation directivity p0165 878-24876

ACOUSTIC STABILITY
U FREQUENCY STABILITY
ACOUSTIC VIBRATIONS
U SOUND WAVES
ACOUSTICS
ST AEROACOUSTICS
Computation of unsteady transonic flows through rotating and stationary cascades. 3: Acoustic far-field analysis [NASA-CR-2902] p0007 878-12035

Acoustic design of the QCSH propulsion systems p0004 878-24067

ACQUISITION
ST DATA ACQUISITION
ACTINOMETERS
ST INFRARED DETECTORS
ST RADIONETERS
ST SPECTROPHOTOMETER
ST ULTRAVIOLET SPECTROPHOTOMETERS
ACTIVATION ANALYSIS
ERDA/NASA advanced thermonuclear technology program [NASA-CR-157248] p0145 878-27552

ACTUATORS
Investigation of means for perturbing the flow field in a supersonic wind tunnel [NASA-TN-78954] p0037 878-27142

ADAPTIVE CONTROL
Analysis and design of a high power laser adaptive phased array transmitter [NASA-CR-134952] p0111 878-13420

ADAPTIVE CONTROL SYSTEMS
U ADAPTIVE CONTROL
ADHESION RESINS
Kinetics of isidisation and crosslinking in PBR-polyiside resin [NASA-TN-78844] p0082 878-23231

ADHESIVES
ST PLASTICISERS

Development of strong and tough cryogenic Fe-12Ni alloys containing reactive metal additions p0076 878-81465

Effectiveness of various organometallics as antiwear additives in mineral oil [NASA-TP-1096] p0080 878-12222

Inhibition of hot salt corrosion by metallic additives [NASA-TN-78966] p0072 878-31208

ADHESION TESTS
U ADHESION TESTS
ADHESION
Role of alloying elements in adhesive transfer and friction of copper-base alloys [NASA-TP-1256] p0071 878-26198

Adhesion of a bimetallic interface --- for Al, Mg, and Zn [NASA-TN-78890] p0071 878-29214

ADHESION TESTS
Adhesive/cohesive strength of a ErO₂-1-2 w/o TiO₂/TiCrAlY thermal barrier coating [NASA-TN-73792] p0057 878-17152

ADHESIVE BONDING
Thermal barrier coating system [NASA-CASR-LEU-12554-1] p0102 878-18355

ADSORPTION
ST CHEMISORPTION
Influence of adsorbed film on the rolling contact deformation of MgO single crystals p0123 878-23447

AERIAL IMAGERY
U AERIAL PHOTOGRAPHY
AERIAL PHOTOGRAPHY
Aerial thermography for energy conservation [NASA-TN-78959] p0129 878-33510

AEROACOUSTICS
Propagation of sound waves through a linear shear layer - A closed form solution [AIAA PAPER 78-196] p0165 878-20738

Far-field multiaxial acoustic radiation directivity p0165 878-24876

Sound production in a moving stream p0165 878-31224

Variation of fan tone steadiness for several inflow conditions [AIAA PAPER 78-1119] p0166 878-81829

Preliminary study of the effect of the turbulent flow field around complex surfaces on their acoustic characteristics [AIAA PAPER 78-1123] p0166 878-85129

Acoustic tests of duct-burning turbofan exhaust nozzles. Comprehensive data report. Volume 1: Model scale acoustic data [NASA-CR-134910-VOL-1] p0002 878-15988

Aero-acoustic tests of duct-burning turbofan exhaust nozzles. Comprehensive data report. Volume 2: Acoustic and aerodynamic data [NASA-CR-134910-VOL-2] p0002 878-15989

Aero-acoustic tests of duct-burning turbofan exhaust nozzles. Comprehensive data report. Volume 3: Acoustic and aerodynamic data curves [NASA-CR-134910-VOL-3] p0002 878-15990

AERODYNAMIC BRAKES
ST WING FLAPS
AERODYNAMIC BUSS
U FLUTTER
AERODYNAMIC CHARACTERISTICS
ST AERODYNAMIC DRAG
E2F noise suppression and aerodynamic penalties --- Externally Blown Flaps [AIAA PAPER 78-240] p0165 878-20763

Effects of film injection on performance of a cooled turbine p0033 878-24902

VSTOL tilt nacelle aerodynamics and its relation to fan blade stresses [AIAA PAPER 78-958] p0007 878-83520

Effect of coolant flow ejection on aerodynamic performance of low-aspect-ratio vanes. 2: Performance with coolant flow ejection at temperature ratios up to 2 [NASA-TP-1057] p0003 878-11008

Effect of cooling-hole geometry on aerodynamic performance of a film-cooled turbine vane tested with cold air in a two-dimensional cascade [NASA-TP-1136] p0004 878-20080

Two-dimensional cold-air cascade study of a film-cooled turbine stator blade. 4: Comparison of experimental and analytical

- aerodynamic results for blade with 12 rows of 0.076-centimeter-(0.030-inch-) diameter holes having streamwise ejection angles
[NASA-TP-1151] p0017 W78-20130
- Two-dimensional cold-air cascade study of a film-cooled turbine stator blade. 5: Comparison of experimental and analytical aerodynamic results for blade with 12 rows of 0.038-centimeter-(0.015 inch) diameter coolant holes having streamwise ejection angles
[NASA-TP-1204] p0017 W78-20133
- Effects of film injection on performance of a cooled turbine
p0029 W78-21147
- Cold-air performance of the compressor-drive turbine of the Department of Energy baseline automobile gas-turbine engine
[NASA-TN-78894] p0005 W78-24098
- VSTOL tilt nacelle aerodynamics and its relation to fan blade stresses
[NASA-TN-78899] p0005 W78-26099
- Aerodynamic performance of conventional and advanced design labyrinth seals with solid-smooth abradable, and honeycomb lands --- gas turbine engines
[NASA-CR-133077] p0122 W78-27427
- Core compressor exit stage study. Volume 1: Blading design --- turbofan engines
[NASA-CR-135191] p0031 W78-29099
- Flight effects on the aerodynamic and acoustic characteristics of inverted profile conical nozzles, volume 1 --- supersonic cruise aircraft research wind tunnel tests
[NASA-CR-135189-VOL-1] p0167 W78-29867
- Flight effects on the aerodynamic and acoustic characteristics of inverted profile conical nozzles, volume 2 --- supersonic cruise aircraft research wind tunnel tests
[NASA-CR-135189-VOL-2] p0167 W78-29868
- Flight effects on the aerodynamic and acoustic characteristics of inverted profile conical nozzles, volume 3 --- supersonic cruise aircraft research wind tunnel tests
[NASA-CR-135189-VOL-3] p0167 W78-29869
- Flight effects on the aerodynamic and acoustic characteristics of inverted profile conical nozzles
[NASA-CR-135189] p0169 W78-32836
- AERODYNAMIC CONFIGURATIONS**
- Preliminary study of the effect of the turbulent flow field around complex surfaces on their acoustic characteristics
[AIAA PAPER 78-1121] p0166 A78-37682
- EBF noise suppression and aerodynamic penalties
[NASA-TN-78893] p0163 W78-35952
- Effect of design changes on aerodynamic and acoustic performance of translating-centerbody sonic inlets
[NASA-TP-11121] p0003 W78-17998
- AERODYNAMIC DRAG**
- Effects of nozzle design and power on cruise drag for upper-surface-blowing aircraft
p0004 W78-24058
- AERODYNAMIC FORCES**
- NT AERODYNAMIC DRAG
NT AERODYNAMIC LOADS
NT DRAG LOADS
- AERODYNAMIC LOADS**
- NT DRAG LOADS
- Effects of rotor location, coning, and tilt on critical loads in large wind turbines
p0141 A78-20476
- Comparison of methods proposed for calculating dynamic loads in wind turbines
p0130 A78-19617
- AERODYNAMIC NOISE**
- EBF noise suppression and aerodynamic penalties --- externally blown flaps
[AIAA PAPER 78-1121] p0166 A78-37682
- Noise of deflectors used for flow attachment with STOL-OTR configurations
p0014 W78-13061
- An empirical model for inverted-velocity-profile jet noise prediction
p0026 W78-10093
- Sound production in a moving stream
p0023 A78-24079
- Numerical spatial averaging techniques for estimating duct attenuation and source pressure profiles
p0166 A78-37682
- Acoustic evaluation of a novel swept-rotor fan
[AIAA PAPER 78-1121] p0166 A78-37682
- Calculation of far-field jet noise spectra from near-field measurements using true source location
[AIAA PAPER 78-1153] p0168 A78-41852
- Effect of forward motion on engine noise
[NASA-CR-134954] p0026 W78-10093
- An empirical model for inverted-velocity-profile jet noise prediction
[NASA-TN-73830] p0014 W78-13061
- Noise of deflectors used for flow attachment with STOL-OTR configurations
[NASA-TN-73809] p0163 W78-13053
- Effectiveness of an inlet flow turbulence control device to simulate flight noise fan in an anechoic chamber
[NASA-TN-73855] p0163 W78-13056
- Simulated flight effects on noise characteristics of a fan inlet with high throat Mach number
[NASA-TP-1109] p0017 W78-20132
- A method for calculating externally blown flap noise
[NASA-CR-2944] p0166 W78-20920
- Preliminary study of the effect of the turbulent flow field around complex surfaces on their acoustic characteristics
[NASA-TN-78944] p0164 W78-28886
- AERONAUTICS**
- NT GEONAUTICS
- AERONAUTIC FLUTTER**
- NT FLUTTER
- AERONAUTICAL ENGINEERING**
- Bibliography of Lewis Research Center technical publications announced in 1977
[NASA-TN-78918] p0177 W78-28986
- AEROSOLS**
- Global measurements of gaseous and aerosol trace species in the upper troposphere and lower stratosphere from daily flights of 747 airliners
p0147 A78-15826
- Global sensing of gaseous and aerosol trace species using automated instrumentation on 747 airliners
[NASA-TN-73810] p0168 W78-13670
- AEROSPACE ENGINEERING**
- NT AERONAUTICAL ENGINEERING
- High-temperature, high-power-density thermionic energy conversion for space
[NASA-TN-73804] p0171 W78-13890
- Making aerospace technology work for the automotive industry, introduction
[NASA-TN-73870] p0179 W78-17941
- Titanium/beryllium laminates: Fabrication, mechanical properties, and potential aerospace applications
[NASA-TN-74891] p0059 W78-21221
- Bibliography of Lewis Research Center technical publications announced in 1977
[NASA-TN-78918] p0177 W78-28986
- Engineering in the 21st century
[NASA-TN-79010] p0105 W78-33380
- AEROSPACE ENVIRONMENTS**
- Materials science experiments in space
[NASA-CP-2842] p0056 W78-16094
- AEROSPACE TECHNOLOGY TRANSFER**
- Making aerospace technology work for the automotive industry - Introduction
p0181 A78-13359
- An overview of aerospace gas turbine technology of relevance to the development of the automotive gas turbine engine
[AIAA PAPER 780675] p0120 A78-33364
- Preliminary engine program test results
[NASA-TN-73732] p0015 W78-15082
- AFTERBURNERS**
- NT AFTERBURNING
- AFTERBURNING**
- A static test of several afterburner configurations on a turbofan engine with a hydrogen heater to simulate an elevated turbine discharge temperature
[NASA-TP-1001] p0014 W78-11106
- AGE HARDENING**
- NT INVESTIGATION HARDENING
- AIR**
- Computer program for obtaining thermodynamic and transport properties of air and products of combustion of ASTR-A-1 fuel and air

AIR BEARINGS

SUBJECT INDEX

[NASA-TP-1160] p0068 N78-20351

AIR BEARINGS

U GAS BEARINGS

AIR BEARINGS ENGINES

WT DOCTED FAN ENGINES

WT GAS TURBINE ENGINES

WT J-85 ENGINE

WT JET ENGINES

WT TURBOFAN ENGINES

WT TURBOJET ENGINES

WT TURBOPROP ENGINES

Normal shock and restart controls for a supersonic airbreathing propulsion system p0019 N78-23023

AIR CONDITIONING

Simulation model of a single-stage lithium bromide-water absorption cooling unit [NASA-TP-1296] p0072 N78-30205

Development of flat-plate solar collectors for the heating and cooling of buildings: Executive summary [NASA-CR-134804-2] p0146 N78-33527

AIR COOLING

A computer program for the transient thermal analysis of an impingement cooled turbine blade [AIAA PAPER 78-92] p0106 N78-20682

Effects of film injection on performance of a cooled turbine p0031 N78-24902

Effect of endwall cooling on secondary flows in turbine stator vanes p0014 N78-11098

Cold-air performance of free-power turbine designed for 112-kilowatt automotive gas-turbine engine. 1: Design Stator-vane-chord setting angle of 35 deg [NASA-TP-1007] p0015 N78-16053

Effects of film injection on performance of a cooled turbine p0029 N78-21147

Emergency and microfog lubrication and cooling of bearings for Army helicopters [NASA-CR-135195] p0122 N78-27429

AIR DUCTS

Design of an air ejector for boundary-layer bleed of an acoustically treated turbofan engine inlet during ground testing [NASA-TN-78917] p0037 N78-27143

AIR FLOW

Variable cycle gas turbine engines [NASA-CASP-LEW-12916-1] p0113 N78-17384

Oil-air mix lubrication for helicopter gearing [NASA-CR-135081] p0010 N78-25080

Gas turbine engine with recirculating bleed [NASA-CASE-LEW-12852-1] p0014 N78-25089

AIR INTAKES

WT ENGINE INTAKES

WT SUPERSONIC INTAKES

AIR POLLUTION

Global measurements of gaseous and aerosol trace species in the upper troposphere and lower stratosphere from daily flights of 747 airliners p0147 N78-14826

Preliminary QCSPP program - Test results --- Quiet Clean Short-haul Experimental Engine [SAP PAPER 77106R] p0023 N78-23840

Aircraft engine emissions --- conference [NASA-CP-2021] p0012 N78-11064

Emissions reduction technology program p0012 N78-11064

Summary of emissions reduction technology program p0013 N78-1107

Emissions control for ground power gas turbines p0013 N78-11072

General aviation piston-engine exhaust emission reduction p0011 N78-11073

Global atmospheric sampling program p0013 N78-11076

Stratospheric cruise emission reduction program p0013 N78-11077

QCSPP task 2: Engine and installation preliminary design [NASA-CR-134718] p0010 N78-23089

Combustor concepts for aircraft gas turbine low-power emissions reduction [NASA-TN-78875] p0020 N78-24143

Gas turbine engine emission reduction technology program p0013 N78-11071

p0001 N78-27058

Effect of inlet temperature on the performance of a catalytic reactor --- air pollution control [NASA-TN-78977] p0141 N78-31534

AIR QUALITY

Description and review of global measurements of atmospheric species from GASP p0148 N78-24893

AIR SEA INTERACTIONS

U AIR WATER INTERACTIONS

AIR WATER INTERACTIONS

Numerical computation of three-dimensional circulation in Lake Erie - A comparison of a free-surface model and a rigid-lid model p0151 N78-47223

AIRCRAFT APPROPRIAS

An airborne meteorological data collection system using satellite relay (ASDAR) [NASA-TN-78992] p0093 N78-33283

AIRCRAFT BRAKES

WT WING FLAPS

AIRCRAFT CONFIGURATIONS

ZBP noise suppression and aerodynamic penalties --- Externally Blown Flaps [AIAA PAPER 78-240] p0165 N78-20763

Noise of deflectors used for flow attachment with STOL-OTW configurations p0023 N78-24877

Noise of deflectors used for flow attachment with STOL-OTW configurations [NASA-TN-73809] p0163 N78-13853

AIRCRAFT DESIGN

Lightning protection of aircraft [NASA-SP-1008] p0009 N78-11024

Preliminary study of propulsion systems and airplane wing parameters for a US Navy subsonic V/STOL aircraft [NASA-TN-73652] p0010 N78-17041

Aerodynamic design and performance testing of an advanced 30 deg swept, eight bladed propeller at Mach numbers from 0.2 to 0.85 [NASA-CR-3047] p0008 N78-32066

AIRCRAFT ENGINES

WT TP-30 ENGINE

WT VARIABLE CYCLE ENGINE

A review of NASA's propulsion programs for civil aviation [AIAA PAPER 78-43] p0023 N78-20651

Minimum-time acceleration of aircraft turbofan engines p0024 N78-21892

The promise of ducted fans for aircraft turbines p0074 N78-24882

Progress in advanced high temperature turbine materials, coatings, and technology p0004 N78-24910

'Chain pooling' model selection as developed for the statistical analysis of a rotor burst protection experiment p0160 N78-29327

General aviation energy-conservation research program at NASA-Lewis Research Center --- for non-turbine general aviation engines p0024 N78-29330

Design approaches to more energy efficient engines [AIAA PAPER 78-931] p0025 N78-43504

General aviation internal combustion engine research program at NASA-Lewis Research Center [AIAA PAPER 78-932] p0026 N78-43505

Combustor concepts for aircraft gas turbine low-power emissions reduction [AIAA PAPER 78-929] p0024 N78-43506

Methods for calculating the transonic boundary layer separation for V/STOL inlets at high incidence angles [AIAA 78-1780] p0067 N78-46537

WAC engine system technology program - An overview [AIAA PAPER 78-928] p0025 N78-44452

The promise of ducted fans for aircraft turbines [NASA-TN-73714] p0012 N78-16098

Aircraft engine emissions --- conference [NASA-CP-2021] p0012 N78-11063

Emissions reduction technology program p0012 N78-11065

Summary of emissions reduction technology program p0013 N78-11071

General aviation piston-engine exhaust emission reduction p0013 N78-11071

SUBJECT INDEX

ALGORITHMS

Global atmospheric sampling program p0013 878-11076
 Stratospheric cruise emission reduction program p0013 878-11077
 Advanced low-NO(x) combustors for supersonic high-altitude gas turbines p0018 878-11078
 Cost benefit study of advanced materials technology for aircraft turbine engines [NASA-CR-135235] p0026 878-11081
 Cost/benefit analysis of advanced material technologies for small aircraft turbine engines [NASA-CR-135265] p0027 878-12083
 An overview of aerospace gas turbine technology of relevance to the development of the automotive gas turbine engine [NASA-TN-73889] p0018 878-13062
 Temperature distributions and thermal stresses in a graded zirconia/metal gas path seal system for aircraft gas turbine engines [NASA-TN-73818] p0015 878-15094
 An analytical study of thermal barrier coated first stage blades in a JT9D engine [NASA-CR-135360] p0028 878-16054
 Analytical study of thermal barrier coated first-stage blades in an F100 engine [NASA-CR-135354] p0028 878-17058
 General aviation energy-conservation research programs at NASA-Lewis Research Center [NASA-TN-73884] p0016 878-17060
 P-15/nonaxisymmetric nozzle system integration study support program [NASA-CR-135252] p0028 878-18070
 Lightweight, low compression aircraft diesel engine -- converting a spark ignition engine to the diesel cycle [NASA-CR-135300] p0121 878-21871
 Impact of future fuel properties on aircraft engines and fuel systems [NASA-TN-74466] p0089 878-24369
 Combustor concepts for aircraft gas turbine low-power emissions reduction [NASA-TN-78875] p0020 878-26141
 ACEE propulsion overview p0004 878-27088
 Propulsion systems noise technology p0001 878-27056
 Advanced materials research for long-haul aircraft turbine engines p0001 878-27057
 Gas turbine engine emission reduction technology program p0001 878-27058
 Impact of broad-specification fuels on future jet aircraft -- engine components and performance p0089 878-27059
 Fuel conservative aircraft engine technology [NASA-TN-78962] p0021 878-27127
 Effect of air temperature and relative humidity at various fuel-air ratios on exhaust emissions on a per-cycle basis of an AVCO Lycoming O-320 diesel light aircraft engine: Volume 1: Results and plotted data [NASA-TN-73507-VOL-1] p0021 878-29100
 Effect of steady flight loads on JT9D-7 performance deterioration [NASA-CR-135407] p0011 878-29105
 Aircraft gas turbine low-power emissions reduction technology program [NASA-CR-135434] p0032 878-32097
 Results and status of the NASA aircraft engine emission reduction technology programs [NASA-TN-79009] p0022 878-34102
 Evaluation of cyclic behavior of aircraft turbine disk alloys [NASA-CR-139833] p0128 878-34478
AIRCRAFT EQUIPMENT
 An airborne meteorological data collection system using satellite relay (ASDAR) [NASA-TN-72992] p0093 878-33284
AIRCRAFT FUEL SYSTEMS
 Oil cooling system for a gas turbine engine [NASA-CR-135121-1] p0113 878-10467
 Alternative aircraft fuels [NASA-TN-73836] p0088 878-17229
AIRCRAFT FUELS
 Propulsion -- NASA program for aircraft fuel consumption reduction p0025 878-48360
 Alternative fuels p0013 878-11074
 Effect of fuel properties on performance of single aircraft turbojet combustor at simulated idle, cruise, and takeoff conditions [NASA-TN-73780] p0018 878-13056
 Development of an experiment for determining the autoignition characteristics of aircraft-type fuels [NASA-CR-135379] p0090 878-16194
 Alternative aircraft fuels [NASA-TN-73836] p0088 878-17229
 Jet aircraft hydrocarbon fuels technology [NASA-CR-2033] p0088 878-19325
 Characteristics and combustion of future hydrocarbon fuels -- aircraft fuels [NASA-TN-78865] p0089 878-24370
AIRCRAFT HERADS
 Simultaneous measurements of ozone outside and inside cabin of two B-747 airliners and a Gates Learjet business jet [NASA-TN-78983] p0009 878-31061
AIRCRAFT INSTRUMENTS
WT ANEMOMETERS
AIRCRAFT NOISE
WT JET AIRCRAFT NOISE
 Propagation of sound waves through a linear shear layer - A closed form solution [AIAA PAPER 76-196] p0165 878-20738
 EBF noise suppression and aerodynamic penalties [NASA-TN-73823] p0163 878-15852
AIRCRAFT PERFORMANCE
WT HELICOPTER PERFORMANCE
 EBF noise suppression and aerodynamic penalties -- Externally Blown Flaps [AIAA PAPER 78-240] p0165 878-70763
 Impact of broad-specification fuels on future jet aircraft -- engine components and performance p0089 878-27059
AIRCRAFT POWER SOURCES
WT AIRCRAFT ENGINES
AIRCRAFT RELIABILITY
 Concepts for the development of light-weight composite structures for rotor burst containment p0012 878-10084
 Turbine disks for improved reliability p0012 878-10089
AIRCRAFT SAFETY
 Lightning protection of aircraft [NASA-SP-1008] p0009 878-11024
AIRCRAFT STRUCTURES
WT AIRFRAMES
AIRFOILS
WT EXTERNALLY BLOWN FLAPS
WT FLAPS (CONTROL SURFACES)
WT PROPELLER BLADES
WT TILTING ROTORS
WT TIP DRIVE ROTORS
WT WING FLAPS
WT WINGS
AIRFRAMES
 Airflow and thrust calibration of an F100 engine, S/N 85A0059, at selected flight conditions [NASA-TN-1069] p0018 878-21112
AIRLINE OPERATIONS
 Global measurements of gaseous and aerosol trace species in the upper troposphere and lower stratosphere from daily flights of B747 airliners p0167 878-15826
AIRSPEED
 On the use of relative velocity experiments for jet engine exhaust noise p0024 878-37683
AIRBORNENESS
WT AIRCRAFT RELIABILITY
AIRBORNENESS REQUIREMENTS
WT AIRCRAFT RELIABILITY
ALARMS
WT WARNING SYSTEMS
ALCOHOLS
WT ETHYL ALCOHOL
WT METHYL ALCOHOL
WT POLYVINYL ALCOHOL
ALGEBRA
WT MATRICES (MATHEMATICS)
WT NONLINEAR EQUATIONS
WT STATE VECTORS
ALGORITHMS
 Diagonal dominance using function minimization

ALIPHATIC COMPOUNDS

algorithms -- multivariable control system design
p0159 A78-16304
Method of fan sound mode structure determination
computer program user's manual: Microphone
location program
[NASA-CR-135294] p0028 W78-17065

ALIPHATIC COMPOUNDS

BT ETHYL ALCOHOL
BT METHYL ALCOHOLS
BT PROPANE
BT TRIOLS

ALKALI HALIDES

BT SODIUM CHLORIDES

ALKALI METAL COMPOUNDS

Formation of Na₂SO₄ and K₂SO₄ in flames doped with
sulfur and alkali chlorides and carbonates
[NASA-TN-73794] p0064 W78-13157

ALKALI METALS

BT CESIUM VAPOR
BT LIQUID LITHIUM
BT LIQUID POTASSIUM

Laser absorption phenomena in flowing gas devices
[NASA-CR-135294] p0112 W78-18411

ALKALINE BATTERIES

Determination of the zincate diffusion coefficient
and its application to alkaline battery problems
[NASA-TN-73879] p0134 W78-19648
Inorganic-organic separators for alkaline batteries
[NASA-CASR-LEU-12649-1] p0136 W78-25530

ALKALINE EARTH METALS

Inhibition of hot salt corrosion by metallic
additives
[NASA-TN-78966] p0072 W78-31208

ALKALINE EARTH OXIDES

BT MAGNESIUM OXIDES

ALKANES

BT PROPANE

ALLOYS

BT ALUMINUM ALLOYS
BT AUSTENITIC STAINLESS STEELS
BT BEARING ALLOYS
BT BINARY ALLOYS
BT BRONZES
BT CARBON STEELS
BT CAST ALLOYS
BT CHROMIUM ALLOYS
BT CHROMIUM STEELS
BT COBALT ALLOYS
BT COPPER ALLOYS
BT EUTECTIC ALLOYS
BT FERRITIC STAINLESS STEELS
BT GERMANIUM ALLOYS
BT HEAT RESISTANT ALLOYS
BT HIGH STRENGTH ALLOYS
BT INDIUM ALLOYS
BT IRON ALLOYS
BT LANTHANUM ALLOYS
BT MARAGING STEELS
BT POLYMER/IRON ALLOYS
BT NICKEL ALLOYS
BT NIOBIUM ALLOYS
BT STAINLESS STEELS
BT STEELS
BT TANTALUM ALLOYS
BT TERNARY ALLOYS
BT TIN ALLOYS
BT TITANIUM ALLOYS
BT TUNGSTEN ALLOYS
BT UDIMET ALLOYS
BT WROUGHT ALLOYS
BT YTTRIUM ALLOYS
BT ZIRCONIUM ALLOYS

Mechanical properties on ion-beam-textured
surgical implant alloys p0075 A78-36045

Thermal fatigue and oxidation data for alloy/braze
combinations [NASA-CR-135299] p0078 W78-16149

Cyclic oxidation of coated Oxide Dispersion
Strengthened (ODS) alloys in high velocity gas
streams at 1100 deg C [NASA-TN-78877] p0071 W78-24336

Effects of thermomechanical processing on strength
and toughness of iron - 12-percent-nickel -
reactive metal alloys at -196 C [NASA-TP-1308] p0073 W78-31213

ALTERNATING CURRENT GENERATORS

U AC GENERATORS

SUBJECT INDEX

ALTERNATORS (GENERATORS)

U AC GENERATORS

ALTITUDE TESTS

Altitude test of several afterburner
configurations on a turbofan engine with a
hydrogen heater to simulate an elevated turbine
discharge temperature [NASA-TP-1068] p0014 W78-11106
Altitude calibration of an F100, S/N P680063,
turbofan engine [NASA-TP-1228] p0019 W78-23095

ALUMINA

U ALUMINUM OXIDES

ALUMINIUM

Experimental transient and permanent deformation
studies of steel-sphere-impacted or
explosively-impulsed aluminum panels
[NASA-CR-135315] p0078 W78-15234
Thermal environment effects on strength and impact
properties of boron-aluminum composites
[NASA-TN-73885] p0058 W78-17155
Evaluation of commercially-available
spacecraft-type heat pipes [NASA-TN-78826] p0103 W78-20459
Friction and wear of selected metals and alloys in
sliding contact with AISI 304 C stainless steel
in liquid methane and in liquid natural gas
[NASA-TP-1150] p0114 W78-20512
Wear of single-crystal silicon carbide in contact
with various metals in vacuum [NASA-TP-1198] p0082 W78-21295
Pressureless sintered Sialons with low amounts of
sintering aid [NASA-TP-1246] p0082 W78-25215
Adhesion of a bimetallic interface --- for Al, Mg,
and Zn [NASA-TN-78890] p0071 W78-29214

ALUMINIUM ALLOYS

Cryogenic properties of a new tough-strong iron
alloy p0073 A78-15825
Comparisor of equivalent energy and energy per
unit area /W bar/A/ data with valid fracture
toughness data for iron, aluminum, and titanium
alloys p0074 A78-24372
Oxide morphology and spalling model for Mill
[NASA-TP-1246] p0075 A78-30112
Investigation of the fracture mechanism of
Ti-5Al-2.5Sn at cryogenic temperatures p0075 A78-32319
Surface-crack shape change in bending fatigue
using an inexpensive resonant fatiguing apparatus
p0075 A78-35394
New alloys to conserve critical elements ---
replacing chromium in steels p0076 A78-37680
The cyclic oxidation resistance of cobalt
chromium-aluminum alloys at 1100 and 1200 C and
a comparison with the nickel-chromium-aluminum
alloy system p0077 A78-50086

Analysis and test of deep flaws in thin sheets of
aluminum and titanium. Volume 1: Program
summary and data analysis [NASA-CR-135369] p0127 W78-21493

Analysis and test of deep flaws in thin sheets of
aluminum and titanium. Volume 2: Crack opening
displacement and stress-strain data [NASA-CR-135370] p0127 W78-21494

Rub tolerance evaluation of two sintered NiCrAl
gas path seal materials --- wear tests of gas
turbine engine seals [NASA-TN-78967] p0071 W78-29215

ALUMINUM BORON/BRIDES

Design of impact-resistant boron/aluminum large
fan blade [NASA-CR-135417] p0031 W78-29104

ALUMINUM BORON COMPOSITES

Thermal environment effects on strength and impact
properties of boron-aluminum composites p0060 A78-33204

Measurement of the time-temperature dependent
dynamic mechanical properties of boron/aluminum
composites p0061 A78-33222

Impact resistant boron/aluminum composites for
large fan blades [NASA-CR-135274] p0062 W78-14099

C-3

5

SUBJECT INDEX

AQUEOUS SOLUTIONS

- ALUMINUM COMPOUNDS**
NT ALUMINUM BOROHYDRIDES
NT ALUMINUM OXIDES
 Development of Sialon materials
 [NASA-CR-135290] p0087 W78-21289
- ALUMINUM HYDRIDES**
NT ALUMINUM BOROHYDRIDES
ALUMINUM OXIDES
 Microstructure of hot-pressed Al₂O₃-Si₃N₄ mixtures
 as a function of holding temperature p0084 A78-17456
 The effect of NaCl/g/ on the Na₂SO₄-induced hot
 corrosion of NiAl p0079 A78-24901
 Oxide morphology and spalling model for NiAl p0075 A78-30112
 Fabrication of thin layer beta alumina p0077 W78-14143
 [NASA-CR-135308]
 High resolution masks for ion milling pores
 through substrates of biological interest p0092 W78-29276
 [NASA-CR-135435]
- AMBIENT TEMPERATURE**
 High temperature environmental effects on metals
 [NASA-TN-73878] p0017 W78-19158
- ANIDES**
NT POLYIMIDES
- ANINES**
NT DIAMINES
- AMPLIFIER**
U ELECTRIC CURRENT
AMPLIFIERS
NT CROSSED FIELD AMPLIFIERS
NT MICROWAVE AMPLIFIERS
- AMPLITUDE MODULATION**
 Carrier-interference ratios for frequency sharing
 between frequency-modulated
 amplitude-modulated-vestigial-sideband
 television systems p0043 W78-28159
 [NASA-TP-1264]
- AMPS (SATELLITE PAYLOAD)**
 The Plasma Interaction Experiment /PIX/ -
 Description and flight qualification test program
 [AIAA PAPER 78-674] p0051 A78-32752
- ANALOG CIRCUITS**
 Measurement of control system response using an
 analog operational circuit p0104 W78-27386
 [NASA-TN-78937]
- ANALOG COMPUTERS**
NT UNIVAC 1100 SERIES COMPUTERS
- ANALOG DATA**
 Instrument to average 100 data sets
 [NASA-TP-1055] p0096 W78-11301
- ANALOG TO DIGITAL CONVERTERS**
 A data acquisition and handling system for the
 measurement of radial plasma transport rates
 [NASA-TN-78849] p0155 W78-23751
- ANALYSIS (MATHEMATICS)**
NT APPROXIMATION
NT FINITE DIFFERENCE THEORY
NT FINITE ELEMENT METHOD
NT INTEGRAL EQUATIONS
NT INTERPOLATION
NT LEAST SQUARES METHOD
NT NONLINEAR EQUATIONS
NT NUMERICAL ANALYSIS
NT NUMERICAL INTEGRATION
NT SINGULARITY (MATHEMATICS)
- ANALYZERS**
NT SIGNAL ANALYZERS
- ANECHOIC CHAMBERS**
 Effectiveness of an inlet flow turbulence control
 device to simulate flight fan noise in an
 anechoic chamber p0024 A78-24880
 Reduction of fan noise in an anechoic chamber by
 reducing chamber wall induced inlet flow
 disturbances p0166 A78-37681
 Effectiveness of an inlet flow turbulence control
 device to simulate flight noise fan in an
 anechoic chamber p0163 W78-13856
 [NASA-TN-73855]
 Reduction of fan noise in an anechoic chamber by
 reducing chamber wall induced inlet flow
 disturbances p0164 W78-22860
 [NASA-TN-78854]
- ANEMOMETERS**
 Miniature drag force anemometer p0109 A78-17397
- ANEMOMETRY**
U VELOCITY MEASUREMENT
- ANESTHETICS**
NT ETHYL CHLORIDE
- ANIONS**
 Anion exchange membranes for electrochemical
 oxidation-reduction energy storage system
 [NASA-TN-73751] p0131 W78-14631
 Anion permeable membrane
 [NASA-CR-135316] p0144 W78-18515
- ANISOTROPIC PLATES**
 Impact on multilayered composite plates
 [NASA-CR-135247] p0062 W78-16103
- ANNEALING**
 The influence of composition, annealing treatment,
 and texture on the fracture toughness of
 Ti-5Al-2.5Sn plate at cryogenic temperatures
 [NASA-TN-73872] p0069 W78-15235
 The design of an Fe-12Ni-0.2Ti alloy steel for low
 temperature use p0078 W78-20310
 [NASA-CR-135310]
- ANNULAR FLOW**
 End-wall boundary layer prediction for axial
 compressors p0007 A78-45133
 [AIAA PAPER 78-1139]
 Performance characteristics of two annular dump
 diffusers using suction-stabilized vortex flow
 control p0004 W78-19057
 [NASA-TN-73857]
- ANNULAR NOZZLES**
 An empirical model for inverted-velocity-profile
 jet noise prediction p0023 A78-28879
 Performance characteristics of two annular dump
 diffusers using suction-stabilized vortex flow
 control p0107 A78-45431
 Performance of a short annular dump diffuser using
 suction-stabilized vortices at inlet Mach
 numbers to 0.41 p0017 W78-20131
 [NASA-TP-1194]
 Wind tunnel performance tests of conical plug
 nozzles --- in the Langley 8 x 6 ft. supersonic
 wind tunnel p0002 W78-21044
 [NASA-CR-2990]
 Flight effects on the aerodynamic and acoustic
 characteristics of inverted profile conical
 nozzles, volume 1 --- supersonic cruise aircraft
 research wind tunnel tests p0167 W78-29867
 [NASA-CR-135189-VOL-1]
 Flight effects on the aerodynamic and acoustic
 characteristics of inverted profile conical
 nozzles, volume 2 --- supersonic cruise aircraft
 research wind tunnel tests p0167 W78-29868
 [NASA-CR-135189-VOL-2]
 Flight effects on the aerodynamic and acoustic
 characteristics of inverted profile conical
 nozzles, volume 3 --- supersonic cruise aircraft
 research wind tunnel tests p0167 W78-29869
 [NASA-CR-135189-VOL-3]
- ANTENNAS**
NT AIRCRAFT ANTENNAS
- ANTI-FRICTION BEARINGS**
NT BALL BEARINGS
NT ROLLER BEARINGS
- ANTIREFLECTION COATINGS**
 Evaluation of glass resin coatings for solar cell
 applications p0145 W78-27540
 [NASA-CR-159392]
- APPLICATIONS OF MATHEMATICS**
 Method of fan sound mode structure determination
 computer program user's manual: Modal
 calculation program p0028 W78-17066
 [NASA-CR-135295]
- APPROXIMATION**
NT FINITE DIFFERENCE THEORY
NT FINITE ELEMENT METHOD
NT LEAST SQUARES METHOD
 The application of the Routh approximation method
 to turbofan engine model: p0023 A78-23891
 Applied Routh approximation
 [NASA-TP-1231] p0091 W78-22257
- APPROXIMATION METHODS**
U APPROXIMATION
- AQUEOUS SOLUTIONS**
 Release of dissolved nitrogen from water during
 depressurization p0065 W78-17172
 [NASA-TN-73822]

ARC DISCHARGES

SUBJECT INDEX

ARC DISCHARGES

A sustained-arc ignition system for internal combustion engines
[NASA-TN-73833] p0096 W78-13331

ARCOU
12-cm magneto-electrostatic containment argon/neon ion source development
[NASA PAPER 78-681] p0039 A78-32756

ARCOU FLASHS
Preliminary results on the conversion of laser energy into electricity p0173 A78-34631

ARID (IMPACT PREDICTION)
U COMPUTERIZED SIMULATION
ARIZONA
Design and fabrication of a photovoltaic power system for the Papago Indian village of Schuchali (Sunlight), Arizona
[NASA-TN-78948] p0139 W78-26555

ARRAYS
BT PHASED ARRAYS
BT SOLAR ARRAYS
Status of wraparound contact solar cells and arrays
[NASA-TN-78911] p0177 W78-26543

ARTIFICIAL SATELLITES
BT ATS 1
BT ATS 3
BT ATS 5
BT ATS 6
BT COMMUNICATION SATELLITES
BT COMMUNICATIONS TECHNOLOGY SATELLITE
BT METEOROLOGICAL SATELLITES
BT SOLAR SATELLITES
BT SYNCHROUS SATELLITES
Design, fabrication and testing of a CFA for use in the solar power satellite
[NASA-CN-159410] p0042 W78-31143

ASPECT RATIO
BT LOW ASPECT RATIO

ASSEMBLING
DOE LERC photovoltaic systems test facility
[NASA-TN-78923] p0138 W78-26549

ASSESSMENTS
BT TECHNOLOGY ASSESSMENT
ASTROLOGY (TRANSMISSION)
Interpolation and extrapolation of creep rupture data by the minimum commitment method. II - Oblique translation p0076 A78-45426
Manufacture of astroloy turbine disk shapes by hot isostatic pressing, volume 1
[NASA-CN-135409] p0079 W78-25166

ASTRONOMICAL MODELS
Charging characteristics of materials: Comparison of experimental results with simple analytical models p0036 W78-10157

ATMOSPHERIC AND MAGNETOSPHERIC PAYLOAD
U ASFS (SATELLITE PAYLOAD)
ATMOSPHERIC CHEMISTRY
Measurement of tropospheric 300 nm solar ultraviolet flux for determination of O₃/D₀ photoproduction rate p0148 A78-38835

ATMOSPHERIC COMPOSITION
Description and review of global measurements of atmospheric species from GASP p0148 A78-24893
Atmospheric ozone measurements made from B-747 airliners - Spring 1975 p0148 A78-24894
Ultraviolet spectrophotometer for measuring columnar atmospheric ozone from aircraft p0110 A78-35826
The fluorination of cobalt and zinc
[NASA-TN-X-73478] p0064 W78-15211
Simultaneous measurements of ozone outside and inside cabins of two B-747 airliners and a Gates Learjet business jet
[NASA-TN-78983] p0009 W78-31061

ATMOSPHERIC EFFECTS
Atmospheric effects on inlets for supersonic cruise aircraft
[NASA-TN-X-73647] p0003 W78-10026

ATMOSPHERIC IMPURITIES
U AIR POLLUTION
ATMOSPHERIC MODELS
BT BREADBOARD MODELS
BT DYNAMIC MODELS

Models for some aspects of atmospheric vortices p0150 A78-14581

ATMOSPHERIC IRRADIATION

BT WHISTLERS

ATMOSPHERIC TEMPERATURE

Effect of air temperature and relative humidity at various fuel-air ratios on exhaust emissions on a per-mode basis of an ATCO Lycoming O-320 diad light aircraft engine: Volume 1: Results and plotted data
[NASA-TN-73507-VOL-1] p0021 W78-29100

ATMOSPHERIC TUBULANCE

BT GUSTS

Models for some aspects of atmospheric vortices p0150 A78-14581

ATMOSPHERICS

BT AISS

BT WHISTLERS

ATOM CONCENTRATION

Atomic hydrogen storage method and apparatus --- cryotrapping and magnetic field strength
[NASA-CN-288-12081-2] p0169 W78-19907

ATOMIC GASES

U NONATOMIC GASES

ATOMIZATION

U ATOMIZING

ATOMISING

BT LIQUID ATOMIZATION

Effect of airstream velocity on mean drop diameters of water sprays produced by pressure and air atomizing nozzles --- for combustion studies p0024 A78-33111

ATOMS

BT HYDROGEN ATOMS

BT OXYGEN ATOMS

ATS

BT ATS 1

BT ATS 3

BT ATS 5

BT ATS 6

ATS 1

Continuation of the compendium of applications technology satellite and communications technology satellite user experiments 1967-1977, volume 1
[NASA-CN-135416-VOL-1] p0042 W78-31141

Continuation of the compendium of applications technology satellite and communications technology satellite user experiments 1967-1977, volume 2 --- bibliography
[NASA-CN-135416-VOL-2] p0042 W78-31142

ATS 3

Continuation of the compendium of applications technology satellite and communications technology satellite user experiments 1967-1977, volume 2 --- bibliography
[NASA-CN-135416-VOL-2] p0042 W78-31142

ATS 5

Active control of spacecraft charging on ATS-5 and ATS-6 p0036 W78-10136

Continuation of the compendium of applications technology satellite and communications technology satellite user experiments 1967-1977, volume 1
[NASA-CN-135416-VOL-1] p0042 W78-31141

Continuation of the compendium of applications technology satellite and communications technology satellite user experiments 1967-1977, volume 2 --- bibliography
[NASA-CN-135416-VOL-2] p0042 W78-31142

ATS 6

Active control of spacecraft charging on ATS-5 and ATS-6 p0036 W78-10136

Continuation of the compendium of applications technology satellite and communications technology satellite user experiments 1967-1977, volume 1
[NASA-CN-135416-VOL-1] p0042 W78-31141

Continuation of the compendium of applications technology satellite and communications technology satellite user experiments 1967-1977, volume 2 --- bibliography
[NASA-CN-135416-VOL-2] p0042 W78-31142

ATTACK AIRCRAFT

BT B-57 AIRCRAFT

BT F-15 AIRCRAFT

- NT P-100 AIRCRAFT
 NT P-102 AIRCRAFT
 NT TP-12 AIRCRAFT
ATTENUATION
 NT ACOUSTIC ATTENUATION
 Methods of attenuating wind turbine ac generator
 output variations p0133 W78-19632
ATTENUATORS
 Use of a simple external nonreciprocal attenuator
 in coupled-cavity TWT's p0098 A78-10282
ATTITUDE (INCLINATION)
 Variation of solar cell sensitivity and solar
 radiation on tilted surfaces
 [NASA-TN-78921] p0130 W78-26547
ATTITUDE STABILITY
 Provisional specification for satellite time in a
 geomagnetic environment p0036 W78-10173
ABRITION (MATERIALS)
 U COMBUSTION
AUDIO EQUIPMENT
 NT MICROPHONES
AUSTENITIC STAINLESS STEELS
 Substitution for chromium in 304 stainless steel
 --- effects on oxidation and corrosion resistance
 p0077 A78-51714
AUTOCALVING
 Effect of processing parameters on autoclaved PBR
 polyimide composites p0060 A78-25191
 Strength enhancement process for prealloyed powder
 superalloys p0075 A78-33216
AUTOCOLLIMATORS
 U COLLIMATORS
AUTOMATIC CONTROL
 NT ADAPTIVE CONTROL
 NT FEEDBACK CONTROL
 NT NUMERICAL CONTROL
 NT OFF-ON CONTROL
 NT OPTIMAL CONTROL
 NT TIME OPTIMAL CONTROL
 Automated meteorological data from commercial
 aircraft via satellite: Present experience and
 future implications p0150 W78-17558
 Method for producing solar energy panels by
 automation
 [NASA-CASE-LEU-12541-1] p0136 W78-25529
AUTOMATIC CONTROL VALVES
 NT PRESSURE REGULATORS
 NT RELIEF VALVES
AUTOMATIC DATA PROCESSING
 U DATA PROCESSING
AUTOMATIC ROCKET IMPACT PREDICTORS
 U COMPUTERIZED SIMULATION
AUTOMATIC TEST EQUIPMENT
 Sound separation probes for flowing duct noise
 measurements --- jet engine diagnostics
 p0033 A78-17396
 Instrumentation for propulsion systems development
 --- high speed fans and turbines
 [NASA-TN-73840] p0011 W78-17052
AUTOMOBILE ENGINES
 An overview of aerospace gas turbine technology of
 relevance to the development of the automotive
 gas turbine engine p0120 A78-33364
 [SAE PAPER 790075]
 Experimental evaluation of fuel preparation
 systems for an automotive gas turbine catalytic
 combustor p0120 A78-37677
 An overview of aerospace gas turbine technology of
 relevance to the development of the automotive
 gas turbine engine p0014 W78-13062
 [NASA-TN-73849]
 Improved ceramic heat exchanger material
 [NASA-CR-135492] p0086 W78-13209
 Performance and emissions of a catalytic reactor
 with propane, diesel, and Jet A fuels
 [NASA-TN-73786] p0088 W78-14177
 Cold-air performance of free-power turbine
 designed for 112-kilowatt automotive gas-turbine
 engine. 1: Design Stator-vane-chord setting
 angle of 35 deg p0015 W78-16053
 [NASA-TP-1007]
 Hydrodynamic air lubricated compliant surface
 bearing for an automotive gas turbine engine.
 1: Journal bearing performance
 [NASA-CN-135366] p0121 W78-21472
 Experimental evaluation of fuel preparation
 systems for an automotive gas turbine catalytic
 combustor p0082 W78-22243
 [NASA-TN-78856]
 Automotive Stirling engine development program ---
 fuel economy assessment
 [NASA-CN-135331] p0181 W78-22970
 Automotive gas turbine fuel control p0115 W78-24545
 [NASA-CASE-LEU-12785-1]
 Cold-air performance of the compressor-drive
 turbine of the Department of Energy baseline
 automobile gas-turbine engine p0005 W78-26090
 [NASA-TN-78694]
 Ceramic regenerator systems development program
 [NASA-CN-135430] p0181 W78-26997
 Hydrodynamic air lubricated compliant surface
 bearing for an automotive gas turbine engine.
 2: Materials and coatings p0122 W78-29449
 [NASA-CN-135402]
 Gas turbine project status p0091 W78-30303
 Stirling engine project status p0117 W78-30314
 Initial test results with single cylinder rhombic
 drive Stirling engine p0117 W78-30316
 Materials technology assessment for Stirling engines
 p0117 W78-30318
 Initial test results with a single-cylinder
 rhombic-drive Stirling engine --- to be applied
 to automobile engine design to conserve energy
 [NASA-TN-78919] p0140 W78-31533
AUTOMOBILES
 NT ELECTRIC AUTOMOBILES
 Making aerospace technology work for the
 automotive industry - Introduction p0181 A78-33359
 Renault 5
 Baseline tests of the C. H. Waterson
 electric passenger vehicle p0178 W78-16928
 [NASA-TN-72759]
 Making aerospace technology work for the
 automotive industry, introduction p0179 W78-17941
 [NASA-TN-73870]
 Ceramic regenerator systems development program
 --- for automobile gas turbine engines p0181 W78-25988
 [NASA-CN-135330]
 State-of-the-art assessment of electric and hybrid
 vehicles p0180 W78-27003
 [NASA-TN-79509]
 Catalytic combustion for the automotive gas
 turbine engine p0092 W78-30333
AUXILIARY POWER SOURCES
 NT SPACE POWER REACTORS
AUXILIARY PROPULSION
 Planned flight test of a mercury ion auxiliary
 propulsion system. I - Objectives, systems
 descriptions, and mission operations p0050 A78-32734
 [AIAA PAPER 78-647-I]
 Planned flight test of a mercury ion auxiliary
 propulsion system. II - Integration with host
 spacecraft p0050 A78-32735
 [AIAA PAPER 78-647-II]
 Evolution of the 1-1/2 mercury ion thruster
 subsystem p0051 A78-32776
 [NASA PAPER 78-7118]
 Planned flight test of a mercury ion auxiliary
 propulsion system. 1: Objectives, systems
 descriptions, and mission operations p0047 W78-21204
 [NASA-TN-78859]
 Planned flight test of a mercury ion auxiliary
 propulsion system. Part 2: Integration with
 host spacecraft p0048 W78-21209
 [NASA-TN-78864]
AXIAL COMPRESSORS
 U TURBOCOMPRESSORS
AXIAL FLOW
 Computation of unsteady transonic flow through
 rotating and stationary cascades. 1: Method of
 analysis p0008 W78-20082
 [NASA-CN-2900]
AXIAL FLOW COMPRESSORS
 U TURBOCOMPRESSORS
AXIAL FLOW PUMPS
 NT TURBINE PUMPS

AXIAL FLOW TURBINES

- Liquid rocket engine axial-flow turbopumps
[NASA-SP-8125] p0050 W78-31164
- AXIAL FLOW TURBINES**
- Design and performance of a
427-meter-per-second-tip-speed two-stage fan
having a 2.80 pressure ratio
[NASA-TP-1314] p0022 W78-33109
- AXIAL STRAIN**
- The effects of eccentricities on the fracture of
off-axis fiber composites --- carbon fiber
reinforced plastics
[NASA-TN-73826] p0057 W78-17153
- AXIAL STRESS**
- The effects of eccentricities on the fracture of
off-axis fiber composites --- carbon fiber
reinforced plastics
[NASA-TN-73826] p0057 W78-17153
- Axial residual stresses in boron fibers
[NASA-TN-73894] p0058 W78-19204
- AXISYMMETRIC DEFORMATION**
- U AXIAL STRAIN**
- AXISYMMETRIC FLOW**
- U AXIPLANAR FLOW**
- AXLES**
- U SHAFTS (MACHINE ELEMENTS)**

B

- B-57 AIRCRAFT**
- An improved technique for the calibration of solar
cells using a high altitude aircraft
[NASA-TN-78871] p0138 W78-26546
- BALANCING**
- Balancing techniques for high-speed flexible rotors
[NASA-CR-2975] p0121 W78-20514
- BALL BEARINGS**
- Rolling-element fatigue life of A57-785 corrosion
resistant, high temperature bearing steel
[ASME PAPER 77-LUB-30] p0075 A78-28423
- Statistical model for asperity-contact time
fraction in elastohydrodynamic lubrication
[NASA-TP-1130] p0194 W78-18429
- Predicted and experimental performance of
jet-lubricated 120-millimeter-bore ball bearings
operating to 2.5 million CM
[NASA-TP-1196] p0114 W78-20513
- Rolling-element fatigue life of AISI M-50 and
18-8-1 balls
[NASA-TP-1202] p0115 W78-21473
- Some effects of composition on friction and wear
of graphite-fiber-reinforced polyimide liners in
plain spherical bearings
[NASA-TP-1229] p0115 W78-25433
- Some load limits and self-lubricating properties
of plain spherical bearings with sintered graphite
fiber reinforced polyimide liners to 320 C
[NASA-TN-78935] p0116 W78-26445
- Filtration effects on ball bearing life and
condition in a contaminated lubricant
[NASA-TN-78907] p0116 W78-26446
- Graphite-fiber-reinforced polyimide liners of
various compositions in plain spherical bearings
[NASA-TN-78908] p0116 W78-26447
- BALLS**
- Characterization of wear debris generated in
accelerated rolling-element fatigue tests
[NASA-TP-1203] p0115 W78-21470
- BAND STRUCTURE OF SOLIDS**
- Physics and chemistry of MoS₂ intercalation
compounds
p0175 A78-27727
- BANDWIDTH**
- U SPECTRAL LINE WIDTH**
- BAWG-JAWG CONTROL**
- U OFF-ON CONTROL**
- BARRIER APPROXIMATION**
- U BARRIER LAYERS**
- U ELECTRICAL PROPERTIES**
- U SURFACE PROPERTIES**
- BARRIER LAYERS**
- Feasibility study of tungsten as a diffusion
barrier between nickel-chromium-aluminum and
Gamma/Gamma prime - Delta eutectic alloys
[NASA-TP-1131] p0068 W78-5230
- BASES (FOUNDATIONS)**
- U FOUNDATIONS**
- BATTERIES**
- U ELECTRIC BATTERIES**

SUBJECT INDEX

- BATTERY CHARGERS**
- Pulse battery charger employing 1000 ampere
transistor switches
p0145 A78-31974
- BATTERY SEPARATORS**
- U SEPARATORS**
- BEAMS (RADIATION)**
- U ELECTRON BEAMS**
- U ION BEAMS**
- U NEUTRAL BEAMS**
- BEAMS (SUPPORTS)**
- Nonlinear flap-lag-axial equations of a rotating
beam with arbitrary precone angle
[AIAA 78-491] p0127 A78-29798
- BEARING BELLOWS**
- Rolling-element fatigue life of AMS 5749 corrosion
resistant, high temperature bearing steel
[ASME PAPER 77-LUB-30] p0075 A78-28423
- Long-term hot-hardness characteristics of five
through-hardened bearing steels
[NASA-TP-1341] p0073 W78-33196
- Rolling element fatigue testing of gear materials
[NASA-CR-135450] p0124 W78-33463
- BEARINGS**
- U BALL BEARINGS**
- U FOIL BEARINGS**
- U GAS BEARINGS**
- U JOURNAL BEARINGS**
- U ROLLER BEARINGS**
- U THRUST BEARINGS**
- Bearing, gearing, and lubrication technology
[SAE PAPER 780077] p0120 A78-33366
- Bearing, gearing, and lubrication technology
[NASA-TN-73851] p0114 W78-17389
- Emergency and microfog lubrication and cooling of
bearings for Army helicopters
[NASA-CR-135195] p0122 W78-27429
- Effect of geometry on hydrodynamic film thickness
[NASA-TP-1287] p0117 W78-30585
- BEAT**
- U SYNCHRONISM**
- BELLOWS**
- Liquid rocket lines, bellows, flexible hoses, and
filters
[NASA-SP-8123] p0047 W78-16089
- BENDING FATIGUE**
- Effect of wall thickness and material on flexural
fatigue of hollow rolling elements
[ASME PAPER 77-LUB-14] p0126 A78-23355
- Load-displacement measurement and work
determination in three-point bend tests of
notched or precracked specimens
p0089 A78-24370
- Comparison of equivalent energy and energy per
unit area /W bar/A/ data with valid fracture
toughness data for iron, aluminum, and titanium
alloys
p0074 A78-24372
- Surface-crack shape change in bending fatigue
using an inexpensive resonant fatiguing apparatus
p0075 A78-35394
- BENDING VIBRATION**
- Unsteady flow in a supersonic cascade with strong
in-passage shocks
p0006 A78-17270
- BERYLLIUM**
- Friction and wear of selected metals and alloys in
sliding contact with AISI 440 C stainless steel
in liquid methane and in liquid natural gas
[NASA-TP-1150] p0114 W78-20512
- Titanium/beryllium laminates: Fabrication,
mechanical properties, and potential aerospace
applications
[NASA-TN-73891] p0059 W78-21221
- BIBLIOGRAPHIES**
- Bibliography of Lewis Research Center technical
contributions announced in 1976
[NASA-TN-73860] p0177 W78-17921
- Bibliography of Lewis Research Center technical
publications announced in 1977
[NASA-TN-78918] p0177 W78-28986
- Continuation of the compendium of applications
technology satellite and communications
technology satellite user experiments 1967-1977,
volume 2 --- bibliography
[NASA-CR-135416-VOL-2] p0042 W78-31142
- BICARBONATES**
- U CARBONATES**

SUBJECT INDEX

BOUNDARY VALUE PROBLEMS

BIMETALS
Adhesion of a bimetallic interface --- for Al, Mg, and Cu [NASA-TN-78890] p0071 N78-29210

BINARY ALLOYS
Some properties of low-vapor-pressure braze alloys for thermionic converters [NASA-TN-78867] p0130 N78-22471

BINARY MIXTURES
BT EUTECTIC ALLOYS
BT EUTECTICS

BINARY SYSTEMS (DIGITAL)
D DIGITAL SYSTEMS

BINARY SYSTEMS (MATERIALS)
BT BINARY ALLOYS
BT EUTECTIC ALLOYS
BT EUTECTICS

BIOENGINEERING
BT BIOINSTRUMENTATION

BIOINSTRUMENTATION
BT IMPLANTED ELECTRODES (BIOLOGY)
The use of an ion-beam source to alter the surface morphology of biological implant materials [NASA-TN-78866] p0061 A78-37686

BIOLOGICAL EFFECTS
The use of an ion-beam source to alter the surface morphology of biological implant materials [NASA-TN-78851] p0152 N78-22618

BIOSENSORS
U BIOINSTRUMENTATION

BIPROPELLANTS
U LIQUID ROCKET PROPELLANTS

BLACKOUT (PROPAGATION)
BT HISS
BT SHOT NOISE
BT WHISTLERS

BLADE TIPS
A parasitic investigation of an existing supersonic relative tip speed propeller noise model --- turbo-prop airplane [NASA-TN-78116] p0163 N78-13850
In-place recalibration technique applied to a capacitance-type system for measuring rotor blade tip clearance [NASA-TP-1110] p0019 N78-22161
Advanced optical blade tip clearance measurement system [NASA-CR-159402] p0032 N78-31106
Compressor seal rub energetics study [NASA-CR-159426] p0032 N78-32096

BLADES
Impact absorbing blade mounts for variable pitch blades [NASA-CASE-LHN-12313-1] p0113 N78-10469
Impact behavior of filament wound graphite/epoxy fan blades [NASA-TN-78805] p0016 N78-22097

BLADES (CUTTERS)
Tissue macerating instrument [NASA-CASE-LHN-12068-1] p0153 N78-10773

BLASTOFF
U ROCKET LAUNCHING

BLEED-OFF
U PRESSURE REDUCTION

BLOW FLAPS
U EXTERNALLY BLOWN FLAPS

BODIES OF REVOLUTION
BT CYLINDRICAL BODIES

BORING AIRCRAFT
BT BOEING 747 AIRCRAFT

BOEING 747 AIRCRAFT
Atmospheric ozone measurements made from B-747 airliners - Spring 1975 p0146 A78-24890

BOILING
BT FILM BOILING
BT LEIDENFROST PHENOMENON
BT NUCLEATE BOILING
Boiling incidence and convective boiling of neon and nitrogen p0105 A78-15820
Conceptual design for spacelab pool boiling experiment [NASA-CR-135178] p0037 N78-20150

BOMBARDMENT
Sensitivity of 30-cs mercury bombardment ion thruster characteristics to accelerator grid design [NASA-TN-78861] p0049 A78-21140

BOMBEN AIRCRAFT
BT B-57 AIRCRAFT
BT F-100 AIRCRAFT

BONDING
BT ADHESIVE BONDING
BT METAL BONDING
BT METAL-METAL BONDING

BORIDES
Friction and wear of radiofrequency-sputtered borides, silicides, and carbides [NASA-TP-1156] p0081 N78-20338
Cesium thermionic converters having improved electrodes [NASA-CASE-LHN-12038-3] p0137 N78-25555

BORON
BT ALUMINUM BOROHYDRIDES

BORON
Mechanical and physical properties of modern boron fibers p0085 A78-33206
Mechanical and physical properties of modern boron fibers [NASA-TN-73682] p0058 N78-17158

BORON COMPOUNDS
BT ALUMINUM BOROHYDRIDES

BORON HYDRIDES
BT ALUMINUM BOROHYDRIDES

BORON REINFORCED MATERIALS
In situ ply strengths - An initial assessment p0061 A78-33223
Mechanical and physical properties of modern boron fibers [NASA-TN-73682] p0058 N78-17158
Thermal environment effects on strength and impact properties of boron-aluminum composites [NASA-TN-73885] p0058 N78-17155
Tial residual stresses in boron fibers [NASA-TN-73898] p0058 N78-19208
Measurement of the time-temperature dependent dynamic mechanical properties of boron/aluminum composites [NASA-TN-78837] p0058 N78-20254

BOSONS
BT PROTONS

BOUNDARIES
BT FREE BOUNDARIES
BT GAS-SOLID INTERFACES
BT LIQUID-SOLID INTERFACES

BOUNDARY LAYER CONTROL
Development and test of an inlet and duct to provide airflow for a wing boundary layer control system [AIAA PAPER 73-141] p0006 A78-20701

BOUNDARY LAYER FLOW
BT BOUNDARY LAYER SEPARATION
BT SECONDARY FLOW
Velocity and temperature profiles in near-critical nitrogen flowing past a horizontal flat plate [AIAA PAPER 77-87-7] p0106 A78-17681
Turbulence processes and simple closure schemes p0107 A78-40983
Flow of liquid jets through closely woven screens p0108 A78-42877
Design of an air ejector for boundary-layer bleed of an acoustically treated turbofan engine inlet during ground testing [NASA-TN-78917] p0037 N78-27113

BOUNDARY LAYER NOISE
U AERODYNAMIC NOISE
U BOUNDARY LAYERS

BOUNDARY LAYER SEPARATION
Methods for calculating the transonic boundary layer separation for V/STOL inlets at high incidence angles [AIAA 78-1340] p0007 A78-46537

BOUNDARY LAYERS
BT THREE DIMENSIONAL BOUNDARY LAYER
BT TURBULENT BOUNDARY LAYER
Boundary layer analysis of a Centaur standard shroud [NASA-TN-78883] p0103 N78-21804
End-wall boundary layer prediction for axial compressors [NASA-TN-78928] p0020 N78-26104

BOUNDARY VALUE PROBLEMS
The use of parabolic variations and the direct determination of stress intensity factors using the BIE method --- Boundary Integral Equation p0126 A78-24903

SUBJECT INDEX

CONTENTS

- Three-dimensional effects on pure tone fan noise due to inflow distortion
[AIAA PAPER 78-1120] p0166 78-41830
- Effect of coolant flow ejection on aerodynamic performance of low-aspect-ratio vanes. 2: Performance with coolant flow ejection at temperature ratios up to 2
[NASA-TP-1057] p0003 78-11008
- Computation of unsteady transonic flow through rotating and stationary cascades. 1: Method of analysis
[NASA-CR-2900] p0008 78-20082
- Two-dimensional cold-air cascade study of a film-cooled turbine stator blade. 8:
Comparison of experimental and analytical aerodynamic results for blade with 12 rows of 0.076-centimeter-(0.030-inch) diameter holes having streamwise ejection angles
[NASA-TP-1151] p0017 78-20130
- Two-dimensional cold-air cascade study of a film-cooled turbine stator blade. 5:
Comparison of experimental and analytical aerodynamic results for blade with 12 rows of 0.038-centimeter-(0.015 inch) diameter coolant holes having streamwise ejection angles
[NASA-TP-1204] p0017 78-20133
- CASCADE WIND TUNNELS
Effect of cooling-hole geometry on aerodynamic performance of a film-cooled turbine vane tested with cold air in a two-dimensional cascade
[NASA-TP-1136] p0004 78-20080
- CASCADES
Computation of unsteady transonic flows through rotating and stationary cascades. 2: User's guide to FORTRAN program B2DATA
[NASA-CR-2901] p0007 78-12034
- CAST ALLOYS
Effects of silicon on the oxidation, hot-corrosion, and mechanical behavior of two cast nickel-base superalloys
p0074 78-21439
- Volume fraction determination in cast superalloys and directionally solidified eutectic alloys by a new manual point count practice
p0089 78-24369
- CASTING
Shape of two-dimensional solidification interface during directional solidification by continuous casting
p0119 78-31829
- CASTING SOLVENTS
O PLASTICIZERS
- CATALYSIS
Experimental evaluation of fuel preparation systems for an automotive gas turbine catalytic combustor
p0120 78-37677
- CATALYSTS
Performance and emissions of a catalytic reactor with propane, diesel, and Jet A fuels
[NASA-TN-73786] p0088 78-14177
- Experimental evaluation of fuel preparation systems for an automotive gas turbine catalytic combustor
[NASA-TN-78856] p0382 78-22243
- Catalytic combustion for the automotive gas turbine engine
p0092 78-30333
- CATALYTIC ACTIVITY
Experimental evaluation of premixing-prevaporizing fuel injection concepts for a gas turbine catalytic combustor
[NASA-TN-73755] p0101 78-14313
- Catalytic decomposition of methanol for onboard hydrogen generation
[NASA-TP-1247] p0083 78-25236
- Effect of inlet temperature on the performance of a catalytic reactor --- air pollution control
[NASA-TN-78977] p0141 78-31534
- CATHODES
HT HOLLOW CATHODES
Noise as a tool for evaluating the activation of cathodes
[NASA-TN-73895] p0096 78-17298
- CATIONS
HT METAL IONS
- CAVITY RESONATORS
Use of a simple external nonreciprocal attenuator in coupled-cavity TWT's
- CELESTIAL DYNAMICS
HT BALLETT'S COMET
CENTRO-LAUNCH VEHICLE
ADJUST - An automated system for steering Centaur launch vehicles in measured winds
p0098 78-16282
p0085 78-14991
- CESTRA
Boundary layer analysis of a Centaur standard shroud
[NASA-TN-78843] p0103 78-21404
- CENTRAUR VEHICLE
O CENTRAUR LAUNCH VEHICLE
CENTRAL PROCESSING UNITS
Electric prototype power processor for a 30cm ion thruster
[NASA-CR-135287] p0054 78-19200
- CENTRIFUGAL COMPRESSORS
Calculation of 3-dimensional choking mass flow in turbomachinery with 2-dimensional flow models
p0006 78-12289
- Splitter-bladed centrifugal compressor impeller designed for automotive gas turbine application --- at the Lewis Research Center
[NASA-CR-135237] p0121 78-10472
- Experimental performance of a 13.6-centimeter-tip-diameter tandem-bladed sweepback centrifugal compressor designed for a pressure ratio of 6
[NASA-TP-1091] p0003 78-11002
- CENTRIFUGAL FORCE
Counter pumping debris excluder and separator --- gas turbine shaft seals
[NASA-CR-LEW-11855-1] p0020 78-25090
- CERAMAL PROTECTIVE COATINGS
O PROTECTIVE COATINGS
- CERAMIC COATINGS
Development of a plasma sprayed ceramic gas path seal for high pressure turbine application
[NASA-CR-135387] p0030 78-24141
- Emission and absorptance of NASA ceramic thermal barrier coating system --- for turbine cooling
[NASA-TP-1190] p0020 78-26148
- Investigation of the effect of ceramic coatings on rocket thrust chamber life
[NASA-TN-78892] p0049 78-26173
- CERAMICS
Directionally solidified ceramic eutectics
p0084 78-11547
- Improved performance of silicon nitride-based high temperature ceramics
p0087 78-24881
- Consolidation of silicon nitride without additives --- for gas turbine engine efficiency increase
p0085 78-24895
- Ceramics in gas turbines - Powder and process characterization
p0085 78-29328
- High temperature compressive cracking in hot-pressed silicon nitride
p0085 78-36706
- Pressureless sintered beta-prime-Si3N4 solid solution - Fabrication, microstructure, and strength
p0086 78-47595
- Substitution of ceramics for high temperature alloys
p0086 78-47596
- Consolidation of silicon nitride without additives
[NASA-TN-73693] p0057 78-10217
- Improved ceramic heat exchange material
[NASA-CR-135262] p0086 78-10291
- Improved performance of silicon nitride-based high temperature ceramics
[NASA-TN-73719] p0080 78-10294
- Improved ceramic heat exchanger material
[NASA-CR-135292] p0086 78-13209
- Ceramics in gas turbine: Powder and process characterization
[NASA-TN-73875] p0016 78-17059
- Development of SiAlON materials
[NASA-CR-135290] p0087 78-21289
- Pressureless sintered SiAlONs with low amounts of sintering aid
[NASA-TP-1246] p0082 78-25215
- Ceramic regenerator systems development program --- for automobile gas turbine engines
[NASA-CR-135330] p0181 78-25988
- Ceramic regenerator systems development program
[NASA-CR-135430] p0181 78-26997

- Study and program plan for improved heavy duty gas turbine engine ceramic component development (NASA-CN-135239) p0122 178-28266
- Substitution of ceramics for high temperature alloys --- advantages of using silicon carbide and silicon nitride in gas turbine engines (NASA-TN-78831) p0088 178-29246
- Materials technology assessment for Stirling engines p0117 178-30318
- Advanced ceramic material for high temperature turbine tip seals (NASA-CN-135319) p0087 178-31230
- CBSIUM**
BT CERION VAPOR
CERION SIEMENS
 Experiments with enhanced soda thermionic converters p0146 178-29636
- CBSIUM VAPOR**
 Cesium thermionic converters having improved electrodes (NASA-CN-135319) p0137 178-25555
- CFRP**
U CARBON FIBER REINFORCED PLASTICS
CHARCOALINIDES
WT ALUMINUM OXIDES
WT CARBON MONOXIDE
WT CEROSITES
WT CERONION OXIDES
WT COPPER SULFIDES
WT DISULFIDES
WT MAGNESIUM OXIDES
WT NITRAL OXIDES
WT NOLYDENUM DISULFIDES
WT NOLYDENUM SULFIDES
WT NITRIC OXIDE
WT NITROGEN OXIDES
WT OXIDES
WT SILICON DIOXIDE
WT SULFIDES
WT ZIRCONIUM OXIDES
- CHANNEL FLOW**
 Calculation of 3-dimensional choking mass flow in turbomachinery with 2-dimensional flow models p0006 178-12289
- CHAPMAN SHEAR LAYER**
U SHEAR LAYERS
CHAPMAN-JOUGET FLAME
U CHEMICAL EQUILIBRIUM
U DETONATION
U FLAME PROPAGATION
CHARGE DISTRIBUTION
 Impurity concentrations and surface charge densities on the heavily doped face of silicon solar cell p0130 178-13534
- CHARGE EXCHANGE**
 Model for interpreting Doppler broadened optical line emission measurements on axially symmetric plasma p0174 178-46189
- Charge-exchange plasma generated by an ion thruster (NASA-CN-135318) p0052 178-13123
- CHARGED PARTICLES**
WT ANIONS
WT ARGON PLASMA
WT COLLISIONLESS PLASMAS
WT ELECTRON PLASMA
WT HYDROGEN PLASMA
WT LASER PLASMAS
WT METAL IONS
WT PHOTONLECTRONS
WT PLASMAS (PHYSICS)
WT TOROIDAL PLASMAS
 Interaction of large, high power systems with operational orbit charged particle environments (NASA-TN-73867) p0037 178-16076
- CHARGING**
 Proceedings of the Spacecraft Charging Technology Conference (NASA-TN-X-73537) p0036 178-10129
- Active control of spacecraft charging on ATS-5 and ATS-6 p0036 178-10136
- CHARTS**
WT GRAPHS (CHARTS)
CHECKOUT EQUIPMENT
U TEST EQUIPMENT
CHEMICAL ANALYSIS
WT ELECTROPHOTOMETRY
- WT QUANTITATIVE ANALYSIS**
WT QUANTITATIVE ANALYSIS
WT QUANTITATIVE ANALYSIS
 Hydrocarbon group type determination in jet fuels by high performance liquid chromatography p0089 178-24906
- Principles of MSCA and applications to metal corrosion, coating and lubrication --- Electron Spectroscopy for Chemical Analysis p0081 178-33213
- Hydrocarbon group type determination in jet fuels by high performance liquid chromatography (NASA-TN-73829) p0088 178-13233
- Principles of MSCA and application to metal corrosion, coating and lubrication (NASA-TN-78839) p0070 178-19262
- CHEMICAL ATTACK**
 Burner rig alkali salt corrosion of several high temperature alloys p0073 178-18793
- Interaction of NaCl/g/ and HCl/g/ with condensed H₂SO₄ --- in hot corrosion processes p0066 178-28888
- CHEMICAL BONDS**
 Friction and metal transfer for single-crystal silicon carbide in contact with various metals in vacuum (NASA-TP-1191) p0082 178-21294
- CHEMICAL COMPOSITION**
 Composition of RF-sputtered refractory compounds determined by X-ray photoelectron spectroscopy p0085 178-30301
- CHEMICAL EFFECTS**
 Definition and effect of chemical properties of surfaces in friction, wear, and lubrication p0121 178-45436
- CHEMICAL ELEMENTS**
WT ALKALI METALS
WT ALKALINE EARTH METALS
WT ALUMINUM
WT ARGON
WT BERYLLIUM
WT BORON
WT CARBON
WT CERIUM VAPOR
WT CELOSINE
WT CHROMIUM
WT COBALT
WT COPPER
WT GOLD
WT HELIUM
WT HYDROGEN ATOMS
WT HYDROGEN IONS
WT HYDROGEN PLASMA
WT IRON
WT ISOTOPES
WT LIQUID LITHIUM
WT LIQUID NEON
WT LIQUID NITROGEN
WT LIQUID POTASSIUM
WT MAGNESIUM
WT MERCURY (METAL)
WT MERCURY VAPOR
WT NICKEL
WT NITROGEN
WT OXYGEN
WT OXYGEN ATOMS
WT RARE GASES
WT REFRACTORY METALS
WT SILICON
WT SULFUR
WT TELLURIUM
WT TITANIUM
WT TUNGSTEN
WT ZENON
WT ZIRCONIUM
WT ZINC
- CHEMICAL EQUILIBRIUM**
 Computer program for calculation of complex chemical equilibrium compositions, rocket performance, incident and reflected shocks, and Chapman-Jouguet detonations (NASA-SP-273) p0156 178-17724
- CHEMICAL FUELS**
WT AIRCRAFT FUELS
WT DIESEL FUELS
WT HYDROCARBON FUELS
WT HYDROGEN FUELS

SUBJECT INDEX

CLEAN ENERGY

HT JET ENGINE FUELS
HT SYNTHETIC FUELS
CHEMICAL MODIFICATIONS
 Hydrocarbon group type determination in jet fuels
 by high performance liquid chromatography
 p0089 A78-24906

CHEMICAL KINETICS
U REACTION KINETICS
CHEMICAL PROPERTIES
HT HEAT OF VAPORIZATION
HT THERMOCHEMICAL PROPERTIES
 Definition and effect of chemical properties of
 surfaces in friction, wear, and lubrication
 [NASA-TN-73806] p0065 A78-19237

CHEMICAL PROPULSION
HT HYBRID PROPULSION
CHEMICAL REACTIONS
HT FLUORINATION
HT OXIDATION
HT OXIDATION-REDUCTION REACTIONS
HT PHOTOCHEMICAL REACTIONS
HT REDUCTION (CHEMISTRY)
HT TITRATION
 Formation of Na2SO4 and K2SO4 in flames doped with
 sulfur and alkali chlorides and carbonates
 p0066 A78-24889
 Reactions of yttria-stabilized zirconia with
 oxides and sulfates of various elements
 [NASA-TN-78982] p0071 A78-29216
 Synthesis of perfluoroalkylene aromatic diamines
 [NASA-CR-159403] p0087 A78-31235

CHEMICAL SPLIT
U CHEMICAL EQUILIBRIUM
CHEMICAL TESTS
HT CHEMICAL ANALYSIS
HT ELECTROPHOTOMETRY
HT OSZONOMETRY
HT QUALITATIVE ANALYSIS
HT QUANTITATIVE ANALYSIS
HT VOLUMETRIC ANALYSIS
CHEMISORPTION
 Shear strength of metal - SiO2 contacts
 p0061 A78-33209

CHILLING
U COOLING
CHLORIDES
HT HYDROGEN CHLORIDES
HT POTASSIUM CHLORIDES
HT SODIUM CHLORIDES
CHLORINE
 Effect of trichlorofluoromethane and molecular
 chlorine on ozone formation by simulated solar
 radiation
 [NASA-TP-1093] p0064 A78-12167

CHLORINE COMPOUNDS
HT CHLOROCARBONS
HT POTASSIUM CHLORIDES
HT SODIUM CHLORIDES
 Effect of trichlorofluoromethane and molecular
 chlorine on ozone formation by simulated solar
 radiation
 [NASA-TP-1093] p0064 A78-12167

CHLOROCARBONS
 Effect of nitric oxide on photochemical ozone
 formation in mixtures of air with molecular
 chlorine and with trichlorofluoromethane
 [NASA-TP-1192] p0065 A78-20281

CHOKE
 Two phase choke flow in tubes with very large L/D
 p0105 A78-15824

CHOPPERS (ELECTRIC)
U ELECTRIC CHOPPERS
CHROMATOGRAPHY
HT LIQUID CHROMATOGRAPHY
CHROME
U CHROMIUM
CHROMITES
 Volatile products from the interaction of KCl(g)
 with Cr2O3 and LaCrO3 in oxidizing environments
 [NASA-TN-73795] p0064 A78-13158

CHROMIUM
 Substitution for chromium in 304 stainless steel
 --- effects on oxidation and corrosion resistance
 p0077 A78-51714
 Plack chrome on commercially electroplated tin as
 a solar selecting coating
 [NASA-TN-73799] p0131 A78-15562
 Selective coating for solar panels --- using black
 chrome and black nickel

[NASA-CR-LEW-12159-1] p0132 A78-19589
CHROMIUM ALLOYS
HT ALUMINUM (THERMAL)
HT CHROMIUM STEELS
 The cyclic oxidation resistance of cobalt
 chromium-aluminum alloys at 1100 and 1200 C and
 a comparison with the nickel-chromium-aluminum
 alloy system
 p0077 A78-50086
 New alloys to conserve critical elements
 [NASA-TN-78840] p0070 A78-24335
 Sub tolerance evaluation of two sintered NiCrAl
 gas path seal materials --- wear tests of gas
 turbine engine seals
 [NASA-TN-78967] p0071 A78-29215

CHROMIUM CARBIDES
 Microstructural and wear properties of sputtered
 carbides and silicides
 p0084 A78-23445

CHROMIUM COMPOUNDS
HT CHROMITES
HT CHROMIUM CARBIDES
HT CHROMIUM OXIDES
CHROMIUM OXIDES
HT CHROMITES
 Volatile products from the interaction of KCl(g)/
 with Cr2O3 and LaCrO3 in oxidizing environments
 --- gas turbine engines
 p0066 A78-24887
 Volatile products from the interaction of KCl(g)
 with Cr2O3 and LaCrO3 in oxidizing environments
 [NASA-TN-73795] p0064 A78-13158

CHROMIUM STEELS
 New alloys to conserve critical elements ---
 replacing chromium in steels
 p0076 A78-37680

CHROMOTROPS
U TIME LAG
CHUCKING
U COMBUSTION STABILITY
CINEFLUOROGRAPHY
U RADIOLIOGRAPHY
CINEFLUOROGRAPHY
U RADIOGRAPHY
CIRCUIT PROTECTION
 Potential damage to dc superconducting magnets due
 to high frequency electromagnetic waves
 p0098 A78-39902
 Multi-cell battery protection system
 [NASA-CR-LEW-12039-1] p0130 A78-14625

CIRCUIT RELIABILITY
 Summary of the CTS Transient Event Counter data
 after one year of operation --- Communication
 Technology Satellite
 p0046 A78-19566

CIRCUITS
HT ANALOG CIRCUITS
HT COMPARATOR CIRCUITS
HT FLUIDIC CIRCUITS
HT INTEGRATED CIRCUITS
HT POWER SUPPLY CIRCUITS
HT SWITCHING CIRCUITS
HT TRANSISTOR CIRCUITS
CIRCULAR CYLINDERS
 A visual investigation of turbulence in stagnation
 flow about a circular cylinder
 [NASA-CR-3019] p0108 A78-33386

CIRCULAR PLATES
 Mode I stress intensity factors for round compact
 specimens
 p0126 A78-13817

CIRCULATION
HT WATER CIRCULATION
CIVIL AVIATION
 A review of NASA's propulsion programs for civil
 aviation
 [AIAA PAPER 78-4..] p0023 A78-20651
 A review of NASA's propulsion programs for aviation
 [NASA-TN-73831] p0016 A78-16055

CLADDING
 Fabrication of stainless steel clad tubing --- gas
 pressure bonding
 [NASA-CR-135307] p0079 A78-21265

CLEAN ENERGY
 A simulation model for wind energy storage
 systems. Volume 2: Operation manual
 [NASA-CR-135284] p0157 A78-20803
 A simulation model for wind energy storage
 systems. Volume 3: Program descriptions

CARDINAL

SUBJECT INDEX

(NASA-CR-135265)	p0177 878-20000	Morphology of gold and copper ion-plated coatings [NASA-TP-1263]	p0071 878-26199
CLEANING		Hydrodynamic air lubricated compliant surface bearing for an automotive gas turbine engine. 2: Materials and coatings [NASA-CR-135402]	p0122 878-29489
Cleaning process for contaminated supersonic powders [NASA-TR-78933]	p0076 878-47000 p0083 878-27257	COATING TRANSMISSION U. J. ANSHUSSTON	
The use of ion beam cleaning to obtain high quality cold welds with minimal deformation [NASA-TR-78933]	p0083 878-27257	COBALT	
CLEARANCES		The fluorination of cobalt and zinc [NASA-TR-X-73470]	p0068 878-15211
High stiffness seals for rotor critical speed control [ASME PAPER 77-DET-10]	p0118 878-20591	COBALT ALLOYS	
Gas path sealing in turbine engine [NASA-TR-73890]	p0010 878-21109	WT ASTROLOY (TRABERRE)	
In-place recalibration technique applied to a capacitance-type system for measuring rotor blade tip clearance [NASA-TP-1110]	p0015 878-22101	The cyclic oxidation resistance of cobalt, chromium-aluminum alloys at 1100 and 1200 C and a comparison with the nickel-chromium-aluminum alloy system	p0077 878-30086
Advanced optical blade tip clearance measurement system [NASA-CR-159402]	p0032 878-31106	Reaction diffusion in the NiCrAl and CoCrAl systems	p0077 878-33063
CLOSED CYCLES		COCKS	
Closed cycle electric discharge laser design investigation [NASA-CR-135408]	p0112 878-25407	Self-acting shaft seals [NASA-TR-73856]	p0114 878-19513
CLOSED LOOP SYSTEMS		CODES	
U FEEDBACK CONTROL		Comparison of computer codes for calculating dynamic loads in wind turbines	p0132 878-19617
CLOSURE LAW		CODING	
Turbulence processes and simple closure schemes	p0107 878-40983	Comparison of computer codes for calculating dynamic loads in wind turbines [NASA-TR-73773]	p0135 878-23556
CLOUD COVER		COEFFICIENT OF FRICTION	
Cloud effects on middle ultraviolet global radiation	p0190 878-42952	Definition and effect of chemical properties of surfaces in friction, wear, and lubrication [NASA-TP-1096]	p0080 878-12222
COAL		Effectiveness of various organometallics as antiwear additives in mineral oil [NASA-TP-1096]	p0080 878-12222
Fluidized bed combustor modeling [NASA-CR-135164]	p0067 878-14119	Friction and wear of several compressor gas-path seal assemblies [NASA-TP-1128]	p0068 878-15229
Energy Conversion Alternatives Study (ECAS) [NASA-TR-73871]	p0135 878-24659	Friction and wear of polyethylene oxide polymer having a range of molecular weights [NASA-TP-1129]	p0080 878-15278
Erosion/corrosion of turbine airfoil materials in the high-velocity effluent of a pressurized fluidized coal combustor [NASA-TP-1274]	p0071 878-28225	Friction and metal transfer for single-crystal silicon carbide in contact with various metals in vacuum [NASA-TP-1191]	p0082 878-21294
COAL GASIFICATION		Friction and wear of carbon-graphite materials for high-energy brakes [NASA-TR-78904]	p0056 878-26178
Performance potential of combined cycles integrated with low-Btu gasifiers for future electric utility applications [NASA-TR-73775]	p0135 878-23557	Effect of oxygen and nitrogen interactions on friction of single-crystal silicon carbide [NASA-TP-1265]	p0083 878-28247
COAL LIQUEFACTION		COEFFICIENTS	
Jet fuels from synthetic crudes	p0090 878-43415	WT COEFFICIENT OF FRICTION	
COAL UTILIZATION		WT DIFFUSION COEFFICIENT	
ECAS Phase I fuel cell results --- Energy Conservation Alternatives Study	p0142 878-26110	WT HEAT TRANSFER COEFFICIENTS	
Design and calculated performance and cost of the ECAS Phase II open cycle MHD power generation system [ASME PAPER 77-WA/ENER-5]	p0174 878-33143	COHESION	
Open-Cycle Gas Turbine/Steam Turbine Combined Cycles with synthetic fuels from coal [ASME PAPER 77-WA/ENER-9]	p0146 878-33147	Adhesive/cohesive strength of a CrO ₂ -1-2 w/o TiO ₂ /NiCrAlY thermal barrier coating [NASA-TR-73792]	p0057 878-17152
Effluent characterization from a conical pressurized fluid bed	p0066 878-33221	COLD PRESSING	
Performance and economics of advanced energy conversion systems for coal and coal-derived fuels [NASA-TR-73897]	p0146 878-34078 p0134 878-21596	Development of SiAlON materials [NASA-CR-135290]	p0087 878-21289
COATING		COLD STRENGTHS	
WT ENCAPSULATING		Development of strong and tough cryogenic Fe-12Ni alloys containing reactive metal additions	p0076 878-41465
Method of forming metal hydride films [NASA-CASE-LEW-12083-1]	p0113 878-13436	COLD WELDING	
Principles of ESCA and application to metal corrosion, coating and lubrication [NASA-TR-78839]	p0070 878-19262	The use of ion beam cleaning to obtain high quality cold welds with minimal deformation [NASA-TR-78933]	p0083 878-27257
Selective coating for solar panels --- using black chrome and black nickel [NASA-CASE-LEW-12159-1]	p0132 878-19599	Method of cold welding using ion beam technology [NASA-CASE-LEW-12982-1]	p0117 878-28459
COATINGS		COLLEGES	
WT ANTIREFLECTION COATINGS		U UNIVERSITIES	
WT CERAMIC COATINGS		COLLIMATORS	
WT ENCAPSULATING		Some basic considerations of measurements involving collimated direct sunlight [NASA-TR-74947]	p0130 878-13608
WT GLASS COATINGS		COLLISION WARNING DEVICES	
WT METAL COATINGS		U WARNING SYSTEMS	
WT NICKEL COATINGS		COLLISIONLESS PLASMAS	
WT PROTECTIVE COATINGS		Dynamic modeling of spacecraft in a collisionless plasma	p0037 878-10150
WT THERMAL CONTROL COATINGS		COLLOIDS	
		WT AEROSOLS	

- COMBUSTION**
- VT AFTERBURNING**
- VT FUEL COMBUSTION**
- VT HYDROCARBON COMBUSTION**
- VT PROPELLANT COMBUSTION**
- VT SUPERSONIC COMBUSTION**
- Investigation of the burning configuration of a coaxial injector in a combustion chamber [NASA-CR-135383] p0054 N78-22188
- Pollution Reduction Technology Program for small jet aircraft engines, phase 2 [NASA-CR-159415] p0032 N78-33104
- COMBUSTION CHAMBERS**
- Burner rig alkali salt corrosion of several high temperature alloys p0073 N78-18793
- Combustor fluctuating pressure measurements in-engine and in a component test facility - a preliminary comparison p0023 N78-24878
- Design and preliminary results of a semitranspiration cooled /Lavalloy/ liner for a high-pressure high-temperature combustor [AIAA PAPER 78-997] p0025 N78-83540
- Combustor concepts for aircraft gas turbine low-power emissions reduction [AIAA PAPER 78-999] p0025 N78-83546
- Degree of vaporization using an airblast type fuel injector for a premixed-prevaporized combustor p0107 N78-50322
- Fuel combustor [NASA-CASE-LEW-12137-1] p0064 N78-10224
- Pollution reduction technology program for class TA(J78D) engines p0013 N78-11067
- Advanced low-NO(x) combustors for supersonic high-altitude gas turbines p0014 N78-11078
- Combustor fluctuating pressure measurements in engine and in a component test facility: A preliminary comparison [NASA-TN-73805] p0035 N78-13077
- Experimental evaluation of premixing-prevaporizing fuel injection concepts for a gas turbine catalytic combustor [NASA-TN-73755] p0101 N78-14313
- Experimental clean combustor program: turbulence characteristics of compressor discharge flows [NASA-CR-135277] p0027 N78-15041
- Liquid rocket engine self-cooled combustion chambers [NASA-SP-8124] p0048 N78-21211
- Effluent characterization from a conical pressurized fluid bed [NASA-TN-73897] p0131 N78-21596
- Lean combustion limits of a confined premixed-prevaporized propane jet [NASA-TN-78868] p0019 N78-22099
- Investigation of the burning configuration of a coaxial injector in a combustion chamber [NASA-CR-135383] p0054 N78-22188
- Design and preliminary results of a semitranspiration cooled (Lavalloy) liner for a high-pressure high-temperature combustor [NASA-TN-78874] p0011 N78-24138
- Degree of vaporization using an airblast type injector for a premixed-prevaporized combustor [NASA-TN-78836] p0107 N78-24494
- YF 102 in-duct combustor noise measurement, volume 1 [NASA-CR-135404-VOL-1] p0167 N78-25827
- YF 102 in-duct combustor noise measurement, volume 2 [NASA-CR-135404-VOL-2] p0167 N78-25828
- YF 102 in-duct combustor noise measurement, volume 3 [NASA-CR-135404-VOL-3] p0167 N78-25829
- Combustor concepts for aircraft gas turbine low-power emissions reduction [NASA-TN-78875] p0020 N78-26183
- Preliminary concept, specifications, and requirements for a zero-gravity combustion facility for spacelab [NASA-TN-78910] p0041 N78-26166
- Reverse-flow combustor for small gas turbines with pressure-atomizing fuel injectors [NASA-TP-1260] p0021 N78-27130
- Direct heating surface combustor [NASA-CR-SP-128-11877-1] p0097 N78-27357
- Correlation of combustor acoustic power levels inferred from internal fluctuating pressure measurements [NASA-TN-78986] p0165 N78-31871
- Aircraft gas turbine low-power emissions reduction technology program [NASA-CR-135434] p0032 N78-32097
- COMBUSTION EFFICIENCY**
- Effect of fuel properties on performance of single aircraft turbojet combustor at simulated idle, cruise, and takeoff conditions [NASA-TN-73780] p0014 N78-13056
- Fluidized bed combustor modeling [NASA-CR-135164] p0067 N78-14119
- Fuel conservative aircraft engine technology [NASA-TN-78962] p0021 N78-27127
- Experimental study of the effect of cycle pressure on lean combustion emissions [NASA-CR-3032] p0031 N78-26098
- Effect of inlet temperature on the performance of a catalytic reactor --- air pollution control [NASA-TN-78977] p0141 N78-31534
- COMBUSTION INSTABILITY**
- U COMBUSTION STABILITY**
- COMBUSTION PHYSICS**
- Burning of liquid pools in reduced gravity [NASA-CR-135234] p0067 N78-25150
- COMBUSTION PRODUCTS**
- Formation of Na2SO4 and K2SO4 in flames doped with sulfur and alkali chlorides and carbonates p0066 N78-24889
- Computer program for obtaining thermodynamic and transport properties of air and products of combustion of ASTM-A-1 fuel and air [NASA-TP-1160] p0088 N78-20351
- Characteristics and combustion of future hydrocarbon fuels --- aircraft fuels [NASA-TN-78865] p0089 N78-24370
- Experimental study of the effects of flameholder geometry on emissions and performance of lean premixed combustors [NASA-CR-135424] p0030 N78-26147
- Erosion/corrosion of turbine airfoil materials in the high-velocity effluent of a pressurized fluidized coal combustor [NASA-TP-1274] p0071 N78-28225
- COMBUSTION STABILITY**
- Investigation of the burning configuration of a coaxial injector in a combustion chamber [NASA-CR-135383] p0054 N78-22149
- COMBUSTION WAVES**
- U PLANE PROPAGATION**
- COMBUSTORS**
- U COMBUSTION CHAMBERS**
- COMETS**
- VT HALLEY'S COMET**
- COMMERCIAL AIRCRAFT**
- VT BOEING 747 AIRCRAFT**
- Automated meteorological data from commercial aircraft via satellite: Present experience and future implications [NASA-TN-73750] p0150 N78-17558
- COMMERCIAL AVIATION**
- U CIVIL AVIATION**
- U COMMERCIAL AIRCRAFT**
- COMBUSTION**
- Effect of attrition milling on the reaction sintering of silicon nitride p0086 N78-50324
- Effect of attrition milling on the reaction sintering of silicon nitride [NASA-TN-78965] p0086 N78-31236
- COMMUNICATING**
- VT POINT TO POINT COMMUNICATIONS**
- COMMUNICATION**
- An airborne meteorological data collection system using satellite relay (ASDAR) [NASA-TN-78997] p0093 N78-33283
- COMMUNICATION EQUIPMENT**
- VT DIGITAL SPACECRAFT TELEVISION**
- VT SATELLITE TELEVISION**
- Low cost satellite land mobile service for nationwide applications p0095 N78-43173
- COMMUNICATION SATELLITES**
- VT COMMUNICATIONS TECHNOLOGY SATELLITE**
- A forecast of broadcast satellite communications p0094 N78-15615
- Performance of the 12 GHz, 200 watt Transmitter Experiment Package for the Hermes Satellite p0098 N78-24883
- Low cost Ku-band earth terminals for voice/data/facsimile

COMMUNICATION SYSTEMS

SUBJECT INDEX

Communication satellite services for special purposes usara p0094 A78-31970

Disaster warning system study summary --- cost estimates using NOAA satellites [NASA-TN-73797] p0094 A78-31971

Millimeter wave satellite concepts, volume 1 [NASA-CR-135227] p0093 A78-10366

[NASA-CR-135227] p0041 A78-15144

COMMUNICATION SYSTEMS
U TELECOMMUNICATIONS
COMMUNICATIONS TECHNOLOGY SATELLITE

Summary of the CTS Transient Event Counter data after one year of operation --- Communication Technology Satellite p0046 A78-19566

A digitally implemented communications experiment utilizing the Hermes /CTS/ satellite p0094 A78-24884

Utilization of NASA Lewis mobile terminals for the Hermes satellite p0094 A78-24885

CTS /Hermes/ - United States experiments and operations summary --- Communications Technology Satellite p0094 A78-24886

Preliminary report on the CTS transient event counter performance through the 1976 spring eclipse season p0136 A78-10135

CTS (Hermes): United States experiments and operations summary [NASA-TN-73830] p0041 A78-13107

Performance of the 12GHz, 200 watt transmitter experiment package for the Hermes satellite [NASA-TN-73804] p0093 A78-13282

A digitally implemented communications experiment utilizing the Hermes (CTS) satellite [NASA-TN-73827] p0093 A78-13283

Utilization of NASA Lewis mobile terminals for the Hermes satellite [NASA-TN-73859] p0093 A78-15326

Accelerated life tests of specimen heat pipe from Communication Technology Satellite (CTS) project [NASA-TN-73846] p0102 A78-17341

CTS TEP thermal anomalies: Heat pipe system performance [NASA-CR-159413] p0108 A78-29410

Continuation of the compendium of applications technology satellite and communications technology satellite user experiments 1967-1977, volume 1 [NASA-CR-135416-VOL-1] p0042 A78-31141

Continuation of the compendium of applications technology satellite and communications technology satellite user experiments 1967-1977, volume 2 --- bibliography [NASA-CR-135416-VOL-2] p0042 A78-31142

Thermal characteristics of the 12-gigahertz, 200-watt output stage tube for the communications technology satellite [NASA-TP-1344] p0043 A78-33137

CONNOTATORS

Photovoltaic power system tests on an 8-kilowatt single-phase line-commutated inverter [NASA-TN-74424] p0134 A78-19657

COMPARATOR CIRCUITS

Multi-cell battery protection system [NASA-CASE-LPN-12039-1] p0130 A78-14625

COMPARISON

Mechanical behavior and fracture characteristics of off-axis fiber composites. 2: Theory and comparisons [NASA-TP-1082] p0057 A78-16098

COMPARTMENTS
 NT ANECHOIC CHAMBERS
 NT VACUUM CHAMBERS

COMPLEX SYSTEMS

Diagonal dominance using function minimization algorithms --- multivariable control system design p0159 A78-16304

COMPLEX VARIABLES
 NT SINGULARITY (MATHEMATICS)

COMPLIANCE (ELASTICITY)
 U MODULUS OF ELASTICITY

COMPOSITE MATERIALS
 NT ALUMINUM BORON COMPOSITES
 NT BORON REINFORCED MATERIALS
 NT CARBON FIBER REINFORCED PLASTICS

NT GLASS FIBER REINFORCED PLASTICS
NT GRAPHITE-EPOXY COMPOSITE MATERIALS
NT LAMINATES
NT METAL MATRIX COMPOSITES
NT PLYWOOD

Evaluation of low cost/high temperature fiber and blanket insulation p0063 A78-16903

Effect of processing parameters on autoclaved PFR polyimide composites p0060 A78-25191

Recent advances in lightweight, filament-wound composite pressure vessel technology p0061 A78-33436

Aspects of composite mechanics on test methods for fiber composites p0062 A78-50325

Analysis of delamination in unidirectional and crossplied fiber composites containing surface cracks [NASA-CR-135248] p0062 A78-11117

Fracture surface characteristics of off-axis composites [NASA-TN-73700] p0057 A78-13137

Mechanical behavior and fracture characteristics of off-axis fiber composites. 1: Experimental investigation --- at the Lewis Research Center [NASA-TP-1081] p0057 A78-13138

An integrated theory for predicting the hydrothermomechanical response of advanced composite structural components [NASA-TN-73612] p0125 A78-13477

Residual stresses in angleplied laminates and their effects on laminate behavior [NASA-TN-78835] p0058 A78-19206

Atomic hydrogen storage method and apparatus [NASA-CASE-LEW-12081-1] p0089 A78-24365

Fiber reinforced PFR polyimide composites [NASA-CR-135377] p0063 A78-25132

Some effects of composition on friction and wear of graphite-fiber-reinforced polyimide liners in plain spherical bearings [NASA-TP-1229] p0115 A78-24433

Advanced materials research for long-haul aircraft turbine engines p0001 A78-27057

Aspects of composite mechanics on test methods for fiber composites [NASA-TN-78979] p0126 A78-37464

COMPOSITE STRUCTURES
NT LAMINATES
NT PLYWOOD

An integrated theory for predicting the hydrothermomechanical response of advanced composite structural components p0060 A78-24905

Evaluation of flawed composite structure under static and cyclic loading p0063 A78-26483

Diagnostic evaluations of a beam-shielded 8-cm mercury ion thruster [AIAA PAPER 78-702] p0051 A78-32768

Concepts for the development of light-weight composite structures for rotor burst containment p0012 A78-10094

Impact on multilayered composite plater [NASA-CR-135247] p0062 A78-16103

Analysis/design of strip reinforced random composites (strip hybrids) [NASA-TN-74945] p0059 A78-31149

Acoustic emission testing of composite vessels under sustained loading [NASA-TN-78981] p0059 A78-31150

COMPOSITES
 U COMPOSITE MATERIALS
COMPOSITION (PROPERTY)
 NT ATMOSPHERIC COMPOSITION
 NT ATOM CONCENTRATION
 NT CHEMICAL COMPOSITION
 NT CONCENTRATION (COMPOSITION)
 NT MOISTURE CONTENT

COMPRESSED GAS
 NT HIGH PRESSURE OXYGEN

COMPRESSIBLE FLOW
 NT TRANSONIC FLOW

COMPRESSION LOADS
 NT IMPACT LOADS

Simplified solution for elliptical-contact deformation between two elastic solids

- an ultralightweight, evacuated, load-bearing,
 high-performance insulation system --- for
 cryogenic propellant tanks
 [AIAA PAPER 78-878] p0045 A78-36005
 Evacuated load-bearing high performance insulation
 study
 [NASA-CR-135342] p0092 W78-18251
- COMPRESSION TESTS**
U COMPRESSION TESTS
COMPRESSION TESTS
 High temperature compressive cracking in
 hot-pressed silicon nitride
 p0085 A78-38706
- COMPRESSOR BLADES**
 Perturbation solutions for blade-to-blade surfaces
 of a transonic compressor
 p0008 A78-12307
 Unsteady flow in a supersonic cascade with strong
 in-passage shocks
 p0006 A78-17270
 Instrumentation for propulsion systems development
 [SAE PAPER 780076] p0109 A78-33365
 Perturbation solutions for transonic flow on the
 blade-to-blade surface of compressor blade rows
 [NASA-CR-29411] p0001 W78-15987
 Core compressor exit stage study. Volume 1:
 Blading design --- turbofan engines
 [NASA-CR-135391] p0031 W78-29099
 Compressor seal rub energetics study
 [NASA-CR-159424] p0032 W78-32096
 Blade row dynamic digital compression program.
 Volume 2: J85 circumferential distortion
 redistribution model, effect of stator
 characteristics, and stage characteristics
 sensitivity study
 [NASA-CR-134953] p0032 W78-33103
- COMPRESSOR EFFICIENCY**
 Design and overall performance of four highly
 loaded, high speed inlet stages for an advanced
 high-pressure-ratio core compressor
 [NASA-TP-1337] p0022 W78-33108
- COMPRESSOR ROTORS**
 Composite hub/metal blade compressor rotor
 [NASA-CR-135343] p0062 W78-18131
 Core compressor exit stage study. Volume 1:
 Blading design --- turbofan engines
 [NASA-CR-135391] p0031 W78-29099
 Performance of a transonic fan stage designed for
 a low meridional velocity ratio
 [NASA-TP-1298] p0022 W78-33107
 Design and overall performance of four highly
 loaded, high speed inlet stages for an advanced
 high-pressure-ratio core compressor
 [NASA-TP-1337] p0022 W78-33108
 Design and performance of a
 427-meter-per-second-tip-speed two-stage fan
 having a 2.40 pressure ratio
 [NASA-TP-1314] p0022 W78-33109
- COMPRESSORS**
NT CENTRIFUGAL COMPRESSORS
NT TRANSONIC COMPRESSORS
NT THERMOCOMPRESSORS
 Experimental clean combustor program: Turbulence
 characteristics of compressor discharge flows
 [NASA-CR-135277] p0027 W78-15041
 Friction and wear of several compressor gas-path
 seal movements
 [NASA-TP-1128] p0068 W78-15229
 F100(3) parallel compressor computer code and
 user's manual
 [NASA-CR-135388] p0029 W78-22096
- COMPUTER GRAPHICS**
 Escort: A data acquisition and display system to
 support research testing
 [NASA-TN-78909] p0154 W78-24807
- COMPUTER METHODS**
U COMPUTER PROGRAMS
COMPUTER PROGRAMMING
NT ON-LINE PROGRAMMING
COMPUTER PROGRAMS
NT COMPUTER SYSTEMS PROGRAMS
NT MASTRAN
 MASCAP, a three-dimensional Charging Analyzer
 Program for complex spacecraft
 p0044 A78-19567
 A computer program for the transient thermal
 analysis of an impingement cooled turbine blade
 [AIAA PAPER 78-92] p0106 A78-20682
- ing elastic distortion of the flanged inner ring
 of a high-speed cylindrical roller bearing
 [AIAA PAPER 77-LUB-8] p0118 A78-23352
 NASA Charging Analyzer Program - A computer tool
 that can evaluate electrostatic contamination
 --- of spacecraft during geomagnetic substorms
 p0044 A78-33220
 Comparison of computer codes for calculating
 dynamic loads in wind turbines
 p0142 A78-37678
 A viscous-inviscid interactive compressor
 calculation
 [AIAA PAPER 78-1140] p0006 A78-41843
 Methods for calculating the transonic boundary
 layer separation for V/STOL inlets at high
 incidence angles
 [AIAA 78-1340] p0007 A78-46537
 Computation of unsteady transonic flows through
 rotating and stationary cascades. 2: User's
 guide to FORTRAN program B2DATL
 [NASA-CR-2901] p0007 W78-12034
 Computer program for calculation of a gas
 temperature profile by infrared emission:
 Absorption spectroscopy
 [NASA-TN-73848] p0015 W78-15043
 A computer program for the transient thermal
 analysis of an impingement cooled turbine blade
 [NASA-TN-73819] p0015 W78-15045
 Computer program for calculation of complex
 chemical equilibrium compositions, rocket
 performance, incident and reflected shocks, and
 Chapman-Jouguet detonations
 [NASA-SP-273] p0156 W78-17724
 Computer program for the analysis of the cross
 flow in a radial inflow turbine scroll
 [NASA-CR-135321] p0029 W78-19154
 Computer model for refinery operations with
 emphasis on jet fuel production. Volume 2:
 Data and technical bases
 [NASA-CR-135334] p0090 W78-20326
 Comparison of computer codes for calculating
 dynamic loads in wind turbines
 p0132 W78-19617
 Computer model for refinery operations with
 emphasis on jet fuel production. Volume 1:
 Program description
 [NASA-CR-135333] p0090 W78-20350
 Computer program for obtaining thermodynamic and
 transport properties of air and products of
 combustion of ASTM-A-1 fuel and air
 [NASA-TP-1160] p0088 W78-20351
 Predicted and experimental performance of
 jet-lubricated 120-millimeter-bore ball bearings
 operating to 2.5 million DN
 [NASA-TP-1196] p0114 W78-20513
 A simulation model for wind energy storage
 systems. Volume 1: Technical report
 [NASA-CR-135283] p0156 W78-20802
 In site ply strength: An initial assessment ---
 using laminate fracture data and a least squares
 method
 [NASA-TN-73771] p0059 W78-21220
 NASA charging analyzer program: A computer tool
 that can evaluate electrostatic contamination
 [NASA-TN-78889] p0096 W78-21372
**FLOWNET: A computer program for calculating
 secondary flow conditions in a network of
 turbomachinery**
 [NASA-TN-73774] p0156 W78-21791
 Comparison of computer codes for calculating
 dynamic loads in wind turbines
 [NASA-TN-73773] p0135 W78-23556
 Heliocentric interplanetary low thrust trajectory
 optimization program, supplement 1, part 2
 [NASA-CR-135414-APP] p0038 W78-25106
 Computer model for refinery operations with
 emphasis on jet fuel production. Volume 3:
 Detailed systems and programming documentation
 [NASA-CR-135335] p0090 W78-25235
 Computer programs for calculating two-dimensional
 potential flow in and about propulsion system
 inlets
 [NASA-TN-78930] p0005 W78-27083
 A computer program for full-coverage film-cooled
 blading analysis including the effects of a
 thermal barrier coating
 [NASA-TN-78951] p0021 W78-27126
 FORTRAN program for calculating coolant flow and
 metal temperatures of a

COMPUTER SIMULATION

SUBJECT INDEX

full-coverage-film-cooled vane or blade
[NASA-TP-1259] p0021 N78-28099

TACT1, a computer program for the transient thermal analysis of a cooled turbine blade or vane equipped with a coolant insert. V. Users manual
[NASA-TP-1271] p0104 N78-28374

A Stirling engine computer model for performance calculations
[NASA-TN-78894] p0180 N78-29994

Derivation and evaluation of an approximate analysis for three-dimensional viscous subsonic flow with large secondary velocities --- finite difference method
[NASA-CR-159430] p0008 N78-33044

DYGABCD: A program for calculating linear A, B, C, and D matrices from a nonlinear dynamic engine simulation
[NASA-TP-1295] p0022 N78-33110

COMPUTER SIMULATION
U COMPUTERIZED SIMULATION
COMPUTER STORAGE DEVICES
BT READ-ONLY MEMORY DEVICES
COMPUTER SYSTEMS DESIGN
Escort - A data acquisition and display system to support research testing
p0155 A78-37685

COMPUTER SYSTEMS PROGRAMS
A data acquisition and handling system for the measurement of radial plasma transport rates
[NASA-TN-78849] p0155 N78-23751

COMPUTER TECHNIQUES
ADJUST - An automated system for steering Centaur launch vehicles in measured winds
p0085 A78-14991

Diagonal dominance using function minimization algorithms --- multivariable control system design
p0159 A78-16304

COMPUTERIZED CONTROL
U NUMERICAL CONTROL
COMPUTERIZED DESIGN
Use of a simple external nonreciprocal attenuator in coupled-cavity TWT's
p0098 A78-18282

COMPUTERIZED SIMULATION
BT DIGITAL SIMULATION
Discrete time domain modelling and analysis of dc-dc converters with continuous and discontinuous inductor current
p0100 A78-18796

MASCAP, a three-dimensional Charging Analyzer Program for complex spacecraft
p0044 A78-19567

'Chain pooling' model selection as developed for the statistical analysis of a rotor burst protection experiment
p0160 A78-29327

Evaluation of an F100 multivariable control using a real-time engine simulation
[NASA-TN-X-73648] p0024 N7-10397

High frequency dynamic engine simulation --- FV-30 engine
[NASA-CR-135313] p0027 N78-13059

MASCAP user's manual
[NASA-CR-135259] p0099 N78-13329

Chain Pooling modeling selection as developed for the statistical analysis of a rotor burst protection experiment
[NASA-TN-73874] p0160 N78-16735

A simulation model for wind energy storage systems. Volume 1: Technical report
[NASA-CR-135281] p0156 N78-20802

A simulation model for wind energy storage systems. Volume 2: Operation manual
[NASA-CR-135284] p0157 N78-20803

A simulation model for wind energy storage systems. Volume 3: Program descriptions
[NASA-CR-135285] p0157 N78-20804

Computer model for refinery operations with emphasis on jet fuel production. Volume 3: Detailed systems and programming documentation
[NASA-CR-135335] p0090 N78-25735

Simulation model of a single-stage lithium bromide-water absorption cooling unit
[NASA-TP-12961] p0072 N78-30205

Procedures for generation and reduction of linear models of a turbopfan engine
[NASA-TP-12611] p0161 N78-30896

DYGABCD: A program for calculating linear A, B, C, and D matrices from a nonlinear dynamic engine simulation
[NASA-TP-1295] p0022 N78-33110

COMPUTERS
BT HYBRID COMPUTERS
U ANALOG COMPUTERS
BT UNIVAC 1100 SERIES COMPUTERS
CONCENTRATION (COMPOSITION)
BT ATOM CONCENTRATION
BT MOISTURE CONTENT
Effects of compositional changes on the performance of a thermal barrier coating system --- yttria-stabilized zirconia coatings on gas turbine engine blades
[NASA-TN-78976] p0072 N78-31212

CONCENTRATORS
Design and fabrication of a low-specific-weight parabolic dish solar concentrator
[NASA-TP-1152] p0046 N78-17145

CONDITIONS
BT NONADIABATIC CONDITIONS
CONDUCTING MEDIA
U CONDUCTORS
CONDUCTORS
BT BUS CONDUCTORS
BT FLAT CONDUCTORS
BT ION EXCHANGE MEMBRANE ELECTROLYTES
BT SUPERCONDUCTORS
Secondary-electron-emission properties of conducting surfaces with application to multistage depressed collectors for microwave amplifiers
[NASA-TP-1097] p0068 N78-11230

CONFERENCES
Proceedings of the Spacecraft Charging Technology Conference
[NASA-TN-X-73537] p0036 N78-10129

Aircraft engine emissions --- conference
[NASA-CR-2021] p0012 N78-11063

Solar Cell High Efficiency and Radiation Damage
[NASA-CR-2020] p0130 N78-13527

Preliminary QCSEE program test results
[NASA-TN-73732] p0015 N78-15042

New alloys to conserve critical elements
[NASA-TN-78840] p0070 N78-24335

Catalytic combustion for the automotive gas turbine engine
p0092 N78-30333

CONFLUENCE
U CONVERGENCE
CONSERVATION
BT ENERGY CONSERVATION
CONSTANT SPEED PROPELLERS
U VARIABLE PITCH PROPELLERS
CONSTRUCTION MATERIALS
Design and preliminary results of a salttranspiration cooled /Lamilly/ liner for a high-pressure high-temperature combustor
[AIAA PAPER 78-997] p0025 A78-43544

CONSUMPTION
BT ENERGY CONSUMPTION
BT FUEL CONSUMPTION
CONTACT RESISTANCE
Elastohydrodynamic lubrication of elliptical contacts for materials of low elastic modulus. 2: Starved conjunction
[NASA-TP-1273] p0117 N78-28454

CONTACTORS
Simplified solution for elliptical-contact deformation between two elastic solids
p0118 A78-12737

CONTACTS (ELECTRIC)
U ELECTRIC CONTACTS
CONTAMINANTS
BT TRACE CONTAMINANTS
Filtration effects on ball bearing life and condition in a contaminated lubricant
[NASA-TN-78907] p0116 N78-26446

CONTAMINATION
BT SPACECRAFT CONTAMINATION
Effect of ice contamination on liquid-nitrogen drops in film boiling
p0105 A78-15821

CONTRAST
BT IMAGE CONTRAST
CONTROL
Application of fluidics to new control components
p0109 N78-23026

SUBJECT INDEX

CORROSION RESISTANCE

- Measurement of control system response using an analog operational circuit
[NASA-TN-78937] p0104 W78-27386
- CONTROL DEVICES**
U CONTROL EQUIPMENT
CONTROL EQUIPMENT
WT PRESSURE REGULATORS
 Variable cycle gas turbine engines
[NASA-CASE-LRW-12916-1] p0111 W78-17384
 Fabrication and test of digital output interface devices for gas turbine electronic controls
[NASA-CR-135427] p0030 W78-27129
- CONTROL SIMULATION**
 Minus-time acceleration of aircraft turbofan engines
p0023 A78-23892
 Real time digital propulsion system simulation for manned flight simulators
[AIAA PAPER 78-927] p0035 A78-85095
 Evaluation of an F100 multivariable control using a real-time engine simulation
[NASA-TN-1-73648] p0012 W78-10097
- CONTROL SURFACES**
WT EXTERNALLY FLOWING FLAPS
WT FLAPS (CONTROL SURFACES)
WT WING FLAPS
 Preliminary study of the effect of the turbulent flow field around complex surfaces on their acoustic characteristics
[NASA-TN-78944] p0164 W78-28886
- CONTROL SYSTEMS**
U CONTROL
CONTROL THEORY
 Diagonal dominance using function minimization algorithms --- multivariable control system design
p0159 A78-16304
- CONTROLLED ATMOSPHERES**
WT CABIN ATMOSPHERES
CONTROLLED POSITION
 A hollow cathode hydrogen ion source --- for controlled fusion
p0173 A78-39835
- CONTROLLED STABILITY**
U CONTROL
CONVECTION
WT FORCED CONVECTION
 Convection due to surface-tension gradients --- in reduced gravity spacecraft environments
p0108 A78-48716
- CONVECTIVE FLOW**
 Mean velocity, turbulence intensity and turbulence convection velocity measurements for a convergent nozzle in a free jet wind tunnel
[NASA-CR-2949] p0008 W78-21058
- CONVECTIVE HEAT TRANSFER**
 Boiling inception and convective boiling of neon and nitrogen
p0105 A78-15820
 Simulation of the heat transfer characteristics of LOX
[ASME PAPER 77-HT-9] p0089 A78-17482
 Method for calculating convective heat-transfer coefficients over turbine vane surfaces
[NASA-TN-1134] p0102 W78-17338
- CONVERGENCE**
 Interpolation and extrapolation of creep rupture data by the minus commitment method. Part 1: focal-point convergence
[NASA-TN-78881] p0125 W78-23471
- CONVERGENT NOZZLES**
 Mean velocity, turbulence intensity and turbulence convection velocity measurements for a convergent nozzle in a free jet wind tunnel. Comprehensive data report
[NASA-CR-115234] p0007 W78-17991
 Mean velocity, turbulence intensity and turbulence convection velocity measurements for a convergent nozzle in a free jet wind tunnel
[NASA-CR-2949] p0008 W78-21058
- CONVERTIBLE PLANES**
U V/STOL AIRCRAFT
COOLING
WT AIR COOLING
WT FILM COOLING
WT LIQUID COOLING
WT REGENERATIVE COOLING
WT SOLAR COOLING
 A computer program for the transient thermal analysis of an impingement cooled turbine blade
[NASA-TN-73819] p0015 W78-15045
 Progress in advanced high temperature turbine materials, coatings, and technology
p0018 W78-21122
- COOLING SYSTEMS**
 Design and preliminary results of a subtranspiration cooled /Laval/ liner for a high-pressure high-temperature combustor
[AIAA PAPER 78-997] p0025 A78-83548
 Oil cooling system for a gas turbine engine
[NASA-CASE-LRW-12321-1] p0113 W78-10467
 Closed loop spray cooling apparatus --- for particle accelerator targets
[NASA-CASE-LRW-11981-1] p0091 W78-17237
 Effect of cooling-hole geometry on aerodynamic performance of a film-cooled turbine vane tested with cold air in a two-dimensional cascade
[NASA-TN-1136] p0004 W78-20880
 Liquid rocket engine self-cooled combustion chambers
[NASA-SP-8124] p0048 W78-21211
 Simulation model of a single-stage lithium bromide-water absorption cooling unit
[NASA-TN-1296] p0072 W78-30205
- COORDINATES**
WT OBLIQUE COORDINATES
COPPER
 Friction and wear of selected metals and alloys in sliding contact with AISI 440 C stainless steel in liquid methane and in liquid natural gas
[NASA-TN-1150] p0114 W78-20512
 Wear of single-crystal silicon carbide in contact with various metals in vacuum
[NASA-TN-1198] p0082 W78-21295
 Morphology of gold and copper ion-plated coatings
[NASA-TN-1262] p0071 W78-26199
- COPPER ALLOYS**
WT BROWNS
 Friction and wear of selected metals and alloys in sliding contact with AISI 440 C stainless steel in liquid methane and in liquid natural gas
[NASA-TN-1150] p0114 W78-20512
 Role of alloying elements in adhesive transfer and friction of copper-base alloys
[NASA-TN-1256] p0071 W78-26198
- COPPER COMPOUNDS**
WT COPPER SULFIDES
COPPER SULFIDES
 Critical currents and scaling laws in spattered copper molybdenum sulfide
p0175 A78-45500
 Upper critical field of copper molybdenum sulfide
p0175 A78-53626
- CORPUSCULAR RADIATION**
WT CYCLOTRON RADIATION
WT ELECTRON BEAMS
CORRECTION
WT OPTICAL CORRECTION PROCEDURE
CORRELATION
WT DATA CORRELATION
CORROSION
WT FUEL CORROSION
 High temperature environmental effects on metals
p0075 A78-29329
 Two-phase working fluids for the temperature range 50 to 350 C
[NASA-CR-135255] p0107 W78-16329
 Principles of ESCA and application to metal corrosion, coating and lubrication
[NASA-TN-78839] p0070 W78-19262
 Thermal barrier coatings
[NASA-TN-78848] p0059 W78-24291
- CORROSION PREVENTION**
 Inhibition of hot salt corrosion by metallic additives
[NASA-TN-78966] p0072 W78-31208
- CORROSION RESISTANCE**
WT OXIDATION RESISTANCE
 Effects of silicon on the oxidation, hot-corrosion, and mechanical behavior of two cast nickel-base superalloys
p0074 A78-21439
 Rolling-element fatigue life of AMS 5749 corrosion resistant, high temperature bearing steel
[ASME PAPER 77-LOB-30] p0075 A78-28423
 Effluent characterization from a conical pressurized fluid bed
p0066 A78-33221
 Substitution for chromium in 304 stainless steel --- effects on oxidation and corrosion resistance

CORROSION TESTS

Improved ceramic heat exchange material
[NASA-CR-135262] p0077 A78-51714
Characterization of wear debris generated in
accelerated rolling-element fatigue tests
[NASA-TP-1203] p0086 W78-10291
Erosion/corrosion of turbine airfoil materials in
the high-velocity effluent of a pressurized
fluidized coal combustor
[NASA-TP-1274] p0115 W78-21470

CORROSION TESTS

Burner rig alkali salt corrosion of several high
temperature alloys p0071 W78-28225
Effluent characterization from a conical
pressurized fluid bed
[NASA-TN-73897] p0073 W78-18793
p0134 W78-21596

CORROSION

U ALUMINUM OXIDES

COST ANALYSIS

Cost analysis of advanced turbine blade
manufacturing processes
[NASA-CR-135203] p0026 W78-10092
Cost benefit study of advanced materials
technology for aircraft turbine engines
[NASA-CR-135235] p0026 W78-11081
Impact of Balance Of System (BOS) costs on
photovoltaic power systems
[NASA-TN-78939] p0138 W78-26550
Cost of photovoltaic energy systems as determined
by balance-of-system costs
[NASA-TN-78957] p0139 W78-27539

COST EFFECTIVENESS

Cost/benefit analysis of advanced material
technologies for small aircraft turbine engines
[NASA-CR-135265] p0027 W78-12083

COST ESTIMATES

Disaster warning system study Summary --- cost
estimates using NOAA satellites
[NASA-TN-73797] p0093 W78-10346
Energy Conversion Alternatives Study (ECAS)
[NASA-TN-73871] p0135 W78-28659

COST REDUCTION

A combined potential and viscous flow solution for
V/STOL engine inlets
[AIAA PAPER 78-142] p0006 W78-20702

COSTS

WT LOW COST

COMPUTERS

WT RADIATION COMPUTERS

Summary of the CTS Transient Event Counter data
after one year of operation --- Communication
Technology Satellite p0086 W78-19566

COUPLING

WT HIGH WAVE COUPLING

COWELL METHOD

U NUMERICAL INTEGRATION

CRACK FORMATION

U CRACK INITIATION

CRACK INITIATION

Application of a flight-line disk crack detector
to a small engine p0012 W78-10088

Analysis and test of deep flaws in thin sheets of
aluminum and titanium. Volume 1: Program
summary and data analysis
[NASA-CR-135369] p0127 W78-21493

Analysis and test of deep flaws in thin sheets of
aluminum and titanium. Volume 2: Crack opening
displacement and stress-strain data
[NASA-CR-135370] p0127 W78-21494

CRACK PROPAGATION

Load-displacement measurement and work
determination in three-point bend tests of
notched or precracked specimens p0029 W78-24370

High temperature compressive cracking in
hot-pressed silicon nitride p0085 W78-38706

CRACKING (FRACTURING)

Room temperature crack growth rates and -20 deg F
fracture toughness of welded 1/4 inch A-285
steel plate
[NASA-TN-73847] p0068 W78-13182

Influence of fretting on flexural fatigue of 304
stainless steel and mild steel
[NASA-TP-1193] p0070 W78-21269

SUBJECT INDEX

Ultraviolet irradiation at elevated temperatures
and thermal cycling in vacuum of PEP-A covered
silicon solar cells
[NASA-TN-78926] p0137 W78-26545

CRACKS

WT SURFACE CRACKS

The use of parabolic variations and the direct
determination of stress intensity factors using
the BII method --- Boundary Integral Equation
[NASA-TN-78903] p0126 W78-24903

Displacement coefficients along the inner
boundaries of radially cracked ring segments
subject to forces and couples p0127 W78-35396

CRACKING

U SURFACE CRACKS

CREEP ANALYSIS

Interpolation and extrapolation of creep rupture
data by the minimum commitment method. II -
Oblique translation p0076 W78-45426

CREEP PROPERTIES

Tensile and creep properties of the experimental
oxide dispersion strengthened iron-base sheet
alloy NA-956E at 1365 K p0074 W78-21858

Elevated-temperature tensile and creep properties
of several ferritic stainless steels
[NASA-TN-73853] p0069 W78-17189

CREEP RESISTANCE

U CREEP STRENGTH

CREEP RUPTURE STRENGTH

Interpolation and extrapolation of creep rupture
data by the minimum commitment method. II -
Oblique translation p0076 W78-45426

Interpolation and extrapolation of creep rupture
data by the minimum commitment method. I -
Focal-point convergence p0076 W78-45427

Interpolation and extrapolation of creep rupture
data by the minimum commitment method. III -
Analysis of multibeats p0076 W78-45428

Interpolation and extrapolation of creep rupture
data by the minimum commitment method. Part 1:
Focal-point convergence
[NASA-TN-78981] p0125 W78-23471

Interpolation and extrapolation of creep rupture
data by the minimum commitment method. Part 2:
Oblique translation
[NASA-TN-78882] p0125 W78-23472

Interpolation and extrapolation of creep rupture
data by the minimum commitment method. Part 3:
Analysis of multibeats
[NASA-TN-78883] p0126 W78-23473

CREEP STRENGTH

Effect of prior creep at 1365 K on the room
temperature tensile properties of several oxide
dispersion strengthened alloys p0074 W78-21431

Ductility normalized-strain-range partitioning
life relations for creep-fatigue life predictions
p0077 W78-51739

Elevated-temperature flow strength, creep
resistance and diffusion welding characteristics
of Ti-6Al-2Nb-1Ta-0.8Zr
[NASA-TN-73854] p0069 W78-17190

CRESTATIONS

U TRAVELING WAVE TUBES

CREVICES

U CRACKS

CRITERIA

WT STRUCTURAL DESIGN CRITERIA

CRITICAL FLOW

Velocity and temperature profiles in near-critical
nitrogen flowing past a horizontal flat plate
[ASME PAPER 77-HT-7] p0106 W78-17481

CRITICAL LOADING

Effects of rotor location, coning, and tilt on
critical loads in large wind turbines p0141 W78-20476

CRITICAL MACH NUMBER

U CRITICAL VELOCITY

U MACH NUMBER

CRITICAL REYNOLDS NUMBER

U CRITICAL VELOCITY

U REYNOLDS NUMBER

SUBJECT INDEX

DAMPING

- CRITICAL SPEED**
J CRITICAL VELOCITY
CRITICAL STRESS
U CRITICAL LOADING
CRITICAL VELOCITY
 High stiffness seals for rotor critical speed control
 [ASME PAPER 77-DET-10] p0118 A78-20591
- CROSS FLOW**
 analysis of the cross flow in a radial inflow turbine scroll
 [NASA-CR-135320] p0029 W78-19153
 Computer program for the analysis of the cross flow in a radial inflow turbine scroll
 [NASA-CR-135321] p0029 W78-19154
- CROSSED FIELD AMPLIFIERS**
 Design, fabrication and testing of a CPA for use in the solar power satellite
 [NASA-CR-159410] p0082 W78-31143
- CROSSLINKING**
 Kinetics of isidization and crosslinking in PBR-polyimide resin --- Polymerization of Monomer Reactants
 p0061 A78-33210
 Trimerization of aromatic nitriles
 [NASA-CASE-LEW-12053-1] p0080 W78-15276
 Kinetics of isidization and crosslinking in PBR-polyimide resin
 [NASA-TN-78844] p0082 W78-23231
- CRUDE OIL**
 Impact of future fuel properties on aircraft engines and fuel systems
 [NASA-TN-78866] p0089 W78-24369
 Computer model for refinery operations with emphasis on jet fuel production. Volume 3: Detailed systems and programming documentation
 [NASA-CR-135335] p0090 W78-25235
- CRUISING FLIGHT**
 Effects of nozzle design and power on cruise drag for upper-surface-blowing aircraft
 p0004 W78-24058
- CRYOGENIC EQUIPMENT**
 Evacuated load-bearing high performance insulation study
 [NASA-CR-135342] p0092 W78-18251
- CRYOGENIC FLUID STORAGE**
 Purging of a tank-mounted multilayer insulation system by gas diffusion
 [NASA-TP-1127] p0041 W78-17127
- CRYOGENIC FLUIDS**
NT LIQUID NITROGEN
NT LIQUID OXYGEN
 Effect of ice contamination on liquid-nitrogen drops in film boiling
 p0105 A78-15821
- CRYOGENIC MAGNETS**
 Design and prototype fabrication of a 30 tesla cryogenic magnet
 p0097 A78-15823
- CRYOGENICS**
 cryogenic properties of a new tough-strong iron alloy
 p0073 A78-15825
 Investigation of the fracture mechanism of Ti-5Al-2.5Sn at cryogenic temperatures
 p0075 A78-52319
 Development of strong and tough cryogenic Fe-12Ni alloys containing reactive metal additions
 p0076 A78-41865
 Comparison of reusable insulation systems for cryogenically-tanked earth-based space vehicles
 [NASA-TN-73668] p0041 W78-21190
- CRYOTRAPPING**
 Atomic hydrogen storage method and apparatus --- cryotrapping and magnetic field strength
 [NASA-CASE-LEW-12081-2] p0169 W78-19907
- CRYSTAL DEFECTS**
NT CRYSTAL DISLOCATIONS
NT EDGE DISLOCATIONS
 Solar Cell High Efficiency and Radiation Damage
 [NASA-CP-2020] p0130 W78-13527
 Photon degradation effects in terrestrial solar cells
 [NASA-TN-78924] p0136 W78-25551
- CRYSTAL DISLOCATIONS**
NT EDGE DISLOCATIONS
 Influence of adsorbed fluids on the rolling contact deformation of MgO single crystals
 p0123 A78-23447
- CRYSTAL GROWTH**
NT DIRECTIONAL SOLIDIFICATION (CRYSTALS)
NT EPITAXY
 Directionally solidified ceramic eutectics
 p0084 A78-11587
 Dendritic web silicon for solar cell application
 p0146 A78-53489
- CRYSTAL LATTICES**
NT FACE CENTERED CUBIC LATTICES
 Crystal field and magnetic properties of ErH3
 p0175 A78-24907
- CRYSTAL STRUCTURE**
 Crystal field and magnetic properties
 [NASA-TN-73837] p0175 W78-13916
- CRYSTALLITES**
 Metastable states of small rare gas crystallites
 p0169 A78-16069
- CRYSTALLINATION**
NT DIRECTIONAL SOLIDIFICATION (CRYSTALS)
CRYSTALS
NT CRYSTALLITES
NT DENDRITIC CRYSTALS
NT POLYCRYSTALS
NT SINGLE CRYSTALS
CUBIC LATTICES
NT FACE CENTERED CUBIC LATTICES
CURRENT DENSITY
 Critical current in sputtered Pb80S8
 p0175 A78-45368
 High-temperature, high-power-density thermionic energy conversion for space
 [NASA-TN-73844] p0171 W78-13890
- CURVE FITTING**
 Instrument to average 100 data sets
 [NASA-TP-1055] p0096 W78-11301
- CURVED SURFACES**
U SHAPES
U SURFACES
- CUTTERS**
NT BLADES (CUTTERS)
- CUTTING**
NT MILLING (MACHINING)
- CYCLES**
NT BRAYTON CYCLE
NT STIRLING CYCLE
 The 5200 cycle test of an 8-cm diameter Hg ion thruster
 [NASA-TN-78860] p0048 W78-21208
- CYCLIC LOADS**
 Evaluation of flawed composite structure under static and cyclic loading
 p0063 A78-26683
 Effect of preload on the fatigue and static strength of composite laminates with defects
 p0061 A78-40310
- CYCLING**
U CYCLES
- CYCLOTRON RADIATION**
 Targets for producing high parity I-123
 [NASA-CASE-LEW-10518-3] p0065 W78-27226
- CYLINDRICAL AFTERBODIES**
J CYLINDRICAL BODIES
CYLINDRICAL BODIES
 Technological development of cylindrical and flat shaped high energy density capacitors --- using polymeric films
 [NASA-CR-135286] p0099 W78-24458
- CYLINDRICAL CHAMBERS**
 Investigation of the effect of ceramic coatings on rocket thrust chamber life
 [NASA-TN-78892] p0049 W78-26173
- CYLINDRICAL TANKS**
 Liquid propellant reorientation in a low-gravity environment
 [NASA-TN-78969] p0105 W78-29407
- CYLINDROIDS**
U CYLINDRICAL BODIES

D

- DABNO (DATA ANALYSIS)**
U DATA PROCESSING
U DATA REDUCTION
- DAMAGE**
NT RADIATION DAMAGE
- DAMPING**
NT ELASTIC DAMPING
NT VISCOELASTIC DAMPING
NT VISCOUS DAMPING

DAMPING FACTOR

Stiffness and damping of elastomeric O-ring bearing mounts [NASA-CR-135328] p0127 W78-18860

DAMPING FACTOR
 U DAMPING
 DAMPING IN FITCH
 U DAMPING
 DAMPING IN HOLL
 U DAMPING
 DAMPING IN TAU
 U DAMPING
 DAMPING TESTS
 Steady-state unbalance response of a three-disk flexible rotor on flexible, damped supports p0119 W78-29326

DAMPNESS
 U MOISTURE CONTENT
 DART TURBOPROP ENGINES
 U TURBOPROP ENGINES
 DATA ACQUISITION
 Escort - 1 data acquisition and display system to support research testing p0155 W78-37685
 Escort: 1 data acquisition and display system to support research testing [NASA-TN-78909] p0154 W78-24807

DATA ADAPTIVE EVALUATOR/MONITOR
 U DATA PROCESSING
 U DATA REDUCTION
 DATA ANALYSIS
 U DATA PROCESSING
 U DATA REDUCTION
 DATA CONVERTERS
 NT ANALOG TO DIGITAL CONVERTERS
 DATA CORRELATION
 Correlations between ultrasonic and fracture toughness factors in metallic materials p0077 W78-45438
 Instrument to average 100 data sets [NASA-TN-1055] p0096 W78-11301
 Correlation of combustor acoustic power levels inferred from internal fluctuating pressure measurements [NASA-TN-78986] p0165 W78-31871

DATA HANDLING SYSTEMS
 U DATA SYSTEMS
 DATA LINKS
 A digitally implemented communications experiment utilizing the Hermes /CTS/ satellite p0094 W78-24884

DATA MANAGEMENT
 Modeling and Analysis of Power Processing Systems (MAPPS), initial phase 2 [NASA-CR-135173] p0100 W78-29350

DATA PROCESSING
 NT DATA CORRELATION
 NT DATA REDUCTION
 Interpolation and extrapolation of creep rupture data by the minimum commitment method. III - Analysis of multiheats p0076 W78-45428
 Interpolation and extrapolation of creep rupture data by the minimum commitment method. Part 1: Focal-point convergence [NASA-TN-78881] p0125 W78-23471
 Interpolation and extrapolation of creep rupture data by the minimum commitment method. Part 2: Oblique translation [NASA-TN-78882] p0125 W78-23472
 Interpolation and extrapolation of creep rupture data by the minimum commitment method. Part 3: Analysis of multiheats [NASA-TN-78883] p0126 W78-23473
 A data acquisition and handling system for the measurement of radial plasma transport rates [NASA-TN-78849] p0155 W78-23751

DATA PROCESSING EQUIPMENT
 NT DATA PROCESSING TERMINALS
 NT HYBRID COMPUTERS
 NT MINICOMPUTERS
 NT UNIVAC 1100 SERIES COMPUTERS
 DATA PROCESSING TERMINALS
 Low cost Ku-band earth terminals for voice/data/facsimile p0094 W78-31970

DATA READOUT SYSTEMS
 U DATA SYSTEMS
 U DISPLAY DEVICES

SUBJECT INDEX

DATA REDUCTION
 Analysis and test of deep flaws in thin sheets of aluminum and titanium. Volume 1: Program summary and data analysis [NASA-CR-135369] p0127 W78-21493

DATA SYSTEMS
 An airborne meteorological data collection system using satellite relay (ASDAR) [NASA-TN-78992] p0093 W78-33283

DC (CURRENT)
 U DIRECT CURRENT
 DEADWEIGHT
 U STATIC LOADS
 DEBRIS
 Counter pumping debris excluder and separator --- gas turbine shaft seals [NASA-CR-13511855-1] p0020 W78-25090

DEBRIS TEMPERATURE
 U SPECIFIC HEAT
 DECAY
 NT ACOUSTIC EMISSION
 NT ELECTRON EMISSION
 NT EMISSION
 NT FIELD EMISSION
 NT ION EMISSION
 NT MICROWAVE EMISSION
 NT PARTICLE EMISSION
 NT PHOTOPRODUCTION
 NT RADIO EMISSION
 NT SECONDARY EMISSION
 NT SPECTRAL EMISSION
 NT THERMIONIC EMISSION
 DECELERATORS
 U BRAKES (FOR ARRESTING MOTION)
 DECOMPOSITION
 NT PHOTODISSOCIATION
 Catalytic decomposition of methanol for onboard hydrogen generation [NASA-TN-1247] p0083 W78-25236

DECOMPRESSION
 U PRESSURE REDUCTION
 DEFECTS
 NT CRYSTAL DEFECTS
 NT CRYSTAL DISLOCATIONS
 NT EDGE DISLOCATIONS
 NT SURFACE DEFECTS
 Evaluation of flawed composite structure under static and cyclic loading p0063 W78-26683
 Effect of preload on the fatigue and static strength of composite laminates with defects p0061 W78-40310

DEFLATING
 U PRESSURE REDUCTION
 DEFLECTORS
 Noise of deflectors used for flow attachment with STOL-OTW configurations p0023 W78-24877
 Noise of deflectors used for flow attachment with STOL-OTW configurations [NASA-TN-73809] p0163 W78-13853

DEFORMATION
 NT AXIAL STRAIN
 NT ELASTIC DEFORMATION
 NT PLASTIC DEFORMATION
 Friction, deformation and fracture of single-crystal silicon carbide [ASLE PREPRINT 77-LC-5C-3] p0085 W78-28438
 The use of ion beam cleaning to obtain high quality cold welds with minimal deformation [NASA-TN-78933] p0083 W78-27257

DEGRADATION
 NT THERMAL DEGRADATION
 Photon degradation effects in terrestrial solar cells [NASA-TN-78924] p0136 W78-25551

DEKATONS
 U COUNTERS
 DELTA DARTER AIRCRAFT
 U F-102 AIRCRAFT
 DENDRITIC CRYSTALS
 Dendritic web silicon for solar cell application p0146 W78-53489

DENSITY (MASS/VOLUME)
 NT GAS DENSITY
 DENSITY (NUMBER/VOLUME)
 NT ELECTRON DENSITY (CONCENTRATION)
 NT ION DENSITY (CONCENTRATION)
 NT PLASMA DENSITY

- DENSITY (MASS/VOLUME)**
 U FLUX DENSITY
- DEPENDENCE**
 NT TIME DEPENDENCE
- DEPOSITION**
 NT VACUUM DEPOSITION
 NT VAPOR DEPOSITION
 Industrial ion source technology --- for ion beam etching, surface texturing, and deposition [NASA-CR-135353] p0169 W78-18883
- DEPRESSURIZATION**
 U PRESSURE REDUCTION
- DESIGN ANALYSIS**
 Dynamic tooth loads and stressing for high contact ratio spur gears [AIAA PAPER 77-DRT-101] p0123 A78-20606
 Up-date of traveling wave tube improvements p0098 A78-33208
 Design considerations in mechanical face seals for improved performance. 1: Basic configurations [NASA-TN-73735] p0113 W78-13839
 Design study of wind turbines 50 kW to 3000 kW for electric utility applications. Volume 2: Analysis and design [NASA-CR-134935] p0143 W78-17462
 Design study of wind turbines 50 kW to 3000 kW for electric utility applications. Volume 3: Supplementary design and analysis tasks [NASA-CR-135121] p0144 W78-17463
 Design study of wind turbines, 50 kW to 3000 kW for electric utility applications: Executive summary [NASA-CR-134936] p0144 W78-23559
 Design study of wind turbines 50 kW to 3000 kW for electric utility applications: Analysis and design [NASA-CR-134937] p0144 W78-23560
- DESIGN OF EXPERIMENTS**
 U EXPERIMENTAL DESIGN
- DETERIORATION**
 Effect of steady flight loads on JT9D-7 performance deterioration [NASA-CR-135407] p0031 W78-29105
- DETONATION**
 Computer program for calculation of complex chemical equilibrium compositions, rocket performance, incident and reflected shocks, and Chapman-Jouquet detonations [NASA-SP-272] p0156 W78-17724
- DEVELOPING NATIONS**
 Energy resources of the developing countries and some priority markets for the use of solar energy p0142 A78-24400
 Utilization of solar energy in developing countries - Identifying some potential markets p0142 A78-45437
 Utilization of solar energy in developing countries: Identifying some potential markets [NASA-TN-78964] p0140 W78-29578
- DEWAR SYSTEMS**
 U CRYOGENIC EQUIPMENT
- DIAGRAMS**
 NT STRESS-STRAIN DIAGRAMS
- DIAMINES**
 Synthesis of perfluoroalkylene aromatic diamines [NASA-CR-159403] p0087 W78-31235
- DIATOMIC MOLECULES**
 Excimer lasers [NASA-CR-155949] p0112 W78-19480
- DIESEL ENGINES**
 General aviation internal combustion engine research programs at NASA-Lewis Research Center [AIAA PAPER 78-932] p0025 A78-43505
 Lightweight, low compression aircraft diesel engine --- converting a spark ignition engine to the diesel cycle [NASA-CR-135300] p0121 W78-21471
 General aviation internal-combustion engine research programs at NASA-Lewis Research Center [NASA-TN-78891] p0011 W78-24139
- DIESEL FUELS**
 Performance and emissions of a catalytic reactor with propane, diesel, and Jet A fuels [NASA-TN-71786] p0088 W78-14177
- DIFFERENTIAL ALGEBRA**
 U MATRICES (MATHEMATICS)
- DIFFUSERS**
 Performance characteristics of two annular dump diffusers using suction-stabilized vortex flow control p0107 A78-45431
 Performance characteristics of two annular dump diffusers using suction-stabilized vortex flow control [NASA-TN-73857] p0004 W78-19057
- DIFFUSION**
 NT GASEOUS DIFFUSION
 NT PARTICLE DIFFUSION
 NT PLASMA DIFFUSION
 NT TURBULENT DIFFUSION
 Feasibility study of tungsten as a diffusion barrier between nickel-chromium-aluminum and Gamma/Gamma prime - Delta eutectic alloys [NASA-TN-1131] p0068 W78-15230
- DIFFUSION BONDING**
 U DIFFUSION WELDING
- DIFFUSION COEFFICIENT**
 Determination of the sinter diffusion coefficient and its application to alkaline battery problems [NASA-TN-73879] p0138 W78-19648
- DIFFUSION EFFECT**
 U DIFFUSION
- DIFFUSION WELDING**
 Development and fabrication of a diffusion welded Columbus alloy heat exchanger --- for space power generation [AIAA PAPER A78-61] p0123 A78-31500
 Elevated-temperature flow strength, creep resistance and diffusion welding characteristics of Ti-6Al-2Nb-1Ta-0.8Bz [NASA-TN-73854] p0069 W78-17190
- DIFLUORO COMPOUNDS**
 NT POLYTETRAFLUOROETHYLENE
- DIGITAL COMMUNICATION**
 U PULSE COMMUNICATION
- DIGITAL COMPUTERS**
 NT BICOINTEGRATED
 NT UNIVAC 1100 SERIES COMPUTERS
- DIGITAL DATA**
 Digital enhancement of computerized axial tomograms [NASA-TN-78974] p0152 W78-31690
- DIGITAL SIMULATION**
 Synchronization of wind turbine generators against an infinite bus under gusting wind conditions [IEEE PAPER P 77 675-2] p0142 A78-30196
 Real time digital propulsion system simulation for manned flight simulators [AIAA PAPER 78-927] p0035 A78-45095
- DIGITAL SPACECRAFT TELEVISION**
 A digitally implemented communications experiment utilizing the Hornes (CTS) satellite [NASA-TN-73827] p0093 W78-13283
- DIGITAL SYSTEMS**
 A data acquisition and handling system for the measurement of radial plasma transport rates [NASA-TN-78849] p0155 W78-23751
 Fabrication and test of digital output interface devices for gas turbine electronic controls [NASA-CR-135427] p0030 W78-27129
- DIGITAL TELEVISION**
 NT DIGITAL SPACECRAFT TELEVISION
- DIGITIZERS**
 U ANALOG TO DIGITAL CONVERTERS
- DILATOMETERS**
 U EXTENSOMETERS
- DIMENSIONLESS NUMBERS**
 NT MACH NUMBER
 NT REYNOLDS NUMBER
- DIMENSIONS**
 NT FILM THICKNESS
 Some basic considerations of measurements involving collimated direct sunlight [NASA-TN-74947] p0130 W78-13608
- DIODES**
 NT CESIUM DIODES
 High frequency capacitor-diode voltage multiplier dc-dc converter development [NASA-CR-135309] p0099 W78-15401
 Extended performance solar electric propulsion thrust system study. Volume 5. Capacitor-diode voltage multiplier: Technology evaluation [NASA-CR-135281-VOL-5] p0053 W78-19195
 A 10-cw mercury ion thruster performance with a 1 kW capacitor-diode voltage multiplier beam supply [NASA-TN-78864] p0049 W78-23143
 Medium power voltage multipliers with a large number of stages [NASA-TN-78900] p0093 W78-26373

DIOXIDES

SUBJECT INDEX

Regulated high efficiency, lightweight capacitor-diode multiplier dc to dc converter [NASA-CASR-LEN-12791-1] p0097 A78-32361

DIOXIDES

UT SILICON DIOXIDE

DIRECT CURRENT

Solid State Remote Power Controllers for high voltage DC distribution systems p0100 A78-15574

Electric vehicle power train instrumentation - Some constraints and considerations [RVC PAPER 7704] p0097 A78-16922

A model for particle confinement in a toroidal plasma subject to strong radial electric fields p0173 A78-24891

Experiments with enhanced mode thermionic converters p0146 A78-29636

Potential damage to dc superconducting magnets due to high frequency electromagnetic waves p0098 A78-39902

Preliminary power train design for a state-of-the-art electric vehicle [NASA-CR-135341] p0182 A78-29992

DIRECT POWER GENERATORS

UT ALKALINE BATTERIES

UT FUEL CELLS

UT MAGNETOHYDRODYNAMIC GENERATORS

UT NICKEL ZINC BATTERIES

UT SOLAR CELLS

UT THERMIONIC CONVERTERS

DIRECTIONAL SOLIDIFICATION (CRYSTALS)

Directionally solidified ceramic eutectics p0084 A78-11547

Volume fraction determination in cast superalloys and directionally solidified eutectic alloys by a new manual point count practice p0089 A78-24369

Shape of two-dimensional solidification interface during directional solidification by continuous casting p0119 A78-31829

DIRECTIVITY

Far-field multimodal acoustic radiation directivity --- from ducted bodies [NASA-TN-73839] p0163 A78-13855

DISASTERS

Disaster warning system study summary --- cost estimates using NOAA satellites [NASA-TN-73797] p0093 A78-10346

DISCONTINUITY

Effect of discontinuities as a means to alleviate thermal expansion mismatch damage in laminar composites [NASA-TN-73739] p0057 A78-13136

DISHS

PARABOLIC REFLECTORS

DISILICIDES

Microstructural and wear properties of sputtered carbides and silicides p0084 A78-23445

DISKS (SHAPES)

UT ROTATING DISKS

Liquid jet impingement normal to a disk in zero gravity [ASME PAPER 78-NA/FE-1] p0107 A78-41154

DISLOCATIONS (MATERIALS)

UT CRYSTAL DISLOCATIONS

UT EDGE DISLOCATIONS

DISPERSION PRECIPITATION HARDENING

PRECIPITATION HARDENING

DISPERSIONS

UT AEROSOLS

UT SMOKE

DISPLACEMENT MEASUREMENT

Load-displacement measurement and work determination in three-point bend tests of notched or precracked specimens p0089 A78-24370

Displacement coefficients along the inner boundaries of radially cracked ring segments subject to forces and couples p0127 A78-35396

DISPLAY DEVICES

UT ANEMOMETERS

UT WIND VANES

Escort - A data acquisition and display system to support research testing p0155 A78-37685

Fabrication and characteristics of experimental radiographic amplifier screens --- image transducers with improved image contrast and resolution [NASA-CR-2937] p0124 A78-15501

Particle parameter analyzing system --- x-y plotter circuits and display [NASA-CASR-ILR-06094] p0096 A78-17293

Escort: A data acquisition and display system to support research testing [NASA-TN-78909] p0154 A78-24807

DISPLAY SYSTEMS

DISPLAY DEVICES

DISSOCIATION

UT PHOTODISSOCIATION

DISSOLUTION

DISSOLVING

DISSOLVING

Release of dissolved nitrogen from water during depressurization p0066 A78-33224

DISTORTION

UT FLOW DISTORTION

DISTRIBUTION (PROPERTY)

UT CHARGE DISTRIBUTION

UT FLOW DISTRIBUTION

UT FREQUENCY DISTRIBUTION

UT HOLD DISTRIBUTION (MECHANICS)

UT PRESSURE DISTRIBUTION

UT RADIAL DISTRIBUTION

UT RADIATION DISTRIBUTION

UT STRESS CONCENTRATION

UT TEMPERATURE DISTRIBUTION

UT VELOCITY DISTRIBUTION

UT VERTICAL DISTRIBUTION

DISTURBANCE THEORY

PERTURBATION THEORY

DISULFIDES

X-ray photoelectron spectroscopic study of surface chemistry of dibenzyl disulfide on steel under mild and severe wear conditions p0066 A78-31839

DITHIOLS

UT THIOLS

DIURNAL VARIATIONS

Variability of ozone near the tropopause from GASP data [NASA-CR-135405] p0148 A78-23648

DOCUMENTS

UT ABSTRACTS

UT BIBLIOGRAPHIES

UT USER MANUALS (COMPUTER PROGRAMS)

DOMESTIC ENERGY

Marshall Space Flight Center development program for solar heating and cooling systems p0110 A78-11368

DOMESTIC SATELLITE COMMUNICATIONS SYSTEMS

A forecast of broadcast satellite communications p0094 A78-15615

The 20/30 GHz satellite systems technology needs assessment [NASA-TN-78975] p0093 A78-31323

DOPIING (ADDITIVES)

UT ADDITIVES

DOPPLER EFFECT

Model for interpreting Doppler broadened optical line emission measurements on axially symmetric plasma p0174 A78-46189

DOVAP

UT DOPPLER EFFECT

DRAG

UT AERODYNAMIC DRAG

DRAG COEFFICIENT

UT AERODYNAMIC DRAG

DRAG DEVICES

UT WING FLAPS

DRAG MEASUREMENT

Miniature drag force anemometer p0109 A78-17397

DRAGULATORS

UT BRAKES (FOR ARRESTING MOTION)

DRIFT (INSTUMENTATION)

Development of a drift-correction procedure for a photoelectric spectrometer p0109 A78-23525

DRILLING

UT LASER DRILLING

SUBJECT INDEX

EARTH SATELLITES

DRONE HELICOPTERS
U HELICOPTERS
DROP SIZE
 Effect of airstream velocity on mean drop diameters of water sprays produced by pressure and air atomizing nozzles --- for combustion studies p0024 A78-33111
 The role of drop velocity in statistical spray description p0107 A78-50323
 Effect of airstream velocity on mean drop diameters of water sprays produced by pressure and air atomizing nozzles [NASA-TN-73740] p0101 A78-13369
DROPS (LIQUIDS)
 Effect of ice contamination on liquid-nitrogen drops in film boiling p0105 A78-15821
 Thermally driven oscillations and wave motion of a liquid drop p0106 A78-17508
 The role of drop velocity in statistical spray description [NASA-TN-73887] p0102 A78-20458
DRUGS
 NT METHYL CHLORIDE
DRY CELLS
 NT NICKEL ZINC BATTERIES
DUAL MODE PROPULSION
 U HYBRID PROPULSION
DUCTED BODIES
 Far-field multimodal acoustic radiation directivity --- from ducted bodies [NASA-TN-73839] p0163 A78-13855
DUCTED FAN ENGINES
 Development and test of an inlet and duct to provide airflow for a wing boundary layer control system [AIAA PAPER 78-141] p0006 A78-20701
DUCTED FANS
 Numerical spatial searching techniques for estimating duct attenuation and source pressure profiles [NASA-TN-78857] p0103 A78-22329
DUCTED FLOW
 Sound separation probes for flowing duct noise measurements --- jet engine diagnostics p0033 A78-17396
 Velocity, temperature, and electrical conductivity profiles in hydrogen-oxygen HED duct flows [NASA-TN-78968] p0108 A78-28372
DUCTILITY
 Ductility normalized-strain-range partitioning, life relations for creep-fatigue life predictions p0077 A78-51739
DUCTS
 NT ACOUSTIC DUCTS
 NT AIR DUCTS
 Some flow phenomena in a constant area duct with a Forda type inlet including the critical region [NASA-TN-78943] p0104 A78-27367
DUNGETS WIND SHEAR MECHANISM
 U WIND SHEAR
DURABILITY
 Endurance testing of first generation (Block 1) commercial solar cell modules [NASA-TN-78922] p0138 A78-26548
DYNAMIC CHARACTERISTICS
 NT AERODYNAMIC DRAG
 NT ATTITUDE STABILITY
 NT COMBUSTION STABILITY
 NT FLOW CHARACTERISTICS
 NT FLOW DISTRIBUTION
 NT FLOW VELOCITY
 NT FREQUENCY STABILITY
 NT MAGNETOHYDRODYNAMIC STABILITY
 NT SPACECRAFT STABILITY
 NT TRANSIENT RESPONSE
 Measurement of the time-temperature dependent dynamic mechanical properties of boron/aluminum composites p0061 A78-33222
 High frequency dynamic engine simulation --- TP-30 engine [NASA-CR-135313] p0027 A78-13059
 Measurement of the time-temperature dependent dynamic mechanical properties of boron/aluminum composites

[NASA-TN-78837] p0058 A78-20254
 Development of procedures for calculating stiffness and damping properties of elastomers in engineering applications. Part 4: Testing of elastomers under a rotating load --- resonance testing [NASA-CR-135355] p0127 A78-22402
 Oil-air mist lubrication for helicopter gearing [NASA-CR-135081] p0010 A78-25080
 Study of dynamic emission spectra from lubricant films in an elastohydrodynamic contact using Fourier transform spectroscopy [NASA-CR-159418] p0162 A78-32809
DYNAMIC LOADS
 NT AERODYNAMIC LOADS
 NT CYCLIC LOADS
 NT GUST LOADS
 NT IMPACT LOADS
 NT ROLLING CONTACT LOADS
 NT VIBRATORY LOADS
 Dynamic tooth loads and stressing for high contact ratio spur gears [ASME PAPER 77-DGT-101] p0123 A78-20606
 Comparison of computer codes for calculating dynamic loads in wind turbines p0142 A78-37678
 Wind Turbine Structural Dynamics [NASA-CR-2034] p0132 A78-19616
 Comparison of computer codes for calculating dynamic loads in wind turbines [NASA-TN-73773] p0135 A78-23556
DYNAMIC MODELS
 Dynamic modeling of spacecraft in a collisionless plasma p0037 A78-110150
 Blade row dynamic digital compression program. Volume 2: J85 circumferential distortion redistribution model, effect of stator characteristics, and stage characteristics sensitivity study [NASA-CR-134953] p0032 A78-33103
DYNAMIC PROPERTIES
 U DYNAMIC CHARACTERISTICS
DYNAMIC RESPONSE
 NT TRANSIENT RESPONSE
 Nonlinear flap-lag-axial equations of a rotating beam with arbitrary precone angle [AIAA 78-491] p0127 A78-29798
 Atmospheric effects on inlets for supersonic cruise aircraft [NASA-TN-I-73667] p0003 A78-10026
 Wind tunnel evaluation of YF-12 inlet response to internal airflow disturbances with and without control --- Lewis 10 by 10 ft supersonic wind tunnel tests p0006 A78-32062
DYNAMIC STABILITY
 NT ATTITUDE STABILITY
 NT COMBUSTION STABILITY
 NT FREQUENCY STABILITY
 NT MAGNETOHYDRODYNAMIC STABILITY
 NT SPACECRAFT STABILITY
DYNAMIC STRUCTURAL ANALYSIS
 Wind Turbine Structural Dynamics [NASA-CR-2034] p0132 A78-19616
 Proposed design procedure for transmission shafting under fatigue loading [NASA-TN-78927] p0115 A78-26444

E

EARTH ATMOSPHERE
 NT TROPOPAUSE
 NT TROPOSPHERE
EARTH ORBITS
 Interaction of large, high power systems with operational orbit charged particle environments [NASA-TN-73867] p0037 A78-16076
EARTH RESOURCES
 NT COAL
 NT CRUDE OIL
 NT FOSSIL FUELS
 NT GEYSERS
 NT WATER RESOURCES
 Energy resources of the developing countries and some priority markets for the use of solar energy p0142 A78-24400
EARTH SATELLITES
 NT ATS 1

- NT ATS 3
 NT ATS 5
 NT ATS 6
 NT COMMUNICATION SATELLITES
 NT COMMUNICATIONS TECHNOLOGY SATELLITE
 NT METEOROLOGICAL SATELLITES
 NT NOAA SATELLITES
 NT SYNCHRONOUS SATELLITES
 EDP
 U INTERNALLY BLOWN FLAPS
 EBULLITION
 U BOILING
 ECCENTRICITY
 The effects of eccentricities on the fracture of off-axis fiber composites --- carbon fiber reinforced plastics
 [NASA-TN-73826] p0057 W78-17153
 ECONOMIC ANALYSIS
 Performance and economics of advanced energy conversion systems for coal and coal-derived fuels
 p0146 A78-34078
 Economics of ion propulsion for large space systems
 [AIAA PAPER 78-698] p0040 A78-37441
 Technical and economic feasibility study of solar/fossil hybrid power systems
 [NASA-TN-73820] p0132 W78-17486
 Engineering in the 21st century
 [NASA-TN-79010] p0105 W78-33380
 EDDIES
 U VORTICES
 EDDY DIFFUSION
 U TURBULENT DIFFUSION
 EDGE DISLOCATIONS
 Influence of adsorbed fluids on the rolling contact deformation of MgO single crystals
 p0123 A78-23447
 EDGES
 NT LEADING EDGES
 EFFECTIVENESS
 NT COST EFFECTIVENESS
 NT SYSTEM EFFECTIVENESS
 EFFECTORS
 U CONTROL EQUIPMENT
 EFFICIENCY
 NT COMBUSTION EFFICIENCY
 NT COMPRESSOR EFFICIENCY
 NT ENERGY CONVERSION EFFICIENCY
 NT POWER EFFICIENCY
 NT PROPULSIVE EFFICIENCY
 NT THERMODYNAMIC EFFICIENCY
 NT TRANSMISSION EFFICIENCY
 Baseline tests of the AM General DJ-5B electric delivery van
 [NASA-TN-73758] p0178 W78-17933
 EFFLUENTS
 Effluent characterization from a conical pressurized fluid bed
 p0066 A78-33221
 Effluent characterization from a conical pressurized fluid bed
 [NASA-TN-73897] p0134 W78-21596
 EFFLUX
 Ion beam plume and efflux measurements of an 8-cm mercury ion thruster
 [AIAA PAPER 78-676] p0055 A78-32753
 A review of electron bombardment thruster systems/spacecraft field and particle interfaces
 [AIAA PAPER 78-677] p0051 A78-32754
 ELASTIC DAMPING
 NT VISCOELASTIC DAMPING
 Development of procedures for calculating stiffness and damping properties of elastomers in engineering applications. Part 2: Testing of elastomers under a rotating load --- resonance testing
 [NASA-CR-135355] p0127 W78-22402
 ELASTIC DEFORMATION
 Simplified solution for elliptical-contact deformation between two elastic solids
 p0118 A78-12737
 The elastic distortion of the flanged inner ring of a high-speed cylindrical roller bearing
 [ASME PAPER 77-LUB-8] p0118 A78-23352
 Simplified contact analysis
 p0127 A78-28200
 Experimental transient and permanent deformation studies of steel-sphere-impacted or explosively-impulsed aluminum panels
 [NASA-CR-135315] p0078 W78-15234
 ELASTIC MODULUS
 U MODULUS OF ELASTICITY
 ELASTIC PROPERTIES
 NT ELASTOPLASTICITY
 NT MODULUS OF ELASTICITY
 NT VISCOELASTICITY
 ELASTIC STABILITY
 U DAMPING
 ELASTIC WAVES
 NT AERODYNAMIC NOISE
 NT AIRCRAFT NOISE
 NT ENGINE NOISE
 NT JET AIRCRAFT NOISE
 NT NOISE (SOUND)
 NT NORMAL SHOCK WAVES
 NT SHOCK WAVES
 NT SOUND WAVES
 NT STRESS WAVES
 ELASTICIZERS
 U PLASTICIZERS
 ELASTODYNAMICS
 NT ELASTIC DAMPING
 NT ELASTOHYDRODYNAMICS
 ELASTOHYDRODYNAMICS
 Elastohydrodynamic lubrication of elliptical contacts for materials of low elastic modulus. I - Fully flooded conjunction
 [ASME PAPER 77-LUB-10] p0119 A78-28414
 Bearing, gearing, and lubrication technology
 [SAE PAPER 780077] p0120 A78-33366
 Traction and lubricant film temperature as related to the glass transition temperature and solidification --- using infrared spectroscopy on EHD contacts
 p0087 A78-40997
 Additional aspects of elastohydrodynamic lubrication
 p0120 A78-45430
 Statistical model for asperity-contact time fraction in elastohydrodynamic lubrication
 [NASA-TP-1130] p0114 W78-18429
 Ferrographic analysis of wear particles from sliding elastohydrodynamic experiments
 [NASA-TP-1230] p0115 W78-22377
 Additional aspects of elastohydrodynamic lubrication
 [NASA-TN-78898] p0115 W78-26443
 Elastohydrodynamic film thickness measurements of artificially produced surface dents and grooves --- using optical interferometry
 [NASA-TN-78949] p0116 W78-27428
 Study of dynamic emission spectra from lubricant films in an elastohydrodynamic contact using Fourier transform spectroscopy
 [NASA-CR-159418] p0162 W78-32809
 The practical impact of elastohydrodynamic lubrication
 [NASA-TN-78987] p0117 W78-33445
 Minimum film thickness in elliptical contacts for different regimes of fluid-film lubrication
 [NASA-TP-1342] p0117 W78-33447
 ELASTOMERS
 Development of procedures for calculating stiffness and damping properties of elastomers in engineering applications. Part 4: Testing of elastomers under a rotating load --- resonance testing
 [NASA-CR-135355] p0127 W78-22402
 ELASTOMETERS
 Stiffness and damping of elastomeric O-ring bearing mounts
 [NASA-CR-135328] p0127 W78-18460
 ELASTOPLASTICITY
 Experimental transient and permanent deformation studies of steel-sphere-impacted or explosively-impulsed aluminum panels
 [NASA-CR-135315] p0078 W78-15234
 ELECTRIC ARCS
 Interaction of large, high power systems with operational orbit charged particle environments --- large solar arrays in space
 [AAS 77-243] p0044 A78-36719
 ELECTRIC AUTOMOBILES
 New batteries and their impact on electric vehicles
 p0141 A78-16923
 Baseline tests of the AM General DJ-5E electric delivery van
 [NASA-TN-73758] p0178 W78-17933
 Baseline tests of the Zagato Elcar electric passenger vehicle
 [NASA-TN-73764] p0178 W78-17934

SUBJECT INDEX

ELECTRIC MOTOR VEHICLES

- Test and evaluation of 23 electric vehicles for state-of-the-art assessment [NASA-TN-75850] p0178 W78-17937
- Baseline tests of the EVA change-of-pace coupe electric passenger vehicle [NASA-TN-73763] p0178 W78-17938
- Baseline tests of the EVA contractor electric passenger vehicle [NASA-TN-73762] p0179 W78-17939
- Baseline tests of the C. S. Waterson DAF electric passenger vehicle [NASA-TN-73757] p0179 W78-17942
- State-of-the-art assessment of electric vehicles and hybrid vehicles [NASA-TN-73756] p0179 W78-18988
- Baseline tests of the Volkswagen transporter electric delivery van [NASA-TN-73766] p0179 W78-20021
- Baseline tests of the EPC Buntingbird electric passenger vehicle [NASA-TN-73760] p0180 W78-21010
- Baseline tests of the Kordesh hybrid passenger vehicle [NASA-TN-73769] p0138 W78-26551
- ELECTRIC BATTERIES**
- WT ALKALINE BATTERIES
- WT LEAD ACID BATTERIES
- WT NICKEL ZINC BATTERIES
- WT STORAGE BATTERIES
- New batteries and their impact on electric vehicles p0181 W78-16923
- Baseline tests of the C. S. Waterson DAF electric passenger vehicle [NASA-TN-73757] p0179 W78-17942
- Baseline tests of the Volkswagen transporter electric delivery van [NASA-TN-73766] p0179 W78-20021
- Response of lead-acid batteries to chopper-controlled discharge: Preliminary results [NASA-TN-73834] p0180 W78-20023
- Rapid, efficient charging of lead-acid and nickel-zinc traction cells [NASA-TN-78901] p0135 W78-24616
- Baseline tests of the Kordesh hybrid passenger vehicle [NASA-TN-73769] p0138 W78-26551
- ELECTRIC CHARGE**
- WT ELECTROSTATIC CHARGE
- ELECTRIC CHOPPERS**
- Electric vehicle power train instrumentation - Some constraints and considerations [EVC PAPER 7744] p0097 W78-16922
- Response of lead-acid batteries to chopper-controlled discharge: Preliminary results [NASA-TN-73834] p0180 W78-20023
- Response of lead-acid batteries to chopper-controlled discharge [NASA-TN-73834-REV] p0180 W78-25010
- ELECTRIC COILS**
- WT MAGNETIC COILS
- ELECTRIC CONTACTS**
- Shear strength of metal - SiO2 contacts p0061 W78-33209
- ELECTRIC CONTROL**
- Response of lead-acid batteries to chopper-controlled discharge: Preliminary results [NASA-TN-73834] p0180 W78-20023
- ELECTRIC CURRENT**
- WT ARC DISCHARGES
- WT DIRECT CURRENT
- WT ELECTRIC ARCS
- WT ELECTRIC DISCHARGES
- WT GAS DISCHARGES
- WT LIGHTNING
- WT PENNING DISCHARGE
- WT RADIO FREQUENCY DISCHARGE
- WT THRESHOLD CURRENTS
- Response of lead-acid batteries to chopper-controlled discharge [NASA-TN-73834-REV] p0180 W78-25010
- ELECTRIC DISCHARGES**
- WT ARC DISCHARGES
- WT ELECTRIC ARCS
- WT GAS DISCHARGES
- WT LIGHTNING
- WT PENNING DISCHARGE
- WT RADIO FREQUENCY DISCHARGE
- Distribution of E/W and W sub e in a cross-flow electric discharge laser [NASA-TN-73807] p0111 W78-14386
- Closed cycle electric discharge laser design investigation [NASA-CP-135400] p0112 W78-25407
- ELECTRIC ENERGY STORAGE**
- Electrochemical cell for rebalancing redox flow system [NASA-CASB-LEW-13150-1] p0136 W78-25554
- ELECTRIC FIELD STRUCTURES**
- A model for particle confinement in a toroidal plasma subject to strong radial electric fields [NASA-TN-73814] p0171 W78-10884
- ELECTRIC FIELDS**
- A possible pole problem in the formula for klystron gap fields p0098 W78-18287
- Inward transport of a toroidally confined plasma subject to strong radial electric fields p0172 W78-24890
- A model for particle confinement in a toroidal plasma subject to strong radial electric fields p0173 W78-24891
- Distribution of E/W and W/e/ in a cross-flow electric discharge laser --- electric field to neutral gas density and electron number density p0111 W78-24896
- Effects of applied dc radial electric fields on particle transport in a bumpy torus plasma p0173 W78-36956
- Distribution of E/W and W sub e in a cross-flow electric discharge laser [NASA-TN-73807] p0111 W78-14386
- ELECTRIC GENERATORS**
- WT AC GENERATORS
- WT ALKALINE BATTERIES
- WT FUEL CELLS
- WT MAGNETOHYDRODYNAMIC GENERATORS
- WT NICKEL ZINC BATTERIES
- WT SOLAR CELLS
- WT SOLAR GENERATORS
- WT THERMIONIC CONVERTERS
- WT TURBOGENERATORS
- Experiments with enhanced mode thermionic converters p0186 W78-29636
- ELECTRIC IMPULSES**
- WT ELECTRIC PULSES
- ELECTRIC MOTOR VEHICLES**
- Electric vehicle power train instrumentation - Some constraints and considerations [EVC PAPER 7744] p0097 W78-16922
- Pulse battery charger employing 1000 ampere transistor switches p0146 W78-31974
- Test and evaluation of 23 electric vehicles for state-of-the-art assessment [SAE PAPER 780290] p0181 W78-33382
- Baseline tests of the C. S. Waterson Renault 5 electric passenger vehicle [NASA-TN-73759] p0178 W78-16928
- Baseline tests of the power-train electric delivery van [NASA-TN-73765] p0178 W78-17936
- Baseline tests of the batronic Minivan electric delivery van [NASA-TN-73761] p0179 W78-17940
- Performance of conventionally powered vehicles tested to an electric vehicle test procedure [NASA-TN-73768] p0179 W78-20022
- Response of lead-acid batteries to chopper-controlled discharge: Preliminary results [NASA-TN-73834] p0180 W78-20023
- Response of lead-acid batteries to chopper-controlled discharge [NASA-TN-73834-REV] p0180 W78-25010
- A cycle timer for testing electric vehicles [NASA-TN-78934] p0180 W78-26996
- State-of-the-art assessment of electric and hybrid vehicles [NASA-TN-79509] p0180 W78-27003
- Solubility, stability, and electrochemical studies of sulfur-sulfide solutions in organic solvents [NASA-TP-1245] p0140 W78-28624
- Preliminary power train design for a state-of-the-art electric vehicle [NASA-CR-135340] p0185 W78-29584
- Preliminary power train design for a state-of-the-art electric vehicle [NASA-CR-135341] p0182 W78-29992

ELECTRIC MOTORS

ELECTRIC MOTORS
WT INDUCTION MOTORS
 Preliminary power train design for a state-of-the-art electric vehicle [NASA-CR-135341] p0182 W78-29992

ELECTRIC POTENTIAL
WT PHOTOVOLTAICS
ELECTRIC POWER
 Power oscillation of the Mod-0 wind turbine p0133 W78-19629

ELECTRIC POWER CONVERSION
U ELECTRIC GENERATORS
ELECTRIC POWER PLANTS
 RCAS Phase I fuel cell results --- Energy Conservation Alternatives Study p0142 A78-26110
 Design and calculated performance and cost of the RCAS Phase II open cycle HHD power generation system [ASME PAPER 77-WA/ENER-5] p0174 A78-33183
 Performance and economics of advanced energy conversion systems for coal and coal-derived fuels p0146 A78-34078
 Thermal energy storage heat exchanger: Solten salt heat exchanger design for utility power plants [NASA-CR-135244] p0143 W78-14632
 Thermal energy storage heat exchanger: Solten salt heat exchanger design for utility power plants [NASA-CR-135245] p0143 W78-14633
 Design study of wind turbines, 50 kW to 3000 kW for electric utility applications: Executive summary [NASA-CR-134936] p0144 W78-23559

ELECTRIC POWER SUPPLIES
WT SPACECRAFT POWER SUPPLIES
 Solid State Serote Power Controllers for high voltage DC distribution systems p0100 A78-15574
 Design and operating experience on the US Department of Energy experimental Mod-0 100-kW wind turbine [NASA-TN-78915] p0138 W78-26552
 DOE/NASA Mod-0A wind turbine performance [NASA-TN-78916] p0139 W78-26553
 Description and status of NASA-LERC/DOE photovoltaic applications systems [NASA-TN-78936] p0139 W78-26554
 An inverter/controller subsystem optimized for photovoltaic applications [NASA-TN-78903] p0180 W78-26995

ELECTRIC POWER TRANSMISSION
 A review of the Thermo-electronic Laser Energy Converter /TELX/ program at Lewis Research Center p0182 A78-33217
 Closed cycle electric discharge laser design investigation [NASA-CR-135408] p0112 W78-25407

ELECTRIC PROPULSION
U ION PROPULSION
WT SOLAR ELECTRIC PROPULSION
 Ion beam plume and efflux measurements of an 8-cm mercury ion thruster [AIAA PAPER 78-676] p0055 A78-32753
 Evolution of the 1-1/2 lb mercury ion thruster subsystem [AIAA PAPER 78-7118] p0051 A78-32776
 Charge-exchange plasma generated by an ion thruster [NASA-CR-135318] p0052 W78-13123
 Inert gas thrusters [NASA-CR-135226] p0053 W78-19198
 Electric prototype power processor for a 30cm ion thruster [NASA-CR-135287] p0054 W78-19200
 The 30-cm ion thruster power processor [NASA-CR-135401] p0054 W78-24280

ELECTRIC PULSES
 Pulse ignition characterization of mercury ion thruster hollow cathode using an improved pulse ignitor [AIAA PAPER 78-709] p0051 A78-32773
 Pulse ignition characterization of mercury ion thruster hollow cathode using an improved pulse ignitor [NASA-TN-78858] p0047 W78-21203

ELECTRIC RELAYS
 Multi-cell battery protection system [NASA-CASE-LEW-12039-1] p0130 W78-14625

SUBJECT INDEX

ELECTRIC ROCKET ENGINES
WT ION ENGINES
WT MERCURY ION ENGINES
 Electric prototype power processor for a 30cm ion thruster [NASA-CR-135287] p0054 W78-19200
 Extended performance electric propulsion power processor design study. Volume 1: Executive summary [NASA-CR-135357] p0054 W78-20250

ELECTRICAL BREAKDOWNS
U ELECTRICAL FAULTS
ELECTRICAL CONDUCTIVITY
U ELECTRICAL RESISTIVITY
ELECTRICAL ENERGY
U ELECTRIC POWER
ELECTRICAL ENGINEERING
 A mechanical, thermal and electrical packaging design for a prototype power management and control system for the 30 cm mercury ion thruster [NASA-TN-78862] p0049 W78-23142

ELECTRICAL FAULTS
 Transient response to three-phase faults on a wind turbine generator [NASA-TN-78902] p0137 W78-26542

ELECTRICAL IMPEDANCE
WT CONTACT RESISTANCE
ELECTRICAL MEASUREMENT
 Results of module electrical measurement of the DOE 46-kilowatt procurement [NASA-TN-78829] p0138 W78-19658

ELECTRICAL PROPERTIES
WT CAPACITANCE
WT CARRIER MOBILITY
WT CHARGE DISTRIBUTION
WT CONTACT RESISTANCE
WT ELECTRICAL RESISTIVITY
WT MAGNETORESISTIVITY
WT PHOTOVOLTAIC EFFECT
WT PLASMA CONDUCTIVITY
WT SUPERCONDUCTIVITY
 Optical and electrical properties of ion beam textured Kapton and Teflon [NASA-TN-73778] p0162 W78-13848
 Charging of flexible solar array substrates in kilovolt electron beams [NASA-TN-73865] p0044 W78-21199

ELECTRICAL RESISTANCE
WT CONTACT RESISTANCE
ELECTRICAL RESISTIVITY
WT MAGNETORESISTIVITY
WT PLASMA CONDUCTIVITY
WT SUPERCONDUCTIVITY
 Upper limit for magnetoresistance in silicon bronze and phosphor bronze wire p0175 A78-14423
 Optical and electrical properties of ion beam textured Kapton and Teflon p0085 A78-24908

ELECTRO-OPTICS
 Advanced optical blade tip clearance measurement system [NASA-CR-159402] p0032 W78-31106

ELECTROACOUSTIC TRANSDUCERS
WT MICROPHONES
ELECTROCHEMICAL CELLS
WT ALKALINE BATTERIES
WT ELECTRIC BATTERIES
WT FUEL CELLS
WT LEAD ACID BATTERIES
WT NICKEL ZINC BATTERIES
WT STORAGE BATTERIES
 Multi-cell battery protection system [NASA-CASE-LEW-12039-1] p0130 W78-14625
 Redox flow cell development and demonstration project, calendar year 1976 [NASA-TN-73873] p0138 W78-19656
 Electrochemical cell for rebalancing redox flow system [NASA-CASE-LEW-13150-1] p0136 W78-25554
 Solubility, stability, and electrochemical studies of sulfur-sulfide solutions in organic solvents [NASA-TP-1245] p0140 W78-28624

ELECTROCHEMISTRY
WT ELECTROLYSIS
 Anion exchange membranes for electrochemical oxidation-reduction energy storage system [NASA-TN-73751] p0131 W78-14631

SUBJECT INDEX

ELECTROPHOTOOMETRY

ELECTRODES

WT CATHODES
 WT HOLLOW CATHODES
 WT IMPLANTED ELECTRODES (BIOLOGY)
 Secondary electron emission properties of
 conducting surfaces for use in multistage
 depressed collectors p0098 A78-23635
 Secondary-electron-emission properties of
 conducting surfaces with application to
 multistage depressed collectors for microwave
 amplifiers
 [NASA-TP-1097] p0068 W78-11230
 Cesium thermionic converters having improved
 electrodes p0137 W78-25555
 [NASA-CASE-LEW-12038-3]
ELECTROGENERATORS
 U ELECTRIC GENERATORS
ELECTROHYDRAULIC CONTROL
 U ELECTRIC CONTROL
ELECTROLYSIS
 Status of the DOE /STOR/-sponsored national
 program on hydrogen production from water via
 thermochemical cycles p0102 A78-29331

ELECTROLYTES

WT ION EXCHANGE MEMBRANE ELECTROLYTES
ELECTROMAGNETIC ABSORPTION
 WT INFRARED ABSORPTION
ELECTROMAGNETIC CONTROL
 U REMOTE CONTROL
ELECTROMAGNETIC FIELDS
 WT FAR FIELDS
ELECTROMAGNETIC INTERACTIONS
 WT PLASMA-ELECTROMAGNETIC INTERACTION
ELECTROMAGNETIC INTERFERENCE
 WT HISS
 WT SHOT NOISE
 WT WHISTLERS
 Carrier-interference ratios for frequency sharing
 between frequency-modulated
 amplitude-modulated-vestigial-sideband
 television systems p0043 W78-26159
 [NASA-TP-1264]

ELECTROMAGNETIC NOISE

WT HISS
 WT SHOT NOISE
 WT WHISTLERS
ELECTROMAGNETIC PROPERTIES
 WT CAPACITANCE
 WT ELECTRICAL PROPERTIES
 WT OPTICAL PROPERTIES
 WT PHOTOVOLTAIC EFFECT
ELECTROMAGNETIC RADIATION
 WT BREMSSTRAHLUNG
 WT CYCLOTRON RADIATION
 WT GAMMA RAYS
 WT MICROWAVE EMISSION
 WT HILLIARY WAVES
 WT RADIO EMISSION
 WT SUNLIGHT
 WT ULTRAVIOLET RADIATION
 Potential damage to DC superconducting magnets due
 to the high frequency electromagnetic waves
 [NASA-TN-73808] p0096 W78-13330

ELECTROMAGNETIC SHIELDING

Diagnostic evaluations of a beam-shielded 8-cm
 mercury ion thruster p0051 A78-32768
 [AIAA PAPER 78-702]

ELECTROMAGNETIC WAVE TRANSMISSION

WT LIGHT TRANSMISSION
 WT MICROWAVE TRANSMISSION
ELECTROMAGNETIC WAVES
 U ELECTROMAGNETIC RADIATION
ELECTROMAGNETS
 WT HIGH FIELD MAGNETS
 WT SUPERCONDUCTING MAGNETS

ELECTROMETERS

The Plasma Interaction Experiment (PIX)
 description and test program --- electrometers
 [NASA-TN-78863] p0041 W78-21188

ELECTRON BEAMS

Compact electron-beam source for formation of
 neutral beams of very low vapor pressure materials
 p0110 A78-41464

ELECTRON BOMBARDMENT

Secondary electron emission properties of
 conducting surfaces for use in multistage
 depressed collectors

p0098 A78-23635
 A review of electron bombardment thruster
 systems/spacecraft field and particle interfaces
 [AIAA PAPER 78-677] p0051 A78-32750
 Mechanical properties on ion-beam-textured
 surgical implant alloys p0075 A78-36045
 Mechanical properties of ion-beam-textured
 surgical implant alloys
 [NASA-TN-73742] p0068 W78-13181
 A review of electron bombardment thruster
 systems/spacecraft field and particle interfaces
 [NASA-TN-78850] p0048 W78-21206

ELECTRON DENSITY (CONCENTRATION)

Distribution of E/N and E/e/ in a cross-flow
 electric discharge laser --- electric field to
 neutral gas density and electron number density
 p0111 A78-26896

ELECTRON EMISSION

WT FIELD EMISSION
 WT SECONDARY EMISSION
 Secondary-electron-emission properties of
 conducting surfaces with application to
 multistage depressed collectors for microwave
 amplifiers
 [NASA-TP-1097] p0068 W78-11230

ELECTRON GUNS

Up-date of traveling wave tube improvements
 p0098 A78-33208

ELECTRON PLASMA

Microwave radiation measurements near the electron
 plasma frequency of the NASA Lewis bumpy torus
 plasma
 [NASA-TN-78940] p0172 W78-27914

ELECTRON RADIATION

WT ELECTRON BEAMS

ELECTRON SOURCES

Compact electron-beam source for formation of
 neutral beams of very low vapor pressure materials
 p0110 A78-41464

ELECTRON SPECTROSCOPY

Composition of RF-sputtered refractory compounds
 determined by X-ray photoelectron spectroscopy
 p0085 A78-30301
 X-ray photoelectron spectroscopic study of surface
 chemistry of dibenzyl disulfide on steel under
 mild and severe wear conditions p0066 A78-31439

Principles of ESCA and applications to metal
 corrosion, coating and lubrication --- Electron
 Spectroscopy for Chemical Analysis p0061 A78-33213

Principles of ESCA and application to metal
 corrosion, coating and lubrication
 [NASA-TN-78839] p0070 W78-19262

ELECTRON TRANSITIONS

Excimer lasers
 [NASA-CR-155949] p0112 W78-19480

ELECTRON TUBES

WT KLYSTRONS
 WT MICROWAVE TUBES
 WT TRAVELING WAVE TUBES

ELECTRONIC CONTROL

Real time digital propulsion system simulation for
 manned flight simulators
 [AIAA PAPER 78-927] p0035 A78-45095
 Design and performance of heart assist or
 artificial heart control systems p0185 W78-23032

ELECTRONIC EQUIPMENT

WT ELECTRONIC MODULES
 WT METAL OXIDE SEMICONDUCTORS
 WT PHOTOVOLTAIC CELLS
 WT SOLID STATE DEVICES
 WT SPACECRAFT ELECTRONIC EQUIPMENT
 Lightning protection of aircraft
 [NASA-RP-1008] p0009 W78-11024

ELECTRONIC MODULES

Method of making encapsulated solar cell modules
 [NASA-CASE-LEW-1-1985-1] p0136 W78-25528

ELECTRONIC SIGNAL MEASUREMENT

U SIGNAL MEASUREMENT
ELECTRONIC SWITCHES
 U SWITCHING CIRCUITS
ELECTRONS

WT PHOTOELECTRONS
ELECTROPHOTOOMETRY
 Development of a drift-correction procedure for a
 photoelectric spectrometer

ELECTROPHYSICS

SUBJECT INDEX

- ELECTROPHYSICS p0109 A78-23525
 WT ELECTRO-OPTICS
 ELECTROSTATIC EFFECT
 U ELECTRIC CURRENT
 ELECTROSTATIC CHARGE
 NASA Charging Analyzer Program - A computer tool that can evaluate electrostatic contamination --- of spacecraft during geomagnetic substorms p0084 A78-33220
 Charging characteristics of materials: Comparison of experimental results with simple analytical models p0036 W78-10157
 Viking and STP P78-2 electrostatic charging designs and testing p0037 W78-10175
 A three dimensional dynamic study of electrostatic charging in materials [NASA-CR-135256] p0099 W78-13328
 NASA charging analyzer program: A computer tool that can evaluate electrostatic contamination [NASA-TN-73889] p0096 W78-21372
 ELECTROSTATIC FIELDS
 U ELECTRIC FIELDS
 ELECTROSTATIC FLASHES
 U PLASMAS (PHYSICS)
 ELECTROSTATIC PROPULSION
 WT ION PROPULSION
 ELECTROSTATICS
 12-cm magneto-electrostatic containment argon/xenon ion source development [AIAA PAPER 78-681] p0039 A78-32756
 ELEMENTARY PARTICLES
 WT PHOTOELECTRONS
 WT PROTONS
 ELLIPTICITY
 Simplified solution for elliptical-contact deformation between two elastic solids p0118 A78-12737
 EMISSION
 U EMISSION
 EMISSION
 WT ACOUSTIC EMISSION
 WT ELECTRON EMISSION
 WT FIELD EMISSION
 WT ION EMISSION
 WT MICROWAVE EMISSION
 WT PARTICLE EMISSION
 WT RADIO EMISSION
 WT SECONDARY EMISSION
 WT SPECTRAL EMISSION
 WT THERMIONIC EMISSION
 Evaluation of Federal Aviation Administration ion engine exhaust sampling rake [NASA-CR-135213] p0029 W78-21111
 EMISSION SPECTRA
 Computer program for calculation of a gas temperature profile by infrared emission: Absorption spectroscopy [NASA-TN-73888] p0015 W78-15043
 Lower hybrid emission diagnostics on the NASA Lewis bumpy torus [NASA-TN-73858] p0171 W78-19938
 Temperature distributions of a cesium-seeded hydrogen-oxygen supersonic free jet [NASA-TP-1162] p0171 W78-20959
 Microwave radiation measurements near the electron plasma frequency of the NASA Lewis bumpy torus plasma [NASA-TN-78940] p0172 W78-27914
 Study of dynamic emission spectra from lubricant films in an elastohydrodynamic contact using Fourier transform spectroscopy [NASA-CR-159418] p0162 W78-32809
 EMITTANCE
 A low cost, portable instrument for measuring emittance p0109 A78-11392
 EMITTERS
 WT THERMIONIC EMITTERS
 A methodology for experimentally-based determination of gap shrinkage and effective lifetimes in the emitter and base of p-n junction solar cells p0181 A78-10903
 EMPLOYMENT
 The NIRE project: Minority Involvement in NASA Engineering p0176 W78-13938
 [NASA-TN-73811]
 ENCAPSULATING
 Method of making encapsulated solar cell modules [NASA-CASR-LEU-12185-1] p0136 W78-25528
 ENCODING
 U CODING
 ENERGETIC PARTICLES
 WT FLASHES (PHYSICS)
 ENERGY CONSERVATION
 ECAS Phase I fuel cell results --- Energy Conservation Alternatives Study p0142 A78-26110
 Propulsion --- NASA program for aircraft fuel consumption reduction p0025 A78-43360
 Alternative fuels p0013 W78-11074
 General aviation energy-conservation research programs at NASA-Lewis Research Center [NASA-TN-73884] p0016 W78-17060
 Performance of conventionally powered vehicles tested to an electric vehicle test procedure [NASA-TN-73768] p0179 W78-20022
 Design approaches to more energy efficient engines [NASA-TN-78893] p0115 W78-26442
 ACEE propulsion overview p0001 W78-27048
 Fuel conservative aircraft engine technology [NASA-TN-78962] p0027 W78-27127
 Lewis Research Center support of Chrysler "Advanced" engine program p0117 W78-30305
 Initial test results with a single-cylinder rhombic-drive Stirling engine --- to be applied to automobile engine design to conserve energy [NASA-TN-78919] p0180 W78-31533
 Aerodynamic design and performance testing of an advanced 30 deg swept, eight bladed propeller at Mac numbers from 0.2 to 0.85 [NASA-CR-1047] p0008 W78-32066
 Aerial thermography for energy conservation [NASA-TN-78959] p0129 W78-33510
 ENERGY CONSUMPTION
 Energy resources of the developing countries and some priority markets for the use of solar energy p0182 A78-24400
 Alternative aircraft fuels [NASA-TN-73836] p0038 W78-17229
 ENERGY CONVERSION
 WT SOLAR ENERGY CONVERSION
 A review of the Thermoelectronic Laser Energy Converter /TELEC/ Program at Lewis Research Center p0142 A78-33217
 Hydrogen turbine power conversion system assessment [NASA-CR-135298] p0144 W78-20621
 A review of the thermoelectronic laser energy converter (TELEC) program at Lewis Research Center [NASA-TN-73888] p0111 W78-21841
 Design study of wind turbines 50 kw to 3000 kw for electric utility applications: Analysis and design [NASA-CR-134937] p0144 W78-23560
 Diode thermionic energy conversion with lanthanum-hexaboride electrodes [NASA-TN-78887] p0135 W78-24617
 Energy Conversion Alternatives Study (ECAS) [NASA-TN-73871] p0135 W78-24659
 ENERGY CONVERSION EFFICIENCY
 Evaluation of initial collector field performance at the Langley Solar Building Test Facility p0181 A78-11391
 ECAS Phase I fuel cell results --- Energy Conservation Alternatives Study p0142 A78-26110
 Experiments with enhanced mode thermionic converters p0146 W78-24636
 Design and calculated performance and cost of the ECAS Phase II open cycle MHD power generation system [ASME PAPER 77-WA/ENER-5] p0174 A78-33143
 Open-Cycle Gas Turbine/Steam Turbine Combined Cycles with synthetic fuels from coal [ASME PAPER 77-WA/ENER-9] p0166 W78-33147
 Update of traveling wave tube improvements p0098 A78-33208
 Performance and economics of advanced energy conversion systems for coal and coal-derived fuels p0146 W78-34078

SUBJECT INDEX

ENGINE CONTROL

Preliminary results on the conversion of laser energy into electricity p0173 A78-34631

Comment on 'Heat-pipe reactors for space power applications' p0052 A78-40826

Design approaches to more energy efficient engines [IAA PAPER 78-931] p0025 A78-43504

Solar Cell High Efficiency and Radiation Damage [NASA-CP-2020] p0130 A78-13527

Optimize out-of-core thermionic energy conversion for nuclear electric propulsion [NASA-TN-73892] p0170 A78-17856

Experimental data and theoretical analysis of an operating 100 kW wind turbine [NASA-TN-73893] p0133 A78-19642

Solar cell system having alternating current output [NASA-CASE-LEW-12806-1] p0136 A78-25553

Self-reconfiguring solar cell system [NASA-CASE-LEW-12586-1] p0139 A78-27520

Energy efficient engine: Preliminary design and integration studies [NASA-CR-135444] p0032 A78-31108

ENERGY DENSITY
 O FLOW DENSITY

ENERGY EXCHANGE
 J ENERGY TRANSFER

ENERGY POLICY
 Alternative fuels p0013 A78-11074

Solar Cell High Efficiency and Radiation Damage [NASA-CP-2020] p0130 A78-13527

Design study of wind turbines 50 kW to 3000 kW for electric utility applications. Volume 2: Analysis and design [NASA-CR-134935] p0143 A78-17462

Baseline tests of the AM General DJ-5E electric truck electric delivery van [NASA-TM-73758] p0178 A78-17933

Photovoltaic highway applications: Assessment of the near-term market [NASA-TM-73863] p0178 A78-17935

Baseline tests of the power-train electric delivery van [NASA-TM-73765] p0178 A78-17936

Test and evaluation of 23 electric vehicles for state-of-the-art assessment [NASA-TM-73850] p0178 A78-17937

Baseline tests of the EVA change-of-pace coupe electric passenger vehicle [NASA-TM-73763] p0178 A78-17938

Baseline tests of the EVA contractor electric passenger vehicle [NASA-TM-73762] p0179 A78-17939

State-of-the-art assessment of electric vehicles and hybrid vehicles [NASA-TM-73756] p0179 A78-18988

Selective coating for solar panels --- using black chrome and black nickel [NASA-CASE-LEW-12159-1] p0132 A78-19599

Experimental data and theoretical analysis of an operating 100 kW wind turbine [NASA-TM-73883] p0133 A78-19642

Photovoltaic village power application: Assessment of the near-term market [NASA-TM-73893] p0133 A78-19643

Photovoltaic water pumping applications: Assessment of the near-term market [NASA-TM-78847] p0134 A78-19644

Baseline tests of the EPC Hummingbird electric passenger vehicle [NASA-TM-73760] p0180 A78-21010

Performance potential of combined cycles integrated with low-Btu gasifiers for future electric utility applications [NASA-TM-73775] p0135 A78-23557

Transient response to three-phase faults on a wind turbine generator [NASA-TM-78902] p0137 A78-26542

Cost of photovoltaic energy systems as determined by balance-of-system costs [NASA-TM-78957] p0139 A78-27539

Study and program plan for improved heavy duty gas turbine engine ceramic component development [NASA-CR-135230] p0122 A78-28466

Large wind turbine generators [NASA-TM-73767] p0140 A78-29575

Thermal energy storage for industrial waste heat recovery [NASA-TM-78953] p0140 A78-29576

Storage systems for solar thermal power [NASA-TM-78952] p0140 A78-29577

The 200-kilowatt wind turbine project [NASA-TM-79757] p0140 A78-29593

Development of flat-plate solar collectors for the heating and cooling of buildings: Executive summary [NASA-CR-134804-2] p0146 A78-33527

ENERGY SOURCES
 Energy resources of the developing countries and some priority markets for the use of solar energy p0142 A78-24400

Solar Cell High Efficiency and Radiation Damage [NASA-CP-2020] p0130 A78-13527

Computer model for refinery operations with emphasis on jet fuel production. Volume 3: Detailed systems and programming documentation [NASA-CR-135335] p0090 A78-25235

Photon degradation effects in terrestrial solar cells [NASA-TM-78924] p0136 A78-25551

Design and operating experience on the US Department of Energy experimental Mod-0 100-kW wind turbine [NASA-TM-78915] p0138 A78-26552

DOE/NASA Mod-0A wind turbine performance [NASA-TM-78916] p0139 A78-26553

An inverter/controller subsystem optimized for photovoltaic applications [NASA-TM-78903] p0180 A78-26995

ENERGY SPECTRA
 Turbulence processes and simple closure schemes p0107 A78-40983

ENERGY STORAGE
 HT ELECTRIC ENERGY STORAGE
 HT HEAT STORAGE

The Redox Flow System for solar photovoltaic energy storage p0141 A78-11019

Status of the DOE/STOR/-sponsored national program on hydrogen production from water via thermochemical cycles p0142 A78-29331

Anion exchange membranes for electrochemical oxidation-reduction energy storage system [NASA-TM-73751] p0131 A78-14631

The ERDA/LeRC photovoltaic systems test facility [NASA-TM-73787] p0035 A78-15059

Hydrogen turbine power conversion system assessment [NASA-CR-135298] p0144 A78-20621

A simulation model for wind energy storage systems. Volume 1: Technical report [NASA-CR-135283] p0156 A78-20802

A simulation model for wind energy storage systems. Volume 2: Operation manual [NASA-CR-135284] p0157 A78-20803

A simulation model for wind energy storage systems. Volume 3: Program descriptions [NASA-CR-135281] p0157 A78-20804

Storage systems for solar thermal power [NASA-TM-78952] p0140 A78-29577

ENERGY STORAGE DEVICES
 O ENERGY STORAGE

ENERGY TECHNOLOGY
 Application of thick-film technology to solar cell fabrication p0146 A78-10947

A simulation model for wind energy storage systems. Volume 2: Operation manual [NASA-CR-135284] p0157 A78-20803

A simulation model for wind energy storage systems. Volume 3: Program descriptions [NASA-CR-135283] p0157 A78-20804

Method for producing solar energy panels by automation [NASA-CASE-LEW-12541-1] p0136 A78-25529

Utilization of solar energy in developing countries: Identifying some potential markets [NASA-TM-78964] p0140 A78-29578

ENERGY TRANSFER
 On the localness of the spectral energy transfer in turbulence p0106 A78-24909

On the localness of the spectral energy transfer in turbulence [NASA-TM-73874] p0101 A78-13361

ENGINE CONTROL
 HT ROCKET ENGINE CONTROL

ENGINE DESIGN

SUBJECT INDEX

- WT TURBOJET ENGINE CONTROL**
 The application of the fourth approximation method to turbofan engine models p0023 A78-23891
 Optimal controls for an advanced turbofan engine p0033 A78-23893
 Design of turbofan engine controls using output feedback regulator theory p0023 A78-23907
 Real time digital propulsion system simulation for manned flight simulators [AIAA PAPER 78-927] p0035 A78-45095
 Normal shock and restart controls for a supersonic airbreathing propulsion system p0019 W78-23023
- ENGINE DESIGN**
WT ROCKET ENGINE DESIGN
 A review of NASA's propulsion programs for civil aviation p0023 A78-20651
 Preliminary QCSER program - Test results --- Quiet Clean Short-haul Experimental Engine [SAR PAPER 771008] p0023 A78-23840
 Design of turbofan engine controls using output feedback regulator theory p0023 A78-23907
 General aviation energy-conservation research programs at NASA-Lewis Research Center --- for non-turbine general aviation engines p0024 A78-29330
 Evolution of the 1-1/2 lb mercury ion thruster subsystem [AIAA PAPER 78-7118] p0051 A78-32776
 Gas path sealing in turbine engines p0024 A78-33218
 An overview of aerospace gas turbine technology of relevance to the development of the automotive gas turbine engine [SAR PAPER 780075] p0120 A78-33364
 Engineering Model 8-cu Thruster System [AIAA PAPER 78-646] p0055 A78-37434
 Comparison of computer codes for calculating dynamic loads in wind turbines p0142 A78-37678
 Propulsion --- NASA program for aircraft fuel consumption reduction p0025 A78-43360
 Design approaches to more energy efficient engines [AIAA PAPER 78-931] p0025 A78-43504
 General aviation internal combustion engine research programs at NASA-Lewis Research Center [AIAA PAPER 78-932] p0025 A78-43505
 Combustor concepts for aircraft gas turbine low-power emissions reduction [AIAA PAPER 78-999] p0025 A78-43546
 Inlet-engine matching for SCAR including application of a biconic variable geometry inlet --- Supersonic Cruise Aircraft Research [AIAA PAPER 78-961] p0007 A78-45096
 NASA engine system technology programs - An overview [AIAA PAPER 78-928] p0025 A78-48452
 Evaluation of a low aspect ratio small axial compressor stage, volume 1 [NASA-CR-135240] p0026 W78-12081
 Evaluation of a low aspect ratio small axial compressor stage, volume 2 [NASA-CR-135241] p0026 W78-12082
 High frequency dynamic engine simulation --- TP-30 engine [NASA-M-135313] p0027 W78-13059
 Cold-air performance of a tip turbine designed to drive a lift fan. 3: Effect of simulated fan leakage on turbine performance [NASA-TP-1109] p0003 W78-16001
 Cold-air performance of free-power turbine designed for 112-kilowatt automotive gas-turbine engine. 1: Design Stator-vane-chord setting angle of 35 deg [NASA-TP-1007] p0015 W78-16053
 F-15/asymmetric nozzle system integration study support program [NASA-CR-135252] p0028 W78-18070
 State-of-the-art assessment of electric vehicles and hybrid vehicles [NASA-TN-73756] p0179 W78-18988
 VCE testbed program planning and definition study [NASA-CR-135362] p0028 W78-19160
 Effects of film injection on performance of a cooled turbine p0029 W78-21147
 Automotive Stirling engine development program --- fuel economy assessment [NASA-CR-135331] p0181 W78-22970
 QCSER task 2: Engine and installation preliminary design [NASA-CR-134738] p0030 W78-23089
 Stirling engine design annual [NASA-CR-135382] p0181 W78-23999
 Acoustic design of the QCSER propulsion systems p0004 W78-24067
 Advanced space engine powerhead breadboard assembly system study [NASA-CR-135232] p0054 W78-25127
 Design approaches to more energy efficient engines [NASA-TN-78893] p0115 W78-26442
 ACEE propulsion overview p0001 W78-27048
 Status of advanced turboprop technology p0001 W78-27055
 Gas turbine engine emission reduction technology program p0001 W78-27058
 Impact of broad-specification fuels on future jet aircraft --- engine components and performance p0089 W78-27059
 Core compressor exit stage study. Volume 1: Blading design --- turbofan engines [NASA-CR-135391] p0031 W78-29099
 Lewis Research Center support of Chrysler upgraded engine program p0117 W78-30305
 Energy efficient engine: Preliminary design and integration studies [NASA-CR-135444] p0032 W78-31108
 Liquid rocket engine axial-flow turbopumps [NASA-SP-8125] p0050 W78-31164
 Initial test results with a single-cylinder rhombic-drive Stirling engine --- to be applied to automobile engine design to conserve energy [NASA-TN-78919] p0140 W78-31533
 Aircraft gas turbine low-power emissions reduction technology program [NASA-CR-135434] p0032 W78-32097
 Design and overall performance of four highly loaded, high speed inlet stages for an advanced high-pressure-ratio core compressor [NASA-TP-1337] p0022 W78-33108
- ENGINE FAILURE**
 Failure detection and correction for turbofan engines p0033 A78-23918
 A 30-cu mercury ion thruster performance with a 1 kv capacitor-diode voltage multiplier beam supply [NASA-TN-78864] p0049 W78-23143
- ENGINE INLETS**
 A combined potential and viscous flow solution for V/STOL engine inlets [AIAA PAPER 78-142] p0006 A78-20702
 Methods for calculating the transonic boundary layer separation for V/STOL inlets at high incidence angles [AIAA 78-1340] p0007 A78-46537
 Predicted inlet gas temperatures for tungsten fiber reinforced superalloy turbine blades [NASA-TN-73842] p0017 W78-19157
 Inlet technology for powered-lift aircraft p0005 W78-24069
- ENGINE MONITORING INSTRUMENTS**
 Application of a flight-line disk crack detector to a small engine p0012 W78-10088
- ENGINE NOISE**
 Propagation of sound waves through a linear shear layer - A closed form solution [AIAA PAPER 78-196] p0165 A78-20738
 Combustor fluctuating pressure measurements in-engine and in a component test facility - A preliminary comparison p0023 A78-24878
 Effectiveness of an inlet flow turbulence control device to simulate flight fan noise in an anechoic chamber p0024 A78-24880
 State-of-the-art of turbofan engine noise control p0024 A78-24858
 Reduction of fan noise in an anechoic chamber by reducing chamber wall induced inlet flow disturbances

SUBJECT INDEX

ENVIRONMENT EFFECTS

- p0166 A78-37681
 Of the use of relative velocity exponents for jet engine exhaust noise
- p0024 A78-37683
 Effect of forward motion on engine noise
 [NASA-CR-134954]
- p0026 A78-10093
 Light-effects on predicted fan fly-by noise
 [NASA-TN-73798]
- p0018 A78-13060
 Combustor fluctuating pressure measurements in engine and in a component test facility: A preliminary comparison
 [NASA-TN-73885]
- p0035 A78-13077
 Variable thrust nozzle for quiet turbofan engine and method of operating same
 [NASA-CASR-LRW-12317-1]
- p0016 A78-17055
 Method of fan sound mode structure determination computer program user's manual: Microphone location program
 [NASA-CR-135294]
- p0028 A78-17065
 Method of fan sound mode structure determination computer program user's manual: Modal calculation program
 [NASA-CR-135295]
- p0028 A78-17066
 A method for calculating strut and splitter plate noise in exit ducts: Theory and verification
 [NASA-CR-2955]
- p0167 A78-20921
 Propulsion systems noise technology
- p0001 A78-27056
ENGINE PARTS
- Two-layer thermal barrier coating for high temperature components
 [ACS PAPER 31-BH-76P]
- p0084 A78-18787
 Temperature distributions and thermal stresses in a graded zirconia/metal gas path seal system for aircraft gas turbine engines
 [AIAA PAPER 79-93]
- p0118 A78-20683
 Consolidation of silicon nitride without additives --- for gas turbine engine efficiency increase
- p0085 A78-28895
 Progress in advanced high temperature turbine materials, coatings, and technology
- p0056 A78-24910
 NASA/General Electric Engine Component Improvement Program
 [AIAA PAPER 79-929]
- p0025 A78-45098
 Substitution of ceramics for high temperature alloys
- p0086 A78-47596
 Turbine disks for improved reliability
- p0012 A78-10089
 Cost/benefit analysis of advanced material technologies for small aircraft turbine engines
 [NASA-CR-135265]
- p0027 A78-12083
 Gas turbine engine with convertible accessories
 [NASA-CASR-LRW-12390-1]
- p0016 A78-17056
 Development of spiral-groove self-acting face seals
 [NASA-CR-135303]
- p0121 A78-17387
 Analysis of the cross flow in a radial inflow turbine scroll
 [NASA-CR-135320]
- p0029 A78-19153
 A method for calculating strut and splitter plate noise in exit ducts: Theory and verification
 [NASA-CR-2955]
- p0167 A78-20921
 Gas path sealing in turbine engines
 [NASA-TN-73890]
- p0018 A78-21109
 Advanced materials research for long-haul aircraft turbine engines
- p0001 A78-27057
 Impact of broad-specification fuels on future jet aircraft --- engine components and performance
- p0089 A78-27059
 Study and program plan for improved heavy duty gas turbine engine ceramic component development
 [NASA-CR-135210]
- p0122 A78-28466
 Long-term CP6 engine performance deterioration: Evaluation of engine S/N 451-380
 [NASA-CR-159390]
- p0031 A78-29103
ENGINE STARTERS
- Normal shock and restart controls for a supersonic airbreathing propulsion system
- p0019 A78-23023
ENGINE TESTING LABORATORIES
- Review of experimental work on transonic flow in turbomachinery
- p0006 A78-12312
 General aviation energy-conservation research programs at NASA-Lewis Research Center
 [NASA-TN-73884]
- p0016 A78-17060
ENGINE TESTS
- Sound separation probes for flowing duct noise
- measurements --- jet engine diagnostics
- p0033 A78-17396
 Preliminary QCSRE program - Test results --- Quiet Clean Short-haul Experimental Engine
 [SAR PAPER 771000]
- p0023 A78-23840
 Combustor fluctuating pressure measurements in-engine and in a component test facility - A preliminary comparison
- p0023 A78-24078
 'Chain pooling' model selection as developed for the statistical analysis of a rotor burst protection experiment
- p0160 A78-29327
 Planned flight test of a mercury ion auxiliary propulsion system. I - Objectives, systems descriptions, and mission operations
 [AIAA PAPER 78-647-I]
- p0050 A78-32734
 Planned flight test of a mercury ion auxiliary propulsion system. II - Integration with host spacecraft
 [AIAA PAPER 78-647-II]
- p0050 A78-32735
 Instrumentation for propulsion systems development
 [SAR PAPER 780076]
- p0109 A78-33365
 Extended-performance thruster technology evaluation
 [AIAA PAPER 78-666]
- p0055 A78-37436
 Manufacture and engine test of advanced oxide dispersion strengthened alloy turbine vanes --- for space shuttle thermal protection
 [NASA-CR-135269]
- p0077 A78-11232
 Effect of fuel properties on performance of single aircraft turbojet combustor at simulated idle, cruise, and takeoff conditions
 [NASA-TN-73780]
- p0014 A78-13056
 Long-term CP6 engine performance deterioration: Evaluation of engine S/N 451-479
 [NASA-CR-135381]
- p0029 A78-20129
 Lightweight, low compression aircraft diesel engine --- converting a spark ignition engine to the diesel cycle
 [NASA-CR-135300]
- p0121 A78-21471
 Altitude calibration of an F100, S/N P680063, turbofan engine
 [NASA-TN-1228]
- p0019 A78-23095
 Stirling engine design manual
 [NASA-CR-135382]
- p0181 A78-23999
 Long-term CP6 engine performance deterioration: Evaluation of engine S/N 451-380
 [NASA-CR-159390]
- p0031 A78-29103
 Initial test results with single cylinder rhombic drive Stirling engine
- p0117 A78-30316
 Initial test results with a single-cylinder rhombic-drive Stirling engine --- to be applied to automobile engine design to conserve energy
 [NASA-TN-78919]
- p0140 A78-31533
ENVIRONMENT EFFECTS
- WT AIR BREATHING ENGINES
 WT DIESEL ENGINES
 WT DUCTED FAN ENGINES
 WT ELECTRIC ROCKET ENGINES
 WT GAS TURBINE ENGINES
 WT HYBRID PROPELLANT ROCKET ENGINES
 WT HYDROGEN OXIDEN ENGINES
 WT INTERNAL COMBUSTION ENGINES
 WT ION ENGINES
 WT J-85 ENGINES
 WT JET ENGINES
 WT LIQUID PROPELLANT ROCKET ENGINES
 WT MERCURY ION ENGINES
 WT PISTON ENGINES
 WT ROCKET ENGINES
 WT TP-30 ENGINE
 WT TURBINE ENGINES
 WT TURBOFAN ENGINES
 WT TURBOJET ENGINES
 WT TURBOPROP ENGINES
 WT VARIABLE CYCLE ENGINES
 WT WATER ENGINES
- Materials technology assessment for Stirling engines
 [NASA-TN-73769]
- p0049 A78-17187
 Evaluation of Federal Aviation Administration ion engine exhaust sampling rake
 [NASA-CR-135213]
- p0029 A78-21111
ENVIRONMENT EFFECTS
- Summary of the CTS Transient Event Counter data after one year of operation --- Communication Technology Satellite
- p0046 A78-19566

ENVIRONMENT POLLUTION

SUBJECT INDEX

ENVIRONMENT POLLUTION
BT AIR POLLUTION
ENVIRONMENT SIMULATION
BT THERMAL SIMULATION
 Simulation of the heat transfer characteristics of
 LOX [ASME PAPER 77-HT-9] p0089 A78-17482
 Compressor seal rub energetics study [NASA-CN-159424] p0032 A78-32096

ENVIRONMENTAL MONITORING
 Development of environmental charging effect
 monitors for operational satellites p0037 A78-10174

ENVIRONMENTAL QUALITY
BT AIR QUALITY
ENVIRONMENTAL TEMPERATURE
U AMBIENT TEMPERATURE
ENVIRONMENTAL TESTS
BT CORROSION TESTS
BT HIGH TEMPERATURE TESTS
 Real-time and accelerated outdoor endurance
 testing of solar cells p0142 A78-52837
 Endurance testing of first generation (Block 1)
 commercial solar cell modules [NASA-TN-78922] p0138 A78-26548

ENVIRONMENTAL TESTS
BT AEROSPACE ENVIRONMENTAL TESTS
BT HIGH TEMPERATURE ENVIRONMENTAL TESTS
BT SPACECRAFT ENVIRONMENTAL TESTS

EPITAXY
 Analysis of epitaxial drift field n on p silicon
 solar cells p0141 A78-10904

EPOXIDES
U SPORT COMPOUNDS
EPOXY COMPOUNDS
 Impact behavior of filament wound graphite/epoxy
 fan blades [NASA-TN-78845] p0018 A78-22097

EPOXY RESINS
 In situ ply strengths - An initial assessment
 Effects of hydrothermal exposure on a
 low-temperature cured epoxy [NASA-TN-73841] p0081 A78-17220

EQUATIONS OF MOTION
 Analysis of the cross flow in a radial inflow
 turbine scroll [NASA-CN-135320] p0029 A78-19153

EQUIPMENT SPECIFICATIONS
 Study of 87 and 85 GHz coupled cavity
 traveling-wave tubes for space use [NASA-CN-134670] p0098 A78-11295
 Some basic considerations of measurements
 involving collimated direct sunlight [NASA-TN-74947] p0130 A78-13608

ERRORS COMPOUNDS
 Crystal field and magnetic properties of ErCl_3
 Crystal field and magnetic properties [NASA-TN-73837] p0175 A78-24947
 p0175 A78-13916

EROSION
 Effect of facility background gases on internal
 erosion of the 30-cm Hg ion thruster [AIAA PAPER 78-665] p0050 A78-32745
 Hydrogen film cooling of a small hydrogen-oxygen
 thrust chamber and its effect on erosion rates
 of various ablative materials [NASA-TP-1098] p0047 A78-13124
 Effect of facility background gases on internal
 erosion of the 30-cm Hg ion thruster [NASA-TN-73803] p0048 A78-21205

ESTIMATES
BT COST ESTIMATES

ETCHING
 Ion beam sputter etching and deposition of
 fluoropolymers p0085 A78-37684
 Industrial ion source technology --- for ion beam
 etching, surface texturing, and deposition
 [NASA-CN-135353] p0169 A78-18883
 Ion beam sputter etching and deposition of
 fluoropolymers [NASA-TN-78886] p0088 A78-24358
 Ion beam sputtering of fluoropolymers --- etching
 polymer films and target surfaces [NASA-TN-79000] p0060 A78-33151

ETHEL ALCOHOL
 PBI polyimide prepreg with improved tack
 characteristics [NASA-TN-73898] p0081 A78-17221

EUTECTIC ALLOYS
 Volume fraction determination in cast superalloys
 and directionally solidified eutectic alloys by
 a new manual point count practice p0089 A78-24369
 Thermal fatigue and oxidation data of superalloys
 including directionally solidified eutectics
 [NASA-CN-135272] p0078 A78-15233
 Directionally solidified eutectic gamma-gamma
 nickel-base superalloys [NASA-CASR-LBN-12905-1] p0069 A78-18183
 Longitudinal shear behavior of several oxide
 dispersion strengthened alloys [NASA-TN-78973] p0072 A78-31211

EUTECTICS
BT EUTECTIC ALLOYS
 Directionally solidified ceramic eutectics
 The promise of eutectics for aircraft turbines
 The promise of eutectics for aircraft turbines
 Feasibility study of tungsten as a diffusion
 barrier between nickel-chromium-aluminum and
 gamma/gamma prime - Delta eutectic alloys [NASA-TP-1131] p0068 A78-15230

EVAPORATION
BT TRANSPIRATION
EVAPORATIVE COOLING
BT FILM COOLING

EXCHANGING
BT CHANGE EXCHANGE

EXCITATION
BT ACOUSTIC EXCITATION
 Employing static excitation control and tie line
 reactance to stabilize wind turbine generators
 [NASA-CN-135344] p0144 A78-20603

EXCITED STATES
U EXCITATION

EXCLUSION
 Counter pumping debris excluder and separator ---
 gas turbine shaft seals [NASA-CASR-LBN-11855-1] p0020 A78-25090

EXCLUSIVE AIRCRAFT
J GENERAL AVIATION AIRCRAFT
EXHAUST FLOW SIMULATION
BT FLIGHT SIMULATION
EXHAUST GASES
 Aircraft engine emissions --- conference
 Exhaust reduction technology program
 Summary of emissions reduction technology programs
 Emissions control for ground power gas turbines
 General aviation piston-engine exhaust emission
 reduction
 Global atmospheric sampling program
 Stratospheric cruise emission reduction program
 Augmentor emissions reduction technology program
 --- for turbofan engines
 Wide range operation of advanced low NOx
 combustors for supersonic high-altitude aircraft
 gas turbines
 Performance and emissions of a catalytic reactor
 with propane, diesel, and Jet A fuels
 Experimental clean combustor program: Turbulence
 characteristics of compressor discharge flows
 Evaluation of Federal Aviation Administration ion
 engine exhaust sampling rake
 Reduction of aircraft gas turbine engine pollutant
 emissions
 Gas turbine engine with recirculating bleed

Gas turbine engine emission reduction technology program p0001 878-27858

Supercritical fuel injection system [NASA-CASR-LEW-12990-1] p0020 878-27122

Experimental study of the effect of cycle pressure on lean combustion emissions [NASA-CR-3032] p0031 878-28098

Effect of air temperature and relative humidity at various fuel-air ratios on exhaust emissions on a per-node basis of an AVCO Lycoming O-320 diad light aircraft engine: Volume 1: Results and plotted data [NASA-TN-73507-VOL-1] p0021 878-29100

Results and status of the NASA aircraft engine emission reduction technology programs [NASA-TN-79009] p0022 878-33102

Pollution Reduction Technology Program for small jet aircraft engines, phase 2 [NASA-CR-159415] p0032 878-33104

EXHAUST JETS
EXHAUST GASES
EXHAUST NOZZLES
EXHAUST NOZZLES

Aero-acoustic tests of duct-burning turbofan exhaust nozzles. Comprehensive data report. Volume 1: Model scale acoustic data [NASA-CR-138910-VOL-1] p0002 878-15988

Aero-acoustic tests of duct-burning turbofan exhaust nozzles. Comprehensive data report. Volume 2: Acoustic and aerodynamic data [NASA-CR-138910-VOL-2] p0002 878-15989

Aero-acoustic tests of duct-burning turbofan exhaust nozzles. Comprehensive data report. Volume 3: Acoustic and aerodynamic data curves [NASA-CR-138910-VOL-3] p0002 878-15990

Flight effects on the aerodynamic and acoustic characteristics of inverted profile coaxial nozzles [NASA-CR-3018] p0169 878-32836

EXHAUST SYSTEMS
 Characterization, shaping, and joining of SiC/superalloy sheet for exhaust system components [NASA-CR-135301] p0062 878-13134

A method for calculating strut and splitter plate noise in exit ducts: Theory and verification [NASA-CR-2955] p0167 878-20921

EXHAUST VELOCITY
 On the use of relative velocity exponents for jet engine exhaust noise p0024 878-37683

EXPANDABLE STRUCTURES
EX BELLOWS
EXPANSION
EX GAS EXPANSION
EX THERMAL EXPANSION
EXPERIMENTAL DESIGN

Ion beam plane and efflux characterization flight experiment study --- space shuttle payload [NASA-CR-135275] p0052 878-12140

Conceptual design for spacelab two-phase flow experiments [NASA-CR-135327] p0034 878-14063

Conceptual design for spacelab pool boiling experiment [NASA-CR-135378] p0037 878-20150

The Plasma Interaction Experiment (PIX) description and test program --- electrostatics [NASA-TN-78863] p0041 878-21198

EXTRINSICITIES
 Experimental determination of transient strain in a thermally-cycled simulated turbine blade utilizing a non-contact technique [NASA-TN-73886] p0017 878-19161

EXTERNALLY BLOWN FLAPS
EX UPPER SURFACE BLOWN FLAPS

HPF noise suppression and aerodynamic penalties --- Externally Blown Flaps [AIAA PAPER 78-2401] p0155 878-20763

Noise of deflectors used for flow attachment with STOL-OTW configurations [NASA-TN-73809] p0163 878-13853

HPF noise suppression and aerodynamic penalties [NASA-TN-73827] p0163 878-15852

A method for calculating externally blown flap noise [NASA-CR-2954] p0166 878-20920

Analytical modeling of under-the-wing externally blown flap powered-lift noise p0004 878-24063

EXTRACCTIONS
EX 108 EXTRACCTIONS
EXTRAPOLATION

Interpolation and extrapolation of creep rupture data by the minimum commitment method. II - Oblique translation p0076 878-45426

Interpolation and extrapolation of creep rupture data by the minimum commitment method. I - Focal-point convergence p0076 878-45427

Interpolation and extrapolation of creep rupture data by the minimum commitment method. Part 1: Focal-point convergence [NASA-TN-78881] p0125 878-23471

Interpolation and extrapolation of creep rupture data by the minimum commitment method. Part 2: Oblique translation [NASA-TN-78882] p0125 878-23472

Interpolation and extrapolation of creep rupture data by the minimum commitment method. Part 3: Analysis of multiboats [NASA-TN-78883] p0126 878-23473

EXTRATERRESTRIAL RADIATION
EX SOLAR RADIATION
EX SUNLIGHT

F

F-15 AIRCRAFT
 F-15/axisymmetric nozzle system integration study support program [NASA-CR-135252] p0028 878-18070

F-100 AIRCRAFT
 Evaluation of an F100 multivariable control using a real-time engine simulation [NASA-TN-X-73648] p0012 878-10097

Analytical study of thermal barrier coated first-stage blades in an F100 engine [NASA-CR-135359] p0028 878-17058

Airflow and thrust calibration of an F100 engine, S/W P680059, at selected flight conditions [NASA-TN-1069] p0018 878-21112

F100(3) parallel compressor computer code and user's manual [NASA-CR-135389] p0029 878-22096

Altitude calibration of an F100, S/W P680063, turbofan engine [NASA-TN-1228] p0019 878-23095

F-102 AIRCRAFT
 F102 in-duct combustor noise measurement, volume 1 [NASA-CR-135404-VOL-1] p0167 878-25827

F102 in-duct combustor noise measurement, volume 2 [NASA-CR-135404-VOL-2] p0167 878-25828

F102 in-duct combustor noise measurement, volume 3 [NASA-CR-135404-VOL-3] p0167 878-25829

FAB (PROGRAMMING LANGUAGE)
F FORTRAN
FABRICATION

Application of thick-film technology to solar cell fabrication p0146 878-10947

Consolidation of silicon nitride without additives --- for gas turbine engine efficiency increase p0085 878-24895

Development and fabrication of a diffusion welded Columbian alloy heat exchanger --- for space power generation [AIAA PAPER 78-61] p0123 878-31500

Cost/benefit analysis of advanced material technologies for small aircraft turbine engines [NASA-CR-135265] p0027 878-12083

Design and fabrication of a low-specific-weight parabolic dish solar concentrator [NASA-TN-1152] p0046 878-17145

Titanium/beryllium laminates: Fabrication, mechanical properties, and potential aerospace applications [NASA-TN-73891] p0059 878-21221

Fabrication of stainless steel clad tubing --- gas pressure bonding [NASA-CR-135347] p0079 878-21265

Technological development of cylindrical and flat shaped high energy density capacitors --- using polymeric films [NASA-CR-135286] p0099 878-24458

FABRY-PEROT LASERS
F LASERS

FACE CENTERED CUBIC LATTICES

SUBJECT INDEX

FACE CENTERED CUBIC LATTICES

Effects of heat treating PH Base' 95 slightly below the gamma-prime solvus p0073 A78-10792

FACTS
U FLY SURFACES
FAILURES
WT ENGINE FAILURES
FAILURE ANALYSIS
 Effect of wall thickness and material on flexural fatigue of hollow rolling elements [ASME PAPER 77-LUB-10] p0126 A78-23355
 Failure detection and correction for turbofan engines p0033 A78-23918
 Strain-range partitioning behavior of the nickel-base superalloys, Base 80 and 100 p0075 A78-33214
 Lubrication and failure mechanisms of graphite fluoride films [NASA-TP-1197] p0081 A78-20337

FAILURE MODES
 Mode I stress intensity factors for round compact specimens p0126 A78-13817
 Design considerations in mechanical face seals for improved performance. I - Basic configurations [ASME PAPER 77-NA/LUB-3] p0119 A78-33103

FAULT DETECTORS
U LIFT FANS
FANS
 Three-dimensional effects on pure tone fan noise due to inflow distortion [AIAA PAPER 78-1120] p0166 A78-41830
 Impact behavior of filament wound graphite/epoxy fan blades [NASA-TN-780845] p0018 A78-22097

FAR FIELDS
 Far-field multimodal acoustic radiation directivity p0165 A78-24876
 Calculation of far-field jet noise spectra from near-field measurements using true source location [AIAA PAPER 78-1153] p0160 A78-41852

FAST FOURIER TRANSFORMATIONS
 A fluctuation-induced plasma transport diagnostic based upon fast-Fourier transform spectral analysis [NASA-TN-78932] p0172 A78-26926

FATIGUE (MATERIALS)
WT BENDING FATIGUE
WT TENSILE FATIGUE
WT STRUCTURAL STRAIN
WT THERMAL FATIGUE
 Reliability analysis of forty-five strain-gage systems mounted on the first fan stage of a TP-100 engine [NASA-TN-73724] p0109 A78-13407
 Fractographic evaluation of creep effects on strain-controlled fatigue-cracking of AISI 304LC and 316 stainless steel [NASA-TN-78913] p0126 A78-27453
 Rolling element fatigue testing of gear materials [NASA-CR-135450] p0124 A78-33463

FATIGUE LIFE
 Experimental and analytical load-life relation for AISI 9310 steel spur gears [ASME PAPER 77-DPT-121] p0118 A78-20609
 Rolling-element fatigue life of ANS 5749 corrosion resistant, high temperature bearing steel [ASME PAPER 77-LUB-30] p0075 A78-28423
 Effect of preload on the fatigue and static strength of composite laminates with defects p0061 A78-40310
FASTSPAN use for cyclic response and fatigue analysis of wind turbine towers p0125 A78-12459
 Influence of fretting on flexural fatigue of 304 stainless steel and mild steel [NASA-TP-1193] p0070 A78-21269
 Rolling-element fatigue life of AISI M-50 and 18-8-1 balls [NASA-TP-1202] p0115 A78-21473
 Effect of filtration on rolling-element bearing life in contaminated lubricant environment [NASA-TP-1272] p0116 A78-28457
 Review of the AGARD 5 and M panel evaluation program of the NASA-Lewis SRP approach to high-temperature LCF life prediction [NASA-TN-78679] p0072 A78-31209

FATIGUE TESTING MACHINES

Effect of wall thickness and material on flexural fatigue of hollow rolling elements [ASME PAPER 77-LUB-10] p0126 A78-23355

FATIGUE TESTS
 Ferrographic analysis of wear debris generated in accelerated rolling element fatigue tests p0119 A78-28425
 Surface-crack shape change in bending fatigue using an inexpensive resonant fatiguing apparatus p0075 A78-35394
 Influence of fretting on flexural fatigue of 304 stainless steel and mild steel [NASA-TP-1193] p0070 A78-21269
 Characterization of wear debris generated in accelerated rolling-element fatigue tests [NASA-TP-1203] p0115 A78-21470
 Rolling-element fatigue life of AISI M-50 and 18-8-1 balls [NASA-TP-1202] p0115 A78-21473
 Filtration effects on ball bearing life and condition in a contaminated lubricant [NASA-TN-78907] p0116 A78-28446
 Rolling element fatigue testing of gear materials [NASA-CR-135411] p0122 A78-31427

FAULT MECHANISMS
U FRACTURE MECHANISMS
FCC LATTICES
U FACE CENTERED CUBIC LATTICES
FEASIBILITY ANALYSIS
 Feasibility study of negative lift circumferential type seal for helicopter transmissions [NASA-CR-135302] p0121 A78-17390

FED SYSTEMS
 Liquid rocket lines, bellows, flexible hoses, and filters [NASA-SP-8123] p0047 A78-16089

FEEDBACK CONTROL
 Design of turbofan engine controls using output feedback regulator theory p0023 A78-23907
 Failure detection and correction for turbofan engines p0033 A78-23918
 Output feedback regulator design for jet engine control systems p0024 A78-24898
 Closed loop spray cooling apparatus for particle accelerator targets [NASA-CASE-LEW-11981-1] p0091 A78-17237

FERRITES
 Friction and wear of single-crystal and polycrystalline manganese-zinc ferrite in contact with various metals [NASA-TP-1059] p0080 A78-10295

FERRITIC STAINLESS STEELS
 Elevated-temperature tensile and creep properties of several ferritic stainless steels [NASA-TN-73853] p0069 A78-17189

FERROMAGNETIC MATERIALS
 Magnetic heat pumping [NASA-CASE-LEW-12508-1] p0102 A78-17335

FERROMAGNETISM
 Characterization of wear debris generated in accelerated rolling-element fatigue tests [NASA-TP-1203] p0115 A78-21470
 Ferrographic analysis of wear particles from sliding elastohydrodynamic experiments [NASA-TP-1230] p0115 A78-22377

FFT
U FAST FOURIER TRANSFORMATIONS
FIBER COMPOSITES
WT CARBON FIBER REINFORCED PLASTICS
WT GLASS FIBER REINFORCED PLASTICS
FIBER ORIENTATION
 Impact of composite mechanics on test methods for fiber composites p0062 A78-50325

FIBER STRENGTH
 Evaluation of low cost/high temperature fiber and blanket insulation p0063 A78-16903
 A Weibull characterization for tensile fracture of multicomponent brittle fibers p0060 A78-24892
 Mechanical and physical properties of modern boron fibers p0085 A78-33206

- Correlation of fiber composite tensile strength with the ultrasonic stress wave factor
p0060 A78-33207
- The effects of eccentricities on the fracture of off-axis fiber composites --- carbon fiber reinforced plastics
[NASA-TN-73826] p0057 W78-17153
- Use of an ultrasonic-acoustic technique for nondestructive evaluation of fiber composite strength
[NASA-TN-73813] p0128 W78-17397
- FIBERS**
- NT METAL FIBERS**
- NT REINFORCING FIBERS**
- Mechanical and physical properties of modern boron fibers
[NASA-TN-73882] p0058 W78-17158
- FIBROUS MATERIALS**
- FIBERS**
- FIELD EMISSION**
- Spacecraft charging control by thermal, field emission with lanthanum-hexaboride emitters
[NASA-TN-78990] p0183 W78-32014
- FIELD STRENGTH**
- NT ELECTRIC FIELD STRENGTH**
- FIGHTER AIRCRAFT**
- NT F-15 AIRCRAFT**
- NT F-100 AIRCRAFT**
- NT F-102 AIRCRAFT**
- NT F-12 AIRCRAFT**
- FILAMENT WINDING**
- Recent advances in lightweight, filament-wound composite pressure vessel technology
p0061 A78-33436
- Filament-winding fabrication of QCSEE configuration fan blades
[NASA-CR-135332] p0028 W78-16052
- Impact behavior of filament wound graphite/epoxy fan blades
[NASA-TN-78845] p0018 W78-22097
- FILAMENT WOUND CONSTRUCTION**
- FILAMENT WINDING**
- FILLING**
- Filling of orbital fluid management systems
[NASA-CR-159404] p0108 W78-31380
- FILE BOILING**
- Effect of ice contamination on liquid-nitrogen drops in film boiling
p0105 A78-15821
- Thermally driven oscillations and wave motion of a liquid drop
p0106 A78-17508
- FILE COOLING**
- Effects of film injection on performance of a cooled turbine
p0033 A78-24902
- Hydrogen film cooling of a small hydrogen-oxygen thrust chamber and its effect on erosion rates of various ablative materials
[NASA-TP-1098] p0047 W78-13124
- Effects of film injection angle on turbine vane cooling
[NASA-TP-1095] p0101 W78-13379
- Effect of cooling-hole geometry on aerodynamic performance of a film-cooled turbine vane tested with cold air in a two-dimensional cascade
[NASA-TP-1136] p0004 W78-20080
- Two-dimensional cold-air cascade study of a film-cooled turbine stator blade. 4:
Comparison of experimental and analytical aerodynamic results for blade with 12 rows of 0.076-centimeter-(0.030-inch-) diameter holes having streamwise ejection angles
[NASA-TP-1151] p0017 W78-20130
- Two-dimensional cold-air cascade study of a film-cooled turbine stator blade. 5:
Comparison of experimental and analytical aerodynamic results for blade with 12 rows of 0.038-centimeter-(0.015 inch) diameter coolant holes having streamwise ejection angles
[NASA-TP-1204] p0017 W78-20133
- Effects of film injection on performance of a cooled turbine
p0029 W78-21147
- A computer program for full-coverage film-cooled blading analysis including the effects of a thermal barrier coating
[NASA-TN-78951] p0021 W78-27126
- FORTRAN program for calculating coolant flow and metal temperatures of a full-coverage-film-cooled vane or blade
[NASA-TP-1259] p0021 W78-28099
- Analysis of metal temperature and coolant flow with a thermal-barrier coating on a full-coverage-film-cooled turbine vane
[NASA-TP-1310] p0022 W78-31109
- FILE THICKNESS**
- Elastohydrodynamic lubrication of elliptical contacts for materials of low elastic modulus. 1 - Fully flooded conjunction
[ASME PAPER 77-LUB-10] p0119 A78-28414
- Elastohydrodynamic film thickness measurements of artificially produced surface dents and grooves --- using optical interferometry
[NASA-TN-78949] p0116 W78-27428
- Elastohydrodynamic lubrication of elliptical contacts for materials of low elastic modulus. 2: Starved conjunction
[NASA-TP-1273] p0117 W78-28458
- Effect of geometry on hydrodynamic film thickness
[NASA-TP-1287] p0117 W78-30585
- Minimum film thickness in elliptical contacts for different regimes of fluid-film lubrication
[NASA-TP-1342] p0117 W78-33447
- FILTRING**
- FILTRATION**
- FILTRATION**
- Filtration effects on ball bearing life and condition in a contaminated lubricant
[NASA-TN-78907] p0116 W78-26446
- Effect of filtration on rolling-element-bearing life in contaminated lubricant environment
[NASA-TP-1272] p0116 W78-28457
- FINITE DIFFERENCE THEORY**
- Derivation and evaluation of an approximate analysis for three-dimensional viscous subsonic flow with large secondary velocities --- finite difference method
[NASA-CR-159430] p0008 W78-33044
- FINITE ELEMENT METHOD**
- The elastic distortion of the flanged inner ring of a high-speed cylindrical roller bearing
[ASME PAPER 77-LUB-8] p0118 A78-23352
- Simplified modeling for wind turbine modal analysis using NASTRAN
p0132 W78-19619
- Analysis/design of strip reinforced random composites (strip hybrids)
[NASA-TN-78985] p0059 W78-33149
- FIXED-WING AIRCRAFT**
- U AIRCRAFT CONFIGURATIONS**
- FLAME FRONTS**
- U FLAME PROPAGATION**
- FLAME HOLDERS**
- Experimental study of the effects of flameholder geometry on emissions and performance of lean premixed combustors
[NASA-CR-135424] p0030 W78-26147
- FLAME INTERACTION**
- U CHEMICAL REACTIONS**
- U FLAME PROPAGATION**
- FLAME PROPAGATION**
- Analytical study of laser-supported combustion waves in hydrogen
[AIAA PAPER 78-1219] p0067 A78-41901
- Analytical study of laser supported combustion waves in hydrogen
[NASA-CR-135349] p0112 W78-20489
- FLAME TEMPERATURE**
- Direct heating surface combustor
[NASA-CASE-LEN-11877-1] p0097 W78-27357
- FLAMES**
- NT PREMIXED FLAMES**
- Formation of Fe₂SO₄ and K₂SO₄ in flames doped with sulfur and alkali chlorides and carbonates
[NASA-TN-73794] p0064 W78-13157
- FLAP CONTROL**
- U FLAPS (CONTROL SURFACES)**
- FLAPS (CONTROL SURFACES)**
- NT EXTERNALLY BLOWN FLAPS**
- NT WING FLAPS**
- Nonlinear flap-lag-axial equations of a rotating beam with arbitrary precone angle
[AIAA 78-891] p0127 A78-29798
- FLAT CONDUCTORS**
- Technology development of cylindrical and flat shaped high energy density capacitors --- using

FLAT PLATES

SUBJECT INDEX

polymeric films
[NASA-CR-135286] p0099 W78-24458

FLAT PLATES
Velocity and temperature profiles in near-critical nitrogen flowing past a horizontal flat plate [ASME PAPER 77-HT-7] p0106 W78-17481
Comparison of three experimental methods used in determining the thermal performance of flat-plate solar collectors [NASA-TN-78929] p0139 W78-28614
Development of flat-plate solar collectors for the heating and cooling of buildings: Executive summary [NASA-CR-134804-2] p0146 W78-33527

FLAT SURFACES
Evaluation of models to predict insolation on tilted surfaces [NASA-TN-78842] p0184 W78-25025

FLAW DETECTION
NONDESTRUCTIVE TESTS
FLAWS
DEFFECTS

FLEXIBILITY
Balancing techniques for high-speed flexible rotors [NASA-CR-2975] p0121 W78-20514

FLEXIBLE BODIES
Nonlinear flap-lag-axial equations of a rotating beam with arbitrary precone angle [AIAA 78-491] p0127 W78-29798
Influence of oil-squeeze-film damping on steady-state response of flexible rotor operating to supersonic speeds [NASA-TP-1094] p0015 W78-13064

FLIGHT CHARACTERISTICS
Flight-effects on predicted fan fly-by noise [NASA-TN-73798] p0014 W78-13060

FLIGHT LOAD RECORDERS
JT9D engine diagnostics. Task 2: Feasibility study of measuring in-service flight loads --- 747 aircraft performance [NASA-CR-135395] p0030 W78-27124

FLIGHT PERFORMANCE
FLIGHT CHARACTERISTICS

FLIGHT SIMULATION
Variation of fan tone steadiness for several inflow conditions [AIAA PAPER 78-1119] p0166 W78-41829
Effectiveness of an inlet flow turbulence control device to simulate flight noise fan in an anechoic chamber [NASA-TN-73855] p0163 W78-13856
Simulated flight effects on noise characteristics of a fan inlet with high throat Mach number [NASA-TP-1159] p0017 W78-20132
Real time digital propulsion system simulation for manned flight simulators [NASA-TN-78958] p0034 W78-27137

FLIGHT SIMULATORS
Real time digital propulsion system simulation for manned flight simulators [AIAA PAPER 78-427] p0035 W78-45095

FLIGHT TESTS
Planned flight test of a mercury ion auxiliary propulsion system. I - Objectives, systems descriptions, and mission operations [AIAA PAPER 78-647-I] p0050 W78-32734
Planned flight test of a mercury ion auxiliary propulsion system. II - Integration with host spacecraft [AIAA PAPER 78-647-II] p0050 W78-32735
The Plasma Interaction Experiment /PIX/ - Description and flight qualification test program [AIAA PAPER 78-674] p0051 W78-32752
Planned flight test of a mercury ion auxiliary propulsion system. Part 2: Integration with host spacecraft [NASA-TN-78869] p0048 W78-21209

FLOW CHARACTERISTICS
WT FLOW DISTRIBUTION
WT FLOW VELOCITY
WT MAGNETOHYDRODYNAMIC STABILITY
Characteristics of the unsteady motion on transversely sheared mean flows p0106 W78-23246
Theoretical flow characteristics of inlets for tilting-nacelle VTOL aircraft [NASA-TP-1205] p0018 W78-21114
Wake characteristics of an eight-leg tower for a MOD-0 type wind turbine

[NASA-TN-73868] p0135 W78-24615

FLOW REFLECTION
Noise of deflectors used for flow attachment with STOL-OTW configurations p0023 W78-24877
Noise of deflectors used for flow attachment with STOL-OTW configurations [NASA-TN-73809] p0163 W78-13853

FLOW DIRECTION INDICATORS
WT WIND VANES
FLOW DISTORTION
Three-dimensional effects on pure tone fan noise due to inflow distortion [AIAA PAPER 78-1120] p0166 W78-41830

FLOW DISTRIBUTION
Investigation of means for perturbing the flow field in a supersonic wind tunnel [NASA-TN-78954] p0037 W78-27142
Preliminary study of the effect of the turbulent flow field around complex surfaces on their acoustic characteristics [NASA-TN-78944] p0164 W78-28886
Wind tunnel evaluation of YF-12 inlet response to internal airflow disturbances with and without control --- Lewis 10 by 10 ft supersonic wind tunnel tests p0006 W78-32062

FLOW EQUATIONS
Velocity, temperature, and electrical conductivity profiles in hydrogen-oxygen HD duct flows [NASA-TN-78968] p0104 W78-28372

FLOW FIELDS
U FLOW DISTRIBUTION
FLOW MEASUREMENT
Review of experimental work on transonic flow in turbomachinery p0006 W78-12312
Signature drag force anemometer p0109 W78-17397
Instrumentation for propulsion systems development [SAE PAPER 780076] p0109 W78-33365
TACT1, a computer program for the transient thermal analysis of a cooled turbine blade or vane equipped with a coolant insert. 1. Users manual [NASA-TP-1271] p0104 W78-28374

FLOW PATTERNS
U FLOW DISTRIBUTION
FLOW RATE
U FLOW VELOCITY
FLOW REGULATORS
Performance characteristics of two annular dump diffusers using suction-stabilized vortex flow control [NASA-TN-73857] p0004 W78-19057
Automotive gas turbine fuel control [NASA-CASE-LEW-12785-1] p0115 W78-24545

FLOW RESISTANCE
WT AERODYNAMIC DRAG
FLOW SEPARATION
U BOUNDARY LAYER SEPARATION
FLOW STABILITY
WT MAGNETOHYDRODYNAMIC STABILITY
FLOW VELOCITY
Lubrication of high-speed, large bore tapered-roller bearings [ASME PAPER 77-LUB-13] p0118 W78-23354
Flow of liquid jets through closely woven screens p0108 W78-42877
Performance characteristics of two annular dump diffusers using suction-stabilized vortex flow control p0107 W78-45431
Effect of airstream velocity on mean drop diameters of water sprays produced by pressure and air atomizing nozzles [NASA-TN-71740] p0101 W78-13369
Small-signal gain diagnostic measurements in a flowing CO2 pin discharge laser [NASA-TN-73843] p0111 W78-13421
The role of drop velocity in statistical spray description [NASA-TN-73887] p0102 W78-20458
Mean velocity, turbulence intensity and turbulence convection velocity measurements for a convergent nozzle in a free jet wind tunnel [NASA-CR-2949] p0008 W78-21058
Some flow phenomena in a constant area duct with a Borda type inlet including the critical region

SUBJECT INDEX

FOKKEB BOND TESTERS

- (NASA-TN-78943) p0104 W78-27367
Derivation and evaluation of an approximate analysis for three-dimensional viscous subsonic flow with large secondary velocities --- finite difference method
(NASA-CR-159430) p0008 W78-33044
- FLOW VISUALIZATION
NT SPHERICAL FLOW VISUALIZATION
A visual investigation of turbulence in stagnation flow about a circular cylinder
(NASA-CR-3019) p0108 W78-33386
- FLUCTUATION THEORY
Low-frequency fluctuation spectra and associated particle transport in the NASA Lewis bumpy-torus plasma
(NASA-TP-1252) p0172 W78-30944
- FLUID BOUNDARIES
NT GAS-SOLID INTERFACES
NT LIQUID-SOLID INTERFACES
- FLUID DYNAMICS
NT ELASTOHYDRODYNAMICS
NT HYDRODYNAMICS
- FLUID FILMS
Sealing, gearing, and lubrication technology
(SAE PAPER 780077) p0120 W78-33366
Traction and lubricant film temperature as related to the glass transition temperature and solidification --- using infrared spectroscopy on EHD contacts
p0087 W78-40997
Minimum film thickness in elliptical contacts for different regimes of fluid-film lubrication
(NASA-TP-1342) p0117 W78-33447
- FLUID FILTERS
Liquid rocket lines, bellows, flexible hoses, and fillers
(NASA-SP-8123) p0047 W78-16089
- FLUID FLOW
NT AIR FLOW
NT ANNULAR FLOW
NT AXIAL FLOW
NT BOUNDARY LAYER FLOW
NT BOUNDARY LAYER SEPARATION
NT CASCADE FLOW
NT CHANNEL FLOW
NT CONVECTIVE FLOW
NT CRITICAL FLOW
NT CROSS FLOW
NT DUCTED FLOW
NT GAS FLOW
NT INLET FLOW
NT INVISCID FLOW
NT JET FLOW
NT MAGNETOHYDRODYNAMIC FLOW
NT MASS FLOW
NT NOZZLE FLOW
NT OSCILLATING FLOW
NT PIPE FLOW
NT POTENTIAL FLOW
NT PROPELLANT TRANSPORT
NT RADIAL FLOW
NT REVERSED FLOW
NT SECONDARY FLOW
NT SHEAR FLOW
NT STAGNATION FLOW
NT SUBSONIC FLOW
NT SUPERCRITICAL FLOW
NT SUPERSONIC FLOW
NT THREE DIMENSIONAL FLOW
NT TRANSONIC FLOW
NT TURBULENT FLOW
NT TWO DIMENSIONAL FLOW
NT TWO PHASE FLOW
NT UNIFORM FLOW
NT UNSTEADY FLOW
NT VISCOUS FLOW
NT WALL FLOW
Two-phase working fluids for the temperature range 50 to 350 C
(NASA-CR-135255) p0107 W78-16329
Flow compensating pressure regulator
(NASA-CASE-LEN-12718-1) p0104 W78-25351
Some flow phenomena in a constant area duct with a Borda type inlet including the critical region
(NASA-TN-78943) p0104 W78-27367
- FLUID INJECTION
NT GAS INJECTION
Effects of film injection on performance of a cooled turbine
- FLUID JETS
NT FREE JETS
NT HYDRAULIC JETS
- FLUID MECHANICS
NT ELASTOHYDRODYNAMICS
NT HYDRODYNAMICS
NT HYDROMECHANICS
Liquid propellant reorientation in a low-gravity environment
(NASA-TN-78969) p0105 W78-29407
- FLUID PRESSURE
Flow compensating pressure regulator
(NASA-CASE-LEN-12718-1) p0104 W78-25351
- FLUID TRANSPORTATION
U TRANSPORTATION
- FLUIDIC CIRCUITS
The design of hydraulic pressure regulators that are stable without the use of sensing line restrictors or frictional dampers
p0164 W78-24897
- FLUIDICS
Application of fluidics to new control components
p0109 W78-23026
- FLUIDIZED BED PROCESSORS
Effluent characterization from a conical pressurized fluid bed
p0066 W78-33221
Fluidized bed combustor modeling
(NASA-CR-135164) p0067 W78-14119
- FLUORIDES
NT OZONE FLUORIDE
Effect of thermal exposure on lubricating properties of polyimide films and polyimide-bonded graphite fluoride films
(NASA-TP-1125) p0030 W78-15277
A comparison of the lubricating mechanisms of graphite fluoride and molybdenum disulfide films
(NASA-TN-78897) p0083 W78-26215
- FLUORINATION
The fluorination of cobalt and zinc
(NASA-TN-X-73478) p0064 W78-15211
- FLUORINE COMPOUNDS
NT FLUORIDES
NT FLUOROPOLYMERS
NT OZONE FLUORIDE
NT POLYTETRAFLUOROETHYLENE
- FLUORINE ORGANIC COMPOUNDS
NT FLUOROPOLYMERS
- FLUORO COMPOUNDS
NT FLUOROPOLYMERS
NT POLYTETRAFLUOROETHYLENE
- FLUOROPOLYMERS
NT POLYTETRAFLUOROETHYLENE
NT TEFLON (TRADEMARK)
Ion beam sputtering of fluoropolymers --- etching polymer films and target surfaces
(NASA-TN-79000) p0060 W78-33151
- FLUTTER
Synthesis of blade flutter vibratory patterns using stationary transducers
(NASA-TN-73821) p0003 W78-17001
- FLUX (RATE PER UNIT AREA)
U FLUX DENSITY
- FLUX (WATTS)
NT HEAT FLUX
NT SOLAR FLUX
- FLUX DENSITY
NT CURRENT DENSITY
Variability of ozone near the tropopause from GASP data
(NASA-CR-135405) p0148 W78-23648
Technological development of cylindrical and flat shaped high energy density capacitors --- using polymeric films
(NASA-CR-135286) p0099 W78-24458
- FLUX MAPPING
U FLUX DENSITY
- FLUXMETERS
U MEASURING INSTRUMENTS
- FLYING QUALITIES
U FLIGHT CHARACTERISTICS
- FOIL BEARINGS
Hydrodynamic air lubricated compliant surface bearing for an automotive gas turbine engine.
2: Materials and coatings
(NASA-CR-135402) p0122 W78-29449
- FOKKEB BOND TESTERS
U ADHESION TESTS

FORCED CONVECTION

SUBJECT INDEX

FORCED CONVECTION

Boiling inception and convective boiling of neon and nitrogen p0105 A78-15820
 Estimating surface temperature in forced convection nucleate boiling - A simplified method p0105 A78-15822

FORECASTING

WT PERFORMANCE PREDICTION
 WT PREDICTION ANALYSIS TECHNIQUES
 WT TECHNOLOGICAL FORECASTING

FOREIGN POLICY

WT INTERNATIONAL COOPERATION

FORMS

U SHAPES

FORMING TECHNIQUES

WT CASTING

WT PRESSING (FORGING)

Method of forming metal hydride films [NASA-CASE-LTR-12083-1] p0113 A78-13436

FOURMAN

User's guide to SPTRAM/1100 [NASA-TP-1200] p0156 A78-20806

FOSSIL FUELS

WT COAL

WT CRUDE OIL

Alternative aircraft fuels [NASA-TN-73836] p0088 A78-17229

Technical and economic feasibility study of solar/fossil hybrid power systems [NASA-TN-73820] p0132 A78-17886

FOUNDATIONS

Influence of wind turbine foundation p0133 A78-19626

FOURIER TRANSFORMATION

WT FAST FOURIER TRANSFORMATIONS

FRACTURE MECHANICS

Mode I stress intensity factors for round compact specimens p0126 A78-13817

Friction, deformation and fracture of single-crystal silicon carbide [ASLE PREPRINT 77-IC-5C-3] p0085 A78-28838

Investigation of the fracture mechanism of Ti-5Al-2.5Sn at cryogenic temperatures p0075 A78-32319

Correlation of fiber composite tensile strength with the ultrasonic stress wave factor p0060 A78-33207

Fracture surface characteristics of off-axis composites p0067 A78-80371

Impetus of composite mechanics on test methods for fiber composites p0062 A78-50325

Fracture surface characteristics of off-axis composites [NASA-TN-73700] p0057 A78-13137

Mechanical behavior and fracture characteristics of off-axis fiber composites. 1: Experimental investigation --- at the Lewis Research Center [NASA-TP-1081] p0057 A78-13138

The effects of eccentricities on the fracture of off-axis fiber composites --- carbon fiber reinforced plastics [NASA-TN-73826] p0057 A78-17153

Fractographic evaluation of creep effects on strain-controlled fatigue-cracking of AISI 304LC and 316 stainless steel [NASA-TN-78913] p0126 A78-27453

FRACTURE RESISTANCE

U FRACTURE STRENGTH

FRACTURE STRENGTH

Stress analysis and stress-intensity factors for finite geometry solids containing rectangular surface cracks [ASME PAPER 77-WA/APR-5] p0126 A78-10531

Cryogenic properties of a new tough-strong iron alloy p0073 A78-15825

Load-displacement measurement and work determination in three-point bend tests of notched or precracked specimens p0089 A78-24370

Comparison of equivalent energy and energy per unit area /W bar/A/ data with valid fracture toughness data for iron, aluminum, and titanium alloys p0074 A78-24372

A Weibull characterization for tensile fracture of multicomponent brittle fibers p0060 A78-24892

Evaluation of flawed composite structure under static and cyclic loading p0063 A78-26683

Investigation of the fracture mechanism of Ti-5Al-2.5Sn at cryogenic temperatures p0075 A78-32319

Thermal environment effects on strength and impact properties of boron-aluminum composites p0060 A78-33204

In situ ply strengths - An initial assessment p0061 A78-33223

Development of strong and tough cryogenic Fe-12Ni alloys containing reactive metal additions p0076 A78-41465

Correlations between ultrasonic and fracture toughness factors in metallic materials p0077 A78-45434

Room temperature crack growth rates and -20 deg F fracture toughness of welded 1 1/4 inch A-285 steel plate [NASA-TN-73847] p0068 A78-13182

The influence of composition, annealing treatment, and texture on the fracture toughness of Ti-5Al-2.5Sn plate at cryogenic temperatures [NASA-TN-73872] p0069 A78-15235

Mechanical behavior and fracture characteristics of off-axis fiber composites. 2: Theory and comparisons [NASA-TP-1082] p0057 A78-16098

The effect of microstructure and strength on the fracture toughness of an 18 Ni, 300 grade saragium steel [NASA-CN-135288] p0078 A78-16150

Thermal environment effects on strength and impact properties of boron-aluminum composites [NASA-TN-73885] p0058 A78-17155

Development of Si3N4 and SiC of improved toughness --- for gas turbine engines [NASA-CN-135306] p0087 A78-17216

The effect of minor additions of titanium on the fracture toughness of Fe-12Ni alloys at 77K [NASA-CN-135351] p0078 A78-19259

Correlations between ultrasonic and fracture toughness factors in metallic materials [NASA-TN-73805] p0069 A78-19261

In situ ply strength: An initial assessment --- using laminate fracture data and a least squares method [NASA-TN-73771] p0059 A78-21220

Pressureless sintered beta prime-Si3N4 solid solution: Fabrication, microstructure, and strength [NASA-TN-78950] p0083 A78-29245

FRACTURE TOUGHNESS

U FRACTURE STRENGTH

FRAGMENTATION

Concepts for the development of light-weight composite structures for rotor burst containment p0012 A78-10084

FRAMES

WT AIRFRAMES

FRANCOISIER REGION

U FAN FIELDS

FREE BOUNDARIES

Liquid jet impingement normal to a disk in zero gravity [ASME PAPER 78-WA/VE-1] p0107 A78-41154

FREE JETS

Mean velocity, turbulence intensity and turbulence convection velocity measurements for a convergent nozzle in a free jet wind tunnel [NASA-CR-2949] p0008 A78-21058

FREE OSCILLATIONS

U FREE VIBRATION

FREE RADICALS

WT HYDROXYL RADICALS

FREE VIBRATION

Approximate method for calculating free vibrations of a large-wind-turbine tower structure [NASA-TN-73754] p0131 A78-16434

FREQUENCIES

WT HIGH FREQUENCIES

WT PLASMA FREQUENCIES

WT RESONANT FREQUENCIES

WT SUPERHIGH FREQUENCIES

WT VERY LOW FREQUENCIES

- FREQUENCY DISTRIBUTION**
Power oscillation of the Rod-0 wind turbine
p0133 W78-19629
- FREQUENCY MEASUREMENT**
Influence of wind turbine foundation
p0133 W78-19626
- Applied South approximation
[NASA-TP-1231] p0091 W78-22257
- FREQUENCY MODULATION**
Carrier-interference ratios for frequency sharing
between frequency-modulated
amplitude-modulated-vestigial-modulated
television systems
[NASA-TP-1264] p0043 W78-28159
- FREQUENCY RESPONSE**
The application of the South approximation method
to turbofan engine models
p0023 A78-23891
- FREQUENCY STABILITY**
Variation of fan tone steadiness for several
inflow conditions
[AIAA PAPER 78-1119] p0166 A78-41829
- FREQUENCY SYNCHRONIZATION**
Synchronization of wind turbine generators against
an infinite bus under gusting wind conditions
[IEEE PAPER P 77 675-2] p0142 A78-30196
- FRETTING**
Influence of fretting on flexural fatigue of 304
stainless steel and mild steel
[NASA-TP-1193] p0070 W78-21269
- FRICTION**
WT AERODYNAMIC DRAG
WT SLIDING FRICTION
Definition and effect of chemical properties of
surfaces in friction, wear, and lubrication
[NASA-TN-73806] p0065 W78-19237
- Friction and wear of radiofrequency-sputtered
borides, silicides, and carbides
[NASA-TP-1156] p0081 W78-20338
- Effect of oxygen and nitrogen interactions on
friction of single-crystal silicon carbide
[NASA-TP-1265] p0083 W78-28247
- FRICTION COEFFICIENT**
μ COEFFICIENT OF FRICTION
FRICTION DRAG
WT AERODYNAMIC DRAG
FRICTION FACTOR
Friction and wear of sintered fibermetal abrasible
seal materials
p0074 A78-23451
- FRICTION LOSS COEFFICIENT**
μ FRICTION FACTOR
FRICTION MEASUREMENT
Some effects of composition on friction and wear
of graphite-fiber-reinforced polyimide liners in
plain spherical bearings
[NASA-TP-1229] p0115 W78-25433
- FRICTION REDUCTION**
Effect of oxygen, methyl mercaptan, and methyl
chloride on friction behavior of copper-iron
contacts
[NASA-TP-1309] p0072 W78-30206
- FUEL CELLS**
ECAS Phase 1 fuel cell results --- Energy
Conservation Alternatives Study
p0142 A78-26110
- FUEL COMBUSTION**
Effluent characterization from a conical
pressure fluid bed
p0066 A78-33221
- Degree of vaporization using an airblast type fuel
injector for a premixed-prevaporized combustor
p0107 A78-50322
- Fuel combustor
[NASA-CASE-LEW-12137-1] p0064 W78-10224
- Effect of fuel properties on performance of single
aircraft turbojet combustor at simulated idle,
cruise, and takeoff conditions
[NASA-TN-73780] p0014 W78-13056
- Computer program for obtaining thermodynamic and
transport properties of air and products of
combustion of ASTM-A-1 fuel and air
[NASA-TP-1160] p0088 W78-20351
- Characteristics and combustion of future
hydrocarbon fuels --- aircraft fuels
[NASA-TN-78865] p0089 W78-24370
- Results and status of the NASA aircraft engine
emission reduction technology program
[NASA-TN-79009] p0022 W78-33102
- FUEL CONSUMPTION**
General aviation energy-conservation research
programs at NASA-Lewis Research Center --- for
non-turbine general aviation engines
p0024 A78-29330
- Propulsion --- NASA program for aircraft fuel
consumption reduction
p0025 A78-43360
- Fuel consumption improvement in current transport
engines
[AIAA PAPER 78-930] p0033 A78-45097
- NASA/General Electric Engine Component Improvement
Program
[AIAA PAPER 78-929] p0025 A78-45098
- General aviation energy-conservation research
programs at NASA-Lewis Research Center
[NASA-TN-73884] p0016 W78-17060
- Automotive Stirling engine development program ---
fuel economy assessment
[NASA-CR-135331] p0181 W78-22970
- Design approaches to more energy efficient engines
[NASA-TN-78893] p0115 W78-26442
- ACEE propulsion overview
p0001 W78-27048
- Study and program plan for improved heavy duty gas
turbine engine ceramic component development
[NASA-CR-135230] p0122 W78-28466
- FUEL CONTROL**
General aviation internal-combustion engine
research programs at NASA-Lewis Research Center
[NASA-TN-78891] p0011 W78-24139
- Automotive gas turbine fuel control
[NASA-CASE-LEW-12785-1] p0115 W78-24545
- FUEL CORROSION**
The effect of NaCl/g/ on the Na2SO4-induced hot
corrosion of NiAl
p0079 A78-24901
- The effect of fuel-to-air ratio on burner-rig hot
corrosion
[NASA-TN-78960] p0072 W78-31210
- FUEL FLOW**
WT PROPELLANT TRANSFER
FUEL INJECTION
Effect of airstream velocity on sea drop
diameters of water sprays produced by pressure
and air atomizing nozzles --- for combustion
studies
p0028 A78-33111
- Experimental evaluation of fuel preparation
systems for an automotive gas turbine catalytic
combustor
p0120 A78-37677
- Degree of vaporization using an airblast type fuel
injector for a premixed-prevaporized combustor
p0107 A78-50322
- Experimental evaluation of preheating-prevaporizing
fuel injection concepts for a gas turbine
catalytic combustor
[NASA-TN-73755] p0101 W78-14313
- Photographic characterization of spark-ignition
engine fuel injectors
[NASA-TN-78830] p0018 W78-21110
- Degree of vaporization using an airblast type
injector for a premixed-prevaporized combustor
[NASA-TN-78836] p0103 W78-24894
- Supercritical fuel injection system
[NASA-CASE-LEW-12990-1] p0020 W78-27122
- Reverse-flow combustor for small gas turbines with
pressure-atomizing fuel injectors
[NASA-TP-1260] p0021 W78-27130
- FUEL SYSTEMS**
WT AIRCRAFT FUEL SYSTEMS
Experimental evaluation of fuel preparation
systems for an automotive gas turbine catalytic
combustor
p0120 A78-37677
- Fuel combustor
[NASA-CASE-LEW-12137-1] p0064 W78-10224
- Experimental evaluation of fuel preparation
systems for an automotive gas turbine catalytic
combustor
[NASA-TN-78856] p0082 W78-22243
- Impact of future fuel properties on aircraft
engines and fuel systems
[NASA-TN-78866] p0089 W78-24369
- Supercritical fuel injection system
[NASA-CASE-LEW-12990-1] p0020 W78-27122
- Fuel conservative aircraft engine technology
[NASA-TN-78962] p0021 W78-27127

FUEL-AIR RATIO

SUBJECT INDEX

FUEL-AIR RATIO

Effect of air temperature and relative humidity at various fuel-air ratios on exhaust emissions on a per-node basis of an AVCO Lycoming O-320 diad light aircraft engine: Volume 1: Results and plotted data
 [NASA-TN-73507-VOL-1] p0021 #78-29100
 The effect of fuel-to-air ratio on burner-rig hot corrosion
 [NASA-TN-78960] p0072 #78-31210

FUELS

- NT AIRCRAFT FUELS
- NT COAL
- NT DIESEL FUELS
- NT FOSSIL FUELS
- NT HYDROCARBON FUELS
- NT HYDROGEN FUELS
- NT JET ENGINE FUELS
- NT LIQUID ROCKET PROPELLANTS
- NT SYNTHETIC FUELS
- FUNCTIONAL ANALYSIS
- NT INTEGRAL EQUATIONS
- FUNCTIONS (MATHEMATICS)
- NT STRESS FUNCTIONS
- NT TRANSFER FUNCTIONS
- NT VELOCITY FUNCTIONS
- FORMS RESINS
- NT POLYARIDE RESINS
- FUSION WELDING
- NT BRASSING

G

GAGES

U MEASURING INSTRUMENTS
 GAMMA RADIATION
 U GAMMA RAYS
 GAMMA RAYS
 Considerations to achieve directionality for gamma ray lasers
 p0116 #78-26A70

GARP

GLOBAL ATMOSPHERIC RESEARCH PROGRAM

GAS ANALYSIS

NT OROGRAPHY

GAS BEARINGS

Hydrodynamic air lubricated compliant surface bearing for an automotive gas turbine engine. 2: Materials and coatings
 [NASA-CR-135402] p0122 #78-29449

GAS COOLED REACTORS

NT HIGH TEMPERATURE NUCLEAR REACTORS

GAS DENSITY

Distribution of E/W and N sub e in a cross-flow electric discharge laser
 [NASA-TN-73807] p0111 #78-14386

GAS DISCHARGE COUNTERS

C COUNTERS

GAS DISCHARGES

Distribution of E/W and N sub e in a cross-flow electric discharge laser --- electric field to neutral gas density and electron number density
 p0111 #78-24896

GAS EXPANSION

Performance of a short annular dump diffuser using suction-stabilized vortices at inlet Mach numbers to 0.41
 [NASA-TP-1194] p0017 #78-20131

GAS FLOW

NT AIR FLOW

NT PIPE FLOW

Small-signal gas diagnostic measurements in a flowing CO2 pl. discharge laser
 [NASA-TN-73843] p0111 #78-13421

Variable cycle gas turbine engines
 [NASA-CASE-LEW-12916-1] p0113 #78-17384

Laser absorption phenomena in flowing gas devices
 [NASA-CR-135129] p0112 #78-18411

Stiffness of straight and tapered annular gas path seals
 [NASA-TN-78872] p0103 #78-23385

GAS GENERATOR ENGINES

1 ENGINES

GAS INJECTION

In-situ laser retorting of oil shale
 [NASA-CASE-LEW-12217-1] p0124 #78-18452
 Gas turbine engine with recirculating bleed
 [NASA-CASE-LEW-12452-1] p0019 #78-25089

GAS LASERS

NT CARBON DIOXIDE LASERS

GAS LUBRICATED BEARINGS

U GAS BEARINGS

GAS MIXTURES

NT AIR

Lean combustion limits of a confined premixed-prevaporized propane jet
 [NASA-TN-78868] p0019 #78-22099

GAS PRESSURE

Fabrication of stainless steel clad tubing --- gas pressure bonding
 [NASA-CR-135347] p0079 #78-21265

GAS STREAMS

Sound production in a moving stream
 p0165 #78-31224

Variable mixer propulsion cycle
 [NASA-CASE-LEW-12917-1] p0016 #78-18067

Cyclic oxidation of coated Oxide Dispersion Strengthened (ODS) alloys in high velocity gas streams at 1100 deg C
 [NASA-TN-78877] p0071 #78-24336

GAS TEMPERATURE

Predicted inlet gas temperatures for tungsten fiber reinforced superalloy turbine blades
 p0060 #78-33203

Computer program for calculation of a gas temperature profile by infrared emission: Absorption spectroscopy
 [NASA-TN-73848] p0015 #78-15043

Recovery and radiation corrections and time constants of several sizes of shielded and unshielded thermocouple probes for measuring gas temperature
 [NASA-TP-1099] p0109 #78-15463

Predicted inlet gas temperatures for tungsten fiber reinforced superalloy turbine blades
 [NASA-TN-73842] p0017 #78-19157

GAS TURBINE ENGINES

NT DUCTED FAN ENGINES

NT J-85 ENGINE

NT JET ENGINES

NT TP-30 ENGINE

NT TURBOFAN ENGINES

NT TURBOJET ENGINES

NT TURBOPROP ENGINES

Temperature distributions and thermal stresses in a graded zirconia/metal gas path seal system for aircraft gas turbine engines
 [AIAA PAPER 78-93] p0118 #78-20683

Friction and wear of sintered fibermetal abrasible seal materials
 p0074 #78-21451

The promise of eutectics for aircraft turbines
 p0074 #78-24882

Volatile products from the interaction of KCl/g/ with Cr2O3 and LaCrO3 in oxidizing environments --- gas turbine engines
 p0066 #78-24887

Consolidation of silicon nitride without additives --- for gas turbine engine efficiency increase
 p0085 #78-24895

Effects of film injection on performance of a cooled turbine
 p0033 #78-24902

Progress in advanced high temperature turbine materials, coatings, and technology
 p0056 #78-24910

High temperature environmental effects on metals
 p0075 #78-29329

Self-acting shaft seals
 p0120 #78-33219

An overview of aerospace gas turbine technology of relevance to the development of the automotive gas turbine engine
 [SAE PAPER 780075] p0120 #78-33364

Experimental evaluation of fuel preparation systems for an automotive gas turbine catalytic combustor
 p0120 #78-37677

Combustor concepts for aircraft gas turbine low-power emissions reduction
 [AIAA PAPER 78-999] p0025 #78-43546

Substitution of ceramics for high temperature alloys
 p0086 #78-47596

Cost analysis of advanced turbine blade manufacturing processes
 [NASA-CR-135203] p0026 #78-10092

SUBJECT INDEX

GAS WELDING

Oil cooling system for a gas turbine engine
 [NASA-CASE-LEW-12321-1] p0113 N78-10457
 Splitter-bladed centrifugal compressor impeller
 designed for automotive gas turbine application
 --- at the Lewis Research Center
 [NASA-CR-135237] p0121 N78-10472
 Experimental performance of a
 13.65-centimeter-tip-diameter tandem-bladed
 sweptback centrifugal compressor designed for a
 pressure ratio of 6
 [NASA-TP-1091] p0003 N78-11002
 An overview of aerospace gas turbine technology of
 relevance to the development of the automotive
 gas turbine engine
 [NASA-TN-73849] p0014 N78-13062
 Temperature distributions and thermal stresses in
 a graded zirconia/metal gas path seal system for
 aircraft gas turbine engines
 [NASA-TN-73818] p0015 N78-15040
 Preliminary study of cyclic thermal shock
 resistance of plasma-sprayed zirconium oxide
 turbine outer air seal shrouds
 [NASA-TN-73852] p0080 N78-15280
 Cold-air performance of free-power turbine
 designed for 112-kilowatt automotive gas-turbine
 engine. 1: Design Stator-vane-chord setting
 angle of 35 deg
 [NASA-TP-1007] p0015 N78-16053
 Ceramics in gas turbine: Powder and process
 characterization
 [NASA-TN-73875] p0016 N78-17059
 Variable cycle gas turbine engines
 [NASA-CASE-LEW-12916-1] p0113 N78-17384
 Development of spiral-groove self-acting face seals
 [NASA-CR-135303] p0121 N78-17387
 Integrated gas turbine engine-nacelle
 [NASA-CASE-LEW-12389-2] p0016 N78-18066
 Variable mixer propulsion cycle
 [NASA-CASE-LEW-12917-1] p0016 N78-18067
 Progress in advanced high temperature turbine
 materials, coatings, and technology
 p0018 N78-21122
 Effects of film injection on performance of a
 cooled turbine p0029 N78-21147
 Hydrodynamic air lubricated compliant surface
 bearing for an automotive gas turbine engine.
 1: Journal bearing performance
 [NASA-CR-135368] p0121 N78-21472
 Experimental evaluation of fuel preparation
 systems for an automotive gas turbine catalytic
 combustor
 [NASA-TN-78858] p0082 N78-22243
 Automotive gas turbine fuel control
 [NASA-CASE-LEW-12785-1] p0115 N78-24545
 Gas turbine engine with recirculating bleed
 [NASA-CASE-LEW-12452-1] p0019 N78-25089
 YF 102 in-duct combustor noise measurement, volume 1
 [NASA-CR-135404-VOL-1] p0167 N78-25827
 YF 102 in-duct combustor noise measurement, volume 2
 [NASA-CR-135404-VOL-2] p0167 N78-25828
 YF 102 in-duct combustor noise measurement, volume 3
 [NASA-CR-135404-VOL-3] p0167 N78-25829
 Ceramic regenerator systems development program
 --- for automobile gas turbine engines
 [NASA-CR-135330] p0181 N78-25988
 Cold-air performance of the compressor-drive
 turbine of the Department of Energy baseline
 automobile gas-turbine engine
 [NASA-TN-78994] p0005 N78-26098
 Combustor concepts for aircraft gas turbine
 low-power emissions reduction
 [NASA-TN-78875] p0020 N78-26143
 Liquid-cooling technology for gas turbines review
 and status
 [NASA-TN-78906] p0020 N78-26145
 Ceramic regenerator systems development program
 [NASA-CR-135410] p0181 N78-26997
 Advanced materials research for long-haul aircraft
 turbine engines p0011 N78-27057
 Gas turbine engine emission reduction technology
 program p0001 N78-27058
 Fabrication and test of digital output interface
 devices for gas turbine electronic controls
 [NASA-CR-135427] p0020 N78-27129
 Reverse-flow combustor for small gas turbines with
 pressure-atomizing fuel injectors

[NASA-TP-1260] p0021 N78-27130
 Aerodynamic performance of conventional and
 advanced design labyrinth seals with
 solid-smooth, abrasible, and honeycomb lands ---
 gas turbine engines
 [NASA-CR-135307] p0122 N78-27427
 Study and program plan for improved heavy duty gas
 turbine engine ceramic component development
 [NASA-CR-135230] p0122 N78-28466
 Long-term CP6 engine performance deterioration:
 Evaluation of engine S/W 451-380
 [NASA-CR-159390] p0031 N78-29103
 Rob tolerance evaluation of two sintered NiCrAl
 gas path seal materials --- wear tests of gas
 turbine engine seals
 [NASA-TN-78967] p0071 N78-29215
 Substitution of ceramics for high temperature alloys
 --- advantages of using silicon carbides and
 silicon nitrides in gas turbine engines
 [NASA-TN-78931] p0040 N78-29246
 Hydrodynamic air lubricated compliant surface
 bearing for an automotive gas turbine engine.
 2: Materials and coatings
 [NASA-CR-135402] p0122 N78-29449
 Catalytic combustion for the automotive gas
 turbine engine p0092 N78-30333
 Advanced optical blade tip clearance measurement
 system
 [NASA-CR-159402] p0032 N78-31106
 Aircraft gas turbine low-power emissions reduction
 technology program
 [NASA-CR-135434] p0032 N78-32097
 Redundant disc
 [NASA-CASE-LEW-12496-1] p0022 N78-33101
GAS TURBINES
 Two-layer thermal barrier coating for gas
 temperature components
 [ACS PAPER 31-BEW-76P] p0084 A78-18787
 Burner rig alkali salt corrosion of several high
 temperature alloys p0073 A78-18793
 Ceramics in gas turbines - Powder and process
 characterization p0085 A78-23328
 Open-Cycle Gas Turbine/Steam Turbine Combined
 Cycles with synthetic fuels from coal
 [ASME PAPER 77-WA/ENER-9] p0146 A78-33147
 Degree of vaporization using an airblast type fuel
 injector for a premixed-prevaporized combustor
 p0107 A78-50322
 Improved ceramic heat exchange material
 [NASA-CR-135262] p0086 N78-10291
 Emissions control for ground power gas turbines
 p0013 N78-11072
 Advanced low-NO(x) combustors for supersonic
 high-altitude gas turbines p0014 N78-11070
 Experimental evaluation of premixing-prevaporizing
 fuel injection concepts for a gas turbine
 catalytic combustor p0101 N78-14313
 Experimental clean combustor program: Turbulence
 characteristics of compressor discharge flows
 [NASA-CR-135277] p0027 N78-15041
 Gas turbine engine with convertible accessories
 [NASA-CASE-LEW-12390-1] p0016 N78-17056
 High temperature surface protection --- 10 gas
 turbines p0102 N78-17340
 Reduction of aircraft gas turbine engine pollutant
 emissions
 [NASA-TN-78870] p0019 N78-22098
 Thermal barrier coatings
 [NASA-TN-78848] p0059 N78-24291
 Counter pumping debris excluder and separator ---
 gas turbine shaft seals
 [NASA-CASE-LEW-11855-1] p0020 N78-25090
 Experimental study of the effects of flameholder
 geometry on emissions and performance of lean
 premixed combustors
 [NASA-CR-135424] p0030 N78-26147
 Direct heating surface combustor
 [NASA-CASE-LEW-11877-1] p0047 N78-27147
 Gas turbine project status p0091 N78-30303

GAS WELDING
 MET BRAZING

GAS-LIQUID INTERACTIONS

SUBJECT INDEX

**GAS-LIQUID INTERACTIONS
WT AIR WATER INTERACTIONS
GAS-SOLID INTERFACES**

The role of thermal shock in cyclic oxidation
p0076 A78-37676

GASDYNAMIC LASERS
Distribution of I/V and μ sub e in a cross-flow electric discharge laser
[NASA-TN-73807] p0111 W78-14386

**GASEOUS CAVITATION
U GAS FLOW**

GASEOUS DIFFUSION
Purging of a tank-mounted multilayer insulation system by gas diffusion
[NASA-TP-1127] p0041 W78-17127

GASEOUS ROCKET PROPELLANTS
Analytical study of laser-supported combustion waves in hydrogen
[AIAA PAPER 78-1219] p0067 A78-41901
Inert gas thrusters
[NASA-CN-135226] p0053 W78-19198

GASES

WT AIR

WT ARGON

WT CARBON MONOXIDE

WT CHARGED PARTICLES

WT COLLISIONLESS PLASMAS

WT EXHAUST GASES

WT GAS MIXTURES

WT GAS STREAMS

WT HELIUM

WT HIGH PRESSURE OXYGEN

WT HYDROGEN ATOMS

WT HYDROGEN IONS

WT HYDROGEN PLASMA

WT IONIZED GASES

WT LASER PLASMAS

WT LIQUID NITROGEN

WT LIQUID NITROGEN

WT LIQUID OXYGEN

WT MONATOMIC GASES

WT NITROGEN

WT OXYGEN

WT OXYGEN ATOMS

WT OZONE

WT RARE GASES

WT XENON

Study of the effects of gaseous environments on sulfidation attack of superalloys
[NASA-CN-135388] p0079 W78-21268

GASIFICATION

WT COAL GASIFICATION

GASP
U GLOBAL AIR SAMPLING PROGRAM

GEAR TEETH

Dynamic tooth loads and stressing for high contact ratio spur gears
[ASME PAPER 77-DET-101] p0123 A78-20606
Study of lubricant jet flow phenomena in spur gears - Out of mesh condition
[ASME PAPER 77-DET-104] p0118 A78-20608
Experimental and analytical load-life relation for AISI 9310 steel spur gears
[ASME PAPER 77-DET-121] p0118 A78-20609

GEARS

Dynamic tooth loads and stressing for high contact ratio spur gears
[ASME PAPER 77-DET-101] p0123 A78-20606
Experimental and analytical load-life relation for AISI 9310 steel spur gears
[ASME PAPER 77-DET-121] p0118 A78-20609
Bearing, gearing, and lubrication technology
[SAE PAPER 780077] p0120 A78-33366
Bearing, gearing, and lubrication technology
[NASA-TN-73851] p0114 W78-17389
Oil-air mist lubrication for helicopter gearing
[NASA-CN-135081] p0010 W78-25080
Rolling element fatigue testing of gear materials
[NASA-CN-135411] p0122 W78-31427
Rolling element fatigue testing of gear materials
[NASA-CN-135.50] p0124 W78-33463

GENERAL AVIATION AIRCRAFT

General aviation energy-conservation research programs at NASA-Lewis Research Center --- for non-turbine general aviation engines
p0024 W78-29330
General aviation piston-engine exhaust emission reduction
p0013 W78-11073

General aviation energy-conservation research programs at NASA-Lewis Research Center
[NASA-TN-73884] p0016 W78-17060

GENERAL DYNAMICS AIRCRAFT

WT P-102 AIRCRAFT

**GEOMAGNETIC EFFECTS
U MAGNETIC EFFECTS**

**GEOMAGNETIC FIELD
U GEOMAGNETISM**

**GEOMAGNETIC STORMS
U MAGNETIC STORMS**

GEOMAGNETISM
The Lewis Research Center geomagnetic substorm simulation facility
p0036 W78-10155

GEOMETRY

WT TANK GEOMETRY

**GEOSTATIONARY SATELLITES
U SYNCHRONOUS SATELLITES**

GEOSYNCHRONOUS ORBITS
Provisional specification for satellite time in a geomagnetic environment
p0036 W78-10173

GEOTHERMAL RESOURCES

WT GEYSERS

**GERMINE ARC HEATERS
U HEATING EQUIPMENT**

GERMANIDES
Superconducting Nb3Ge for high-field magnets
p0175 A78-41922

GERMANIUM ALLOYS

Niobium-germanium superconducting tapes for high-field magnet applications
[NASA-CN-135364] p0099 W78-19392

GERMANIUM COMPOUNDS

WT GERMANIUM DISELENIDES

Liquid propellant reorientation in a low-gravity environment
[NASA-TN-78969] p0105 W78-29407

GLASS

Traction and lubricant film temperature as related to the glass transition temperature and solidification --- using infrared spectroscopy on EHD contacts
p0087 A78-40947
Preliminary evaluation of Glass Resin materials for solar cell cover use
[NASA-TN-78925] p0137 W78-26544

GLASS COATINGS

Evaluation of glass resin coatings for solar cell applications
[NASA-CN-159392] p0145 W78-27440

GLASS FIBER REINFORCED PLASTICS

In situ ply strength - An initial assessment
p0061 A78-33223

GLAUBERT COEFFICIENT

U HACH NUMBER

GLOBAL AIR SAMPLING PROGRAM

Global measurements of gaseous and aerosol trace species in the upper troposphere and lower stratosphere from daily flights of 747 airliners
p0147 A78-15826
Description and review of global measurements of atmospheric species from GASP
p0148 A78-24893

Atmospheric ozone measurements made from B-747 airliners - Spring 1975
p0148 A78-24894

Global atmospheric sampling program
p0013 W78-11076

GLOBAL ATMOSPHERIC RESEARCH PROGRAM

An analysis of the first two years of GASP data
[NASA-TN-73817] p0148 W78-13669

GOLD

Morphology of gold and copper ion-plated coatings
[NASA-TP-1242] p0071 W78-26199

GOVERNMENT/INDUSTRY RELATIONS

Making aerospace technology work for the automotive industry, introduction
[NASA-TN-73870] p0179 W78-17941

GRADUATION

U CALIBRATING

GRAVULAR MATERIALS

Petrographic analysis of wear particles from sliding elastohydrodynamic experiments
[NASA-TP-1230] p0115 W78-22377

GRAPHITE

Effect of thermal exposure on lubricating

SUBJECT INDEX

HEAT EXCHANGERS

properties of polyimide films and polyimide-bonded graphite fluoride films [NASA-TP-1125] p0080 N78-15277

Impact behavior of filament wound graphite/epoxy fan blades [NASA-TN-78945] p0018 N78-22097

Fiber reinforced PPH polyimide composites [NASA-CR-135377] p0063 N78-25132

Some effects of composition on friction and wear of graphite-fiber-reinforced polyimide liners in plain spherical bearings [NASA-TP-1229] p0115 N78-25433

Friction and wear of carbon-graphite materials for high-energy brakes [NASA-TN-78908] p0056 N78-26178

A comparison of the lubricating mechanisms of graphite fluoride and molybdenum disulfide films [NASA-TN-78897] p0083 N78-26215

Graphite-fiber-reinforced polyimide liners of various compositions in plain spherical bearings [NASA-TN-78908] p0116 N78-26447

GRAPHITE-EPOXY COMPOSITE MATERIALS

Lamination residual strains and stresses in hybrid laminates p0128 A78-12071

Correlation of fiber composite tensile strength with the ultrasonic stress wave factor p0060 A78-33207

In situ ply strengths - An initial assessment p0061 A78-33223

Effect of preload on the fatigue and static strength of composite laminates with defects p0061 A78-40310

Fracture surface characteristics of off-axis composites p0067 A78-40371

Mechanical behavior and fracture characteristics of off-axis fiber composites. 1: Experimental investigation --- at the Lewis Research Center [NASA-TP-10811] p0057 N78-13138

Filament-winding fabrication of QCSEE configuration fan blades [NASA-CR-135332] p0028 N78-16052

Mechanical behavior and fracture characteristics of off-axis fiber composites. 2: Theory and comparisons [NASA-TP-1082] p0057 N78-16098

Composite hub/metal blade compressor rotor [NASA-CR-135383] p0062 N78-18131

Correlation of fiber composite tensile strength with the ultrasonic stress wave factor [NASA-TN-78946] p0056 N78-20255

Effects of moisture profiles and laminate configuration on the hydro stresses in advanced composites --- graphite-epoxy composites [NASA-TN-78978] p0059 N78-32191

GRAPHS (CHARTS)

Aero-acoustic tests of duct-burning turbofan exhaust nozzles. Comprehensive data report. Volume 3: Acoustic and aerodynamic data curves [NASA-CR-134910-VOL-3] p0032 N78-15990

GRAVITATION

NT REDUCED GRAVITY

GRAVITY GRADIENT SATELLITES

NT ATS 1

NT ATS 2

NT ATS 3

NT ATS 4

GREAT LAKES (NORTH AMERICA)

NT LAKE ERIE

GRIDS

Sensitivity of 30-cw mercury bombardment ion thruster characteristics to accelerator grid design [NASA PAPER 78-668] p0050 A78-32747

Sensitivity of 30-cw mercury bombardment ion thruster characteristics to accelerator grid design [NASA-TN-78861] p0049 N78-23144

GROUND STATIONS

Utilization of NASA Lewis mobile terminals for the Hermes satellite p0094 A78-24885

Low cost Ku-band earth terminals for voice/data/facsimile p0094 A78-31970

GROUND SUPPORT EQUIPMENT

Emissions control for ground power gas turbines p0013 N78-11072

GROUP 1A COMPOUNDS

U ALKALI METAL COMPOUNDS

GROWTH

NT CRYSTAL GROWTH

NT DIRECTIONAL SOLIDIFICATION (CRYSTALS)

NT EPITAXY

GUST LOADS

Synchronization of wind turbine generators against an infinite bus under gusting wind conditions [IEEE PAPER Y 77 675-2] p0142 A78-30196

DOE/NASA Mod-0 100KW wind turbine test results p0133 N78-19628

GUSTS

Characteristics of the unsteady action on transversely sheared mean flows p0106 A78-23246

GYROPLANES

U HELICOPTERS

H

HALIDES

NT FLUORIDES

NT HYDROGEN CHLORIDES

NT CHLORINE FLUORIDE

NT POTASSIUM CHLORIDES

NT SODIUM CHLORIDES

HALL CURRENTS

HALLEY'S COMET

Extended performance electric propulsion power processor design study. Volume 1: Executive summary [NASA-CR-135357] p0054 N78-20250

SEP EVOLVE and Halley rendezvous studies and improved model implementation in HILTOP [NASA-CR-135414] p0038 N78-25105

HALOCARBONS

NT CHLOROCARBONS

HALOGEN COMPOUNDS

NT CHLORINE COMPOUNDS

NT FLUOROPOLYMERS

NT HYDROGEN CHLORIDES

NT CHLORINE FLUORIDE

NT POLYTETRAFLUOROETHYLENE

NT POTASSIUM CHLORIDES

NT SODIUM CHLORIDES

HALOGENATION

NT FLUORINATION

HALOGENS

NT CHLORINE

HARDBOOKS

NT USER MANUALS (COMPUTER PROGRAMS)

HARDENING (MATERIALS)

NT HOT PRESSING

NT PRECIPITATION HARDENING

HARDNESS TESTS

Long-term hot-hardness characteristics of five through-hardened bearing steels [NASA-TP-1341] p0073 N78-33196

HARDWARE

EPDA/NASA advanced thermionic technology program [NASA-CR-157117] p0145 N78-24674

HAZARDS

NT AIRCRAFT HAZARDS

NT TOXIC HAZARDS

HEALTH

Toxic substances alert program [NASA-TN-73866] p0153 N78-20755

HEART FUNCTION

Design and performance of heart assist or artificial heart control systems p0185 N78-23032

HEAT CAPACITY

1 SPECIFIC HEAT

HEAT DISSIPATION

1 COOLING

HEAT DISSIPATION CHILLING

1 COOLING

HEAT EFFECTS

1 TEMPERATURE EFFECTS

HEAT EXCHANGERS

Development and fabrication of a diffusion welded Columbian alloy heat exchanger --- for space power generation [AIME PAPER A78-61] p0123 A78-31500

Improved ceramic heat exchange material [NASA-CR-135262] p0086 N78-10291

HEAT FLUX

SUBJECT INDEX

- Improved ceramic heat exchanger material
[NASA-CR-135292] p0086 W78-13209
- Ceramic regenerator systems development program
--- for automobile gas turbine engines
[NASA-CR-135330] p0181 W78-25988
- Ceramic regenerator systems development program
[NASA-CR-135430] p0181 W78-26997
- Preliminary design study of an alternate heat
source assembly for a Brayton isotope power system
[NASA-CR-135428] p0185 W78-28608
- HEAT FLUX**
- Conceptual design for spacelab pool boiling
experiment
[NASA-CR-135378] p0037 W78-20150
- HEAT GENERATION**
- Lubrication of high-speed, large bore
tapered-roller bearings
[ASME PAPER 77-LUB-13] p0118 W78-23354
- HEAT OF VAPORIZATION**
- Degree of vaporization using an airblast type
injector for a premixed-prevaporized combustor
[NASA-TN-78836] p0103 W78-24494
- HEAT PIPES**
- Evaluation of commercially-available
spacecraft-type heat pipes
[AIAA 78-397] p0044 W78-35590
- High temperature heat pipe research at NASA Lewis
Research Center
[AIAA 78-438] p0106 W78-35618
- Comment on 'Heat-pipe reactors for space power
applications'
p0052 W78-40826
- Two-phase working fluids for the temperature range
50 to 350 C
[NASA-CR-135255] p0107 W78-16329
- Accelerated life tests of specimen heat pipe from
Communication Technology Satellite (CTS) project
[NASA-TN-78846] p0102 W78-17341
- High temperature heat pipe research at NASA Lewis
Research Center
[NASA-TN-78832] p0103 W78-23384
- Performance of a thermionic converter module
utilizing emitter and collector heat pipes
[NASA-TN-78841] p0049 W78-27174
- CTS TEP thermal anomalies: Heat pipe system
performance
[NASA-CR-134413] p0108 W78-29410
- HEAT PUMPS**
- Magnetic heat pumping
[NASA-CR-135250-1] p0102 W78-17335
- HEAT RADIATORS**
- BY SPACECRAFT RADIATORS**
- HEAT REGULATION**
- TEMPERATURE CONTROL**
- HEAT RESISTANCE**
- INTERNAL RESISTANCE**
- HEAT RESISTANT ALLOYS**
- NI MOLYBDENUM ALLOYS**
- NI NIOBIUM ALLOYS**
- NI TANTALUM ALLOYS**
- NI TUNGSTEN ALLOYS**
- NI UDIALYT ALLOYS**
- An experimental P/W wrought superalloy for
advanced temperature service
p0073 W78-15335
- Volatilization of oxides during oxidation of some
superalloys at 1200 C
p0074 W78-18631
- Effects of heat treating on Rene' 95 slightly
below the gamma-prime solvus
p0073 W78-18792
- Burner rig alkali salt corrosion of several high
temperature alloys
p0073 W78-18791
- Effects of silicon on the oxidation,
hot-corrosion, and mechanical behavior of two
cast nickel-base superalloys
p0074 W78-21019
- Volume fraction determination in cast superalloys
and directionally solidified eutectic alloys by
a new manual point count practice
p0089 W78-24369
- Progress in advanced high temperature turbine
materials, coatings, and technology
p0056 W78-24910
- Rolling-element fatigue life of AMS 5789 corrosion
resistant, high temperature bearing steel
[ASME PAPER 77-LUB-10] p0075 W78-28423
- Strainrange partitioning behavior of the
nickel-base superalloys, Rene 80 and 100
p0075 W78-33214
- Strength enhancement process for prealloyed powder
superalloys
p0075 W78-33216
- Cleaning process for contaminated superalloy powders
p0078 W78-41400
- Substitution of ceramics for high temperature alloys
p0086 W78-47596
- 10,000-hour cyclic oxidation behavior at 815 C
/1500 P/ of 33 high-temperature alloys
p0077 W78-51716
- Thermal fatigue and oxidation data of superalloys
including directionally solidified eutectics
[NASA-CR-135272] p0078 W78-15233
- Directionally solidified eutectic gamma-gamma
nickel-base superalloys
[NASA-CR-135272] p0069 W78-18183
- Predicted inlet gas temperatures for tungsten
fiber reinforced superalloy turbine blades
[NASA-TN-78842] p0017 W78-19157
- Strength enhancement process for prealloyed powder
superalloys
[NASA-TN-78842] p0070 W78-21266
- Strainrange partitioning behavior of the
nickel-base superalloys, Rene' 80 and 100
[NASA-TN-78828] p0070 W78-21267
- Study of the effects of gaseous environments on
sulfidation attack of superalloys
[NASA-CR-135148] p0079 W78-21268
- The effect of microstructure on hydrogen
embrittlement of the nickel-base superalloy,
Udiate 700
[NASA-TN-73772] p0082 W78-22232
- The role of thermal shock in cyclic oxidation
[NASA-TN-78876] p0070 W78-23193
- Advanced materials research for long-haul aircraft
turbine engines
p0001 W78-27057
- Erosion/corrosion of turbine airfoil materials in
the high-velocity effluent of a pressurized
fluidized coal combustor
[NASA-TP-1274] p0071 W78-28225
- Substitution of ceramics for high temperature alloys
--- advantages of using silicon carbide and
silicon nitride in gas turbine engines
[NASA-TN-78931] p0084 W78-29246
- Longitudinal shear behavior of several oxide
dispersion strengthened alloys
[NASA-TN-78973] p0072 W78-31211
- Evaluation of cyclic behavior of aircraft turbine
disk alloys
[NASA-CR-134933] p0128 W78-33478
- HEAT SHIELDING**
- Recovery and radiation corrections and time
constants of several sizes of shielded and
unshielded thermocouple probes for measuring gas
temperature
[NASA-TP-1094] p0104 W78-15463
- HEAT SINKS**
- A model for particle confinement in a toroidal
plasma subject to strong radial electric fields
[NASA-TN-78814] p0171 W78-10884
- HEAT SOURCES**
- NI GENIUMS**
- Preliminary design study of an alternate heat
source assembly for a Brayton isotope power system
[NASA-CR-135428] p0185 W78-28608
- HEAT STORAGE**
- Thermal energy storage heat exchanger: Molten
salt heat exchanger design for utility power
plants
[NASA-CR-135244] p0143 W78-14632
- Thermal energy storage heat exchanger: Molten
salt heat exchanger design for utility power
plants
[NASA-CR-135244] p0143 W78-14633
- Thermal energy storage for industrial waste heat
recovery
[NASA-TN-78941] p0140 W78-29576
- HEAT TESTS**
- INTERNAL TEMPERATURE TESTS**
- HEAT TRANSFER**
- NI CONVECTIVE HEAT TRANSFER**
- A computer program for the transient thermal
analysis of an impingement cooled turbine blade
[AIAA PAPER 78-92] p0106 W78-20682

SUBJECT INDEX

HIGH TEMPERATURE TESTS

- Shape of two-dimensional solidification interface during directional solidification by continuous casting p0119 A78-31829
- Effects of film injection angle on turbine vane cooling [NASA-TP-1095] p0101 A78-13379
- Supercritical oxygen heat transfer --- regenerative cooling [NASA-CR-135339] p0108 A78-17302
- FORTRAN program for calculating coolant flow and metal temperatures of a full-coverage-film-cooled vane or blade [NASA-TP-1259] p0021 A78-28099
- Analysis of metal temperature and coolant flow with a thermal-barrier coating on a full-coverage-film-cooled turbine vane [NASA-TP-1310] p0022 A78-31109
- Filling of orbital fluid management systems [NASA-CR-159401] p0108 A78-31380
- Thermal characteristics of the 12-gigahertz, 200-watt output stage tube for the communications technology satellite [NASA-TP-1344] p0043 A78-33137
- HEAT TRANSMISSION COEFFICIENTS**
- Boiling incipience and convective boiling of neon and nitrogen p0105 A78-15820
- Method for calculating convective heat-transfer coefficients over turbine vane surfaces [NASA-TP-1134] p0102 A78-17338
- HEAT TRANSMISSION**
- HT CONVECTIVE HEAT TRANSFER**
- HT HEAT TRANSFER**
- HEAT TREATMENT**
- HT ANNEALING**
- Effects of heat treating PH Rene' 95 slightly below the gamma-prime solvus p0073 A78-18792
- Rolling element fatigue testing of gear materials [NASA-CR-135411] p0122 A78-31427
- HEATING**
- HT LASER HEATING**
- HT PLASMA HEATING**
- HT RADIO FREQUENCY HEATING**
- HT SOLAR HEATING**
- HEATING EQUIPMENT**
- Development of flat-plate solar collectors for the heating and cooling of buildings: Executive summary [NASA-CR-134804-2] p0146 A78-33527
- HELICOPTER ATTITUDE INDICATORS**
- HELICOPTERS**
- HELIUM**
- Purging of a tank-mounted multilayer insulation system by gas diffusion [NASA-TP-1127] p0041 A78-17127
- HELIX TUBES**
- U TRAVELLING WAVE TUBES**
- HERMES SATELLITE**
- U COMMUNICATIONS TECHNOLOGY SATELLITE**
- HIGH ACCELERATION**
- Minimum-time acceleration of aircraft turbofan engines p0023 A78-23892
- HIGH FIELD MAGNETS**
- Design and prototype fabrication of a 30 tesla cryogenic magnet p0097 A78-15823
- Superconducting Nb₃Ge for high-field magnets p0175 A78-41922
- HIGH FREQUENCIES**
- High frequency dynamic engine simulation --- TP-30 engine [NASA-CR-135313] p0027 A78-13059
- Potential damage to DC superconducting magnets due to the high frequency electromagnetic waves [NASA-TN-73808] p0096 A78-13330
- HIGH MELTING COMPOUNDS**
- U REFRACTORY MATERIALS**
- HIGH PRESSURE**
- Design and preliminary results of a semitranspiration cooled (Lamilloy) liner for a high-pressure high-temperature combustor [NASA-TN-78874] p0011 A78-24138
- HIGH PRESSURE OXYGEN**
- Supercritical oxygen heat transfer --- regenerative cooling [NASA-CR-135339] p0108 A78-17302
- HIGH SPEED**
- Balancing techniques for high-speed flexible rotors [NASA-CR-2975] p0121 A78-20514
- HIGH SPEED FLIGHT**
- U HIGH SPEED**
- HIGH STRENGTH ALLOYS**
- HT ASTEROLOY (TRADEMARK)**
- HT HARAGING STEELS**
- Cryogenic properties of a new tough-strong iron alloy p0073 A78-15825
- Effects of heat treating PH Rene' 95 slightly below the gamma-prime solvus p0073 A78-18792
- Manufacture and engine test of advanced oxide dispersion strengthened alloy turbine vanes --- for space shuttle thermal protection [NASA-CP-135269] p0077 A78-11232
- HIGH STRENGTH STEELS**
- HT HARAGING STEELS**
- HIGH TEMPERATURE**
- Effect of prior creep at 1365 K on the room temperature tensile properties of several oxide dispersion strengthened alloys p0074 A78-21431
- Elevated-temperature flow strength, creep resistance and diffusion welding characteristics of Ti-6Al-2Nb-1Ta-0.8Mo [NASA-TN-73854] p0069 A78-17190
- Design and preliminary results of a semitranspiration cooled (Lamilloy) liner for a high-pressure high-temperature combustor [NASA-TN-78874] p0011 A78-24138
- HIGH TEMPERATURE ALLOYS**
- U HEAT RESISTANT ALLOYS**
- HIGH TEMPERATURE ENVIRONMENTS**
- High temperature environmental effects on metals p0075 A78-29329
- High temperature surface protection --- 10 gas turbines [NASA-TN-73877] p0102 A78-17340
- High temperature environmental effects on metals [NASA-TN-73878] p0017 A78-19158
- HIGH TEMPERATURE MATERIALS**
- U REFRACTORY MATERIALS**
- HIGH TEMPERATURE NUCLEAR REACTORS**
- High-temperature, high-power-density thermonuclear energy conversion for space [NASA-TN-73844] p0171 A78-13890
- HIGH TEMPERATURE RESEARCH**
- High temperature heat pipe research at NASA Lewis Research Center [AIAA 78-438] p0106 A78-35618
- Review of the ICARD S and M panel evaluation program of the NASA-Lewis SRP approach to high-temperature LCF life prediction [NASA-TN-78979] p0072 A78-31209
- HIGH TEMPERATURE TESTS**
- An experimental P/M wrought superalloy for advanced temperature service p0073 A78-15335
- Evaluation of low cost/high temperature fiber and blanket insulation p0063 A78-16903
- Volatilization of oxides during oxidation of some superalloys at 1200 C p0073 A78-18631
- Two-layer thermal barrier coating for high temperature components [ACS PAPER 31-BE-76P] p0088 A78-18787
- High temperature environmental effects on metals p0075 A78-29329
- High temperature compressive cracking in hot-pressed silicon nitride p0085 A78-38706
- Elevated-temperature tensile and creep properties of several ferritic stainless steels [NASA-TN-73853] p0069 A78-17189

HIGH VOLTAGES

SUBJECT INDEX

HIGH VOLTAGES

Solid State Remote Power Controllers for high voltage DC distribution systems p0100 A78-15574

Spacecraft-generated plasma interaction with high voltage solar array [ATAA PAPER 78-673] p0055 A78-32751

Potential damage to dc superconducting magnets due to high frequency electromagnetic waves p0098 A78-39902

Medium power voltage multipliers with a large number of stages p0098 A78-45435

High frequency capacitor-diode voltage multiplier dc-dc converter development [NASA-CR-135309] p0099 A78-15400

Interaction of large, high power systems with operational orbit charged particle environments [NASA-TN-73867] p0037 A78-16076

Investigation of high voltage spacecraft system interactions with plasma environments [NASA-TN-78831] p0097 A78-21373

HIGHWAYS
Photovoltaic highway applications: Assessment of the near-term market [NASA-TN-73863] p0178 A78-17935

HISS
Experiments on whistler wave filamentation and VLF hiss in a laboratory plasma p0149 A78-41788

HOLDERS
WT FILAR HOLDERS
SOLE DISTRIBUTION (MECHANICS)
Effect of cooling-hole geometry on aerodynamic performance of a film-cooled turbine vane tested with CO₂ air in a two-dimensional cascade [NASA-TN-1136] p0008 A78-20080

HOLLOW CATHODES
Pulse ignition characterization of mercury ion thruster hollow cathode using an improved pulse ignitor [ATAA PAPER 78-709] p0051 A78-32772

A hollow cathode hydrogen ion source --- for controlled fusion p0173 A78-39835

Pulse ignition characterization of mercury ion thruster hollow cathode using an improved pulse ignitor [NASA-TN-78858] p0047 A78-21203

HOMOGENEOUS TURBULENCE
On the localness of the spectral energy transfer in turbulence p0106 A78-24939

On the localness of the spectral energy transfer in turbulence [NASA-TN-73824] p0101 A78-13361

HONEYCOMB STRUCTURES
Aerodynamic performance of conventional and advanced design labyrinth seals with solid-smooth shradable, and honeycomb lands --- gas turbine engines [NASA-CR-135307] p0122 A78-27427

HOSBS
Liquid rocket lines, bellows, flexible hoses, and filters [NASA-SP-8123] p0047 A78-16089

HOT CYCLE PROPULSION SYSTEM
U TIP DRIVEN ROTORS
HOT JET EXHAUST
U JET EXHAUST
HOT JETS
U JET FLOW
HOT PRESSING
Microstructure of hot-pressed Al₂O₃-Si₃N₄ mixtures as a function of holding temperature p0084 A78-17456

Effects of pressure and temperature on hot pressing a sialon [NASA-TN-78945] p0083 A78-27274

HOT-WIRE TURBULENCE METERS
U TURBULENCE METERS
HUMIDITY
Effect of air temperature and relative humidity at various fuel-air ratios on exhaust emissions on a per-mile basis of an AVCO Lycoming O-320 diad light aircraft engine: Volume 1: Results and plotted data [NASA-TN-73507-VOL-1] p0021 A78-29100

HYBRID COMBUSTION

U HYBRID PROPELLANT ROCKET ENGINES
HYBRID COMPUTERS
An automated procedure for calculating system matrices from perturbation data generated by an HAI Facor and 100 hybrid computer system [NASA-TN-73869] p0156 A78-15729

HYBRID PROPELLANT ROCKET ENGINES
Linear aerospace engine study --- for reusable launch vehicles [NASA-CR-135231] p0026 A78-11082

HYBRID PROPULSION
State-of-the-art assessment of electric and hybrid vehicles [NASA-TN-79509] p0180 A78-27003

HYBRID STRUCTURES
Analysis/design of strip reinforced random composites (strip hybrids) [NASA-TN-78985] p0059 A78-33149

HYDRAULIC ACTUATORS
U ACTUATORS
U HYDRAULIC EQUIPMENT
HYDRAULIC EQUIPMENT
The design of hydraulic pressure regulators that are stable without the use of sensing line restrictors or frictional dampers p0164 A78-24897

The design of hydraulic pressure regulators that are stable without the use of sensing line restrictors or frictional dampers [NASA-TN-X-73687] p0101 A78-10415

HYDRAULIC HEATING SOURCES
U HEAT SOURCES
U HYDRAULIC EQUIPMENT
HYDRAULIC JETS
Flow of liquid jets through closely woven screens p0108 A78-42877

Effect of airstream velocity on beam drop diameters of water sprays produced by pressure and air atomizing nozzles [NASA-TN-73740] p0101 A78-13369

HYDRAULIC PUMPS
U HYDRAULIC EQUIPMENT
HYDRAULIC SYSTEMS
U HYDRAULIC EQUIPMENT
HYDRAULIC VALVES
U HYDRAULIC EQUIPMENT
HYDRIDES
WT ALUMINUM BOROXYGENIDES
WT METAL HYDRIDES
HYDROCARBON COMBUSTION
In-situ laser retorting of oil shale [NASA-CASE-LEW-12217-1] p0129 A78-14452

HYDROCARBON FUELS
WT DIESEL FUELS
WT FOSSIL FUELS
WT JET ENGINE FUELS
Jet aircraft hydrocarbon fuels technology [NASA-CP-2033] p0088 A78-19325

Characteristics and combustion of future hydrocarbon fuels --- aircraft fuels [NASA-TN-78865] p0089 A78-24370

HYDROCARBONS
WT PROPANE
Hydrocarbon group type determination in jet fuels by high performance liquid chromatography p0089 A78-24406

Hydrocarbon group type determination in jet fuels by high performance liquid chromatography [NASA-TN-73829] p0088 A78-11213

Experimental study of the effect of cycle pressure on lean combustion emissions [NASA-CR-3032] p0031 A78-28098

HYDRODYNAMICS
WT FLASTOHYDRODYNAMICS
Conceptual design for spacelab pool boiling experiment [NASA-CR-135378] p0037 A78-20150

Effect of geometry on hydrodynamic film thickness [NASA-PP-1287] p0117 A78-30585

HYDROGEN
WT HYDROGEN ATOMS
WT HYDROGEN IONS
WT HYDROGEN PLASMA
HYDROGEN ATOMS
Atomic hydrogen storage method and apparatus --- cryotrapping and magnetic field strength [NASA-CAS2-LEW-12081-2] p0169 A78-19907

SUBJECT INDEX

IMPEDANCE PROBES

- Atomic hydrogen storage method and apparatus
[NASA-CASR-188-12081-1] p0089 W78-24365
- HYDROGEN CHLORIDES**
Interaction of NaCl(g) and HCl(g) with condensed
H₂SO₄ --- in hot corrosion processes p0066 W78-24488
Interaction of NaCl(g) and HCl(g) with condensed
H₂SO₄
[NASA-TN-73796] p0064 W78-13159
- HYDROGEN COMPOUNDS**
BT ALUMINUM BOMBYDRIDES
BT METAL HYDRIDES
HYDROGEN BRITTLENESS
The effect of microstructure on hydrogen
embrittlement of the nickel base superalloy,
Udian-700 p0076 W78-37075
The effect of microstructure on hydrogen
embrittlement of the nickel-base superalloy,
Udian-700
[NASA-TN-73772] p0082 W78-22232
- HYDROGEN FUELS**
Analytical study of laser-supported combustion
waves in hydrogen
[AIAA PAPER 78-1219] p0067 W78-41901
Analytical study of laser supported combustion
waves in hydrogen
[NASA-CR-135389] p0112 W78-20489
Hydrogen turbine power conversion system assessment
[NASA-CR-135298] p0108 W78-20621
- HYDROGEN IONS**
A hollow cathode hydrogen ion source --- for
controlled fusion p0173 W78-39835
- HYDROGEN OXYGEN ENGINES**
Hydrogen film cooling of a small hydrogen-oxygen
thrust chamber and its effect on erosion rates
of various ablative materials
[NASA-TP-1098] p0087 W78-13124
Hydrogen turbine power conversion system assessment
[NASA-CR-135298] p0108 W78-20621
Advanced space engine powerhead breadboard
assembly system study
[NASA-CR-135232] p0054 W78-25127
- HYDROGEN PLASMA**
Parametric dependence of ion temperature and
relative density in the NASA Lewis SORNA facility
p0173 W78-37679
- HYDROGEN PRODUCTION**
Status of the DOE /STOR/-sponsored national
program on hydrogen production from water via
thermochemical cycles p0102 W78-29331
Status of the DOE (STOR)-sponsored national
program on hydrogen production from water via
thermochemical cycles
[NASA-TN-78825] p0132 W78-17469
- HYDROLYTICS**
1 HYDROMECHANICS
HYDROMAGNETIC FLOW
2 MAGNETOHYDRODYNAMIC FLOW
HYDROMAGNETIC STABILITY
3 MAGNETOHYDRODYNAMIC STABILITY
HYDROMECHANICS
4T ELASTIC HYDRODYNAMICS
4* HYDRODYNAMICS
An integrated theory for predicting the
hydrothermochemical response of advanced
composite structural components p0060 W78-24905
- HYDROX ENGINES**
7 HYDROGEN OXYGEN ENGINES
HYDROXIDES
An improved method for analysis of hydroxide and
carbonate in alkaline electrolytes containing zinc
[NASA-TN-78961] p0139 W78-28607
- HYDROXYL COMPOUNDS**
BT ETHYL ALCOHOL
BT N-ETHYL ALCOHOLS
BT POLYVINYL ALCOHOL
HYDROXYL RADICALS
Measurement of tropospheric 300 nm solar
ultraviolet flux for determination of O₃/D₀
photoproduction rate p0148 W78-38835
- HYPERSONIC WIND TUNNELS**
BT CASCADE WIND TUNNELS
HYPERVERLOCITY WIND TUNNELS
BT CASCADE WIND TUNNELS
- ICE**
Effect of ice contamination on liquid-nitrogen
drops in film boiling p0105 W78-15021
- IGNITERS**
Preburner of staged combustion rocket engine
[NASA-CR-135356] p0054 W78-24279
- IGNITION**
BT SPARK IGNITION
Development of an experiment for determining the
autoignition characteristics of aircraft-type
fuels
[NASA-CR-135329] p0090 W78-16194
- IGNITION SYSTEMS**
Pulse ignition characterization of mercury ion
thrustor hollow cathode using an improved pulse
ignitor
[AIAA PAPER 78-709] p0051 W78-32773
Pulse ignition characterization of mercury ion
thrustor hollow cathode using an improved pulse
ignitor
[NASA-TN-78858] p0047 W78-21203
- IMAGE CONTRAST**
Fabrication and characteristics of experimental
radiographic amplifier screens --- image
transducers with improved image contrast and
resolution
[NASA-CR-2937] p0124 W78-15501
- IMAGE ENHANCEMENT**
Digital enhancement of computerized axial tomograms
[NASA-TN-78974] p0152 W78-31690
- IMAGE TRANSDUCERS**
Fabrication and characteristics of experimental
radiographic amplifier screens --- image
transducers with improved image contrast and
resolution
[NASA-CR-2937] p0124 W78-15501
- IMAGERY**
BT AERIAL PHOTOGRAPHY
BT RADIOGRAPHY
BT TOPOGRAPHY
IMAGING TECHNIQUES
BT IMAGE ENHANCEMENT
IMIDES
Kinetics of imidization and crosslinking in
PBI-polyimide resin --- Polymerization of
Monomer Reactants p0061 W78-33210
- IMMISCIBILITY**
0 SOLUBILITY
IMPACT LOADS
Experimental transient and permanent deformation
studies of steel-sphere-impacted or
explosively-impacted aluminum panels
[NASA-CR-135315] p0078 W78-15234
- IMPACT PRESSURES**
3 IMPACT LOADS
IMPACT RESISTANCE
Impact resistant boron/aluminum composites for
large fan blades
[NASA-CR-135274] p0062 W78-14099
Impact on multilayered composite plates
[NASA-CR-135247] p0062 W78-16103
Thermal environment effects on strength and impact
properties of boron-aluminum composites
[NASA-TN-73885] p0058 W78-17155
Development of Si₃N₄ and SiC of improved toughness
--- for gas turbine engines
[NASA-CR-135306] p0087 W78-17216
Design of impact-resistant boron/aluminum large
fan blade
[NASA-CR-135417] p0031 W78-29104
- IMPACT SENSITIVITY**
2 IMPACT RESISTANCE
IMPACT STRENGTH
Thermal environment effects on strength and impact
properties of boron-aluminum composites
p0060 W78-33204
- IMPEDANCE**
BT ACOUSTIC IMPEDANCE
BT CONTACT RESISTANCE
IMPEDANCE PROBES
BT RADIO FREQUENCY IMPEDANCE PROBES
Probe studies in a modified penning discharge
[NASA-TN-X-73631] p0171 W78-15905

INPELLER BLADES

SUBJECT INDEX

INPELLER BLADES
 O ROTOR BLADES (TURBOCHARGER)
INPELLERS
 Splitter-bladed centrifugal compressor impeller designed for automotive gas turbine application --- at the Lewis Research Center [NASA-CR-135237] p0121 W78-10472

IMPERFECTIONS
 O DEFECTS
IMPIINGEMENT
 WT JET IMPIINGEMENT
 A computer program for the transient thermal analysis of an impingement cooled turbine blade [NASA-TN-73849] p0015 W78-15045

IMPLANTATION
 The use of an ion-beam source to alter the surface morphology of biological implant materials [NASA-TN-78851] p0152 W78-22618

IMPLANTED ELECTRODES (BIOLOGY)
 The use of an ion-beam source to alter the surface morphology of biological implant materials p0061 A78-37686
 Effect of surface texture by ion beam sputtering on implant biocompatibility and soft tissue attachment [NASA-CR-135311] p0152 W78-18672

IMPURITIES
 Impurity concentrations and surface charge densities on the heavily doped face of a silicon solar cell p0130 W78-13534

IN-FLIGHT MONITORING
 Application of a flight-line disk crack detector to a small engine p0012 W78-10088
 JT9D engine diagnostics. Task 2: Feasibility study of measuring in-service flight loads --- 747 aircraft performance [NASA-CR-135395] p0030 W78-27124

INDICATING INSTRUMENTS
 WT ANEMOMETERS
 WT WIND VANES
INDIUM ALLOYS
 Solar cell collector [NASA-CASE-LEW-12552-1] p0136 W78-25527

INDUCED FLUID FLOW
 J FLUID FLOW
INDUCTION MOTORS
 Baseline tests of the power-train electric delivery van [NASA-TN-73765] p0178 W78-17936

INDUCTION SYSTEMS
 J INTAKE SYSTEMS
INDUSTRIAL MANAGEMENT
 Computer model for refinery operations with emphasis on jet fuel production. Volume 1: Program description [NASA-CR-135333] p0090 W78-20350

INDUSTRIAL WASTES
 Thermal energy storage for industrial waste heat recovery [NASA-TN-78953] p0140 W78-29576

INDUSTRIES
 Industrial ion source technology --- for ion beam etching, surface texturing, and deposition [NASA-CR-135353] p0169 W78-18883

INERT GASES
 O RARE GASES
INFRARED ABSORPTION
 Computer program for calculation of a gas temperature profile by infrared emission: Absorption spectroscopy [NASA-TN-73848] p0015 W78-15043

INFRARED DETECTORS
 A low cost, portable instrument for measuring exitance p0109 A78-11392

INFRARED INSTRUMENTS
 WT INFRARED DETECTORS
INFRARED LASERS
 Preliminary results on the conversion of laser energy into electricity p0173 A78-34631

INFRARED LASERS
 O INFRARED LASERS
INFRARED SPECTROSCOPY
 Traction and lubricant film temperature as related to the glass transition temperature and solidification --- using infrared spectroscopy

on ESD contacts p0087 A78-40997

Study of dynamic emission spectra from lubricant films in an elastohydrodynamic contact using Fourier transform spectroscopy [NASA-CR-159418] p0162 W78-32809

INHIBITORS
 WT GEAR INHIBITORS
INITIAL VALUE PROBLEMS
 O BOUNDARY VALUE PROBLEMS
INJECTION
 WT FLUID INJECTION
 WT FUEL INJECTION
 WT GAS INJECTION
INJECTION CARBUSETORS
 O FUEL INJECTION
INJECTORS
 Photographic characterization of spark-ignition engine fuel injectors [NASA-TN-78830] p0018 W78-21110
 Investigation of the burning configuration of a coaxial injector in a combustion chamber [NASA-CR-135383] p0054 W78-22148

INLET FLOW
 A combined potential and viscous flow solution for V/STOL engine inlets [AIAA PAPER 78-142] p0006 A78-20702
 Effectiveness of an inlet flow turbulence control device to simulate flight fan noise in an anechoic chamber p0024 A78-24880
 Predicted inlet gas temperatures for tungsten fiber reinforced superalloy turbine blades p0060 A78-33203
 Reduction of fan noise in an anechoic chamber by reducing chamber wall induced inlet flow disturbances p0166 A78-37681
 Variation of fan tone steadiness for several inflow conditions [AIAA PAPER 78-1119] p0166 A78-41829
 Acoustic evaluation of a novel swept-rotor fan [AIAA PAPER 78-1121] p0166 A78-41831
 Inlet-engine matching for SCAR including application of a bicone variable geometry inlet --- Supersonic Cruise Aircraft Research [AIAA PAPER 78-961] p0007 A78-45096
 Computation of unsteady transonic flows through rotating and stationary cascades. 3: Acoustic far-field analysis [NASA-CR-2902] p0007 W78-12035
 Mechanical characteristics of stability-bleed valves for a supersonic inlet --- for the YF-12 aircraft [NASA-TN-X-3483] p0015 W78-13063
 Effectiveness of an inlet flow turbulence control device to simulate flight noise fan in an anechoic chamber [NASA-TN-73855] p0163 W78-13856
 Effect of design changes on aerodynamic and acoustic performance of translating-centerbody sonic inlets [NASA-TP-1132] p0003 W78-17998
 Simulated flight effects on noise characteristics of a fan inlet with high throat Mach number [NASA-TP-1199] p0017 W78-20132
 Theoretical flow characteristics of inlets for tilting-nacelle VTOL aircraft [NASA-TP-1205] p0018 W78-21114
 Reduction of fan noise in an anechoic chamber by reducing chamber wall induced inlet flow disturbances [NASA-TN-78854] p0164 W78-22860
 Acoustic evaluation of a novel swept-rotor fan --- noise reduction in turbofan engines [NASA-TN-78878] p0164 W78-24897
 Gas turbine engine with recirculating bleed [NASA-CASE-LEW-12452-1] p0019 W78-25089
 Variation of fan tone steadiness for several inflow conditions [NASA-TN-78886] p0164 W78-26878
 Computer program for calculating two-dimensional potential flow in and about propulsion system inlets [NASA-TN-78930] p0005 W78-27083
 Effect of inlet temperature on the performance of a catalytic reactor --- air pollution control [NASA-TN-78977] p0141 W78-31544

SUBJECT INDEX

INVENTIONS

- Wind tunnel evaluation of IP-12 inlet response to internal airflow disturbances with and without control --- Lewis 10 by 10 ft supersonic wind tunnel tests p0006 N78-32062
- INLETS (DEVICES)**
 U INTAKE SYSTEMS
- ISOBARIC COATINGS**
 U CERAMIC COATINGS
INORGANIC COMPOUNDS
 Inorganic-organic separators for alkaline batteries [NASA-CASE-LRW-12649-1] p0136 N78-25530
- INORGANIC SULFIDES**
 U COPPER SULFIDES
 U BILYBDENON DISULFIDES
 U BILYBDENON SULFIDES
- INSULATION**
 Cloud effects on middle ultraviolet global radiation p0150 A78-42952
 Solar energy meter [NASA-TN-73791] p0131 N78-14630
 Evaluation of models to predict insulation on tilted surfaces [NASA-TN-78842] p0184 N78-25025
 Variation of solar cell sensitivity and solar radiation on tilted surfaces [NASA-TN-78921] p0138 N78-26547
- INSTRUMENT COMPENSATION**
 Development of a drift-correction procedure for a photoelectric spectrometer p0109 A78-23525
- INSTRUMENT DRIFT**
 U DRIFT (INSTRUMENTATION)
- INSTRUMENT PACKAGES**
 Performance of the 12 GHz, 200 watt Transmitter Experiment Package for the Hermes Satellite p0098 A78-24883
- INSULATION**
 U MULTILAYER INSULATION
 U THERMAL INSULATION
- INTAKE SYSTEMS**
 U ENGINE INLETS
 U SUPERSONIC INLETS
 Development and test of an inlet and duct to provide airflow for a wing boundary layer control system [AIAA PAPER 78-141] p0006 A78-20701
 Atmospheric effects on inlets for supersonic cruise aircraft [NASA-TN-X-73647] p0003 N78-10026
 Comparison of the noise characteristics of two low pressure ratio fans with a high throat Mach number inlet [NASA-TN-73880] p0018 N78-21108
 Performance with and without inlet radial distortion of a transonic fan stage designed for reduced loading in the tip region [NASA-TP-1294] p0005 N78-30057
 Design and overall performance of four highly loaded, high speed inlet stages for an advanced high-pressure-ratio core compressor [NASA-TP-1337] p0022 N78-33108
- INTEGRAL EQUATIONS**
 The use of parabolic variations and the direct determination of stress intensity factors using the RIP method --- Boundary Integral Equation p0126 A78-24903
- INTEGRAL TRANSFORMATIONS**
 U FAST FOURIER TRANSFORMATIONS
- INTEGRATED CIRCUITS**
 Solar cell system having alternating current output [NASA-CASE-LRW-12606-1] p0136 N78-25533
- INTEGRAL DIFFERENTIAL EQUATIONS**
 U INTEGRAL EQUATIONS
- INTERFACES**
 U GAS-SOLID INTERFACES
 U LIQUID-SOLID INTERFACES
 U SOLID-SOLID INTERFACES
- INTERFACIAL ENERGY**
 Friction and metal transfer for single-crystal silicon carbide in contact with various metals in vacuum [NASA-TP-11911] p0082 N78-21294
- INTERFACIAL STRAIN**
 U INTERFACIAL TENSION
- INTERFACIAL TENSION**
 Revised international representations for the viscosity of water and steam and new representations for the surface tension of water p0105 A78-13725
 Convection due to surface-tension gradients --- in reduced gravity spacecraft environments p0108 A78-48716
- INTERFEROMETERS**
 Elastohydrodynamic film thickness measurements of artificially produced surface dents and grooves --- using optical interferometry [NASA-TN-78949] p0116 N78-27428
- INTERLAYERS**
 U MULTILAYER INSULATION
 Status of wraparound contact solar cells and arrays [NASA-TN-78911] p0137 N78-26543
- INTERMETALLICS**
 The promise of eutectics for aircraft turbines p0074 A78-24882
- INTERNAL COMBUSTION ENGINES:**
 U DIESEL ENGINES
 U DUCTED FAN ENGINES
 U GAS TURBINE ENGINES
 U J-85 ENGINE
 U JET ENGINES
 U TP-30 ENGINE
 U TURBOPAN ENGINES
 U TURBOJET ENGINES
 U TURBOPROP ENGINES
 U WANKEL ENGINES
 General aviation internal combustion engine research program at NASA-Lewis Research Center [AIAA PAPER 78-932] p0025 A78-43505
 A sustained-arc ignition system for internal combustion engines [NASA-TN-73833] p0096 N78-13331
 State-of-the-art assessment of electric vehicles and hybrid vehicles [NASA-TN-73756] p0179 N78-18988
 Performance of conventionally powered vehicles tested to an electric vehicle test procedure [NASA-TN-73768] p0179 N78-20022
 Supercritical fuel injection system [NASA-CASE-LRW-12490-1] p0020 N78-27122
 Catalytic combustion for the automotive gas turbine engine p0092 N78-30333
- INTERNAL PRESSURE**
 Correlation of combustor acoustic power levels inferred from internal fluctuating pressure measurements [NASA-TN-78986] p0165 N78-31871
- INTERNAL STRESS**
 U RESIDUAL STRESS
- INTERNATIONAL COOPERATION**
 U CTS/Hermes/ - United States experiments and operations summary --- Communications Technology Satellite p0094 A78-24886
- INTERNATIONAL RELATIONS**
 U INTERNATIONAL COOPERATION
- INTERPLANETARY PROPULSION**
 U ROCKET ENGINES
- INTERPLANETARY SPACECRAFT**
 U VIKING LANDER SPACECRAFT
- INTERPLANETARY TRAJECTORIES**
 Helio-centric interplanetary low thrust trajectory optimization program, supplement 1, part 2 [NASA-CR-135418-APP] p0038 N78-25106
- INTERPOLATION**
 Interpolation and extrapolation of creep rupture data by the sinus commitment method. II - Oblique translation p0076 A78-45426
 Interpolation and extrapolation of creep rupture data by the sinus commitment method. I - Focal-point convergence p0076 A78-45427
 Interpolation and extrapolation of creep rupture data by the sinus commitment method. Part 1: Focal-point convergence [NASA-TN-78881] p0125 N78-23471
 Interpolation and extrapolation of creep rupture data by the sinus commitment method. Part 2: Oblique translation [NASA-TN-78882] p0125 N78-23472
 Interpolation and extrapolation of creep rupture data by the sinus commitment method. Part 3: Analysis of antitheats [NASA-TN-78883] p0126 N78-23473
- INVENTIONS**
 Gas path seal

INVERTED CONVERTERS (DC TO AC)

SUBJECT INDEX

(NASA-CASE-LEW-12131-2) p0021 W78-31103
INVERTED CONVERTERS (DC TO AC)
 An inverter/controller subsystem optimized for photovoltaic applications [NASA-TN-78903] p0180 W78-26995
INVERTERS
 Photovoltaic power system tests on an 8-kilowatt single-phase line-commutated inverter [NASA-TN-78824] p0134 W78-19657
INVISCID FLOW
VT STAGNATION FLOW
 A viscous-inviscid interactive compressor calculation [AIAA PAPER 78-1140] p0006 A78-41843
 A viscous-inviscid interactive compressor calculations [NASA-TN-78920] p0005 W78-26100
ION ACCELERATORS
 Sensitivity of 30-cm mercury bombardment ion thruster characteristics to accelerator grid design [AIAA PAPER 78-666] p0050 A78-32747
ION BEAMS
 Optical and electrical properties of ion beam textured Kapton and Teflon p0085 A78-24908
 Ion beam plume and efflux measurements of an 8-cm mercury ion thruster [AIAA PAPER 78-676] p0055 A78-32753
 30-cm mercury ion thruster performance with a 1 kW capacitor-diode voltage multiplier beam supply [AIAA PAPER 78-686] p0051 A78-32760
 Diagnostic evaluations of a beam-shielded 8-cm mercury ion thruster [AIAA PAPER 78-702] p0051 A78-32768
 Mechanical properties on ion-beam-textured surgical implant alloys p0075 A78-36045
 Ion beam sputter etching and deposition of fluoropolymers p0085 A78-37684
 The use of an ion-beam source to alter the surface morphology of biological implant materials p0061 A78-37686
 A hollow cathode hydrogen ion source --- for controlled fusion p0172 A78-39835
 Ion beam plume and efflux characterization flight experiment study --- space shuttle payload [NASA-CR-135275] p0052 W78-12140
 Charge-exchange plasma generated by an ion thruster [NASA-CR-135318] p0052 W78-13123
 Optical and electrical properties of ion beam textured Kapton and Teflon [NASA-TN-73778] p0162 W78-13848
 Mercury ion thruster research, 1977 --- plasma acceleration [NASA-CR-135317] p0052 W78-15167
 Adaptation of ion beam technology to microfabrication of solid state devices and transducers [NASA-CR-135314] p0099 W78-15397
 Effect of surface texture by ion beam sputtering on implant biocompatibility and soft tissue attachment [NASA-CR-135311] p0152 W78-18672
 Industrial ion source technology --- for ion beam etching, surface texturing, and deposition [NASA-CR-135353] p0169 W78-18883
 The use of an ion-beam source to alter the surface morphology of biological implant materials [NASA-TN-78851] p0152 W78-22618
 Ion beam sputter etching and deposition of fluoropolymers [NASA-TN-78888] p0088 W78-24358
 Targets for producing high purity I-123 [NASA-CASE-LEW-10518-3] p0065 W78-27226
 The use of ion beam cleaning to obtain high quality cold welds with minimal deformation [NASA-TN-78933] p0083 W78-27257
 Method of cold welding using ion beam technology [NASA-CASE-LEW-12982-1] p0117 W78-28459
 Ion beam sputtering of fluoropolymers --- etching polymer films and target surfaces [NASA-TN-79000] p0060 W78-33151
ION CHAMBERS
U IONIZATION CHAMBERS
ION CURRENTS
VT ION BEAMS

ION DENSITY (CONCENTRATION)
 Parametric dependence of ion temperature and relative density in the NASA Lewis 500MA facility p0173 A78-37679
 Parametric dependence of ion temperature and relative density in the NASA Lewis 500MA facility --- superconducting magnetic mirror [NASA-TN-73770] p0172 W78-23923
ION EMISSION
 Ion beam plume and efflux characterization flight experiment study --- space shuttle payload [NASA-CR-135275] p0052 W78-12140
ION ENGINES
VT MERCURY ION ENGINES
 Status of SERT II spacecraft and ion thrusters - 1978 [AIAA PAPER 78-662] p0050 A78-32743
 A review of electron bombardment thruster systems/spacecraft field and particle interfaces [AIAA PAPER 78-677] p0051 A78-32754
 Extended-performance thruster technology evaluation [AIAA PAPER 78-666] p0055 A78-37436
 Ion engine auxiliary propulsion applications and integration study [NASA-CR-135312] p0053 W78-15168
 Electric prototype power processor for a 30cm ion thruster [NASA-CR-135287] p0054 W78-19200
 Extended performance electric propulsion power processor design study. Volume 1: Executive summary [NASA-CR-135357] p0054 W78-20250
 A mechanical, thermal and electrical packaging design for a prototype power processor and control system for the 30 cm mercury ion thruster [NASA-TN-78862] p0049 W78-23142
 A 30-cm mercury ion thruster performance with a 1 kW capacitor-diode voltage multiplier beam supply [NASA-TN-78864] p0049 W78-23143
 Sensitivity of 30-cm mercury bombardment ion thruster characteristics to accelerator grid design [NASA-TN-78861] p0049 W78-23144
ION EXCHANGE MEMBRANE ELECTROLYTES
 Anion permselective membrane [NASA-CR-135316] p0144 W78-18515
 Formulated plastic separators for soluble electrode cells [NASA-CASE-LEW-12358-2] p0065 W78-25149
ION EXCHANGE RESINS
 Inorganic-organic separators for alkaline batteries [NASA-CASE-LEW-12649-1] p0136 W78-25530
ION EXTRACTION
 Apparatus for extraction and separation of a preferentially photo-dissociated molecular isotope into positive and negative ions by means of an electric field [NASA-CASE-LEW-12465-1] p0065 W78-25148
ION PROPULSION
 Diagnostic evaluations of a beam-shielded 8-cm mercury ion thruster [AIAA PAPER 78-702] p0051 A78-32768
 Economics of ion propulsion for large space systems [AIAA PAPER 78-698] p0040 A78-37441
 Extended performance solar electric propulsion thrust system study. Volume 1: Executive summary [NASA-CR-135281-VOL-1] p0052 W78-10205
 Ion beam plume and efflux characterization flight experiment study --- space shuttle payload [NASA-CR-135275] p0052 W78-12140
 Mercury ion thruster research, 1977 --- plasma acceleration [NASA-CR-135317] p0052 W78-15167
 Extended performance solar electric propulsion thrust system study. Volume 4: Thruster technology evaluation [NASA-CR-135281-VOL-4] p0053 W78-16090
 Electric prototype power processor for a 30cm ion thruster [NASA-CR-135287] p0054 W78-19200
 Status of SERT II spacecraft and ion thrusters, 1978 [NASA-TN-78827] p0047 W78-20251
 Evolution of the 1-mlb mercury ion thruster subsystem [NASA-TN-73733] p0047 W78-21202
 Planned flight test of a mercury ion auxiliary propulsion system. 1: Objectives, systems descriptions, and mission operations [NASA-TN-78859] p0047 W78-21204

SUBJECT INDEX

JET AIRCRAFT

- Effect of facility background gases on internal erosion of the 30-cm Hg ion thruster
[NASA-TN-73803] p0048 N78-21205
- A review of electron bombardment thruster systems/spacecraft field and particle interfaces
[NASA-TN-78850] p0048 N78-21206
- Diagnostic evaluations of a beam-shielded 8-cm mercury ion thruster
[NASA-TN-78855] p0048 N78-21207
- Closed loop solar array-ion thruster system with power control circuitry
[NASA-CASE-LEW-12780-1] p0048 N78-22149
- A mechanical, thermal and electrical packaging design for a prototype power management and control system for the 30 cm mercury ion thruster
[NASA-TN-78862] p0049 N78-23142
- The 30-cm ion thruster power processor
[NASA-CR-135401] p0054 N78-28280
- Ion propulsion for spacecraft
[NASA-TN-79502] p0056 N78-26172
- ION SOURCES**
- 12-cm magneto-electrostatic containment argon/xenon ion source development
[AIAA PAPER 78-681] p0039 A78-32756
- A hollow cathode hydrogen ion source controlled fusion
p0173 A78-39835
- Industrial ion source technology --- for ion beam etching, surface texturing, and deposition
[NASA-CR-135353] p0169 N78-18883
- ION TEMPERATURE**
- Parametric dependence of ion temperature and relative density in the NASA Lewis SORHA facility
p0173 A78-37679
- Parametric dependence of ion temperature and relative density in the NASA Lewis SORHA facility --- superconducting magnetic mirror
[NASA-TN-73770] p0172 N78-23923
- IONIC PROPELLANTS**
- U ION ENGINES**
- IONIZATION CHAMBERS**
- 5200 cycle of an 8-cm diameter Hg ion thruster
[AIAA PAPER 78-649] p0050 A78-32736
- IONIZATION COUNTERS**
- U IONIZATION CHAMBERS**
- U RADIATION COUNTERS**
- IONIZED GASES**
- NT CHARGED PARTICLES**
- NT COLLISIONLESS PLASMAS**
- NT ELECTRON PLASMA**
- NT LASER PLASMAS**
- NT PLASMA JETS**
- NT PLASMAS (PHYSICS)**
- NT TOROIDAL PLASMAS**
- Apparatus for extraction and separation of a preferentially photo-dissociated molecular isotope into positive and negative ions by means of an electric field
[NASA-CASE-LEW-12465-1] p0065 N78-25148
- IONIZED PLASMAS**
- U PLASMAS (PHYSICS)**
- IONIZING RADIATION**
- NT GAMMA RAYS**
- NT ULTRAVIOLET RADIATION**
- IONOSPHERIC NOISE**
- NT WHISTLERS**
- IONOSPHERICS**
- NT HISS**
- IONS**
- NT ANIONS**
- NT HYDROGEN IONS**
- NT METAL IONS**
- IP (IMPACT PREDICTION)**
- U COMPUTERIZED SIMULATION**
- IRASERS**
- U INFRARED LASERS**
- IRON**
- Friction and wear of selected metals and alloys in sliding contact with AISI 440 C stainless steel in liquid methane and in liquid natural gas
[NASA-TP-1150] p0114 N78-20512
- Effects of thermomechanical processing on strength and toughness of iron - 12-percent-nickel - reactive metal alloys at -196 C
[NASA-TP-1308] p0073 N78-31213
- IRON ALLOYS**
- NT AUSTENITIC STAINLESS STEELS**
- NT CARBON STEELS**
- NT CHROMIUM STEELS**
- NT FERRITIC STAINLESS STEELS**
- NT HARDENING STEELS**
- NT STAINLESS STEELS**
- NT STEELS**
- Cryogenic properties of a new tough-strong iron alloy
p0073 A78-15825
- Tensile and creep properties of the experimental oxide dispersion strengthened iron-base sheet alloy NA-956E at 1365 F
p0074 A78-21858
- Comparison of equivalent energy and energy per unit area /W bar/A/ data with valid fracture toughness data for iron, aluminum, and titanium alloys
p0074 A78-24372
- Development of strong and tough cryogenic Fe-12Ni alloys containing reactive metal additions
p0076 A78-41465
- Tantalum modified ferritic iron base alloys
[NASA-CASE-LEW-12095-1] p0069 N78-18182
- The effect of minor additions of titanium on the fracture toughness of Fe-12Ni alloys at 77K
[NASA-CR-135351] p0078 N78-19259
- The design of an Fe-12Ni-0.2Ti alloy steel for low temperature use
[NASA-CR-135310] p0078 N78-20310
- High toughness-high strength iron alloy
[NASA-CASE-LEW-12542-2] p0070 N78-22205
- IRON COMPOUNDS**
- NT CHROMITES**
- NT FERRITES**
- IRON OXIDES**
- NT CHROMITES**
- IRROTATIONAL FLOW**
- U POTENTIAL FLOW**
- ISING MODEL**
- U FERROMAGNETISM**
- U MATHEMATICAL MODELS**
- ISOTHERMS**
- Metastable states of small rare gas crystallites
p0169 A78-16069
- ISOSTATIC PRESSURE**
- Manufacture of astroloy turbine disk shapes by hot isostatic pressing, volume 1
[NASA-CR-135409] p0079 N78-25166
- ISOTHERMAL PROCESSES**
- Effect of geometry on hydrodynamic film thickness
[NASA-TP-1287] p0117 N78-30585
- ISOTHERMS**
- Interpolation and extrapolation of creep rupture data by the minimum commitment method. II - Oblique translation
p0076 A78-45426
- ISOTOPES**
- NT CESIUM VAPOR**
- NT TELLURIUM**
- Preliminary design study of an alternate heat source assembly for a Brayton isotope power system
[NASA-CR-135428] p0145 N78-28608
- ITERATION**
- NT ITERATIVE SOLUTION**
- ITERATIVE SOLUTION**
- A viscous-inviscid interactive compressor calculations
[NASA-TN-78920] p0005 N78-26100
- J**
- J-85 ENGINE**
- Blade row dynamic digital compression program. Volume 2: J85 circumferential distortion redistribution model, effect of Stator characteristics, and stage characteristics sensitivity study
[NASA-CR-134953] p0032 N78-33103
- JEEPS**
- U AUTOMOBILES**
- JET AIRCRAFT**
- NT B-57 AIRCRAFT**
- NT BOEING 747 AIRCRAFT**
- NT F-15 AIRCRAFT**
- NT F-100 AIRCRAFT**
- NT F-102 AIRCRAFT**
- NT TURBOPAN AIRCRAFT**
- NT TURBOPROP AIRCRAFT**
- Jet aircraft hydrocarbon fuels technology
[NASA-CP-2033] p0088 N78-19325

JET AIRCRAFT NOISE

SUBJECT INDEX

- Lean combustion limits of a confined premixed-prevaporized propane jet [NASA-TN-78868] p0019 N78-22099
- JET AIRCRAFT NOISE**
State-of-the-art of turbofan engine noise control p0024 A78-35658
- On the use of relative velocity exponents for jet engine exhaust noise p0024 A78-37683
- Acoustic evaluation of a novel swept-rotor fan [AIAA PAPER 78-1121] p0166 A78-41831
- Calculation of far-field jet noise spectra from near-field measurements using true source location [AIAA PAPER 78-1153] p0168 A78-41852
- Effect of forward motion on engine noise [NASA-CR-134954] p0026 N78-10093
- Flight-effects on predicted fan fly-by noise [NASA-TN-73798] p0014 N78-13060
- An empirical model for inverted-velocity-profile jet noise prediction [NASA-TN-73838] p0014 N78-13061
- A parametric investigation of an existing supersonic relative tip speed propeller noise model --- turboprop aircraft [NASA-TN-73816] p0163 N78-13854
- Analytical modeling of under-the-wing externally blown flap powered-lift noise p0004 N78-24063
- On the use of relative velocity exponents for jet engine exhaust noise [NASA-TN-78873] p0011 N78-24137
- Propulsion systems noise technology p0001 N78-27056
- Acoustic tests of duct-burning turbofan jet noise simulation [NASA-CR-2966] p0002 N78-28043
- Acoustic tests of duct-burning turbofan jet noise simulation: Comprehensive data report. Volume 1, section 2: Full size data [NASA-CR-135239-VOL-1-SECT-2] p0030 N78-28095
- Acoustic tests of duct-burning turbofan jet noise simulation: Comprehensive data report. Volume 1, section 3: Data plots [NASA-CR-135239-VOL-1-SECT-3] p0030 N78-28096
- Acoustic tests of duct-burning turbofan jet noise simulation: Comprehensive data report. Volume 2: Model design and aerodynamic test results [NASA-CR-135239-VOL-2] p0031 N78-28097
- Flight effects on the aerodynamic and acoustic characteristics of inverted profile conannular nozzles, volume 1 --- supersonic cruise aircraft research wind tunnel tests [NASA-CR-135189-VOL-1] p0167 N78-29867
- Flight effects on the aerodynamic and acoustic characteristics of inverted profile conannular nozzles, volume 2 --- supersonic cruise aircraft research wind tunnel tests [NASA-CR-135189-VOL-2] p0167 N78-29868
- Flight effects on the aerodynamic and acoustic characteristics of inverted profile conannular nozzles, volume 3 --- supersonic cruise aircraft research wind tunnel tests [NASA-CR-135189-VOL-3] p0167 N78-29869
- JET AUGMENTED WING FLAPS**
U WING FLAPS
- JET DAMPING**
U DAMPING
- JET DRIVE**
U JET PROPULSION
- JET ENGINE FUELS**
Hydrocarbon group type determination in jet fuels by high performance liquid chromatography p0089 A78-24906
- Jet fuels from synthetic crudes p0090 A78-43415
- Fuel consumption improvement in current transport engines [AIAA PAPER 78-930] p0033 A78-45097
- Hydrocarbon group type determination in jet fuels by high performance liquid chromatography [NASA-TN-73829] p0088 N78-13233
- Jet aircraft hydrocarbon fuels technology [NASA-CR-2033] p0088 N78-19325
- Computer model for refinery operations with emphasis on jet fuel production. Volume 2: Data and technical bases [NASA-CR-135334] p0090 A78-19326
- Computer model for refinery operations with emphasis on jet fuel production. Volume 1: Program description [NASA-CR-135333] p0090 N78-20350
- Computer model for refinery operations with emphasis on jet fuel production. Volume 3: Detailed systems and programming documentation [NASA-CR-135335] p0090 N78-25235
- Impact of broad-specification fuels on future jet aircraft --- engine components and performance p0089 N78-27059
- JET ENGINES**
WT DOCTED FAN ENGINES
WT J-85 ENGINE
WT TP-30 ENGINE
WT TURBOFAN ENGINES
WT TURBOJET ENGINES
WT TURBOPROP ENGINES
- Sound separation probes for flowing duct noise measurements --- jet engine diagnostics p0033 A78-17396
- Reliability analysis of forty-five strain-gage systems mounted on the first fan stage of a TP-100 engine [NASA-TN-73724] p0109 N78-13407
- Composite hub/metal blade compressor rotor [NASA-CR-135343] p0062 N78-18131
- JT9D engine diagnostics. Task 2: Feasibility study of measuring in-service flight loads --- 747 aircraft performance [NASA-CR-135395] p0030 N78-27124
- JET EXHAUST**
On the use of relative velocity exponents for jet engine exhaust noise p0024 A78-37683
- On the use of relative velocity exponents for jet engine exhaust noise [NASA-TN-78873] p0011 N78-24137
- Gas turbine engine with recirculating bleed [NASA-CASE-LRW-12452-1] p0019 N78-25089
- JET FLAMES**
U FLAMES
U JET FLOW
JET FLIGHT
U JET AIRCRAFT
JET FLOW
Study of lubricant jet flow phenomena in spur gears - Out of mesh condition [ASME PAPER 77-DET-104] p0118 A78-20608
- An empirical model for inverted-velocity-profile jet noise prediction p0023 A78-24879
- Sound production in a moving stream p0165 A78-31224
- Flow of liquid jets through closely woven screens p0108 A78-42877
- An empirical model for inverted-velocity-profile jet noise prediction [NASA-TN-73838] p0014 N78-13061
- JET FUELS**
U JET ENGINE FUELS
- JET IMPINGEMENT**
Study of lubricant jet flow phenomena in spur gears - Out of mesh condition [ASME PAPER 77-DET-104] p0118 A78-20608
- A computer program for the transient thermal analysis of an impingement cooled turbine blade [AIAA PAPER 78-92] p0106 A78-20682
- Liquid jet impingement normal to a disk in zero gravity [ASME PAPER 78-SA/FE-1] p0107 A78-41154
- Flow of liquid jets through closely woven screens p0108 A78-42877
- JET NOISE**
U JET AIRCRAFT NOISE
- JET PROPULSION**
A review of NASA's propulsion programs for aviation [NASA-TN-73831] p0016 N78-16055
- JOINTS (JUNCTIONS)**
WT METAL JOINTS
- JOURNAL BEARINGS**
Hydrodynamic air lubricated compliant surface bearing for an automotive gas turbine engine. 1: Journal bearing performance [NASA-CR-135368] p0121 N78-21472
- Hydrodynamic air lubricated compliant surface bearing for an automotive gas turbine engine. 2: Materials and coatings [NASA-CR-135402] p0122 N78-29449
- JOURNALS (SHAFTS)**
U SHAFTS (MACHINE ELEMENTS)

SUBJECT INDEX

LATTICE IMPERFECTIONS

K

KALMAN FILTERS
Failure detection and correction for turbofan engines
p0033 A78-23910

KAPTON (TRADEMARK)
Optical and electrical properties of ion beam textured Kapton and Teflon
p0085 A78-24908

Optical and electrical properties of ion beam textured Kapton and Teflon
[NASA-TN-73778]
p0162 W78-13848

KINETIC FRICTION
NT SLIDING FRICTION

KINETIC THEORY
NT TRANSPORT THEORY

KINETICS
NT REACTION KINETICS

KIRCHHOFF-HELMHOLTZ FLOW
U PIPE FLOW

KIRCHHOFF-HUYGENS PRINCIPLE
U WAVE PROPAGATION

KLYSTRONS
A possible pole problem in the formula for klystron gap fields
p0098 A78-18287

KU BAND
U SUPERHIGH FREQUENCIES

L

LABORATORIES
NT ENGINE TESTING LABORATORIES

LAG (DELAY)
U TIME LAG

LAKE ERIE
Numerical computation of three-dimensional circulation in Lake Erie - A comparison of a free-surface model and a rigid-lid model
p0151 A78-47223

LAKES
NT LAKE ERIE

LAMINA
U LAYERS

LAMINAR FLAMES
U FLAMES

LAMINAR FLOW CONTROL
U BOUNDARY LAYER CONTROL

LAMINAR JETS
U JET FLOW

LAMINATED MATERIALS
U LAMINATES

LAMINATES
NT PLYWOOD

Lamination residual strains and stresses in hybrid laminates
p0128 A78-12071

Evaluation of flawed composite structure under static and cyclic loading
p0063 A78-26683

Residual stresses in angleplied laminates and their effects on laminate behavior
p0060 A78-33201

Effect of preload on the fatigue and static strength of composite laminates with defects
p0061 A78-40310

Impact of composite mechanics on test methods for fiber composites
p0062 A78-50325

Analysis of delamination in unidirectional and crossplied fiber composites containing surface cracks
[NASA-CR-135248]
p0062 W78-11197

Effect of discontinuities as a means to alleviate thermal expansion mismatch damage in laminar composites
[NASA-TN-73739]
p0057 W78-13136

Impact on multilayered composite plates
[NASA-CR-135247]
p0062 W78-16103

Residual stresses in angleplied laminates and their effects on laminate behavior
[NASA-TN-78835]
p0058 W78-19206

In situ ply strength: An initial assessment --- using laminate fracture data and a least squares method
[NASA-TN-73771]
p0059 W78-21220

Titanium/beryllium laminates: Fabrication, mechanical properties, and potential aerospace applications
[NASA-TN-73891]
p0059 W78-21221

Method for alleviating thermal stress damage in laminates
[NASA-CASE-LEW-12493-1]
p0059 W78-22163

Effects of moisture profiles and laminate configuration on the hygro stresses in advanced composites --- graphite-epoxy composites
[NASA-TN-78976]
p0059 W78-32191

LAMINATIONS
U LAMINATES

LANGUAGES
NT FORTRAN
NT PROGRAMMING LANGUAGES

LANTHANUM ALLOYS
Spacecraft charging control by thermal, field emission with lanthanum-hexaboride emitters
[NASA-TN-78990]
p0183 W78-32018

LANTHANUM COMPOUNDS
Volatile products from the interaction of KCl(g) with Cr2O3 and LaCrO3 in oxidizing environments --- gas turbine engines
p0066 A78-24887

Volatile products from the interaction of KCl(g) with Cr2O3 and LaCrO3 in oxidizing environments
[NASA-TN-73795]
p0068 W78-13158

Disinide thermal energy conversion with lanthanum-hexaboride electrodes
[NASA-TN-78887]
p0135 W78-24617

Cesium thermionic converters having improved electrodes
[NASA-CASE-LEW-12038-3]
p0137 W78-25555

LARGE SPACE STRUCTURES
Interaction of large, high power systems with operational orbit charged particle environments --- large solar arrays in space
[NAS 77-243]
p0044 A78-36719

Economics of ion propulsion for large space systems
[AIAA PAPER 78-698]
p0040 A78-37441

LASER APPLICATIONS
Review of experimental work on transonic flow in turbomachinery
p0006 A78-12312

A review of the Thermoelectronic Laser Energy Converter /TELEC/ Program at Lewis Research Center
p0142 A78-33217

A review of the thermoelectronic laser energy converter (TELEC) program at Lewis Research Center
[NASA-TN-73886]
p0111 W78-21941

Apparatus for extraction and separation of a preferentially photo-dissociated molecular isotope into positive and negative ions by means of an electric field
[NASA-CASE-LEW-12465-1]
p0065 W78-25148

Closed cycle electric discharge laser design investigation
[NASA-CR-135408]
p0112 W78-25407

LASER DRILLING
In-situ laser retorting of oil shale
[NASA-CASE-LEW-12217-1]
p0129 W78-14452

LASER HEATING
Analytical study of laser-supported combustion waves in hydrogen
[AIAA PAPER 78-1219]
p0067 A78-41901

LASER OUTPUTS
Distribution of E/N and W/e in a cross-flow electric discharge laser --- electric field to neutral gas density and electron number density
p0111 A78-24896

LASER PLASMAS
Preliminary results on the conversion of laser energy into electricity
p0173 A78-34631

LASERS
NT CARBON DIOXIDE LASERS
NT GASDYNAMIC LASERS
NT INFRARED LASERS

Analysis and design of a high power laser adaptive phased array transmitter
[NASA-CR-134952]
p0111 W78-13470

Excimer lasers
[NASA-CR-155949]
p0112 W78-19480

Considerations to achieve directionality for gamma ray lasers
p0116 W78-26870

LATTICE IMPERFECTIONS
U CRYSTAL DEFECTS

LAUNCH VEHICLES

SUBJECT INDEX

LAUNCH VEHICLES
NT CERTAIN LAUNCH VEHICLE
LAUNCHING
NT POCKET LAUNCHING
LAWS
NT CLOSURE LAW
NT SCALING LAWS
LAYERS
 Atomic hydrogen storage method and apparatus
 [NASA-CASE-LEW-12061-1] p0089 W78-24365
LEAD ACID BATTERIES
 Rapid, efficient charging of lead-acid and
 nickel-zinc traction cells
 [NASA-TN-78901] p0135 W78-24616
 Response of lead-acid batteries to
 chopper-controlled discharge
 [NASA-TN-73834-REV] p0180 W78-25010
LEAD COMPOUNDS
 Critical currents in sputtered PbMo6S8
 p0175 A78-45368
LEADING EDGES
 Experimental determination of transient strain in
 a thermally-cycled simulated turbine blade
 utilizing a non-contact technique
 [NASA-TN-73886] p0017 W78-19161
LEAKAGE
 Liquid rocket engine turbopump rotating-shaft seals
 [NASA-SP-8121] p0117 W78-30584
LEAST SQUARES METHOD
 In situ ply strength: An initial assessment ---
 using laminate fracture data and a least squares
 method
 [NASA-TN-73771] p0059 W78-21220
LEIDENFROST PHENOMENON
 Thermally driven oscillations and wave motion of a
 liquid drop
 p0106 A78-17508
LIFE (DURABILITY)
NT FATIGUE LIFE
NT SERVICE LIFE
 Effect of facility background gases on internal
 erosion of the 30-cs Hg ion thruster
 [AIAA PAPER 78-665] p0050 A78-32745
 Strain-rate partitioning behavior of the
 nickel-base superalloys, Rene 80 and 100
 p0075 A78-33214
 Real-time and accelerated outdoor endurance
 testing of solar cells
 [NASA-TN-73783] p0130 W78-14628
 Investigation of the effect of ceramic coatings on
 rocket thrust chamber life
 [NASA-TN-78892] p0049 W78-26173
 Filtration effects on ball bearing life and
 condition in a contaminated lubricant
 [NASA-TN-78907] p0116 W78-26446
 The practical impact of elastohydrodynamic
 lubrication
 [NASA-TN-78987] p0117 W78-33445
LIFETIME (DURABILITY)
U LIFE (DURABILITY)
LIFT AUGMENTATION
 Noise of deflectors used for flow attachment with
 STOL-OTW configurations
 p0023 A78-24877
 Effects of nozzle design and power on cruise drag
 for upper-surface-blowing aircraft
 p0004 W78-24058
 Analytical modeling of under-the-wing externally
 blown flap powered-lift noise
 p0004 W78-24063
 Overview of the QCSEE program
 p0004 W78-24066
 Acoustic design of the QCSEE propulsion systems
 p0004 W78-24067
 Inlet technology for powered-lift aircraft
 p0005 W78-24069
 Reverse-thrust technology for variable-pitch fan
 propulsion systems
 p0005 W78-24070
LIFT FANS
 Cold-air performance of a tip turbine designed to
 drive a lift fan
 [NASA-TP-1126] p0003 W78-14998
 Cold-air performance of a tip turbine designed to
 drive a lift fan. 3: Effect of simulated fan
 leakage on turbine performance
 [NASA-TP-1105] p0003 W78-16001
LIFTING SURFACES
U SURFACES

LIGHT (VISIBLE RADIATION)
NT SUNLIGHT
LIGHT AIRCRAFT
 Cost/benefit analysis of advanced material
 technologies for small aircraft turbine engines
 [NASA-CN-135265] p0027 W78-12083
LIGHT ALLOYS
NT ALUMINUM ALLOYS
LIGHT TRANSMISSION
 Optical and electrical properties of ion beam
 textured Kapton and Teflon
 p0085 A78-24908
LIGHTING
 Lightning protection of aircraft
 [NASA-EP-1008] p0009 W78-11024
LINEAR FILTERS
NT KALMAN FILTERS
LINEAR SYSTEMS
 Optical controls for an advanced turbofan engine
 p0033 A78-23693
LINERS
U LININGS
LININGS
 Optimum wall impedance for spinning modes - A
 correlation with mode cut-off ratio
 [AIAA PAPER 78-193] p0165 A78-20735
 Design and preliminary results of a
 semitranspiration cooled /Lamilly/ liner for a
 high-pressure high-temperature combustor
 [AIAA PAPER 78-957] p0025 A78-43544
 Some load limits and self-lubricating properties
 of plain spherical bearings with molded graphite
 fiber reinforced polyimide liners to 320 C
 [NASA-TN-78935] p0116 W78-26445
 Graphite-fiber-reinforced polyimide liners of
 various compositions in plain spherical bearings
 [NASA-TN-78908] p0116 W78-26447
LIQUEFACTION
NT COAL LIQUEFACTION
LIQUEFIED GASES
NT LIQUID BROW
NT LIQUID NITROGEN
NT LIQUID OXYGEN
LIQUID ATOMIZATION
 Effect of airstream velocity on mean drop
 diameters of water sprays produced by pressure
 and air atomizing nozzles
 [NASA-TN-73740] p0101 W78-13369
LIQUID CHROMATOGRAPHY
 Hydrocarbon group type determination in jet fuels
 by high performance liquid chromatography
 p0089 A78-24906
 Hydrocarbon group type determination in jet fuels
 by high performance liquid chromatography
 [NASA-TN-73829] p0088 W78-13233
LIQUID COOLING
NT FILM COOLING
 Effect of coolant flow ejection on aerodynamic
 performance of low-aspect-ratio vanes. 2:
 Performance with coolant flow ejection at
 temperature ratios up to 2
 [NASA-TP-1057] p0003 W78-11008
 Closed loop spray cooling apparatus --- for
 particle accelerator targets
 [NASA-CASE-LEW-11981-1] p0091 W78-17237
 Liquid-cooling technology for gas turbines review
 and status
 [NASA-TN-78906] p0020 W78-26145
LIQUID DROPS
U DROPS (LIQUIDS)
LIQUID LITHIUM
 Lithium and potassium heat pipes for thermionic
 converters
 [NASA-TN-78946] p0104 W78-26390
LIQUID MERCURY
U MERCURY (METAL)
LIQUID METALS
NT LIQUID LITHIUM
NT LIQUID POTASSIUM
NT MERCURY (METAL)
NT MERCURY VAPOR
 Shape of two-dimensional solidification interface
 during directional solidification by continuous
 casting
 p0119 A78-31829
 Liquid metal slip ring
 [NASA-CASE-LEW-12277-2] p0097 W78-25323
LIQUID NEON
 Boiling incipience and convective boiling of neon

SUBJECT INDEX

LUBRICANTS

- and nitrogen
 Design and prototype fabrication of a 30 tesla cryogenic magnet p0105 A78-15820
 p0097 A78-15823
- LIQUID NITROGEN**
 Boiling incipience and convective boiling of neon and nitrogen p0105 A78-15820
 Effect of ice contamination on liquid-nitrogen drops in film boiling p0105 A78-15821
 Simulation of the heat transfer characteristics of LOX [ASME PAPER 77-HT-9] p0089 A78-17482
- LIQUID OXYGEN**
 Simulation of the heat transfer characteristics of LOX [ASME PAPER 77-HT-9] p0089 A78-17482
- LIQUID POTASSIUM**
 Lithium and potassium heat pipes for thermionic converters [NASA-TN-78946] p0104 A78-26390
- LIQUID PROPELLANT ROCKET ENGINES**
WT HYDROGEN OXYGEN ENGINES
 Liquid rocket lines, bellows, flexible hoses, and filters [NASA-SP-8123] p0047 A78-16089
 Liquid rocket engine self-cooled combustion chambers [NASA-SP-8124] p0048 A78-21211
 Investigation of the burning configuration of a coaxial injector in a combustion chamber [NASA-CR-135383] p0054 A78-22148
 Preburner of staged combustion rocket engine [NASA-CR-135356] p0054 A78-24279
 Liquid rocket engine axial-flow turbopumps [NASA-SP-8125] p0050 A78-31164
- LIQUID ROCKET PROPELLANTS**
 Ion engine auxiliary propulsion applications and integration study [NASA-CR-135312] p0053 A78-15168
 Liquid propellant reorientation in a low-gravity environment [NASA-TN-78969] p0105 A78-29407
- LIQUID SLOSHING**
 Constrained sloshing of liquid mercury in a flexible spherical tank [AIAA PAPER 78-670] p0104 A78-32749
 Constrained sloshing of liquid mercury in a flexible spherical tank [NASA-TN-78833] p0103 A78-21403
- LIQUID-GAS MIXTURES**
WT AEROSOLS
LIQUID-SOLID INTERFACES
 Shape of two-dimensional solidification interface during directional solidification by continuous casting p0119 A78-31829
 Flow of liquid jet through closely woven screens p0108 A78-42877
- LIQUIDS**
 WT CRYOGENIC FLUIDS
 WT LIQUID LITHIUM
 WT LIQUID METALS
 WT LIQUID NEON
 WT LIQUID NITROGEN
 WT LIQUID OXYGEN
 WT LIQUID POTASSIUM
 WT LIQUID ROCKET PROPELLANTS
 WT MERCURY (METAL)
 WT MERCURY VAPOR
- LITHIUM**
 WT LIQUID LITHIUM
- LOAD TESTS**
 Experimental and analytical load-life relation for AISI 9310 steel spur gears [ASME PAPER 77-DET-121] p0118 A78-20609
 Load-displacement measurement and work determination in three-point bend tests of notched or precracked specimens p0089 A78-24370
 Displacement coefficients along the inner boundaries of radially cracked ring segments subject to forces and couples p0127 A78-35396
 Acoustic emission testing of composite vessels under sustained loading [NASA-TN-789811] p0051 A78-33150
- LOADS (FORCES)**
 WT AERODYNAMIC LOADS
 WT COMPRESSION LOADS
 WT CRITICAL LOADING
 WT CYCLIC LOADS
 WT DYNAMIC LOADS
 WT GUST LOADS
 WT IMPACT LOADS
 WT ROLLING CONTACT LOADS
 WT STATIC LOADS
 WT VIBRATORY LOADS
- LOCALIZATION**
 U POSITION (LOCATION)
LOCATION
 U POSITION (LOCATION)
LONG TERM EFFECTS
 Long-term CP6 engine performance deterioration: Evaluation of engine S/N 451-380 [NASA-CR-159390] p0031 A78-29103
 Long-term hot-hardness characteristics of five through-hardened bearing steels [NASA-TP-1341] p0073 A78-33196
- LOS ALAMOS TURBINE REACTOR**
U HIGH TEMPERATURE NUCLEAR REACTORS
- LOW ASPECT RATIO**
 Evaluation of a low aspect ratio small axial compressor stage, volume 1 [NASA-CR-135240] p0026 A78-12081
 Evaluation of a low aspect ratio small axial compressor stage, volume 2 [NASA-CR-135241] p0026 A78-12082
- LOW COST**
 Low cost satellite land mobile service for nationwide applications p0095 A78-43173
 Summary of the NASA space photovoltaic research and technology program p0130 A78-13528
 Wind turbine generator rotor blade concepts with low cost potential [NASA-TN-73835] p0131 A78-17466
- LOW FREQUENCIES**
 WT VERY LOW FREQUENCIES
- LOW FREQUENCY BASES**
 WT VERY LOW FREQUENCIES
- LOW GRAVITY**
 U REDUCED GRAVITY
- LOW PRESSURE CHAMBERS**
 U VACUUM CHAMBERS
- LOW TEMPERATURE**
 The influence of composition, annealing treatment, and texture on the fracture toughness of Ti-5Al-2.5Sn plate at cryogenic temperatures [NASA-TN-73872] p0069 A78-15235
 Effects of hydrothermal exposure on a low-temperature cured epoxy [NASA-TN-73841] p0081 A78-17220
 High toughness-high strength iron alloy [NASA-CR-158-12542-2] p0070 A78-22205
- LOW THRUST PROPULSION**
 WT ION PROPULSION
 WT SOLAR ELECTRIC PROPULSION
- LOWER ATMOSPHERE**
 WT TROPOSPHERE
- LOX (OXYGEN)**
 U LIQUID OXYGEN
- LOX-HYDROGEN ENGINES**
 U HYDROGEN OXYGEN ENGINES
- LUBRICANT TESTS**
 Study of lubricant jet flow phenomena in spur gears - Out of mesh condition [ASME PAPER 77-DET-104] p0118 A78-20608
 Lubrication of high-speed, large bore tapered-roller bearings [ASME PAPER 77-LUB-13] p0118 A78-23354
 Traction and lubricant film temperature as related to the glass transition temperature and solidification --- using infrared spectroscopy on EHD contacts p0087 A78-40997
- LUBRICANTS**
 WT LUBRICATING OILS
 WT SOLID LUBRICANTS
 Effect of thermal exposure on lubricating properties of polyimide films and polyimide-bonded graphite fluoride films [NASA-TP-1125] p0080 A78-15277
 Elastohydrodynamic lubrication of elliptical contacts for materials of low elastic modulus.

LUBRICATING OILS

2: Starved conjunction
[NASA-TP-1273] p0117 W78-28458
Study of dynamic emission spectra from lubricant
films in an elastohydrodynamic contact using
Fourier transform spectroscopy
[NASA-CR-759418] p0162 W78-32809

LUBRICATING OILS
Study of lubricant jet flow phenomena in spur
gears - Out of mesh condition
[ASME PAPER 77-DET-104] p0118 W78-20608
Steady-state unbalance response of a three-disk
flexible rotor on flexible, damped supports
p0119 W78-29326

Oil-air mist lubrication for helicopter gearing
[NASA-CR-135081] p0010 W78-25080

LUBRICATION
Elastohydrodynamic lubrication of elliptical
contacts for materials of low elastic modulus. I
- Fully flooded conjunction
[ASME PAPER 77-LUB-10] p0119 W78-28414
Design considerations in mechanical face seals for
improved performance. I - Basic configurations
[ASME PAPER 77-WA/LUB-3] p0119 W78-33183
Design considerations in mechanical face seals for
improved performance. II - Lubrication
[ASME PAPER 77-WA/LUB-4] p0120 W78-33184
Bearing, gearing, and lubrication technology
[SAE PAPER 780077] p0120 W78-33366
Additional aspects of elastohydrodynamic lubrication
p0120 W78-45430
Definition and effect of chemical properties of
surfaces in friction, wear, and lubrication
p0121 W78-45436
Bearing, gearing, and lubrication technology
[NASA-TN-73851] p0114 W78-17389
Statistical model for asperity-contact time
fraction in elastohydrodynamic lubrication
[NASA-TP-1130] p0114 W78-18429
Definition and effect of chemical properties of
surfaces in friction, wear, and lubrication
[NASA-TN-73806] p0065 W78-19237
Principles of PSCA and application to metal
corrosion, coating and lubrication
[NASA-TN-78839] p0070 W78-19262
Lubrication and failure mechanisms of graphite
fluoride films
[NASA-TP-1197] p0081 W78-20337
Oil-air mist lubrication for helicopter gearing
[NASA-CR-135081] p0010 W78-25080
Application of ESCA to the determination of
stoichiometry in sputtered coatings and
interface regions
[NASA-TN-78896] p0065 W78-26185
Additional aspects of elastohydrodynamic lubrication
[NASA-TN-78898] p0115 W78-26443
Emergency and microfog lubrication and cooling of
bearings for Army helicopters
[NASA-TN-135195] p0122 W78-27429
The practical impact of elastohydrodynamic
lubrication
[NASA-TN-78947] p0117 W78-33445
Minimum film thickness in elliptical contacts for
different regimes of fluid-film lubrication
[NASA-TP-1342] p0117 W78-33447

LUBRICATION SYSTEMS
Oil cooling system for a gas turbine engine
[NASA-CASP-LPW-12321-1] p0113 W78-10467
Predicted and experimental performance of
jet-lubricated 120-millimeter-bore ball bearings
operating to 2.5 million DN
[NASA-TP-1196] p0114 W78-20513
A comparison of the lubricating mechanisms of
graphite fluoride and molybdenum disulfide films
[NASA-TN-73897] p0083 W78-26215

LOSER BANDS
O PLASTIC DEFORMATION

M

MACH NUMBER
Simulated flight effects on noise characteristics
of a fan inlet with high throat Mach number
[NASA-TP-1199] p0017 W78-20132

MACHINE LIFE
O SERVICE LIFE

MACHINING
M MILLING (MACHINING)

MAGNESIUM
Adhesion of a bimetallic interface --- for Al, Mg,
and Zn

SUBJECT INDEX

and Zn
[NASA-TN-78890] p0071 W78-29214

MAGNETIC COMPOUNDS
M MAGNETIC OXIDES
M MAGNETIC OXIDES
Influence of adsorbed fluids on the rolling
contact deformation of HgO single crystals
p0123 W78-23447

MAGNET COILS
Design and prototype fabrication of a 30 tesla
cryogenic magnet
p0097 W78-15823

MAGNETIC COILS
Potential damage to dc superconducting magnets due
to high frequency electromagnetic waves
p0098 W78-39902

MAGNETIC DISTURBANCES
M MAGNETIC STORMS
M MAGNETIC EFFECTS
12-cs magnetoelectrostatic containment
argon/xenon ion source development
[AIAA PAPER 78-66'] p0039 W78-32756

MAGNETIC FIELD CONFIGURATIONS
Lower hybrid emission diagnostics on the NASA
Levis Bumpy Torus
p0173 W78-29332

MAGNETIC FIELDS
M GEOMAGNETISM
M TRAPPED MAGNETIC FIELDS
A model for particle confinement in a toroidal
plasma subject to strong radial electric fields
p0173 W78-24891
Upper critical field of copper molybdenum sulfide
p0175 W78-53626
Lightning protection of aircraft
[NASA-RC-1008] p0009 W78-11028
Magnetic heat pumping
[NASA-CASE-LEW-12508-1] p0102 W78-17335
Atomic hydrogen storage method and apparatus ---
cryotrapping and magnetic field strength
[NASA-CASE-LEW-12081-2] p0169 W78-19907

MAGNETIC MATERIALS
M FERROMAGNETIC MATERIALS
M MAGNETIC MEMORIES
M MAGNETIC STORAGE
M MAGNETIC BEHALS
M METALS

MAGNETIC SERRORS
Parametric dependence of ion temperature and
relative density in the NASA Lewis SORNA facility
p0173 W78-37679
Alternative approaches to plasma confinement
p0174 W78-52146
Parametric dependence of ion temperature and
relative density in the NASA Lewis SORNA facility
--- superconducting magnetic mirror
[NASA-TN-73770] p0172 W78-23923

MAGNETIC PERMEABILITY
Crystal field and magnetic properties of FeR3
p0175 W78-24907

MAGNETIC PROPERTIES
M FERROMAGNETISM
M GEOMAGNETISM
M MAGNETIC EFFECTS
M MAGNETIC PERMEABILITY
M MAGNETORESISTIVITY
Crystal field and magnetic properties
[NASA-TN-73837] p0175 W78-13916

MAGNETIC STORAGE
Atomic hydrogen storage method and apparatus
[NASA-CASE-LEW-12081-1] p0099 W78-24365

MAGNETIC STORMS
Summary of the CTS Transient Event Counter data
after one year of operation --- Communication
Technology Satellite
p0046 W78-19564

NASA Charging Analyzer Program - A computer tool
that can evaluate electrostatic contamination
--- of spacecraft during geomagnetic substorm
p0044 W78-34220

The Lewis Research Center geomagnetic substorm
simulation facility
p0036 W78-10154

Testing of typical spacecraft materials in a
simulated substorm environment
p0036 W78-10154

NASA charging analyzer program: A computer tool
that can evaluate electrostatic contamination
[NASA-TN-73889] p0096 W78-21372

SUBJECT INDEX

MATRICES (MATHEMATICS)

- MAGNETIC SUBSTANCES**
MAGNETIC STORES
MAGNETIZATION
 Crystal field and magnetic properties of ErH₃
 p0175 A78-24907
- MAGNETIC ACTIVITY**
NT MAGNETORESISTIVITY
MAGNETOHYDRODYNAMIC ACCELERATION
U PLASMA ACCELERATION
MAGNETOHYDRODYNAMIC FLOW
 Velocity, temperature, and electrical conductivity profiles in hydrogen-oxygen MHD duct flows
 [NASA-TN-78968] p0104 A78-28372
- MAGNETOHYDRODYNAMIC GENERATORS**
 Design and calculated performance and cost of the ECAS Phase II open cycle MHD power generation system
 [ASME PAPER 77-WA/ENERG-5] p0174 A78-33143
 Performance and economics of advanced energy conversion systems for coal and coal-derived fuels
 p0186 A78-34078
- MAGNETOHYDRODYNAMIC STABILITY**
 Experiments on whistler wave filamentation and VLF hiss in a laboratory plasma
 p0149 A78-41788
 A fluctuation-induced plasma transport diagnostic based upon fast-Fourier transform spectral analysis
 [NASA-TN-78932] p0172 A78-26926
 Fluctuation spectra in the NASA Lewis bumpy-torus plasma
 [NASA-TP-1257] p0172 A78-26927
- MAGNETOIONIC PLASMA**
U PLASMAS (PHYSICS)
MAGNETOPLASMAS
U PLASMAS (PHYSICS)
MAGNETORESISTIVITY
 Upper limit for magnetoresistance in silicon bronze and phosphor bronze wire
 p0175 A78-14423
- MAGNETS**
NT CRYOGENIC MAGNETS
NT HIGH FIELD MAGNETS
NT SUPERCONDUCTING MAGNETS
MAN MACHINE SYSTEMS
 A viscous-inviscid interactive compressor calculation
 [AT PAPER 78-1140] p0006 A78-41843
- MANAGEMENT**
NT DATA MANAGEMENT
NT INDUSTRIAL MANAGEMENT
NT PRODUCTION MANAGEMENT
NT PROJECT MANAGEMENT
NT SAFETY MANAGEMENT
MANAGEMENT PLANNING
NT PROJECT PLANNING
MANAGEMENT SYSTEMS
 Filling of orbital fluid management systems
 [NASA-CR-159404] p0108 A78-31380
- HANDBOOKS**
NT USER HANDBOOKS (COMPUTER PROGRAMS)
- MAPPING**
NT THERMAL MAPPING
- MARAGING STEELS**
 The effect of microstructure and strength on the fracture toughness of an 18 Ni, 300 grade maraging steel
 [NASA-CR-135288] p0078 A78-16150
- MARKET RESEARCH**
 Utilization of solar energy in developing countries - Identifying some potential markets
 p0142 A78-45437
 Photovoltaic refrigeration application: Assessment of the near-term market
 [NASA-TN-73874] p0131 A78-16435
 Photovoltaic highway applications: Assessment of the near-term market
 [NASA-TN-73863] p0178 A78-17935
 Photovoltaic village power application: Assessment of the near-term market
 [NASA-TN-73993] p0133 A78-19643
 Photovoltaic water pumping applications: Assessment of the near-term market
 [NASA-TN-78847] p0134 A78-19644
 Photovoltaic remote instrument applications: Assessment of the near-term market
 [NASA-TN-73821] p0150 A78-19710
- MARKETING**
 Utilization of solar energy in developing countries: Identifying some potential markets
 [NASA-TN-78968] p0140 A78-29578
- MASS PROBES**
NT TIKING LADDER SPACECRAFT
GASTIN AIRCRAFT
NT B-57 AIRCRAFT
MASS FILTERS
U FLUID FILTERS
MASS FLOW
 Calculation of 3-dimensional choking mass flow in turbomachinery with 2-dimensional flow models
 p0006 A78-12289
- MASS SPECTROMETRY**
U MASS SPECTROSCOPY
MASS SPECTROSCOPY
 Interaction of NaCl/g/ and RCl/g/ with condensed H₂SO₄ --- in hot corrosion processes
 p0066 A78-24888
- MATERIALS**
 Testing of typical spacecraft materials in a simulated subsonic environment
 p0036 A78-10156
- MATERIALS HANDLING**
NT PROPELLANT TRANSFER
- MATERIALS SCIENCE**
 Cost benefit study of advanced materials technology for aircraft turbine engines
 [NASA-CR-135235] p0026 A78-11081
 Materials science experiments in space
 [NASA-CR-2842] p0056 A78-16094
- MATERIALS TESTS**
 Charging characteristics of materials: Comparison of experimental results with simple analytical models
 p0036 A78-10157
 A three dimensional dynamic study of electrostatic charging in materials
 [NASA-CR-135256] p0099 A78-13328
 Status of the NASA-Lewis Research Center spacecraft charging investigation --- spacecraft materials tests
 [NASA-TN-78938] p0049 A78-27170
- MATHEMATICAL ANALYSIS**
U APPLICATIONS OF MATHEMATICS
MATHEMATICAL LOGIC
NT ALGORITHMS
MATHEMATICAL MODELS
NT DIGITAL SIMULATION
 A forecast of broadcast satellite communications
 p0094 A78-15615
 The application of the Routh approximation method to turbofan engine models
 p0023 A78-21891
 'Chain pooling' model selection as developed for the statistical analysis of a rotor burst protection experiment
 p0160 A78-29327
 Numerical computation of three-dimensional circulation in Lake Erie - A comparison of a free-surface model and a rigid-lid model
 p0151 A78-47223
 A parametric investigation of an existing supersonic relative tip speed propeller noise model --- turboprop aircraft
 [NASA-TN-73816] p0163 A78-13854
 Optimum wall impedance for spinning modes: A correlation with mode cut-off ratio
 [NASA-TN-73862] p0163 A78-15853
 Correlations between ultrasonic and fracture toughness factors in metallic materials
 [NASA-TN-73805] p0069 A78-19261
 Self-acting shaft seals
 [NASA-TN-73856] p0114 A78-19513
 A Stirling engine computer model for performance calculations
 [NASA-TN-78884] p0180 A78-20994
 Procedures for generation and reduction of linear models of a turbofan engine
 [NASA-TP-1261] p0161 A78-30896
- MATHEMATICAL PROGRAMMING**
NT NONLINEAR PROGRAMMING
- MATRICES (MATHEMATICS)**
 An automated procedure for calculating system matrices from perturbation data generated by an EAI Pacer and 100 hybrid computer systems
 [NASA-TN-73869] p0156 A78-15729
 DIGARCD: A program for calculating linear A, B, C, and D matrices from a nonlinear dynamic engine simulation

MATRIX ANALYSIS

SUBJECT INDEX

[NASA-TP-1295] p0022 N78-33110
MATRIX ANALYSIS
 O MATRICES (MATHEMATICS)
MEASUREMENT AND INSTRUMENTATION
 WT NUMERICAL INTEGRATION
MEASURING INSTRUMENTS
 WT AMPS (SATELLITE PAYLOAD)
 WT ANEMOMETERS
 WT COUNTERS
 WT ELASTOMETERS
 WT ELECTROMETERS
 WT ENGINE MONITORING INSTRUMENTS
 WT EXTENSOMETERS
 WT FLIGHT LOAD RECORDERS
 WT IMPEDANCE PROBES
 WT INFRARED DETECTORS
 WT INTERFEROMETERS
 WT PHOTOETERS
 WT PLASMA PROBES
 WT RADIATION COUNTERS
 WT RADIATION MEASURING INSTRUMENTS
 WT RADIO FREQUENCY IMPEDANCE PROBES
 WT RADIONETERS
 WT SIGNAL ANALYZERS
 WT SPECTROPHOTOMETERS
 WT STRAIN GAGES
 WT TEMPERATURE MEASURING INSTRUMENTS
 WT TIMING DEVICES
 WT TURBULENCE METERS
 WT ULTRAVIOLET SPECTROPHOTOMETERS
 WT WEATHER DATA RECORDERS
 WT WIND VANES
 Instrumentation for propulsion systems development [SAE PAPER 780076] p0109 A78-33365
 Instrumentation for propulsion systems development --- high speed fans and turbines [NASA-TN-73840] p0011 N78-17052
MECHANICAL DEVICES
 Design considerations in mechanical face seals for improved performance. 1 - Basic configurations [ASME PAPER 77-WA/LUB-3] p0119 A78-33183
MECHANICAL DRIVES
 WT TRANSMISSIONS (MACHINE ELEMENTS)
 Electric vehicle power train instrumentation - Some constraints and considerations [EVC PAPER 7743] p0097 A78-16922
 Gas turbine engine with convertible accessories [NASA-CASE-LEW-12390-1] p0016 N78-17056
 Wind Turbine Structural Dynamics [NASA-CP-2038] p0132 N78-19616
MECHANICAL ENGINEERING
 A mechanical, thermal and electrical packaging design for a prototype power management and control system for the 30 cm mercury ion thruster [NASA-TN-78862] p0049 N78-23142
 Quantitative ultrasonic evaluation of mechanical properties of engineering materials [NASA-TN-78905] p0128 N78-24565
MECHANICAL MEASUREMENT
 WT DISPLACEMENT MEASUREMENT
 WT DRAG MEASUREMENT
 WT FLOW MEASUREMENT
 WT FRICTION MEASUREMENT
 WT PRESSURE MEASUREMENTS
 WT THRUST MEASUREMENT
 WT VELOCITY MEASUREMENT
 WT VIBRATION MEASUREMENT
MECHANICAL PROPERTIES
 WT ABRASION RESISTANCE
 WT COLD STRENGTH
 WT CREEP PROPERTIES
 WT CREEP RUPTURE STRENGTH
 WT CREEP STRENGTH
 WT DUCTILITY
 WT ELASTOPLASTICITY
 WT FATIGUE LIFE
 WT FIBER STRENGTH
 WT FLEXIBILITY
 WT FRACTURE STRENGTH
 WT IMPACT STRENGTH
 WT MODULUS OF ELASTICITY
 WT SHEAR STRENGTH
 WT STIFFNESS
 WT STRESS RELAXATION
 WT SUPERPLASTICITY
 WT TENSILE PROPERTIES
 WT TENSILE STRENGTH
 WT THERMAL RESISTANCE
 WT TOUGHNESS

WT VICOELASTICITY
WT YIELD STRENGTH
 Effects of silicon on the oxidation, hot-corrosion, and mechanical behavior of two cast nickel-base superalloys p0078 A78-21439
 Ceramics in gas turbines - Powder and process characterization p0085 A78-29328
 Residual stresses in angleplied laminates and their effects on laminate behavior p0060 A78-33201
 Mechanical and physical properties of modern boron fibers p0085 A78-33206
 Measurement of the time-temperature dependent dynamic mechanical properties of boron/aluminum composites p0061 A78-33222
 Mechanical properties on ion-beam-textured surgical implant alloys p0075 A78-14045
 Quantitative ultrasonic evaluation of mechanical properties of engineering materials p0128 A78-45433
 Pressureless sintered beta-prime-Si3N4 solid solution - Fabrication, microstructure, and strength p0086 A78-47595
 An integrated theory for predicting the hydrothermomechanical response of advanced composite structural components [NASA-TN-73812] p0125 N78-13477
 Mechanical behavior and fracture characteristics of off-axis fiber composites. 2: Theory and comparisons [NASA-TP-1082] p0057 N78-16098
 Mechanical and physical properties of modern boron fibers [NASA-TN-73882] p0058 N78-17154
 The design of an Fe-12Mn-0.2Ti alloy steel for low temperature use [NASA-CR-135310] p0078 N78-20310
 Titanium/beryllium laminates: Fabrication, mechanical properties, and potential aerospace applications [NASA-TN-73891] p0059 N78-21221
 Impetus of composite mechanics on test methods for fiber composites [NASA-TN-78979] p0126 N78-32464
MEDICAL EQUIPMENT
 WT PROSTHETIC DEVICES
 Tissue accelerating instrument [NASA-CASE-LEW-12668-1] p0153 N78-14773
 Flow compensating pressure regulator [NASA-CASE-LEW-12718-1] p0104 N78-25351
MEETINGS
 O CONFERENCES
MEISSNER EFFECT
 O SUPERCONDUCTIVITY
MELTING
 WT VACUUM MELTING
MEMBRANE ANALOGY
 O STRUCTURAL ANALYSIS
MEMBRANE THEORY
 O STRUCTURAL ANALYSIS
MEMBRANES
 WT ION EXCHANGE MEMBRANE ELECTROLYTES
 Anion exchange membranes for electrochemical oxidation-reduction energy storage system [NASA-TN-73751] p0131 N78-14631
 Anion permselective membrane [NASA-CR-135314] p0144 N78-18515
MERCAPTAN
 O THIOLS
MERCAPTO COMPOUNDS
 O THIOLS
MERCURY (METAL)
 WT MERCURY VAPOR
 Constrained sloshing of liquid mercury in a flexible spherical tank [AIAA PAPER 78-670] p0106 A78-32749
 Mechanical properties on ion-beam-textured surgical implant alloys p0075 A78-36045
 Evolution of the 1-1lb mercury ion thruster subsystem [NASA-TN-73733] p0047 N78-21202

SUBJECT INDEX

METAL JOINTS

- Planned flight test of a mercury ion auxiliary propulsion system. 1: Objectives, systems descriptions, and mission operations [NASA-TN-78859] p0047 W78-21204
- Effect of facility background gases on internal erosion of the 30-cm Hg ion thruster [NASA-TN-73803] p0048 W78-21205
- Diagnostic evaluations of a beam-shielded 8-cm mercury ion thruster [NASA-TN-78855] p0048 W78-21207
- Constrained sloshing of liquid mercury in a flexible spherical tank [NASA-TN-78833] p0103 W78-21403
- A mechanical, thermal and electrical packaging design for a prototype power management and control system for the 30 cm mercury ion thruster [NASA-TN-78862] p0049 W78-23142
- A 10-cm mercury ion thruster performance with a 1 kW capacitor-diode voltage multiplier beam supply [NASA-TN-78864] p0049 W78-23143
- Sensitivity of 30-cm mercury bombardment ion thruster characteristics to accelerator grid design [NASA-TN-78861] p0049 W78-23144
- MERCURY ION ENGINES**
- Planned flight test of a mercury ion auxiliary propulsion system. I - Objectives, systems descriptions, and mission operations [AIAA PAPER 78-647-I] p0050 A78-32734
- Planned flight test of a mercury ion auxiliary propulsion system. II - Integration with host spacecraft [AIAA PAPER 78-647-II] p0050 A78-32735
- 5200 cycle of an 8-cm diameter Hg ion thruster [AIAA PAPER 78-649] p0050 A78-32736
- Effect of facility background gases on internal erosion of the 30-cm Hg ion thruster [AIAA PAPER 78-685] p0050 A78-32745
- Sensitivity of 30-cm mercury bombardment ion thruster characteristics to accelerator grid design [AIAA PAPER 78-668] p0050 A78-32747
- Ion beam plume and efflux measurements of an 8-cm mercury ion thruster [AIAA PAPER 78-674] p0055 A78-32753
- A mechanical, thermal and electrical packaging design for a prototype power management and control system for the 30 cm mercury ion thruster [AIAA PAPER 78-685] p0051 A78-32754
- 30-cm mercury ion thruster performance with a 1 kW capacitor-diode voltage multiplier beam supply [AIAA PAPER 78-686] p0051 A78-32760
- Diagnostic evaluations of a beam-shielded 8-cm mercury ion thruster [AIAA PAPER 78-702] p0051 A78-32768
- Pulse ignition characterization of mercury ion thruster hollow cathode using an improved pulse ignitor [AIAA PAPER 78-709] p0051 A78-32773
- Evolution of the 1-1/2 mercury ion thruster subsystem [AIAA PAPER 78-711B] p0051 A78-32776
- A mission profile life test facility --- for mercury ion thrusters [AIAA PAPER 78-671] p0040 A78-37431
- Engineering Model 8-cm Thruster System [AIAA PAPER 78-646] p0055 A78-37434
- Electrical Prototype Power Processor for the 30-cm mercury electric propulsion engine [AIAA PAPER 78-644] p0055 A78-37439
- Pulse ignition characterization of mercury ion thruster hollow cathode using an improved pulse ignitor [NASA-TN-78858] p0047 W78-21203
- Effect of facility background gases on internal erosion of the 30-cm Hg ion thruster [NASA-TN-73803] p0048 W78-21205
- A review of electron bombardment thruster systems/spacecraft field and particle interfaces [NASA-TN-78853] p0048 W78-21206
- Diagnostic evaluations of a beam-shielded 8-cm mercury ion thruster [NASA-TN-78855] p0048 W78-21207
- The 5200 cycle test of an 8-cm diameter Hg ion thruster [NASA-TN-78863] p0048 W78-21208
- Planned flight test of a mercury ion auxiliary propulsion system. Part 2: Integration with host spacecraft [NASA-TN-76449] p0048 W78-21209
- Ion propulsion for spacecraft [NASA-TN-79502] p0056 W78-26172
- MERCURY VAPOR**
- Mercury ion thruster research, 1977 --- plasma acceleration [NASA-CN-135317] p0C52 ST2-15147
- METAL BONDING**
- BT METAL-METAL BONDING**
- Shear strength of metal - SiO2 contacts [NASA-TN-78838] p0125 W78-19539
- The use of ion beam cleaning to obtain high quality cold welds with minimal deformation [NASA-TN-78933] p0083 W78-27257
- Adhesion of a bimetallic interface --- for Al, Hg, and Zn [NASA-TN-78890] p0071 W78-29214
- METAL COATINGS**
- BT NICKEL COATINGS**
- Two-layer thermal barrier coating for high temperature components [ACS PAPER 31-BW-76P] p0084 A78-18787
- X-ray photoelectron spectroscopy study of radiofrequency-sputtered refractory compound steel interfaces [NASA-TP-1161] p0081 W78-20336
- Solar cell collector [NASA-CASE-LEW-12552-1] p0136 W78-25527
- Effects of compositional changes on the performance of a thermal barrier coating system --- yttria-stabilized zirconia coatings on gas turbine engine blades [NASA-TN-78976] p0072 W78-31212
- METAL COMPOUNDS**
- Friction and wear of single-crystal and polycrystalline manganese-zinc ferrite in contact with various metals [NASA-TP-1059] p0080 W78-10295
- Emission and absorbance of NASA ceramic thermal barrier coating system --- for turbine cooling [NASA-TP-1190] p0020 W78-26148
- Inhibition of hot salt corrosion by metallic additives [NASA-TN-78966] p0072 W78-31208
- METAL CORROSION**
- BT CORROSION**
- BT FATIGUE**
- Correlations between ultrasonic and fracture toughness factors in metallic materials p0077 A78-45434
- Ductility normalized-strain-range partitioning life relations for creep-fatigue life predictions p0077 A78-51739
- Mechanical properties of ion-beam-textured surgical implant alloys [NASA-TN-73742] p0068 W78-13181
- Proposed design procedure for transmission shafting under fatigue loading [NASA-TN-78927] p0115 W78-26444
- METAL FIBERS**
- Friction and wear of sintered fibermetal abrasible seal materials p0074 A78-23451
- METAL FILMS**
- Method of forming metal hydride films [NASA-CASE-LEW-12083-1] p0113 W78-13436
- METAL FORMING**
- BT FORMING TECHNIQUES**
- METAL HALIDES**
- BT POTASSIUM CHLORIDES**
- BT SODIUM CHLORIDES**
- METAL HYDRIDES**
- BT ALUMINUM BOROHYDRIDES**
- Crystal field and magnetic properties of ErH3 p0175 W78-24907
- Method of forming metal hydride films [NASA-CASE-LEW-12083-1] p0113 W78-13436
- METAL IONS**
- Evolution of the 1-1/2 mercury ion thruster subsystem [NASA-TN-71733] p0047 W78-21202
- Planned flight test of a mercury ion auxiliary propulsion system. 1: Objectives, systems descriptions, and mission operations [NASA-TN-78859] p0047 W78-21204
- METAL JOINTS**
- Method of cold welding using ion beam technology [NASA-CASE-LEW-12982-1] p0117 W78-28459

METAL MATRIX COMPOSITES

SUBJECT INDEX

METAL MATRIX COMPOSITES

Predicted inlet gas temperatures for tungsten fiber reinforced superalloy turbine blades p0060 A78-33203

Thermal environment effects on strength and impact properties of boron-aluminum composites [NASA-TN-73805] p0058 A78-17155

METAL OXIDE SEMICONDUCTORS
Impurity concentrations and surface charge densities on the heavily doped face of a silicon solar cell p0130 A78-13534

Solar cell collector [NASA-CASE-LTR-12552-1] p0136 A78-25527

METAL OXIDES
WT ALUMINUM OXIDES
WT CARBORITES
WT CARBON OXIDES
WT MAGNESIUM OXIDES
WT ZIRCONIUM OXIDES
 Effect of prior creep at 1365 K on the room temperature tensile properties of several oxide dispersion strengthened alloys p0074 A78-21431

Tensile and creep properties of the experimental oxide dispersion strengthened iron-base sheet alloy NA-956E at 1365 K p0074 A78-21858

Reactions of yttria-stabilized zirconia with oxides and sulfates of various elements [NASA-TN-78942] p0071 A78-29216

Longitudinal shear behavior of several oxide dispersion strengthened alloys [NASA-TN-78973] p0072 A78-31211

METAL PARTICLES
WT METAL POWDER
METAL FLATES
 The influence of composition, annealing treatment, and texture on the fracture toughness of Ti-5Al-2.5Sn plate at cryogenic temperatures [NASA-TN-73872] p0069 A78-15235

METAL POWDER
 Cleaning process for contaminated superalloy powders p0076 A78-81400

METAL SHEETS
 Tensile and creep properties of the experimental oxide dispersion strengthened iron-base sheet alloy NA-956E at 1365 K p0074 A78-21858

Analysis and test of deep flaws in thin sheets of aluminum and titanium. Volume 1: Program summary and data analysis [NASA-CR-135369] p0127 A78-21493

Analysis and test of deep flaws in thin sheets of aluminum and titanium. Volume 2: Crack opening displacement and stress-strain data [NASA-CR-135370] p0127 A78-21494

METAL SURFACES
 High temperature environmental effects on metals p0075 A78-29329

Shear strength of metal - SiO₂ contacts p0061 A78-33209

Surface-crack shape change in bending fatigue using an inexpensive resonant fatiguing apparatus p0075 A78-35394

The role of thermal shock in cyclic oxidation p0076 A78-37676

Friction and wear behavior of single-crystal silicon carbide in sliding contact with various metals p0086 A78-44095

Temperature distributions and thermal stresses in a graded zirconia/metal gas path seal system for aircraft gas turbine engines [NASA-TN-73819] p0015 A78-15044

Friction and wear of metals with a single-crystal abrasive grit of silicon carbide: Effect of shear strength of metal p0084 A78-30238

Study of dynamic emission spectra from lubricant films in an elasto-hydrodynamic contact using Fourier transform spectroscopy [NASA-CR-159418] p0162 A78-32809

METAL VAPORS
WT MERCURY VAPOR
 Compact electron-beam source for formation of neutral beams of very low vapor pressure materials p0110 A78-41464

METAL BORING

WT CLADDING
METAL-METAL BORING
 Fabrication of stainless steel clad tubing --- gas pressure bonding [NASA-CR-135347] p0079 A78-21265

METALLOIDS
WT BORON
WT SILICON
WT TELLURIUM
METALORGANIC COMPOUNDS
U ORGANOMETALLIC COMPOUNDS
METALS
WT ALKALI METALS
WT ALKALINE EARTH METALS
WT ALUMINUM
WT BERYLLIUM
WT CESIUM VAPOR
WT CARBORIUM
WT COBALT
WT GOLD
WT IRON
WT LIQUID LITHIUM
WT LIQUID METALS
WT LIQUID POTASSIUM
WT MAGNESIUM
WT MERCURY (METAL)
WT MERCURY VAPOR
WT METAL COATINGS
WT METAL FILMS
WT METAL MATRIX COMPOSITES
WT METAL POWDER
WT METAL VAPORS
WT NICKEL
WT NICKEL COATINGS
WT REFRACTORY METALS
WT TITANIUM
WT TRANSITION METALS
WT TUNGSTEN
WT YTTRIUM
WT ZINC
 Two-phase working fluids for the temperature range 50 to 350 C [NASA-CR-135255] p0107 A78-16329

High temperature environmental effects on metals [NASA-TN-73878] p0017 A78-19158

Correlations between ultrasonic and fracture toughness factors in metallic materials [NASA-TN-73805] p0069 A78-19261

Friction and wear behavior of single-crystal silicon carbide in sliding contact with various metals [NASA-TN-73782] p0114 A78-19512

Materials technology assessment for Stirling engines p0117 A78-30318

METASTABILITY
U METASTABLE STATE
METASTABLE STATE
 Metastable states of small rare gas crystallites p0169 A78-16069

METROLOGICAL COMPRESSION TESTS
U COMPRESSION TESTS
U MECHANICAL PROPERTIES
METROLOGICAL INSTRUMENTS
WT WEATHER DATA RECORDERS
WT WIND VANES
METROLOGICAL SATELLITES
WT NOAA SATELLITES
 Automated meteorological data from commercial aircraft via satellite: Present experience and future implications [NASA-TN-73750] p0150 A78-17558

METERS
U MEASURING INSTRUMENTS
METHYL ALCOHOLS
 PBR polyimide prepreg with improved tack characteristics [NASA-TN-73898] p0081 A78-17221

Catalytic decomposition of methanol for onboard hydrogen generation [NASA-TP-1247] p0083 A78-25236

METHYL CHLORIDE
 Effect of oxygen, methyl mercaptan, and methyl chloride on friction behavior of copper-iron contacts [NASA-TP-1309] p0072 A78-30266

MICROPHONES
 Method of fan sound mode structure determination computer program user's manual: Microphone

SUBJECT INDEX

MODELS

location program
[NASA-CR-135294] p0028 W78-17065

MICROPHOTOGRAPHS
* PHOTOGRAPHS

MICROSTRUCTURE
Microstructure of hot-pressed Al2O3-Si3N4 mixtures
as a function of holding temperature p0084 A78-17456
Microstructural and wear properties of sputtered
carbides and silicides p0084 A78-23445
Oxide morphology and spalling model for SiAl
p0075 A78-30112
The effect of microstructure on hydrogen
embrittlement of the nickel base superalloy,
Udinet 700 p0076 A78-37075
The effect of microstructure and strength on the
fracture toughness of an 18 Ni, 300 grade
aerating steel p0078 W78-16150
[NASA-CR-135288]
The effect of microstructure on hydrogen
embrittlement of the nickel-base superalloy,
Udinet 700 p0082 W78-22272
[NASA-TN-73772]
Pressureless sintered beta prime-Si3N4 solid
solution: Fabrication, microstructure, and
strength p0083 W78-29245
[NASA-TN-78950]

MICROWAVE AMPLIFIERS
Secondary-electron-emission properties of
conducting surfaces with application to
multistage depressed collectors for microwave
amplifiers p0068 W78-11230
[NASA-TP-1097]

MICROWAVE COUPLING
Use of a simple external nonreciprocal attenuator
in coupled-cavity TWT's p0098 A78-18282

MICROWAVE EMISSION
Microwave radiation measurements near the electron
plasma frequency of the NASA Lewis bumpy torus
plasma p0172 W78-27914
[NASA-TN-78940]

MICROWAVE EQUIPMENT
* KLYSTRONS
* MICROWAVE AMPLIFIERS
* MICROWAVE TUBES
* TRAVELING WAVE TUBES

MICROWAVE FREQUENCIES
* SUPERHIGH FREQUENCIES

MICROWAVE TRANSMISSION
Performance of the 12 GHz, 200 watt Transmitter
Experiment Package for the Hermes Satellite
p0096 A78-24883
Design, fabrication and testing of a CPA for use
in the solar power satellite p0042 W78-31143
[NASA-CR-159410]

MICROWAVE TUBES
* KLYSTRONS
* TRAVELING WAVE TUBES
Design, fabrication and testing of a CIA for use
in the solar power satellite p0042 W78-31143
[NASA-CR-159410]

MICROWAVES
* MICROWAVE EMISSION
* MILLIMETER WAVES

MILLIMETER WAVES
Study of 42 and 85 GHz coupled cavity
traveling-wave tubes for space use
[NASA-CR-134670] p0098 W78-11295
Millimeter wave satellite concepts, volume 1
[NASA-CR-135227] p0141 W78-15144
The 20/30 GHz satellite systems technology needs
assessment p0093 W78-31323
[NASA-TN-78975]

MILLING (MACHINING)
Effect of attrition milling on the reaction
sintering of silicon nitride p0096 A78-50324
Effect of attrition milling on the reaction
sintering of silicon nitride p0094 W78-31236
[NASA-TN-78965]

MINERAL OILS
Effectiveness of various organometallics as
antiwear additives in mineral oil p0080 W78-12222
[NASA-TP-1096]
Characterization of wear debris generated in
accelerated rolling-element fatigue tests

[NASA-TP-1203] p0115 W78-21470

MINERALS
* CARBONITES
* GRAPHITE

MINIATURIZATION
Miniature drag force anemometer p0199 A78-17397

MINICOMPUTERS
Escort - A data acquisition and display system to
support research testing p0155 A78-37685
Escort: A data acquisition and display system to
support research testing p0154 W78-24807
[NASA-TN-78909]

MINIEMIZATION
* OPTIMIZATION

MINORITY
The NIRE project: Minority Involvement in NASA
Engineering p0176 W78-13938
[NASA-TN-73811]
Design and fabrication of a photovoltaic power
system for the Papago Indian village of
Schuchell (Gunsight), Arizona p0139 W78-26555
[NASA-TN-78948]

MISROBS
* MAGNETIC MISROBS

MISCIBILITY
* SOLUBILITY

MISSILE CONTROL
ADJUST - An automated system for steering Centaur
launch vehicles in measured winds p0045 A78-14991

MISSILE GUIDANCE
* MISSILE CONTROL

MISSILE STABILIZATION
* MISSILE CONTROL

MISSION PLANNING
Planned flight test of a mercury ion auxiliary
propulsion system. I: Objectives, systems
descriptions, and mission operations p0047 W78-21204
[NASA-TN-78859]

HIST
Oil-air mist lubrication for helicopter gearing
[NASA-CR-135081] p0010 W78-25080

MIXERS
Variable mixer propulsion cycle
[NASA-CASE-LEW-12917-1] p0016 W78-18067

MIXING
* DISSOLVING

MIXTURES
* AEROSOLS
* AQUEOUS SOLUTIONS
* EUTECTIC ALLOYS
* EUTECTICS
* GAS MIXTURES
* METAL MATRIX COMPOSITES
* SMOKE
* SOLID SOLUTIONS

MODELS
* ASTRONOMICAL MODELS
* ATMOSPHERIC MODELS
* BREADBOARD MODELS
* DIGITAL SIMULATION
* DYNAMIC MODELS
* MATHEMATICAL MODELS
* SCALE MODELS

MODES
* FAILURE MODES
* MODES (STANDING WAVES)
* PROPAGATION MODES
Method of fan sound mode structure determination
[NASA-CR-135293] p0028 W78-17064
Method of fan sound mode structure determination
computer program user's manual: Modal
calculation program p0028 W78-17066
[NASA-CR-135295]

MODES (STANDING WAVES)
Interaction of a turbulent jet noise source with
transverse modes in a rectangular duct
[NASA-TN-1248] p0001 W78-25049

MODULATION
* AMPLITUDE MODULATION
* FREQUENCY MODULATION
* PHASE MODULATION
* PULSE DURATION MODULATION

MODULES
* ELECTRONIC MODULES
Results of module electrical measurement of the
DOE 46-kilowatt procurement

MODULES OF ELASTICITY

SUBJECT INDEX

[NASA-TN-78879] p0138 W78-19658
MODULES OF ELASTICITY
 Elastohydrodynamic lubrication of elliptical
 contacts for materials of low elastic modulus. I
 - Fully flooded conjunction
 [ASME PAPER 77-LUB-10] p0119 W78-28418
 Mechanical and physical properties of modern boron
 fibers p0085 W78-33206

SOBE CIRCLES
 J FRACTURE MECHANICS
SOLESTONE COEFFICIENT
 Effects of hydrothermal exposure on a
 low-temperature cured epoxy
 [NASA-TN-73881] p0081 W78-17220
 Effects of moisture profiles and laminate
 configuration on the hygro stresses in advanced
 composites --- graphite-epoxy composites
 [NASA-TN-78978] p0059 W78-32191

MOLECULAR BONDS
 U CRITICAL BONDS
MOLECULAR WEIGHT
 Friction and wear of polyethylene oxide polymer
 having a range of molecular weights
 [NASA-TN-1129] p0080 W78-15278

MOLECULES
 BT DIATOMIC MOLECULES
MOLYBDENUM ALLOYS
 New alloys to conserve critical elements ---
 replacing chromium in steels p0076 W78-37680

MOLYBDENUM COMPOUNDS
 BT MOLYBDENUM DISULFIDES
MOLYBDENUM DISULFIDES
 Physics and chemistry of MoS₂ intercalation
 compounds p0175 W78-27727
 A comparison of the lubricating mechanisms of
 graphite flake and molybdenum disulfide films
 [NASA-TN-78897] p0083 W78-26215

MOLYBDENUM SULFIDES
 BT MOLYBDENUM DISULFIDES
 Critical currents in sputtered PbMoS₆
 p0175 W78-45368
 Critical currents and scaling laws in sputtered
 copper molybdenum sulfide p0175 W78-45500
 Upper critical field of copper molybdenum sulfide
 p0175 W78-53626

MONOMERS
 BT PITCHING MONOMERS
MONOTOMIC GASES
 Atomic hydrogen storage method and apparatus ---
 cryotrapping and magnetic field strength
 [NASA-CASE-LEU-12081-2] p0169 W78-19907

MONOCRYSTALS
 U SINGLE CRYSTALS
MONOLITHIC CIRCUITS
 U INTEGRATED CIRCUITS
MONOMERS
 Kinetics of isodization and crosslinking in
 PMR-polyimide resin --- Polymerization of
 Monomer Reactants p0061 W78-33210

MONOPLAQUES
 WT B-57 AIRCRAFT
 WT F-100 AIRCRAFT
 WT F-102 AIRCRAFT
MOS (SEMICONDUCTORS)
 U METAL OXIDE SEMICONDUCTORS
MOSSBAUER EFFECT
 Considerations to achieve directionality for gamma
 ray lasers p0116 W78-26870

MOTION AFTEREFFECTS
 Effect of forward motion on engine noise
 [NASA-CN-134954] p0026 W78-10093

MOTION EQUATIONS
 U EQUATIONS OF MOTION
MOTION STABILITY
 BT ATTITUDE STABILITY
 WT MAGNETOHYDRODYNAMIC STABILITY
 WT SPACECRAFT STABILITY

MOTOR VEHICLES
 WT AUTOMOBILES
 WT ELECTRIC MOTOR VEHICLES
 WT TRUCKS
 State-of-the-art assessment of electric vehicles
 and hybrid vehicles

[NASA-TN-73756] p0179 W78-18980
MOTORS
 BT ELECTRIC MOTORS
 BT INDUCTION MOTORS
MOUNTING
 Impact absorbing blade mounts for variable pitch
 blades
 [NASA-CASE-LEU-12313-1] p0113 W78-10468

MULTILAYER INSULATION
 An ultralightweight, evacuated, load-bearing,
 high-performance insulation system --- for
 cryogenic propellant tanks
 [AIAA PAPER 78-878] p0045 W78-36005
 Farging of a tank-mounted multilayer insulation
 system by gas diffusion
 [NASA-TN-1127] p0081 W78-17127
 Thermal performance of a customized multilayer
 insulation (MLI). Design and fabrication of
 test facility hardware
 [NASA-CN-157648] p0062 W78-20257
 Comparison of reusable insulation systems for
 cryogenically-tanked earth-based space vehicles
 [NASA-TN-73668] p0061 W78-21190

MULTILAYER STRUCTURES
 U LAMINATES
MULTIPHASE FLOW
 BT TWO PHASE FLOW
MULTIPLIERS
 30-cm mercury ion thruster performance with a 1 kV
 capacitor-diode voltage multiplier beam supply
 [AIAA PAPER 78-686] p0051 W78-32760
 Extended performance solar electric propulsion
 thrust system study. Volume 5. Capacitor-diode
 voltage multiplier: Technology evaluation
 [NASA-CN-135281-VOL-5] p0053 W78-19195
 Medium power voltage multipliers with a large
 number of stages
 [NASA-TN-78900] p0093 W78-26373
 Regulated high efficiency, lightweight
 capacitor-diode multiplier dc to dc converter
 [NASA-CASE-LEU-12791-1] p0097 W78-32341

MULTISTAGE COMPRESSORS
 U TURBOCOMPRESSORS
MULTIVARIATE STATISTICAL ANALYSIS
 BT REGRESSION ANALYSIS

N

N-P JUNCTIONS
 U P-N JUNCTIONS
N-TYPE SEMICONDUCTORS
 Analysis of epitaxial drift field N on P silicon
 solar cells p0141 W78-10904

NACELLES
 VSTOL tilt nacelle aerodynamics and its relation
 to fan blade stresses
 [AIAA PAPER 78-958] p0007 W78-43520
 Integrated gas turbine engine-nacelle
 [NASA-CASE-LEU-12389-2] p0016 W78-18066
 Theoretical flow characteristics of inlets for
 tilting-nacelle VTOL aircraft
 [NASA-TN-1205] p0018 W78-21118
 VSTOL tilt nacelle aerodynamics and its relation
 to fan blade stresses
 [NASA-TN-78899] p0005 W78-26099

NASA PROGRAMS
 BT CENTAUR PROJECT
 WT GLOBAL ATMOSPHERIC RESEARCH PROGRAM
 WT QUIET ENGINE PROGRAM
 WT SUPERSONIC CRUISE AIRCRAFT RESEARCH
 A review of NASA's propulsion programs for civil
 aviation
 [AIAA PAPER 78-43] p0023 W78-20651
 CTS /Nereus/ - United States experiments and
 operations summary --- Communications Technology
 Satellite p0094 W78-24886
 ECAS Phase I fuel cell results --- Energy
 Conservation Alternatives Study p0142 W78-26110
 Making aerospace technology work for the
 automotive industry - Introduction p0181 W78-33359
 NASA/General Electric Engine Component Improvement
 Program
 [AIAA PAPER 78-929] p0025 W78-45098
 NASA engine system technology programs - An overview
 [AIAA PAPER 78-928] p0025 W78-48452

SUBJECT INDEX

NIOBIUM COMPOUNDS

- A three dimensional dynamic study of electrostatic charging in materials
[NASA-CR-135256] p0099 W78-13328
- NASCAP user's manual
[NASA-CR-135259] p0099 W78-13329
- The HIRE project: Minority Involvement in NASA Engineering
[NASA-TN-73811] p0176 W78-13938
- Preliminary QCSSE program test results
[NASA-TN-73732] p0015 W78-15042
- A review of NASA's propulsion programs for aviation
[NASA-TN-73831] p0016 W78-16055
- General aviation energy-conservation research programs at NASA-Lewis Research Center
[NASA-TN-73884] p0016 W78-17060
- Synchronization of the DOE/NASA 100-kilowatt wind turbine generator with a large utility network
[NASA-TN-73861] p0132 W78-17467
- Bibliography of Lewis Research Center technical contributions announced in 1976
[NASA-TN-73860] p0177 W78-17921
- DOE/NASA Mod-0 100KW wind turbine test results
p0133 W78-19628
- Description and status of NASA-LERC/DOE photovoltaic applications systems
[NASA-TN-78936] p0139 W78-26554
- Bibliography of Lewis Research Center technical publications announced in 1977
[NASA-TN-78918] p0177 W78-28986
- Results and status of the NASA aircraft engine emission reduction technology programs
[NASA-TN-79009] p0022 W78-33102
- NASA STRUCTURAL ANALYSIS PROGRAM**
O NASTRAN
NASTRAN
NASTRAN use for cyclic response and fatigue analysis of wind turbing towers
p0125 W78-12459
- Simplified modeling for wind turbine nodal analysis using NASTRAN
p0132 W78-19619
- Effect of steady flight loads on JT9D-7 performance deterioration
[NASA-CR-135407] p0031 W78-29105
- NATIONS**
NT DEVELOPING NATIONS
NATURAL FREQUENCIES
7 RESONANT FREQUENCIES
NEON
NT LIQUID NEON
NETWORK ANALYSIS
Discrete time domain modelling and analysis of dc-dc converters with continuous and discontinuous inductor current
p0100 W78-16796
- FLOWNET: A computer program for calculating secondary flow conditions in a network of turbomachinery
[NASA-TN-73774] p0156 W78-21791
- NEUTRAL BEAMS**
Compact electron-beam source for formation of neutral beams of very low vapor pressure materials
p0110 W78-41464
- NEUTRAL PARTICLES**
Model for interpreting Doppler broadened optical line emission measurements on axially symmetric plasma
p0174 W78-46189
- NICKEL**
Directionally solidified eutectic gamma-gamma nickel-base superalloys
[NASA-CASE-LEW-12905-1] p0069 W78-18183
- Friction and wear of selected metals and alloys in sliding contact with AISI 440 C stainless steel in liquid methane and in liquid natural gas
[NASA-TP-1150] p0114 W78-20512
- Effects of thermomechanical processing on strength and toughness of iron - 12-percent-nickel - reactive metal alloys at -196 C
[NASA-TP-1308] p0073 W78-31213
- NICKEL ALLOYS**
NT ASTROLOY (TRADEMARK)
NT TDIAPT ALLOYS
Cryogenic properties of a new tough-strong iron alloy
p0073 W78-15825
- Burner rig alkali salt corrosion of several high temperature alloys
p0073 W78-18793
- Effect of prior creep at 1365 K on the room temperature tensile properties of several oxide dispersion strengthened alloys
p0074 W78-21431
- Effects of silicon on the oxidation, hot-corrosion, and mechanical behavior of two cast nickel-base superalloys
p0074 W78-21439
- Friction and wear of sintered fibermetal abrasible seal materials
p0074 W78-23451
- The effect of NaCl/g/ on the Na2SO4-induced hot corrosion of NiAl
p0079 W78-24901
- Oxide morphology and spalling model for NiAl
p0075 W78-30112
- Strainrange partitioning behavior of the nickel-base superalloys, Rene 80 and 100
p0075 W78-33214
- Strength enhancement process for prealloyed powder superalloys
p0075 W78-33216
- The role of thermal shock in cyclic oxidation
p0076 W78-37676
- Development of strong and tough cryogenic Fe-12Ni alloys containing reactive metal additions
p0076 W78-41465
- Interpolation and extrapolation of creep rupture data by the minimum commitment method. 1 - Focal-point convergence
p0076 W78-45427
- The cyclic oxidation resistance of cobalt chromium-aluminum alloys at 1100 and 1200 C and a comparison with the nickel-chromium-aluminum alloy system
p0077 W78-50086
- Reaction diffusion in the NiCrAl and CoCrAl systems
p0077 W78-53063
- Feasibility study of tungsten as a diffusion barrier between nickel-chromium-aluminum and Gamma/Gamma prime - Delta eutectic alloys
[NASA-TP-1131] p0068 W78-15230
- The effect of microstructure and strength on the fracture toughness of an 18 Ni, 300 grade maraging steel
[NASA-CR-135288] p0078 W78-16150
- Adhesive/cohesive strength of a ZrO2.1-2 w/o Y2O3/NiCrAl thermal barrier coating
[NASA-TN-73792] p0057 W78-17152
- The effect of minor additions of titanium on the fracture toughness of Fe-12Ni alloys at 77K
[NASA-CR-135351] p0078 W78-19259
- Strainrange partitioning behavior of the nickel-base superalloys, Rene' 80 and in 100
[NASA-TN-78828] p0070 W78-21267
- The effect of microstructure on hydrogen embrittlement of the nickel-base superalloy, Udmet 700
[NASA-TN-73772] p0082 W78-22232
- Rub tolerance evaluation of two sintered NiCrAl gas path seal materials --- wear tests of gas turbine engine seals
[NASA-TN-78967] p0071 W78-29215
- Longitudinal shear behavior of several oxide dispersion strengthened alloys
[NASA-TN-78973] p0072 W78-31211
- Evaluation of cyclic behavior of aircraft turbine disk alloys
[NASA-CR-159433] p0128 W78-33478
- NICKEL COATINGS**
Selective coating for solar panels --- using black chrome and black nickel
[NASA-CASE-LEW-12159-1] p0132 W78-19599
- NICKEL ZINC BATTERIES**
Rapid, efficient charging of lead-acid and nickel-zinc traction cells
[NASA-TN-78901] p0135 W78-24616
- NIOBIUM ALLOYS**
Development and fabrication of a diffusion welded Columbian alloy heat exchanger --- for space power generation
[AIIE PAPER A78-61] p0123 W78-31500
- Niobium-germanium superconducting tapes for high-field magnet applications
[NASA-CR-135364] p0099 W78-19392
- NIOBIUM COMPOUNDS**
Superconducting Nb3Ge for high-field magnets
p0175 W78-41922

NITRIC OXIDE

SUBJECT INDEX

NITRIC OXIDE

Effect of nitric oxide on photochemical ozone formation in mixtures of air with molecular chlorine and with trichlorofluoromethane [NASA-TP-1192] p0065 N78-20281

NITRIDES

NT SILICON NITRIDES
Development of SiAlON materials [NASA-CR-135290] p0087 N78-21289

NITRILES

Trimerization of aromatic nitriles [NASA-CASR-LNU-12053-1] p0080 N78-15276

NITROGEN

NT LIQUID NITROGEN

Velocity and temperature profiles in near-critical nitrogen flowing past a horizontal flat plate [ASME PAPER 77-NV-7] p0106 A78-17881
Release of dissolved nitrogen from water during depressurization p0066 A78-33228

Release of dissolved nitrogen from water during depressurization [NASA-TN-73822] p0065 N78-17172
Effect of oxygen and nitrogen interactions on friction of single-crystal silicon carbide [NASA-TP-1265] p0083 N78-28247

NITROGEN COMPOUNDS

NT NITRIDES

NT NITRIC OXIDE

NT NITRIDES

NT NITROGEN OXIDES

NT POLYIMIDES

NT SILICON NITRIDES

NITROGEN OXIDES

NT NITRIC OXIDE

Stratospheric cruise emission reduction program p0013 N78-11077
Advanced low-NO(x) combustors for supersonic high-altitude gas turbines p0014 N78-11078

Augmentor emissions reduction technology program --- for turbofan engines [NASA-CR-135215] p0027 N78-13057

Wide range operation of advanced low NOx combustors for supersonic high-altitude aircraft gas turbines [NASA-CR-135297] p0027 N78-18047

Experimental study of the effect of cycle pressure on lean combustion emissions [NASA-CR-3032] p0031 N78-28098

NOAA SATELLITES

Disaster warning system study summary --- cost estimates using NOAA satellites [NASA-TN-73797] p0093 N78-10346

NOBLE GASES

U PURE GASES

NOBLE METALS

NT GOLD

NOISE (SOUND)

NT AERODYNAMIC NOISE

NT AIRCRAFT NOISE

NT ENGINE NOISE

NT JET AIRCRAFT NOISE

Interaction of a turbulent-jet noise source with transverse modes in a rectangular duct [NASA-TP-1248] p0001 N78-25049

NOISE ATTENUATION

U NOISE REDUCTION

NOISE ELIMINATION

U NOISE REDUCTION

NOISE GENERATORS

Three-dimensional effects on pure tone fan noise due to inflow distortion [AIAA PAPER 78-1120] p0166 A78-41830
Effect of forward motion on engine noise [NASA-CR-134954] p0026 N78-10093

NOISE HAZARDS

U NOISE (SOUND)

NOISE INTENSITY

Flight-effects on predicted fan fly-by noise [NASA-TN-73798] p0014 N78-13060

NOISE MEASUREMENT

Sound separation probes for flowing duct noise measurements --- jet engine diagnostics p0033 A78-17396

Reduction of fan noise in an anechoic chamber by reducing chamber wall induced inlet flow disturbances: p0166 A78-37681

Calculation of far-field jet noise spectra from near-field measurements using true source location [AIAA PAPER 78-1153] p0168 A78-41852

A method for calculating externally blown flap noise [NASA-CR-2954] p0166 N78-20920

Comparison of the noise characteristics of two low pressure ratio fans with a high throat Mach number inlet [NASA-TN-73880] p0018 N78-21108

YF 102 in-duct combustor noise measurement, volume 1 [NASA-CR-135404-VOL-1] p0167 N78-25827

YF 102 in-duct combustor noise measurement, volume 2 [NASA-CR-135404-VOL-2] p0167 N78-25828

YF 102 in-duct combustor noise measurement, volume 3 [NASA-CR-135404-VOL-3] p0167 N78-25829

Acoustic tests of duct-burning turbofan jet noise simulation [NASA-CR-2966] p0002 N78-28043

NOISE PROPAGATION

Optimum wall impedance for spinning modes: A correlation with mode cut-off ratio [NASA-TN-73862] p0163 N78-15853

NOISE REDUCTION

EBF noise suppression and aerodynamic penalties --- Externally Blown Flaps [AIAA PAPER 78-240] p0165 A78-20763

Effectiveness of an inlet flow turbulence control device to simulate flight fan noise in an anechoic chamber p0024 A78-24880

State-of-the-art of turbofan engine noise control p0024 A78-35658

Reduction of fan noise in an anechoic chamber by reducing chamber wall induced inlet flow disturbances p0166 A78-37681

Acoustic evaluation of a novel swept-rotor fan [AIAA PAPER 78-1121] p0166 A78-41831

EBF noise suppression and aerodynamic penalties [NASA-TN-73823] p0163 N78-15852

Variable thrust nozzle for quiet turbofan engine and method of operating same [NASA-CASR-LNU-12317-1] p0016 N78-17055

Method of fan sound mode structure determination [NASA-CR-135293] p0028 N78-17064

Reduction of fan noise in an anechoic chamber by reducing chamber wall induced inlet flow disturbances [NASA-TN-78854] p0164 N78-22860

QCSEE task 2: Engine and installation preliminary design [NASA-CR-134738] p0030 N78-23089

Acoustic evaluation of a novel swept-rotor fan --- noise reduction in turbofan engines [NASA-TN-78878] p0164 N78-24897

Acoustic tests of duct-burning turbofan jet noise simulation [NASA-CR-2966] p0002 N78-28043

Acoustic tests of duct-burning turbofan jet noise simulation: Comprehensive data report. Volume 1, section 2: Full size data [NASA-CR-135239-VOL-1-SECT-2] p0030 N78-28095

Acoustic tests of duct-burning turbofan jet noise simulation: Comprehensive data report. Volume 1, section 3: Data plots [NASA-CR-135239-VOL-1-SECT-3] p0030 N78-28096

Acoustic tests of duct-burning turbofan jet noise simulation: Comprehensive data report. Volume 2: Model design and aerodynamic test results [NASA-CR-135239-VOL-2] p0031 N78-28097

NOISE SPECTRA

Calculation of far-field jet noise spectra from near-field measurements using true source location [AIAA PAPER 78-1153] p0168 A78-41852

NOISE SUPPRESSORS

U NOISE REDUCTION

NOMINAL VALUES

U APPROXIMATION

NONADIABATIC CONDITIONS

Direct heating surface combustor [NASA-CASR-LNU-11877-1] p0097 N78-27357

NONADIABATIC PROCESSES

U HEAT TRANSFER

NONDESTRUCTIVE TESTS

Quantitative ultrasonic evaluation of mechanical properties of engineering materials p0124 A78-45433

Correlations between ultrasonic and fracture toughness factors in metallic materials

SUBJECT INDEX

OILS

- Use of an ultrasonic-acoustic technique for nondestructive evaluation of fiber composite strength [NASA-TN-73813] p0077 A78-45434
- Acoustic emission testing of composite vessels under sustained loading [NASA-TN-78981] p0124 A78-17397
- ANISOTROPIC PLATES
U ANISOTROPIC PLATES p0059 A78-33150
- NONLINEAR EQUATIONS
Nonlinear flap-lag-axial equations of a rotating beam with arbitrary precone angle [AIAA 78-491] p0127 A78-29798
- NONLINEAR PROGRAMMING
Solution of transient optimization problems by using an algorithm based on nonlinear programming p0158 A78-23909
- NONRIGIDITY
U FLEXIBILITY
- NOVISCOUS FLOW
U TURBULENT FLOW
- NORMAL SHOCK WAVES
Normal shock and restart controls for a supersonic airbreathing propulsion system p0019 A78-23023
- NORTH AMERICAN AIRCRAFT
NT F-100 AIRCRAFT
- NOTATION
U CODING
- NOTCH TESTS
Load-displacement measurement and work determination in three-point bend tests of notched or precracked specimens p0089 A78-24370
- NOTCHED METALS
U NOTCH TESTS
- NOXIOUS MATERIALS
U CONTAMINANTS
- NOZZLE COEFFICIENT
U NOZZLE FLOW
- NOZZLE DESIGN
Variable thrust nozzle for quiet turbofan engine and method of operating same [NASA-CASE-LEW-12317-1] p0016 A78-17055
- F-15/nonaxisymmetric nozzle system integration study support program [NASA-CR-135252] p0028 A78-18070
- Design of an air ejector for boundary-layer bleed of an acoustically treated turbofan engine inlet during ground testing [NASA-TN-78917] p0037 A78-27143
- NOZZLE FLOW
An empirical model for inverted-velocity-profile jet noise prediction p0023 A78-24879
- Performance characteristics of two annular dump diffusers using suction-stabilized vortex flow control p0107 A78-45831
- Wind tunnel performance tests of conannular pipe nozzles --- in the Langley 8 x 6 ft. supersonic wind tunnel [NASA-CR-2990] p0002 A78-21044
- NUCLEAR AUXILIARY POWER UNITS
NT SPACE POWER REACTORS
- NUCLEAR ELECTRIC POWER GENERATION
NT SPACE POWER REACTORS
- NUCLEAR ELECTRIC PROPULSION
Comment on 'Heat-pipe reactors for space power applications' p0052 A78-40826
- Optimize out-of-core thermionic energy conversion for nuclear electric propulsion [NASA-TN-73892] p0170 A78-17856
- NUCLEAR FUSION
NT CONTROLLED FUSION
- NUCLEAR PARTICLES
NT PHOTOELECTRONS
NT PHOTONS
- NUCLEAR POWER REACTORS
NT SPACE POWER REACTORS
- NUCLEAR PROPULSION
NT NUCLEAR ELECTRIC PROPULSION
- NUCLEAR RADIATION
NT GAMMA RAYS
NT SPALLATION
- NUCLEAR REACTIONS
NT CONTROLLED FUSION
- NT PHOTOPRODUCTION
NT SPALLATION
- NUCLEAR REACTORS
NT HIGH TEMPERATURE NUCLEAR REACTORS
NT SPACE POWER REACTORS
NT TOKAMAK DEVICES
High temperature heat pipe research at NASA Lewis Research Center [NASA-TN-78832] p0103 A78-23384
- NUCLEAR RESEARCH AND TEST REACTORS
NT HIGH TEMPERATURE NUCLEAR REACTORS
- NUCLEAR SHIELDING
U RADIATION SHIELDING
- NUCLEATE BOILING
NT LEIDENFROST PHENOMENON
Estimating surface temperature in forced convection nucleate boiling - A simplified method p0105 A78-15822
- NUCLIDES
NT CESIUM VAPOR
NT ISOTOPES
NT TELLOBIUM
- NUMERICAL ANALYSIS
NT APPROXIMATION
NT FINITE DIFFERENCE THEORY
NT FINITE ELEMENT METHOD
NT INTERPOLATION
NT ITERATIVE SOLUTION
NT LEAST SQUARES METHOD
NT NUMERICAL INTEGRATION
Numerical spatial marching techniques for estimating duct attenuation and source pressure profiles p0166 A78-37682
- Interpolation and extrapolation of creep rupture data by the minimum commitment method. I - Focal-point convergence p0076 A78-45427
- Numerical spatial marching techniques for estimating duct attenuation and source pressure profiles [NASA-TN-78857] p0103 A78-22329
- NUMERICAL CONTROL
Real time digital propulsion system simulation for manned flight simulators [AIAA PAPER 78-927] p0035 A78-45095
- NUMERICAL FLOW VISUALIZATION
Computation of unsteady transonic flows through rotating and stationary cascades. 3: Acoustic far-field analysis [NASA-CR-2902] p0007 A78-12035
- NUMERICAL INTEGRATION
Stability of numerical integration techniques for transient rotor dynamics [NASA-TP-1092] p0113 A78-10474
- NUMERICAL STABILITY
Stability of numerical integration techniques for transient rotor dynamics [NASA-TP-1092] p0113 A78-10474
- NYLON RESINS
U POLYAMIDE RESINS
- O RING SEALS
Stiffness and damping of elastomeric O-ring bearing mounts [NASA-CR-135328] p0127 A78-18460
- Stiffness of straight and tapered annular gas path seals [NASA-TP-78872] p0103 A78-23385
- OBLIQUE COORDINATES
Interpolation and extrapolation of creep rupture data by the minimum commitment method. Part 2: Oblique translation [NASA-TN-78882] p0125 A78-23472
- OFF-ON CONTROL
Solution of transient optimization problems by using an algorithm based on nonlinear programming p0158 A78-23909
- 5200 cycle of an 8-cm diameter Hg ion thruster [AIAA PAPER 78-649] p0050 A78-32736
- OIL RECOVERY
In-situ laser retorting of oil shale [NASA-CASE-LEW-12217-1] p0129 A78-14452
- OILS
NT CRUDE OIL
NT LUBRICATING OILS
NT MINERAL OILS

ON-LINE PROGRAMMING

SUBJECT INDEX

WT SHALE OIL
ON-LINE PROGRAMMING
 Escort - A data acquisition and display system to support research testing p0155 A78-37685

ONBOARD EQUIPMENT
WT AIRCRAFT EQUIPMENT
WT SPACECRAFT ELECTRONIC EQUIPMENT
OPERATIONS RESEARCH
 CTS (Hercules): United States experiments and operations summary [NASA-TN-73830] p0041 W78-13107
 Computer model for refinery operations with emphasis on jet fuel production. Volume 1: Program description [NASA-CR-135333] p0090 W78-20350

OPTICAL ABSORPTION
U LIGHT TRANSMISSION
OPTICAL CORRECTION PROCEDURES
 Development of a drift-correction procedure for a photoelectric spectrometer p0109 A78-23525

OPTICAL EMISSION SPECTROSCOPY
 Development of a drift-correction procedure for a photoelectric spectrometer p0109 A78-23525
 Model for interpreting Doppler broadened optical line emission measurements on axially symmetric plasma p0174 A78-46189

OPTICAL EQUIPMENT
WT COLLIMATORS
WT PHOTOMETERS
WT SPECTROPHOTOMETERS
WT ULTRAVIOLET SPECTROPHOTOMETERS
 Analysis and design of a high power laser adaptive phased array transmitter [NASA-CR-134952] p0111 W78-13420

OPTICAL RASERS
U LASERS
OPTICAL MEASUREMENT
WT ELECTROPHOTOMETRY
OPTICAL MEASURING INSTRUMENTS
WT PHOTOMETERS
WT SPECTROPHOTOMETERS
WT ULTRAVIOLET SPECTROPHOTOMETERS
OPTICAL PROPERTIES
WT PHOTOVOLTAIC EFFECT
 Optical and electrical properties of ion beam textured Kapton and Teflon [NASA-TN-73778] p0162 W78-13848

OPTIMAL CONTROL
WT LINE OPTIMAL CONTROL
 Diagonal dominance using function minimization algorithms --- multivariable control system design p0159 A78-16304
 Optimal controls for an advanced turbofan engine p0033 A78-23893
 Solution of transient optimization problems by using an algorithm based on nonlinear programming p0158 A78-23909
 Optimal control of a supersonic inlet to minimize frequency of inlet unstart p0019 W78-23024

OPTIMIZATION
WT OPTIMAL CONTROL
WT LINE OPTIMAL CONTROL
 Heliocentric interplanetary low thrust trajectory optimization program, supplement 1, part 2 [NASA-CR-135414-APP] p0038 W78-25106

OPTIMUM CONTROL
U OPTIMAL CONTROL
ORBITAL MOTION
U ORBITS
ORBITING SATELLITES
U ARTIFICIAL SATELLITES
ORBITS
WT EARTH ORBITS
WT GEOSYNCHRONOUS ORBITS
WT SPACECRAFT ORBITS
 Filling of orbital fluid management systems [NASA-CR-159404] p0108 W78-31380

ORGANIC COMPOUNDS
WT ORGANIC SULFUR COMPOUNDS
ORGANIC SULFUR COMPOUNDS
 Solubility, stability, and electrochemical studies of sulfur-sulfide solutions in organic solvents [NASA-TP-1245] p0140 W78-28624

ORGANOMETALLIC COMPOUNDS
 Effectiveness of various organometallics as antiwear additives in mineral oil [NASA-TP-1096] p0080 W78-12222
 Inhibition of hot salt corrosion by metallic additives [NASA-TN-78966] p0072 W78-31208

ORBITALS
U ASTRONOMICAL MODELS
OSCILLATING FLOW
 Thermally driven oscillations and wave motion of a liquid drop p0106 A78-17508

OSCILLATIONS
WT PRESSURE OSCILLATIONS
 Power oscillation of the Mod-0 wind turbine p0133 W78-19629

OSCILLATORS
WT MICROWAVE TUBES
OUTPUT
WT LASER OUTPUTS
OVERCAST
U CLOUD COVER
OXIDATION
 High temperature environmental effects on metals p0075 A78-29329
 The role of thermal shock in cyclic oxidation p0076 A78-37676
 Volatile products from the interaction of KCl(g) with Cr2O3 and LaCrO3 in oxidizing environments [NASA-TN-73795] p0064 W78-13158
 Thermal fatigue and oxidation data of superalloys including directionally solidified eutectics [NASA-CR-135272] p0078 W78-15233
 Thermal fatigue and oxidation data for alloy/brake combinations [NASA-CR-135299] p0078 W78-16149
 In situ self cross-linking of polyvinyl alcohol battery separators [NASA-CASE-LEW-12972-1] p0056 W78-22157
 The role of thermal shock in cyclic oxidation [NASA-TN-78876] p0070 W78-23193
 Cyclic oxidation of coated Oxide Dispersion Strengthened (ODS) alloys in high velocity gas streams at 1100 deg C [NASA-TN-78977] p0071 W78-24336

OXIDATION RESISTANCE
 Volatilization of oxides during oxidation of some superalloys at 1200 C p0073 A78-18631
 Effects of silicon on the oxidation, hot-corrosion, and mechanical behavior of two cast nickel-base superalloys p0074 A78-21439
 Volatile products from the interaction of KCl(g) with Cr2O3 and LaCrO3 in oxidizing environments --- gas turbine engines p0066 A78-24887
 The cyclic oxidation resistance of cobalt chromium-aluminum alloys at 1100 and 1200 C and a comparison with the nickel-chromium-aluminum alloy system p0077 A78-50086
 Substitution for chromium in 304 stainless steel --- effects on oxidation and corrosion resistance p0077 A78-51714
 10,000-hour cyclic oxidation behavior at 815 C /1500 F/ of 33 high-temperature alloys p0077 A78-51716
 Improved reaction sintered silicon nitride --- protective coatings to improve oxidation resistance [NASA-CR-135291] p0063 W78-22164

OXIDATION-REDUCTION REACTIONS
 The Redox Flow System for solar photovoltaic energy storage p0141 A78-11019
 Anion exchange membranes for electrochemical oxidation-reduction energy storage system [NASA-TN-73751] p0131 W78-14631
 Redox flow cell development and demonstration project, calendar year 1976 [NASA-TN-73873] p0134 W78-19656
 Formulated plastic separators for soluble electrode cells [NASA-CASE-LEW-12358-2] p0065 W78-25149

OXIDE FILMS
 The effect of NaCl/g/ on the Na2SO4-induced hot corrosion of NiAl

SUBJECT INDEX

PAYLOADS

OXIDES p0079 A78-24901

WT ALUMINUM OXIDES
 WT CARBON MONOXIDE
 WT CHROMITES
 WT CHROMIUM OXIDES
 WT MAGNESIUM OXIDES
 WT METAL OXIDES
 WT NITRIC OXIDE
 WT NITROGEN OXIDES
 WT SILICON DIOXIDE
 WT ZIRCONIUM OXIDES

Manufacture and engine test of advanced oxide dispersion strengthened alloy turbine vanes --- for space shuttle thermal protection [NASA-CR-135269] p0077 W78-11232

Friction and wear of polyethylene oxide polymer having a range of molecular weights [NASA-TP-1129] p0080 W78-15278

OXIDIZERS
 WT LIQUID OXYGEN
 OXYGEN
 WT HIGH PRESSURE OXYGEN
 WT LIQUID OXYGEN
 WT OXYGEN ATOMS
 WT OZONE

Development of Silicon materials [NASA-CR-135290] p0087 W78-21289

Effect of oxygen and nitrogen interactions on friction of single-crystal silicon carbide [NASA-TP-1265] p0083 W78-28247

Effect of oxygen, methyl mercaptan, and methyl chloride on friction behavior of copper-iron contacts [NASA-TP-1309] p0072 W78-30206

OXYGEN ATOMS
 Measurement of tropospheric 300 nm solar ultraviolet flux for determination of O₃/I₀/ photoproduction rate p0148 A78-38835

OZONE
 Effect of trichlorofluoromethane and molecular chlorine on ozone formation by simulated solar radiation [NASA-TP-1093] p0064 W78-12167

Effect of nitric oxide on photochemical ozone formation in mixtures of air with molecular chlorine and with trichlorofluoromethane [NASA-TP-1192] p0065 W78-20281

Variability of ozone near the tropopause from GASP data [NASA-CR-135405] p0148 W78-23648

Simultaneous measurements of ozone outside and inside cabins of two B-747 airliners and a Gates Learjet business jet [NASA-TN-78983] p0009 W78-31061

OZONE FLUORIDE
 Effect of trichlorofluoromethane and molecular chlorine on ozone formation by simulated solar radiation [NASA-TP-1093] p0064 W78-12167

OZONEOMETRY
 Atmospheric ozone measurements made from B-747 airliners - Spring 1975 p0148 A78-24894

Ultraviolet spectrophotometer for measuring columnar atmospheric ozone from aircraft p0110 A78-35826

An analysis of the first two years of GASP data [NASA-TN-73817] p0148 W78-13669

P

P-I-N DIODES
 I DIODES
 P-N JUNCTIONS

A methodology for experimentally-based determination of gap shrinkage and effective lifetimes in the emitter and base of p-n-junction solar cells p0141 A78-10903

P-TYPE SEMICONDUCTORS
 Analysis of epitaxial drift field n on p silicon solar cells p0141 A78-10904

PACKAGES
 WT INSTRUMENT PACKAGES
 PANELS

Experimental transient and permanent deformation

studies of steel-sphere-impacted or explosively-impulsed aluminum panels [NASA-CR-135315] p0078 W78-15230

Selective coating for solar panels --- using black chrome and black nickel [NASA-CASE-LEW-12159-1] p0132 W78-19599

PARABOLIC REFLECTORS
 Design and fabrication of a low-specific-weight parabolic dish solar concentrator [NASA-TP-1152] p0046 W78-17145

PARALLEL FLOW
 WT PIPE FLOW
 WT THREE DIMENSIONAL FLOW

PARAMETERIZATION
 A parametric investigation of an existing supersonic relative tip speed propeller noise model --- turboprop aircraft [NASA-TN-73816] p0163 W78-13854

PARTICLE ACCELERATOR TARGETS
 Closed loop spray cooling apparatus --- for particle accelerator targets [NASA-CASE-LEW-11981-1] p0091 W78-17237

PARTICLE ACCELERATORS
 WT ION ACCELERATORS

PARTICLE BEAMS
 WT ELECTRON BEAMS
 WT ION BEAMS
 WT NEUTRAL BEAMS

PARTICLE COUNTERS
 U RADIATION COUNTERS
 PARTICLE DENSITY (CONCENTRATION)
 WT ELECTRON DENSITY (CONCENTRATION)
 WT ION DENSITY (CONCENTRATION)
 WT PLASMA DENSITY

PARTICLE DETECTORS
 U RADIATION COUNTERS
 PARTICLE DIFFUSION
 Reaction diffusion in the NiCrAl and CoCrAl systems p0077 A78-53063

PARTICLE EMISSION
 WT ELECTRON EMISSION
 WT FIELD EMISSION
 WT ION EMISSION
 WT SECONDARY EMISSION
 WT THERMIONIC EMISSION

Combustor concepts for aircraft gas turbine low-power emissions reduction [NASA-TN-78875] p0020 W78-26143

Results and status of the NASA aircraft engine emission reduction technology programs [NASA-TN-79009] p0022 W78-33102

PARTICLE INTERACTIONS
 Interaction of large, high power systems with operational orbit charged particle environments [NASA-TN-73867] p0037 W78-16076

PARTICLES
 WT AEROSOLS
 WT ANIONS
 WT ARGON PLASMA
 WT CHARGED PARTICLES
 WT COLLISIONLESS PLASMAS
 WT CYCLOTRON RADIATION
 WT DROPS (LIQUIDS)
 WT ELECTRON BEAMS
 WT ELECTRON PLASMA
 WT HYDROGEN PLASMA
 WT LASER PLASMAS
 WT METAL IONS
 WT MIST
 WT NEUTRAL PARTICLES
 WT PHOTOELECTRONS
 WT PROTONS
 WT PLASMA JETS
 WT PLASMAS (PHYSICS)
 WT POWDER (PARTICLES)
 WT TOROIDAL PLASMAS
 WT TRAPPED PARTICLES

Particle parameter analyzing system --- x-y plotter circuits and display [NASA-CASE-LEW-06094] p0096 W78-17293

PARTICULATE FILTERS
 U FLUID FILTERS

PASSENGER AIRCRAFT
 WT BOEING 747 AIRCRAFT

PAYLOADS
 WT AMPS (SATELLITE PAYLOAD)
 Ion beam plume and efflux characterization flight experiment study --- space shuttle payload [NASA-CR-135275] p0052 W78-12140

PDB (MODULATION)

SUBJECT INDEX

PDB (MODULATION)

U PULSE DURATION MODULATION

PENNING DISCHARGE

Probe studies in a modified Penning discharge
 p0173 A78-24904
 [NASA-TN-X-73631] p0171 W78-15905

PERFORMANCE

Test and evaluation of 23 electric vehicles for
 state-of-the-art assessment
 [NASA-TN-73850] p0178 W78-17937

PERFORMANCE PREDICTION

WT PREDICTION ANALYSIS TECHNIQUES

Synchronization of wind turbine generators against
 an infinite bus under gusting wind conditions
 [IEEE PAPER P 77 675-2] p0142 A78-30196

Design and calculated performance and cost of the
 ECAS Phase II open cycle RHD power generation
 system
 [ASAE PAPER 77-WA/ENER-5] p0174 A78-33143

Design considerations in mechanical face seals for
 improved performance. I - Basic configurations
 [ASAE PAPER 77-WA/LUB-3] p0119 A78-33183

Up-date of traveling wave tube improvements
 p0098 A78-33208

An overview of aerospace gas turbine technology of
 relevance to the development of the automotive
 gas turbine engine
 [SAE PAPER 780075] p0120 A78-33364

Performance and economics of advanced energy
 conversion systems for coal and coal-derived fuels
 p0146 A78-34078

Comparison of computer codes for calculating
 dynamic loads in wind turbines
 p0142 A78-37678

Medium power voltage multipliers with a large
 number of stages
 p0098 A78-45435

Performance potential of combined cycles
 integrated with low-Btu gasifiers for future
 electric utility applications
 [NASA-TN-73775] p0135 W78-23557

Effect of steady flight loads on JT9D-7
 performance deterioration
 [NASA-CR-135407] p0031 W78-29105

The practical impact of elastohydrodynamic
 lubrication
 [NASA-TN-78987] p0117 W78-33445

PERFORMANCE TESTS

A methodology for experimentally-based
 determination of gap shrinkage and effective
 lifetimes in the emitter and base of
 p-n-junction solar cells
 p0141 A78-10903

Status of the ERDA/NASA Photovoltaic Tests and
 Applications Project
 p0141 A78-11014

Evaluation of initial collector field performance
 at the Langley Solar Building Test Facility
 p0141 A78-11391

Test and evaluation of 23 electric vehicles for
 state-of-the-art assessment
 [SAE PAPER 780290] p0181 A78-33382

Acoustic evaluation of a novel swept-rotor fan
 [AIAA PAPER 78-1121] p0166 A78-41831

Performance characteristics of two annular dump
 diffusers using suction-stabilized vortex flow
 control
 p0107 A78-45431

U.S. terrestrial solar cell calibration and
 measurement procedures
 p0143 A78-52844

Experimental performance of a
 13.65-centimeter-tip-diameter tandem-bladed
 sweptback centrifugal compressor designed for a
 pressure ratio of 6
 [NASA-TP-1091] p0003 W78-11002

Design considerations in mechanical face seals for
 improved performance. 1: Basic configurations
 [NASA-TN-73735] p0113 W78-13439

Cold-air performance of a tip turbine designed to
 drive a lift fan. 3: Effect of simulated fan
 leakage on turbine performance
 [NASA-TP-1109] p0003 W78-16001

Baseline tests of the C. H. Waterman Beault 5
 electric passenger vehicle
 [NASA-TN-73759] p0178 W78-16928

Baseline tests of the AM General DJ-5E electric
 electric delivery van
 p0178 W78-16928

[NASA-TN-73750] p0178 W78-17933
 Baseline tests of the EVA change-of-pace coupe
 electric passenger vehicle
 [NASA-TN-73763] p0178 W78-17938

Baseline tests of the 1. A contractor electric
 passenger vehicle
 [NASA-TN-73762] p0179 W78-17939

Baseline tests of the batronic Minivan electric
 delivery van
 [NASA-TN-73761] p0179 W78-17940

Baseline tests of the C. H. Waterman DAF electric
 passenger vehicle
 [NASA-TN-73757] p0179 W78-17942

Evacuated load-bearing high performance insulation
 study
 [NASA-CR-135342] p0092 W78-18251

Performance characteristics of two annular dump
 diffusers using suction-stabilized vortex flow
 control
 [NASA-TN-73857] p0004 W78-19057

Baseline tests of the Volkswagen transporter
 electric delivery van
 [NASA-TN-73766] p0179 W78-20021

Performance of conventionally powered vehicles
 tested to an electric vehicle test procedure
 [NASA-TN-73768] p0179 W78-20022

Long-term CP6 engine performance deterioration:
 Evaluation of engine S/N 451-479
 [NASA-CR-135381] p0029 W78-20129

Performance of a short annular dump diffuser using
 suction-stabilized vortices at inlet Mach
 numbers to 0.41
 [NASA-TP-1194] p0017 W78-20131

Baseline tests of the BPC Hummingbird electric
 passenger vehicle
 [NASA-TN-73760] p0180 W78-21010

Preliminary evaluation of Glass Resin materials
 for solar cell cover use
 [NASA-TN-78925] p0137 W78-26544

Baseline tests of the Kordeh hybrid passenger
 vehicle
 [NASA-TN-73769] p0138 W78-26551

Long-term CP6 engine performance deterioration:
 Evaluation of engine S/N 451-380
 [NASA-CR-159390] p0031 W78-29103

A stirling engine computer model for performance
 calculations
 [NASA-TN-78884] p0180 W78-29994

Aerodynamic design and performance testing of an
 advanced 30 deg swept, eight bladed propeller at
 Mach numbers from 0.2 to 0.85
 [NASA-CR-3047] p0008 W78-32066

PERFUSSION

U DIFFUSION

PERIODIC ORBITS

U ORBITS

PERIODIC PROCESSES

U CYCLES

PERIODIC VARIATIONS

WT DIURNAL VARIATIONS

An analysis of the first two years of GASP data
 [NASA-TN-73817] p0148 W78-13669

PERIODICITY

U PERIODIC VARIATIONS

PERTURBATION

An automated procedure for calculating system
 matrices from perturbation data generated by an
 PAI Pacer and 100 hybrid computer system
 [NASA-TN-73869] p0156 W78-15729

PERTURBATION THEORY

Perturbation solutions for blade-to-blade surfaces
 of a transonic compressor
 p0008 A78-12307

Perturbation solutions for transonic flow on the
 blade-to-blade surface of compressor blade rows
 [NASA-CR-2941] p0001 W78-15987

PETROLEUM

U CRUDE OIL

PETROLEUM PRODUCTS

WT DIESEL FUELS

WT LUBRICATING OILS

Computer model for refinery operations with
 emphasis on jet fuel production. Volume 2:
 Data and technical bases
 [NASA-CR-135334] p0090 W78-19326

PHASE MODULATION

Closed loop solar array-ion thruster system with
 power control circuitry
 [NASA-CASE-LEW-12780-1] p0048 W78-22149

- PHASE TRANSFORMATIONS**
 NT BOILING
 NT COAL LIQUEFACTION
 NT FILM BOILING
 NT LEIDENFROST PHENOMENON
 NT NUCLEATE BOILING
 NT TRANSPIRATION
 NT VACUUM MELTING
 NT VAPORIZING
 The promise of eutectics for aircraft turbines
 [NASA-TN-73714] p0012 178-10098
- PHASED ARRAYS**
 Analysis and design of a high power laser adaptive
 phased array transmitter
 [NASA-CR-134952] p0111 178-13420
- PHOTOCHEMICAL REACTIONS**
 Effect of nitric oxide on photochemical ozone
 formation in mixtures of air with molecular
 chlorine and with trichlorofluoromethane
 [NASA-TP-1192] p0065 178-20281
 Apparatus for extraction and separation of a
 preferentially photo-dissociated molecular
 isotope into positive and negative ions by means
 of an electric field
 [NASA-CASE-LEU-12465-1] p0065 178-25148
- PHOTOCHEMISTRY**
 7 PHOTOCHEMICAL REACTIONS
- PHOTOCURRENTS**
 0 ELECTRIC CURRENT
- PHOTODETECTORS**
 0 PHOTOMETERS
- PHOTODISSOCIATION**
 Apparatus for extraction and separation of a
 preferentially photo-dissociated molecular
 isotope into positive and negative ions by means
 of an electric field
 [NASA-CASE-LEU-12465-1] p0065 178-25148
- PHOTOELECTRIC CELLS**
 NT PHOTOVOLTAIC CELLS
- PHOTOELECTROMAGNETIC DETECTORS**
 7 RADIATION MEASURING INSTRUMENTS
- PHOTOELECTRON SPECTROSCOPY**
 Principles of ESCA and applications to metal
 corrosion, coating and lubrication --- Electron
 Spectroscopy for Chemical Analysis
 p0061 178-33213
 Application of ESCA to the determination of
 stoichiometry in sputtered coatings and
 interface regions
 [NASA-TN-78896] p0065 178-26185
- PHOTOELECTRONS**
 X-ray photoelectron spectroscopic study of surface
 chemistry of dibenzyl disulfide on steel under
 mild and severe wear conditions
 p0066 178-31439
- PHOTOGRAPHY**
 NT AERIAL PHOTOGRAPHY
- PHOTOMETERS**
 NT ULTRAVIOLET SPECTROPHOTOMETERS
 A low cost, portable instrument for measuring
 exitance
 p0109 178-11392
- PHOTOMETRY**
 NT ELECTROPHOTOMETRY
- PROTONS**
 Solar cell collector
 [NASA-CASE-LEU-12552-1] p0136 178-25527
 Photon degradation effects in terrestrial solar
 cells
 [NASA-TN-78924] p0136 178-25551
- PHOTOPRODUCTION**
 Measurement of tropospheric 300 nm solar
 ultraviolet flux for determination of O₃/10/
 photoproduction rate
 p0148 178-38835
- PHOTOREDUCTION**
 0 PHOTOCHEMICAL REACTIONS
- PHOTOSENSORS**
 0 RADIATION MEASURING INSTRUMENTS
- PHOTOTHERMOTROPISM**
 3 TEMPERATURE EFFECTS
- PHOTOVOLTAGES**
 Photovoltaic village power application:
 Assessment of the near-term market
 [NASA-TN-73781] p0131 178-19647
 Photovoltaic water pumping applications:
 Assessment of the near-term market
 [NASA-TN-78847] p0134 178-19644
- PHOTOVOLTAIC CELLS**
 Real-time and accelerated outdoor endurance
 testing of solar cells
 p0142 178-52837
 The ERDA/LeRC Photovoltaic Systems Test Facility
 p0143 178-52851
 Real-time and accelerated outdoor endurance
 testing of solar cells
 [NASA-TN-73743] p0130 178-14628
 FS terrestrial solar cell calibration and
 measurement procedures
 [NASA-TN-73788] p0130 178-14629
 Solar energy meter
 [NASA-TN-73791] p0131 178-14630
 The ERDA/LeRC photovoltaic systems test facility
 [NASA-TN-73787] p0035 178-15059
 Photovoltaic refrigeration application:
 Assessment of the near-term market
 [NASA-TN-73876] p0131 178-16435
 Photovoltaic highway applications: Assessment of
 the near-term market
 [NASA-TN-73863] p0178 178-17235
 DOE LeRC photovoltaic systems test facility
 [NASA-TN-78923] p0138 178-26549
 Impact of Balance Of System (BOS) costs on
 photovoltaic power systems
 [NASA-TN-78939] p0138 178-26550
 Description and status of NASA-LeRC/DOE
 photovoltaic applications systems
 [NASA-TN-78936] p0139 178-26554
 Design and fabrication of a photovoltaic power
 system for the Papago Indian village of
 Schuchell (Gunsight), Arizona
 [NASA-TN-78948] p0139 178-26555
 An inverter/controller subsystem optimized for
 photovoltaic applications
 [NASA-TN-78903] p0180 178-26995
 Performance and stability analysis of a
 photovoltaic power system
 [NASA-TN-78880] p0140 178-29566
- PHOTOVOLTAIC CONVERSION**
 Status of the ERDA/NASA Photovoltaic Tests and
 Applications Project
 p0141 178-11014
 The Redox Flow System for solar photovoltaic
 energy storage
 p0141 178-11019
 Summary of the NASA space photovoltaic research
 and technology program
 p0130 178-13528
 Description and status of NASA-LeRC/DOE
 photovoltaic applications systems
 [NASA-TN-78936] p0139 178-26554
 Cost of photovoltaic energy systems as determined
 by balance-of-systems costs
 [NASA-TN-78957] p0139 178-27539
- PHOTOVOLTAIC EFFECT**
 Photovoltaic power system tests on an 8-kilowatt
 single-phase line-commutated inverter
 [NASA-TN-78824] p0134 178-19657
 Photovoltaic remote instrument applications:
 Assessment of the near-term market
 [NASA-TN-73881] p0150 178-19710
- PHOENIX OSCILLATIONS**
 0 OSCILLATIONS
- PHYSICAL PROPERTIES**
 Mechanical and physical properties of modern boron
 fibers
 p0085 178-33206
- PIPE FLOW**
 Two phase choke flow in tubes with very large L/D
 p0105 178-15824
 Turbulence processes and simple closure schemes
 p0107 178-40983
- PIPES (TUBES)**
 Fabrication of thin layer beta alumina
 [NASA-CR-135308] p0077 178-14143
 Evaluation of commercially-available
 spacecraft-type heat pipes
 [NASA-TN-78826] p0103 178-20459
 Fabrication of stainless steel clad tubing --- gas
 pressure bonding
 [NASA-CR-135347] p0079 178-21265
- PISTON ENGINES**
 NT DIESEL ENGINES
 General aviation piston-engine exhaust emission
 reduction
 p0013 178-11073

PITCHING ROBBETS

SUBJECT INDEX

PITCHING ROBBETS
 Pivoted pitch wind turbines p0133 W78-19638

PLATFORMS
 NT SIBC PLATFORMS

PLASMOGRAPHY
 U TOPOGRAPHY

PLANNING
 NT MISSION PLANNING
 NT PROJECT PLANNING

PLASMA ACCELERATION
 Mercury ion thruster research, 1977 --- plasma acceleration
 [NASA-CR-135317] p0052 W78-15167

PLASMA ARCS
 U PLASMA JETS

PLASMA CONDUCTIVITY
 Investigation of high voltage spacecraft system interactions with plasma environments
 [AIAA PAPER 78-672] p0050 A78-32750
 Inward transport of a toroidally confined plasma subject to strong radial electric fields
 [NASA-TN-73800] p0171 W78-10883

PLASMA CONFINEMENT
 U PLASMA CONTROL

PLASMA CONTROL
 Inward transport of a toroidally confined plasma subject to strong radial electric fields
 p0172 A78-24890
 A model for particle confinement in a toroidal plasma subject to strong radial electric fields
 p0173 A78-24891
 12-cm magneto-electrostatic containment argon/xenon ion source development
 [AIAA PAPER 78-681] p0039 A78-32756
 Effects of applied dc radial electric fields on particle transport in a bumpy torus plasma
 p0173 A78-36956
 Alternative approaches to plasma confinement
 p0174 A78-52186
 A model for particle confinement in a toroidal plasma subject to strong radial electric fields
 [NASA-TN-73814] p0171 W78-10884
 Parametric dependence of ion temperature and relative density in the NASA Lewis SORNA facility --- superconducting magnetic mirror
 [NASA-TN-73770] p0172 W78-23923

PLASMA DENSITY
 Inward transport of a toroidally confined plasma subject to strong radial electric fields
 p0172 A78-24890
 Lower hybrid emission diagnostics on the NASA Lewis Bumpy Torus
 p0171 A78-29332
 Effects of applied dc radial electric fields on particle transport in a bumpy torus plasma
 p0173 A78-36956

PLASMA DIAGNOSTICS
 Probe studies in a modified Penning discharge
 p0173 A78-24904
 Lower hybrid emission diagnostics on the NASA Lewis Bumpy Torus
 p0173 A78-29332
 Model for interpreting Doppler broadened optical line emission measurements on axially symmetric plasma
 p0174 A78-46189
 Lower hybrid emission diagnostics on the NASA Lewis bumpy torus
 [NASA-TN-73858] p0171 W78-19938
 A fluctuation-induced plasma transport diagnostic based upon fast-Fourier transform spectral analysis
 [NASA-TN-78932] p0172 W78-26926
 Fluctuation spectra in the NASA Lewis bumpy-torus plasma
 [NASA-TP-1257] p0172 W78-26927
 Low-frequency fluctuation spectra and associated particle transport in the NASA Lewis bumpy-torus plasma
 [NASA-TP-1258] p0172 W78-30944

PLASMA DIFFUSION
 Fluctuation spectra in the NASA Lewis bumpy-torus plasma
 [NASA-TP-1257] p0172 W78-26927
 Low-frequency fluctuation spectra and associated particle transport in the NASA Lewis bumpy-torus plasma
 [NASA-TP-1258] p0172 W78-30944

PLASMA DISCHARGES
 U PLASMA JETS

PLASMA DISPERSION
 U PLASMA DIFFUSION

PLASMA DYNAMICS
 Inward transport of a toroidally confined plasma subject to strong radial electric fields
 p0172 A78-24890

PLASMA FLOW
 U MAGNETOHYDRODYNAMIC FLOW

PLASMA FREQUENCIES
 Lower hybrid emission diagnostics on the NASA Lewis bumpy torus
 [NASA-TN-73858] p0171 W78-19938
 Microwave radiation measurements near the electron plasma frequency of the NASA Lewis bumpy torus plasma
 [NASA-TN-78940] p0172 W78-27914

PLASMA GENERATORS
 NT TOKAMAK DEVICES

PLASMA HEATING
 A model for particle confinement in a toroidal plasma subject to strong radial electric fields
 p0173 A78-24891

PLASMA INSTABILITY
 U MAGNETOHYDRODYNAMIC STABILITY

PLASMA INTERACTIONS
 NT PLASMA-ELECTROMAGNETIC INTERACTION
 Investigation of high voltage spacecraft system interactions with plasma environments
 [AIAA PAPER 78-672] p0050 A78-32750
 Spacecraft-generated plasma interaction with high voltage solar array
 [AIAA PAPER 78-673] p0055 A78-32751
 The Plasma Interaction Experiment (PIE) - description and flight qualification test program
 [AIAA PAPER 78-674] p0051 A78-32752
 Solar electric propulsion thruster interactions with solar arrays
 [NASA-CR-135257] p0052 W78-13122
 The effect of environmental plasma interactions on the performance of the solar sail system
 [NASA-CR-135258] p0098 W78-13325
 The Plasma Interaction Experiment (PIE) description and test program --- electrometers
 [NASA-TN-78863] p0041 W78-21188
 Investigation of high voltage spacecraft system interactions with plasma environments
 [NASA-TN-78831] p0097 W78-21373

PLASMA JETS
 Probe studies in a modified Penning discharge
 p0173 A78-24904
 Temperature distributions of a cesium-seeded hydrogen-oxygen supersonic free jet
 [NASA-TP-1162] p0171 A78-20959

PLASMA PHYSICS
 Experiments on whistler wave filamentation and VLF hiss in a laboratory plasma
 p0189 A78-41788
 Charge-exchange plasma generated by an ion thruster
 [NASA-CR-135318] p0052 W78-13123
 ERDA/NASA advanced thermal technology program
 [NASA-CR-157117] p0145 W78-24674

PLASMA PROBES
 Probe studies in a modified Penning discharge
 p0173 A78-24904

PLASMA RADIATION
 Lower hybrid emission diagnostics on the NASA Lewis Bumpy Torus
 p0173 A78-29332

PLASMA RINGS
 U TOROIDAL PLASMAS

PLASMA SPRAYING
 Two-layer thermal barrier coating for high temperature components
 [ACS PAPER 31-BEN-76P] p0084 A78-18787
 Friction and wear of several compressor gas-path seal movements
 [NASA-TP-1128] p0068 W78-15229
 Development of a plasma sprayed ceramic gas path seal for high pressure turbine application
 [NASA-CR-135387] p0030 W78-24141

PLASMA STABILITY
 U MAGNETOHYDRODYNAMIC STABILITY

PLASMA THEORY
 U PLASMA PHYSICS

PLASMA-ELECTROMAGNETIC INTERACTION
 Inward transport of a toroidally confined plasma subject to strong radial electric fields

SUBJECT INDEX

POLYIMIDES

- PH-718001 p0171 A78-10883
 PLASMA (PHYSICS)
 NT COLLISIONLESS PLASMAS
 NT ELECTRON PLASMA
 NT HYDROGEN PLASMA
 NT LASER PLASMAS
 Probe studies in a modified peening discharge
 [NASA-TN-I-73631] p0171 A78-15905
 PLASMAS-IN-SPACE PAYLOAD
 7 ANPS (SATELLITE PAYLOAD)
 PLASMOIDS
 9 PLASMAS (PHYSICS)
 PLASTIC DEFORMATION
 Lamination residual strains and stresses in hybrid
 laminates p0128 A78-12071
 Strength enhancement process for prealloyed powder
 superalloys p0075 A78-33216
 PLASTIC FILMS
 7 POLYMERIC FILMS
 PLASTIC PROPERTIES
 NT ELASTOPLASTICITY
 NT SUPERPLASTICITY
 PLASTIC YIELDING
 3 PLASTIC DEFORMATION
 PLASTICIZERS
 Inorganic-organic separators for alkaline batteries
 [NASA-CASE-LEW-12649-1] p0136 A78-25530
 PLASTICS
 NT ADDITION RESINS
 NT CARBON FIBER REINFORCED PLASTICS
 NT EPOXY RESINS
 NT POLYAMIDE RESINS
 NT POLYETHYLENE
 NT POLYTETRAFLUOROETHYLENE
 NT POLYVINYL ALCOHOL
 NT TEFLON (TFE/DMARK)
 NT THERMOPLASTIC RESINS
 PLASTISOLS
 NT SMOKE
 PLATE (METAL)
 7 METAL PLATES
 PLATES (STRUCTURAL MEMBERS)
 NT ANISOTROPIC PLATES
 NT CIRCULAR PLATES
 PLIES
 3 LAYERS
 PLOTTERS
 NT X-Y PLOTTERS
 PLUG NOZZLES
 Wind tunnel performance tests of conical plug
 nozzles --- in the Langley 8 x 6 ft. supersonic
 wind tunnel [NASA-CR-2990] p0002 A78-21044
 FLUORANE
 7 LEAD COMPOUNDS
 3 METAL HYDRIDES
 FLUORINE
 Ion beam plume and efflux measurements of an 8-cm
 mercury ion thruster [AIAA PAPER 78-676] p0055 A78-32753
 FLYWOOD
 In situ ply strengths - An initial assessment
 p0061 A78-33223
 POINT MATCHING METHOD (MATHEMATICS)
 0 BOUNDARY VALUE PROBLEMS
 POINT TO POINT COMMUNICATIONS
 Millimeter wave satellite concepts, volume 1
 [NASA-CR-135227] p0041 A78-15144
 POLARIZATION CURRENTS
 7 GRAPHENE QUANTUM
 POLICIES
 NT ENERGY POLICY
 POLLUTANTS
 3 CONTAMINANTS
 POLLUTION
 NT AIR POLLUTION
 POLLUTION CONTROL
 Preliminary QCEP program - Test results --- Quiet
 Clean Short-haul Experimental Engine
 [SME PAPER 771009] p0023 A78-23840
 State-of-the-art of turbofan engine noise control
 p0024 A78-35652
 Combustor concepts for aircraft gas turbine
 low-power emissions reduction
 [AIAA PAPER 78-999] p0025 A78-43546
 Aircraft engine emissions --- conference
 [NASA-CR-2021] p0012 A78-11063
 Emissions reduction technology program
 p0012 A78-11065
 Pollution reduction technology program for class
 T4 (JT8D) engines p0013 A78-11067
 Summary of emissions reduction technology programs
 p0013 A78-11071
 Emissions control for ground power gas turbines
 p0013 A78-11072
 General aviation piston-engine exhaust emission
 reduction p0013 A78-11073
 Global atmospheric sampling program p0013 A78-11076
 Stratospheric cruise emission reduction program
 p0013 A78-11077
 Advanced low-NO(x) combustors for supersonic
 high-altitude gas turbines p0014 A78-11078
 Augmentor emissions reduction technology program
 --- for turbofan engines
 [NASA-CR-135215] p0027 A78-13057
 Reduction of aircraft gas turbine engine pollutant
 emissions p0019 A78-22098
 QCEP task 2: Engine and installation preliminary
 design [NASA-CR-134738] p0030 A78-23089
 Gas turbine engine emission reduction technology
 program p0001 A78-27058
 Supercritical fuel injection system
 [NASA-CASE-LEW-12990-1] p0020 A78-27122
 Effect of inlet temperature on the performance of
 a catalytic reactor --- air pollution control
 [NASA-TN-78977] p0141 A78-31534
 Aircraft gas turbine low-power emissions reduction
 technology program [NASA-CR-135434] p0032 A78-32097
 Pollution Reduction Technology Program for small
 jet aircraft engines, phase 2
 [NASA-CR-159415] p0032 A78-33104
 POLLUTION MONITORING
 Description and review of global measurements of
 atmospheric species from GASP p0148 A78-24893
 POLYAMIDE RESINS
 Fiber reinforced PBR polyimide composites
 [NASA-CR-135377] p0063 A78-25132
 Some load limits and self-lubricating properties
 of plain spherical bearings with molded graphite
 fiber reinforced polyimide liners to 320 C
 [NASA-TN-78935] p0116 A78-26445
 POLYATOMIC MOLECULES
 NT DIATOMIC MOLECULES
 POLYCRYSTALS
 Friction and wear of single-crystal and
 polycrystalline manganese-zinc ferrite in contact
 with various metals [NASA-TP-1059] p0080 A78-10295
 POLYETHYLENES
 Friction and wear of polyethylene oxide polymer
 having a range of molecular weights
 [NASA-TP-1129] p0080 A78-15278
 POLYIMIDE RESINS
 Effect of processing parameters on autoclaved PBR
 polyimide composites p0060 A78-25191
 Kinetics of imidization and crosslinking in
 PBR-polyimide resin --- Polymerization of
 Monomer Reactants p0061 A78-33210
 Kinetics of imidization and crosslinking in
 PBR-polyimide resin [NASA-TN-78884] p0082 A78-23231
 Graphite-fiber-reinforced polyimide liners of
 various compositions in plain spherical bearings
 [NASA-TN-78908] p0116 A78-26447
 POLYIMIDES
 NT KAPTON (TRADEMARK)
 Effect of thermal exposure on lubricating
 properties of polyimide films and
 polyimide-bonded graphite fluoride films
 [NASA-TP-1125] p0080 A78-15277
 PBR polyimide prepreg with improved tack
 characteristics [NASA-TN-73898] p0081 A78-17221

POLYMER CHEMISTRY

Some effects of composition on friction and wear of graphite-fiber-reinforced polyimide liners in plain spherical bearings
[NASA-TP-1229] p0115 N78-25433

Synthesis of perfluoroalkylene aromatic diazines
[NASA-CR-159403] p0087 N78-31235

POLYMER CHEMISTRY

Trimerization of aromatic nitriles
[NASA-CASE-LEW-12053-1] p0080 N78-15276

In situ self cross-linking of polyvinyl alcohol battery separators
[NASA-CASE-LEW-12972-1] p0056 N78-22157

POLYMERIC FILMS

NT KAPTON (TRADERMARK)

Ion beam sputter etching and deposition of fluoropolymers
[NASA-TN-78888] p0088 N78-24358

Technological development of cylindrical and flat shaped high energy density capacitors --- using polymeric films
[NASA-CR-135286] p0099 N78-24458

Ion beam sputtering of fluoropolymers --- etching polymer films and target surfaces
[NASA-TN-79000] p0060 N78-33454

POLYMERIZATION

Kinetics of isidization and crosslinking in PBR-polyimide resin --- Polymerization of Monomer Reactants
p0061 A78-33210

Kinetics of isidization and crosslinking in PBR-polyimide resin
[NASA-TN-78844] p0082 N78-23231

POLYTETRAFLUOROETHYLENE

Ion beam sputter etching and deposition of fluoropolymers
p0085 A78-37684

Ion beam sputter etching and deposition of fluoropolymers
[NASA-TN-78888] p0088 N78-24358

POLYVINYL ALCOHOL

In situ self cross-linking of polyvinyl alcohol battery separators
[NASA-CASE-LEW-12972-1] p0056 N78-22157

POROUS MATERIALS

High resolution masks for ion milling pores through substrates of biological interest
[NASA-CR-135435] p0092 N78-29276

PORTABLE EQUIPMENT

Utilization of NASA Lewis mobile terminals for the Hermes satellite
[NASA-TN-73859] p0093 N78-15326

POSITION (LOCAT. ON)

Calculation of far-field jet noise spectra from near-field measurements using true source location
[AIAA PAPER 78-1153] p0168 A78-41852

On the localness of the spectral energy transfer in turbulence
[NASA-TN-73824] p0101 N78-13361

Effects of rotor location, coning, and tilt on critical loads in large wind turbines
p0133 N78-19636

POTASSIUM

NT LIQUID POTASSIUM

POTASSIUM CHLORIDES

Volatile products from the interaction of KCl(g) with Cr₂O₃ and LaCrO₃ in oxidizing environments --- gas turbine engines
p0066 A78-24887

Volatile products from the interaction of KCl(g) with Cr₂O₃ and LaCrO₃ in oxidizing environments
[NASA-TN-73796] p0064 N78-13158

POTASSIUM COMPOUNDS

NT POTASSIUM CHLORIDES

Formation of Na₂SO₄ and K₂SO₄ in flames doped with sulfur and alkali chlorides and carbonates
p0066 A78-24889

POTENTIAL ENERGY

NT PHOTOVOLTAGES

POTENTIAL FLOW

Development and test of an inlet and duct to provide airflow for a wing boundary layer control system
[AIAA PAPER 78-141] p0086 A78-20701

A combined potential and viscous flow solution for V/STOL engine inlets
[AIAA PAPER 78-142] p0086 A78-20702

POWDER (PARTICLES)

NT METAL POWDER

SUBJECT INDEX

Ceramics in gas turbines - Powder and process characterization
p0085 A78-29328

Effect of attrition milling on the reaction sintering of silicon nitride
p0086 A78-50324

Ceramics in gas turbine: Powder and process characterization
[NASA-TN-73875] p0016 N78-17059

POWDER METALLURGY

An experimental P/N wrought superalloy for advanced temperature service
p0073 A78-15335

Improved performance of silicon nitride-based high temperature ceramics
p0087 A78-24881

Strength enhancement process for prealloyed powder superalloys
p0075 A78-33216

Cleaning process for contaminated superalloy powders
p0076 A78-41400

Strength enhancement process for prealloyed powder superalloys
[NASA-TN-78834] p0070 N78-21266

Evaluation of cyclic behavior of aircraft turbine disk alloys
[NASA-CR-159433] p0128 N78-33478

POWDERED METALS

J METAL POWDER

POWER CONDITIONING

Solid State Resonant Power Controllers for high voltage DC distribution systems
p0100 A78-15574

Discrete time domain modelling and analysis of ac-dc converters with continuous and discontinuous inductor current
p0100 A78-18796

A mechanical, thermal and electrical packaging design for a prototype power management and control system for the 30 cm mercury ion thruster
[AIAA PAPER 78-685] p0051 A78-32759

Electrical Prototype Power Processor for the 30-cm Mercury electric propulsion engine
[AIAA PAPER 78-684] p0055 A78-37439

Photovoltaic village power application: Assessment of the near-term market
[NASA-TN-73893] p0133 N78-19643

The 30-cm ion thruster power processor
[NASA-CR-135401] p0054 N78-24280

POWER EFFICIENCY

Medium power voltage multipliers with a large number of stages
p0098 A78-45435

Study of 42 and 85 GHz coupled cavity traveling-wave tubes for space use
[NASA-CR-134670] p0098 N78-11295

POWER GENERATORS

J ELECTRIC GENERATORS

POWER PROCESSING SYSTEMS

J POWER CONDITIONING

POWER SUPPLY CIRCUITS

High frequency capacitor-diode voltage multiplier Jc-dc converter development
[NASA-CR-135309] p0099 N78-15400

Extended performance electric propulsion power processor design study. Volume 1: Executive summary
[NASA-CR-135357] p0054 N78-20250

Closed loop solar array-ion thruster system with power control circuitry
[NASA-CASE-LEW-12780-1] p0048 N78-22149

POWER TRANSMISSION

A mechanical, thermal and electrical packaging design for a prototype power management and control system for the 30 cm mercury ion thruster
[NASA-TN-78862] p0049 N78-23142

POWDERED LIFT AIRCRAFT

Effects of nozzle design and power on cruise drag for upper-surface-blowing aircraft
p0004 N78-24058

Analytical modeling of under-the-wing externally blown flap powered-lift noise
p0004 N78-24063

Overview of the QCSSE program
p0004 N78-24064

Acoustic design of the QCSSE propulsion systems
p0004 N78-24067

Inlet technology for powered-lift aircraft
p0005 N78-24069

- Reverse-thrust technology for variable-pitch fan propulsion systems p0005 W78-24070
- PREBURNERS**
Preburner of staged combustion rocket engine [NASA-CR-135356] p0054 W78-24279
- PRECIPITATION HARDENING**
Tensile and creep properties of the experimental oxide dispersion strengthened iron-base sheet alloy NA-956E at 1365 K p0074 A78-21858
- PREDICTION ANALYSIS TECHNIQUES**
Calculation of far-field jet noise spectra from near-field measurements using true source location [AIAA PAPER 78-1153] p0168 A78-41852
Predicted and experimental performance of jet-lubricated 120-millimeter-bore ball bearings operating to 2.5 million DN [NASA-TP-1196] p0114 W78-20513
A method for calculating strut and splitter plate noise in exit ducts: Theory and verification [NASA-CR-1555] p0167 W78-20921
Three-dimensional effects on pure tone fan noise due to inflow distortion --- rotor blade noise prediction [NASA-TN-78565] p0164 W78-24898
Computer model for refinery operations with emphasis on jet fuel production. Volume 1: Detailed systems and programming documentation [NASA-CR-135335] p0090 W78-25235
- PREDICTIONS**
NT PERFORMANCE PREDICTION
- PREHEATERS**
1 HEATING EQUIPMENT
- PREMIXED FLAMES**
Degree of vaporization using an airblast type fuel injector for a premixed-prevaporized combustor p0107 A78-50322
Experimental study of the effects of flameholder geometry on emissions and performance of lean premixed combustors [NASA-CR-135424] p0030 W78-26147
- PREPOLYMERS**
NT TRIMERS
- PRESENTING**
1 SINTERING
- PRESSING (FORMING)**
Consolidation of silicon nitride without additives [NASA-TN-73693] p0057 W78-10217
- PRESSURE**
NT FLUID PRESSURE
NT GAS PRESSURE
NT HIGH PRESSURE
NT IMPACT LOADS
NT INTERNAL PRESSURE
NT ISOSTATIC PRESSURE
NT SUPERCRITICAL PRESSURES
NT VAPOR PRESSURE
NT WALL PRESSURE
- PRESSURE CHAMBERS**
NT VACUUM CHAMBERS
- PRESSURE DISTRIBUTION**
Numerical spatial marching techniques for estimating duct attenuation and source pressure profiles p0166 A78-37632
Numerical spatial marching techniques for estimating duct attenuation and source pressure profiles [NASA-TN-78957] p0103 W78-21329
Reverse-flow combustor for small gas turbines with pressure-atomizing fuel injectors [NASA-TP-1260] p0021 W78-27130
Elastohydrodynamic lubrication of elliptical contacts for materials of low elastic modulus. 2: Starved conjunction [NASA-TP-1271] p0117 W78-29458
Design and overall performance of four highly loaded, high speed inlet stages for an advanced high-pressure-ratio core compressor [NASA-TP-1337] p0022 W78-33108
- PRESSURE EFFECTS**
Design considerations in mechanical face seals for improved performance. I - Basic configurations [AIAA PAPER 77-WA/LUR-3] p0119 A78-33183
Effects of pressure and temperature on hot pressing a sialon [NASA-TN-78945] p0083 W78-27274
- PRESSURE FIELDS**
0 PRESSURE DISTRIBUTION
PRESSURE MEASUREMENTS
Experimental performance of a 13.65-centimeter-tip-diameter tandem-bladed sweptback centrifugal compressor designed for a pressure ratio of 6 [NASA-TP-1091] p0003 W78-11002
Combustor fluctuating pressure measurements in engine and in a component test facility: A preliminary comparison [NASA-TN-73805] p0035 W78-13077
TACTI, a computer program for the transient thermal analysis of a cooled turbine blade or vane equipped with a coolant insert. 1. Users manual [NASA-TP-1271] p0104 W78-28374
Correlation of combustor acoustic power levels inferred from internal fluctuating pressure measurements [NASA-TN-78986] p0165 W78-31871
- PRESSURE OSCILLATIONS**
Combustor fluctuating pressure measurements in-engine and in a component test facility - A preliminary comparison p0023 A78-24878
- PRESSURE REDUCTION**
Release of dissolved nitrogen from water during depressurization p0066 A78-33224
Release of dissolved nitrogen from water during depressurization [NASA-TN-73822] p0065 W78-17172
- PRESSURE REGULATORS**
The design of hydraulic pressure regulators that are stable without the use of sensing line restrictors or frictional dampers p0154 A78-24897
The design of hydraulic pressure regulators that are stable without the use of sensing line restrictors or frictional dampers [NASA-TN-X-73687] p0101 W78-10415
Applied South approximation [NASA-TP-1231] p0091 W78-22257
Flow compensating pressure regulator [NASA-CASE-LEW-12718-1] p0104 W78-25351
- PRESSURE VESSELS**
NT PREBURNERS
Recent advance in lightweight, filament-wound composite pressure vessel technology p0061 A78-33436
Acoustic emission testing of composite vessels under sustained loading [NASA-TN-78981] p0059 W78-33150
- PRESSURE WELDING**
NT DIFFUSION WELDING
- PRETESTS**
0 TESTS
- PREVENTION**
NT CORROSION PREVENTION
- PRIMARY BATTERIES**
NT ALKALINE BATTERIES
NT NICKEL ZINC BATTERIES
- PRIVATE AIRCRAFT**
1 GENERAL AVIATION AIRCRAFT
- PROBABILITY**
0 PROBABILITY THEORY
PROBABILITY DENSITY FUNCTIONS
NT WEIBULL DENSITY FUNCTIONS
PROBABILITY THEORY
Chain Pooling modeling selection as developed for the statistical analysis of a rotor burst protection experiment [NASA-TN-73874] p0160 W78-16735
- PROBLEM SOLVING**
NT ITERATIVE SOLUTION
- PROCEDURES**
NT FINITE ELEMENT METHOD
NT OPTICAL CORRECTION PROCEDURE
- PROCESSORS (COMPUTERS)**
0 CENTRAL PROCESSING UNITS
- PRODUCTION ENGINEERING**
Dendritic web silicon for solar cell application p0146 A78-53489
Ceramics in gas turbine: Powder and process characterization [NASA-TN-73875] p0016 W78-17059
Computer model for refinery operations with emphasis on jet fuel production. Volume 1:

PRODUCTION MANAGEMENT

SUBJECT INDEX

Program description
[NASA-CR-135333] p0090 W78-20350

PRODUCTION MANAGEMENT

Cost analysis of advanced turbine blade
manufacturing processes
[NASA-CR-135203] p0026 W78-10092

PRODUCTION METHODS

PRODUCTION ENGINEERING

PRODUCTS

WT PETROLEUM PRODUCTS

PROGRAM MANAGEMENT

PROJECT MANAGEMENT

PROGRAMMING LANGUAGES

WT FORTRAN

User's guide for SPTRAW/360
[NASA-TP-1006] p0156 W78-10746

PROGRAMS

WT CENTAUR PROJECT

WT GLOBAL ATMOSPHERIC RESEARCH PROGRAM

WT NASA PROGRAMS

WT QUIET ENGINE PROGRAM

WT SUPERSONIC CROSS AIRCRAFT RESEARCH

PROJECT MANAGEMENT

Pollution reduction technology program for class
T8 (JT8D) engines p0013 W78-11067

PROJECT PLANNING

CTS (Hermes): United States experiments and
operations summary
[NASA-TN-73830] p0041 W78-13107

VCR testbed program planning and definition study
[NASA-CR-135362] p0029 W78-19160

PROJECTS

WT CENTAUR PROJECT

PROPAGATION (EXTENSION)

WT CRACK PROPAGATION

WT PLANE PROPAGATION

PROPAGATION MODES

Optimal wall impedance for spinning modes - A
correlation with mode cut-off ratio
[AIAA PAPER 78-193] p0165 A78-20735

Far-field multimodal acoustic radiation directivity
--- from ducted bodies
[NASA-TN-73839] p0163 W78-13855

PROPANE

Performance and emissions of a catalytic reactor
with propane, diesel, and Jet A fuels
[NASA-TN-73786] p0088 W78-14177

Lean combustion limits of a confined
premixed-prevaporized propane jet
[NASA-TN-78868] p0019 W78-22099

PROPELLANT COMBUSTION

Preburner of staged combustion rocket engine
[NASA-CR-135356] p0054 W78-24279

PROPELLANT TANKS

Constrained sloshing of liquid mercury in a
flexible spherical tank
[AIAA PAPER 78-670] p0106 A78-32749

Comparison of reusable insulation systems for
cryogenically-tanked earth-based space vehicles
[AIAA PAPER 78-877] p0044 W78-36004

An ultralightweight, evacuated, load-bearing,
high-performance insulation system --- for
cryogenic propellant tanks
[AIAA PAPER 78-878] p0045 A78-36005

Purging of a tank-mounted multilayer insulation
system by gas diffusion
[NASA-TP-1127] p0041 W78-17127

PROPELLANT TRANSFER

Effect of vibration on retention characteristics
of screen acquisition system --- for surface
tension propellant acquisition
[AIAA PAPER 78-1030] p0045 A78-43560

PROPELLANTS

WT GASEOUS ROCKET PROPELLANTS

WT LIQUID ROCKET PROPELLANTS

PROPELLER BLADES

A parametric investigation of an existing
supersonic relative tip speed propeller noise
model --- turboprop aircraft
[NASA-TN-73816] p0163 W78-13854

Design of impact-resistant boron/aluminum large
fan blade
[NASA-CR-135417] p0031 W78-29104

Aerodynamic design and performance testing of an
advanced 10 deg swept, eight bladed propeller at
Mach numbers from 0.2 to 0.85
[NASA-CR-1047] p0008 W78-32066

PROPELLER PANS

Variation of fan tone steadiness for several
inflow conditions
[AIAA PAPER 78-1119] p0166 A78-41829

Variation of fan tone steadiness for several
inflow conditions
[NASA-TN-78886] p0164 W78-26878

PROPELLERS

WT PROPELLER PANS

WT VARIABLE PITCH PROPELLERS

PUSPULSION

WT AUXILIARY PUSPULSION

WT ELECTRIC PUSPULSION

WT HYBRID PUSPULSION

WT ION PUSPULSION

WT JET PUSPULSION

WT NUCLEAR ELECTRIC PUSPULSION

WT SOLAR ELECTRIC PUSPULSION

WT SPACECRAFT PUSPULSION

PUSPULSION SYSTEM CONFIGURATIONS

30-cm mercury ion thruster performance with a 1 kV
capacitor-diode voltage multiplier beam supply
[AIAA PAPER 78-686] p0051 A78-32760

NASA engine system technology programs - An overview
[AIAA PAPER 78-928] p0025 A78-88452

Advanced supersonic propulsion study, phase 4
[NASA-CR-135273] p0026 W78-11062

Linear aerospoke engine study --- for reusable
launch vehicles
[NASA-CR-135231] p0026 W78-11082

Evolution of the 1-mlb mercury ion thruster
subsystem
[NASA-TN-73733] p0047 W78-21202

Acoustic design of the QCSEE propulsion systems
p0004 W78-24067

Reverse-thrust technology for variable-pitch fan
propulsion systems p0005 W78-24070

Computer programs for calculating two-dimensional
potential flow in and about propulsion system
inlets
[NASA-TN-78930] p0005 W78-27083

PUSPULSION SYSTEM PERFORMANCE

A review of NASA's propulsion programs for civil
aviation
[AIAA PAPER 78-43] p0023 A78-20651

Planned flight test of a mercury ion auxiliary
propulsion system. II - Integration with host
spacecraft
[AIAA PAPER 78-647-II] p0050 A78-32735

5200 cycle of an 8-cm diameter Hg ion thruster
[AIAA PAPER 78-649] p0050 A78-32736

Instrumentation for propulsion systems development
[SAE PAPER 780076] p0109 A78-33365

Extended performance solar electric propulsion
thrust system design
[AIAA PAPER 78-643] p0055 A78-37430

Extended performance solar electric propulsion
thrust system study. Volume 1: Executive summary
[NASA-CR-135281-VOL-1] p0052 W78-10205

Advanced supersonic propulsion study, phases 3 and 4
--- variable cycle engines
[NASA-CR-135236] p0027 W78-13058

Preliminary study of propulsion systems and
airplane wing parameters for a US Navy subsonic
V/STOL aircraft
[NASA-TN-73652] p0010 W78-17041

Instrumentation for propulsion systems development
--- high speed fans and turbines
[NASA-TN-73840] p0011 W78-17052

Baseline tests of the power-train electric
delivery van
[NASA-TN-73765] p0178 W78-17936

Variable mixer propulsion cycle
[NASA-CASE-LEW-12917-1] p0016 W78-18067

State-of-the-art assessment of electric vehicles
and hybrid vehicles
[NASA-TN-73756] p0179 W78-18988

Airflow and thrust calibration of an F100 engine,
S/N P680059, at selected flight conditions
[NASA-TP-1069] p0018 W78-21112

Planned flight test of a mercury ion auxiliary
propulsion system. 1: Objectives, systems
descriptions, and mission operations
[NASA-TN-73759] p0047 W78-21204

QCSEE task 2: Engine and installation preliminary
design
[NASA-CR-134738] p0030 W78-23089

SUBJECT INDEX

RADIATION DISTRIBUTION

- Impact of future fuel properties on aircraft engines and fuel systems
[NASA-TN-78866] p0089 W78-24369
- JT90 engine diagnostics. Task 2: Feasibility study of measuring in-service flight loads --- 747 aircraft performance
[NASA-CR-135395] p0030 W78-27124
- Real time digital propulsion system simulation for manned flight simulators
[NASA-TN-78958] p0034 W78-27137
- PROPULSIVE EFFICIENCY**
Propulsion --- NASA program for aircraft fuel consumption reduction
p0025 A78-43360
- SEP ENCKE-87 and Halley rendezvous studies and improved S/C model implementation in HILTOP
[NASA-CR-135414] p0038 W78-25105
- ACEE propulsion overview
p0001 W78-27048
- PROSTHETIC DEVICES**
Mechanical properties of ion-beam-textured surgical implant alloys
[NASA-TN-73742] p0068 W78-13181
- PROTECTION**
NT CIRCUIT PROTECTION
NT CORROSION PREVENTION
NT RADIATION SHIELDING
NT THERMAL PROTECTION
- PROTECTIVE COATINGS**
NT CERAMIC COATINGS
Two-layer thermal barrier coating for high temperature components
[ACS PAPER 31-BEN-76P] p0084 A78-18787
- The effect of NaCl/H₂O on the Na2SO4-induced hot corrosion of NiAl
p0079 A78-24901
- Composition of RF-sputtered refractory compounds determined by X-ray photoelectron spectroscopy
p0085 A78-30301
- Reaction diffusion in the NiCrAl and CoCrAl systems
p0077 A78-53063
- High temperature surface protection --- 10 gas turbines
[NASA-TN-73877] p0102 W78-17340
- Coatings for wear and lubrication
[NASA-TN-78841] p0081 W78-20333
- Progress in advanced high temperature turbine materials, coatings, and technology
p0013 W78-21122
- Improved reaction sintered silicon nitride --- protective coatings to improve oxidation resistance
[NASA-CR-135291] p0063 W78-22164
- The friction and wear properties of sputtered hard refractory compounds
[NASA-TN-78895] p0056 W78-26177
- Preliminary evaluation of Glass Resin materials for solar cell cover use
[NASA-TN-78925] p0137 W78-26544
- Evaluation of glass resin coatings for solar cell applications
[NASA-CR-159392] p0145 W78-27540
- High resolution masks for ion milling pores through substrates of biological interest
[NASA-CR-135435] p0092 W78-29276
- PROTOTYPES**
Electrical Prototype Power Processor for the 30-cm Mercury electric propulsion engine
[AIAA PAPER 78-684] p0055 A78-37439
- PULSATING FLOW**
O UNSTEADY FLOW
- PULSE COMMUNICATION**
NT DIGITAL SPACECRAFT TELEVISION
A digitally implemented communications experiment utilizing the Hermes /CTS/ satellite
p0094 A78-24984
- A digitally implemented communications experiment utilizing the Hermes (CTS) satellite
[NASA-TN-73827] p0093 W78-13283
- PULSE DURATION MODULATION**
Electric vehicle power train instrumentation --- some constraints and considerations
[FVC PAPER 7744] p0097 A78-16922
- PULSE MODULATION**
NT PULSE DURATION MODULATION
- PULSE RECORDERS**
O COUNTERS
- PULSE TIME MODULATION**
NT PULSE DURATION MODULATION
- PULSE WIDTH MODULATION**
O PULSE DURATION MODULATION
- PULSES**
NT ELECTRIC PULSES
- PUMPS**
NT AXIAL FLOW PUMPS
NT TURBINE PUMPS
- PURGING**
Purging of a tank-mounted multilayer insulation system by gas diffusion
[NASA-TP-1127] p0041 W78-17127
- PURIFICATION**
Targets for producing high purity I-123
[NASA-CASR-LRW-10518-3] p0065 W78-27226
- PURIFIERS**
J PURIFICATION
- PWM (MODULATION)**
J PULSE DURATION MODULATION
- PYROGRAPHALLOY**
O COMPOSITE MATERIALS
O REFRACTORY MATERIALS
- PYROMETRY**
O TEMPERATURE MEASUREMENT
- Q**
- QUALITATIVE ANALYSIS**
Hydrocarbon group type determination in jet fuels by high performance liquid chromatography
p0089 A78-24906
- QUALITY**
NT AIR QUALITY
- QUANTITATIVE ANALYSIS**
Quantitative ultrasonic evaluation of mechanical properties of engineering materials
[NASA-TN-78905] p0124 W78-24565
- QUANTIFIER**
O COUNTERS
- QUIET ENGINE PROGRAM**
Preliminary QCSEE program - Test results --- Quiet Clean Short-haul Experimental Engine
[SAE PAPER 771008] p0023 A78-23840
- Preliminary QCSEE program test results
[NASA-TN-73732] p0015 W78-15042
- Filament-winding fabrication of QCSEE configuration fan blades
[NASA-CR-135332] p0028 W78-16052
- QCSEE task 2: Engine and installation preliminary design
[NASA-CR-134738] p0030 W78-23089
- Overview of the QCSEE program
p0004 W78-24066
- Acoustic design of the QCSEE propulsion systems
p0004 W78-24067
- R**
- RADIAL DISTRIBUTION**
Effects of applied dc radial electric fields on particle transport in a bumpy torus plasma
p0173 A78-36956
- Low-frequency fluctuation spectra and associated particle transport in the NASA Lewis bumpy-torus plasma
[NASA-TP-1258] p0172 W78-30944
- RADIAL FLOW**
Analysis of the cross flow in a radial inflow turbine scroll
[NASA-CR-135320] p0029 W78-19153
- Computer program for the analysis of the cross flow in a radial inflow turbine scroll
[NASA-CR-135321] p0029 W78-19154
- RADIATION CHEMISTRY**
NT PHOTODISSOCIATION
- RADIATION COUNTERS**
Particle parameter analyzing system --- x-y plotter circuits and display
[NASA-CRSE-ILE-06094] p0096 W78-17293
- RADIATION DAMAGE**
Potential damage to DC superconducting magnets due to the high frequency electromagnetic waves
[NASA-TN-73808] p0096 W78-13330
- Solar Cell High Efficiency and Radiation Damage
[NASA-CR-2020] p0130 W78-13527
- RADIATION DISTRIBUTION**
Far-field multimodal acoustic radiation directivity
p0165 A78-24876
- Far-field multimodal acoustic radiation directivity --- from ducted bodies

RADIATION EFFECTS

SUBJECT INDEX

[NASA-TN-73839] p0163 W78-13855
RADIATION EFFECTS
 WT RADIATION DAMAGE
RADIATION FIELDS
 J RADIATION DISTRIBUTION
RADIATION MEASUREMENT
 Microwave radiation measurements near the electron
 plasma frequency of the NASA Lewis cuspy torus
 plasma
 [NASA-TN-78940] p0172 W78-27914
RADIATION MEASURING INSTRUMENTS
 WT INFRARED DETECTORS
 WT PHOTOEYES
 WT RADIATION COUNTERS
 WT RADIODIODES
 WT SPECTROPHOTOMETERS
 WT ULTRAVIOLET SPECTROPHOTOMETERS
 Development of environmental charging effect
 monitors for operational satellites p0037 W78-10174
RADIATION METERS
 U RADIATION MEASURING INSTRUMENTS
RADIATION PROTECTION
 WT RADIATION SHIELDING
RADIATION SHIELDING
 Diagnostic evaluations of a beam-shielded 8-cm
 mercury ion thruster
 [NASA-TN-78855] p0048 W78-21207
RADIATION SPECTRA
 WT ABSORPTION SPECTRA
 WT EMISSION SPECTRA
RADICALS
 WT HYDROXYL RADICALS
RADIO BROADCASTING
 U BROADCASTING
RADIO COMMUNICATION
 Low cost satellite land mobile service for
 nationwide applications p0095 A78-43173
RADIO EMISSION
 Lower hybrid emission diagnostics on the NASA
 Lewis Bumpy Torus p0173 A78-29332
RADIO EQUIPMENT
 WT RADIO TRANSMITTERS
RADIO FREQUENCIES
 WT HIGH FREQUENCIES
 WT SUPERHIGH FREQUENCIES
 WT VERY LOW FREQUENCIES
RADIO FREQUENCY DISCHARGE
 Lower hybrid emission diagnostics on the NASA
 Lewis bumpy torus
 [NASA-TN-73858] p0171 W78-19938
RADIO FREQUENCY HEATING
 Composition of RF-sputtered refractory compounds
 determined by X-ray photoelectron spectroscopy p0085 A78-30301
RADIO FREQUENCY IMPEDANCE PROBES
 Probe studies in a modified Penning discharge
 p0173 A78-24904
RADIO FREQUENCY INTERFERENCE
 WT HISS
 WT SHOT NOISE
 WT WHISTLERS
RADIO TRANSMISSION
 WT MICROWAVE TRANSMISSION
RADIO TRANSMITTERS
 Performance of the 12 GHz, 200 watt Transmitter
 Experiment Package for the Hermes Satellite p0098 A78-24883
RADIO WAVES
 WT MICROWAVE EMISSION
 WT MILLIMETER WAVES
 WT RADIO EMISSION
 WT WHISTLERS
RADIOGRAPHY
 WT TOMOGRAPHY
 Fabrication and characteristics of experimental
 radiographic amplifier screens --- image
 transducers with improved image contrast and
 resolution p0124 W78-15501
 [NASA-CR-2937]
RADIODIODES
 WT INFRARED DETECTORS
 Effect of airstream velocity on spray drop
 diameters of water sprays produced by pressure
 and air atomizing nozzles --- for combustion
 studies p0024 A78-3311

RANDOM DISTRIBUTIONS
 U STATISTICAL DISTRIBUTIONS
RANDOM LOADS
 WT GUST LOADS
RARE EARTH COMPOUNDS
 WT RARE EARTH COMPOUNDS
RARE EARTH ELEMENTS
 WT YTTRIUM
RARE GASES
 WT ARGON
 WT HELIUM
 WT LIQUID NEON
 WT XENON
 Metastable states of small rare gas crystallites
 p0169 A78-16069
 Inert gas thrusters
 [NASA-CR-135226] p0053 W78-19199
RATE METERS
 U MEASURING INSTRUMENTS
RATES (PER TIME)
 WT AIRSPEED
 WT CRITICAL VELOCITY
 WT CURRENT DENSITY
 WT EXHAUST VELOCITY
 WT FLOW VELOCITY
 WT FLUX DENSITY
 WT HEAT FLUX
 WT HIGH ACCELERATION
 WT HIGH SPEED
 WT PLASMA ACCELERATION
 WT ROTOR SPEED
 WT SOLAR FLUX
 WT STRAIN RATE
 WT SUPERSONIC SPEEDS
 WT TIP SPEED
 WT WIND VELOCITY
RATIOS
 WT FUEL-AIR RATIO
 WT LOW ASPECT RATIO
 WT MACH NUMBER
 WT REYNOLDS NUMBER
RB-57 AIRCRAFT
 U RB-57 AIRCRAFT
REACTION JETS
 J JET FLOW
REACTION KINETICS
 Kinetics of imidization and crosslinking in
 PMP-polyimide resin
 [NASA-TN-78944] p0082 W78-23231
REACTOR DESIGN
 Comment on 'Heat-pipe reactors for space power
 applications' p0052 A78-40826
READ-ONLY MEMORY DEVICES
 A cycle timer for testing electric vehicles
 [NASA-TN-78934] p0180 W78-26996
REAL TIME OPERATION
 Real time digital propulsion system simulation for
 manned flight simulators
 [NASA-TN-78958] p0034 W78-27137
REAL VARIABLES
 WT NONLINEAR EQUATIONS
 WT NUMERICAL INTEGRATION
RECIPROCATING ENGINES
 U PISTON ENGINES
RECORDING INSTRUMENTS
 WT FLIGHT LOAD RECORDERS
 WT WEATHER DATA RECORDERS
 WT X-Y PLOTTERS
RECOVERABLE SPACECRAFT
 WT REUSABLE SPACECRAFT
REDUCED GRAVITY
 Burning of liquid pools in reduced gravity
 [NASA-CR-135234] p0067 W78-25150
 Liquid propellant reorientation in a low-gravity
 environment
 [NASA-TN-78969] p0105 W78-29407
REDUCTION (CHEMISTRY)
 Electrochemical cell for rebalancing redox flow
 system
 [NASA-CASP-LEW-13150-1] p0136 W78-25554
REDUNDANT COMPONENTS
 Redundant disc
 [NASA-CASE-LEW-12496-1] p0022 W78-33101
REDUNDANT STRUCTURES
 U REDUNDANT COMPONENTS
REENTRY VEHICLES
 WT REUSABLE SPACECRAFT

SUBJECT INDEX

REMOTE SENSORS

REFERENCES (STANDARDS)

U STANDARDS

REFINING

- Computer model for refinery operations with emphasis on jet fuel production. Volume 2: Data and technical bases [NASA-CR-135334] p0090 W78-19326
- Computer model for refinery operations with emphasis on jet fuel production. Volume 1: Program description [NASA-CR-135333] p0090 W78-20350
- Computer model for refinery operations with emphasis on jet fuel production. Volume 3: Detailed systems and programming documentation [NASA-CR-135335] p0090 W78-25235

REFLECTORS

- NT PARABOLIC REFLECTORS
- NT SOLAR REFLECTORS

REFRACTORY MATERIALS

- NT CHROMIUM
- NT MOLYBDENUM ALLOYS
- NT NIOBIUM ALLOYS
- NT REFRACTORY METALS
- NT TANTALUM ALLOYS
- NT TUNGSTEN
- NT TUNGSTEN ALLOYS
- Improved performance of silicon nitride-based high temperature ceramics p0087 A78-24881
- Progress in advanced high temperature turbine materials, coatings, and technology p0056 A78-24910
- Composition of RF-sputtered refractory compounds determined by I-ray photoelectron spectroscopy p0085 A78-30301
- Improved performance of silicon nitride-based high temperature ceramics [NASA-TN-73719] p0080 W78-10298
- Materials technology assessment for stirling engines [NASA-TN-73789] p0069 W78-17187
- Development of Si3N4 and SiC of improved toughness --- for gas turbine engines [NASA-CR-135306] p0087 W78-17216
- I-ray photoelectron spectroscopy study of radiofrequency-sputtered refractory compound steel interfaces [NASA-TP-1161] p0081 W78-20336
- Progress in advanced high temperature turbine materials, coatings, and technology p0018 W78-21122
- The friction and wear properties of sputtered hard refractory compounds [NASA-TN-78895] p0056 W78-26177
- Substitution of ceramics for high temperature alloys --- advantages of using silicon carbides and silicon nitrides in gas turbine engines [NASA-TN-78911] p0084 W78-29246

REFRACTORY METAL ALLOYS

- NT MOLYBDENUM ALLOYS
- NT NIOBIUM ALLOYS
- NT TANTALUM ALLOYS
- NT TUNGSTEN ALLOYS

REFRACTORY METALS

- NT CHROMIUM
- NT TUNGSTEN
- High temperature heat pipe research at NASA Lewis Research Center [ATAA 78-838] p0106 A78-35618

REFRASIL (TRADEMARK)

REFRIGERANTS

REFRIGERATING MACHINERY

REFRIGERATORS

- Photovoltaic refrigeration application: Assessment of the near-term market [NASA-TN-73876] p0131 W78-16435

REGENERATIVE COOLING

- Supercritical oxygen heat transfer --- regenerative cooling [NASA-CR-135339] p0108 W78-17342

REGRESSION (STATISTICS)

REGRESSION ANALYSIS

- Chain pooling modeling selection as developed for the statistical analysis of a rotor burst protection experiment [NASA-TN-73874] p0160 W78-16735

REGULATION

U CONTROL

REGULATORS

- NT FLOW REGULATORS
- NT PRESSURE REGULATORS
- NT RELIEF VALVES
- NT VOLTAGE REGULATORS
- Design of turbofan engine controls using output feedback regulator theory p0023 A78-23907
- Output feedback regulator design for jet engine control systems p0024 A78-24898

REIGNITION

U IGNITION

REINFORCED MATERIALS

U COMPOSITE MATERIALS

REINFORCED PLASTICS

NT GLASS FIBER REINFORCED PLASTICS

REINFORCEMENT (STRUCTURES)

- Analysis/design of strip reinforced random composites (strip hybrids) [NASA-TN-78985] p0059 W78-33149

REINFORCING FIBERS

- A Weibull characterization for tensile fracture of multicomponent brittle fibers p0060 A78-24892

- An integrated theory for predicting the hydrothermo-mechanical response of advanced composite structural components p0060 A78-24905

- Effect of processing parameters on autoclaved PBR polyimide composites p0060 A78-25191

- Mechanical and physical properties of modern boron fibers p0085 A78-33206

- Analysis of delamination in unidirectional and crossplied fiber composites containing surface cracks [NASA-CR-135248] p0062 W78-11197

- Predicted inlet gas temperatures for tungsten fiber reinforced superalloy turbine blades [NASA-TN-73882] p0017 W78-19157

- Fiber reinforced PBR polyimide composites [NASA-CR-135377] p0063 W78-25132

- Some effects of composition on friction and wear of graphite-fiber-reinforced polyimide liners in plain spherical bearings [NASA-TP-1277] p0115 W78-25433

- Impact of composite mechanics on test methods for fiber composites [NASA-TN-78979] p0126 W78-32464

RELAXATION (MECHANICS)

NT STRESS RELAXATION

RELIABILITY

NT AIRCRAFT RELIABILITY

NT CIRCUIT RELIABILITY

RELIABILITY ANALYSIS

- Reliability analysis of forty-five strain-gage systems mounted on the first fan stage of a TP-100 engine [NASA-TN-73724] p0109 W78-13407

RELIABILITY CONTROL

RELIABILITY ENGINEERING

- Evaluation of commercially-available spacecraft-type heat pipes [ATAA 78-397] p0094 A78-35590

- Potential damage to dc superconducting magnets due to high frequency electromagnetic waves p0098 A78-19902

- Turbine disks for improved reliability p0012 W78-10089

RELIEF VALVES

- Mechanical characteristics of stability-bleed valves for a supersonic inlet --- for the F-12 aircraft [NASA-TN-X-3483] p0015 W78-13063

REMAGNETIZATION

REMOVAL OF MAGNETIZATION

REMOTE CONTROL

- Sol.J State Remote Power Controllers for high voltage DC distribution systems p0100 A78-16574

REMOTE SENSORS

- Global sensing of gaseous and aerosol trace species using automated instrumentation on 747 airliners

REFERENCES

SUBJECT INDEX

[NASA-TN-73810] p0188 W78-13670
 Photovoltaic remote instrument applications:
 Assessment of the near-term market
 [NASA-TN-73881] p0150 W78-19710

REFERENCES

UT SPACE REFERENCES

RESEARCH

WT HIGH TEMPERATURE RESEARCH

WT MARKET RESEARCH

WT NONLINEAR PROGRAMMING

WT OPERATIONS RESEARCH

RESEARCH AND DEVELOPMENT

Bibliography of Lewis Research Center technical contributions announced in 1976 [NASA-TN-73860] p0177 W78-17921

Bibliography of Lewis Research Center technical publications announced in 1977 [NASA-TN-78918] p0177 W78-28986

RESEARCH PROJECTS

EPDA/NASA advanced thermionic technology program [NASA-CR-157117] p0145 W78-24674

Stirling engine project status p0117 W78-30314

RESIDUAL STRESS

Lamination residual strains and stresses in hybrid laminates p0128 A78-12071

Residual stresses in angleplied laminates and their effects on laminate behavior p0060 A78-33201

Axial residual stresses in boron fibers [NASA-TN-73894] p0058 W78-19204

Residual stresses in angleplied laminates and their effects on laminate behavior [NASA-TN-78835] p0058 W78-19206

RESINS

WT ADDITION RESINS

WT EPOXY RESINS

WT ION EXCHANGE RESINS

WT POLYAMIDE RESINS

WT POLYIMIDE RESINS

WT THERMOPLASTIC RESINS

Preliminary evaluation of Glass Resin materials for solar cell cover use [NASA-TN-78925] p0137 W78-26544

RESISTIVITY

U ELECTRICAL RESISTIVITY

RESOLUTION

Fabrication and characteristics of experimental radiographic amplifier screens --- image transducers with improved image contrast and resolution [NASA-CR-29377] p0124 W78-15501

RESOLVING POWER

U RESOLUTION

RESONANCE TESTING

Development of procedures for calculating stiffness and damping properties of elastomers in engineering applications. Part 4: Testing of elastomers under a rotating load --- resonance testing [NASA-CR-135355] p0127 W78-22402

RESONANT CAVITIES

U CAVITY RESONATORS

RESONANT FREQUENCIES

Constrained sloshing of liquid mercury in a flexible spherical tank [AIAA PAPER 78-670] p0106 A78-32749

RESONATORS

WT CAVITY RESONATORS

Small-signal gain diagnostic measurements in a flowing CO2 pin discharge laser [NASA-TN-73843] p0111 W78-13421

RESOURCES

WT COAL

WT CRUDE OIL

WT EARTH RESOURCES

WT FOSSIL FUELS

WT GEYSERS

WT WATER RESOURCES

RESPONSES

WT DYNAMIC RESPONSE

WT TRANSIENT RESPONSE

REUSABLE SPACECRAFT

Comparison of reusable insulation systems for cryogenically-tanked earth-based space vehicles [AIAA PAPER 78-877] p0044 A78-36004

Preliminary concept, specifications, and requirements for a zero-gravity combustion

facility for spacelab [NASA-TN-78910] p0041 W78-26166

REVERSED FLOW

Reverse-flow combustor for small gas turbines with pressure-atomizing fuel injectors [NASA-TN-1260] p0021 W78-27130

RYTHOLDS NUMBER

On the localness of the spectral energy transfer in turbulence p0106 A78-24909

RIBBONS

Analysis/design of strip reinforced random composites (strip hybrids) [NASA-TN-78985] p0059 W78-33149

RICHARDSON-DUSSEMAN EQUATION

U TEMPERATURE EFFECTS

U THERMIONIC EMISSION

RING STRUCTURES

The elastic distortion of the flanged inner ring of a high-speed cylindrical roller bearing [ASME PAPER 77-LOB-8] p0118 A78-23352

Liquid metal slip ring [NASA-CASE-LEW-12277-2] p0097 W78-25323

ROADS

WT HIGHWAYS

ROCKET CHAMBERS

U THRUST CHAMBERS

ROCKET ENGINE CONTROL

A mechanical, thermal and electrical packaging design for a prototype power management and control system for the 30 cm mercury ion thruster [AIAA PAPER 78-685] p0051 A78-32759

Advanced space engine powerhead breadboard assembly system study [NASA-CR-135232] p0054 W78-25127

ROCKET ENGINE DESIGN

5200 cycle of an 8-cm diameter Hg ion thruster [AIAA PAPER 78-689] p0050 A78-32736

Sensitivity of 30-cm mercury bombardment ion thruster characteristics to accelerator grid design [AIAA PAPER 78-668] p0050 A78-32747

Ion beam plume and efflux measurements of an 8-cm mercury ion thruster [AIAA PAPER 78-676] p0055 A78-32753

Pulse ignition characterization of mercury ion thruster hollow cathode using an improved pulse ignitor [AIAA PAPER 78-709] p0051 A78-32773

Extended performance solar electric propulsion thrust system design [AIAA PAPER 78-643] p0055 A78-37430

Electrical Prototype Power Processor for the 30-cm Mercury electric propulsion engine [AIAA PAPER 78-684] p0055 A78-37439

Linear aerospike engine study --- for reusable launch vehicles [NASA-CR-135231] p0026 W78-11082

Preburner of staged combustion rocket engine [NASA-CR-135356] p0054 W78-24279

ROCKET ENGINES

WT ELECTRIC ROCKET ENGINES

WT HYBRID PROPELLANT ROCKET ENGINES

WT HYDROGEN OXYGEN ENGINES

WT ION ENGINES

WT LIQUID PROPELLANT ROCKET ENGINES

WT MERCURY ION ENGINES

Mercury ion thruster research, 1977 --- plasma acceleration [NASA-CR-135317] p0052 W78-15167

Ion engine auxiliary propulsion applications and integration study [NASA-CR-135312] p0053 W78-15168

Extended performance solar electric propulsion thrust system study. Volume 4: Thruster technology evaluation [NASA-CR-135281-VOL-4] p0053 W78-16090

Extended performance solar electric propulsion thrust system study. Volume 3: Tradeoff studies of alternate thrust system configurations [NASA-CR-135281-VOL-3] p0053 W78-19196

Evolution of the 1-mlb mercury ion thruster subsystem [NASA-TN-73733] p0047 W78-21202

Planned flight test of a mercury ion auxiliary propulsion system. 1: Objectives, systems descriptions, and mission operations [NASA-TN-78859] p0047 W78-21204

SUBJECT INDEX

ROTORS

The 5200 cycle test of an 8-cm diameter Mg ion thruster [NASA-TN-78860] p0048 N78-21208
 Applied tooth approximation [NASA-TP-1231] p0091 N78-22257
ROCKET LAUNCHING
 ADJUST - An automated system for steering Centaur launch vehicles in measured winds p0045 A78-14991
ROCKET PROPELLANT TANKS
 U PROPELLANT TANKS
ROCKET PROPELLANTS
 NT GASEOUS ROCKET PROPELLANTS
 NT LIQUID ROCKET PROPELLANTS
ROCKET TEST FACILITIES
 A mission profile life test facility --- for mercury ion thrusters [AIAA PAPER 78-671] p0040 A78-37431
ROCKET VEHICLES
 NT CENTAUR LAUNCH VEHICLE
ROCKS
 NT COAL
ROLLER BEARINGS
 The elastic distortion of the flanged inner ring of a high-speed cylindrical roller bearing [ASME PAPER 77-LUB-8] p0118 A78-23352
 Lubrication of high-speed, large bore tapered-roller bearings [ASME PAPER 77-LUB-13] p0118 A78-23354
 Effect of wall thickness and material on flexural fatigue of hollow rolling elements [ASME PAPER 77-LUB-14] p0126 A78-23355
 Effect of filtration on rolling-element-bearing life in contaminated lubricant environment [NASA-TP-1272] p0116 N78-28457
 Rolling element fatigue testing of gear materials [NASA-CR-135411] p0122 N78-31427
 The practical impact of elastohydrodynamic lubrication [NASA-TN-78987] p0117 N78-33445
ROLLING CONTACT LOADS
 Influence of adsorbed fluids on the rolling contact deformation of MgO single crystals p0123 A78-23447
 Simplified contact analysis p0127 A78-28200
 Rolling-element fatigue life of AMS 5749 corrosion resistant, high temperature bearing steel [ASME PAPER 77-LUB-30] p0075 A78-28423
 Ferrographic analysis of wear debris generated in accelerated rolling element fatigue tests p0119 A78-28425
 Rolling element fatigue testing of gear materials [NASA-CR-135450] p0124 N78-33463
ROLLUP SOLAR ARRAYS
 U SOLAR ARRAYS
ROOM TEMPERATURE
 Effect of prior creep at 136° K on the room temperature tensile properties of several oxide dispersion strengthened alloys p0074 A78-21431
ROOTS OF EQUATIONS
 A possible pole problem in the formula for klystron gap fields p0098 A78-18287
ROTARY DRIVES
 U MECHANICAL DRIVES
ROTARY WING AIRCRAFT
 NT HELICOPTERS
ROTARY WINGS
 NT TILTING ROTORS
 NT TIP DRIVEN ROTORS
ROTATING BODIES
 NT COMPRESSOR ROTORS
 NT IMPELLERS
 NT ROTATING DISKS
 NT ROTORS
 NT TILTING ROTORS
 NT TIP DRIVEN ROTORS
 NT TURBINE WHEELS
 Development of procedures for calculating stiffness and damping properties of elastomers in engineering applications. Part 4: Testing of elastomers under a rotating load --- resonance testing [NASA-CR-135355] p0127 N78-22402
ROTATING DISKS
 Steady-state unbalance response of a three-disk flexible rotor on flexible, damped supports
 Redundant disc [NASA-CASE-LEW-12496-1] p0022 N78-33101
ROTATING GENERATORS
 NT AC GENERATORS
 NT TURBOGENERATORS
ROTATING SHAFTS
 NT SHAFTS (MACHINE ELEMENTS)
 The elastic distortion of the flanged inner ring of a high-speed cylindrical roller bearing [ASME PAPER 77-LUB-8] p0118 A78-23352
 Nonlinear flap-lag-axial equations of a rotating beam with arbitrary precone angle [AIAA 78-491] p0127 A78-29798
 Stability of numerical integration techniques for transient rotor dynamics [NASA-TP-1092] p0113 N78-10474
ROTATING VEHICLES
 U ROTATING BODIES
ROTATIONAL FLOW
 U FLUID FLOW
 U VORTICES
ROTOR BLADES
 Three-dimensional effects on pure tone fan noise due to inflow distortion [AIAA PAPER 78-1120] p0166 A78-41830
ROTOR BLADES (TURBOCHARGER)
 Acoustic evaluation of a novel swept-rotor fan [AIAA PAPER 78-1121] p0166 A78-41831
 Impact resistant boron/aluminum composites for large fan blades [NASA-CR-135274] p0062 N78-14099
 Synthesis of blade flutter vibratory patterns using stationary transducers [NASA-TN-73821] p0003 N78-17001
 Instrumentation for propulsion systems development --- high speed fans and turbines [NASA-TN-73840] p0011 N78-17052
 Wind turbine generator rotor blade concepts with low cost potential [NASA-TN-73835] p0131 N78-17466
 Effects of rotor location, coning, and tilt on critical loads in large wind turbines p0133 N78-19636
 Fixed pitch wind turbines p0133 N78-19638
 Computation of unsteady transonic flows through rotating and stationary cascades. 1: Method of analysis [NASA-CR-2900] p0008 N78-20082
 In-place recalibration technique applied to a capacitance-type system for measuring rotor blade tip clearance [NASA-TP-1110] p0019 N78-22101
 Acoustic evaluation of a novel swept-rotor fan --- noise reduction in turbofan engines [NASA-TN-78878] p0164 N78-24897
 Three-dimensional effects on pure tone fan noise due to inflow distortion --- rotor blade noise prediction [NASA-TN-78885] p0164 N78-24898
 VSTOL tilt nacelle aerodynamics and its relation to fan blade stresses [NASA-TN-78899] p0005 N78-26099
 Performance with and without inlet radial distortion of a transonic fan stage designed for reduced loading in the tip region [NASA-TP-1294] p0005 N78-30057
 Advanced optical blade tip clearance measurement system [NASA-CR-159402] p0032 N78-31106
ROTOR DISKS
 U TURBINE WHEELS
ROTOR HUBS
 U ROTORS
ROTOR SPEED
 High stiffness seals for rotor critical speed control [ASME PAPER 77-DET-10] p0118 A78-20591
 Lubrication of high-speed, large bore tapered-roller bearings [ASME PAPER 77-LUB-13] p0118 A78-23354
ROTORS
 NT COMPRESSOR ROTORS
 NT IMPELLERS
 NT TILTING ROTORS
 NT TIP DRIVEN ROTORS
 NT TURBINE WHEELS

ROBBER

SUBJECT INDEX

Steady-state unbalance response of a three-disk flexible rotor on flexible, damped supports p0119 A78-29326
 Concepts for the development of light-weight composite structures for rotor burst containment p0012 W78-10084
 Stability of numerical integration techniques for transient rotor dynamics [NASA-TP-1092] p0113 W78-10474
 Influence of oil-squeeze-film damping on steady-state response of flexible rotor operating to supercritical speeds [NASA-TP-1094] p0015 W78-13064
 Balancing techniques for high-speed flexible rotors [NASA-CR-2975] p0121 W78-20514
 Liquid metal slip ring [NASA-CASE-LEN-12277-2] p0097 W78-25323
 Transient dynamics of a flexible rotor with squeeze film dampers [NASA-CR-3050] p0123 W78-32433

**ROBBER
 NT ELASTOMERS**

S

S BAND
 U SUPERHIGH FREQUENCIES
SAFETY
 NT AIRCRAFT SAFETY
SAFETY MANAGEMENT
 Toxic substances alert program [NASA-TM-73866] p0153 W78-20755
SAILS
 NT SOLAR SAILS
SALTS
 Thermal energy storage heat exchanger: Molten salt heat exchanger design for utility power plants [NASA-CR-135244] p0143 W78-14632
 Thermal energy storage heat exchanger: Molten salt heat exchanger design for utility power plants [NASA-CR-135245] p0143 W78-14633
SAMPLING
 Global sensing of gaseous and aerosol trace species using automated instrumentation on 747 airliners [NASA-TM-73810] p0148 W78-13670
SATELLITE ATTITUDE DISTURBANCE
 U ATTITUDE STABILITY
 U SPACECRAFT STABILITY
SATELLITE COMMUNICATIONS
 U SPACECRAFT COMMUNICATION
SATELLITE CONTROL
 Engineering Model 8-cc Thruster System [AIAA PAPER 78-646] p0055 A78-37434
SATELLITE ORBITS
 NT GEOSYNCHRONOUS ORBITS
SATELLITE TELEVISION
 A forecast of broadcast satellite communications p0094 A78-15615
SATELLITE TRANSMISSION
 A digitally implemented communications experiment utilizing the Hermes /CTS/ satellite p0094 A78-24884
 The 20/30 GHz satellite systems technology needs assessment [NASA-TM-78975] p0093 W78-31323
SATELLITE-BORNE INSTRUMENTS
 NT AMPS (SATELLITE PAYLOAD)
SATELLITES
 NT ARTIFICIAL SATELLITES
 NT ATS 1
 NT ATS 3
 NT ATS 5
 NT ATS 6
 NT COMMUNICATION SATELLITES
 NT COMMUNICATIONS TECHNOLOGY SATELLITE
 NT METEOROLOGICAL SATELLITES
 NT NOAA SATELLITES
 NT SYNCHRONOUS SATELLITES
SCALE EFFECT
 Aero-acoustic tests of duct-burning turbofan exhaust nozzles. Comprehensive data report. Volume 2: Acoustic and aerodynamic data [NASA-CR-134910-VOL-2] p0002 W78-15989
SCALE MODELS
 Aero-acoustic tests of duct-burning turbofan exhaust nozzles. Comprehensive data report.

Volume 1: Model scale acoustic data [NASA-CR-134910-VOL-1] p0002 W78-15988
 Effect of design changes on aerodynamic and acoustic performance of translating-centerbody sonic inlets [NASA-TP-1132] p0003 W78-17998
 Applied Booth approximation [NASA-TP-1231] p0091 W78-22257
SCALING LAWS
 Critical currents and scaling laws in sputtered copper molybdenum sulfide p0175 A78-45500
SCAR PROGRAM
 U SUPERSONIC CRUISE AIRCRAFT RESEARCH
SCARS (SROLOGY)
 U EROSION
SCHEDULING
 NT PREDICTION ANALYSIS TECHNIQUES
SCOTTKEY EFFECT
 U WORK FUNCTIONS
SCIENTIFIC SATELLITES
 NT ATS 1
 NT ATS 3
 NT ATS 5
 NT ATS 6
SCREENING
 Effect of vibration on retention characteristics of screen acquisition systems [NASA-CR-135264] p0107 W78-12364
SCREENS
 Effect of vibration on retention characteristics of screen acquisition systems --- for surface tension/propellant acquisition [AIAA PAPER 78-1030] p0045 A78-43560
SEALANTS
 U SEALERS
SEALERS
 Temperature distributions and thermal stresses in a graded zirconia/metal gas path seal system for aircraft gas turbine engines [NASA-TM-73818] p0015 W78-15094
SEALING
 NT SELF SEALING
 Gas path sealing in turbine engines p0024 A78-33218
 Compressor seal rub energetics study [NASA-CR-159424] p0032 W78-32096
SEALS (STOPPERS)
 NT O RING SEALS
 High stiffness seals for rotor critical speed control [ASME PAPER 77-DET-10] p0118 A78-20591
 Temperature distributions and thermal stresses in a graded zirconia/metal gas path seal system for aircraft gas turbine engines [AIAA PAPER 78-93] p0118 A78-20683
 Friction and wear of sintered fibermetal abrasible seal materials p0074 A78-23451
 Design considerations in mechanical face seals for improved performance. I - Basic configurations [ASME PAPER 77-WA/LUB-3] p0119 A78-33183
 Design considerations in mechanical face seals for improved performance. II - Lubrication [ASME PAPER 77-WA/LUB-4] p0120 A78-33184
 Self-acting shaft seals p0120 A78-33219
 Design considerations in mechanical face seals for improved performance. 1: Basic configurations [NASA-TM-73735] p0113 W78-13439
 Friction and wear of several compressor gas-path seal assemblies [NASA-TP-1128] p0068 W78-15229
 Preliminary study of cyclic thermal shock resistance of plasma-sprayed zirconium oxide turbine outer air seal shrouds [NASA-TM-73852] p0080 W78-15280
 Development of spiral-groove self-acting face seals [NASA-CR-135303] p0121 W78-17387
 Feasibility study of negative lift circumferential type seal for helicopter transmissions [NASA-CR-135302] p0121 W78-17390
 Self-acting shaft seals [NASA-TM-73856] p0114 W78-19513
 Gas path sealing in turbine engines [NASA-TM-73890] p0018 W78-21109
 Development of a plasma sprayed ceramic gas path seal for high pressure turbine application [NASA-CR-135387] p0030 W78-24141

SUBJECT INDEX

SHOCK RESISTANCE

Counter pumping debris excluder and separator ---
gas turbine shaft seals
[NASA-CASE-LEW-11855-1] p0020 W78-25090

Aerodynamic performance of conventional and
advanced design labyrinth seals with
solid-smooth abrasible, and honeycomb lands ---
gas turbine engines
[NASA-CR-135307] p0122 W78-27427

Rub tolerance evaluation of two sintered NiCrAl
gas path seal materials --- wear tests of gas
turbine engine seals
[NASA-TN-78967] p0071 W78-29215

Liquid rocket engine turbopump rotating-shaft seals
[NASA-SP-8121] p0117 W78-30584

Gas path seal
[NASA-CASE-LEW-12131-2] p0021 W78-31103

Advanced ceramic material for high temperature
turbine tip seals
[NASA-CR-135319] p0087 W78-31238

SEASONS
Preliminary report on the CTS transient event
counter performance through the 1976 spring
eclipse season p0036 W78-10135

SECONDARY BATTERIES
7 STORAGE BATTERIES

SECONDARY EMISSION
Secondary electron emission properties of
conducting surfaces for use in multistage
depressed collectors p0098 A78-23635

A three dimensional dynamic study of electrostatic
charging in materials
[NASA-CR-135256] p0099 W78-13328

SECONDARY FLOW
End-wall boundary layer prediction for axial
compressors
[AIAA PAPER 78-1139] p0007 A78-45133

Effect of endwall cooling on secondary flows in
turbine stator vanes p0014 W78-11098

**FLOWNET: A computer program for calculating
secondary flow conditions in a network of
turbomachinery
[NASA-TN-73774] p0156 W78-21791**

Derivation and evaluation of an approximate
analysis for three-dimensional viscous subsonic
flow with large secondary velocities --- finite
difference method
[NASA-CR-159430] p0008 W78-33044

SECULAR PERTURBATION
7 LONG TERM EFFECTS

SEDIMENTARY ROCKS
7 COAL

SELF LUBRICATING MATERIALS
Some load limits and self-lubricating properties
of plain spherical bearings with molded graphite
fiber reinforced polyimide liners to 320 C
[NASA-TN-78935] p0116 W78-26445

SELF REGULATING
7 AUTOMATIC CONTROL

SELF SEALING
Self-acting shaft seals
[NASA-TN-73856] p0114 W78-19513

SEMICONDUCTOR DEVICES
7 METAL OXIDE SEMICONDUCTORS
7 PHOTOVOLTAIC CELLS

SEMICONDUCTOR JUNCTIONS
7 P-N JUNCTIONS
7 SILICON JUNCTIONS
Solar Cell High Efficiency and Radiation Damage
[NASA-CP-2020] p0130 W78-13527

Status of wraparound contact solar cells and arrays
[NASA-TN-78911] p0137 W78-26543

SEMICONDUCTORS (MATERIALS)
7 METAL OXIDE SEMICONDUCTORS
7 N-TYPE SEMICONDUCTORS
7 P-TYPE SEMICONDUCTORS

SENDERS
7 TRANSMITTERS

SENSITIVITY
7 IMPACT RESISTANCE

SEPARATED FLOW
7 BOUNDARY LAYER SEPARATION

SEPARATORS
7 FLOW FILTERS
Counter pumping debris excluder and separator ---
gas turbine shaft seals
[NASA-CASE-LEW-11855-1] p0020 W78-25090

Formulated plastic separators for soluble
electrode cells
[NASA-CASE-LEW-12358-2] p0065 W78-25149

Inorganic-organic separators for alkaline batteries
[NASA-CASE-LEW-12649-1] p0136 W78-25530

SEPT 2 SPACECRAFT
Status of SEPT II spacecraft and ion thrusters -
1978
[AIAA PAPER 78-662] p0050 A78-32743

Status of SEPT II spacecraft and ion
thrusters, 1978
[NASA-TN-78827] p0047 W78-20251

SERVICE LIFE
Evaluation of commercially-available
spacecraft-type heat pipes
[AIAA 78-397] p0044 A78-35590

A mission profile life test facility --- for
mercury ion thrusters
[AIAA PAPER 78-671] p0040 A78-37431

Ductility normalized-strain-range partitioning
life relations for creep-fatigue life predictions
p0077 A78-51739

Real-time and accelerated outdoor endurance
testing of solar cells p0142 A78-52837

SHAFTS (MACHINE ELEMENTS)
Self-acting shaft seals p0120 A78-33219

Balancing techniques for high-speed flexible rotors
[NASA-CR-2975] p0121 W78-20514

Rolling-element fatigue life of AISI A-50 and
18-4-1 balls
[NASA-TP-1202] p0115 W78-21473

Counter pumping debris excluder and separator ---
gas turbine shaft seals
[NASA-CASE-LEW-11855-1] p0020 W78-25090

Proposed design procedure for transmission
shafting under fatigue loading
[NASA-TN-78927] p0115 W78-26444

SHAPE OIL
Jet fuels from synthetic crudes p0090 A78-43415

In-situ laser retorting of oil shale
[NASA-CASE-LEW-12217-1] p0129 W78-14452

SHAPES
7 ELLIPTICITY
Experimental study of the effects of flameholder
geometry on emissions and performance of lean
premixed combustors
[NASA-CR-135424] p0030 W78-26147

SHATTERING
7 FRAGMENTATION

SHEAR FLOW
Characteristics of the unsteady motion on
transversely sheared mean flows p0106 A78-23246

Turbulence processes and simple closure schemes
p0107 A78-40983

SHEAR LAYERS
Propagation of sound waves through a linear shear
layer - A closed form solution
[AIAA PAPER 78-196] p0165 A78-20738

Propagation of sound waves through a linear shear
layer: A closed form solution
[NASA-TN-73828] p0164 W78-16766

SHEAR PROPERTIES
7 SHEAR STRENGTH

SHEAR STRENGTH
Shear strength of metal - SiO2 contacts
p0061 A78-33209

Shear strength of metal - SiO2 contacts
[NASA-TN-78838] p0125 W78-19539

Friction and wear of metals with a single-crystal
abrasive grit of silicon carbide: Effect of
shear strength of metal
[NASA-TP-1243] p0084 W78-30238

Longitudinal shear behavior of several oxide
dispersion strengthened alloys
[NASA-TN-78973] p0072 W78-31211

SHEET METAL
7 REPEL SHEETS

SHIELDING
7 ELECTROMAGNETIC SHIELDING
7 HEAT SHIELDING
7 RADIATION SHIELDING
7 SPACECRAFT SHIELDING

SHOCK DIFFUSERS
7 DIFFUSERS

SHOCK RESISTANCE
7 IMPACT RESISTANCE

SHOCK WAVES

SUBJECT INDEX

- Preliminary study of cyclic thermal shock resistance of plasma-sprayed zirconium oxide turbine outer air seal shrouds [NASA-TN-73852] p0080 W78-15280
- SHOCK WAVES**
- WT NORMAL SHOCK WAVES**
- Unsteady flow in a supersonic cascade with strong in-passage shocks p0006 A78-17270
- SHORT HAUL AIRCRAFT**
- Preliminary QCSRE program - Test results --- Quiet Clean Short-haul Experimental Engine [SAB PAPER 771008] p0023 A78-23840
- SHORT TAKEOFF AIRCRAFT**
- ESP noise suppression and aerodynamic penalties --- Externally Blown Flaps [AIAA PAPER 78-240] p0165 A78-20763
- Noise of deflectors used for flow attachment with STOL-OTW configurations p0023 A78-24877
- Real time digital propulsion system simulation for manned flight simulators [AIAA PAPER 78-927] p0035 A78-45095
- Noise of deflectors used for flow attachment with STOL-OTW configurations [NASA-TN-73809] p0163 W78-13853
- SHORT WAVE RADIATION**
- WT MICROWAVE EMISSION**
- WT MILLIMETER WAVES**
- SHOT NOISE**
- Noise as a tool for evaluating the activation of cathodes [NASA-TN-73895] p0096 W78-17298
- SHROUDED BODIES**
- T SHROUDS**
- SEROUDS**
- Preliminary study of cyclic thermal shock resistance of plasma-sprayed zirconium oxide turbine outer air seal shrouds [NASA-TN-73852] p0080 W78-15280
- Boundary layer analysis of a Centaur standard shroud [NASA-TN-78843] p0103 W78-21404
- SHUTTLE ORBITERS**
- T SPACE SHUTTLE ORBITERS**
- SIGNAL ANALYZERS**
- WASCAP, a three-dimensional Charging Analyzer Program for complex spacecraft p0044 A78-19567
- SIGNAL MEASUREMENT**
- Small-signal gain diagnostic measurements in a flowing CO₂ pin discharge laser [NASA-TN-73843] p0111 W78-13421
- SIGNAL TRANSMISSION**
- WT MICROWAVE TRANSMISSION**
- WT SATELLITE TRANSMISSION**
- SILICA**
- O SILICON DIOXIDE**
- SILICIDES**
- WT DISILICIDES**
- Friction and wear of radiofrequency-sputtered borides, silicides, and carbides [NASA-TP-1156] p0081 W78-20338
- SILICON**
- Effects of silicon on the oxidation, hot-corrosion, and mechanical behavior of two cast nickel-base superalloys p0074 A78-21439
- Dendritic web silicon for solar cell application p0146 A78-53489
- Impurity concentrations and surface charge densities on the heavily doped face of a silicon solar cell p0130 W78-13534
- Pressureless sintered Sialons with low amounts of sintering aid [NASA-TP-1246] p0082 W78-25215
- Photon degradation effects in terrestrial solar cells [NASA-TN-78924] p0136 W78-25551
- SILICON CARBIDES**
- Friction, deformation and fracture of single-crystal silicon carbide [ASLE PREPRINT 77-IC-5C-3] p0085 A78-28438
- Ceramics in gas turbines - Powder and process characterization p0085 A78-29328
- Friction and wear behavior of single-crystal silicon carbide in sliding contact with various metals p0086 A78-44095
- Substitution of ceramics for high temperature alloys p0086 A78-47596
- Characterization, shaping, and joining of SiC/superalloy sheet for exhaust system components [NASA-CR-135301] p0062 W78-13134
- Development of Si₃N₄ and SiC of improved toughness --- for gas turbine engines [NASA-CR-135306] p0087 W78-17216
- Friction and wear behavior of single-crystal silicon carbide in sliding contact with various metals [NASA-TN-73782] p0114 W78-19512
- Friction and metal transfer for single-crystal silicon carbide in contact with various metals in vacuum [NASA-TP-1191] p0082 W78-21294
- Wear of single-crystal silicon carbide in contact with various metals in vacuum [NASA-TP-1198] p0082 W78-21295
- Effect of oxygen and nitrogen interactions on friction of single-crystal silicon carbide [NASA-TP-1265] p0083 W78-28247
- Substitution of ceramics for high temperature alloys --- advantages of using silicon carbides and silicon nitrides in gas turbine engines [NASA-TN-78931] p0084 W78-29246
- Friction and wear of metals with a single-crystal abrasive grit of silicon carbide: Effect of shear strength of metal [NASA-TP-1293] p0084 W78-30238
- SILICON COMPOUNDS**
- WT DISILICIDES**
- WT SILICIDES**
- WT SILICON CARBIDES**
- WT SILICON DIOXIDE**
- WT SILICON NITRIDES**
- Development of SIALON materials [NASA-CR-135290] p0087 W78-21289
- SILICON DIOXIDE**
- Shear strength of metal - SiO₂ contacts p0061 A78-33209
- Shear strength of metal - SiO₂ contacts [NASA-TN-78838] p0125 W78-19539
- SILICON FILMS**
- Microstructural and wear properties of sputtered carbides and silicides p0084 A78-23445
- SILICON JUNCTIONS**
- Analysis of epitaxial drift field N on P silicon solar cells p0141 A78-10904
- SILICON NITRIDES**
- Microstructure of hot-pressed Al₂O₃-Si₃N₄ mixtures as a function of holding temperature p0084 A78-17456
- Improved performance of silicon nitride-based high temperature ceramics p0087 A78-24881
- Consolidation of silicon nitride without additives --- for gas turbine engine efficiency increase p0085 A78-24895
- Ceramics in gas turbines - Powder and process characterization p0085 A78-29328
- High temperature compressive cracking in hot-pressed silicon nitride p0085 A78-38706
- Pressureless sintered beta-prime-Si₃N₄ solid solution - Fabrication, microstructure, and strength p0086 A78-47595
- Substitution of ceramics for high temperature alloys p0086 A78-47596
- Effect of attrition milling on the reaction sintering of silicon nitride p0086 A78-50324
- Consolidation of silicon nitride without additives [NASA-TN-73693] p0057 W78-10217
- Improved performance of silicon nitride-based high temperature ceramics [NASA-TN-73719] p0080 W78-10294
- Development of Si₃N₄ and SiC of improved toughness --- for gas turbine engines [NASA-CR-135306] p0087 W78-17216
- Improved reaction sintered silicon nitride --- protective coatings to improve oxidation resistance [NASA-CR-135291] p0063 W78-22164

SUBJECT INDEX

SOLAR ARRAYS

- Pressureless sintered beta prime-Si₃N₄ solid solution: Fabrication, microstructure, and strength [NASA-TN-78950] p0083 W78-29285
- Substitution of ceramics for high temperature alloys --- advantages of using silicon carbides and silicon nitrides in gas turbine engines [NASA-TN-78931] p0084 W78-29286
- Effect of attrition milling on the reaction sintering of silicon nitride [NASA-TN-78965] p0084 W78-31236
- SILICON OXIDES**
- NT SILICON DIOXIDE
- SILICON SOLAR CELLS**
- U SOLAR CELLS
- SIMULATION**
- NT COMPUTERIZED SIMULATION
- NT CONTROL SIMULATION
- NT DIGITAL SIMULATION
- NT ENVIRONMENT SIMULATION
- NT FLIGHT SIMULATION
- NT THERMAL SIMULATION
- The Lewis Research Center geomagnetic substorm simulation facility p0036 W78-10155
- SIMULATORS**
- NT CONTROL SIMULATION
- NT FLIGHT SIMULATORS
- SINGLE CRYSTALS**
- Influence of adsorbed fluids on the rolling contact deformation of MgO single crystals p0123 W78-23447
- Friction, deformation and fracture of single-crystal silicon carbide [ASLE PREPRINT 77-LC-5C-3] p0005 W78-28438
- Friction and wear behavior of single-crystal silicon carbide in sliding contact with various metals p0086 W78-44095
- Friction and wear of single-crystal and polycrystalline manganese-zinc ferrite in contact with various metals [NASA-TP-1059] p0080 W78-10295
- Friction and metal transfer for single-crystal silicon carbide in contact with various metals in vacuum [NASA-TP-1191] p0082 W78-21294
- Wear of single-crystal silicon carbide in contact with various metals in vacuum [NASA-TP-1198] p0082 W78-21295
- Effect of oxygen and nitrogen interactions on friction of single-crystal silicon carbide [NASA-TP-1265] p0083 W78-28247
- SINGULARITY (MATHEMATICS)**
- A possible pole problem in the formula for klystron gap fields p0098 W78-18287
- Interaction of a turbulent-jet noise source with transverse modes in a rectangular duct [NASA-TP-1248] p0001 W78-25049
- SINKS**
- NT HEAT SINKS
- SINTERING**
- Pressureless sintered beta-prime-Si₃N₄ solid solution - Fabrication, microstructure, and strength p0086 W78-47595
- Effect of attrition milling on the reaction sintering of silicon nitride p0086 W78-50324
- Development of SIALON materials [NASA-CP-115290] p0087 W78-21289
- Improved reaction sintered silicon nitride --- protective coatings to improve oxidation resistance [NASA-CP-115291] p0063 W78-22164
- Pressureless sintered Sialons with low amounts of sintering aid [NASA-TP-1248] p0082 W78-25215
- Pressureless sintered beta prime-Si₃N₄ solid solution: Fabrication, microstructure, and strength [NASA-TN-78950] p0083 W78-29285
- Effect of attrition milling on the reaction sintering of silicon nitride [NASA-TN-78965] p0084 W78-31236
- SKIN FRICTION**
- NT AERODYNAMIC DRAG
- SKY WAVES**
- NT WHISTLERS
- SLIDING FRICTION**
- Friction, deformation and fracture of single-crystal silicon carbide [ASLE PREPRINT 77-LC-5C-3] p0085 W78-28438
- Friction and wear behavior of single-crystal silicon carbide in sliding contact with various metals p0086 W78-44095
- Friction and wear of single-crystal and polycrystalline manganese-zinc ferrite in contact with various metals [NASA-TP-1059] p0080 W78-10295
- Friction and wear behavior of single-crystal silicon carbide in sliding contact with various metals [NASA-TN-73782] p0114 W78-19512
- Friction and wear of selected metals and alloys in sliding contact with AISI 440 C stainless steel in liquid methane and in liquid natural gas [NASA-TP-1150] p0114 W78-20512
- Wear of single-crystal silicon carbide in contact with various metals in vacuum [NASA-TP-1198] p0082 W78-21295
- Role of alloying elements in adhesive transfer and friction of copper-base alloys [NASA-TP-1256] p0071 W78-26198
- Effect of oxygen, methyl mercaptan, and methyl chloride on friction behavior of copper-iron contacts [NASA-TP-1309] p0072 W78-30206
- Friction and wear of metals with a single-crystal abrasive grit of silicon carbide: Effect of shear strength of metal [NASA-TP-1293] p0084 W78-30238
- SLIP BANDS**
- U EDGE DISLOCATIONS
- SLOSHING**
- U LIQUID SLOSHING
- SMOKE**
- Evaluation of Federal Aviation Administration ion engine exhaust sampling rake [NASA-CR-138213] p0029 W78-21111
- SNOWFLOW EFFECT**
- U PLASMA DYNAMICS
- SODIUM CHLORIDES**
- Interaction of NaCl/g/ and HCl/g/ with condensed Na₂SO₄ --- in hot corrosion processes p0066 W78-24888
- The effect of NaCl/g/ on the Na₂SO₄-induced hot corrosion of NiAl p0079 W78-24901
- Interaction of NaCl(g) and HCl(g) with condensed Na₂SO₄ [NASA-TN-73796] p0064 W78-13159
- The effect of fuel-to-air ratio on burner-rig hot corrosion [NASA-TN-78960] p0072 W78-31210
- SODIUM COMPOUNDS**
- NT SODIUM CHLORIDES
- NT SODIUM SULFATES
- NT SODIUM SULFITES
- SODIUM SULFATES**
- Interaction of NaCl/g/ and HCl/g/ with condensed Na₂SO₄ --- in hot corrosion processes p0066 W78-24888
- Formation of Na₂SO₄ and K₂SO₄ in flames doped with sulfur and alkali chlorides and carbonates p0066 W78-24889
- The effect of NaCl/g/ on the Na₂SO₄-induced hot corrosion of NiAl p0079 W78-24901
- Formation of Na₂SO₄ and K₂SO₄ in flames doped with sulfur and alkali chlorides and carbonates [NASA-TN-73794] p0064 W78-13157
- Inhibition of hot salt corrosion by metallic additives [NASA-TN-78966] p0072 W78-31208
- SODIUM SULFITES**
- Interaction of NaCl(g) and HCl(g) with condensed Na₂SO₄ [NASA-TN-73796] p0064 W78-13159
- SOFTWARE (COMPUTERS)**
- U COMPUTER PROGRAMS
- U COMPUTER SYSTEMS PROGRAMS
- SOLAR ARRAYS**
- Spacecraft-generated plasma interaction with high voltage solar array

SOLAR CELLS

SUBJECT INDEX

[AIAA PAPER 78-673] p0055 78-32751
 Interaction of large, high power systems with operational orbit charged particle environments --- large solar arrays in space [AAS 77-283] p0048 78-36719
 Solar electric propulsion thruster interactions with solar arrays [NASA-CR-135257] p0052 78-13122
 Summary of the NASA space photovoltaic research and technology program p0130 78-13528
 The ERDA/LeRC photovoltaic systems test facility [NASA-TN-73787] p0035 78-15059
 Results of module electrical measurement of the DOE 46-kilowatt procurement [NASA-TN-78829] p0138 78-19658
 Charging of flexible solar array substrates in kilovolt electron beams [NASA-TN-73865] p0048 78-21199
 Closed loop solar array-ion thruster system with power control circuitry [NASA-CASR-LEW-12780-1] p0048 78-22149

SOLAR CELLS
 A methodology for experimentally-based determination of gap shrinkage and effective lifetimes in the emitter and base of p-n-junction solar cells p0141 78-10903
 Analysis of epitaxial drift field N on P silicon solar cells p0141 78-10904
 Application of thick-film technology to solar cell fabrication p0186 78-10947
 Real-time and accelerated outdoor endurance testing of solar cells p0142 78-52837
 U.S. terrestrial solar cell calibration and measurement procedures p0143 78-52844
 Dendritic web silicon for solar cell application p0146 78-53489
 Solar Cell High Efficiency and Radiation Damage [NASA-CP-2020] p0130 78-13527
 Summary of the NASA space photovoltaic research and technology program p0130 78-13528
 Impurity concentrations and surface charge densities on the heavily doped face of a silicon solar cell p0130 78-13534
 Real-time and accelerated outdoor endurance testing of solar cells [NASA-TN-73743] p0130 78-14628
 US terrestrial solar cell calibration and measurement procedures [NASA-TN-73788] p0130 78-14629
 Results of module electrical measurement of the DOE 46-kilowatt procurement [NASA-TN-78829] p0138 78-19658
 Photovoltaic remote instrument applications: Assessment of the near-term market [NASA-TN-73893] p0150 78-19710
 Method of making encapsulated solar cell modules [NASA-CASR-LEW-12185-1] p0136 78-25528
 Method for producing solar energy panels by automation [NASA-CASR-LEW-12541-1] p0136 78-25529
 Photon degradation effects in terrestrial solar cells [NASA-TN-78928] p0136 78-25551
 Solar cell system having alternating current output [NASA-CASR-LEW-12806-1] p0136 78-25553
 Status of wraparound contact solar cells and arrays [NASA-TN-78911] p0137 78-26543
 Preliminary evaluation of Glass Resin materials for solar cell cover use [NASA-TN-78953] p0137 78-26544
 Ultraviolet irradiation at elevated temperatures and thermal cycling in vacuum of YEP-A covered silicon solar cells [NASA-TN-78926] p0137 78-26545
 An improved technique for the calibration of solar cells using a high altitude aircraft [NASA-TN-78974] p0138 78-26546
 Variation of solar cell sensitivity and solar radiation on tilted surfaces [NASA-TN-78921] p0130 78-26547

Endurance testing of first generation (Block 1) commercial solar cell modules [NASA-TN-78922] p0138 78-26548
 Self-reconfiguring solar cell system [NASA-CASR-LEW-12586-1] p0139 78-27520
 Evaluation of glass resin coatings for solar cell applications [NASA-CR-159392] p0145 78-27540

SOLAR COLLECTORS
ST SOLAR REFLECTORS
 Evaluation of initial collector field performance at the Langley Solar Building Test Facility p0141 78-11391
 A low cost, portable instrument for measuring emittance p0109 78-11392
 Selective coating for solar panels --- using black chrome and black nickel [NASA-CASR-LEW-12159-1] p0132 78-19599
 Solar cell collector [NASA-CASR-LEW-12552-1] p0136 78-25527
 Comparison of three experimental methods used in determining the thermal performance of flat-plate solar collectors [NASA-TN-78929] p0139 78-28614
 Development of flat-plate solar collectors for the heating and cooling of buildings: Executive summary [NASA-CR-134804-2] p0146 78-33527

SOLAR CONVERTERS
U SOLAR GENERATORS
SOLAR COOLING
 Marshall Space Flight Center development program for solar heating and cooling systems p0110 78-11368

SOLAR ELECTRIC PROPULSION
 Status of SERT II spacecraft and ion thrusters - 1978 [AIAA PAPER 78-662] p0050 78-32743
 Constrained sloshing of liquid mercury in a flexible spherical tank [AIAA PAPER 78-670] p0106 78-32749
 Spacecraft-generated plasma interaction with high voltage solar array [AIAA PAPER 78-673] p0055 78-32751
 Extended performance solar electric propulsion thrust system design [AIAA PAPER 78-643] p0055 78-37430
 Extended performance solar electric propulsion thrust system study. Volume 1: Executive summary [NASA-CR-135281-VOL-1] p0052 78-10205
 Solar electric propulsion thruster interactions with solar arrays [NASA-CR-135257] p0052 78-13122
 Extended performance solar electric propulsion thrust system study. Volume 4: Thruster technology evaluation [NASA-CR-135281-VOL-4] p0053 78-16690
 Extended performance solar electric propulsion thrust system study. Volume 5: Capacitor-diode voltage multiplier: Technology evaluation [NASA-CR-135281-VOL-5] p0053 78-19195
 Extended performance solar electric propulsion thrust system study. Volume 3: Tradeoff studies of alternate thrust system configurations [NASA-CR-135281-VOL-3] p0053 78-19196
 Extended performance electric propulsion power processor design study. Volume 1: Executive summary [NASA-CR-135357] p0054 78-20240
 Closed loop solar array-ion thruster system with power control circuitry [NASA-CASR-LEW-12780-1] p0048 78-22149
 SEP ENCKF-87 and Ralley rendezvous studies and improved S/C model implementation in HILTOP [NASA-CR-135414] p0058 78-25105
 Heliocentric interplanetary low thrust trajectory optimization program, supplement 1, part 2 [NASA-CR-135414-APP] p0058 78-25106

SOLAR ENERGY
 Energy resources of the developing countries and some priority markets for the use of solar energy p0142 78-28400
 US terrestrial solar cell calibration and measurement procedures [NASA-TN-74788] p0130 78-14629
 Solar energy meter [NASA-TN-73794] p0131 78-14630

SUBJECT INDEX

SOUND TRANSDUCERS

- Technical and economic feasibility study of solar/fossil hybrid power systems [NASA-TN-73820] p0132 N78-17486
- Status of SERT II spacecraft and ion thrusters, 1978 [NASA-TN-78827] p0047 N78-20251
- Method for producing solar energy panels by automation [NASA-CASE-LEW-12541-1] p0136 N78-25529
- Storage systems for solar thermal power [NASA-TN-78952] p0140 N78-29577
- Utilization of solar energy in developing countries: Identifying some potential markets [NASA-TN-78964] p0140 N78-29578
- SOLAR ENERGY ABSORBERS**
- Black chrome on commercially electroplated tin as a solar selecting coating [NASA-TN-73799] p0131 N78-15562
- SOLAR ENERGY CONVERSION**
- Status of the ERDA/NASA Photovoltaic Tests and Applications Project p0141 N78-11014
- The Redox Flow System for solar photovoltaic energy storage p0141 N78-11019
- Utilization of solar energy in developing countries - Identifying some potential markets p0142 N78-45437
- The ERDA/LeRC Photovoltaic Systems Test Facility p0143 N78-52851
- TS terrestrial solar cell calibration and measurement procedures [NASA-TN-73788] p0130 N78-14629
- Performance and stability analysis of a photovoltaic power system [NASA-TN-78980] p0140 N78-29566
- SOLAR FLUX**
- Ultraviolet spectrophotometer for measuring columnar atmospheric ozone from aircraft p0110 N78-35826
- Measurement of tropospheric 300 nm solar ultraviolet flux for determination of C/1D/ photoprotection p0148 N78-38835
- SOLAR GENERATORS**
- NT SOLAR CELLS**
- Photovoltaic remote instrument applications: Assessment of the near-term market [NASA-TN-73981] p0150 N78-19710
- Impact of Balance of System (BOS) costs on photovoltaic power systems [NASA-TN-78934] p0138 N78-26550
- Design, fabrication and testing of a CFA for use in the solar power satellite [NASA-CR-159410] p0042 N78-21143
- SOLAR HEATING**
- Marshall Space Flight Center development program for solar heating and cooling systems p0110 N78-11368
- Evaluation of initial collector field performance at the Langley Solar Building Test Facility p0141 N78-11391
- SOLAR POWER GENERATION**
- T SOLAR GENERATORS**
- SOLAR POWER SOURCES**
- T SOLAR GENERATORS**
- SOLAR PROPULSION**
- NT SOLAR ELECTRIC PROPULSION**
- SOLAR RADIATION**
- NT SOLAR RADIATION**
- Effect of trichlorofluoromethane and molecular chlorine on ozone formation by simulated solar radiation [NASA-TN-10641] p0064 N78-12167
- Evaluation of models to predict insolation on tilted surfaces [NASA-TN-78942] p0144 N78-25025
- SOLAR REFLECTORS**
- Design and fabrication of a low-specific-weight parabolic dish solar concentrator [NASA-TN-1152] p0046 N78-17145
- SOLAR SAILS**
- The effect of environmental plasma interactions on the performance of the solar sail system [NASA-CR-135258] p0043 N78-17125
- SOLAR SYSTEM**
- NT BALLISTIC CORRECTION**
- SOLID LUBRICANTS**
- Coatings for wear and lubrication [NASA-TN-74841] p0081 N78-20333
- Sputtering technology in solid film lubrication [NASA-TN-78914] p0083 N78-26214
- SOLID ROTATION**
- U ROTATING BODIES**
- SOLID SOLUTIONS**
- Pressureless sintered beta-prime-Si3N4 solid solution - Fabrication, microstructure, and strength p0086 N78-47595
- Pressureless sintered beta prime-Si3N4 solid solution: Fabrication, microstructure, and strength [NASA-TN-78950] p0083 N78-29245
- SOLID STATE DEVICES**
- NT METAL OXIDE SEMICONDUCTORS**
- NT PHOTOVOLTAIC CELLS**
- Adaptation of ion beam technology to microfabrication of solid state devices and transducers [NASA-CR-135314] p0099 N78-15397
- SOLID SURFACES**
- Stress analysis and stress-intensity factors for finite geometry solids containing rectangular surface cracks [ASME PAPER 77-WA/APR-5] p0126 N78-10531
- Definition and effect of chemical properties of surfaces in friction, wear, and lubrication p0121 N78-45436
- Aerodynamic performance of conventional and advanced design labyrinth seals with solid-smooth abradable, and honeycomb lands --- gas turbine engines [NASA-CR-135307] p0122 N78-27427
- SOLID-SOLID INTERFACES**
- Simplified solution for elliptical-contact deformation between two elastic solids p0118 N78-12737
- Simplified contact analysis p0127 N78-28200
- Elastohydrodynamic lubrication of elliptical contacts for materials of low elastic modulus. I - Fully flooded conjunction [ASME PAPER 77-LUB-10] p0119 N78-28414
- Shear strength of metal - SiO2 contacts p0061 N78-33209
- Tribological properties of surfaces p0120 N78-33211
- Effect of oxygen and nitrogen interactions on friction of single-crystal silicon carbide [NASA-TP-1265] p0083 N78-28247
- Effect of oxygen, methyl mercaptan, and methyl chloride on friction behavior of copper-iron contacts [NASA-TP-1309] p0072 N78-30206
- SOLIDIFICATION**
- Traction and lubricant film temperature as related to the glass transition temperature and solidification --- using infrared spectroscopy on EHD contacts p0087 N78-40997
- SOLUBILITY**
- Formulated plastic separators for soluble electrode cells [NASA-CASE-LEW-12358-2] p0065 N78-25149
- SOLUTIONS**
- NT AQUEOUS SOLUTIONS**
- NT GAS MIXTURES**
- NT SOLID SOLUTIONS**
- SONIC FLOW**
- U TRANSONIC FLOW**
- SORPTION**
- NT ADSORPTION**
- NT CHEMISORPTION**
- SOFTIE CAN**
- U SPACELAB**
- SOFTIE LAB**
- T SPACELAB**
- SOUND**
- U ACOUSTICS**
- SOUND DETECTORS**
- U SOUND TRANSDUCERS**
- SOUND MEASUREMENT**
- T ACOUSTIC MEASUREMENTS**
- SCOUND PROPAGATION**
- Propagation of sound waves through a linear shear layer - A closed form solution [AIAA PAPER 78-196] p0165 N78-20738
- SOUND TRANSDUCERS**
- NT MICROPHONES**

SOUND WAVES

Sound separation probes for flowing duct noise measurements --- jet engine diagnostics p0033 A78-17396

SOUND WAVES
 NT AERODYNAMIC NOISE
 NT AIRCRAFT NOISE
 NT ENGINE NOISE
 NT JET AIRCRAFT NOISE
 NT NOISE (SOUND)
 Far-field multimodal acoustic radiation directivity p0165 A78-24876
 Far-field multimodal acoustic radiation directivity --- from ducted bodies [NASA-TN-73839] p0163 A78-13855
 Propagation of sound waves through a linear shear layer: A closed form solution [NASA-TN-73828] p0164 A78-16766

SOUNDING
 NT ACOUSTIC SOUNDING
SPACE COMMUNICATION
 NT SPACECRAFT COMMUNICATION
SPACE ENVIRONMENT
 U AEROSPACE ENVIRONMENTS
SPACE POWER REACTORS
 Lithium and potassium heat pipes for thermionic converters [NASA-TN-78946] p0104 A78-26390

SPACE PROBES
 Extended-performance thruster technology evaluation [AIAA PAPER 78-666] p0055 A78-37836

SPACE PROCESSING
 Convection due to surface-tension gradients --- in reduced gravity spacecraft environments p0108 A78-48716

SPACE RADIATORS
 U SPACECRAFT RADIATORS
SPACE RESEARCH
 SEP EMCKE-87 and Bailey rendezvous studies and improved S/C model implementation in BILTOP [NASA-CR-135818] p0038 A78-25105

SPACE SHUTTLE ORBITERS
 Ion beam plume and efflux characterization flight experiment study --- space shuttle payload [NASA-CR-135275] p0052 A78-12140

SPACE SHUTTLE PAYLOADS
 NT SPACEBORNE EXPERIMENTS
 NT SPACELAB
SPACE SYSTEMS ENGINEERING
 U AEROSPACE ENGINEERING
SPACE TRANSPORTATION SYSTEMS
 NT SPACE SHUTTLE ORBITERS
SPACE VEHICLES
 U SPACECRAFT
SPACEBORNE EXPERIMENTS
 The Plasma Interaction Experiment (PIX) description and test program --- electrometers [NASA-TN-78963] p0041 A78-21189
 Continuation of the compendium of applications technology satellite and communications technology satellite user experiments 1967-1977, volume 1 [NASA-CR-135816-VOL-1] p0042 A78-31101
 Continuation of the compendium of applications technology satellite and communications technology satellite user experiments 1967-1977, volume 2 --- bibliography [NASA-CR-135816-VOL-2] p0042 A78-31102

SPACECRAFT
 Proceedings of the Spacecraft Charging Technology Conference [NASA-TN-X-71537] p0036 A78-10129
 Dynamic modeling of spacecraft in a collisionless plasma p0037 A78-10150
 Testing of typical spacecraft materials in a simulated substorm environment p0036 A78-10156
 Investigation of high voltage spacecraft system interactions with plasma environments [NASA-TN-78831] p0097 A78-21373

SPACECRAFT CHARGING
 Summary of the CTS Transient Event Counter data after one year of operation --- Communication Technology Satellite p0046 A78-19566
 NASCAP, a three-dimensional Charging Analyzer Program for complex spacecraft p0044 A78-19567

SUBJECT INDEX

NASA Charging Analyzer Program - A computer tool that can evaluate electrostatic contamination --- of spacecraft during geomagnetic substorms p0044 A78-33220

Interaction of large, high power systems with operational orbit charged particle environments --- large solar arrays in space [AAS 77-243] p0044 A78-36719

Charging characteristics of materials: Comparison of experimental results with simple analytical models p0036 A78-10157

Provisional specification for satellite time in a geomagnetic environment p0036 A78-10173

Development of environmental charging effect monitors for operational satellites p0037 A78-10174

Viking and STP P78-2 electrostatic charging designs and testing p0037 A78-10175

The effect of environmental plasma interactions on the performance of the solar sail system [NASA-CR-135258] p0098 A78-13325

NASCAF user's manual [NASA-CR-135259] p0099 A78-13329

NASA charging analyzer program: A computer tool that can evaluate electrostatic contamination [NASA-TN-73889] p0096 A78-21372

Status of the NASA-Lewis Research Center spacecraft charging investigation --- spacecraft materials tests [NASA-TN-78938] p0049 A78-27170

Spacecraft charging control by thermal, field emission with lanthanum-hexaboride emitters [NASA-TN-78990] p0183 A78-32014

SPACECRAFT COMMUNICATION
 Utilization of NASA Lewis mobile terminals for the Hermes satellite p0094 A78-24885

CTS /Hermes/ - United States experiments and operations summary --- Communications Technology Satellite p0094 A78-24886

Low cost Ka-band earth terminals for voice/data/facsimile p0094 A78-31970

Low cost satellite land mobile service for nationwide applications p0095 A78-83173

Utilization of NASA Lewis mobile terminals for the Hermes satellite [NASA-TN-78959] p0093 A78-15326

SPACECRAFT COMPONENTS
 The Plasma Interaction Experiment /PIX/ - Description and flight qualification test program [AIAA PAPER 78-674] p0051 A78-32752

Evaluation of commercially-available spacecraft-type heat pipes [AIAA 78-397] p0044 A78-35550

SPACECRAFT CONSTRUCTION MATERIALS
 Status of the NASA-Lewis Research Center spacecraft charging investigation --- spacecraft materials tests [NASA-TN-78938] p0049 A78-27170

SPACECRAFT CONTAMINATION
 NASA Charging Analyzer Program - A computer tool that can evaluate electrostatic contamination --- of spacecraft during geomagnetic substorms p0044 A78-33220

SPACECRAFT CONTROL
 NT SATELLITE CONTROL
SPACECRAFT DESIGN
 Viking and STP P78-2 electrostatic charging designs and testing p0037 A78-10175

Liquid rocket engine axial-flow turbopumps [NASA-SP-8124] p0050 A78-31164

SPACECRAFT ELECTRONIC EQUIPMENT
 Performance of the 12GHz, 200 watt transmitter experiment package for the Hermes satellite [NASA-TN-71904] p0093 A78-13282

SPACECRAFT ENVIRONMENTS
 Investigation of high voltage spacecraft system interactions with plasma environments [AIAA PAPER 78-672] p0050 A78-32750

The Plasma Interaction Experiment /PIX/ - Description and flight qualification test program [AIAA PAPER 78-674] p0051 A78-32752

SUBJECT INDEX

SPECTRUM ANALYSIS

- Convection due to surface-tension gradients --- in reduced gravity spacecraft environments p0108 A78-48716
- Interaction of large, high power systems with operational orbit charged particle environments [NASA-TN-73867] p0037 N78-16076
- SPACECRAFT ORBITS**
- BT GEOSYNCHRONOUS ORBITS**
- Interaction of large, high power systems with operational orbit charged particle environments --- large solar arrays in space [AAS 77-241] p0084 A78-36719
- SPACECRAFT PERFORMANCE**
- Status of SERT II spacecraft and ion thrusters - 1978 [AIAA PAPER 78-662] p0050 A78-32783
- SPACECRAFT POWER SUPPLIES**
- Development and fabrication of a diffusion welded Columbia alloy heat exchanger --- for space power generation [AIAA PAPER 78-61] p0123 A78-31500
- Investigation of high voltage spacecraft system interactions with plasma environments [AIAA PAPER 78-672] p0050 A78-32750
- High temperature heat pipe research at NASA Lewis Research Center [AIAA 78-478] p0106 A78-35618
- Comment on 'Heat-pipe reactors for space power applications' p0052 A78-40826
- SPACECRAFT PROPULSION**
- BT ION PROPULSION**
- BT SOLAR ELECTRIC PROPULSION**
- Planned flight test of a mercury ion auxiliary propulsion system. I - Objectives, systems descriptions, and mission operations [AIAA PAPER 78-647-I] p0050 A78-32734
- Planned flight test of a mercury ion auxiliary propulsion system. II - Integration with host spacecraft [AIAA PAPER 78-647-II] p0050 A78-32735
- A review of electron bombardment thruster systems/spacecraft field and particle interfaces [AIAA PAPER 78-677] p0051 A78-32754
- A mechanical, thermal and electrical packaging design for a prototype power management and control system for the 30 cm mercury ion thruster [AIAA PAPER 78-685] p0051 A78-32759
- 30-cm mercury ion thruster performance with a 1 kw capacitor-diode voltage multiplier beam supply [AIAA PAPER 78-686] p0051 A78-32760
- Evolution of the 1-lb mercury ion thruster subsystem [AIAA PAPER 78-7118] p0051 A78-32776
- Extended-performance thruster technology evaluation [AIAA PAPER 78-688] p0055 A78-37436
- Linear arcjet engine study --- for reusable launch vehicles [NASA-78-15231] p0026 N78-11082
- High-temperature, high-power-density thermionic energy conversion for space [NASA-78-71994] p0171 N78-13890
- Ion engine auxiliary propulsion applications and integration study [NASA-78-15232] p0052 N78-15168
- SPACECRAFT RADIATORS**
- Evaluation of taxially-available spacecraft-type heat pipes [NASA-TN-78836] p0103 N78-20459
- SPACECRAFT RENOVATIONS**
- SPACECRAFT SENSORS**
- SPACECRAFT SHIELDING**
- Evaluation of low cost/high temperature fiber and blanket insulation p0063 A78-16903
- SPACECRAFT STABILITY**
- Effect of vibration on retention characteristics of screen acquisition systems --- for surface mission propellant acquisition [AIAA PAPER 78-1031] p0045 A78-14960
- Provisional specification for satellite time in a geomagnetic environment p0036 N78-10173
- SPACECRAFT STRUCTURES**
- A three dimensional dynamic study of electrostatic charging of materials [NASA-78-15233] p0029 N78-13328
- SPACECRAFT TELEVISION**
- BT OPTICAL SPACECRAFT TELEVISION**
- BT SATELLITE TELEVISION**
- SPACECRAFT TRAJECTORIES**
- BT INTERPLANETARY TRAJECTORIES**
- SPACELAB**
- Burning of liquid pools in reduced gravity [NASA-CR-135234] p0067 N78-25150
- Preliminary concept, specifications, and requirements for a zero-gravity combustion facility for spacelab [NASA-TN-78910] p0041 N78-26166
- SPACELAB PAYLOADS**
- BT ANPS (SATELLITE PAYLOAD)**
- Conceptual design for spacelab two-phase flow experiments [NASA-CR-135327] p0037 N78-14063
- Conceptual design for spacelab pool boiling experiment [NASA-CR-135378] p0037 N78-20150
- SPALLATION**
- Oxide morphology and spalling model for SIAL p0075 A78-30112
- SPARK IGNITION**
- A sustained-arc ignition system for internal combustion engines [NASA-TN-73833] p0096 N78-13331
- Photographic characterization of spark-ignition engine fuel injectors [NASA-TN-78830] p0018 N78-25110
- Light weight, low compression aircraft diesel engine --- converting a spark ignition engine to the diesel cycle [NASA-CR-135300] p0121 N78-21471
- Line tests of the Kordesh hybrid passenger vehicle [NASA-TN-73769] p0138 N78-26551
- SPATIAL ORIENTATION**
- BT ATTITUDE (INCLINATION)**
- SPECIFIC HEAT**
- Interpolation and extrapolation of creep rupture data by the minimum commits it method. III - Analysis of multibeats p0076 A78-45428
- SPECIFICATIONS**
- BT EQUIPMENT SPECIFICATIONS**
- Provisional specification for satellite time in a geomagnetic environment p0036 N78-10173
- Impact of broad-specification fuels on future jet aircraft --- engine components and performance p0089 N78-27059
- SPECTRA**
- BT ABSORPTION SPECTRA**
- BT EMISSION SPECTRA**
- BT ENERGY SPECTRA**
- BT NOISE SPECTRA**
- SPECTRAL ABSORPTION**
- BT ABSORPTION SPECTRA**
- SPECTRAL ANALYSIS**
- BT SPECTRUM ANALYSIS**
- SPECTRAL BANDS**
- BT ABSORPTION SPECTRA**
- SPECTRAL EMISSION**
- On the localness of the spectral energy transfer in turbulence [NASA-TN-73824] p0101 N78-13361
- Emittance and absorptance of NASA ceramic thermal barrier coating system --- for turbine cooling [NASA-TD-1190] p0020 N78-26148
- SPECTRAL LINE WIDTH**
- Model for interpreting Doppler broadened optical line emission measurements on axially symmetric plasma p0174 A78-46189
- SPECTROPHOTOMETERS**
- BT ULTRAVIOLET SPECTROPHOTOMETERS**
- Development of a drift-correction procedure for a photoelectric spectrometer p0109 A78-23525
- SPECTROSCOPY**
- BT ELECTRON SPECTROSCOPY**
- BT INFRARED SPECTROSCOPY**
- BT MASS SPECTROSCOPY**
- BT OPTICAL EMISSION SPECTROSCOPY**
- BT PHOTOELECTRON SPECTROSCOPY**
- BT X RAY SPECTROSCOPY**
- SPECTRUM ANALYSIS**
- A fluctuation-induced plasma transport diagnostic based upon fast-Fourier transforms spectral analysis

SPEED CONTROL

[NASA-TN-78932] p0172 N78-26926
 Fluctuation spectra in the NASA Lewis bumpy-torus
 plasma
 [NASA-TN-1257] p0172 N78-26927

SPEED CONTROL
 High stiffness seals for rotor critical speed
 control
 [ASME PAPER 77-DET-10] p0118 N78-20591
 Response of lead-acid batteries to
 chopper-controlled discharge: Preliminary results
 [NASA-TN-73834] p0180 N78-20023

SPEED INDICATORS
 NT ANEMOMETERS

SPEED REGULATION
 7 SPEED CONTROL

SPHERICAL TANKS
 Constrained sloshing of liquid mercury in a
 flexible spherical tank
 [AIAA PAPER 78-670] p0106 N78-32749

SPRAY CHARACTERISTICS
 The role of drop velocity in statistical spray
 description
 p0107 N78-50323

SPRAY NOZZLES
 Effect of airstream velocity on mean drop
 diameters of water sprays produced by pressure
 and air atomizing nozzles
 [NASA-TN-73740] p0101 N78-13369

SPRAYED PROTECTIVE COATINGS
 3 PROTECTIVE COATINGS

SPRAYERS
 Closed loop spray cooling apparatus --- for
 particle accelerator targets
 [NASA-CASE-1EN-11961-1] p0091 N78-17237
 The role of drop velocity in statistical spray
 description
 [NASA-TN-73887] p0102 N78-20458

SPRAYING
 NT PLASMA SPRAYING

SPRAYING APPARATUS
 3 SPRAYERS

SPRAYS
 3 SPRAYERS

SPUTTERING
 Microstructural and wear properties of sputtered
 carbides and silicides p0084 N78-21445
 Composition of RF-sputtered refractory compounds
 determined by X-ray photoelectron spectroscopy
 p0085 N78-33301
 Effect of facility background gases on internal
 erosion of the 12-cm Hg ion thruster
 [AIAA PAPER 78-665] p0060 N78-32745
 Mechanical properties on ion-beam-textured
 surgical implant alloys p0075 N78-36045
 Ion beam sputter etching and deposition of
 fluoropolymers p0085 N78-37684
 The use of an ion-beam source to alter the surface
 morphology of biological implant materials
 p0061 N78-37686
 Critical currents and scaling laws in sputtered
 copper molybdenum sulfide p0175 N78-45500
 Effect of surface texture by ion beam sputtering
 on implant biocompatibility and soft tissue
 attachment
 [NASA-CR-134711] p0152 N78-18672
 X-ray photoelectron spectroscopy study of
 radiofrequency-sputtered refractory compound
 steel interfaces
 [NASA-TN-11-1] p0081 N78-20336
 Ion beam sputter etching and deposition of
 fluoropolymers
 [NASA-TN-78989] p0086 N78-20358
 The friction and wear properties of sputtered hard
 refractory compounds
 [NASA-TN-78995] p0080 N78-26177
 Application of TSCA to the determination of
 stoichiometry in sputtered coatings and
 interface regions
 [NASA-TN-78806] p0085 N78-26185
 Sputtering technology in solid film lubrication
 [NASA-TN-78114] p0083 N78-26214
 Ion beam sputtering of fluoropolymers --- etching
 polymer films and target surfaces
 [NASA-TN-79000] p0060 N78-33151

SUBJECT INDEX

STABILITY
 NT ACOUSTIC INSTABILITY
 NT ATTITUDE STABILITY
 NT COMBUSTION STABILITY
 NT FREQUENCY STABILITY
 NT MAGNETOHYDRODYNAMIC STABILITY
 NT SPACECRAFT STABILITY
 NT SYSTEMS STABILITY
 NT THERMAL STABILITY
 STABILITY DERIVATIVES
 NT PITCHING MOMENTS
 STACKING FAULTS
 0 CRYSTAL DEFECTS

STAGNATION FLOW
 A visual investigation of turbulence in stagnation
 flow about a circular cylinder
 [NASA-CR-3019] p0108 N78-33386

STAINLESS STEELS
 NT AUSTENITIC STAINLESS STEELS
 NT FERRITIC STAINLESS STEELS
 X-ray photoelectron spectroscopic study of surface
 chemistry of dibenzyl disulfide on steel under
 mild and severe wear conditions
 p0066 N78-31439
 New alloys to conserve critical elements ---
 replacing chromium in steels
 p0076 N78-37680
 Interpolation and extrapolation of creep rupture
 data by the minimum commitment method. III -
 Analysis of multiheats
 p0076 N78-45428
 Evaluation of commercially-available
 spacecraft-type heat pipes
 [NASA-TN-78826] p0103 N78-20459
 Fabrication of stainless steel clad tubing --- gas
 pressure bonding
 [NASA-CR-135347] p0079 N78-21265
 Influence of fretting on flexural fatigue of 304
 stainless steel and mild steel
 [NASA-TN-1193] p0070 N78-21260
 New alloys to conserve critical elements
 [NASA-TN-78840] p0070 N78-24335
 Fractographic evaluation of creep effects on
 strain-controlled fatigue-cracking of AISI 304C
 and 316 stainless steel
 [NASA-TN-78913] p0126 N78-27453

STANDARDS
 Proposed design procedure for transmission
 shafting under fatigue loading
 [NASA-TN-78927] p0115 N78-26444

STARTERS
 NT ENGINE STARTERS

STARTING
 Optimal control of a supersonic inlet to minimize
 frequency of inlet unstart
 p0019 N78-23028

STATE VECTORS
 Discrete time domain modelling and analysis of
 dc-dc converters with continuous and
 discontinuous inductor current
 p0100 N78-18796

STATIC LOADS
 Evaluation of flawed composite structure under
 static and cyclic loading
 p0063 N78-26683
 Influence of wind turbine foundation
 p0133 N78-19626
 Summary of static load test of the Mod-0 blade
 p0133 N78-19627

STATIC TESTS
 Summary of static load test of the Mod-0 blade
 p0133 N78-19627

STATICS
 NT ELECTROSTATICS

STATIONS
 NT GROUND STATIONS

STATISTICAL ANALYSIS
 NT REGRESSION ANALYSIS
 NT WEIBULL DENSITY FUNCTIONS
 'Chain pooling' model selection as developed for
 the statistical analysis of a rotor burst
 protection experiment
 p0160 N78-29327
 Interpolation and extrapolation of creep rupture
 data by the minimum commitment method. III -
 Analysis of multiheats
 p0076 N78-45428
 Chain Pooling modeling selection as developed for
 the statistical analysis of a rotor burst

- protection experiment
[NASA-TN-73878] p0160 W78-16735
- Statistical model for asperity-contact time
fraction in elastohydrodynamic lubrication
[NASA-TP-1130] p0110 W78-18429
- STATISTICAL DISTRIBUTIONS**
The role of drop velocity in statistical spray
description p0107 W78-50323
- STATISTICAL PROBABILITY**
J PROBABILITY THEORY
- STATOR BLADES**
Cold-air performance of free-power turbine
designed for 112-kilowatt automotive gas-turbine
engine. 1: Design stator-vane-chord setting
angle of 35 deg p0015 W78-16053
[NASA-TP-1007]
- Two-dimensional cold-air cascade study of a
film-cooled turbine stator blade. 4:
Comparison of experimental and analytical
aerodynamic results for blade with 12 rows of
0.076-centimeter-(0.030-inch-) diameter holes
having streamwise ejection angles
[NASA-TP-1151] p0017 W78-20130
- Two-dimensional cold-air cascade study of a
film-cooled turbine stator blade. 5:
Comparison of experimental and analytical
aerodynamic results for blade with 12 rows of
0.038-centimeter-(0.015 inch) diameter coolant
holes having streamwise ejection angles
[NASA-TP-1200] p0017 W78-20133
- STATORS**
Effect of endwall cooling on secondary flows in
turbine stator vanes p0014 W78-11076
- Liquid metal slip ring
[NASA-CASE-12W-12277-2] p0057 W78-25323
- STEAM**
Revised international representations for the
viscosity of water and steam and new
representations for the surface tension of water
p0105 W78-15725
- STEAM TURBINES**
Open-Cycle Gas Turbine/Steam Turbine Combined
Cycles with synthetic fuels from coal
[ASME PAPER 77-WA/ENER-9] p0146 W78-33187
- STEELS**
NT AUSTENITIC STAINLESS STEELS
NT CARBON STEELS
NT CHROMIUM STEELS
NT FERRITIC STAINLESS STEELS
NT MARAGING STEELS
NT STAINLESS STEELS
- Experimental and analytical load-life relation for
AISI 52100 steel spur gears
[ASME PAPER 77-DET-121] p0119 W78-20609
- Surface-crack shape change in bending fatigue
using an inexpensive resonant fatiguing apparatus
p0075 W78-35394
- Cyclic stress-strain curve determination for DeAc
steel by three methods
[NASA-TN-73815] p0068 W78-13183
- The effect of microstructure and strength on the
fracture toughness of an 18 Ni, 300 grade
maraging steel
[NASA-CR-115288] p0078 W78-16450
- I-ray photoelectron spectroscopy study of
radiofrequency-sputtered refractory compound
steel interfaces
[NASA-TP-11611] p0081 W78-20336
- High toughness-high strength iron alloy
[NASA-CASE-12W-12542-2] p0070 W78-22205
- The friction and wear properties of sputtered hard
refractory compounds
[NASA-TN-73895] p0056 W78-26177
- Long-term hot-hardness characteristics of five
through-hardened bearing steels
[NASA-TP-11811] p0073 W78-33196
- STEEP GRADIENT AIRCRAFT**
J V-STOL AIRCRAFT
- STELLAR DOPPLER SHIFT**
J DOPPLER EFFECT
- STELLARATORS**
Alternative approaches to plasma confinement
p0174 W78-52146
- STABILIZATION EFFECTS**
NT CHEMICAL EFFECTS
NT THERMAL DEGRADATION
- STIFFNESS**
Stiffness and damping of elastomeric O-ring
beard counts
[NASA-CR-135328] p0127 W78-18460
- Development of procedures for calculating
stiffness and damping properties of elastomers
in engineering applications. Part 4: Testing of
elastomers under a rotating load --- resonance
testing
[NASA-CR-135355] p0127 W78-22402
- Stiffness of straight and tapered annular gas path
seals
[NASA-TN-78872] p0103 W78-23385
- STIMULATED EMISSION DEVICES**
NT CARBON DIOXIDE LASERS
NT GASDYNAMIC LASERS
NT INFRARED LASERS
NT LASERS
- STIRLING CYCLE**
Materials technology assessment for Stirling engines
[NASA-TN-73789] p0065 W78-171.7
- Automotive Stirling engine development program ---
fuel economy assessment
[NASA-CR-135331] p0181 W78-225.6
- Stirling engine design manual
[NASA-CR-135382] p0181 W78-23999
- Ceramic regenerator system development program
--- for automobile gas turbine engines
[NASA-CR-135330] p0181 W78-25988
- A Stirling engine computer model for performance
calculations
[NASA-TN-78864] p0180 W78-29994
- Stirling engine project status
p0117 W78-30314
- Initial test results with single cylinder rhombic
drive Stirling engine
p0117 W78-30316
- Materials technology assessment for Stirling engines
p0117 W78-30318
- Initial test results with a single-cylinder
rhombic-drive Stirling engine --- to be applied
to automobile engine design to conserve energy
[NASA-TN-78919] p0180 W78-31533
- STOICHIOMETRY**
Physics and chemistry of MoS₂ intercalation
compounds p0175 W78-27727
- Application of ESCA to the determination of
stoichiometry in spattered coatings and
interface regions
[NASA-TN-78896] p0065 W78-26185
- STOL AIRCRAFT**
J SHORT TAKEOFF AIRCRAFT
- STOPCOCKS**
J COCKS
- STORABLE PROPELLANTS**
NT AIRCRAFT FUELS
- STORAGE BATTERIES**
NT LEAD ACID BATTERIES
NT NICKEL ZINC BATTERIES
New batteries and their impact on electric vehicles
p0181 W78-16923
- STORMS**
NT MAGNETIC STORMS
NT TORNADOES
- STORMS (METEOROLOGY)**
NT TORNADOES
- STRAIN AGING**
J PRECIPITATION HARDENING
- STRAIN DISTRIBUTION**
J STRESS CONCENTRATION
- STRAIN FATIGUE**
J FATIGUE (MATERIALS)
- STRAIN GAGES**
Reliability analysis of forty-five strain-gage
systems mounted on the first fan stage of a
TF-100 engine
[NASA-TN-73720] p0109 W78-13407
- STRAIN RATE**
Ductility normalized-strain-range partitioning
life relations for creep-fatigue life predictions
p0077 W78-51739
- Strainrange partitioning behavior of the
nickel-base superalloys, Rene' 80 and In 100
[NASA-TN-78828] p0070 W78-21267
- STRAIN SOFTENING**
J PLASTIC DEFORMATION
- STRATOSPHERE**
Global measurements of gaseous and aerosol trace

STRESS FUNCTIONS (FLUIDS)

species in the upper troposphere and lower stratosphere from daily flights of 747 airliners
p0147 A78-15826

Stratospheric cruise emission reduction program
p0013 A78-11077

Global sensing of gaseous and aerosol trace species using automated instrumentation on 747 airliners
[NASA-TN-73610] p0100 A78-13670

STRESS FUNCTIONS (FLUIDS)
VCE testbed program planning and definition study
[NASA-CR-135362] p0029 A78-19160

STRESS
BT GAS STRESS

STRENGTH OF MATERIALS
U MECHANICAL PROPERTIES
STRESS ANALYSIS
Stress analysis and stress-intensity factors for finite geometry solids containing rectangular surface cracks
[ASME PAPER 77-WA/APM-5] p0126 A78-10531

DYNAMIC TOOTH LOADS AND STRESSING FOR HIGH CONTACT RATIO SPUR GEARS
[ASME PAPER 77-DET-101] p0123 A78-10606

VSTOL tilt nacelle aerodynamics and its relation to fan blade stresses
[AIAA PAPER 78-958] p0007 A78-83520

Interpolation and extrapolation of creep rupture data by the minimum commitment method. III - Analysis ofaultboats
p0076 A78-85428

Summary of static load test of the Mod-0 blade
p0133 A78-19627

In situ ply strength: An initial assessment --- using laminate fracture data and a least squares method
[NASA-TN-73771] p0059 A78-21220

Effects of moisture profiles and laminate configuration on the hygro stresses in advanced composites --- graphite-epoxy composites
[NASA-TN-78978] p0059 A78-32191

STRESS CALCULATIONS
U STRESS ANALYSIS
STRESS CONCENTRATION
Stress analysis and stress-intensity factors for finite geometry solids containing rectangular surface cracks
[ASME PAPER 77-WA/APM-5] p0126 A78-10531

Mode I stress intensity factors for round compact specimens
p0126 A78-11817

The use of parabolic variations and the direct determination of stress intensity factors using the BIE method --- Boundary Integral Equation
p0126 A78-24903

STRESS DISTRIBUTION
U STRESS CONCENTRATION

STRESS FUNCTIONS
Displacement coefficients along the inner boundaries of radially cracked ring segments subject to forces and couples
p0127 A78-35396

STRESS PROPAGATION
Correlations between ultrasonic and fracture toughness factors in metallic materials
p0077 A78-45834

STRESS RELAXATION
Method for alleviating thermal stress damage in laminates
[NASA-CASZ-LEN-12493-1] p0059 A78-22163

STRESS RUPTURE STRENGTH
U CREEP RUPTURE STRENGTH

STRESS WAVES
Correlation of fiber composite tensile strength with the ultrasonic stress wave factor
p0060 A78-33207

Impact on multilayered composite plates
[NASA-CR-135247] p0062 A78-16103

STRESS-STRAIN DIAGRAMS
Cyclic stress-strain curve determination for D6AC steel by three methods
[NASA-TN-73815] p0068 A78-13183

Analysis and test of deep flaws in thin sheets of aluminum and titanium. Volume 2: Crack opening displacement and stress-strain data
[NASA-CR-135170] p0127 A78-21494

STRESS-STRAIN DISTRIBUTION
U STRESS CONCENTRATION

SUBJECT INDEX

STRESS-STRAIN RELATIONSHIPS
U STRESS-STRAIN DIAGRAMS

STRESSES
BT AXIAL STRESS
BT CRITICAL LOADING
BT RESIDUAL STRESS
BT TENSILE STRESS
BT THERMAL STRESSES
BT VIBRATIONAL STRESS

STRUCTURAL ANALYSIS
BT DYNAMIC STRUCTURAL ANALYSIS
Gas path sealing in turbine engines
p0028 A78-33218

Room temperature crack growth rates and -20 deg F fracture toughness of welded 1/4 inch A-285 steel plate
[NASA-TN-73847] p0068 A78-13182

Simplified modeling for wind turbine nodal analysis using NASTRAN
p0132 A78-19619

Ferrographic analysis of wear particles from sliding elastohydrodynamic experiments
[NASA-TN-1230] p0115 A78-22377

Analysis/design of strip reinforced random composites (strip hybrids)
[NASA-TN-78985] p0059 A78-33189

STRUCTURAL BEAMS
U BEAMS (SUPPORTS)

STRUCTURAL DESIGN
Design and performance of heart assist or artificial heart control systems
p0185 A78-23032

STRUCTURAL DESIGN CRITERIA
Liquid rocket lines, bellows, flexible hoses, and filters
[NASA-SP-8123] p0047 A78-16089

Preliminary concept, specifications, and requirements for a zero-gravity combustion facility for spacelab
[NASA-TN-78910] p0041 A78-26166

STRUCTURAL DYNAMICS
U DYNAMIC STRUCTURAL ANALYSIS

STRUCTURAL ENGINEERING
Turbine disks for improved reliability
p0012 A78-10089

STRUCTURAL FATIGUE
U FATIGUE (MATERIALS)

STRUCTURAL FOUNDATIONS
U FOUNDATIONS

STRUCTURAL MATERIALS
U CONSTRUCTION MATERIALS

STRUCTURAL MEMBERS
BT ANISOTROPIC PLATES
BT BEAMS (SUPPORTS)
BT CIRCULAR PLATES
BT FLAT PLATE
BT STRUTS
Influence of wind turbine foundation
p0133 A78-19621

STRUCTURAL STRAIN
Experimental determination of transient strain in a thermally-cycled simulated turbine blade utilizing a non-contact technique
[NASA-TN-73886] p0017 A78-19161

STRUCTURAL VIBRATION
BT BENDING VIBRATION
BT FLUTTER
Effect of vibration on retention characteristics of screen acquisition systems --- for surface tension propellant acquisition
[AIAA PAPER 78-1030] p0045 A78-83560

Effect of vibration on retention characteristics of screen acquisition systems
[NASA-CR-135264] p0107 A78-12364

STRUCTURAL WEIGHT
Concepts for the development of light-weight composite structures for rotor burst containment
p0012 A78-10089

STRUTS
A method for calculating strut and splitter plate noise in exit ducts: Theory and verification
[NASA-CR-29855] p0117 A78-20921

SUBGRAVITY
U REDUCED GRAVITY

SUBSONIC FLOW
A combined potential and viscous flow solution for VSTOL engine inlets
[AIAA PAPER 78-142] p0006 A78-28702

SUBJECT INDEX

SUPERSONIC INLETS

- A viscous-inviscid interactive compressor calculation [AIAA PAPER 76-1180] p0006 A78-41843
- A viscous-inviscid interactive compressor calculations [NASA-TN-78920] p0005 A78-26100
- Derivation and evaluation of an approximate analysis for three-dimensional viscous subsonic flow with large secondary velocities --- finite difference method [NASA-CR-159030] p0008 A78-33044
- SUBSTANCES**
- T MATERIALS**
- SULFATES**
- NT SODIUM SULFATES
Reactions of yttria-stabilized zirconia with oxides and sulfates of various elements [NASA-TN-78942] p0071 A78-29216
- SULFIDES**
- NT COPPER SULFIDES
- NT DISULFIDES
- NT MOLYBDENUM DISULFIDES
- NT MOLYBDENUM SULFIDES
Solubility, stability, and electrochemical studies of sulfur-sulfide solutions in organic solvents [NASA-TP-1285] p0180 A78-28624
- SULFITES**
- NT SODIUM SULFITES
- SULFUR**
Study of the effects of gaseous environments on sulfidation attack of superalloys [NASA-CR-135348] p0070 A78-21268
- SULFUR COMPOUNDS**
- NT COPPER SULFIDES
- NT DISULFIDES
- NT MOLYBDENUM DISULFIDES
- NT MOLYBDENUM SULFIDES
- NT ORGANIC SULFUR COMPOUNDS
- NT SODIUM SULFATES
- NT SODIUM SULFITES
- NT SULFATES
- NT SULFIDES
- NT TRIOLS
- SUMMARIES**
- NT ABSTRACTS
- SUNLIGHT**
Some basic considerations of measurements involving collimated direct sunlight [NASA-TN-78947] p0130 A78-11608
- SUPER SABRE AIRCRAFT**
- F-100 AIRCRAFT
- SUPERBALLS**
- T HEAT RESISTANT ALLOYS
- SUPERCONDUCTING MAGNETS**
Parametric dependence of ion temperature and relative density in the NASA Lewis SUMMA facility p0173 A78-37679
- Potential damage to dc superconducting magnets due to high frequency electromagnetic waves p0098 A78-39902
- Superconducting Nb₃Ge for high-field magnets p0175 A78-41922
- Potential damage to DC superconducting magnets due to the high frequency electromagnetic waves [NASA-TN-78908] p0096 A78-13330
- Niobium-germanium superconducting tapes for high-field magnet applications [NASA-CR-135348] p0099 A78-19392
- SUPERCONDUCTIVITY**
Physics and chemistry of MoS₂ intercalation compounds p0175 A78-27727
- Parametric dependence of ion temperature and relative density in the NASA Lewis SUMMA facility --- superconducting magnetic mirror [NASA-TN-78770] p0172 A78-23923
- SUPERCONDUCTORS**
Critical currents and scaling laws in sputtered copper polybismuth sulfide p0175 A78-45500
- Upper critical field of copper polybismuth sulfide p0175 A78-53626
- SUPERCRITICAL CRI FLOW**
Influence of oil-squeeze-film damping on steady-state response of flexible rotor operating at supercritical speeds [NASA-TN-10941] p0015 A78-13064
- SUPERCRITICAL PRESSURES**
Supercritical oxygen heat transfer ---
- regenerative cooling [NASA-CR-135339] p0108 A78-17342
- SUPERHIGH FREQUENCIES**
The 20/30 GHz satellite systems technology needs assessment [NASA-TN-78975] p0093 A78-31323
- SUPERMAGNETS**
- O HIGH FIELD MAGNETS
- SUPERPLASTICITY**
Strength enhancement process for prealloyed powder superalloys p0075 A78-33216
- SUPERSONIC AIRCRAFT**
- NT F-15 AIRCRAFT
- NT F-100 AIRCRAFT
- NT F-102 AIRCRAFT
- NT SUPERSONIC TRANSPORTS
Advanced supersonic propulsion study, phase 4 [NASA-CR-135273] p0026 A78-11062
- SUPERSONIC COMBUSTION**
Wide range operation of advanced low NOx combustors for supersonic high-altitude aircraft gas turbines [NASA-CR-135297] p0027 A78-14007
- SUPERSONIC CRUISE AIRCRAFT RESEARCH**
Inlet-engine matching for SCAR including application of a bicone variable geometry inlet --- Supersonic Cruise Aircraft Research [AIAA PAPER 78-961] p0007 A78-45096
- Atmospheric effects on inlets for supersonic cruise aircraft [NASA-TN-X-73647] p0003 A78-10026
- Advanced supersonic propulsion study, phases 3 and 4 --- variable cycle engines [NASA-CR-135236] p0027 A78-13058
- Aero-acoustic tests of duct-burning turbofan exhaust nozzles. Comprehensive data report. Volume 1: Model scale acoustic data [NASA-CR-134910-VOL-1] p0002 A78-15988
- Aero-acoustic tests of duct-burning turbofan exhaust nozzles. Comprehensive data report. Volume 2: Acoustic and aerodynamic data [NASA-CR-134910-VOL-2] p0002 A78-15989
- Aero-acoustic tests of duct-burning turbofan exhaust nozzles. Comprehensive data report. Volume 3: Acoustic and aerodynamic data curves [NASA-CR-134910-VOL-3] p0002 A78-15990
- Supersonic through-flow fan engines for supersonic cruise aircraft [NASA-TN-78885] p0019 A78-23088
- Inlet-engine matching for SCAR including application of a bicone variable geometry inlet [NASA-TN-78955] p0021 A78-27125
- Flight effects on the aerodynamic and acoustic characteristics of inverted profile coannular nozzles, volume 1 --- supersonic cruise aircraft research wind tunnel tests [NASA-CR-135189-VOL-1] p0167 A78-29867
- Flight effects on the aerodynamic and acoustic characteristics of inverted profile coannular nozzles, volume 2 --- supersonic cruise aircraft research wind tunnel tests [NASA-CR-135189-VOL-2] p0167 A78-29868
- SUPERSONIC FLOW**
Unsteady flow in a supersonic cascade with strong in-passage shocks p0006 A78-17270
- Supersonic through-flow fan engines for supersonic cruise aircraft [NASA-TN-78889] p0019 A78-23088
- SUPERSONIC FLOW INLETS**
- T SUPERSONIC INLETS**
- SUPERSONIC INLETS**
Inlet-engine matching for SCAR including application of a bicone variable geometry inlet --- Supersonic Cruise Aircraft Research [AIAA PAPER 78-961] p0007 A78-45096
- Atmospheric effects on inlets for supersonic cruise aircraft [NASA-TN-X-73647] p0003 A78-10026
- Mechanical characteristics of stability-bleed valves for a supersonic inlet --- for the F-12 aircraft [NASA-TN-X-3483] p0015 A78-13063
- Normal shock and restart controls for a supersonic airbreathing propulsion system p0019 A78-23023
- Optimal control of a supersonic inlet to minimize frequency of inlet unstart

SUPERSONIC SPEEDS

SUBJECT INDEX

Inlet-engine matching for SCAR including application of a bicone variable geometry inlet [NASA-TN-78955] p0021 W78-27125
 Wind tunnel evaluation of YF-12 inlet response to internal airflow disturbances with and without control --- Lewis 10 by 10 ft supersonic wind tunnel tests p0006 W78-32062

SUPERSONIC SPEEDS
 Lean combustion limits of a confined preaired-prevaporized propane jet [NASA-TN-78868] p0017 W78-22099

SUPERSONIC TRANSPORTS
 Advanced supersonic propulsion study, phases 3 and 4 --- variable cycle engines [NASA-CR-135236] p0027 W78-13058

SUPERSONIC TURBINES
 A parametric investigation of an existing supersonic relative tip speed propeller noise model --- turboprop aircraft [NASA-TN-73846] p0163 W76-13854
 Wide range operation of advanced low NOx combustors for supersonic high-altitude aircraft gas turbines [NASA-CR-135297] p0027 W78-14047
 Performance of a transonic fan stage designed for a low meridional velocity ratio [NASA-TN-1290] p0022 W78-33107

SUPERSONIC WIND TUNNELS
 Room temperature crack growth rates and -20 deg F fracture toughness of welded 1/4 inch A-285 steel plate [NASA-TN-73847] p0068 W78-13182
 Wind tunnel performance tests of conannular plug nozzles --- in the Langley 8 x 6 ft. supersonic wind tunnel [NASA-CR-2990] p0002 W78-21044
 Investigation of means for perturbing the flow field in a supersonic wind tunnel [NASA-TN-78954] p0037 W78-27142

SURFACE CRACKS
 Stress analysis and stress-intensity factors for finite geometry solids containing rectangular surface cracks [ASME PAPER 77-WA/APR-5] p0126 W78-10531
 Friction, deformation and fracture of single-crystal silicon carbide [ASLE PREPRINT 77-IC-5C-3] p0085 W78-28438
 Surface-crack shape change in bending fatigue using an inexpensive resonant fatiguing apparatus p0075 W78-35394
 High temperature compressive cracking in hot-pressed silicon nitride p0085 W78-38706
 Analysis of delamination in unidirectional and crossplied fiber composites containing surface cracks [NASA-CR-135248] p0062 W78-11197

SURFACE DEFECTS
 Analysis and test of deep flaws in thin sheets of aluminum and titanium. Volume 1: Program summary and data analysis [NASA-CR-135369] p0127 W78-21093
 Analysis and test of deep flaws in thin sheets of aluminum and titanium. Volume 2: Crack opening displacement and stress-strain data [NASA-CR-135370] p0127 W78-21494

SURFACE FINISHING
 The use of analytical surface tools in the fundamental study of wear p011 W78-23428
 The use of an ion-beam source to alter the surface morphology of biological implant materials p0061 W78-37496
 High temperature surface protection --- 10 gas turbines [NASA-TN-71877] p0102 W78-17340
 Charging of flexible solar array substrates in kilovolt electron beams [NASA-TN-71865] p0044 W78-21199
 Morphology of gold and copper ion-plated coatings [NASA-TN-12421] p0071 W78-26199
 Hydrodynamic air lubricated compliant surface bearing for an automotive gas turbine engine. 2: Materials and coatings [NASA-CR-135402] p0122 W78-28449
 Ion beam sputtering of fluoropolymers --- etching polymer films and target surfaces

[NASA-TN-79000] p0060 W78-33151

SURFACE INTERACTIONS
U SURFACE REACTIONS
SURFACE LAYERS
 Tribological properties of surfaces p0120 W78-33211

SURFACE PROPERTIES
NT ADELSION
NT COEFFICIENT OF FRICTION
NT INTERFACIAL TENSION
NT SURFACE CRACKS
NT SURFACE DEFECTS
NT SURFACE TEMPERATURE
 The use of analytical surface tools in the fundamental study of wear p0119 W78-23428
 Tribological properties of surfaces p0120 W78-33211
 Fracture surface characteristics of off-axis composites p0067 W78-40371
 Definition and effect of chemical properties of surfaces in friction, wear, and lubrication p0121 W78-45436
 Definition and effect of chemical properties of surfaces in friction, wear, and lubrication [NASA-TN-73806] p0065 W78-19237
 Tribological properties of surfaces [NASA-TN-73896] p0114 W78-20511
 The use of an ion-beam source to alter the surface morphology of biological implant materials [NASA-TN-78851] p0122 W78-22618
 ERDA-NASA advanced thermal technology program [NASA-CR-157222] p0145 W78-26579

SURFACE REACTIONS
 I-ray photoelectron spectroscopic study of surface chemistry of dibenzyl disulfide on steel under mild and severe wear conditions p006 W78-21439

SURFACE ROUGHNESS EFFECTS
 Aerodynamic performance of conventional and advanced design labyrinth seals with solid-smooth abradable, and honeycomb lands --- 943 turbine engines [NASA-CR-135307] p0122 W78-27427

SURFACE TEMPERATURE
 Estimating surface temperature in forced convection nucleate boiling - A simplified method p0105 W78-15822
 Method for calculating convective heat-transfer coefficients over turbine vane surfaces [NASA-TN-1134] p0102 W78-17338

SURFACE TENSION
U INTERFACIAL TENSION

SURFACE TREATMENT
U SURFACE FINISHING

SURFACE VEHICLES
NT AUTOMOBILES
NT ELECTRIC AUTOMOBILES
NT ELECTRIC MOTOR VEHICLES
NT MOTOR VEHICLES
NT TRUCKS
 Utilization of NASA Lewis mobile terminals for the Hermes satellite p0094 W78-24885
 Baseline tests of the Zagato Elcar electric passenger vehicle [NASA-TN-71764] p0178 W78-17934

SURFACES
 Variation of solar cell sensitivity and solar radiation on tilted surfaces [NASA-TN-74921] p0138 W78-26547

SURCPHY
 Tissue macerating instrument [NASA-CASE-LPN-1266P-1] p0153 W78-14773

SURGES
 Preliminary report on the CTS transient event counter performance through the 1976 spring eclipse season p0036 W78-10135

SUSCEPTIBILITY (MAGNETISM)
U MAGNETIC PERMEABILITY

SWITCHES
NT ELECTRIC RELAYS
NT SWITCHING CIRCUITS

SWITCHING CIRCUITS
 Pulse battery charger employing 1000 ampere transistor switches p0146 W78-31574

SUBJECT INDEX

TECHNOLOGY ASSESSMENT

- Self-reconfiguring solar cell system
[NASA-CASB-LEW-12586-1] p0139 W78-27520
Modelling, analyses and design of switching
converters
[NASA-CR-135174] p0100 W78-29351
- SWITCHING ELEMENTS
U SWITCHING CIRCUITS
SYMMETRICAL BODIES
NT CYLINDRICAL BODIES
SYNCHRONISM
NT FREQUENCY SYNCHRONIZATION
Synchronization of the DOE/NASA 100-kilowatt wind
turbine generator with a large utility network
[NASA-TN-73861] p0132 W78-17467
- SYNCHRONIZATION
U SYNCHRONISM
SYNCHRONOUS SATELLITES
NASCAP, a three-dimensional Charging Analyzer
Program for complex spacecraft p0044 A78-19567
Preliminary report on the CTS transient event
counter performance through the 1976 spring
eclipse season p0036 W78-10135
- SYNTHETIC FUELS
Open-Cycle Gas Turbine/Steam Turbine Combined
Cycles with synthetic fuels from coal
[ASME PAPER 77-WA/ENER-9] p0146 A78-3147
Jet fuels from synthetic crudes p0090 A78-43415
Effect of fuel properties on performance of single
aircraft turbojet combustor at simulated idle,
cruise, and takeoff conditions
[NASA-TN-73780] p0014 W78-13056
- SYNTHETIC RUBBERS
NT ELASTOMERS
SYSTEM EFFECTIVENESS
Effect of vibration on retention characteristics
of screen acquisition systems --- for surface
tension propellant acquisition
[AIAA PAPER 78-1030] p0045 A78-43560
- SYSTEMS ANALYSIS
Extended performance solar electric propulsion
thrust system study. Volume 1: Executive summary
[NASA-CR-135281-VOL-1] p0052 W78-10205
Disaster warning system study summary --- cost
estimates using NOAA satellites
[NASA-TN-73797] p0093 W78-10346
Advanced space engine powerhead breadboard
assembly system study
[NASA-CR-135232] p0054 W78-25127
- SYSTEMS DESIGN
U SYSTEMS ENGINEERING
SYSTEMS ENGINEERING
NT COMPUTER SYSTEMS DESIGN
Marshall Space Flight Center development program
for solar heating and cooling systems p0110 A78-11368
Diagonal dominance using function minimization
algorithms --- multivariable control system design
p0159 A78-16308
Design and calculated performance and cost of the
PCAS Phase II open cycle HRD power generation
system
[ASME PAPER 77-WA/ENER-5] p0174 A78-33143
Engineering Model 8-cm Thruster System
[AIAA PAPER 78-646] p0055 A78-37874
The FSDA/LORC Photovoltaic Systems Test Facility
p0143 A78-52851
Analysis and design of a high power laser adaptive
phase array transmitter
[NASA-CR-114952] p0111 W78-13420
Instrumentation for propulsion systems development
--- high speed fans and turbines
[NASA-TN-73840] p0011 W78-17052
Design study of wind turbines 50 kw to 3000 kw for
electric utility applications. Volume 2:
Analysis and design p0143 W78-17462
[NASA-CR-134935]
Making aerospace technology work for the
automotive industry, introduction
[NASA-TN-73870] p0175 W78-17941
F-15/sonar/magnetic nozzle system integration
study support program
- [NASA-CR-135252] p0028 W78-18070
Extended performance solar electric propulsion
thrust system study. Volume 5. Capacitor-diode
voltage multiplier: Technology evaluation
[NASA-CR-135281-VOL-5] p0053 W78-19195
Thermal performance of a customized multilayer
insulation (MLI). Design and fabrication of
test facility hardware
[NASA-CR-157648] p0062 W78-20257
Evolution of the 1- α b mercury ion thruster
subsystem
[NASA-TN-73733] p0047 W78-21202
Closed cycle electric discharge laser design
investigation
[NASA-CR-135408] p0112 W78-25407
Design and fabrication of a photovoltaic power
system for the Papago Indian village of
Schuchuli (Gunnight), Arizona
[NASA-TN-78948] p0139 W78-26555
Preliminary design study of an alternate heat
source assembly for a Brayton isotope power system
[NASA-CR-135428] p0145 W78-28608
Liquid rocket engine turbopump rotating-shaft seals
[NASA-SP-8121] p0117 W78-30584
- SYSTEMS STABILITY
The design of hydraulic pressure regulators that
are stable without the use of sensing line
restrictors or frictional dampers
[NASA-TN-X-73687] p0101 W78-13415

T

TABLES (DATA)

- An analysis of the first two years of GASP data
[NASA-TN-73817] p0143 W78-13669
- TAILLESS AIRCRAFT
NT P-102 AIRCRAFT
- TANK GEOMETRY
Constrained sloshing of liquid mercury in a
flexible spherical tank
[NASA-TN-78833] p0103 W78-21403
- TANKS (CONTAINERS)
NT CYLINDRICAL TANKS
NT PROPELLANT TANKS
NT SPHERICAL TANKS
- TANTALUM ALLOYS
Tantalum modified ferritic iron base alloys
[NASA-CASB-LEW-12095-1] p0069 W78-18182
- TARE (DATA REDUCTION)
U DATA REDUCTION
- TARGETS
NT PARTICLE ACCELERATOR TARGETS
Ion beam sputtering of fluoropolymers --- etching
polymer films and target surfaces
[NASA-TN-79300] p0060 W78-33151
- TECHNOLOGICAL FORECASTING
General aviation energy-conservation research
programs at NASA-Lewis Research Center --- for
non-turbine general aviation engines p0024 A78-29330
Engineering in the 21st century
[NASA-TN-79010] p0105 W78-33380
- TECHNOLOGIES
NT ENERGY TECHNOLOGY
Bibliography of Lewis Research Center technical
contributions announced in 1978
[NASA-TN-77940] p0177 W78-17941
- TECHNOLOGY ASSESSMENT
Progress in advanced high temperature turbine
materials, coatings, and technology p0056 A78-24910
Design considerations in mechanical face seals for
improved performance. II - Lubrication
[ASME PAPER 77-WA/LOR-4] p0120 A78-33184
Test and evaluation of 23 electric vehicles for
state-of-the-art assessment
[ASME PAPER 750290] p0181 A78-33382
State-of-the-art of turbofan engine noise control
p0028 A78-35650
Alternative approaches to plasma refinement
p0174 A78-52146
Cost/benefit analysis of advanced material
technologies for small aircraft turbine engines
[NASA-CR-135265] p0027 W78-12083
Reliability analysis of forty-five strain-gage
systems mounted on the first fan stage of a
YF-100 engine
[NASA-TN-73724] p0109 W78-13407

TECHNOLOGY TRANSFER

SUBJECT INDEX

Advanced Thermionic Technology Program
[NASA-CR-155299] p0143 W78-13599

Extended performance solar electric propulsion thrust system study. Volume 4: Thruster technology evaluation
[NASA-CR-135281-VOL-4] p0053 W78-16090

Materials technology assessment for stirling engines
[NASA-TN-73789] p0069 W78-17187

Technical and economic feasibility study of solar/fossil hybrid power systems
[NASA-TN-73820] p0132 W78-17486

State-of-the-art assessment of electric vehicles and hybrid vehicles
[NASA-TN-73756] p0179 W78-18988

Up-date of traveling wave tube improvements
[NASA-TN-78852] p0096 W78-19397

Design study of wind turbines 50 kW to 3000 kW for electric utility applications: Analysis and design
[NASA-CR-134937] p0144 W78-23560

General aviation internal-combustion engine research programs at NASA-Lewis Research Center
[NASA-TN-78891] p0011 W78-24139

Technological development of cylindrical and flat shaped high energy density capacitors --- using polymeric films
[NASA-CR-135286] p0099 W78-24058

Liquid-cooling technology for gas turbines review and status
[NASA-TN-78906] p0020 W78-26145

Sputtering technology in solid film lubrication
[NASA-TN-78914] p0083 W78-26214

Additional aspects of elastohydrodynamic lubrication
[NASA-TN-78898] p0115 W78-26443

Status of wraparound contact solar cells and arrays
[NASA-TN-78911] p0137 W78-26543

EBDA-NASA advanced thermionic technology program
[NASA-CR-157222] p0145 W78-26579

State-of-the-art assessment of electric and hybrid vehicles
[NASA-TN-79509] p0180 W78-27003

Status of advanced turboprop technology
[NASA-TN-79509] p0001 W78-27055

Status of the NASA-Lewis Research Center spacecraft charge investigation --- spacecraft materials tests
[NASA-TN-78938] p0049 W78-27170

Preliminary power train design for a state-of-the-art electric vehicle
[NASA-CR-135340] p0145 W78-29584

Preliminary power train design for a state-of-the-art electric vehicle
[NASA-CR-135341] p0182 W78-29992

Materials technology assessment for Stirling engines
[NASA-TN-78911] p0117 W78-30318

The 20/30 GHz satellite systems technology needs assessment
[NASA-TN-78975] p0093 W78-31323

TECHNOLOGY TRANSFER

WT AEROSPACE TECHNOLOGY TRANSFER

An overview of aerospace gas turbine technology of relevance to the development of the automotive gas turbine engine
[NASA-TN-73849] p0014 W78-13062

TECHNOLOGY UTILIZATION

Communication satellite services for special purpose users
[NASA-TN-78975] p0094 W78-31971

Making aerospace technology work for the automotive industry - Introduction
[NASA-TN-73849] p0181 W78-33359

Utilization of solar energy in developing countries - Identifying some potential markets
[NASA-TN-73849] p0142 W78-45437

Emissions reduction technology program
[NASA-TN-73849] p0012 W78-11065

FRP polyimide prepreg with improved tack characteristics
[NASA-TN-73899] p0081 W78-17221

Photovoltaic highway applications: Assessment of the near-term market
[NASA-TN-73863] p0178 W78-17935

Making aerospace technology work for the automotive industry, introduction
[NASA-TN-73870] p0179 W78-17941

Industrial ion source technology --- for ion beam etching, surface texturing, and deposition
[NASA-CR-135353] p0169 W78-18883

Method of cold welding using ion beam technology
[NASA-CASE-LEW-12982-1] p0117 W78-28459

Continuation of the compendium of applications technology satellite and communications technology satellite user experiments 1967-1977, volume 1
[NASA-CR-135416-VOL-1] p0042 W78-31141

Continuation of the compendium of applications technology satellite and communications technology satellite user experiments 1967-1977, volume 2 --- Bibliography
[NASA-CR-135416-VOL-2] p0042 W78-31142

TEFLON (TRADEMARK)

Optical and electrical properties of ion beam textured Kapton and Teflon
[NASA-TN-73778] p0085 W78-28908

Optical and electrical properties of ion beam textured Kapton and Teflon
[NASA-TN-73778] p0162 W78-13848

TELECOMMUNICATION

WT BROADCASTING

WT COMMUNICATION

WT DATA LINKS

WT DIGITAL SPACECRAFT TELEVISION

WT PULSE COMMUNICATION

WT RADIO COMMUNICATION

WT SATELLITE TELEVISION

WT SPACECRAFT COMMUNICATION

Low cost satellite land mobile service for nationwide applications
[NASA-TN-73778] p0095 W78-31173

TELEVISION SYSTEMS

WT DIGITAL SPACECRAFT TELEVISION

WT SATELLITE TELEVISION

Carrier-interference ratios for frequency sharing between frequency-modulated amplitude-modulated-vestigial-sideband television systems
[NASA-TN-1264] p0043 W78-28159

TELLEGRAPH THEORY

U NETWORK ANALYSIS

TELLURIUM

Targets for producing high purity I-123
[NASA-CASE-LEW-10518-3] p0065 W78-27226

TEMPERATURE

WT AMBIENT TEMPERATURE

WT ATMOSPHERIC TEMPERATURE

WT FLAME TEMPERATURE

WT GAS TEMPERATURE

WT HIGH TEMPERATURE

WT ION TEMPERATURE

WT LOW TEMPERATURE

WT ROOM TEMPERATURE

WT SURFACE TEMPERATURE

WT TRANSITION TEMPERATURE

TEMPERATURE CONTROL

Evaluation of commercially-available spacecraft-type heat pipes
[NASA-TN-78826] p0103 W78-20459

Liquid rocket engine self-cooled combustion chambers
[NASA-SP-8124] p0048 W78-21211

TEMPERATURE DISTRIBUTION

Temperature distributions and thermal stresses in a graded zirconia/metal gas path seal system for aircraft gas turbine engines
[AIAA PAPER 78-93] p0118 W78-20683

Lubrication of high-speed, large bore tapered-roller bearings
[ASME PAPER 77-LCB-13] p0118 W78-23354

Effect of coolant flow ejection on aerodynamic performance of low-aspect-ratio vanes. 2: Performance with coolant flow ejection at temperature ratios up to 2
[NASA-TN-1057] p0003 W78-11008

Room temperature crack growth rates and -20 deg F fracture toughness of welded 1/4 inch A-285 steel plate
[NASA-TN-73847] p0048 W78-13182

Temperature distributions and thermal stresses in a graded zirconia/metal gas path seal system for aircraft gas turbine engines
[NASA-TN-73818] p0015 W78-15044

Temperature distributions of a cesium-seeded hydrogen-oxygen supersonic free jet
[NASA-TN-1162] p0171 W78-20959

TEMPERATURE EFFECTS

Effects of heat treating on BeCu 95 slightly below the gamma-prime solvus
[NASA-TN-73778] p0073 W78-18742

SUBJECT INDEX

THERMAL CONDUCTIVITY

- Thermal environment effects on strength and impact properties of boron-aluminum composites p0060 A78-33204
- Measurement of the time-temperature dependent dynamic mechanical properties of boron/aluminum composites p0061 A78-33222
- Effect of thermal exposure on lubricating properties of polyimide films and polyimide-bonded graphite fluoride films [NASA-TP-1125] p0080 W78-15277
- Thermal environment effects on strength and impact properties of boron-aluminum composites [NASA-TN-73885] p0058 W78-17155
- High temperature environmental effects on metals [NASA-TN-73878] p0017 W78-19158
- Effects of pressure and temperature on hot pressing a sialon [NASA-TN-78945] p0083 W78-27274
- Effect of inlet temperature on the performance of a catalytic reactor --- air pollution control [NASA-TN-78977] p0141 W78-31534
- TEMPERATURE FIELDS**
- TEMPERATURE DISTRIBUTION
- TEMPERATURE INDICATORS**
- TEMPERATURE MEASURING INSTRUMENTS
- TEMPERATURE INSTRUMENTS
- TEMPERATURE MEASURING INSTRUMENTS
- TEMPERATURE INVERSIONS
- TEMPERATURE MEASUREMENT
- Estimating surface temperature in forced convection nucleate boiling - A simplified method p0105 A78-15822
- TACT1, a computer program for the transient thermal analysis of a cooled turbine blade or vane equipped with a coolant insert. 1. Users manual [NASA-TP-12711] p0104 W78-28374
- TEMPERATURE MEASURING INSTRUMENTS
- Aerial thermography for energy conservation [NASA-TN-78959] p0129 W78-33510
- TEMPERATURE PROFILES**
- Velocity and temperature profiles in near-critical nitrogen flowing past a horizontal flat plate [ASME PAPER 77-HT-7] p0106 A78-17481
- Computer program for calculation of a gas temperature profile by infrared emission: Absorption spectroscopy [NASA-TN-73848] p0015 W78-15043
- TEMPERING**
- The design of an Fe-12Mn-0.2Ti alloy steel for low temperature use [NASA-CR-135310] p0078 W78-20310
- Long-term hot-hardness characteristics of five through-hardened bearing steels [NASA-TP-13411] p0073 W78-33196
- TENSILE PROPERTIES**
- Effect of prior creep at 1365 K on the room temperature tensile properties of several oxide dispersion strengthened alloys p0074 A78-21431
- Tensile and creep properties of the experimental oxide dispersion strengthened iron-base sheet alloy WA-956P at 1365 K p0074 A78-21858
- Ball characterization for tensile fracture of multicomponent brittle fibers p0060 A78-24892
- Elevated-temperature tensile and creep properties of several ferritic stainless steels [NASA-TN-73853] p0069 W78-17189
- TENSILE STRENGTHS**
- Thermal environment effects on strength and impact properties of boron-aluminum composites p0060 A78-33204
- Correlation of fiber composite tensile strength with the ultrasonic stress wave factor p0060 A78-33207
- Strength enhancement process for prealloyed powder superalloys p0075 A78-33216
- Correlation of fiber composite tensile strength with the ultrasonic stress wave factor [NASA-TN-78846] p0058 W78-20255
- Strength enhancement process for prealloyed powder superalloys [NASA-TN-78844] p0070 W78-21266
- Quantitative ultrasonic evaluation of mechanical properties of engineering materials [NASA-TN-78905] p0124 W78-24565
- TENSILE STRESSES**
- Effect of wall thickness and material on flexural fatigue of hollow rolling elements [ASME PAPER 77-LUB-14] p0126 A78-23355
- TENSILE TESTS**
- Fracture surface characteristics of off-axis composites p0067 A78-40371
- TERNARY ALLOYS**
- HT ASTROLOY (TRADEMARK) Reaction diffusion in the NiCrAl and CoCrAl systems p0077 A78-13063
- TERNARY SYSTEMS (DIGITAL)**
- DIGITAL SYSTEMS
- TERRSTRAL MAGNETISM**
- GEOMAGNETISM
- TEST BEDS**
- TEST EQUIPMENT
- TEST CHAMBERS**
- HT ANECHOIC CHAMBERS
- HT VACUUM CHAMBERS
- TEST EQUIPMENT**
- VCE testbed program planning and definition study [NASA-CR-135362] p0029 W78-19160
- Thermal performance of a customized multilayer insulation (MLI). Design and fabrication of test facility hardware [NASA-CR-157648] p0062 W78-20257
- Comparison of three experimental methods used in determining the thermal performance of flat-plate solar collectors [NASA-TN-78929] p0139 W78-28614
- TEST FACILITIES**
- HT ANECHOIC CHAMBERS
- HT CASCADE WIND TUNNELS
- HT ENGINE TESTING LABORATORIES
- HT ROCKET TEST FACILITIES
- HT SUPERSONIC WIND TUNNELS
- HT WIND TUNNELS
- Escort - A data acquisition and display system to support research testing p0155 A78-37685
- The ERDA/LeRC Photovoltaic Systems Test Facility p0143 A78-52851
- The ERDA/LeRC photovoltaic system test facility [NASA-TN-73787] p0035 W78-15059
- Thermal performance of a customized multilayer insulation (MLI). Design and fabrication of test facility hardware [NASA-CR-157648] p0062 W78-20257
- DOE LeRC photovoltaic system test facility [NASA-TN-78923] p0138 W78-26549
- Status of the NASA-Lewis Research Center spacecraft charging investigation --- spacecraft materials tests [NASA-TN-78938] p0049 W78-27170
- TEST VEHICLES**
- Test and evaluation of 23 electric vehicles for state-of-the-art assessment [SAE PAPER 780290] p0181 A78-33382
- TESTERS**
- TEST EQUIPMENT
- TESTING**
- TESTS
- TESTING MACHINES**
- TEST EQUIPMENT
- TESTS**
- Impetus of composite mechanics on test methods for fiber composites [NASA-TN-78979] p0126 W78-32464
- TEXTURES**
- Optical and electrical properties of ion beam textured Kapton and Teflon [NASA-TN-73778] p0162 W78-13888
- Industrial ion source technology --- for ion beam etching, surface texturing, and deposition [NASA-CR-135353] p0169 W78-18883
- TP-30 ENGINE**
- High frequency dynamic engine simulation --- TP-30 engine [NASA-CR-135313] p0027 W78-13059
- THERMAL AGITATION**
- THERMAL ENERGY
- THERMAL CONDUCTIVITY**
- Thermal barrier coating system [NASA-CASE-L2U-12554-1] p0102 W78-18355

THERMAL CONTROL COATINGS

SUBJECT INDEX

- Development of a plasma sprayed ceramic gas path seal for high pressure turbine application [NASA-CR-135387] p0030 W78-24141
- THERMAL CONTROL COATINGS**
- Two-layer thermal barrier coating for high temperature components [ACS PAPER 31-BNH-76P] p0086 A78-18787
- An analytical study of thermal barrier coated first stage blades in a JT9D engine [NASA-CR-135360] p0028 W78-16054
- Analytical study of thermal barrier coated first-stage blades in an F100 engine [NASA-CR-135359] p0028 W78-17058
- Adhesive/cohesive strength of a SrO₂-1-2 w/o TiO₂/NiCrAlY thermal barrier coating [NASA-TN-73792] p0057 W78-17152
- Thermal barrier coating system [NASA-CASB-LBN-12554-1] p0102 W78-18355
- Thermal barrier coatings [NASA-TN-78848] p0059 W78-24291
- A computer program for full-coverage film-cooled blading analysis including the effects of a thermal barrier coating [NASA-TN-78951] p0021 W78-27126
- Analysis of metal temperature and coolant flow with a thermal-barrier coating on a full-coverage-film-cooled turbine vane [NASA-TP-1310] p0022 W78-31109
- Effects of compositional changes on the performance of a thermal barrier coating system --- yttria-stabilized zirconia coatings on gas turbine engine blades [NASA-TN-78976] p0072 W78-31212
- THERMAL CURRENTS**
- U CONVECTIVE FLOW**
- THERMAL CYCLING TESTS**
- Evaluation of low cost/high temperature fiber and blanket insulation p0063 A78-16903
- Thermal environment effects on strength and impact properties of boron-aluminum composites p0060 A78-33204
- The cyclic oxidation resistance of cobalt chromium-aluminum alloys at 1100 and 1200 C and a comparison with the nickel-chromium-aluminum alloy system p0077 A78-50086
- 10,000-hour cyclic oxidation behavior at 815 C /1500 % of 33 high-temperature alloys p0077 A78-51716
- Experimental determination of transient strain in a thermally-cycled simulated turbine blade utilizing a non-contact technique [NASA-TN-73886] p0017 W78-19111
- The role of thermal shock in cyclic oxidation [NASA-TN-78876] p0070 W78-23193
- Ultraviolet irradiation at elevated temperatures and thermal cycling in vacuum of PEP-A covered silicon solar cells [NASA-TN-78926] p0137 W78-26545
- THERMAL DEGRADATION**
- Thermal environment effects on strength and impact properties of boron-aluminum composites p0060 A78-33204
- THERMAL EFFECTS**
- U TEMPERATURE EFFECTS**
- THERMAL EFFICIENCY**
- U THERMODYNAMIC EFFICIENCY**
- THERMAL EMISSION**
- WT THERMIONIC EMISSION**
- THERMAL ENERGY**
- CTS TEP thermal anomalies: Heat pipe system performance [NASA-CR-159413] p0108 W78-20410
- THERMAL ENERGY STORAGE**
- U HEAT STORAGE**
- THERMAL EXPANSION**
- Effect of discontinuities as a means to alleviate thermal expansion mismatch damage in laminar composites [NASA-TN-73719] p0057 W78-13136
- THERMAL FATIGUE**
- Thermal fatigue and oxidation data of superalloys including directionally solidified eutectics [NASA-CR-135272] p0078 W78-15233
- Thermal fatigue and oxidation data for alloy/braze combinations [NASA-CR-135299] p0078 W78-16149
- THERMAL INSULATION**
- Evaluation of low cost/high temperature fiber and blanket insulation p0063 A78-16903
- Comparison of reusable insulation systems for cryogenically-tanked earth-based space vehicles [AIAA PAPER 78-877] p0044 A78-36004
- An ultralightweight, evacuated, load-bearing, high-performance insulation system --- for cryogenic propellant tanks [AIAA PAPER 78-878] p0045 A78-36005
- Evacuated load-bearing high performance insulation study [NASA-CR-135342] p0092 W78-18251
- Comparison of reusable insulation systems for cryogenically-tanked earth-based space vehicles [NASA-TN-73668] p0041 W78-21190
- THERMAL MAPPING**
- Aerial thermography for energy conservation [NASA-TN-78959] p0129 W78-33510
- THERMAL POWER**
- U TURBOGENERATORS**
- THERMAL PROPERTIES**
- U THERMODYNAMIC PROPERTIES**
- THERMAL PROTECTION**
- Emittance and absorptance of NASA ceramic thermal barrier coating system -- for turbine cooling [NASA-TP-1190] p0020 W78-26148
- THERMAL RESISTANCE**
- An experimental P/B wrought superalloy for advanced temperature service p0073 A78-15335
- THERMAL RESOURCES**
- WT GEYSERS**
- THERMAL SHIELDING**
- U HEAT SHIELDING**
- THERMAL SHOCK**
- The role of thermal shock in cyclic oxidation p0076 A78-37676
- Preliminary study of cyclic thermal shock resistance of plasma-sprayed zirconia oxide turbine outer air seal shrouds [NASA-TN-73852] p0080 W78-15280
- The role of thermal shock in cyclic oxidation [NASA-TN-78876] p0070 W78-23193
- THERMAL SINSULATION**
- Thermal performance of a customized multilayer insulation (MLI). Design and fabrication of test facility hardware [NASA-CR-157648] p0062 W78-20257
- THERMAL STABILITY**
- Synthesis of perfluoroalkylene aromatic diamines [NASA-CR-159403] p0087 W78-31235
- THERMAL STRESSES**
- Lamination residual strains and stresses in hybrid laminates p0128 W78-12071
- Temperature distributions and thermal stresses in a graded zirconia/metal gas path seal system for aircraft gas turbine engines [AIAA PAPER 78-93] p0118 W78-20683
- Temperature distributions and thermal stresses in a graded zirconia/metal gas path seal system for aircraft gas turbine engines [NASA-TN-73818] p0015 W78-15044
- Method for alleviating thermal stress damage in laminates [NASA-CASE-LEW-12493-1] p0059 W78-22163
- Interpolation and extrapolation of creep rupture data by the minimum commitment method. Part 3: Analysis of multibeats [NASA-TN-78883] p0126 W78-23473
- THERMIONIC CONVERSION SYSTEMS**
- U THERMIONIC POWER GENERATION**
- THERMIONIC CONVERTERS**
- Experiments with enhanced mode thermionic converters p0186 A78-29636
- Advanced Thermionic Technology Program [NASA-CR-155299] p0143 W78-13599
- Some properties of low-vapor-pressure braze alloys for thermionic converters [NASA-TN-78867] p0134 W78-22471
- Dilanthide thermionic energy conversion with lanthanum-hexaboride electrodes [NASA-TN-78887] p0135 W78-24617
- ERDA/NASA advanced thermionic technology program [NASA-CR-157117] p0145 W78-24674
- Cesium thermionic converters having improved electrodes

SUBJECT INDEX

TESE FILES

- [NASA-CASE-LEW-12038-3] p0137 878-25555
Lithium and potassium heat pipes for thermionic converters
[NASA-TN-78946] p0104 878-26390
Performance of a thermionic converter module utilizing emitter and collector heat pipes
[NASA-TN-78941] p0049 878-27174
- THERMIONIC PROBES**
VT CESIUM DIODES
THERMIONIC SECTIONS
ERDA/NASA advanced thermionic technology program
[NASA-CR-157248] p0145 878-27552
- THERMIONIC SECTIONS**
Lithium and potassium heat pipes for thermionic converters
[NASA-TN-78946] p0104 878-26390
Performance of a thermionic converter module utilizing emitter and collector heat pipes
[NASA-TN-78941] p0049 878-27174
Spacecraft charging control by thermal, field emission with lanthanum-hexaboride emitters
[NASA-TN-78990] p0183 878-32014
- THERMIONIC POWER GENERATION**
High temperature heat pipe research at NASA Lewis Research Center
[AIAA 78-438] p0106 878-35618
Advanced Thermionic Technology Program
[NASA-CR-155299] p0143 878-13599
High-temperature, high-power-density thermionic energy conversion for space
[NASA-TN-73884] p0171 878-13890
Optimize out-of-core thermionic energy conversion for nuclear electric propulsion
[NASA-TN-73892] p0170 878-17856
High temperature heat pipe research at NASA Lewis Research Center
[NASA-TN-78832] p0103 878-23388
ERDA/NASA advanced thermionic technology program
[NASA-CR-157248] p0145 878-27552
- THERMIONIC REACTORS**
U ION ENGINES
THERMIONICS
ERDA-NASA advanced thermionic technology program
[NASA-CR-157222] p0145 878-26579
- THERMOCHEMICAL PROPERTIES**
VT HEAT OF VAPORIZATION
Status of the DOE /STOR/-sponsored national program on hydrogen production from water via thermochemical cycles
p0142 878-29331
- THERMOCHEMISTRY**
Status of the DOE (STOR)-sponsored national program on hydrogen production from water via thermochemical cycles
[NASA-TN-78825] p0132 878-17469
- THERMOCOUPLES**
Recovery and radiation corrections and time constants of several sizes of shielded and unshielded thermocouple probes for measuring gas temperature
[NASA-TP-1099] p0109 878-15463
- THERMODYNAMIC CYCLES**
VT BRAYTON CYCLE
VT STIRLING CYCLE
THERMODYNAMIC EFFICIENCY
Comparison of three experimental methods used in determining the thermal performance of flat-plate solar collectors
[NASA-TN-78929] p0139 878-28614
- THERMODYNAMIC EQUILIBRIUM**
Computer program for calculation of complex chemical equilibrium compositions, rocket performance, incident and reflected shocks, and Chapman-Jouquet detonations
[NASA-SP-273] p0156 878-17724
- THERMODYNAMIC PROPERTIES**
VT HEAT OF VAPORIZATION
VT SPECIFIC HEAT
VT SUPERCRITICAL PRESSURES
VT THERMAL CONDUCTIVITY
VT THERMAL EXPANSION
VT THERMAL STABILITY
VT THERMOCHEMICAL PROPERTIES
VT VAPOR PRESSURE
VT VOLATILITY
An integrated theory for predicting the hydrothermomechanical response of advanced composite structural components
p0060 878-24906
- An integrated theory for predicting the hydrothermomechanical response of advanced composite structural components
[NASA-TN-78912] p0123 878-19477
A computer program for the transient thermal analysis of an impingement cooled turbine blade
[NASA-TN-73819] p0015 878-15045
Computer program for obtaining thermodynamic and transport properties of air and products of combustion of ALF8-A-1 fuel and air
[NASA-TP-1160] p0088 878-20351
Characteristics and combustion of future hydrocarbon fuels --- aircraft fuels
[NASA-TN-78885] p0089 878-24370
Comparison of three experimental methods used in determining the thermal performance of flat-plate solar collectors
[NASA-TN-78929] p0139 878-28614
A Stirling engine computer model for performance calculations
[NASA-TN-78884] p0180 878-29994
Effects of thermomechanical processing on strength and toughness of iron - 12-percent-nickel - reactive metal alloys at -196 C
[NASA-TP-1308] p0073 878-31213
- THERMODYNAMICS**
VT COMBUSTION PHYSICS
THERMOELECTRIC CONVERSION SYSTEMS
U THERMOELECTRIC POWER GENERATION
THERMOELECTRIC POWER GENERATION
Development and fabrication of a diffusion welded Columbian alloy heat exchanger --- for space power generation
[AIRE PAPER 878-61] p0123 878-31500
Preliminary results on the conversion of laser energy into electricity
p0173 878-34631
A review of the thermoelectronic laser energy converter (TELEC) program at Lewis Research Center
[NASA-TN-73888] p0111 878-21841
- THERMOGRAMS**
U TEMPERATURE MEASURING INSTRUMENTS
THERMOGRAVIMETRY
Interaction of NaCl/g/ and HCl/g/ with condensed Na2SO4 --- in hot corrosion processes
p0066 878-24688
- THERMOMETRY**
U TEMPERATURE MEASUREMENT
THERMONUCLEAR REACTIONS
VT CONTROLLED FUSION
THERMOPHYSICAL PROPERTIES
VT SPECIFIC HEAT
VT SUPERCRITICAL PRESSURES
VT THERMAL CONDUCTIVITY
VT THERMAL STABILITY
VT VAPOR PRESSURE
VT VOLATILITY
THERMOPLASTIC RESINS
Formulated plastic separators for soluble electrode cells
[NASA-CASE-LEW-12358-2] p0065 878-25149
- THERMOSETTING RESINS**
VT EPOXY RESINS
VT POLYANIDE RESINS
THERMOSTABILITY
U THERMAL STABILITY
THERMOTROPISM
U TEMPERATURE EFFECTS
THICK FILMS
Application of thick-film technology to solar cell fabrication
p0146 878-10947
- THIN FILMS**
Method of forming metal hydride films
[NASA-CASE-LEW-12083-1] p0113 878-13436
Effect of thermal exposure on lubricating properties of polyimide films and polyimide-bonded graphite fluoride films
[NASA-TP-1125] p0080 878-15277
Lubrication and failure mechanisms of graphite fluoride films
[NASA-TP-1197] p0081 878-20337
Tribological properties of surfaces
[NASA-TN-73896] p0114 878-20511
Application of ESCA to the determination of stoichiometry in sputtered coatings and interface regions
[NASA-TN-78896] p0065 878-24185

THIS PLATES

Sputtering technology in solid film lubrication
[NASA-TN-78914] p0083 W78-26214

A comparison of the lubricating mechanisms of graphite fluoride and molybdenum disulfide films
[NASA-TN-73897] p0083 W78-26215

Transient dynamics of a flexible rotor with squeeze film dampers
[NASA-CR-3050] p0123 W78-32433

THIS PLATES

Analysis and test of deep flaws in thin sheets of aluminum and titanium. Volume 1: Program summary and data analysis
[NASA-CR-135369] p0127 W78-21493

Analysis and test of deep flaws in thin sheets of aluminum and titanium. Volume 2: Crack opening displacement and stress-strain data
[NASA-CR-135370] p0127 W78-21494

THIOLS

Effect of oxygen, methyl mercaptan, and methyl chloride on friction behavior of copper-iron contacts
[NASA-TP-1209] p0072 W78-30206

THREE DIMENSIONAL BOUNDARY LAYER

End-wall boundary layer prediction for axial compressors
[AIAA PAPER 78-1139] p0007 W78-45133

THREE DIMENSIONAL FLOW

WT SECONDARY FLOW

Calculation of 3-dimensional choking mass flow in turbomachinery with 2-dimensional flow models
p0006 W78-12289

Three-dimensional effects on pure tone fan noise due to inflow distortion
[AIAA PAPER 78-1120] p0166 W78-41830

Three-dimensional effects on pure tone fan noise due to inflow distortion --- rotor blade noise prediction
[NASA-TN-78885] p0164 W78-24898

Derivation and evaluation of an approximate analysis for three-dimensional viscous subsonic flow with large secondary velocities --- finite difference method
[NASA-CR-159430] p0008 W78-33044

THREE DIMENSIONAL MOTION

WT SECONDARY FLOW

WT THREE DIMENSIONAL FLOW

THRESHOLD CURRENTS

Critical currents and scaling laws in spotted copper molybdenum sulfide
p0175 W78-45500

THRUST

WT VARIABLE THRUST

Extended performance solar electric propulsion thrust system study. Volume 3: Tradeoff studies of alternate thrust system configurations
[NASA-CR-135281-VOL-3] p0053 W78-19196

THRUST BEARINGS

Self-acting shaft seals
p0120 W78-33219

THRUST CHAMBERS

Effect of facility background gases on internal erosion of the 30-cm Hg ion thruster
[AIAA PAPER 78-665] p0050 W78-32745

Hydrogen film cooling of a small hydrogen-oxygen thrust chamber and its effect on erosion rates of various ablative materials
[NASA-TP-1098] p0047 W78-13124

Investigation of the effect of ceramic coatings on rocket thrust chamber life
[NASA-TN-78892] p0049 W78-26173

THRUST MEASUREMENT

Airflow and thrust calibration of an F100 engine, S/W P680059, at selected flight conditions
[NASA-TP-1069] p0018 W78-21112

Altitude calibration of an F100, S/W P680063, turbofan engine
[NASA-TP-1228] p0019 W78-21095

THRUST POWER

U THRUST

THRUSTORS

U ROCKET ENGINES

TILT

U ATTITUDE (INCLINATION)

TILTING

U ATTITUDE (INCLINATION)

TILTING MOTORS

Effects of rotor location, coning, and tilt on critical loads in large wind turbines
p0133 W78-19676

SUBJECT INDEX

TIME DELAY

U TIME LAG

TIME DEFERENCE

Measurement of the time-temperature dependent dynamic mechanical properties of boron/aluminum composites
p0061 W78-33222

TIME LAG

Development of an experiment for determining the autoignition characteristics of aircraft-type fuels
[NASA-CR-135329] p0090 W78-16194

TIME MEASURING INSTRUMENTS

U TIMING DEVICES

TIME OPTIMAL CONTROL

Minimum-time acceleration of aircraft turbofan engines
p0023 W78-23892

TIME RESPONSE

The application of the South approximation method to turbofan engine models
p0023 W78-23891

TIGERS

U TIMING DEVICES

TIMING DEVICES

A cycle timer for testing electric vehicles
[NASA-TN-78934] p0180 W78-26996

TIN ALLOYS

Investigation of the fracture mechanism of Ti-5Al-2.5Sn at cryogenic temperatures
p0075 W78-32319

TIP DRIVEN MOTORS

Cold-air performance of a tip turbine designed to drive a lift fan. 3: Effect of simulated fan leakage on turbine performance
[NASA-TP-1109] p0003 W78-16001

TIP SPEED

Design and performance of a 427-meter-per-second-tip-speed two-stage fan having a 2.40 pressure ratio
[NASA-TP-1314] p0022 W78-33100

TIPS

WT BLADE TIPS

TISSUES (BIOLOGY)

Effect of surface texture by ion beam sputtering on implant biocompatibility and soft tissue attachment
[NASA-CR-135311] p0152 W78-18672

TITANIUM

The effect of minor addition of titanium on the fracture toughness of Fe-12Ni alloys at 77K
[NASA-CR-135351] p0078 W78-19259

Friction and wear of selected metals and alloys in sliding contact with AISI 440 C stainless steel in liquid methane and in liquid natural gas
[NASA-TP-1150] p0114 W78-20512

Titanium/beryllium laminates: Fabrication, mechanical properties, and potential aerospace applications
[NASA-TN-73891] p0059 W78-21221

Compressor seal rub energetics study
[NASA-CR-159024] p0032 W78-32996

TITANIUM ALLOYS

Comparison of equivalent energy and energy per unit area /W bar/A/ data with valid fracture toughness data for iron, aluminum, and titanium alloys
p0074 W78-24172

Investigation of the fracture mechanism of Ti-5Al-2.5Sn at cryogenic temperatures
p0075 W78-32319

The influence of composition, annealing treatment, and texture on the fracture toughness of Ti-5Al-2.5Sn plate at cryogenic temperatures
[NASA-TN-73872] p0069 W78-15235

Elevated-temperature flow strength, creep resistance and diffusion welding characteristics of Ti-4Al-2Nb-1Ta-0.8Mo
[NASA-TN-73854] p0069 W78-17140

Analysis and test of deep flaws in thin sheets of aluminum and titanium. Volume 1: Program summary and data analysis
[NASA-CR-135369] p0127 W78-21493

Analysis and test of deep flaws in thin sheets of aluminum and titanium. Volume 2: Crack opening displacement and stress-strain data
[NASA-CR-135370] p0127 W78-21494

TITRATION

An improved method for analysis of hydroxide and

SUBJECT INDEX

TRANSMISSION EFFICIENCY

- carbonate in alkaline electrolytes containing zinc
[NASA-TN-78961] p0139 W78-28607
- TORUS DEVICES**
Alternative approaches to plasma confinement
p0174 W78-52146
- TOROGRAPHY**
Digital enhancement of computerized axial tomograms
[NASA-TN-78974] p0152 W78-31190
- TOROSITY**
PRESSURE MEASUREMENTS
- TORNADOES**
Models for some aspects of atmospheric vortices
p0150 W78-14581
- TOROIDAL PLASMAS**
Inward transport of a toroidally confined plasma
subject to strong radial electric fields
p0172 W78-24890
A model for particle confinement in a toroidal
plasma subject to strong radial electric fields
p0173 W78-24891
Lower hybrid emission diagnostics on the NASA
Lewis Busby Torus
p0173 W78-29332
Effects of applied dc radial electric fields on
particle transport in a busby torus plasma
p0173 W78-36956
Alternative approaches to plasma confinement
p0174 W78-52146
Inward transport of a toroidally confined plasma
subject to strong radial electric fields
[NASA-TN-73800] p0171 W78-10883
A model for particle confinement in a toroidal
plasma subject to strong radial electric fields
[NASA-TN-73814] p0171 W78-10884
Lower hybrid emission diagnostics on the NASA
Lewis busby torus
[NASA-TN-73858] p0171 W78-19938
Fluctuation spectra in the NASA Lewis busby-torus
plasma
[NASA-TN-1257] p0172 W78-26927
Microwave radiation measurements near the electron
plasma frequency of the NASA Lewis busby torus
plasma
[NASA-TN-78940] p0172 W78-27914
- TOUGHNESS**
High toughness-high strength iron alloy
[NASA-CASE-LEN-12542-2] p0070 W78-22205
- TOWED TARGETS**
O TARGETS
- TOWERS**
Approximate method for calculating free vibrations
of a large-wind-turbine tower structure
[NASA-TN-73758] p0131 W78-14434
Wake characteristics of a tower for the DOE-NASA
MOD-1 wind turbine
[NASA-TN-78853] p0135 W78-23558
- TOWSEED DISCHARGE**
WT GAS DISCHARGES
- TOXIC HAZARDS**
Toxic substances alert program
[NASA-TN-73866] p0153 W78-20755
- TOXICITY**
Toxic substances alert program
[NASA-TN-73866] p0153 W78-20755
- TRACE CONTAMINANTS**
Global measurements of gaseous and aerosol trace
species in the upper troposphere and lower
stratosphere from daily flights of 747 airliners
p0147 W78-15826
- TRALBOPPS**
Extended performance solar electric propulsion
thrust system study. Volume 3: Tradeoff
studies of alternate thrust system configurations
[NASA-CR-135281-VOL-3] p0053 W78-19196
- TRAINING SIMULATORS**
WT FLIGHT SIMULATORS
- TRAJECTORIES**
WT INTERPLANETARY TRAJECTORIES
- TRANSDUCERS**
WT IMAGE TRANSDUCERS
WT MICROPHONES
WT SOUND TRANSDUCERS
Adaptation of ion beam technology to
microfabrication of solid state devices and
transducers
[NASA-CR-135314] p0099 W78-15397
Synthesis of blade flutter vibratory patterns
using stationary transducers
[NASA-TN-73821] p0003 W78-17001
- TRANSFER FUNCTIONS**
On the localness of the spectral energy transfer
in turbulence
p0106 W78-24909
- TRANSFORMATIONS (MATHEMATICS)**
WT FAST FOURIER TRANSFORMATIONS
- TRANSIENT LOADS**
WT GUST LOADS
WT IMPACT LOADS
- TRANSIENT RESPONSE**
Summary of the CTS Transient Event Counter data
after one year of operation --- Communication
Technology Satellite
p0046 W78-19566
A computer program for the transient thermal
analysis of an impingement cooled turbine blade
[AIAA PAPER 78-92] p0106 W78-20682
Stability of numerical integration techniques for
transient rotor dynamics
[NASA-TN-1092] p0113 W78-10474
A computer program for the transient thermal
analysis of an impingement cooled turbine blade
[NASA-TN-73819] p0015 W78-15045
Transient response to three-phase faults on a wind
turbine generator
[NASA-TN-78902] p0137 W78-26542
Transient dynamics of a flexible rotor with
squeeze film dampers
[NASA-CR-3050] p0123 W78-32433
- TRANSIENTS (SURGES,**
O SURGES
- TRANSISTOR CIRCUITS**
Pulse battery charger employing 1000 ampere
transistor switches
p0146 W78-31974
- TRANSITION METALS**
WT CHROMIUM
WT COBALT
WT GOLD
WT IRON
WT NICKEL
WT REFRACTORY METALS
WT TITANIUM
WT TUNGSTEN
WT YTTRIUM
WT ZINC
Friction and metal transfer for single-crystal
silicon carbide in contact with various metals
in vacuum
[NASA-TN-1191] p0082 W78-21294
Wear of single-crystal silicon carbide in contact
with various metals in vacuum
[NASA-TN-1198] p0082 W78-21295
- TRANSITION POINTS**
Upper critical field of copper silybdenum sulfide
p0175 W78-53626
- TRANSITION TEMPERATURE**
Traction and lubricant film temperature as related
to the glass transition temperature and
solidification --- using infrared spectroscopy
on EHD contacts
p0087 W78-40997
- TRANSLATIONAL MOTION**
WT SECONDARY FLOW
WT THREE DIMENSIONAL FLOW
- TRANSMISSION**
WT ACOUSTIC PROPAGATION
WT CONVECTIVE HEAT TRANSFER
WT ELECTRIC POWER TRANSMISSION
WT HEAT TRANSFER
WT LIGHT TRANSMISSION
WT MICROWAVE TRANSMISSION
WT SATELLITE TRANSMISSION
WT STRESS PROPAGATION
WT WAVE PROPAGATION
Proposed design procedure for transmission
shafting under fatigue loading
[NASA-TN-78927] p0115 W78-26444
- TRANSMISSION EFFICIENCY**
Use of a simple external nonreciprocal attenuator
in coupled-cavity TWT's
p0098 W78-18282
Performance of the 12 GHz, 200 watt Transmitter
Experiment Package for the Hermes Satellite
p0098 W78-24883
Analysis and design of a high power laser adaptive
phased array transmitter
[NASA-CR-38952] p0111 W78-13820

TRANSMISSIONS (MACHINE ELEMENTS)

SUBJECT INDEX

TRANSMISSIONS (MACHINE ELEMENTS)

Feasibility study of negative lift circumferential type seal for helicopter transmissions
[NASA-CR-135302] p0121 N78-17390

Preliminary power train design for a state-of-the-art electric vehicle
[NASA-CR-135300] p0145 N78-29584

TRANSMITTERS

KT RADIO TRANSMITTERS

Performance of the 12GHz, 200 watt transmitter experiment package for the Hermes satellite
[NASA-TN-73804] p0093 N78-13282

Analysis and design of a high power laser adaptive phased array transmitter
[NASA-CN-134952] p0111 N78-13420

TRANSONIC AIRCRAFT

U SUPERSONIC AIRCRAFT

TRANSONIC COMPRESSORS

Perturbation solutions for blade-to-blade surfaces of a transonic compressor
p0008 A78-12307

Performance with and without inlet radial distortion of a transonic fan stage designed for reduced loading in the tip region
[NASA-TP-1294] p0005 N78-30057

TRANSONIC FLOW

Review of experimental work on transonic flow in turbomachinery
p0006 A78-12312

Methods for calculating the transonic boundary layer separation for V/STOL inlets at high incidence angles
[AIAA 78-1380] p0007 A78-46537

Computation of unsteady transonic flows through rotating and stationary cascades. 2: User's guide to FORTRAN program BZDAT1
[NASA-CN-2901] p0007 N78-12034

Perturbation solutions for transonic flow on the blade-to-blade surface of compressor blade rows
[NASA-CN-2941] p0001 N78-15987

Computation of unsteady transonic flows through rotating and stationary cascades. 1: Method of analysis
[NASA-CN-2900] p0008 N78-20082

TRANSONIC INLETS

U SUPERSONIC INLETS

TRANSONIC TURBINES

U SUPERSONIC TURBINES

TRANSONICS

U TRANSONIC FLOW

TRANSPARATION

Design and preliminary results of a semitranspiration cooled (Lasilloy) liner for a high-pressure high-temperature combustor
[NASA-TN-78874] p0011 N78-24138

TRANSPORT AIRCRAFT

WT BOEING 747 AIRCRAFT

WT SHORT HAUL AIRCRAFT

Fuel consumption improvement in current transport engines
[AIAA PAPER 78-910] p0031 A78-45097

Energy efficient engine: Preliminary design and integration studies
[NASA-CN-135444] p0032 N78-31108

TRANSPORT COEFFICIENTS

U TRANSPORT PROPERTIES

TRANSPORT PROPERTIES

WT CARRIER MOBILITY

WT DIFFUSION COEFFICIENT

WT ELECTRICAL RESISTIVITY

WT GASEOUS DIFFUSION

WT MAGNETORESISTIVITY

WT PLASMA CONDUCTIVITY

WT SUPERCONDUCTIVITY

WT THERMAL CONDUCTIVITY

WT VISCOSITY

Inward transport of a toroidally confined plasma subject to strong radial electric fields
p0172 A78-24890

Computer program for obtaining thermodynamic and transport properties of air and products of combustion of ASTM-A-1 fuel and air
[NASA-TP-1160] p0088 N78-20351

TRANSPORT THEORY

Low-frequency fluctuation spectra and associated particle transport in the NASA Lewis dusty-torus plasma
[NASA-TP-1258] p0172 N78-30944

TRANSPORTATION

WT URBAN TRANSPORTATION

TRANSPORTATION ENERGY

New batteries and their impact on electric vehicles
p0141 A78-16923

TRAPPED MAGNETIC FIELDS

Inward transport of a toroidally confined plasma subject to strong radial electric fields
[NASA-TN-73800] p0171 N78-10883

TRAPPED PARTICLES

A model for particle confinement in a toroidal plasma subject to strong radial electric fields
[NASA-TN-73814] p0171 N78-10884

TRAPPING

WT CRYOTRAPPING

TRAVELING WAVE TUBES

Use of a simple external nonreciprocal attenuator in coupled-cavity TWT's
p0098 A78-16282

Performance of the 12 GHz, 200 watt Transmitter Experiment Package for the Hermes Satellite
p0098 A78-24883

Up-date of traveling wave tube improvements
p0098 A78-33208

Study of 42 and 85 GHz coupled cavity traveling-wave tubes for space use
[NASA-CN-134670] p0098 N78-11295

Up-date of traveling wave tube improvements
[NASA-TN-78852] p0096 N78-19397

Thermal characteristics of the 12-gigahertz, 200-watt output stage tube for the communications technology satellite
[NASA-TP-1344] p0043 N78-33137

TRIBOLOGY

Tribological properties of surfaces
p0120 A78-33211

Additional aspects of elastohydrodynamic lubrication
p0120 A78-45430

Tribological properties of surfaces
[NASA-TN-73896] p0114 N78-20511

TRIGGERS

U ACTUATORS

TRIGGERS

Trimerization of aromatic nitriles
[NASA-CASE-LBN-12053-1] p0080 N78-15276

TRIPROPELLANTS

U LIQUID ROCKET PROPELLANTS

TROPOPAUSE

Variability of ozone near the tropopause from GASP data
[NASA-CN-135405] p0148 N78-23648

TROPOSPHERE

Global measurements of gaseous and aerosol trace species in the upper troposphere and lower stratosphere from daily flights of 747 airliners
p0147 A78-15826

Measurement of tropospheric 300 nm solar ultraviolet flux for determination of O₃/D₀/ photoproduction rate
p0148 A78-38835

Global sensing of gaseous and aerosol trace species using automated instrumentation on 747 airliners
[NASA-TN-73810] p0148 N78-13670

TROUGHS

Supersonic through-flow fan engines for supersonic cruise aircraft
[NASA-TN-78889] p0019 N78-23088

TROCKS

Baseline tests of the power-train electric delivery van
[NASA-TN-73765] p0178 N78-17936

TRONCTION (MATHEMATICS)

U APPROXIMATION

TROUBIONS

U SHAFTS (MACHINE ELEMENTS)

TUBING

U PIPES (TUBES)

TUNGSTEN

Feasibility study of tungsten as a diffusion barrier between nickel-chromium-aluminum and Gamma/Gamma prime - Delta eutectic alloys
[NASA-TP-1111] p0068 N78-15230

TUNGSTEN ALLOYS

Predicted inlet gas temperatures for tungsten fiber reinforced superalloy turbine blades
[NASA-TN-73842] p0017 N78-19147

TURBINE BLADES

Calculation of 3-dimensional choking mass flow in

- turbomachinery with 2-dimensional flow models
 p0006 A78-12289
 A computer program for the transient thermal
 analysis of an impingement cooled turbine blade
 [NASA PAPER 78-92] p0186 A78-20602
 The promise of esthetics for aircraft turbines
 p0070 A78-24802
 Effluent characterization from a conical
 pressurized fluid bed p0066 A78-33221
 Comparison of computer codes for calculating
 dynamic loads in wind turbines p0142 A78-37678
 Cost analysis of advanced turbine blade
 manufacturing processes p0026 A78-10092
 [NASA-CR-135203]
 The promise of esthetics for aircraft turbines
 [NASA-TN-73714] p0012 A78-10098
 Effects of film injection angle on turbine vane
 cooling p0101 A78-13379
 [NASA-TN-1095]
 A computer program for the transient thermal
 analysis of an impingement cooled turbine blade
 [NASA-TN-73819] p0015 A78-15045
 Filament-winding fabrication of OCSEB
 configuration fan blades p0028 A78-16052
 [NASA-CR-135732]
 An analytical study of thermal barrier coated
 first stage blades in a JT9D engine p0028 A78-16054
 [NASA-CR-135360]
 Analytical study of thermal barrier coated
 first-stage blades in an F100 engine p0028 A78-17058
 [NASA-CR-135159]
 Method for calculating convective heat-transfer
 coefficients over turbine vane surfaces p0102 A78-17338
 [NASA-TN-1134]
 Wind turbine generator rotor blade concepts with
 low cost potential p0131 A78-17466
 [NASA-TN-73835]
 Predicted inlet gas temperatures for tungsten
 fiber reinforced superalloy turbine blades p0017 A78-19157
 [NASA-TN-73842]
 Experimental determination of transient strain in
 a thermally-cycled insulated turbine blade
 utilizing a non-contact technique p0017 A78-19161
 [NASA-TN-73886]
 Summary of static load test of the Mod-0 blade
 p0133 A78-19627
 DOE/NASA Mod-0 100KW wind turbine test results
 p0131 A78-19628
 Effect of cooling-hole geometry on aerodynamic
 performance of a film-cooled turbine vane tested
 with cold air in a two-dimensional cascade
 [NASA-TN-1116] p0004 A78-20080
 Two-dimensional cold-air cascade study of a
 film-cooled turbine stator blade. 4:
 Comparison of experimental and analytical
 aerodynamic results for blade with 12 rows of
 0.076-centimeter-(0.030-inch-) diameter holes
 having streamwise ejection angles p0017 A78-20130
 [NASA-TN-1151]
 Two-dimensional cold-air cascade study of a
 film-cooled turbine stator blade. 5:
 Comparison of experimental and analytical
 aerodynamic results for blade with 12 rows of
 0.038-centimeter-(0.015 inch) diameter coolant
 holes having streamwise ejection angles p0017 A78-20133
 [NASA-TN-1204]
 Effluent characterization from a conical
 pressurized fluid bed p0134 A78-21596
 [NASA-TN-73897]
 A computer program for full-coverage film-cooled
 blading analysis including the effects of a
 thermal barrier coating p0021 A78-27126
 [NASA-TN-74951]
 FORTRAN program for calculating coolant flow and
 metal temperatures of a
 full-coverage-film-cooled vane or blade p0021 A78-28099
 [NASA-TN-1259]
 Erosion/corrosion of turbine airfoil materials in
 the high-velocity effluent of a pressurized
 fluidized coal combustor p0071 A78-28224
 [NASA-TN-1274]
 Gas path seal p0021 A78-31103
 [NASA-CASE-LWU-12131-2]
 Analysis of metal temperature and coolant flow
 with a thermal-barrier coating on a
 full-coverage-film-cooled turbine vane p0022 A78-31109
 [NASA-TN-1310]
- Advanced ceramic material for high temperature
 turbine tip seals p0087 A78-31238
 [NASA-CR-135319]
TURBINE ENGINES
 WT DUCTED FAN ENGINES
 WT GAS TURBINE ENGINES
 WT J-85 ENGINE
 WT JET ENGINES
 WT TP-30 ENGINES
 WT TURBOPAW ENGINES
 WT TURBOJET ENGINES
 WT TURBOPROP ENGINES
 'Chain pooling' model selection as developed for
 the statistical analysis of a rotor burst
 protection experiment p0160 A78-29327
 Gas path sealing in turbine engines p0024 A78-33218
 Cost benefit study of advanced materials
 technology for aircraft turbine engines p0026 A78-11081
 [NASA-CR-135235]
 Cost/benefit analysis of advanced material
 technologies for small aircraft turbine engines
 [NASA-CR-135265] p0027 A78-12083
 Cold-air performance of a tip turbine designed to
 drive a lift fan. 3: Effect of insulated fan
 leakage on turbine performance p0003 A78-16001
 [NASA-TN-1109]
 Preliminary study of propulsion systems and
 airplane wing parameters for a US Navy subsonic
 V/STOL aircraft p0010 A78-17041
 [NASA-TN-73652]
 Gas path seal p0021 A78-31103
 [NASA-CASE-LWU-12131-2]
 Evaluation of cyclic behavior of aircraft turbine
 disk alloys p0128 A78-33474
 [NASA-CR-139433]
- TURBINE INSTRUMENTS**
 Instrumentation for propulsion systems development
 [SAE PAPER 780076] p0109 A78-33365
- TURBINE PUMPS**
 Two phase choke flow in tubes with very large L/D
 p0105 A78-15824
 Liquid rocket engine turbopump rotating-shaft seals
 [NASA-SP-8121] p0117 A78-30584
- TURBINE WHEELS**
 Effects of rotor location, coning, and tilt on
 critical loads in large wind turbines p0141 A78-20476
 Concepts for the development of light-weight
 composite structures for rotor burst containment
 p0012 A78-10084
 Application of a flight-line disk crack detector
 to a small engine p0012 A78-10088
 Turbine disks for improved reliability p0012 A78-10089
 Manufacture of astroloy turbine disk shapes by hot
 isostatic pressing, volume 1 p0079 A78-25166
 [NASA-CR-135409]
- TURBINES**
 WT AXIAL FLOW TURBINES
 WT GAS TURBINES
 WT STEAM TURBINES
 WT SUPERSONIC TURBINES
 Manufacture and engine test of advanced oxide
 dispersion strengthened alloy turbine vanes ---
 for space shuttle thermal protection p0077 A78-11232
 [NASA-CR-135269]
 NASTRAW use for cyclic response and fatigue
 analysis of wind turbine towers p0125 A78-12459
 Design study of wind turbines 50 kW to 3000 kW for
 electric utility applications. Volume 1:
 Summary report p0143 A78-12524
 [NASA-CR-134934]
 Cold-air performance of a tip turbine designed to
 drive a lift fan p0001 A78-14998
 [NASA-TN-1126]
 Instrumentation for propulsion systems development
 --- high speed fans and turbines p0011 A78-17052
 [NASA-TN-73840]
 Design study of wind turbines 50 kW to 3000 kW for
 electric utility applications. Volume 2:
 Analysis and design p0143 A78-17862
 [NASA-CR-134935]
 Design study of wind turbines 50 kW to 3000 kW for
 electric utility applications. Volume 3:
 Supplementary design and analysis tasks

TURBOCHARGERS

SUBJECT INDEX

[NASA-CR-135121] p0144 W78-17463
 Wind Turbine Structural Dynamics
 [NASA-TP-2034] p0132 W78-19616
 Comparison of computer codes for calculating
 dynamic loads in wind turbines p0132 W78-19617
 Simplified modeling for wind turbine nodal
 analysis using NASTRAN p0132 W78-19619
 DOE/NASA Mod-0 100KW wind turbine test results p0133 W78-19620
 Power oscillation of the Mod-0 wind turbine p0133 W78-19629
 Methods of attenuating wind turbine ac generator
 output variations p0133 W78-19632
 Fixed pitch wind turbines p0133 W78-19630
 Experimental data and theoretical analysis of a
 operating 100 kW wind turbine [NASA-TP-78083] p0133 W78-19642
 Wake characterization of a tower for the DOE-NASA
 MOD-1 wind turbine [NASA-TP-78053] p0135 W78-23558
 Design and operating experience on the US
 Department of Energy experimental Mod-0 100-kW
 wind turbine [NASA-TP-78915] p0138 W78-26552
 DOE/NASA Mod-0A wind turbine performance [NASA-TP-78916] p0139 W78-26553

TURBOCHARGERS

U TURBOCOMPRESSORS

TURBOCOMPRESSORS

A viscous-inviscid interactive compressor
 calculation [AIAA PAPER 78-1140] p0006 W78-41043
 End-wall boundary layer prediction for axial
 compressors [AIAA PAPER 78-1139] p0007 W78-45133
 Evaluation of a low aspect ratio small axial
 compressor stage, volume 1 [NASA-CR-135240] p0026 W78-12081
 Evaluation of a low aspect ratio small axial
 compressor stage, volume 2 [NASA-CR-135241] p0026 W78-12082
 Cold-air performance of the compressor-drive
 turbine of the Department of Energy baseline
 automobile gas-turbine engine [NASA-TP-78894] p0005 W78-26098
 A viscous-inviscid interactive compressor
 calculations [NASA-TP-78920] p0005 W78-26100
 End-wall boundary layer prediction for axial
 compressors [NASA-TP-78928] p0020 W78-26104
 Core compressor exit stage study, Volume 1:
 Blading design --- turbofan engines [NASA-CR-135391] p0031 W78-29099

TURBOCONVERTERS

U TURBOGENERATORS

TURBOELECTRIC CONVERSION

U TURBOGENERATORS

TURBOFAN AIRCRAFT

Altitude calibration of an F100, S/W P680063,
 turbofan engine [NASA-TP-1228] p0019 W78-23095

TURBOFAN ENGINES

HT TP-70 ENGINES

The application of the Mouth approximation method
 to turbofan engine models p0023 W78-23891
 Minimum-time acceleration of aircraft turbofan
 engines p0023 W78-23892
 Optimal controls for an advanced turbofan engine p0033 W78-23893
 Design of turbofan engine controls using output
 feedback regulator theory p0023 W78-33907
 Failure detection and correction for turbofan
 engines p0033 W78-23918
 Combustor fluctuating pressure measurements
 in-engine and in a component test facility - A
 preliminary comparison p0023 W78-24878
 Effectiveness of an inlet flow turbulence control
 device to simulate flight fan noise in an
 anechoic chamber

Output feedback regulator design for jet engine
 control systems p0024 W78-24880
 State-of-the-art of turbofan engine noise control p0024 W78-24898
 Reduction of fan noise in an anechoic chamber by
 reducing chamber wall induced inlet flow
 disturbance p0024 W78-35658
 Design approaches to more energy efficient engines
 [AIAA PAPER 78-931] p0166 W78-37681
 VTOL tilt nacelle aerodynamics and its relation
 to fan blade stresses [AIAA PAPER 78-958] p0025 W78-43504
 Fuel consumption improvement in current transport
 engines [AIAA PAPER 78-930] p0007 W78-43520
 NASA/General Electric Engine Component Improvement
 Program [AIAA PAPER 78-929] p0033 W78-45097
 Evaluation of an F100 multivariable control using
 a real-time engine simulation [NASA-TP-78648] p0025 W78-45098
 Pollution reduction technology program for class
 T8(J78D) engines p0012 W78-10097
 Altitude test of several afterburner
 configurations on a turbofan engine with a
 hydrogen heater to simulate an elevated turbine
 discharge temperature [NASA-TP-1068] p0013 W78-11067
 Augmentor emissions reduction technology program
 --- for turbofan engines [NASA-CR-135215] p0014 W78-11106
 Aero-acoustic tests of duct-burning turbofan
 exhaust nozzles. Comprehensive data report.
 Volume 1: Model scale acoustic data p0027 W78-13057
 Aero-acoustic tests of duct-burning turbofan
 exhaust nozzles. Comprehensive data report.
 Volume 2: Acoustic and aerodynamic data [NASA-CR-134910-VOL-1] p0002 W78-15988
 Aero-acoustic tests of duct-burning turbofan
 exhaust nozzles. Comprehensive data report.
 Volume 3: Acoustic and aerodynamic data [NASA-CR-134910-VOL-2] p0002 W78-15989
 Aero-acoustic tests of duct-burning turbofan
 exhaust nozzles. Comprehensive data report.
 Volume 3: Acoustic and aerodynamic data curves [NASA-CR-134910-VOL-3] p0002 W78-15990
 Variable thrust nozzle for quiet turbofan engine
 and method of operating same [NASA-CR-135217-1] p0016 W78-17055
 Method of fan sound mode structure determination
 [NASA-CR-135293] p0028 W78-17064
 Method of fan sound mode structure determination
 computer program user's manual: Microphone
 location program [NASA-CR-135294] p0028 W78-17065
 Method of fan sound mode structure determination
 computer program user's manual: Modal
 calculation program [NASA-CR-135295] p0028 W78-17066
 Supersonic through-flow fan engines for supersonic
 cruise aircraft [NASA-TP-78889] p0019 W78-23088
 Acoustic evaluation of a novel swept-rotor fan ---
 noise reduction in turbofan engines [NASA-TP-78878] p0164 W78-24897
 Propulsion systems noise technology p0001 W78-27056
 Design of an air ejector for boundary-layer bleed
 of an acoustically treated turbofan engine inlet
 during ground testing [NASA-TP-78917] p0037 W78-27103
 Acoustic tests of duct-burning turbofan jet noise
 simulation [NASA-CR-2966] p0062 W78-28043
 Acoustic tests of duct-burning turbofan jet noise
 simulation: Comprehensive data report. Volume
 1, section 2; Full size data [NASA-CR-135239-VOL-1-SECT-2] p0030 W78-28095
 Acoustic tests of duct-burning turbofan jet noise
 simulation: Comprehensive data report. Volume
 1, section 3; Data plots [NASA-CR-135239-VOL-1-SECT-3] p0030 W78-28096
 Acoustic tests of duct-burning turbofan jet noise
 simulation: Comprehensive data report. Volume
 2; Model design and aerodynamic test results [NASA-CR-135239-VOL-2] p0031 W78-28097
 Core compressor exit stage study, Volume 1:
 Blading design --- turbofan engines

SUBJECT INDEX

TURBULENT FLOW

- (NASA-CR-135391) p0031 W78-29099
Effect of steady flight loads on JT9D-7 performance deterioration
(NASA-CR-135407) p0031 W78-29105
Procedures for generation and reduction of linear models of a turbofan engine
(NASA-TP-1261) p0161 W78-30896
Energy efficient engine: Preliminary design and integration studies
(NASA-CR-135444) p0032 W78-31108
Pollution Reduction Technology Program for small jet aircraft engines, phase 2
(NASA-CR-159415) p0032 W78-33104
DYABCD: A program for calculating linear A, B, C, and D matrices from a nonlinear dynamic engine simulation
(NASA-TP-1295) p0022 W78-33110
- TURBOFANS**
Acoustic evaluation of a novel swept-rotor fan
(AIAA PAPER 78-1121) p0166 A78-41831
Effectiveness of an inlet flow turbulence control device to simulate flight noise fan in an anechoic chamber
(NASA-TN-73855) p0163 W78-13856
Method of fan sound mode structure determination
(NASA-CR-135291) p0020 W78-17064
Method of fan sound mode structure determination computer program user's manual: Microphone location program
(NASA-CR-135294) p0020 W78-17065
Method of fan sound mode structure determination computer program user's manual: Nodal calculation program
(NASA-CR-135295) p0020 W78-17066
Comparison of the noise characteristics of two low pressure ratio fans with a high throat Mach number inlet
(NASA-TN-73880) p0010 W78-21108
Reduction of fan noise in an anechoic chamber by reducing chamber wall induced inlet flow disturbances
(NASA-TN-78854) p0164 W78-22860
On the use of relative velocity exponents for jet engine exhaust noise
(NASA-TN-78873) p0011 W78-24137
Acoustic evaluation of a novel swept-rotor fan --- noise reduction in turbofan engines
(NASA-TN-78878) p0164 W78-24897
Design of impact-resistant boron/aluminum large fan blade
(NASA-CR-135417) p0031 W78-29104
Performance of a transonic fan stage designed for a low meridional velocity ratio
(NASA-TP-1298) p0022 W78-33107
- TURBOGENERATORS**
Open-Cycle Gas Turbine/Steam Turbine Combined Cycles with synthetic fuels from coal
(ASME PAPER 77-WA/FWHR-9) p0146 A78-33147
- TURBOJET AIRCRAFT**
U JET AIRCRAFT
TURBOJET ENGINE CONTROL
Solution of transient optimization problems by using an algorithm based on nonlinear programming
p0150 A78-23909
Output feedback regulator design for jet engine control systems
p0020 W78-24898
- TURBOJET ENGINES**
NT DUCTED FAN ENGINES
NT J-84 ENGINE
NT TF-10 ENGINE
NT TURBOFAN ENGINES
NT TURBOPROP ENGINES
Effect of fuel properties on performance of single aircraft turbojet combustor at simulated idle, cruise, and takeoff conditions
(NASA-TN-73760) p0014 W78-13056
DYABCD: A program for calculating linear A, B, C, and D matrices from a nonlinear dynamic engine simulation
(NASA-TP-1295) p0022 W78-33110
- TURBOCHARGE BLADES**
NT COMPRESSOR BLADES
NT ROTOR BLADES (THERMOCHARGE)
NT STATOR BLADES
NT TURBINE BLADES
Predicted inlet gas temperatures for tungsten fiber reinforced superalloy turbine blades
p0060 A78-33203
- VSTOL tilt nacelle aerodynamics and its relation to fan blade stresses
(AIAA PAPER 78-958) p0007 A78-43520
- TURBOCHARGER**
NT AXIAL FLOW TURBINES
NT CENTRIFUGAL COMPRESSORS
NT GAS TURBINES
NT STEAM TURBINES
NT SUPERSONIC TURBINES
NT TURBINE PUMPS
NT TURBINES
NT TURBOCOMPRESSORS
NT TURBOFANS
NT TURBOGENERATORS
Review of experimental work on transonic flow in turboachinery
p0004 A78-12312
Analysis of the cross flow in a radial inflow turbine scroll
(NASA-CR-135320) p0029 W78-19153
FLOWNET: A computer program for calculating secondary flow conditions in a network of turboachinery
(NASA-TN-73774) p0156 W78-21791
Design and performance of a 427-meter-per-second-tip-speed two-stage fan having a 2.40 pressure ratio
(NASA-TP-1310) p0022 W78-33109
- TURBOPROP AIRCRAFT**
A parametric investigation of an existing supersonic relation tip speed propeller noise model --- turboprop aircraft
(NASA-TN-73816) p0163 W78-13854
Aerodynamic design and performance testing of an advanced 30 deg swept, eight bladed propeller at Mach numbers from 0.2 to 0.65
(NASA-CR-3047) p0008 W78-32066
- TURBOPROP ENGINES**
Propulsion --- NASA program for aircraft fuel consumption reduction
p0025 A78-43360
Status of advanced turboprop technology
p0001 W78-27055
- TURBOPUMPS**
U TURBINE PUMPS
- TURBOROTORS**
U TURBINE WHEELS
- TURBULENCE**
NT ATMOSPHERIC TURBULENCE
NT GUSTS
NT HOMOGENEOUS TURBULENCE
Experimental clean combustor program: Turbulence characteristics of compressor discharge flows
(NASA-CR-135277) p0027 W78-15041
Mean velocity, turbulence intensity and turbulence convection velocity measurements for a convergent nozzle in a free jet wind tunnel. Comprehensive data report
(NASA-CR-135230) p0007 W78-17991
- TURBULENCE EFFECTS**
Preliminary study of the effect of the turbulent flow field around complex surfaces on their acoustic characteristics
(AIAA PAPER 78-1123) p0166 A78-45129
- TURBULENCE METERS**
Mean velocity, turbulence intensity and turbulence convection velocity measurements for a convergent nozzle in a free jet wind tunnel
(NASA-CR-2949) p0008 W78-21058
- TURBULENT BOUNDARY LAYER**
A visual investigation of turbulence in stagnation flow about a circular cylinder
(NASA-CR-1019) p0108 W78-33386
- TURBULENT DIFFUSION**
Performance of a short annular dump diffuser using suction-stabilized vortices at inlet Mach numbers to 0.41
(NASA-TP-1194) p0017 W78-20131
- TURBULENT FLOW**
Effectiveness of an inlet flow turbulence control device to simulate flight fan noise in an anechoic chamber
p0024 A78-24880
Turbulence processes and simple closure schemes
p0107 A78-40983
Preliminary study of the effect of the turbulent flow field around complex surfaces on their acoustic characteristics
(AIAA PAPER 78-1123) p0166 A78-45129

TURBULENT JETS

Effectiveness of an inlet flow turbulence control device to simulate flight noise fan in an anechoic chamber
 [NASA-TN-73855] p0163 N78-13856

A method for calculating strut and splitter plate noise in exit ducts: Theory and verification
 [NASA-CR-29551] p0167 N78-20921

Reduction of fan noise in an anechoic chamber by reducing chamber wall induced inlet flow disturbances
 [NASA-TN-78854] p0164 N78-22860

Investigation of means for perturbing the flow field in a supersonic wind tunnel
 [NASA-TN-78958] p0037 N78-27182

Preliminary study of the effect of the turbulent flow field around complex surfaces on their acoustic characteristics
 [NASA-TN-78984] p0164 N78-28886

TURBULENT JETS

Interaction of a turbulent-jet noise source with transverse modes in a rectangular duct
 [NASA-TN-1248] p0001 N78-25049

TWO DIMENSIONAL FLOW

Calculation of 3-dimensional choking mass flow in turbomachinery with 2-dimensional flow models
 [NASA-TN-78958] p0066 N78-12289

Computer programs for calculating two-dimensional potential flow in and about propulsion system inlets
 [NASA-TN-78910] p0005 N78-27083

Velocity, temperature, and electrical conductivity profiles in hydrogen-oxygen SHD duct flows
 [NASA-TN-78968] p0104 N78-28372

TWO PHASE FLOW

Two phase choke flow in tubes with very large L/D
 [NASA-TN-78958] p0105 N78-15824

Conceptual design for spacelab two-phase flow experiments
 [NASA-CR-135127] p0037 N78-14061

Two-phase working fluids for the temperature range 5G to 350 C
 [NASA-CR-135255] p0107 N78-16329

U

UDINET ALLOYS

The effect of microstructure on hydrogen embrittlement of the nickel base superalloy, Udinet 700
 [NASA-TN-78958] p0076 N78-37075

OTHER (NUCLEAR REACTORS)

1 HIGH TEMPERATURE NUCLEAR REACTORS

ULTRASONIC TESTS

Correlation of fiber composite tensile strength with the ultrasonic stress wave factor
 [NASA-TN-78958] p0060 N78-33207

Quantitative ultrasonic evaluation of mechanical properties of engineering materials
 [NASA-TN-78958] p0128 N78-45433

Correlations between ultrasonic and fracture toughness factors in metallic materials
 [NASA-TN-78958] p0077 N78-45438

Use of an ultrasonic-acoustic technique for nondestructive evaluation of fiber composite strength
 [NASA-TN-73813] p0128 N78-17397

Correlation of fiber composite tensile strength with the ultrasonic stress wave factor
 [NASA-TN-78884] p0054 N78-20255

Quantitative ultrasonic evaluation of mechanical properties of engineering materials
 [NASA-TN-78904] p0128 N78-24565

ULTRASONICS

Correlations between ultrasonic and fracture toughness factors in metallic materials
 [NASA-TN-73805] p0069 N78-19261

ULTRAVIOLET LIGHT

U ULTRAVIOLET RADIATION

ULTRAVIOLET RADIATION

Measurement of tropospheric 300 nm solar ultraviolet flux for determination of O₃/D₂ photoproduction rate
 [NASA-TN-78958] p0144 N78-38814

Cloud effects on middle ultraviolet global radiation
 [NASA-TN-78958] p0140 N78-42952

Preliminary evaluation of Glass Resin materials for solar cell cover use
 [NASA-TN-78975] p0137 N78-26540

SUBJECT INDEX

Ultraviolet irradiation at elevated temperatures and thermal cycling in vacuum of PEP-4 covered silicon solar cells
 [NASA-TN-78926] p0137 N78-26545

ULTRAVIOLET SPECTROPHOTOMETRY

Ultraviolet spectrophotometer for measuring columnar atmospheric ozone from an aircraft
 [NASA-TN-78958] p0110 N78-35826

UNIAXIAL STRAIN

U AXIAL STRAIN

UNIFORM FLOW

Characteristics of the unsteady motion on transversely sheared mean flows
 [NASA-TN-78958] p0106 N78-23246

UNITED STATES OF AMERICA

UT ARIZONA

UNIVAC COMPUTERS

UT UNIVAC 1100 SERIES COMPUTERS

UNIVAC 1100 SERIES COMPUTERS

Computer program for calculation of a gas temperature profile by infrared emission: Absorption spectroscopy
 [NASA-TN-73844] p0015 N78-15043

User's guide to SPTRAN/1100
 [NASA-TN-1200] p0156 N78-20886

UNIVERSITIES

The SINE project: Minority Involvement in NASA Engineering
 [NASA-TN-73811] p0176 N78-13938

UNMANNED SPACECRAFT

UT SPACE PROBE

UNSTEADY FLOW

UT OSCILLATING FLOW

Unsteady flow in a supersonic cascade with strong in-passage shocks
 [NASA-TN-78958] p0006 N78-17270

Characteristics of the unsteady motion on transversely sheared mean flows
 [NASA-TN-78958] p0106 N78-23246

Computation of unsteady transonic flows through rotating and stationary cascades. 2: User's guide to PORTAN program B2DAT1
 [NASA-CR-2901] p0007 N78-12034

Computation of unsteady transonic flows through rotating and stationary cascades. 1: Method of analysis
 [NASA-CR-2900] p0008 N78-20082

Three-dimensional effects on pure tone fan noise due to inflow distortion --- rotor blade noise prediction
 [NASA-TN-78885] p0164 N78-24898

UPPER SURFACE BLOWN FLAPS

Effects of cone design and power on cruise drag for upper-surface-blowing aircraft
 [NASA-TN-78958] p0004 N78-24058

URBAN TRANSPORTATION

An overview of aerospace gas turbine technology of relevance to the development of the automotive gas turbine engine
 [SAE PAPER 780075] p0120 N78-33364

Baseline tests of the Sagato Elcar electric passenger vehicle
 [NASA-TN-73764] p0174 N78-17934

USER MANUALS (COMPUTER PROGRAMS)

User's guide for SPTRA /360
 [NASA-TN-1006] p0156 N78-10786

Computation of unsteady transonic flows through rotating and stationary cascades. 2: User's guide to PORTAN program B2DAT1
 [NASA-CR-2901] p0007 N78-12034

WASCAP user's manual
 [NASA-CR-135259] p0099 N78-13329

Method of fan sound mode structure determination computer program user's manual: Microphone location program
 [NASA-CR-135294] p0028 N78-17065

Method of fan sound mode structure determination computer program user's manual: Modal calculation program
 [NASA-CR-135295] p0028 N78-17066

User's guide to SPTRAN/1100
 [NASA-TN-1200] p0156 N78-20886

F100(3) parallel compressor computer code and user's manual
 [NASA-CR-135388] p0029 N78-22096

USER REQUIREMENTS

Communication satellite services for special purpose users
 [NASA-TN-78958] p0094 N78-31971

SUBJECT INDEX

VECTORS (MATHEMATICS)

UTILITIES

Design study of wind turbines 50 kW to 3000 kW for electric utility applications. Volume 1: Summary report [NASA-CR-738934] p0143 W78-12529
 Performance potential of combined cycles integrated with low-Btu gasifiers for future electric utility applications [NASA-TN-73775] p0135 W78-23557

UTILIZATION

BT COAL UTILIZATION
 BT LASER APPLICATIONS
 BT NASTR ENERGY UTILIZATION
 BT WINDPOWER UTILIZATION

V

V/STOL AIRCRAFT

BT HELICOPTERS
 BT SHORT TAKEOFF AIRCRAFT
 BT VERTICAL TAKEOFF AIRCRAFT
 A combined potential and viscous flow solution for V/STOL engine inlets [AIAA PAPER 78-182] p0006 W78-20702
 VSTOL tilt nacelle aerodynamics and its relation to fan blade stresses [AIAA PAPER 78-958] p0007 W78-83520
 Methods for calculating the transonic boundary layer separation for V/STOL inlets at high incidence angles [AIAA 78-1380] p0007 W78-86537
 Cold-air performance of a tip turbine designed to drive a lift fan [NASA-TP-1126] p0003 W78-14998
 Preliminary study of propulsion systems and airplane wing parameters for a US Navy subsonic V/STOL aircraft [NASA-TN-73652] p0010 W78-17041
 VSTOL tilt nacelle aerodynamics and its relation to fan blade stresses [NASA-TN-78899] p0005 W78-26049

VACUUM APPARATUS

BT VACUUM CHAMBERS

VACUUM CHAMBERS

Atomic hydrogen storage method and apparatus --- cryotrapping and magnetic field strength [NASA-CASE-LEW-12081-2] p0169 W78-19907
 Effect of facility background gases on internal erosion of the 30-cm Hg ion thruster [NASA-TN-738011] p0048 W78-21205

VACUUM DEPOSITION

Ion beam sputter etching and deposition of fluoropolymers [NASA-TN-78888] p0018 W78-28358

VACUUM MELTING

Rolling element fatigue testing of gear materials [NASA-CR-135411] p0124 W78-31427

VACUUM TESTS

Friction and metal transfer for single-crystal silicon carbide in contact with various metals in vacuum [NASA-TP-1191] p0082 W78-21294

VACUUM TUBE OSCILLATORS

BT KLYSTRONS
 BT MICROWAVE TUBES
 BT TRAVELING WAVE TUBES

VACUUM TUBES

BT KLYSTRONS
 BT MICROWAVE TUBES
 BT TRAVELING WAVE TUBES

VALVES

BT COCKS
 BT PRESSURE REGULATORS
 BT RELIEF VALVES

VANES

BT BEND VANES
 Effect of coolant flow ejection on aerodynamic performance of low-aspect-ratio vanes. 2: Performance with coolant flow ejection at temperature ratios up to 2 [NASA-TP-1047] p0033 W78-11008
 Effect of endwall cooling on secondary flows in turbine stator vanes p0014 W78-11098
 Manufacture and engine test of advanced oxide dispersion strengthened alloy turbine vanes --- for space shuttle thermal protection [NASA-CR-135269] p0077 W78-11232

Method for calculation of convective heat-transfer coefficients over turbine vane surfaces [NASA-TP-1134] p0102 W78-17338
 Effect of cooling-hole geometry on aerodynamic performance of a film-cooled turbine vane tested with cold air in a two-dimensional cascade [NASA-TP-1136] p0004 W78-20080

VANES

BT TRUCKS
 VAPOR DEPOSITION
 BT VACUUM DEPOSITION
 Superconducting Nb₃Ge for high-field magnets p0175 W78-41922

VAPOR PRESSURE

Compact electron-beam source for formation of neutral beams of very low vapor pressure materials p0110 W78-41464
 Some properties of low-vapor-pressure brass alloys for thermionic converters [NASA-TN-78867] p0134 W78-22471

VAPORIZATION HEAT

BT HEAT OF VAPORIZATION
 VAPORIZING
 BT BOILING
 BT COAL GASIFICATION
 BT FILM BOILING
 BT LEIDENFROST PHENOMENON
 BT NUCLEATE BOILING
 BT TRANSPIRATION
 Volatilization of oxides during oxidation of some superalloys at 1200 C p0073 W78-18631
 Degree of vaporization using an airblast type fuel injector for a preoxidized-prevaporized combustor p0107 W78-50322

VAPORS

BT CESIUM VAPOR
 BT MERCURY VAPOR
 BT METAL VAPORS

VARIABLE CYCLE ENGINES

Inlet-engine matching for SCAR including application of a bicone variable geometry inlet --- Supersonic Cruise Aircraft Research [AIAA PAPER 78-961] p0007 W78-45096
 Advanced supersonic propulsion study, phase 4 [NASA-CR-135273] p0026 W78-11062
 Advanced supersonic propulsion study, phases 3 and 4 --- variable cycle engines [NASA-CR-135236] p0027 W78-13058
 A review of NASA's propulsion programs for aviation [NASA-TN-73831] p0016 W78-16055
 Variable cycle gas turbine engines [NASA-CASE-LEW-12916-1] p0113 W78-17380
 Variable mixer propulsion cycle [NASA-CASE-LEW-12917-1] p0016 W78-18067
 VCE testbed program planning and definition study [NASA-CR-135362] p0029 W78-19160
 Inlet-engine matching for SCAR including application of a bicone variable geometry inlet [NASA-TN-78955] p0021 W78-27125

VARIABLE GEOMETRY STRUCTURES

Inlet-engine matching for SCAR including application of a bicone variable geometry inlet [NASA-TN-78955] p0021 W78-27125

VARIABLE PITCH PROPELLERS

Impact absorbing blade mounts for variable pitch blades [NASA-CASE-LEW-12313-1] p0113 W78-10468
 Reverse-thrust technology for variable-pitch fan propulsion systems p0005 W78-24070

VARIABLE THRUST

Variable thrust nozzle for quiet turbofan engine and method of operating same [NASA-CASE-LEW-12317-1] p0016 W78-17055

VARIANCE (STATISTICS)

BT REGRESSION ANALYSIS

VARIATIONS

BT SIGNAL VARIATIONS
 BT PERIODIC VARIATIONS
 BT WIND VARIATIONS

VCR

BT VARIABLE CYCLE ENGINES

VECTOR SPACES

BT MATRICES (MATHEMATICS)
 BT STATE VECTORS
 VECTORS (MATHEMATICS)
 BT STATE VECTORS

VELOCITY

SUBJECT INDEX

VELOCITY

VT AIRSPEED
 VT CRITICAL VELOCITY
 VT EXHAUST VELOCITY
 VT FLOW VELOCITY
 VT HIGH SPEED
 VT MOTOR SPEED
 VT SUPERSONIC SPEEDS
 VT TIP SPEED
 VT WIND VELOCITY
 VELOCITY DISTRIBUTION
 Velocity and temperature profiles in near-critical nitrogen flowing past a horizontal flat plate [ASME PAPER 77-HT-7] p0186 A78-17461
 Optimum wall impedance for spinning codes - A correlation with mode out-off ratio [AIAA PAPER 78-193] p0165 A78-20735
 An empirical model for inverted-velocity-profile jet noise prediction p0023 A78-24879
 End-wall boundary layer prediction for axial compressors [AIAA PAPER 78-1139] p0907 A78-45133
 An empirical model for inverted-velocity-profile jet noise prediction [NASA-TN-73038] p0014 A78-13061
 VELOCITY FIELDS
 U VELOCITY DISTRIBUTION
 VELOCITY MEASUREMENT
 Miniature drag force anemometer p0109 A78-17397
 The role of drop velocity in statistical spray description p0107 A78-50323
 Heat velocity, turbulence intensity and turbulence convection velocity measurements for a convergent nozzle in a free jet wind tunnel. Comprehensive data report [NASA-CN-135238] p0007 A78-17991
 VELOCITY PROFILES
 U VELOCITY DISTRIBUTION
 VERTICAL DISTRIBUTION
 Ultraviolet spectrophotometer for measuring colinear atmospheric ozone from aircraft p0110 A78-35826
 VERTICAL TAKEOFF AIRCRAFT
 Theoretical flow characteristics of inlets for tilting-nacelle VTOL aircraft [NASA-TP-1205] p0018 A78-21114
 VERY LOW FREQUENCIES
 Experiments on whistler wave filamentation and VLF hiss in a laboratory plasma p0149 A78-41788
 VIBRATION
 VT BENDING VIBRATION
 VT FLUTTER
 VT FREE VIBRATION
 VT STRUCTURAL VIBRATION
 VIBRATION EFFECTS
 Effect of vibration on retention characteristics of screen acquisition systems --- for surface tension propellant acquisition [AIAA PAPER 78-1030] p0045 A78-43560
 VIBRATION MEASUREMENT
 Synthesis of blade flutter vibratory patterns using stationary transducers [NASA-TN-73821] p0003 A78-17001
 VIBRATION TESTS
 VT DAMPING TESTS
 Measurement of the time-temperature dependent dynamic mechanical properties of boron/aluminum composites p0061 A78-33222
 VIBRATIONAL STRESS
 VTOL tilt nacelle aerodynamics and its relation to fan blade stresses [NASA-TN-78899] p0005 A78-26099
 VIBRATORY LOADS
 Transient dynamics of a flexible rotor with squeeze film dampers [NASA-CN-3050] p0123 A78-32433
 VIKING LAUNDS SPACECRAFT
 Viking and STP P78-2 electrostatic charging designs and testing p0037 A78-10175
 VIKING SPACECRAFT
 VT VIKING LAUNDS SPACECRAFT
 VIKING 1 SPACECRAFT
 VT VIKING LAUNDS SPACECRAFT

VIKING 2 SPACECRAFT

VT VIKING LAUNDS SPACECRAFT
 VISCOELASTIC DAMPING
 Transient dynamics of a flexible rotor with squeeze film dampers [NASA-CN-3050] p0123 A78-32433
 VISCOELASTIC FLOW
 U VISCOELASTICITY
 VISCOELASTICITY
 Development of procedures for calculating stiffness and damping properties of elastomers in engineering applications. Part 4: Testing of elastomers under a rotating load --- resonance testing [NASA-CN-135355] p0127 A78-22402
 VISCOSITY
 Revised international representations for the viscosity of water and steam and new representations for the surface tension of water p0105 A78-15725
 VISCOUS DAMPING
 VT VISCOELASTIC DAMPING
 Influence of oil-squeeze-film damping on steady-state response of flexible rotor operating to supercritical speeds [NASA-TP-1094] p0015 A78-13064
 VISCOUS FLOW
 VT BOUNDARY LAYER FLOW
 VT BOUNDARY LAYER SEPARATION
 VT SECONDARY FLOW
 A combined potential and viscous flow solution for V/STOL engine inlets [AIAA PAPER 78-142] p0006 A78-20702
 A viscous-inviscid interactive compressor calculation [AIAA PAPER 78-1140] p0006 A78-41843
 A viscous-inviscid interactive compressor calculation [NASA-TN-78920] p0005 A78-26100
 End-wall boundary layer prediction for axial compressors [NASA-TN-78928] p0020 A78-26144
 VISUAL DISPLAYS
 U DISPLAY DEVICES
 VISUALIZATION OF FLOW
 U FLOW VISUALIZATION
 VOLATILITY
 Volatile products from the interaction of KCl(g) with Cr2O3 and LaCrO3 in oxidizing environments [NASA-TN-73795] p0064 A78-13158
 VOLATILIZATION
 U VAPOURING
 VOLT-AMPERE CHARACTERISTICS
 Preliminary results on the conversion of laser energy into electricity p0173 A78-34631
 VOLTAGE BREAKDOWNS
 U ELECTRICAL FAILURES
 VOLTAGE CONVERTERS (DC TO DC)
 Discrete time domain modelling and analysis of dc-dc converters with continuous and discontinuous inductor current p0100 A78-18796
 Medium power voltage multipliers with a large number of stages p0098 A78-45435
 High frequency capacitor-diode voltage multiplier dc-dc converter development [NASA-CN-135309] p0099 A78-15400
 Medium power voltage multipliers with a large number of stages [NASA-TN-78900] p0093 A78-26373
 Modeling and Analysis of Power Processing Systems (MAPPS), initial phase 2 [NASA-CN-135173] p0100 A78-29350
 Modelling, analysis and design of switching converters [NASA-CN-135174] p0100 A78-29351
 Regulated high efficiency, lightweight capacitor-diode multiplier dc to dc converter [NASA-CASE-LW-12791-1] p0097 A78-32341
 VOLTAGE GENERATORS
 VT PHOTOVOLTAIC CELLS
 Extended performance solar electric propulsion thrust system study. Volume 5. Capacitor-diode voltage multiplier: Technology evaluation [NASA-CN-135281-VOL-5] p0053 A78-19195
 VOLTAGE MEASUREMENT
 U ELECTRICAL MEASUREMENT

SUBJECT INDEX

WEAR TESTS

VOLTAGE REGULATORS
 30-cm mercury ion thruster performance with a 1 kV capacitor-diode voltage multiplier beam supply (AIAA PAPER 78-686; p0051 178-32760)

VOLUNTARY ANALYSIS
 Volume fraction determination in cast superalloys and directionally solidified eutectic alloys by a new manual point count practice p0069 178-24369

VON KISES THEORY
 V STRESS FUNCTIONS

VORTEX COLUMNS
 V VORTICES

VORTEX DISTURBANCES
 V VORTICES

VORTEX FLOW
 V VORTICES

VORTEX SHEETS
 Sound production in a moving stream p0165 178-31224

VORTEX TUBES
 V VORTICES

VORTICES
 Models for some aspects of atmospheric vortices p0150 178-14581
 Performance characteristics of two annular dump diffusers using suction-stabilized vortex flow control p0107 178-45431
 Performance characteristics of two annular dump diffusers using suction-stabilized vortex flow control [NASA-TN-73857] p0004 178-19057
 Performance of a short annular dump diffuser using suction-stabilized vortices at inlet Mach numbers to 0.41 [NASA-TN-1194] p0017 178-20131

VTOL AIRCRAFT
 V VERTICAL TAKEOFF AIRCRAFT

W

WAKES
 Wake characteristics of a tower for the DOE-NASA MOD-1 wind turbine [NASA-TN-78853] p0135 178-23558
 Wake characteristics of an eight-leg tower for a MOD-0 type wind turbine [NASA-TN-73868] p0135 178-24615

WALL FLOW
 End-wall boundary layer prediction for axial compressors (AIAA PAPER 78-1139) p0007 178-45133
 Reduction of fan noise in an anechoic chamber by reducing chamber wall induced inlet flow disturbances [NASA-TN-78854] p0164 178-22860

WALL PRESSURE
 End-wall boundary layer prediction for axial compressors [NASA-TN-78928] p0020 178-26144

WAKEFIELD ENGINES
 General aviation internal combustion engine research programs at NASA-Lewis Research Center (AIAA PAPER 78-932) p0025 178-43505

WARNING DEVICES
 W WARNING SYSTEMS

WARNING SIGNALS
 W WARNING SYSTEMS

WARNING SYSTEMS
 Disaster warning system study summary --- cost estimates using NOAA satellites [NASA-TN-73797] p0093 178-10346

WASTE ENERGY UTILIZATION
 Thermal energy storage for industrial waste heat recovery [NASA-TN-78953] p0140 178-29576

WASTES
 WT INDUSTRIAL WASTES

WATER
 Revised international representations for the viscosity of water and steam and new representations for the surface tension of water p0105 178-15725
 Status of the DOE (TOB)-sponsored national program on hydrogen production from water via thermochemical cycles [NASA-TN-78825] p0132 178-17469

Catalytic decomposition of methanol for onboard hydrogen generation [NASA-TN-1287] p0083 178-25236

WATER CIRCULATION
 Numerical computation of three-dimensional circulation in Lake Erie - a comparison of a free-surface model and a rigid-lid model p0151 178-47223

WATER CONTENT
 W MOISTURE CONTENT

WATER JETS
 W HYDRAULIC JETS

WATER PURIFICATION
 W WATER TREATMENT

WATER RESOURCES
 Photovoltaic water pumping applications: Assessment of the near-term market [NASA-TN-78847] p0134 178-19644

WATER TREATMENT
 Release of dissolved nitrogen from water during depressurization p0066 178-33224

WAVE ATTENUATION
 WT ACOUSTIC ATTENUATION

WAVE EXCITATION
 WT ACOUSTIC EXCITATION

WAVE PROPAGATION
 WT ACOUSTIC PROPAGATION
 Impact on multilayered composite plates [NASA-CN-135247] p0062 178-16103

WAVE RADIATION
 W ELECTROMAGNETIC RADIATION

WEAR
 The use of analytical surface tools in the fundamental study of wear p0119 178-23428
 Definition and effect of chemical properties of surfaces in friction, wear, and lubrication p0121 178-45436
 Friction and wear of single-crystal and polycrystalline manganese-zinc ferrite in contact with various metals [NASA-TN-1059] p0080 178-10295
 Friction and wear of several compressor gas-path seal movements [NASA-TN-1128] p0068 178-15229
 Friction and wear of polyethylene oxide polymer having a range of molecular weights [NASA-TN-1129] p0080 178-15278
 Definition and effect of chemical properties of surfaces in friction, wear, and lubrication [NASA-TN-73806] p0065 178-19237
 Friction and wear behavior of single-crystal silicon carbide in sliding contact with various metals [NASA-TN-73782] p0114 178-19512
 Lubrication and failure mechanisms of graphite fluoride films [NASA-TN-1197] p0081 178-20337
 Friction and wear of radiofrequency-sputtered borides, silicides, and carbides [NASA-TN-1156] p0081 178-20338
 Friction and wear of selected metals and alloys in sliding contact with AISI 440 C stainless steel in liquid methane and in liquid natural gas [NASA-TN-1150] p0114 178-20512
 Ferrographic analysis of wear particles from sliding elastohydrodynamic experiments [NASA-TN-1230] p0115 178-22377
 Friction and wear of carbon-graphite materials for high-energy brakes [NASA-TN-78904] p0054 178-26178

WEAR INHIBITORS
 Microstructural and wear properties of sputtered carbides and silicides p0084 178-23445
 Coatings for wear and lubrication [NASA-TN-78841] p0081 178-20333

WEAR TESTS
 Friction and wear of sintered fibermetal abradable seal materials p0074 178-23451
 Ferrographic analysis of wear debris generated in accelerated rolling element fatigue tests p0119 178-28425
 I-ray photoelectron spectroscopic study of surface chemistry of dibenzyl disulfide on steel under mild and severe wear conditions p0066 178-31439

WEATHER DATA RECORDERS

SUBJECT INDEX

Friction and wear behavior of single-crystal silicon carbide in sliding contact with various metals	p0086 A78-84095	VSTOL tilt nacelle aerodynamics and its relation to fan blade stresses	p0007 A78-83520
Wear of single-crystal silicon carbide in contact with various metals in vacuum	p0082 A78-21295	Wind tunnel performance tests of conical plug nozzles --- in the Langley 8 x 6 ft. supersonic wind tunnel	p0002 A78-21088
Some effects of composition on friction and wear of graphite-fiber-reinforced polyimide liners in plain spherical bearings	p0115 A78-25433	Wake characteristics of an eight-leg tower for a MOD-0 type wind turbine	p0135 A78-28615
Sub tolerance evaluation of two sintered NiCrAl gas path seal materials --- wear tests of gas turbine engine seals	p0071 A78-29215	Flight effects on the aerodynamic and acoustic characteristics of inverted profile conical nozzles, volume 1 --- supersonic cruise aircraft research wind tunnel tests	p0167 A78-29867
WEATHER DATA RECORDERS		Wind tunnel evaluation of YF-12 inlet response to internal airflow disturbances with and without control --- Lewis 10 by 10 ft supersonic wind tunnel tests	p0008 A78-21058
Automated meteorological data from commercial aircraft via satellite: Present experience and future implications	p0150 A78-17558		
WINDS (HEADWINDS)		WIND TUNNELS	
WINDS (SUPPORTS)		WT CASCADE WIND TUNNELS	
Integrated gas turbine engine-nacelle	p0016 A78-18066	WT SUPERSONIC WIND TUNNELS	
[NASA-CASE-118-12389-2]		Mean velocity, turbulence intensity and turbulence convection velocity measurements for a convergent nozzle in a free jet wind tunnel.	
WINDMILL DENSITY FUNCTIONS		Comprehensive data report	p0007 A78-17991
A Weibull characterization for tensile fracture of multicomponent brittle fibers	p0060 A78-24892	WIND TUNNELS	
		Effects of rotor location, coning, and tilt on critical loads in large wind turbines	p0181 A78-20476
WEIGHT (MASS)		WIND VARIATIONS	
WT STRUCTURAL WEIGHT		Methods of attenuating wind turbine ac generator output variations	p0133 A78-19632
WEIGHT ANALYSIS		WIND VELOCITY	
Consent on 'Heat-pipe reactors for space power applications'	p0052 A78-40826	Mean velocity, turbulence intensity and turbulence convection velocity measurements for a convergent nozzle in a free jet wind tunnel.	
WEIGHT REDUCTION		Comprehensive data report	p0007 A78-17991
Recent advances in lightweight, filament-wound composite pressure vessel technology	p0061 A78-33436	WINDING	
An ultralightweight, evacuated, load-bearing, high-performance insulation system --- for cryogenic propellant tanks	p0085 A78-36005	WT FILAMENT WINDING	
[AIAA PAPER 78-878]		WINDMILLS (WINDPOWERED MACHINES)	
WEIGHTLESSNESS		Comparison of computer codes for calculating dynamic loads in wind turbines	p0142 A78-37678
Liquid jet impingement normal to a disk in zero gravity	p0107 A78-81154	Design study of wind turbines 50 kW to 3000 kW for electric utility applications. Volume 1: Summary Report	p0143 A78-12529
[ASME PAPER 78-WA/FE-1]		[NASA-CR-138938]	
Conceptual design for spacelab two-phase flow experiments	p0037 A78-14063	Design study of wind turbines 50 kW to 3000 kW for electric utility applications. Volume 2: Analysis and design	p0143 A78-17842
[NASA-CR-135127]		[NASA-CR-138938]	
Materials science experiments in space	p0056 A78-16094	Design study of wind turbines 50 kW to 3000 kW for electric utility applications. Volume 3: Supplementary design and analysis tasks	p0184 A78-17863
[NASA-CR-2842]		[NASA-CR-135121]	
Preliminary concept, specifications, and requirements for a zero-gravity combustion facility for spacelab	p0041 A78-26166	Wake characteristics of a tower for the DOE-WASA MOD-1 wind turbine	p0135 A78-23558
[NASA-TN-78910]		[NASA-TN-78853]	
WELD STRENGTH		WINDPOWER UTILIZATION	
Cryogenic properties of a new tough-strong iron alloy	p0073 A78-15825	WASRA use for cyclic response and fatigue analysis of wind turbine towers	p0125 A78-12459
WELDING		EPDA/WASA 100 kilowatt mod-0 wind turbine operations and performance --- at the NASA Plum Brook Station, Ohio	p0131 A78-15563
WT BRAZING		[NASA-TN-73825]	
WT COLD WELDING		Design study of wind turbines 50 kW to 3000 kW for electric utility applications. Volume 3: Supplementary design and analysis tasks	p0184 A78-17863
WT DIFFUSION WELDING		[NASA-CR-135121]	
WETNESS		Synchronization of the DOE/WASA 100-kilowatt wind turbine generator with a large utility network	p0132 A78-17467
WETNESS CONTENT		[NASA-TN-73861]	
WHEELS		Comparison of computer codes for calculating dynamic loads in wind turbines	p0132 A78-19617
WT TURBINE WHEELS		Experimental data and theoretical analysis of an operating 100 kW wind turbine	p0173 A78-19682
WHISTLES		[NASA-TN-73883]	
Experiments on whistler wave filamentation and VLF hiss in a laboratory plasma	p0189 A78-81788		
WIND (METEOROLOGY)			
WT GUSTS			
WIND EFFECTS			
Numerical computation of three-dimensional circulation in Lake Erie - A comparison of a free-surface model and a rigid-lid model	p0151 A78-87223		
Effects of rotor location, coning, and tilt on critical loads in large wind turbines	p0133 A78-19636		
WIND SHEAR			
Models for some aspects of atmospheric vortices	p0150 A78-14581		
WIND TUNNEL TESTS			
Variation of fan tone steadiness for several inflow conditions	p0166 A78-81829		
[AIAA PAPER 78-1119]			

SUBJECT INDEX

Y28228

A simulation model for wind energy storage systems. Volume 1: Technical report [NASA-CN-135283] p0156 W78-20802

A simulation model for wind energy storage systems. Volume 2: Operation manual [NASA-CN-135284] p0157 W78-20803

A simulation model for wind energy storage systems. Volume 3: Program descriptions [NASA-CN-135285] p0157 W78-20804

Design and operating experience on the US Department of Energy experimental Mod-0 100-kw wind turbine [NASA-TN-78915] p0138 W78-26552

DOE/NASA Mod-0A wind turbine performance [NASA-TN-78916] p0139 W78-26553

WINDPOWERED GENERATORS

Effects of rotor location, coning, and tilt on critical loads in large wind turbines p0141 W78-20476

Synchronization of wind turbine generators against an infinite bus under gusting wind conditions [IEEE PAPER P 77 675-2] p0142 W78-30196

ERDA/NASA 100 kilowatt mod-0 wind turbine operations and performance --- at the NASA Ples Brook Station, Ohio [NASA-TN-73825] p0131 W78-15563

Appropriate method for calculating free vibrations of a large-wind-turbine tower structure [NASA-TN-73754] p0131 W78-16434

Design study of wind turbines 50 kw to 3000 kw for electric utility applications. Volume 2: Analysis and design [NASA-CN-134935] p0143 W78-17462

Synchronization of the DOE/NASA 100-kilowatt wind turbine generator with a large utility network [NASA-TN-73861] p0132 W78-17467

Wind Turbine Structural Dynamics [NASA-CN-2034] p0132 W78-19616

Simplified modeling for wind turbine nodal analysis using NASTRAN p0132 W78-19619

Influence of wind turbine foundation p0133 W78-19626

Summary of static load test of the Mod-0 blade p0133 W78-19627

DOE/NASA Mod-0 100KW wind turbine test results p0133 W78-19628

Power oscillation of the Mod-0 wind turbine p0133 W78-19629

Methods of attenuating wind turbine ac generator output variations p0133 W78-19632

Effects of rotor location, coning, and tilt on critical loads in large wind turbines p0133 W78-19636

Fixed pitch wind turbines p0133 W78-19638

Experimental data and theoretical analysis of an operating 100 kW wind turbine [NASA-TN-73883] p0133 W78-19682

Employing static excitation control and tie line reactance to stabilize wind turbine generators [NASA-CN-135388] p0188 W78-20403

Comparison of computer codes for calculating dynamic loads in wind turbines [NASA-TN-73771] p0135 W78-21556

Design study of wind turbines, 50 kw to 3000 kw for electric utility applications: Executive summary [NASA-CN-134936] p0188 W78-21559

Design study of wind turbines 50 kw to 3000 kw for electric utility applications: Analysis and design [NASA-CN-134937] p0188 W78-21560

Transient response to three-phase faults on a wind turbine generator [NASA-TN-78902] p0137 W78-26542

Large wind turbine generators [NASA-TN-73767] p0180 W78-29574

The 200-kilowatt wind turbine project [NASA-TN-79757] p0180 W78-29583

WIND FLAPS

Analytical modeling of under-the-wing externally blown flap powered-lift noise p0006 W78-24063

WIND PLATEFORMS

Preliminary study of propulsion systems and airplane wing parameters for a US Navy subsonic V/STOL aircraft

[NASA-TN-73652] p0010 W78-17001

WINGS

WT TILTING ROTORS

WT TIP DRIVEN ROTORS

Development and test of an inlet and duct to provide airflow for a wing boundary layer control system [AIAA PAPER 78-141] p0006 W78-20701

WIRES

Upper limit for sagtoreistance in silicon bronze and phosphor bronze wire p0175 W78-14423

WIRE CLOTS

Flow of liquid jets through closely spaced screens p0108 W78-42677

WIRE MESH

U WIRE CLOT

WOOD

WT PLYWOOD

WORK FUNCTIONS

ERDA-NASA advanced thermonuclear technology program [NASA-CN-157222] p0145 W78-26579

WORKING FLUIDS

Evaluation of commercially-available spacecraft-type heat pipes [AIAA 78-397] p0064 W78-35590

WRAPAROUND CONTACT SOLAR CELLS

U SOLAR CELLS

WROUGHT ALLOYS

An experimental P/W wrought superalloy for advanced temperature service p0073 W78-15335

Effect of prior creep at 1365 K on the room temperature tensile properties of several oxide dispersion strengthened alloys p0074 W78-21431

X

X BAND

U SUPERHIGH FREQUENCIES

X RAY SPECTROGRAPHY

U X RAY SPECTROSCOPY

X RAY SPECTROMETRY

U X RAY SPECTROSCOPY

X RAY SPECTROSCOPY

Principles of ESCA and applications to metal corrosion, coating and lubrication --- Electron Spectroscopy for Chemical Analysis p0061 W78-33213

X-ray photoelectron spectroscopy study of radiofrequency-sputtered refractory compound steel interfaces [NASA-TN-1161] p0081 W78-20336

X-Y PLOTTERS

Particle parameter analyzing system --- x-y plotter circuits and display [NASA-CASE-REP-06098] p0096 W78-17293

XENON

12-cw magneto-electrostatic containment argon/xenon ion source development [AIAA PAPER 78-681] p0039 W78-32756

Y

YF-102 AIRCRAFT

U F-102 AIRCRAFT

YF-12 AIRCRAFT

Mechanical characteristics of stability-bleed valves for a supersonic inlet --- for the YF-12 aircraft [NASA-TN-X-1483] p0015 W78-11063

Wind tunnel evaluation of YF-12 inlet response to internal airflow disturbances with and without control --- Lewis 10 by 10 ft supersonic wind tunnel tests p0006 W78-12742

YIELD STRENGTH

Effects of thermomechanical processing on strength and toughness of iron - 12-percent-nickel - reactive metal alloys at -196 C [NASA-CP-1108] p0073 W78-31213

YJ-93 ENGINE

U J-85 ENGINE

YOUNG MODULUS

J MODULUS OF ELASTICITY

YTTBIUM

Pre-arcless sintered Sialons with low amounts of sintering aid

TITANIUM ALLOYS

SUBJECT INDEX

[NASA-TN-1246] p0082 W78-25215
TITANIUM ALLOYS
 Adhesive/cohesive strength of a ErO_2 -1-2 w/o
 Y2O3/NiCrAlY thermal barrier coating
 [NASA-TN-73792] p0081 W78-17152
 Effects of compositional changes on the
 performance of a thermal barrier coating system
 --- yttria-stabilized zirconia coatings on gas
 turbine engine blades
 [NASA-TN-78976] p0072 W78-31212
TITANIUM COMPOUNDS
 Reactions of yttria-stabilized zirconia with
 oxides and sulfates of various elements
 [NASA-TN-78982] p0071 W78-29216

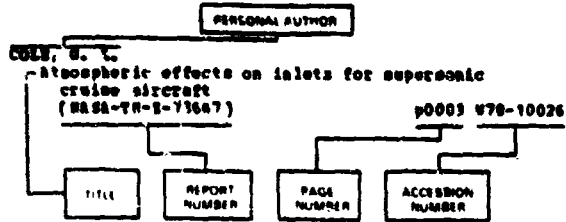
Z

ZINC CROSSINGS
Z ROOTS OF EQUATIONS
ZINC GRAVITY
Z ZINCZLSSZZZZS

ZINC
 The fluorination of orbital and zinc
 [NASA-TN-X-73878] p0064 W78-15211
 Determination of the zincate diffusion coefficient
 and its application to alkaline battery problems
 [NASA-TN-73879] p0134 W78-19648
 Adhesion of a metallic interface --- for Al, Mg,
 and Zn
 [NASA-TN-78890] p0071 W78-29216
ZINC NICKEL BATTERIES
Z NICKEL ZINC BATTERIES
ZIRCONIUM ALLOYS
 Adhesive/cohesive strength of a ErO_2 -1-2 w/o
 Y2O3/NiCrAlY thermal barrier coating
 [NASA-TN-73792] p0057 W78-17152
 Reactions of yttria-stabilized zirconia with
 oxides and sulfates of various elements
 [NASA-TN-78982] p0071 W78-29216
ZIRCONIUM COMPOUNDS
WT ZIRCONIUM OXIDES
ZIRCONIUM OXIDES
 Temperature distributions and thermal stresses in
 a graded zirconia/metal gas path seal system for
 aircraft gas turbine engines
 [AIAA PAPER 78-93] p0118 W78-20681
 Temperature distributions and thermal stresses in
 a graded zirconia/metal gas path seal system for
 aircraft gas turbine engines
 [NASA-TN-73818] p0015 W78-15044
 Preliminary study of cyclic thermal shock
 resistance of plasma-sprayed zirconium oxide
 turbine outer air seal shrouds
 [NASA-TN-73852] p0080 W78-15280
 Effects of compositional changes on the
 performance of a thermal barrier coating system
 --- yttria-stabilized zirconia coatings on gas
 turbine engine blades
 [NASA-TN-78976] p0072 W78-31212

PERSONAL AUTHOR INDEX

Typical Personal Author Index Listing



Listings in this index are arranged alphabetically by personal author. The title of the document provides the user with a brief description of the subject matter. The report number helps to indicate the type of document listed (e.g. NASA report, translation, NASA contractor report). The page and accession numbers are located beneath and to the right of the title (e.g. p0003 N78-10026). Under any one author's name the accession numbers are arranged in sequence with the AIAA accession numbers appearing first.

A

- ABBOTT, J. B.**
Simulated flight effects of noise characteristics of a fan inlet with high throat Mach number (NASA-TN-1199) p0017 N78-23132
Comparison of the noise characteristics of two low pressure ratio fans with a high throat Mach number inlet (NASA-TN-73800) p0018 N78-21100
- ABDILLAH, S.**
Analysis of the cross flow in a radial inflow turbine scroll (NASA-CR-135320) p0129 N78-19153
Computer program for the analysis of the cross flow in a radial inflow turbine scroll (NASA-CR-135321) p0029 N78-19154
- ADAMCHIK, J. J.**
Unsteady flow in a supersonic cascade with strong in-passage shocks p0006 N78-17270
- ADAMSON, A. P.**
Impact absorbing blade mounts for variable pitch blades (NASA-CASR-LEW-12313-1) p0113 N78-10460
Variable thrust nozzle for quiet turbofan engine and method of operating same (NASA-CASR-LEW-12317-1) p0116 N78-17055
Can turbine engine with convertible accessories (NASA-CASR-LEW-12390-1) p0016 N78-17056
Integrated gas turbine engine nacelle (NASA-CASR-LEW-12389-2) p0016 N78-18066
Can turbine engine with recirculating bleed (NASA-CASR-LEW-12452-1) p0019 N78-24089
- ADUJA, K. K.**
Calculation of far-field jet noise spectra from near-field measurements using true source location (AIAA PAPER 78-1153) p0168 N78-81852
- AKIN, L. S.**
Study of lubricant jet flow phenomena in spur gears - Out of mesh condition (AIAA PAPER 77-DPT-106) p0110 N78-20608
- ALBERT, A. J.**
NASA/General Electric Engine Component Improvement Program (AIAA PAPER 78-929) p0025 N78-85098
- ALBUQUERQUE, S.**
Thin permeable membrane (NASA-CR-135116) p0108 N78-18515
- ALBUQUERQUE, S. E.**
Performance of the 12 GHz, 200 watt Transmitter Experiment Package for the Hermes Satellite p0098 N78-24883
- ALLEN, D. L.**
Performance of the 12GHz, 200 watt transmitter experiment package for the Hermes satellite (NASA-TN-7380-1) p0092 N78-13282
A review of the Thermo-electronic Laser Energy Converter (TELPEC) Program at Lewis Research Center p0142 N78-33217
Preliminary results on the conversion of laser energy into electricity p0173 N78-34631
Method of forming metal hydride films (NASA-CASR-LEW-12083-1) p0113 N78-13636
Closed loop spray cooling apparatus (NASA-CASR-LEW-11981-1) p0091 N78-17237
A review of the thermo-electronic laser energy converter (TELPEC) program at Lewis Research Center (NASA-TN-73804) p0111 N78-21601
- ALLAN, R. B.**
Advanced supersonic propulsion study, phases 3 and 4 (NASA-CN-135736) p0027 N78-13058
- ALLAN, R., JR.**
The NISE project: Minority Involvement in NASA Engineering (NASA-TN-73811) p0176 N78-13938
- ALLEN, J. L.**
Preliminary study of propulsion systems and airplane wing parameters for a US Navy subsonic V/STOL aircraft (NASA-TN-73852) p0010 N78-17081
- ALTSHOVITZ, S. A.**
Critical currents in sputtered PbMo6S8 p0175 N78-85368
Critical currents and scaling laws in sputtered copper molybdenum sulfide p0175 N78-85500
Upper critical field of copper molybdenum sulfide p0175 N78-53626
- ALVERN, S.**
Computation of unsteady transonic flow through rotating and stationary cascades. 2: User's guide to POSTSAR program W2DAT (NASA-CR-2901) p0007 N78-12038
Computation of unsteady transonic flow through rotating and stationary cascades. 1: Method of analysis (NASA-CR-2900) p0008 N78-20082
- ANASTASIOU, S.**
Real-time and accelerated outdoor endurance testing of solar cells p0142 N78-52837
Real-time and accelerated outdoor endurance testing of solar cells (NASA-TN-73783) p0130 N78-14628
Method of making encapsulated solar cell modules (NASA-CASR-LEW-12185-1) p0136 N78-25528
Endurance testing of first generation (Block 1) commercial solar cell modules (NASA-TN-78922) p0138 N78-26548
- ANDERSON, D. E.**
Emissions control for ground power gas turbines p0013 N78-11072
Performance and emissions of a catalytic reactor with propane, diesel, and Jet A fuels (NASA-TN-73786) p0088 N78-14177
Catalytic combustion for the automotive gas turbine engine p0092 N78-30333
Effect of inlet temperature on the performance of a catalytic reactor (NASA-TN-78977) p0181 N78-31534
- ANDERSON, D. E.**
Long-term hot-hardness characteristics of five through-hardened bearing steels (NASA-TN-1381) p0073 N78-32196

- ANDERSON, O. L.**
Derivation and evaluation of an approximate analysis for three-dimensional viscous subsonic flow with large secondary velocities [NASA-CR-159430] p0008 W78-33044
- ANDERSON, W. D.**
Experimental data and theoretical analysis of an operating 100 kW wind turbine [NASA-TN-73883] p0133 W78-19442
- ANDERSON, W. J.**
Bearing, gearing, and lubrication technology [SAE PAPER 780077] p0120 W78-33366
Bearing, gearing, and lubrication technology [NASA-TN-73851] p0118 W78-17389
The practical impact of elastohydrodynamic lubrication [NASA-TN-78987] p0117 W78-33445
- ANDREWS, D. E.**
Analytical study of thermal barrier coated first-stage blades in an F100 engine [NASA-CR-135359] p0028 W78-17058
- ANDREWS, C. W.**
Volume fraction determination in cast superalloys and directionally solidified eutectic alloys by a new manual point count practice p0089 W78-24369
- ANGLIN, A. E.**
Cleaning process for contaminated superalloy powders p0076 W78-41400
- ANTOINE, A. C.**
Hydrocarbon group type determination in jet fuels by high performance liquid chromatography p0089 W78-24906
Jet fuels from synthetic crudes p0090 W78-43415
Alternative fuels p0013 W78-11074
Hydrocarbon group type determination in jet fuels by high performance liquid chromatography [NASA-TN-73829] p0088 W78-13233
- ARIAS, A.**
Pressureless sintered Sialons with low amounts of sintering aid [NASA-TP-1246] p0082 W78-25215
- ASHBROOK, E. L.**
Directionally solidified ceramic eutectics p0084 W78-11547
Improved performance of silicon nitride-based high temperature ceramics p0087 W78-24881
Improved performance of silicon nitride-based high temperature ceramics [NASA-TN-73719] p0080 W78-10294
- AULT, G. E.**
Progress in advanced high temperature turbine materials, coatings, and technology p0056 W78-24910
Progress in advanced high temperature turbine materials, coatings, and technology p0018 W78-21122
- AYDENO, J. C.**
Effect of vibration on retention characteristics of screen acquisition systems [AIAA PAPER 78-1030] p0045 W78-43560
- B**
- BACHLE, C. F.**
Lightweight, low compression aircraft diesel engine [NASA-CR-135300] p0121 W78-21471
- BADNER, E. P.**
Tissue macerating instrument [NASA-CASE-LEW-12668-1] p0153 W78-14773
Flow compensating pressure regulator [NASA-CASE-LEW-12718-1] p0104 W78-25351
- BAGWELL, J. W.**
An airborne meteorological data collection system using satellite relay (A²DAR) [NASA-TN-78992] p0093 W78-33283
- BAIR, D. W.**
Augmentor emissions reduction technology program [NASA-CR-135215] p0027 W78-13057
Aircraft gas turbine low-power emissions reduction technology program [NASA-CR-135434] p0032 W78-32097
- BAILEY, P. G.**
Manufacture and engine test of advanced oxide dispersion strengthened alloy turbine vanes [NASA-CR-135269] p0077 W78-11232
- BAILY, P. E.**
Closed cycle electric discharge laser design investigation [NASA-CR-135408] p0112 W78-25407
- BAIR, V. L.**
Some properties of low-vapor-pressure braze alloys for thermionic converters [NASA-TN-78867] p0134 W78-22471
Dinialoxide thermionic energy conversion with lanthanum-hexaboride electrodes [NASA-TN-78887] p0135 W78-24617
- BAKER, C. E.**
Status of the DOE (STOR)-sponsored national program on hydrogen production from water via thermochemical cycles p0142 W78-29331
Status of the DOE (STOR)-sponsored national program on hydrogen production from water via thermochemical cycles [NASA-TN-78825] p0132 W78-17469
- BALONOV, J. E.**
Variation of fan tone steadiness for several inflow conditions [AIAA PAPER 78-1119] p0166 W78-41829
Variation of fan tone steadiness for several inflow conditions [NASA-TN-78886] p0164 W78-26878
- BANDSCHNEIDER, E. E.**
Effect of wall thickness and material on flexural fatigue of hollow rolling elements [ASME PAPER 77-LUB-14] p0126 W78-23355
- BANKS, B. A.**
Evolution of the 1-slb mercury ion thruster subsystem [AIAA PAPER 78-711B] p0051 W78-32776
Ion beam sputter etching and deposition of fluoropolymers p0085 W78-37684
Evolution of the 1-slb mercury ion thruster subsystem [NASA-TN-73733] p0047 W78-21202
Ion beam sputter etching and deposition of fluoropolymers [NASA-TN-78888] p0088 W78-24354
- BARACK, W. E.**
Redundant disc [NASA-CASE-LEW-12496-1] p0022 W78-33101
- BARANOV, C. E.**
Analysis of epitaxial drift field on P silicon solar cells p0141 W78-10904
Status of wraparound contact solar cells and arrays [NASA-TN-78911] p0137 W78-26543
Preliminary evaluation of Glass Resin materials for solar cell cover use [NASA-TN-78925] p0137 W78-26544
- BARBER, J. E.**
Comparison of reusable insulation systems for cryogenically-tanked earth-based space vehicles [AIAA PAPER 78-877] p0044 W78-36004
Comparison of reusable insulation systems for cryogenically-tanked earth-based space vehicles [NASA-TN-73668] p0041 W78-21190
- BARBUS, S. P.**
Carrier-interference ratios for frequency sharing between frequency-modulated amplitude-modulated-vestigial-sideband television systems [NASA-TP-1264] p0043 W78-28159
- BARRANGER, J. P.**
Application of a flight-line disk crack detector to a small engine p0012 W78-10088
In-place recalibration technique applied to a capacitance-type system for measuring rotor blade tip clearance [NASA-TP-1110] p0019 W78-22101
- BARRETT, C. A.**
The cyclic oxidation resistance of cobalt chromium-aluminum alloys at 1100 and 1200 C and a comparison with the nickel-chromium-aluminum alloy system p0077 W78-50086
Substitution for chromium in 304 stainless steel p0077 W78-51714
10,000-hour cyclic oxidation behavior at 815 C /1500 F/ of 33 high-temperature alloys p0077 W78-51716

- BARBOUR, R. G.**
A Weibull characterization for tensile fracture of multicomponent brittle fibers p0060 A78-24892
- BARTO, C. F.**
Cost analysis of advanced turbine blade manufacturing processor [NASA-CR-135203] p0026 W78-10092
- BARTLEY, R. G.**
Active control of spacecraft charging on ATS-5 and ATS-6 p0036 W78-10136
- BAUGHNSTER, E. J.**
Effect of ice contamination on liquid-nitrogen drops in film boiling p0105 A78-15821
Thermally driven oscillations and wave motion of a liquid drop p0106 A78-17506
Numerical spatial marching techniques for estimating duct attenuation and source pressure profiles p0166 A78-37682
Numerical spatial marching techniques for estimating duct attenuation and source pressure profiles [NASA-TN-78057] p0103 W78-22329
Interaction of a turbulent-jet noise source with transverse modes in a rectangular duct [NASA-TN-1248] p0001 W78-25049
- BAUGHNSTER, R. R.**
Improved reaction sintered silicon nitride [NASA-CR-135291] p0063 W78-22164
- BEATTIE, J. R.**
Extended-performance thruster technology evaluation [AIAA PAPER 78-666] p0055 A78-37436
Extended performance solar electric propulsion thrust system study. Volume 4: Thruster technology evaluation [NASA-CR-135281-VOL-4] p0053 W78-16090
- BECHTEL, R.**
A mission profile life test facility [AIAA PAPER 78-671] p0040 A78-37431
- BECHTEL, R. T.**
Extended-performance thruster technology evaluation [AIAA PAPER 78-666] p0055 A78-37436
- BERKMAN, S. W.**
Redundant disc [NASA-CASE-LEW-12496-1] p0022 W78-33101
- BERRENDT, D. R.**
Axial residual stresses in boron fibers [NASA-TN-73894] p0058 W78-19204
- BENSON, G. C.**
Extended performance solar electric propulsion thrust system study. Volume 4: Thruster technology evaluation [NASA-CR-135281-VOL-4] p0053 W78-16090
- BERRENDT, D. G.**
Direct heating surface combustor [NASA-CASE-LEW-11877-1] p0097 W78-27357
- BERROPEC, F. D.**
Investigation of high voltage spacecraft system interactions with plasma environments [AIAA PAPER 78-672] p0050 A78-32750
Interaction of large, high power systems with operational orbit charged particle environments [AAS 77-243] p0044 A78-36719
The Lewis Research Center geomagnetic substorm simulation facility p0036 W78-10155
Testing of typical spacecraft materials in a simulated substorm environment p0036 W78-10156
Development of environmental charging effect monitors for operational satellites p0037 W78-10174
Interaction of large, high power systems with operational orbit charged particle environments [NASA-TN-73867] p0037 W78-16076
Investigation of high voltage spacecraft system interactions with plasma environments [NASA-TN-78831] p0097 W78-21373
Liquid metal slip ring [NASA-CASE-LEW-12277-2] p0097 W78-25323
Status of the NASA-Lewis Research Center spacecraft charging investigation [NASA-TN-78938] p0049 W78-27170
- BRUSHAN, B.**
Hydrodynamic air lubricated compliant surface bearing for an automotive gas turbine engine. 2: Materials and coatings [NASA-CR-135402] p0122 W78-29449
- BIRCHBOUGH, A. G.**
Airflow and thrust calibration of an F100 engine, S/W W80099, at selected flight conditions [NASA-TN-1069] p0018 W78-21112
Altitude calibration of an F100, S/W W80095, turbofan engine [NASA-TN-1228] p0019 W78-23095
- BISS, J. J.**
Electrical Prototype Power Processor for the 30-cm Mercury electric propulsion engine [AIAA PAPER 78-684] p0055 A78-37439
Electric prototype power processor for a 30cm ion thruster [NASA-CR-135287] p0054 W78-19200
Extended performance electric propulsion power processor design study. Volume 1: Executive summary [NASA-CR-135357] p0054 W78-20250
- BIPARO, W. J.**
Photovoltaic refrigeration application: Assessment of the near-term market [NASA-TN-73876] p0131 W78-16435
Photovoltaic highway applications: Assessment of the near-term market [NASA-TN-73863] p0178 W78-17935
Photovoltaic village power application: Assessment of the near-term market [NASA-TN-73893] p0133 W78-19643
Photovoltaic water pumping applications: Assessment of the near-term market [NASA-TN-78847] p0134 W78-19644
Photovoltaic remote instrument applications: Assessment of the near-term market [NASA-TN-73881] p0150 W78-19710
Design and fabrication of a photovoltaic power system for the Papago Indian village of Schuchuli (Gunsight), Arizona [NASA-TN-78548] p0139 W78-26555
- BILL, R. C.**
Temperature distributions and thermal stresses in a graded zirconia/metal gas path seal system for aircraft gas turbine engines [AIAA PAPER 78-93] p0118 A78-20683
Friction and wear of sintered fibrous sintered seal materials p0074 A78-23851
Temperature distributions and thermal stresses in a graded zirconia/metal gas path seal system for aircraft gas turbine engines [NASA-TN-73818] p0015 W78-15044
Friction and wear of several compressor gas-path seal movements [NASA-TN-1128] p0068 W78-15229
Preliminary study of cyclic thermal shock resistance of plasma-sprayed zirconium oxide turbine outer air seal shrouds [NASA-TN-73852] p 780 W78-15280
Influence of fretting on flexural fatigue of 304 stainless steel and mild steel [NASA-TN-1193] p0070 W78-21269
Friction and wear of carbon-graphite materials for high-energy brakes [NASA-TN-78904] p0056 W78-26178
Rub tolerance evaluation of two sintered NiCrAl gas path seal materials [NASA-TN-78967] p0071 W78-29215
Gas path seal [NASA-CASE-LEW-12131-2] p0021 W78-31103
- BILLINGS, W. F.**
Solid State Remote Power Controllers for high voltage DC distribution systems p0100 A78-15574
- BIRCHBOUGH, A. G.**
Instrument to average 100 data sets [NASA-TN-1055] p0096 W78-11301
A sustained-arc ignition system for internal combustion engines [NASA-TN-73833] p0096 W78-13331
Design and fabrication of a low-specific-weight parabolic dish solar concentrator [NASA-TN-1152] p0046 W78-17145
Baseline tests of the EPC Hummingbird electric passenger vehicle [NASA-TN-73760] p0180 W78-21010
Design and operating experience on the OS Department of Energy experimental Mod-0 100-kW

wind turbine
[NASA-TN-78915] p0138 N78-26552

RITTER, D. A.
Effect of trichlorofluoromethane and molecular chlorine on ozone formation by simulated solar radiation
[NASA-TP-1093] p0064 N78-12167
Effect of nitric oxide on photochemical ozone formation in mixtures of air with molecular chlorine and with trichlorofluoromethane
[NASA-TP-1192] p0065 N78-20201

RISCH, P. T.
Experimental determination of transient strain in a thermally-cycled simulated turbine blade utilizing a non-contact technique
[NASA-TN-73886] p0017 N78-19161

BLACK, D. E.
Aerodynamic design and performance testing of an advanced 30 deg swept, eight bladed propeller at Mach numbers from 0.2 to 0.85
[NASA-CR-3067] p0008 N78-32066

BLANK, R. J.
Performance and stability analysis of a photovoltaic power system
[NASA-TN-78880] p0140 N78-29566

BLANK, D. E.
Cost analysis of advanced turbine blade manufacturing processes
[NASA-CR-135203] p0026 N78-10092

BLANKENSHIP, C. V.
Tantalum modified ferritic iron base alloys
[NASA-CASE-LEW-12095-1] p0069 N78-18102
Advanced materials research for long-haul aircraft turbine engines
p0001 N78-27057

BLANKENSHIP, G. L.
Effect of forward motion on engine noise
[NASA-CR-136954] p0026 N78-10093

BLATT, H. W.
Filling of orbital fluid management systems
[NASA-CR-159404] p0108 N78-31380

BLICK, R. A.
Testing of typical spacecraft materials in a simulated subsonic environment
p0036 N78-10156
Small-signal gain diagnostic measurements in a flowing CO₂ pin discharge laser
[NASA-TN-73843] p0111 N78-13421

BLOOMFIELD, R. S.
In-situ laser retorting of oil shale
[NASA-CASE-LEW-12217-1] p0129 N78-18452
Technical and economic feasibility study of solar/fossil hybrid power systems
[NASA-TN-73820] p0132 N78-17486

BLUB, J. W.
Considerations to achieve directionality for gamma ray lasers
p0116 N78-26870
Targets for producing high purity I-123
[NASA-CASE-LEW-10518-3] p0065 N78-27226

BOLDMAN, D.
Preliminary study of the effect of the turbulent flow field around complex surfaces on their acoustic characteristics
[NASA PAPER 78-1123] p0166 N78-45129
Preliminary study of the effect of the turbulent flow field around complex surfaces on their acoustic characteristics
[NASA-TN-78944] p0164 N78-28896

BOLES, W. A.
Theoretical flow characteristics of inlets for tilting-nacelle VTOL aircraft
[NASA-TP-1205] p0018 N78-21110

BOBKOWSKI, J.
Cloud effects on middle ultraviolet global radiation
p0150 N78-32952

BOHNSTEIN, B. S.
The effect of NaCl/g on the Na₂SO₄-induced hot corrosion of NiAl
p0079 N78-24901
Study of the effects of gaseous environments on sulfidation attack of superalloys
[NASA-CR-135348] p0079 N78-21268

BOTTRELL, W. S.
Lightweight, low compression aircraft diesel engine
[NASA-CR-115300] p0121 N78-21471

BOYDEN, J. E.
Impact resistant boron/aluminum composites for large fan blades
[NASA-CR-135274] p0062 N78-14099

BOYLES, E. J.
Use of an ultrasonic-acoustic technique for nondestructive evaluation of fiber composite strength
[NASA-TN-73813] p0124 N78-17397
Impact behavior of filament wound graphite/epoxy fan blades
[NASA-TN-78845] p0018 N78-22097

BOYD, C. E.
A data acquisition and handling system for the measurement of radial plasma transport rates
[NASA-TN-78849] p0155 N78-23751

BOYER, E. O.
An improved technique for the calibration of solar cells using a high altitude aircraft
[NASA-TN-78871] p0138 N78-26546

BOYLE, R. J.
Evaluation of initial collector field performance at the Langley Solar Building Test Facility
p0141 N78-11391

BOSEK, J. E.
Baseline tests of the power-train electric delivery van
[NASA-TN-73765] p0178 N78-17936
Baseline tests of the EVA change-of-pace coupe electric passenger vehicle
[NASA-TN-73763] p0178 N78-17938
Baseline tests of the EVA contractor electric passenger vehicle
[NASA-TN-73762] p0179 N78-17939
Baseline tests of the batronic Minivan electric delivery van
[NASA-TN-73761] p0179 N78-17940
Baseline tests of the Volkswagen transporter electric delivery van
[NASA-TN-73766] p0179 N78-20021
Baseline tests of the Kordest hybrid passenger vehicle
[NASA-TN-73769] p0138 N78-26551

BRADBS, T.
Catalytic decomposition of methanol for onboard hydrogen generation
[NASA-TP-1247] p0083 N78-25236

BRADSHAW, S. D.
Conceptual design for spacelab two-phase flow experiments
[NASA-CR-135327] p0037 N78-14063

BRAGINSKI, A. I.
Superconducting Nb₃Ge for high-field magnets
p0175 N78-41922
Niobium-germanium superconducting tapes for high-field magnet applications
[NASA-CR-135324] p0099 N78-19392

BRAIBAND, W. A.
Composition of RF-sputtered refractory compounds determined by I-ray photoelectron spectroscopy
p0085 N78-30301
I-ray photoelectron spectroscopy study of radiofrequency-sputtered refractory compound steel interfaces
[NASA-TP-1161] p0081 N78-20336
Friction and wear of radiofrequency-sputtered borides, silicides, and carbides
[NASA-TP-1156] p0081 N78-20338
The friction and wear properties of sputtered hard refractory compounds
[NASA-TN-78895] p0056 N78-26177

BRALEY, E. C.
Disaster warning system study summary
[NASA-TN-73797] p0093 N78-10346

BRANDENBURG, R. A.
Analysis and design of a high power laser adaptive phased array transmitter
[NASA-CR-134952] p0111 N78-13420

BRANDHORST, S. W., JR.
A methodology for experimentally-based determination of gap shrinkage and effective lifetimes in the emitter and base of p-n-junction solar cells
p0141 N78-10903
Analysis of epitaxial drift field on P silicon solar cells
p0141 N78-10904
Status of the BRDA/NASA Photovoltaic Tests and Applications Project
p0141 N78-11014
U.S. terrestrial solar cell calibration and measurement procedures

PERSONAL AUTHOR INDEX

BURNS, R. E.

- Summary of the NASA space photovoltaic research and technology program p0143 A78-52044
- US terrestrial solar cell calibration and measurement procedures [NASA-TN-73768] p0130 W78-13528
- Photon degradation effects in terrestrial solar cells [NASA-TN-78924] p0136 W78-25551
- BRAUER, E. J.
A visual investigation of turbulence in stagnation flow about a circular cylinder [NASA-CR-3019] p0108 W78-33386
- BRAWN, W.
Unsteady flow in a supersonic cascade with strong in-passage shocks p0006 A78-17270
- BRAUSCH, J. F.
Acoustic tests of duct-burning turbofan jet noise simulation [NASA-CR-2966] p0002 W78-28043
- Acoustic tests of duct-burning turbofan jet noise simulation: Comprehensive data report. Volume 1, section 2: Full size data [NASA-CR-135239-VOL-1-SECT-2] p0030 W78-28095
- Acoustic tests of duct-burning turbofan jet noise simulation: Comprehensive data report. Volume 1, section 3: Data plots [NASA-CR-135239-VOL-1-SECT-3] p0030 W78-28096
- Acoustic tests of duct-burning turbofan jet noise simulation: Comprehensive data report. Volume 2: Model design and aerodynamic test results [NASA-CR-135239-VOL-2] p0031 W78-28097
- BRENNAN, J. J.
Development of S13H4 and SIC of improved toughness [NASA-CR-135306] p0087 W78-17216
- BRENN, D. E.
Simplified solution for elliptical-contact deformation between two elastic solids p0118 A78-12737
- Simplified contact analysis p0127 A78-28200
- Effect of geometry on hydrodynamic film thickness [NASA-TP-1287] p0117 W78-30585
- BRISSEL, D.
Description and review of global measurements of atmospheric species from GASP p0148 W78-24893
- BRISSEL, D. C.
Ultraviolet spectrophotometer for measuring columnar atmospheric ozone from aircraft p0110 A78-35826
- BRISL, D.
Simultaneous measurements of ozone outside and inside cabins of two B-747 airliners and a Gates Learjet business jet [NASA-TN-78983] p0009 W78-31061
- BRILEY, W. B.
Derivation and evaluation of an approximate analysis for three-dimensional viscous subsonic flow with large secondary velocities [NASA-CR-159430] p0008 W78-33044
- BRODER, J. D.
Photon degradation effects in terrestrial solar cells [NASA-TN-78924] p0136 W78-25551
- Ultraviolet irradiation at elevated temperatures and thermal cycling in vacuum of PEP-A covered silicon solar cells [NASA-TN-78926] p0137 W78-26545
- BROWN, G. V.
Design and prototype fabrication of a 30 tesla cryogenic magnet p0097 A78-15823
- Magnetic heat pumping [NASA-CASE-LEW-12508-1] p0102 W78-17335
- BROWN, R. B.
Variable mixer propulsion cycle [NASA-CASE-LEW-12917-1] p0016 W78-18067
- BROWN, V. C.
Design, fabrication and testing of a CPA for use in the solar power satellite [NASA-CR-159410] p0042 W78-31143
- BROWNELL, D. W., JR.
A three dimensional dynamic study of electrostatic charging in materials [NASA-CR-135256] p0099 W78-13328
- BUCCH, T. W.
Pollution Reduction Technology Program for small jet aircraft engines, phase 2 [NASA-CR-159415] p0032 W78-33108
- BUCKLE, R. E.
Computer program for calculation of a gas temperature profile by infrared emission: Absorption spectroscopy [NASA-TN-73848] p0015 W78-15043
- BUCK, E.
Up-date of traveling wave tube improvements p0098 A78-33208
- Up-date of traveling wave tube improvements [NASA-TN-78852] p0096 W78-19397
- BUCKLEY, D. E.
The use of analytical surface tools in the fundamental study of wear p0119 A78-23428
- Friction, deformation and fracture of single-crystal silicon carbide [ASLE PREPRINT 77-LE-5C-3] p0085 A78-28438
- Tribological properties of surfaces p0120 A78-33211
- Friction and wear behavior of single-crystal silicon carbide in sliding contact with various metals p0086 A78-44095
- Definition and effect of chemical properties of surfaces in friction, wear, and lubrication p0121 A78-45436
- Friction and wear of single-crystal and polycrystalline sapphire-zinc ferrite in contact with various metals [NASA-TP-1059] p0080 W78-10295
- Effectiveness of various organometallics as antiwear additives in mineral oil [NASA-TP-1096] p0080 W78-12222
- Friction and wear of polyethylene oxide polymer having a range of molecular weights [NASA-TP-1129] p0080 W78-15278
- Definition and effect of chemical properties of surfaces in friction, wear, and lubrication [NASA-TN-73806] p0065 W78-19237
- Friction and wear behavior of single-crystal silicon carbide in sliding contact with various metals [NASA-TN-73782] p0118 W78-19512
- Tribological properties of surfaces [NASA-TN-73896] p0118 W78-20511
- Friction and metal transfer for single-crystal silicon carbide in contact with various metals in vacuum [NASA-TP-1191] p0082 W78-21294
- Wear of single-crystal silicon carbide in contact with various metals in vacuum [NASA-TP-1198] p0082 W78-21295
- Role of alloying elements in adhesive transfer and friction of copper-base alloys [NASA-TP-1256] p0071 W78-26198
- Effect of oxygen and nitrogen interactions on friction of single-crystal silicon carbide [NASA-TP-1265] p0083 W78-28247
- Effect of oxygen, methyl mercaptan, and methyl chloride on friction behavior of copper-iron contacts [NASA-TP-1309] p0072 W78-30206
- Friction and wear of metals with a single-crystal abrasive grit of silicon carbide: Effect of shear strength of metal [NASA-TP-1293] p0084 W78-30238
- BURHO, D. F.
Transient dynamics of a flexible rotor with squeeze film dampers [NASA-CR-3050] p0123 W78-32433
- BURCHAN, R. E.
Liquid rocket engine turbopump rotating-shaft seals [NASA-SP-8121] p0117 W78-30584
- BURKHART, J. A.
Potential damage to dc superconducting magnets due to high frequency electromagnetic waves p0098 A78-39902
- BURBETT, J. E.
Tissue necrating instrument [NASA-CASE-LEW-12666-1] p0153 W78-14773
- BURNS, R. E.
Performance potential of combined cycles integrated with low-Btu gasifiers for future electric utility applications [NASA-TN-73775] p0135 W78-23557

- BURNHUGH, J. D.
 A simulation model for wind energy storage systems. Volume 2: Operation manual [NASA-CR-135284] p0157 W78-20803
 A simulation model for wind energy storage systems. Volume 3: Program descriptions [NASA-CR-135285] p0157 W78-20804
- BUTTS, H. P.
 Alternative fuels p0013 W78-11074
 Effect of fuel properties on performance of single aircraft turbojet combustor at simulated idle, cruise, and takeoff conditions [NASA-TN-73780] p0014 W78-13056
- BUSSARD, R. J.
 Load-displacement measurement and work determination in three-point bend tests of notched or precracked specimens p0089 A78-24370
- BYRNE, D. C.
 A review of electron bombardment thruster systems/spacecraft field and particle interfaces [AIAA PAPER 78-677] p0051 A78-32754
 A review of electron bombardment thruster systems/spacecraft field and particle interfaces [NASA-TN-78850] p0048 W78-21206
- C**
- CABILL, T. P.
 Wind turbine generator rotor blade concepts with low cost potential [NASA-TN-73835] p0131 W78-17466
- CAIVELLI, J. E.
 Initial test results with single cylinder rhombic drive Stirling engine p0117 W78-30716
 Initial test results with a single-cylinder rhombic-drive Stirling engine [NASA-TN-78919] p0140 W78-31533
- CARR, J. E.
 Extended performance solar electric propulsion thrust system design [AIAA PAPER 78-643] p0055 A78-37430
- CALVO, F. D.
 Experimental determination of transient strain in a thermally-cycled simulated turbine blade utilizing a non-contact technique [NASA-TN-73886] p0017 W78-19161
- CALOGERAS, J. E.
 Technical and economic feasibility study of solar/fossil hybrid power systems [NASA-TN-73820] p0132 W78-17486
 Storage systems for solar thermal power [NASA-TN-78952] p0140 W78-29577
- CAMPBELL, J.
 Hydrogen turbine power conversion system assessment [NASA-CR-135298] p0144 W78-20621
- CAMPBELL, R. G.
 Advanced space engine powerhead breadboard assembly system study [NASA-CR-135232] p0054 W78-25127
- CASH, B.
 Marshall Space Flight Center development program for solar heating and cooling systems p0110 A78-11368
- CAVALDO, E. L.
 Response of lead-acid batteries to chopper-controlled discharge: Preliminary results [NASA-TN-73838] p0180 W78-20023
 Response of lead-acid batteries to chopper-controlled discharge [NASA-TN-73838-B2V] p0180 W78-25010
- CAVANO, P. J.
 Fiber reinforced FRB polyimide composites [NASA-CR-135377] p0063 W78-25132
- CHAI, A. T.
 Some basic considerations of measurements involving collimated direct sunlight [NASA-TN-74947] p0130 W78-13608
- CHAI, A.-T.
 Cloud effects on middle ultraviolet global radiation p0150 A78-42952
- CHANNY, A. J.
 QCSEE task 2: Engine and installation preliminary design [NASA-CR-134738] p0030 W78-23089
- CHARRIS, C. C.
 An integrated theory for predicting the hydrothermomechanical response of advanced composite structural components p0060 A78-24905
 Residual stresses in angleplied laminates and their effects on laminate behavior p0060 A78-33201
 In situ ply strengths - An initial assessment p0061 A78-33223
 Fracture surface characteristics of off-axis composites p0067 A78-40171
 Impact of composite mechanics on test methods for fiber composites p0062 A78-50325
 FASTRAN use for cyclic response and fatigue analysis of wind turbine towers p0125 W78-12459
 Fracture surface characteristics of off-axis composites [NASA-TN-73700] p0057 W78-13137
 Mechanical behavior and fracture characteristics of off-axis fiber composites. 1: Experimental investigation [NASA-TN-1081] p0057 W78-13138
 An integrated theory for predicting the hydrothermomechanical response of advanced composite structural components [NASA-TN-73812] p0125 W78-13477
 Mechanical behavior and fracture characteristics of off-axis fiber composites. 2: Theory and comparisons [NASA-TN-1082] p0057 W78-16098
 The effects of eccentricities on the fracture of off-axis fiber composites [NASA-TN-73826] p0057 W78-17153
 Residual stresses in angleplied laminates and their effects on laminate behavior [NASA-TN-78835] p0058 W78-19206
 In situ ply strength: An initial assessment [NASA-TN-73771] p0059 W78-21220
 Titanium/beryllium laminates: Fabrication, mechanical properties, and potential aerospace applications [NASA-TN-73891] p0059 W78-21221
 Effects of moisture profiles and laminate configuration on the hygro stresses in advanced composites [NASA-TN-78978] p0059 W78-32191
 Impact of composite mechanics on test methods for fiber composites [NASA-TN-78979] p0126 W78-32464
 Analysis/design of strip reinforced random composites (strip hybrids) [NASA-TN-78985] p0059 W78-33149
- CHAN, Y. K.
 A simulation model for wind energy storage systems. Volume 1: Technical report [NASA-CR-135283] p0156 W78-20802
- CHAPMAN, G. B., II
 Development of a drift-correction procedure for a photoelectric spectrometer p0109 A78-23525
- CHAPMAN, P. E.
 Laser absorption phenomena in flowing gas devices [NASA-CR-135129] p0112 W78-18411
- CHAUSSE, D. S.
 Perturbation solutions for blade-to-blade surfaces of a transonic compressor p0008 A78-12307
 Perturbation solutions for transonic flow on the blade-to-blade surface of compressor blade rows [NASA-CR-2941] p0001 W78-15987
- CHENIELEWSKI, C. E.
 Effect of ice contamination on liquid-nitrogen drops in film boiling p0105 A78-15821
- CHOW, D. C.
 Methods for calculating the transonic boundary layer separation for V/STOL inlets at high incidence angles [AIAA 78-1340] p0007 A78-46537
- CISPLUCH, C. C.
 Preliminary QCSEE program - Test results [SAE PAPER 771008] p0023 A78-23840
 Preliminary QCSEE program test results [NASA-TN-73732] p0015 W78-15042
 Overview of the QCSEE program p0004 W78-24066

PERSONAL AUTHOR INDEX

CURRAN, A. E.

- CLARK, B. J.
Flight-effects on predicted fan fly-by noise
[NASA-TN-73798] p0018 W78-13060
- CLARK, J. S.
Thermal barrier coatings
[NASA-TN-78048] p0059 W78-24291
- CLARK, T. A.
Y100(3) parallel compressor computer code and user's manual
[NASA-CR-135388] p0029 W78-22096
- COB, B. B.
Predicted and experimental performance of jet-lubricated 120-millimeter-bore ball bearings operating to 2.5 million DN
[NASA-TP-1196] p0114 W78-20513
- COFFINBERY, G. A.
Oil cooling system for a gas turbine engine
[NASA-CASE-LW-12321-1] p0113 W78-10467
- COLE, A.
Ion beam plume and efflux characterization flight experiment study
[NASA-CR-135275] p0052 W78-12140
- COLE, G. L.
Atmospheric effects on inlets for supersonic cruise aircraft
[NASA-TN-X-73647] p0003 W78-10026
Mechanical characteristics of stability-bleed valves for a supersonic inlet
[NASA-TN-X-3483] p0015 W78-13063
Normal shock and restart controls for a supersonic airbreathing propulsion system
p0019 W78-23023
Investigation of means for perturbing the flow field in a supersonic wind tunnel
[NASA-TN-78954] p0037 W78-27142
Wind tunnel evaluation of YF-12 inlet response to internal airflow disturbances with and without control
p0006 W78-32062
- COLLADAY, B. S.
Design approaches to more energy efficient engines
[AIAA PAPER 78-931] p0025 A78-43504
Computer program for obtaining thermodynamic and transport properties of air and products of combustion of ASTM-A-1 fuel and air
[NASA-TP-1160] p0088 W78-20351
Design approaches to more energy efficient engines
[NASA-TN-78893] p0115 W78-26442
- COLLETT, C. B.
Engineering Model 8-cs Thruster System
[AIAA PAPER 78-646] p0055 A78-37434
- COLLEY, W. C.
Augmentor emissions reduction technology program
[NASA-CR-135215] p0027 W78-13057
- COBBY, D. B.
Cost/benefit analysis of advanced material technologies for small aircraft turbine engines
[NASA-CR-135265] p0027 W78-12083
- COBBOLLY, D. J.
Use of a simple external nonreciprocal attenuator in coupled-cavity TWT's
p0096 A78-18282
- CONRAD, E. W.
NASA engine system technology programs - An overview
[AIAA PAPER 78-928] p0025 A78-48452
- CONRAD, R.
The effect of minor additions of titanium on the fracture toughness of Fe-12Ni alloys at 77K
[NASA-CR-135351] p0078 W78-19259
- COOK, J. A.
Ceramic regenerator systems development program
[NASA-CR-135330] p0181 W78-25988
Ceramic regenerator systems development program
[NASA-CR-135430] p0181 W78-26997
- COOPER, D. B.
Method of forming metal hydride films
[NASA-CASE-LW-12051-1] p0113 W78-13436
- COOPER, L. P.
Supercritical fuel injection system
[NASA-CASE-LW-12990-1] p0020 W78-27122
- COLEBY, R. C.
Failure detection and correction for turbofan engines
p0033 A78-23918
- CORRAN, J. C.
Open-Cycle Gas Turbine/Steam Turbine Combined Cycles with synthetic fuels from coal
[ASME PAPER 77-WA/ENER-9] p0146 A78-33147
- Performance and economics of advanced energy conversion systems for coal and coal-derived fuels
p0146 A78-34078
- CORNWELL, B. B.
Dynamic tooth loads and stressing for high contact ratio spur gears
[ASME PAPER 77-DET-101] p0123 A78-20606
- CORWIN, J. S.
Characterization, shaping, and joining of SiC/superalloy sheet for exhaust system components
[NASA-CR-135301] p0062 W78-13134
- COSMOVIE, B. V.
Effect of air temperature and relative humidity at various fuel-air ratios on exhaust emissions on a per-node basis of an AVCO Lycoming O-320 diad light aircraft engine: Volume 1: Results and plotted data
[NASA-TN-73507-VOL-1] p0021 W78-29100
- COX, B. B.
Aerodynamic performance of conventional and advanced design labyrinth seals with solid-smooth abrasible, and honeycomb lands
[NASA-CR-135307] p0122 W78-27427
- COY, J. J.
Experimental and analytical load-life relation for AISI 9310 steel spur gears
[ASME PAPER 77-DET-121] p0118 A78-20609
Statistical model for asperity-contact time fraction in elastohydrodynamic lubrication
[NASA-TP-1130] p0114 W78-18429
- CRABBALL, K. S.
Ion beam sputter etching and deposition of fluoropolymers
p0085 A78-37684
Ion beam sputter etching and deposition of fluoropolymers
[NASA-TN-78888] p0088 W78-24358
- CROFT, W. J.
Materials technology assessment for stirling engines
[NASA-TN-73739] p0069 W78-17187
- CUK, S. B.
Modelling, analyses and design of switching converters
[NASA-CR-135174] p0100 W78-29351
- CULL, R. C.
DOE LeRC photovoltaic systems test facility
[NASA-TN-78923] p0138 W78-26549
- CULLOH, B. B.
Altitude test of several afterburner configurations on a turbofan engine with a hydrogen heater to simulate an elevated turbine discharge temperature
[NASA-TP-1066] p0014 W78-11106
- CULP, D. B.
The Plasma Interaction Experiment (PIX) - Description and flight qualification test program
[AIAA PAPER 78-678] p0051 A78-32752
The Plasma Interaction Experiment (PIX) description and test program
[NASA-TN-78863] p0041 W78-21188
Liquid metal slip ring
[NASA-CASE-LW-12277-2] p0097 W78-25323
- CURRAN, A. E.
Design and performance of a 427-meter-per-second-tip-speed two-stage fan having a 2.40 pressure ratio
[NASA-TP-1314] p0022 W78-33109
- CUNNINGHAM, B. E.
Steady-state unbalance response of a three-disk flexible rotor on flexible, damped supports
p0119 A78-29326
Influence of oil-squeeze-film damping on steady-state response of flexible rotor operating to supercritical speeds
[NASA-TP-1094] p0015 W78-13064
- CUNNINGTON, G. B.
Evacuated load-bearing high performance insulation study
[NASA-CR-135342] p0092 W78-18251
- CUNNINGTON, G. B., JR.
An ultralightweight, evacuated, load-bearing, high-performance insulation system
[AIAA PAPER 78-878] p0045 A78-36005
- CURRAN, A. E.
Thermal characteristics of the 12-gigahertz, 200-watt output stage tube for the communications technology satellite
[NASA-TP-1344] p0043 W78-33137

CURTIS, R. B.
Results of module electrical measurement of the
DOE 46-kilowatt procurement
[NASA-TN-78829] p0134 W78-19658

CUSANO, C.
Elastohydrodynamic film thickness measurements of
artificially produced surface dents and grooves
[NASA-TN-78949] p0116 W78-27428

CUSICK, J. F.
Photovoltaic water pumping applications:
Assessment of the near-term market
[NASA-TN-78847] p0134 W78-19644

Impact of Balance of System (BOS) costs on
photovoltaic power systems
[NASA-TN-78939] p0138 W78-26550

CUTNER, D. S.
Procedures for generation and reduction of linear
models of a turbofan engine
[NASA-TN-1261] p0161 W78-30896

D

DAVIEL, L. B.
Lamination residual strains and stresses in hybrid
laminates p0128 A78-12071

DAVIEL, R. E.
Superconducting Nb3Ge for high-field magnets
p0175 A78-41922

Niobium-germanium superconducting tapes for
high-field magnet applications
[NASA-CN-135364] p0099 W78-19392

DAVILOVICH, B.
Metastable states of small rare gas crystallites
p0169 A78-16069

DARLOW, H. S.
Development of procedures for calculating
stiffness and damping properties of elastomers
in engineering applications. Part 1: Testing of
elastomers under a rotating load
[NASA-CN-135355] p0127 W78-22402

DAS, S. C.
Approximate method for calculating free vibrations
of a large-wind-turbine tower structure
[NASA-TN-73754] p0131 W78-16434

DAVIS, F. G.
Pollution Reduction Technology Program for small
jet aircraft engines, phase 2
[NASA-CN-159415] p0032 W78-33104

DEADWORE, D.
Burner rig alkali salt corrosion of several high
temperature alloys p0073 A78-18793

DEADWORE, D. L.
The role of thermal shock in cyclic oxidation
p0076 A78-37676

The role of thermal shock in cyclic oxidation
[NASA-TN-78876] p0070 W78-23193

Inhibition of hot salt corrosion by metallic
additives
[NASA-TN-78966] p0072 W78-31208

The effect of fuel-to-air ratio on burner-rig hot
corrosion
[NASA-TN-78960] p0072 W78-31210

DECRESCENTIS, S. A.
The effect of NaCl/g/ on the Na2SO4-induced hot
corrosion of NiAl p0079 A78-24901

DEFOREST, S. E.
Active control of spacecraft charging on ATS-5 and
ATS-6 p0036 W78-10136

The effect of environmental plasma interactions on
the performance of the solar sail system
[NASA-CN-135258] p0098 W78-13325

DEISSLER, R. G.
Models for some aspects of atmospheric vortices
p0150 A78-14581

On the localness of the spectral energy transfer
in turbulence p0106 A78-24909

Turbulence processes and simple closure schemes
p0107 A78-40983

On the localness of the spectral energy transfer
in turbulence
[NASA-TN-73824] p0101 W78-13361

DELVIGS, P.
PBN polyimide prepreg with improved tack
characteristics

[NASA-TN-73898] p0081 W78-17221

DEHICHTER, R. J.
Test and evaluation of 23 electric vehicles for
state-of-the-art assessment
[SAR PAPER 780290] p0101 A78-33382

Test and evaluation of 23 electric vehicles for
state-of-the-art assessment
[NASA-TN-73850] p0178 W78-17937

Baseline tests of the Kordash hybrid passenger
vehicle
[NASA-TN-73769] p0138 W78-26551

DEHITT, K. J.
Liquid jet impingement normal to a disk in zero
gravity
[ASME PAPER 78-WA/PT-1] p0107 A78-41154

DEHITT, R. L.
Preliminary concept, specifications, and
requirements for a zero-gravity combustion
facility for spacelab
[NASA-TN-78910] p0041 W78-26166

DEHO, J. H.
Status of the ERDA/NASA Photovoltaic Tests and
Applications Project p0141 A78-11014

DICARLO, J. L.
Mechanical and physical properties of modern boron
fibers p0085 A78-33206

Measurement of the time-temperature dependent
dynamic mechanical properties of boron/aluminum
composites p0061 A78-33222

Mechanical and physical properties of modern boron
fibers
[NASA-TN-73882] p0058 W78-17154

Measurement of the time-temperature dependent
dynamic mechanical properties of boron/aluminum
composites
[NASA-TN-78837] p0058 W78-20254

DICUS, J.
Synthesis of blade flutter vibratory patterns
using stationary transducers
[NASA-TN-73821] p0003 W78-17001

DIERL, L. A.
Pollution reduction technology program for class
74 (J78D) engines p0013 W78-11067

Stratospheric cruise emission reduction program
p0013 W78-11077

Reduction of aircraft gas turbine engine pollutant
emissions
[NASA-TN-78870] p0019 W78-22098

Gas turbine engine emission reduction technology
program p0001 W78-27058

Results and status of the NASA aircraft engine
emission reduction technology programs
[NASA-TN-79009] p0022 W78-33102

DINN, W. G.
Linear aerospike engine study
[NASA-CN-135231] p0026 W78-11082

DISTRICH, D. A.
Simulated flight effects on noise characteristics
of a fan inlet with high throat Mach number
[NASA-TP-1199] p0017 W78-20132

Comparison of the noise characteristics of two low
pressure ratio fans with a high throat Mach
number inlet
[NASA-TN-73880] p0018 W78-21108

Reverse-thrust technology for variable-pitch fan
propulsion systems p0005 W78-24070

DILLARD, J. G.
Volatile products from the interaction of KCl/g/
with Cr2O3 and LaCrO3 in oxidizing environments
p0066 A78-24887

Volatile products from the interaction of KCl (g)
with Cr2O3 and LaCrO3 in oxidizing environments
[NASA-TN-73795] p0064 W78-13158

DILL, B. B.
Experimental clean combustor program: Turbulence
characteristics of compressor discharge flows
[NASA-CN-135277] p0027 W78-15041

DITTMER, J. H.
Reduction of fan noise in an anechoic chamber by
reducing chamber wall induced inlet flow
disturbances p0166 A78-37681

PERSONAL AUTHOR INDEX

EDLBAW, E. A.

- A parametric investigation of an existing supersonic relative tip speed propeller noise model
[NASA-TN-73816] p0163 178-13854
Reduction of fan noise in an anechoic chamber by reducing chamber wall induced inlet flow disturbances
[NASA-TN-78854] p0164 178-22860
- DOBLE, C. S.
Impact resistant boron/aluminum composites for large fan blades
[NASA-CR-135274] p0062 178-18099
- DOBBS, W. J.
Combustor concepts for aircraft gas turbine low-power emissions reduction
[AIAA PAPER 78-999] p0025 178-43546
Combustor concepts for aircraft gas turbine low-power emissions reduction
[NASA-TN-78875] p0020 178-26143
Aircraft gas turbine low-power emissions reduction technology program
[NASA-CR-135434] p0032 178-32097
- DODGE, F. T.
Flow of liquid jets through closely woven screens
p0108 178-42877
- DOBBS, P. A.
Redundant disc
[NASA-CASE-LEW-12496-1] p0022 178-33101
- DOEING, E. J.
The Plasma Interaction Experiment (PIX) - Description and flight qualification test program
[AIAA PAPER 78-674] p0051 178-32752
The Plasma Interaction Experiment (PIX) description and test program
[NASA-TN-78863] p0041 178-21188
- DOHMAN, E. E.
Experimental data and theoretical analysis of an operating 100 kW wind turbine
[NASA-TN-73883] p0133 178-19642
- DOHONGHE, P. L.
CTS/Hermes/ - United States experiments and operations summary
p0094 178-24886
CTS (Hermes): United States experiments and operations summary
[NASA-TN-73830] p0041 178-13107
- DOHMAN, S. S.
High resolution masks for ion milling pores through substrates of biological interest
[NASA-CR-135435] p0092 178-29276
- DOHOVON, E. M.
Large wind turbine generators
[NASA-TN-73767] p0140 178-29575
- DOUGLAS, E.
The effect of environmental plasma interactions on the performance of the solar sail system
[NASA-CR-135258] p0098 178-13325
- DOHLING, R. P.
Sound production in a moving stream
p0165 178-31224
- DOHSON, D.
Flastrohydrodynamic lubrication of elliptical contacts for materials of low elastic modulus. I - Fully flooded conjunction
[ASME PAPER 77-LUB-10] p0119 178-28414
Elastohydrodynamic lubrication of elliptical contacts for materials of low elastic modulus. 2: Starved conjunction
[NASA-TP-1273] p0117 178-28458
Minimum film thickness in elliptical contacts for different regimes of fluid-film lubrication
[NASA-TP-1342] p0117 178-33447
- DRESHFELD, R. L.
Effects of heat treating PM Rene' 95 slightly below the gamma-prime solvus
p0073 178-18792
- DUDENSTADT, E. C.
Development and fabrication of a diffusion welded Columbus alloy heat exchanger
[ASME PAPER 178-61] p0123 178-31500
- DUPRANE, W. F.
Influence of adsorbed fluids on the rolling contact deformation of MgO single crystals
p0123 178-23847
- DUGAN, J. F.
Status of advanced turboprop technology
p0001 178-27055
- DUKY, L. C.
General aviation piston-engine exhaust emission reduction
p0013 178-11073
- DULGEROFF, C. S.
Engineering Model 8-cm Thruster System
[AIAA PAPER 78-646] p0055 178-37434
- DUNBAR, D. E.
Computer model for refinery operations with emphasis on jet fuel production. Volume 2: Data and technical bases
[NASA-CR-135334] p0090 178-19326
Computer model for refinery operations with emphasis on jet fuel production. Volume 1: Program description
[NASA-CR-135333] p0090 178-20350
Computer model for refinery operations with emphasis on jet fuel production. Volume 3: Detailed systems and programming documentation
[NASA-CR-135335] p0090 178-25235
- DUNZING, J. E., JR.
Distribution of R/W and W/e in a cross-flow electric discharge laser
p0111 178-24896
Small-signal gain diagnostic measurements in a flowing CO2 pin discharge laser
[NASA-TN-73843] p0111 178-13421
Distribution of R/W and W sub e in a cross-flow electric discharge laser
[NASA-TN-73807] p0111 178-14386
- DUSCHA, E. A.
Thermal energy storage for industrial waste heat recovery
[NASA-TN-78953] p0140 178-29576
- DUSTIN, H. G.
Test and evaluation of 23 electric vehicles for state-of-the-art assessment
[SAE PAPER 780290] p0181 178-33382
Mechanical characteristics of stability-bleed valves for a supersonic inlet
[NASA-TN-X-3483] p0015 178-13063
Baseline tests of the AN General DJ-5R electric delivery van
[NASA-TN-73758] p0178 178-17933
Baseline tests of the power-train electric delivery van
[NASA-TN-73765] p0178 178-17936
Test and evaluation of 23 electric vehicles for state-of-the-art assessment
[NASA-TN-73850] p0178 178-17937
Baseline tests of the EVA change-of-pace coupe electric passenger vehicle
[NASA-TN-73763] p0178 178-17938
Baseline tests of the batronic Minivan electric delivery van
[NASA-TN-73761] p0179 178-17940
Performance of conventionally powered vehicles tested to an electric vehicle test procedure
[NASA-TN-73768] p0179 178-20022
Application of fluidics to new control components
p0109 178-23026
Baseline tests of the Kordeah hybrid passenger vehicle
[NASA-TN-73769] p0138 178-26551
Wind tunnel evaluation of YP-12 inlet response to internal airflow disturbances with and without control
p0006 178-32062
- DUTTA, S.
Ceramics in gas turbines - Powder and process characterization
p0085 178-29328
Pressureless sintered beta-prime-513N6 solid solution - Fabrication, microstructure, and strength
p0086 178-47595
Ceramics in gas turbine: Powder and process characterization
[NASA-TN-73875] p0016 178-17059
Pressureless sintered beta prime-513N6 solid solution: Fabrication, microstructure, and strength
[NASA-TN-78950] p0083 178-29245

E

- EAGLE, C. D.
Lightweight, low compression aircraft diesel engine
[NASA-CR-135300] p0121 178-21471
- EDLBAW, E. A.
Utilization of NASA Lewis mobile terminals for the

- Hermes satellite
Utilization of NASA Lewis mobile terminals for the
Hermes satellite
{NASA-TN-73859} p0093 W78-15326
- EDSINGER, R. W.
A simulation model for wind energy storage
systems. Volume 1: Technical report
{NASA-CR-135283} p0156 W78-20802
A simulation model for wind energy storage
systems. Volume 2: Operation manual
{NASA-CR-135284} p0157 W78-20103
A simulation model for wind energy storage
systems. Volume 3: Program descriptions
{NASA-CR-135285} p0157 W78-20804
- KISUMATSU, J. E.
Effects of film injection on performance of a
cooled turbine p0033 A78-24902
Effects of film injection on performance of a
cooled turbine p0029 W78-21147
- EL-WAKIL, M. N.
The role of drop velocity in statistical spray
description p0107 A78-50323
The role of drop velocity in statistical spray
description
{NASA-TN-73887} p0102 W78-20458
- ENG, S. D.
Manufacture of astroloy turbine disk shapes by hot
isostatic pressing, volume 1
{NASA-CR-135409} p0079 W78-25166
- ENGLEN, S. A.
Continuation of the compendium of applications
technology satellite and communications
technology satellite user experiments 1967-1977,
volume 1
{NASA-CR-135416-VOL-1} p0042 W78-31141
Continuation of the compendium of applications
technology satellite and communications
technology satellite user experiments 1967-1977,
volume 2
{NASA-CR-135416-VOL-2} p0042 W78-31142
- ENGLETT, G. W.
Model for interpreting Doppler broadened optical
line emission measurements on axially symmetric
plasma p0174 A78-46189
- ENGLISH, R. E.
Comment on 'Heat-pipe reactors for space power
applications' p0052 A78-40826
- ENGLUND, P. E.
Global atmospheric sampling program p0013 W78-11076
- ESSIGN, C. E.
Interpolation and extrapolation of creep rupture
data by the sinus commitment method. II -
Oblique translation p0076 A78-45426
Interpolation and extrapolation of creep rupture
data by the sinus commitment method. I -
Focal-point convergence p0076 A78-45427
Interpolation and extrapolation of creep rupture
data by the sinus commitment method. III -
Analysis of subheats p0076 A78-45428
Interpolation and extrapolation of creep rupture
data by the sinus commitment method. Part 1:
Focal-point convergence
{NASA-TN-78881} p0125 W78-23471
Interpolation and extrapolation of creep rupture
data by the sinus commitment method. Part 2:
Oblique translation
{NASA-TN-78882} p0125 W78-23472
Interpolation and extrapolation of creep rupture
data by the sinus commitment method. Part 3:
Analysis of subheats
{NASA-TN-78883} p0126 W78-23473
- ENDOS, J. I.
Computation of unsteady transonic flows through
rotating and stationary cascades. 3: Acoustic
far-field analysis
{NASA-CR-2902} p0007 W78-12015
Computation of unsteady transonic flows through
rotating and stationary cascades. 1: Method of
analysis {NASA-CR-2900} p0008 W78-20882
- ETTES, R. B.
Metastable states of small rare gas crystallites
p0169 A78-16069
- EVANICH, P. L.
Photographic characterization of spark-ignition
engine fuel injectors
{NASA-TN-78830} p0018 W78-21110
- EVANS, D. G.
An overview of aerospace gas turbine technology of
relevance to the development of the automotive
gas turbine engine
{SAB PAPER 780075} p0120 A78-33364
An overview of aerospace gas turbine technology of
relevance to the development of the automotive
gas turbine engine
{NASA-TN-73849} p0014 W78-13062
- EVANS, D. J.
Manufacture of astroloy turbine disk shapes by hot
isostatic pressing, volume 1
{NASA-CR-135409} p0079 W78-25166
- EVANS, J. C., JR.
Solar cell collector
{NASA-CASE-LEU-12552-1} p0134 W78-25527
"Echo" for producing solar energy panels by
automation
{NASA-CASE-LEU-12541-1} p0136 W78-25529
Solar cell system having alternating
current output
{NASA-CASE-LEU-12806-1} p0136 W78-25553

F

- FALCONER, F. D.
Atmospheric ozone measurements made from B-747
airliners - Spring 1975 p0188 A78-24894
An analysis of the first two years of GASP data
{NASA-TN-73817} p0148 W78-13669
- FARQUHAN, J.
Liquid rocket engine axial-flow turbopumps
{NASA-SP-8125} p0050 W78-31164
- FARRELL, C. A., JR.
Computer program for calculating two-dimensional
potential flow in and about propulsion system
inlets
{NASA-TN-78930} p0005 W78-27083
- FEILNER, C. E.
Propulsion system noise technology p0001 W78-27056
- FELDMAN, R.
Upper limit for magneto-resistance in silicon
bronze and phosphor bronze wire p0175 A78-14423
- FENN, D. B.
Fixed pitch wind turbines p0133 W78-19638
- FERRARA, A.
Thermal energy storage heat exchanger: Molten
salt heat exchanger design for utility power
plants
{NASA-CR-135244} p0143 W78-14632
Thermal energy storage heat exchanger: Molten
salt heat exchanger design for utility power
plants
{NASA-CR-135245} p0143 W78-14633
- FERRAWAY, J.
Adhesion of a bimetallic interface
{NASA-TN-78890} p0071 W78-29214
- FESSLER, T. E.
User's guide for SPTRAV/360
{NASA-TP-1006} p0156 W78-10746
User's guide to SPTRAV/1100
{NASA-TP-1200} p0156 W78-20806
- FFORDS WILLIAMS, J. E.
Sound production in a moving stream p0125 A78-31224
- FIALA, J.
A digitally implemented communications experiment
utilizing the Hermes /CTS/ satellite p0094 A78-24884
- FIALA, J. L.
Utilization of NASA Lewis mobile terminals for the
Hermes satellite p0094 A78-24885
A digitally implemented communications experiment
utilizing the Hermes (CTS) satellite
{NASA-TN-73827} p0093 W78-13283
Utilization of NASA Lewis mobile terminals for the
Hermes satellite

PERSONAL AUTHOR INDEX

FRYBURG, G. C.

- [NASA-TN-73859] p0093 W78-15326
FIELD, S. S.
 Application of thick-film technology to solar cell fabrication p0146 A78-10947
 Evaluation of glass resin coatings for solar cell applications [NASA-CR-159392] p0145 W78-27540
FIELDER, G. L.
 Solubility, stability, and electrochemical studies of sulfur-sulfide solutions in organic solvents [NASA-TP-12451] p0180 W78-28624
FIGURE, R. U.
 Analysis and test of deep flaws in thin sheets of aluminum and titanium. Volume 1: Program summary and data analysis [NASA-CR-135369] p0127 W78-21493
 Analysis and test of deep flaws in thin sheets of aluminum and titanium. Volume 2: Crack opening displacement and stress-strain data [NASA-CR-135370] p0127 W78-21494
FINN, R. E.
 A method for calculating externally blown flap noise [NASA-CR-2954] p0166 W78-20920
 A method for calculating strut and splitter plate noise in exit ducts: Theory and verification [NASA-CR-2955] p0167 W78-20921
FIORENTINO, S. J.
 Pollution reduction technology program for class 74 (JT8D) engines p0013 W78-11067
 Evaluation of Federal Aviation Administration ion engine exhaust sampling rate [NASA-CR-135213] p0029 W78-21111
FIORITO, R. J.
 Wide range operation of advanced low NOx combustors for supersonic high-altitude aircraft gas turbines [NASA-CR-135297] p0027 W78-14047
FISCHER, D.
 Computation of unsteady transonic flows through rotating and stationary cascades. 3: Acoustic far-field analysis [NASA-CR-2932] p0007 W78-12035
FISCHER, R. E.
 High frequency dynamic engine simulation [NASA-CR-135313] p0027 W78-13059
FISCHBACH, L. E.
 Preliminary study of propulsion systems and airplane wing parameters for a US Navy subsonic V/STOL aircraft [NASA-TN-73652] p0010 W78-17041
FISHER, D. S.
 Load-displacement measurement and work determination in three-point bend tests of notched or precracked specimens p0089 A78-24370
FISHER, P. A.
 Lightning protection of aircraft [NASA-EP-1006] p0009 W78-11024
FLEHING, D. P.
 High stiffness seals for rotor critical speed control [ASME PAPER 77-DET-10] p0118 W78-20591
 Stiffness of straight and tapered annular gas path seals [NASA-TN-78872] p0103 W78-23185
FLOOD, D. J.
 Crystal field and magnetic properties of ErH₃ p0175 A78-24907
 Crystal field and magnetic properties [NASA-TN-73877] p0175 W78-13916
FOLLOWSBEE, P. S.
 Experimental clean combustor program: Turbulence characteristics of compressor discharge flows [NASA-CR-135277] p0027 W78-15081
FORD, R. J.
 Advanced optical blade tip clearance measurement system [NASA-CR-159402] p0032 W78-31106
FORD, W. F.
 User's guide for SPTRAW/360 [NASA-TP-1006] p0156 W78-10746
 User's guide to SPTRAW/1100 [NASA-TP-1200] p0156 W78-20806
FORESTIERI, A. P.
 Status of the ERDA/NASA Photovoltaic Tests and Applications Project p0141 A78-11014
 Seal-time and accelerated outdoor endurance testing of solar cells p0142 A78-52837
 The ERDA/LeRC Photovoltaic Systems Test Facility p0143 A78-52851
 Seal-time and accelerated outdoor endurance testing of solar cells [NASA-TN-73783] p0130 W78-14628
 The ERDA/LeRC photovoltaic systems test facility [NASA-TN-73787] p0035 W78-15059
 Method of making encapsulated solar cell modules [NASA-CASB-LSU-12185-1] p0136 W78-29528
 Endurance testing of first generation (Block 1) commercial solar cell modules [NASA-TN-78922] p0138 W78-26548
 DOE LeRC photovoltaic systems test facility [NASA-TN-78923] p0138 W78-26549
FORNAB, E.
 Secondary electron emission properties of conducting surfaces for use in multistage depressed collectors p0098 A78-23635
 Secondary-electron-emission properties of conducting surfaces with application to multistage depressed collectors for microwave amplifiers [NASA-TP-1097] p0068 W78-11230
POSTER, T.
 Variable cycle gas turbine engines [NASA-CASB-LSU-12916-1] p0113 W78-17384
 Variable mixer propulsion cycle [NASA-CASB-LSU-12917-1] p0016 W78-18067
FOX, G. E.
 Performance and economics of advanced energy conversion systems for coal and coal-derived fuels p0146 A78-34078
FRALICK, G. C.
 Miniature drag force anemometer p0109 A78-17397
FRANCISCO, L. C.
 Supersonic through-flow fan engines for supersonic cruise aircraft [NASA-TN-78889] p0019 W78-23088
FRASER, L. H.
 Reliability analysis of forty-five strain-gage systems mounted on the first fan stage of a YF-100 engine [NASA-TN-73724] p0109 W78-13407
FRICKE, J. C.
 Progress in advanced high temperature turbine materials, coatings, and technology p0056 A78-24910
 Strength enhancement process for prealloyed powder superalloys p0075 A78-33216
 Progress in advanced high temperature turbine materials, coatings, and technology p0018 W78-21122
 Strength enhancement process for prealloyed powder superalloys [NASA-TN-78834] p0070 W78-21266
FRISMAN, S.
 Alternative fuels p0013 W78-11074
FRISMAN, H.
 Extended performance solar electric propulsion thrust system study. Volume 4: Thruster technology evaluation [NASA-CR-135281-VOL-4] p0053 W78-16090
FRYBURG, G. C.
 Volatile products from the interaction of HCl(g) with Cr₂O₃ and LaCrO₃ in oxidizing environments p0066 A78-24887
 Interaction of NaCl(g) and HCl(g) with condensed Na₂SO₄ p0066 A78-24888
 Formation of Na₂SO₄ and K₂SO₄ in flames doped with sulfur and alkali chlorides and carbonates p0066 A78-24889
 Formation of Na₂SO₄ and K₂SO₄ in flames doped with sulfur and alkali chlorides and carbonates [NASA-TN-73794] p0066 W78-13157
 Volatile products from the interaction of HCl(g) with Cr₂O₃ and LaCrO₃ in oxidizing environments [NASA-TN-73795] p0066 W78-13158
 Interaction of NaCl(g) and HCl(g) with condensed Na₂SO₄ [NASA-TN-73796] p0066 W78-13159

FRYE, E. J.

PERSONAL AUTHOR INDEX

- FRYE, E. J.
Electrical Prototype Power Processor for the 30-cm
Mercury electric propulsion engine
[AIAA PAPER 78-684] p0055 178-37439
- FUCIENSKI, C. A.
Ceramic regenerator systems development program
[NASA-CR-135330] p0181 178-25988
- Ceramic regenerator systems development program
[NASA-CR-135430] p0181 178-26997
- FOLMERTSON, S. A.
P100(3) parallel compressor computer code and
user's manual
[NASA-CR-135388] p0029 178-22096
- FURMAN, E. B.
Closed loop spray cooling apparatus
[NASA-CR-135-11981-1] p0091 178-17237
- FURMAN, E. B.
Effect of thermal exposure on lubricating
properties of polyimide films and
polyimide-bonded graphite fluoride films
[NASA-TP-1125] p0080 178-15277
- Lubrication and failure mechanisms of graphite
fluoride films
[NASA-TP-1197] p0081 178-20337
- A comparison of the lubricating mechanisms of
graphite fluoride and molybdenum disulfide films
[NASA-TN-78897] p0083 178-26215
- FUTRAL, S. W., JR.
Cold-air performance of a tip turbine designed to
drive a lift fan. 3: Effect of simulated fan
leakage on turbine performance
[NASA-TP-1109] p0003 178-16001

G

- GABBIEL, G. J.
Potential damage to dc superconducting magnets due
to high frequency electromagnetic waves
p0098 178-39902
- Potential damage to DC superconducting magnets due
to the high frequency electromagnetic waves
[NASA-TN-73808] p0096 178-13330
- GANN, E. F.
The Redox Flow System for solar photovoltaic
energy storage
p0141 178-11019
- Anion exchange membranes for electrochemical
oxidation-reduction energy storage systems
[NASA-TN-73751] p0131 178-18631
- GALLAGHER, J. G.
Millimeter wave satellite concepts, volume 1
[NASA-CR-135227] p0041 178-15104
- GALLAGHER, J. F.
Jet fuels from synthetic crudes
p0090 178-43415
- GAUGLES, E. E.
A computer program for the transient thermal
analysis of an impingement cooled turbine blade
[AIAA PAPER 78-92] p0106 178-20682
- A computer program for the transient thermal
analysis of an impingement cooled turbine blade
[NASA-TN-73819] p0015 178-15065
- TACT1, a computer program for the transient
thermal analysis of a cooled turbine blade or
vane equipped with a coolant insert. 1. Users
manual
[NASA-TP-1271] p0104 178-28374
- GAUNTHER, D. J.
Description and review of global measurements of
atmospheric species from GASP
p0148 178-24893
- Global atmospheric sampling program
p0013 178-11076
- Method for calculating convective heat-transfer
coefficients over turbine vane surfaces
[NASA-TP-1134] p0102 178-17338
- GAUNTHER, J. W.
Effects of film injection angle on turbine vane
cooling
[NASA-TP-10951] p0101 178-13379
- GAYDON, F. J.
Lightweight, low compression aircraft diesel engine
[NASA-CR-135300] p0121 178-21471
- GIBSON, V. D.
Application of fluidics to new control components
p0109 178-23026
- Design and performance of heart assist or
artificial heart control systems
p0185 178-23032

- GESBON, L.
A mechanical, thermal and electrical packaging
design for a prototype power management and
control system for the 30 cm mercury ion thruster
[AIAA PAPER 78-685] p0081 178-32759
- A mechanical, thermal and electrical packaging
design for a prototype power management and
control system for the 30 cm mercury ion thruster
[NASA-TN-78862] p0049 178-23142
- GESBURY, E. T.
Numerical computation of three-dimensional
circulation in Lake Erie - a comparison of a
free-surface model and a rigid-lid model
p0151 178-47223
- GESHILL, S. A.
Cyclic oxidation of coated Oxide Dispersion
Strengthened (ODS) alloys in high velocity gas
streams at 1100 deg C
[NASA-TN-78877] p0071 178-24336
- GELLES, S. U.
Materials science experiments in space
[NASA-CR-2842] p0056 178-16094
- GERSTENHAIN, W. E.
Inlet-engine matching for SCAR including
application of a bicone variable geometry inlet
[AIAA PAPER 78-961] p0007 178-45096
- Inlet-engine matching for SCAR including
application of a bicone variable geometry inlet
[NASA-TN-78955] p0021 178-27125
- GESSEN, E. S.
Wind turbine generator rotor blade concepts with
low cost potential
[NASA-TN-73835] p0131 178-17466
- GETZEL, L. C.
Optical control of a supersonic inlet to minimize
frequency of inlet unstart
p0019 178-23024
- DYABCD: A program for calculating linear A, B,
C, and D matrices from a nonlinear dynamic
engine simulation
[NASA-TP-1295] p0022 178-33110
- GIBSON, D. F.
Effect of surface texture by ion beam sputtering
on implant biocompatibility and soft tissue
attachment
[NASA-CR-135311] p0152 178-18672
- GIBSSON, R. C.
Materials science experiments in space
[NASA-CR-2842] p0056 178-16094
- GILBERT, L. J.
Synchronization of wind turbine generators against
an infinite bus under gusting wind conditions
[EPRI PAPER 77 575-2] p0142 178-30196
- Synchronization of the DOE/NASA 100-kilowatt wind
turbine generator with a large utility network
[NASA-TN-73861] p0132 178-17467
- Transient response to three-phase faults on a wind
turbine generator
[NASA-TN-78902] p0137 178-26542
- GLASGOW, J. C.
DOE/NASA Mod-0 100kW wind turbine test results
p0133 178-19628
- Experimental data and theoretical analysis of an
operating 100 kW wind turbine
[NASA-TN-73883] p0133 178-19642
- Design and operating experience on the US
Department of Energy experimental Mod-0 100-kw
wind turbine
[NASA-TN-78915] p0138 178-26542
- GLASGOW, T. K.
Effect of attrition sintering on the reaction
sintering of silicon nitride
p0086 178-50324
- Longitudinal shear behavior of several oxide
dispersion strengthened alloys
[NASA-TN-78973] p0072 178-31211
- Effect of attrition sintering on the reaction
sintering of silicon nitride
[NASA-TN-78965] p0084 178-31236
- GLASS, G. E.
Recovery and radiation corrections and time
constants of several sizes of shielded and
unshielded thermocouple probes for measuring gas
temperature
[NASA-TP-1099] p0109 178-15463
- GLEASON, C. C.
Combustor concepts for aircraft gas turbine
low-power emissions reduction
[AIAA PAPER 78-999] p0025 178-43546

PERSONAL AUTHOR INDEX

GROSSBECK, D.

Combustor concepts for aircraft gas turbine
low-power emissions reduction
[NASA-TN-78875] p0020 N78-26143
Aircraft gas turbine low-power emissions reduction
technology program
[NASA-TN-135338] p0032 N78-32097

GLICKSMAN, S. S.
Materials science experiments in space
[NASA-CN-2882] p0056 N78-16098

GODFREY, S. P.
A methodology for experimentally-based
determination of gap shrinkage and effective
lifetimes in the emitter and base of
p-n-junction solar cells p0181 A78-10903

GODSTON, J.
VCR method program planning and definition study
[NASA-CN-135362] p0029 N78-19160

GOSTIN, S. E.
Gas turbine project status p0091 N78-30303

GOLD, M.
The design of hydraulic pressure regulators that
are stable without the use of sensing line
restrictors or frictional dampers p0168 A78-28897
The design of hydraulic pressure regulators that
are stable without the use of sensing line
restrictors or frictional dampers
[NASA-TN-73687] p0101 N78-10815
Methods of attenuating wind turbine ac generat-
output variations p0133 N78-19632
Automotive gas turbine fuel control
[NASA-CASE-LEW-12785-1] p0115 N78-28545

GOLDSMAN, L. J.
Effect of endwall cooling on secondary flows in
turbine stator vanes p0018 N78-11098

GOLDSTEIN, S. E.
Feasibility study of negative lift circumferential
type seal for helicopter transmissions
[NASA-CN-135302] p0121 N78-17390

GOLDSTEIN, S. E.
Unsteady flow in a supersonic cascade with strong
in-passage shocks p0006 A78-17270
Characteristics of the unsteady motion on
transversely sheared shear flows p0106 A78-23286
Fouling production in a moving stream p0165 A78-31224

GOODALE, D. S.
Performance of a thermionic converter module
utilizing emitter and collector heat pipes
[NASA-TN-78941] p0049 N78-27178

GORDON, L. E.
Storage systems for solar thermal power
[NASA-TN-78952] p0140 N78-29577

GORDON, S.
Computer program for calculation of complex
chemical equilibria compositions, rocket
performance, incident and reflected shocks, and
Chapman-Jouquet detonations
[NASA-SP-273] p0156 N78-17724

GORDON, S. A.
Development of a drift-correction procedure for a
photoelectric spectrometer p0109 A78-23525

GORE, J. V.
Summary of the CTS Transient Event Counter data
after one year of operation p0086 A78-19566

GOURASH, V.
Baseline tests of the Volkswagen transporter
electric delivery van
[NASA-TN-73766] p0179 N78-20021

GRAY, H. B.
The promise of eutectics for aircraft turbines p0078 A78-28882
The effect of microstructure on hydrogen
embrittlement of the nickel base superalloy,
Alloy 700 p0076 A78-17075
The promise of eutectics for aircraft turbines
[NASA-TN-73714] p0012 N78-10098
The effect of microstructure on hydrogen
embrittlement of the nickel-base superalloy,
Alloy 700

[NASA-TN-73772] p0082 N78-22232

GRAY, S.
Hydrodynamic air lubricated compliant surface
bearing for an automotive gas turbine engine.
1: Journal bearing performance p0121 N78-21672
[NASA-CN-135368]
Hydrodynamic air lubricated compliant surface
bearing for an automotive gas turbine engine.
2: Materials and coatings p0122 N78-29689
[NASA-CN-135402]

GREEN, A. E. G.
Cloud effects on middle ultraviolet global radiation
p0150 A78-82952

GREENE, S.
Evaluation of Federal Aviation Administration ion
engine exhaust sampling rake
[NASA-CN-135213] p0029 N78-21111

GREINER, S. F.
Design considerations in mechanical face seals for
improved performance. I - Basic configurations
[ASME PAPER 77-SA/LUB-3] p0119 A78-33183
Design considerations in mechanical face seals for
improved performance. II - Lubrication
[ASME PAPER 77-SA/LUB-8] p0120 A78-33184
Design considerations in mechanical face seals for
improved performance. 1: Basic configurations
[NASA-TN-73735] p0113 N78-13439

GRITWALL, S. H.
Velocity, temperature, and electrical conductivity
profiles in hydrogen-oxygen RSD duct flows
[NASA-TN-78968] p0108 A78-28372

GRISH, S.
Investigation of high voltage spacecraft system
interactions with plasma environments
[NASA PAPER 78-672] p0050 A78-32750
Investigation of high voltage spacecraft system
interactions with plasma environments
[NASA-TN-78831] p0097 N78-21373

GRIFFIN, D. G., JR.
Wind turbine generator rotor blade concepts with
low cost potential
[NASA-TN-73835] p0131 N78-17866

GRINES, S. E.
Thermal environment effects on strength and impact
properties of boron-aluminum composites p0060 A78-33208
Thermal environment effects on strength and impact
properties of boron-aluminum composites
[NASA-TN-73885] p0058 N78-17155

GRISAFFE, S. J.
High temperature environmental effects on metals
p0075 A78-29329
High temperature environmental effects on metals
[NASA-TN-73878] p0017 N78-19158
Thermal barrier coatings
[NASA-TN-78848] p0059 N78-28291

GROBMAN, J. E.
Alternative fuels p0013 N78-11078
Alternative aircraft fuels
[NASA-TN-73836] p0088 N78-17229
Impact of future fuel properties on aircraft
engines and fuel system
[NASA-TN-78846] p0089 N78-28369
Characteristics and combustion of future
hydrocarbon fuels
[NASA-TN-78865] p0089 N78-28370
Impact of broad-specification fuels on future jet
aircraft p0089 N78-27059

Results and status of the NASA aircraft engine
emission reduction technology program
[NASA-TN-79009] p0022 N78-33102

GROBMAN, J. F.
State-of-the-art of turbofan engine noise control
p0028 A78-35658
The role of drop velocity in statistical spray
description p0107 A78-50323
The role of drop velocity in statistical spray
description
[NASA-TN-73887] p0102 N78-20856

GROSSBECK, D.
Noise of deflectors used for flow attachment with
STOL-OTS configurations p0023 A78-28877
Noise of deflectors used for flow attachment with
STOL-OTS configurations

- [NASA-TN-73809] p0163 A78-13853
- GROSS, B.
Mode I stress intensity factors for round compact specimens p0126 A78-13817
- Displacement coefficients along the inner boundaries of radially cracked ring segments subject to forces and couples p0127 A78-35396
- GRUBER, B. P.
Pulse ignition characterization of mercury ion thruster hollow cathode using an improved pulse ignitor [AIAA JOURNAL 76-709] p0051 A78-32773
- Pulse Ignition characterization of mercury ion thruster hollow cathode using an improved pulse ignitor [NASA-TN-78858] p0047 A78-21203
- Closed loop solar array-ion thruster system with power control circuitry [NASA-CASR-LRU-12780-1] p0088 A78-22149
- Self-reconfiguring solar cell system [NASA-CASR-LRU-12586-1] p0139 A78-27520
- GUNBARSON, B. W.
Development and test of an inlet and duct to provide airflow for a wing boundary layer control system [AIAA PAPER 78-141] p0006 A78-20701
- GUO, S.
Employing static excitation control and tie line reactance to stabilize wind turbine generators [NASA-CN-135384] p0144 A78-20603
- GYSSEBYNSKI, J. P.
Stress analysis and stress-intensity factors for finite geometry solids containing rectangular surface cracks [ASME PAPER 77-WA/EPH-5] p0126 A78-10531

H

- HAS, J. H.
Cold-air performance of a tip turbine designed to drive a lift fan [NASA-TN-1126] p0003 A78-14998
- Cold-air performance of a tip turbine designed to drive a lift fan. 3: Effect of simulated fan leakage on turbine performance [NASA-TN-1109] p0003 A78-16001
- HADDAB, D. S.
F100(3) parallel compressor computer code and user's manual [NASA-CN-135388] p0029 A78-22096
- HANE, S. P.
Preliminary power train design for a state-of-the-art electric vehicle [NASA-CN-135381] p0182 A78-24992
- HARLEY, P. S.
The Plasma Interaction Experiment (PIE) - Description and flight qualification test program [AIAA PAPER 78-674] p0051 A78-32752
- The Plasma Interaction Experiment (PIE) description and test program [NASA-TN-78843] p0081 A78-21188
- HALFORD, G. S.
Strain-range partitioning behavior of the nickel-base superalloys, Rene 80 and 100 p0075 A78-33214
- Ductility normalized-strain-range partitioning life relations for creep-fatigue life predictions p0077 A78-44739
- Strain-range partitioning behavior of the nickel-base superalloys, Rene 80 and 100 [NASA-TN-78828] p0070 A78-21157
- HALL, B. G., III
Transient dynamics of a flexible rotor with squeeze film dampers [NASA-CN-3050] p0123 A78-32433
- HANSEN, A.
Analysis of the cross flow in a radial inflow turbine scroll [NASA-CN-135320] p0029 A78-19153
- Computer program for the analysis of the cross flow in a radial inflow turbine scroll [NASA-CN-135321] p0029 A78-19154
- HANCOCK, B. J.
Simplified solution for elliptical-contact deformation between two elastic solids p0118 A78-12737

- Simplified contact analysis p0127 A78-20200
- Elastohydrodynamic lubrication of elliptical contacts for materials of low elastic modulus. 1 - Fully flooded conjunction [ASME PAPER 77-LUB-10] p0119 A78-29414
- Additional aspects of elastohydrodynamic lubrication [NASA-TN-78898] p0120 A78-45830
- Additional aspects of elastohydrodynamic lubrication [NASA-TN-78898] p0115 A78-26483
- Elastohydrodynamic lubrication of elliptical contacts for materials of low elastic modulus. 2: Starved conjunction [NASA-TN-1271] p0117 A78-26458
- Effect of geometry on hydrodynamic film thickness [NASA-TN-1287] p0117 A78-30585
- Minimum film thickness in elliptical contacts for different regimes of fluid-film lubrication [NASA-TN-1342] p0117 A78-33447
- HANSEN, W.
Hydrogen film cooling of a small hydrogen-oxygen thrust chamber and its effect on erosion rates of various ablative materials [NASA-TN-1098] p0047 A78-13124
- HANSEN, D. O.
Particle parameter analyzing system [NASA-CASR-ILR-06094] p0096 A78-17293
- HANSEN, I. S.
Electric vehicle power train instrumentation - Some constraints and considerations [AVC PAPER 7744] p0097 A78-16922
- HANSEN, V. A.
Ultraviolet spectrophotometer for measuring columnar atmospheric ozone from aircraft p0110 A78-35810
- Measurement of tropospheric 300 nm solar ultraviolet flux for determination of O₃/D₀/ photoproduction rate p0148 A78-38835
- HARRISILL, S. T.
Radial power voltage multipliers with a large number of stages p0098 A78-45435
- Radial power voltage multipliers with a large number of stages [NASA-TN-78900] p0093 A78-26373
- HARRISILL, S. T., JR.
10-cu mercury ion thruster performance with a 1 kV capacitor-diode voltage multiplier beam supply [AIAA PAPER 78-686] p0051 A78-32760
- A 30-cu mercury ion thruster performance with a 1 kV capacitor-diode voltage multiplier beam supply [NASA-TN-78844] p0049 A78-23143
- Regulated high efficiency, lightweight capacitor-diode multiplier dc to dc converter [NASA-CASR-LRU-12781-1] p0097 A78-32341
- HARRIS, L. P.
Design and calculated performance and cost of the ECAS Phase II open cycle HRD power generation system [ASME PAPER 77-WA/EPH-5] p0174 A78-33143
- HART, C. E.
Real time digital propulsion system simulation for manned flight simulators [AIAA PAPER 78-927] p0035 A78-45095
- Real time digital propulsion system simulation for manned flight simulators [NASA-TN-78959] p0038 A78-27137
- HART, S. S.
Photon degradation effects in terrestrial solar cells [NASA-TN-78924] p0134 A78-25551
- HASSEN, J. H.
HASC - a three-dimensional charging analyzer Program for complex spacecraft p0044 A78-19547
- A three dimensional dynamic study of electrostatic charging in materials [NASA-CN-135256] p0044 A78-13320
- HASCAP user's manual [NASA-CN-135259] p0044 A78-13320
- HASLETT, S.
Thermal energy storage heat exchanger: Molten salt heat exchanger design for utility power plants [NASA-CN-135244] p0143 A78-18632
- Thermal energy storage heat exchanger: Molten salt heat exchanger design for utility power plants

PERSONAL AUTHOR INDEX

HOLANDA, B.

- [NASA-CN-135245] p0143 #78-14633
- HASE, J. S.**
Effect of coolant flow ejection on aerodynamic performance of low-aspect-ratio vanes. 2: Performance with coolant flow ejection at temperature ratios up to 2 [NASA-TN-1057] p0003 #78-11008
- HASE, J. S.**
Computer program for calculating two-dimensional potential flow in and about propulsion system inlet [NASA-TN-78930] p0005 #78-27083
- HAYWOOD, E. I.**
Extended performance solar electric propulsion thrust system design [AIAA PAPER 78-643] p0055 #78-17430
Extended performance solar electric propulsion thrust system study. Volume 1: Executive Summary [NASA-CN-135281-VOL-1] p0052 #78-10705
Extended performance solar electric propulsion thrust system study. Volume 2: Thruster technology evaluation [NASA-CN-135281-VOL-2] p0053 #78-16090
Extended performance solar electric propulsion thrust system study. Volume 3: Tradeoff studies of alternate thrust system configurations [NASA-CN-135281-VOL-3] p0053 #78-19196
- HAYES, C. L.**
Analysis and design of a high power laser adaptive phased array transmitter [NASA-CN-134952] p0111 #78-13420
- HECK, P. B.**
Acoustic tests of duct-burning turbofan jet noise simulation [NASA-CN-2866] p0002 #78-28043
Acoustic tests of duct-burning turbofan jet noise simulation: Comprehensive data report. Volume 1, section 2: Full size data [NASA-CN-135239-VOL-1-SECT-2] p0030 #78-28095
Acoustic tests of duct-burning turbofan jet noise simulation: Comprehensive data report. Volume 1, section 3: Data plots [NASA-CN-135239-VOL-1-SECT-3] p0030 #78-28094
Acoustic tests of duct-burning turbofan jet noise simulation: Comprehensive data report. Volume 2: Model design and aerodynamic test results [NASA-CN-135239-VOL-2] p0031 #78-28097
- HEIDHANN, H. F.**
Flight-effects on predicted fan fly-by noise [NASA-TN-73799] p0014 #78-13060
- HEIN, G. F.**
Energy resources of the developing countries and some priority markets for the use of solar energy p0182 #78-28400
Utilization of solar energy in developing countries - Identifying some potential markets p0182 #78-85437
Impact of balance of system (BOS) costs on photovoltaic power systems [NASA-TN-78439] p0138 #78-26550
Utilization of solar energy in developing countries: Identifying some potential markets [NASA-TN-78464] p0140 #78-29478
- HELMS, B. E.**
Study and program plan for improved heavy duty gas turbine engine ceramic component development [NASA-CN-135230] p0122 #78-28466
- HENDRICKS, E. C.**
Revised international representations for the viscosity of water and steam and new representations for the surface tension of water p0105 #78-15725
Boiling incipience and convective boiling of neon and nitrogen p0105 #78-15820
Estimating surface temperature in forced convection nucleate boiling - A simplified method p0105 #78-15822
Two phase choke flow in tubes with very large L/D p0105 #78-15824
Simulation of the heat transfer characteristics of LOX [ASME PAPER 77-WT-9] p0089 #78-17482
Thermally driven oscillations and wave motion of a liquid drop p0106 #78-17504
Some flow phenomena in a constant area duct with aorda type inlet including the critical region [NASA-TN-78643] p0108 #78-27367
- HENSHALL, T. P.**
Effect of attrition milling on the reaction sintering of silicon nitride p0006 #78-30324
Effect of attrition milling on the reaction sintering of silicon nitride [NASA-TN-78965] p0004 #78-31236
- HERSON, D. G.**
Engineering Model 8-cs Thruster System [AIAA PAPER 78-646] p0055 #78-37434
The 30-cs ion thruster power processor [NASA-CN-135401] p0054 #78-24280
- HESS, L. S.**
Excimer lasers [NASA-CN-155949] p0112 #78-19480
- HIBBERD, D. E.**
Transient dynamics of a flexible rotor with squeeze film dampers [NASA-CN-3050] p0123 #78-32433
- HILL, V. L.**
Thermal fatigue and oxidation data of superalloys including directionally solidified eutectics [NASA-CN-135272] p0078 #78-15233
Thermal fatigue and oxidation data for alloy/brake combinations [NASA-CN-135299] p0078 #78-16149
- HILBERT, E. V.**
Cost benefit study of advanced materials technology for aircraft turbine engines [NASA-CN-135235] p0026 #78-11081
- HILSHO, B. S.**
Millimeter wave satellite concepts, volume 1 [NASA-CN-135227] p0041 #78-15184
- HINES, B. W.**
Fuel consumption improvement in current transport engines [AIAA PAPER 78-930] p0033 #78-45097
- HINSHY, W. E.**
Boundary layer analysis of a Centaur standard shroud [NASA-TN-78843] p0103 #78-27404
Investigation of seams for perturbing the flow field in a supersonic wind tunnel [NASA-TN-78954] p0037 #78-27142
- HIPPENSTIEL, S. A.**
Computer program for obtaining thermodynamic and transport properties of air and products of combustion of ASTA-A-1 fuel and air [NASA-TN-1160] p0008 #78-20351
- HIRSCHBERG, H. S.**
Ductility normalised-strain-range partitioning life relations for creep-fatigue life predictions p0077 #78-51739
Review of the AGARD 5 and 8 panel evaluation program of the NASA-Levin SPP approach to high-temperature LCF life prediction [NASA-TN-78879] p0072 #78-31209
- HIRSCHBERG, H.**
Energy efficient engine: Preliminary design and integration studies [NASA-CN-135444] p0032 #78-31108
- HODDER, B. S.**
Boiling-element fatigue life of AMS 5749 corrosion resistant, high temperature bearing steel [ASME PAPER 77-LUB-30] p0075 #78-28423
- HODSDON, S. B.**
Anion permselective membrane [NASA-CN-135316] p0144 #78-34415
- HOPFMAN, C. A.**
Effect of discontinuities as a means to alleviate thermal expansion mismatch damage in laminar composites [NASA-TN-73719] p0057 #78-11136
Method for alleviating thermal stress damage in laminates [NASA-CASE-LEM-12493-1] p0059 #78-22163
- HOPFMAN, S. E.**
Thermal energy storage for industrial waste heat recovery [NASA-TN-78953] p0140 #78-24474
- HOLANDA, B.**
Reliability analysis of forty-five strain-gauge systems mounted on the first fan stage of a TP-100 engine [NASA-TN-73724] p0109 #78-13407
Recovery and radiation corrections and time constants of several sizes of shielded and unshielded thermocouple probes for measuring gas temperature [NASA-TN-1049] p0104 #78-15463

- TOLSON, J. D.**
Description and review of global measurements of atmospheric species from GASP p0148 A78-24893
Atmospheric ozone measurements made from B-747 airliners - Spring 1975 p0148 A78-24894
Global atmospheric sampling program p0013 A78-11076
An analysis of the first two years of GASP data [NASA-TN-73817] p0148 A78-13669
- HOLLAND, L. B.**
Millimeter wave satellite concepts, volume 1 [NASA-CR-135227] p0041 A78-15144
- HOLLN, G. F.**
Aerodynamic performance of conventional and advanced design labyrinth seals with solid-smooth abradable, and honeycomb leads [NASA-CR-135307] p0122 A78-27427
- HOLMS, A. G.**
'Chain pooling' model selection as developed for the statistical analysis of a rotor burst protection experiment p0160 A78-29327
Concepts for the development of light-weight composite structures for rotor burst containment p0012 A78-10084
Chain Pooling modeling selection as developed for the statistical analysis of a rotor burst protection experiment [NASA-TN-73874] p0160 A78-16735
- HORNECUTT, R. E.**
Advanced optical blade tip clearance measurement system [NASA-CR-159402] p0032 A78-31106
- HONG, J.**
Inward transport of a toroidally confined plasma subject to strong radial electric fields p0172 A78-24890
Inward transport of a toroidally confined plasma subject to strong radial electric fields [NASA-TN-738000] p0171 A78-10883
- HONG, J. Y.**
A data acquisition and handling system for the measurement of radial plasma transport rates [NASA-TN-78849] p0155 A78-23751
A fluctuation-induced plasma transport diagnostic based upon fast-Fourier transform spectral analysis [NASA-TN-78932] p0172 A78-26926
Fluctuation spectra in the NASA Lewis bumpy-torus plasma [NASA-TP-1257] p0172 A78-26927
Low-frequency fluctuation spectra and associated particle transport in the NASA Lewis bumpy-torus plasma [NASA-TP-1258] p0172 A78-30944
- HOPPER, B. J.**
Engineering Model 8-cs Thruster System [AIAA PAPER 78-646] p0055 A78-37434
The 30-cs ion thruster power processor [NASA-CR-135401] p0054 A78-24280
- HORIO, H.**
Fluidized bed combustor modeling [NASA-CR-135164] p0067 A78-14119
- HORSEWOOD, J. L.**
SEP ENCRE-87 and Halley rendezvous studies and improved S/C model implementation in HILTOP [NASA-TP-135414] p0038 A78-25105
Heliocentric interplanetary low thrust trajectory optimization program, supplement 1, part 2 [NASA-CR-135414-APP] p0038 A78-25106
- HOTCHKISS, G. B.**
Comparison of three experimental methods used in determining the thermal performance of flat-plate solar collectors [NASA-TN-78929] p0139 A78-28614
- HOTZ, G. H.**
Cold-air performance of a tip turbine designed to drive a lift fan [NASA-TP-1126] p0003 A78-14998
Cold-air performance of a tip turbine designed to drive a lift fan. 3: Effect of simulated fan leakage on turbine performance [NASA-TP-1109] p0003 A78-16001
- HOUTMAN, W. E.**
General aviation piston-engine exhaust emission reduction p0013 A78-11073
- HUELTZ, B. A.**
Advanced supersonic propulsion study, phase 4 [NASA-CR-135273] p0026 A78-11062
- HUN, L. C.**
Impurity concentrations and surface charge densities on the heavily doped face of a silicon solar cell p0130 A78-13534
Trimerization of aromatic nitriles [NASA-CASE-LEW-12053-1] p0080 A78-15276
In situ self cross-linking of polyvinyl alcohol battery separators [NASA-CASE-LEW-12972-1] p0056 A78-22157
- HUCK, K. L.**
Lean combustion limits of a confined premixed-propanized propane jet [NASA-TN-78868] p0019 A78-22099
- HULSE, C. O.**
Development of Si3N4 and SiC of improved toughness [NASA-CR-135306] p0087 A78-17216
- HUNDEK, F. B.**
Description and review of global measurements of atmospheric species from GASP p0148 A78-24893
- HUNPHREYS, V. E.**
Thermal fatigue and oxidation data of superalloys including directionally solidified eutectics [NASA-CR-135272] p0078 A78-15233
Thermal fatigue and oxidation data for alloy/brake combinations [NASA-CR-135299] p0078 A78-16149
- HUNCEAR, H. B.**
CTS/Bernes/ - United States experiments and operations summary p0094 A78-24886
CTS (Bernes): United States experiments and operations summary [NASA-TN-73830] p0041 A78-13107
- HUPPERT, V. C.**
Liquid rocket engine axial-flow turbopumps [NASA-SP-8125] p0050 A78-31164
- HUSSEMAN, P. W.**
Experiments with enhanced mode thermionic converters p0146 A78-29636
- HUANG, H. H.**
Synchronization of wind turbine generators against an infinite bus under gusting wind conditions [IEEE PAPER P 77 675-2] p0142 A78-30196
Employing static excitation control and tie line reactance to stabilize wind turbine generators [NASA-CR-135344] p0144 A78-20603
- HUANG, S. K.**
The design of an Fe-12Ni-0.2Ti alloy steel for low temperature use [NASA-CR-135310] p0078 A78-20310
- HYMAN, J., JR.**
Engineering Model 8-cs Thruster System [AIAA PAPER 78-646] p0055 A78-37434
- ICB, W. J.**
Design and fabrication of a photovoltaic power system for the Papago Indian village of Schuchuli (Gunsight), Arizona [NASA-TN-78948] p0139 A78-26555
- IGNACIAR, L. B.**
Status of SERT II spacecraft and ion thrusters - 1978 [AIAA PAPER 78-662] p0050 A78-32743
The Plasma Interaction Experiment (PIE) - Description and flight qualification test program [AIAA PAPER 78-674] p0051 A78-32752
Status of SERT II spacecraft and ion thrusters, 1978 [NASA-TN-78827] p0047 A78-20251
The Plasma Interaction Experiment (PIE) description and test program [NASA-TN-78863] p0041 A78-21188
- INGARD, K. U.**
Interaction of a turbulent-jet noise source with transverse modes in a rectangular duct [NASA-TP-1248] p0001 A78-25049
- INGERSO, R. D.**
Effect of airstream velocity on mean drop diameters of water sprays produced by pressure and air atomizing nozzles p0074 A78-33111
Effect of airstream velocity on mean drop diameters of water sprays produced by pressure

- and air atomizing nozzles
[NASA-TN-73780] p0101 W78-13369
- INDOYR, L. V.
Electric prototype power processor for a 30cm ion
thruster
[NASA-CN-135287] p0054 W78-19200
Extended performance electric propulsion power
processor design study. Volume 1: Executive
summary
[NASA-CN-135357] p0054 W78-20250
- IKO, T. I.
Synthesis of perfluoroalkylene aromatic diamines
[NASA-CN-159803] p0087 W78-31235
- IRMS, R. P.
Discrete time domain modelling and analysis of
dc-dc converters with continuous and
discontinuous inductor current
p0100 A78-18796
- J**
- JACK, J. E.
Aerial thermography for energy conservation
[NASA-TN-78959] p0129 W78-33510
- JACKSON, B. B.
A digitally implemented communications experiment
utilizing the Hermes /CTS/ satellite
p0094 A78-28884
A digitally implemented communications experiment
utilizing the Hermes (CTS) satellite
[NASA-TN-73827] p0093 W78-13283
- JACKSON, B. B.
Directionally solidified eutectic gamma-gamma
nickel-base superalloys
[NASA-CASB-LEW-12905-1] p0069 W78-18183
- JACOBSON, T. P.
Some effects of composition on friction and wear
of graphite-fiber-reinforced polyimide liners in
plain spherical bearings
[NASA-TP-1229] p0115 W78-25433
Graphite-fiber-reinforced polyimide liners of
various compositions in plain spherical bearings
[NASA-TN-78908] p0116 W78-26447
- JAMES, E.
A mission profile life test facility
[AIAA PAPER 78-671] p0040 A78-37831
- JANNEY, D. C.
Effects of rotor location, coning, and tilt on
critical loads in large wind turbines
p0141 A78-20476
Effects of rotor location, coning, and tilt on
critical loads in large wind turbines
p0133 W78-19636
- JAY, A.
Effect of steady flight loads on JT9D-7
performance deterioration
[NASA-CN-135407] p0031 W78-29105
- JEFFERIES, K.
A stirling engine computer model for performance
calculations
[NASA-TN-78888] p0180 W78-29994
- JENSEN, E. W.
Evaluation of initial collector field performance
at the Langley Solar Building Test Facility
p0141 A78-11391
- JHA, S.
Considerations to achieve directionality for gamma
ray lasers
p0116 W78-26870
- JOHNSON, R. L.
Altitude test of several afterburner
configurations on a turbofan engine with a
hydrogen heater to simulate an elevated turbine
discharge temperature
[NASA-TP-1068] p0014 W78-11106
- JOHNSON, R. W.
A review of NASA's propulsion programs for civil
aviation
[AIAA PAPER 78-43] p0023 A78-20651
NASA engine system technology programs - An overview
[AIAA PAPER 78-928] p0025 A78-88452
A review of NASA's propulsion programs for aviation
[NASA-TN-73831] p0016 W78-16055
- JOHNSON, J. E.
Variable cycle gas turbine engines
[NASA-CASB-LEW-12916-1] p0113 W78-17384
- JOHNSTON, J. E.
Materials technology assessment for stirling engines
[NASA-TN-73789] p0069 W78-17187
- JOHNSTON, R. P.
Cost benefit study of advanced materials
technology for aircraft turbine engines
[NASA-CN-133235] p0025 W78-11081
Energy efficient engine: Preliminary design and
integration studies
[NASA-CN-133444] p0032 W78-31188
- JOHNSTON, R.
A viscous-inviscid interactive compressor
calculations
[NASA-TN-78920] p0005 W78-26100
- JOHNSTON, R. A.
A viscous-inviscid interactive compressor
calculation
[AIAA PAPER 78-1144] p0006 A78-81843
- JOHNS, R. E.
Design and preliminary results of a
semitranspiration cooled /Lasilloy/ liner for a
high-pressure high-temperature combustor
[AIAA PAPER 78-997] p0025 A78-43544
Emissions reduction technology program
p0012 W78-11065
Design and preliminary results of a
semitranspiration cooled (Lasilloy) liner for a
high-pressure high-temperature combustor
[NASA-TN-78874] p0011 W78-24138
Results and status of the NASA aircraft engine
emission reduction technology program
[NASA-TN-79009] p0022 W78-33102
- JOHNS, W. L.
State-of-the-art of turbofan engine noise control
p0028 A78-35658
- JONES, W. E., JR.
Petrographic analysis of wear debris generated in
accelerated rolling element fatigue tests
p0119 A78-28425
Characterization of wear debris generated in
accelerated rolling-element fatigue tests
[NASA-TP-1203] p0115 W78-21470
Petrographic analysis of wear particles from
sliding elastohydrodynamic experiments
[NASA-TP-1230] p0115 W78-22377
- JOY, F.
Advanced supersonic propulsion study, phases 3 and 4
[NASA-CN-135236] p0027 W78-13058
- JUNASE, A. J.
Performance characteristics of two annular dump
diffusers using suction-stabilized vortex flow
control
p0107 A78-45431
Emissions control for ground power gas turbines
p0013 W78-11072
Performance characteristics of two annular dump
diffusers using suction-stabilized vortex flow
control
[NASA-TN-73857] p0004 W78-19057
Performance of a short annular dump diffuser using
suction-stabilized vortices at inlet Mach
numbers to 0.41
[NASA-TP-1194] p0017 W78-20131
- JURGO, T. L.
Toxic substances alert program
[NASA-TN-73866] p0153 W78-20755
- K**
- KARLBERG, J.
Metastable states of small rare gas crystallites
p0169 A78-16069
- KAPPA, P. E.
JT9D engine diagnostics. Task 2: Feasibility
study of measuring in-service flight loads
[NASA-CN-135395] p0030 W78-27124
- KILBEN, F. P.
Computation of unsteady transonic flows through
rotating and stationary cascades. 2: User's
guide to FORTRAN program BIDATL
[NASA-CN-2901] p0007 W78-12034
- KARNDTNER, L.
Critical currents in sputtered PbMoS8
p0175 A78-45368
Critical currents and scaling laws in sputtered
copper molybdenum sulfide
p0175 A78-45500
- KARUNY, A. E.
Burning of liquid pools in reduced gravity
[NASA-CN-135236] p0067 W78-25150
- KARCHNER, A.
Combustor fluctuating pressure measurements

- in-engine and in a component test facility - A preliminary comparison p0023 178-24878
- Combustor fluctuating pressure measurements in engine and in a component test facility: A preliminary comparison [NASA-TN-73845] p0035 178-13077
- KASCAR, A. P.
Stability of numerical integration techniques for transient rotor dynamics [NASA-TN-1092] p0113 178-10474
- KASPER, E. J.
Investigation of the effect of ceramic coatings on rocket thrust chamber life [NASA-TN-78892] p0049 178-26173
- KAST, W. B.
Oil cooling system for a gas turbine engine [NASA-CASE-LEM-12321-1] p0113 178-10467
- KATSANIS, T.
Calculation of 3-dimensional choking mass flow in turbomachinery with 2-dimensional flow models p0006 178-12289
- KATE, I.
NASCAP, a three-dimensional Charging Analyzer Program for complex spacecraft p0084 178-19567
- Spacecraft-generated plasma interaction with high voltage solar array [AIAA PAPER 78-673] p0055 178-32751
- Dynamic modeling of spacecraft in a collisionless plasma p0037 178-10150
- Solar electric propulsion thruster interactions with solar arrays [NASA-CN-135257] p0052 178-13122
- A three dimensional dynamic study of electrostatic charging in materials [NASA-CN-135256] p0099 178-13328
- NASCAP user's manual [NASA-CN-135259] p0099 178-13329
- KAZEMIAN, A.
Turbine disks for improved reliability p0012 178-10089
- KAZEMIAN, H. H.
Charge-exchange plasma generated by an ion thruster [NASA-CN-135318] p0052 178-13123
- Industrial ion source technology [NASA-CN-135353] p0169 178-18883
- Inert gas thrusters [NASA-CN-135226] p0053 178-19198
- KAZEMIAN, W. B.
Evaluation of commercially-available spacecraft-type heat pipes [AIAA 78-397] p0044 178-35590
- High temperature heat pipe research at NASA Lewis Research Center [AIAA 78-438] p0106 178-35618
- Accelerated life tests of specimen heat pipe from Communication Technology Satellite (CTS) project [NASA-TN-73846] p0102 178-17341
- Evaluation of commercially-available spacecraft-type heat pipes [NASA-TN-78826] p0103 178-20459
- High temperature heat pipe research at NASA Lewis Research Center [NASA-TN-78832] p0103 178-23388
- KAZI, K. B. V.
Nonlinear flap-lag-axial equations of a rotating beam with arbitrary precone angle [AIAA 78-491] p0127 178-29798
- KAZAROFF, J. W.
Investigation of the effect of ceramic coatings on rocket thrust chamber life [NASA-TN-78892] p0049 178-26173
- KEDL, E. J.
Thermal energy storage for industrial waste heat recovery [NASA-TN-78953] p0140 178-29576
- KELLEY, R. B., JR.
Liquid rocket engine turbopump rotating-shaft seals [NASA-SP-8121] p0117 178-30584
- Liquid rocket engine axial-flow turbopumps [NASA-SP-8125] p0050 178-31164
- KELLEY, R. L.
Low cost Ku-band earth terminals for voice/data/facsimile p0094 178-31970
- KEMP, W. H.
Analytical study of laser-supported combustion waves in hydrogen [AIAA PAPER 78-1219] p0067 178-41901
- Analytical study of laser supported combustion waves in hydrogen [NASA-CN-135345] p0112 178-20489
- KENPE, R. E., JR.
Effect of air temperature and relative humidity at various fuel-air ratios on exhaust emissions on a per-node basis of an ATCO Lycoming 4-320 diad light aircraft engine: Volume 1: Results and plotted data [NASA-TN-73507-VOL-1] p0021 178-29100
- KESPER, E. E., JR.
General aviation piston-engine exhaust emission reduction p0013 178-11073
- KENNEDY, J. E.
Study of 61 and 85 GHz coupled cavity traveling-wave tubes for space use [NASA-CN-134670] p0098 178-11295
- KENT, E. B.
An experimental P/W wrought superalloy for advanced temperature service p0073 178-15335
- KERBERT, R. J.
Augmentor emissions reduction technology program [NASA-CN-135215] p0027 178-13057
- KESSELER, W. S.
Status of SERT II spacecraft and ion thrusters - 1978 [AIAA PAPER 78-662] p0050 178-32743
- Evolution of the 1-1/2 lb mercury ion thruster subsystem [AIAA PAPER 78-7118] p0051 178-32776
- Status of SERT II spacecraft and ion thrusters, 1978 [NASA-TN-78827] p0047 178-20251
- Evolution of the 1-1/2 lb mercury ion thruster subsystem [NASA-TN-73733] p0047 178-21202
- Ion propulsion for spacecraft [NASA-TN-79502] p0056 178-26172
- KIRSHING, J. D.
Communication satellite services for special purpose users p0094 178-31971
- KIN, B. S.
Impact on multilayered composite plates [NASA-CN-135247] p0062 178-16103
- KIN, Y.
Inward transport of a toroidally confined plasma subject to strong radial electric fields p0172 178-24890
- KIN, Y. C.
A fluctuation-induced plasma transport diagnostic based upon fast-Fourier transform spectral analysis [NASA-TN-78932] p0172 178-26926
- Low-frequency fluctuation spectra and associated particle transport in the NASA Lewis dump-torus plasma [NASA-TN-1258] p0172 178-30944
- KIN, Y. S.
Inward transport of a toroidally confined plasma subject to strong radial electric fields [NASA-TN-73800] p0171 178-10883
- KING, C. D.
Conceptual design for spacelab two-phase flow experiments [NASA-CN-135127] p0037 178-14063
- KIRBY, P. W.
Linear aerospine engine study [NASA-CN-135231] p0026 178-11082
- KISCH, J. J.
High frequency capacitor-diode voltage multiplier dc-dc converter development [NASA-CN-135309] p0099 178-15400
- KITNER, E. W.
Automotive Stirling engine development program [NASA-CN-135331] p0181 178-22970
- KLASSIN, E. A.
Experimental performance of a 13.65-centimeter-tip-diameter tandem-bladed sweptback centrifugal compressor designed for a pressure ratio of 6 [NASA-TN-10911] p0003 178-11002
- KLIFF, J. F.
Effect of cooling-hole geometry on aerodynamic performance of a film-cooled turbine vane tested with cold air in a two-dimensional cascade

PERSONAL AUTHOR INDEX

KRAUSE, L. E.

- [NASA-TP-1136] p0004 W78-20080
KLINCKT, V. G.
 Summary of the CTS transient Event Counter data after one year of operation p0006 A78-19566
 Preliminary report on the CTS transient event counter performance through the 1976 spring eclipse season p0036 W78-10135
- KLOCHER, T. S.**
 Evaluation of models to predict insolation on tilted surfaces [NASA-TN-78842] p0184 W78-25025
 Variation of solar cell sensitivity and solar radiation on tilted surfaces [NASA-TN-78921] p0138 W78-26547
- KWIGHT, B. S.**
 Planned flight test of a mercury ion auxiliary propulsion syst. II - Integration with host spacecraft [AIAA PAPER 78-647-II] p0050 A78-32735
 Planned flight test of a mercury ion auxiliary propulsion system. Part 2: Integration with host spacecraft [NASA-TN-78869] p0048 W78-21209
- KROLL, E. S.**
 Evaluation of initial collector field performance at the Langley Solar Building Test Facility p0141 A78-11391
- KUOTT, P. S.**
 Acoustic tests of duct-burning turbofan jet noise simulation [NASA-CR-2966] p0002 W78-28043
 Acoustic tests of duct-burning turbofan jet noise simulation: Comprehensive data report. Volume 1, section 2: Full size data [NASA-CR-135239-VOL-1-SRCT-2] p0030 W78-28095
 Acoustic tests of duct-burning turbofan jet noise simulation: Comprehensive data report. Volume 1, section 3: Data plots [NASA-CR-135239-VOL-1-SRCT-3] p0030 W78-28096
 Acoustic tests of duct-burning turbofan jet noise simulation: Comprehensive data report. Volume 2: Model design and aerodynamic test results [NASA-CR-135239-VOL-2] p0031 W78-28097
- KOBAYASHI, S.**
 Three-dimensional effects on pure tone fan noise due to inflow distortion [AIAA PAPER 78-1120] p0166 A78-41830
 Three-dimensional effects on pure tone fan noise due to inflow distortion [NASA-TN-78885] p0164 W78-24898
- KOCH, C. C.**
 Energy efficient engine: Preliminary design and integration studies [NASA-CR-135478] p0032 W78-31108
- KOENIG, E. W.**
 Fabrication and test of digital output interface devices for gas turbine electronic controls [NASA-CR-135427] p0030 W78-27129
- KOPSENY, S. G.**
 Effect of coolant flow ejection on aerodynamic performance of low-aspect-ratio vanes. 2: Performance with coolant flow ejection at temperature ratios up to 2 [NASA-TP-1057] p0003 W78-11008
 Cold-air performance of a tip turbine designed to drive a lift fan [NASA-TP-1126] p0003 W78-14998
 Cold-air performance of a tip turbine designed to drive a lift fan. 3: Effect of simulated fan leakage on turbine performance [NASA-TP-1109] p0003 W78-16001
 Cold-air performance of free-power turbine designed for 112-kilowatt automotive gas-turbine engine. 1: Design Stator-vane-chord setting angle of 35 deg [NASA-TP-1007] p0015 W78-16053
- KOHL, F. J.**
 Volatile products from the interaction of HCl(g)/with Cr2O3 and LaCrO3 in oxidizing environments p0066 A78-24887
 Interaction of NaCl(g) and HCl(g) with condensed H2SO4 p0066 A78-24888
 Formation of H2SO4 and K2SO4 in flames doped with sulfur and alkali chlorides and carbonates p0066 A78-24889
- Formation of H2SO4 and K2SO4 in flames doped with sulfur and alkali chlorides and carbonates [NASA-TN-73794] p0064 W78-13157
 Volatile products from the interaction of HCl(g) with Cr2O3 and LaCrO3 in oxidizing environments [NASA-TN-73795] p0064 W78-13158
 Interaction of NaCl(g) and HCl(g) with condensed H2SO4 [NASA-TN-73796] p0064 W78-13159
 The effect of fuel-to-air ratio on burner-rig hot corrosion [NASA-TN-78960] p0072 W78-31210
- KONATSO, G. E.**
 Ion beam plume and efflux measurements of an 8-cm mercury ion thruster [AIAA PAPER 78-676] p0055 A78-32753
 Ion beam plume and efflux characterization flight experiment study [NASA-CR-135275] p0052 W78-12140
- KONCSER, J. L.**
 VSTOL tilt nacelle aerodynamics and its relation to fan blade stresses [AIAA PAPER 78-958] p0007 A78-83520
 VSTOL tilt nacelle aerodynamics and its relation to fan blade stresses [NASA-TN-78899] p0005 W78-26099
- KOSHARL, E.**
 Noise as a tool for evaluating the activation of cathodes [NASA-TN-73895] p0096 W78-17298
- KOSHARL, S. G.**
 A possible pole problem in the formula for klystron gap fields p0098 A78-18287
- KOSSON, S.**
 Thermal energy storage heat exchanger: Molten salt heat exchanger design for utility power plants [NASA-CR-135244] p0143 W78-14632
 The mol energy storage heat exchanger: Molten salt heat exchanger design for utility power plants [NASA-CR-135245] p0143 W78-14633
- KOVACH, C. W.**
 Fabrication of stainless steel clad tubing [NASA-CR-135347] p0079 W78-21265
- KOZLOWSKI, S.**
 Aero-acoustic tests of duct-burning turbofan exhaust nozzles. Comprehensive data report. Volume 1: Model scale acoustic data [NASA-CR-134910-VOL-1] p0002 W78-15988
 Aero-acoustic tests of duct-burning turbofan exhaust nozzles. Comprehensive data report. Volume 2: Acoustic and aerodynamic data [NASA-CR-134910-VOL-2] p0002 W78-15989
 Aero-acoustic tests of duct-burning turbofan exhaust nozzles. Comprehensive data report. Volume 3: Acoustic and aerodynamic data curves [NASA-CR-134910-VOL-3] p0002 W78-15990
 Flight effects on the aerodynamic and acoustic characteristics of inverted profile coannular nozzles, volume 1 [NASA-CR-135189-VOL-1] p0167 W78-29867
 Flight effects on the aerodynamic and acoustic characteristics of inverted profile coannular nozzles, volume 2 [NASA-CR-135189-VOL-2] p0167 W78-29868
 Flight effects on the aerodynamic and acoustic characteristics of inverted profile coannular nozzles, volume 3 [NASA-CR-135189-VOL-3] p0167 W78-29869
 Flight effects on the aerodynamic and acoustic characteristics of inverted profile coannular nozzles [NASA-CR-3018] p0169 W78-32836
- KRABER, S. S.**
 Long-term CP6 engine performance deterioration: Evaluation of engine S/N 451-479 [NASA-CR-135381] p0029 W78-20129
 Long-term CP6 engine performance deterioration: Evaluation of engine S/N 451-380 [NASA-CR-159390] p0031 W78-29103
- KRATZER, S. S.**
 Synthesis of perfluoroalkylene aromatic diamines [NASA-CR-159403] p0007 W78-31235
- KRAUSE, L. E.**
 Miniature drag force anemometer p0109 A78-17397

- Recovery and radiation corrections and time constants of several sizes of shielded and unshielded thermocouple probes for measuring gas temperature
[NASA-TF-1099] p0109 878-15463
- KRAUCOBER, W. S.**
Inward transport of a toroidally confined plasma subject to strong radial electric fields
p0172 878-24890
- Inward transport of a toroidally confined plasma subject to strong radial electric fields
[NASA-TF-73800] p0171 878-10883
- A data acquisition and handling system for the measurement of radial plasma transport rates
[NASA-TF-78849] p0155 878-23751
- A fluctuation-induced plasma transport diagnostic based upon fast-Fourier transform spectral analysis
[NASA-TF-78932] p0172 878-26926
- Fluctuation spectra in the NASA Lewis bumpy-torus plasma
[NASA-TF-1257] p0172 878-26927
- Low-frequency fluctuation spectra and associated particle transport in the NASA Lewis bumpy-torus plasma
[NASA-TF-1258] p0172 878-30944
- KRISHNAN, R.**
Fluidized bed combustor modeling
[NASA-CR-135164] p0067 878-14119
- KROGER, E. W.**
Diniodide thermionic energy conversion with lanthanum-hexaboride electrodes
[NASA-TF-78887] p0135 878-24617
- Lithium and potassium heat pipes for thermionic converters
[NASA-TF-78946] p0104 878-26390
- Performance of a thermionic converter module utilizing emitter and collector heat pipes
[NASA-TF-78941] p0049 878-27174
- KROSEL, S. W.**
An automated procedure for calculating system matrices from perturbation data generated by an EAI Pacor and 100 hybrid computer system
[NASA-TF-73869] p0156 878-15729
- KUHN, T. E.**
Pollution Reduction Technology Program for small jet aircraft engines, phase 2
[NASA-CR-159415] p0032 878-33104
- KURKOV, A.**
Synthesis of blade flutter vibratory patterns using stationary transducers
[NASA-TF-73821] p0003 878-17001
- KVATZBERG, R. G.**
Nonlinear flap-lag-axial equations of a rotating beam with arbitrary precone angle
[AIAA 78-491] p0127 878-29798
- L**
- LADUS, T. L.**
Liquid jet impingement normal to a disk in zero gravity
[ASME PAPER 78-WA/FE-1] p0107 878-41154
- LAD, R. A.**
Thermal environment effects on strength and impact properties of boron-aluminum composites
p0060 878-33204
- Thermal environment effects on strength and impact properties of boron-aluminum composites
[NASA-TF-73885] p0058 878-17155
- LALLI, V. R.**
Measurement of control system response using an analog operational circuit
[NASA-TF-78937] p0104 878-27386
- LANNETT, S. W.**
Photon degradation effects in terrestrial solar cells
[NASA-TF-78924] p0136 878-25551
- LAWCASHIRE, R. D.**
Distribution of E/N and E sub e in a cross-flow electric discharge laser
p0111 878-24896
- Distribution of E/N and E sub e in a cross-flow electric discharge laser
[NASA-TF-73807] p0111 878-14386
- LAQUAY, R.**
The effect of environmental plasma interactions on the performance of the solar sail system
[NASA-CR-135258] p0098 878-13325
- LARK, E. P.**
An integrated theory for predicting the hydrothermomechanical response of advanced composite structural components
p0060 878-24905
- Correlation of fiber composite tensile strength with the ultrasonic stress wave factor
p0060 878-33207
- Recent advances in lightweight, filament-wound composite pressure vessel technology
p0061 878-33436
- An integrated theory for predicting the hydrothermomechanical response of advanced composite structural components
[NASA-TF-73812] p0125 878-13477
- Correlation of fiber composite tensile strength with the ultrasonic stress wave factor
[NASA-TF-78846] p0058 878-20255
- Titanium/beryllium laminates: Fabrication, mechanical properties, and potential aerospace applications
[NASA-TF-73891] p0059 878-21221
- Effects of moisture profiles and laminate configuration on the hygro stresses in advanced composites
[NASA-TF-78978] p0059 878-32191
- Acoustic emission testing of composite vessels under sustained loading
[NASA-TF-78981] p0059 878-33150
- LARSON, R. E.**
Mean velocity, turbulence intensity and turbulence convection velocity measurements for a convergent nozzle in a free jet wind tunnel. Comprehensive data report
[NASA-CR-135238] p0007 878-17991
- Mean velocity, turbulence intensity and turbulence convection velocity measurements for a convergent nozzle in a free jet wind tunnel
[NASA-CR-2949] p0008 878-21058
- LATHAM, D.**
Acoustic tests of duct-burning turbofan jet noise simulation
[NASA-CR-2966] p0002 878-28043
- Acoustic tests of duct-burning turbofan jet noise simulation: Comprehensive data report. Volume 1, section 2: Full size data
[NASA-CR-135239-VOL-1-SECT-2] p0030 878-28095
- Acoustic tests of duct-burning turbofan jet noise simulation: Comprehensive data report. Volume 1, section 3: Data plots
[NASA-CR-135239-VOL-1-SECT-3] p0030 878-28096
- Acoustic tests of duct-burning turbofan jet noise simulation: Comprehensive data report. Volume 2: Model design and aerodynamic test results
[NASA-CR-135239-VOL-2] p0031 878-28097
- LAUER, J. L.**
Traction and lubricant film temperature as related to the glass transition temperature and solidification
p0087 878-40997
- Study of dynamic emission spectra from lubricant films in an elastohydrodynamic contact using Fourier transform spectroscopy
[NASA-CR-159418] p0162 878-32809
- LAVERGNE, R. R.**
Parametric dependence of ion temperature and relative density in the NASA Lewis SUHRA facility
[NASA-TF-73770] p0172 878-23523
- LAVERGNE, R. W.**
Kinetics of imidization and crosslinking in PNB-polyimide resin
p0061 878-33210
- Effects of hydrothermal exposure on a low-temperature cured epoxy
[NASA-TF-73841] p0081 878-17220
- Kinetics of imidization and crosslinking in PNB-polyimide resin
[NASA-TF-78844] p0082 878-23231
- LAVERGNE, R. P.**
Compressor seal rub energetics study
[NASA-CR-159426] p0032 878-32096
- LAYDEN, G. K.**
Development of SiALON materials
[NASA-CR-135290] p0087 878-21289
- LEE, D.**
Airflow and thrust calibration of an F100 engine,

PERSONAL AUTHOR INDEX

LOW, J. R., JR.

- S/N P680059, at selected flight conditions
[NASA-TP-1069] p0018 878-21112
Altitude calibration of an F100, S/W P680063,
turbofan engine
[NASA-TP-1228] p0019 878-23095
- LEE, F. C.
Discrete time domain modelling and analysis of
dc-dc converters with continuous and
discontinuous inductor current p0100 878-18796
Modeling and Analysis of Power Processing Systems
(NAPPS), initial phase 2
[NASA-CR-135173] p0100 878-29350
- LEE, M. C.
Methods for calculating the transonic boundary
layer separation for V/STOL inlets at high
incidence angles
[AIAA 78-1340] p0007 878-86537
- LEE, J. C.
Hydrogen turbine power conversion system assessment
[NASA-CR-135298] p0104 878-20621
- LEE, R.
QCSEE task 2: Engine and installation preliminary
design
[NASA-CR-134738] p0030 878-23089
- LEEVISHEN, B.
Optimal control of a supersonic inlet to minimize
frequency of inlet unstart p0019 878-23024
- LEHNER, C. B.
Thermal barrier coating system
[NASA-CASE-LEW-12554-1] p0102 878-18355
- LEHNINGER, G. G.
Diagonal dominance using function minimization
algorithms p0159 878-16304
- LEHWARD, D. J.
NASA/General Electric Engine Component Improvement
Program
[AIAA PAPER 78-929] p0025 878-85098
- LEHS, R. C., JR.
A forecast of broadcast satellite communications
p0098 878-15615
- LEHWARD, K. E.
Thermal performance of a customized multilayer
insulation (MLI). Design and fabrication of
test facility hardware
[NASA-CR-157648] p0062 878-20257
- LEROY, B. F.
Disaster warning system study summary
[NASA-TN-73797] p0093 878-10346
- LESTYINGI, J.
Constrained sloshing of liquid mercury in a
flexible spherical tank
[AIAA PAPER 78-670] p0106 878-32749
Constrained sloshing of liquid mercury in a
flexible spherical tank
[NASA-TN-78833] p0103 878-21403
- LEWIS, S. B.
Reaction diffusion in the NiCrAl and CoCrAl systems
p0077 878-53063
Adhesive/cohesive strength of a ZrO₂-1-2 w/c
TZ03/NiCrAl thermal barrier coating
[NASA-TN-73792] p0057 878-17152
High temperature surface protection
[NASA-TN-73877] p0102 878-17340
Thermal barrier coatings
[NASA-TN-78648] p0059 878-24291
- LEWIS, G. W., JR.
Performance of a transonic fan stage designed for
a low meridional velocity ratio
[NASA-TP-1298] p0022 878-33107
- LEWIS, R. O., JR.
Viking and STP P78-2 electrostatic charging
designs and testing p0037 878-10175
- LEWIS, E. A.
Global atmospheric sampling program p0013 878-11076
- LILES, T.
Lamination residual strains and stresses in hybrid
laminates p0128 878-12071
- LICK, W.
Numerical computation of three-dimensional
circulation in Lake Erie - A comparison of a
free-surface model and a rigid-lid model
p0151 878-87223
- LIEN, D. P.
Performance of a thermionic converter module
utilizing emitter and collector heat pipes
[NASA-TN-78941] p0045 878-27174
- LIEBERT, C. E.
Emitance and absorptance of NASA ceramic thermal
barrier coating system
[NASA-TP-1190] p0020 878-26148
- LIEBHARD, J. H.
Conceptual design for spacelab pool boiling
experiment
[NASA-CR-135378] p0037 878-20150
- LIEBOWITZ, P. A.
A methodology for experimentally-based
determination of gap shrinkage and effective
lifetimes in the emitter and base of
p-n-junction solar cells p0141 878-10903
- LIEBOW, B. G.
An airborne meteorological data collection system
using satellite relay (ASDAR)
[NASA-TN-78992] p0093 878-33283
- LIEBSCHNEIT, J. E.
Ceramic regenerator systems development program
[NASA-CR-135330] p0181 878-25988
Ceramic regenerator systems development program
[NASA-CR-135430] p0181 878-26997
- LIESCOTT, B. S.
Approximate method for calculating free vibrations
of a large-wind-turbine tower structure
[NASA-TN-73754] p0131 878-16434
Experimental data and theoretical analysis of an
operating 100 kW wind turbine
[NASA-TN-73883] p0133 878-19642
- LIESENHARDT, T. L.
Extended performance solar electric propulsion
thrust system study. Volume 4: Thruster
technology evaluation
[NASA-CR-135281-VOL-4] p0053 878-16090
- LOEFFLER, I. J.
Acoustic design of the QCSEE propulsion systems
p0004 878-24067
- LOEWENTHAL, S. B.
Proposed design procedure for transmission
shafting under fatigue loading
[NASA-TN-78927] p0115 878-26444
Filtration effects on ball bearing life and
condition in a contaminated lubricant
[NASA-TN-78907] p0116 878-26446
Effect of filtration on rolling-element-bearing
life in contaminated lubricant environment
[NASA-TP-1272] p0116 878-28457
- LOEWELL, J. P.
Alternative aircraft fuels p0088 878-17229
Jet aircraft hydrocarbon fuels technology
[NASA-CP-2033] p0058 878-19325
- LOVE, B. A.
Method of fan sound mode structure determination
computer program user's manual: Microphone
location program
[NASA-CR-135298] p0028 878-17065
Method of fan sound mode structure determination
computer program user's manual: Modal
calculation program
[NASA-CR-135295] p0028 878-17066
- LOVELL, B. B.
Proceedings of the Spacecraft Charging Technology
Conference
[NASA-TN-8-73537] p0036 878-10129
Preliminary report on the CTS transient event
counter performance through the 1976 spring
eclipse season p0036 878-10135
Provisional specification for satellite time in a
geomagnetic environment p0036 878-10173
Liquid metal slip ring
[NASA-CASE-LEW-12277-2] p0097 878-25323
- LOW, J. R. C.
Effect of forward motion on engine noise
[NASA-CR-136954] p0026 878-10093
- LOW, J. R., JR.
Investigation of the fracture mechanics of
Ti-5Al-2.5Sn at cryogenic temperatures
p0075 878-32319
The influence of composition, annealing treatment,
and texture on the fracture toughness of
Ti-5Al-2.5Sn plate at cryogenic temperatures

- [NASA-TN-73672] p0069 N78-15235
The effect of microstructure and strength on the fracture toughness of an 18 Ni, 300 grade maraging steel
- [NASA-CN-135288] p0078 N78-16150
LOWELL, C.
Burner rig alkali salt corrosion of several high temperature alloys
- p0073 N78-18793
- LOWELL, C. B.
High temperature environmental effects on metals p0075 N78-29329
The role of thermal shock in cyclic oxidation p0076 N78-37676
The cyclic oxidation resistance of cobalt chromium-aluminum alloys at 1100 and 1200 C and a comparison with the nickel-chromium-aluminum alloy system p0077 N78-50086
High temperature environmental effects on metals [NASA-TN-73878] p0017 N78-19158
The role of thermal shock in cyclic oxidation [NASA-TN-78876] p0070 N78-23193
Erosion/corrosion of turbine airfoil materials in the high-velocity effluent of a pressurized fluidized coal combustor [NASA-TP-1278] p0071 N78-28225
Inhibition of hot salt corrosion by metallic additives [NASA-TN-78966] p0072 N78-31208
The effect of fuel-to-air ratio on burner-rig hot corrosion [NASA-TN-78960] p0072 N78-31210
- LUCAS, J. G.
Acoustic evaluation of a novel swept-rotor fan [AIAA PAPER 78-1121] p0166 N78-41931
Acoustic evaluation of a novel swept-rotor fan [NASA-TN-78878] p0164 N78-24897
- LUCCI, A. D.
Hydrogen turbine power conversion system assessment [NASA-CN-135298] p0144 N78-20621
- LUDWIG, L. F.
Design considerations in mechanical face seals for improved performance. I - Basic configurations [ASME PAPER 77-WA/LUB-3] p0119 N78-33183
Design considerations in mechanical face seals for improved performance. II - Lubrication [ASME PAPER 77-WA/LUB-4] p0120 N78-33184
Gas path sealing in turbine engines p0024 N78-33218
Self-acting shaft seals p0120 N78-33219
Design considerations in mechanical face seals for improved performance. I: Basic configurations [NASA-TN-73735] p0113 N78-13439
Self-acting shaft seals [NASA-TN-73856] p0114 N78-19513
Gas path sealing in turbine engines [NASA-TN-73890] p0018 N78-21109
Counter pumping debris excluder and separator [NASA-CASE-LEW-11855-1] p0020 N78-25090
Gas path seal [NASA-CASE-LEW-12131-2] p0021 N78-31103
- LUDWIG, R. W.
Methods for calculating the transonic boundary layer separation for V/STOL inlets at high incidence angles [AIAA 78-1340] p0007 N78-86537
Theoretical flow characteristics of inlets for tilting-nacelle VTOL aircraft [NASA-TP-1205] p0018 N78-21114
Inlet technology for powered-lift aircraft p0005 N78-24069
- LUNANWICK, S.
Baseline tests of the power-train electric delivery van [NASA-TN-73765] p0178 N78-17936
Performance of conventionally powered vehicles tested to an electric vehicle test procedure [NASA-TN-73768] p0179 N78-20022
- LUO, H.-L.
Critical currents in sputtered PbMo6S8 p0175 N78-45368
Critical currents and scaling laws in sputtered copper molybdenum sulfide p0175 N78-45500
- M**
- MACIOCE, L. E.
Design approaches to more energy efficient engines [AIAA PAPER 78-931] p0025 N78-43504
Design approaches to more energy efficient engines [NASA-TN-78893] p0115 N78-26442
- MACKINNON, R. J.
Effectiveness of an inlet flow turbulence control device to simulate flight fan noise in an anechoic chamber p0115 N78-26442
Reduction of fan noise in an anechoic chamber by reducing chamber wall induced inlet flow disturbances p0166 N78-37681
Acoustic evaluation of a novel swept-rotor fan [AIAA PAPER 78-1121] p0166 N78-41831
Effectiveness of an inlet flow turbulence control device to simulate flight noise in an anechoic chamber [NASA-TN-73855] p0163 N78-13856
Reduction of fan noise in an anechoic chamber by reducing chamber wall induced inlet flow disturbances [NASA-TN-78854] p0164 N78-22860
Acoustic evaluation of a novel swept-rotor fan [NASA-TN-78878] p0164 N78-24897
- MAISEL, J. E.
Thermal environment effects on strength and impact properties of boron-aluminum composites p0060 N78-33204
Measurement of the time-temperature dependent dynamic mechanical properties of boron/aluminum composites p0061 N78-33222
Thermal environment effects on strength and impact properties of boron-aluminum composites [NASA-TN-73885] p0058 N78-17155
Measurement of the time-temperature dependent dynamic mechanical properties of boron/aluminum composites [NASA-TN-78837] p0058 N78-20254
- MALLAVARPU, N.
Lower hybrid emission diagnostics on the NASA Lewis Bumpy Torus p0173 N78-29332
Lower hybrid emission diagnostics on the NASA Lewis bumpy torus [NASA-TN-73858] p0171 N78-19938
Microwave radiation measurements near the electron plasma frequency of the NASA Lewis bumpy torus plasma [NASA-TN-78940] p0172 N78-27914
- MALOY, J. E.
Disaster warning system study summary [NASA-TN-73797] p0093 N78-10346
- MARDELL, J. F.
Analysis of delamination in unidirectional and crossplied fiber composites containing surface cracks [NASA-CN-135248] p0062 N78-11197
- MARDELL, S. J.
MASCAP, a three-dimensional Charging Analyzer Program for complex spacecraft p0044 N78-19567
MASCAP Charging Analyzer Program - A computer tool that can evaluate electrostatic contamination p0044 N78-33220
A three dimensional dynamic study of electrostatic charging in materials [NASA-CN-135256] p0099 N78-13328
MASCAP user's manual [NASA-CN-135259] p0099 N78-13329
MASCAP charging analyzer program: A computer tool that can evaluate electrostatic contamination [NASA-TN-73889] p0096 N78-21372
- MARISTA, E. J.
Distribution of E/N and W/e in a cross-flow electric discharge laser p0111 N78-24896
A review of the Thermo-electronic Laser Energy Converter /TELEC/ Program at Lewis Research Center p0142 N78-33217
Preliminary results on the conversion of laser energy into electricity p0173 N78-34631

- Small-signal gain diagnostic measurements in a flowing CO₂ pin discharge laser
[NASA-TN-73843] p0111 N78-13821
- Distribution of E/N and N sub e in a cross-flow electric discharge laser
[NASA-TN-73887] p0111 N78-14386
- A review of the thermoelectric laser energy converter (TELEC) program at Lewis Research Center
[NASA-TN-73888] p0111 N78-21441
- HARR, P. I.
SEP TUCKER-87 and Halley rendezvous studies and improved S/C model implementation in HILTOP
[NASA-CR-135414] p0038 N78-25105
- Heliocentric interplanetary low thrust trajectory optimization program, supplement 1, part 2
[NASA-CR-135414-APP] p0038 N78-25106
- HAROS, P.
WASTRAW use for cyclic response and fatigue analysis of wind turbing towers p0125 N78-12459
- HARSON, S. S.
Interpolation and extrapolation of creep rupture data by the sinus commitment method. II - Oblique translation p0076 A78-45426
- Interpolation and extrapolation of creep rupture data by the sinus commitment method. I - Focal-point convergence p0076 A78-45427
- Interpolation and extrapolation of creep rupture data by the sinus commitment method. III - Analysis of subheats p0076 A78-45428
- Interpolation and extrapolation of creep rupture data by the sinus commitment method. Part 1: Focal-point convergence
[NASA-TN-78881] p0125 N78-23471
- Interpolation and extrapolation of creep rupture data by the sinus commitment method. Part 2: Oblique translation
[NASA-TN-78882] p0125 N78-23472
- Interpolation and extrapolation of creep rupture data by the sinus commitment method. Part 3: Analysis of subheats
[NASA-TN-78883] p0126 N78-23473
- HARTWIGERS, B. A.
5200 cycle of an 8-cm diameter Hg ion thruster
[AIAA PAPER 78-649] p0050 A78-32736
- Effect of facility background gases on internal erosion of the 30-cm Hg ion thruster
[AIAA PAPER 78-665] p0050 A78-32745
- Effect of facility background gases on internal erosion of the 30-cm Hg ion thruster
[NASA-TN-73803] p0048 N78-21205
- The 5200 cycle test of an 8-cm diameter Hg ion thruster
[NASA-TN-78860] p0048 N78-21208
- HARCUS, B. D.
CTS TFR thermal anomalies: Heat pipe system performance
[NASA-CR-159413] p0108 N78-29410
- HAREK, C. J.
Fuel combustor
[NASA-CASE-LEW-12137-1] p0064 N78-10224
- Stratospheric cruise emission reduction program p0013 N78-11077
- Lean combustion limits of a confined premixed-prevaporized propane jet
[NASA-TN-78868] p0019 N78-22099
- Supercritical fuel injection system
[NASA-CASE-LEW-12990-1] p0020 N78-27122
- HARGRAVE, J. L.
Materials science experiments in space
[NASA-CR-2842] p0056 N78-16094
- HARKOVITS, B.
Materials science experiments in space
[NASA-CR-2842] p0056 N78-16094
- HARQUIS, G. A.
Design and fabrication of a low-specific-weight parabolic dish solar concentrator
[NASA-TP-1152] p0046 N78-17145
- HARSIN, S. J.
Preliminary evaluation of Glass Resin materials for solar cell cover use
[NASA-TN-78925] p0137 N78-26544
- Ultraviolet irradiation at elevated temperatures and thermal cycling in vacuum of PEP-A covered silicon solar cells
[NASA-TN-78926] p0137 N78-26545
- HARTWELL, B. E.
High frequency capacitor-diode voltage multiplier dc-dc converter development
[NASA-CR-135309] p0099 N78-15400
- Extended performance solar electric propulsion thrust system study. Volume 2: Thruster technology evaluation
[NASA-CR-135281-VOL-4] p0053 N78-16090
- Extended performance solar electric propulsion thrust system study. Volume 3: Capacitor-diode voltage multiplier: Technology evaluation
[NASA-CR-135281-VOL-5] p0053 N78-19195
- HARTWILL, B. E.
Stirling engine design manual
[NASA-CR-135382] p0181 N78-23999
- HARTING, J. B.
A forecast of broadcast satellite communications p0094 A78-15615
- HASER, T. D.
Economics of ion propulsion for large space systems
[AIAA PAPER 78-698] p0040 A78-37441
- HASLOVSKI, E. A.
Baseline tests of the Sagato Elcar electric passenger vehicle
[NASA-TN-73764] p0178 N78-17934
- Baseline tests of the EVA change-of-pace coupe electric passenger vehicle
[NASA-TN-73763] p0178 N78-17938
- Baseline tests of the batronic Minivan electric delivery van
[NASA-TN-73761] p0179 N78-17990
- Baseline tests of the C. H. Waterson DAF electric passenger vehicle
[NASA-TN-73757] p0179 N78-17942
- Baseline tests of the EPC Hummingbird electric passenger vehicle
[NASA-TN-73760] p0180 N78-21010
- HASSEL, H. A.
Analysis and design of a high power laser adaptive phased array transmitter
[NASA-CR-134952] p0111 N78-13420
- HASTBS, B. B.
Solar energy meter
[NASA-TN-73791] p0131 N78-14630
- HAY, C. E.
Determination of the zincate diffusion coefficient and its application to alkaline battery problems
[NASA-TN-73879] p0134 N78-19648
- HASSAW, B. S.
P100(3) parallel compressor computer code and user's manual
[NASA-CR-135388] p0029 N78-22096
- HARDLE, J. C.
Development and test of an inlet and duct to provide airflow for a wing boundary layer control system
[AIAA PAPER 78-141] p0006 A78-20701
- HCBRIDE, B. J.
Computer program for calculation of complex chemical equilibrium compositions, rocket performance, incident and reflected shocks, and Chapman-Jouguet detonations
[NASA-SP-273] p0156 N78-17724
- HCBRINE, E. P.
Baseline tests of the C. H. Waterson Renault 5 electric passenger vehicle
[NASA-TN-73759] p0178 N78-16928
- Baseline tests of the Volkswagen transporter electric delivery van
[NASA-TN-73766] p0179 N78-20021
- HCCANTON, J. F., JR.
Engineering in the 21st century
[NASA-TN-79010] p0105 N78-33380
- HCLLIWOCK, R. B.
Revised international representations for the viscosity of water and steam and new representations for the surface tension of water p0105 A78-17725
- MCCOLLAM, C. J.
Mean velocity, turbulence intensity and turbulence convection velocity measurements for a convergent nozzle in a free jet wind tunnel. Comprehensive data report
[NASA-CR-135238] p0007 N78-17591
- Mean velocity, turbulence intensity and turbulence convection velocity measurements for a convergent nozzle in a free jet wind tunnel
[NASA-CR-2949] p0008 N78-21058

- SCOLLISTER, E. L.
Improved ceramic heat exchange material
[NASA-CN-135262] p0086 878-10291
- SCODNICK, J.
Hydrodynamic air lubricated compliant surface
bearing for an automotive gas turbine engine.
1: Journal bearing performance
[NASA-CN-135368] p0121 878-21472
- SCOWELL, G.
A low cost, portable instrument for measuring
emittance p0109 878-11392
- SCOWELL, G. E.
Black chrome on commercially electroplated tin as
a solar selecting coating
[NASA-TN-73799] p0131 878-15562
Selective coating for solar panels
[NASA-CASB-LTR-12159-1] p0132 878-19599
- SCOWELL, E.
Derivation and evaluation of an approximate
analysis for three-dimensional viscous subsonic
flow with large secondary velocities
[NASA-CN-159830] p0C08 878-24088
- SCOWELL, J. E.
Effects of film injection on performance of a
cooled turbine p0033 878-24902
Effects of film injection on performance of a
cooled turbine p0029 878-21147
- SCRAFF, R. J.
Extended performance solar electric propulsion
thrust system study. Volume 8: Thruster
technology evaluation
[NASA-CN-135281-VOL-8] p0053 878-16090
- SCROGAN, F.
Oil-air mist lubrication for helicopter gearing
[NASA-CN-135081] p0010 878-25080
- SCWAGE, D. P.
Variable mixer propulsion cycle
[NASA-CASB-LTR-12917-1] p0016 878-18067
- SCYKIN, D. J., JR.
BPF noise suppression and aerodynamic penalties
[NASA-TN-73823] p0163 878-15852
Analytical modeling of under-the-wing externally
blown flap powered-lift noise p0004 878-24063
- SCYKIN, L. J., JR.
BPF noise suppression and aerodynamic penalties
[AIAA PAPER 78-240] p0165 878-20763
- MCALLAN, E. L.
Effect of endwall cooling on secondary flows in
turbine stator vanes p0014 878-11098
Cold-air performance of the compressor-drive
turbine of the Department of Energy baseline
automobile gas-turbine engine
[NASA-TN-78894] p0005 878-26098
- MCALWELLS, P. E.
High frequency dynamic engine simulation
[NASA-CN-135313] p0027 878-13059
- MCHELLY, G. D.
Review of experimental work on transonic flow in
turbomachinery p0006 878-12312
- MCITNER, P. L.
FORTRAN program for calculating coolant flow and
metal temperatures of a
full-coverage-film-cooled vane or blade
[NASA-TN-1259] p0021 878-28099
Analysis of metal temperature and coolant flow
with a thermal-barrier coating on a
full-coverage-film-cooled turbine vane
[NASA-TN-1310] p0022 878-31109
- MCLEASON, E. T.
Effects of nozzle design and power on cruise drag
for upper-surface-blowing aircraft p0004 878-24058
- MCLENN, P.
Impact resistant boron/aluminum composites for
large fan blades
[NASA-CN-135278] p0062 878-14099
- MCNEELSON, A.
Stress analysis and stress-intensity factors for
finite geometry solids containing rectangular
surface cracks
[ASME PAPER 77-WA/APP-5] p0126 878-10531
The use of parabolic variations and the direct
determination of stress intensity factors using
the BIS method p0126 878-24903
- MESE, P. E.
Effect of air temperature and relative humidity at
various fuel-air ratios on exhaust emissions on
a per-mode basis of an AVCO Lycoming O-328 diad
light aircraft engine: Volume 1: Results and
plotted data
[NASA-TN-73507-VOL-1] p0021 878-29100
- MEYER, E. W.
Aerodynamic design and performance testing of an
advanced 30 deg swept, eight bladed propeller at
Mach numbers from 0.2 to 0.85
[NASA-CN-3047] p0008 878-32066
- MEYER, F.
Filling of orbital fluid management system
[NASA-CN-159808] p0108 878-31380
- MEYER, F.
Experimental transient and permanent deformation
studies of steel-sphere-impacted or
explosively-impacted aluminum panels
[NASA-CN-135315] p0078 878-15238
- MEYER, W.
Output feedback regulator design for jet engine
control systems p0024 878-24898
- MEYER, W. C.
The application of the South approximation method
to turbofan engine models p0023 878-23891
Design of turbofan engine controls using output
feedback regulator theory p0023 878-23907
Applied South approximation
[NASA-TN-1231] p0091 878-22257
An inverter/controller subsystem optimized for
photovoltaic applications
[NASA-TN-78902] p0180 878-26995
Performance and stability analysis of a
photovoltaic power system
[NASA-TN-78880] p0140 878-29566
- MEYER, J. E.
Effect of forward motion on engine noise
[NASA-CN-134954] p0026 878-10093
- MEYER, G. E.
Analysis and design of a high power laser adaptive
phased array transmitter
[NASA-CN-134952] p0111 878-13420
- MEYER, D.
A stirling engine computer model for performance
calculations
[NASA-TN-78884] p0180 878-29998
Simulation model of a single-stage lithium
bromide-water absorption cooling unit
[NASA-TN-1296] p0072 878-30205
- MEYER, E. E.
Modelling, analyses and design of switching
converters
[NASA-CN-135174] p0100 878-29351
- MEYER, P.
Preliminary power train design for a
state-of-the-art electric vehicle
[NASA-CN-135311] p0182 878-29992
- MEYER, J. E.
Real time digital propulsion system simulation for
sanned flight simulators
[AIAA PAPER 78-927] p0035 878-45095
Real time digital propulsion system simulation for
sanned flight simulators
[NASA-TN-78958] p0034 878-27137
- MILLER, E. A.
Effect of design changes on aerodynamic and
acoustic performance of translating-centerbody
sonic inlets
[NASA-TN-1132] p0003 878-17998
Status of advanced turboprop technology p0001 878-27055
- MILLER, D. E.
Wind Turbine Structural Dynamics
[NASA-CN-2034] p0132 878-19616
Summary of static load test of the Rod-0 blade
p0133 878-19627
- MILLER, E. F.
Carrier-interference ratios for frequency sharing
between frequency-modulated
amplitude-modulated-vestigial-sideband
television systems
[NASA-TN-1264] p0043 878-28159

- HILLES, S. S.
Volatile products from the interaction of KCl(g)/
with Cr₂O₃ and LaCrO₃ in oxidizing environments
p0066 A78-24887
Interaction of NaCl(g) and KCl(g) with condensed
H₂SO₄ p0066 A78-24888
Formation of H₂SO₄ and K₂SO₄ in flames doped with
sulfur and alkali chlorides and carbonates
p0066 A78-24889
Formation of H₂SO₄ and K₂SO₄ in flames doped with
sulfur and alkali chlorides and carbonates
[NASA-TN-73794] p0064 A78-13157
Volatile products from the interaction of KCl(g)
with Cr₂O₃ and LaCrO₃ in oxidizing environments
[NASA-TN-73795] p0064 A78-13158
Interaction of NaCl(g) and KCl(g) with condensed
H₂SO₄
[NASA-TN-73796] p0064 A78-13159
- HILLES, B. L.
Escort - A data acquisition and display system to
support research testing p0155 A78-37685
Escort: A data acquisition and display system to
support research testing
[NASA-TN-78909] p0154 A78-24807
- HILLES, T. B.
Ion beam sputter etching and deposition of
fluoropolymers p0085 A78-37684
Ion beam sputter etching and deposition of
fluoropolymers
[NASA-TN-78886] p0088 A78-24358
- HILLES, T. J.
An overview of aerospace gas turbine technology of
relevance to the development of the automotive
gas turbine engine
[SAB PAPER 780075] p0120 A78-33364
An overview of aerospace gas turbine technology of
relevance to the development of the automotive
gas turbine engine
[NASA-TN-73849] p0014 A78-13062
- HILLES, E. J.
An automated procedure for calculating system
matrices from perturbation data generated by an
RAY Pacer and 100 hybrid computer system
[NASA-TN-73849] p0156 A78-15729
- HINCH, B. V.
An experimental P/W wrought superalloy for
advanced temperature service p0073 A78-15335
- HINCH, B. V., JR.
Effects of silicon on the oxidation,
hot-corrosion, and mechanical behavior of two
cast nickel-base superalloys p0074 A78-21439
- HINTICH, E. J.
Optical and electrical properties of ion beam
textured Kapton and Teflon p0085 A78-24908
A hollow cathode hydrogen ion source
p0173 A78-39835
Optical and electrical properties of ion beam
textured Kapton and Teflon
[NASA-TN-73778] p0162 A78-13848
- HISKOLCHY, G.
Lithium and potassium heat pipes for thermionic
converters
[NASA-TN-78946] p0104 A78-26390
Performance of a thermionic converter module
utilizing emitter and collector heat pipes
[NASA-TN-78941] p0049 A78-27174
- HIYOSHI, K.
Friction, deformation and fracture of
single-crystal silicon carbide
[ASLE PREPRINT 77-LC-5C-3] p0085 A78-28438
Friction and wear behavior of single-crystal
silicon carbide in sliding contact with various
metals p0086 A78-44095
Friction and wear of single-crystal and
polycrystalline manganese-zinc ferrite in contact
with various metals
[NASA-TN-1059] p0080 A78-10295
Friction and wear behavior of single-crystal
silicon carbide in sliding contact with various
metals
[NASA-TN-73782] p0114 A78-19512
- Friction and metal transfer for single-crystal
silicon carbide in contact with various metals
in vacuum
[NASA-TN-1191] p0092 A78-21294
Wear of single-crystal silicon carbide in contact
with various metals in vacuum
[NASA-TN-1190] p0082 A78-21295
Effect of oxygen and nitrogen interactions on
friction of single-crystal silicon carbide
[NASA-TN-1265] p0083 A78-28247
Friction and wear of metals with a single-crystal
abrasive grit of silicon carbide: Effect of
shear strength of metal
[NASA-TN-1293] p0084 A78-30238
- HO, T.
Cloud effects on middle ultraviolet global radiation
p0150 A78-42952
- HOFFITE, T. P.
Effect of cooling-hole geometry on aerodynamic
performance of a film-cooled turbine vane tested
with cold air in a two-dimensional cascade
[NASA-TN-1136] p0004 A78-20880
- HOLLS, P. B.
Numerical computation of three-dimensional
circulation in Lake Erie - a comparison of a
free-surface model and a rigid-lid model
p0151 A78-47223
- HORSIA, E. C.
Pollution Reduction Technology Program for small
jet aircraft engines, phase 2
[NASA-CN-159415] p0032 A78-33104
- HOVE, F. C.
Impact on multilayered composite plates
[NASA-CN-135247] p0062 A78-16103
- HOORN, H. Y.
Sound separation probes for flowing duct noise
measurements p0033 A78-17396
- HOORN, B. D.
Performance of a transonic fan stage designed for
a low meridional velocity ratio
[NASA-TN-1298] p0022 A78-33107
Design and overall performance of four highly
loaded, high speed inlet stages for an advanced
high-pressure-ratio core compressor
[NASA-TN-1337] p0022 A78-33108
- HOORN, F. J.
Elevated-temperature flow strength, creep
resistance and diffusion welding characteristics
of Ti-6Al-2Nb-1Ta-0.8W
[NASA-TN-73854] p0069 A78-17190
The use of ion beam cleaning to obtain high
quality cold welds with minimal deformation
[NASA-TN-78933] p0083 A78-27257
- HOORNHAD, P. E.
Acoustic emission testing of composite vessels
under sustained loading
[NASA-TN-78961] p0059 A78-33150
- HORRIS, J. P.
High-temperature, high-power-density thermionic
energy conversion for space
[NASA-TN-73844] p0171 A78-13690
Optimize out-of-core thermionic energy conversion
for nuclear electric propulsion
[NASA-TN-73892] p0170 A78-17856
Disinfect thermionic energy conversion with
lanthanum-hexaboride electrodes
[NASA-TN-78887] p0135 A78-24617
Cesium thermionic converters having improved
electrodes
[NASA-CASH-LEN-12030-3] p0137 A78-25555
Performance of a thermionic converter module
utilizing emitter and collector heat pipes
[NASA-TN-78941] p0049 A78-27174
Spacecraft charging control by thermal, field
emission with lanthanum-hexaboride emitters
[NASA-TN-78940] p0183 A78-32014
- HORRIS, J. W., JR.
The design of an Fe-12Ni-0.2Ti alloy steel for low
temperature use
[NASA-CN-135310] p0078 A78-20310
- NOTER, D. W.
Filtration effects on ball bearing life and
condition in a contaminated lubricant
[NASA-TN-78907] p0116 A78-26466
Effect of filtration on rolling-element-bearing
life in contaminated lubricant environment
[NASA-TN-1272] p0116 A78-28857

ROSENCO, R. V.
Employing static excitation control and tie line reactance to stabilize wind turbine generators [NASA-CR-135344] p0144 W78-20603

ROSE, T. E.
Emissions control for ground power gas turbines p0013 W78-11072
Design and fabrication of a low-specific-weight parabolic dish solar concentrator [NASA-TP-1152] p0086 W78-17145
Direct heating surface combustor [NASA-CASE-LRW-11877-1] p0097 W78-27357

RULAKE, R. J.
Combustor concepts for aircraft gas turbine low-power emissions reduction [AIAA PAPER 78-999] p0025 A78-43546
Emissions control for ground power gas turbines p0013 W78-11072
Combustor concepts for aircraft gas turbine low-power emissions reduction [NASA-TN-78875] p0020 W78-26143
Reverse-flow combustor for small gas turbines with pressure-atomizing fuel injectors [NASA-TP-1260] p0021 W78-27130

RYERS, I. T.
Medium power voltage multipliers with a large number of stages p0098 A78-45435
Medium power voltage multipliers with a large number of stages [NASA-TN-78900] p0093 W78-26373
Regulated high efficiency, lightweight capacitor-diode multiplier dc to dc converter [NASA-CASE-LRW-12791-1] p0097 W78-32341

RYERS, P. S.
The role of drop velocity in statistical spray description p0107 W78-50323
The role of drop velocity in statistical spray description [NASA-TN-73807] p0102 W78-20458

N

NACHTIGALL, L. J.
Strainrange partitioning behavior of the nickel-base superalloys, Rene 80 and 100 p0075 A78-33214
Cyclic stress-strain curve determination for D6AC steel by three methods [NASA-TN-73815] p0068 W78-13183
Strainrange partitioning behavior of the nickel-base superalloys, Rene 80 and 100 [NASA-TN-78628] p0070 W78-21267

NAGARAJ, R. S.
Petrographic analysis of wear particles from sliding elastohydrodynamic experiments [NASA-TP-1230] p0115 W78-22377

NAGLE, W. J.
Multi-cell battery protection system [NASA-CASE-LRW-12039-1] p0130 W78-14625

NASH, A. E.
Rolling element fatigue testing of gear materials [NASA-CR-135411] p0122 W78-31427
Rolling element fatigue testing of gear materials [NASA-CR-135450] p0124 W78-33463

NAWIGER, J. J.
Performance potential of combined cycles integrated with low-P_{ta} gasifiers for future electric utility applications [NASA-TN-73775] p0135 W78-23557

NARAWARA, J. W.
Synthesis of perfluoroalkylene aromatic diamines [NASA-CR-159403] p0087 W78-31235

NAKAWISHI, S.
Diagnostic evaluations of a beam-shielded 8-cs mercury ion thruster [AIAA PAPER 78-702] p0051 A78-32768
Diagnostic evaluations of a beam-shielded 8-cs mercury ion thruster [NASA-TN-78815] p0068 W78-21207

NARCISO, S. J.
Testing of typical spacecraft materials in a simulated subzero environment p0036 W78-10156
Charging of flexible solar array substrates in kilovolt electron beams [NASA-TN-73865] p0044 W78-21199

NASH, J. F.
Continuation of the compendium of applications technology satellite and communications technology satellite user experiments 1967-1977, volume 1 [NASA-CR-135416-VOL-1] p0062 W78-31141
Continuation of the compendium of applications technology satellite and communications technology satellite user experiments 1967-1977, volume 2 [NASA-CR-135416-VOL-2] p0062 W78-31142

NASH, S.
Wake characteristics of a tower for the DOE-WASA MOD-1 wind turbine [NASA-TN-78853] p0135 W78-23558

NASTROM, G. B.
An analysis of the first two years of GASP data [NASA-TN-73817] p0148 W78-13669
Variability of ozone near the tropopause from GASP data [NASA-CR-135405] p0148 W78-23648

NEIFER, G. E.
Mechanical characteristics of stability-bleed valves for a supersonic inlet [NASA-TN-1-3483] p0015 W78-13063
Normal shock and restart controls for a supersonic airbreathing propulsion system p0019 W78-23023
Wind tunnel evaluation of YP-12 inlet response to internal airflow disturbances with and without control p0006 W78-32062

NEITZEL, R. E.
OCSEE task 2: Engine and installation preliminary design [NASA-CR-134738] p0030 W78-23089
Energy efficient engine: Preliminary design and integration studies [NASA-CR-135488] p0032 W78-31108

NEUGROSCHEL, A.
A methodology for experimentally-based determination of gap shrinkage and effective lifetimes in the emitter and base of p-n-junction solar cells p0141 A78-10903

NEUSTADTER, R. E.
DOE/WASA Mod-0A wind turbine performance [NASA-TN-78916] p0139 W78-26553

NEWIRTH, D. S.
Fabrication and test of digital output interface devices for gas turbine electronic controls [NASA-CR-135427] p0030 W78-27129

NIEDERWICHL, R. S.
Summary of emissions reduction technology progress p0013 W78-11071

NOBLDUD, R. E.
Advanced optical blade tip clearance measurement system [NASA-CR-159402] p0032 W78-31106

NOBIS, D. L.
Propulsion p0025 A78-43360
ACER propulsion overview p0001 W78-27048
Fuel conservative aircraft engine technology [NASA-TN-78962] p0021 W78-27127

NORBERT, C. T.
Reverse-flow combustor for small gas turbines with pressure-atomizing fuel injectors [NASA-TP-1260] p0021 W78-27130

NOVICK, A. S.
Materials science experiments in space [NASA-CR-2842] p0056 W78-16094

NUSBAUM, W. J.
Cold-air performance of free-power turbine designed for 112-kilowatt automotive gas-turbine engine. 1: Design Stator-vane-chord setting angle of 35 deg [NASA-TP-1007] p0015 W78-16053

O

OBBINS, S.
Development of spiral-groove self-acting face seals [NASA-CR-135303] p0121 W78-17387

ODONWELL, P.
The Redox Flow System for solar photovoltaic energy storage p0141 A78-11019

- OSBURN, P. S.**
Anion exchange membranes for electrochemical oxidation-reduction energy storage system [NASA-TN-73751] p0131 N78-14631
The fluorination of cobalt and zinc [NASA-TN-X-73678] p0068 N78-15211
- OSTYNSKI, P. S.**
Experiments with enhanced mode thermionic converters p0146 N78-29636
- OSLEBY, J. C.**
A mechanical, thermal and electrical packaging design for a prototype power management and control system for the 30 cm mercury ion thruster [AIAA PAPER 78-685] p0051 N78-32759
Charging characteristics of materials: Comparison of experimental results with simple analytical models p0036 N78-10157
A mechanical, thermal and electrical packaging design for a prototype power management and control system for the 30 cm mercury ion thruster [NASA-TN-78862] p0049 N78-23142
- OSARA, J.**
Investigation of the burning configuration of a coaxial injector in a combustion chamber [NASA-CN-135383] p0054 N78-22148
- OLDRIEVE, S. S.**
Tantalum modified ferritic iron base alloys [NASA-CASE-LEW-12095-1] p0069 N78-18182
Fractographic evaluation of creep effects on strain-controlled fatigue-cracking of AISI 304LC and 316 stainless steel [NASA-TN-78913] p0126 N78-27453
- OLLEN, T. L.**
Impact resistant boron/aluminum composites for large fan blades [NASA-CN-135274] p0062 N78-14099
- OLSEN, W. A.**
Preliminary study of the effect of the turbulent flow field around complex surfaces on their acoustic characteristics [AIAA PAPER 78-1123] p0166 N78-45129
Preliminary study of the effect of the turbulent flow field around complex surfaces on their acoustic characteristics [NASA-TN-78944] p0164 N78-28886
- OLSON, W. T.**
Making aerospace technology work for the automotive industry - Introduction p0181 N78-33359
Making aerospace technology work for the automotive industry, introduction [NASA-TN-73870] p0179 N78-17941
- ORTU, W. W.**
Method for alleviating thermal stress damage in laminates [NASA-CASE-LEW-12491-1] p0059 N78-22163
- OSBORN, S. S.**
Performance of a transonic fan stage designed for a low meridional velocity ratio [NASA-TP-1298] p0022 N78-33107
- OSTRACH, S.**
Convection due to surface-tension gradients p0108 N78-48716
- OSULLIVAN, G.**
An inverter/controller subsystem optimized for photovoltaic applications [NASA-TN-78903] p0180 N78-26995
- OTIS, J. E.**
Laser absorption phenomena in flowing gas devices [NASA-CN-135126] p0112 N78-18411
- OWENSKI, P. C.**
Two-phase working fluids for the temperature range 50 to 350 C [NASA-CN-135255] p0107 N78-16329
- P**
- PACTORNE, S. I.**
Synthesis of perfluoroalkylene aromatic fluorines [NASA-CN-159403] p0087 N78-31235
- PACHAUS, A. B.**
Aero-acoustic tests of duct-burning turbofan exhaust nozzles. Comprehensive data report. Volume 1: Mode scale acoustic data [NASA-CN-134910-VOL-1] p0002 N78-15988
Aero-acoustic tests of duct-burning turbofan exhaust nozzles. Comprehensive data report. Volume 2: Acoustic and aerodynamic data [NASA-CN-134910-VOL-2] p0002 N78-15989
- PALMER, A. J.**
Excimer lasers [NASA-CN-155949] p0112 N78-19480
- PANPHEW, S. C.**
Splitter-bladed centrifugal compressor impeller designed for automotive gas turbine application [NASA-CN-135237] p0121 N78-10472
- PAPATHANAS, L. C.**
Global scanning of gaseous and aerosol trace species using automated instrumentation on 747 airliners [NASA-TN-73810] p0146 N78-13670
- PAPILL, S. S.**
Boiling incipience and convective boiling of neon and nitrogen p0105 N78-15820
Estimating surface temperature in forced convection nucleate boiling - A simplified method p0105 N78-15822
- PARK, A. C.**
Effect of vibration on retention characteristics of screen acquisition systems [NASA-CN-135264] p0107 N78-12764
- PARKER, S. B.**
Technological development of cylindrical and flat shaped high energy density capacitors [NASA-CN-135286] p0099 N78-24458
- PARKER, S. J.**
Lubrication of high-speed, large bore tapered-roller bearings [ASME PAPER 77-LUB-13] p0118 N78-23354
Effect of wall thickness and material on flexural fatigue of hollow rolling elements [ASME PAPER 77-LUB-14] p0126 N78-23355
Rolling-element fatigue life of AISI 52100 corrosion resistant, high temperature bearing steel [ASME PAPER 77-LUB-30] p0075 N78-28423
Perforographic analysis of wear debris generated in accelerated rolling element fatigue tests p0119 N78-28425
Characterization of wear debris generated in accelerated rolling-element fatigue tests [NASA-TP-1203] p0115 N78-21470
Rolling-element fatigue life of AISI M-50 and 18-8-1 balls [NASA-TP-1202] p0115 N78-21473
- PARKS, D. E.**
WASCAP, a three-dimensional Charging Analyzer Program for complex spacecraft p0044 N78-19567
Spacecraft-generated plasma interaction with high voltage solar array [AIAA PAPER 78-673] p0055 N78-32751
Dynamic modeling of spacecraft in a collisionless plasma p0037 N78-10150
Solar electric propulsion thruster interactions with solar arrays [NASA-CN-135257] p0052 N78-13122
A three dimensional dynamic study of electrostatic charging of materials [NASA-CN-135256] p0099 N78-13328
- PARKLEY, R. T.**
An ultralightweight, evacuated, load-bearing, high-performance insulation system [AIAA PAPER 78-878] p0045 N78-34005
Evacuated load-bearing high performance insulation study

- (NASA-CN-135302) p0092 878-18231
PATCH, R. S.
 Efficient characterization from a conical pressurized fluid bed p0046 878-32221
 Parametric dependence of ion temperature and relative density in the NASA Lewis SUSEM facility p0173 878-37679
 Model for interpreting Doppler broadened optical line emission measurements on axially symmetric plasmas p0178 878-45189
 Efficient characterization from a conical pressurized fluid bed (NASA-TN-73997) p0138 878-21596
 Parametric dependence of ion temperature and relative density in the NASA Lewis SUSEM facility (NASA-TN-73770) p0172 878-23923
PAVLOVICH, V. J.
 Normal shock and restart controls for a super sonic airbreathing propulsion system p0019 878-23023
PECK, R. E.
 Conceptual design for spacelab pool boiling experiment (NASA-CN-135378) p0037 878-20150
PEPPER, D. S.
 Excimer lasers (NASA-CN-155949) p0112 878-19880
PEPPER, S. V.
 Shear strength of metal - SiO2 contacts p0061 878-33209
 Shear strength of metal - SiO2 contacts (NASA-TN-78838) p0125 878-19539
PERRINO, P. J.
 Global measurements of gaseous and aerosol trace species in the upper troposphere and lower stratosphere from daily flights of 747 airliners p0147 878-15826
 Global atmospheric sampling program p0013 878-11076
 Global sampling of gaseous and aerosol trace species using automated instrumentation on 747 airliners (NASA-TN-73810) p0148 878-13670
 Simultaneous measurements of ozone outside and inside cabins of two B-747 airliners and a Gates Learjet business jet (NASA-TN-78983) p0009 878-31061
PETREKIN, R. E.
 Traction and lubricant film temperature as related to the glass transition temperature and solidification p0087 878-80997
PETRASHIN, D. S.
 Predicted inlet gas temperatures for tungsten fiber reinforced superalloy turbine blades p0060 878-33203
 Predicted inlet gas temperatures for tungsten fiber reinforced superalloy turbine blades (NASA-TN-73842) p0017 878-19157
PETRASHIN, D. A.
 Gas turbine engine emission reduction technology program p0001 878-27058
 Results and status of the NASA aircraft engine emission reduction technology programs (NASA-TN-79009) p0022 878-33102
PFRIFFER, R.
 The Redox Flow System for solar photovoltaic energy storage p0181 878-11019
PHILLIPS, J. E.
 In situ self cross-linking of polyvinyl alcohol battery separators (NASA-CR-135-12972-1) p0056 878-22157
PIAN, C. C. P.
 Velocity, temperature, and electrical conductivity profiles in hydrogen-oxygen MHD duct flows (NASA-TN-78968) p0108 878-28372
PICKERT, G. P.
 Method of fan sound mode structure determination (NASA-CN-135293) p0028 878-17068
 Method of fan sound mode structure determination computer program user's manual: Microphone location program (NASA-CN-135294) p0028 878-17065
 Method of fan sound mode structure determination computer program user's manual: Model calculation program (NASA-CN-135295) p0028 878-17066
PICKRELL, R. L.
 An inverter/controller subsystem optimized for photovoltaic applications (NASA-TN-78993) p0180 878-26995
 Performance and stability analysis of a photovoltaic power system (NASA-TN-78888) p0140 878-29566
PIECH, G. S.
 Surface-crack shape change in bending fatigue using an incompressive resonant fatiguing apparatus p0075 878-35398
 The influence of composition, annealing treatment, and texture on the fracture toughness of Ti-3Al-2.5Sn plate at cryogenic temperatures (NASA-TN-73872) p0069 878-15235
PIER, C. P.
 Proceedings of the Spacecraft Charging Technology Conference (NASA-TN-X-73537) p0036 878-10129
PISHCH, J. A.
 Lightning protection of aircraft (NASA-SP-1008) p0009 878-11028
POBSCHEK, R. L.
 Extended performance solar electric propulsion thrust system design (AIAA PAPER 78-643) p0055 878-37430
 Extended-performance thruster technology evaluation (AIAA PAPER 78-666) p0055 878-37436
 Extended performance solar electric propulsion thrust system study. Volume 1: Executive summary (NASA-CN-135281-VOL-1) p0052 878-10205
 Extended performance solar electric propulsion thrust system study. Volume 2: Thruster technology evaluation (NASA-CN-135281-VOL-2) p0053 878-16090
POLNY, R. A.
 Photovoltaic refrigeration application: Assessment of the near-term market (NASA-TN-73876) p0131 878-16435
 Photovoltaic highway applications: Assessment of the near-term market (NASA-TN-73863) p0178 878-17935
 Photovoltaic village power application: Assessment of the near-term market (NASA-TN-73893) p0133 878-19663
 Photovoltaic water pumping applications: Assessment of the near-term market (NASA-TN-78947) p0176 878-19444
 Photovoltaic remote instrument applications: Assessment of the near-term market (NASA-TN-73881) p0150 878-19710
 Impact of Balance Of System (BOS) costs on photovoltaic power systems (NASA-TN-78939) p0138 878-26550
POP, R. G.
 Evaluation of cyclic behavior of aircraft turbine disk alloys (NASA-CN-159833) p0128 878-33878
PORTER, T. E.
 Evaluation of flawed composite structure under static and cyclic loading p0063 878-26683
 Effect of preload on the fatigue and static strength of composite laminates with defects p0064 878-40310
POWER, J. C.
 Planned flight test of a mercury ion auxiliary propulsion system. 1: Objectives, systems descriptions, and mission operations (NASA-TN-78859) p0047 878-21208
POWER, J. L.
 Planned flight test of a mercury ion auxiliary propulsion system. 1 - Objectives, systems descriptions, and mission operations (AIAA PAPER 78-647-1) p0050 878-12734
POWERS, R. J.
 Inward transport of a toroidally confined plasma subject to strong radial electric fields p0172 878-28890
 Inward transport of a toroidally confined plasma subject to strong radial electric fields (NASA-TN-73800) p0171 878-10088
 A data acquisition and handling system for the measurement of radial plasma transport rates (NASA-TN-78849) p0155 878-23751
 A fluctuation-induced plasma transport diagnostic based upon fast-Fourier transform spectral

- analysis
[NASA-TN-78932] p0172 878-26928
- Fluctuation spectra in the NASA Lewis bangy-torus
plasma
[NASA-TN-1257] p0172 878-26927
- Low-frequency fluctuation spectra and associated
particle transport in the NASA Lewis bangy-torus
plasma
[NASA-TN-1258] p0172 878-30990
- PHINE, R. J.
Effluent characterization from a conical
pressurized fluid bed p0066 878-33221
- Emissions control for ground power gas turbines
[NASA-TN-73897] p0013 878-11072
- Effluent characterization from a conical
pressurized fluid bed
[NASA-TN-73897] p0124 878-21596
- PROBST, R. B.
Substitution of ceramics for high temperature alloys
[NASA-TN-78931] p0086 878-29246
- Substitution of ceramics for high temperature alloys
[NASA-TN-78931] p0086 878-29246
- PROK, G. B.
Design and prototype fabrication of a 30 tesla
cryogenic magnet p0097 878-15823
- PROVENCER, C. E.
Diameter scaling system study summary
[NASA-TN-73797] p0093 878-10346
- PROST, R. B., JR.
Two-dimensional cold-air cascade study of a
film-cooled turbine stator blade. 4:
Comparison of experimental and analytical
aerodynamic results for blade with 12 rows of
0.076-centimeter-(0.030-inch-) diameter holes
having streamwise ejection angles
[NASA-TN-1151] p0017 878-20130
- Two-dimensional cold-air cascade study of a
film-cooled turbine stator blade. 5:
Comparison of experimental and analytical
aerodynamic results for blade with 12 rows of
0.116-centimeter-(0.075 inch) diameter coolant
holes having streamwise ejection angles
[NASA-TN-1204] p0017 878-20133
- PSIDRA, J. A.
The effect of microstructure and strength on the
fracture toughness of an 18 Ni, 300 grade
maraging steel
[NASA-CN-135288] p0078 878-16150
- PURVIS, C. E.
Investigation of high voltage spacecraft system
interactions with plasma environments
[NASA PAPER 78-672] p0050 878-32750
- Interaction of large, high power systems with
operational orbit charged particle environments
[NAS 77-243] p0044 878-36719
- Active control of spacecraft charging on ATS-5 and
ATS-6 p0036 878-10136
- Charging characteristics of materials: Comparison
of experimental results with simple analytical
models p0036 878-10157
- Provisional specification for satellite time in a
geomagnetic environment p0036 878-10173
- Interaction of large, high power systems with
operational orbit charged particle environments
[NASA-TN-73867] p0037 878-16076
- Investigation of high voltage spacecraft system
interactions with plasma environments
[NASA-TN-78831] p0097 878-21373
- Status of the NASA-Lewis Research Center
spacecraft charging investigation
[NASA-TN-78938] p0049 878-27170
- Q**
- QUENTENBERG, R. J.
Investigation of the effect of ceramic coatings on
rocket thrust chamber life
[NASA-TN-78892] p0049 878-26173
- R**
- RAGSBALL, R. G.
Stirling engine project status p0117 878-30316
- RANBY, C. J.
Ceramic regenerator systems development program
[NASA-CN-135330] p0181 878-25988
- Ceramic regenerator systems development program
[NASA-CN-135430] p0181 878-26997
- RANBY, R. B.
12-cm magneto-electrostatic containment
argon/torus ion source development
[AIAA PAPER 78-681] p0039 878-32756
- RAO, V. B.
Ceramic regenerator systems development program
[NASA-CN-135430] p0181 878-26997
- RATNAPARKHI, R. V.
Description and status of NASA-LeRC/DOE
photovoltaic applications systems
[NASA-TN-78936] p0129 878-26554
- Design and fabrication of a photovoltaic power
system for the Pungo Indian village of
Scheffels (Sunlight), Arizona
[NASA-TN-78948] p0139 878-26555
- RAUCH, R. B.
Improved ceramic heat exchanger material
[NASA-CN-135292] p0086 878-13209
- RAVENHILL, R.
Impact absorbing blade mounts for variable pitch
blades
[NASA-CASR-LEU-12313-1] p0111 878-10458
- RAULIN, V. E.
Effect of facility background gases on internal
erosion of the 30-cm Hg ion thruster
[AIAA PAPER 78-665] p0050 878-32785
- Sensitivity of 30-cm mercury bombardment ion
thruster characteristics to accelerator grid
design
[AIAA PAPER 78-668] p0050 878-32787
- Economics of ion propulsion for large space systems
[AIAA PAPER 78-698] p0060 878-37041
- Effect of facility background gases on internal
erosion of the 30-cm Hg ion thruster
[NASA-TN-73803] p0088 878-21205
- Sensitivity of 30-cm mercury bombardment ion
thruster characteristics to accelerator grid
design
[NASA-TN-78861] p0069 878-23144
- RECH, G. B.
Stratospheric cruise emission reduction program
p0013 878-11077
- REID, L.
Design and overall performance of four highly
loaded, high speed inlet stages for an advanced
high-pressure-ratio core compressor
[NASA-TN-1337] p0022 878-33138
- REID, R. A.
An improved method for analysis of hydroxide and
carbonate in alkaline electrolytes containing zinc
[NASA-TN-78961] p0139 878-28607
- REISSMAN, J. J.
Model for interpreting Doppler broadened optical
line emission measurements on axially symmetric
plasma p0174 878-86189
- REYERBAJAN, P.
Fluidized bed combustor modeling
[NASA-CN-135164] p0067 878-14119
- REYNOLDS, R.
Combustor fluctuating pressure measurements
in-engine and in a component test facility - a
preliminary comparison p0023 878-24878
- Combustor fluctuating pressure measurements in
engine and in a component test facility: A
preliminary comparison
[NASA-TN-73845] p0035 878-13077
- REYNOLDS, T. G.
Alternative fuels p0013 878-11078
- REY, R. J.
General aviation piston-engine exhaust emission
reduction p0013 878-11073
- REYNOLDS, R. E.
A combined potential and viscous flow solution for
V-STOL engine inlets
[AIAA PAPER 78-142] p0006 878-20702
- RICH, R. J.
Optimum wall impedance for spinning modes - A
correlation with mode cut-off ratio
[AIAA PAPER 78-193] p0165 878-20735

- Far-field multimodal acoustic radiation directivity
p0165 A78-24876
- Far-field multimodal acoustic radiation directivity
[NASA-TN-73839] p0163 W78-13655
- Optimum wall impedance for spinning modes: A
correlation with mode cut-off ratio
[NASA-TN-73862] p0163 W78-15253
- RICE, W. J.
Instrument to average 100 data sets
[NASA-TP-10554] p0096 W78-11201
- RICHARDS, T. E.
ERDA/NASA 100 kilowatt mod-w wind turbine
operations and performance
[NASA-TN-73825] p0131 W78-15563
- DOE/NASA mod-0A wind turbine performance
[NASA-TN-78916] p0139 W78-26553
- RICHTER, C. W.
Design and fabrication of a low-specific-weight
parabolic dish solar concentrator
[NASA-TP-1152] p0046 W78-17145
- RICKER, J. E.
Flow of liquid jets through closely woven screens
p0008 A78-42877
- RIDDLEBAUGH, S. E.
Reverse-flow combustor for small gas turbines with
pressure-atomizing fuel injectors
[NASA-TP-1260] p0021 W78-27130
- RIZZO, L.
Utilization of NASA Lewis mobile terminals for the
Hermes satellite
p0094 A78-24885
- Utilization of NASA Lewis mobile terminals for the
Hermes satellite
[NASA-TN-73859] p0093 W78-15326
- ROBERTS, E., JR.
Digital enhancement of computerized axial tomograms
[NASA-TN-78974] p0152 W78-31690
- ROBERTS, P. B.
Advanced low γ combustors for supersonic
high-altitude gas turbines
p0014 W78-11078
- Wide range operation of advanced low γ
combustors for supersonic high-altitude aircraft
gas turbines
[NASA-CR-132297] p0027 W78-14047
- ROBERTS, R.
Pollution reduction technology program for class
T4 (JT8D) engines
p0013 W78-11067
- Evaluation of Federal Aviation Administration ion
engine exhaust sampling rake
[NASA-CR-135213] p0029 W78-21111
- ROBERTS, W. E.
Hydrogen film cooling of a small hydrogen-oxygen
thrust chamber and its effect on erosion rates
of various ablative materials
[NASA-TP-10981] p0047 W78-13124
- ROBINSON, W. W.
Advanced optical blade tip clearance measurement
system
[NASA-CR-159402] p0032 W78-31106
- ROCHE, J. C.
WASCAP, a three-dimensional Charging Analyzer
Program for complex spacecraft
p0044 A78-19567
- NASA Charging Analyzer Program - A computer tool
that can evaluate electrostatic contamination
p0044 A78-33220
- NASA charging analyzer program: A computer tool
that can evaluate electrostatic contamination
[NASA-TN-73889] p0096 W78-21372
- RODAL, J. J. A.
Experimental transient and permanent deformation
studies of steel-sphere-impacted or
explosively-impulsed aluminum panels
[NASA-CR-135315] p0078 W78-15234
- RODRIGUEZ, J. B.
Airflow and thrust calibration of an F100 engine,
S/N P680059, at selected flight conditions
[NASA-TP-1069] p0018 W78-21112
- Altitude calibration of an F100, S/N P680063,
turbofan engine
[NASA-TP-1228] p0019 W78-23095
- ROELKE, E. J.
Cold-air performance of the compressor-drive
turbine of the Department of Energy baseline
automobile gas-turbine engine
[NASA-TN-78894] p0005 W78-26093
- ROFFE, G.
Experimental study of the effects of flameholder
geometry on emissions and performance of lean
premixed combustors
[NASA-CR-135424] p0030 W78-26147
- Experimental study of the effect of cycle pressure
on lean combustion emissions
[NASA-CR-3032] p0031 W78-28098
- ROHM, D. A.
Influence of fretting on flexural fatigue of 304
stainless steel and mild steel
[NASA-TP-1193] p0070 W78-21269
- ROJESKI, E.
Upper limit for sagittoresistance in silicon
bronze and phosphor bronze wire
p0175 A78-14423
- ROLAND, C. W.
Superconducting Nb₃Ge for high-field magnets
p0175 A78-41922
- ROLAND, G. W.
Niobium-germanium superconducting tapes for
high-field magnet applications
[NASA-CR-135364] p0099 W78-19392
- ROLLBUEHLER, E. J.
Effluent characterization from a conical
pressurized fluid bed
p0066 A78-33221
- Effluent characterization from a conical
pressurized fluid bed
[NASA-TN-73897] p0134 W78-21596
- ROOT, E. C.
Analytical study of laser-supported combustion
waves in hydrogen
[AIAA PAPER 78-1219] p0067 A78-41901
- Analytical study of laser supported
waves in hydrogen
[NASA-CR-135349] p0112 W78-20489
- ROSE, J. B.
FLOWNET: A computer program for calculating
secondary flow conditions in a network of
turbomachinery
[NASA-TN-73774] p0156 W78-21791
- ROSEWALD, L.
Photovoltaic refrigeration application:
Assessment of the near-term market
[NASA-TN-73876] p0131 W78-16435
- Photovoltaic highway applications: Assessment of
the near-term market
[NASA-TN-73863] p0178 W78-17935
- Photovoltaic village power application:
Assessment of the near-term market
[NASA-TN-73893] p0133 W78-19643
- Photovoltaic water pumping applications:
Assessment of the near-term market
[NASA-TN-78847] p0134 W78-19644
- Photovoltaic remote instrument applications:
Assessment of the near-term market
[NASA-TN-73881] p0150 W78-19710
- Cost of photovoltaic energy systems as determined
by balance-of-system costs
[NASA-TN-78957] p0139 W78-27539
- ROSENLEIB, J. W.
Emergency and microfog lubrication and cooling of
bearings for Army helicopters
[NASA-CR-135195] p0122 W78-27429
- ROSIAK, G.
Ion beam plume and efflux characterization flight
experiment study
[NASA-CR-135275] p0052 W78-12140
- ROSS, J. A.
Preliminary power train design for a
state-of-the-art electric vehicle
[NASA-CR-135340] p0145 W78-29584
- ROTHBERG, W.
A three dimensional dynamic study of electrostatic
charging in materials
[NASA-CR-135256] p0099 W78-13328
- ROTH, J. E.
Inward transport of a toroidally confined plasma
subject to strong radial electric fields
p0172 A78-24890
- A model for particle confinement in a toroidal
plasma subject to strong radial electric fields
p0173 A78-24891
- Effects of applied dc radial electric fields on
particle transport in a bumpy torus plasma
p0173 A78-36956
- Alternative approaches to plasma confinement
p0174 A78-52146

PERSONAL AUTHOR INDEX

SCHREB, D. D.

- Inward transport of a toroidally confined plasma subject to strong radial electric fields
[NASA-TN-73800] p0171 N78-10883
- A model for particle confinement in a toroidal plasma subject to strong radial electric fields
[NASA-TN-73818] p0171 N78-10884
- A fluctuation-induced plasma transport diagnostic based upon fast-Fourier transform spectral analysis
[NASA-TN-78932] p0172 N78-26926
- Fluctuation spectra in the NASA Lewis bumpy-torus plasma
[NASA-TP-1257] p0172 N78-26927
- Microwave radiation measurements near the electron plasma frequency of the NASA Lewis bumpy torus plasma
[NASA-TN-78940] p0172 N78-27914
- Low-frequency fluctuation spectra and associated particle transport in the NASA Lewis bumpy-torus plasma
[NASA-TP-1258] p0172 N78-30944
- BOOSER, B. C.
Supercritical oxygen heat transfer
[NASA-CR-135339] p0108 N78-17342
- BOWE, A. P.
Erosion/corrosion of turbine airfoil materials in the high-velocity effluent of a pressurized fluidized coal combustor
[NASA-TP-1274] p0071 N78-28225
- BOY, W. L.
Particle parameter analyzing system
[NASA-CASE-LEW-06094] p0096 N78-17293
- BUDEY, R. A.
Impact of future fuel properties on aircraft engines and fuel systems
[NASA-TN-78866] p0089 N78-24369
- Characteristics and combustion of future hydrocarbon fuels
[NASA-TN-78865] p0089 N78-24370
- BUDNEY, R. A.
Fissions control for ground power gas turbines
p0013 N78-11072
- BUCCERI, B. S.
Performance with and without inlet radial distortion of a transonic fan stage designed for reduced loading in the tip region
[NASA-TP-1294] p0005 N78-10057
- BUNDLE, D. J.
Variable mixer propulsion cycle
[NASA-CASE-LEW-12917-1] p0016 N78-18067
- RUSCITTO, D.
Hydrodynamic air lubricated compliant surface bearing for an automotive gas turbine engine. 1: Journal bearing performance
[NASA-CR-135368] p0221 N78-21472
- Hydrodynamic air lubricated compliant surface bearing for an automotive gas turbine engine. 2: Materials and coatings
[NASA-CR-135402] p0122 N78-29449
- RUSSELL, L. B.
Hydrogen film cooling of a small hydrogen-oxygen thrust chamber and its effect on erosion rates of various ablative materials
[NASA-TP-1098] p0047 N78-13124
- RUTHERFORD, J. A.
Compact electron-beam source for formation of neutral beams of very low vapor pressure materials
p0110 A78-81444
- IZASHIKI, M.
Pore temperature crack growth rates and -20 deg F fracture toughness of welded 1 1/4 inch A-285 steel plate
[NASA-TN-73847] p0068 N78-13182
- SAASKI, E. W.
Two-phase working fluids for the temperature range 50 to 350 C
[NASA-CP-135255] p0107 N78-16320
- SADLER, R. E.
A visual investigation of turbulence in stagnation flow about a circular cylinder
[NASA-CR-10119] p0108 N78-33386
- SAGRESE, D. A.
Reverse-thrust technology for variable-pitch fan propulsion systems
p0005 N78-24070
- Status of advanced turboprop technology
p0001 N78-27055
- SAN, C. T.
A methodology for experimentally-based determination of gap shrinkage and effective lifetimes in the emitter and base of p-n-junction solar cells
p0141 A78-10903
- SALISBERY, C. T.
Impact absorbing blade mounts for variable pitch blades
[NASA-CASE-LEW-12313-1] p0113 N78-10468
- Impact resistant boron/aluminum composites for large fan blades
[NASA-CR-135274] p0062 N78-14099
- Design of impact-resistant boron/aluminum large fan blade
[NASA-CR-135417] p0031 N78-29104
- SALTSMAN, J. P.
Ductility normalized-strain-range partitioning life relations for creep-fatigue life predictions
p0077 A78-51739
- SAUNDERS, W. A.
High temperature compressive cracking in hot-pressed silicon nitride
p0085 A78-38706
- SARGENT, G.
The effect of minor additions of titanium on the fracture toughness of Fe-12Ni alloys at 77K
[NASA-CR-135351] p0078 N78-19259
- SARGENT, W. B.
Baseline tests of the C. N. Waterson Renault 5 electric passenger vehicle
[NASA-TN-73759] p0178 N78-16928
- Baseline tests of the AM General DJ-5E electruck electric delivery van
[NASA-TN-73758] p0178 N78-17933
- Baseline tests of the Zagato Elcar electric passenger vehicle
[NASA-TN-73763] p0178 N78-17934
- Baseline tests of the C. N. Waterson DAP electric passenger vehicle
[NASA-TN-73757] p0179 N78-17942
- Baseline tests of the EPC Hummingbird electric passenger vehicle
[NASA-TN-73760] p0180 N78-21010
- SARGISSOW, D. P.
Gas turbine engine with convertible accessories
[NASA-CASE-LEW-12390-1] p0016 N78-17056
- Integrated gas turbine engine nacelle
[NASA-CASE-LEW-12389-2] p0016 N78-18066
- SATRE, B. L.
The use of ion beam cleaning to obtain high quality cold welds with minimal deformation
[NASA-TN-78933] p0083 N78-27257
- Method of cold welding using ion beam technology
[NASA-CASE-LEW-12942-1] p0117 N78-24444
- SAUL, A. V.
Far-field multimodal acoustic radiation directivity
p0165 A78-24876
- Far-field multimodal acoustic radiation directivity
[NASA-TN-73819] p0163 N78-13855
- SAUNDERS, W. T.
Design approaches to more energy efficient engines
[AIAA PAPER 76-931] p0025 A78-33434
- Design approaches to more energy efficient engines
[NASA-TN-78891] p0114 N78-26442
- SAVINO, J. M.
Wake characteristics of a tower for the DOE-NASA NCP-1 wind turbine
[NASA-TN-78853] p0115 N78-23558
- Wake characteristics of an eight leg tower for a NCP-0 type wind turbine
[NASA-TN-73868] p0115 N78-24615
- SAYLER, C. W., III
Evaluation of a low aspect ratio small axial compressor stage, volume 1
[NASA-CR-135280] p0026 N78-12081
- Evaluation of a low aspect ratio small axial compressor stage, volume 2
[NASA-CR-135281] p0026 N78-12082
- SCHARF, J. W.
Reverse-thrust technology for variable-pitch fan propulsion systems
p0005 N78-24070
- SCHREB, D. D.
Liquid rocket engine axial-flow turbopumps
[NASA-SP-8125] p0050 N78-31164

SCHLITZER, L. B.

PERSONAL AUTHOR INDEX

- SCHLITZER, L. B.
Transient dynamics of a flexible rotor with
squeeze film dampers
[NASA-CN-3050] p0123 878-32433
- SCHMIDT, J. V.
Performance with and without inlet radial
distortion of a transonic fan stage designed for
reduced loading in the tip region
[NASA-TN-1294] p0005 878-30057
- SCHNEIDER, A. B.
Electric prototype power processor for a 30cm ion
thruster
[NASA-CN-135267] p0054 878-19200
Extended performance electric propulsion power
processor design study. Volume 1: Executive
summary
[NASA-CN-135357] p0054 878-20250
- SCHNEIDER, G. J.
Effect of ice contamination on liquid-nitrogen
drops in film boiling
p0105 878-15821
Thermally driven oscillations and wave motion of a
liquid drop
p0106 878-17508
- SCHNEIDER, J. A.
High frequency dynamic engine simulation
[NASA-CN-135313] p0027 878-13059
- SCHUBB, R. E.
Baseline tests of the C. H. Waterman DAF electric
passenger vehicle
[NASA-TN-73757] p0179 878-17942
- SCHUBERT, S. A.
Diameter varying system study summary
[NASA-TN-73797] p0093 878-10346
- SCHUBERT, L. F.
Experimental performance of a
13.65-centimeter-tip-diameter tandem-bladed
sweptback centrifugal compressor designed for a
pressure ratio of 6
[NASA-TN-1091] p0003 878-11002
- SCHUBB, W. B.
Closed loop spray cooling apparatus
[NASA-CASR-LEN-11981-1] p0091 878-17237
- SCHWARTZ, E. J.
New batteries and their impact on electric vehicles
p0141 878-16923
- SCOTT, J. E.
Propagation of sound waves through a linear shear
layer - A closed form solution
[AIAA PAPER 78-196] p0165 878-20738
Propagation of sound waves through a linear shear
layer: A closed form solution
[NASA-TN-73828] p0164 878-16766
- SCUDDER, L. B.
Application of thick-film technology to solar cell
fabrication
p0146 878-10947
Photovoltaic refrigeration application:
Assessment of the near-term market
[NASA-TN-73876] p0131 878-16435
Photovoltaic highway applications: Assessment of
the near-term market
[NASA-TN-73863] p0178 878-17935
Photovoltaic village power application:
Assessment of the near-term market
[NASA-TN-73893] p0133 878-19643
Photovoltaic water pumping applications:
Assessment of the near-term market
[NASA-TN-78847] p0134 878-19644
Photovoltaic remote instrument applications:
Assessment of the near-term market
[NASA-TN-73881] p0150 878-19710
- SKIDEL, R. C.
Power oscillation of the Hod-0 wind turbine
p0133 878-19629
- SHENSTICKER, E. G.
Dendritic web silicon for solar cell application
p0146 878-53489
- SHLUBER, K.
Procedures for generation and reduction of linear
models of a turbofan engine
[NASA-TN-1261] p0161 878-30896
- SELLER, J. E., JR.
Ion beam plume and efflux measurements of an 8-cm
mercury ion thruster
[AIAA PAPER 78-676] p0055 878-32753
Ion beam plume and efflux characterization flight
experiment study
[NASA-CN-135275] p0052 878-12140
- SELLER, B.
Ultraviolet spectrophotometer for measuring
colossal atmospheric ozone from aircraft
p0110 878-35826
Measurement of tropospheric 340 nm solar
ultraviolet flux for determination of O₃/10/
photo-production rate
p0148 878-38835
- SEN, C.
Probe studies in a modified Penning discharge
p0173 878-24904
Probe studies in a modified penning discharge
[NASA-TN-1-73631] p0171 878-15905
- SERAFINI, T. T.
FBR polyimide prepreg with improved tack
characteristics
[NASA-TN-73898] p0081 878-17221
- SEWCIE, W. E.
An analytical study of the thermal barrier coated
first stage blades in a JT9D engine
[NASA-CN-135360] p0028 878-16054
- SHAN, R. F.
Open-Cycle Gas Turbine/Steam Turbine Combined
Cycles with synthetic fuels from coal
[ASME PAPER 77-BA/ESER-9] p0146 878-33147
- SHARAF, V.
Evaluation of cyclic behavior of aircraft turbine
disk alloys
[NASA-CN-159433] p0128 878-33478
- SHARPE, P. J.
The Plasma Interaction Experiment (PIX) -
Description and flight qualification test program
[AIAA PAPER 78-674] p0051 878-32752
The Plasma Interaction Experiment (PIX)
description and test program
[NASA-TN-78863] p0041 878-21188
- SHARPE, P. S.
A mechanical, thermal and electrical packaging
design for a prototype power management and
control system for the 30 cm mercury ion thruster
[AIAA PAPER 78-685] p0051 878-32759
A mechanical, thermal and electrical packaging
design for a prototype power management and
control system for the 30 cm mercury ion thruster
[NASA-TN-78862] p0049 878-23142
- SHARROW, J. L., JR.
Investigation of the fracture mechanism of
Ti-5Al-2.5Sn at cryogenic temperatures
p0075 878-32519
Surface-crack shape change in bending fatigue
using an inexpensive resonant fatiguing apparatus
p0075 878-35394
Room temperature crack growth rates and -20 deg F
fracture toughness of welded 1/4 inch A-285
steel plate
[NASA-TN-73847] p0068 878-13182
The influence of composition, annealing treatment,
and texture on the fracture toughness of
Ti-5Al-2.5Sn plate at cryogenic temperatures
[NASA-TN-73872] p0069 878-15235
- SHARPE, G. B.
A mechanical, thermal and electrical packaging
design for a prototype power management and
control system for the 30 cm mercury ion thruster
[AIAA PAPER 78-685] p0051 878-32759
A mechanical, thermal and electrical packaging
design for a prototype power management and
control system for the 30 cm mercury ion thruster
[NASA-TN-78862] p0049 878-23142
- SHAW, L. E.
Effectiveness of an inlet flow turbulence control
device to simulate flight fan noise in an
anechoic chamber
p0024 878-24880
Effectiveness of an inlet flow turbulence control
device to simulate flight fan noise in an
anechoic chamber
[NASA-TN-73855] p0163 878-13856
- SHAW, E. J.
VSTOL tilt nacelle aerodynamics and its relation
to fan blade stresses
[AIAA PAPER 78-958] p0007 878-43520
VSTOL tilt nacelle aerodynamics and its relation
to fan blade stresses
[NASA-TN-78899] p0005 878-26099
- SHIBBLEY, D. S.
Anion exchange membranes for electrochemical
oxidation-reduction energy storage system
[NASA-TN-73751] p0131 878-14631

- In situ self cross-linking of polyvinyl alcohol battery separators [NASA-CASB-LRU-12973-1] p0056 W78-22157
- Formulated plastic separators for soluble electrode cells [NASA-CASB-LRU-12350-2] p0065 W78-25149
- Inorganic-organic separators for alkaline batteries [NASA-CASB-LRU-12649-1] p0136 W78-25530
- SHENG, Y. P.
Numerical computation of three-dimensional circulation in Lake Erie - A comparison of a free-surface model and a rigid-lid model p0151 A78-47223
- SHERLOCK, J. J.
Effect of filtration on rolling-element-bearing life in contaminated lubricant environment [NASA-TP-1272] p0116 W78-20457
- SHIENGOB, L. T.
Friction and wear of sintered fibermetal abrasible seal materials p0074 A78-23457
- Development of a plasma sprayed ceramic gas path seal for high pressure turbine application [NASA-CR-135387] p0030 W78-24141
- SHIRE, L. I.
Direct heating surface combustor [NASA-CASB-LRU-11877-1] p0097 W78-27357
- SIDDIQI, T. A.
Energy resources of the developing countries and some priority markets for the use of solar energy p0142 A78-24400
- Utilization of solar energy in developing countries - Identifying some potential markets p0142 A78-45637
- Utilization of solar energy in developing countries: Identifying some potential markets [NASA-TN-78964] p0140 W78-29578
- SIDIK, S. H.
Statistical model for asperity-contact time fraction in elastohydrodynamic lubrication [NASA-TP-1130] p0114 W78-18429
- SIEGEL, R.
Shape of two-dimensional solidification interface during directional solidification by continuous casting p0119 A78-31829
- SIGBERT, C. E.
A mechanical, thermal and electrical packaging design for a prototype power management and control system for the 30 cm mercury ion thruster [AIAA PAPER 78-685] p0051 A78-32759
- A mechanical, thermal and electrical packaging design for a prototype power management and control system for the 30 cm mercury ion thruster [NASA-TN-78862] p0049 W78-23142
- SIGHER, R. E.
Lubrication of high-speed, large bore tapered-roller bearings [ASME PAPER 77-LWB-13] p0118 A78-23354
- SIGNORELLI, R. A.
Advanced materials research for long-haul aircraft turbine engines p0001 W78-27057
- SIKORA, P. F.
Consolidation of silicon nitride without additives p0085 A78-24895
- Consolidation of silicon nitride without additives [NASA-TN-73693] p0057 W78-10217
- SILVESTRI, G. J.
Revised international representations for the viscosity of water and steam and new representations for the surface tension of water p0105 A78-15725
- SIMONHAU, H. J.
Two phase choke flow in tubes with very large L/D p0105 A78-15824
- Velocity and temperature profiles in near-critical nitrogen flowing past a horizontal flat plate [ASME PAPER 77-HT-7] p0106 A78-17481
- Release of dissolved nitrogen from water during depressurization p0066 A78-13224
- Release of dissolved nitrogen from water during depressurization [NASA-TN-73822] p0065 W78-17172
- Some flow phenomena in a constant area duct with a Ford type inlet including the critical region [NASA-TN-78943] p0104 W78-27367
- SINCLAIR, B.
Wake characteristics of an eight-leg tower for a MOD-0 type wind turbine [NASA-TN-73868] p0135 W78-24615
- SINCLAIR, J. E.
An integrated theory for predicting the hydrothermomechanical response of advanced composite structural components p0060 A78-24905
- Fracture surface characteristics of off-axis composites p0067 A78-40371
- FASTRAK use for cyclic response and fatigue analysis of wind turbine towers p0125 W78-12659
- Fracture surface characteristics of off-axis composites [NASA-TN-73700] p0057 W78-13137
- Mechanical behavior and fracture characteristics of off-axis fiber composites. 1: Experimental investigation [NASA-TP-1081] p0057 W78-13138
- An integrated theory for predicting the hydrothermomechanical response of advanced composite structural components [NASA-TN-73812] p0125 W78-13477
- Mechanical behavior and fracture characteristics of off-axis fiber composites. 2: Theory and comparisons [NASA-TP-1022] p0057 W78-16098
- The effects of eccentricities on the fracture of off-axis fiber composites [NASA-TN-73826] p0057 W78-17153
- Effects of moisture profiles and laminate configuration on the hygro stresses in advanced composites [NASA-TN-78978] p0059 W78-32191
- Analysis/design of strip reinforced random composites (strip hybrids) [NASA-TN-78985] p0059 W78-33149
- SINGER, J.
Solubility, stability, and electrochemical studies of sulfur-sulfide solutions in organic solvents [NASA-TP-1245] p0140 W78-28624
- SINON, C. E.
Fluctuation spectra in the NASA Lewis bumpy-torus plasma [NASA-TP-1257] p0172 W78-26927
- Low-frequency fluctuation spectra and associated particle transport in the NASA Lewis bumpy-torus plasma [NASA-TP-1258] p0172 W78-30944
- SKIBO, H. A.
JT9D engine diagnostics. Task 2: Feasibility study of measuring in-service flight loads [NASA-CR-135395] p0030 W78-27124
- SKIBA, C.
Evaluation of an F100 multivariable control using a real-time engine simulation [NASA-TN-X-73648] p0012 W78-10097
- SKROBATCZYI, B.
Effect of air temperature and relative humidity at various fuel-air ratios on exhaust emissions on a per-node basis of an AVCO Lycoming O-320 diad light aircraft engine: Volume 1: Results and plotted data [NASA-TN-73507-VOL-1] p0021 W78-29100
- SLATER, G. L.
Optimal controls for an advanced turbofan engine p0033 A78-23893
- SLAVICK, R. J.
Baseline tests of the C. H. Watman Renault 5 electric passenger vehicle [NASA-TN-73759] p0178 W78-16928
- Baseline tests of the Zagato Elcar electric passenger vehicle [NASA-TN-73764] p0178 W78-17934
- Baseline tests of the EVA contractor electric passenger vehicle [NASA-TN-73762] p0179 W78-17939
- Performance of conventionally powered vehicles tested to an electric vehicle test procedure [NASA-TN-73768] p0179 W78-20022
- Baseline tests of the EPC Hunningbird electric passenger vehicle [NASA-TN-73760] p0180 W78-21010
- SLIWET, H. E.
Some effects of composition on friction and wear

- of graphite-fiber-reinforced polyimide liners in plain spherical bearings
[NASA-TP-1229] p0115 W78-25833
- Some load limits and self-lubricating properties of plain spherical bearings with sintered graphite fiber reinforced polyimide liners to 320 C
[NASA-TN-78935] p0116 W78-26845
- Graphite-fiber-reinforced polyimide liners of various compositions in plain spherical bearings
[NASA-TN-78908] p0116 W78-26847
- SLUTSKY, S.**
Computation of unsteady transonic flows through rotating and stationary cascades. 3: Acoustic far-field analysis
[NASA-CR-2902] p0007 W78-12035
- SMALLEY, A. J.**
Stiffness and damping of elastomeric O-ring bearing mounts
[NASA-CR-135328] p0127 W78-18860
- Balancing techniques for high-speed flexible rotors
[NASA-CR-2975] p0127 W78-20514
- Development of procedures for calculating stiffness and damping properties of elastomers in engineering applications. Part 4: Testing of elastomers under a rotating load
[NASA-CR-135355] p0127 W78-22402
- SMEGILL, J. G.**
The effect of NaCl/g/ on the Na2SO4-induced hot corrosion of NiAl
p0079 W78-24901
- Study of the effects of gaseous environments on sulfidation attack of superalloys
[NASA-CR-135388] p0079 W78-21268
- SHYALAK, J. L.**
Oxide morphology and spalling model for NiAl
p0075 W78-30112
- SHYTH, A. L.**
Effect of fuel properties on performance of single aircraft turbojet combustor at simulated idle, cruise, and takeoff conditions
[NASA-TN-73780] p0018 W78-13056
- SHYTH, E. E.**
Acoustic design of the QCSEE propulsion systems
p0004 W78-24067
- SHYTH, G. T.**
Effect of preload on the fatigue and static strength of composite laminates with defects
p0061 W78-40310
- SHYTH, J. J.**
Long-term CP6 engine performance deterioration: Evaluation of engine S/W 451-479
[NASA-CR-135381] p0029 W78-20129
- Long-term CP6 engine performance deterioration: Evaluation of engine S/W 451-380
[NASA-CR-159390] p0031 W78-29103
- SHYTH, J. B.**
Design and preliminary results of a semitranspiration cooled /Lamilloy/ liner for a high-pressure high-temperature combustor
[AIAA PAPER 78-997] p0025 W78-43544
- Performance characteristics of two annular dump diffusers using suction-stabilized vortex flow control
p0107 W78-45431
- Performance characteristics of two annular dump diffusers using suction-stabilized vortex flow control
[NASA-TN-73857] p0004 W78-19057
- Performance of a short annular dump diffuser using suction-stabilized vortices at inlet Mach numbers to 0.41
[NASA-TP-1194] p0017 W78-20131
- Temperature distributions of a cesium-seeded hydrogen-oxygen supersonic free jet
[NASA-TP-1162] p0171 W78-20959
- Design and preliminary results of a semitranspiration cooled (Lamilloy) liner for a high-pressure high-temperature combustor
[NASA-TN-78874] p0011 W78-24138
- SHYTH, R. C.**
Closed cycle electric discharge laser design investigation
[NASA-CR-135408] p0112 W78-25407
- SHYTHICK, J. J.**
Rapid, efficient charging of lead-acid and nickel-zinc traction cells
[NASA-TN-78901] p0135 W78-24616
- SHYTH, A.**
Parametric dependence of ion temperature and relative density in the NASA Lewis SUMMA facility
p0173 W78-37679
- Parametric dependence of ion temperature and relative density in the NASA Lewis SUMMA facility
[NASA-TN-73770] p0172 W78-23923
- SOCROB, F. B.**
A viscous-inviscid interactive compressor calculation
[AIAA PAPER 78-1140] p0006 W78-41843
- End-wall boundary layer prediction for axial compressors
[AIAA PAPER 78-1139] p0007 W78-45133
- A viscous-inviscid interactive compressor calculation
[NASA-TN-78920] p0005 W78-26100
- End-wall boundary layer prediction for axial compressors
[NASA-TN-78928] p0020 W78-26144
- SOEDER, J. F.**
Evaluation of an F100 multivariable control using a real-time engine simulation
[NASA-TN-73648] p0012 W78-10097
- SOPRIN, T. G.**
Method of fan sound mode structure determination
[NASA-CR-135293] p0028 W78-17064
- SOLOMON, W. G.**
Advanced ceramic material for high temperature turbine tip seals
[NAS.-CR-135319] p0087 W78-31238
- SOLTIS, R. F.**
Baseline tests of the Zagato Elcar electric passenger vehicle
[NASA-TN-73764] p0178 W78-17934
- Baseline tests of the batronic Minivan electric delivery van
[NASA-TN-73761] p0179 W78-17940
- Baseline tests of the C. E. Waterman DAF electric passenger vehicle
[NASA-TN-73757] p0179 W78-17942
- Baseline tests of the Volkswagen transporter electric delivery van
[NASA-TN-73766] p0179 W78-20021
- Baseline tests of the Kordesh hybrid passenger vehicle
[NASA-TN-73769] p0138 W78-26551
- A cycle timer for testing electric vehicles
[NASA-TN-78934] p0180 W78-26996
- SOSOLNO, R. B.**
Physics and Chemistry of MoS2 intercalation compounds
p0175 W78-27727
- SOONOO, J. P.**
Analysis and design of a high power laser adaptive phased array transmitter
[NASA-CR-134952] p0111 W78-13420
- SOUTHWELL, W. H.**
Analysis and design of a high power laser adaptive phased array transmitter
[NASA-CR-134952] p0111 W78-13420
- SOVET, J. S.**
Optical and electrical properties of ion beam textured Kapton and Teflon
p0085 W78-24908
- Ion beam sputter etching and deposition of fluoropolymers
p0085 W78-37648
- A hollow cathode hydrogen ion source
p0173 W78-39835
- Optical and electrical properties of ion beam textured Kapton and Teflon
[NASA-TN-73778] p0162 W78-13848
- Ion beam sputter etching and deposition of fluoropolymers
[NASA-TN-78888] p0088 W78-24358
- Ion beam sputtering of fluoropolymers
[NASA-TN-79000] p0060 W78-33151
- SOBERS, W. D.**
Acoustic design of the QCSEE propulsion system
p0004 W78-24067
- SPADACCINI, L. J.**
Development of an experiment for determining the autoignition characteristics of aircraft-type fuels
[NASA-CR-135329] p0090 W78-16194
- SPALVINS, T.**
Microstructural and wear properties of sputtered carbides and silicides
p0084 W78-23445

PERSONAL AUTHOR INDEX

STEPHENS, J. B.

- Coatings for wear and lubrication
[NASA-TN-78841] p0081 W78-20333
Morphology of gold and copper ion-plated coatings
[NASA-TP-1262] p0071 W78-26199
Sputtering technology in solid film lubrication
[NASA-TN-78914] p0083 W78-26214
- SPANG, E. A., III
Failure detection and correction for turbofan
engines p0033 A78-23918
- SPENCER, E. G.
Supercritical oxygen heat transfer
[NASA-CR-135339] p0108 W78-17342
- SPINA, B. A.
Effects of rotor location, coning, and tilt on
critical loads in large wind turbines p0141 A78-20476
Comparison of computer codes for calculating
dynamic loads in wind turbines p0142 A78-37678
Comparison of computer codes for calculating
dynamic loads in wind turbines p0132 W78-19617
Effects of rotor location, coning, and tilt on
critical loads in large wind turbines p0133 W78-19636
Comparison of computer codes for calculating
dynamic loads in wind turbines
[NASA-TN-73773] p0135 W78-23556
- SPREITER, J. E.
Perturbation solutions for blade-to-blade surfaces
of a transonic compressor p0008 A78-12307
Perturbation solutions for transonic flow on the
blade-to-blade surface of compressor blade rows
[NASA-CR-2941] p0001 W78-15987
- STABE, E. G.
Effect of cooling-hole geometry on aerodynamic
performance of a film-cooled turbine vane tested
with cold air in a two-dimensional cascade
[NASA-TP-1136] p0004 W78-20080
- STAGLIANO, T. E.
Experimental transient and permanent deformation
studies of steel-sphere-impacted or
explosively-impulsed aluminum panels
[NASA-CR-135315] p0078 W78-15234
- STARARA, S. S.
Perturbation solutions for blade-to-blade surfaces
of a transonic compressor p0008 A78-12307
Perturbation solutions for transonic flow on the
blade-to-blade surface of compressor blade rows
[NASA-CR-2941] p0001 W78-15987
- STAUD, P. S.
Wind tunnel performance tests of conical plug
nozzles p0002 W78-21044
Acoustic tests of duct-burning turbofan jet noise
simulation p0002 W78-28043
Acoustic tests of duct-burning turbofan jet noise
simulation: Comprehensive data report. Volume
1, section 2: Full size data p0030 W78-28095
[NASA-CR-135239-VOL-1-SECT-2]
Acoustic tests of duct-burning turbofan jet noise
simulation: Comprehensive data report. Volume
1, section 3: Data plots p0030 W78-28096
[NASA-CR-135239-VOL-1-SECT-3]
Acoustic tests of duct-burning turbofan jet noise
simulation: Comprehensive data report. Volume
2: Model design and aerodynamic test results
[NASA-CR-135239-VOL-2] p0031 W78-28097
- STAROLICH, E. G.
Design of an air ejector for boundary-layer bleed
of an acoustically treated turbofan engine inlet
during ground testing p0037 W78-27143
[NASA-TN-78917]
- STASKUS, J.
Investigation of high voltage spacecraft system
interactions with plasma environments
[AIAA PAPER 78-672] p0050 A78-32750
- STASKUS, J. V.
Testing of typical spacecraft materials in a
simulated substora environment p0036 W78-10156
Charging of flexible solar array substrates in
kilovolt electron beams p0044 W78-21199
[NASA-TN-73865]
- Investigation of high voltage spacecraft system
interactions with plasma environments
[NASA-TN-78831] p0097 W78-21373
- STARRIS, C. A.
Volatile products from the interaction of HCl(g)/
with Cr2O3 and LaCrO3 in oxidizing environments
p0066 A78-24687
Interaction of NaCl(g) and HCl(g) with condensed
H2SO4 p0066 A78-24688
Formation of Na2SO4 and K2SO4 in flames doped with
sulfur and alkali chlorides and carbonates
p0066 A78-24689
High temperature environmental effects on metals
p0075 A78-29329
Formation of Na2SO4 and K2SO4 in flames doped with
sulfur and alkali chlorides and carbonates
[NASA-TN-73794] p0064 W78-13157
Volatile products from the interaction of HCl(g)
with Cr2O3 and LaCrO3 in oxidizing environments
[NASA-TN-73795] p0064 W78-13158
Interaction of NaCl(g) and HCl(g) with condensed
H2SO4 p0064 W78-13159
[NASA-TN-73796]
High temperature environmental effects on metals
[NASA-TN-73878] p0017 W78-19158
- STECURA, S.
Two-layer thermal barrier coating for high
temperature components p0084 A78-18787
[ACS PAPER 31-BW-76P]
Thermal barrier coating system p0102 W78-18355
[NASA-CASE-LEW-12554-1]
Effects of compositional changes on the
performance of a thermal barrier coating system
[NASA-TN-78976] p0072 W78-31212
- STENKIN, W. G.
Blade row dynamic digital compression program.
Volume 2: J85 circumferential distortion
redistribution model, effect of stator
characteristics, and stage characteristics
sensitivity study p0032 W78-33103
[NASA-CR-134953]
- STEIGERWALD, R. L.
Pulse battery charger employing 1000 ampere
transistor switches p0146 A78-31974
- STEINBERG, R.
Method of forming metal hydride films p0113 W78-13436
[NASA-CASE-LEW-12083-1]
Automated meteorological data from commercial
aircraft via satellite: Present experience and
future implications p0150 W78-17558
[NASA-TN-73750]
- STELSON, T. S.
Cost analysis of advanced turbine blade
manufacturing processes p0026 W78-10092
[NASA-CR-135203]
- STENZEL, R. L.
Experiments on whistler wave filamentation and VLF
hiss in a laboratory plasma p0149 A78-41788
- STEPHENS, J. B.
Cryogenic properties of a new tough-strong iron
alloy p0073 A78-15825
Comparison of equivalent energy and energy per
unit area /W bar/A/ data with valid fracture
toughness data for iron, aluminum, and titanium
alloys p0074 A78-24372
New alloys to conserve critical elements p0076 A78-37680
Development of strong and tough cryogenic Fe-12Ni
alloys containing reactive metal additions p0076 A78-41465
Substitution for chromium in 304 stainless steel
p0077 A78-51714
Materials technology assessment for Stirling engines
[NASA-TN-73789] p0069 W78-17187
High toughness-high strength iron alloy p0070 W78-22205
[NASA-CASE-LEW-12542-2]
New alloys to conserve critical elements p0070 W78-24315
[NASA-TN-78840]
Materials technology assessment for Stirling engines
p0117 W78-30318
Effects of thermochemical processing on strength
and toughness of iron - 12-percent-nickel -
reactive metal alloys at -196 C p0073 W78-31213
[NASA-TP-1308]

- STEPHENS, E. E.
Facinet lasers
[NASA-CN-135989] p0112 W78-19480
- STEPHA, F. S.
Liquid-cooling technology for gas turbines review
and status
[NASA-TN-78906] p0020 W78-26145
- STEVENS, W.
Design and performance of a
427-meter-per-second-tip-speed two-stage fan
having a 2.00 pressure ratio
[NASA-TP-1314] p0022 W78-33109
- STEVENS, G.
The 20/30 GHz satellite systems technology needs
assessment
[NASA-TN-78975] p0093 W78-31323
- STEVENS, W. L.
F-15/nonaxisymmetric nozzle system integration
study support program
[NASA-CN-135252] p0028 W78-18070
- STEVENS, W. J.
Summary of the CTS Transient Event Counter data
after one year of operation p0046 W78-19566
- Investigation of high voltage spacecraft system
interactions with plasma environments
[AIAA PAPER 78-672] p0050 W78-32750
- NASA Charging Analyzer Program - A computer tool
that can evaluate electrostatic contamination
p0044 W78-33220
- Interaction of large, high power systems with
operational orbit charged particle environments
[NAS 77-243] p0044 W78-36719
- Preliminary Report on the CTS transient event
counter performance through the 1976 spring
eclipse season p0036 W78-10135
- The Lewis Research Center geomagnetic substora
simulation facility p0036 W78-10155
- Testing of typical spacecraft materials in a
simulated substora environment p0036 W78-10156
- Charging characteristics of materials: Comparison
of experimental results with simple analytical
models p0036 W78-10157
- Provisional specification for satellite time in a
geomagnetic environment p0036 W78-10173
- Development of environmental charging effect
monitors for operational satellites p0037 W78-10174
- Interaction of large, high power systems with
operational orbit charged particle environments
[NASA-TN-73867] p0037 W78-16076
- NASA charging analyzer program: A computer tool
that can evaluate electrostatic contamination
[NASA-TN-73889] p0096 W78-21372
- Investigation of high voltage spacecraft system
interactions with plasma environments
[NASA-TN-78831] p0097 W78-21373
- Status of the NASA-Lewis Research Center
spacecraft charging investigation
[NASA-TN-78938] p0049 W78-27170
- STEWART, W. L.
A review of NASA's propulsion programs for civil
aviation
[AIAA PAPER 78-43] p0023 W78-20651
- A review of NASA's propulsion programs for aviation
[NASA-TN-73831] p0016 W78-16055
- STOCKER, W. L.
Aerodynamic performance of conventional and
advanced design labyrinth seals with
solid-smooth abrasable, and honeycomb lands
[NASA-CN-135307] p0122 W78-27427
- STOCKHARD, W. O.
A combined potential and viscous flow solution for
V/STOL engine inlets
[AIAA PAPER 78-142] p0006 W78-20702
- Methods for calculating the transonic boundary
layer separation for V/STOL inlets at high
incidence angles
[AIAA 78-1340] p0007 W78-46537
- Theoretical flow characteristics of inlets for
tilting-nacelle VTOL aircraft
[NASA-TP-1205] p0018 W78-21114
- Computer programs for calculating two-dimensional
potential flow in and about propulsion system
inlets
[NASA-TN-78930] p0005 W78-27083
- STONE, J. E.
An empirical model for inverted-velocity-profile
jet noise prediction p0023 W78-24879
- On the use of relative velocity exponents for jet
engine exhaust noise p0024 W78-37683
- An empirical model for inverted-velocity-profile
jet noise prediction
[NASA-TN-73838] p0014 W78-13061
- On the use of relative velocity exponents for jet
engine exhaust noise
[NASA-TN-78873] p0011 W78-24137
- STONE, E. L.
An analytical study of thermal barrier coated
first stage blades in a JT9D engine
[NASA-CN-135360] p0028 W78-16054
- STOLLER, C. L., JR.
Integrated gas turbine engine-nacelle
[NASA-CASR-LEW-12389-2] p0016 W78-18066
- STOVER, J. E.
Photovoltaic power system tests on an 8-kilowatt
single-phase line-commutated inverter
[NASA-TN-78824] p0134 W78-19657
- STRANGE, J. D.
Continuation of the compendium of applications
technology satellite and communications
technology satellite user experiments 1967-1977,
volume 1
[NASA-CN-135416-VOL-1] p0042 W78-31141
- Continuation of the compendium of applications
technology satellite and communications
technology satellite user experiments 1967-1977,
volume 2
[NASA-CN-135416-VOL-2] p0042 W78-31142
- STRAUSS, E. L.
Evaluation of low cost/high temperature fiber and
blanket insulation p0063 W78-16903
- STRINGSAS, E. J.
Acoustic tests of duct-burning turbofan jet noise
simulation
[NASA-CN-2966] p0002 W78-28043
- Acoustic tests of duct-burning turbofan jet noise
simulation: Comprehensive data report. Volume
1, section 2: Full size data
[NASA-CN-135239-VOL-1-SECT-2] p0030 W78-28095
- Acoustic tests of duct-burning turbofan jet noise
simulation: Comprehensive data report. Volume
1, section 3: Data plots
[NASA-CN-135239-VOL-1-SECT-3] p0030 W78-28096
- Acoustic tests of duct-burning turbofan jet noise
simulation: Comprehensive data report. Volume
2: Model design and aerodynamic test results
[NASA-CN-135239-VOL-2] p0031 W78-28097
- STRONOFF, H. J.
Preliminary design study of an alternate heat
source assembly for a Brayton isotope power system
[NASA-CN-135428] p0145 W78-28608
- STURMAN, J. C.
The Lewis Research Center geomagnetic substora
simulation facility p0036 W78-10155
- Development of environmental charging effect
monitors for operational satellites p0037 W78-10174
- SUCCI, G. P.
Interaction of a turbulent-jet noise source with
transverse modes in a rectangular duct
[NASA-TP-1248] p0001 W78-25049
- SUCHEC, J.
Method for calculating convective heat-transfer
coefficients over turbine vane surfaces
[NASA-TP-1134] p0102 W78-17338
- SULLIVAN, T. L.
In situ ply strengths - An initial assessment
p0061 W78-33223
- Wind turbine generator rotor blade concepts with
low cost potential
[NASA-TN-73835] p0111 W78-17466
- Simplified modeling for wind turbine nodal
analysis using WASTRAN p0132 W78-19619
- In situ ply strength: An initial assessment
[NASA-TN-73771] p0059 W78-21220
- SURBER, I. E.
Comparison of reusable insulation systems for

- cryogenically-tanked earth-based space vehicles
 [AIAA PAPER 78-877] p0048 A78-36008
 Purging of a tank-mounted multilayer insulation
 system by gas diffusion p0041 A78-17127
 [NASA-TP-1127]
 Comparison of reusable insulation systems for
 cryogenically-tanked earth-based space vehicles
 [NASA-TN-73668] p0081 A78-21190
 Liquid propellant reorientation in a low-gravity
 environment p0105 A78-29407
 [NASA-TN-78969]
- SUDDERS, G. B.**
 Solid State Remote Power Controllers for high
 voltage DC distribution systems p0100 A78-15574
- SWANSON, D. C.**
 ADJUST - An automated system for steering Centaur
 launch vehicles in measured winds p0041 A78-14991
- SWANSON, M. C.**
 Design and prototype fabrication of a 30 tesla
 cryogenic magnet p0097 A78-15823
- SWARTZ, C. R.**
 Preliminary evaluation of Glass Resin materials
 for solar cell cover use p0137 A78-26548
 [NASA-TN-78925]
- SWANISWLO, A. J.**
 Stratospheric cruise emission reduction program
 p0013 A78-11077
- TEPESI, S.**
 Fabrication and characteristics of experimental
 radiographic amplifier screens p0124 A78-15501
 [NASA-CR-2937]
- THORN, J. R.**
 Evaluation of an F100 multivariable control using
 a real-time engine simulation p0012 A78-10097
 [NASA-TN-X-73648]
- T**
- TABAKOFF, W.**
 Analysis of the cross flow in a radial inflow
 turbine scroll p0029 A78-19153
 [NASA-CR-135320]
 Computer program for the analysis of the cross
 flow in a radial inflow turbine scroll p0029 A78-19154
 [NASA-CR-135321]
- TACIBA, R. R.**
 Experimental evaluation of fuel preparation
 systems for an automotive gas turbine catalytic
 combustor p0120 A78-37677
 Degree of vaporization using an airblast type fuel
 injector for a premixed-prevaporized combustor
 p0107 A78-50372
 Experimental evaluation of premixing-prevaporizing
 fuel injection concepts for a gas turbine
 catalytic combustor p0101 A78-18313
 [NASA-TN-73755]
 Experimental evaluation of fuel preparation
 systems for an automotive gas turbine catalytic
 combustor p0082 A78-22243
 [NASA-TN-78856]
 Degree of vaporization using an airblast type
 injector for a premixed-prevaporized combustor
 [NASA-TN-78836] p0103 A78-24494
- TALLEY, L.**
 Upper limit for magnetoresistance in silicon
 bronze and phosphor bronze wire p0175 A78-14423
- TANABARO, I.**
 Study of 82 and 85 GHz coupled cavity
 traveling-wave tubes for space use p0098 A78-11295
 [NASA-CR-134670]
- TANWA, M. K.**
 Calculation of far-field jet noise spectra from
 near-field measurements using true source location
 [AIAA PAPER 78-1153] p0168 A78-41852
- TAYLOR, A. D.**
 Atmospheric ozone measurements made from B-747
 airliners - Spring 1975 p0148 A78-24894
- TAYLOR, C. B.**
 Temperature distributions and thermal stresses in
 a graded zirconia/metal gas path seal system for
 aircraft gas turbine engines p0118 A78-20683
 [AIAA PAPER 78-93]
- The elastic distortion of the flanged inner ring
 of a high-speed cylindrical roller bearing
 [ASME PAPER 77-LUB-8] p0118 A78-23352
 Temperature distributions and thermal stresses in
 a graded zirconia/metal gas path seal system for
 aircraft gas turbine engines p0015 A78-15044
 [NASA-TN-73818]
 Effect of geometry on hydrodynamic film thickness
 [NASA-TP-1287] p0117 A78-30585
- TEGANT, J. R.**
 Effect of vibration on retention characteristics
 of screen acquisition systems p0045 A78-83560
 [AIAA PAPER 78-1030]
 Effect of vibration on retention characteristics
 of screen acquisition systems p0107 A78-12364
 [NASA-CR-135264]
- TEUBENHOUSE, G. J.**
 Fabrication of thin layer beta alumina
 [NASA-CR-135308] p0077 A78-14143
- TERDAV, P. P.**
 30-cm mercury ion thruster performance with a 1 kW
 capacitor-diode voltage multiplier beam supply
 [AIAA PAPER 78-686] p0051 A78-32760
 30-cm mercury ion thruster performance with a 1
 kW capacitor-diode voltage multiplier beam supply
 [NASA-TN-78864] p0049 A78-23143
- THEISS, P.**
 Minimum-time acceleration of aircraft turbofan
 engines p0023 A78-23892
 Solution of transient optimization problems by
 using an algorithm based on nonlinear programming
 p0158 A78-23909
- THSCH, W. A.**
 Blade row dynamic digital compression program.
 Volume 2: J85 circumferential distortion
 redistribution model, effect of stator
 characteristics, and stage characteristics
 sensitivity study p0032 A78-33103
 [NASA-CR-134953]
- TESTER, B. J.**
 Calculation of far-field jet noise spectra from
 near-field measurements using true source location
 [AIAA PAPER 78-1153] p0168 A78-41852
- THE, B.**
 A Stirling engine computer model for performance
 calculations p0180 A78-29994
 [NASA-TN-78884]
- THALLER, L. E.**
 Electrochemical cell for rebalancing redox flow
 system p0136 A78-25554
 [NASA-CASE-LEW-13150-1]
- THIRRE, L. G.**
 Initial test results with a single-cylinder
 rhombic-drive Stirling engine p0140 A78-31533
 [NASA-TN-78919]
- THIES, W. C.**
 Filling of orbital fluid management systems
 [NASA-CR-159404] p0108 A78-31380
- THOMAS, R. D.**
 Multi-cell battery protection system
 [NASA-CASE-LEW-12039-1] p0130 A78-14625
- THOMAS, R. E.**
 Millimeter wave satellite concepts, volume 1
 [NASA-CR-135227] p0041 A78-15144
- THOMAS, R. L.**
 ERDA/NASA 100 kilowatt sod-o wind turbine
 operations and performance p0131 A78-15563
 [NASA-TN-73825]
 Large wind turbine generators p0140 A78-29575
 [NASA-TN-73767]
- THOMPSON, R. W.**
 A review of the Thermo-electronic Laser Energy
 Converter (TELEC) Program at Lewis Research Center
 p0142 A78-33217
 Preliminary results on the conversion of laser
 energy into electricity p0173 A78-34631
 A review of the thermo-electronic laser energy
 converter (TELEC) program at Lewis Research Center
 [NASA-TN-73888] p0111 A78-21441
- TITMAN, R. E.**
 Development and fabrication of a diffusion welded
 Columbian alloy heat exchanger p0123 A78-31500
 [AIME PAPER A78-61]
- TODD, R. S.**
 Effect of steady flight loads on J79D-7
 performance deterioration p0031 A78-29105
 [NASA-CR-135407]

TOPICH, J. A.

PERSONAL AUTHOR INDEX

TOPICH, J. A.
Adaptation of ion beam technology to microfabrication of solid state devices and transducers [NASA-CR-135314] p0099 W78-15397

TOWNE, L. E.
Evaluation of commercially-available spacecraft-type heat pipes [AIAA 78-397] p0044 A78-35590
High temperature heat pipe research at NASA Lewis Research Center [AIAA 78-438] p0106 A78-35618
Accelerated life tests of specimen heat pipe from Communication Technology Satellite (CTS) project [NASA-TN-73886] p0102 W78-17341
Evaluation of commercially-available spacecraft-type heat pipes [NASA-TN-78826] p0103 W78-20859
High temperature heat pipe research at NASA Lewis Research Center [NASA-TN-78832] p0103 W78-23304

TOUNE, C. E.
Boundary layer analysis of a Centaur standard shroud [NASA-TN-78843] p0103 W78-21404

TOUNSEND, F. P.
Study of lubricant jet flow phenomena in spur gears - Out of mesh condition [ASME PAPER 77-DET-104] p0118 A78-20608
Experimental and analytical load-life relation for AISI 9310 steel spur gears [ASME PAPER 77-DET-121] p0118 A78-20609

TRIBER, J. E.
Electric vehicle power train instrumentation - Some constraints and considerations [EVC PAPER 7784] p0097 A78-16922
Discrete time domain modelling and analysis of dc-dc converters with continuous and discontinuous inductor current p0100 A78-18796

TROUT, A. W.
Design and preliminary results of a semitranspiration cooled /Lasilloy/ liner for a high-pressure high-temperature combustor [AIAA PAPER 78-997] p0025 A78-43544
Design and preliminary results of a semitranspiration cooled (Lasilloy) liner for a high-pressure high-temperature combustor [NASA-TN-78874] p0011 W78-24138

TRION, E. B.
Baseline tests of the AM General DJ-5E electric truck electric delivery van [NASA-TN-73758] p0178 W78-17933
Baseline tests of the EVA contractor electric passenger vehicle [NASA-TN-73762] p0179 W78-17939

TUHA, G. B.
Instrument to average 100 data sets [NASA-TP-1055] p0096 W78-11301

TOHMAN, B. G.
Computer model for refinery operations with emphasis on jet fuel production. Volume 2: Data and technical bases [NASA-CR-135338] p0090 W78-19324
Computer model for refinery operations with emphasis on jet fuel production. Volume 1: Program description [NASA-CR-135331] p0090 W78-20350
Computer model for refinery operations with emphasis on jet fuel production. Volume 3: Detailed systems and programming documentation [NASA-CR-135335] p0090 W78-25235

U

URASER, D. C.
Design and performance of a 427-meter-per-second-tip-speed two-stage fan having a 2.40 pressure ratio [NASA-TP-1314] p0022 W78-13109

UYEKAWA, O. E.
The role of drop velocity in statistical spray description p0107 A78-50323
The role of drop velocity in statistical spray description [NASA-TN-73887] p0102 W78-20458

V

VALGODA, S. E.
Disaster warning system study summary [NASA-TN-73797] p0093 W78-10346

VAN STONE, S. W.
Investigation of the fracture mechanism of Ti-5Al-2.5Sn at cryogenic temperatures p0075 A78-32319

VANPOSSEN, G. J., JR.
Liquid-cooling technology for gas turbines review and status [NASA-TN-78906] p0020 W78-26145

VANUCCI, E. D.
Effect of processing parameters on autoclaved FRP polyimide composites p0060 A78-25191

VANSTONE, S. W.
The influence of composition, annealing treatment, and texture on the fracture toughness of Ti-5Al-2.5Sn plate at cryogenic temperatures [NASA-TN-73872] p0069 W78-15235

VARY, A.
Correlation of fiber composite tensile strength with the ultrasonic stress wave factor p0060 A78-33207
Quantitative ultrasonic evaluation of mechanical properties of engineering materials p0124 A78-45433
Correlations between ultrasonic and fracture toughness factors in metallic materials p0077 A78-45434
Use of an ultrasonic-acoustic technique for nondestructive evaluation of fiber composite strength [NASA-TN-73813] p0124 W78-17397
Correlations between ultrasonic and fracture toughness factors in metallic materials [NASA-TN-73805] p0069 W78-19261
Correlation of fiber composite tensile strength with the ultrasonic stress wave factor [NASA-TN-78846] p0058 W78-20255
Quantitative ultrasonic evaluation of mechanical properties of engineering materials [NASA-TN-78905] p0124 W78-24565

VENKATARAMAN, K. S.
Experimental study of the effects of flameholder geometry on emissions and performance of lean premixed combustors [NASA-CR-135424] p0030 W78-26147
Experimental study of the effect of cycle pressure on lean combustion emissions [NASA-CR-3032] p0031 W78-28098

VERHOFFEN, J. D.
Materials science experiments in space [NASA-CR-2842] p0056 W78-16094

VETROUS, E.
A mission profile life test facility [AIAA PAPER 78-671] p0040 A78-37431

VINSON, P. W.
Energy efficient engine: Preliminary design and integration studies [NASA-CR-135444] p0032 W78-31108

VITERI, P.
Liquid rocket engine axial-flow turbopumps [NASA-SP-4125] p0050 W78-31164

VITTEBA, L. A.
Fixed pitch wind turbines p0133 W78-19638

VOGAS, J. W.
Advanced ceramic material for high temperature turbine tip seals [NASA-CR-135319] p0087 W78-31236

VOLD, T.
Upper limit for magnetoresistance in silicon bronze and phosphor bronze wire p0175 A78-14423

VON GLASS, U.
Noise of deflectors used for flow attachment with STOL-OTW configurations p0023 A78-24877

VONGLASS, U. H.
Noise of deflectors used for flow attachment with STOL-OTW configurations [NASA-TN-73809] p0163 W78-13653
Correlation of combustor acoustic power levels inferred from internal fluctuating pressure measurements

{NASA-TN-78986} p0165 W78-31871
VROON, D. A.
 Compact electron-beam source for formation of
 neutral beams of very low vapor pressure materials
 p0110 A78-81868

W

WAGNER, L. S.
 Wake characteristics of a tower for the DOE-NASA
 MOD-1 wind turbine
 {NASA-TN-78853} p0135 W78-23558
 Wake characteristics of an eight-leg tower for a
 MOD-0 type wind turbine
 {NASA-TN-73868} p0135 W78-24615

WAIWASUKI, M. S.
 Aerodynamic design and performance testing of an
 advanced 30 deg swept, eight bladed propeller at
 Mach numbers from 0.2 to 0.85
 {NASA-CR-3087} p0008 W78-32066

WALLACE, B. W.
 Millimeter wave satellite concepts, volume 1
 {NASA-CR-135227} p0061 W78-15188

WALLSCHLAG, B. E.
 Application of fluidics to new control elements
 p0109 W78-23026

WALTER, R. J.
 Initial test results with a single-cylinder
 rhombic-drive Stirling engine
 {NASA-TN-78919} p0180 W78-31533

WANG, S. S.
 WASCAP, a three-dimensional Charging Analyzer
 Program for complex spacecraft
 p0044 A78-19567
 Dynamic modeling of spacecraft in a collisionless
 plasma p0037 W78-10150
 Analysis of delamination in unidirectional and
 crossplied fiber composites containing surface
 cracks
 {NASA-CR-135288} p0062 W78-11197
 A three dimensional dynamic study of electrostatic
 charging in materials
 {NASA-CR-135256} p0099 W78-13328

WANG, S. Y.
 Temperature distributions of a cesium-seeded
 hydrogen-oxygen supersonic free jet
 {NASA-TP-1162} p0171 W78-20959

WANGSUNSHIN, H.
 Modeling and Analysis of Power Processing Systems
 (MAPP5), initial phase 2
 {NASA-CR-135173} p0100 W78-29350

WARD, J. W.
 Economics of ion propulsion for large space systems
 {AIAA PAPER 78-698} p0080 A78-37481

WARREN, A. W.
 A simulation model for wind energy storage
 systems. Volume 1: Technical report
 {NASA-CR-135283} p0156 W78-20802
 A simulation model for wind energy storage
 systems. Volume 2: Operation manual
 {NASA-CR-135284} p0157 W78-20803
 A simulation model for wind energy storage
 systems. Volume 3: Program descriptions
 {NASA-CR-135285} p0157 W78-20804

WARREN, D.
 Modeling and Analysis of Power Processing Systems
 (MAPP5), initial phase 2
 {NASA-CR-135173} p0100 W78-29350

WARREN, E. L.
 Lewis Research Center support of Chrysler upgraded
 engine program
 p0117 W78-30305

WARSHAWSKY, I.
 Instrumentation for propulsion systems development
 {SAE PAPER 780076} p0109 A78-33365
 Instrumentation for propulsion systems development
 {NASA-TN-73880} p0011 W78-17052

WARSHAY, G.
 ECA Phase I fuel cell results
 p0142 A78-26110

WASSERBAUM, J. F.
 Inlet-engine matching for SCAR including
 application of a bicone variable geometry inlet
 {AIAA PAPER 78-961} p0007 A78-45096
 Inlet-engine matching for SCAR including
 application of a bicone variable geometry inlet
 {NASA-TN-78955} p0021 W78-27125

WATERS, G. J.
 Strength enhancement process for prealloyed powder
 superalloys p0075 A78-33216
 Strength enhancement process for prealloyed powder
 superalloys
 {NASA-TN-78834} p0070 W78-21266

WATKINS, J. A.
 Effect of forward motion on engine noise
 {NASA-CR-138954} p0026 W78-10093

WATSON, G. E.
 Materials technology assessment for stirling engines
 {NASA-TN-73789} p0069 W78-17187

WASTHAR, J. A.
 Effectiveness of an inlet flow turbulence control
 device to simulate flight fan noise in an
 anechoic chamber p0024 A78-24880
 Effectiveness of an inlet flow turbulence control
 device to simulate flight noise fan in an
 anechoic chamber
 {NASA-TN-73855} p0163 W78-13856

WEAR, J. D.
 Design and preliminary results of a
 semitranspiration cooled/Lanilloy liner for a
 high-pressure high-temperature combustor
 {AIAA PAPER 78-997} p0025 A78-43588
 Design and preliminary results of a
 semitranspiration cooled (Lanilloy) liner for a
 high-pressure high-temperature combustor
 {NASA-TN-78874} p0011 W78-24136

WEBB, J. A., JR.
 Design and performance of heart assist or
 artificial heart control systems p0185 W78-23032

WEBER, R. J.
 A review of NASA's propulsion programs for civil
 aviation
 {AIAA PAPER 78-43} p0023 A78-20651
 A review of NASA's propulsion programs for aviation
 {NASA-TN-73831} p0016 W78-16055

WEDEVEN, L. D.
 Elastohydrodynamic film thickness measurements of
 artificially produced surface dents and grooves
 {NASA-TN-78949} p0116 W78-27428

WESTON, J. W.
 Method for alleviating thermal stress damage in
 laminates
 {NASA-CASE-LEW-12493-1} p0059 W78-22163

WRIGHT, A. J.
 Mechanical properties on ion-beam-textured
 surgical implant alloys p0075 A78-36085
 The use of an ion-beam source to alter the surface
 morphology of biological implant materials
 p0061 A78-37686
 Mechanical properties of ion-beam-textured
 surgical implant alloys
 {NASA-TN-73782} p0068 W78-13181
 The use of an ion-beam source to alter the surface
 morphology of biological implant materials
 {NASA-TN-78851} p0152 W78-22618

WEIN, B.
 Development and fabrication of a diffusion welded
 Columbian alloy heat exchanger
 {AIAA PAPER 78-61} p0123 A78-31500

WEINBERG, I.
 Impurity concentrations and surface charge
 densities on the heavily doped face of a silicon
 solar cell p0130 W78-13534

WEISMAN, Y. C.
 Extended performance solar electric propulsion
 thrust system study. Volume 8: Thruster
 technology evaluation
 {NASA-CR-135281-VOL-8} p0053 W78-16090

WEISS, J. A.
 Low cost satellite land mobile service for
 nationwide applications p0095 A78-43173

WEISER, V. G.
 Photon degradation effects in terrestrial solar
 cells
 {NASA-TN-78924} p0136 W78-25551

WELLS, R. A.
 Method of fan sound mode structure determination
 computer program user's manual: Microphone
 location program
 {NASA-CR-135294} p0028 W78-17065

- Method of fan sound mode structure determination
computer program user's manual: Model
calculation program
{NASA-CN-135295} p0028 W78-17066
- WELLS, E. W.
Method of fan sound mode structure determination
{NASA-CN-135293} p0028 W78-17064
- WEN, C. Y.
Fluidized bed combustor modeling
{NASA-CN-135164} p0067 W78-14119
- WENSKY, S. L.
Simulated flight effects on noise characteristics
of a fan inlet with high throat Mach number
{NASA-TF-1129} p0017 W78-20132
- Comparison of the noise characteristic of two low
pressure ratio fans with a high throat Mach
number inlet
{NASA-TN-73880} p0018 W78-21108
- WESTERVELT, W. G.
Dynamic tooth loads and stressing for high contact
ratio spur gears
{AIAA PAPER 77-DET-101} p0123 A78-20606
- WESTFALL, L. J.
Predicted inlet gas temperatures for tungsten
fiber reinforced superalloy turbine blades
p0060 A78-33203
- Predicted inlet gas temperatures for tungsten
fiber reinforced superalloy turbine blades
{NASA-TN-73842} p0017 W78-19157
- WESTFIELD, W. T.
General aviation piston-engine exhaust emission
reduction p0013 W78-11073
- WESTROBLAND, J. S.
VCE tested program planning and definition study
{NASA-CN-135362} p0029 W78-19160
- WESLER, B. S.
Composition of RF-sputtered refractory compounds
determined by I-ray photoelectron spectroscopy
p0085 A78-30301
- I-ray photoelectron spectroscopic study of surface
chemistry of dibenzyl disulfide on steel under
mild and severe wear conditions p0066 A78-31439
- Principles of ESCA and applications to metal
corrosion, coating and lubrication p0061 A78-33213
- Principles of ESCA and application to metal
corrosion, coating and lubrication
{NASA-TN-78839} p0070 W78-19262
- I-ray photoelectron spectroscopy study of
radiofrequency-sputtered refractory compound
steel interfaces
{NASA-TF-1161} p0081 W78-20336
- Friction and wear of radiofrequency-sputtered
borides, silicides, and carbides
{NASA-TF-1156} p0081 W78-20338
- Application of ESCA to the determination of
stoichiometry in sputtered coatings and
interface regions
{NASA-TN-78694} p0065 W78-26185
- WHITE, J. L.
JT9D engine diagnostics. Task 2: Feasibility
study of measuring in-service flight loads
{NASA-CN-135395} p0030 W78-27124
- WHITE, W. F., JR.
Nonlinear flap-lag-axial equations of a rotating
beam with arbitrary precone angle
{AIAA 78-891} p0127 A78-29798
- WITTEWENGER, J. D.
Effect of prior creep at 1365 K on the room
temperature tensile properties of several oxide
dispersion strengthened alloys p0074 A78-21831
- Tensile and Creep properties of the experimental
oxide dispersion strengthened iron-base sheet
alloy Na-9561 at 1365 K p0074 A78-21858
- Elevated-temperature tensile and creep properties
of several ferritic stainless steels
{NASA-TN-73853} p0069 W78-17189
- Elevated-temperature flow strength, creep
resistance and diffusion welding characteristics
of Ti-6Al-2Nb-1Ta-0.8Mo
{NASA-TN-73854} p0069 W78-17190
- WILSON, P. J.
Mercury ion thruster research, 1977
{NASA-CN-135317} p0052 W78-15167
- WILHELM, S. E.
Apparatus for extraction and separation of a
preferentially photo-dissociated molecular
isotope into positive and negative ions by means
of an electric field
{NASA-CASR-LEU-12465-1} p0065 W78-25148
- WILLIAMS, R. C.
VSTOL tilt nacelle aerodynamics and its relation
to fan blade stresses
{AIAA PAPER 78-958} p0007 A78-43520
- VSTOL tilt nacelle aerodynamics and its relation
to fan blade stresses
{NASA-TN-78899} p0005 W78-26099
- WILLIAMS, S. S.
Engineering Model 8-cv Thruster System
{AIAA PAPER 78-646} p0055 A78-37434
- WILLIS, E. A.
General aviation energy-conservation research
programs at NASA-Lewis Research Center
p0024 A78-29330
- General aviation internal combustion engine
research programs at NASA-Lewis Research Center
{AIAA PAPER 78-932} p0025 A78-43505
- General aviation energy-conservation research
programs at NASA-Lewis Research Center
{NASA-TN-73884} p0016 W78-17060
- General aviation internal-combustion engine
research programs at NASA-Lewis Research Center
{NASA-TN-78891} p0011 W78-24139
- WILSON, A.
Dynamic modeling of spacecraft in a collisionless
plasma p0037 W78-10150
- WILSON, C. A.
YP 102 in-duct combustor noise measurement, volume 1
{NASA-CN-135404-VOL-1} p0167 W78-25827
- YP 102 in-duct combustor noise measurement, volume 2
{NASA-CN-135404-VOL-2} p0167 W78-25828
- YP 102 in-duct combustor noise measurement, volume 3
{NASA-CN-135404-VOL-3} p0167 W78-25829
- WISBILLE, J. E.
NASA's use for cyclic response and fatigue
analysis of wind turbine towers p0125 W78-12459
- WISER, W. O.
Petrographic analysis of wear particles from
sliding elastohydrodynamic experiments
{NASA-TF-1710} p0115 W78-22377
- WISOCUP, J.
Analysis and design of a high power laser adaptive
phased array transmitter
{NASA-CN-134952} p0111 W78-13420
- WINSA, E. A.
Predicted inlet gas temperatures for tungsten
fiber reinforced superalloy turbine blades
p0060 A78-33203
- Predicted inlet gas temperatures for tungsten
fiber reinforced superalloy turbine blades
{NASA-TN-73842} p0017 W78-19157
- WITTEBS, W. E.
Fiber reinforced FRB polyimide composites
{NASA-CN-135377} p0063 W78-25132
- WITUCKY, E. G.
5200 cycle of an 8-cm diameter Hg ion thruster
{AIAA PAPER 78-649} p0050 A78-32736
- Pulse ignition characterization of mercury ion
thruster hollow cathode using an improved pulse
ignitor
{AIAA PAPER 78-709} p0051 A78-32773
- Pulse ignition characterization of mercury ion
thruster hollow cathode using an improved pulse
ignitor
{NASA-TN-78858} p0047 W78-21203
- The 5200 cycle test of an 8-cm diameter Hg ion
thruster
{NASA-TN-78860} p0048 W78-21208
- WISARD, D. W.
Friction and wear of several compressor gas-path
seal movements
{NASA-TF-1128} p0068 W78-15229
- Preliminary study of cyclic thermal shock
resistance of plasma-sprayed zirconium oxide
turbine outer air seal shrouds
{NASA-TN-73852} p0080 W78-15280
- Friction and wear of selected metals and alloys in
sliding contact with AISI 440 C stainless steel
in liquid methane and in liquid natural gas
{NASA-TF-1150} p0114 W78-20512

- WISLER, S. C.
Core compressor exit stage study. Volume 1:
Blading design
[NASA-CR-135391] p0031 W78-29099
- WITBEK, S. E.
High toughness-high strength iron alloy
[NASA-CASR-LTU-125a2-2] p0070 W78-22205
- WITBEK, S. E.
Experimental transient and permanent deformation
studies of steel-sphere-impacted or
explosively-impelled aluminum panels
[NASA-CR-135315] p0076 W78-15236
- WITT, A. F.
Materials science experiments in space
[NASA-CR-2842] p0056 W78-16094
- WITBEK, S. E.
Cryogenic properties of a new tough-strong iron
alloy p0073 W78-15825
- Comparison of equivalent energy and energy per
unit area / σ bar/ data with valid fracture
toughness data for iron, aluminum, and titanium
alloys p0074 W78-24372
- Development of strong and tough cryogenic Fe-12Ni
alloys containing reactive metal additions
p0076 W78-21465
- Materials technology assessment for stirling engines
[NASA-TN-73789] p0069 W78-17187
- Effects of thermochemical processing on strength
and toughness of iron - 12-percent-nickel -
reactive metal alloys at -196 C
[NASA-TP-1308] p0073 W78-31213
- WOLCOTT, P. S.
Study of 42 and 85 GHz coupled cavity
traveling-wave tubes for space use
[NASA-CR-134670] p0098 W78-11295
- WONG, E. L.
Effect of trichlorofluoromethane and molecular
chlorine on ozone formation by simulated solar
radiation [NASA-TP-1093] p0064 W78-12167
- Effect of nitric oxide on photochemical ozone
formation in mixtures of air with molecular
chlorine and with trichlorofluoromethane
[NASA-TP-1192] p0065 W78-20281
- WOOD, J. E.
Experimental performance of a
13.65-centimeter-tip-diameter tandem-bladed
sweptback centrifugal compressor designed for a
pressure ratio of 6
[NASA-TP-1091] p0003 W78-11002
- WOODWARD, E. P.
Effectiveness of an inlet flow turbulence control
device to simulate flight fan noise in an
anechoic chamber p0024 W78-24880
- Reduction of fan noise in an anechoic chamber by
reducing chamber wall induced inlet flow
disturbances p0166 W78-37681
- Acoustic evaluation of a novel swept-rotor fan
[AIAA PAPER 78-1121] p0166 W78-41831
- Effectiveness of an inlet flow turbulence control
device to simulate flight fan noise in an
anechoic chamber [NASA-TN-73855] p0163 W78-13856
- Reduction of fan noise in an anechoic chamber by
reducing chamber wall induced inlet flow
disturbances [NASA-TN-78854] p0164 W78-22860
- Acoustic evaluation of a novel swept-rotor fan
[NASA-TN-78878] p0164 W78-24897
- WOOLAN, J. A.
Niobium-germanium superconducting tapes for
high-field magnet applications [NASA-CR-135364] p0099 W78-19392
- Atomic hydrogen storage method and apparatus
[NASA-CASR-LTU-12081-2] p0169 W78-19907
- WOOLDRIDGE, G. E.
Preliminary power train design for a
state-of-the-art electric vehicle
[NASA-CR-135340] p0185 W78-29584
- WOOLMAN, J. A.
Upper limit for magnetoresistance in silicon
bronze and phosphor bronze wire p0174 W78-14623
- Physics and chemistry of MoS₂ intercalation
compounds p0175 W78-27727
- Superconducting Nb₃Ge for high-field magnets
p0175 W78-41922
- Critical currents in sputtered PbMoS₆
p0175 W78-45368
- Critical currents and scaling laws in sputtered
copper molybdenum sulfide p0175 W78-48500
- Upper critical field of copper molybdenum sulfide
p0175 W78-53626
- Atomic hydrogen storage method and apparatus
[NASA-CASR-LTU-12081-1] p0089 W78-24365
- WRIGHT, D.
The 20/30 GHz satellite system technology needs
assessment [NASA-TN-78975] p0093 W78-31323
- WRIGHT, D. E.
Hydrogen turbine power conversion system assessment
[NASA-CR-135298] p0144 W78-20621
- WRIGHT, D. L.
Communication satellite services for special
purpose users p0094 W78-31971

Y

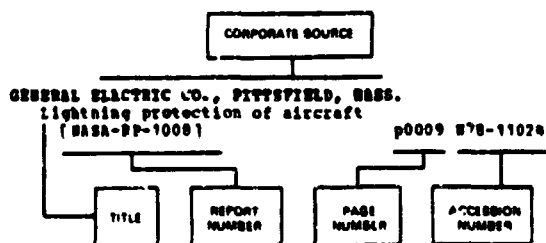
- YAO, S.
Filament-winding fabrication of QCSR
configuration fan blades
[NASA-CR-135332] p0028 W78-16052
- Composite hub/metal blade compressor
rotor [NASA-CR-135343] p0022 W78-18131
- YARBRA, A. E.
A combined potential and viscous flow solution for
V/STOL engine inlets [AIAA PAPER 78-142] p0006 W78-20702
- YEE, S. T.
Influence of wind turbine foundation p0133 W78-19626
- YEH, B. C.
Microstructure of hot-pressed Al₂O₃-Si₃N₄ mixtures
as a function of holding temperature p0084 W78-17456
- Consolidation of silicon nitride without additives
p0085 W78-24895
- Effect of attrition milling on the reaction
sintering of silicon nitride p0086 W78-50324
- Consolidation of silicon nitride without additives
[NASA-TN-73693] p0057 W78-10217
- Effects of pressure and temperature on hot
pressing a silicon [NASA-TN-78945] p0083 W78-27274
- Effect of attrition milling on the reaction
sintering of silicon nitride [NASA-TN-78945] p0084 W78-31236
- YEBUTCH, G.
Thermal energy storage heat exchanger: Molten
salt heat exchanger design for utility power
plants [NASA-CR-135244] p0183 W78-16632
- Thermal energy storage heat exchanger: Molten
salt heat exchanger design for utility power
plants [NASA-CR-135245] p0183 W78-16633
- YIB, C.
The effect of minor additions of titanium on the
fracture toughness of Fe-12Ni alloys at 77K
[NASA-CR-135351] p0078 W78-19259
- YOKEL, S. A.
Design of impact-resistant boron/aluminum large
fan blade [NASA-CR-135417] p0031 W78-29104
- YOST, B. C.
Preburner of staged combustion rocket engine
[NASA-CR-135356] p0054 W78-24279
- YOUNG, L. E.
Status of wraparound contact solar cells and arrays
[NASA-TN-78911] p0137 W78-26543
- YOUNG, S. G.
Feasibility study of tungsten as a diffusion
barrier between nickel-chromium-aluminum and
Gama/Gama prime - Delta eutectic alloys
[NASA-TP-1131] p0068 W78-15230
- YU, Y.
Modeling and Analysis of Power Processing Systems
(MAPPS), initial phase 2
[NASA-CR-135173] p0100 W78-29350

Z

- ZAFRAN, S.
 Ion beam plume and efflux measurements of an 8-cm
 mercury ion thruster
 [AIAA PAPER 78-676] p0099 A78-12753
 Ion beam plume and efflux characterization flight
 experiment study
 [NASA-CN-135275] p0052 W78-12140
 Ion engine auxiliary propulsion applications and
 integration study
 [NASA-CN-135312] p0053 W78-15168
- ZAPLATONSKI, I.
 Volatilization of oxides during oxidation of some
 superalloys at 1200 C
 p0073 A78-18631
 Reactions of yttria-stabilized zirconia with
 oxides and sulfates of various elements
 [NASA-TN-78942] p0071 W78-29216
- ZARITSKY, E. V.
 Experimental and analytical load-life relation for
 AISI 5310 steel spur gears
 [ASME PAPER 77-PET-121] p0118 A78-20609
 Predicted and experimental performance of
 jet-lubricated 120-millimeter-bore ball bearings
 operating to 7.5 million DW
 [NASA-TP-1196] p0118 W78-20513
 Rolling-element fatigue life of AISI 5-50 and
 18-8-1 balls
 [NASA-TP-1202] p0115 W78-21473
- ZAVENET, R.
 Constrained sloshing of liquid mercury in a
 flexible spherical tank
 [AIAA PAPER 78-670] p0106 A78-32749
 Constrained sloshing of liquid mercury in a
 flexible spherical tank
 [NASA-TN-78833] p0103 W78-21403
- ZELIN, J. A.
 Technological development of cylindrical and flat
 shaped high energy density capacitors
 [NASA-CN-135286] p0099 W78-28456
- ZELLARS, G. B.
 Feasibility study of tungsten as a diffusion
 barrier between nickel-chromium-aluminum and
 Gamma/Gamma prime - Delta eutectic alloys
 [NASA-TP-1111] p0068 W78-12230
 Erosion/corrosion of turbine airfoil materials in
 the high-velocity effluent of a pressurized
 fluidized coal combustor
 [NASA-TP-1274] p0071 W78-28225
- ZELLSER, J. B.
 Optimal control of a supersonic inlet to minimize
 frequency of inlet unstart
 p0019 W78-23024
- ZISNIBASHVILI, J. A.
 Fuel consumption improvement in current transport
 engines
 [AIAA PAPER 78-940] p0033 A78-45097
 NASA/General Electric Engine Component Improvement
 Program
 [AIAA PAPER 78-929] p0025 A78-45098
- ZIMMERMAN, S. F.
 Development and fabrication of a diffusion welded
 Columbian alloy heat exchanger
 [AIAA PAPER 78-61] p0123 A78-31500
- ZOLA, C. L.
 Preliminary study of propulsion systems and
 airplane wing parameters for a US Navy subsonic
 V/STOL aircraft
 [NASA-TN-73652] p0010 W78-17081

CORPORATE SOURCE INDEX

Typical Corporate Source Index Listing



The title of the document is used to provide a brief description of the subject matter. The page number and NASA or AIAA accession number are included in each entry to assist the user in locating the abstract in the abstract section. If applicable, a report number is also included as an aid in identifying the document.

A

- ADVANCED TECHNOLOGY LABS., INC., WESTBURY, N. Y.
Computation of unsteady transonic flows through rotating and stationary cascades. 2: User's guide to FORTRAN program B2D4TL [NASA-CR-2901] p0007 N78-12034
- Computation of unsteady transonic flows through rotating and stationary cascades. 1: Acoustic far-field analysis [NASA-CR-2902] p0007 N78-12035
- Computation of unsteady transonic flows through rotating and stationary cascades. 1: Method of analysis [NASA-CR-2900] p0008 N78-20082
- ASSOCIATED LIQUID JACKET CO., SACRAMENTO, CALIF.
Supercritical oxygen heat transfer [NASA-CR-135339] p0108 N78-17342
- AIRRESEARCH SFG. CO., FROBNIH, ARIZ.
Cost/benefit analysis of advanced aerobion technologies for small aircraft turbine engines [NASA-CR-135265] p0077 N78-12083
- Pollution Reduction Technology Program for small jet aircraft engines, phase 2 [NASA-CR-159815] p0232 N78-33104
- AIRRESEARCH SFG. CO., TORRANCE, CALIF.
Preliminary design study of an alternate heat source assembly for a Brayton isotopw power system [NASA-CR-135428] p0145 N78-28600
- ARMON SIV., OHIO.
Constrained sloshing of liquid mercury in a flexible spherical tank [AIAA PAPER 78-670] p0106 A78-32749
- ASTHEDAN UNIV. (HEYHEBLAUS).
Metastable states of small rare gas crystallites p0149 A78-16069
- ARMY AIR MOBILITY RESEARCH AND DEVELOPMENT LAB., CLEVELAND, OHIO.
Simplified solution for elliptical-contact deformation between two elastic solids p0118 A78-12717
- Fraction and wear of sintered fibermetal abradable seal materials p0278 A78-23451
- A Weibull characterization for tensile fracture of multicomponent brittle fibers p0060 A78-24892
- Combustor concepts for aircraft gas turbine low-power emissions reduction [AIAA PAPER 78-999] p0024 A78-83544
- ARMY AIR MOBILITY RESEARCH AND DEVELOPMENT LAB., HANPTON, VA.
Nonlinear flap-lag-azial equations of a rotating beam with arbitrary precone angle [AIAA 78-491] p0127 A78-29798
- ARMY AVIATION RESEARCH AND DEVELOPMENT COMMAND, ST. LOUIS, MO.
Long-term hot-hardness characteristics of five through-hardened bearing steels [NASA-TP-1201] p0073 N78-33196
- ATLANTIC BECHFIELD CO., SARVEY, ILL.
Jet fuel's free synthetic grades p0090 A78-43415
- AVCO-EVERETT RESEARCH LAB., MASS.
Laser absorption phenomena in firing gas devices [NASA-CR-135129] p0112 N78-18411
- AVCO LYCOMING DIV., STRATFORD, CONN.
TF 102 in-duct combustor noise measurement, volume 1 [NASA-CR-135404-VOL-1] p0167 N78-25827
- TF 102 in-duct combustor noise measurement, volume 2 [NASA-CR-135404-VOL-2] p0167 N78-25828
- TF 102 in-duct combustor noise measurement, volume 3 [NASA-CR-135404-VOL-3] p0167 N78-25829
- AVCO LYCOMING ENGINE GROUP, STRATFORD, CONN.
Development of spiral-groove self-acting face seals [NASA-CR-135303] p0521 N78-17387

B

- BATTELLE COLUMBUS LABS., OHIO.
Influence of adsorbed fluids on the rolling contact deformation of MgO single crystals p0123 A78-23447
- BOEING AEROSPACE CO., SEATTLE, WASH.
Evaluation of flawed composite structure under static and cyclic loading p0063 A78-26683
- Effect of preload on the fatigue and static strength of composite laminates with defects p0061 A78-40310
- Analysis and test of deep flaws in thin sheets of aluminum and titanium. Volume 1: Program summary and data analysis [NASA-CR-135369] p0127 N78-21493
- Analysis and test of deep flaws in thin sheets of aluminum and titanium. Volume 2: Crack opening displacement and stress-strain data [NASA-CR-135370] p0127 N78-21494
- BOEING COMMERCIAL AIRPLANE CO., SEATTLE, WASH.
Development and test of an inlet and duct to provide airflow for a wing boundary layer control system [AIAA PAPER 78-141] p0004 A78-20701
- J79D engine diagnostics. Task 2: Feasibility study of measuring in-service flight loads [NASA-CR-135195] p0030 N78-27124
- BOEING COMPUTER SERVICES, INC., SEATTLE, WASH.
A simulation model for wind energy storage systems. Volume 1: Technical report [NASA-CR-135281] p0156 N78-20802
- A simulation model for wind energy storage systems. Volume 2: Operation manual [NASA-CR-135284] p0157 N78-20803
- A simulation model for wind energy storage systems. Volume 3: Program descriptions [NASA-CR-135285] p0157 N78-20804
- BOEING MILITARY AIRPLANE DEVELOPMENT, SEATTLE, WASH.
VSTOL tilt nacelle aerodynamics and its relation to fan blade stresses [AIAA PAPER 78-458] p0007 A78-43520
- BOOS-ALLEN AND HAMILTON, INC., CLEVELAND, OHIO.
Preliminary power train design for a state-of-the-art electric vehicle

[NASA-CR-135381] p0182 W78-29992
BUSINESS AND TECHNOLOGICAL SYSTEMS, INC., SHARROCK,
MD.

SEP EUCKE-87 and Halley rendezvous studies and
improved S/C model implementation in EILTOP
[NASA-CR-135418] p0038 W78-25105
Heliocentric interplanetary low thrust
trajectory optimization program, supplement 1,
part 2
[NASA-CR-135418-APP] p0038 W78-25106

C

CALIFORNIA INST. OF TECH., PASADENA.
Modelling, analyses and design of switching
converters
[NASA-CR-135178] p0100 W78-29351

CALIFORNIA UNIV., BERKELEY. LAWRENCE BERKELEY LAB.
The design of an Fe-12Mn-0.2Ti alloy steel for
low temperature use
[NASA-CR-135310] p0078 W78-20310

CALIFORNIA UNIV., LA JOLLA.
Critical currents in sputtered PbMoSS
[NASA-CR-135308] p0175 A78-45368
Critical currents and scaling laws in sputtered
copper molybdenum sulfide
[NASA-CR-135309] p0175 A78-45500

CALIFORNIA UNIV., LOS ANGELES.
Experiments on whistler wave filamentation and
VLF hiss in a laboratory plasma
[NASA-CR-135307] p0149 A78-41788

CAMBRIDGE UNIV. (ENGLAND).
Sound production in a moving stream
[NASA-CR-135306] p0165 A78-31224

CARNEGIE-MELLON UNIV., PITTSBURGH, PA.
The effect of microstructure and strength on the
fracture toughness of an 18 Ni, 300 grade
maraging steel
[NASA-CR-135288] p0078 W78-16150

CASE WESTERN RESERVE UNIV., CLEVELAND, OHIO.
A viscous-inviscid interactive compressor
calculation
[AIAA PAPER 78-1140] p0006 A78-41843

Interpolation and extrapolation of creep rupture
data by the minimum commitment method. II -
Oblique translation
[NASA-CR-135287] p0076 A78-45426

Interpolation and extrapolation of creep rupture
data by the minimum commitment method. I -
Focal-point convergence
[NASA-CR-135286] p0076 A78-45427

Interpolation and extrapolation of creep rupture
data by the minimum commitment method. III -
Analysis of multibeats
[NASA-CR-135285] p0076 A78-45428

Numerical computation of three-dimensional
circulation in Lake Erie - A comparison of a
free-surface model and a rigid-lid model
[NASA-CR-135284] p0151 A78-47223

Convection due to surface-tension gradients
[NASA-CR-135283] p0108 A78-48716

Adaptation of ion beam technology to
microfabrication of solid state devices and
transducers
[NASA-CR-135314] p0099 W78-15397

Effect of surface texture by ion beam sputtering
on implant biocompatibility and soft tissue
attachment
[NASA-CR-135311] p0152 W78-18672

CHEVSELER CORP., DETROIT, MICH.
Splitter-bladed centrifugal compressor impeller
designed for automotive gas turbine application
[NASA-CR-135237] p0121 W78-10472

CINCINNATI UNIV., OHIO.
Optimal controls for an advanced turbofan engine
[NASA-CR-135236] p0033 A78-23893

Analysis of the cross flow in a radial inflow
turbine scroll
[NASA-CR-135320] p0029 W78-19153

Computer program for the analysis of the cross
flow in a radial inflow turbine scroll
[NASA-CR-135321] p0029 W78-19154

CLEVELAND STATE UNIV., OHIO.
Microstructure of hot-pressed Al₂O₃-Si₃N₄
mixtures as a function of holding temperature
[NASA-CR-135322] p0084 A78-17456
Consolidation of silicon nitride without additives
[NASA-CR-135323] p0085 A78-24895

Thermal environment effects on strength and
impact properties of boron-aluminum composites
[NASA-CR-135324] p0050 A78-33204
Effect of attrition milling on the reaction
sintering of silicon nitride
[NASA-CR-135325] p0086 A78-50324

COLORADO STATE UNIV., FORT COLLINS.
Metastable states of small rare gas crystallites
[NASA-CR-135326] p0169 A78-16069

Charge-exchange plasma generated by an ion
thruster
[NASA-CR-135318] p0052 W78-13123

Mercury ion thruster research, 1977
[NASA-CR-135317] p0052 W78-15167

Industrial ion source technology
[NASA-CR-135353] p0169 W78-18883

Inert gas thrusters
[NASA-CR-135226] p0053 W78-19198

Apparatus for extraction and separation of a
preferentially photo-dissociated molecular
isotope into positive and negative ions by
means of an electric field
[NASA-CR-135227] p0065 W78-25148

A visual investigation of turbulence in
stagnation flow about a circular cylinder
[NASA-CR-3019] p0108 W78-33386

COLT INDUSTRIES, INC., PITTSBURGH, PA.
Fabrication of stainless steel clad tubing
[NASA-CR-135347] p0079 W78-21265

CONTROL DATA CORP., MINNEAPOLIS, MINN.
Variability of ozone near the tropopause from
GASP data
[NASA-CR-135405] p0148 W78-23648

CORNELL UNIV., ITHACA, N. Y.
Impact on multilayered composite plates
[NASA-CR-135287] p0042 W78-16103

CYCLOPS CORP., BRIDGEVILLE, PA.
An experimental P/B wrought superalloy for
advanced temperature service
[NASA-CR-135288] p0073 A78-15335

D

DAYTON UNIV., OHIO.
Continuation of the compendium of applications
technology satellite and communications
technology satellite user experiments
1967-1977, volume 1
[NASA-CR-135416-VOL-1] p0042 W78-31141

Continuation of the compendium of applications
technology satellite and communications
technology satellite user experiments
1967-1977, volume 2
[NASA-CR-135416-VOL-2] p0042 W78-31142

DAYTON UNIV. RESEARCH INST., OHIO.
A forecast of broadcast satellite communications
[NASA-CR-135417] p0094 A78-15615

DEPARTMENT OF COMMUNICATIONS, OTTAWA (ONTARIO).
Summary of the CTS Transient Event Counter data
after one year of operation
[NASA-CR-135418] p0046 A78-19566

DETROIT DIESEL ALLISON, INDIANAPOLIS, IND.
Aerodynamic performance of conventional and
advanced design labyrinth seals with
solid-smooth abrasible, and honeycomb lands
[NASA-CR-135307] p0122 W78-27427

DOUGLAS AIRCRAFT CO., INC., LONG BEACH, CALIF.
Effect of forward motion on engine noise
[NASA-CR-134954] p0026 W78-10093

F

FAIRCHILD SPACE AND ELECTRONICS CO., GERRANTOWN, MD.
Low cost Ku-band earth terminals for
voice/data/facsimile
[NASA-CR-135419] p0094 A78-31970

Communication satellite services for special
purpose users
[NASA-CR-135420] p0094 A78-31971

Low cost satellite land mobile service for
nationwide applications
[NASA-CR-135421] p0095 A78-43173

FIBER SCIENCE, INC., GARDENA, CALIF.
Filament-winding fabrication of QCSE
configuration fan blades
[NASA-CR-135332] p0028 W78-16052
Composite hub/metal blade compressor rotor
[NASA-CR-135343] p0062 W78-18131

FLORIDA UNIV., GAINESVILLE.

A methodology for experimentally-based determination of gap shrinkage and effective lifetimes in the emitter and base of p-n-junction solar cells

p0181 A78-10903

Effect of ice condensation on liquid-nitrogen drops in film boiling

p0105 A78-15621

Thermally driven oscillations and wave motion of a liquid drop

p0106 A78-17508

Cold effects on middle ultraviolet global radiation

p0150 A78-82952

FORD MOTOR CO., DEARBORN, MICH.

Fabrication of thin layer beta alumina

[NASA-CR-135308] p0077 W78-14143

Automotive Stirling engine development program

[NASA-CR-135331] p0181 W78-22970

Ceramic regenerator systems development program

[NASA-CR-135330] p0181 W78-25988

Ceramic regenerator systems development program

[NASA-CR-135430] p0181 W78-26997

G

GELLES (S. N.) ASSOCIATES, COLUMBUS, OHIO.

Materials science experiments in space

[NASA-CR-2842] p0056 W78-16094

GENERAL APPLIED SCIENCE LABS., INC., WESTBURY, N. Y.

Experimental study of the effects of flameholder geometry on emissions and performance of lean

premixed combustors

[NASA-CR-135428] p0030 W78-26147

Experimental study of the effect of cycle pressure on lean combustion emissions

[NASA-CR-3032] p0031 W78-28098

GENERAL DYNAMICS/CONVAIR, SAN DIEGO, CALIF.

Conceptual design for spacelab two-phase flow experiments

[NASA-CR-135327] p0037 W78-18063

Thermal performance of a customized multilayer insulation (MLI). Design and fabrication of

test facility hardware

[NASA-CR-157648] p0062 W78-20257

Filling of orbital fluid management systems

[NASA-CR-159404] p0108 W78-31380

GENERAL DYNAMICS CORP., SAN DIEGO, CALIF.

ADJUST - An automated system for steering

Centaur launch vehicles in measured winds

p0045 A78-14991

GENERAL ELECTRIC CO., CINCINNATI, OHIO.

Sound separation probes for flowing duct noise

measurements

p0033 A78-17396

Failure detection and correction for turbofan

engines

p0033 A78-23918

NASA/General Electric Engine Component

Improvement Program

[AIAA PAPER 78-929] p0025 A78-85098

Oil cooling system for a gas turbine engine

[NASA-CASE-LEW-12321-1] p0113 W78-10467

Impact absorbing blade mounts for variable pitch

blades

[NASA-CASE-LEW-12313-1] p0113 W78-10468

Cost benefit study of advanced materials

technology for aircraft turbine engines

[NASA-CR-135235] p0026 W78-11081

Manufacture and engine test of advanced oxide

dispersion strengthened alloy turbine vanes

[NASA-CR-135269] p0077 W78-11232

Augmentor emissions reduction technology program

[NASA-CR-135215] p0027 W78-13057

Advanced supersonic propulsion study, phases 3

and 4

[NASA-CR-135236] p0027 W78-13058

Impact resistant boron/aluminum composites for

large fan blades

[NASA-CR-135278] p0062 W78-14099

Variable thrust nozzle for quiet turbofan engine

and method of operating same

[NASA-CASE-LEW-12317-1] p0016 W78-17055

Gas turbine engine with convertible accessories

[NASA-CASE-LEW-12390-1] p0016 W78-17056

Variable cycle gas turbine engines

[NASA-CASE-LEW-12916-1] p0113 W78-17384

Long-term CP6 engine performance deterioration:

Evaluation of engine S/W 451-479

[NASA-CR-135381] p0029 W78-20129

Wind tunnel performance tests of conical plug

nozzles

[NASA-CR-2990] p0002 W78-21044

QCSEE task 2: Engine and installation

preliminary design

[NASA-CR-138738] p0030 W78-23089

Gas turbine engine with recirculating bleed

[NASA-CASE-LEW-12452-1] p0019 W78-25089

Acoustic tests of duct-burning turbofan jet

noise simulation

[NASA-CR-2966] p0002 W78-28043

Acoustic tests of duct-burning turbofan jet

noise simulation: Comprehensive data report.

Volume 1, section 2: Full size data

[NASA-CR-135239-VOL-1-SECT-2] p0030 W78-28095

Acoustic tests of duct-burning turbofan jet

noise simulation: Comprehensive data report.

Volume 1, section 3: Data plots

[NASA-CR-135239-VOL-1-SECT-3] p0030 W78-28096

Acoustic tests of duct-burning turbofan jet

noise simulation: Comprehensive data report.

Volume 2: Model design and aerodynamic test

results

[NASA-CR-135239-VOL-2] p0031 W78-28097

Core compressor exit stage study. Volume 1:

Blading design

[NASA-CR-135391] p0031 W78-29099

Long-term CP6 engine performance deterioration:

Evaluation of engine S/W 451-380

[NASA-CR-159390] p0031 W78-29103

Design of impact-resistant boron/aluminum large

fan blade

[NASA-CR-135417] p0031 W78-29104

Energy efficient engine: Preliminary design and

integration studies

[NASA-CR-135444] p0032 W78-31108

Rolling element fatigue testing of gear materials

[NASA-CR-135411] p0122 W78-31427

Aircraft gas turbine low-power emissions

reduction technology program

[NASA-CR-135434] p0032 W78-32097

Redundant disc

[NASA-CASE-LEW-12496-1] p0022 W78-33101

Blade row dynamic digital compression program.

Volume 2: J85 circumferential distortion

redistribution model, effect of stator

characteristics, and stage characteristics

sensitivity study

[NASA-CR-134953] p0032 W78-33103

Rolling element fatigue testing of gear materials

[NASA-CR-135450] p0124 W78-33463

Evaluation of cyclic behavior of aircraft

turbine disk alloys

[NASA-CR-159433] p0128 W78-33478

GENERAL ELECTRIC CO., CLEVELAND, OHIO.

Integrity of the fracture mechanism of

Ti-5Al-2.5Sn at cryogenic temperatures

p0075 A78-32319

Variable mixer propulsion cycle

[NASA-CASE-LEW-12917-1] p0016 W78-18067

GENERAL ELECTRIC CO., EVANSDALE, OHIO.

Effect of wall thickness and material on

flexural fatigue of hollow rolling elements

[ASME PAPER 77-LUB-78] p0126 A78-23355

Effects of film injection on performance of a

cooled turbine

p0033 A78-28902

Development and fabrication of a diffusion

welded Columbian alloy heat exchanger

[AIME PAPER 78-61] p0123 W78-31500

Combustor concepts for aircraft gas turbine

low-power emissions reduction

[AIAA PAPER 78-999] p0025 A78-83546

Effects of film injection on performance of a

cooled turbine

p0029 W78-21147

GENERAL ELECTRIC CO., PHILADELPHIA, PA.

Design study of wind turbines 50 kW to 3000 kW

for electric utility applications. Volume 1:

Summary report

[NASA-CR-138934] p0143 W78-12529

Improved ceramic heat exchanger material

[NASA-CR-135292] p0086 W78-13209

Design study of wind turbines 50 kW to 3000 kW

for electric utility applications. Volume 2:

Analysis and Design

[NASA-CR-134935] p0143 W78-17462
 Design study of wind turbines 50 kw to 3000 kw
 for electric utility applications. Volume 3:
 Supplementary design and analysis tasks
 [NASA-CR-135121] p0144 W78-17463

GENERAL ELECTRIC CO., PITTSFIELD, MASS.
 Lightning protection of aircraft
 [NASA-RP-1008] p0009 W78-11024

GENERAL ELECTRIC CO., SCHENECTADY, N. Y.
 Revised international representations for the
 viscosity of water and steam and new
 representations for the surface tension of water
 p0105 A78-15725

Failure detection and correction for turbofan
 engines p0033 A78-23918

Pulse battery charger employing 1000 ampere
 transistor switches p0146 A78-31974

Design and calculated performance and cost of
 the ECAS Phase II open cycle NHD power
 generation system p0174 A78-33143
 [ASME PAPER 77-WA/ENR-5]

Open-Cycle Gas Turbine/Steam Turbine Combined
 Cycles with synthetic fuels from coal
 [ASME PAPER 77-WA/ENR-9] p0146 A78-33147

Performance and economics of advanced energy
 conversion systems for coal and coal-derived
 fuels p0146 A78-34078

GENERAL MOTORS CORP., INDIANAPOLIS, IND.
 Study and program plan for improved heavy duty
 gas turbine engine ceramic component development
 [NASA-CR-135230] p0122 W78-28466

GEORGIA INST. OF TECH., ATLANTA.
 Millimeter wave satellite concepts, volume 1
 [NASA-CR-135227] p0041 W78-15144

GORDIAN ASSOCIATES, INC., NEW YORK.
 Computer model for refinery operations with
 emphasis on jet fuel production. Volume 2:
 Data and technical bases p0090 W78-19326
 [NASA-CR-135334]

Computer model for refinery operations with
 emphasis on jet fuel production. Volume 1:
 Program description p0090 W78-20350
 [NASA-CR-135331]

Computer model for refinery operations with
 emphasis on jet fuel production. Volume 3:
 Detailed systems and programming documentation
 [NASA-CR-135335] p0090 W78-25235

GRUMMAN AEROSPACE CORP., BETHPAGE, N.Y.
 Thermal energy storage heat exchanger: Molten
 salt heat exchanger design for utility power
 plants p0143 W78-14632
 [NASA-CR-135244]

Thermal energy storage heat exchanger: Molten
 salt heat exchanger design for utility power
 plants p0143 W78-14633
 [NASA-CR-135245]

H

HAMILTON STANDARD, WINDSOR LOCKS, CONN.
 Dynamic tooth loads and stressing for high
 contact ratio spur gears p0123 A78-20606
 [ASME PAPER 77-DGT-101]

Aerodynamic design and performance testing of an
 advanced 30 deg swept, eight bladed propeller
 at Mach numbers from 0.2 to 0.85 p000F W78-32066
 [NASA-CR-13471]

HAWAII UNIV., HONOLULU.
 Synchronization of wind turbine generators
 against an infinite bus under gusting wind
 conditions p0142 A78-30196
 [IEEE PAPER 77 675-2]

Employing static excitation control and tie line
 reactance to stabilize wind turbine generators
 [NASA-CR-135344] p0144 W78-20603

HONEYWELL, INC., MINNEAPOLIS, MINN.
 Development of flat-plate solar collectors for
 the heating and cooling of buildings:
 Executive summary p0146 W78-33527
 [NASA-CR-134804-2]

HOBIOUS RESEARCH, INC., CLEVELAND, OHIO.
 High resolution masks for ion milling pores
 through substrates of biological interest
 [NASA-CR-135435] p0002 W78-29276

HUGHES AIRCRAFT CO., CULVER CITY, CALIF.
 High frequency capacitor-diode voltage

multiplier dc-dc converter development
 [NASA-CR-135399] p0099 W78-15400

Technological development of cylindrical and
 flat shaped high energy density capacitors
 [NASA-CR-135284] p0099 W78-24458

Closed cycle electric discharge laser design
 investigation p0112 W78-25407
 [NASA-CR-135408]

HUGHES AIRCRAFT CO., EL SEGUNDO, CALIF.
 Engineering Model 8-cs Thruster System
 [AIAA PAPER 78-646] p0055 A78-37434

HUGHES AIRCRAFT CO., LOS ANGELES, CALIF.
 Extended performance solar electric propulsion
 thrust system design p0055 A78-37430
 [AIAA PAPER 78-643]

HUGHES AIRCRAFT CO., TORRANCE, CALIF.
 Study of 42 and 85 GHz coupled cavity
 traveling-wave tubes for space use
 [NASA-CR-134670] p0098 W78-11295

HUGHES RESEARCH LABS., MALIBU, CALIF.
 Extended performance solar electric propulsion
 thrust system design p0055 A78-37430
 [AIAA PAPER 78-643]

Engineering Model 8-cs Thruster System
 [AIAA PAPER 78-646] p0055 A78-37434

Extended-performance thruster technology
 evaluation p0055 A78-37436
 [AIAA PAPER 78-666]

Economics of ion propulsion for large space
 systems p0040 A78-37441
 [AIAA PAPER 78-698]

Extended performance solar electric propulsion
 thrust system study. Volume 1: Executive
 summary p0052 W78-10205
 [NASA-CR-135281-VOL-1]

Extended performance solar electric propulsion
 thrust system study. Volume 4: Thruster
 technology evaluation p0053 W78-16090
 [NASA-CR-135281-VOL-4]

Extended performance solar electric propulsion
 thrust system study. Volume 5:
 Capacitor-diode voltage multiplier:
 Technology evaluation p0053 W78-19195
 [NASA-CR-135281-VOL-5]

Extended performance solar electric propulsion
 thrust system study. Volume 3: Tradeoff
 studies of alternate thrust system
 configurations p0053 W78-19196
 [NASA-CR-135281-VOL-3]

Excimer lasers p0112 W78-19480
 [NASA-CR-155949]

The 30-cm ion thruster power processor
 [NASA-CR-135401] p0054 W78-24280

HUGHES SPACE AND COMMUNICATIONS GROUP, LOS ANGELES,
 CALIF.
 Extended performance solar electric propulsion
 thrust system study. Volume 4: Thruster
 technology evaluation p0053 W78-16090
 [NASA-CR-135281-VOL-4]

I

IIT RESEARCH INST., CHICAGO, ILL.
 Lamination residual strains and stresses in
 hybrid laminates p0128 A78-12071

Thermal fatigue and oxidation data of
 superalloys including directionally solidified
 eutectics p0078 W78-15233
 [NASA-CR-135272]

Thermal fatigue and oxidation data for
 alloy/brake combinations p0078 W78-16149
 [NASA-CR-135299]

ILLINOIS UNIV., URBANA.
 A methodology for experimentally-based
 determination of gas shrinkage and effective
 lifetimes in the emitter and base of
 p-n-junction solar cells p0141 A78-10903

INDUSTRIAL TECTONICS, INC., CORPTON, CALIF.
 Lubrication of high-speed, large bore
 tapered-roller bearings p0118 A78-23354
 [ASME PAPER 77-LUB-13]

INTERNATIONAL HARVESTER CO., SAN DIEGO, CALIF.
 Advanced ceramic material for high temperature
 turbine tip seals p0087 W78-31238
 [NASA-CR-135319]

IONICS, INC., WATERBURY, MASS.
 Anion permselective membrane

[NASA-CR-135316] p0144 W78-18515
 IOWA UNIV., IOWA CITY.
 Methods for calculating the transonic boundary layer separation for V-STOL inlets at high incidence angles
 [AIAA 78-1340] p0007 A78-46537
 IRT CORP., SAN DIEGO, CALIF.
 Compact electron-beam source for formation of neutral beams of very low vapor pressure materials p0110 A78-41464

J

JET PROPULSION LAB., CALIF. INST. OF TECH., PASADENA.
 Physics and chemistry of MoS₂ intercalation compounds p0175 A78-27727
 JOINT CENTER FOR GRADUATE STUDY, RICHLAND, WASH.
 Stirling engine design manual [NASA-CR-135382] p0181 W78-23999

K

KAWASAWA CORP., BLOOMFIELD, CONN.
 Design study of wind turbines, 50 kW to 3000 kW for electric utility applications: Executive summary [NASA-CR-134936] p0144 W78-23559
 Design study of wind turbines 50 kW to 3000 kW for electric utility applications: Analysis and design [NASA-CR-134937] p0144 W78-23560
 KAWASAWA UNIV. (JAPAN).
 Friction, deformation and fracture of single-crystal silicon carbide [ASLE PREPRINT 77-IC-5C-3] p0085 A78-28438
 KENTUCKY UNIV., LEXINGTON.
 The effect of minor additions of titanium on the fracture toughness of Fe-12Ni alloys at 77K [NASA-CR-135351] p0078 W78-19259
 Conceptual design for spacelab pool boiling experiment [NASA-CR-135378] p0037 W78-20150

L

LEEDS UNIV. (ENGLAND).
 Temperature distributions and thermal stresses in a graded zirconia/metal gas path seal system for aircraft gas turbine engines [AIAA PAPER 78-93] p0118 A78-20683
 Elastohydrodynamic lubrication of elliptical contacts for materials of low elastic modulus. I - Fully flooded conjunction [ASME PAPER 77-LUB-10] p0119 A78-28414
 LOCKHEED AIRCRAFT CORP., PALO ALTO, CALIF.
 An ultralightweight, evacuated, load-bearing, high-performance insulation system [AIAA PAPER 78-878] p0045 A78-36005
 LOCKHEED-GEOORGIA CO., MARIETTA.
 Calculation of far-field jet noise spectra from near-field measurements using true source location [AIAA PAPER 78-1153] p0168 A78-41852
 LOCKHEED MISSILES AND SPACE CO., PALO ALTO, CALIF.
 Evacuated load-bearing high performance insulation study [NASA-CR-135342] p0092 W78-18251

M

MARTIN MARIETTA AEROSPACE, DENVER, COLO.
 Evaluation of low cost/high temperature fiber and blanket insulation p0063 A78-16903
 Effect of vibration on retention characteristics of screen acquisition systems [AIAA PAPER 78-1030] p0045 A78-43560
 MARTIN MARIETTA CORP., DENVER, COLO.
 Effect of vibration on retention characteristics of screen acquisition systems [NASA-CR-135264] p0107 W78-12364
 MASSACHUSETTS INST. OF TECH., CAMBRIDGE.
 Analysis of delamination in unidirectional and crossplied fiber composites containing surface cracks [NASA-CR-135248] p0062 W78-11197

Experimental transient and permanent deformation studies of steel-sphere-impacted or explosively-impulsed aluminum panels [NASA-CR-135315] p0078 W78-15234
 MAYA DEVELOPMENT CORP., SAN DIEGO, CALIF.
 The effect of environmental plasma interactions on the performance of the solar sail system [NASA-CR-135258] p0098 W78-13325
 MECHANICAL TECHNOLOGY, INC., LATHAU, N. Y.
 Stiffness and damping of elastomeric O-ring bearing mounts [NASA-CR-135328] p0127 W78-18460
 Balancing techniques for high-speed flexible rotors [NASA-CR-2975] p0121 W78-20514
 Hydrodynamic air lubricated compliant surface bearing for an automotive gas turbine engine. 1: Journal bearing performance [NASA-CR-135368] p0121 W78-21472
 Development of procedures for calculating stiffness and damping properties of elastomers in engineering applications. Part 8: Testing of elastomers under a rotating load [NASA-CR-135355] p0127 W78-22402
 Hydrodynamic air lubricated compliant surface bearing for an automotive gas turbine engine. 2: Materials and coatings [NASA-CR-135402] p0122 W78-29449
 MICHIGAN UNIV., ANN ARBOR.
 Lightweight, low compression aircraft diesel engine [NASA-CR-135300] p0121 W78-21471

N

NATIONAL AERONAUTICS AND SPACE ADMINISTRATION, WASHINGTON, D. C.
 A review of NASA's propulsion programs for civil aviation [AIAA PAPER 78-83] p0023 A78-20651
 NASA engine system technology programs - An overview [AIAA PAPER 78-928] p0025 A78-48452
 NATIONAL AERONAUTICS AND SPACE ADMINISTRATION, GODDARD INST. FOR SPACE STUDIES, NEW YORK.
 Cloud effects on middle ultraviolet global radiation p0150 A78-42952
 NATIONAL AERONAUTICS AND SPACE ADMINISTRATION, LANGLEY RESEARCH CENTER, HAMPTON, VA.
 Evaluation of initial collector field performance at the Langley Solar Building Test Facility p0141 A78-11391
 Nonlinear flap-lag-axial equations of a rotating beam with arbitrary precone angle [AIAA 78-491] p0127 A78-29798
 NATIONAL AERONAUTICS AND SPACE ADMINISTRATION, MARSHALL SPACE FLIGHT CENTER, HUNTSVILLE, ALA.
 Marshall Space Flight Center development program for solar heating and cooling systems p0110 A78-11368
 NATIONAL AEROSPACE LAB., TOKYO (JAPAN).
 Three-dimensional effects on pure tone fan noise due to inflow distortion [AIAA PAPER 78-1120] p0166 A78-41830
 NATIONAL OCEANIC AND ATMOSPHERIC ADMINISTRATION, SILVER SPRING, MD.
 Atmospheric ozone measurements made from B-747 airliners - Spring 1975 p0148 A78-24894
 NIELSEN ENGINEERING AND RESEARCH, INC., MOUNTAIN VIEW, CALIF.
 Perturbation solutions for blade-to-blade surfaces of a transonic compressor p0008 A78-12307
 Perturbation solutions for transonic flow on the blade-to-blade surface of compressor blade rows [NASA-CR-2941] p0001 W78-15987
 NORTON CO., SOMERSET, MASS.
 Improved reaction sintered silicon nitride [NASA-CR-135291] p0063 W78-22164
 NOTRE DAME UNIV., IND.
 Potential damage to dc superconducting magnets due to high frequency electromagnetic waves p0094 A78-34902
 Burning of liquid pools in reduced gravity [NASA-CR-135234] p0067 W78-25150

O

OBERLIN COLL., OHIO.
Upper limit for magnetoresistance in silicon
bronze and phosphor bronze wire
p0175 A78-14423

OWENS-ILLINOIS, INC., TOLEDO, OHIO.
Application of thick-film technology to solar
cell fabrication
p0186 A78-10947
Improved ceramic heat exchange material
[NASA-CR-135262] p0086 W78-10291

P

PANASTYRICS, INC., WALTHAM, MASS.
Ultraviolet spectrophotometer for measuring
columnar atmospheric ozone from aircraft
p0110 A78-35826

PASTER INTERNATIONAL CORP., LEWISTOWN, PA.
Evaluation of glass resin coatings for solar
cell applications
[NASA-CR-159392] p0145 W78-27540

PANASTYRICS, INC., WALTHAM, MASS.
Measurement of tropospheric 300 nm solar
ultraviolet flux for determination of O₃/ID/
photoproduction rate
p0148 A78-38835

PHYSICAL SCIENCES, INC., WOBURN, MASS.
Analytical study of laser-supported combustion
waves in hydrogen
[AIAA PAPER 78-1219] p0067 A78-41901
Analytical study of laser supported combustion
waves in hydrogen
[NASA-CR-135349] p0112 W78-20889

PRATT AND WHITNEY AIRCRAFT, EAST HARTFORD, CONN.
Aero-acoustic tests of duct-burning turbofan
exhaust nozzles. Comprehensive data report.
Volume 1: Model scale acoustic data
[NASA-CR-134910-VOL-1] p0002 W78-15988
Aero-acoustic tests of duct-burning turbofan
exhaust nozzles. Comprehensive data report.
Volume 2: Acoustic and aerodynamic data
[NASA-CR-134910-VOL-2] p0002 W78-15989
Aero-acoustic tests of duct-burning turbofan
exhaust nozzles. Comprehensive data report.
Volume 3: Acoustic and aerodynamic data curves
[NASA-CR-134910-VOL-3] p0002 W78-15990
Mean velocity, turbulence intensity and
turbulence convection velocity measurements
for a convergent nozzle in a free jet wind
tunnel. Comprehensive data report
[NASA-CR-135238] p0007 W78-17991
VCE testbed program planning and definition study
[NASA-CR-135362] p0029 W78-19160

PRATT AND WHITNEY AIRCRAFT, WEST PALM BEACH, FLA.
Analytical study of thermal barrier coated
first-stage blades in an F100 engine
[NASA-CR-135359] p0028 W78-17358

PRATT AND WHITNEY AIRCRAFT GROUP, EAST HARTFORD,
CONN.
Friction and wear of sintered fibermetal
abradable seal materials
p0074 A78-23451

Advanced supersonic propulsion study, phase 4
[NASA-CR-135273] p0026 W78-11062

High frequency dynamic engine simulation
[NASA-CR-135313] p0077 W78-13059

Experimental clean combustor program:
Turbulence characteristics of compressor
discharge flows
[NASA-CR-135277] p0027 W78-15041

An analytical study of thermal barrier coated
first stage blades in a JT9D engine
[NASA-CR-135360] p0028 W78-16054

Method of fan sound mode structure
determination [NASA-CR-135293] p0028 W78-17064

Method of fan sound mode structure
determination computer program user's manual:
Microphone location program
[NASA-CR-135294] p0028 W78-17065

Method of fan sound mode structure
determination computer program user's manual:
Modal calculation program
[NASA-CR-135295] p0028 W78-17066

Mean velocity, turbulence intensity and
turbulence convection velocity measurements
for a convergent nozzle in a free jet wind
tunnel
[NASA-CR-29499] p0008 W78-21058

Evaluation of Federal Aviation Administration
ion engine exhaust sampling rake
[NASA-CR-135213] p0029 W78-21111

F100(3) parallel compressor computer code and
user's manual
[NASA-CR-135388] p0029 W78-22096

Development of a plasma sprayed ceramic gas path
seal for high pressure turbine application
[NASA-CR-135387] p0030 W78-24181

Manufacture of astroloy turbine disk shapes by
hot isostatic pressing, volume 1
[NASA-CR-135409] p0079 W78-25166

Fabrication and test of digital output interface
devices for gas turbine electronic controls
[NASA-CR-135427] p0030 W78-27129

Effect of steady flight loads on JT9D-7
performance deterioration
[NASA-CR-135407] p0031 W78-29105

Flight effects on the aerodynamic and acoustic
characteristics of inverted profile coannular
nozzles, volume 1
[NASA-CR-135189-VOL-1] p0167 W78-29867

Flight effects on the aerodynamic and acoustic
characteristics of inverted profile coannular
nozzles, volume 2
[NASA-CR-135189-VOL-2] p0167 W78-29868

Flight effects on the aerodynamic and acoustic
characteristics of inverted profile coannular
nozzles, volume 3
[NASA-CR-135189-VOL-3] p0167 W78-29869

Compressor seal rub energetics study
[NASA-CR-159424] p0032 W78-32096

Flight effects on the aerodynamic and acoustic
characteristics of inverted profile coannular
nozzles
[NASA-CR-3018] p0169 W78-32836

PRATT AND WHITNEY AIRCRAFT GROUP, WEST PALM BEACH,
FLA.
Evaluation of a low aspect ratio small axial
compressor stage, volume 1
[NASA-CR-135240] p0026 W78-12081

Evaluation of a low aspect ratio small axial
compressor stage, volume 2
[NASA-CR-135241] p0026 W78-12082

F-15/nonaxisymmetric nozzle system integration
study support program
[NASA-CR-135252] p0028 W78-18070

Advanced optical blade tip clearance measurement
system
[NASA-CR-159402] p0032 W78-31106

R

RAYTHEON CO., WAYLAND, MASS.
Design, fabrication and testing of a CPA for use
in the solar power satellite
[NASA-CR-159410] p0042 W78-31143

ROCKETDYNE, CANOGA PARK, CALIF.
Linear aerospike engine study
[NASA-CR-135231] p0026 W78-11082

Liquid rocket lines, bellows, flexible hoses,
and filters
[NASA-SP-8123] p0047 W78-16089

Hydrogen turbine power conversion system
assessment
[NASA-CR-135298] p0144 W78-20621

Preburner of staged combustion rocket engine
[NASA-CR-135356] p0054 W78-24279

Advanced space engine powerhead breadboard
assembly system study
[NASA-CR-135232] p0054 W78-25127

Liquid rocket engine turbopump rotating-shaft
seals
[NASA-SP-8121] p0117 W78-30584

ROCKWELL INTERNATIONAL CORP., ANAHEIM, CALIF.
Analysis and design of a high power laser
adaptive phased array transmitter
[NASA-CR-134952] p0111 W78-13420

ROHR INDUSTRIES, INC., CHULA VISTA, CALIF.
Preliminary power train design for a
state-of-the-art electric vehicle
[NASA-CR-135340] p0145 W78-29584

S

- SEALOL, INC., PROVIDENCE, R. I.**
Design considerations in mechanical face seals for improved performance. I - Basic configurations
[ASME PAPER 77-WA/LUB-3] p0119 A78-33183
Design considerations in mechanical face seals for improved performance. II - Lubrication
[ASME PAPER 77-WA/LUB-4] p0120 A78-33184
- SIGMA RESEARCH, INC., RICHLAND, WASH.**
Two-phase working fluids for the temperature range 50 to 350 C
[NASA-CR-135255] p0107 W78-16329
- SIBIRSKY AIRCRAFT, STRATFORD, CONN.**
Oil-air mist lubrication for helicopter gearing
[NASA-CR-135081] p0010 W78-25080
- SKF INDUSTRIES, INC., KING OF PRUSSIA, PA.**
Emergency and microfog lubrication and cooling of bearings for Army helicopters
[NASA-CR-135195] p0122 W78-27429
- SOLAR TURBINES INTERNATIONAL, SAN DIEGO, CALIF.**
Wide range operation of advanced low NOx combustors for supersonic high-altitude aircraft gas turbines
[NASA-CR-135297] p0027 W78-14047
- SOUTHWEST RESEARCH INST., SAN ANTONIO, TEX.**
Flow of liquid jets through closely woven screens
p0108 A78-42877
- STANFORD UNIV., CALIF.**
Perturbation solutions for blade-to-blade surfaces of a transonic compressor
p0008 A78-12307
- STEIN SEAL CO., PHILADELPHIA, PA.**
Feasibility study of negative lift circumferential type seal for helicopter transmissions
[NASA-CR-135302] p0121 W78-17390
- SUBTECH, INC., BARCLAY HOOK, PA.**
Traction and lubricant film temperature as related to the glass transition temperature and solidification
p0087 A78-40997
- Study of dynamic emission spectra from lubricant films in an elastohydrodynamic contact using Fourier transform spectroscopy
[NASA-CR-159418] p0162 W78-32809
- SYSTEMS SCIENCE AND SOFTWARE, LA JOLLA, CALIF.**
NASCAP, a three-dimensional Charging Analyzer Program for complex spacecraft
p0044 A78-19567
- Spacecraft-generated plasma interaction with high voltage solar array
[AIAA PAPER 78-673] p0055 A78-32751
- NASA Charging Analyzer Program - A computer tool that can evaluate electrostatic contamination
p0044 A78-33220
- Dynamic modeling of spacecraft in a collisionless plasma
p0037 W78-10150
- Solar electric propulsion thruster interactions with solar arrays
[NASA-CR-135257] p0052 W78-13122
- A three dimensional dynamic study of electrostatic charging in materials
[NASA-CR-135256] p0099 W78-13328
- NASCAP user's manual
[NASA-CR-135259] p0099 W78-13329
- ERDA/NASA advanced thermionic technology program**
[NASA-CR-157117] p0145 W78-24674
- THERMO ELECTRON ENGINEERING CORP., WALTHAM, MASS.**
Advanced Thermionic Technology Program
[NASA-CR-155299] p0143 W78-13599
- ERDA/NASA advanced thermionic technology program**
[NASA-CR-157222] p0145 W78-26579
- ERDA/NASA advanced thermionic technology program**
[NASA-CR-157248] p0145 W78-27552
- TOLEDO UNIV., OHIO.**
Diagonal dominance using function minimization algorithms
p0159 A78-16304
- Nonlinear flap-lag-axial equations of a rotating beam with arbitrary precone angle
[AIAA 78-491] p0127 A78-29790
- Liquid jet impingement normal to a disk in zero gravity
[ASME PAPER 78-WA/FE-1] p0107 A78-41154
- TRW DEFENSE AND SPACE SYSTEMS GROUP, REDONDO BEACH, CALIF.**
Discrete time domain modelling and analysis of dc-dc converters with continuous and discontinuous inductor current
p0100 A78-18796
- Ion beam plume and efflux measurements of an 8-cm mercury ion thruster
[AIAA PAPER 78-676] p0055 A78-32753
- Electrical Prototype Power Processor for the 30-cm Mercury electric propulsion engine
[AIAA PAPER 78-684] p0055 A78-37439
- Ion beam plume and efflux characterization flight experiment study
[NASA-CR-135275] p0052 W78-12140
- Ion engine auxiliary propulsion applications and integration study
[NASA-CR-135312] p0053 W78-15168
- Electric prototype power processor for a 30cm ion thruster
[NASA-CR-135287] p0054 W78-19200
- Extended performance electric propulsion power processor design study. Volume 1: Executive summary
[NASA-CR-135357] p0054 W78-20250
- Modeling and Analysis of Power Processing Systems (MAPPS), initial phase 2
[NASA-CR-135173] p0100 W78-29350
- Modeling, analyses and design of switching converters
[NASA-CR-135174] p0100 W78-29351
- CTS TEP thermal anomalies: Heat pipe system performance
[NASA-CR-159413] p0108 W78-29410
- TRW EQUIPMENT LABS., CLEVELAND, OHIO.**
Fiber reinforced PPR polyimide composites
[NASA-CR-135377] p0063 W78-25132
- TRW, INC., CLEVELAND, OHIO.**
Cost analysis of advanced turbine blade manufacturing processes
[NASA-CR-135203] p0026 W78-10092
- TRW, INC., REDONDO BEACH, CALIF.**
Metastable states of small rare gas crystallites
p0169 A78-16069
- Particle parameter analyzing system
[NASA-CASE-ILE-06094] p0096 W78-17293
- TRW SYSTEMS, REDONDO BEACH, CALIF.**
Experiments on whistler wave filamentation and VLF hiss in a laboratory plasma
p0149 A78-41788

T

- TENNESSEE UNIV. SPACE INST., TULLAHOMA.**
Transient dynamics of a flexible rotor with squeeze film dampers
[NASA-CR-3050] p0123 W78-32433
- TEXAS A&I UNIV., KINGSVILLE.**
Investigation of the burning configuration of a coaxial injector in a combustion chamber
[NASA-CR-135383] p0054 W78-22148
- TEXAS UNIV., AUSTIN.**
Inward transport of a toroidally confined plasma subject to strong radial electric fields
p0172 A78-24890
- THERMO ELECTRON CORP., WALTHAM, MASS.**
Experiments with enhanced mode thermionic converters
p0146 A78-29636
- ULTRASYSTEMS, INC., IRVINE, CALIF.**
Synthesis of perfluoroalkylene aromatic diamines
[NASA-CR-159403] p0087 W78-31235
- UNITED TECHNOLOGIES CORP., EAST HARTFORD, CONN.**
Fuel consumption improvement in current transport engines
[AIAA PAPER 78-930] p0033 A78-45097
- UNITED TECHNOLOGIES RESEARCH CENTER, EAST HARTFORD, CONN.**
The effect of NaCl/g/ on the Na2SO4-induced hot corrosion of NiAl
p0079 A78-24901

U

- Development of an experiment for determining the autoignition characteristics of aircraft-type fuels
 [NASA-CR-135329] p0090 W78-16198
 Development of Si3N4 and SiC of improved toughness
 [NASA-CR-135306] p0087 W78-17216
 A method for calculating externally blown flap noise
 [NASA-CR-2954] p0166 W78-20920
 A method for calculating strut and splitter plate noise in exit ducts: Theory and verification
 [NASA-CR-2955] p0167 W78-20921
 Study of the effects of gaseous environments on sulfidation attack of superalloys
 [NASA-CR-135348] p0079 W78-21268
 Development of SiAlON materials
 [NASA-CR-135290] p0087 W78-21289
 Derivation and evaluation of an approximate analysis for three-dimensional viscous subsonic flow with large secondary velocities
 [NASA-CR-159430] p0008 W78-33044

V

- VOUGHT CORP., DALLAS, TEX.
 A combined potential and viscous flow solution for V/STOL engine inlets
 [AIAA PAPER 78-142] p0006 A78-20702

W

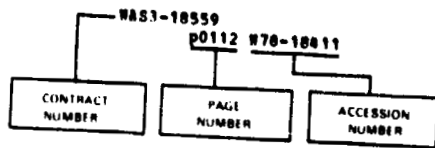
- WARSAW UNIV. (POLAND).
 Cloud effects on middle ultraviolet global radiation
 p0150 A78-82952
 WEST VIRGINIA UNIV., MORGANTOWN.
 Fluidized bed combustor modeling
 [NASA-CR-135164] p0067 W78-14119
 WESTERN GEAR CORP., LYNNWOOD, CALIF.
 Study of lubricant jet flow phenomena in spur gears - Out of mesh condition
 [ASME PAPER 77-DET-104] p0118 A78-20608
 WESTINGHOUSE ELECTRIC CORP., LIMA, OHIO.
 Solid State Remote Power Controllers for high voltage DC distribution systems
 p0100 A78-15574
 WESTINGHOUSE ELECTRIC CORP., PHILADELPHIA, PA.
 Revised international representations for the viscosity of water and steam and new representations for the surface tension of water
 p0105 A78-15725
 WESTINGHOUSE ELECTRIC CORP., PITTSBURGH, PA.
 Superconducting Nb3Ge for high-field magnets
 p0175 A78-41922
 Characterization, shaping, and joining of SiC/superalloy sheet for exhaust system components
 [NASA-CR-135301] p0062 W78-13130
 Fabrication and characteristics of experimental radiographic amplifier screens
 [NASA-CR-2937] p0124 W78-15501
 Niobium-germanium superconducting tapes for high-field magnet applications
 [NASA-CR-135364] p0099 W78-19392
 WESTINGHOUSE RESEARCH LABS., PITTSBURGH, PA.
 Dendritic web silicon for solar cell application
 p0146 A78-53489
 WICHITA STATE UNIV., WANS.
 Velocity, temperature, and electrical conductivity profiles in hydrogen-oxygen HHD duct flows
 [NASA-TN-78968] p0104 W78-28372
 WISCONSIN UNIV., MADISON.
 The role of drop velocity in statistical spray description
 p0107 A78-50323

X

- XEROX ELECTRO-OPTICAL SYSTEMS, PASADENA, CALIF.
 12-cm magneto-electrostatic containment argon/xenon ion source development
 [AIAA PAPER 78-681] p0039 A78-32756
 A mission profile life test facility
 [AIAA PAPER 78-671] p0040 A78-37431

CONTRACT NUMBER INDEX

Typical Contract Number Index Listing



Listings in this index are arranged alphabetically by contract number. Under each contract number, the accession numbers denoting documents that have been produced as a result of research done under that contract are arranged in ascending order with the /AA accession numbers appearing first. Preceding the accession number is the page number in the abstract section in which the citation may be found.

AF PROJ. 7661
p0036 W78-10129

DNW-3-8
p0181 W78-25988
p0181 W78-26997

DNA001-76-C-0121
p0037 W78-10150

DOT-FA77WAI-708
p0029 W78-21111

F(40-1)-5134
p0181 A78-10903

Z(49-18)-1751
p0135 W78-24659

E(49-26)-1004
p0125 W78-12459
p0144 W78-20603
p0139 W78-26553

E(49-26)-1010
p0143 W78-12529
p0144 W78-23559
p0144 W78-23560

E(49-26)-1022
p0130 W78-14628
p0130 W78-14629
p0131 W78-14630
p0035 W78-15059
p0131 W78-16435
p0178 W78-17435
p0133 W78-19641
p0134 W78-19644
p0134 W78-19657
p0134 W78-19658
p0150 W78-19710
p0184 W78-25025
p0136 W78-26551
p0138 W78-26547
p0138 W78-26548
p0138 W78-26549
p0138 W78-26550
p0139 W78-26554
p0139 W78-26555
p0180 W78-26995
p0140 W78-29566

Z(49-26)-1028
p0131 W78-15563
p0131 W78-16434
p0131 W78-17866
p0132 W78-17867
p0133 W78-19642
p0135 W78-23556
p0135 W78-23558
p0135 W78-24615
p0138 W78-26552

Z(49-26)-1059
p0140 W78-29575

X(49-28)-1002
p0111 W78-18431
p0134 W78-19656

E(49-28)-1022
p0147 A78-45437
p0140 W78-29578

E(49-28)-1024
p0156 W78-20802
p0157 W78-20803
p0157 W78-20804

EC-77-A-31-1011
p0107 A78-50322
p0086 W78-10291
p0086 W78-13209
p0088 W78-14177
p0101 W78-14313
p0178 W78-16928
p0069 W78-17187
p0178 W78-17933
p0178 W78-17934
p0178 W78-17936
p0178 W78-17937
p0178 W78-17938
p0179 W78-17939
p0179 W78-17940
p0179 W78-17942
p0179 W78-18988
p0179 W78-20321
p0179 W78-20022
p0180 W78-21010
p0181 W78-23999
p0101 W78-24494
p0135 W78-24616
p0005 W78-26098
p0138 W78-26551
p0180 W78-26946
p0180 W78-29994

EC-77-A-31-1034
p0140 W78-29574
p0140 W78-29577

EC-77-A-31-1040
p0086 A78-50324
p0121 W78-21472
p0181 W78-26997
p0122 W78-29449
p0084 W78-31236
p0180 W78-31533
p0141 W78-31534

EC-77-A-31-1044
p0180 W78-25010
p0145 W78-29584
p0182 W78-29992

EC-77-C-02-4396
p0181 W78-22970

EC-77-11-1044
p0180 W78-20023

EP-77-A-01-2593
p0071 W78-29216
p0072 W78-31208

EP-77-A-01-2647
p0104 W78-28372

EX-76-A-29-1022
p0130 W78-13608

EX-76-A-31-1011
p0180 W78-27003
p0122 W78-28466

EX-76-29-1060
p0111 W78-15562

ET-76-C-02-3056
p0143 W78-13594
p0145 W78-24674
p0145 W78-26579
p0145 W78-27552

P44620-78-C-0014
p0087 A78-40997

P44620-78-C-0042
p0175 A78-41922

NAS3-2953
p0149 A78-41788

NAS3-1175
p0149 A78-41788

NAS3-6263
p0123 A78-23447

NAS3-10094
p0144 W78-23560

NAS3-13514
p0045 A78-14991

NAS3-14302
p0122 W78-31427
p0124 W78-33463

NAS3-16726
p0030 W78-23089

NAS3-16732
p0033 A78-24902
p0029 W78-21147

NAS3-16766
p0128 A78-12071

NAS3-16807
p0007 W78-12034
p0007 W78-12035
p0008 W78-20082

NAS3-17223
p0054 W78-24280

NAS3-17343
p0122 W78-27429

NAS3-17756
p0062 W78-20257

NAS3-17759
p0110 A78-41464

NAS3-17768
p0087 A78-24881

NAS3-17787
p0078 W78-15233

NAS3-17817
p0045 A78-36005
p0092 W78-18251

NAS3-17826
p0159 A78-16304

NAS3-17859
p0123 A78-20606

NAS3-17862
p0146 W78-33527

NAS3-17863
p0166 W78-20920
p0167 W78-20921

NAS3-17866
p0002 W78-15988
p0002 W78-15989
p0002 W78-15990
p0007 W78-17991
p0008 W78-21058
p0167 W78-29867
p0167 W78-29868
p0169 W78-32836

NAS3-18008
p0002 W78-28043
p0030 W78-28095
p0030 W78-28096
p0031 W78-28097

NAS3-18021
p0033 A78-17396
p0033 A78-23893
p0033 A78-23914

NAS3-18034
p0146 A78-53489

NAS3-18520
p0121 W78-20514

NAS3-18523
p0123 W78-32433

NAS3-18526
p0032 W78-33103

NAS3-18538
p0010 W78-25080

NAS3-18541
p0123 A78-31500

NAS3-18546
p0127 W78-22402

NAS3-18559
p0112 W78-18411

NAS3-18900
p0063 A78-16903

NAS3-18915
p0077 W78-11232

NAS3-18917
p0055 A78-37434

NAS3-18918
p0100 A78-18756

NAS3-18926
p0062 W78-18131

NAS3-18937
p0111 W78-13420

NAS3-18942
p0078 W78-16149

NAS3-19080
p0009 W78-11024

NAS3-19403
p0143 W78-12529
p0143 W78-17462
p0144 W78-17463

NAS3-19404
p0144 W78-23559

NAS3-19406
p0174 A78-33143
p0146 A78-33147
p0146 A78-34078

NAS3-19424
p0026 W78-12081
p0026 W78-12082

NAS3-19427
p0121 W78-21472
p0122 W78-29479

NAS3-19439
p0146 A78-53489

NAS3-19441
p0146 A78-10947

NAS3-19447
p0027 W78-15041
p0029 W78-21111

NAS3-19540
p0026 W78-11062

NAS3-19544
p0027 W78-13058

NAS3-19690
p0100 W78-29350
p0100 W78-29351

NAS3-19697
p0127 W78-21493
p0127 W78-21494

NAS3-19698
p0086 W78-13209

NAS3-19701
p0098 W78-11295

NAS3-19707
p0112 W78-19480

NAS3-19709
p0063 A78-26683

NAS3-19712
p0087 A78-24881
p0087 W78-21289

NAS3-19713
p0054 W78-24279

NAS3-19723
p0087 A78-24881
p0063 W78-22164

NAS3-19725
p0067 W78-14119

NAS3-19729
p0062 W78-14099

NAS3-19730
p0055 A78-37439
p0054 W78-19200

NAS3-19731
p0087 A78-24881
p0087 W78-17216

NAS3-19733
p0086 W78-10291

NAS3-19735
p0062 W78-13134

NAS3-19737
p0027 W78-13057

NAS3-19738
p0008 A78-12307
p0001 W78-15987

CONTRACT NUMBER INDEX

NAS3-19747
 p0090 A78-43415
 NAS3-19750
 p0146 A78-31974
 NAS3-19751
 p0127 W78-18460
 NAS3-19752
 p0008 W78-33044
 NAS3-19758
 p0087 A78-40997
 p0162 W78-32809
 NAS3-19770
 p0027 W78-14047
 NAS3-19772
 p0121 W78-17387
 NAS3-19777
 p0002 W78-21044
 NAS3-19782
 p0077 W78-14143
 NAS3-19898
 p0030 W78-27129
 NAS3-20031
 p0026 W78-10093
 NAS3-20039
 p0079 A78-24901
 p0079 W78-21268
 NAS3-20044
 p0032 W78-33104
 NAS3-20047
 p0028 W78-17064
 p0028 W78-17065
 p0028 W78-17066
 NAS3-20048
 p0029 W78-19160
 NAS3-20049
 p0056 W78-16094
 NAS3-20050
 p0168 A78-41852
 NAS3-20051
 p0121 W78-21471
 NAS3-20052
 p0167 W78-25827
 p0167 W78-25828
 p0167 W78-25829
 NAS3-20056
 p0122 W78-27427
 NAS3-20059
 p0121 W78-10472
 NAS3-20064
 p0122 W78-28466
 NAS3-20066
 p0090 W78-16194
 NAS3-20070
 p0031 W78-29099
 NAS3-20072
 p0079 W78-25166
 NAS3-20073
 p0027 W78-12083
 NAS3-20074
 p0026 W78-11081
 NAS3-20081
 p0087 W78-31238
 NAS3-20083
 p0100 A78-15574
 NAS3-20086
 p0108 A78-42877
 NAS3-20087
 p0067 W78-25150
 NAS3-20090
 p0099 W78-24458
 NAS3-20097
 p0045 A78-43560
 p0107 W78-12364
 NAS3-20098
 p0079 W78-21265
 NAS3-20099
 p0028 W78-16052
 NAS3-20100
 p0112 W78-25407
 NAS3-20101
 p0040 A78-37441
 NAS3-20102
 p0100 W78-29351
 NAS3-20108
 p0144 W78-18515
 NAS3-20110
 p0041 W78-15144
 NAS3-20111
 p0099 W78-15400
 NAS3-20113
 p0055 A78-32753

p0053 W78-15168
 NAS3-20114
 p0026 W78-11082
 NAS3-20117
 p0143 W78-14632
 p0143 W78-14633
 NAS3-20119
 p0055 A78-32751
 p0037 W78-10150
 p0052 W78-13122
 p0098 W78-13325
 p0099 W78-13328
 p0099 W78-13329
 NAS3-20219
 p0008 W78-32066
 NAS3-20222
 p0107 W78-16329
 NAS3-20233
 p0175 A78-41922
 p0099 W78-19392
 NAS3-20270
 p0104 W78-26390
 p0049 W78-27174
 NAS3-20292
 p0027 W78-13059
 NAS3-20302
 p0146 A78-29636
 p0143 W78-13599
 p0145 W78-24674
 NAS3-20365
 p0094 A78-15615
 NAS3-20366
 p0063 W78-25132
 NAS3-20368
 p0128 W78-33478
 NAS3-20374
 p0042 W78-31143
 NAS3-20378
 p0026 W78-10092
 NAS3-20381
 p0067 A78-41901
 p0112 W78-20489
 NAS3-20384
 p0108 W78-17342
 NAS3-20385
 p0156 W78-20802
 p0157 W78-20803
 p0157 W78-20804
 NAS3-20386
 p0054 W78-25127
 NAS3-20388
 p0144 W78-20621
 NAS3-20389
 p0037 W78-14063
 NAS3-20392
 p0042 W78-31141
 p0042 W78-31142
 NAS3-20393
 p0039 A78-32756
 NAS3-20395
 p0055 A78-37430
 p0055 A78-37436
 p0052 W78-10205
 p0053 W78-16090
 p0053 W78-19195
 p0053 W78-19196
 NAS3-20397
 p0037 W78-20150
 NAS3-20399
 p0040 A78-37431
 NAS3-20400
 p0087 W78-31235
 NAS3-20403
 p0055 A78-37439
 p0054 W78-20250
 NAS3-20472
 p0144 W78-38835
 NAS3-20479
 p0032 W78-31104
 NAS3-20580
 p0025 A78-43546
 p0032 W78-32097
 NAS3-20561
 p0031 W78-28096
 NAS3-20592
 p0145 W78-29584
 NAS3-20595
 p0182 W78-29992
 NAS3-20598
 p0121 W78-17390

NAS3-20603
 p0030 W78-26147
 NAS3-20608
 p0028 W78-18070
 NAS3-20610
 p0029 W78-22096
 NAS3-20613
 p0032 W78-32096
 NAS3-20618
 p0148 W78-23640
 NAS3-20620
 p0090 W78-19326
 p0090 W78-20350
 p0090 W78-25235
 NAS3-20623
 p0030 W78-24141
 NAS3-20627
 p0032 W78-31108
 NAS3-20629
 p0025 A78-45098
 NAS3-20630
 p0033 A78-45097
 NAS3-20631
 p0025 A78-45098
 p0029 W78-20129
 p0031 W78-29103
 NAS3-20632
 p0033 A78-45097
 p0030 W78-27124
 p0031 W78-29105
 NAS3-20742
 p0124 W78-15501
 NAS3-20816
 p0145 W78-28604
 NAS3-20950
 p0038 W78-25105
 p0038 W78-25106
 NAS3-20958
 p0145 W78-27500
 NAS3-20959
 p0145 W78-26579
 p0145 W78-27552
 NAS3-21012
 p0108 W78-29410
 NAS3-21021
 p0108 W78-31380
 NAS3-21023
 p0055 A78-37434
 NAS3-21032
 p0028 W78-17058
 NAS3-21033
 p0028 W78-16054
 NAS3-21041
 p0031 W78-29104
 NAS3-21046
 p0108 A78-48716
 NAS3-21054
 p0092 W78-29274
 NAS3-23064
 p0094 A78-31970
 p0094 A78-31971
 p0095 A78-43173
 NAS3-30287
 p0052 W78-12140
 NGR-05-003-562
 p0078 W78-20310
 NGR-06-002-112
 p0052 W78-15167
 NGR-06-002-159
 p0144 A78-16069
 NGR-22-009-339
 p0078 W78-15234
 NGR-39-087-003
 p0078 W78-16150
 NGR-39-087-047
 p0075 A78-32319
 NSP ENT-76-23902
 p0144 W78-38835
 MSG-3011
 p0053 W78-19198
 MSG-3018
 p0141 A78-10903
 MSG-3038
 p0052 W78-13123
 MSG-3044
 p0062 W78-11197
 MSG-3063
 p0159 A78-16304
 MSG-3066
 p0029 W78-19153
 p0029 W78-19154

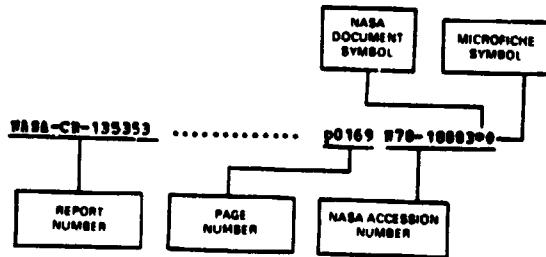
MSG-3080
 p0062 W78-16103
 MSG-3086
 p0169 W78-18883
 MSG-3091
 p0116 W78-26870
 MSG-3103
 p0175 A78-45500
 MSG-3112
 p0054 W78-22148
 MSG-3117
 p0007 A78-46537
 MSG-3125
 p0078 W78-19259
 MSG-3126
 p0152 W78-18672
 MSG-3127
 p0108 W78-33186
 MSG-3131
 p0099 W78-15397
 MSG-3132
 p0144 W78-20603
 MSG-3152
 p0181 W78-23999
 MSG-3186
 p0104 W78-28372
 N00014-73-C-0316
 p0148 W78-38835
 W-7405-ENG-26
 p0140 W78-29576
 198-10
 p0064 W78-12167
 p0065 W78-20281
 505-01
 p0156 W78-10746
 p0068 W78-15230
 p0156 W78-20806
 p0082 W78-25215
 505-03
 p0096 W78-11301
 p0001 W78-25049
 505-03-12
 p0167 W78-25827
 p0167 W78-25828
 p0167 W78-25829
 505-03-32
 p0032 W78-31104
 505-04
 p0113 W78-10474
 p0003 W78-11002
 p0003 W78-11008
 p0014 W78-11106
 p0015 W78-13064
 p0101 W78-13379
 p0068 W78-15224
 p0008 W78-15277
 p0004 W78-20080
 p0017 W78-20170
 p0017 W78-20171
 p0017 W78-20133
 p0081 W78-20337
 p0088 W78-20351
 p0114 W78-20513
 p0070 W78-21269
 p0115 W78-21470
 p0115 W78-21473
 p0019 W78-22101
 p0115 W78-22377
 p0020 W78-26188
 p0021 W78-27130
 p0021 W78-28099
 p0104 W78-28374
 p0116 W78-28457
 p0117 W78-28458
 p0005 W78-30057
 p0117 W78-30585
 p0022 W78-11109
 p0022 W78-33107
 p0022 W78-33108
 p0022 W78-33109
 p0073 W78-33196
 p0117 W78-33447
 505-05
 p0003 W78-14998
 p0003 W78-16001
 p0018 W78-21112
 p0018 W78-21114
 p0091 W78-22257
 p0019 W78-24095
 p0161 W78-30896
 p0022 W78-33110
 505-05-22
 p0032 W78-33103
 505-16
 p0114 W78-20512
 506-16
 p0080 W78-10295
 p0081 W78-20336

CONTRACT NUMBER 12021

p0081 #78-20338
p0082 #78-21294
p0082 #78-21295
p0115 #78-25433
p0071 #78-26198
p0084 #78-10238
p0073 #78-31213
506-17 p0057 #78-13138
p0057 #78-16098
506-20 p0068 #78-11230
506-21 p0047 #78-13124
p0041 #78-17127
506-23 p0140 #78-28624
506-25 p0171 #78-20959
p0172 #78-26927
p0172 #78-30944
511-55-01
p0027 #78-15041
610-22 p0043 #78-33137
643-10 p0043 #78-28159
716-01-02
p0032 #78-31108
718-01 p0017 #78-20132
743-03 p0015 #78-13063
776-71 p0083 #78-25236
778-11 p0135 #78-24659
778-32 p0046 #78-17145
778-63 p0071 #78-28225

REPORT/ACCESSION NUMBER INDEX

Typical Report/Accession Number Index Listing



Listings in this index are arranged alphanumerically by report number. The page number indicates the page in the abstract section in which the citation is located. The accession number denotes the number by which the citation is identified. An asterisk (*) indicates that the item is a NASA report. A pound sign (#) indicates that the item is available on microfiche.

AAS 77-243	p0044	A78-36719*	
ACS PAPER 31-DEW-76P	p0088	A78-18787*	
AFGL-TR-77-0051	p0036	#78-10129**	
AFSO-364	p0074	#78-10129**	
AIAA PAPER 78-83	p0023	A78-20651**	
AIAA PAPER 78-92	p0106	A78-20682**	
AIAA PAPER 78-93	p0118	A78-20683**	
AIAA PAPER 78-101	p0006	A78-20701**	
AIAA PAPER 78-102	p0006	A78-20702**	
AIAA PAPER 78-103	p0165	A78-20735**	
AIAA PAPER 78-104	p0165	A78-20738**	
AIAA PAPER 78-120	p0165	A78-20763**	
AIAA PAPER 78-643	p0055	A78-37430**	
AIAA PAPER 78-644	p0055	A78-37430**	
AIAA PAPER 78-647-I	p0050	A78-32738**	
AIAA PAPER 78-647-II	p0050	A78-32735**	
AIAA PAPER 78-649	p0050	A78-32736**	
AIAA PAPER 78-662	p0050	A78-32743**	
AIAA PAPER 78-665	p0050	A78-32745**	
AIAA PAPER 78-666	p0055	A78-37436**	
AIAA PAPER 78-668	p0050	A78-32747**	
AIAA PAPER 78-670	p0106	A78-32749**	
AIAA PAPER 78-671	p0040	A78-37431**	
AIAA PAPER 78-672	p0050	A78-32750**	
AIAA PAPER 78-673	p0055	A78-32751**	
AIAA PAPER 78-674	p0055	A78-32752**	
AIAA PAPER 78-676	p0055	A78-32753**	
AIAA PAPER 78-677	p0051	A78-32754**	
AIAA PAPER 78-681	p0039	A78-32756**	
AIAA PAPER 78-684	p0055	A78-37439**	
AIAA PAPER 78-685	p0051	A78-32759**	
AIAA PAPER 78-686	p0051	A78-32760**	
AIAA PAPER 78-690	p0080	A78-37441**	
AIAA PAPER 78-702	p0051	A78-32768**	
AIAA PAPER 78-709	p0051	A78-32773**	
AIAA PAPER 78-711B	p0051	A78-32776**	
AIAA PAPER 78-877	p0044	A78-36008**	
AIAA PAPER 78-878	p0045	A78-36005**	
AIAA PAPER 78-927	p0035	A78-45095**	
AIAA PAPER 78-928	p0025	A78-48452**	
AIAA PAPER 78-929	p0025	A78-45098**	
AIAA PAPER 78-930	p0033	A78-45097**	
AIAA PAPER 78-931	p0025	A78-43504**	
AIAA PAPER 78-932	p0025	A78-43505**	
AIAA PAPER 78-948	p0007	A78-43520**	
AIAA PAPER 78-961	p0007	A78-45096**	
AIAA PAPER 78-997	p0025	A78-41544**	
AIAA PAPER 78-999	p0025	A78-43546**	
AIAA PAPER 78-1030	p0045	A78-43560**	
AIAA PAPER 78-1119	p0166	A78-41829**	
AIAA PAPER 78-1120	p0166	A78-41830**	
AIAA PAPER 78-1121	p0166	A78-41831**	
AIAA PAPER 78-1123	p0166	A78-45139**	
AIAA PAPER 78-1139	p0007	A78-45133**	
AIAA PAPER 78-1140	p0006	A78-41843**	
AIAA PAPER 78-1153	p0168	A78-41852**	
AIAA PAPER 78-1219	p0067	A78-41911**	
AIAA 78-397	p0044	A78-35590**	
AIAA 78-438	p0106	A78-35618**	
AIAA 78-491	p0127	A78-29798**	
AIAA 78-1340	p0007	A78-46537**	
AIAA-PAPER-78-668	p0049	#78-23188**	
AIAA-PAPER-78-686	p0049	#78-23183**	
AIAA-PAPER-78-999	p0020	#78-26143**	
AIAA-PAPER-78-1034	p0049	#78-26173**	
AIAA-PAPER-78-1119	p0164	#78-26878**	
AIAA-PAPER-78-1121	p0164	#78-26897**	
AIAA-78-665	p0048	#78-21205**	
AIAA-78-1123	p0164	#78-28886**	
AINE PAPER A78-61	p0123	A78-31500**	
AIRSEARCH-21-2391	p0027	#78-12083**	
AIRSEARCH-21-2817	p0032	#78-33104**	
AIRSEARCH-78-15171	p0145	#78-28608**	
AR-1	p0152	#78-18672**	
ASLB PREPRINT 77-LC-5C-3	p0085	A78-28438*	
ASME PAPER 77-DET-10	p0118	A78-20591**	
AIAA-PAPER-78-686	p0123	A78-20606**	
ASME PAPER 77-DET-104	p0118	A78-20608**	
ASME PAPER 77-DET-121	p0118	A78-20609**	
ASME PAPER 77-DET-7	p0106	A78-17481**	
ASME PAPER 77-DET-9	p0089	A78-17482**	
ASME PAPER 77-LUB-8	p0118	A78-23352**	
ASME PAPER 77-LUB-10	p0119	A78-28414**	
ASME PAPER 77-LUB-13	p0118	A78-23354**	
ASME PAPER 77-LUB-14	p0126	A78-23355**	
ASME PAPER 77-LUB-30	p0075	A78-28423**	
ASME PAPER 77-WA/ENR-5	p0126	A78-10531**	
ASME PAPER 77-WA/ENR-5	p0174	A78-33143**	
ASME PAPER 77-WA/ENR-9	p0146	A78-33147**	
ASME PAPER 77-WA/LUB-3	p0119	A78-33183**	
ASME PAPER 77-WA/LUB-4	p0120	A78-33184**	
ASME PAPER 78-WA/ENR-4	p0107	A78-41154**	
ASRL-TR-154-12	p0078	#78-15234**	
ATL-TR-205-VOL-1	p0008	#78-20082**	
ATL-TR-205-VOL-2	p0007	#78-12034**	
ATL-TR-205-VOL-3	p0007	#78-12035**	
AVRADCON-TR-78-18	p0117	#78-30585**	
AVRADCON-TR-78-19 (PL)	p0021	#78-28099**	
AVRADCON-TR-78-20	p0022	#78-31109**	
AVRADCON-TR-78-22 (PL)	p0021	#78-27130**	
AVRADCON-TR-78-23 (PL)	p0020	#78-26143**	
AVRADCON-TR-78-26 (PL)	p0020	#78-26145**	
AVRADCON-TR-78-27 (PL)	p0056	#78-26178**	
AVRADCON-TR-78-31 (PL)	p0021	#78-27126**	
AVRADCON-TR-78-39 (PL)	p0071	#78-29215**	
BCS-40180-1-VOL-1	p0156	#78-20802**	
BCS-40180-2-VOL-2	p0157	#78-20803**	
BCS-40180-3-VOL-3	p0157	#78-20804**	
BTS-TR-78-54-59PPL-1-PT-2	p0038	#78-25106**	
BTS-TR-78-55-PT-1	p0038	#78-25105**	

REPORT/ACCESSION NUMBER INDEX

CASD-WAS-75-006 p0062 W78-2025700
 CASD-WAS-77-025 p0017 W78-1806300
 CASD-WAS-78-010 p0100 W78-3130000
 CEB-77-78028-001322 p0100 W78-3338600
 CRD-WASA-8 p0078 W78-1615000
 CORP-761129-8 p0130 W78-1360800
 CONS/0008-1 p0181 W78-2598000
 CONS/0008-3 p0181 W78-2699700
 CONS/0068-1 p0122 W78-2846600
 CONS/0385-1 p0156 W78-2080200
 CONS/0385-2 p0157 W78-2080300
 CONS/0385-3 p0157 W78-2080400
 CONS/1002-3 p0138 W78-1965600
 CONS/1011-1 p0179 W78-1998800
 CONS/1011-2 p0179 W78-1998200
 CONS/1011-3 p0178 W78-1993300
 CONS/1011-4 p0178 W78-1992800
 CONS/1011-5 p0180 W78-2101000
 CONS/1011-6 p0179 W78-1998000
 CONS/1011-7 p0179 W78-1993900
 CONS/1011-8 p0178 W78-1993800
 CONS/1011-9 p0178 W78-1993800
 CONS/1011-10 p0178 W78-1993600
 CONS/1011-11 p0179 W78-2002100
 CONS/1011-12 p0015 W78-1605300
 CONS/1011-13 p0179 W78-2002200
 CONS/1011-14 p0138 W78-2655100
 CONS/1011-18 p0101 W78-1831300
 CONS/1011-20 p0088 W78-1817700
 CONS/1011-21 p0178 W78-1993700
 CONS/1011-22 p0069 W78-1718700
 CONS/1044-1 p0180 W78-2002300
 CONS/1044-1 p0180 W78-2501000
 CONS/4396-1 p0181 W78-2297000
 CONS/9427-1 p0121 W78-2147200
 CONS/9427-2 p0122 W78-2944900
 CONS/9498-1 p0086 W78-1120900
 CONS/9733-1 p0086 W78-1029100
 COO-3056-23 p0183 W78-1359900
 COO-3056-25 p0185 W78-2467800
 COO-3056-28 p0185 W78-2657900
 COO-3056-29 p0185 W78-2755200
 CSO-PHREP-WASLBC-1 p0108 W78-3338600
 C75-537/501 p0111 W78-1342000
 D-9179 p0080 W78-1527700
 DDA-EDR-9068 p0122 W78-2846600
 DDC-W77AEG400-VOL-1 p0031 W78-2909900
 DDC-W77AEG524 p0002 W78-2804300
 DDC-W78AEG289 p0122 W78-1142700
 DDC-W78AEG408 p0012 W78-3209700
 DOC-76SD54287-VOL-1 p0183 W78-1252900
 DOE-CORP-771188 p0132 W78-1961600
 DOE/WASA/0592-78/1 p0185 W78-2958000
 DOE/WASA/0595-78/1 p0182 W78-2999200
 DOE/WASA/1004-78/13 p0139 W78-2655300
 DOE/WASA/1011-78/23 p0082 W78-2224300
 DOE/WASA/1011-78/24 p0180 W78-2998800
 DOE/WASA/1011-78/25 p0005 W78-2609800
 DOE/WASA/1011-78/26 p0135 W78-2861600
 DOE/WASA/1011-78/27 p0180 W78-2699600
 DOE/WASA/1022-77/22 p0178 W78-1793500
 DOE/WASA/1022-77/23 p0131 W78-1643500
 DOE/WASA/1022-77/28 p0150 W78-1971000
 DOE/WASA/1022-78/25 p0131 W78-1968300
 DOE/WASA/1022-78/26 p0134 W78-1965700
 DOE/WASA/1022-78/27 p0134 W78-1965800
 DOE/WASA/1022-78/29 p0138 W78-1964800
 DOE/WASA/1022-78/30 p0180 W78-2956600
 DOE/WASA/1022-78/31 p0180 W78-2699500
 DOE/WASA/1022-78/32 p0138 W78-2654700
 DOE/WASA/1022-78/34 p0138 W78-2654800
 DOE/WASA/1022-78/38 p0138 W78-2654900
 DOE/WASA/1022-78/39 p0136 W78-2654900
 DOE/WASA/1022-78/39 p0139 W78-2654900
 DOE/WASA/1022-78/39 p0139 W78-2655500

DOE/WASA/1022-78/40 p0138 W78-2655000
 DOE/WASA/1022-78/41 p0180 W78-2957800
 DOE/WASA/1028-77/10 p0132 W78-1746700
 DOE/WASA/1028-77/13 p0131 W78-1746600
 DOE/WASA/1028-77/14 p0135 W78-2461500
 DOE/WASA/1028-78/15 p0133 W78-1964200
 DOE/WASA/1028-78/16 p0135 W78-2355600
 DOE/WASA/1028-78/17 p0135 W78-2355800
 DOE/WASA/1028-78/18 p0138 W78-2655200
 DOE/WASA/1034-78/1 p0180 W78-2957700
 DOE/WASA/1034-78/2 p0180 W78-2957600
 DOE/WASA/1040-78/1 p0180 W78-3153300
 DOE/WASA/1040-78/2 p0088 W78-3123600
 DOE/WASA/1040-78/3 p0141 W78-3153400
 DOE/WASA/1050-78/1 p0180 W78-2957500
 DOE/WASA/2593-78/1 p0071 W78-2921600
 DOE/WASA/2593-78/2 p0072 W78-3120800
 DOE/WASA/3132-78/1 p0144 W78-2060300
 DOE/WASA/3152-78/1 p0181 W78-2359900
 DOE/WASA/9404-78/1 p0144 W78-2355900
 DOE/WASA/9404-78/2 p0180 W78-2356000
 D6-48664 p0030 W78-2712800
 D180-24613-1 p0127 W78-2199300
 D180-24613-2 p0127 W78-2199400
 E-0671 p0005 W78-2708300
 E-1411-1 p0065 W78-1717200
 E-8233 p0064 W78-1521100
 E-8259-1 p0056 W78-2617800
 E-8556 p0135 W78-2465900
 E-8696 p0172 W78-2692700
 E-8852 p0015 W78-1306300
 E-8909 p0047 W78-1312400
 E-8916-2 p0021 W78-2910000
 E-8964 p0015 W78-1605300
 E-8994 p0022 W78-3310700
 E-9005 p0022 W78-3310900
 E-9056-1 p0068 W78-1318100
 E-9078 p0064 W78-1216700
 E-9085 p0057 W78-1313800
 E-9085-2 p0057 W78-1313700
 E-9091 p0015 W78-1306800
 E-9114 p0091 W78-2225700
 E-9124 p0171 W78-1590500
 E-9154 p0003 W78-1002600
 E-9155 p0012 W78-1009700
 E-9159 p0096 W78-1130100
 E-9174 p0008 W78-2008000
 E-9187 p0017 W78-2013000
 E-9192 p0041 W78-2119000
 E-9195 p0114 W78-2051200
 E-9203 p0164 W78-1676600
 E-9207 p0014 W78-1110600
 E-9213 p0003 W78-1100800
 E-9220 p0101 W78-1041500
 E-9222 p0131 W78-1463100
 E-9229 p0057 W78-1021700
 E-9233 p0068 W78-1123000
 E-9236 p0059 W78-2122000
 E-9246 p0005 W78-3085700
 E-9252 p0113 W78-1047800
 E-9253 p0017 W78-2013200
 E-9254 p0101 W78-1337900
 E-9257 p0018 W78-2111200
 E-9258 p0012 W78-1009800
 E-9259 p0057 W78-1313600
 E-9260 p0115 W78-2147000
 E-9261 p0080 W78-1527800
 E-9262 p0012 W78-1104300
 E-9264 p0156 W78-1074600
 E-9265 p0114 W78-1842900
 E-9267 p0171 W78-2095900
 E-9268 p0080 W78-1028800
 E-9269 p0057 W78-1609800
 E-9269-1 p0057 W78-1715300
 E-9271 p0068 W78-1523000
 E-9274 p0109 W78-1340700
 E-9276 p0068 W78-1522900
 E-9278 p0047 W78-2120200
 E-9283 p0003 W78-1799800
 E-9284 p0041 W78-1712700
 E-9288 p0114 W78-2051100
 E-9289 p0109 W78-1546300
 E-9293 p0003 W78-1499800
 E-9294 p0115 W78-2483300
 E-9296 p0114 W78-2644700
 E-9297 p0065 W78-2028100
 E-9298-1 p0113 W78-1343500

REPORT/ACCESSION NUMBER INDEX

Z-9300	p0115	878-2237700	Z-9484	p0153	878-2075500
Z-9301	p0101	878-1631300	Z-9487	p0088	878-1932500
Z-9302	p0022	878-3310000	Z-9488	p0021	878-2713000
Z-9304	p0101	878-1336900	Z-9489	p0037	878-1607800
Z-9307	p0082	878-2129800	Z-9490	p0161	878-1089600
Z-9308	p0179	878-1898800	Z-9492	p0001	878-2364900
Z-9310	p0120	878-1862800	Z-9493	p0135	878-2461500
Z-9323	p0150	878-1753000	Z-9494	p0022	878-3311000
Z-9324	p0102	878-1733000	Z-9495	p0156	878-1572900
Z-9329	p0162	878-1304800	Z-9496	p0178	878-1793000
Z-9330	p0175	878-1391600	Z-9497	p0170	878-1793800
Z-9331	p0003	878-1600100	Z-9498	p0071	878-2615000
Z-9332	p0017	878-2013100	Z-9499	p0083	878-2523600
Z-9336	p0018	878-1305600	Z-9500	p0020	878-2618000
Z-9337	p0198	878-1951200	Z-9501	p0016	878-1705900
Z-9339	p0046	878-1718500	Z-9502	p0131	878-1683500
Z-9342	p0017	878-2013300	Z-9503	p0102	878-1734000
Z-9346	p0081	878-2033700	Z-9504	p0043	878-2618900
Z-9347	p0117	878-3058500	Z-9505	p0160	878-1673500
Z-9349	p0088	878-1817700	Z-9506	p0005	878-2609800
Z-9350	p0115	878-2187300	Z-9507	p0179	878-1793900
Z-9353	p0130	878-1862900	Z-9508	p0079	878-2002200
Z-9354	p0134	878-1965600	Z-9509	p0180	878-1790100
Z-9355	p0019	878-2309500	Z-9510	p0170	878-2101000
Z-9356	p0069	878-1718700	Z-9511	p0134	878-1968000
Z-9358	p0131	878-1863000	Z-9512	p0018	878-2110800
Z-9359	p0057	878-1715200	Z-9513	p0021	878-2609900
Z-9360	p0052	878-2129500	Z-9514	p0150	878-1971000
Z-9366	p0093	878-1038600	Z-9515	p0058	878-1715800
Z-9367	p0062	878-2618500	Z-9516	p0112	878-1964200
Z-9368	p0056	878-2617700	Z-9517	p0058	878-1715500
Z-9371	p0088	878-2035100	Z-9518	p0088	878-3023000
Z-9372	p0125	878-1387700	Z-9519	p0017	878-1916100
Z-9374	p0081	878-2033600	Z-9520	p0102	878-2085000
Z-9375	p0131	878-1556200	Z-9521	p0111	878-2188100
Z-9376	p0101	878-1336100	Z-9522	p0018	878-2117000
Z-9381	p0178	878-1793300	Z-9523	p0179	878-2002100
Z-9384	p0081	878-2033800	Z-9524	p0071	878-2822500
Z-9385	p0093	878-1328200	Z-9525	p0059	878-2122100
Z-9387	p0018	878-2111800	Z-9526	p0133	878-1968300
Z-9388	p0179	878-1794200	Z-9527	p0020	878-2618500
Z-9390	p0111	878-1838600	Z-9528	p0132	878-1961600
Z-9392	p0163	878-1385300	Z-9529	p0010	878-1708100
Z-9395	p0019	878-2210100	Z-9530	p0096	878-1720800
Z-9396	p0148	878-1367000	Z-9531	p0082	878-2521500
Z-9397	p0176	878-1393800	Z-9532	p0134	878-2159600
Z-9400	p0124	878-1739700	Z-9533	p0096	878-2137200
Z-9401	p0171	878-1088400	Z-9534	p0138	878-1965700
Z-9402	p0068	878-1318300	Z-9535	p0071	878-2619900
Z-9404	p0080	878-1528000	Z-9536	p0132	878-1786900
Z-9405	p0163	878-1385400	Z-9537	p0047	878-2025100
Z-9406	p0144	878-1366900	Z-9538	p0073	878-3319600
Z-9409	p0132	878-1788600	Z-9539	p0134	878-1965000
Z-9410	p0003	878-1700100	Z-9540	p0018	878-2111000
Z-9412	p0163	878-1585200	Z-9541	p0097	878-2137300
Z-9414	p0070	878-2126900	Z-9542	p0103	878-2338400
Z-9416	p0088	878-1323300	Z-9543	p0103	878-2180300
Z-9418	p0116	878-2648600	Z-9544	p0070	878-2126600
Z-9419	p0116	878-2845700	Z-9545	p0103	878-2449800
Z-9420	p0096	878-1333100	Z-9546	p0072	878-3020500
Z-9421	p0140	878-2002300	Z-9547	p0056	878-2025800
Z-9421	p0180	878-2501000	Z-9548	p0070	878-2413500
Z-9422	p0131	878-1746600	Z-9549	p0180	878-2862400
Z-9424	p0083	878-2824700	Z-9550	p0180	878-2957500
Z-9425	p0014	878-1306100	Z-9551	p0104	878-2837400
Z-9426	p0163	878-1385500	Z-9552	p0188	878-2502500
Z-9428	p0081	878-1722000	Z-9553	p0101	878-2180800
Z-9430	p0111	878-1342100	Z-9554	p0117	878-2845800
Z-9431	p0171	878-1389000	Z-9555	p0043	878-3313700
Z-9432	p0035	878-1307700	Z-9556	p0082	878-2323100
Z-9433	p0102	878-1738100	Z-9557	p0018	878-2209700
Z-9434	p0178	878-1692800	Z-9558	p0172	878-2392300
Z-9435	p0068	878-1318200	Z-9559	p0058	878-2025500
Z-9436	p0015	878-1506300	Z-9560	p0172	878-3098400
Z-9438	p0178	878-1793700	Z-9561	p0134	878-1968400
Z-9440	p0069	878-1718900	Z-9562	p0135	878-2355700
Z-9441	p0069	878-1719000	Z-9563	p0048	878-2120400
Z-9442	p0178	878-1793800	Z-9564	p0096	878-1939700
Z-9444	p0163	878-1385600	Z-9565	p0152	878-2261800
Z-9445	p0154	878-2080600	Z-9566	p0082	878-2223200
Z-9447	p0171	878-1993800	Z-9567	p0135	878-2355800
Z-9448	p0091	878-1532600	Z-9568	p0103	878-2338500
Z-9449	p0177	878-1792100	Z-9569	p0135	878-2355600
Z-9449-2	p0177	878-2898600	Z-9570	p0156	878-2179100
Z-9450	p0132	878-1746700	Z-9571	p0164	878-2286000
Z-9451	p0161	878-1585300	Z-9572	p0048	878-2120700
Z-9452	p0178	878-1793500	Z-9573	p0073	878-3121300
Z-9453	p0019	878-2209900	Z-9574	p0048	878-2120500
Z-9455	p0044	878-2119900	Z-9575	p0082	878-2224300

REPORT/ACCESSION NUMBER INDEX

F-9586	p0103	878-2232000	F-9719	p0021	878-2712700
F-9589	p0047	878-2120400	F-9723	p0088	878-3123000
F-9590	p0048	878-2120800	F-9728	p0072	878-3120000
F-9591	p0049	878-2314400	F-9726	p0071	878-2921500
F-9592	p0047	878-2120300	F-9733	p0059	878-3314900
F-9593	p0049	878-2314200	F-9734	p0126	878-3264000
F-9594	p0041	878-2118000	F-9746	p0072	878-3121100
F-9595	p0049	878-2314300	F-9748	p0152	878-3169000
F-9596	p0089	878-2437000	F-9750	p0093	878-3123300
F-9597	p0089	878-2436900	F-9751	p0072	878-3121200
F-9598	p0134	878-2247100	F-9752	p0181	878-3153000
F-9599	p0048	878-2120900	F-9755	p0059	878-3314900
F-9601	p0049	878-2209000	F-9759	p0059	878-3315000
F-9603	p0138	878-2654600	F-9760	p0009	878-3106100
F-9604	p0138	878-2655100	F-9764	p0165	878-3107100
F-9605	p0011	878-2413700	F-9766	p0117	878-3344500
F-9606	p0072	878-3020400	F-9768	p0093	878-3320300
F-9607	p0011	878-2413800	F-9772	p0072	878-3120900
F-9609	p0140	878-2954600	F-9773	p0183	878-3201400
F-9610	p0070	878-2319300	F-9784	p0060	878-3315100
F-9611	p0071	878-2433600	F-9793	p0022	878-3310200
F-9612	p0164	878-2489700			
F-9613	p0180	878-2999400	EDB-9339	p0122	878-2742700
F-9614	p0125	878-2347100			
F-9615	p0125	878-2347200	ERDA/NASA-1002/77/2	p0131	878-1463100
F-9616	p0126	878-2347300	ERDA/NASA-1022/76/5	p0130	878-1308000
F-9618	p0164	878-2689800	ERDA/NASA-1022/77/17	p0130	878-1462800
F-9621	p0164	878-2687800	ERDA/NASA-1022/77/19	p0035	878-1505900
F-9622	p0135	878-2461700	ERDA/NASA-1022/77/20	p0130	878-1462900
F-9626	p0019	878-2300800	ERDA/NASA-1022/77/21	p0131	878-1463000
F-9629	p0011	878-2413900	ERDA/NASA-1028/77/9	p0131	878-1554300
F-9630	p0049	878-2417300	ERDA/NASA-1028/77/12	p0131	878-1643800
F-9631	p0083	878-2621500	ERDA/NASA-1060/77/1	p0131	878-1556200
F-9634	p0115	878-2644300	ERDA/NASA-9403/76/1-VOL-1	p0143	878-1252900
F-9635	p0005	878-2609900	ERDA/NASA-9403/76/2-VOL-2	p0143	878-1746200
F-9636	p0093	878-2637300	ERDA/NASA-9403/76/3-VOL-3	p0144	878-1746300
F-9637	p0135	878-2461600			
F-9638	p0137	878-2654200	EVC PAPER 7744	p0097	878-1692200
F-9639	p0180	878-2699500			
F-9640	p0124	878-2456500	FAB-8D-77-115	p0029	878-2111100
F-9644	p0154	878-2480700			
F-9645	p0041	878-2416600	FR-9232	p0018	878-1807000
F-9646	p0137	878-2654300	FR-9609	p0028	878-1705800
F-9648	p0126	878-2745300	FR-10200A	p0032	878-3110600
F-9649	p0072	878-3121000			
F-9652	p0138	878-2655200	GASL-78-248	p0031	878-2809800
F-9654	p0114	878-2655300	GASL-78-249	p0030	878-2614700
F-9655	p0037	878-2714300			
F-9656	p0140	878-3153300	GE-SD-76SD34288-VOL-2	p0143	878-1746200
F-9658	p0005	878-2410000			
F-9661	p0118	878-2654700	GT-A1855-VOL-1	p0041	878-1514400
F-9662	p0118	878-2654800			
F-9663	p0118	878-2654900	HCP/H1011-01	p0180	878-2700300
F-9664	p0116	878-2555100			
F-9665	p0137	878-2654400	HBI-391	p0092	878-2927600
F-9666	p0117	878-2654500			
F-9667	p0115	878-2644400	ICED PAPER P 77 675-2	p0147	878-3019600
F-9668	p0020	878-2614800			
F-9669	p0139	878-2861400	IITRI-86124-48	p0078	878-1523300
F-9672	p0139	878-2655500	IITRI-86134-25	p0078	878-1614900
F-9674	p0084	878-2924600			
F-9675	p0172	878-2692600	LBSC-D564116	p0092	878-1825100
F-9676	p0083	878-2725700			
F-9677	p0180	878-2499400	LTC-77-41	p0121	878-1738700
F-9678	p0116	878-2644400	LTC-77-56-VOL-1	p0167	878-2582700
F-9679	p0139	878-2655800	LTC-77-46-VOL-2	p0167	878-2582800
F-9680	p0104	878-2714600	LTC-77-56-VOL-3	p0167	878-2582900
F-9681	p0049	878-2717000			
F-9685	p0134	878-2655000	HCB-77-253	p0107	878-1234400
F-9687	p0172	878-2791400			
F-9687	p0117	878-1384700	HDC-J7708	p0024	878-1009300
F-9689	p0071	878-2421600			
F-9690	p0104	878-2736700	NTI-77TR2	p0121	878-2051400
F-9691	p0164	878-2480600	NTI-78TR17	p0127	878-1846000
F-9692	p0061	878-2727400	NTI-78TR18-PT-4	p0127	878-2240200
F-9693	p0116	878-2742800			
F-9695	p0104	878-2639000	NASA-CASE-LEW-10518-3	p0065	878-2722600
F-9696	p0021	878-2712600	NASA-CASE-LEW-11845-1	p0020	878-2509000
F-9698	p0140	878-2957700	NASA-CASE-LEW-11877-1	p0097	878-2735700
F-9702	p0180	878-2957600	NASA-CASE-LEW-11981-1	p0091	878-1723700
F-9703	p0037	878-2714200	NASA-CASE-LEW-12038-1	p0137	878-2555900
F-9705	p0049	878-2717400	NASA-CASE-LEW-12039-1	p0130	878-1462500
F-9706	p0021	878-2712500	NASA-CASE-LEW-12051-1	p0080	878-1527600
F-9708	p0139	878-2753900	NASA-CASE-LEW-12081-1	p0089	878-2036500
F-9710	p0014	878-2713700	NASA-CASE-LEW-12081-2	p0149	878-1990700
F-9711	p0129	878-1351000	NASA-CASE-LEW-12083-1	p0113	878-1343600
F-9714	p0105	878-1338000	NASA-CASE-LEW-12095-1	p0067	878-1818200
F-9716	p0105	878-2940700	NASA-CASE-LEW-12131-2	p0021	878-3110300
F-9717	p0104	878-2837200	NASA-CASE-LEW-12137-1	p0064	878-1022400

REPORT/ACCESSION NUMBER INDEX

NASA-CASE-LEV-12159-1	p0132	W78-19599*	NASA-CR-135232	p0054	W78-25127**
NASA-CASE-LEV-12185-1	p0136	W78-25528*	NASA-CR-135234	p0067	W78-25150**
NASA-CASE-LEV-12217-1	p0129	W78-14452*	NASA-CR-135235	p0026	W78-11881**
NASA-CASE-LEV-12277-2	p0097	W78-25323**	NASA-CR-135236	p0027	W78-13058**
NASA-CASE-LEV-12313-1	p0113	W78-10468*	NASA-CR-135237	p0121	W78-10472**
NASA-CASE-LEV-12317-1	p0016	W78-17055*	NASA-CR-135238	p0007	W78-17991**
NASA-CASE-LEV-12321-1	p0113	W78-10467*	NASA-CR-135239-VOL-1-SMCT-2	p0030	W78-28095**
NASA-CASE-LEV-12358-2	p0065	W78-25149**	NASA-CR-135239-VOL-1-SMCT-3	p0030	W78-28096**
NASA-CASE-LEV-12389-2	p0016	W78-18066**	NASA-CR-135239-VOL-2	p0031	W78-28097**
NASA-CASE-LEV-12390-1	p0016	W78-17056*	NASA-CR-135240	p0026	W78-12881**
NASA-CASE-LEV-12452-1	p0019	W78-25089**	NASA-CR-135241	p0026	W78-12882**
NASA-CASE-LEV-12465-1	p0065	W78-25149**	NASA-CR-135244	p0143	W78-14632**
NASA-CASE-LEV-12493-1	p0059	W78-22163**	NASA-CR-135245	p0143	W78-14633**
NASA-CASE-LEV-12496-1	p0022	W78-33101*	NASA-CR-135247	p0062	W78-16103**
NASA-CASE-LEV-12508-1	p0102	W78-17335*	NASA-CR-135248	p0062	W78-11197**
NASA-CASE-LEV-12541-1	p0136	W78-25529**	NASA-CR-135252	p002*	W78-18070**
NASA-CASE-LEV-12542-2	p0070	W78-22205**	NASA-CR-135255	p010	W78-16329**
NASA-CASE-LEV-12552-1	p0136	W78-25527**	NASA-CR-135256	p0099	W78-13328**
NASA-CASE-LEV-12554-1	p0102	W78-18355**	NASA-CR-135257	p0052	W78-13122**
NASA-CASE-LEV-12586-1	p0139	W78-27520**	NASA-CR-135258	p0098	W78-13325**
NASA-CASE-LEV-12649-1	p0136	W78-25530**	NASA-CR-135259	p0099	W78-13329**
NASA-CASE-LEV-12668-1	p0153	W78-14773*	NASA-CR-135262	p0086	W78-10291**
NASA-CASE-LEV-12718-1	p0104	W78-25351*	NASA-CR-135264	p0167	W78-12364**
NASA-CASE-LEV-12780-1	p0048	W78-22149**	NASA-CR-135265	p0027	W78-12083**
NASA-CASE-LEV-12785-1	p0115	W78-24545*	NASA-CR-135269	p0077	W78-11232**
NASA-CASE-LEV-12791-1	p0097	W78-32341*	NASA-CR-135272	p0078	W78-15233**
NASA-CASE-LEV-12806-1	p0136	W78-25533**	NASA-CR-135273	p0026	W78-11062**
NASA-CASE-LEV-12905-1	p0069	W78-18183*	NASA-CR-135274	p0062	W78-14099**
NASA-CASE-LEV-12916-1	p0113	W78-17384**	NASA-CR-135275	p0052	W78-12140**
NASA-CASE-LEV-12917-1	p0016	W78-18067*	NASA-CR-135277	p0027	W78-15041**
NASA-CASE-LEV-12972-1	p0056	W78-22157**	NASA-CR-135281-VOL-1	p0052	W78-10205**
NASA-CASE-LEV-12982-1	p0117	W78-28459**	NASA-CR-135281-VOL-3	p0053	W78-19196**
NASA-CASE-LEV-12990-1	p0020	W78-27122**	NASA-CR-135281-VOL-4	p0053	W78-16040**
NASA-CASE-LEV-13150-1	p0136	W78-25554**	NASA-CR-135281-VOL-5	p0053	W78-19195**
NASA-CASE-LEV-06094	p0096	W78-17293*	NASA-CR-135283	p0156	W78-20802**
NASA-CP-2020	p0130	W78-13527**	NASA-CR-135284	p0157	W78-20803**
NASA-CP-2021	p0012	W78-11063**	NASA-CR-135285	p0157	W78-20804**
NASA-CP-2033	p0088	W78-19325**	NASA-CR-135286	p0099	W78-24458**
NASA-CP-2034	p0132	W78-19616**	NASA-CR-135287	p0054	W78-19200**
NASA-CR-2842	p0056	W78-16094**	NASA-CR-135288	p0078	W78-16150**
NASA-CR-2900	p0008	W78-20082**	NASA-CR-135290	p0087	W78-21289**
NASA-CR-2901	p0007	W78-12038**	NASA-CR-135291	p0063	W78-22164**
NASA-CR-2902	p0007	W78-12035**	NASA-CR-135292	p0086	W78-13209**
NASA-CR-2937	p0124	W78-15501**	NASA-CR-135293	p0028	W78-17064**
NASA-CR-2941	p0001	W78-15987**	NASA-CR-135294	p0028	W78-17065**
NASA-CR-2949	p0008	W78-21058**	NASA-CR-135295	p0028	W78-17066**
NASA-CR-2954	p0166	W78-20920**	NASA-CR-135297	p0027	W78-14047**
NASA-CR-2955	p0167	W78-20921**	NASA-CR-135298	p0144	W78-20621**
NASA-CR-2966	p0002	W78-28083**	NASA-CR-135299	p0078	W78-16149**
NASA-CR-2975	p0121	W78-20514**	NASA-CR-135300	p0121	W78-21471**
NASA-CR-2990	p0002	W78-21044**	NASA-CR-135301	p0062	W78-13134**
NASA-CR-3019	p0169	W78-32836**	NASA-CR-135302	p0121	W78-17387**
NASA-CR-3019	p0108	W78-33386**	NASA-CR-135303	p0087	W78-17216**
NASA-CR-3032	p0031	W78-28098**	NASA-CR-135306	p0122	W78-27827**
NASA-CR-3047	p0008	W78-32066**	NASA-CR-135307	p0077	W78-14143**
NASA-CR-3050	p0123	W78-32433**	NASA-CR-135308	p0099	W78-15400**
NASA-CR-134670	p0098	W78-11295**	NASA-CR-135309	p0078	W78-20310**
NASA-CR-134738	p0030	W78-23089**	NASA-CR-135310	p0152	W78-18672**
NASA-CR-134804-2	p0146	W78-33527**	NASA-CR-135311	p0053	W78-15168**
NASA-CR-134910-VOL-1	p0002	W78-15988**	NASA-CR-135312	p0027	W78-13059**
NASA-CR-134910-VOL-2	p0002	W78-15989**	NASA-CR-135313	p0099	W78-15397**
NASA-CR-134910-VOL-3	p0002	W78-15990**	NASA-CR-135314	p0078	W78-15234**
NASA-CR-134934	p0143	W78-12529**	NASA-CR-135315	p0144	W78-18515**
NASA-CP-134935	p0143	W78-17462**	NASA-CR-135316	p0052	W78-15167**
NASA-CP-134936	p0144	W78-23559**	NASA-CR-135317	p0052	W78-13123**
NASA-CP-134937	p0144	W78-23560**	NASA-CR-135318	p0087	W78-31238**
NASA-CP-134952	p0111	W78-13420**	NASA-CR-135319	p0029	W78-19153**
NASA-CP-134953	p0032	W78-33103**	NASA-CR-135320	p0029	W78-19154**
NASA-CP-134954	p0026	W78-10093**	NASA-CR-135321	p0037	W78-14063**
NASA-CP-135011	p0010	W78-25080**	NASA-CR-135322	p0127	W78-18460**
NASA-CP-135121	p0144	W78-17463**	NASA-CR-135323	p0090	W78-16194**
NASA-CP-135129	p0112	W78-18411**	NASA-CR-135324	p0181	W78-25988**
NASA-CP-135164	p0067	W78-14119**	NASA-CR-135325	p0181	W78-22970**
NASA-CP-135173	p0100	W78-29350**	NASA-CR-135327	p0028	W78-16052**
NASA-CP-135174	p0100	W78-29351**	NASA-CR-135328	p0090	W78-20350**
NASA-CP-135189-VOL-1	p0167	W78-29867**	NASA-CR-135329	p0090	W78-19326**
NASA-CP-135189-VOL-2	p0167	W78-29868**	NASA-CR-135330	p0090	W78-25235**
NASA-CP-135189-VOL-3	p0167	W78-29869**	NASA-CR-135331	p0108	W78-17342**
NASA-CP-135195	p0122	W78-27429**	NASA-CR-135332	p0145	W78-29584**
NASA-CP-135203	p0026	W78-10092**	NASA-CR-135333	p0182	W78-29992**
NASA-CP-135213	p0029	W78-21111**	NASA-CP-135334	p0092	W78-18251**
NASA-CP-135215	p0027	W78-13057**	NASA-CR-135335	p0062	W78-18131**
NASA-CP-135226	p0053	W78-19198**	NASA-CR-135336	p0144	W78-20603**
NASA-CP-135227	p0041	W78-15144**	NASA-CR-135337	p0079	W78-21265**
NASA-CP-135230	p0122	W78-28466**	NASA-CR-135338	p0079	W78-21266**
NASA-CP-135231	p0026	W78-11082**	NASA-CR-135339	p0112	W78-20489**
			NASA-CR-135341	p0078	W78-19259**
			NASA-CR-135342	p0169	W78-18883**

REPORT/ACCESSION NUMBER INDEX

NASA-CR-135355	p0127	W78-2280200	NASA-TN-73780	p0101	W78-1336900
NASA-CR-135356	p0054	W78-2427900	NASA-TN-73742	p0068	W78-1318100
NASA-CR-135357	p0054	W78-2025000	NASA-TN-73743	p0130	W78-1462800
NASA-CR-135359	p0028	W78-1705800	NASA-TN-73750	p0150	W78-1755800
NASA-CR-135360	p0028	W78-1605800	NASA-TN-73751	p0131	W78-1463100
NASA-CR-135362	p0029	W78-1916000	NASA-TN-73754	p0131	W78-1643800
NASA-CR-135364	p0099	W78-1939200	NASA-TN-73755	p0101	W78-1431300
NASA-CR-135366	p0121	W78-2147200	NASA-TN-73756	p0179	W78-1898800
NASA-CR-135369	p0127	W78-2149300	NASA-TN-73757	p0179	W78-1798200
NASA-CR-135370	p0127	W78-2149400	NASA-TN-73758	p0178	W78-1793300
NASA-CR-135377	p0063	W78-2513200	NASA-TN-73759	p0178	W78-1692800
NASA-CR-135378	p0037	W78-2015000	NASA-TN-73760	p0178	W78-2101000
NASA-CR-135381	p0029	W78-2012900	NASA-TN-73761	p0179	W78-1798000
NASA-CR-135382	p0181	W78-2399900	NASA-TN-73762	p0179	W78-1793900
NASA-CR-135383	p0054	W78-2214800	NASA-TN-73763	p0178	W78-1793800
NASA-CR-135387	p0030	W78-2414100	NASA-TN-73764	p0178	W78-1793800
NASA-CR-135388	p0029	W78-2209600	NASA-TN-73765	p0178	W78-1793600
NASA-CR-135391	p0031	W78-2909900	NASA-TN-73766	p0179	W78-2002100
NASA-CR-135395	p0030	W78-2712800	NASA-TN-73767	p0180	W78-2957500
NASA-CR-135401	p0054	W78-2428000	NASA-TN-73768	p0179	W78-2002200
NASA-CR-135402	p0122	W78-2944900	NASA-TN-73769	p0138	W78-2655100
NASA-CR-135408-VOL-1	p0167	W78-2582700	NASA-TN-73770	p0172	W78-2392300
NASA-CR-135408-VOL-2	p0167	W78-2582800	NASA-TN-73771	p0059	W78-2122000
NASA-CR-135408-VOL-3	p0167	W78-2582900	NASA-TN-73772	p0082	W78-2223200
NASA-CR-135405	p0148	W78-2364800	NASA-TN-73773	p0135	W78-2355600
NASA-CR-135407	p0031	W78-2910500	NASA-TN-73774	p0156	W78-2179100
NASA-CR-135408	p0112	W78-2540700	NASA-TN-73775	p0135	W78-2355700
NASA-CR-135409	p0079	W78-2516600	NASA-TN-73778	p0162	W78-1384800
NASA-CR-135411	p0122	W78-3142700	NASA-TN-73780	p0014	W78-1305600
NASA-CR-135414	p0038	W78-2510500	NASA-TN-73782	p0114	W78-1951200
NASA-CR-135418-APP	p0038	W78-2510600	NASA-TN-73786	p0088	W78-1417700
NASA-CR-135416-VOL-1	p0042	W78-3114100	NASA-TN-73787	p0035	W78-1505900
NASA-CR-135416-VOL-2	p0042	W78-3114200	NASA-TN-73788	p0130	W78-1462900
NASA-CR-135417	p0031	W78-2910400	NASA-TN-73789	p0069	W78-1718700
NASA-CR-135424	p0030	W78-2614700	NASA-TN-73791	p0131	W78-1463000
NASA-CR-135427	p0010	W78-2712900	NASA-TN-73792	p0057	W78-1715200
NASA-CR-135428	p0145	W78-2860800	NASA-TN-73794	p0064	W78-1315700
NASA-CR-135430	p0181	W78-2699700	NASA-TN-73795	p0064	W78-1315800
NASA-CR-135431	p0032	W78-3209700	NASA-TN-73796	p0064	W78-1315900
NASA-CR-135435	p0092	W78-2927600	NASA-TN-73797	p0093	W78-1038600
NASA-CR-135444	p0032	W78-3110800	NASA-TN-73798	p0011	W78-1306000
NASA-CR-135450	p0124	W78-3306100	NASA-TN-73799	p0131	W78-1556200
NASA-CR-155299	p0143	W78-1359900	NASA-TN-73800	p0171	W78-1088300
NASA-CR-155949	p0112	W78-1948000	NASA-TN-73803	p0048	W78-2120500
NASA-CR-157117	p0145	W78-2467800	NASA-TN-73804	p0093	W78-1328200
NASA-CR-157222	p0145	W78-2657900	NASA-TN-73805	p0069	W78-1926100
NASA-CR-157248	p0145	W78-2755200	NASA-TN-73806	p0065	W78-1923700
NASA-CR-157648	p0062	W78-2025700	NASA-TN-73807	p0111	W78-1438600
NASA-CR-159390	p0031	W78-2910300	NASA-TN-73808	p0096	W78-1333000
NASA-CR-159392	p0145	W78-2754000	NASA-TN-73809	p0163	W78-1385300
NASA-CR-159402	p0032	W78-3110600	NASA-TN-73810	p0148	W78-1367000
NASA-CR-159403	p0087	W78-3123500	NASA-TN-73811	p0176	W78-1393800
NASA-CR-159404	p0108	W78-3138000	NASA-TN-73812	p0125	W78-1347700
NASA-CR-159410	p0047	W78-1114300	NASA-TN-73813	p0124	W78-1739700
NASA-CR-159413	p0108	W78-2941000	NASA-TN-73814	p0171	W78-1088400
NASA-CR-159415	p0012	W78-3310600	NASA-TN-73815	p0068	W78-1318300
NASA-CR-159418	p0142	W78-3280900	NASA-TN-73816	p0163	W78-1385400
NASA-CR-159424	p0012	W78-3209600	NASA-TN-73817	p0148	W78-1366900
NASA-CR-159430	p0008	W78-3304400	NASA-TN-73818	p0015	W78-1504800
NASA-CR-159433	p0128	W78-3347800	NASA-TN-73819	p0015	W78-1504900
NASA-RP-100H	p0009	W78-1102400	NASA-TN-73820	p0132	W78-1748600
NASA-SP-273	p0156	W78-1772400	NASA-TN-73821	p0003	W78-1700100
NASA-SP-A121	p0117	W78-3058400	NASA-TN-73822	p0065	W78-1717200
NASA-SP-A123	p0047	W78-1408900	NASA-TN-73823	p0163	W78-1585200
NASA-SP-A128	p0048	W78-2121100	NASA-TN-73824	p0101	W78-1336100
NASA-SP-A125	p0050	W78-3116400	NASA-TN-73825	p0111	W78-1556300
NASA-TN-X-3483	p0015	W78-1301300	NASA-TN-73826	p0057	W78-1715300
NASA-TN-X-71478	p0064	W78-1521100	NASA-TN-73827	p0093	W78-1428300
NASA-TN-X-73547	p0036	W78-1012900	NASA-TN-73828	p0164	W78-1676600
NASA-TN-X-73641	p0171	W78-1590500	NASA-TN-73829	p0088	W78-1323300
NASA-TN-X-73647	p0003	W78-1002600	NASA-TN-73830	p0041	W78-1310700
NASA-TN-X-73648	p0012	W78-1009700	NASA-TN-73831	p0016	W78-1605500
NASA-TN-X-73647	p0101	W78-1041500	NASA-TN-73833	p0096	W78-1333100
NASA-TN-73507-VOL-1	p0021	W78-2910000	NASA-TN-73834	p0180	W78-2002300
NASA-TN-73652	p0010	W78-1704100	NASA-TN-73834-REV	p0180	W78-2501000
NASA-TN-73666	p0041	W78-2114000	NASA-TN-73835	p0131	W78-1746600
NASA-TN-73693	p0057	W78-1021700	NASA-TN-73836	p0088	W78-1722900
NASA-TN-73700	p0047	W78-1113700	NASA-TN-73837	p0175	W78-1391600
NASA-TN-73714	p0012	W78-1009400	NASA-TN-73838	p0014	W78-1306100
NASA-TN-73719	p0040	W78-1029400	NASA-TN-73839	p0163	W78-1385500
NASA-TN-73724	p0109	W78-1340700	NASA-TN-73840	p0011	W78-1705200
NASA-TN-73732	p0015	W78-1504200	NASA-TN-73841	p0041	W78-1722000
NASA-TN-73733	p0047	W78-2120200	NASA-TN-73843	p0017	W78-1915700
NASA-TN-73735	p0113	W78-1343900	NASA-TN-73844	p0111	W78-1342100
NASA-TN-73739	p0057	W78-1313600	NASA-TN-73845	p0171	W78-1389000
			NASA-TN-73846	p0035	W78-1307700
			NASA-TN-73847	p0102	W78-1718100
			NASA-TN-73848	p0068	W78-1318200
				p0015	W78-1504300

REPORT/ACCESSION NUMBER INDEX

NASA-TN-73809	p0014	N78-1306200	NASA-TN-78863	p0041	N78-2118800
NASA-TN-73850	p0178	N78-1793700	NASA-TN-78864	p0089	N78-2314300
NASA-TN-73851	p0114	N78-1738900	NASA-TN-78865	p0089	N78-2437000
NASA-TN-73852	p0080	N78-1528000	NASA-TN-78866	p0089	N78-2436900
NASA-TN-73853	p0069	N78-1718900	NASA-TN-78867	p0134	N78-2247100
NASA-TN-73854	p0069	N78-1719000	NASA-TN-78868	p0019	N78-2209900
NASA-TN-73855	p0163	N78-1385600	NASA-TN-78869	p0048	N78-2120900
NASA-TN-73856	p0114	N78-1951300	NASA-TN-78870	p0019	N78-2209800
NASA-TN-73857	p0004	N78-1905700	NASA-TN-78871	p0138	N78-2654600
NASA-TN-73858	p0171	N78-1993800	NASA-TN-78872	p0103	N78-2338500
NASA-TN-73859	p0093	N78-1532600	NASA-TN-78873	p0011	N78-2413700
NASA-TN-73860	p0177	N78-1792100	NASA-TN-78874	p0011	N78-2413800
NASA-TN-73861	p0132	N78-1746700	NASA-TN-78875	p0020	N78-2614300
NASA-TN-73862	p0163	N78-1585300	NASA-TN-78876	p0070	N78-2319300
NASA-TN-73863	p0178	N78-1793500	NASA-TN-78877	p0071	N78-2433600
NASA-TN-73865	p0044	N78-2119900	NASA-TN-78878	p0164	N78-2489700
NASA-TN-73866	p0153	N78-2075500	NASA-TN-78879	p0072	N78-3120900
NASA-TN-73867	p0037	N78-1607600	NASA-TN-78880	p0140	N78-2956600
NASA-TN-73868	p0135	N78-2461500	NASA-TN-78881	p0125	N78-2347100
NASA-TN-73869	p0156	N78-1572900	NASA-TN-78882	p0125	N78-2347200
NASA-TN-73870	p0179	N78-1794100	NASA-TN-78883	p0126	N78-2347300
NASA-TN-73871	p0135	N78-2465900	NASA-TN-78884	p0180	N78-2999800
NASA-TN-73872	p0069	N78-1523500	NASA-TN-78885	p0164	N78-2489800
NASA-TN-73873	p0134	N78-1965600	NASA-TN-78886	p0164	N78-2687800
NASA-TN-73874	p0160	N78-1673500	NASA-TN-78887	p0135	N78-2461700
NASA-TN-73875	p0016	N78-1705900	NASA-TN-78888	p0088	N78-2435800
NASA-TN-73876	p0131	N78-1643500	NASA-TN-78889	p0019	N78-2308800
NASA-TN-73877	p0102	N78-1738000	NASA-TN-78890	p0071	N78-2421800
NASA-TN-73878	p0017	N78-1915800	NASA-TN-78891	p0011	N78-2413900
NASA-TN-73879	p0134	N78-1964800	NASA-TN-78892	p0049	N78-2617300
NASA-TN-73880	p0018	N78-2110800	NASA-TN-78893	p0115	N78-2644200
NASA-TN-73881	p0150	N78-1971000	NASA-TN-78894	p0005	N78-2609800
NASA-TN-73882	p0058	N78-1715400	NASA-TN-78895	p0056	N78-2617700
NASA-TN-73883	p0133	N78-1964200	NASA-TN-78896	p0065	N78-2618500
NASA-TN-73884	p0016	N78-1706000	NASA-TN-78897	p0083	N78-2621500
NASA-TN-73885	p0058	N78-1715500	NASA-TN-78898	p0115	N78-2644300
NASA-TN-73886	p0017	N78-1916100	NASA-TN-78899	p0005	N78-2609900
NASA-TN-73887	p0102	N78-2045800	NASA-TN-78900	p0093	N78-2637300
NASA-TN-73888	p0111	N78-2144100	NASA-TN-78901	p0135	N78-2461600
NASA-TN-73889	p0096	N78-2137200	NASA-TN-78902	p0137	N78-2654200
NASA-TN-73890	p0018	N78-2110900	NASA-TN-78903	p0180	N78-2699500
NASA-TN-73891	p0059	N78-2122100	NASA-TN-78904	p0056	N78-2617800
NASA-TN-73892	p0170	N78-1785600	NASA-TN-78905	p0124	N78-2456500
NASA-TN-73893	p0133	N78-1964300	NASA-TN-78906	p0020	N78-2614500
NASA-TN-73894	p0058	N78-1920400	NASA-TN-78907	p0116	N78-2644600
NASA-TN-73895	p0096	N78-1729800	NASA-TN-78908	p0116	N78-2644700
NASA-TN-73896	p0114	N78-2051100	NASA-TN-78909	p0154	N78-2480700
NASA-TN-73897	p0134	N78-2159600	NASA-TN-78910	p0041	N78-2616600
NASA-TN-73898	p0081	N78-1722100	NASA-TN-78911	p0137	N78-2654300
NASA-TN-73899	p0130	N78-1360800	NASA-TN-78912	p0126	N78-2745300
NASA-TN-73900	p0134	N78-1965700	NASA-TN-78913	p0083	N78-2621400
NASA-TN-73901	p0132	N78-1744900	NASA-TN-78914	p0138	N78-2655200
NASA-TN-73902	p0103	N78-2045900	NASA-TN-78915	p0139	N78-2655300
NASA-TN-73903	p0047	N78-2025100	NASA-TN-78916	p0017	N78-2714300
NASA-TN-73904	p0070	N78-2126700	NASA-TN-78917	p0177	N78-2898600
NASA-TN-73905	p0134	N78-1965800	NASA-TN-78918	p0140	N78-3153300
NASA-TN-73906	p0018	N78-2111000	NASA-TN-78919	p0005	N78-2610000
NASA-TN-73907	p0097	N78-2137300	NASA-TN-78920	p0138	N78-2654700
NASA-TN-73908	p0103	N78-2338400	NASA-TN-78921	p0138	N78-2654800
NASA-TN-73909	p0103	N78-2140300	NASA-TN-78922	p0138	N78-2654900
NASA-TN-73910	p0070	N78-2126600	NASA-TN-78923	p0116	N78-2555100
NASA-TN-73911	p0058	N78-1920600	NASA-TN-78924	p0137	N78-2654400
NASA-TN-73912	p0103	N78-2449400	NASA-TN-78925	p0137	N78-2654500
NASA-TN-73913	p0058	N78-2025400	NASA-TN-78926	p0115	N78-2644400
NASA-TN-73914	p0125	N78-1953900	NASA-TN-78927	p0020	N78-2614400
NASA-TN-73915	p0070	N78-1926200	NASA-TN-78928	p0139	N78-2861400
NASA-TN-73916	p0070	N78-2431500	NASA-TN-78929	p0005	N78-2708100
NASA-TN-73917	p0081	N78-2031400	NASA-TN-78930	p0084	N78-2924600
NASA-TN-73918	p0184	N78-2502500	NASA-TN-78931	p0172	N78-2692600
NASA-TN-73919	p0103	N78-2140000	NASA-TN-78932	p0083	N78-2725700
NASA-TN-73920	p0082	N78-2323100	NASA-TN-78933	p0180	N78-2699600
NASA-TN-73921	p0018	N78-2209100	NASA-TN-78934	p0116	N78-2644500
NASA-TN-73922	p0058	N78-2025500	NASA-TN-78935	p0139	N78-2655400
NASA-TN-73923	p0134	N78-1964400	NASA-TN-78936	p0104	N78-2738600
NASA-TN-73924	p0059	N78-2429100	NASA-TN-78937	p0044	N78-2717000
NASA-TN-73925	p0155	N78-2335100	NASA-TN-78938	p0138	N78-2655000
NASA-TN-73926	p0048	N78-2120600	NASA-TN-78939	p0172	N78-2791400
NASA-TN-73927	p0152	N78-2261800	NASA-TN-78940	p0049	N78-2717800
NASA-TN-73928	p0096	N78-1919700	NASA-TN-78941	p0071	N78-2921600
NASA-TN-73929	p0135	N78-2358800	NASA-TN-78942	p0104	N78-2736700
NASA-TN-73930	p0164	N78-2286300	NASA-TN-78943	p0164	N78-2848600
NASA-TN-73931	p0048	N78-2120700	NASA-TN-78944	p0081	N78-2727400
NASA-TN-73932	p0082	N78-2324100	NASA-TN-78945	p0104	N78-2639000
NASA-TN-73933	p0103	N78-2123400	NASA-TN-78946	p0139	N78-2655500
NASA-TN-73934	p0047	N78-2120300	NASA-TN-78947	p0116	N78-2742800
NASA-TN-73935	p0049	N78-2120800	NASA-TN-78948	p0083	N78-2924500
NASA-TN-73936	p0049	N78-2314400	NASA-TN-78949	p0021	N78-2712600
NASA-TN-73937	p0049	N78-2314400	NASA-TN-78950	p0140	N78-2957700
NASA-TN-73938	p0049	N78-2314200	NASA-TN-78951	p0140	N78-2957600
NASA-TN-73939	p0049	N78-2314200	NASA-TN-78952		
NASA-TN-73940	p0049	N78-2314200	NASA-TN-78953		

REPORT/ACCESSION NUMBER INDEX

NASA-TR-78954	p0037	N78-2714200	NASA-TP-1231	p0091	N78-2225700
NASA-TR-78955	p0021	N78-2712500	NASA-TP-1245	p0140	N78-2862800
NASA-TR-78957	p0139	N78-2753900	NASA-TP-1246	p0082	N78-2521500
NASA-TR-78958	p0034	N78-2713700	NASA-TP-1247	p0083	N78-2523600
NASA-TR-78959	p0129	N78-3351000	NASA-TP-1248	p0001	N78-2504900
NASA-TR-78960	p0072	N78-3121000	NASA-TP-1256	p0071	N78-2619800
NASA-TR-78961	p0139	N78-2860700	NASA-TP-1257	p0172	N78-2692700
NASA-TR-78962	p0021	N78-2712700	NASA-TP-1258	p0172	N78-3098400
NASA-TR-78964	p0140	N78-2957800	NASA-TP-1259	p0021	N78-2809900
NASA-TR-78965	p0084	N78-3123600	NASA-TP-1260	p0021	N78-2713000
NASA-TR-78966	p0072	N78-3120800	NASA-TP-1261	p0161	N78-3089600
NASA-TR-78967	p0071	N78-2921500	NASA-TP-1262	p0071	N78-2619900
NASA-TR-78968	p0104	N78-2837200	NASA-TP-1264	p0043	N78-2815900
NASA-TR-78969	p0105	N78-2940700	NASA-TP-1265	p0063	N78-2824700
NASA-TR-78973	p0072	N78-3121100	NASA-TP-1271	p0104	N78-2837400
NASA-TR-78974	p0152	N78-3169000	NASA-TP-1272	p0116	N78-2845700
NASA-TR-78975	p0093	N78-3132300	NASA-TP-1273	p0117	N78-2845800
NASA-TR-78976	p0072	N78-3121200	NASA-TP-1274	p0071	N78-2822500
NASA-TR-78977	p0141	N78-3153400	NASA-TP-1287	p0117	N78-3058500
NASA-TR-78978	p0059	N78-3219100	NASA-TP-1293	p0084	N78-3023800
NASA-TR-78979	p0126	N78-3246400	NASA-TP-1294	p0005	N78-3005700
NASA-TR-78981	p0059	N78-3315000	NASA-TP-1295	p0022	N78-3311000
NASA-TR-78983	p0009	N78-3106100	NASA-TP-1296	p0072	N78-3020500
NASA-TR-78985	p0059	N78-3314900	NASA-TP-1298	p0022	N78-3310700
NASA-TR-78986	p0165	N78-3187100	NASA-TP-1308	p0073	N78-3121300
NASA-TR-78987	p0117	N78-3344500	NASA-TP-1309	p0072	N78-3020600
NASA-TR-78990	p0183	N78-3201400	NASA-TP-1310	p0022	N78-3110900
NASA-TR-78992	p0093	N78-3328300	NASA-TP-1314	p0022	N78-3310900
NASA-TR-79000	p0060	N78-3315100	NASA-TP-1337	p0022	N78-3310800
NASA-TR-79009	p0022	N78-3310200	NASA-TP-1341	p0073	N78-3319600
NASA-TR-79010	p0105	N78-3338000	NASA-TP-1342	p0117	N78-3344700
NASA-TR-79502	p0056	N78-2617200	NASA-TP-1344	p0043	N78-3313700
NASA-TR-79509	p0140	N78-2700300			
NASA-TR-79757	p0140	N78-2958100			
NASA-TP-1006	p0156	N78-1074600	NEAR-TR-136	p0001	N78-1598700
NASA-TP-1007	p0015	N78-1605300	PR-22	p0143	N78-1359900
NASA-TP-1055	p0096	N78-1130100	PR-23	p0145	N78-2467400
NASA-TP-1057	p0003	N78-1100700	PR-26	p0145	N78-2657900
NASA-TP-1059	p0040	N78-1029500	PR-27	p0145	N78-2755200
NASA-TP-1068	p0014	N78-1110600			
NASA-TP-1069	p0018	N78-2111200	PSI-TR-97	p0112	N78-2048900
NASA-TP-1081	p0047	N78-1313800	PT-5228	p0042	N78-3114300
NASA-TP-1082	p0057	N78-1609300			
NASA-TP-1091	p0003	N78-1100200	PWA-PP-8499-VOL-1	p0026	N78-1208100
NASA-TP-1092	p0113	N78-1047400	PWA-PR-8499-VOL-2	p0026	N78-1208200
NASA-TP-1093	p0064	N78-1216700			
NASA-TP-1094	p0015	N78-1106400	PWA-5336	p0002	N78-1598800
NASA-TP-1095	p0101	N78-1337900	PWA-5336	p0002	N78-1598900
NASA-TP-1096	p0040	N78-1222200	PWA-5336	p0002	N78-1599000
NASA-TP-1097	p0068	N78-1123200	PWA-5501	p0169	N78-3283600
NASA-TP-1098	p0047	N78-1312400	PWA-5506	p0008	N78-2105800
NASA-TP-1099	p0109	N78-1546300	PWA-5509-VOL-1	p0167	N78-2986700
NASA-TP-1109	p0003	N78-1600100	PWA-5509-VOL-2	p0167	N78-2986800
NASA-TP-1110	p0019	N78-2210100	PWA-5509-VOL-3	p0167	N78-2986900
NASA-TP-1125	p0040	N78-1527700	PWA-5512-24	p0031	N78-2910500
NASA-TP-1126	p0003	N78-1499800	PWA-5516	p0007	N78-1799100
NASA-TP-1127	p0041	N78-1712700	PWA-5534	p0029	N78-2111100
NASA-TP-1128	p0008	N78-1522900	PWA-5540	p0027	N78-1504100
NASA-TP-1129	p0040	N78-1527800	PWA-5543	p0027	N78-1305900
NASA-TP-1130	p0114	N78-1842900	PWA-5544-13	p0030	N78-2712900
NASA-TP-1131	p0068	N78-1523000	PWA-5544-7	p0029	N78-1916000
NASA-TP-1132	p0003	N78-1799400	PWA-5547-4	p0026	N78-1106200
NASA-TP-1134	p0102	N78-1713800	PWA-5548-9	p0123	N78-3243300
NASA-TP-1136	p0004	N78-2034000	PWA-5549-8	p0029	N78-2202400
NASA-TP-1150	p0114	N78-2051200	PWA-5554-3	p0028	N78-1706400
NASA-TP-1151	p0017	N78-2011300	PWA-5554-4	p0028	N78-1706500
NASA-TP-1152	p0046	N78-1714500	PWA-5554-5	p0028	N78-1706600
NASA-TP-1156	p0041	N78-2031400	PWA-5559-12	p0030	N78-2414100
NASA-TP-1160	p0048	N78-2035100	PWA-5570-12-VOL-1	p0079	N78-2516600
NASA-TP-1161	p0041	N78-2031600	PWA-5593	p0028	N78-1605800
NASA-TP-1162	p0171	N78-2095000	PWA-5616	p0032	N78-3209600
NASA-TP-1190	p0070	N78-2414800			
NASA-TP-1191	p0092	N78-2129400	P77-437	p0099	N78-1540000
NASA-TP-1192	p0065	N78-2024100	P77-544	p0099	N78-2445400
NASA-TP-1193	p0070	N78-2126400	P78-128	p0112	N78-2540700
NASA-TP-1194	p0017	N78-2011100			
NASA-TP-1194	p0114	N78-2051100	CTPR-1	p0181	N78-2297000
NASA-TP-1197	p0041	N78-2031700			
NASA-TP-1199	p0042	N78-2129500	R-1382	p0144	N78-2355900
NASA-TP-1199	p0017	N78-2013200	R-1382	p0144	N78-2356000
NASA-TP-1200	p0156	N78-2083600			
NASA-TP-1202	p0115	N78-2147300	RADC-TR-77-216	p0027	N78-1208300
NASA-TP-1203	p0115	N78-2147000			
NASA-TP-1234	p0017	N78-2011300	RDR-1817-22	p0027	N78-1404700
NASA-TP-1205	p0018	N78-2111400	RDR-1931-23	p0047	N78-3121800
NASA-TP-1228	p0019	N78-2109500			
NASA-TP-1229	p0115	N78-2541300	REPT-904-NASIC-R1	p0062	N78-1313400
NASA-TP-1230	p0115	N78-2237700	REPT-77-9F1-HYSUC-R9	p0099	N78-1939200

REPORT/ACCESSION NUMBER INDEX

REPT-77-979-BAPEX-R1	p0124	W78-1550100	US-PATENT-APPL-SH-676432	p0089	W78-243650
REPT-77ARG596	p0002	W78-2104400	US-PATENT-APPL-SH-677353	p0153	W78-147
REPT-1099-1	p0090	W78-1932600	US-PATENT-APPL-SH-684171	p0069	W78-181830
REPT-1099-1-VOL-1	p0090	W78-2035000	US-PATENT-APPL-SH-686449	p0102	W78-183550
REPT-1099-1-VOL-3	p0090	W78-2523500	US-PATENT-APPL-SH-687822	p0130	W78-146250
RR-78-035	p0105	W78-2958000	US-PATENT-APPL-SH-692413	p0065	W78-251480
FI/RD77-170	p0026	W78-1108200	US-PATENT-APPL-SH-695513	p0019	W78-250890
FI/RD77-192	p0054	W78-2512700	US-PATENT-APPL-SH-708660	p0097	W78-273570
FI/RD77-252	p0140	W78-2062100	US-PATENT-APPL-SH-720521	p0136	W78-255300
FI/RD78-114	p0050	W78-2427900	US-PATENT-APPL-SH-739909	p0115	W78-245450
RR-1	p0148	W78-2364800	US-PATENT-APPL-SH-746269	p0136	W78-255280
R76ARG484-VOL-2	p0032	W78-3310300	US-PATENT-APPL-SH-746580	p0102	W78-173350
R77-911739-17	p0166	W78-2092000	US-PATENT-APPL-SH-763753	p0129	W78-144520
R77-911739-18	p0167	W78-2092100	US-PATENT-APPL-SH-770869	p0136	W78-255270
R77-912184-21	p0087	W78-2128900	US-PATENT-APPL-SH-779428	p0104	W78-253510
R77-912252-23	p0087	W78-1721600	US-PATENT-APPL-SH-790637	p0136	W78-255290
R77-912613-5	p0079	W78-2126800	US-PATENT-APPL-SH-801432	p0097	W78-323410
R77ARG569	p0077	W78-1123200	US-PATENT-APPL-SH-837794	p0169	W78-1990700
R77ARG593	p0027	W78-1305700	US-PATENT-APPL-SH-848428	p0065	W78-2514900
R77ARG635	p0027	W78-1305800	US-PATENT-APPL-SH-860405	p0070	W78-2220500
R77ARG667	p0062	W78-1409900	US-PATENT-APPL-SH-863280	p0065	W78-272260
R78-912881-2	p0090	W78-1619400	US-PATENT-APPL-SH-891370	p0049	W78-2214900
R78ARG476	p0124	W78-3386300	US-PATENT-APPL-SH-893857	p0059	W78-2216300
R78ARG510	p0032	W78-1110800	US-PATENT-APPL-SH-896955	p0097	W78-2532300
SAE PAPER 771008	p0023	W78-238400	US-PATENT-APPL-SH-897829	p0056	W78-2215700
SAE PAPER 780075	p0120	W78-3336400	US-PATENT-APPL-SH-901892	p0137	W78-2555500
SAE PAPER 780076	p0109	W78-3336500	US-PATENT-APPL-SH-910260	p0136	W78-2555400
SAE PAPER 780077	p0120	W78-3336600	US-PATENT-APPL-SH-915050	p0136	W78-2555300
SAE PAPER 780290	p0181	W78-3338200	US-PATENT-APPL-SH-916654	p0020	W78-2712200
SAE PAPER 780290	p0181	W78-3338200	US-PATENT-APPL-SH-916655	p0139	W78-2752000
SAE PAPER 780290	p0181	W78-3338200	US-PATENT-APPL-SH-929084	p0117	W78-2845900
SAE PAPER 780290	p0181	W78-3338200	US-PATENT-APPL-SH-931090	p0021	W78-3110300
SER-50959	p0010	W78-2508000	US-PATENT-CLASS-29-463	p0022	W78-331010
SKP-AL77T021	p0122	W78-2742900	US-PATENT-CLASS-29-572	p0136	W78-255270
SN-8320-F	p0087	W78-3123500	US-PATENT-CLASS-29-572	p0136	W78-255280
SSS-R-77-3367	p0099	W78-1332900	US-PATENT-CLASS-29-572	p0136	W78-255290
SSS-R-77-3368	p0099	W78-1332900	US-PATENT-CLASS-29-628	p0136	W78-255280
SSS-R-78-3420	p0052	W78-1312200	US-PATENT-CLASS-34-15	p0089	W78-243650
TE-8217/4220-123-77	p0143	W78-1759900	US-PATENT-CLASS-55-2	p0065	W78-251480
TE-8217/4220-140-77	p0145	W78-2467400	US-PATENT-CLASS-55-100	p0065	W78-251480
TE-4220/4233-24-78	p0145	W78-2647900	US-PATENT-CLASS-55-101	p0065	W78-251480
TF9220/4233-44-78	p0145	W78-2755200	US-PATENT-CLASS-60-39.28R	p0113	W78-104670
TR-2-6	p0130	W78-1360800	US-PATENT-CLASS-60-39.29R	p0115	W78-245450
TR-77-33	p0067	W78-2515000	US-PATENT-CLASS-60-39.31	p0016	W78-180640
TRW-A72042-RRBE	p0100	W78-2935100	US-PATENT-CLASS-60-39.51B	p0064	W78-102240
TRW-D04803-CFCH	p0100	W78-2935100	US-PATENT-CLASS-60-39.52	p0019	W78-250890
TRW-FR-7884-F	p0063	W78-2513200	US-PATENT-CLASS-60-39.65	p0097	W78-273570
TRW-1EP-7910	p0026	W78-1009200	US-PATENT-CLASS-60-39.66	p0113	W78-104670
TRW-27744.000	p0100	W78-2935000	US-PATENT-CLASS-60-39.69B	p0097	W78-273570
TRW-28014-R001-T0-00	p0054	W78-1970000	US-PATENT-CLASS-60-204	p0016	W78-170550
TRW-29999-R011-R0-00	p0053	W78-1516800	US-PATENT-CLASS-60-204	p0016	W78-180670
TRW-31526.000-VOL-1	p0054	W78-2025000	US-PATENT-CLASS-60-226R	p0016	W78-170550
TRW-31526.000-VOL-1	p0054	W78-2025000	US-PATENT-CLASS-60-226R	p0016	W78-170560
TRW-31526.000-VOL-1	p0054	W78-2025000	US-PATENT-CLASS-60-226R	p0016	W78-180660
TRW-31526.000-VOL-1	p0054	W78-2025000	US-PATENT-CLASS-60-226R	p0019	W78-250890
TRW-31526.000-VOL-1	p0054	W78-2025000	US-PATENT-CLASS-60-261	p0113	W78-173840
TRW-31526.000-VOL-1	p0054	W78-2025000	US-PATENT-CLASS-60-262	p0113	W78-173840
TRW-31526.000-VOL-1	p0054	W78-2025000	US-PATENT-CLASS-60-262	p0016	W78-180670
TRW-31526.000-VOL-1	p0054	W78-2025000	US-PATENT-CLASS-60-271	p0016	W78-170550
TRW-31526.000-VOL-1	p0054	W78-2025000	US-PATENT-CLASS-60-271	p0113	W78-173840
TRW-31526.000-VOL-1	p0054	W78-2025000	US-PATENT-CLASS-62-3	p0102	W78-173350
TRW-31526.000-VOL-1	p0054	W78-2025000	US-PATENT-CLASS-62-48	p0089	W78-243650
TRW-31526.000-VOL-1	p0054	W78-2025000	US-PATENT-CLASS-62-100	p0089	W78-243650
TRW-31526.000-VOL-1	p0054	W78-2025000	US-PATENT-CLASS-62-376	p0091	W78-172370
TRW-31526.000-VOL-1	p0054	W78-2025000	US-PATENT-CLASS-62-514R	p0091	W78-172370
TRW-31526.000-VOL-1	p0054	W78-2025000	US-PATENT-CLASS-74-185	p0016	W78-170560
TRW-31526.000-VOL-1	p0054	W78-2025000	US-PATENT-CLASS-74-417	p0016	W78-170560
TRW-31526.000-VOL-1	p0054	W78-2025000	US-PATENT-CLASS-74-572	p0022	W78-331010
TRW-31526.000-VOL-1	p0054	W78-2025000	US-PATENT-CLASS-75-124	p0069	W78-181820
TRW-31526.000-VOL-1	p0054	W78-2025000	US-PATENT-CLASS-75-126P	p0069	W78-181820
TRW-31526.000-VOL-1	p0054	W78-2025000	US-PATENT-CLASS-75-126P	p0069	W78-181820
TRW-31526.000-VOL-1	p0054	W78-2025000	US-PATENT-CLASS-75-128G	p0069	W78-181820
TRW-31526.000-VOL-1	p0054	W78-2025000	US-PATENT-CLASS-75-128G	p0069	W78-181820
TRW-31526.000-VOL-1	p0054	W78-2025000	US-PATENT-CLASS-75-128T	p0069	W78-181820
TRW-31526.000-VOL-1	p0054	W78-2025000	US-PATENT-CLASS-75-170	p0069	W78-181820
TRW-31526.000-VOL-1	p0054	W78-2025000	US-PATENT-CLASS-123-41.33	p0113	W78-104670
TRW-31526.000-VOL-1	p0054	W78-2025000	US-PATENT-CLASS-123-122E	p0113	W78-104670
TRW-31526.000-VOL-1	p0054	W78-2025000	US-PATENT-CLASS-126-270	p0132	W78-195900
TRW-31526.000-VOL-1	p0054	W78-2025000	US-PATENT-CLASS-128-105	p0153	W78-147730
TRW-31526.000-VOL-1	p0054	W78-2025000	US-PATENT-CLASS-136-89CC	p0136	W78-255270
TRW-31526.000-VOL-1	p0054	W78-2025000	US-PATENT-CLASS-136-89CC	p0136	W78-255290
TRW-31526.000-VOL-1	p0054	W78-2025000	US-PATENT-CLASS-136-89H	p0136	W78-255280
TRW-31526.000-VOL-1	p0054	W78-2025000	US-PATENT-CLASS-136-89H	p0136	W78-255290
TRW-31526.000-VOL-1	p0054	W78-2025000	US-PATENT-CLASS-136-89P	p0136	W78-255280
TRW-31526.000-VOL-1	p0054	W78-2025000	US-PATENT-CLASS-136-89P	p0136	W78-255290
TRW-31526.000-VOL-1	p0054	W78-2025000	US-PATENT-CLASS-137-108	p0136	W78-255280
TRW-31526.000-VOL-1	p0054	W78-2025000	US-PATENT-CLASS-137-108	p0136	W78-255290
TRW-31526.000-VOL-1	p0054	W78-2025000	US-PATENT-CLASS-137-501	p0113	W78-104670
TRW-31526.000-VOL-1	p0054	W78-2025000	US-PATENT-CLASS-137-505.16	p0104	W78-253510
TRW-31526.000-VOL-1	p0054	W78-2025000	US-PATENT-CLASS-137-505.16	p0104	W78-253510

REPORT/ACCESSION NUMBER INDEX

US-PATENT-CLASS-148-32	p0069	N78-18183*	US-PATENT-4,068,470	p0016	N78-17056*
US-PATENT-CLASS-148-32.5	p0069	N78-18183*	US-PATENT-4,068,495	p0091	N78-17237*
US-PATENT-CLASS-156-633	p0136	N78-25529*	US-PATENT-4,069,028	p0102	N78-17335*
US-PATENT-CLASS-165-105	p0064	N78-10224*	US-PATENT-4,069,661	p0016	N78-18067*
US-PATENT-CLASS-166-248	p0129	N78-14452*	US-PATENT-4,077,788	p0089	N78-24365*
US-PATENT-CLASS-166-259	p0129	N78-14452*	US-PATENT-4,078,378	p0115	N78-24545*
US-PATENT-CLASS-176-11	p0065	N78-27226*	US-PATENT-4,083,569	p0136	N78-25527*
US-PATENT-CLASS-176-16	p0065	N78-27226*	US-PATENT-4,083,097	p0136	N78-25528*
US-PATENT-CLASS-244-53A	p0016	N78-18066*	US-PATENT-4,083,181	p0019	N78-25089*
US-PATENT-CLASS-244-54	p0016	N78-18066*	US-PATENT-4,084,612	p0104	N78-25351*
US-PATENT-CLASS-250-400	p0065	N78-27226*	US-PATENT-4,084,825	p0020	N78-25090*
US-PATENT-CLASS-250-423P	p0065	N78-25148*	US-PATENT-4,084,985	p0136	N78-25529*
US-PATENT-CLASS-250-429	p0065	N78-27226*	US-PATENT-4,085,241	p0136	N78-25530*
US-PATENT-CLASS-250-492B	p0065	N78-27226*	US-PATENT-4,085,332	p0065	N78-25148*
US-PATENT-CLASS-250-499	p0089	N78-24365*	US-PATENT-4,085,962	p0097	N78-27357*
US-PATENT-CLASS-250-499	p0113	N78-13436*	US-PATENT-4,088,532	p0065	N78-27226*
US-PATENT-CLASS-250-528	p0065	N78-25148*	US-PATENT-4,092,712	p0097	N78-32341*
US-PATENT-CLASS-250-531	p0065	N78-25148*	US-PATENT-4,097,194	p0022	N78-33101*
US-PATENT-CLASS-260-2R	p0080	N78-15276*				
US-PATENT-CLASS-277-25	p0020	N78-25090*				
US-PATENT-CLASS-277-13A	p0020	N78-25090*				
US-PATENT-CLASS-313-22	p0091	N78-17237*				
US-PATENT-CLASS-313-61S	p0113	N78-13436*				
US-PATENT-CLASS-315-22	p0096	N78-17293*				
US-PATENT-CLASS-320-6	p0130	N78-14625*				
US-PATENT-CLASS-320-15	p0130	N78-14625*				
US-PATENT-CLASS-320-18	p0130	N78-14625*				
US-PATENT-CLASS-320-40	p0130	N78-14625*				
US-PATENT-CLASS-357-30	p0136	N78-25527*				
US-PATENT-CLASS-357-65	p0136	N78-25527*				
US-PATENT-CLASS-357-67	p0136	N78-25527*				
US-PATENT-CLASS-363-16	p0097	N78-32341*				
US-PATENT-CLASS-363-6C	p0097	N78-32341*				
US-PATENT-CLASS-363-101	p0097	N78-32341*				
US-PATENT-CLASS-415-1A0	p0113	N78-10467*				
US-PATENT-CLASS-416-135	p0113	N78-10468*				
US-PATENT-CLASS-416-141	p0113	N78-10468*				
US-PATENT-CLASS-416-218A	p0022	N78-33101*				
US-PATENT-CLASS-416-220R	p0113	N78-10468*				
US-PATENT-CLASS-416-244A	p0022	N78-33101*				
US-PATENT-CLASS-416-248	p0113	N78-10468*				
US-PATENT-CLASS-423-648R	p0089	N78-24365*				
US-PATENT-CLASS-423-3A	p0102	N78-18355*				
US-PATENT-CLASS-427-75	p0136	N78-25527*				
US-PATENT-CLASS-427-124	p0113	N78-13436*				
US-PATENT-CLASS-427-126	p0113	N78-13436*				
US-PATENT-CLASS-427-160	p0132	N78-19599*				
US-PATENT-CLASS-427-248E	p0113	N78-13436*				
US-PATENT-CLASS-427-250	p0113	N78-13436*				
US-PATENT-CLASS-427-255	p0113	N78-13436*				
US-PATENT-CLASS-427-261	p0136	N78-25527*				
US-PATENT-CLASS-427-395B	p0136	N78-25530*				
US-PATENT-CLASS-427-395C	p0136	N78-25530*				
US-PATENT-CLASS-427-405	p0102	N78-18355*				
US-PATENT-CLASS-427-419A	p0102	N78-18355*				
US-PATENT-CLASS-427-423	p0102	N78-18355*				
US-PATENT-CLASS-428-633	p0102	N78-18355*				
US-PATENT-CLASS-428-652	p0102	N78-18355*				
US-PATENT-CLASS-428-652	p0132	N78-19599*				
US-PATENT-CLASS-428-667	p0102	N78-18355*				
US-PATENT-CLASS-428-667	p0132	N78-19599*				
US-PATENT-CLASS-428-679	p0132	N78-19599*				
US-PATENT-CLASS-429-254	p0136	N78-25530*				
US-PATENT-CLASS-431-7	p0097	N78-27357*				
US-PATENT-CLASS-431-10	p0097	N78-27357*				
US-PATENT-CLASS-431-15R	p0064	N78-10224*				
US-PATENT-CLASS-431-328	p0097	N78-27357*				
US-PATENT-CLASS-431-352	p0064	N78-10224*				
US-PATENT-CLASS-526-193	p0080	N78-15276*				
US-PATENT-CLASS-526-225	p0080	N78-15276*				
US-PATENT-CLASS-544-193	p0080	N78-15276*				
US-PATENT-3,423,627	p0096	N78-17293*				
US-PATENT-3,694,313	p0065	N78-27226*				
US-PATENT-4,041,697	p0113	N78-10467*				
US-PATENT-4,047,840	p0113	N78-10468*				
US-PATENT-4,052,144	p0064	N78-10224*				
US-PATENT-4,055,041	p0016	N78-18066*				
US-PATENT-4,055,416	p0069	N78-18183*				
US-PATENT-4,055,467	p0069	N78-18183*				
US-PATENT-4,055,686	p0113	N78-13436*				
US-PATENT-4,055,705	p0102	N78-18355*				
US-PATENT-4,055,747	p0132	N78-19599*				
US-PATENT-4,061,146	p0153	N78-14774*				
US-PATENT-4,061,190	p0129	N78-14452*				
US-PATENT-4,061,856	p0080	N78-15276*				
US-PATENT-4,061,955	p0130	N78-14625*				
US-PATENT-4,064,692	p0113	N78-17384*				
US-PATENT-4,068,469	p0016	N78-17055*				
UTRC78-106	p0008	N78-33044**				
W-06553	p0098	N78-11295**				